Geological, mineralogical and geochemical characterisation of the Heavy Rare Earth-rich carbonatites at Lofdal, Namibia.

Submitted by Vistorina Nandigolo Do Cabo
to the University of Exeter
as a thesis for the degree of
Doctor of Philosophy in Earth Resources
In April 2013

certify that all material in this thesis which is not my own work has been identified and that no material has previously been submitted and approved for the award of a degree by this or any other University.

Signature: ……..

Abstract

This study considered the geology, mineralogy, geochemistry, formation and evolution of the heavy rare earth element (HREE) mineralised Lofdal alkaline carbonatite complex (LACC), which is located on the Bergville and Lofdal farms northwest of Khorixas, in the Kunene Region of the Republic of Namibia. .

Field methods used included mapping, ground and hyperspectral airborne geophysics, and sampling. Analytical techniques used were optical petrography and CL, XRF, ICP-AES, backscattered and secondary electron imaging, electron microprobe, LA-ICP-MS, leaching, as well as carbon and oxygen stable isotope determination.

The LACC comprises a swarm of dykes, mainly calcite carbonatite but also dolomite and ankerite carbonatite dykes (classified into five types) and two newly discovered plugs of calcite carbonatite ('Main' and 'Emanya'), with associated dykes and plugs of phonolites, syenites and rare mafic rocks. These all intrude into the Huab Metamorphic Complex basement rocks within a NE-SW shear zone over 30 km long.

The main HREE host mineral is xenotime-(Y). It occurs in highly oxidised iron-rich calcite carbonatite dykes mantling and replacing zircon, associated with hematite, thorite and apatite, or associated with monazite-(Ce), synchysite-(Ce), and parisite-(Ce), replacing the fluorocarbonates; it also forms aggregates in ankerite carbonatite. Although xenotime-(Y) occurs throughout the paragenetic sequence, there is much evidence for hydrothermal fluid activity at Lofdal, altering the dykes, and taking xenotime-(Y) into brecciated carbonate veins in albitised country rock (fenite). Radiogenic (Sr, Nd-Sm, U-Pb) and C and O stable isotope studies confirm that the carbonatite, derived from an enriched mantle, is the source of the REE. Mineralisation was contemporaneous with carbonatite emplacement at 765 ±16 Ma. Magmatic fluids >300°C were diluted with cool meteoric fluids. Abundant fluorite and carbonate indicate roles for F- and CO_3^{2-} in addition to Cl^- in REE transport. These ligands form the most stable complexes with HREE and since xenotime is soluble in concentrated alkali halide solutions, they could have preferentially transported and then deposited xenotime.

Many of the features of Lofdal are common to other REE-rich carbonatite complexes but the xenotime-(Y) abundance is so far unique. The high amount of fluid activity in shear zones around the dyke swarm and probably a higher proportion of HREE in the original magmas seem to be the main differentiating features.

Acknowledgements

I thank the Ministry of Mines and Energy through the Geological Survey of Namibia, Ministry of Education and Energy Africa (PTY) Ltd for the financial support to carry out this study.

Many thanks to my supervisors Prof. Frances Wall, Dr. Ben Williams from Camborne School of Mines and Prof. Hillary Downes Birkbeck, University College of London who assisted to make this project possible. Their encouragement and help during study and their advices contributed to the success of this project.

I thank Dr. Rainer Ellmies who supported this project work and shared the heat and rain in the field. I thank you for the valuable discussions we had around fire in the field.

My special thanks go to Etruscan and Namibia Rare Earth for their generosity to share their valuable data with me and for the logistical support during the field trips.

The assistance of A.M. van den Kerkhof during acquisition of CL spectra at the Geowissenschaftliches Zentrum Göttingen is highly acknowledged.

In particular, I thank Prof. Reimar Seltmann and Dr.Tony Mariano for the advice and encouragement for the project.

Thanks are due to Dr. Baruch Spiro for helping with isotope analysis, Dr. Maria Sitnikova for reflected light microscopy and Bundesanstalt für Geowissenschaften und Rohstoffe (BGR) team for the various chemical analyses.

I thank Dr. Scott Swinden, Dr. Gabi Schneider, Dr. Fredy Kamona and Ms. Linda Scotty for the support and very helpful comments on the draft manuscript.

I also thank my family, Tony and Johanna who supported me during the proctracted time of my studies.

TABLE OF CONTENTS

LIST OF TABLES

LIST OF FIGURES

Figure 9.3 Schematic diagram illustrating the carbonatite only association and seven alkali silicate rock associations occurring with carbonatite Woolley and Kjarsgaard (2008). Relative depths of magma generation in the mantle and, in particular, two levels of carbonatite generation are also illustrated, i.e., directly in the mantle (stars) and by differentiation processes at shallower depths (open white boxes). Note that carbonatite originating in the mantle can pass directly to the surface, and need not be involved in differentiation at a higher level (open white boxes). Ultramafic cumulate rocks are depicted by the solid black rectangles. Known alkali silicate differentiation series are represented by the thin black lines with arrowheads indicating the sequence from primary magma to differentiate. The red box indicates the fit to the Lofdal Alkaline Carbonatite Complex. The red dashed line indicates the possible source region of the LACC magma. 296

Chapter 1: Introduction; Aim of study, summary of approach and methodology

The study of carbonatites with respect to their variety of origin, formation and occurrence, their geotectonic positions and economic importance as carriers of strategic commodities has been a challenge since they were identified as a unique rock type.

The initial aim of the project was to study in detail the swarm of carbonatite dykes around the Lofdal area, which had been identified as being highly unusual in containing the heavy rare earth mineral, xenotime-(Y). The focus was on petrography, stratigraphy, age, mineral chemistry and relationship to the alkaline felsic dykes and the syenites plugs at Lofdal and Oas. During the course of the field investigation, several carbonatite bodies were discovered by the author. The discovery includes two carbonatite plugs extending up to 2 km^2. Consequently, the newly discovered carbonatites became part of the research project. Alkaline rocks associated with the carbonatites were also investigated and form part of this study.

The overall aims of the study were to determine the field geology, geochemistry, geochronology and mineralogy of the carbonatite complex in order to determine how the xenotime formed and in particular to differentiate between the three most likely scenarios for xenotime formation: precipitation directly from the carbonatite magma, formation by late-stage carbonatitic processes in a pegmatoid or hydrothermal environment, or crystallization as a result of much later metamorphic alteration of the carbonatite. A better understanding of xenotime at Lofdal will help future exploration for rare earths at the Lofdal complex and also help target valuable heavy rare earths associated with other carbonatite complexes worldwide.

The specific objectives and approach were:

1. To map and describe the field geology, including the use of innovative remote sensing methods such as hyperspectral imaging;
2. To define the unusual mineralogy and geochemistry of Lofdal including analysis by whole rock geochemical methods, stable isotope analysis and spatially-resolved mineral analysis;
3. To use state of the art analytical methods of geochronology of xenotime-(Y), pyrochlore and zircon minerals to determine the formation age of the Lofdal complex permitting to put it into its geotectonic context;

4. To combine the geochemistry, mineralogy and geochronology to give a first contribution describing this rare type of heavy REE mineralisation and drawing preliminary conclusions for its origin and evolution
5. To formulate a comprehensive deposit model for Lofdal, to aid exploration, based upon criteria collected through the author's professional experience, tested and verified on the example of the Namibian carbonatite and alkaline rock complexes.
6. To determine the hydrothermal processes, origin of the fluids and their chemical effects.
7. To compare with other HREE ore deposits and describe the origins of the HREE mineralization.

The thesis begins with a literature review of rare earths and carbonatites. It then reviews Namibian carbonatites in some detail. Chapter 4 gives details of the field and analytical methods used during the study. The results and interpretation of the field mapping are given in Chapter 5. Chapter 6 concentrates on whole rock geochemistry of the carbonatites and alkaline rocks before the mineralogy and mineral paragenesis of the rare earth and rock forming minerals is investigated in detail in Chapter 7. The results of both radiogenic and stable isotope studies are presented in Chapter 8. Radiogenic isotope analyses of minerals in carbonatites and associated feldspathoid rocks were carried out using K-Ar analysis of whole rock samples and spatially-resolved analysis of zircon and xenotime-(Y) using U–Pb methods. Analyses of carbon and oxygen isotopes were used to consider the source of mineralizing fluids and potential contributions from circulating groundwater. The results from the various sections are brought together and discussed in Chapter 9 to produce a model for Lofdal. The main conclusions of the thesis are summarized in Chapter 10.

Chapter 2: Overview of Rare Earth Elements (REE) and Global carbonatites.

2.1 Overview of Rare Earth Elements (REE)

2.1.1 Definition of REE

As defined by International Union of Pure and Applied Chemistry (IUPAC), rare earth elements (REE) or rare earth metals are a collection of seventeen chemical elements in the periodic table, namely the fifteen lanthanides, plus scandium and yttrium (Connelly and Damhus, 2005). Scandium and yttrium are considered rare earths since they tend to occur in the same ore deposits as the lanthanides and exhibit similar chemical properties. Rare earth metals are divided into light (LREE), medium (MREE) and heavy rare earth elements (HREE), Table 2.1. The LREE are - La = Lanthanum, Ce = Cerium, Pr = Praseodymium and Nd = Neodymium. Medium REE are - Pr = Promethium, Sm = Samarium, Eu = Europium, Gd = Gadolinium, while the HREE are - Tb = Terbium, Dy = Dysprosium, Ho = Holmium, Er = Erbium, Tm = Thulium, Yb = Ytterbium, Lu = Lutetium and Y = Yttrium. The REE elements share similar chemical properties and tend to occur in the same ore deposits. Sometimes L REE said to be La to Sm while HREE are Eu to Y.

2.1.2 Characteristics and properties of REE

Rare earth elements became known to the world with the discovery of the black mineral ytterbite (also known as gadolinite) in 1787, in a quarry in the village of Ytterby, Sweden. The ytterbite was renamed to gadolinite in 1800, by Johann Gadolin, a University of Turku professor, and his analysis yielded an unknown oxide which he called Ytteria (Dean and Dean, 1996).

Rare earth elements are characterised by high density, high melting point, high conductivity and high thermal conductance. A number of rare-earth minerals contain thorium and uranium in variable amounts but thorium and uranium do not constitute essential components in the composition of the minerals.

Table 2.1 Selected properties of the REE. Compiled from Gupta and Krishnamurthy (2004) and modified after BGS (2011) http://www.bgs.ac.uk

REE Division	Symbol	Atomic Number	Atomic Weight	Density (g/cm^3)	Melting Point (^0C)	Vicker's Hardness, 10 kg load, kg/mm^2
Light or Ceric	La	57	138.90	6.146	918	37
	Ce	58	140.11	8.160	798	24
	Pr	59	140.90	6.773	931	37
	Nd	60	144.24	7.008	1021	35
Medium	Pm	61	145.00	7.264	1042	-
	Sm	62	150.36	7.520	1074	45
	Eu	63	151.96	5.244	822	17
	Gd	64	157.25	7.901	1313	57
Heavy or Yttric	Tb	65	158.92	8.230	1356	46
	Dy	66	162.50	8.551	1412	42
	Ho	67	164.93	8.795	1474	42
	Er	68	167.26	9.066	1529	44
	Tm	69	168.93	9.321	1545	48
	Yb	70	173.04	6.966	819	21
	Lu	71	174.97	9.841	1663	77
	Y	39	88.90	4.469	1522	38

The common properties applying to both the lanthanides and actinides are that the rare earths are silver, silvery-white, or gray metals, have a high luster, but tarnish readily in air and high electrical conductivity. There are very small differences in solubility and complex formation between the rare earths. The REE naturally occur together in minerals (e.g., monazite is a mixed rare earth phosphate). The rare earths share many common properties. This makes them difficult to separate or even to distinguish from each other.

Rare earth elements are found with non-metals, usually in the $^{3+}$ oxidation state. There is little tendency to vary the valence (europium has also a valence of $^{2+}$ in nature and cerium has also a valence of $^{4+}$ (Kanazawa and Kamitani 2006).

2.1.3. Source of REE

The REE are not, in fact, truly rare. Gold, for instance, is much more rare and even lead is less common than some REE. What is rare, though, is their occurrence in economic quantities compared with other mineral commodities.

The principal sources of rare earth elements in commercial quantities are the minerals bastnäsite-(Ce) (Ce, La)(CO_3)F, monazite-(Ce) (Ce, La)PO_4, xenotime-(Y) YPO_4, loparite-(Ce) ($Na_{0.5}Ce_{0.5}$)TiO_3 and the RE-bearing ion-adsorption clays (Table 2.2) (Kanazawa and Kamitani 2006). About 200 rare earth (RE) minerals are distributed in a wide variety of mineral classes, such as halides, carbonates, oxides, phosphates, silicates, etc. Due to their large ionic radii and trivalent oxidation state, RE ions in the minerals have large coordination numbers (c.n.) 6–10 by anions (O, F, OH) (Kanazawa and Kamitani 2006). Light rare earth elements (LREEs) tend to occupy the larger sites of 8–10 c.n. and concentrate in carbonates and phosphates (Kanazawa and Kamitani 2006). On the other hand, heavy rare earth elements (HREEs) and Y occupy 6–8 c.n. sites and are abundant in oxides and some phosphates.

The smaller ion size of the yttrium group allows it a greater solid solubility in the rock-forming minerals that comprise the Earth's mantle, and thus Y and the HREE show less enrichment in the Earth's crust, relative to chondritic abundance, than does cerium and the LREE. This has economic consequences: large ore bodies of the LREE are known around the world, and are being actively exploited. Ore bodies for Y and HREE tend to be rarer, smaller, and less concentrated. Current supply of Y originates in the "ion adsorption clay" ores of Southern China. Well-known minerals that contain Y include gadolinite, xenotime-(Y), samarskite, euxenite, fergusonite, yttrotantalite, yttrotungstite, yttrofluorite (a variety of fluorite), thalenite, yttrialite (mindat.org). Xenotime-(Y) is occasionally recovered as a byproduct of processing heavy mineral sand, but has never been nearly as abundant as the similarly recovered monazite-(Ce).

Table 2.2 Illustration of the variable natural distribution of REE minerals at some key known deposits and the 000 total tonnes rare earth oxide (REO) at each of the deposits Sources: IMCOA, Technology Metals Research estimates (2008).

Rare Earth Mineral	**Bastnäsite**		**Ion adsorption Clays**		**Monazite**		**Loparite**
REO	Bayan Obo (China)	Mountain Pass (USA)	Xunwu, Jiangxi (China)	Lognan, Jiangxi (China)	Mount Weld (Australia)	Guangdong (China)	Lovozersky (Russia)
La_2O_3	23	33.2	43.4	1.82	25.5	23	28
CeO_2	50	49.1	2.4	0.4	46.7	42.7	57.5
Pr_6O_{11}	6.2	4.3	9	0.7	5.3	4.1	3.8
Nd_2O_3	18.5	12	31.7	18.5	18.5	18.5	8.8
Eu_2O_3	18.5	12	31.7	3	18.5	17	8.8
Tb_4O_7	0.1	trace	trace	1.3	0.1	0.7	0.1
Dy_2O_3	0.1	trace	trace	6.7	0.1	0.8	0.1
Y_2O_3	trace	0.1	8	65	0.3	2.4	Trace

2.1.4. Producers of REE

China produces over 97% of the world's rare earths, with 77% of world production coming from one mine (i.e., Bayan Obo). Other producers are India, Brazil and Malaysia (Figure 2.1). The United States of America used to produce approximately 6% of the world's supply from one of the only in-situ rare earth mines in the world, at Mountain Pass, California. However, Mountain Pass, the only producing mine in North America ceased operations in 2006, creating a situation where there is no REE production taking place anywhere significant outside of China (http://crowlee.proboards.com).

The world reserves are summarised below and it is important to note that most of these deposits are not exploited. Reserves are defined by USGS as that part of the reserve base which could be economically extracted or produced at the time of determination. The term reserves does not signify that extraction facilities are in place and operative. Reserves include only recoverable materials.

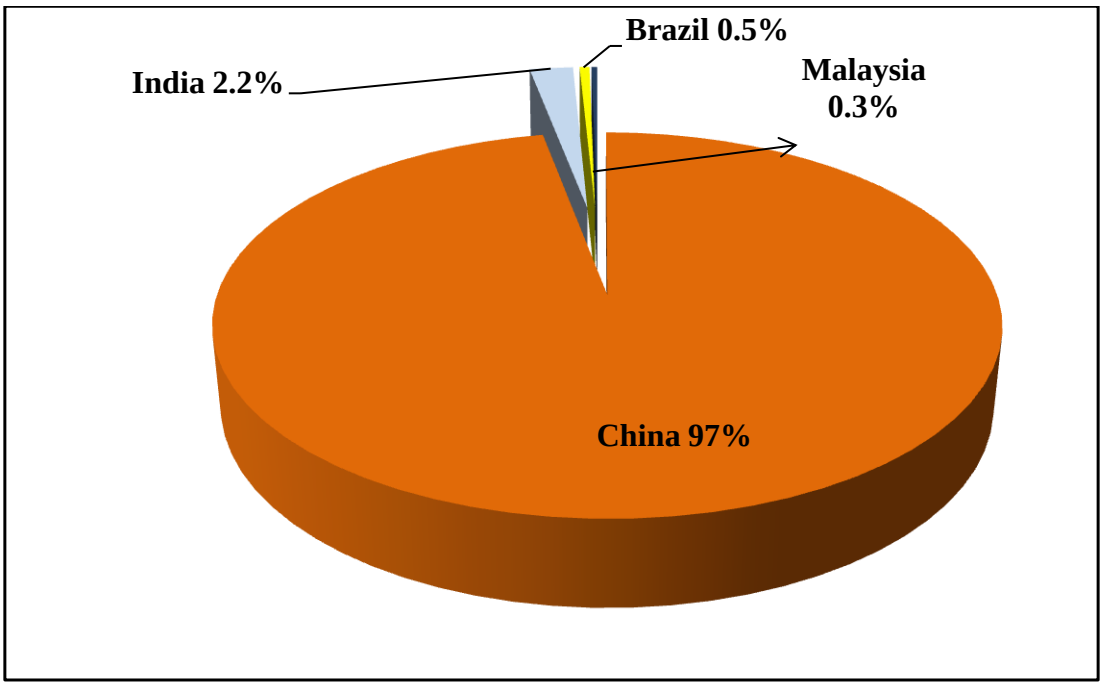

Figure 2.1 World REE Mineral Production (Source: U.S. Geological Survey 2010)

Namibia has known monazite reserves located in carbonatite veins at Eureka farm, about 30 km southwest of Usakos. The drilling by Dunai (1989) established proven reserves of 30,000 tons of ore to a depth of 20 m, containing 1,900 tons of REE. Carbonatites of Kalkfeld complex and iron ore in Namibia show enrichment in La (0.1 to 0.25%), Ce (0.05 to 0.5%), Nd (0.1 to 0.25%), P_2O_5 (7 to 8 and above 10% Mn and Fe) Japan International Cooperation Agency- Metal Mining Agency of Japan 1995).

2.1.5 Supply

Currently, China dominates the supply of the REE metals (Figure 2.2). Between 1999 and 2011 more than 90% of the separated REE used in the United States, as a previous producer, was imported from China. In fact, some countries normally import their plant feed materials from China. This supply trend appears to continuing for the near future because the largest REE deposits are found in China (Humphries 2012).

There is increasing pressure placed on the limited REE supply, mainly driven by their use and demand in modern technology development as indicated by (Table 2.3). Currently, supplies of key HREE (Y, Dy and Tb) remains tight, and China imposed export quotas and tariffs on REE. China's restriction on REE pushes the REE prices and gives chances to develop long known projects in order to maintain balance in the market place (Figure 2.3).

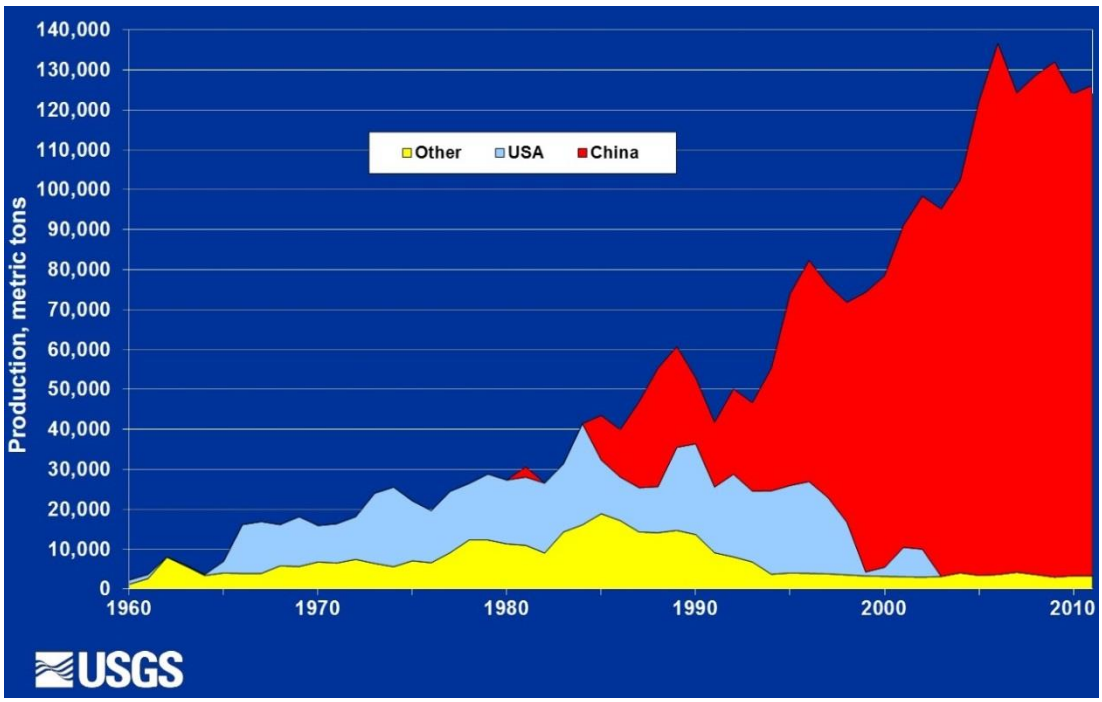

Figure 2.2 Global rare-earth-oxide production trends, Pui-Kwan Tse (USGS 2011).

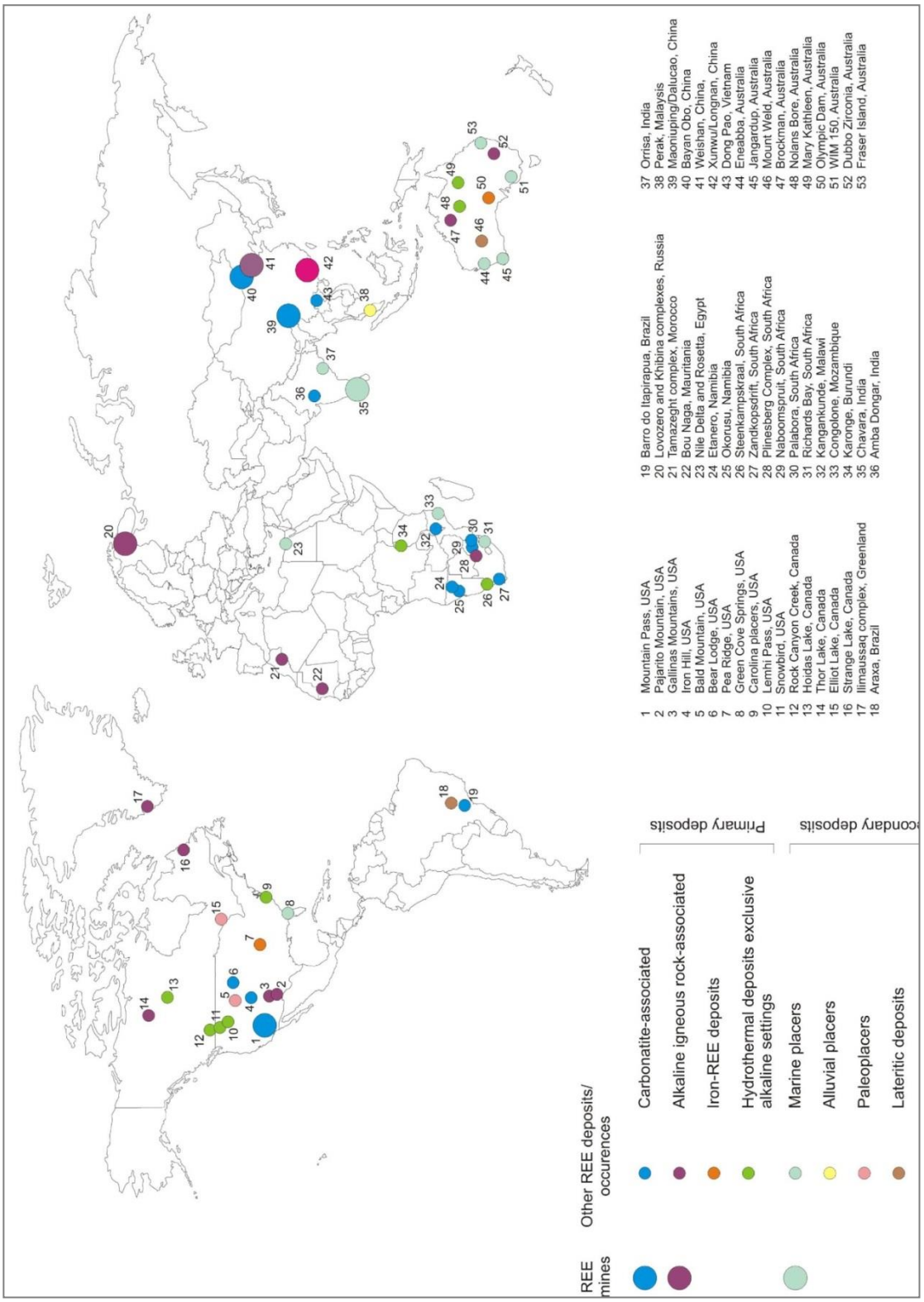

Figure 2.3 Global distributions of REE deposits and occurrences BGS (2010) (Source: http://www.bgs.ac.uk/research/highlights/documents/Global_REE_Deposits.pdf)

2.1.6 Use and applications of the Rare Earth Elements

Rare earth elements are used in a wide range of applications from everyday household items, to cutting-edge technologies (e.g. rechargeable cell phone batteries to super alloys used in the aerospace industry). The versatility and specificity of the REE has given them a level of technological, environmental, and economic importance considerably greater than expected from their relative obscurity. Specificity is not limited to the more exotic REE, such as Eu or Er.

The use of REE per element is varied in modern technologies and societal development (table 2.3 and Figure 2.4). REE are used extensively, in the defense industry. Some of their specific defense applications include: anti-missile defense, aircraft parts, communications systems, electronic countermeasures, jet engines, rockets, underwater mine detection, missile guidance systems and space based satellite power (Vulcan 2008).

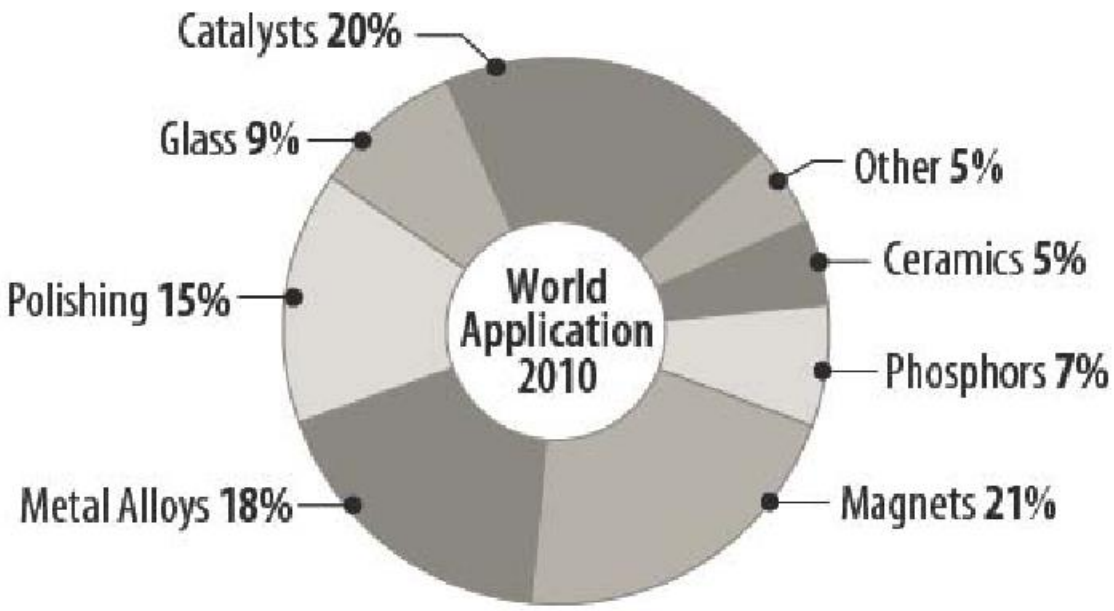

Figure 2.4 Major world REE applications, (Source: IMCOA 2011).

Table 2.3 Summary of REE metal oxides, their principal uses and price US$/kg in December 2012. Source: http://www.mineralprices.com/

REE	Metal Oxide	Price US$/kg	Key Application
La	Lanthanum Oxide ≥ 99.5%	13.00	FCC catalysts, alloy mischmetal (for NiMH batteries, hydrogen absorption, & creep resistant magnesium), optical glass, additive to produce nodular cast iron, lighter flints, phosphors
Ce	Cerium Oxide ≥ 99.5%	12.00	Catalytic converters, glass, ceramic & plastic pigments, polishing, de-oxidant and desulfurizer in the steel industry, self-cleaning ovens, carbon-arc lighting, mischmetal
Pr	Praseodymium Oxide ≥ 99.5%	95.00	NdFeB magnet corrosion resistance, high-strength metals, yellow glass and ceramic pigment
Nd	Neodymium Oxide ≥ 99.5%	77.00	NdFeB magnets, glass and ceramic pigments, autocatalysts, lasers
Sm		-	Magnets, carbon arc lighting, lasers, biofuel catalysts, mischmetal, geological dating, nuclear applications, medical uses, optical glass
Eu	Europium Oxide ≥ 99.5%	2,150.00	Phosphors, lighting, neutron absorbers
Gd	Gadolinium Oxide ≥ 99.5%	75.00	Contrast agents to enhance MRI imaging, Gd-Y garnets, superconductors, phosphors, glass and ceramics, fuel cells, lighting, magnets
Tb	Terbium Oxide ≥ 99.5%	1,750.00	Phosphors, fuel cells, lighting, magnets
Dy	Dysprosium Oxide ≥ 99.5%	975.00	NdFeB magnets, lasers, chalcogenide sources of infrared radiation, ceramics, nuclear applications, phosphors, lighting, catalysts
Ho		-	Magnets, nuclear (control rods, medical uses), lasers, red & yellow pigments in glass & zirconia, calibration of gamma ray spectrometers
Yb		-	Fiber optics, radiation source for x-ray machines, stress gauges, lasers, doping of stainless steel, doping of optical materials
Lu		-	Specialist X-ray phosphor, single crystal scintillators (baggage scanners, oil exploration)
Er	Erbium Oxide ≥ 99.5%	-	Colorant in glassware & ceramics, metal alloys, repeaters in fiber optic cables, nuclear applications (medical)
Tm		-	medical imaging, phosphors, lasers, possible use in ferrites
Y	Yttrium Oxide ≥ 99.95%	50.00	Phosphors, stabilized zirconia, metal alloys, garnets, lasers, catalyst for ethylene polymerization, ceramics, radar technology, superconductors

2.1.7 REE Demand

The revival of automotive and electronics industry has boosted great demand of the rare earth industry. Automotive catalytic converter and permanent magnets are expected to keep strong demands for Ce and Nd.

At present, the global demand for REE, calculated in REO, is up to approximately 80,000-90,000 tons annually (Table 2.4). Yet, in China, the treatment capacity of rare earth has reached 200,000 tons per year; smelting and separating capacity exceeds 200,000 tons annually.

The global demand for rare earth is forecasted to increase specially for the use of REE in hydrogen fuel vehicle, hybrid vehicle and electric vehicle (Figure 2.5), half of which will come from China. Magnets will continue to show the highest rates of growth in demand in the years to 2015 (USGS, 2012).

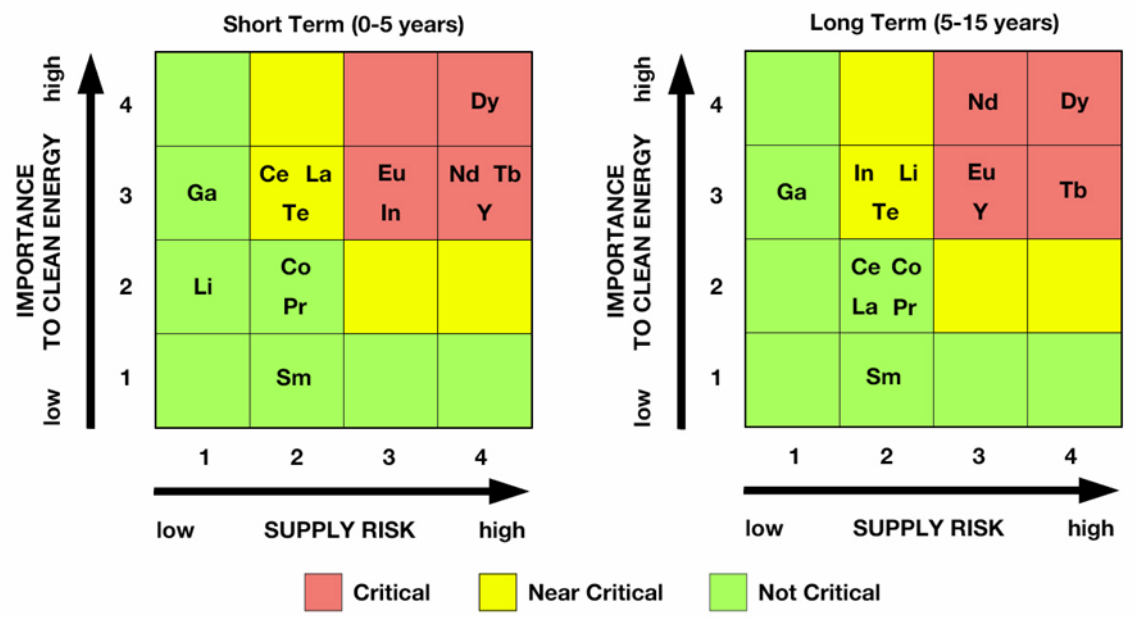

Figure 2.5 Short- and medium-term criticality matrices for select elements (source: TMR, after Bauer et al. 2010).

Table 2.4 Estimated global rare-earth demand in 2015 (tonnes of REO ± 15%) *(may not add to 100% due to rounding).* Sources: IMCOA, Technology Metals Research estimates (2012).

Application	China	Japan & SE Asia	USA	Others	Total	Market Share	Market Value
Permanent Magnets	37,000	6,000	3,000	2,000	**48,000**	**26%**	**44%**
Catalysts	12,500	3,000	10,000	3,000	**28,500**	**15%**	**12%**
Metal Alloys	25,000	7,000	2,000	1,000	**35,000**	**19%**	**13%**
Polishing Compounds	12,500	10,000	4,000	4,000	**30,500**	**16%**	**10%**
Glass	7,000	2,000	1,000	1,000	**11,000**	**6%**	**3%**
Phosphors	8,000	3,000	1,000	1,000	**13,000**	**7%**	**14%**
Ceramics	3,000	3,000	2,000	1,500	**9,500**	**5%**	**2%**
Other	6,000	2,500	500	500	**9,500**	**5%**	**2%**
Total	**111,000**	**36,500**	**23,500**	**14,000**	**185,000**	**100%**	**100%**
Market Share	**60%**	**20%**	**13%**	**8%**	**100%**	-	-

2.1.8 Market of the Rare Earth Industry

The REE are said to be strategic and vital to the security of a nation but must be procured entirely or in large part from foreign sources for most countries. The future of REE is predicted to follow the following trends;

- An industry expansion and exploration of rare earth in the world, emergency non-Chinese REE production and formation of supply chain between mining companies and end users.
- Quality, proximity to market and security of supply are the major selling points with consumers. However, the best strategy for establishing an REE industry is to pursue a "mine-to-market" philosophy with the "market" being those products with a significant value-added component targeted to specific users and industries (Mariano 2010).

For the last two years REE maintains a major topic in mining and exploration industries. This is mainly because of the following developments (Chegwidden & Shaw 2011);

- China unofficially temporarily suspends shipments of rare earths to Japan (September and October 2010)
- Chinese export quotas reduced significantly in July2010 and further reduced in January 2011
- China declares 'heavy' rare earths resources are finite (approximately 15-20 years)
- Chinese rare earths industry consolidation
- Western producers - Mt Weld & Mountain Pass – establishing production capacity of at least 20,000 tpa REO each.

2.2.9 REE Consumption

The major consumers of rare earths are Southeast Asia (Japan, Korea, Thailand, and China) and the USA. The USA used to be the world's largest single consumer of rare earths, at approximately 27% of the world's total. However the USA currently imports nearly 100% of its REE requirement and the value of rare earth products consumed in the USA is estimated to be in excess of US$1 billion per year (Murkowski and Alaska 2009). During the past few years, China has become the world's largest consumer, surpassing even USA consumption (http://crowlee.proboards.com).

2.1.10 Chinese Rare Earth Industry

2.1.10.1 China's control over the world's Rare Earths industry

The Institute for the Analysis of Global Security (IAGS) 2010 announced that the main accessible concentrations of the rare earths are found in China, where more than 97% of rare earths supplies to the world are now produced. Until 1998, the United States was the second largest producer of rare earths from the Molycorp mine in Mountain Pass, California. The facility was closed in December 1998 allowing China to be the main producer till now (Morrison and Tang 2012). China deposits are HREE dominated while the USA deposit at Mountain Pass is LREE (Figure 2.6).

Causative factors that led USA to a complete dependence on imports from a single country are (Gordon et al. 2002):

- The lower labour and regulatory costs in China compared to those in the United States.
- Continued expansion of electronics and other manufacturing in Asia.

- The favourable number, size, and HREE content of Chinese deposits and
- The ongoing environmental and regulatory problems at Mountain Pass, California.

China's dominance of world REE markets raises several important issues of REE supply for the western markets especially after China is continuous reduction of the amount of rare earths available for export. China's gradual reduction of its export of raw ores and ore concentrates has forced the rare earth refining, separating, metal and alloy production industries to move to China. Western industry, both civilian and military, could be cut off with little notice from these elements at a time when there is no alternative supplier. China currently restricts export quotas on dysprosium, terbium, thulium, lutetium, yttrium, and the heavy and scarcer rare earths (Figure 2.7). This reduction of export quotas has pushed up the international price of key rare earths, including Nd which is so critical for neodymium-iron-boron permanent magnets as reported by "China's Grip Tightens on Rare-Earth Metal Neodymium", The New York Times Global business 2009).

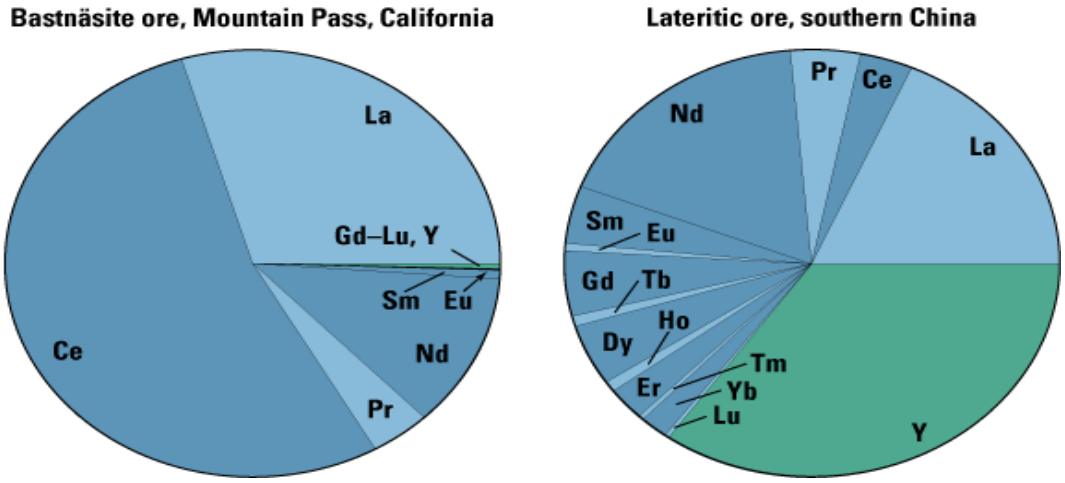

Figure 2.6 Proportions of individual REE in two representative ores: bastnäsite, and lateritic ion-adsorption ore (Source: USGS Source Facts 2008).

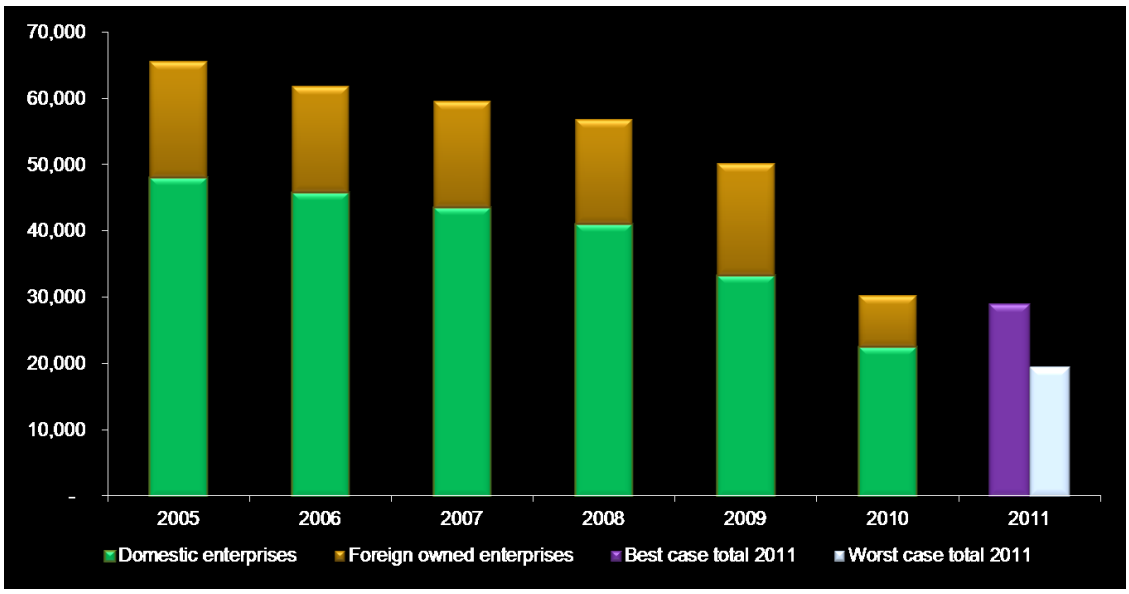

Figure 2.7 Evolution of Chinese exports quotas from 2005 to 2011 (Note: tonnes of product – not REO). Source: Chinese Ministry of Commerce, Roskil and IMCOA (2010)

According to the statistics, there are 154 million tons of exploitable rare earth reserves globally, among which 89 million tons (about 58%) are distributed in China (www.researchinchina.com).

Recent statistics show that 89 million tons of REO in China are with a complete establishment of production systems from exploiting, selecting, smelting, separating, analyzing and testing. It can produce over 100 kinds of rare earth products. However, China lags far behind the developed countries in hi-tech rare earth development and application.

According to Wang (2009), China used 70,000 tons of rare earth elements in 2008. Global consumption was 130,000 tons. China exported 10,000 tons of rare earth magnets worth $400 million and 34,600 tons of other rare earth products worth $500 million.

2.1.10.2 Chinese REE Mining regions/provinces

China has hard rock, placer and ion adsorption clay deposits. The Bayan Obo deposit contains an estimated 70% of the world's known REE resources. The total reserves for Bayan Obo are reported as at least 1.65 billion short tons of 35% Fe, 6% REO, and 0.13% Nb. The ore is primarily enriched in LREE and the deposit has an extremely high LREE/HREE ratio (Chao et al. 1997, Smith and Henderson 2000).

The mining and processing of rare earths is widespread across China, but has become concentrated in nine provinces and regions, specifically:

• **Fujian** (a southeastern province - capital & largest city is **Fuzhou**)

• **Guangdong** (a southern province - capital & largest city is **Guangzhou**)
• **Guangxi** (a southern autonomous region - capital & largest city is **Nanning**)
• **Hunan** (a southern province - capital & largest city is **Changsha**)
• **Inner Mongolia** (a northern autonomous region - capital is **Hohhot** & largest city is **Baotou**)
• **Jiangxi** (a southeastern province - capital & largest city is **Nanchang**)
• **Shandong** (an eastern province - capital is **Jinan** & largest city is **Qingdao**)
• **Sichuan** (a southern province - capital & largest city is **Chengdu**)
• **Yunnan** (a southern province - capital & largest city is **Kunming**)

Ion adsorption clay deposits, which are most important for HREE, are at Mianning. Placer deposits are largely found in the coastal areas of west Guangdong and Hainan Island and associated with alkaline rocks in Shandong Province (Figure 2.8).

Because of the scattered distribution of rare earth resources, it is difficult to carry out efficient oversight of the industry. Table 2.5 is a short summary of the major Chinese producers listed in figure 2.5.

Table 2.5 Chinese REE producers. Source: Rare Earths Elements Letter, Pieterse G. M. (2011).

Name of deposit	**Bayan Obo**	**The Maoniuping REE deposit**	**Ion adsorption clay**
Location (Producer)	Inner Mongolia Autonomous Province	Located in the Panxi rift, Sichuan Province	In the Guangdong, Hunan, Jianxi and Jiangsu provinces
Nature of occurrence	Tabular and/or lenticular bodies of REO bearing magnetite and hematite iron ores. Sheets, dykes and sedimentary-volcanic series	Hosted in a carbonatite syenite complex. The deposit is characterized by large scale, shallow buried and coarse-grained bastnäsite; hydrothermal-metasomatic and vein deposits	In situ weathering of the alkali granite forming residues of ion adsorption clays
Type of ores produced	Polymetallic deposit producing iron and REO	Bastnäsite is the primary mineral, dominated by the light rare earths, cerium, lanthanum and neodymium, which together account for over 90% of the total REO content.	Ion adsorption clays are rich in HREE and yttrium. Rare Earths produced are mainly europium, terbium, dysprosium and yttrium
Reserves and ore grade	Total reserves of 1.5 billion tons of 35% Fe ore and 48 million tons of 6% Rare Earth Oxides and 1 million t niobium (average grade 0.13%).	The Maoniuping REE deposit is the second largest light rare earth elements deposit (1.45 million tons of REO).	Estimates range from 35,000 – 55,000 tonnes REO (Rare Earth Element International, 2011).
Mineral associations	Columbite and REE minerals such as bastnäsite, monazite, REE–Nb minerals, aeschynite and fergusonite are closely associated with iron ore	Most of REE ore bodies are composed of pegmatitic bastnäsite ores, pegmatitic calcite veins and networks of ores, with the gangue minerals of fluorite, barite, calcite, quartz, mica and aegirine-augite. Fluorite occurs in all ore bodies	Heavy Rare Earths (europium, terbium, dysprosium and yttrium) associated with ion adsorption clays
Isotopic composition	Pb and Nd isotopes from Bayan Obo ore and gangue minerals indicate a crustal origin for the REE (Wang et al., 1994)	Present day Pb isotope ratios for the carbonatite, syenite, fluorite, galena, pyrite, and feldspar samples are considered to approximate initial ratios because of relatively young age of the complex (~30 Ma) and low U/Pb (0.03–0.09, 0.001–0.002, 0.007–0.04, 0.02), Xu et al. (2004)	N/A
Ore genesis	Related to a rift system. Hydrothermal alkaline-carbonatite fluid derived from the upper mantle overprinted the REE–Nb of the original iron ore body. See the model for Bayan Obo formation under section 2.1.10. 3.	Located on the north margin of the Panxi (Panzhihua-Xichang) rift, and is tectonically located in the middle zone of the NE-trending Haha fault. Mineralisation is hydrothermal-metasomatic and vein deposits	Mineable deposits form as a result of in situ weathering of host alkali granite rich in rare earth oxides (REO)

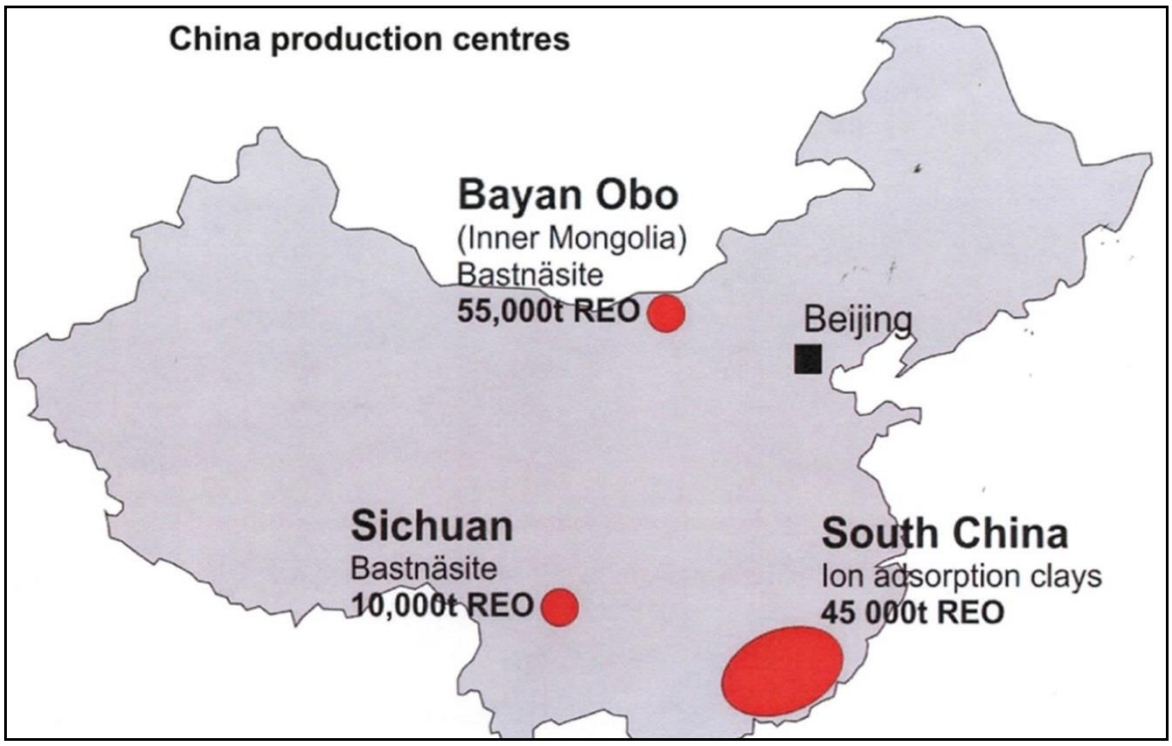

Figure 2.8 Map of the Chinese REE production centres. Note that the figures as indicated are annual production of REO in tonnes. (Source: http://www.bgs.ac.uk/research/highlights/documents/Global_REE_Deposits.pdf)

2.1.10. 3 Models for Bayan Obo Formation

The Fe–REE–Nb deposit at Bayan Obo, Inner Mongolia, China, is the world's largest known rare-earth element (REE) resource.

Several models on the genesis of Bayan Obo REE deposit have been proposed: (1) It is genetically related to carbonatite magmatism (Li 1983, Liu 1986, Zhou et al. 1986, Le Bas et al. 1992, Le Bas et al. 1997, Yuan et al. 2000, Hao et al. 2002, Yang and Le Bas 2004); (2) it was formed as a result of hydrothermal alteration of carbonate sedimentary rocks (Meng 1982, Tu et al. 1985, Huo 1987 Anon 1988, Meng and Drew 1992, Chao et al. 1993, 1997, Tu 1998, Smith et al. 1999, 2000, Smith and Henderson 200, Smith 2007); (3) it was formed by the interaction of carbonatitic fluids from the mantle or from the lower crust (Yuan et al. 1992a,b, 1995); (4) it formed due to deposition on the sea floor accompanied by simultaneous metasomatism caused by sea floor volcanic eruptions (Huo 1989, Cao and Wang 1994, Ren et al. 1994). These models, to some extent, reflect the complexity of the Bayan Obo deposit;

(5) Multistage nature of mineralisation with a direct involvement of carbonatite derived fluids during ore genesis Smith (2006). All these models indicate the complexity of the Bayan Obo deposit.

2.1.10.4 Rare-earth production outside of China

The revamping of the Mountain Pass mine in California, add to a significant number of new projects at advanced stages of development outside of China,

• Lahat (located in Malaysia)

• Karnasurt (located in the Kola Peninsula of the Russian Federation)

• Buena Norte (located in eastern Brazil)

• Orissa-Kerala (located in various coastal regions of India) [TMR Advanced Rare-Earth Projects Index (2012).

2.2 Global Review of Carbonatites

2.2.1. Nomenclature and Classification

Carbonatites are igneous (plutonic or volcanic) rocks composed of more than 50% primary (i.e., magmatic) carbonate (sensu lato) and containing less than 20 wt% SiO_2 (Le Maitre 2002). Carbonatites are most commonly composed of one of the carbonate minerals: calcite ($CaCO_3$), dolomite-ankerite ($Ca(Mg,Fe^{+2})(CO_3)$) and siderite ($Fe^{+2}CO_3$). Carbonatite magma differs greatly from the more prevalent silicate magma and these two different types of magma are immiscible at crustal temperatures and pressures depending on their compositions (Wyllie and Huang 1976). Such magmas possess a very low viscosity because the lack of silica prevents extensive silicate polymerization (Treiman 1989).

Carbonatites are classified using the IUGS system (Le Maitre 2002), summarised in Table 2.6. This provides two classification schemes as reviewed by Woolley and Kempe (1989):

a) Mineralogical: where the modal mineralogy is known, the carbonatite is named by its principal carbonate mineral and mineralogically the following classes of carbonatites may be distinguished:

- **Calcite-carbonatite -** where the main carbonate is calcite. If the rock is coarse - grained it may be called **sövite**; if medium to fine-grained, **alvikite**.
- **Dolomite-carbonatite**-where the main carbonate is dolomite. This may also be called **beforsite.**
- **Ferrocarbonatite -** where the main carbonate is rich in iron.
- **Natrocarbonatite -** essentially composed of sodium, potassium, and calcium carbonates. At present this unusual rock type is only found at the Oldoinyo Lengai volcano in Tanzania.

Where a carbonatite is composed of more than one carbonate mineral a composite name is formed with the minerals listed in order of increasing modal abundance: a dolomite calcite carbonatite is a calcite carbonatite containing dolomite; a calcite ankerite carbonatite has ankerite in greater modal abundance than calcite. Important non carbonate minerals can also be included in the name for example magnetite dolomite carbonatite; phlogopite magnetite calcite carbonatite. Igneous rocks containing from 10 to 50% of carbonate minerals are referred to using the mineral modifier ―carbonatitic (e.g., carbonatitic ijolite) (Le Maitre 2002). Carbonatites containing in excess of 20 wt.% SiO_2 are termed silicocarbonatites (Le Maitre 2002).

b) Chemical: where the modal mineralogy is not known, a chemical classification is adopted which uses the relative abundances of MgO, CaO and ($FeO+Fe_2O_3+MnO$) to define calciocarbonatites, magnesiocarbonatites and ferrocarbonatites using **CCMF** (CaO/CaO+MgO+FFM) to denote the ratio in weight percent where FFM is ($FeO+Fe_2O_3+MnO$). Calciocarbonatites have CCMF>0.8; magnesiocarbonatites have CCMF<0.8 and MgO/FFM > 0.5; ferrocarbonatites have CCMF<0.8 and MgO/FFM<0.5 (Table 2.6).

Evidently, the term **ferrocarbonatite** has two meanings in the IUGS scheme: it denotes a carbonatite predominantly composed of iron carbonate minerals or it could indicate one with FFM, MgO and CCMF>0.8. It is possible to demonstrate (e.g. Gittins and Harmer 1996) that these two options will not always be equivalent. The chemical classification produces reasonably consistent and logical nomenclature when applied to iron-poor carbonatites. However, serious inconsistencies occur in iron-rich carbonatites. The IUGS ignores the oxidation state of the iron, as it does not distinguish between Fe present in carbonate phases and the Fe in oxide (magnetite) and silicate (aegirine, sodic amphibole, mica) phases, (IUGS 2008).

Table 2.6 Carbonatite nomenclature based on mineralogy and/or chemistry as per IUGS recommendations

Mineralogical classification scheme	**Chemical and dominant Minerals classification**	**Alternative name****	**Other identification criteria**
Calcite-carbonatite	Calcite	Sövite Alvikite	Coarse-grained Fine-medium grained
Dolomite-carbonatite	Dolomite	Rauhaugite Beforsite	
Natrocarbonatite	K-Na-Ca-carbonates (dominant alkali/carbonate mineral		Only found at Oldoinyo Lengai volcano, Tanzania
*Calciocarbonatite	C/(C+M+F) > 0.8		< 20% SiO_2
*Ferrocarbonatite	Iron-rich, C/(C+M+F) < 0.8 and MgO/FFM<0.5		< 20% SiO_2
*Magnesiocarbonatite	C/(C+M+F) < 0.8 and MgO/FFM.0.5	Mostly Beforsite & Rauhaugites	< 20% SiO_2
*Silicocarbonatite	excess of 20 wt. % SiO_2		> 20% SiO_2
Calcite-bearing ijolite etc.			< 10% carbonates
Calcitic ijolite etc.			10 -50% carbonates

**Names given on the basis of chemical analysis where (C = CaO, M = MgO, F = $FeO+Fe_2O_3$+MnO, in weight) (Lee et al., 2000).*
***Old names that appear mostly in old literature*

It is recommended by Gittins and Harmer (1997) that:

"The term ferrocarbonatite be used only in the chemical sense; that carbonatites rich in iron-bearing carbonates be named according to the constituent mineral phases; that a modified chemical classification be adopted (but to be used only when it is impossible to determine the mineralogy) in which analyses are plotted in molar proportions and only FeO is used".

Recently, an alternative carbonatite definition has been proposed using also a mineralogical-genetic classification and is divided into two groups: primary carbonatites and carbothermal residua (Mitchell 2005).

Primary carbonatites in terms of mineralogical-genetic classifications rather than modal classification can be divided into a group of magmatic carbonatites formed from diverse mantle-derived magmas: i.e. carbonatites associated with;

(a) melilitite,

(b) nepheline, ailikite, and

(c) kimberlites rocks.

Carbothermal carbonatites are those carbonate-rich rocks associated with diverse potassic or sodic peralkaline saturated to undersaturated magmas derived predominantly from metasomatised lithospheric mantle, together with REE-carbonatite-rich rocks of undetermined genesis (Mitchell 2005). Here the IUGS classification of carbonatite is used also with consideration of Gittins and Harmer (1997) because some Lofdal carbonatites are Fe-rich. The term ignores carbonatite that are not associated with silicate rocks e.g. those associated with kimberlites.

Although most carbonatites are intrusive, **extrusive carbonatites** are dominantly pyroclastic and many are lapilli tuffs (Keller 1989, Woolley and Church 2005), for example Melkfontein near Cedarville in East Griqualand in South Africa (Boctor et al. 1984). This tuff is spatially associated with kimberlites but tuffs appear to be significantly younger than kimberlite bodies. The active volcano with lava flows at Oldoinyo Lengai, Tanzania has been continuously erupting natrocarbonatite "lengaite" lava since the 1980s. Other known extrusive carbonatites referred to as ignimbrites and lapilli tuffs are found at Fort Portal, Uganda (Barker and Nixon 1883) and Kaiserstuhl Germany (Keller 1981, 2000). Apart from the natrocarbonatite at Oldoinyo Lengai, extrusive carbonatite is almost always calcitic (Woolley and Church 2005).

2.2.2 Tectonic settings

Carbonatite and alkaline igneous complexes occur mainly in intraplate settings.

1) Carbonatites are commonly found in stable cratonic, intraplate areas (Le Bas 1987) and are associated with rift valleys or continental deep fault structures and with structural domes, where rifting and faulting can occur in response to doming, for example the East African Rift system and Kola Alkaline Province, situated on topographic high elevations, which has been interpreted as the outcome of crustal doming (Woolley 1989).
2) Environments of rifted continental margins such as Brazil and Namibia and these are related to asthenospheric mantle & plumes (Pirajno 2004a).
3) Fold belts, even amongst ophiolites in the Arab Emirates (Woolley et al. 1991).
4) Carbonatites can be found in areas of partially melted oceanic crust such as the Cape Verde and Canary Islands (Le Bas 1980; Silva et al. 1981).
5) Syn-tectonic carbonatites are also known from the accreted terrains of the Western Cordillera of British Columbia (Pell and Hoy 1989) and the frontal nappe complex of the 1000 Ma Natal Metamorphic Province at the Bull's Run Complex (Scogings and Forster 1978).

In Africa carbonatites are related to hot spots and rifts and are expressed clearly by 15 large provinces of alkaline magmatism and more than 130 carbonatite occurrences that can be outlined by Van Alstine and Schruben (1980) in figure 2.9.

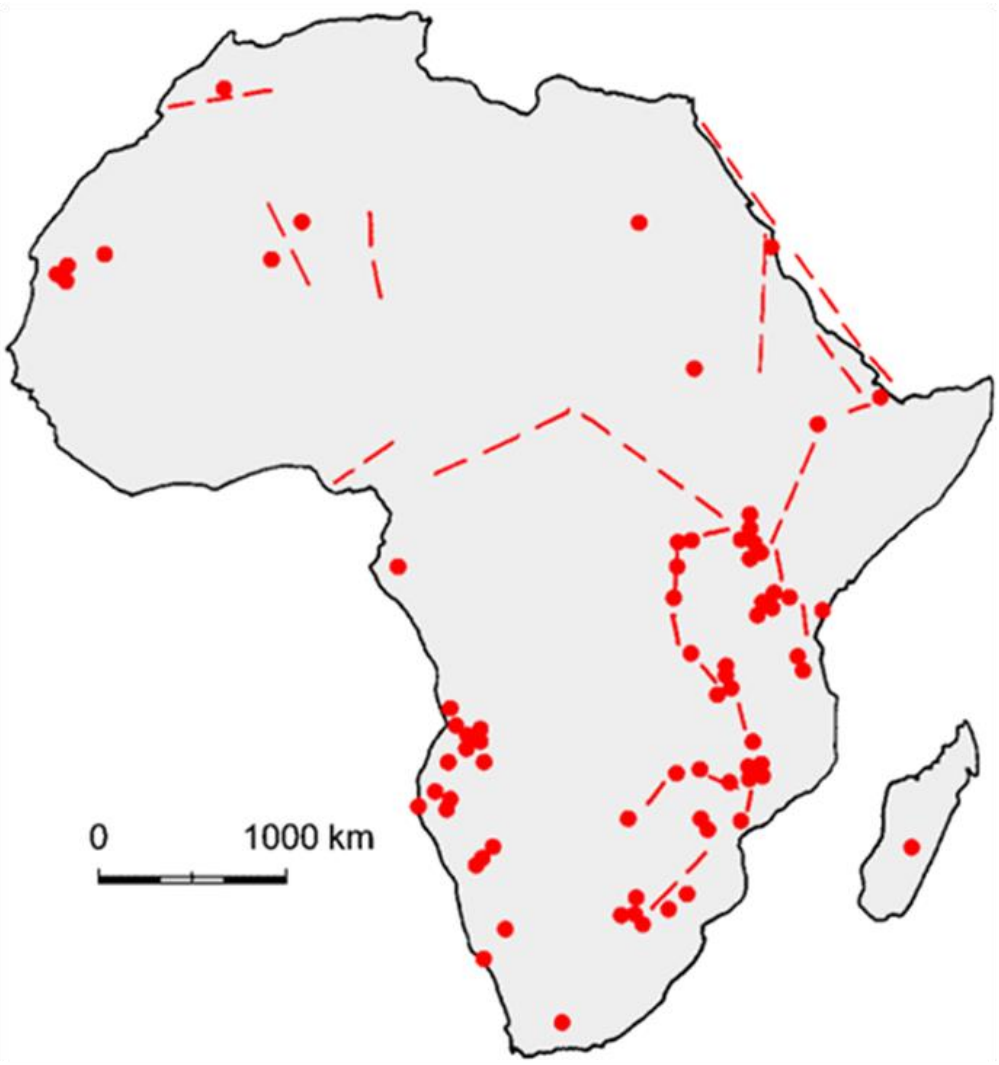

Figure 2.9 Location of carbonatite complexes in Africa modified after Van Alstine and Schruben (1980). Dashed lines represent rift structures.

2.2.3 Rock associations and field relationship

Following are the rock association of the carbonatites as found in different geological environments;

- Carbonatites are spatially associated with wide variety of feldspathic silicate rocks (Figure 2.10) such as ijolite, nepheline syenite, melilitite, nephelinite, ailikite and the kimberlite clans (Mitchell 2005). The association both locally and regionally of carbonatites with alkali-rich, silica-poor igneous rocks implies a strong genetic relationship (Ehlers and Blatt 1982).

- Carbonatites can also occur on their own without silicate rocks associations. *e.g.*, Sarfartoq (Greenland), Bulhoek (South Africa), Newania (India), and not all alkaline rocks are associated with carbonatites, *e.g.*, nepheline syenite at Mt. Brome (Canada) or Kangerdlugssuaq (Greenland), lamproite (Leucite Hills),

katungite (Toro–Ankole), and leucitite (Vesuvius). The significance of these associations has been briefly discussed by Mitchell (2005). Woolley (2003) has noted that there are at least 68 intrusive and 10 extrusive carbonatite localities with no associated intrusive or extrusive silicate rocks.

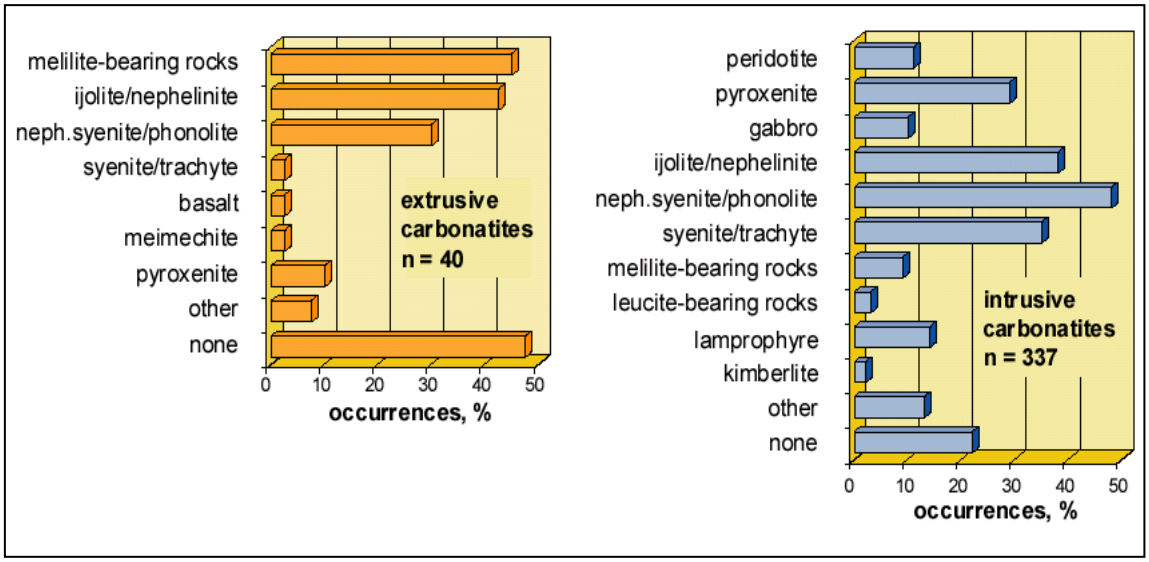

Figure 2.10 Silicate rocks associated with carbonatites (Mitchell 2005).

There are no entirely reliable or universally applicable criteria to identify a rock as a carbonatite but most carbonatites have some or all of the following field characteristics among which the most important one is evidence for magmatic features, including preservation of cross-cutting and chilled contacts. Intrusive styles in carbonatite magma are indicated by ring dykes, cone sheets, diatremes, radial dykes, and dykes swarms that never form large homogenous bodies. Metasomatic invasion of earlier silicate and carbonatite rocks is a common feature of carbonatites. Other magmatic textures observed are flow alignment of constituent phases and schlieren, layered chilled margins, comb and spinifex textures, xenoliths and xenocrysts of crustal and mantle material (Bailey 1993, Woolley et al. 1991, Barker 1989).

A genetic definition of carbonatite must be combined with observational criteria as summarised in Table 2.7.

A fenitization halo (alkali metasomatised country rocks) commonly surrounds carbonatite intrusions; mineral alteration depends largely on the composition of the host rock. Typical minerals are sodic amphibole, wollastonite, nepheline, mesoperthite, antiperthite, aegirine-augite, pale brown biotite, phlogopite and albite. Most fenites are zones of desilicification with addition of Fe^{3+}, Na and K (Birkett and Simandl 1999).

Table 2.7 Criteria for magmatic heritage of carbonatites (Barker 1989).

Associated rocks	**Accessory minerals and Chemical composition**	**Isotopic composition**
1. Feldspathoid-bearing (nephelinites, phonolites, nepheline syenite and urtite-ijolite-melteigite series)	pyrochlore, melilite, nepheline, sodic clinopyroxene	$\delta^{13}C$ = -1 to - 9 per mil relative to PDB
2. Melilite-bearing (melilites, okaites, turjaites, uncompahgrites) kimberlites	Trace element enrichment with Sr, Ba, Zr, Nb, Th, REEs	$\delta^{18}O$ = +6 to +12 per mil relative to SMOW
3. Fenites (wall rocks.)	metasomatically enriched in Fe and alkalis, and commonly depleted in Si	Initial $^{87}Sr/^{86}Sr$ <0.706

2.2.4 Mineralogical composition

By definition carbonatites are composed mainly of carbonate minerals. The most common carbonates are;

a) Calcite $CaCO_3$, often with significant Mg substitution to magnesian calcite (Ca, Mg)CO_3 (Reeder 1983). In general, however, only minor substitution occurs. Only manganese and magnesium are known to substitute extensively for the calcium: manganocalcite and calcium rhodochrosite (i.e., calcium-bearing $MnCO_3$) have been identified, and solid solution has been shown (http://webmineral.com/), to be possible from pure $CaCO_3$ to 40 percent $MnCO_3$ and from pure MnCO3 to about 25 percent $CaCO_3$.

b) Dolomite-ankerite solid solutions (Ca(Mg,Fe^{+2})(CO_3). Following the terminology adapted by Chang et al. (1996), the name dolomite is used for $CaMg(CO_3)_2$, ferroan dolomite for Ca(Mg,Fe+2)$(CO_3)_2$ compositions with Fe/Fe+Mg)<0.25 and ankerite for the compositions where 0.25<Fe/Fe+Mg)<0.75.

c) Siderite Fe+CO_3 are far rarer than either of the above species and are generally restricted to late stage carbonatites (Harmer and Gittins 1997).

d) Only one occurrence of an alkali carbonatite is known – the so called natrocarbonatite erupting from the volcano of Oldoinyo Lengai in northern Tanzania.

This carbonatite is made up of predominantly of the alkali carbonate phases nyerereite ($Na_{0.8}K_{0.2}CaO_3$) and gregoryite ($Na_{1.6}K_{0.1}Ca_{0.15}CO_3$). Natrocarbonatite does not survive in the geological record but alters to calcite carbonatite (Zaitsev 2008).

Other common minerals found in carbonatites are;

a) Magnetite, constituting the most common oxide mineral and occurring as euhedral phenocysts, in grain clusters and streaks (schlieren). Magnetite occurs in modal abundance of 5 to 10%. Carbonatite magnetites are usually low in TiO_2.

b) Apatite is a characteristic component of many carbonatites. It is frequently present in sufficient amounts to constitute an economic phosphate resource. Known economic carbonatite phosphorite deposits occur at Phalaborwa, South Africa, Siilinjarvi, Finland and Kovdor, Russia.

c) Phlogopite is a minor phase and occurs as coarse-grained individual euhedral crystals and as schlieren and streaks.

d) Alkali amphiboles include arfvedsonite, riebeckite and magnesio-kataphorite varieties. Pyroxene, such as aegirine is less common but is reported, for example, in the Xiluvo Complex, Mozambique.

e) Accessory phases are abundant with over 200 different minerals reported from carbonatites. Common accessories minerals found in carbonatites are olivine (fosterite), diopside, phlogopite, calcic amphiboles, magnetite and pyrochlore, sodic-calcic amphiboles, monticellite, aegirine-augite, andradite, chlorite, titanite and perovskite (Chakhmouradian and Zaitsev 2002, Chakhmouradian 2004, Le Bas 1981). Sulphides are rare with pyrite most common. Chalcopyrite, bornite and related copper minerals are unusual. They are concentrated in the Phalaborwa carbonatite and are abundant in the Glenover Complex, South Africa Verwoerd (1986).

f) REE minerals constitute a distinctive aspect of carbonatites. The REE are present in anomalously high amounts and for some geologists Sr and REEs are the most reliable geochemical indicators of igneous carbonatites (Mariano 1989). Potential economic REE-bearing minerals are baddeleyite, monazite, bastnäsite, zircon, ancylite, apatite, fluorite, strontianite, and pyrochlore.

Minerals of economic importance hosted by carbonatites are further discussed in section 2.2.10.

2.2.5 Whole rock geochemistry

Most carbonatites have geochemical signatures distinct from sedimentary carbonates and other igneous rocks. Carbonatites contain elevated levels of Sr, Ba, Nb, Zr, Ta, U and Th and are characterised by REE higher than most other rock types (Cullers and Graaf, 1984) (e.g., concentrations of Sr, Ba are usually in the range of 1000 ppm, Nb and Y are above 100 ppm). The ranges of major and trace-element compositions of carbonatites are variable (Table 2.8; Woolley and Kempe 1989).

Table 2.8 Major and trace element composition of carbonatites, (after Woolley and Kempe 1989).

Wt%	**Calciocarbonatite**		**Magnesiocarbonatite**		**Ferrocarbonatite**	
	Average	**Range**	**Average**	**Range**	**Average**	**Range**
SiO_2	2.72	0.00 - 8.93	3.63	0.60 - 9.40	4.70	0.36 - 9.00
TiO_2	0.15	0.00 - 1.09	0.33	0.00 - 1.98	0.42	0.00 - 2.30
Al_2O_3	1.06	0.00 - 6.89	0.99	0.00 - 4.41	1.46	0.01 - 5.60
Fe_2O_3	2.25	0.00 - 9.28	2.41	0.00 - 9.57	7.44	0.46 - 17.84
FeO	1.01	0.00 - 4.70	3.93	0.00 - 10.40	5.28	0.00 - 20.28
MnO	0.52	0.00 - 2.57	0.96	0.02 - 5.47	1.65	0.23 - 5.53
MgO	1.80	0.00 - 8.11	15.06	9.25 - 24.82	6.05	0.10 - 14.50
CaO	49.12	39.24 - 55.40	30.12	20.80 - 47.00	32.77	9.20 - 46.43
Na_2O	0.29	0.00 - 1.73	0.29	0.00 - 0.39	0.39	0.00 - 1.52
K_2O	0.26	0.00 - 1.47	0.28	0.00 - 1.89	0.39	0.00 - 2.80
H_2O	0.76	0.00 - 4.49	1.20	0.08 - 9.61	1.25	0.04 - 4.52
P_2O_5	2.10	0.00 - 10.41	1.90	0.00 - 11.30	1.97	0.00 - 11.56
CO_2	36.64	11.02 - 47.83	36.81	16.93 - 47.88	30.74	20.56 - 41.81
BaO	0.34	0.00 - 5.00	0.64	0.01 - 4.30	3.25	0.02 - 20.60
SrO	0.86	0.00 - 3.29	0.69	0.06 - 1.50	0.88	0.01 - 5.95
F	0.29	0.00 - 2.66	0.31	0.03 - 2.10	0.45	0.02 - 1.20
Cl	0.08	0.00 - 0.45	0.07	N/A	0.02	0.01 - 0.04
S	0.14	0.02 - 2.29	0.35	0.03 - 1.30	0.96	0.12 - 5.40
SO_3	0.88	0.02 - 3.87	1.08	0.06 - 2.86	4.14	0.06 - 17.10
(ppm)						
Li	0.1	N/A	N/A	N/A	10	N/A
Be	2.4	0.4 - 0.80	<5	N/A	12	N/A
Sc	7	0.6 - 18.00	14	10 - 17	10	56 - 340
V	80	0 - 300.0	89	7 - 280	191	56 - 340
Cr	13	2 - 479	55	2 - 175	62	15 - 135
Co	11	2 - 26	17	4 - 39	26	11 - 54
Ni	18	5 - 30	33	21 - 60	26	10 - 63
Cu	24	4 - 80	27	4 - 94	16	4 - 45
Zn	188	20 - 1120	251	15 - 851	606	35 - 1800
Ga	<5	N/A	5	N/A	12	N/A
Rb	14	4 - 35	31	2 - 80	N/A	N/A
Y	119	25 - 346	61	5 - 120	204	28 - 535
Zr	189	4 - 2320	165	0 - 550	127	0 - 900
Nb	1204	1 - 15000	569	10 - 3000	1292	10 - 5033
Ta	5	N/A	21	10 - 16780	0.9	N/A
Pb	56	30 - 108	89	30 - 244	217	46 - 400
Th	52	5 - 168	93	4 - 315	276	100 - 723
U	8.7	0.3 - 29	13	1 - 42	7.2	1 - 20

2.2.6 Isotopic composition

A feature of most carbonatites is their rather distinctly radiogenic isotopes with ε_{Nd} values ranging from -7.5 to -1. Calciocarbonatites have ε_{Sr} similar to silicate rocks ranging from 0 to 35, whilst most of magnesiocarbonatite have lower ε_{Sr} (e.g. Bell and Blenkinsop 1989, Harmer and Gittins 1998). Initial isotope ratios for Sr, Nd and Pb are consistent with a mantle origin, usually from a depleted sub continental mantle (Nelson et al. 1988, Bell and Blenkinsop 1989). Involvement of at least two end member compositions is suggested in the carbonatite magma. Some carbonatites, Phalaborwa for example, have anomalous non-mantle-like isotopic compositions (Eriksson 1989), and reflect contribution from sources having long lived (>1Ga) enrichments in Rb/Sr and LREE/HREE- values that conventionally are attributed to crust rather than mantle. Another known carbonatite complex with similar enriched isotopic signature is the Ihouhaouene complex in Algeria (Bernard-Griffiths et al. 1988) which, coincidentally, at 2.0 Ga is similar to Phalaborwa. Diamond-bearing lamproites from Australia (McCulloch et al. 1983) have similar isotopic signatures.

Carbon and oxygen stable isotope values in unaltered carbonatites are consistent with a mantle origin but are easily altered by processes of magmatic differentiation and sub-solidus alteration. The usual values range from $\delta\ ^{13}C$ = -1 to - 9‰ relative to PDB $\delta^{18}O$ = +6 +12‰ relative to SMOW (Deines, 1989). Other processes capable of changing the initial mantle-like isotopic signature of carbonatites include degassing and assimilation of crustal carbonate (Demény et al. 2004).

2.2.7 Petrogenesis

Bell (1998) discussed the following models that have been proposed for the origin of carbonatites;

(i) Carbonatite magmas are residual melts derived from ‘carbonated alkali peridotite magmas’ (King and Sutherland 1960).

(ii) Carbonatite magmas are *‘primary’,* the result of direct generation by very low degree of partial melts in the mantle and travelling from the mantle as carbonatite magmas (von Eckermann 1948). Primary carbonatite magmas might be rich in alkali carbonates, with the alkalis being responsible for the fenitisation and the development of the associated alkaline igneous rocks.

Some carbonatites are thought to have originated as direct partial melts from mantle rocks, such as carbonated peridotite, or as partial melts from subducted oceanic lithosphere (e.g., Wallace and Green 1988, Frezzotti et al. 2002, Ducea et al. 2005 and Walter et al. 2008).

(iii) Carbonatite magmas represent an immiscible liquid fraction which has separated from a parent, ultrabasic or basic magma in the crust (Lee and Wyllie 1998).

It has been shown experimentally (Kjaarsgard and Hamilton 1989, Panina and Motorina 2008) that at a temperature of around 1250°C -1230°C and at a pressure of 5 kbar a magma possessing a high carbon dioxide (CO_2) content will divide into separate, immiscible silicate and carbonatite magmas. Magmatic carbonatites are formed at a late stage in the crystallisation of peralkaline magma (Nielsen and Veksler 2002).

Evidence for each process exists, but the key is that these are unusual phenomenon. A direct mantle source is often invoked when geochemical data (in particular, trace-element ratios) rule out any consanguinity between carbonatites and their associated silicate rocks. For example, Harmer (1999) reported that in the Spitskop complex (South Africa), trace-element and isotopic geochemical data are inconsistent with the derivation of carbonatitic and silicate rocks from a single source by either immiscibility or fractional crystallization. He proposed that the Spitskop carbonatite originated from primary melts of mantle provenance. A similar conclusion was reached for the carbonatite-phonolite association at Khibina, Russia (Sindern et al. 2004).

Another hypothesis is that carbonatites form as cumulates from carbonate-rich silicate magma. Fractional crystallization from a silicate melt would produce compositionally intermediate (i.e. carbonate-silicate and silicate-carbonate) rocks, with both silicate and carbonate components having identical radiogenic isotope signatures (Bell and Rukhlov 2004). For example, at Dicker Willem (Namibia), ijolite and sövite are intercalated and show diffuse contacts, which is consistent with fractional crystallization theory (Cooper and Reid 1998). Progressive fractionation of carbonatitic magma will initially produce calcite carbonatites, followed by dolomite/ankerite or, in some cases, siderite carbonatites (Le Bas 1987, Bell and Rukhlov 2004).

The liquid immiscibility hypothesis states that a carbonate-rich silicate melt separates into two discrete phases. This model has been used to explain the genesis of many carbonatite-silicate rock associations around the globe. Experimental data show that immiscible carbonate liquids can form from carbonate-rich silicate melts at crustal pressures and that immiscibility is limited to alkali-carbonatite systems (Lee et al. 1994,

Lee and Wyllie 1997a, Harmer 1999). One of the most commonly cited lines of evidence for liquid immiscibility in silicate–carbonate systems is textural, i.e. the presence of rounded globules or ocelli of carbonate in silicate units or vice versa (Lapin and Vartiainen 1983, Vichi et al 2005). However, Lee et al. (1994) have shown in their experiments that round carbonate globules represent calcite crystals, and not quenched carbonate liquids. Experimental evidence (Lee and Wyllie 1997) also shows that dolomitic carbonatites cannot be formed by liquid immiscibility. Validity of liquid immiscibility relationships between carbonatites and spatially associated silicate rocks have been outlined by Bell and Rukhlov (2004). These criteria include: the lack of compositionally intermediate carbonate-silicate rocks, compositional similarity of mineral phases in both types of rock, consistency of element distribution between the carbonate and silicate phases with the experimentally determined partition coefficients, and similar radio-isotopic compositions of the two conjugate phases. It is worth noting that none of these criteria are conclusive, they simply do not rule out the possibility of a liquid-immiscibility relationship.

2.2.8 Carbonatite-associated ore deposits

Carbonatite-associated ore deposits may be of magmatic (primary), replacement/hydrothermal, and residual or weathering type of mineralisation as described below and in Table 2.9

a) Magmatic or primary mineralisation: Intrusive form and cooling history control primary igneous deposits (fractional crystallization). The best known primary deposits are those at Mountain Pass, California where carbonatites contain REE minerals that are of primary igneous crystallisation (Mariano 1989). Another example of a primary carbonatite deposit is the dolomitic carbonatite at Kangakunde Hill, Malawi that contains up to 7% monazite as green euhedral crystals (Wall and Mariano 1996). The most common primary minerals of economic interest in carbonatites are bastnäsite, pyrochlore, apatite, zircon, baddeleyite, magnetite, monazite and parisite. Fersmite and xenotime are rare.

Table 2.9 Key characteristics and examples of the major REE deposits types. Specific deposits listed may fall into more than one mineral deposit class*. Number of documented occurrences, compiled from Orris and Grauch (2002), Grauch and Mariano (2008) **(Doc. No** = Documented number of occurrences).

Deposit type	Brief description	Doc. No.	Typical grades and tonnage	Major example
Primary deposits				
Carbonatite associated	Deposits associated with carbonatite and alkaline provinces and zones of major faulting	107	A few thousands of tonnes to several hundred million tonnes, 0.1 - 10% REO, e.g. Bayan Obo (750 million tonnes at 4.1 % REO)	Mountain Pass, USA; Bayan Obo, China; Okorusu, Namibia; Amba Dongar, India; Barra do Itapiragua, Brazil; Iron Hill, USA
Associated with alkaline rocks	Deposits associated with igneous rocks characterised by abundant alkali minerals and enrichment in HFSE	122	Typical <100 million tonnes (Lovozero >1000 million tonnes), grade variable, typically <5% REO, e.g. Thor Lake (64.2 million tonnes at 1.96% REO)	Greenland; Khibina and Lovozero, Russia; Thor Lake and Strange Lake, Canada; Weishan, China; Brockman, Australia; Pajarito Mountain, USA
Iron-REE deposits (iron oxide-copper-gold deposits)	Copper-gold deposits rich in iron oxide and diverse in character and form	4	E.g. Olympic Dam: 200 Million tonnes at 0.3295% REO (Orris and Grauch 2002)	Olympic Dam, Australia; Pea Ridge, USA
Hydro-thermal deposits (unrelated to alkaline rocks)	Typical quartz, fluorite, polymetallic veins and pegmatites of diverse origin	63 (a)	Typical <1million tones, rarely up to 50 million tonnes, grade variable, typically 0.5-4.0 rarely up to 12%; REO e.g. Lemhi Pass, 37 million tonnes at 0.516% REO (Orris and Grauch 2002)	Karonge, Burundi; Naboomspruit and Steenkampskraal, South Africa; Lemhi Pass, Snowbird and Bear Lodge, USA; Hoidas Lake, Canada

Table 2.9 (cont.)

Deposit type	Brief description	Doc No.	Typical grades and tonnage	Major example
Secondary Deposits				
Marine placers	Accumulations of resistant, heavy minerals, concentrated by coastal processes and found along or close to existing coastlines	264 (b)	Highly variable tonnage, commonly in the order of tens to 1-3 hundred million tonnes, generally 0.1% monazite, e.g. Jangardup 30 million tonnes at 0.046% monazite (Orris and Grauch 2002)	Eneabba, Jangardup, Capel, WIM 150, Australia; Green Cove Spring, USA; Richards Bay, South Africa; Chavara, India
Alluvial placers	Ancient placers deposits typically forming consolidated cemented rocks	78(b)	10s to <200 million tonnes, typically <0.1% monazite e.g. Horse Greek: 19 million tonnes at 0.041% monazite (Orris and Grauch 2002)	Perak, Malaysia; Chavara, India; Carolina monazite belt and Horse Creek, USA; Guangdong, China
Paleo-placers	Ancient placer deposits typically forming consolidated cemented rocks	13(b)	Tens of million tonnes up to 100 million tonnes, typically <0.1% REO	Elliot Lake, Canada; Bald Mountain, USA
Lateritic deposits	Residual surface deposits formed from intense chemical weathering of REE-enriched igneous rocks	42(b)	A few ten thousands of tonnes to several hundred of million tonnes, 0.1-10% REO e.g. Mount Weld: 12.24 million tonnes at 9.7% REO (up to 40% REO)	Mount Weld, Australia; Araxa, Brazil; Kangankunde, Malawi
Ion-adsorption clays	Residual clay deposits formed from the weathering of REE-enriched granites	>100	Most 10 000 tonnes, low grade (0.03-0.35% REO)	Longnan, Xunwu, China

b) Replacement veins or hydrothermal mineralisation: Tectonic and local structural controls influence the forms of metasomatic mineralisation. Genetic models indicate

mineralisation within carbonatites to be syn to post-intrusion and commonly occuring in several different types or stages of mineralisation such as: Fluorite along fractures, barite veins, U-Th minerals + silicification, calcite veining and reprecipitation of Fe oxides (hematite).

c) Hydrothermal and weathering type mineralisation: usually forms within the complex however, the mineralisation can form outside of the complex if the elements are sufficiently mobile. The gangue mineralogy associated with these deposits is mostly well defined and consists of the following minerals: calcite, dolomite, siderite, ferroan calcite, ankerite, hematite, biotite, titanite, and olivine.

2.2.9 Exploration criteria for carbonatite deposits

The exploration for carbonatites includes three main approaches that are described below as geochemical, geophysical and others**.**

*a) Geochemical signature***:** Resistant niobium or phosphate minerals in soils and stream sediments; F, Th and U in waters.

*b) Geophysical signature***:** Magnetic and radiometric expressions and sometimes anomalous radon gas concentrations can identify primary targets**.**

c) Other exploration guides: Carbonatites are commonly found over broad provinces, but individual intrusions may be isolated. Fenitization increases the size of target in regional exploration for carbonatite-hosted deposits. U-Th radioactivity associated with fluorite and baryte within carbonatites are considered as indirect REE indicators.

2.2.10 Economic importance of carbonatite deposits

Minerals hosted in carbonatites and of substantial proportions to the world reserves Mariano (1989) are:

1. **Phosphates** – generally as concentrations of apatite. At present apatite is challenged by various reserves of sedimentary phosphate. These sedimentary ores, particularly those in Morocco, contain significant quantities of Cd, an extremely dangerous heavy metal. Environmental pressure together with the current phosphate demand has increased the demand for carbonatite-hosted apatite. Apatite is an easily beneficiated resource which can be exploited using low level of technologies. As such it is extremely important in an African context. Zimbabwe's total demand for agricultural super-phosphate is satisfied by apatite from the Dorowa carbonatites. Namibia has seen increase in the number

of applications for mineral rights with regard to phosphate deposits from only 3 applicants in 2007 to 11in 2008 and 33 by 2012.

2. **Niobium (Nb):** primarily in pyrochlore and related minerals and their hydrothermal and lower temperature alteration products. At present Araxa (Brazil) produces most of the world's niobium.
3. **Industrial minerals** such as vermiculite; feldspar and nepheline in associated fenites and nepheline-bearing silicate rocks are a potential source of fluxes for the ceramic industry. Calcite itself is a relatively rare commodity in Southern Africa. Carbonatites are also mined for copper (Phalaborwa, RSA), iron (Kovdor, Russia) and fluorite (Amba Dongar, India; Okorusu, Namibia (Figure 2.11).
4. **Rare earth elements:** Carbonatites are important sources of rare-earth elements (REE) in the form of rare-earth carbonate minerals, phosphates and oxides. Because of their vital importance in today's development for a wide range of technological applications, such as electronics, high-performance magnets, petroleum cracking catalysts and high-efficiency fluorescent lighting (Pell 1996) these are discussed separately in this thesis and summarised in (Figure 2.4).

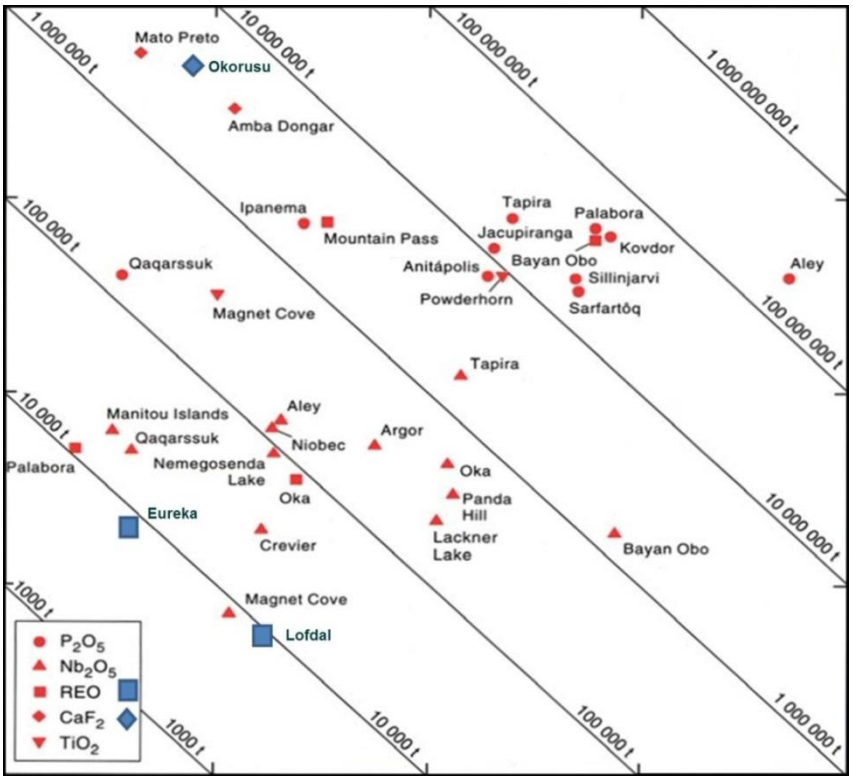

Figure 2.11 World economic resources related to carbonatites (Source: Natural Resources Canada, Goodfellow (2006), compared with Namibian carbonatite deposits

Chapter 3: Investigation of the spatial and temporal location of Namibian carbonatites in the context of regional geological settings

The purpose of the present chapter is to briefly describe the occurrence of carbonatites in Namibia, giving basic information on their distribution, geology, petrology and ages. Some of them are of considerable economic interest, as will be described, and an attempt has been made to give approximate coordinates of the carbonatites. Some have very limited data available. A number have been visited by the author during this study, their locations records were improved and their geochemical data used for comparison to Lofdal.

3.1 Namibia geological settings in the context of the spatial and temporal location of Namibian carbonatites

The oldest rocks in Namibia are late Archean and occupy a small area near Sesfontein, North western part of Namibia. Several Paleoproterozoic metamorphic complexes ranging between 2 – 1.8 Ma can be found scattered in different places in Namibia. These include the Huab Metamorphic Complex, into which the Lofdal Carbonatite Alkaline Complex has intruded. The Huab Metamorphic Complex is associated with slightly younger cover sequences of volcanic and sedimentary rocks such as the Khobedus group and the associated Fransfontein Granitic Suite.

In the southern Namibia, extensive Mesoproterozoic successions occur and include the syntectonic, granulite to amphibolite facies gneisses of the Namaqua Metamorphic Complex.

The Marienhof Formation is an older, Mesoproterozoic stand-alone unit in the Rehoboth area Miller (2008), in the central part of Namibia.

The most extensive stratigraphic unit in Namibia is the Damara supergroup, deposited in the NE trending Damara belt of central Namibia and the North-trending Kaoko Belt of North West Namibia (Figure3.1). Damara evolution began at approximately 850 Ma with the deposition of up to 6000 m of sediments and bimodal, peralkaline volcanic rocks of the Nosib group (Miller 2008). At about 780 – 760 Ma there was rifting, together with rift-related sedimentation and volcanism. A period of mainly marine deposition followed from 730 -600 Ma till subsequent crustal convergence between

Congo and Kalahari Cratons from 600 - 580 Ma to the final collision at 550 -540 Ma (Miller 2008).

Episodic high-temperature metamorphic events and granitic intrusions followed in the northern and central part of the Damara Belt and the youngest pan-African metamorphic rocks yield an age of 465 Ma. The final uplift of the central parts of the orogen is said to have taken place from 470 - 465 Ma (Miller 1983). Based on the lithologies, metamorphic characteristics and the structures, the Damara orogeny is subdivided into several tectono-stratigraphic zones. Lofdal area belongs to the Northern Zone according to Miller (1983).

The Neoproterozoic rocks that are not related to Damara and Gariep succession are the granitic and syenitic rocks forming the intrusive, anorogenic Wetterkopf complex of the Richtersveld suite. The Lofdal complex also falls under this group of rocks.

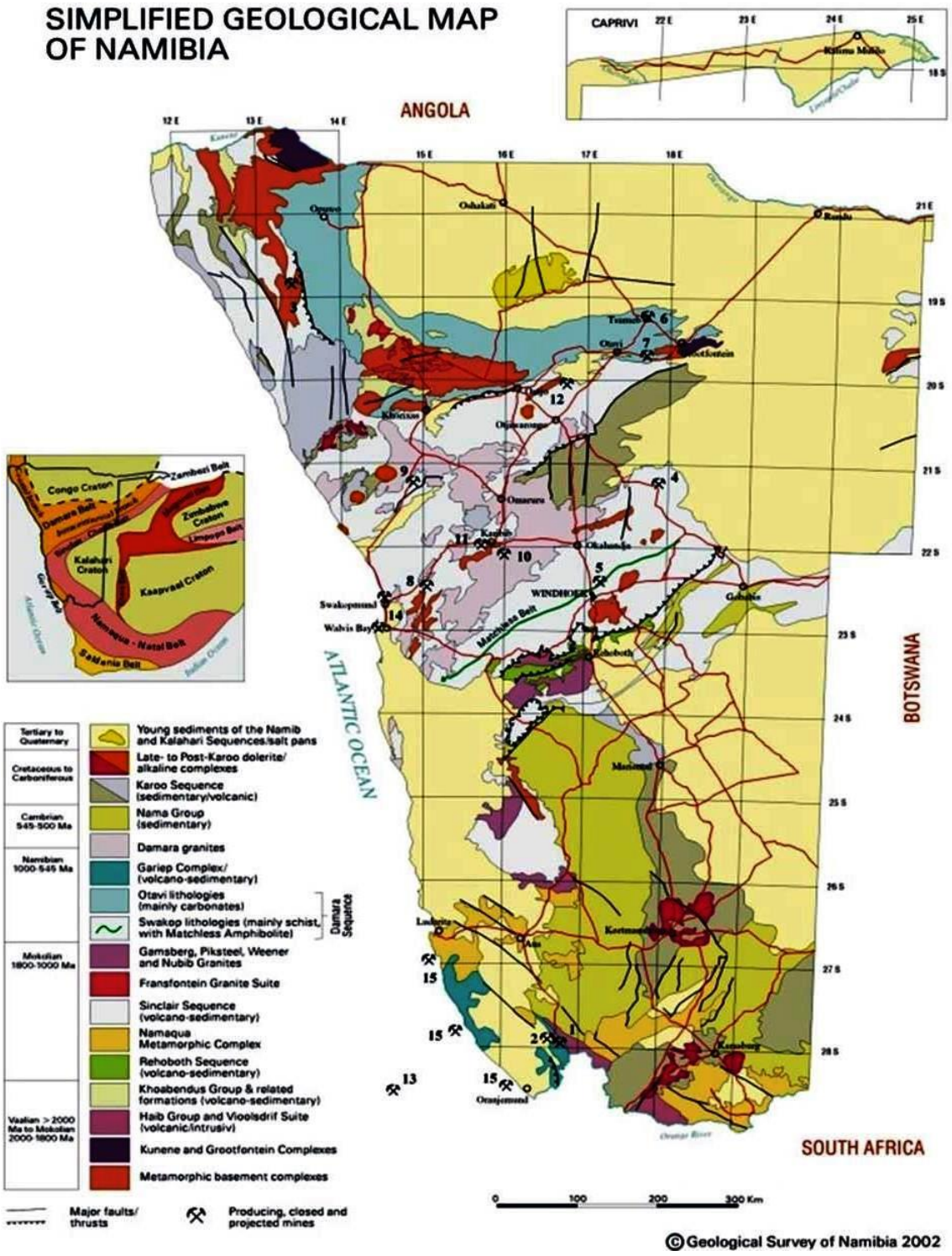

Figure 3.1 General geology of Namibia showing the belts that define the collisional triple junction nature of the Damara Orogen (insert) and showing the main geological units, the major faults and the distribution of plutonic. Source: Geological Survey of Namibia (2002).

3.2 Overview of the Namibian carbonatites and their economic potential

In the Southern African region carbonatites occur over a period of 2000 million years from early Proterozoic to Tertiary. Five different groups are distinguished that show very limited overlap in time and space (Verwoerd 1993). Here the carbonatites in Namibia are put into four age groups (Figure 3.2); Mesoproterozoic 1600 to 1000 Ma; Damaran1000 to 465 Ma; Early Cretaceous ±130 Ma and late Cretaceous to early Tertiary 80 – 50 Ma. Carbonatites belonging to late Cretaceous and early Tertiary are related to the extensional regime of the opening of the southern Atlantic (Marsh 1972, Pirajno 2004a).

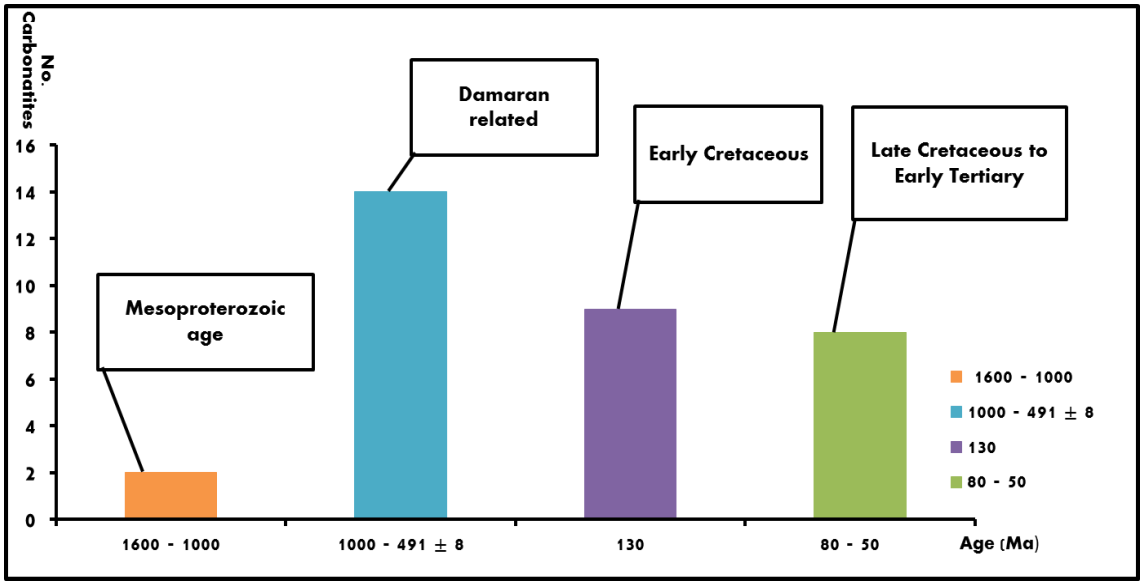

Figure 3.2 Age distribution of Namibian carbonatites

More than 53 alkaline and carbonatite complexes are known in Namibia (Figure 3.3). The carbonatites are described here according to their age groups.

Namibian carbonatites are mainly associated with alkaline intrusions forming complexes. However, Eureka, Keishohe, Kaukasib and Teufelskuppe carbonatites are not associated with any alkaline bodies. Woolley and Kjarsgaard (2008a) found that 21% of carbonatites, in a world database including >500 occurrences, have no association with silicate rocks.

There are four major provinces of alkaline rocks and carbonatites in Namibia. Three of these comprise linear distributions of occurrences defining NE-SW trending lines (Figure 3.3) correlated these provinces with transform faults in the South Atlantic (Marsh 1972). The Alkaline Provinces are 1) Kunene; 2) Damaraland; 3) Luderitz and 4) Kuboos Bremen. These are divided according to their locations rather than their geological ages.

Some new carbonatite discoveries such as Florence, Summas and findings in Kaokoland and Otavi Mountain land are in an early stage of study and not yet displayed.

In the North West of Namibia is the Kunene Alkaline Province where four carbonatites are known. Most carbonatites of Namibia are located on the western central part of Namibia known as the Damaraland province. A third large group are the Luderitz and Kuboos Bremen provinces located in the south most part of Namibia, the later extending into South Africa. Most carbonatites under this group occur along the EW transform zones, formed during the extensional stress field after the main Karoo deposition and during the break up of Gondwana. The fourth group comprised of few alkaline and carbonatite bodies that fall outside these linear zones.

Namibian carbonatites occur as plugs, dykes, domes, and complexes associated with alkaline rocks and pyroclastics, for the latter especially those associated with kimberlite intrusions. Little is known of the geochemistry of the Namibia carbonatites. Some ages of the carbonatites have been correlated to the regional geological settings of adjacent rocks or correlated to known alkaline rocks in their vicinities. Some data collected from less known carbonatites during this study shall be illustrated and used for comparison with that of Lofdal carbonatite data. There are numerous carbonatites in Angola and Brazil that reveal same ages to the Namibian (Comin-Chiaramonti and Gomes 1999) giving insights of geological processes in the southern hemisphere before the Gondwana breakup. In brief, Namibian carbonatites are dominantly calcitic with several occurrences comprised of dolomite with no calcite and with varying degrees of alterations and/or fenitisation.

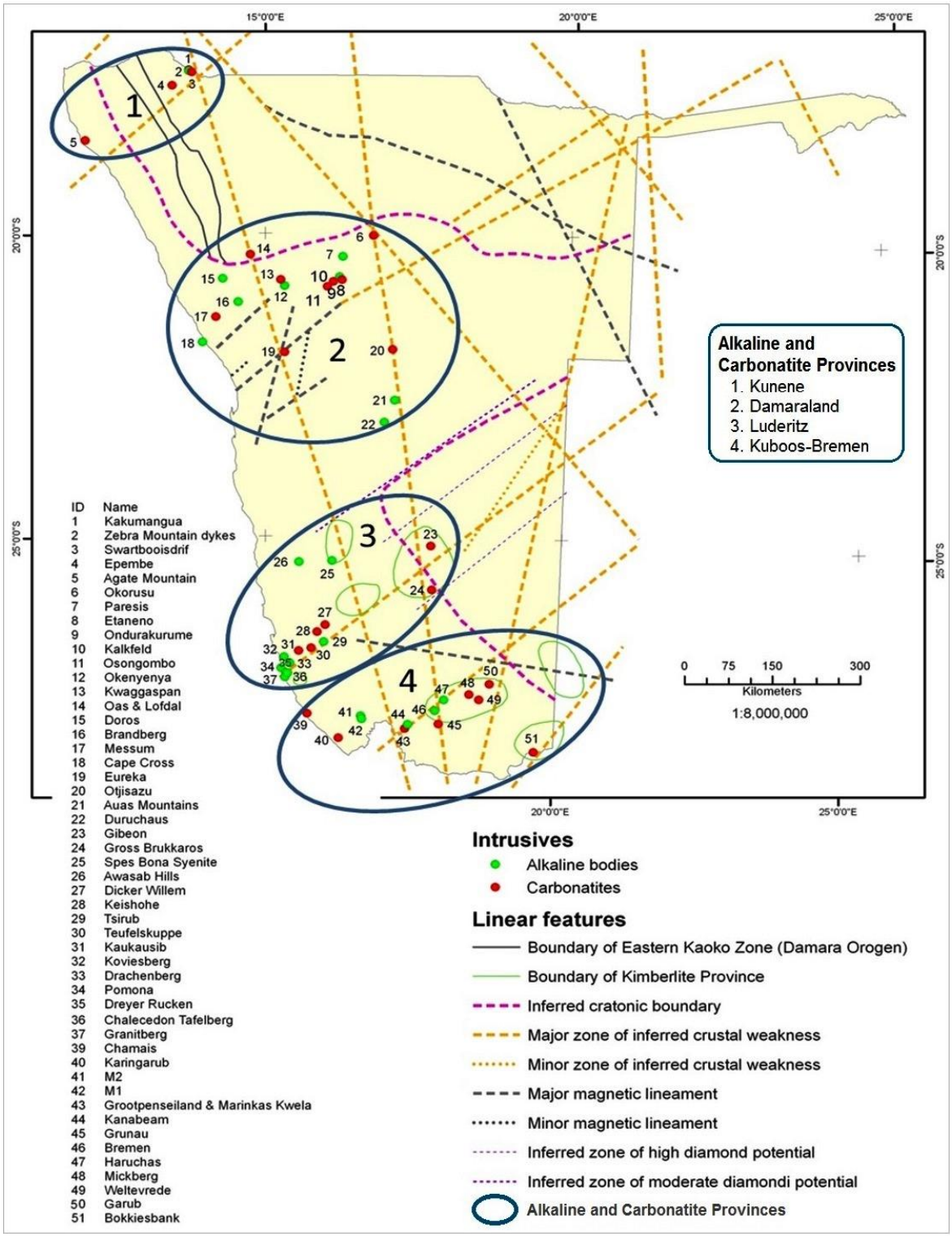

Figure 3.3 Distribution of carbonatite and alkaline rocks in Namibia Early. Cretaceous occurrences are restricted to EW transform faults modified after GSN (2001).The Alkaline Provinces are 1) Kunene; 2) Damaraland; 3) Luderitz and 4) Kuboos Bremen. These are divided according to their locations and not their geological ages.

Ferrocarbonatites are also described from a number of occurrences. The accessory minerals are characterised, typically, by their broad range and as listed in table 1. Apart from typical carbonatite minerals such as apatite, magnetite, phlogopite and pyrochlore, carbonatites contain other accessory minerals such as feldspars, amphiboles, micas and olivine, as well as sulphides.

Accessory species include bastnäsite, monazite, sodalite and REE bearing minerals. The ranges of igneous silicate rocks with which the carbonatites of Namibia are associated are variable (table 1). Most complexes in Namibia are associated with syenites, ijolites and occasionally also with kimberlites. Many carbonatites of Namibia are dated (Table 2). Their ages range between 1600 – 32 Ma (Figure 3.2).

3.3. Descriptions of Namibian carbonatites

A brief description of each reported carbonatite occurrence, including key reference is summarized in Table 3.1 for comparison.

Table 3.1 Brief description of Namibian carbonatites.

NO.	*Carbonatite/alkaline complex name*	*Carbonatite type*	*Whole rock/mineral*	*Method*	*Age (Ma)*	*Geological period*	*Reference*
1	Epembe (Otjitanga)	Ferro carbonatite	Zircon	U-Pb	1600 - 1000	Mesoproterozoic	Verwoerd (1967) Menge and Miller (1968) Toerien (1965) Ferguson et al. (1975).
2	Kakumangua	Ferro carbonatite	N/A		1600 - 1000	Mesoproterozoic	Verwoerd (1967) Menge and Miller 1968 Toerien 1965 Ferguson et al. 1975.
3	Swaartbooisdrif	Ferro carbonatite	Biotite; pyrochlore	K-Ar; U-Pb	1600-1000; 1140-1120	Neoproterozoic	Menge and Miller (1968), Toerien (1965), Ferguson et al. (1975, Thompson et al. (2002), Verwoerd (1967), S. Littmann (written communication (2005), Drüppel et al. (2006)
4	Lofdal carbonatite dykes	Various	xenotime-(Y)	U-Pb	765	Neoproterozoic	Wall et.al. (2008)
5	Otjisazu	calcitic carbonatite			(837 + 601/ - 49 Ma	Neoproterozoic to Cambrian	Bühn (1999)
6	Mickberg				(1000 - 570) to (570 - 510)	Neoproterozoic to Cambrian	Verwoerd (1967)
7	Weltevrede				(1000 - 570) to (570 - 510)	Neoproterozoic to Cambrian	Verwoerd (1967)
8	Eureka		Monazite	Pb	500 ±20	Cambrian	Burger et al. (1965)

Table 3.1 (cont.) Brief descriptions of Namibian carbonatites.

NO.	*Carbonatite name*	*Carbonatite type*	*Whole rock/mineral*	*Method*	*Age (Ma)*	*Geological period*	*Reference*
9	Marinkas Quellen		whole rock	Rb - Sr	529 ±24, 514 ±26	Cambrian	Smiethies and Marsh 1996
10	Garub		biotite/whole rock	Rb - Sr	491 ±8	Cambrian	Allsopp et al. 1979
11	Kalkfeld	Ferro carbonatite		K -Ar	153.6 - 172.8	Early Cretaceous	Ziegler 1992
12	Okorusu	calcitic carbonatite		Rb - Sr	126.6 ±7.3	Early Cretaceous	Milner et al. 1995
13	Ondurakorume				±130	Early Cretaceous	Verwoerd 1967
14	Osongombo		NA		±130	Early Cretaceous	Verwoerd 1967
15	Kwaggaspan	Ferro carbonatite			±130	Early Cretaceous	Verwoerd 1967
16	Karingarub				±130	Early Cretaceous	Verwoerd 1967
17	Chameis*		while rock	K- Ar	37 ; 133 ± 2	Early Cretaceous	Mathias 1974
18	Agate Mountain	calcitic carbonatite			Post early cretaceous	Early Cretaceous	Miller 1999
19	Messum	calcitic carbonatite	Biotite, Mica and calcite	Rb - Sr, Ar/Ar , Rb Sr	132 ± 2.2, 149 ± 1, 126.8 ± 1.3	Early Cretaceous	Allsopp et al. 1984 Fitch and Milner 1984 Milner et al. 1995
20	Okenjenje			K - Ar, Rb - Sr	133 - 128, 128.6 ±1 - 123.4 ±1.4	Early Cretaceous	Watkins et al. 1994 Milner et al 1993
21	Brukarros		phlogopite	K - Ar, Rb - Sr	77 ± 2 , 84	Late Cretaceous to Early Tertiary	Reid et al. 1990 Allsopp and Barrett 1975
22	Dicker Willem	calcitic carbonatite	Biotite	K - Ar Rb - Sr	48 ± 2, 49. 8 ± 0.8	Late Cretaceous to Early Tertiary	Reid et al. 1990
23	Grunau				80 - 50	Late Cretaceous to Early Tertiary	Verwoerd 1993
24	Bokkiesbank				80 - 50	Late Cretaceous to Early Tertiary	Verwoerd 1993
25	Teufelskuppe	dolomitic carbonatite	Considered to coeval with Dicker Willem		80 - 50	Late Cretaceous to Early Tertiary	Verwoerd 1993
26	Kaukasib				80 - 50	Late Cretaceous to Early Tertiary	Verwoerd 1993
27	Hatzium				80 - 50	Late Cretaceous to Early Tertiary	Verwoerd 1993
29	Keishohe	calcitic carbonatite	NA	NA	80 - 50	Late Cretaceous to Early Tertiary	Verwoerd 1993

3.4 Carbonatites of Mesoproterozoic age (1600 – 1000 Ma)

Two carbonatites have been linked to belong to the same alkaline province, the Kunene alkaline complex. These are the Swartbooidrift and Epembe carbonatites which are the oldest carbonatites in Namibia (Figure 3.5).

3.4.1 Swartbooidrift and Epembe $17^0$20'S; $13^0$49'E and $17^0$33'S; $13^0$30'E

A swarm of sodalite rich carbonatite dykes occurs near Swartbooidrift on the Namibia/Angola border (Menge 1986) (Figure 3.4).

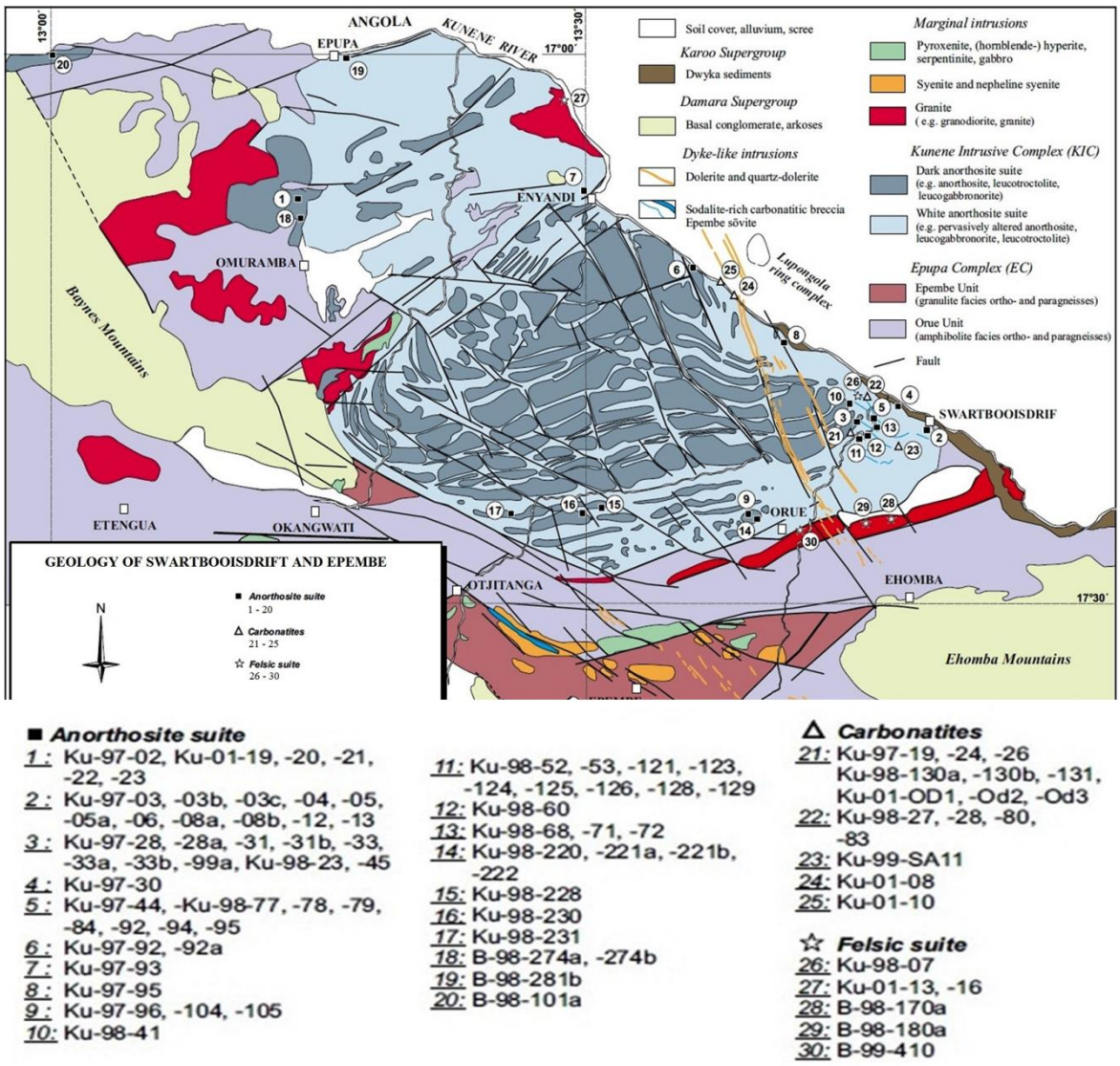

■ ***Anorthosite suite***

1: Ku-97-02, Ku-01-19, -20, -21, -22, -23
2: Ku-97-03, -03b, -03c, -04, -05, -05a, -06, -08a, -08b, -12, -13
3: Ku-97-28, -28a, -31, -31b, -33, -33a, -33b, -99a, Ku-98-23, -45
4: Ku-97-30
5: Ku-97-44, -Ku-98-77, -78, -79, -84, -92, -94, -95
6: Ku-97-92, -92a
7: Ku-97-93
8: Ku-97-95
9: Ku-97-96, -104, -105
10: Ku-98-41
11: Ku-98-52, -53, -121, -123, -124, -125, -126, -128, -129
12: Ku-98-60
13: Ku-98-68, -71, -72
14: Ku-98-220, -221a, -221b, -222
15: Ku-98-228
16: Ku-98-230
17: Ku-98-231
18: B-98-274a, -274b
19: B-98-281b
20: B-98-101a

Δ ***Carbonatites***

21: Ku-97-19, -24, -26 Ku-98-130a, -130b, -131, Ku-01-OD1, -Od2, -Od3
22: Ku-98-27, -28, -80, -83
23: Ku-99-SA11
24: Ku-01-08
25: Ku-01-10

☆ ***Felsic suite***

26: Ku-98-07
27: Ku-01-13, -16
28: B-98-170a
29: B-98-180a
30: B-99-410

Figure 3.4 Geological map of Swartbooidrift (Geological Survey of Namibia 2001).

They consist of banded ankerite, sodalite, analcite, cancrinite, albite and magnetite as principal constituents, and were intruded along pre-existing lamprophyre and syenite dykes. The sodalite has been exploited as semi-precious stone.

At Epembe 40 km southwest of Swartbooidrift a broad apatite-bearing sövite dyke cuts across an oblong body of nepheline syenite accompanied by several smaller syenites and nepheline syenites stocks (Menge 1986, Ferguson et al. 1975). The sövite is 6.5 km long and up to 250 m wide. Minor constituents are biotite, K-feldspar, plagioclase, magnetite, epidote, aegirine, riebeckite, and a betafite-like mineral.

These two occurrences have been linked as belonging to one alkaline igneous province but there is considerable doubt about their age. SACS (1980) classified Epembe as

Phanerozoic. This was challenged by Menge (1986) on the basis of preliminary U-Pb zircon and K-Ar biotite data pointing to a minimum age of 1110 Ma for the alkaline rocks.

The carbonatites are therefore included here in the Mesoproterozoic group despite their isolated position and the fact that all the others are situated on the Kaapvaal Craton. It should be noted that composite syenite carbonatite dykes have been described from across the border in Angola, and are genetically connected with the Lupongola carbonatite ring complex only about 25 km from Swartbooidrift (Lapido-Loureiro 1973).

Lupongola has not been dated, but the Angolan volcano-plutonic complexes are generally considered to be Cretaceous or younger similar to their Namibian counterparts further South. This is supported by Sr-Rb isochron age of 104.3 +-0.8 Ma and 130.8 +-1.4 Ma for the Njoio and Tchivira nepheline syenites respectively (Allsopp & Hargraves 1985).

Economic importance:

a) **<u>Swartboois drift:</u> T**he sodalite rich carbonatite has been quarried for decades to be used as ornament and dimension stone. Production in 1964 was about 6 350 kg and increased to 140 000 kg in 1985 and most of their products are exported to foreign markets (Menge, 1986). Until 2011 small scale miners have been operating these quarries. The large operation was abandoned owing to unfavorable rock properties.
b) **<u>Epembe:</u>** sampling of the carbonatite on 30 – 30 m grid gave P_2O_5 values of 0.1 – 6.3wt% with an average value of 1.5wt% (Woolley, 2001; Menge, 1986).

3.5 Carbonatites of Neoproterozoic (1000 – 570 Ma 550) to Cambrian age (570 – 510 Ma)

Seven carbonatites and their associated alkaline rocks are grouped under the Neoproterozoic age group. They are found throughout Namibia in different geological terrains.

3.5.1 Lofdal complex $20^0$21'S; $14^0$45'E

A large swarm of north-eastern trending carbonatite dykes (Miller, 1983a) is associated with the Lofdal nepheline syenite complex west of Khorixas near the northern edge of the Damara mobile belt in Namibia. Other associated intrusive rocks are gabbro, peridotite anorthosite, syenites and quartz-feldspar porphyry. The carbonatite carries

abundant fluorite in places and contains up to 180 thorium ppm, 260 ppm W, and 1500 ppm Zn while up to 460 ppm Nb is recorded in the nepheline syenites (Miller, 1983b). One sample of a carbonatite dyke indicated the presence of rare earth element mineralisation; cerium 0.87 wt%, lanthanum 1.5 wt%, and neodymium 0.74 wt% (Barbour, 1982).

Hawkesworth et al. (1983) obtained an Rb-Sr whole rock isochron age of 764 $\pm$ 60 Ma for the nepheline syenites. Although exposed within pre-Damara basement and not in contact with any Damara rocks, the Lofdal intrusion belongs to an early magmatic event and is pre-orogenic related to an intra-continental rift environment (Miller, 1983).

Several more carbonatite bodies were identified by the author and her colleague R. Ellmies between 2002 and 2010. These bodies are described in details in the following chapters.

Economic importance: Locally the carbonatite has HREE concentrations up to 8% although the average of the carbonatite dykes at Lofdal is 1.2 wt% total REE (Figure 3.6). The main body of the carbonatite contains lower levels of REE that rarely exceed 0.02wt%.

3.5.2. Otjisazu carbonatite $21^0$55'S; $17^0$06'E

This major carbonatite complex is located 20 km east northeast of Okahandja, near the southern boundary of the highly deformed central zone of the Damara Orogen. It has not been dated isotopically but can be bracketed rather closely on geological grounds. It is younger than the syntectonic granites of the major phase of deformation (550 Ma) and the Donkerhoek granites (523 Ma, Miller 1983a).

The complex is elongated and approximately 12 km^2 in surface area. A core of sövite is surrounded by alkali pyroxenite and subordinate ijolitic and gabbroic rocks, all of which are intruded by leucocratic syenite and syenite pegmatite. K-feldspar, garnet, apatite, titanite, calcite and accessory monazite are encountered in the carbonatite. The sövite has a complex mega breccia-like structure Verwoerd (1993). It is locally rich in aegirine-augite, garnet and apatite and contains xenoliths of schistose garnet-wollastonite rock. Apatite concentrations associated with traces of Cu sulphides are localised within both pyroxenite and sövite (Gunthorpe et al., 1986).

Both pyroxenite and sövite are titanite rich but devoid of magnetite, perhaps indicating crystallisation under iron-poor reducing conditions. Large titanite and apatite crystals are confined to the sövite and alkali pyroxenite as a late phase. Fenitisation of the surrounding porphyritic and semi-pelitic schists of the Swakop Group is very limited Verwoerd, (1993).

Economic importance: Large tonnages of P_2O_5 ore with an average grade of 3 to 5 P_2O_5 wt% have been established for the carbonatites. Apatite is concentrated patchily in the alkali pyroxenite, some segregations of pure apatite rock being 50 cm in diameter, and is also concentrated in the sövite. Geochemical sampling of soils defined areas of about 3 wt % P_2O_5 and 200 ppm copper, Woolley (2001); Gunthorpe and Buerger, (1989).

3.5.3. Eureka carbonatite $21^0$58'S; $15^0$19'E

Eureka is approximately 13 km from Usakos and 6.5 km north-northeast of Ebony siding on the Usakos-Swakopmund road. Previously differences of opinion whether this famous monazite locality is related to marble, skarn or carbonatite (Verwoerd, 1967a) have now been resolved with a PhD study by T. Dunai (Dunai et al., 1989; Ziegler and Dunai, 1991).

Low thorium, high cerium monazite, varying from minute rounded grains to platy aggregates up to 13 cm in length, occurs in several medium to coarse grained beforsite dykes with an average thickness of 1 – 2 m (maximum 7 m). The dykes intrude feldspathic quartzite inter-fingering with calc–silicate layers of the Nosib Group, and are intersected in turn by a tourmaline-bearing pegmatite of late Pan-African age. This leads to the conclusion that Eureka carbonatites were emplaced at a time between 450 and 500 Ma. Selvages of orthoclase up to 20 cm thick are interpreted as the result of fenitisation. A Sr-isotope study of four carefully selected carbonatite samples yielded a Sr content of 2.46 to 3.06 wt % Sr and initial $^{87}Sr/^{86}Sr$ in the range 0,70286 – 0.70318 (Dunai et al. 1989).

Economic importance: Analyses of four carbonatite samples by Dunai et al. (1989) indicated 2.3 – 3 wt % Sr.

3.5.4. Marinkas Quelle $28^0$10'S; $17^0$25'E

The Marinkas Quelle carbonatite complex occurs within the Kuboos-Bremen line of alkaline complexes in southern Namibia and the northwestern Cape Province of the RSA (Smithies et al. 1998). This carbonatite complex was discovered only in 1972.

It was indicated on the regional geological map of Blignault (1976), and briefly mentioned as a member of the Kuboos-Bremen line of intrusive rocks by Kröner and Blignault (1976) without description. The main body of carbonatite is a circular plug, 600 m in diameter cropping out as a prominent brown peak. A second arcuate body occurs to the northeast and sends off numerous dyke-like apophyses into the country rock and associated nepheline syenites (Fig 3.5). A third carbonatite occurrence has

been also identified Verwoerd (1993), although it needs confirmation as it does not appear on later publications. The complex comprises beforsite, sövite, syenite, nepheline syenite, trachyte and fenite, associated with three overlapping centres. The Nb-Ta, Y, Th and rare earth carriers reported in the Marinkas Quelle carbonatite complex in minerals such as synchysite, monazite and yttrio-fluorite. Phlogopite-fenite carries disseminated pyrochlore, ankerite, beforsite, apatite (Smithies et al. 1998).

The Marinkas Quelle Carbonatite Complex is related to magmatism with an uncontaminated depleted mantle signature in a continental setting ((Smithies et al. 1998).

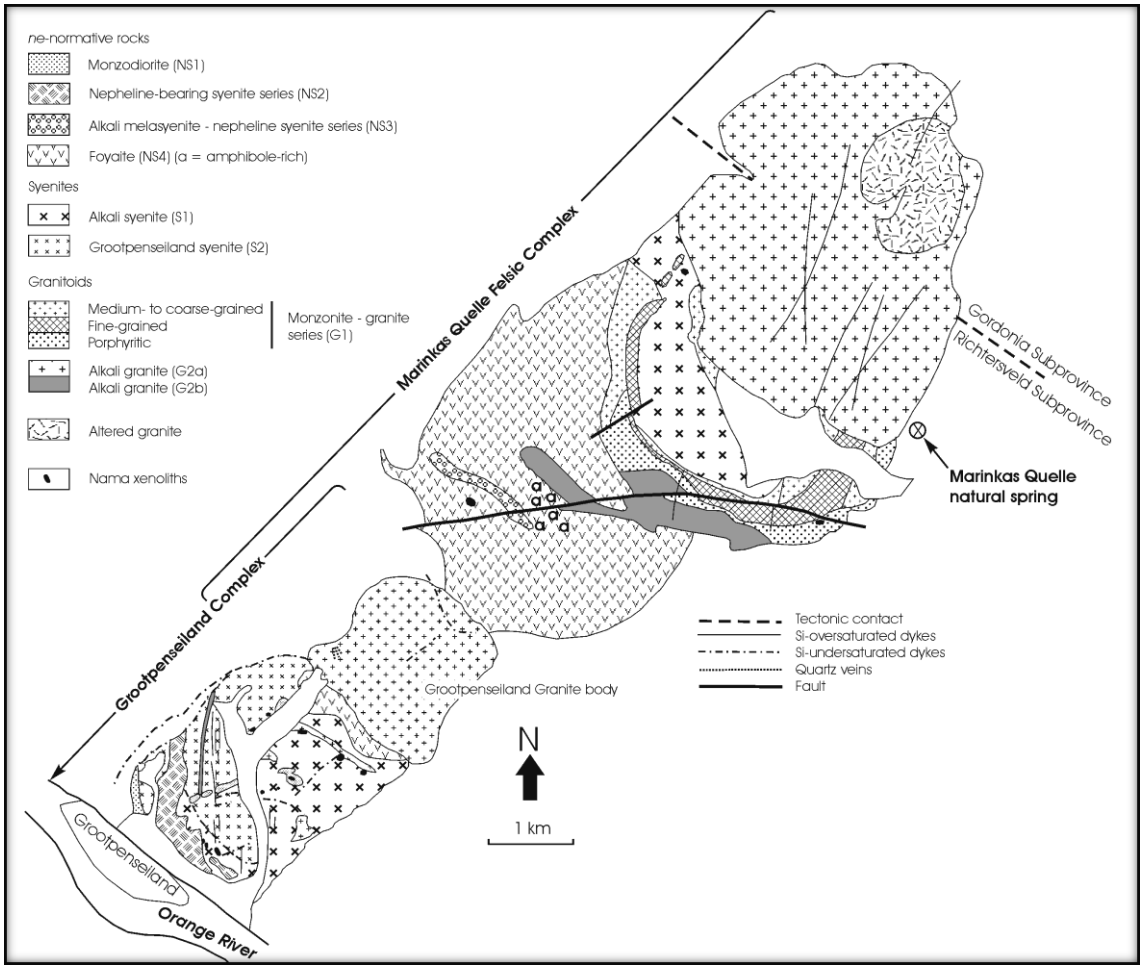

Figure 3.5 Geological map of the Marinkas Quelle (Geological Survey of Namibia 2008).

Economic importance: The Japan International Cooperation Agency- Metal Mining Agency of Japan 1995) indicated the beforsite rock to contain 0.1% of REO, 0.1% Nb and 1% phosphate content. The mineral descriptions as stated by Schommarz (1999) are of possible economic interest in relation to REE deposits.

3.5.5. Mickberg $27^0$35'S; $18^0$31'E

This carbonatite was first described by Schreuder (1975). Mickberg is located on the farm Mickberg 262; 20 km northeast of Grunau in Southern Namibia. It is a double-crested hill, elongated in a north-north-eastern direction and rising about 100 m above the surrounding plain. It is built of gneiss that is brecciated in places and intruded by irregular bodies of dark brown ankeritic beforsite. Inclusions of gneiss grit and quartzite of the Kuibis formation are embedded in the carbonatite. Some fragments of quartzite are light blue in colours as a result of fenitisation. The interlinking grains of quartz are seen under the microscope to be replaced by tuffs and a mosaic of new feldspar (microcline perthite and albite/oligoclase). Blue sodium amphibole also occurs in carbonatite north of the hill top. The main constituent of the carbonatite are ankerite, ferroan calcite, apatite, magnetite, biotite, and chlorite, as well as zircon, quartz and feldspar derived from the surrounding gneiss. Insignificant amounts of malachite and chrysocolla occur at the southern tip of the composite plug (Schreuber 1975, Verwoerd 1993).

A remarkable feature of the largest carbonatite body is in places the presence of spheroidal inclusions up to 15 cm in diameter. They consist of concentric shells made of fine grained ankerite and angular fragments around a lithic nucleus that may vary from 1 to 7 cm in diameter. Between these orbicules there is often a medium grained silica rich matrix consisting of quartz, microcline, and albite in a mosaic texture (Schreuber 1975).

Economic importance: The economic potential of this carbonatite has not been evaluated.

3.5.6. Weltevrede $27^0$40'S; $18^0$41'E

On the farm Weltevrede 302 adjacent to Mickberg 262 there are two breccia plugs forming low rounded hills in a sandy flat. The northern most measures 1 km in diameter, with several smaller subsidiary outcrops, and consist of gneissic rock fragments set in a gritty matrix with variable brown weathering carbonate content. Beforsite dykes cut across the breccias and their boundaries, and are also full of clasts. The second occurrence is similar with less ankeritic carbonate in the matrix.

Several blocks of Kuibis quartzite and conglomerate, meters in diameter, are found in the breccias below the projected stratigraphic level where this formation used to be present. This plug is also associated with beforsite veins and a calcitic dyke up to 2 m wide that follows a zig zag course along strike of the carbonatite dyke that contains

sporadic galena, chalcopyrite, limonite, malachite, chrysocolla, and quartz (Schreuder 1975) and Verwoerd (personal communication).

Economic importance: The economic potential of this carbonatite has not been evaluated.

3.5.7. Garub carbonatites dykes and sills $27^0$25'-$27^0$46'S; $18^0$40- $19^0$00'E

A series of ankeritic diatreme dykes, and sills that are known to extend over an area of 3000 km^2 toward Bremen and Jaruchas Complexes, occur in farm Garub 266 in the Great Karas Mountain. Verwoerd (1967a), in unpublished report recorded about 60 separate occurrences and designated them as carbonatites of doubtful status. A subsequent field and laboratory investigation carried out by Schreuder in 1997 identified approximately 100 occurrences and studied 82 of them. The majority, 65%, are intrusive into the Schwarzrand Formation of the Nama Group, 41% sills, and 25% occur as pipe-like bodies (Schreuber 1975).

Most of the diatremes and some of the dykes are filled with coarse breccia. The nature of the clasts proves that they were carried both upward and downward in the pipes (Schreuber 1975, Verwoerd 1993).

Some breccia clasts are well rounded. In addition, accretionary lapilli and other spherical bodies 5 – 10 mm in size are common in many dykes, pipes, and sills, giving rise to pisolitic structure. The groundmass and the pisoliths consist of medium-grained ankerite and subordinate calcite, chlorite, biotite, albite and Fe-hydrates. Veinlets of non-dilatational type with similar composition penetrate the county rock.

Evidence for a relationship with carbonatite is somewhat equivocal. Most sills and dykes consist at least in part of relatively homogenous, greenish-grey rock type with 10wt% to 20 wt% P_2O_5 and about 25 wt% SiO_2. Under the microscope both phenocrysts and microcrysts of biotite, augite, kaersutitic hornblende and ilmenite are seen in a matrix of ankerite. Carbonatised lath shaped pseudomorphs (original melilite or feldspar?) are common. Irregular ferruginous patches may represent large olivines. Minor constituents are apatite, zircon, magnetite leucoxene, pyrite garnet, and quartz. On major element variation diagrams the Garub rocks do not coincide with South African olivine-melilites or kimberlites. Trace elements (Ba, Sr, Nb, Zr, Y and Rb) are low and do not show clear geochemical similarities with either carbonatite or kimberlite (Schreuder 1997) Apart from their high carbonate content, they do show a similarity with alnoite. However, in the course of their geochronological study, Allsopp et al. (1978) noted that the high Sr content (>1000 ppm) of the whole rock sample from one of the hills supported a carbonatitic affinity.

They also found that the initial Sr/Sr ratio of c. 0.708 is unusually high for carbonatite and in view of the high Sr content, cannot have been seriously altered by contamination or internal isotopic observation of fenitisation effects at two localities (replacement of quartz in the wall rock by blue amphibole plus K-feldspar).

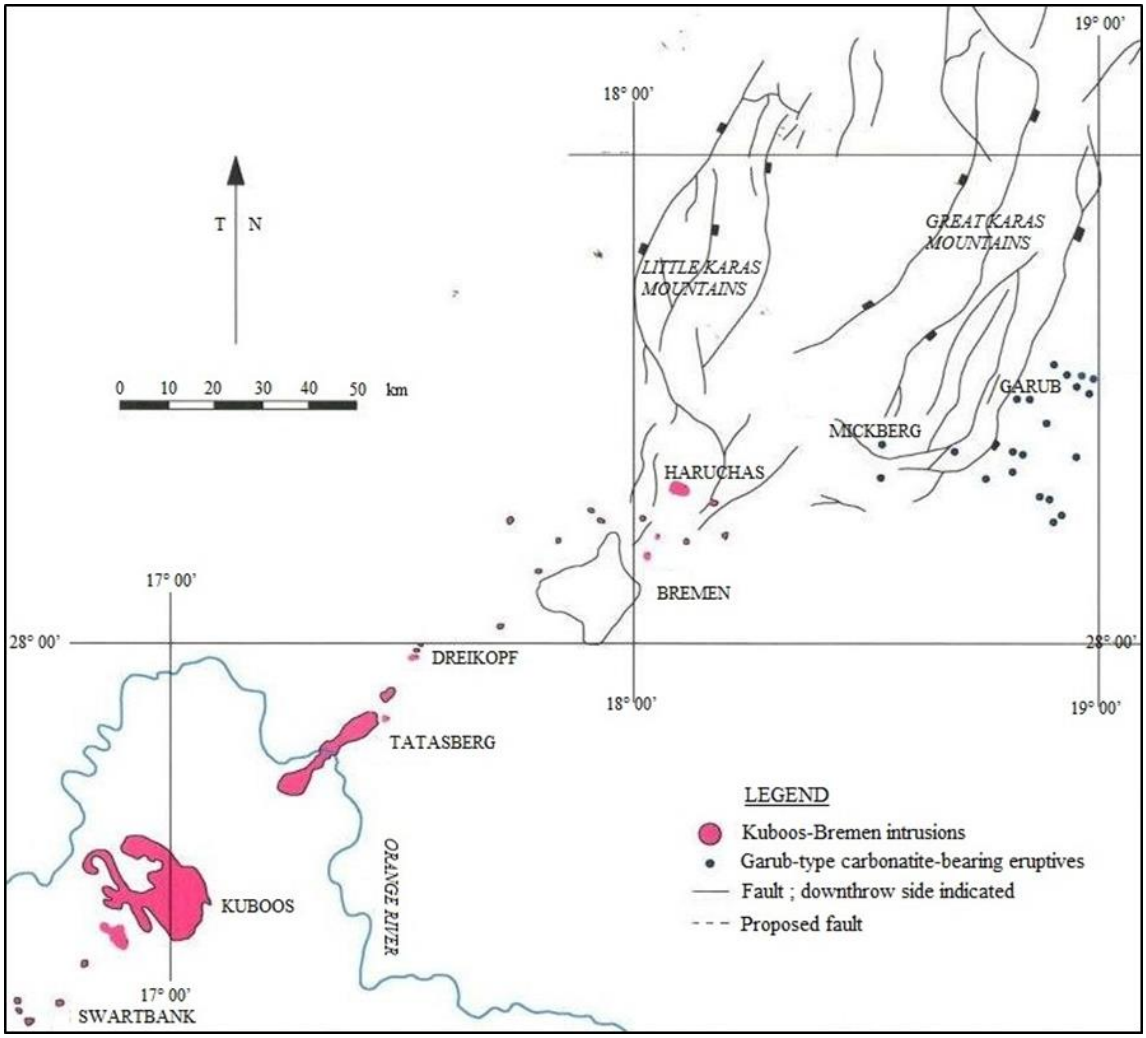

Figure 3.6 Geological Map of Kuboos-Bremen intrusions including Garub (modified after Geological Survey 2002)

The ages of the Garub eruptives are not well constrained. According to Allsopp et al. (1979) the calculated Rb-Sr isochron age of 491 $\pm$ 8 Ma, which they obtained from one whole rock and two impure (calcite-impregnated) biotite samples, should be interpreted as the minimum age for the emplacement of the sill. Likewise, their figures for the Nama Group, namely 518 $\pm$ 15 Ma (definite) and 553$\pm$13 Ma (probable) are minimum ages.

This implies that the Garub eruptives may perhaps postdate the rocks onto which they were emplaced by approximately 50 million years, but that pene contemporaneity is not excluded (Verwoerd 1967a, Schreuder 1975). It seems more likely that they belong to the alkaline magmatism of the Kuboos-Bremen line of intrusions. In view of many

similarities, a detailed comparison of this field with Miocene to Pleistocene Urach-Hegau-Kaiserstuhl volcanic district in Germany would be interesting (Verwoerd 1967a).

Economic importance: fluorite which is not directly associated with the carbonatite was mined in the early 1960s from Garub mine. This occurrence is unique for its blue fluorite.

3.6. Early Cretaceous ca.130 Ma

The next four localities are well-known in the geological literature (cf. earlier references in Verwoerd, 1967a). They are aligned along the east northeast-trending Cape Cross lineament in Damaraland, northern Namibia (Figure 3.7), and are assumed to be of similar age to other volcano-plutonic complexes along this lineament that have been dated e.g. Messum (123 Ma) and Paresis 135 Ma (Milner et al. 1995). Prins (1981) presented results of a comparative geochemical investigation of the carbonatites and their associated rocks. These rocks coincide with the breakup of Gondwanaland suggesting a thermal activity as a result of break up (Milner et al. 1995, Le Roux 1996).

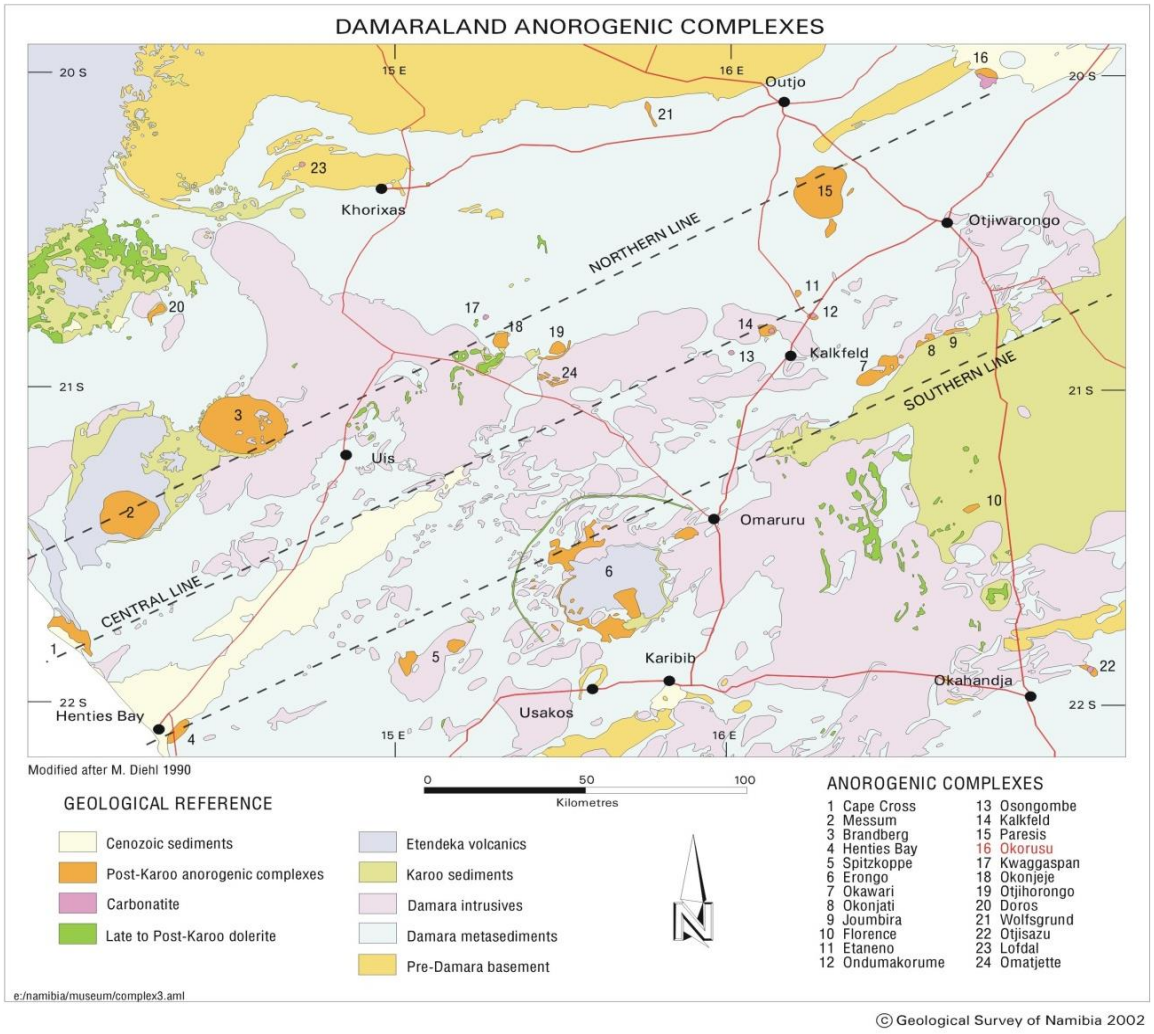

Figure 3.7 Anorogenic alkaline rocks trends associated with defined lineaments produced during the Gondwana breakup. Cretaceous rocks indicated include lamprophyres, Nephelinites, carbonatites and all known alkaline rocks and granites (Geological Survey of Namibia 2002)

3.6.1 Okorusu 20002'S; 16046'E

Okorusu is a poorly exposed ring complex 5 x 6 km in diameter, consisting of syenites, nepheline syenites and very subordinate carbonatite (Figure 3.8). The carbonatite occurs in the form of several isolated intrusions in the fenitised aureole but, according to Prins (1981), it occupies a larger area than previously thought. It is medium grained sövite with apatite, aegirine augite, pyrite, magnetite, celestine, quartz, and feldspar as accessory minerals. Trace elements (Sr, Ba, Y, Zr, Nb, La, Ce, and Nd) fall in the range typical of sövite, but Zr is rather low (Prins, 1981).

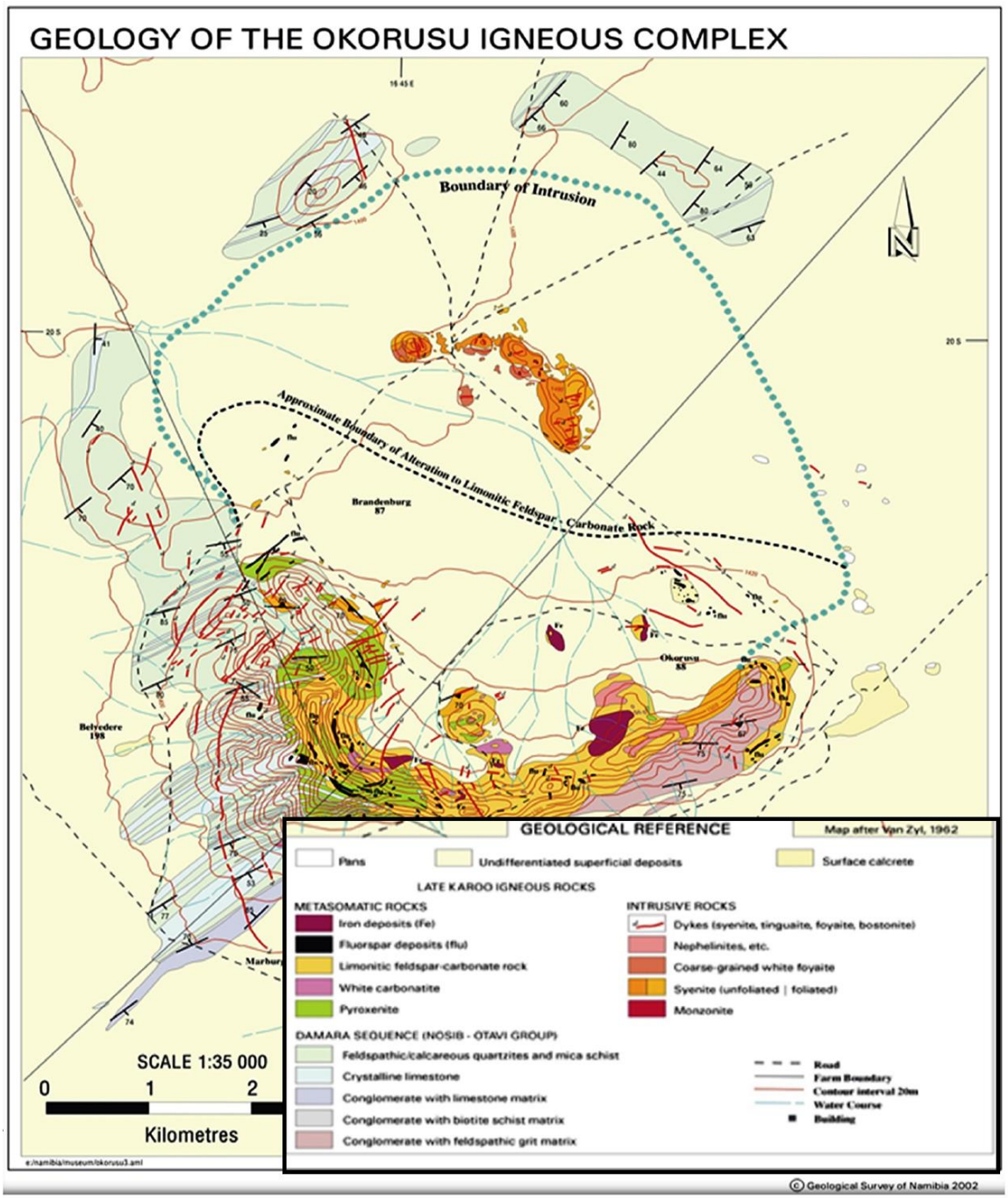

Figure 3.8 Geological map of Okorusu Geological Survey of Namibia ,2002)

Prins (1981) found relatively low REE contents in the associated alkaline rocks compared to Kalkfeld and Ondurakorume. He suggested that the silicate magma at Okorusu retained large quantities of REE due to relative high Na, F, and CO_2 contents, whereas a more complete extraction of the REE into the carbonate liquid took place at Kalkfeld and Ondurakorume.

Two features of particular interest at Okorusu are:

- The transformation of country rock quartzite and greywacke by pervasive metasomatism first to aegirine augite fenite and afterwards to K-feldspar fenite.
- The widespread introduction of fluorite as replacements, veins, and disseminations. After a lapse of 34 years fluorite mining at Okorusu was resumed in 1989; further particulars about the ore bodies are given by Notholt et al. (1990).

Economic importance: Fluorite has been mined intermittently since 1949. Van Zijl (1962) estimated reserves at 7 - 10 million tonnes at 35% CaF_2 and these are being mined to date. The possible existence of undiscovered niobium and rare earth mineralisation are currently explored at Okorusu.

3.6.2 Ondurakorume $20^0$46'S; $16^0$15'E

This is a composite carbonatite complex rising (Figure 3.9) above the surrounding plain as a prominent inselberg. It is 1.4 km in diameter and sends dyke like apophyses into the country rock of Damara marble, quartzite, schist, and granite. It is the only plug associated with leucocratic nepheline syenites (Figure 3.7). The consecutive phases of intrusion are micaceous sövite, sövite, beforsite (in part apatite rich) and REE bearing riebeckite, beforsite. This was followed by replacement bodies of radioactive hematite. The geological map (Verwoerd 1976a) has been revised, one difference being the recognition of the REE beforsite as a separate set of intrusions (Prins 1981). Mineralogically, this late phase is characterised by a variety of carbonate (dolomite, calcite, pistomesite, strontianite, ancyllite, carbocernaite) as well as riebeckite, pyrochlore, monazite, apatite and cerianite.

Economic importance: Ondurakorume has potential for phosphate, niobium, rare earth, strontium and thorium/uranium (Verwoerd 1986). The early micaceous sövite has the lowest Zr and highest Nb contents of the members of this complex, and there is a regular increase of Sr, Zr, Ce, and Ce/Y ratio with differentiation (Prins 1981). Systematic sampling for phosphate has been undertaken, 350 samples assaying up to 17.3% P_2O_3 with an average of 7% and Nb_2O_5 assaying up to 2.5%(Verwoerd 1967, Japan International Cooperation Agency- Metal Mining Agency of Japan 1995). REE and strontium are also present in interesting quantities.

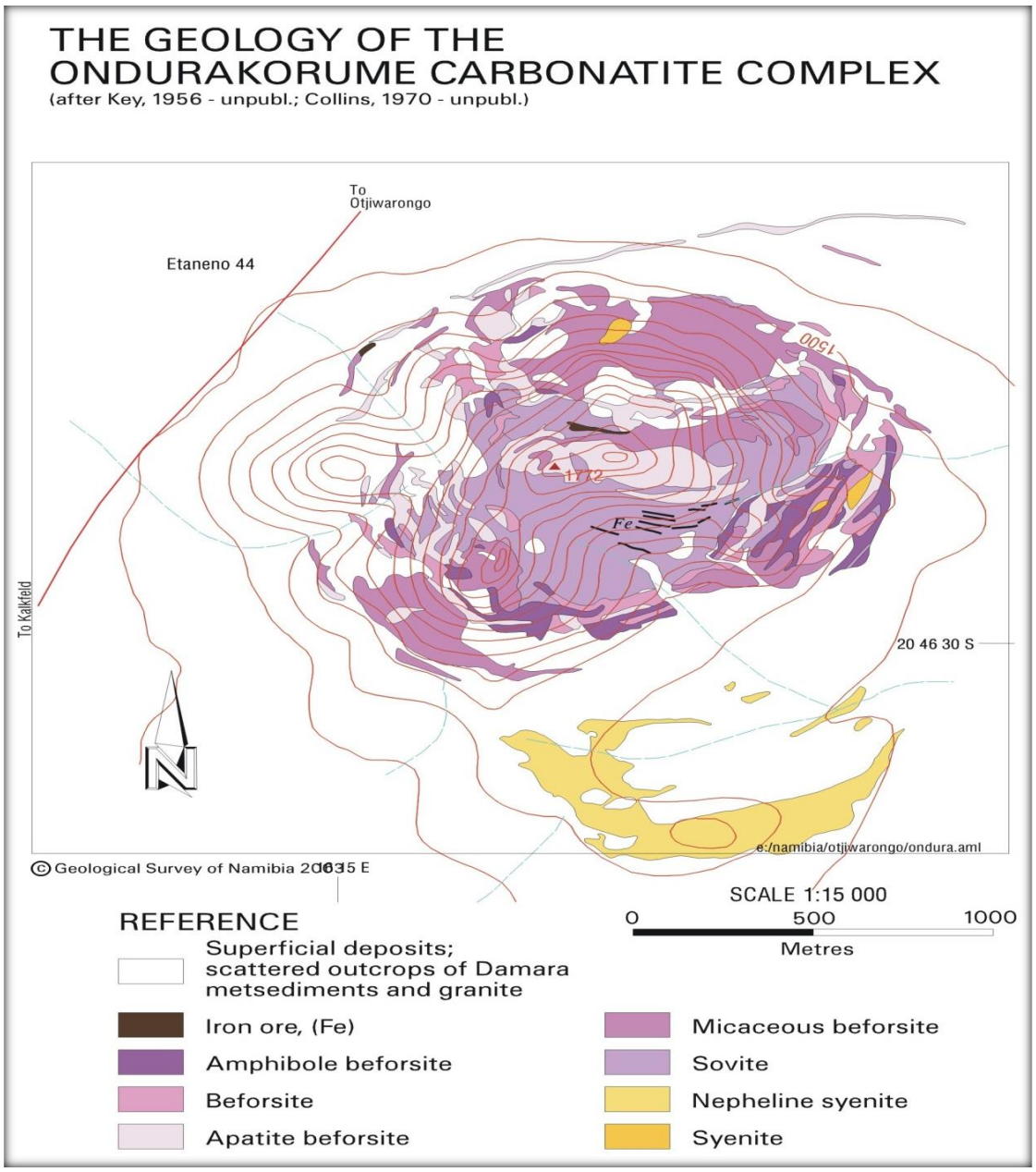

Figure 3.9 The geology of Ondurakorume carbonatite complex. Source: unpublished data from Key (1976) and Collins (1970)

3.6.3. Kalkfeld $20^0$48'S; $16^0$07'E

The Kalkfeld complex about 15 km southwest of Ondurakorume, consists of a carbonatite plug followed outward by incomplete concentric rings of nepheline syenites, syenites and fenite, accompanied by alkaline and sub alkaline dykes (Figure 3.10). Prins (1981) and Verwoerd (1967a) consider associated granites to be part of the country rock.

The complex is approximately 6 km in diameter and the carbonatite is oval with diameters of 2 m and 1.5 km. The carbonatite is a sövite with micaceous and apatite rich

zones. Accessory minerals are chlorite, albite, ankerite, apatite, pyrochlore, monazite, carbocernaite, barite, pyrite, and quartz. A replacement deposit of hematite iron ore with a content of 0.5% ThO_2 occurs in the centre of the carbonatite and was mined in the past (Verwoerd 1967a). Prins (1981) found evidence of a Fe, Mg, Sr, Ba and LREE enrichment trend in the Kalkfeld carbonatites, coupled with a decrease in Nb, Zr and Y (Prins 1981).

Economic importance: The iron ore possesses good fluxing properties and was formerly used in the smelting of the iron poor Tsumeb copper-lead ore. Operations resumed in 1963 (Verwoerd 1967) but are no longer active. Syenite with >12% K_2O and 1% Na_2O and negligible dark minerals could be of interest for ceramics. Verwoerd reported values of 6, 7 wt% P_2O_5 obtained from analysis of the rock yield.

3.6.4. Osongombo $20^0$53'S; $16^0$01'E

This occurrence is somewhat similar to Ondurakorume but much smaller (0.5 km). It differs in the relative importance of breccias (presumed to represent a volcanic level of exposure), which are intruded by beforsite containing radioactive hematite ore (Verwoerd 1993). The beforsite consists of manganiferrous ankerite, apatite, quartzite, feldspar, pyrochlore, rutile, calcite, and baryte (Verwoerd 1993). Prins (1981) also analysed sövite from Osongombo and found that it is depleted in Sr, compared to the associated iron ore, but enriched in Nb, Zr, La, Ce, Nd and Y.

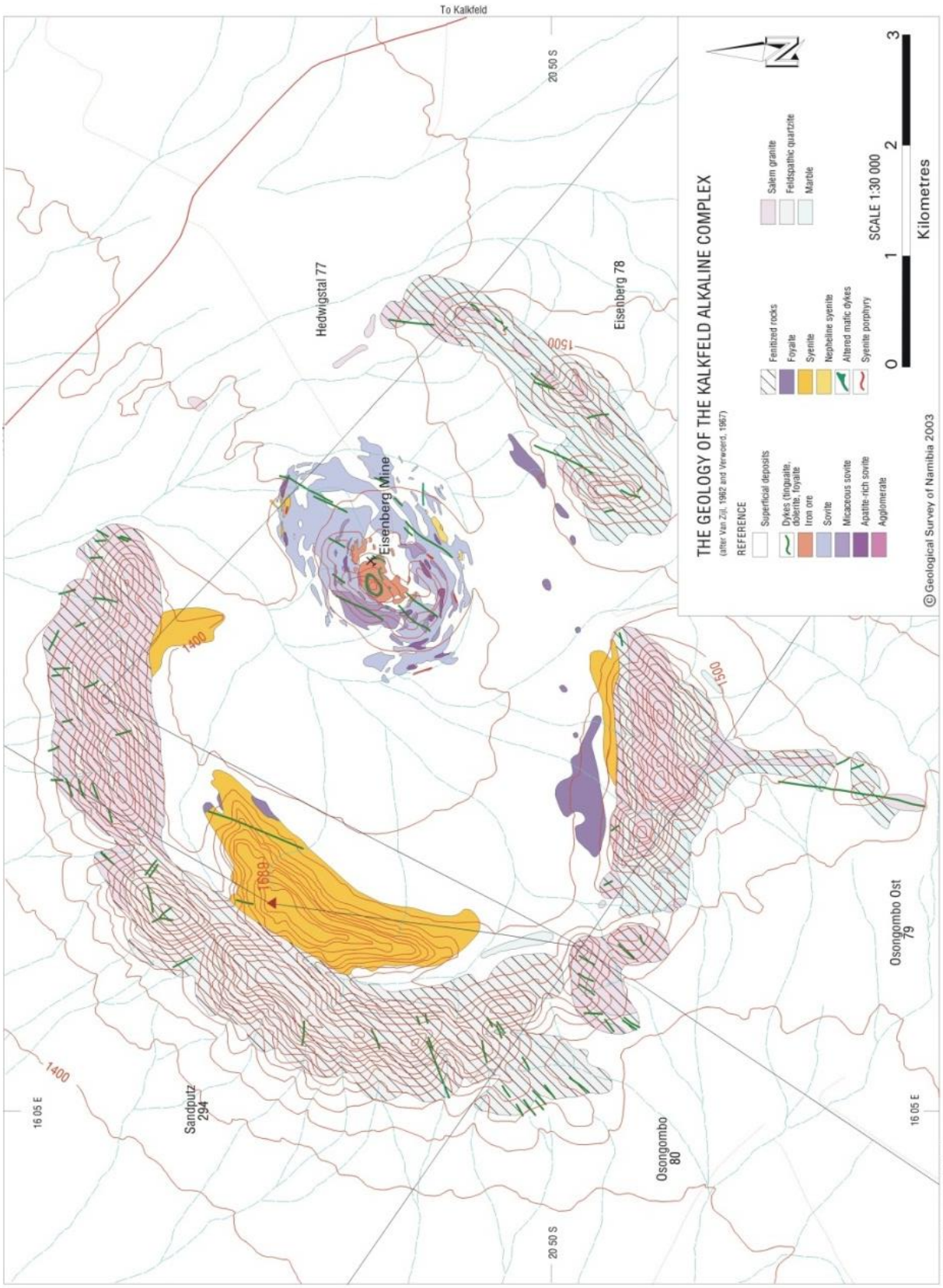

Figure 3.10 The geology of the Kalkfeld alkaline complex (Geological Survey of Namibia 2003).

Economic importance: The Osongombo complex shows a predominance of the mid-REE (Sm, Eu and Tb). Other element such as Th, Mn, Sr and Fe are also noted (Japan International Cooperation Agency- Metal Mining Agency of Japan 1995).

3.6.5. Kwaggaspan $20^0$46'S; $15^0$15'E

Kwaggaspan is located at approximately 90 km west of Kalkfeld and 7 km northeast of Omanzongaku in Khorixas district. It consists of several small plugs and associated calcite veins aligned along 1.3 km long gently curving east-west oriented breccia zone in Kuiseb schist Verwoerd (1993). The largest plug has a diameter of 150 m; it is mainly sövite associated with hematite. The carbonatite is assumed to be post Karoo age (Miller 1980).

Economic importance: A small high-grade hematite ore body of about 10m in diameter (Miller 1980) occurs near the northwestern edge of the calciocarbonatite plug.

3.6.6. Karingarub $28^0$5'S; $16^0$11'E

Not much is known about the carbonatite at this locality in the southern Namib, approximately 40 km northeast of Oranjemund Verwoerd (1993). Its age is uncertain but it may be linked to the carbonatite at Chameis 90 km distant. New geophysical data by the Geological survey 2009 clearly outline the intrusion line and indicate a good radiometric response along the existing geological structures.

Economic importance: The economic potential of this carbonatite has not been evaluated.

3.6.7. Chameis $27^0$56'S; $15^0$43'E

Chameis (spelling adapted from the 1:1000 000 geological map of SWA/Namibia, 1980) was described by Verwoerd (1967a) as a minor plug 100 m long and 50 m wide, 100 km northwest of Oranjemund. It is clearly intrusive in schist of the Gariep complex, but differs from Tertiary carbonatites of the Lüderitz area in composition and texture. It is therefore tentatively grouped with the great foyaite massif of the southern Namib called Granitberg (dated 133 ± 2 Ma, Reid et al. 1990) and with the early Cretaceous carbonatites of Damaraland. It is magnesio-carbonatite with a miarolitic texture containing quartz, perthite, pyrite, zircon, rutile, amphibole and biotite as accessories Verwoerd (1993).

Economic importance: The economic potential of this carbonatite has not been evaluated.

3.7. Carbonatites of Late Cretaceous to Early Tertiary age (70 – 40 Ma)

3.7.1 Gross Brukkaros $25^0$52'S; $17^0$50'E

Brukkaros Mountain is a prominent landmark 83 km north northwest of Keetmanshoop, Namibia. Its 3 km wide crater-like aspect is the result of differential erosion, but geological investigations have shown that it was undoubtedly formed by explosive eruption Janse (1969), Stachel (1995). The absence of igneous material among the ejecta is striking. The best estimate of age is 77 +_ 2 Ma based on K-Ar data obtained from mica in the closely associated monticellite-bearing peridotite at Blue hills (Reid et al. 1990).

Brukkaros was described as a carbonatite volcano by Janse (1969) and as a kimberlite carbonatite volcano by Ferguson et al. (1975a). The link with carbonatite is rather indirect: it rests on 1) numerous narrow carbonatite (beforsite) dykes that radiate from the mountain for distance of a least 90 km; 2) about 45 breccia filled satellite vents with carbonate matrix, sometimes closely associated with the dykes; 3) chemical and petrographic evidence of fenitisation effects in the micro breccias and tuffs of the central crater; 4) late composite veins of dolomite, calcite, quartz, and baryte in these sediments and 5) the updoming and eventual rupturing of the surrounding strata which are indicative of a volatile-rich magma. The postulated relationship with the kimberlite is equally tenuous. It is supported by 1) the Gibeon swarm of non-diamondiferous kimberlites and other ultramafic intrusion in the same general area and of the same age Reid et al., (1990); 2) pseudomorphic textures indicating that at least some of the radial dykes are carbonatised lamprophyres rather than carbonatites and 3) enrichment of trace elements characteristic of both ultramafic and highly evolved magmas, in both micro breccias and dyke rocks, as well as in kimberlite. The conclusion seems justified that mantle derived volatile-rich magmas shaped the late Cretaceous magmatism in this tectonic environment at the craton margin, controlling both carbonatites and kimberlites.

Economic importance: The economic potential of this carbonatite has not been evaluated.

3.7.2. Dicker Willem

Ijolites show only half the LREE concentrations of the nepheline sövite (206–269 C1), and have lower LREE enrichment, with La/Yb_n ranging from 4 to 24.

Dicker Willem is a 5 km sub volcanic intrusion complex (Figure 3.11 and 3.12) of Eocene age (49 Ma. It consists of rock types ranging from early nepheline sövite through sövite and dolomite alvikite to late-stage ferroan carbonatites.

Early sövite forms a 2.5 km long diameter concentric intrusion with inclusions of banded alvikite that contains magnetite, apatite and pyrochlore (up to 60 m long segregations); fragments with wollastonite; alvikite with magnetite, pyrochlore and Fe-Mn-dolomite.

Late stage carbonates represent recrystallised carbonatites in equilibrium with low-temperature (<100C) fluids (Reid and Cooper 2002).

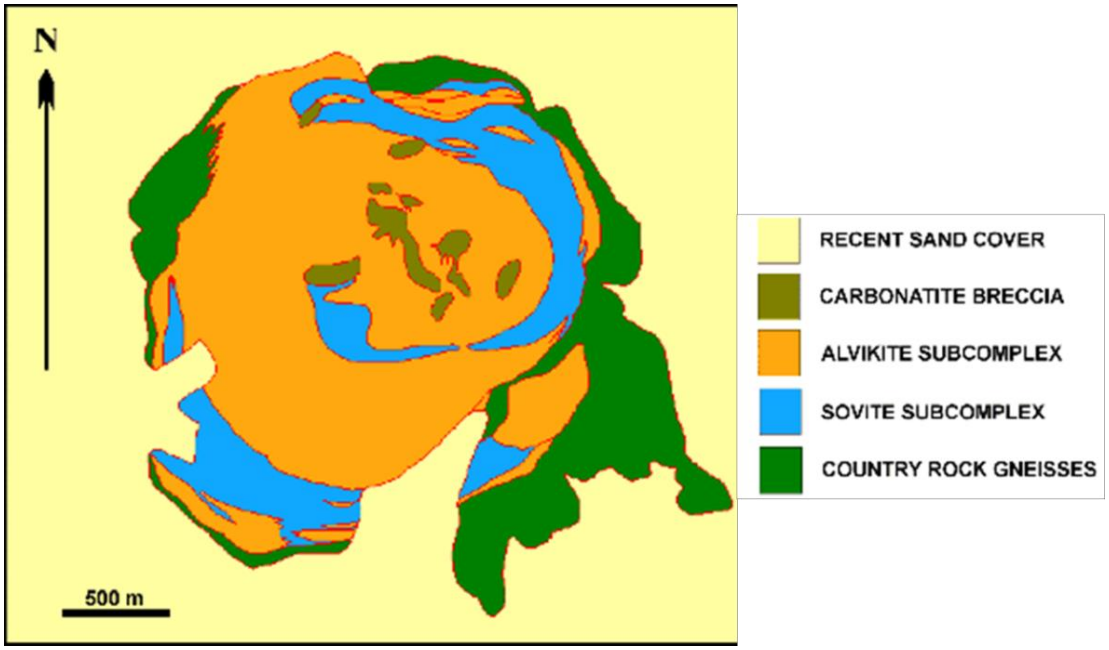

Figure 3.11 Geological map of Dicker Willem Reid et al., (1990)

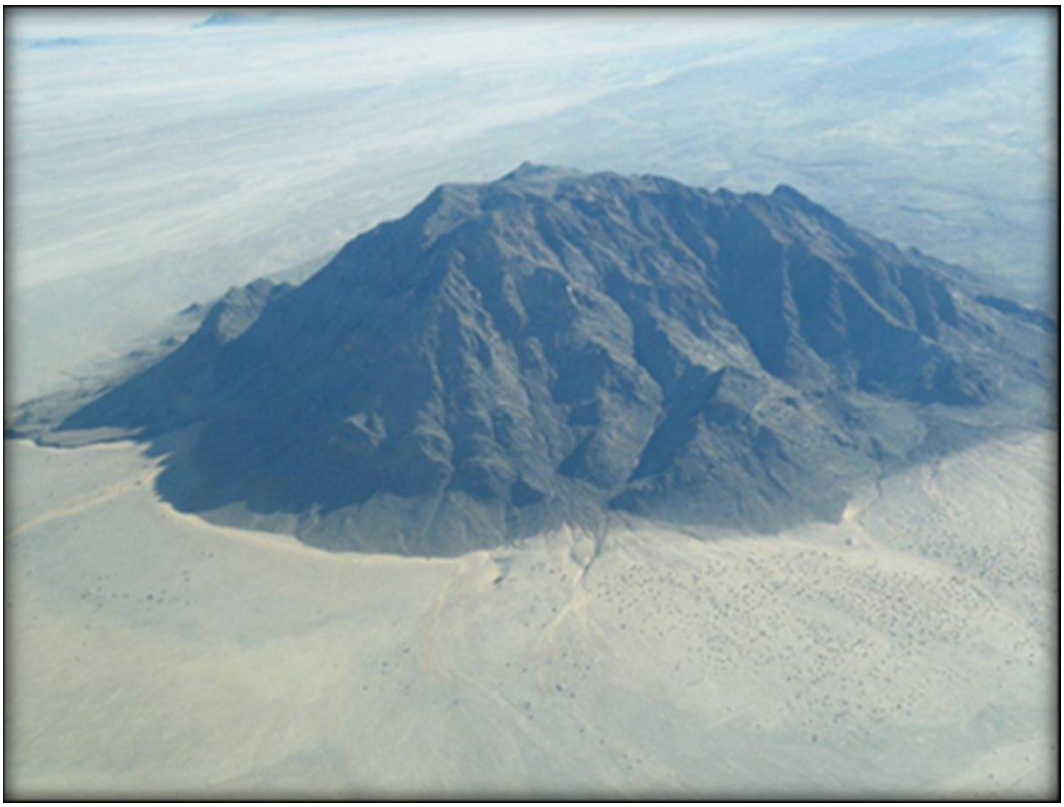

Figure 3.12 Aerial view of the Dicker Willem alkaline complex outcrop (photo by Ljung 2010).

Nepheline sövite show both the lowest absolute concentrations of REE, and the least degree of LREE enrichment. La/Ybn values for nepheline sövite range 29 to 50 (La is 564–607 times C1), compared with values of 84–172 for dolomite alvikite and more evolved beforsite and late-stage carbonatites. Ijolites show only half the LREE concentrations of the nepheline sövite (206–269 C1), and have lower LREE enrichment, with La/Ybn ranging from 4 to 24.

Economic importance: Low values of REE are reported however, the outcrop is large enough so that it would be likely to have sufficient tonnage of any particular ore deposit that was found (Cooper and Reid 1998). Sample collected during this study indicate high values of P_2O_5 up 2 wt % and REE content up to 4 wt %.

3.7.3. Hatzium

The Hatzium dome almost 100 km to the North of Brukkaros has been interpreted as a closely related to Brukkaros crypto-volcanic structure 2.4 km in diameter (Heath and Toerien, 1962). Numerous small plugs and dykes of kimberlitic and carbonatitic affinity are known in the area. Consolidated Diamond Mines Ltd drilled some boreholes here prior to 1988 but no further details are available; the core was stored at Kimberley.

Economic importance: The economic potential of this carbonatite has not been evaluated.

3.7.4. Grunau $26^0$05'S; $18^0$00'E

According to Schreuder (1975) an oval-shaped pipe and two sinuous dykes of carbonatite were encountered in farm Grunau 16 in Southern Namibia by G. Genis during a regional survey. They are 30 m in diameter and consist of country rock fragments in a weathered matrix of calcite, apatite, and limonite Verwoerd (1993). The dykes emanate from the pipe and extend for about 120 m to the southwest and northeast. This occurrence is not related to the northeast because it is post Karoo in age: the carbonatite intruded tillite, boulder shale, and limestone of the Dwyka Formation. A correlation with Brukkaros or Salpeterkop seems most likely (Schreuder 1975).

Economic importance: The economic potential of this carbonatite has not been evaluated.

3.7.5. Bokiesbank $28^0$30'S; $19^0$40'E

Haughton and Frommurze mentioned in an unpublished report at GSN in 1936 the existence of thin limestone veins, sometimes composite, cutting across the gneisses and amphibolites on the farms Blydeverwacht 72, Hogeis 83 and Bokiesbank Ost 79 in the Warmbad district, southern Namibia. At the latter locality the veins are folded and

sometimes broken by minor faulting. They are generally fine-grained but occasionally a coarse grain size was seen Verwoerd (1993). Here these are fine grained, they weather to a rusty brown, but the coarse-grained varieties remain grey. The veins are sometimes zoned, the central portion containing inclusions of angular feldspar, quartz, mica, and galena fragments. On either side are narrow pegmatites with brick red feldspar. A thin section shows set in a matrix of granular calcite, abundant large and small prisms of apatite, fragments of strained orthoclase showing secondary twinning, and a little limonite.

Elsewhere in the Warmbad district these authors described marble with garnet, quartz, and apatite and iron ores. Verwoerd (1967) thought that, except for the folding, the brown weathered veins resembled the ankeritic beforsite dyke of Brukkaros, but he never had the opportunity of visiting the locality. It was designated as a possible carbonatite.

The existence of carbonatite dykes and dykelets at Bokiesbank has since been confirmed. Early in 1993 Dr. M.D Mcmillan submitted a suite of samples including ankeritic beforsite from three 45 cm dykes near Ariamsvlei road on Bokiesbank. Under the microscope the rock shows many of the features previously described in the Brukkaros dykes; pseudomorphs after olivine and biotite, scattered crystals of perovskite and magnetite, xenocrysts of K-feldspar and quartz, and chlorite intergrowth with quartz and fluorite. Major and trace elements analyses leave little doubt that the rock is a carbonatite (1810 ppm Sr, 328 Ce, 223 ppm Zr, and 196 ppm Nb) but it is enriched in the ultramafic indicator elements (281 ppm Cr and 206 ppm Ni) (Verwoerd 1993).

In the vicinity of these dykes there are outcrops of granite and gneiss impregnated with calcite having no geochemical affinities with carbonatite. The analysed specimen consist of 42% calcite, 33% albite (neglecting minimal anorthosite), and 25% orthoclase with no quartz. From their description, Haughton and Frommurze (1936) obviously confused the two types of carbonate rock. The origin of the calcite feldspar rock is problematic.

It must be concluded that there is likely to be an undiscovered volcanic centre of similar type to Brukkaros dykes extending for 300 km southwards almost as far as the Orange River (Verwoerd 1993).

Economic importance: The economic potential of this carbonatite has not been evaluated.

3.7.6 Keishohe $26^0$35'S; $15^0$53'E

In an area of 1.3 x 0.6 km there are low scattered outcrops of brown weathering dolomite carbonatite. Several shallow-dipping sills up to 2 m thick are cut by thin beforsite dykes that trend towards Dicker Willem 20 km to the North East (Verwoerd 1993).

Economic importance: The economic potential of this carbonatite has not been evaluated. Samples collected during this study indicate an elevated amount of LREE and MREE.

3.7.7 Kaukasib $26^0$54'S; $15^0$34'E

This occurrence comprises a low hill 150 m in diameter strewn with lateritic talus and a few outcrops of ferruginous silicified carbonatite. There are probably a few minor beforsite dykes (Verwoerd 1993)

Economic importance: The economic potential of this carbonatite has not been evaluated.

3.7.8 Teufelkuppe $26^0$54'S; $15^0$34'E

The Teufelkuppe carbonatite is a roughly circular group of hills, 1 km in diameter and 120 m height, in the Diamond Area No. 1, Southern Namibia. The carbonatite intruded biotite schists and amphibolites of the Namaqualand Metamorphic Complex (Verwoerd 1993). The carbonatite consist of principally medium to fine grained calciocarbonatite (alvikite). High Sr concentrations have been reported, and magnetite and apatite occur as minor minerals.

Economic importance: The economic potential of this carbonatite has not been evaluated.

Chapter 4: Methodology

This chapter describes the methods used during the field and analytical studies. The list of samples collected by the author and used in this study are included (Appendix 1), the samples collected by Etruscan and Namibia Rare Earth (Pty) Ltd (NRE) and used in this study are listed (Appendix 2).

4.1 Field methods

4.1.1 Mapping

Mapping the area constituted the first phase of the field work that started in 2003 and continued to 2010 (Table 1). Mapping was done by noting outcrops and recording their coordinates. At the same time rocks representing different lithologies, textures and colours were collected for further analysis. About 3000 sampling points are indicated in Fig 5.1 and their analytical results attached as appendix.

A hand held gamma ray counter spectrometer was used for recording radiometric response of rocks, mainly the carbonatites. Mapping of the alkaline dykes and plugs required advanced remote sensing methods (Hyperspectral Survey) for the purpose of enhancing mapping and understanding the distribution of alkaline rocks in the study area, defining the extension of the intrusions and regional trends.

Integrated data sets of methods were used such as the radiometrical geophysical survey maps, existing geological maps, Landsat images and hyperspectral survey in order to interpret structures and geological regional settings (Figure 5.1). Later verification by ground truthing of the remote sensing methods used was carried out. Field documentation and reconstruction of regional geological setting of the area around Lofdal comprise author's observations and the published literature. The Lofdal carbonatite complex was remapped and resampled in order to establish the regional settings and the tectonic deformations in the area. Namibia Rare Earth contributed to the understanding of the geology of the area through detailed mapping of the exploration area.

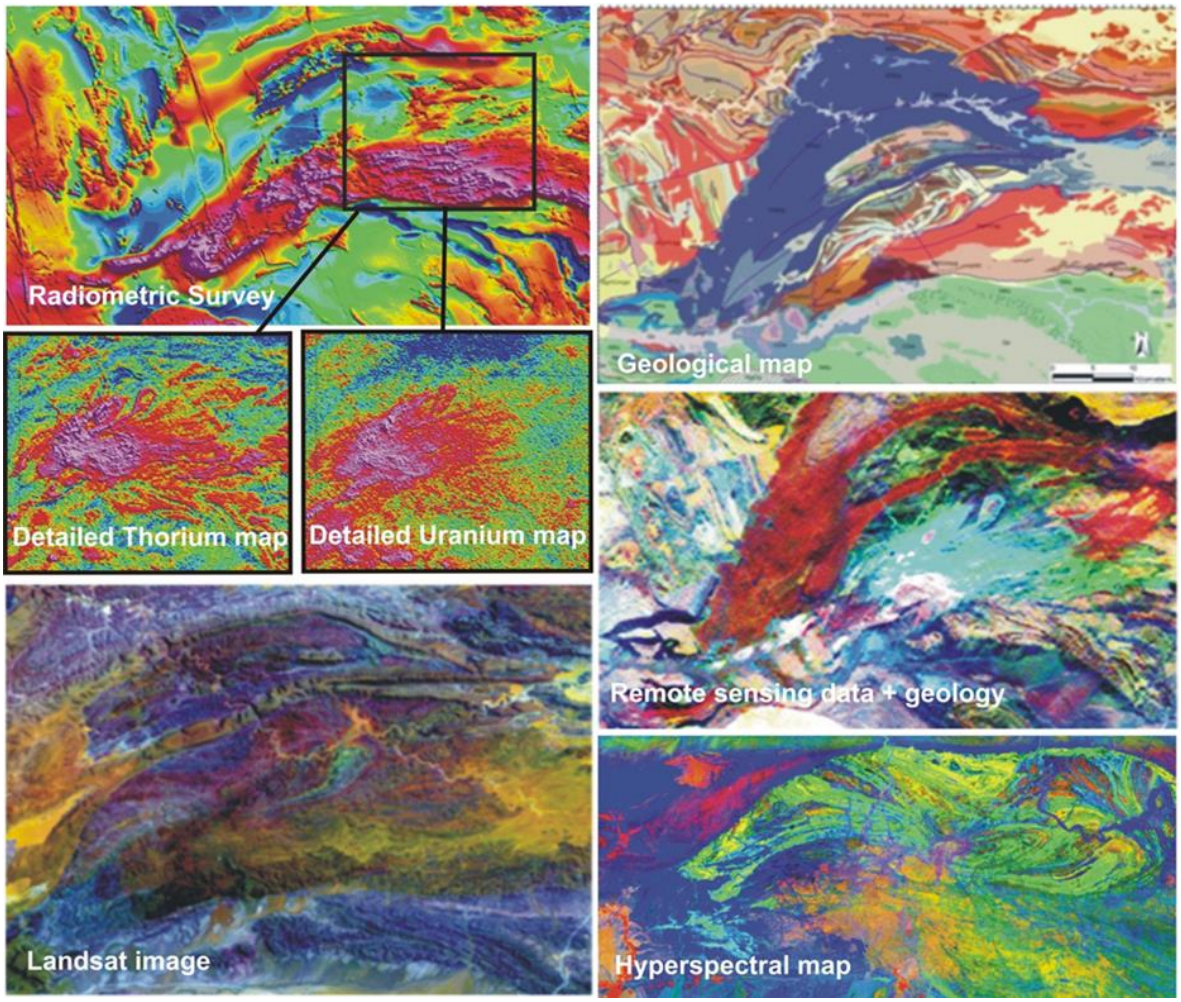

Figure 4.1 Integration of data used for the mapping at Lofdal. Landsat image and the hyperspectral analysis were useful in highlighting regional deformation.

Table 4.1 Field Mapping from year 2003 to 2010

2001	Reconnaissance and introduction to Lofdal by Dr. A. Mariano
2002 - 2003	• Field mapping and sample collection based on carbonatite and alkalic rocks lithologies VNP 1 to VNP 140. • Traverses mapping of the newly discovered main calcite carbonatite plug Measuring of radiometric response of different rocks in the area total counts
2004 - 2005	• Preparation of thin sections for petrographic studies. • Microscopic studies of the samples collected (transmitted and reflected light microscopy). • 207 samples analysed using, X-ray fluorescence (XRF) for whole-rock major and trace element analyses at the GSN. • X-ray diffraction for mineral identification • 35 samples analysed using cathodoluminescence and scanning electron microscope, electron-microprobe analysis (EPMA) for mineral analysis (NHM, London), inductively-coupled-plasma mass-spectrometry (LA-ICP-MS) for trace-element and REE analysis (NHM, London). • Laser-ablation inductively-coupled-plasma mass-spectrometry (LA-ICP-MS), geochronology, trace element and REE analyses of minerals (NHM, London).
2006	• More sampling from areas not sampled during 2002 – 2003 sampling Programme. Sampled VNP 140 to VNP 320. • 6 dated using the K-Ar method in Hungary
2007	• Commissioning of a hyperspectral survey of the area by GSN, to determine the extension of alkaline intrusion at Lofdal. Follow up sampling based on the new data obtained. • Ground truthing and field mapping based on hyperspectral data. • Mapping: extent of intrusion to the west and south and spatial distribution of dykes and indications for stratification of intrusion (syenite, carbonatites)
2008 - 2010	• Detailed mapping and selective sampling of the representative carbonatite samples based on their REE geochemical patterns. • analysis of strategically important samples based on REE trends (major, minor elements, REE) using Electron-microprobe analysis (EPMA) for mineral analysis (BGR, Germany), Inductively-coupled-plasma mass-spectrometry (LA-ICP-MS) for trace-element and REE analysis (BGR, Germany),Laser-ablation inductively-coupled-plasma mass-spectrometry (LA-ICP-MS), geochronology, trace element and REE analyses of minerals (BGR and Birkbeck College, London). • Differentiate carbonatite types (REE bound to oxidised varieties or metasomatism)

Ground magnetic and radiometric surveys were carried out by the Geological Survey of Namibia and also later by Etruscan. Field mapping results are indicated in the geological map (Fig 7.8).

Modification has been made as a result of this mapping in an effort to improve the boundaries of the units and also by revising units that were incorrectly presented.

4.1.2 Ground Geophysics methods

A handheld Gamma Surveyor spectrometer (Gf instruments, s.r.o) was used for recording radiometric response of the rocks; mainly the carbonatites. Gamma surveyor is a group of multi-channel gamma-ray spectrometer designed for measurements of Natural and artificial radioisotope in ground, boreholes and laboratories. It is used for searching radiation sources, dose rate and measurable gamma-ray spectra and determination of concentrations of elements (especially K, U and Th). The results are available in the appendix 3. The interpretation of the results is discussed along with the petrography of the dykes. The main purpose of the ground geophysics survey was to identify carbonatite dykes with high radiometric values as these were initially considered to be rich in heavy rare earth elements associated with thorium.

4.1.3 Hyperspectral Airborne methods

The hyperspectral airborne survey method is based on the principle that the earth's surface reflects light in a characteristic pattern; the manner in which light of different wavelengths is reflected or absorbed from each material is known as its reflectance spectrum. Many minerals show specific absorption features in the visible and infrared wavelengths, which can be used as a diagnostic tool to identify and map these mineral and chemical variations. (Goetz et al. 1985, Lang et al. 1987, Pieters and Mustard 1988, Kruse 1988, Kruse et al. 1993a, Crowley 1993, Boardman and Kruse 1994, Clark et al. 1996, Boardman and Huntington 1996, Crowley and Zimbelman 1996). Imaging spectrometers or "Hyperspectral Sensors" collect unique data that are both a set of spatially contiguous spectra and a set of spectrally contiguous images (Goetz et al. 1985).

The Geological Survey of Namibia (GSN) in 2008 contracted an Australian company, Hyvista Corporation (PTY) Ltd, to acquire hyperspectral data in order to delineate areas of carbonatite plugs and dykes intrusions, define regional geological structures and interpretation of such data. Image and data processing was carried out on satellite and airborne imagery as well as supplementary information provided through a training course by Dr. Ingrid Stengel (NamibGeoVista GeoConsult & Imaging) to distinguish signals from carbonatite and phonolite dykes. Below is the explanation of the spectrum and the processing method used.

4.1.3.1 Hyperspectral spectrum and processing methods for the surveys at Lofdal alkaline complex

The hyperspectral data is processed up to level three and is used in conjunction with other data for mapping and interpretation purposes.

Level 1 a / pre-processing of data and calibrations

The HyMap scanner data is collected and stored on a DLT flight tape and converted to ENVI-compatible image files (16-bit integer, BIL data file with an ASCII header file) during pre-processing of the data, The HyMap stores the intensity of light reflected from the surface of the earth as digital numbers (DN). The intensity recorded is the net effect of the wavelength-dependent atmospheric absorption and scattering, solar irradiance, light scattered back from the earth surface, and background voltages from the scanner electronics. Pre-processing involves two corrections:

1. Dark Current Subtraction to removes the "zero light" spectrum in all image pixels and

2. Calibration – Radiometric, Spectral and Scaling. The scanner is calibrated using a standard light source so the response of each detector is known. Every pixel of each band has been scaled by this band constant and a multiplier has been applied so that the data is stored as a 16-bit integer. When the pre-processing corrections described above have been applied, the data are in radiance units of microwatts/cm2/steradian/nm before the multiplier of 1000 is applied to convert it to a 16-bit integer.

Level 1 b – atmospheric, cross track and geometric correction

1. Atmospheric Correction

The data has been processed using the HyCorr program that determines a model of a subset of atmospheric properties that are appropriate for the time (UTC), date, latitude/longitude and acquisition height (AGL) for HyMap data that has been radiance corrected. The output of HyCorr is an apparent surface reflectance image from which spectra can be compared to relative reflectance library spectra.

2. Cross Track Correction and Strip Levelling

Prior to geometric correction each strip is processed to remove the effect of bi-directional reflectance that results from non-uniform illumination across the image when the azimuth is to the side of the flight line. The levelling correction adjusts each data strip to the same data ranges. These corrections improve processing and ensure that the final mosaic images are seamless.

3. Geometric Correction

Variations in the aircraft orientation, speed and altitude during image acquisition result in spatial distortions of the images, even though the scanner is mounted in a tri-axial, gyro-stabilised platform that compensates for some of these motion effects. An IMU/GPS unit is attached to the scanner and it provides data that can be used to remove these distortions which would otherwise result in positional errors of several hundred metres. Using these data with the appropriate software permits geo-correction to be completed without the need for control point picking and, depending on terrain variation; this can reduce positional errors to below 20m.

Software developed by HyVista is used for to produce a ray traced image (.glt) file from combining the output from the IMU/GPS with a DEM (SRTM 90m image). The glt file is then used to georectify the image products produced to the UTM/WGS84 map projection using proprietary HyVista software.

Level 1c product – mosaices and data cubes

In this survey the cross track corrected and levelled reflectance data have been mosaiced into data cubes for the SWIR and VNIR bands. This data cube image has then been masked to eliminate and reduce pixels that contain predominately shadow, green/dry vegetation and water. This masked image is used as the input for Level 2/3 processing, apart from the production of the overview colour composite images.

Level 2 processing - standard colour composites, decorrelation stretch index images and mnf transform

1. Overview Colour Composite Mosaics and Standard Colour Composites

Three colour composite images are produced from the reflectance data consisting of:

Landsat TM 741 equivalent: RGB = 2.208um/0.851um/0.488um (HyMap bands 109, 28, 03 respectively)

False Colour: RGB =0.851um/0.664um/0.488um (HyMap bands 28, 15, 03 respectively)

True Colour: RGB=0.664um/0.577um/0.488um (HyMap bands 15, 09, 03 respectively)

The contrast in these colour composites has been enhanced by applying a combination of interactive ENVI stretches (square root, linear 2%, Gaussian, equalize) to the images.

2. Decorrelation Stretch (DCS) Colour Composites

The SWIR bands 115 (2.30um), 109(2.191um) and VNIR band 30(0.87) are combined into an RGB colour composite image and the ENVI de-correlation stretch function applied to it. The resultant image maps the distribution of mineral classes that absorb at these wavelengths i.e. Mg-OH/Carbonates, Al-OH, and Iron Oxides respectively.

However, since it is absorption features being mapped the resultant colours are confusing, for example Mg-OH absorptions (displayed as red) are mapped as not red. However, by taking the negative of the bands (i.e. inverting the RGB colour image planes) an image results in which:

Red = Mg-OH/CO3 bearing minerals (including - Amphibole, talc, chlorite, calcite, dolomite)

Green = Al-OH bearing minerals (including - White mica, kaolinite, montmorillonite)

Blue = FeOx bearing minerals (including - hematite, goethite, Jarosite, siderite).

Hence areas of argillic alteration are green in this image, where they co-occur with iron they will by cyan.

3. Index Images

By calculating the depths of the absorption features at specific wavelengths it is possible to produce images that show the overall abundance of groups of minerals that have a primary absorption feature at the specified wavelength. In this case the band depths for seven (7) SWIR absorption features have been mapped to show the distribution of:

2.173um - Argillic (alunite, pyrophyllite, dickite, ordered kaolinite)

2.190um - AlOH-2189 (kaolinite, aluminium rich white mica (paragonite / illite), Al-smectite)

2.204um - AlOH-2204 (kaolinite, white mica (sericite / muscovite / illite) Al-smectite)

2.219um - AlOH-2219 (aluminium poor white mica (sericite / phengite / Illite), Al-smectite)

2.2246um – FeOH-2246(nontronite, chlorite, Fe / Mg smectite)

2.259um – FeOH-2259 (jarosite, nontronite, chlorite, Fe / Mg smectite

2.305um – MgOH (MgOH minerals and MgCO3: actinolite / talc / dolomite)

2.326um - CaCO3 (Calcite and biotite / chlorite)

0.87um – FeOX-Hematite

0.89um – FeOX Goethite

These images are termed Index Images and have been produced as greyscale, grey scale rainbow coloured images, and combined into RGB colour composites.

4. MNF Transform

An MNF transform has been applied to the SWIR bands and from this images colour composites have been produced. The bands selected show the greatest variation is surface materials producing images that highlight geological and regolith variation within the area.

Level 3 processing – minerals mapping

Hyperspectral remote sensing is essentially a mineral mapping technology. Its fundamental principles are based on spectroscopy, so an understanding of the spectral signatures of surface materials is required for its application. Briefly, each pixel of a hyperspectral image contains a spectrum which forms the basis for determining the materials present in a scene. Surface mineralogy and other components are mapped using algorithms which either de-convolve a scene into component end-member signatures (unsupervised un-mixing) or specifically target spectral signatures of known materials (supervised match filtering). A combination of these approaches has been applied in the project. The Fugro NPA study involved several stages from a regional Landsat ETM image interpretation of the Lofdal Carbonatite Complex to a more detailed interpretation of hyperspectral data.

The applied method includes the following steps:

- Landsat ETM+ (15m resolution, Pan-sharpened) – regional geological assessment.
- ASTER (15m spatial/30m spectral resolution) – geological information assessment and field truthing of analysed information. Hymap airborne hyperspectral survey (4-6m resolution) – detailed mineralogical mapping.
- Airborne aeromagnetic and radiometric–supplementary information for integration and analysis. Results from field-sampling campaigns – supplementary information for integration and analysis.

4.1.4 Sampling

The sampling rationale was at first based on lithologies of different intrusive rock types at Lofdal. Later these rock types and a large number of samples from Etruscan (Fig 4.2) were used for setting up different types of carbonatites at Lofdal. Prudent sample selection based on the geochemical distribution of elements in the carbonatites enabled further sampling to have a representative sample of each group well studied in detail.

Chemically investigating the composition of carbonatite dykes that are less than 0.5 m is problematic. Country rock inclusions and xenoliths that were not fully resorbed in the carbonatite give variable composition made of carbonatite melt and the silicate xenoliths. The rocks referred here as ‘others’ are those containing less than 50 wt% $CaCO_3$ too low to be classified as a carbonatite, and also high amounts of silica and a high loss on ignition. A large number of 3250 rock grab samples were collected by

Etruscan and Namibia Rare Earth (Pty) Ltd (NRE), and analysed. They form part of database processed for this study. The chronologies of the investigation around the Lofdal is described.

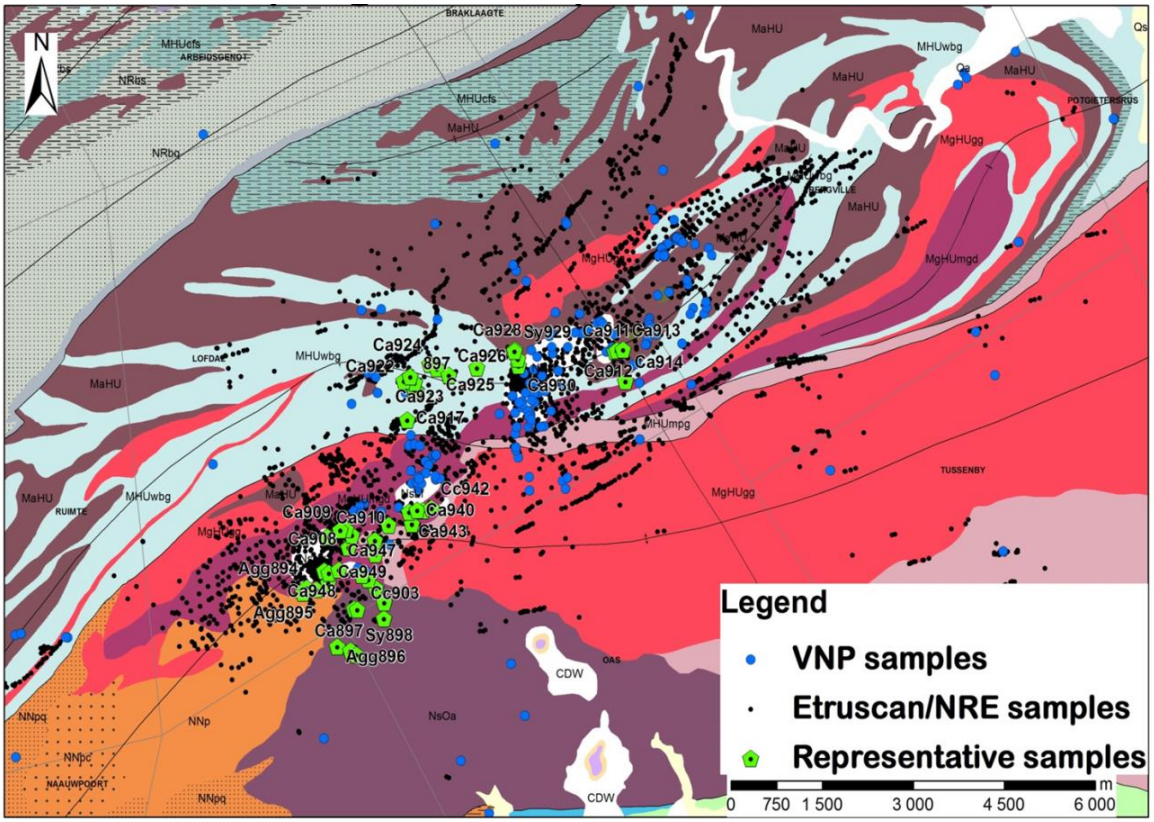

Figure 4.2 Simplified Geological map of the Lofdal area after GSN (2008) indicating different sample locations.

4.1.5 Selection of samples for whole rock analysis

Some data presented in this research were collected during the field mapping program conducted between 2002 and 2010. A large portion of data also presented was obtained from Etruscan and later Namibia Rare Earth (NRE) (Pty) Ltd., who is the mineral right holder of the study area at the time of carrying out this research work. A total number of 3250 samples were used for this study. Plotting the large data set from NRE and those collected by the author allowed identifying nine (9) REE patterns. Judicious sample selection based on the geochemical distribution of elements in the carbonatites enabled further sampling to have a representative of each group well studied in detail.

Resampling was based on geochemical characteristics and detailed studies were done on dykes that showed the following characteristics:

(i) > 5% TREE+Y,

(ii) High REE contents with HREE=LREE and

(iii) HREE>>LREE

The rationale for this approach was to understand the mineralogy of those representative samples which significantly contributed to the understanding of the geochemical and mineralisation processes of the Lofdal carbonatite deposit. In total 12 representative samples were studied in detail.

4.2 Analytical techniques

4.2.1 Optical petrography and Cathodoluminescence (CL)

Preliminary mineralogical and textural analysis of the syenites and phonolite samples was determined using transmitted- and reflected-light microscopy. For the carbonatite using transmitted- and reflected-light microscopy was not possible due to small mineral grain sizes and the intense iron stains of the calcite carbonatite samples which impeded visibility of the rock/mineral textures. Thus, mineralogical and textural analysis of Lofdal carbonatites was determined using mainly cathodoluminescence microscopy and backscattered electron imaging coupled with electron microprobe analyses.

Cathodoluminescence (CL) imagery was carried out on a CITL MKIV cold cathodoluminescence system at 13 kV and 300 mA at the Natural History Museum, London.

CL spectrometry was carried out using the Simon-Neuser's "hot-cathodoluminescence-microscope" HC2-LM (Neuser et al. 1995) at the Geowissenschaftliches Zentrum Göttingen, Germany. The acceleration voltage was 14 keV and the filament current 0.18 mA. CL spectra were recorded with a triple-grating (100, 1200, and 1800 lines/mm^{-1}) spectrograph TRIAX 320 equipped with a liquid N_2-cooled charge coupled device (CCD) camera. The 100-lines/mm^{-1} grating was used to detect the emitted spectra between 400 and 900 nm. The integration time of spectrum acquisition was 20 s for fluorite, 60 s for apatite and 120 s for xenotime-(Y) and zircon. The spectra are not corrected for detector response. Therefore, the spectra are suppressed in the regions 400-450 nm and 600-900 nm. For collecting the CL signal the 32x objective was chosen for fluorite and 50 x objectives for apatite, xenotime-(Y) and zircon. The diameter of the sample area from which the CL signal was collected, was about 500 µm for fluorite and 300 µm for the three other minerals. Therefore, the collected spectra represent an average CL signal of the fine-scale oscillatory zoned minerals (apatite, xenotime-(Y), and zircon). Cathodoluminescence spectrometry provides information about emission centres and their spatial distribution of minerals. The recorded CL spectra are from fluorite, apatite, xenotime-(Y) and zircon.

4.2.2 X-ray Fluorescence analysis (XRF)

Representative rock samples were reduced to fine powder using a jaw crusher (with hardened steel plates); later with a rotary pulverizer with ceramic plates, and final reduction was done by hand grinding in an agate mortar. Major elements were determined using (XRF) analysis of fused beads using standard techniques, while trace elements were determined by XRF on pressed powders, all at the GSN using a wave length depressive XRF spectrometer Philips 2404. The software used is SuperQ and SemiQ. The standards and blanks were run after every 10 samples.

4.2.3 ICP-AES

Whole rock analyses were carried out by the analytical laboratory at the Natural History Museum, London, using lithium metaborate fusion dissolved in platinum crucibles plus ICP-AES in a Varian VISTA PRO instrument for major elements and HF/HClO4 dissolution plus ICP-AES and ICP-MS on a Varian 810 instrument for trace elements. F and Cl were analysed by pyrohyrdrolysis and ion chromatography, FeO was determined by titration and H_2O, C and S by elemental analyser. The modal composition of rocks was used for their classification on the basis of the IUGS-approved classification principles (Le Maitre 2002).

4.2.4 Backscattered and secondary electron imaging

Backscattered electron imaging and phase identification was carried out on a Jeol 5900LV equipped with an Oxford Instruments INCA EDS system operated at 20 kV and 2 nA. Some micro textural observations, major-element compositions of rock-forming and accessory minerals from the Lofdal carbonatite complex were made in back-scattered electron images using a Cameca SX-100 electron microprobe at the Bundesanstalt für Geowissenschaften und Rohstoffe (BGR), Hannover, Germany.

4.2.5 Electron Microprobe analyses

Electron microprobe analysis (EMPA) is a micro-analytical technique capable of quantifying mineral chemistry on a micro scale with detection limits generally in the range of 0.01 to 0.05 wt%. Electron microprobe analyses were performed on a Cameca SX50 WDS electron microprobe at the Natural History Museum, London, operated at 20 kV and 20 nA with a PAP φρz matrix correction and empirical corrections for REE interferences (see Williams 1996). A mixture of natural and synthetic standards was used and monazite-(Ce) from Manangoutry, Madagascar (donated by F. Poitrasson) was used as a quality control standard for the REE phosphates. Additional analyses were carried out at Camborne School of Mines, UK using a JEOL JXA-8200 Superprobe and

the BGR, Hannover, Germany using a CAMECA SX100 Electron Probe Microanalyzer. The operating conditions for the electron beam are an accelerating voltage of 15 kV beam currents for carbonates and 20 kV for the silicate minerals. The beam diameter of is 10 microns. Principles of EMPA are provided in Potts et al. (1995). X-ray emissions can be analyzed by wavelength-dispersive spectrometry (WDS) or energy-dispersive spectrometry (EDS), and standardized to natural or synthetic materials of known composition. In the present work, EDS was used for qualitative analysis and mineral identification, and WDS was used for quantitative analysis of selected minerals.

4.2.6 Laser ablation inductively coupled plasma mass spectrometry (LA-ICP-MS)

Laser ablation inductively coupled plasma mass spectrometry (LA-ICP-MS) was used during this study to date fine xenotime-(Y) overgrowths on zircon for the first time. The technique uses high energy laser that ablates a solid mineral sample that is than carried into the plasma through argon gas media. The sample is then ionized for the mass spectrometer analyses.

Polished thin sections about 150μm thick were prepared and studied using the methods described above. The sections were then cleaned using a weak HNO_3 solution, dried and mounted in the cell of a New-Wave Research UP213 UV frequency quintupled Nd: YAG laser operating at 213nm wavelength, linked to a PlasmaQuad 3 quadrupole ICP-MS at the Natural History Museum, London. All LA-ICP-MS analyses were conducted in a He atmosphere, mixed with Ar before arrival at the Ar plasma (Jeffries et al. 2003). In this study, we used zircon geostandard 91500 (Wiedenbeck et al. 1995) to calibrate the Pb/U isotope ratios for age calculation. Unlike for ion microprobe U-Pb analysis, we further demonstrate here that matrix matching is not a strict requirement for U-Pb geochronology by LA-ICP-MS, in agreement with several studies (Horstwood et al. 2003, Smith et al. 2004, Storey et al. 2006) which is particularly pertinent since a homogeneous xenotime-(Y) standard has yet to be characterised (Fletcher et al. 2004). Machine drift was monitored by racketing 12 unknown analyses with 4 standards at the start and end of the run Wall et al. (2008).

Selective minerals were analysed using the Laser Ablation Inductively Coupled Mass Spectrometry (LA ICP MS) to analyse for REE and other trace elements at the Birkbeck College, London. Spot ablation diameter employed was 50 μm. Raw count data for each element was corrected by subtracting the background counts and processed using GLITTER Software. It was also used to calculate the trace element concentrations normalised to chondrite values of Evenson et al. (1978). The minimum detection limits

were at 99% confidence. All values are reported in ppm. Different certified NIST standards were used as internal standards. Calcium as internal standard was used for the analyses of calcite, LREE-fluoro-carbonates and pyrochlore. Calcite and thorite were corrected with CaO 49.5 wt%. Y_2O_3 was used as internal standard for the analyses of xenotime, 65.5 wt% for ZrO_2 in zircons and 16wt% La_2O_3 for monazite.

Apatite was also analysed but the section was too thin for the analyses and contamination resulted from the glass, thus those results are not used in this study.

New U-Pb age determinations were carried out on zircon and pyrochlore by Laser ablation magnetic sector field inductively coupled plasma mass spectrometry (LA-SF-ICP-MS) at the University of Frankfurt, Germany. The method is used as a low-cost alternative to ion-microprobe techniques for highly precise and accurate *in situ* U–Th–Pb age dating, using an Element 2 coupled to a RESOlution M-50 Excimer laser.

4.2.7 Leaching of the samples

The trial to mechanically separate the two (2) fractions of pure main rock-forming carbonate and REE-carbonates and phosphates were not possible because of the very fine-grained material. The separation would allow easy determination of the isotopes distributions in heavy and light minerals. To assess the amount ^{87}Sr and ^{86}Sr of Sr soluble in sequential leaches in a diluted solution, the samples were leached firstly with a weak acids dissolved in 0.3M HNO_3, that dissolved the rock-forming carbonate – calcite. Accurately known sequential volumes were added to each sample in the order of tens of microlitres of 0.3M HNO_3, the sample was ultrasonically agitated until reaction ceased. The supernatant was separated by pipette after double centrifugation and was analysed for Sr concentration ^{87}Sr and ^{86}Sr. The aim for the leaches was to determine the isotope compositions of the easily solute s and the residue solutions

The residues were further leached using HF-HNO_3 acid to dissolve the REE-carbonates and phosphates for 24 h at room temperature. A supernatant was separated for measurement. Analyses of Sr and Nd were carried out using a VG354 five collector mass spectrometer at BGR, Hannover, Germany. Sr and Nd were separated using standard ion exchange techniques, before being loaded onto single Ta filaments (Sr) and either single Re filaments (Nd).

4.2.8 Carbon and Oxygen stable isotope determination on carbonates

Determination of the stable isotope composition of carbon and carbonate from the Lofdal carbonatite was done at the Bundesanstalt für Geowissenschaften und Rohstoffe (BGR) and the Natural History Museum (NHM) by Dr. Baruch Spiro.

Carbon and oxygen isotope analysis based on 15 samples from the Lofdal Alkaline Carbonatite Complex are presented (Table10.1). These have been corrected to Vienna Pee Dee Belemnite (VPDB) and Vienna Standard Mean Ocean Water (VSMOW) respectively (expressed in delta notation).

Carbonate minerals were selected by looking at different appearance of the carbonate minerals. The samples were treated with 100% phosphoric acid. CO_2 was measured by mass spectrometry with a Finnigan Mat 251.Values of $\delta^{13}C$ and $\delta^{18}O$ are here expressed as per mil differences relative to the Peedee Belemnite (PDB) and Standard Mean Ocean Water (SMOW) respectively.

Chapter 5: Mapping of the Lofdal Carbonatite Complex

This chapter starts with a review of the geological background and setting of the Lofdal area. It then gives the results of the different methods (radiometric survey, landsat images, hyperspectral imaging, and fieldwork) used to map the Lofdal Alkaline Carbonatite Complex and its structural setting and tectonic features. Details of the methods are given in Chapter 4. The mapping was undertaken by the author, with help from colleagues at the Geological Survey of Namibia. Namibia Rare Earths Ltd also contributed to the understanding of the geology through detailed mapping of local geological structures during their exploration programme. Field descriptions of the main rock types are presented in this chapter and the mapping results are then used for the interpretation of the evolution of the structure and intrusion sequence at Lofdal.

5.1 Location, geological and tectonic setting of the Lofdal Alkaline Carbonatite Complex

The Lofdal Alkaline Carbonatite Complex (LACC) is located on farms Lofdal 491, Bergville 490, Oas no: 486 and Ruimte 510: approximately 14^0 31'20, 14^0 47'0; 14^0 31'30, 14^0 47'0 longitude and $20^0$15'0S $20^0$15'15 S Latitude, 36 km Northwest of Khorixas in Damaraland, Kunene Region, Namibia.

On the regional scale the complex is situated on the southern rift margin of the Congo craton, at the intersection of the Northern Platform Zone of the central Damara belt with both the eastern Kaoko Zone and the Northern Margin Zone, but more specifically between the Northern zone and the Ugab tectono Zone as defined by Goscombe (2008) (Figure 5.1).

The LACC occupies an area of about 24 km^2. The complex consists of carbonatite dykes, phonolite dykes, nepheline syenites and breccias associated with the intrusions plus some mafic dykes, including at least one lamprophyre. Some researchers have extended the complex to include the Naauwpoort Formation and the Khorixas intrusive suites as described by Miller (2008) that comprise the Bloukranz Bostonite, mainly the nepheline syenite, the Bergville swarm of alkaline dykes and the Buschhöhe Gabbro.

Geologically and temporally, the complex also forms part of an alkaline magmatic province of the Nosib Group that in part records the intra-continental orogenic stages of the Damara belt rift and faulting systems, possibly related to the last stage of the last

major uplifting episode that ended at around 700 Ma and to an early onset of the Damara Orogeny as defined by Miller (1983).

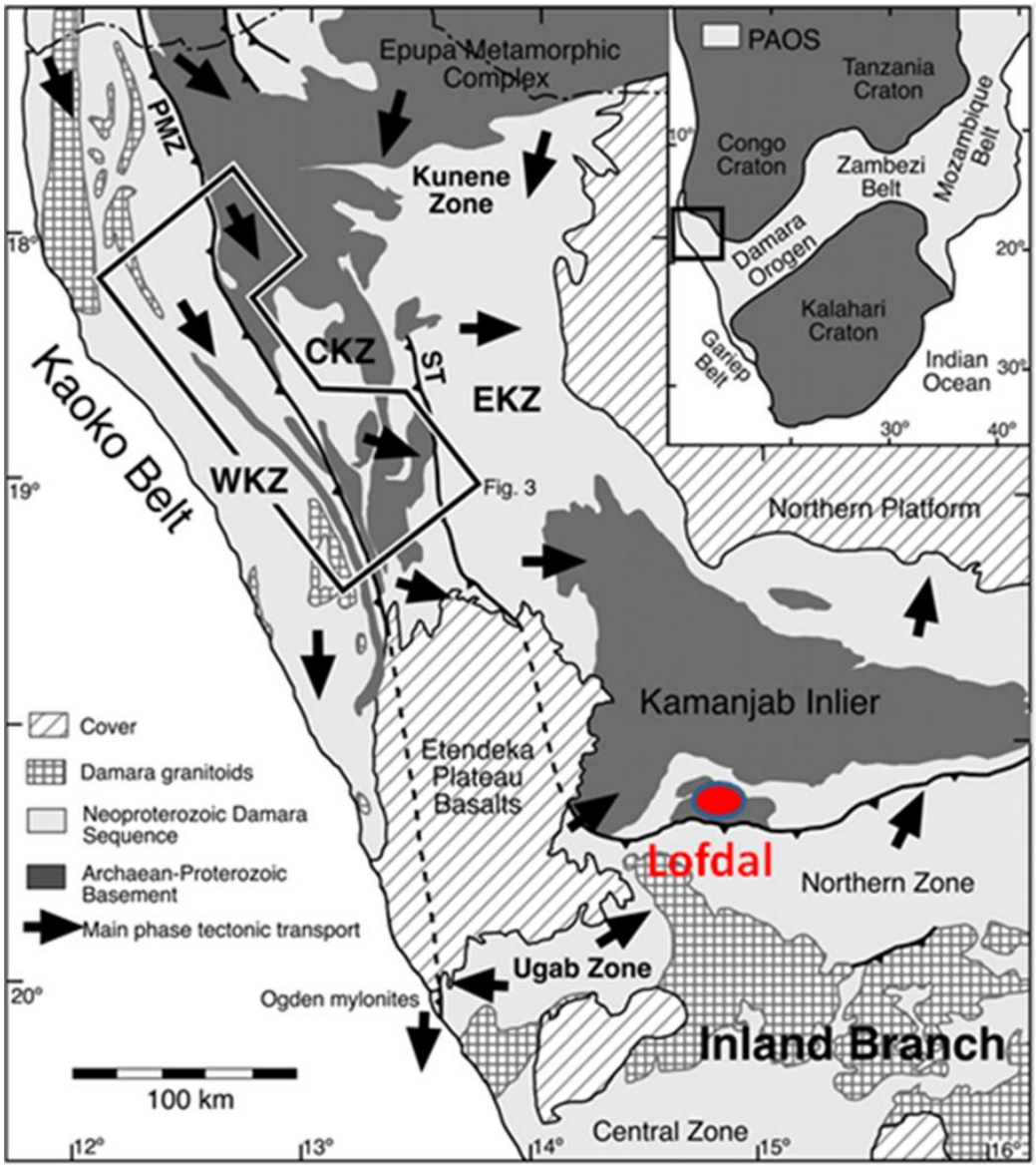

Figure 5.1 Map indicating the location of the Lofdal Alkaline Complex with relation to Damaran and Kaoko Belts (Goscombe 2008)

Frets (1969) broadly also considered the Oas and Lofdal syenites to belong to the Naauwpoort Formation. The Naauwpoort formation is made up of widespread alkaline to peralkaline volcanism ranging from sodic to potassic and basic centres, along the northern boundary fault of the northern graben. These rocks were mainly erupted at two principal volcanic centres; the east of Khorixas (Miller 1980) and between the farm Naauwpoort 515 and Austerlitz 515, west of Khorixas. Generally the association of coeval and chemically similar volcanic and intrusive rocks implies a strong genetic relationship (Ehlers and Blat 1982).

The LACC has intruded the gneisses, amphibolites and schists of the Welwitschia Inlier composed of pre-Damaran basement rocks of the Huab Metamorphic Complex HMC (Figure.5.2). It is emplaced in a dominantly NW – SE orientation, similar to the dominant direction of the country rock foliation.

Erosional processes in the area have completely stripped out the Damara rocks resulting in exposure of the older Huab basement in a window, which is bordered by younger rocks of the Damara ages. Namibian age rocks of the Mulden Group lie to the North and the Oas syenite intrusion to the South, unconformably bordering the Lofdal alkaline complex. Complex compressional structures, observed in addition to the rift-related structures may also play a major role in the location of the alkaline and carbonatite rocks (Figure 5.2)

5.2 Introduction to the host rocks of the Lofdal Alkaline Carbonatite Complex

On a regional scale the rocks around the Lofdal complex record the Damara Orogeny, Neoproterozoic and early Paleozoic tectonics that resulted in repeated deformations and metamorphic phases. It is bordered by the Sesfontein rift to the West, the northern platform made of carbonates and schists to the North and the Northern rift to the south and eastern part of the area (Figure 5.2).

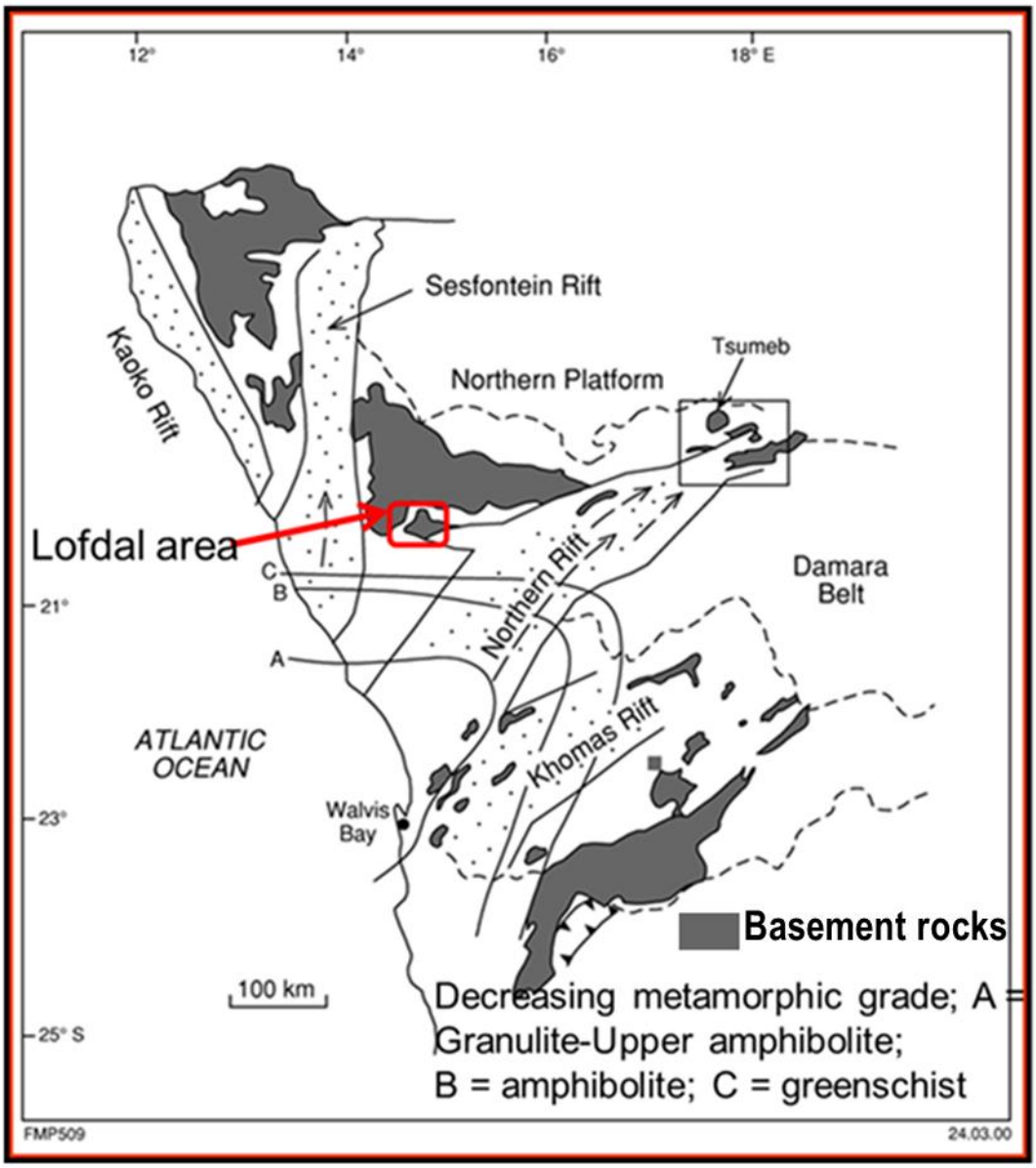

Figure 5.2 Simplified geological map showing the rifts, the metamorphism of the Damara Orogen around Lofdal, major faults and Location of Lofdal. Source: Pirajno (1998). Dashed lines indicate major local rifts boundaries and solid colour shows the Damara belts boundaries.

5.3 Host rocks

The oldest rocks in the area consist of the gneisses, amphibolites and schists of the Welwitschia Inlier, composed of pre-Damaran basement rocks of the Huab Metamorphic Complex HMC. These rocks host the Lofdal Alkaline Carbonatite complex. The host rocks are estimated at about 1.2 Ga old and are variably metamorphosed and folded. The study area is covered by several stratigraphic sequences of different ages and is described here in the sequence of their age groups. Consideration is given to those formations found within the distance of 50 km from the study area.

The area is well exposed and strongly affected by tectonics, thus, various metasediments that cover the area are intensely metamorphosed and deformed, resulting in gneisses and schists. The region consists of a mosaic of Paleoproterozoic and Meso-Proterozoic metamorphic basement rocks and igneous complexes, which form the margins of the Archean Congo Craton. These are unconformably overlain by the Neoproterozoic Damara rock sequences.

5.3.1 Paleoproterozoic Basement Rocks

Lofdal is located within the Kamanjab Inlier. The Kamanjab Inlier consist of metamorphic sequences 1811 $\pm$ 35 Ma (Tegtmeyer and Kröner, 1985), 1871 ± 30 Ma and 1730 Ma (Frets, 1996), belonging to an early Mokolian age of (2.7 – 1.9 Ga). The Kamanjab inlier is composed of three main units: the Huab metamorphic complex (HMC), the volcano sedimentary rocks of the Khoabendus formation (KF) and the Fransfontein granitic suite (FFG).

5.3.1.1. The Huab Metamorphic Complex

The Huab Metamorphic Complex (HMC) is a collective term including rocks of different origins and ages, partly sedimentary, igneous and of intermediate and metasomatic origin. HMC comprises of granites, granitic gneisses altered basic igneous, felsic and mafic volcanic rocks, quartzites, amphibolites, para- and augen-gneisses as well as lesser meta-volcanic rocks and meta-conglomerates. The red rectangle indicates the Lofdal area (Figure 5.3).

Orthogneisses are the predominant rock types in the area of interest in this study. Some authors attempted to subdivide the orthogneisses into coarse-grained to porphyritic granodioritic orthogneisses and equigranular medium- to fine-grained red orthogneisses of granitic composition (Schneider 2008). He also noted light gneisses containing layers of quartzites, mica schists and amphibolites as the main rock types of the HMC.

The granitic gneisses mainly are intercalated by quartzite and amphibolite bands (Miller 2008). The Huab Metamorphic Complex is metamorphosed at amphibolite grade.

These rocks all have in common that they represent the oldest rocks in this part of Namibia, estimated at >1700 Ma (Frets, 1969). GUJ (1970) distinguished the HMC in an upper and a lower sequence.

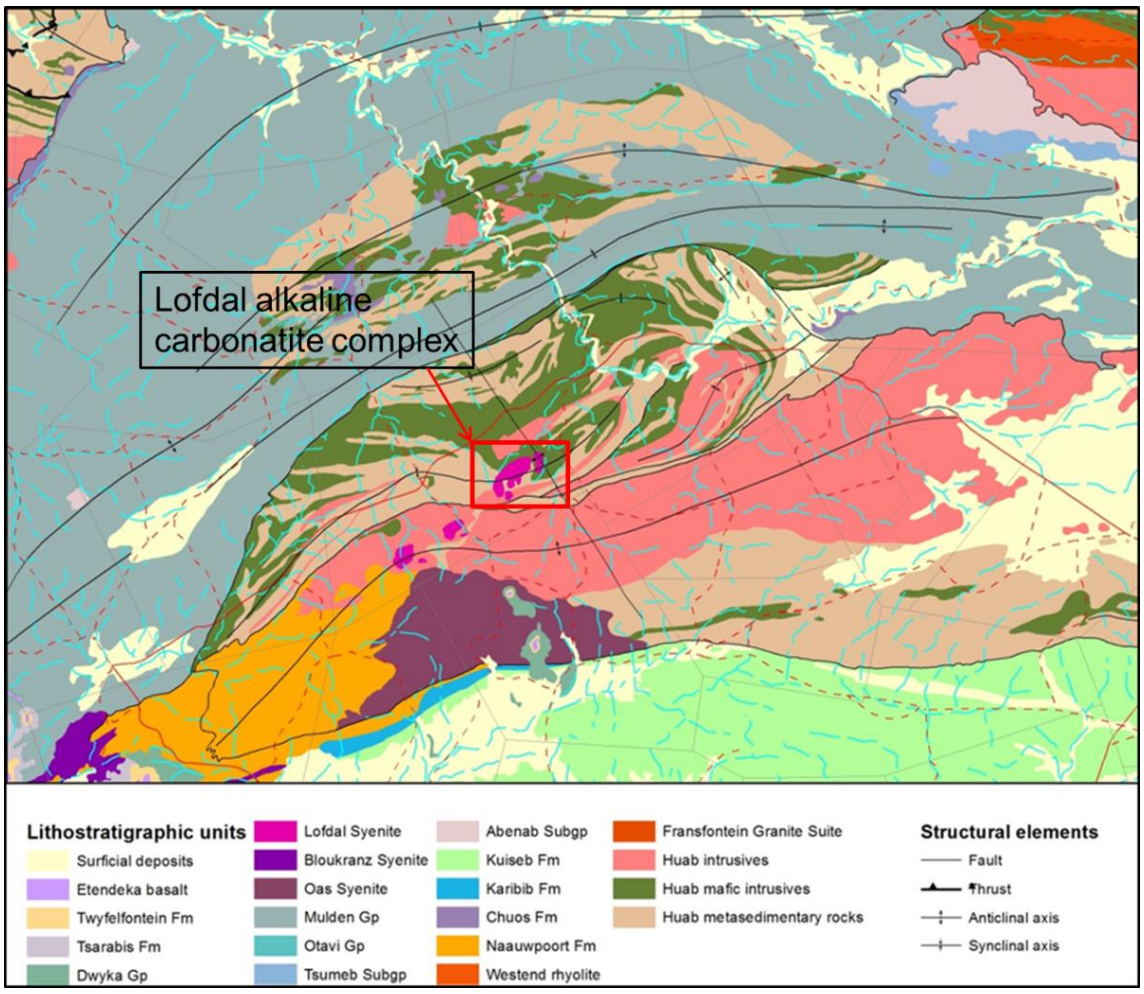

Figure 5.3 Map showing the Huab Welwitchia Basement rocks GSN (2012)

Frets (1969) mapped the area in detail and gave a description from the region west of Khorixas and reported amphibolite-grade banded gneisses (metavolcanics and metasediments). This is supported by Seth et al. (1998) with the characterisation of HMC rocks as amphibolite-facies para- and orthogneisses. Similar amphibolites are largely exposed in the Bergville and Lofdal areas. The para and orthogneisses and metasediments are well exposed at Lofdal farm and the surrounding areas.

These rocks revealed polyphase deformations occasionally turned into migmatites. The deformation suffered by these rocks is believed to be before 1.8 Ma intrusion of the Fransfontein granites (Frets 1969). Such intense and repeated folding, metamorphism, anatexis and the reworking structurally makes it difficult to determine sedimentary units and quite impossible to define stratigraphic sequences in the metasediments of Huab Formation. The basement is additionally intensely reworked by the Damara orogeny episode. Frets (1969) and Miller (1983) have best described the deformational sequence of events in the area. The Carbonatite plugs and dykes and the associated alkaline rocks have intruded the HMC.

5.3.1.2 The Fransfontein Granite Suite

The Fransfontein Archean granitic terrain and Orthogneisses (2- 1.8 Ma) are located to the northeast of the study area. The Fransfontein granitic suite intruded both Khoabendus formation and the early Damara successions (Miller 2008). These granitic rocks show deformation and illustrate some schistocity. The entire basement in the area is Paleoproterozoic and younger Mesoproterozoic and dominated by granitoids and orthogneisses. The Fransfontein granites and granodiorites are coarse-grained and pink in colour. This granite suite is affected by later widespread granitization and occurs mainly within the Huab Metamorphic Complex and the Khoabendus Group.

5.3.2 Damara Sequence

The Damara Orogen forms part of the pan African network of Neoproterozoic belts that partially surround Africa. The Pan-African Damara Orogen of southern Africa is the result of temporally distinct, high-angle and oblique convergence in different parts of what appears to be a three-pronged orogenic system (Coward 1981, 1983). The tectonic evolution of the Damaran belt started off with an intra-continental rifting episode between 1000 and 900 Ma at a triple ridge junction with north-south and north-east-trending arms (Miller 1983). Damara Orogen Belts evolved through phases of intra-continental rifting, spreading, subduction and continental collision lasting from approximately 800 Ma to 460 Ma.

The Damara Orogen belt has three arms: the Kaoko belt, the central Damara Belt and the Gariep Belt that meet at a triple junction centred approximately at Swakopmund. The Kaoko belt is the North-North Western coastal arm and dominated by two major, sinistral strike-slip shear zones within high grade amphibolite facies Damara Supergroup turbidites, incorporating basement slivers and sheared Pan-African age granitoids (Dürr and Dingeldey 1996, Passchier et al. 2002, Goscombe et al. 2003a,b). Goscombe et al. (2003a, b) subdivided the Kaoko Belt into contrasting tectono-stratigraphic zones with degree of metamorphism increasing from the margins of the belts to the granite facies that have intruded central zones. The Kaoko belt is further subdivided into the Eastern (EKZ), Central (CKZ), Western (WKZ) and Southern Kaoko Zone (SKZ). Lofdal Complex is located within the Kaoko Belt, at the juncture of the Damara Belt and the Ugab Zone of the Kaoko Belt (Figure 5.1). The Damara stratigraphic unit represented by Nosib, the Mulden, Otavi, Swakop and Zerissene Groups.

The deposition of the Nosib Group and emplacement of alkaline and peralkaline mantle derived volcanics and plutonics along major faults or linear features that formed the rift margins formed part of the episode between 840 and 730 Ma Miller (1983). Several large bodies intruded into the basement including the Oas Syenite and Lofdal Alkaline Complex as part of the intra-continental orogenic stage of the Damara belt and are classified as part of the Nosib Group by the GSN (1992), deposited during the period of spreading and uplifting and at the time of Damara sediments deposition. The rifting episode ended at around 700 Ma and was followed by a compressional period as a result of subduction of the Kalahari Craton below the Congo Craton that ended at 540 Ma (Miller 1983).

The detailed deformational sequence of events has been described by Frets (1969) and Miller (1983). The Damaran rocks are overlain by syn-orogenically deposited Nama rocks (deposited between 600 Ma and 540 Ma ago (Schneider 2008), most observed in the Southern Zone. The Damaran orogeny was followed by a period of intense erosion that exposed the Huab basement and pre-Damaran rocks. Damaran rock sequences found around Lofdal alkaline complex are described below.

5.3.2.1 The Nosib Group

The Naauwpoort formation is a unit within the Nosib Group and is made of large scale alkaline to peralkaline volcanism from sodic, potassic and basic centres along the northern boundary fault of the northern graben. The rocks produced at this structure are ignimbrite volcanic piles in the graben structure over 6600 m thick, which were erupted at two main volcanic centres; to the east of Khorixas (Miller 1980) and between the farm Naauwpoort 515 and Austerlitz 515 west of Khorixas. The volcanic rocks at both localities are interbedded with the sedimentary rocks of the Ombombo and Ugab Subgroup of the Otavi Group.

Nosib Group stratigraphic unit is deposited during the rifting phase. The accumulation of the Nosib age sedimentary rocks were deposited at around 900 to 760 Ma and are found on the graben rift shoulders on the Northern Platform and in the eastern Kaoko Zone. Nosib group is represented by two main units in the area, mainly arenaceous rocks, conglomerates and a number of alkaline intrusive rocks mainly belonging to the Naauwpoort formation. The Nosib group quartzites are intruded by the Oas syenite. The quartzites have been baked to dark silicified hornfels along the contact.

Syenite, nepheline syenite, carbonatite and gabbro intruded north of the northern rift shoulder to this graben close to sodic volcanic centre. These intrusions are mostly referred to as Khorixas intrusive suites (Miller 2008). Most of these rocks occur in close

association with the Naauwpoort volcanic rocks of the Khorixas area including the Oas syenite, the Blaukranz bostonite (mainly the nepheline syenite), the Bergville swarm of alkaline dykes and the Buschhöhe Gabbro are in a broader sense belonging to the Naauwpoort Formation (Frets 1969). The Lofdal Alkaline Complex is part of the Naauwpoort Formation considering the depositional and intrusion age of 765 Ma (Wall et al. 2008).

5.3.2.2 The Otavi Group

The Otavi Group overlies the Nosib group and is composed of dolomite and limestone with intercalations of quartzite and shale. The Ugab Subgroup of the Otavi Group is limited to the eastern flank of the inlier where it wedges in above the Naauwpoort volcanics of the central core and below the Chuos diamictite. The unit was also observed North of Lofdal close to the rocks of Mulden Group.

5.3.2.3 The Mulden Group

The Mulden group is confined to the Northern Zone of the Damara Orogen and is the third succession on the Northern platform overlying unconformable the Otavi Group. The top of the Mulden Group consists mainly of quartzite and conglomerate but also contains substantial intercalations of shale, marl and phyllite (Miller 2008).

At Lofdal the Mulden Group overlies Nosib, other earlier Damara rocks and rests directly on the Huab Metamorphic Complex basement. The Mulden Group forms a series of very prominent hills as synclinal structures, locally thrusted but usually unconformable with the Huab Metamorphic Complex (Figure 5.8 and 5.10).

It rises steeply above the surrounding Huab Basement gneisses forming some of the highest ridges of the whole area, covering the whole northern part of the study area. Further south at Naauwpoort the Mulden group rests on Naauwpoort extrusive and intrusive rocks.

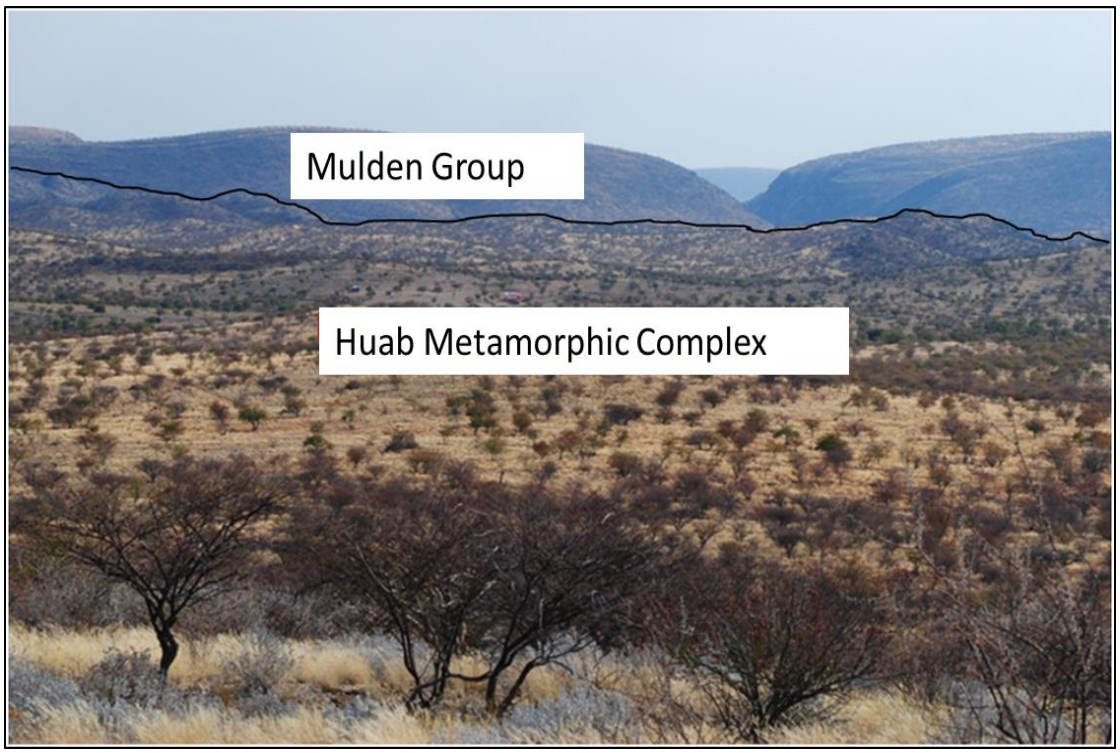

Figure 5.4 View of the Mulden Group unconformity with relation to Huab basement.

5.3.3 Other Granitic Intrusion

Also some rare granitic dykes and granitic orthogneisses sills are present in the area and these are believed to belong to similar granitoids described by Goscombe (2003) to the North West of the study area. Several meters scale lenticular shaped granitoid bodies are observed, extending parallel to the direction of younger intrusive dykes of the phonolitic and carbonatitic affinity. Magmatic segregations and a variety of coeval S-type granitic orthogneisses bodies of 580-552 Ma are said to belong to the Damaran age (Seth 1998).

5.3.4 Early Cretaceous Etendeka volcanics

The name Etendeka means a place of flat topped mountains (Figure 5.11) in the language of the local Himba people and refers to the characteristic table-topped hillocks dotting the plateau. Covering ca. 78 000 km^2 between the Huab River in the south and the Hoanib River in the north, it towers some 700 to 800 metres above the deeply eroded gneisses and metasedimentary rocks of the Paleoproterozoic Huab Metamorphic Complex to the east, while rising gradually out of the coastal plain in the west (Figure 5.5). The Etendeka volcanics are related to the opening of the South Atlantic Ocean.

Figure 5.5 Etendeka table mountains around Lofdal

Together with the Paraná volcanics of Brazil they formed a large igneous province in western Gondwanaland just before continental break-up, with an estimated extruded volume of some 1.3 million cubic kilometres (Marsh 1972, Pirajno 2004a).

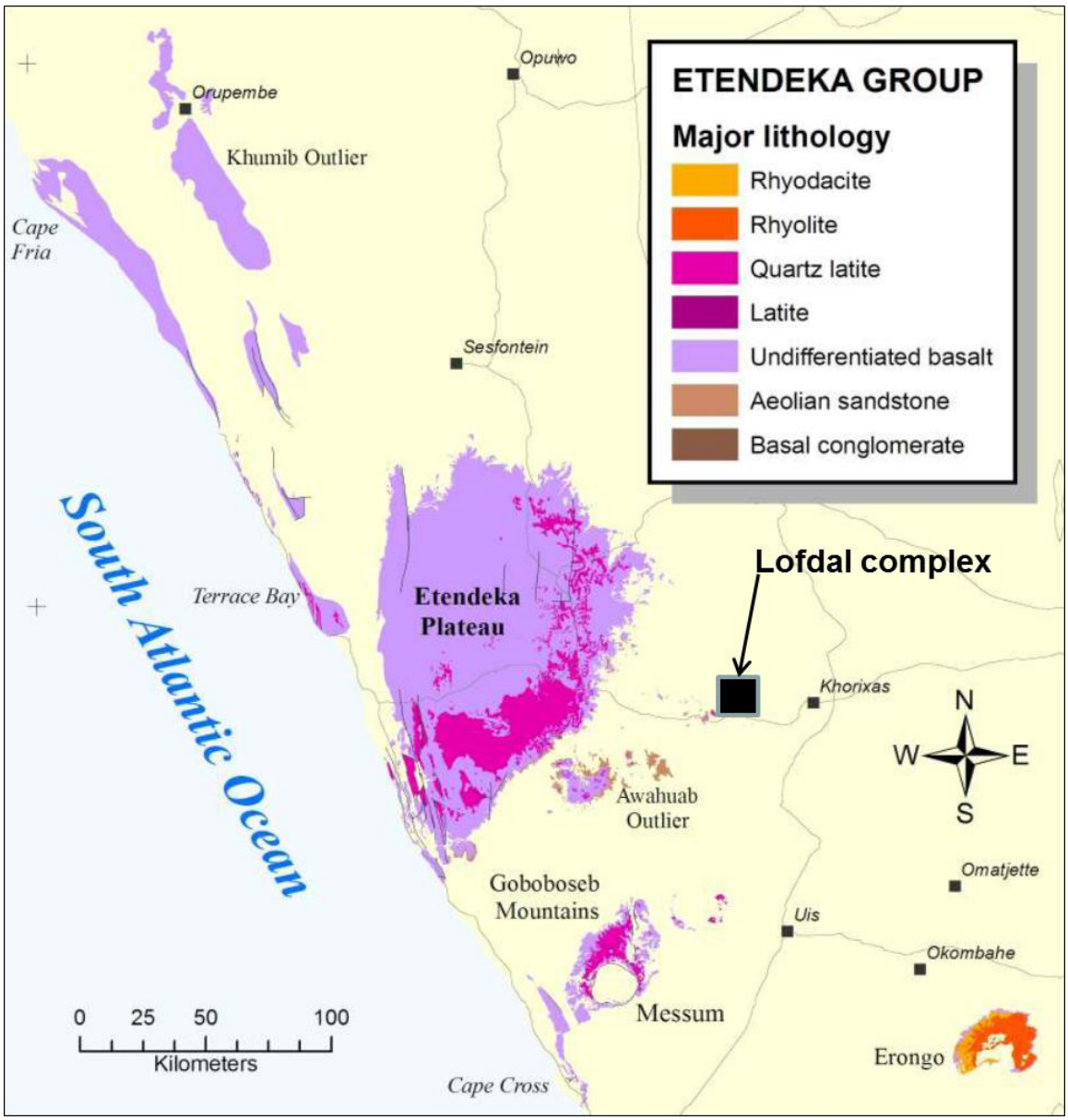

Figure 5.6 Distribution of the Etendeka Group in the north-western part of Namibia after Milner (1997).

The province had an extensive post-flow surface area (Figure 5.6). The basalt samples at Paraná and Etendeka have an age of about 132 Ma and it could be the origin of the Gough and Tristan da Cunha Islands as it is connected by the Walvis Ridge; Courtillot and Renneb 2003, Fodor et al. 1989). The plateau of north western Namibia consists of volcanic rocks of the Cretaceous period. The Etendeka Group consists of a bimodal association of mafic to intermediate (51-59 wt% Si_2O content) tholeiitic lavas interbedded with more felsic (66-69 wt% Si_2O content) quartz latites and minor latites.

5.3.5 Karoo Supergroup

The Karoo Supergroup overlays the Damaran rocks and consists of the Kalahari Group, which are the terrestrial sediments such as aeolian and alluvial sand, calcrete as well as silcrete. These rocks were deposited on a continental erosion surface and present day drainage. They are mainly observed south west of the region of interest. The Karoo lithology can be summarised below in Table 5.1 according to lithology details described by Hodgson (1970).

Table 5.1 Geological sequences of the Karoo Supergroup

Formation	**Lithology**	**Thickness**
Etjo	Dune bedded, fine to medium grained, yellow-Orange Aeolian sandstone	125 m
Prince Albert	Sandstones and carbonaceous shales	10 – 70 m
Dwyka	Tillite with quartz, schist and quartzite	Variable and localised

5.4 Mapping results

Hyperspectral digital imagery was successfully used to map the area, understand spectral reflectance of the carbonatite rocks and interpret geological features, mainly the magnitude of the Lofdal carbonatite complex intrusion and the different lithologies in the area. By filtering specific wavelengths of the electromagnetic spectrum minerals images were created that enhanced the ability to delineate different geological features.

Composite bands 180, 28, 3 and 15, 9, 3 were used to produce hyperspectral colour images that highlight calcitic carbonate and the content of iron oxides in red respectively. The ratio bands used also highlighted the NE-trending sinistral shear zones that coincidence with the dyke's direction (as discussed in subsection 5.5).

The interpretations of the hyperspectral maps led to the generation of follow up targets for ground sampling. Large than 1.0 m phonolite/carbonatite dykes were seen extending up to 15 km along strike. Carbonatite dykes less than a meter wide could not be observed in the hyperspectral maps.

Careful analyses of the spectral reflectance properties of the Main calciocarbonatite plug were used as a standard to compare and delineate areas with similar reflections. The exercise led to the discovery of the Emanya calciocarbonatite plug (Figure 5.5). Areas covered by calcrete showed similar properties to the areas with carbonatite intrusions.

Measurements of spectral reflectance showed various lithologies and the distribution of the minerals in the area, allowing identification of the alteration zones in the area, particularly the iron oxides, argillic distribution and felsic minerals (Figure 5.7 and 5.8). Structural features such as faults observed in the spectral images provided valuable information adding to the existing geological data in updating the geological map of the area. Visible fault zones concurred with earlier geological mapping work by Frets (1969). Although the directions of dykes and their extent were clearly visible, it was difficult to differentiate between phonolite and carbonatite dykes. It was also impossible to differentiate carbonatite of different compositions mainly because of the small size of the dykes.

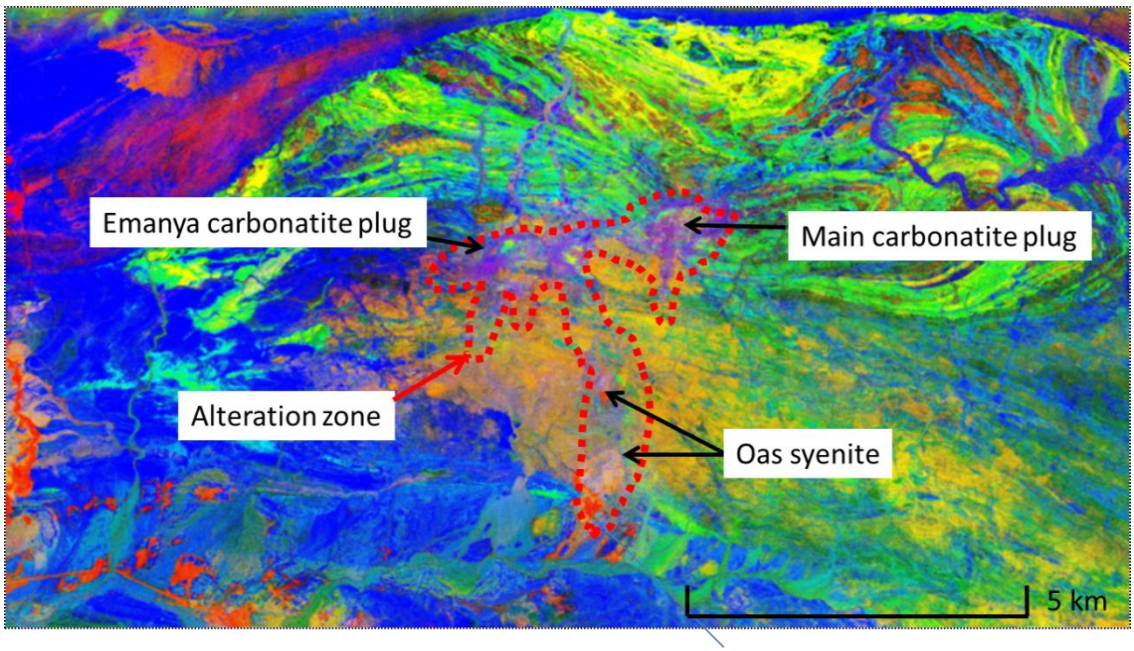

Figure 5.7 Hyperspectral highlighting argillic alterations (red dots) around the Lofdal Alkaline carbonatite Complex and the Oas.

A reconnaissance radiometric survey using a hand-held scintillometer was carried out by the author with assistance of the division of geophysics at the Geological Survey of Namibia. The survey led to the discovery of some carbonatite dykes that have radioactive anomalies reaching up to 46 000TCPS.

Most readings obtained on the carbonatite dykes were higher than the background and/or the intruded Huab Basement rocks although the carbonatite dykes gave variable readings. This was interpreted to mean that the radiometric minerals are not uniformly disseminated. The red and yellow coloured carbonatite dykes exhibited the highest readings. The grey coloured carbonatites did not exceed 2000 TCPS.

Quartzites and granitic rocks that are adjacent to the highly radioactive carbonatite dykes also exhibited anomalous high values. These rocks are red in colour with visible patches of a red mineral. It is evident that these rocks have been affected by late hydrothermal activities.

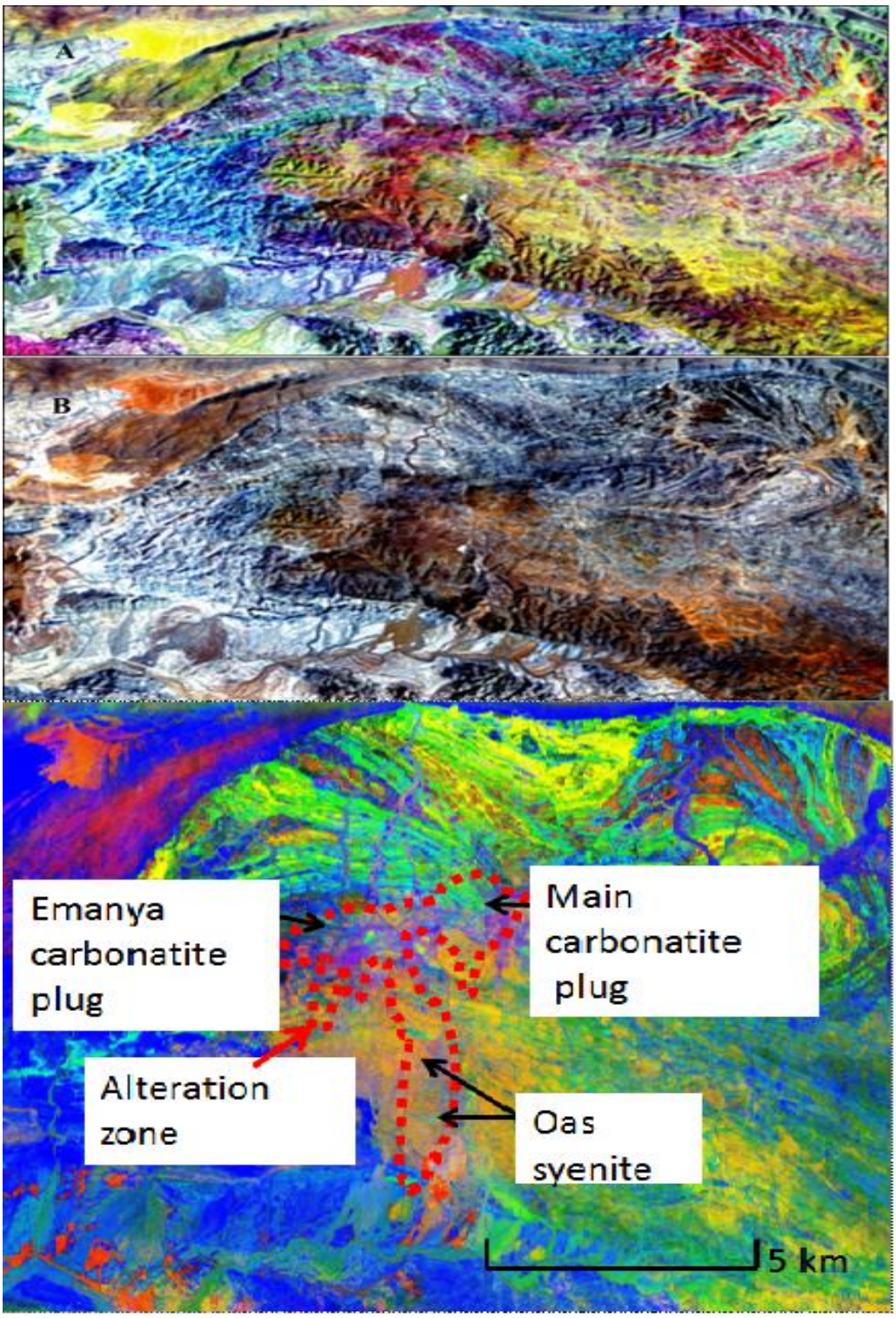

Figure 5.8 Hyperspectral colour image with a) false colour, b) true colour, and c) composite. Bottom image highlights iron oxides in red and granitic gneisses in green. The black circles indicate mapped calcitic carbonatite intrusions. Note the NE-trending sinistral shears coincidence with the dyke's direction.

The source of most radioactive anomalies could be identified in the outcrop, as a lustrous shiny red mineral, that forms disseminated patches up to 2 cm in diameter. The mineral was identified as thorite, using X-ray diffraction.

Field observations and the magnetic survey images indicate an extension of the Lofdal alkaline complex. The complex has a general ENE trend and seems to extend further for at least 2 km to the SSW which could give the complex an overall length of 6.5 km (Figure 5.9).

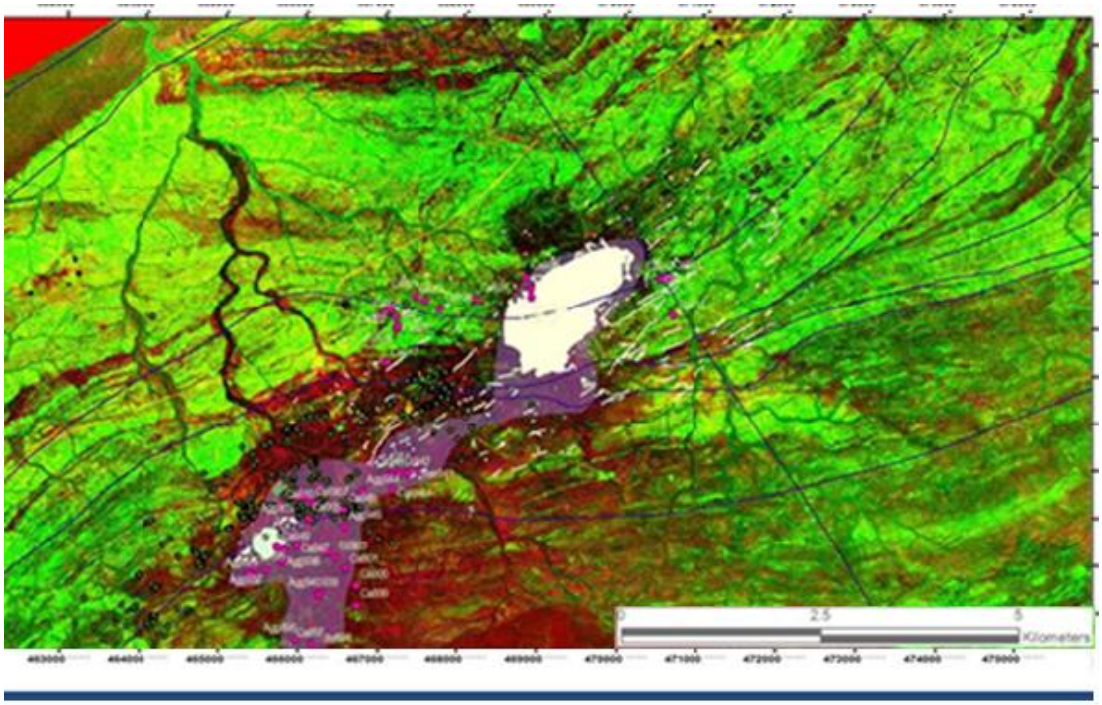

Figure 5.9 Possible extension of the carbonatite bodies in the Lofdal alkaline carbonatite complex, marked in purple. Also indicated with black and magenta colour are sample points. The white regions represent the carbonatite plugs.

5.5 The structure of the Lofdal complex

Locally, Lofdal is tectonically located in a zone of sinistral shear NE-trending Ruimte-Bergville fault that traverses south of the main syenite and carbonatite intrusion. This major structure is transected and cross cut by various faults with a NW – SE dominant direction. Other structural features include a long fault originating from the Naauwpoort farm 511, extending through to the Bergville farm 490, referred to as the Naauwpoort-Bergville fault [(Figure 5.10) that appears to have a major impact on the origin of the Lofdal alkaline carbonatite complex.

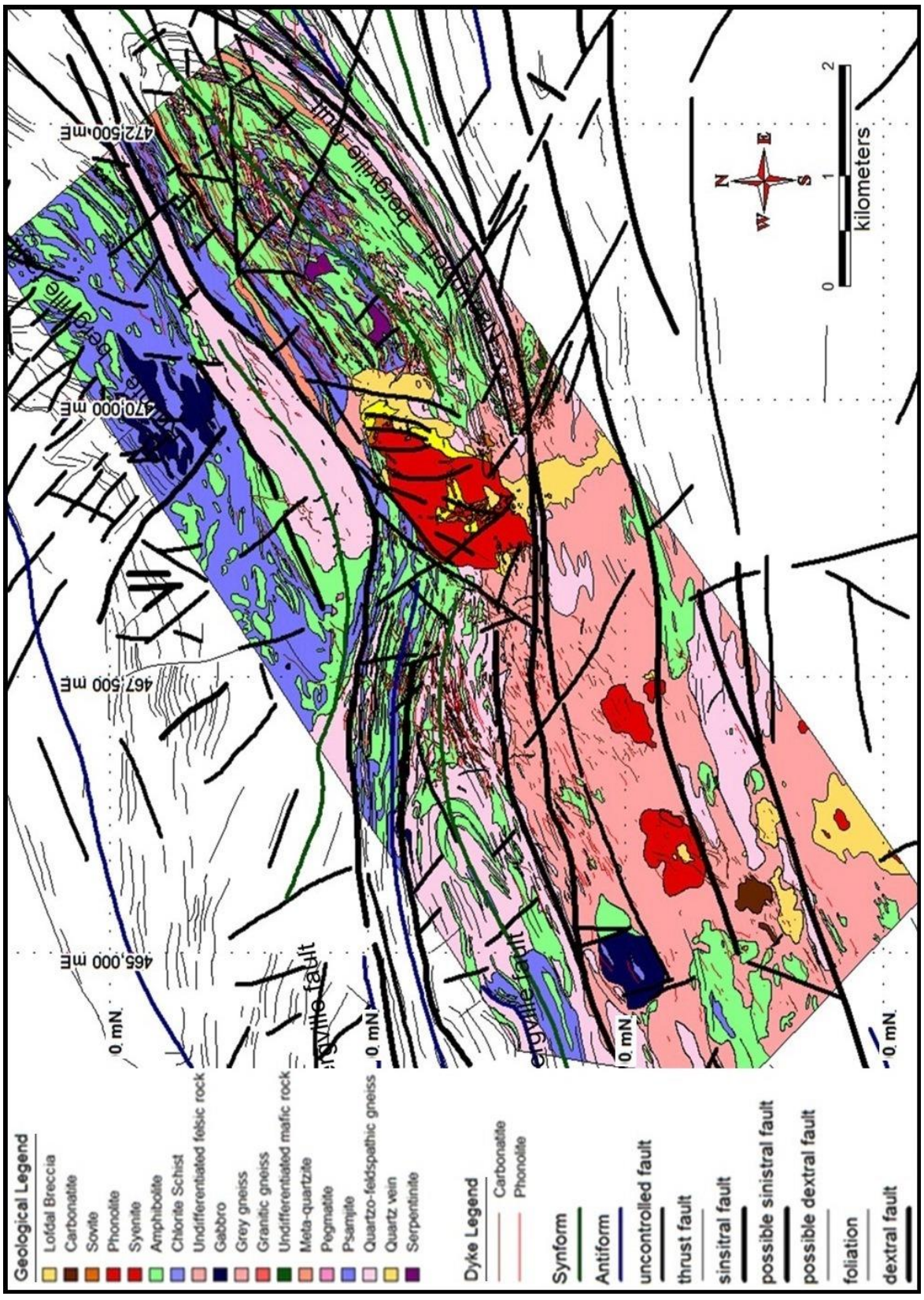

Figure 5.10 Structural map of Lofdal edited after Namibia Rare Earth Ltd.

The Naauwpoort-Bergville fault occurs within a graben area north of the carbonatite and syenite plugs. Frets (1969) described similar structures in the vicinity of Lofdal e.g. the

Bethanis fault that represents a weakness zone along the southern margin of the stable Congo Craton.

The dominant NE - SW direction of the intrusion and foliation is perpendicular to maximum stress. This could possibly have played an important role in allowing the intrusion of the dykes and plugs. The rift system that developed in the Northern Platform of the graben rift shoulders in the eastern Kaoko Zone (Miller 2008) possibly also contributed to create favorite tectonic conditions for the intrusion of the Lofdal carbonatite complex and other related rocks in the area.

A small number of dykes (carbonatites, phonolites, mafics (including lamprophyres) and dolerites) have a direction perpendicular to the dominant direction possibly representing the tension joints. The two directional dykes seemed to have been produced at the same time, although displacement at the dyke intersections is typical at Lofdal.

Structures within and around the carbonatite and syenite main intrusions record both extensional and transpressional events. The transtensional features are recognised in the fault zone where strike slip movement is combined with extensional movements. The transpression event is indicated by the local changes of the strike-slip fault direction, creating a zone where the fault trend is oblique to the to the strike-slip fault movement direction. The combinations of folds and faults at the local zones of transpression or transtension produced the flower structures and a strike slip duplex zone as observed in Figure 5.8. The duplex zone formed at bends in a strike slip fault, as a possibly result of progressive migration of the active fault into one wall. It is at the duplex bend zone where syenites and carbonatite plugs have intruded. The intrusion of carbonatites along the fault structure has a significance because it suggests that the observed structures have crustal-scale magnitude with deep roots through the crust, allowing the passage of the different alkaline magmas from sub crustal levels. The fault structures served as access channels to the surface, tapping the upper mantle over a period of time to provide the different alkaline suite of rocks with access to the surface.

5.6 The Geology of the Lofdal complex

The complex has an ellipsoidal shape in plan with a NE-trending elongation (Figure 5.11). The topographic landscapes around the main intrusion plugs are controlled by the more resistant silicate rocks, mainly the syenites. The Main calciocarbonatite plug form subdued topography. The Emanya calciocarbonatite carbonatite plug, which is altered and brecciated, forms a high hill.

The low relief of the Main calciocarbonatite plug makes it difficult to be readily noticed and distinguished from a distance.

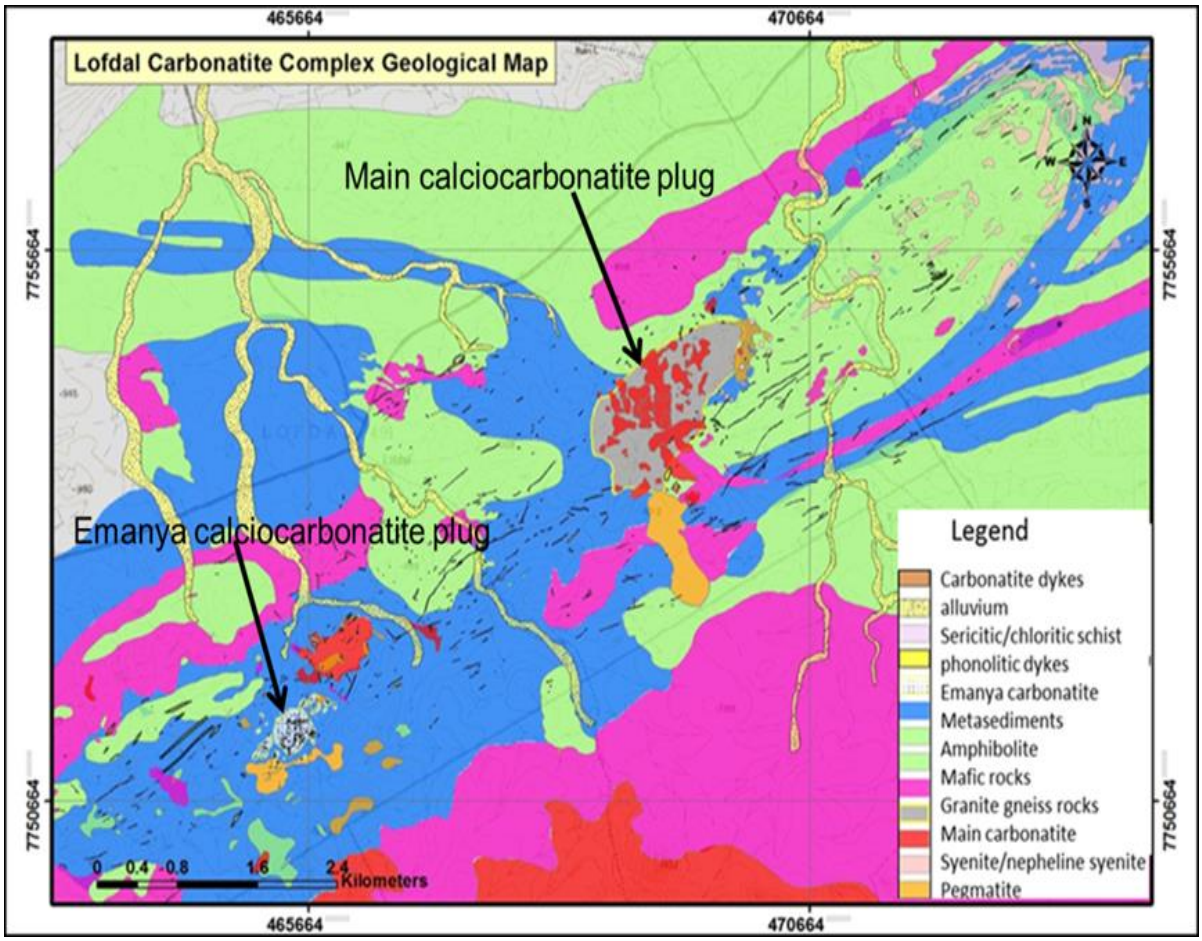

Figure 5.11 Geology of the Lofdal area, after GSN (2006b), and Namibia Rare Earths Ltd., unpublished data.

However, the carbonatite dykes are resistant to weathering in comparison to the intruded basement rocks and, therefore, stand out as 'wall-like' structures. The largest calciocarbonatite intrusion in the area is the Main carbonatite intrusion of about 4 km^2. The other sizable intrusion is the Emanya calciocarbonatite. These are coarse-grained and sövite plugs. Syenitic rocks and coarse polymictic breccias are closely associated with the calciocarbonatite intrusions.

A thin marginal zone of alkali metasomatised syenite and basement rocks forms the contact zone between the calciocarbonatite and the syenite intrusion and or the country rocks. This zone extends several meters from the carbonatite intrusions. Small satellite intrusions of calciocarbonatite no larger than 100 m^2 in diameter crop out in the area.

Phonolite and carbonatite dykes range from few centimeters to up 30m wide and extend up to 15 km along strike. The phonolite and carbonatite dykes crosscut, interfinger, run in parallel with one another, at places may thin out completely, and/or cross-cut other intrusions mainly the syenites, granites and the earlier phonolites.

5.6.1 Igneous rocks, breccias and cross-cutting relationships

Lofdal Alkaline Carbonatite Complex consists of a varied of intrusive suite made of feldspathic silicate rocks such as nepheline syenite, syenites, phonolites, mafic rocks that are spatially associated with carbonatite plugs and dykes. As with most carbonatite complexes, silicate rocks were emplaced before the carbonatites, which are almost the last phase to be emplaced al at Lofdal. Mafic dykes, including at least one lamprophyre, postdate the carbonatites. Lamprophyre rocks have been described around the Lofdal alkaline carbonatite complex (Fritz 1968, Miller 2008). Quartz syenites are also encountered in the vicinity, represented by the Oas quartz syenite (Jung et al. 2007).

Granites encountered in the area represent an earlier stage of intrusions as they predate the phonolites and the carbonatites. Phonolites and carbonatites are emplaced on the same strike as granite and these at places cut the granitic dykes forming a dyke swarm that outcrops normally sub-parallel to the regional foliation of the schist and gneissic basement rocks. The dykes vary in size and length. Nepheline syenite represents the principal member of intrusive series while phonolite plays a secondary role and represents the extrusive fine-grained equivalent series.

Directional stress is inferred in both the phonolite and carbonatite dykes, giving the rocks a pronounced layering. A number of volcanic breccias along the contacts between the syenite and carbonatite bodies and also within the syenite and country rocks are encountered.

The western side of the Lofdal Alkaline Carbonatite Complex is covered by polymictic chaotic breccias and white carbonatite intrusions topped by syenite. The calcitic carbonatite intrusions are obviously widespread if not everywhere beneath the whole complex.

5.6.2.1 Oas and Lofdal nepheline syenite plugs

The Lofdal syenites are well delineated bodies forming several well exposed small hypabyssal plugs of nepheline syenite up to 2 km^2 and isolated clusters intruding the gneisses of the Huab Basement Complex. The number of individual syenite outcrop exceeds eight (8) separate intrusions. The syenites are coarse to medium grained leucocratic nepheline syenite. Fine grained varieties are observed at contacts with the gneisses of the basement rocks (Fig 5.12a). Major syenite rock types at Lofdal and Oas are mildly sodic nepheline normative and quartz-normative syenites and are interpreted as primarily generated by fractional crystallization from a mantle-derived alkaline magma (Jung 2007).

The syenites are closely associated with carbonatite plugs as well as the phonolite and carbonatite dykes. Carbonatite plugs are mostly found at the base of the syenites. Xenoliths of the syenites have been observed in the carbonatites (Figure5.13).

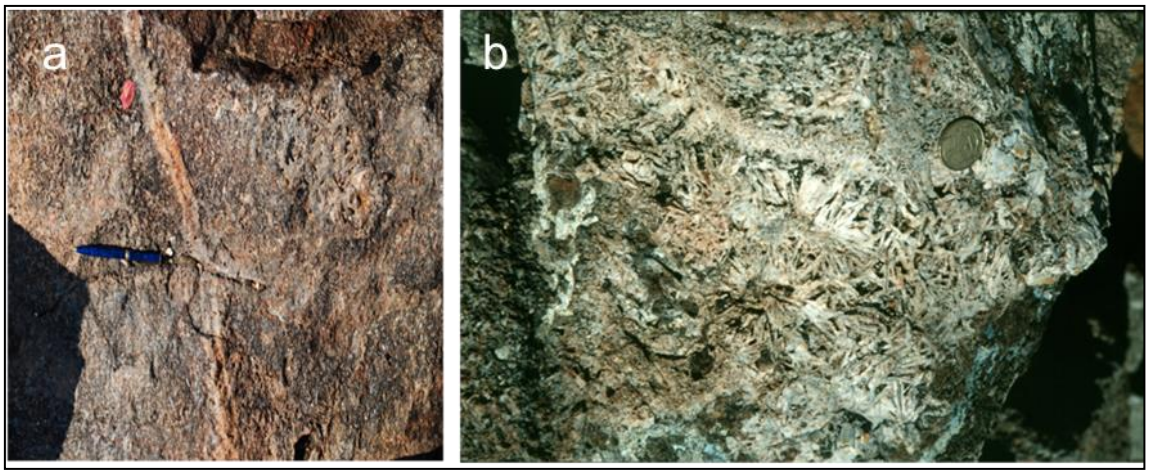

Figure 5.12 (a) Fine-grained variety of syenite and (b) nepheline syenite pegmatite from Lofdal

Figure 5.13 Syenite xenolith in the carbonatites

Some varieties of sodalite rich syenite were observed west of the main plug in the Lofdal farm. The sodalite rich syenite exhibits a bluish colour that gives these rocks a distinct appearance.

Local features include coarse-grained or pegmatite syenite with vugs that contain amphiboles, pyroxenes, nepheline and euhedral zircon crystals that are easily observed on the weathered surfaces, where carbonate materials fill the vugs. The carbonates in the vugs are partially resorbed, permitting the view and preservation of the resistant zircons. Trachytic texture is a common local feature within the syenite. The porphyritic texture is formed by alkali feldspar, plagioclase and nepheline. Cancrinite is a replacement after nepheline and at times pyroxenes. In places cancrinite replaces nepheline completely or partially forms pseudomorphs. Nepheline forms equigranular grains enclosed in feldspar with relict nepheline and large interstitial cancrinite. The potash-feldspar is perthitic. Other minerals in syenites include amphibole, biotite, pyroxene, titanite, apatite and pyrochlore found as phenocysts (Appendix 14). The phenocryst phases are also found in the matrix. Mineral content variation in several syenite samples is defined by the presence or absence of minerals such as amphibole, biotite, pyroxene, titanite, apatite and pyrochlore.

Apatite is localised in zones close to the contacts with carbonatite plugs. The apatite forms flow textures that are elongated, poikilitic and up to 2mm long. Sample 288d from the contact zone between the carbonatites and the syenite comprised of up to 40% apatite in thin section (Figure 5.14). Samples with large amounts of apatite also contained isolated grains of pyrochlore.

Many calcite carbonatite veinlets of different sizes are sporadically spread in all directions at the contacts between the syenites and the carbonatite plugs. These dykes near the contact exhibit a white colour in contrast to other dykes further from the syenites and carbonatite plugs.

Carbonatite dykes in proximity to the syenite plugs have low radioactivity and low REE total contents. Phonolite dykes with variable textures cut through the syenite plugs, an indication that the syenites are older than the phonolite dykes found at Lofdal. Several chaotic polymictic breccias are developed locally along the contact with the gneisses and the syenite bodies and also within the syenites. The breccia consist of closely packed, 1-150 cm angular fragments of a varied origin, embedded in a fine-grained, contaminated facies of the syenites and carbonatites.

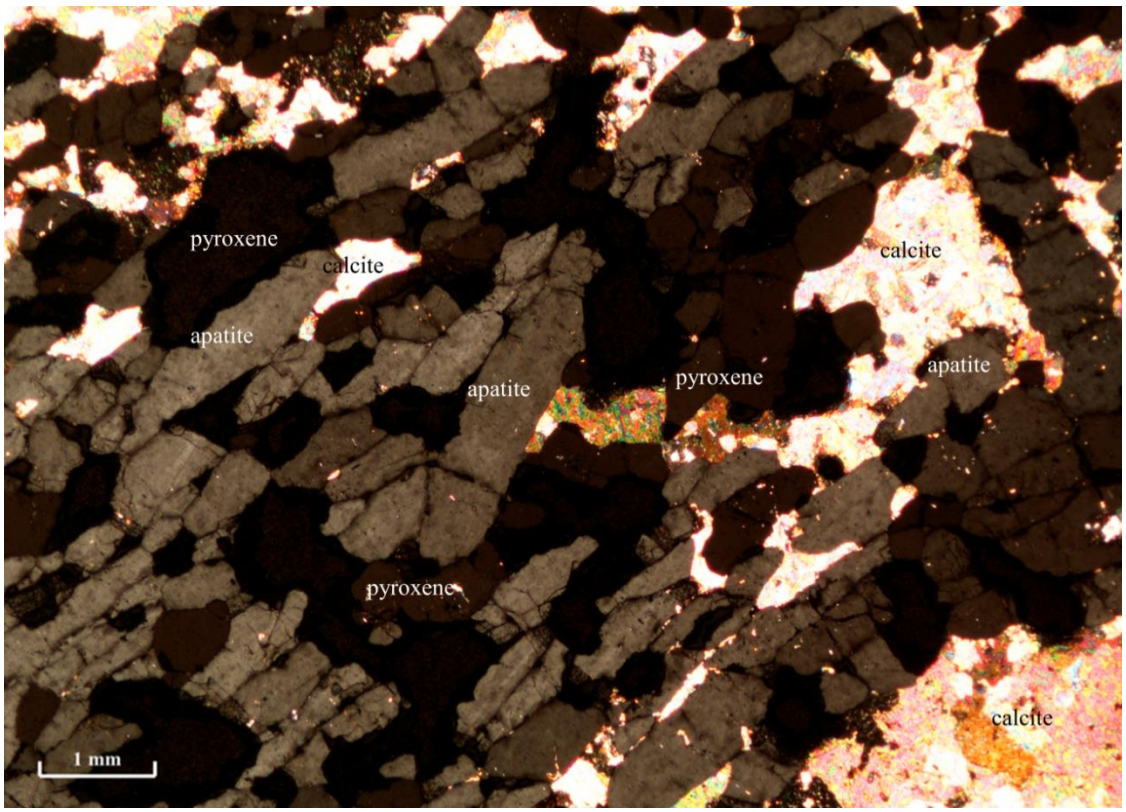

Figure 5.14 Photomicrograph of apatite concentration at the carbonatite-syenite contacts.

No mantle xenoliths were observed in the syenites although some rocks contain inclusions of the mafic series similar in composition to gabbros.

Dating of the alkaline rocks around Lofdal has been well documented and various ages obtained inferred the age of intrusion of the Lofdal and Oas syenites approximately 750 to 760 Ma. Various age data is compiled in Table 5.2. The ages of the Oas-Lofdal syenites concur with the timing of the rifting in the region at around 700 Ma.

The dates that tie down the age of the syenites are published by Hoffman et al. (1996), De Kock (2000) and Jung et al. (2007). The xenotime date given in Wall et al. (2008) is good evidence for the carbonatites being coeval with the syenites but not a very precise age for the complex overall.

Table 5.2 Ages of the Naauwpoort Formation

Oas syenite	756 +/- 2 Ma	Zircon	(Hoffman et al. 1996)
Oas quartz normative syenite	840 +/- 13 Ma	Rb-Sr	(Kröner 1982)
Oas/Lofdal syenite	764 ± 60 Ma	Rb-Sr whole rock	Hawkesworth et al. (1983)
Oas quartz normative syenite	783 +133/-141	U-Pb	Tegtmeyer and Kröner (1985)
Oas intrusive and metamorphic ages	783 ± 18 Ma	U-Pb	Tegtmeyer and Kröner (1985)
Oas	764 ± 60 Ma	the Rb-Sr whole rock	Hawkesworth et al. (1983).
alkali rhyolite Naawport Formation	726 ± 40 and 750 ± 65	U-Pb zircon	Miller and Burger (1983)
Oas quartz normative syenite	756 ± 2 Ma	U – Pb zircon	Hoffman et al. (1996)
quartz porphyries	752 ± 7 Ma	U- Pb zircon	De Kock et al. (2000)
Lofdal syenites	715 ± 9 to 751 ± 4 Ma	U – Pb titanite	Jung et al. (2007)
Oas quartz syenites	759 ± 4 Ma	U-Pb titanite	Jung et al. (2007)
Lofdal carbonatite	765 +/-16 Ma	U-Pb xenotime	Wall et al. (2008)

5.6.2.2 Breccias

Several breccia pipes are recognized and these are quite abundant and localised within the Huab metamorphic basement to the south of the study area, around the main syenite/carbonatite intrusions, in the syenite plug and along the contact with the syenites and the carbonatite plugs.

Breccia zones along the syenite and within the country rock are spectacular containing a wide variety of different rocks types, sizes and colours (Figure 5.15). Most fragments in the breccia can be easily recognized and related to different metamorphic rocks that outcrop in the surrounding areas. These breccias are interpreted to have formed at shallow depths because of the local origin of the fragments some of which are very large, and the local origin of all clasts.

Figure 5.15 Breccia zone marginal to the Main intrusion with fragments of different country rock types mainly schists, amphibolites, mafic rocks and cut by narrow veins of brown carbonatite

Fragments of carbonatite and syenite are also recognized and these increase towards the contacts between carbonatites and syenites. The shape of the brecciated fragments varies from tabular to angular, with larger fragments more angular than the smaller size. Field observations indicate that the magmatic breccia preceded the syenite intrusions but not the carbonatites. The breccia was probable produced by exsolution of magmatic gases that produced column of ascending fluids advancing ahead of carbonatite magma and exerting pressure upon the roof rocks.

5.6.2.3 Phonolites and Mafic rocks

Mineralogically varied phonolite dykes form part of the dyke swarm at Lofdal. The phonolite dykes cut the basement rocks and also the syenite plugs. They were rarely found to cut carbonatite although there is one location where a felsic dyke cross-cuts a carbonatite dyke. Their relationship with the basement, syenites and carbonatite rocks indicates that felsic dykes are younger than the basement rocks and the syenites, but older than the carbonatite plugs and dykes. Contacts of the phonolite dykes are generally sharp with chilled margins observed locally.

Chilled margins were best observed at the largest felsic dyke south of the farm Lofdal 491. The dyke has a wide variety of different sizes and lithologies of angular mafic and phonolitic xenoliths. Trachytic texture is well developed by the large laths of feldspar minerals that are aligned and emphasised by weathering. The dyke was evidently emplaced after the syenite plugs.

Most of the alkaline felsic dykes in the area are fine grained and porphyritic formed by feldspar and nepheline laths that are accentuated by weathering. The phonolite dykes have a general North-East direction with a steep dip (60^{o}C) towards the south and are fresh and undeformed and mostly parallel and or adjacent to the carbonatite dykes.

The minerals that make up the dykes are mainly potash feldspars, pyroxenes, biotite, chlorite, cancrinite, fluorite and magnetite. The pyroxene is ragged, dispersed and highly altered between the felsic minerals. All these minerals can be encountered forming the phenocysts in the trachytic texture. Minerals such as nepheline, alkali feldspar: plagioclase titanite, apatite calcite- mica (sericite), micas and cancrinite aggregates dominate the phenocrysts phases.

The interstitial material mainly consists of leucocratic minerals that are substantially, a mixture of fine grained sericite, carbonate, prismatic opaque, anhedral amphibole, altered feldspars and cancrinite.

5.6.2.4 Field features of carbonatites

Two carbonatite plugs, the largest carbonatite plugs in the area, are described here for the first time, namely the Main and Emanya carbonatites. They are both sövite (coarse-grained calcite carbonatite); both follow a regional sinistral NE-trending shear fault zone and are locally enclosed by breccias.

The relationship of the carbonatites and the nepheline syenites is of interest as these are closely related (Figure 5.16). Field relations indicate that the carbonatites postdate and fracture the nepheline syenite, indicative that both carbonatite and nepheline syenite may have exploited the same dilatational fracture systems.

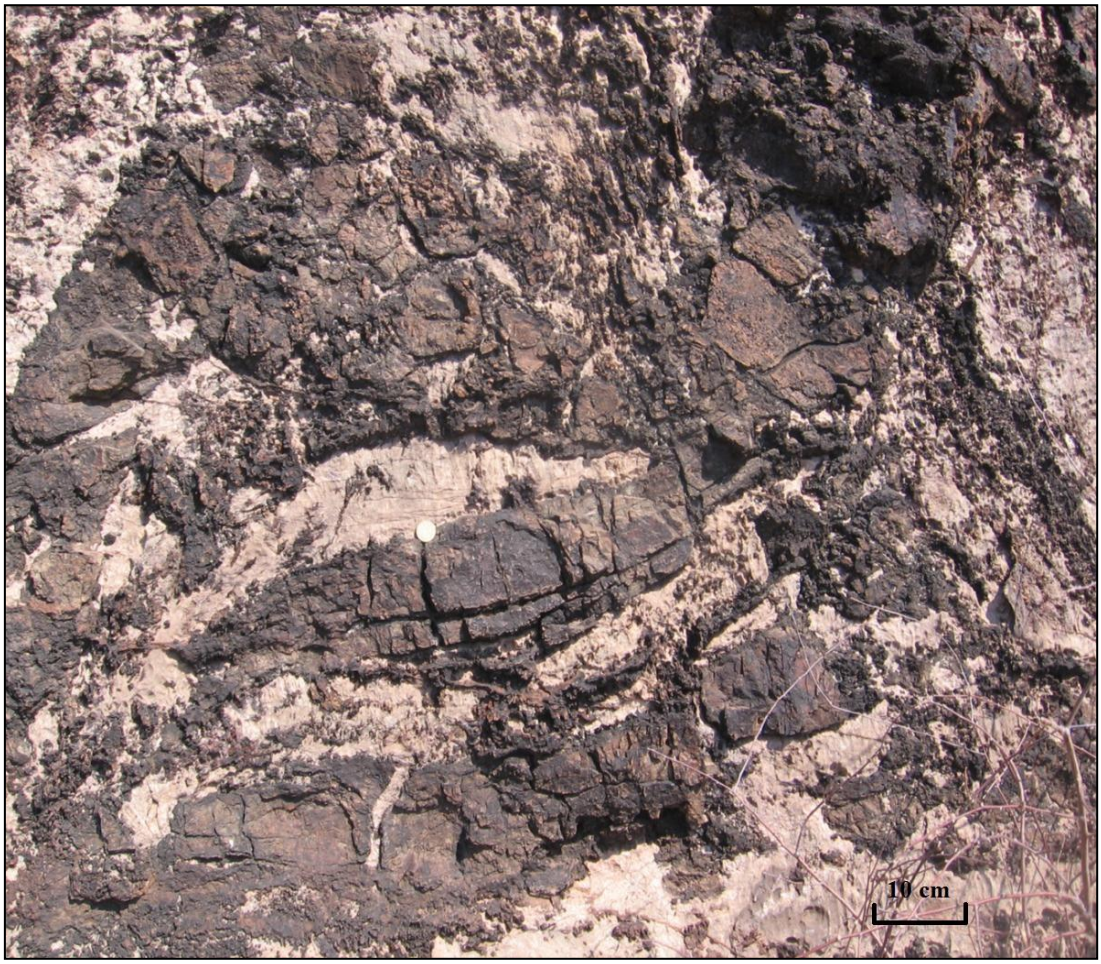

Figure 5.16 Contact between nepheline syenite (brown) and the carbonatite (cream) plugs forming stoping.

5.6.2.5 Main calciocarbonatite plug

The Main calciocarbonatite plug is the largest in volume among the calciocarbonatite plugs in the area. It is located on farm Bergville 490 approximately 2 km south of National Road D2625.

The author made the discovery of the Main carbonatite during field work in 2003, and subsequently discovered the second carbonatite body in the area (Emanya) together with Dr. R. Ellmies, a geologist of the Geological Survey at the time and a geologist from Etruscan Resources Ltd.

The Main calciocarbonatite trends a NNW-SSE direction and exclusively intrude the nepheline syenite plugs (Figure 5.14), forming patches below small hypabyssal plugs of nepheline syenite (Figure 5.15 and 5.17).

The main carbonatite attracted no special attention to other workers who mapped earlier the area, due to a low relieve and its coverage by the syenites. Also the difficulties to access the area, since there was no road passing nears the carbonatite outcrop, made their discoveries difficult. The intrusion has a shallow depth and has been weathered down. This weathering makes it appear in the field difficult to recognise from a distance as the only visible outcrops are the nepheline syenite apophyres that are found cropping above the carbonatite plugs.

The intrusion overall has an ellipsoidal shape in plain view with a core of sövite, that is surrounded by a marginal zone of metasomatised/fenitised syenites and country rock gneisses. Carbonatite and phonolite dykes occur in the fenite zone as well as in the country rock away from the main intrusion. A narrow rim of fenite occurs at the immediate contacts between the carbonatites and syenite plugs. The zone is rich in aegirine, pyrochlore and apatite. Further away the fenites are of varying intensity and can be identified in the country rocks around the intrusion with zones rich in chlorite and iron oxides. No contact with the country basement rocks was observed.

Syenite plugs at contacts with carbonatites stand high on top of the carbonatite (Figure. 5.16). The contacts with the syenite ranges are generally sharp but at places are gradational with increased sövite calcite veins cutting the syenites within about 5 m from the contact and dying out away from the contacts.

In places the nepheline syenite and carbonatites contacts are sharp (Figure. 5.17 and 5.19), with an observed zone of alteration in the syenites. The alteration zone extends up to tens of meters in the syenites. Feldspar minerals in this zone are altered and form large crystals. The nepheline syenite away from the contacts with the carbonatite appears fresh.

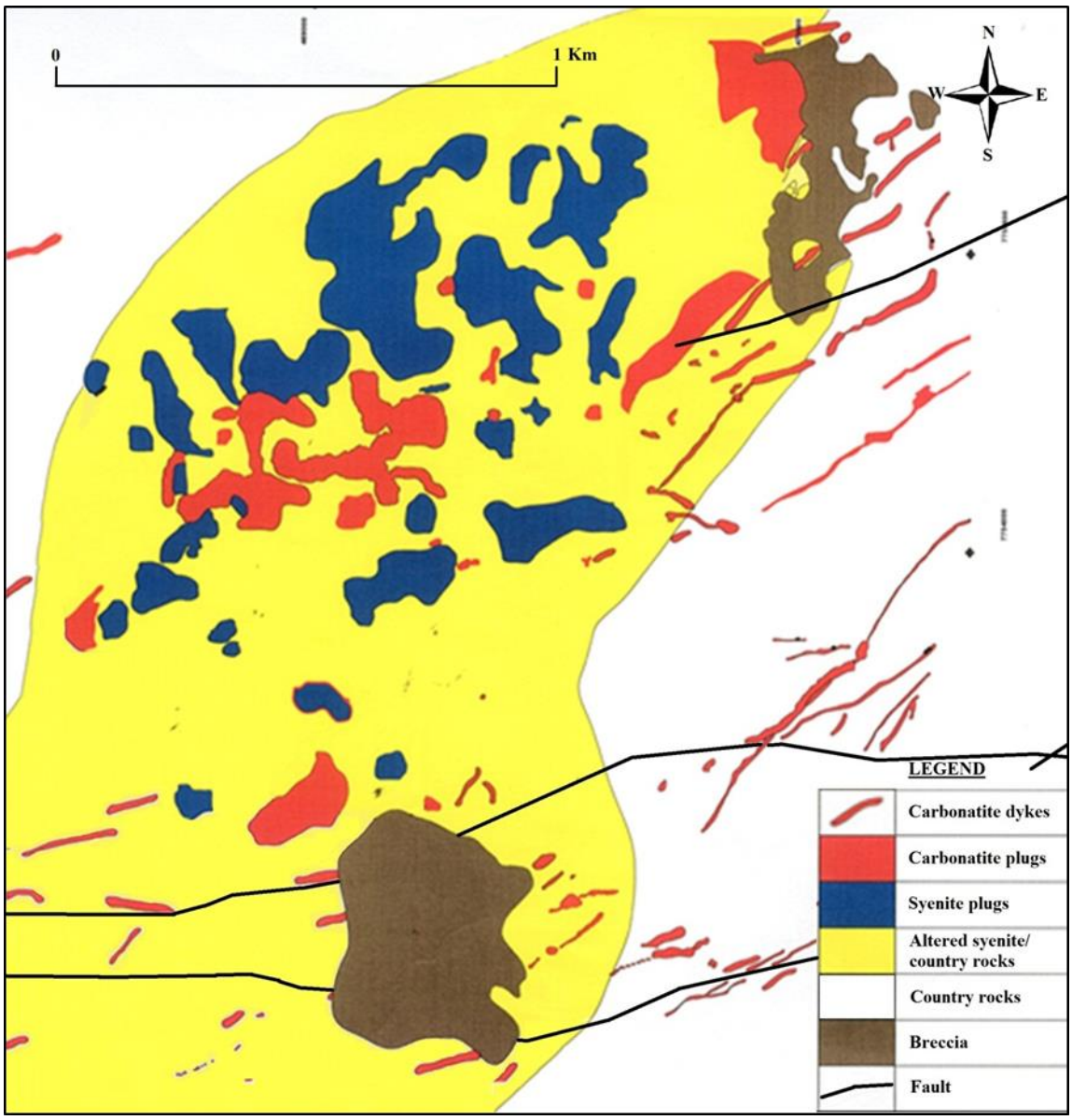

Figure 5.17 Geological map of the Main calciocarbonatite plug

Where the contacts are sharp the calcite grain sizes are larger. Clearly observation indicates that the carbonatites are of intrusive nature rather than replacement of earlier rocks. The texture of the carbonatite can however be described as variable because at places carbonatites are very coarse grained between 2 - 4 mm and at other places fine grained > 2 mm grain sized. Where calcite grain size is finer, there are a number of secondary micro calcite dykes that are brown in colour with higher concentrations of magnesium.

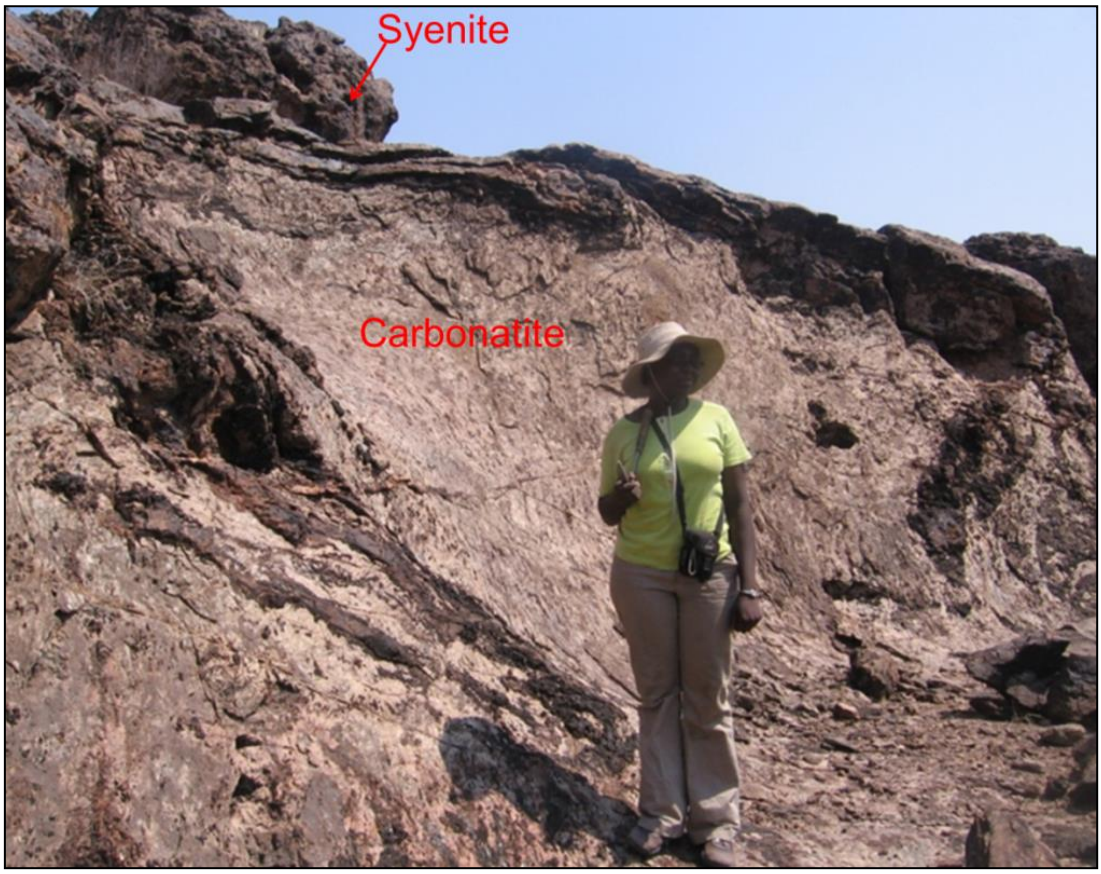

Figure 5.18 Calciocarbonatite plug capped by syenite

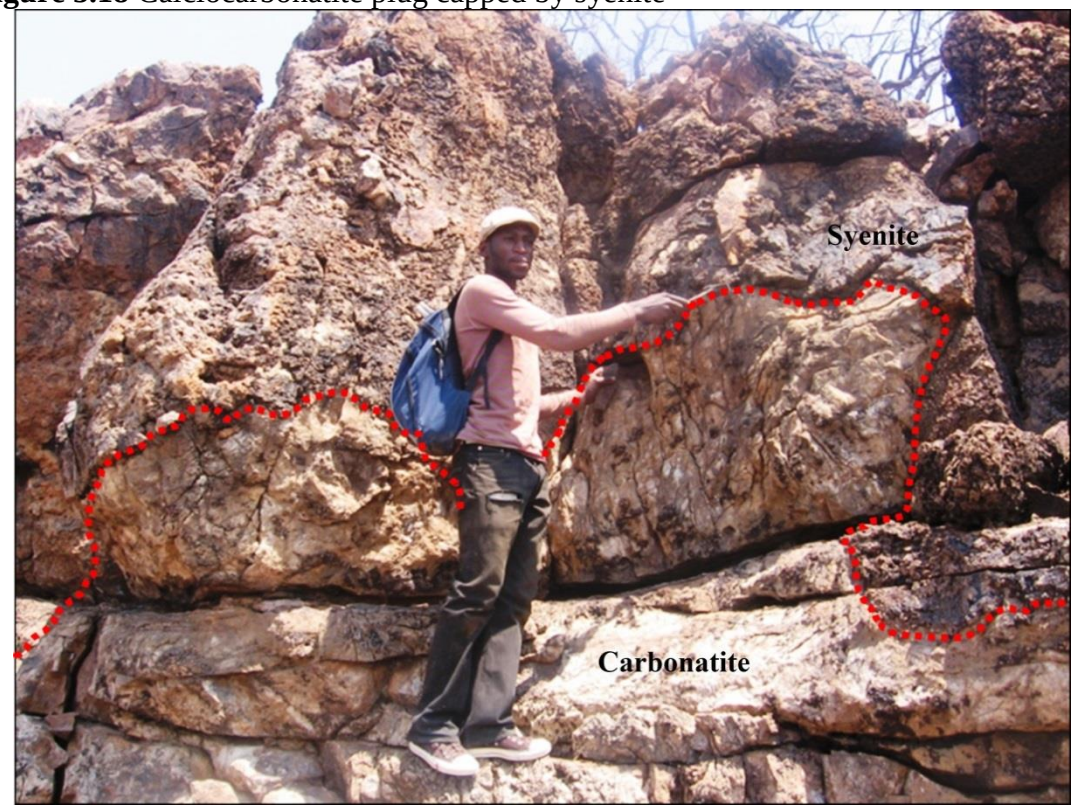

Figure 5.19 Sharp contacts (red dots) between syenite and carbonatite plugs

5.6.2.6 Emanya carbonatite plug

Recent mapping by the Geological Survey of Namibia and NRE, revealed the Emanya calciocarbonatite plug. Its discovery was guided by the observations from the

hyperspectral map in 2008. Emanya calciocarbonatite is a sövite intrusion of up to 0.7 km in diameter.

Like the Main calciocarbonatite, the Emanya intrusion follows a NE – SW direction similar to the regional structures and observed also in the dyke directions. Emanya has intruded into the Huab basement rock (Figure 5.20). The contacts are poorly exposed except to the North-West of the intrusion, where the carbonatite is in contact with the syenites.

The geology of Emanya calciocarbonatite is simple. It is dominantly made up of dark brown to reddish brown calciocarbonatite with abundant iron oxide and varying degrees of oxidation (Figure 5.11 and 5.22).

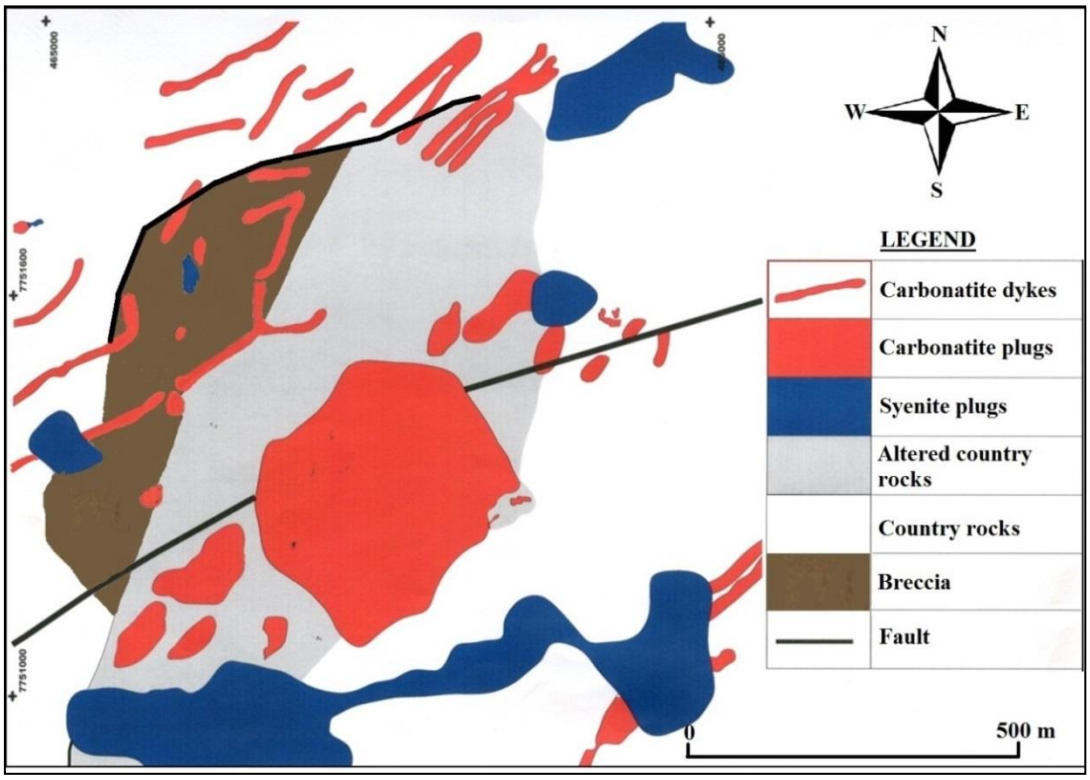

Figure 5.20 The geological map of Emanya calciocarbonatite after Swinden and Siegfried (2012).

Figure 5.21 Outcrop of the Emanya carbonatite plug

The Emanya carbonatite is dominantly a dark brown to reddish brown rock on weathered surfaces, with abundant iron oxide throughout the whole area and varying degrees of oxidation of the carbonatite (Figure 5.19). The rocks are brecciated and oxidized in the breccia joints **(**Figure 5.22). Oxidation gives a brown or less commonly a red colour to the weathered surface.

Metasomatic mineralisation along the much fractured zones on top of the calcitic intrusions is not observed. The gneissic schist is cut on the east of the Emanya intrusion by swarms of very close and up to 4m thick dark brown carbonatite dykes containing up to 25 % fluorite. The observation is unique to this location.

Figure 5.22 Brecciated and oxidised calciocarbonatite of the Emanya plug

5.6.2.7 Carbonatite dykes

The xenotime-(Y)-bearing carbonatite dykes are found mainly in the Bergville and Lofdal farms.

The Lofdal calciocarbonatite dykes are part of a swarm of about one thousand carbonatite and phonolite dykes which stretch over a strike length of up to 30 km. Individual dykes typically range from 0.5 –5 m wide but can be up to a maximum of 10 m wide and up to 15 km long. Many thousands of very narrow micro dykes with a width from only a few cm to less than 0.5 m are scattered in the areas mainly north and south of the Main carbonatite intrusion.

These dykes generally dip almost vertically (Figure 5.23) and generally intrude the basement rocks estimated at >1700 Ma (Frets 1969). Most of the carbonatites have intruded parallel and adjacent to, or even into the centre of the phonolite dykes and earlier granitic pegmatite dykes. The carbonatite dykes clearly cross cut all of the other rocks in the area, indicating that they represent the youngest intrusion event in the area. The dykes cutting the syenites are few but a stockwork of carbonatite dykes is observed at the contacts between the syenites and carbonatite plugs.

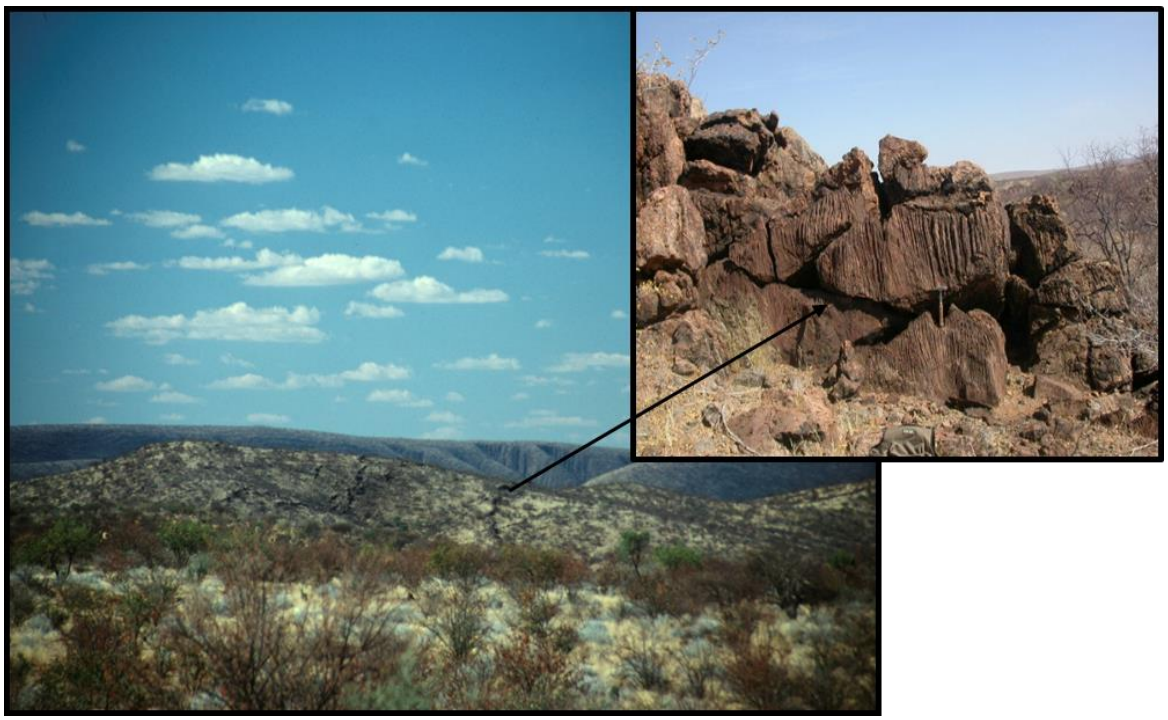

Figure 5.23 Narrow wall- like ridges formed by phonolites and carbonatite dykes

The narrow wall-like nature of the dykes makes them easily identifiable in the field and on the hyperspectral map. These narrow wall-like structures result from the resistance of carbonatites dykes to weathering compared to the surrounding basement gneisses

The biggest dyke stretches from the NE up to 15 km towards the main intrusion branching at about 7 km from the main carbonatite into NE and ENE branches. The composition at the branching point is mainly phonolite, while near the calciocarbonatite intrusion the dyke is a carbonatite, thus phonolite and carbonatite contemporaneous in one dyke. The direction is parallel to the observed faulting and shear structure in the area. There are also a number of small sub parallel dykes observed mainly in the hyperspectral maps. SE of the main calciocarbonatite intrusion, the dykes strike mainly a NNW-SSE direction forming two sets of dykes, especially in the east and southeast as seen in the hyperspectral maps.

The contacts are generally sharp with local breccia developed at places. In places the carbonatite dykes show folding structures (Figure 7.24), probably a result of the Damara event. Some carbonatite dykes contain inclusions of the phonolite, syenites and the country rocks. There are also local leakages of carbonatites into cracks in the country rocks and some carbonatisation.

A marked vvariable characteristic of the dykes is the colours that range from white to grey and through shades of brown, red and yellow colours. The variable colours seem to reflect the abundance and state of iron oxidation and the relative degree of hydrothermal alteration (Figure 5.25).

The intense yellow and red colours are observed in the most oxidised rocks and there appears to be no systematic relationship between colour and the amount of REE.

Carbonatites are variably deformed with some dykes clearly showing Damaran deformation, while most appear fresher. Textures in the carbonatite dykes are also variable as is their REE content. Multiple phases of carbonatite intrusion are observed within the dykes. Some dykes are brecciated, a characteristic only recognised in fresh rock samples (Figure 5.26).

Figure 5.24 Folding structures within the carbonatite dykes

Figure 5.25 Altered and oxidised carbonatite dykes from Lofdal

The minerals observed in the rocks are mainly calcite, hematite and magnetite, fluorite and minor sulphides. Highly sheared carbonatite dykes of calcitic, dolomitic or ankeritic composition show elevated radiometric readings.

The xenotime-(Y)-bearing carbonatite dykes have a stronger reddish-yellowish brown colour than the carbonatites plugs with some dark coloured banding, reflecting higher iron contents.

Figure 5.26 Brecciated dykes from Lofdal.

5.7 Fenitisation

Fenitisation has been recognized within the immediate contacts with varied mineral formation. Aegirine-augite up to 50 mm long is observed between the carbonatites and the syenites forming the fenite zone. Large albite-rich areas are also observed at the contacts with the carbonatites where oxidation of the carbonatite dykes is evident thorite crystals are observed in country rocks near the contacts with carbonatites and also in the carbonatite dykes.

The recognised types of fenites include:

I. Subordinate alkali feldspar, alkali amphibole and sodic pyroxenes (aegirine-augite) up to 50 mm long (Figure 5.27). In places large feldspar crystals reach up to 4 cm long with perthitic textures.

II. Albitite zones are observed at contacts between the country rocks and the carbonatite dykes. In places where oxidation of carbonatite dykes is evident

III. Thorite crystals are observed in the country rocks near contacts with the carbonatite dykes.

IV. Dissolution of carbonate and residual concentration of iron oxide are the dominant secondary phases. Partial dissolution and reprecipitation of apatite is also observed at the contact between the carbonatite and syenite.

V. Massive albitite with green phlogopite fenite. The brown stained albitite breccias are infused with carbonatite (dolomite) in the country rocks, but mainly are calcite and altered schist that has been carbonatised. Variably albitised iron stained carbonatites veins are intruded by late calcite carbonate veinlets.

VI. Chloritisation of ferromagnesian minerals observed in some dykes.

VII. Fenitisation has been recognized at immediate contacts of carbonatites and syenites with varied rock formation. At the contact between carbonatites and syenites, the fenites are observed by the presence

VIII. Other lithological alteration zones apart from hyperspectral images reveal a wide zone of iron and argillic alteration to the south and southeast of the main intrusion.

Figure 5.27 Aegirine-augite crystal at contacts between carbonatite and syenite plug.

5.8 Interpretation: Structural evolution and intrusion sequence

Combining field observations, the result of the applied remote sensing combined with other geological and geophysical methods indicates four main phases of intrusive phases and a sequence of tectonic events as following:

I. Uplifting and updoming creating ductile shear fracture zones
II. Compressional deformation and development of thrust faults, formation of a locked point leading to the formation of a duplex structure, which transects south of the Main intrusion. At the same time multiple uncontrolled faults were produced resulting from the compressional tensions.
III. Rise of the syenite and phonolite magmas, filling the created fault space. Some local breccia associated with these intrusions.
IV. Intrusion of syenite plugs and phonolite dykes.
V. Intrusion of the carbonatite plugs and dykes, which also produced further brecciation and subsequently filling of the existing faults and weak zones, including those in the country rocks.
VI. Further shearing, carbonatite intrusion and expulsion of the REE- rich carbonatite fluids along the existing shear zones within earlier carbonatite dykes and along the joint and fractures of the country rocks.

Syenite and phonolite associations are the most common in carbonatite complexes and are estimated to be present in 48% overall of 147 known occurrences (Woolley 2003). The association can be nepheline/sodalite/syenite; phonolite/tinguaite, gabbros, basanite and tephrite similar to those encountered at Lofdal.

5.9 Summary and conclusions

- Mapping of the alkaline dykes and plugs at Lofdal was aided by remote sensing methods, radiometrical geophysical survey maps, existing geological map, landsat images and a hyperspectral survey.
- Two calciocarbonatites bodies were discovered during the mapping programme: A sövite carbonatite referred to as the Main calciocarbonatite and the Emanya calciocarbonatite plugs.
- Interpretation of the hyperspectral maps led to the generation of follow up targets for ground sampling. Spectral reflectance properties of the Main calciocarbonatite plug were used as a standard to compare and delineate areas with similar reflections, leading to the discovery of the Emanya calciocarbonatite plug.
- Measurements of spectral reflectance showed various lithologies, mineral distributions, zones of alteration and structural features such as faults.
- Carbonatite dykes have higher and variable radiometric signatures than the carbonatite plug and the Huab Basement rocks. The source of most radioactive anomalies is thorite.
- Lofdal is situated on the southern rift margin of the Congo craton, at the intersection of the Northern Platform Zone of the central Damara belt with both the eastern Kaoko Zone and the Northern Margin Zone, but more specifically between the Northern zone and the Ugab tectonic Zone.
- The Lofdal alkaline carbonatite complex consists of carbonatite and nepheline syenites plugs, phonolite and carbonatite dykes. The complex has an ellipsoidal shape in plan with a NE-trending elongation.
- A thin marginal zone of alkali metasomatised syenite and basement rocks forms the contact zone between the calciocarbonatite and the syenite intrusion and/or the country rocks. The zone extends several meters from the carbonatite intrusions.
- Combined field observations, remote sensing, geological and geophysical methods indicate a sequence of tectonic events and they are as follows:

- As with most carbonatite complexes silicate rocks were emplaced before the carbonatites, which are the last phase to be emplaced at Lofdal.
- Several breccia pipes are localised within the Huab metamorphic basement, around the main syenite/carbonatite intrusions, in the syenite plug and along the contact with the syenites and the carbonatite plugs. These contain a wide variety of different rocks types, sizes and colours.
- Phonolite dykes are younger than the basement rocks and the syenites, but older than the carbonatite plugs and dykes. These are fine-grained and porphyritic formed by feldspar and nepheline laths and accentuated by weathering.
- The phonolite dykes have a general North-East direction with a steep dip (60^{o}C) towards the south. They are fresh, undeformed and mostly parallel and/or adjacent to the carbonatite dykes. The minerals that make up the dykes are potash feldspars, pyroxenes, biotite, chlorite, cancrinite, fluorite and magnetite.
- Both the Main and Emanya carbonatite plugs are sövites, following a regional sinistral NE-trending shear fault zone and are locally enclosed by breccias.
- The Main calciocarbonatite plug is the largest in volume among the calciocarbonatite plugs in the area. It exclusively intruded the syenite plugs. No contact with the country basement rocks was observed.
- The Lofdal calciocarbonatite dykes are part of a swarm of about one thousand carbonatite and phonolite dykes that stretch over a strike length of up to 30 km.
- The dykes generally dip almost vertically and intrude the basement rocks.
- Some carbonatite dykes strike in a NE direction, while others have a dominant SE striking direction.
- Variable characteristics of the dykes include colours ranging from white to grey, through shades of brown, red and yellow. The variable colours reflect the abundance, state of iron oxidation and the relative degree of alteration.
- Fenitisation occurs at immediate contacts with varied rock formations.
- Dissolution of carbonate and residual concentration of iron oxide are the dominant secondary phases. Partial dissolution and reprecipitation of apatite and pyrochlore is also observed at the contact between the carbonatite and syenite.

- Other lithological alteration zones are albitite, localized zones of green phlogopite fenite; brown stained albitite breccias infused with carbonatite (dolomite) in the country rocks, calcite and altered schist that has been carbonatised and chloritisation of ferromagnesian.
- Hyperspectral images reveal a wide zone of iron and argillic alteration to the south and southeast of the main intrusion.

Chapter 6: Whole rock geochemistry of the Lofdal alkaline carbonatite complex

6.1 Introduction

The major emphasis of this chapter is the geochemical characterization of the silicate intrusive alkaline and carbonatite rocks in the Lofdal complex, some related mafic rocks and dykes.

All analyses of the silicate rocks were obtained specifically for this project from samples collected in the field and analysed at the GSN. Representative samples of the carbonatites were also collected for the purpose of this thesis and analysed at the BGR and NHM. Additionally, a large number of analyses of surface grab samples were made available by Namibia Rare Earths Inc. (NRE) from their exploration programme. Drill sample number 58 was also used as a representative sample and the Mesopotamie hydrothermal carbonate samples obtained from NRE are included in the classification as some of the representative samples, while Mesopotamie is used for grouping purposes according to their REE distribution in carbonatites. Mesopotamie hydrothermal carbonates are included here for their doubtful origin and their high content of base metals. Appendix 2 (a and b) includes analyses of all samples provided by NRE that form part of this thesis. Analytical methods used for the different representative samples are described in appendix 1.

The felsic silicate intrusive rocks are part of the Bergville dyke swarm described by Frets (1969) and Miller (2008) and in this thesis are considered to be associated with carbonatite intrusions at Lofdal. These are mainly phonolites and nepheline syenites. The mafic rocks of the lamproic composition are also found intruding the felsic silicate rocks.

The alkaline dykes are younger than the intrusive plugs, cutting the Lofdal syenite but not the carbonatites. In this chapter, the whole rock compositions of the silicate rocks are compared with REE-rich carbonatites at Lofdal. The compositions of the silicate rocks are consistent with silicate rocks associated with carbonatites elsewhere as described by Woolley 2003.

Major element analyses were also used to geochemically classify the Lofdal carbonatites. REE distribution is used to group the Lofdal carbonatites into 8 major types. The various plugs and dykes of the Lofdal carbonatites are then compared with each other and with calciocarbonatites in the literature (e.g.Woolley and Kempe 1989).

The Lofdal carbonatite rocks are also compared with other REE-rich carbonatites elsewhere in the world. Below is the introduction of the samples studied in detail. The samples are grouped into 8 main groups and specially colour coded. These colour codes are used through the rest of the chapters (Figure 6.1).

Table 6.1 Eight (8) main carbonatite groups at Lofdal and their colour coding.

SAMPLE	Group	REE description
08-68, 326, 269	Main Calcio-carbonatite plug and Zero sample (269)	Relatively high LREE, low HREE
881R, 881G, 949	Emanya Calcio-carbonatite plug	Relatively high LREE, elevated HREE and low Y
119, 114	Dolomite dykes	Very low LREE and high HREE
813, 907, 115, 5769G	Type 1 dyke	Very high LREE, relatively low HREE (dykes); LREE>>HREE
927, 189	Type 2dyke	Very high Mid REE, High LREE and HREE; LREE<<MREE>=HREE
15769, 15769LG, 15796	Type 3 dyke	Very high LREE and HREE; LREE>>HREE<<MREE
914	Type 4 dyke	Very high LREE, relatively low HREE and elevated Y (LREE>>HREE); LREE>>=HREE
924	Type 5 dyke	High overall REE; LREE>>>HREE

6.2 Geochemistry of the silicate and ultramafic intrusive rocks

The major and trace element concentrations in 25 phonolites, mafic and ultramafic dykes and syenite plugs from Lofdal are presented in Table 6.2.

Most intrusive silicate rocks associated with the carbonatites were not analysed for the rare earth elements (REE), thus their REE content is not discussed here. The geochemistry of both Lofdal and the Oas syenite has been described in detail by Jung et al. (2007).

6.2.1 Major element geochemistry of the silicate and ultramafic rocks

The total alkalis range between 11.7 wt% and 18.6wt% in the phonolites but are more variable in the syenites ranging between 13 wt% and 23 wt%. The phonolites and the different types of syenites have between 44 and 50 wt% SiO_2.

Mafic inclusions have very high total alkali contents ranging from 12 to 15 wt% while the total alkalis in the mafic rocks are ranging from 3.2 to 3.7 wt%. Their SiO_2 content ranges from 39 to 45 wt %, the lowest of any silicate rocks in this study. Mafic rocks are relatively magnesian–rich (>7 wt % MgO), whereas evolved rock types such as phonolites and syenites have lower magnesia contents (0.2 –4 wt. % MgO).

The different rock types were classified based on whole-rock chemistry using SiO_2 versus K_2O and the TAS diagram (Peccerillo and Taylor, 1976 and Cox et al., 1979), respectively.

Table 6.2 Representative whole rock major (wt %) and trace element (ppm) compositions of alkaline silicate rocks associated with carbonatites at Lofdal. Values below the detection limit are indicated as "<" before the detection limit. Elements that were not detected are indicated with the sign ("-").

	phonolites													
Sample	VNP27	VNP30	VNP36	VNP38	VNP39	VNP50	VNP51	VNP114	VNP120	VNP128	VNP131	VNP139	VNP41	VNP31
SiO_2	47.7	50.4	47.8	50.5	50.8	48.2	49.8	48.8	49.5	50.6	49.7	44.5	50.5	41.0
TiO_2	0.4	0.5	0.3	0.3	0.4	0.3	0.3	0.4	0.4	0.4	0.6	0.4	0.3	1.4
Al_2O_3	24.6	14.8	21.2	20.0	20.4	21.7	22.2	22.3	22.9	22.0	21.3	21.3	21.8	20.2
Fe_2O_3	6.9	13.9	6.6	7.3	6.2	6.0	6.1	6.0	7.4	7.4	6.7	6.2	5.8	8.6
MnO	0.3	0.5	0.3	0.4	0.3	0.3	0.2	0.3	0.3	0.2	0.2	0.2	0.2	0.3
MgO	0.7	0.8	0.1	0.1	0.2	0.1	0.1	0.9	0.5	0.2	2.3	0.4	0.1	1.7
CaO	4.4	2.6	1.4	1.8	1.8	1.4	1.7	2.4	2.5	2.8	3.7	3.7	1.7	7.3
Na_2O	8.6	8.1	14.1	12.4	10.1	15.2	11.6	12.7	6.5	5.6	6.9	13.6	11.0	11.8
K_2O	3.2	5.0	4.5	3.2	5.7	3.3	4.9	1.6	6.2	7.0	5.4	5.2	4.9	3.5
P_2O_5	0.1	0.1	0.0	0.0	0.0	0.0	0.0	0.3	0.1	0.1	0.3	0.3	0.1	0.9
SO_3	2.2	2.3	2.5	2.7	3.1	2.3	2.3	3.4	2.9	2.7	2.1	2.8	2.3	2.5
Cl	0.1	0.2	0.5	0.4	0.2	0.6	0.1	0.2	0.2	0.1	0.1	0.1	0.3	0.3
F	0.3	0.3		0.1	0.1	0.5		0.2		0.1	0.3	0.9	0.2	0.2
TOTAL	99.3	99.6	99.3	99.4	99.4	99.7	99.3	99.5	99.3	99.3	99.7	99.6	99.4	99.6
As	<2.3	<2.3	<2.3	<2.3	<2.3	<2.3	<2.3	<2.3	<2.3	<2.3	<2.3	<2.3	<2.3	<2.3
Ba	2152	480	260	290	388	169	445	692	877	1174	938	1247	475	1214
Bi	< 5	< 5	< 5	< 5	< 5	< 5	< 5	< 5	< 5	< 5	< 5	< 5	< 5	< 5
Ce	469	81	227	242	102	50	44	95	366	113	45	106	134	170
Co	3.6	7	3.6	3.6	3.6	3.6	3.6	8	6	4	12	10	3.6	10
Cr	<2.3	<2.3	<2.3	<2.3	<2.3	<2.3	<2.3	32	<2.3	<2.3	137	<2.3	<2.3	<2.3
Cs	27	43	16	25	35	16	33	16	16	16	16	23	16	16
Cu	28	24	31	28	25	24	34	29	18	31	33	26	26	22
Ga	41	26	38	62	43	47	41	39	36	34	31	31	48	21
Hf	31	51	47	24	41	50	54	24	61	48	24	30	58	21
La	397	65	194	198	81	49	29	87	250	122	51	78	122	116
Mo	11	4	12	12	13	13	16	14	12	10	12	12	12	12
Nb	546	335	715	1758	925	762	786	546	548	638	359	510	724	365
Nd	134	39	66	82	43	28	28	44	170	90	28	54	68	114
Ni	2.6	2.6	2.6	2.6	2.6	2.6	2.6	6	2.6	2.6	45	2.6	2.6	2.6
Pb	64	14	35	20	15	17	51	34	63	103	10	20	15	4.5
Pr	115	38	64	61	33	30	30	54	87	30	46	46	38	40
Rb	83	165	172	162	224	132	162	73	213	274	255	194	160	100
Sb	40	40	40	40	42	40	40	40	59	40	40	64	40	40
Sc	< 5	< 5	< 5	< 5	< 5	< 5	8	< 5	< 5	< 5	< 5	< 5	< 5	< 5
Sm	<22	<22	<22	<22	<22	<22	<22	<22	<22	<22	<22	<22	<22	<22
Sn	24	24	24	24	24	24	24	24	24	24	24	24	24	26
Sr	963	382	1944	1587	1142	807	1272	2063	401	893	435	2181	1474	1109
Ta	15	13	14	49	27	17	21	25	23	17	18	17	16	20
Th	16	4.4	27	65	28	21	6	14	45	9	12	6	12	4.4
U	33	58	49	80	37	41	37	21	28	16	18	24	41	4.2
V	<8.7	53	<8.7	<8.7	<8.7	<8.7	<8.7	13	<8.7	<8.7	15	<8.7	<8.7	99
W	<4.3	<4.3	<4.3	<4.3	<4.3	<4.3	<4.3	<4.3	<4.3	<4.3	<4.3	<4.3	<4.3	<4.3
Y	64	19	34	84	28	27	20	38	90	38	27	35	12	31
Zn	149	226	289	368	190	265	242	215	267	162	174	176	230	124
Zr	1390	2149	1970	853	1733	2180	2231	1125	2401	2026	926	1315	2422	764

Table 6.2 (Cont.) Representative whole rock major (wt %) and trace element (ppm) compositions of alkaline silicate rocks associated with carbonatites at Lofdal. Values below the detection limit are indicated as "<" before the detection limit. Elements that were not detected are indicated with the sign ("-").

	Mafic rocks					Mafic inclusions in Syenite		Syenites			Sodalite syenite
Sample	VNP40	VNP44	VNP53	VNP18	VNP118	VNP31	VNP140	VNP34	VNP37	VNP68	VNP33
SiO_2	45.0	41.7	41.0	43.6	43.6	39.6	42.9	50.4	50.2	46.7	40.0
TiO_2	0.4	0.8	0.9	2.8	0.6	1.6	1.1	0.3	0.3	0.4	0.2
Al_2O_3	21.6	15.3	14.0	16.3	17.7	20.5	19.1	25.7	22.4	21.8	25.1
Fe_2O_3	5.9	9.1	9.6	13.7	12.5	10.2	8.7	5.9	3.6	7.9	4.0
MnO	0.2	0.4	0.7	0.2	0.1	0.3	0.3	0.2	0.2	0.2	0.3
MgO	0.4	6.9	4.4	7.5	8.8	2.2	3.3	0.5	0.3	0.3	0.4
CaO	3.7	14.3	13.3	8.4	10.5	7.4	4.6	1.4	1.4	6.1	2.0
Na_2O	13.8	5.6	8.4	2.4	2.9	10.8	11.2	9.4	12.3	9.3	19.2
K_2O	4.9	1.2	2.1	1.3	0.3	2.9	4.3	3.2	5.6	2.8	3.6
P_2O_5	0.2	0.3	0.5	0.6	0.1	1.1	0.3	0.1	0.0	0.1	0.0
SO_3	2.3	2.8	2.3	2.7	2.5	2.6	3.0	2.2	2.0	2.7	2.0
Cl	0.5	0.2	0.1	0.1	0.2	0.2	0.6	0.1	1.0	0.1	3.2
F	0.9	0.9	3.7	0.2	0.0	0.3	0.6	0.3	0.6	1.8	0.5
TOTAL	99.7	99.4	101.0	99.8	99.9	99.8	100.0	99.8	100.0	100.3	100.6
As	<2.3	<2.3	10	4	<2.3	<2.3	<2.3	<2.3	<2.3	<2.3	<2.3
Ba	1047	307	700	340	80	450	925	577	254	1206	225
Bi	< 5	< 5	< 5	< 5	< 5	< 5	< 5	< 5	< 5	< 5	< 5
Ce	210	442	359	123	5	180	90	106	317	115	139
Co	3.6	25	22	56	68	18	20	6	3.6	3.6	3.6
Cr	<2.3	213	<2.3	<2.3	320	<2.3	29	<2.3	<2.3	<2.3	<2.3
Cs	33	51	16	16	42	16	16	16	16	16	16
Cu	30	36	47	237	62	40	42	31	23	29	23
Ga	30	26	19	16	13	21	16	43	37	36	32
Hf	29	32	4	15	5	21	8	4	25	24	21
La	153	290	242	83	5	127	78	91	265	113	135
Mo	13	12	15	6	3	4	6	15	13	8	14
Nb	461	538	178	55	0	365	157	155	523	301	121
Nd	69	185	179	45	14	71	45	28	96	40	64
Ni	2.6	113	6	27	80	2.6	28	2.6	2.6	2.6	2.6
Pb	22	71	16	4.5	3	4.5	12	28	21	4.5	16
Pr	45	62	35	50	6	52	41	43	30	30	48
Rb	189	77	179	52	4	118	147	95	255	73	179
Sb	40	52	40	40	34	40	40	40	40	40	40
Sc	< 5	13	9	28	26	< 5	7	< 5	< 5	< 5	< 5
Sm	<22	34	<22	<22	<22	<22	<22	<22	<22	<22	<22
Sn	24	24	24	24	-4	24	24	24	24	24	24
Sr	2239	3957	2192	65	139	1027	1310	934	998	900	475
Ta	11	18	5.3	9	3	17	9	5.3	18	5	5.3
Th	10	79	20	4.4	14	4.4	4.4	4.4	4.4	4.4	5.3
U	19	23	6	5	1	8	4.2	8	105	17	12
V	<8.7	63	80	386	203	113	66	<8.7	<8.7	<8.7	<8.7
W	<4.3	<4.3	<4.3	<4.3	33	<4.3	<4.3	<4.3	<4.3	<4.3	<4.3
Y	29	117	119	38	22	34	19	20	9	46	13
Zn	188	142	224	72	220	135	116	476	137	60	147
Zr	1272	1349	61	384	45	717	278	195	969	880	779

Silicate intrusive rocks associated with carbonatites at Lofdal are classified as alkalic based on the SiO_2 versus K_2O diagram after Peccerillo and Taylor (1976) (Figure 6.1).

On the total alkalis versus silica (TAS) diagram (Cox et al. 1979), silicate intrusive rocks plot in the phonolite and phonolitic nephelinite fields, while the mafic rocks plot in the tephrite and basalt fields (Fig 6.2). The phonolite rocks vary in composition from phonotephrites through to phonolites (Figure 6.2). Alkali values are extremely high even for phonolites and as a result some points fall outside the defined boundaries on the TAS diagram. The sodalite syenite is much too alkali-rich (22.9 wt %) to display on this diagram.

On the CNK ternary diagram ($CaO + Na_2O + K_2O$), all samples except the mafic rocks plot in the Na_2O-rich part of the diagram, while the mafic rocks plot near the CaO end-member (Fig 6.3).

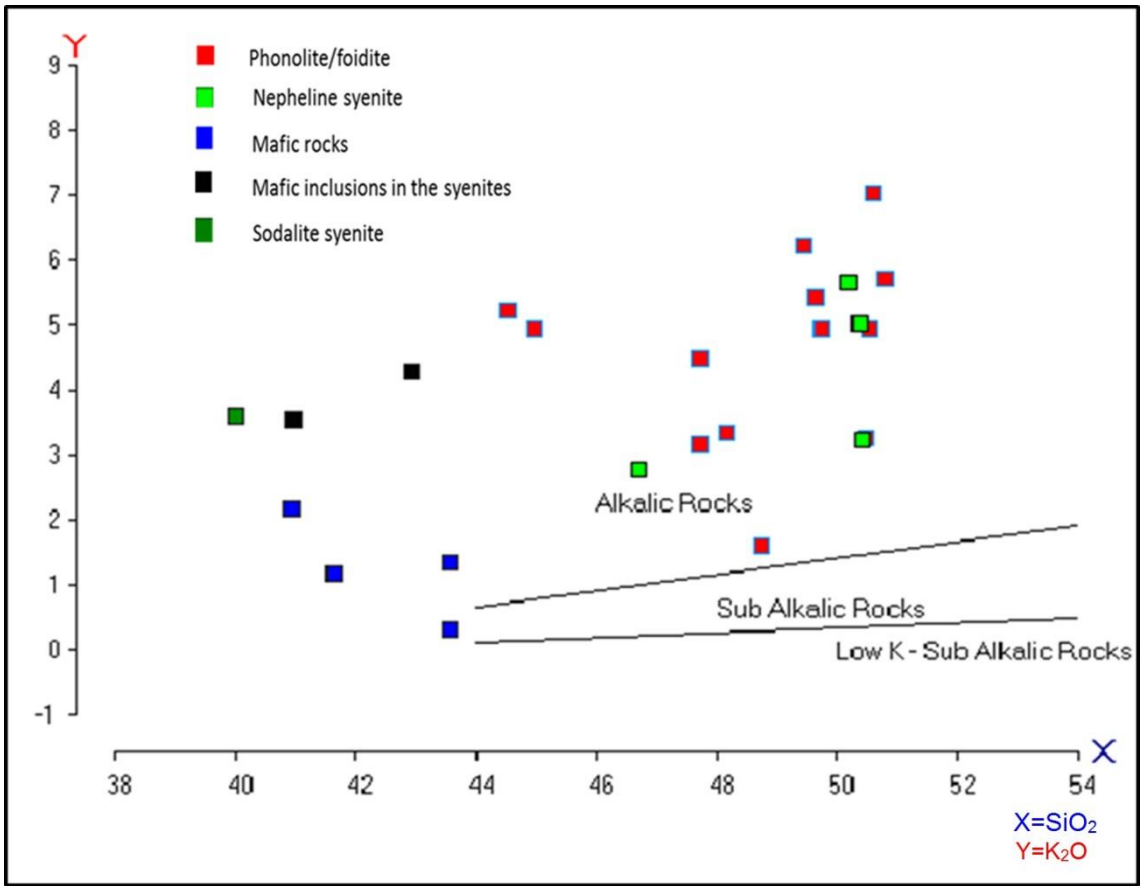

Figure 6.1 Classification of Lofdal alkaline rocks: K_2O versus SiO_2 after Peccerillo and Taylor (1976)

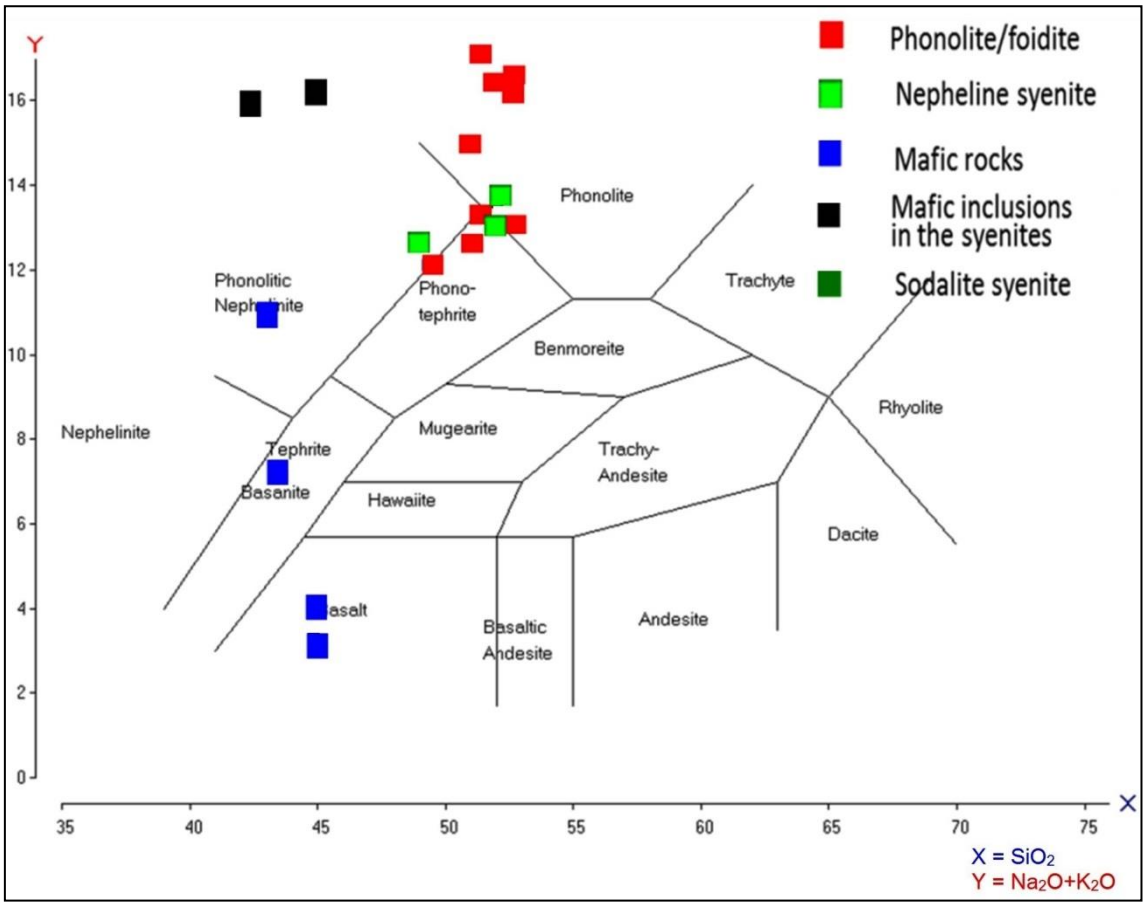

Figure 6.2 Classification of Lofdal alkaline rocks: Total alkalies versus silica (TAS) after Cox et al. (1979).

The concentrations of SiO_2 and $Na_2O + K_2O$ (total alkalis) increases from the mafic rocks to the phonolites and syenites. The Al_2O_3 versus total alkalis is typically considerably greater than one, indicating that the rocks are miaskitic (Figure 6.4). Total alkalis for the mafic rocks show a range between 3.2 -3.7 wt %.

Interestingly, the mafic rocks excluding the inclusions have SiO_2 contents similar to the mafic rocks, but their $K_2O + Na_2O$ content is similar to that of syenites and phonolites.

As expected mafic rocks have higher CaO contents than the syenites and phonolites. The phonolites, mafic inclusions and syenites are more sodic than potassic (Figure 6.3), a characteristic similar to the alkaline volcanic rocks of the Naauwpoort Formation of the Nosib Group (Miller, 2008).

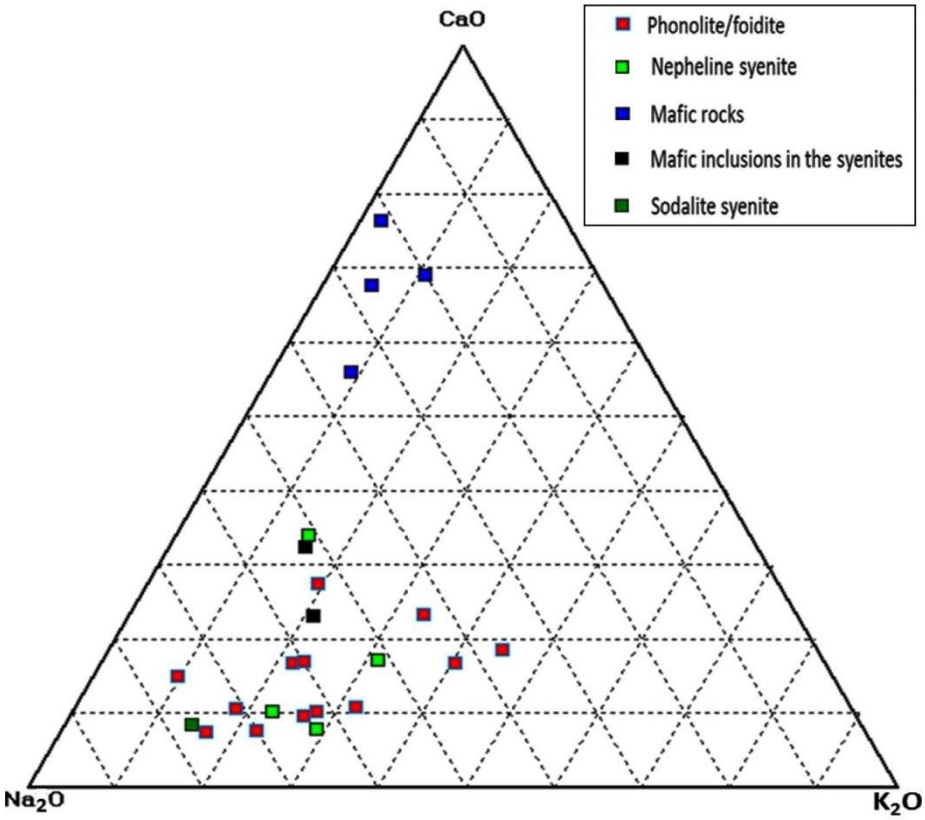

Figure 6.3 Na, K and Ca content in silicate rocks associated with the Lofdal carbonatites

Fenitisation is not clearly displayed in the mafic inclusions due to their small sizes but their high alkali contents suggest a degree of fenitisation. On the basis of Al_2O_3 – CaO – MgO content (Figure 6.5), the Lofdal felsic rocks are more aluminous than the associated mafic rocks. As expected, the phonolites and syenites plot near the Al_2O_3 apex, the inclusions from the syenites and phonolites in the upper middle, while the mafic rocks plot towards more CaO and MgO-rich compositions (Figure 6.5).

The phonolites, syenites and the mafic inclusions show high concentrations of Na_2O + K_2O and Al_2O_3 in comparison to the mafic members of the group. Nepheline syenite rocks have the highest concentrations of Na_2O + K_2O but Al_2O_3 plots more towards CaO and MgO-rich compositions (Figure 6.5) and the mafic rocks have the lowest values of Al_2O_3 (Figure 6.5).

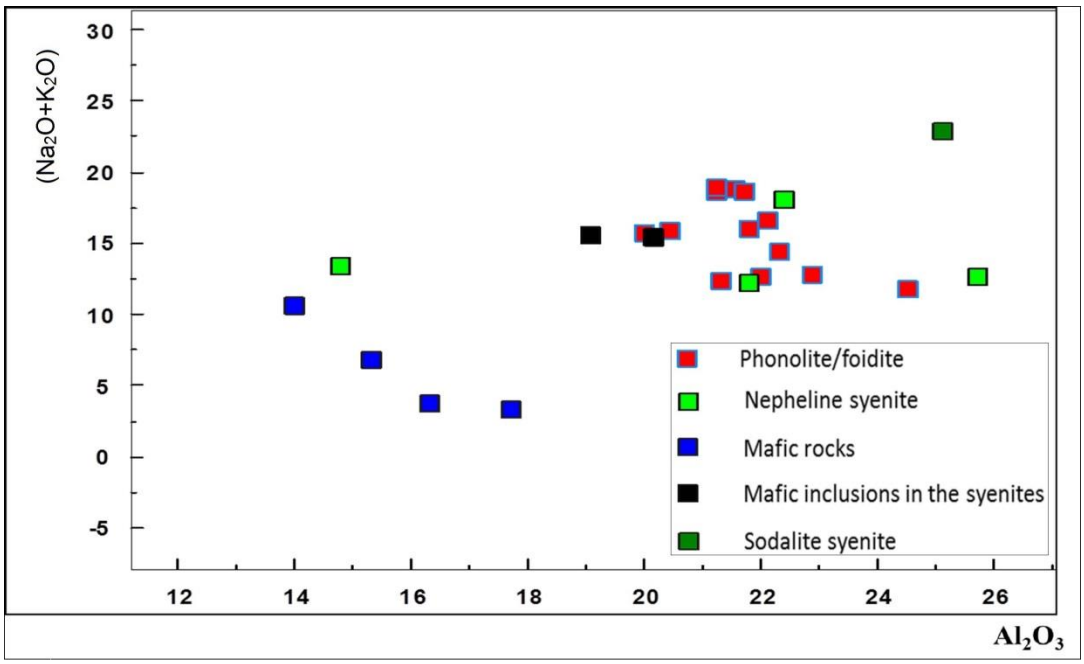

Figure 6.4 $Na_2O + K_2O$ versus Al_2O_3 plot of the Lofdal silicate rocks at Lofdal.

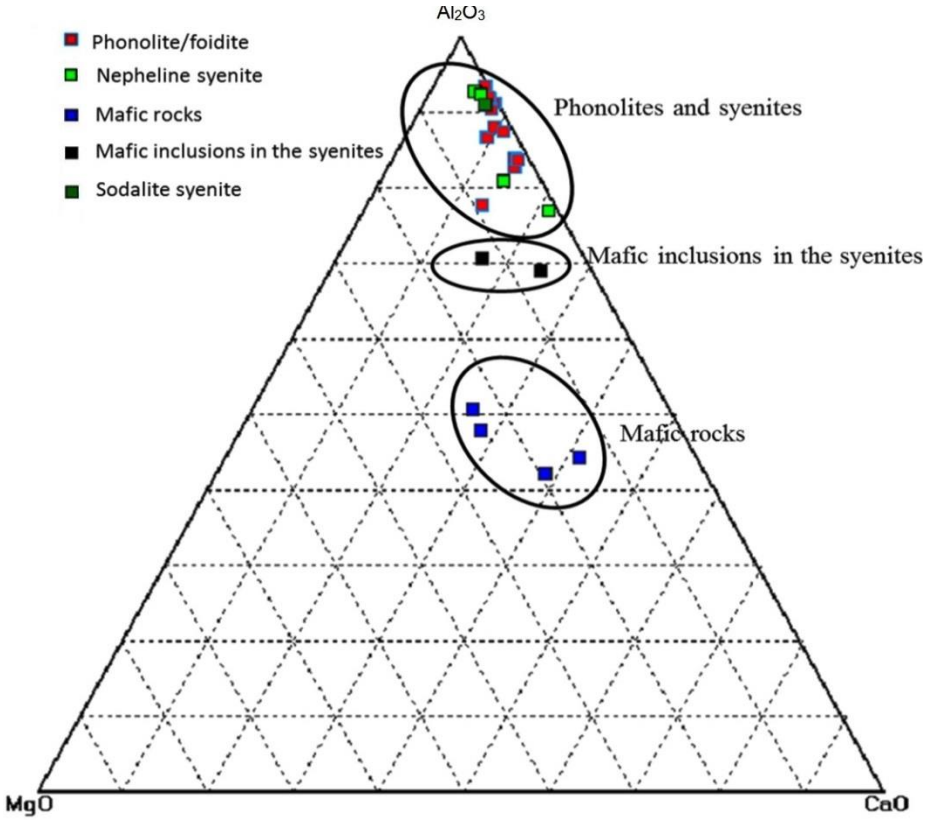

Figure 6.5 Al_2O_3 – CaO – MgO (wt %) ternary plots of the different silicate rock types associated with carbonatites at Lofdal, adapted from Rock (1987).

Harker diagrams show considerable dispersion of the data, especially Na_2O and K_2O which are particularly mobile during alteration. There is an indistinct decrease in P_2O_5, Na_2O, MgO and CaO with increasing SiO_2.

K_2O, MnO and Al_2O_3 show a slight increase with SiO_2 for the phonolites and syenites (Figure 6.6).

TiO_2, Fe_2O_3 and MgO are similar across the silica range of the phonolites and syenites except for the sodalite syenite sample. Such a gap between the sodalite syenite, the phonolites and the nepheline syenites suggests either contamination or separate origin for the sodalite syenite.

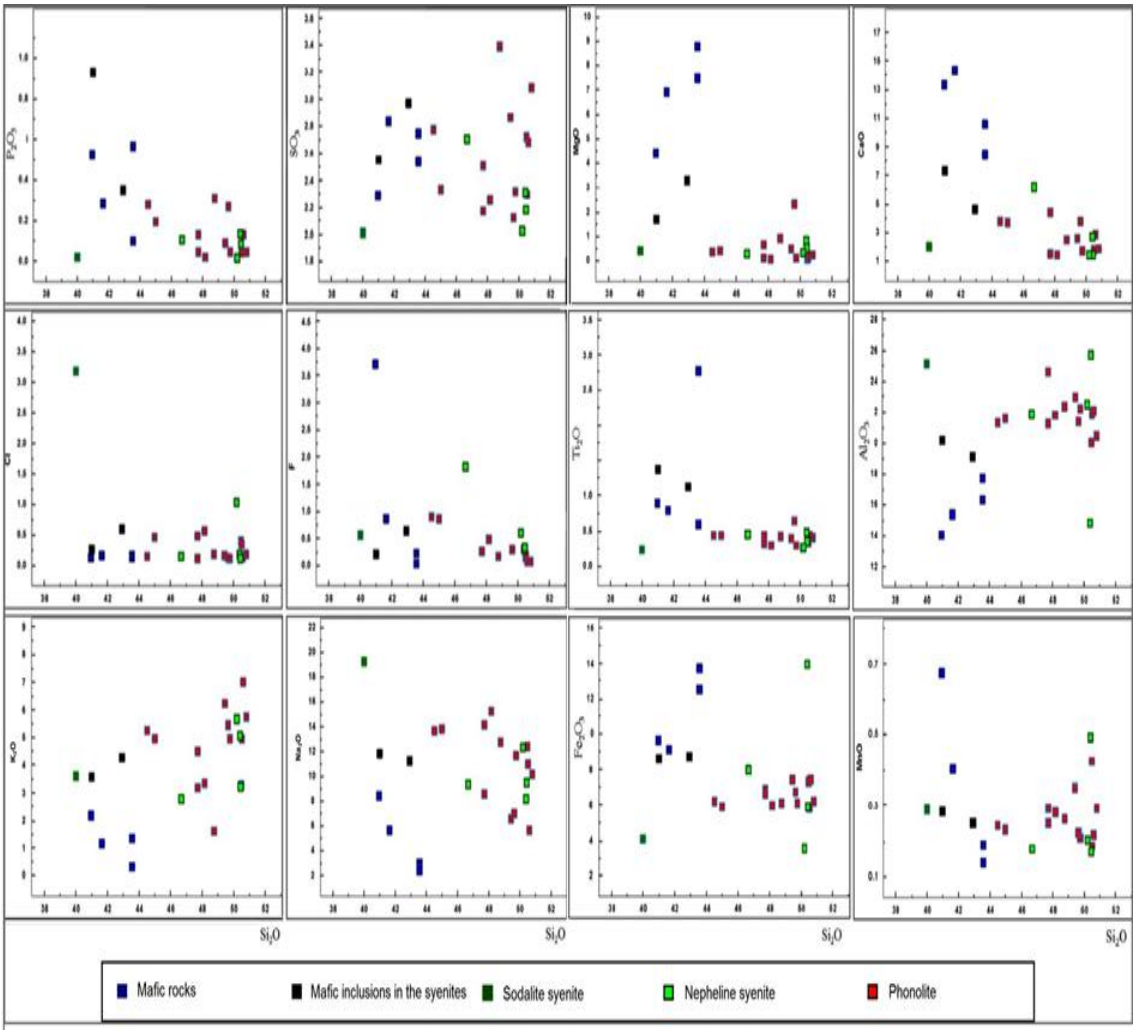

Figure 6.6 Major oxides versus SiO_2 (Harker) plots of the Lofdal alkalic rocks, showing variations in major element geochemistry

6.2.2 Trace element geochemistry of intrusive silicate and ultramafic rocks

The primitive mantle-normalized trace element diagrams for phonolites and syenites show very similar patterns (Figure 6.7a) supporting the interpretations from major elements that they are petrogenetically related. However, the mafic dykes at Lofdal have similar trace element distribution patterns to felsic rocks (Figure 6.7b) showing enrichment of Cs, U, Nb, Pb and Y. Th, Hf and Zr enrichment is observed only in some dykes. Elements such as K and Ti are depleted in all the mafic dykes, whereas Zr depletion is only observed in a few mafic dykes.

The three mafic dykes display a variable level of enrichment in Cs, Rb, Ba, U, Nb, Ce, Pr, Sr, Zr and Ti. High Ba contents in the mafic rocks is consistent with observed micas (phlogopite) in the lampropyres Elements such as Th, Ta, Pb, Nd, Sm and Y are similarly enriched. Yttrium displays the most uniform concentration in all the dykes, possibly due to its low concentration in these rocks and the log scale.

Major and trace element concentration from suite of 21 samples representing different lithological units of the silicate rocks, associated with carbonatite at Lofdal has permitted the following conclusions:

1. All intrusive silicate rocks, associated with carbonatite at Lofdal are classified as alkaline.
2. Geochemical classification using the TAS diagram classifies alkaline intrusive rocks at Lofdal as phonolite/ syenites, basanite and basalts. The basalts classification here includes the lamprophyres as these plots in TAS diagrams as basalts. The association of phonolite/ syenites, basanites and lamprophyres is common.
3. The data show considerable dispersion, especially Na_2O and K_2O reflecting a degree of fractionation or alteration.
4. The syenite plugs and phonolite dykes have very similar chemical characteristics and appear to be part of the same magma system.
5. The rocks are dominantly sodic rather than potassic and with total alkalis less than alumina, are not peralkaline (miaskitic).

The variety of trace element patterns shown by the nepheline syenites and phonolites of the Lofdal complex have also been observed in a number of other alkaline provinces (Foley et al. 1987, Gleason et al. 1994, Miller et al. 1999) that have moderate depletions of Pb, Rb and Th relative to Ba and U and their association to carbonatite is consistent with silicate rocks usually associated with carbonatites (Woolley 2010).

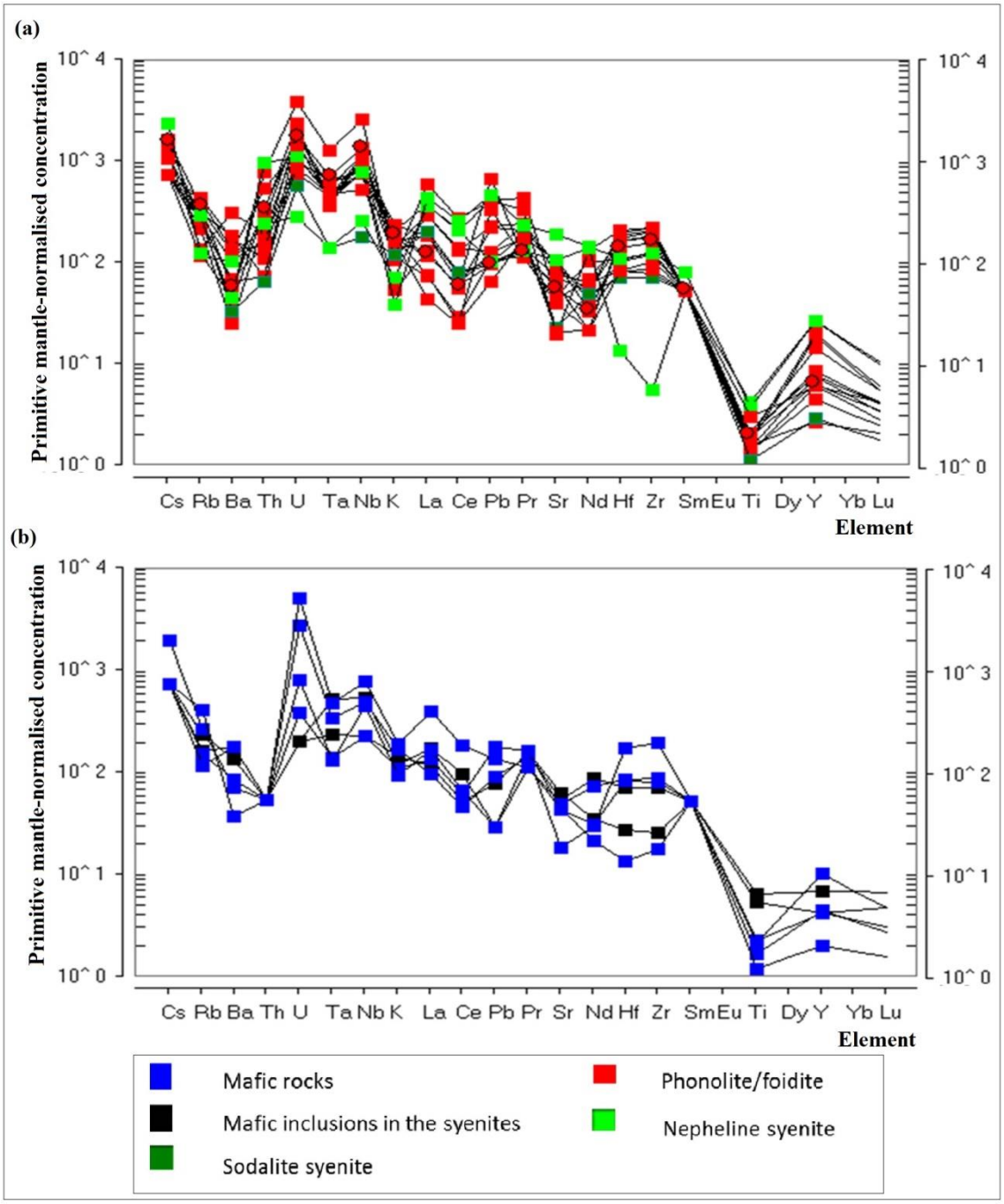

Figure 6.7 Primitive mantle-normalized trace element spider diagram (McDonough and Sun 1995) for the Lofdal silicate rocks showing only slight variability.

6.3 Geochemistry of the Carbonatites

The major and trace element compositions of the Lofdal carbonatite rocks are discussed here and used for their subdivision, classification and for comparison with other carbonatites in Namibia and worldwide. Analytical methods are discussed in Chapter 4. Diagrams summarizing the geochemical characteristics of Lofdal carbonatites are presented in this chapter.

6.3.1 Geochemical distribution/subdivision of the Lofdal Carbonatites

Geochemical data indicate major differences between carbonatite rocks from the Lofdal complex. Whole-rock, major- trace and rare earth element concentrations for representative Lofdal carbonatite samples are presented in Tables 6.3 and 6.4. For many years attempts have been made to systematise the geochemistry of carbonatites, (Samoilov, 1984, Nelson et al, 1988, Woolley and Kempe 1989, Rass 1998 and Chakhmouradian 2009). These studies revealed a number of important geochemical characteristics that can be used to track the evolutionary history of carbonatites. These characteristics together with specific geochemical patterns of the distinct REE patterns of Lofdal, allowed their classification into nine main groups: The Main and Emanya calciocarbonatite plugs, the dolomite Dykes, Types 1 to 5 dykes and the Mesopotamie hydrothermal carbonate dyke. The Main and Emanya plugs as well as Type 1, 4 and 5 dykes are overall LREE-enriched and differ from each other in absolute concentrations of the REE and degree of LREE-enrichment (i.e. slope of the chondrite-normalized pattern). Dolomite dykes and Type 2 and 3 Dykes are characterized by an overall LREE-depletion and a distinctive increase in normalized REE concentrations between Nd and Eu. They differ from each other in absolute REE concentrations and the relative enrichment in the HREE (i.e. slope of the chondrite-normalized trends from Eu to Lu). The Mesopotamie hydrothermal dyke is unlike any of the Lofdal carbonatites, with a relatively flat overall chondrite-normalized pattern and a small negative Eu anomaly. The nine geochemical groupings are here based on chondrite-normalized REE patterns and the ratios of LREE, MREE and HREE contents which are presented in Table 6.3 and Figure 6.8. The LREE are La, Ce, Pr and Nd, MREE are Sm, Eu, Gd, while the HREE are Tb, Dy, Ho, Er, Tm, Yb and Lu. Their REE compositions are compared in Table 6.5.

Table 6.3 Major and trace element composition (Wt %) of Carbonatites rocks at Lofdal. Values below the detection limit are indicated with "< "before the detection limit value. Elements that were not detected are indicated with ("-").

Sample Group	Main calcio carbonatite plug			Emanya calcio carbonatite plug			Dolomite dykes		Type 4 dyke	Type 5 dyke
Sample No:	58	326	269	881G	881R	949	114	119	914	924
SiO_2	2.57	0.18	1.72	2.13	1.13	2.24	30.29	12.47	2.96	1.30
TiO_2	0.01	<0.001	0.26	0.39	0.07	0.33	0.05	0.30	0.19	0.12
Al_2O_3	0.47	<0.05	0.51	<0.05	0.31	0.45	7.42	3.53	0.48	<0.05
Fe_2O_3	1.48	1.35	9.51	2.53	20.96	16.16	5.56	9.62	13.13	10.09
MnO	0.41	1.10	2.74	1.59	2.45	2.59	0.15	0.27	5.02	1.53
MgO	0.08	0.13	0.71	0.29	0.72	5.14	8.62	10.79	0.58	0.55
CaO	50.87	52.91	43.41	51.33	40.60	36.45	17.63	23.48	37.63	52.55
Na_2O	0.21	<0.01	0.08	<0.01	<0.01	<0.01	4.23	1.96	<0.01	<0.01
K_2O	0.22	<0.005	0.09	0.01	0.09	0.25	0.07	0.05	0.07	<0.005
P_20_5	0.11	0.04	1.23	0.17	0.03	0.02	0.12	1.41	1.10	1.78
(SO_3)	0.21	0.01	0.28	0.02	0.06	0.04	<0.01	0.01	0.13	0.11
(Cl)	0.01	0.02	0.01	0.01	0.01	0.00	0.00	0.01	0.01	0.00
(F)	0.08	0.08	1.08	0.28	<0.05	0.15	<0.05	<0.05	0.75	13.68
LOI	41.00	42.63	34.85	40.87	33.29	35.26	25.39	33.84	31.82	21.43
Sum	97.73	98.44	96.47	99.65	99.69	99.06	99.52	97.74	93.81	103.18
Trace Elements (ppm)										
(As)	<2	<2	43	8	8	13	9	27	<2	133
Ba	717	290	4472	132	48	24	25	17	51	134
Bi	<3	<3	20	4	4	<3	<2	<3	<3	4
Ce	400	471	3408	353	210	3129	46	21	25450	4721
Co	<3	<3	8	6	28	12	40	239	<6	67
Cr	<5	<5	<5	<5	<5	<5	58	122	<6	47
Cs	<4	<4	<4	<4	<4	8	<3	<3	45	6
Cu	28	19	22	34	52	25	3	<3	14	<4
Ga	2	<2	3	<2	<2	<2	7	<2	<3	<2
Hf	<7	<7	<8	<7	<8	<8	7	<7	14	<8
La	235	263	2115	217	152	2081	<15	16	14160	3375
Mo	<3	<3	46	<3	10	21	<3	<4	19	165
Nb	78	8	166	185	38	135	22	73	65	145
Nd	126	159	1157	87	63	878	<13	37	8525	1503
Ni	<3	<3	<3	<3	6	8	34	51	<4	12
Pb	7	8	64	9	<4	6	5	10	32	71
Rb	12	6	15	9	14	18	8	10	17	16
Sb	<12	<12	<12	<12	<11	<11	<9	<9	<11	<13
Sc	<3	<3	5	6	8	6	12	17	7	33
Sm	16	23	110	<16	<20	60	<15	23	754	262
Sn	<5	<5	<5	<5	<5	5	<4	<4	<5	<5
Sr	16810	11490	18640	1465	457	427	357	676	2482	1585
Ta	<5	<5	<6	<5	<6	<6	<5	<6	<7	<6
Th	40	30	190	51	19	80	98	412	330	3224
U	<5	<5	<5	6	6	7	10	21	<5	56
W	7	<7	31	n/a	n/a	20	n/a	n/a	17	64
V	<4	<5	37	44	40	19	36	73	37	241
Y	59	77	662	150	76	135	1117	13980	808	4327
Zn	11	9	864	16	65	31	18	19	18	31
Zr	85	33	352	14	13	12	460	210	19	38

Dyke type	Main calcio carbonatite plug			Emanya calcio carbonatite plug			Dolomite dykes		Type 1 Dyke				Type 2 Dyke		Type 3 Dyke			Type 4 Dyke	Type 5 Dyke
Sample:	58	326	269	881G	881R	949	114	119	813	15769G	907	115	189	927	15769	15769LG	15796	914	924
La	238	265	2032	228	141	2089	19	8	546	893	287	3126	190	68	394	998	533	13850	2952
Ce	442	512	3488	357	234	3312	35	17	923	1494	548	4462	341	198	719	1562	925	26334	4458
Pr	45	53	351	34	25	299	4	2	89	148	57	376	38	30	89	161	100	2612	420
Nd	150	172	1133	104	79	892	12	10	275	489	185	1027	158	152	420	594	404	8305	1362
Sm	22	23	143	17	11	79	6	12	33	66	28	91	227	128	497	536	455	908	280
Eu	6	6	38	6	4	19	3	12	9	18	8	18	102	71	139	230	191	194	123
Gd	16	18	103	18	9	43	16	71	23	46	24	56	291	286	237	602	531	461	419
Tb	2	3	16	3	1	5	5	25	3	5	4	9	41	60	17	73	73	42	61
Dy	13	15	107	24	10	27	36	206	17	27	23	67	180	353	59	286	359	160	278
Y	60	72	642	129	50	130	236	1538	88	116	146	473	584	1835	216	863	1325	742	1276
Ho	2	3	24	5	2	5	8	48	3	4	5	16	26	66	8	38	55	23	43
Er	6	9	72	19	8	17	26	146	10	12	14	56	57	175	21	82	134	52	109
Tm	1	1	11	4	2	3	4	23	1	2	2	9	7	25	3	10	17	6	15
Yb	5	8	70	29	15	22	33	143	9	10	15	61	38	161	17	60	103	33	95
Lu	1	1	10	5	3	3	4	19	1	2	2	8	5	23	2	8	14	5	13
ΣLREE	875	1002	7004	724	478	6592	70	37	1833	3024	1077	8991	727	448	1622	3315	1962	51101	9192
ΣMREE	45	47	284	41	24	140	25	95	64	129	59	165	620	485	874	1367	1177	1563	822
ΣHREE	90	111	951	219	91	212	352	2149	133	178	211	701	937	2698	344	1420	2079	1062	1889
ΣREE	1010	1160	8239	983	593	6944	446	2281	2031	3331	1347	9857	2284	3631	2840	6102	5219	53726	11903
La/Lu	355	219	213	49	53	604	4	0	407	582	138	378	41	3	170	125	39	3031	232
(La/Yb)n	32	22	20	5	7	67	0	0	41	59	14	35	3	0	16	11	4	294	21

Table 6.4 Representative REE (ppm) compositions of carbonatites rocks at Lofdal

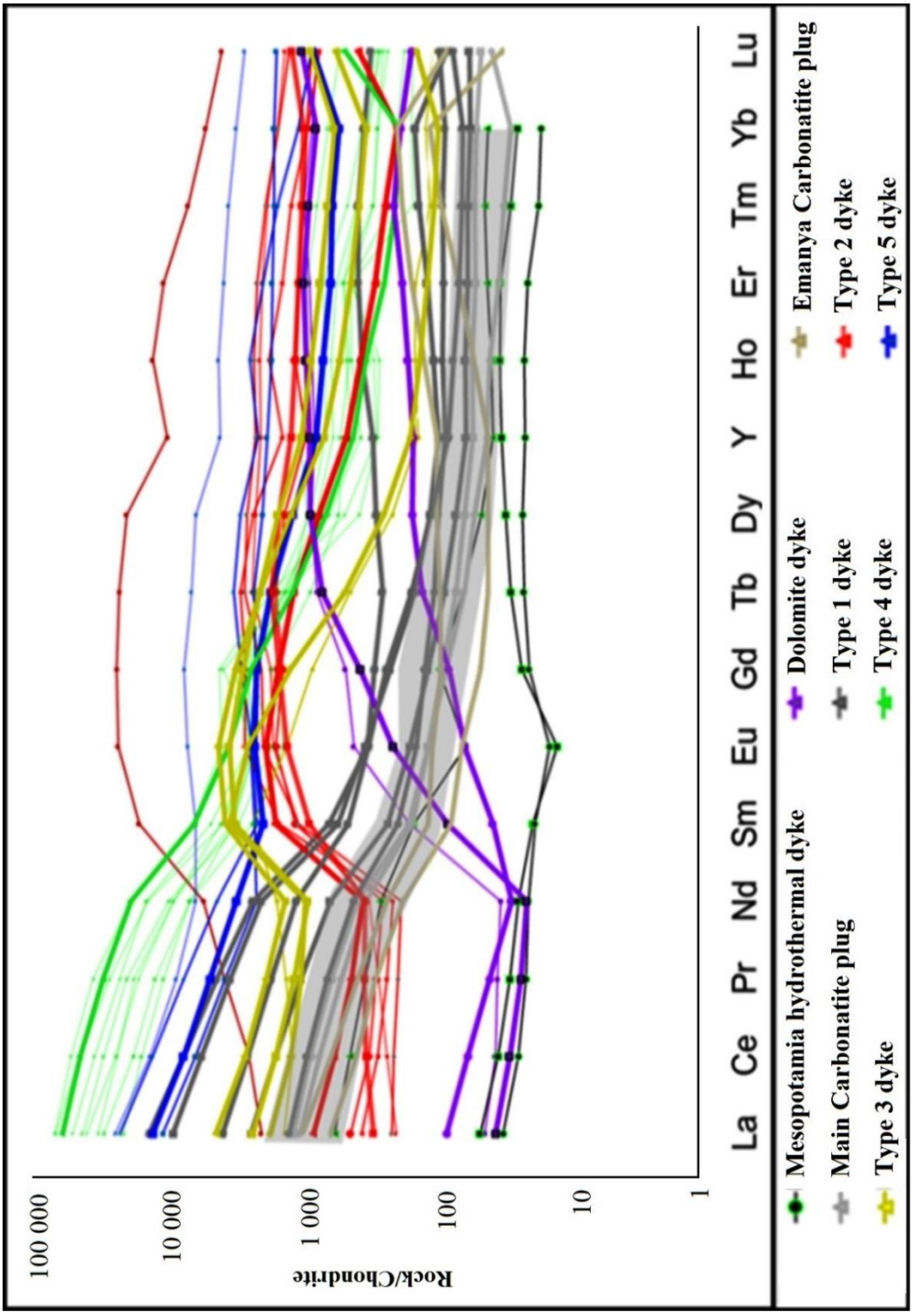

Figure 6.8 Chondrite-normalized REE-patterns of Lofdal carbonatites. The samples represented by thin lines and the grey shaded area (main carbonatite plug) represent 2970 samples from the Lofdal complex analysed by NRE while the bold lines are for the representative samples used in this thesis.

Table 6.5 Lofdal carbonatite groups based on REE content, REE patterns and LREE/HREE ratios. Concentrations in ppm (the numbers for LREE, MREE, HREE and TREE are averages). Colours used are consistent with the carbonatites subdivision at Lofdal.

SAMPLE	Group	LREE	MREE	HREE	ΣREE	MIN - MAX ΣREE	REE description
08-68, 326, 269	Main Calcio-carbonatite plug and Zero sample (269)	3352	141	384	3931	1009-8238	Relatively high LREE, low HREE
881R, 881G, 949	Emanya Calcio-carbonatite plug	2973	74	167	3211	2104-21729	Relatively high LREE, elevated HREE and low Y
119, 114	Dolomite dykes	53	60	1251	1364	446 - 2281	Very low LREE and high HREE
813, 907, 115, 5769G	Type 1 dyke	4165	107	343	4628	1347 - 9857	Very high LREE, relatively low HREE (dykes); LREE>>HREE
927, 189	Type 2dyke	588	553	1817	3182	2284 - 3631	Very high Mid REE, High LREE and HREE; LREE<<MREE>=HREE
15769, 15769LG, 15796	Type 3 dyke	2367	1132	1253	4621	2840 - 6102	Very high LREE and HREE; LREE>>HREE<<MREE
914	Type 4 dyke	51101	1563	1062	53726	53726 (5%)	Very high LREE, relatively low HREE and elevated Y (LREE>>HREE); LREE>>=HREE
924	Type 5 dyke	9192	822	1889	11903	11903(1.1 %)	High overall REE; LREE>>>HREE

The grouping and classification of carbonatite in this thesis is unusual and has not been noted elsewhere in the literature. Lofdal carbonatites have unique REE contents and distributions, especially with regards to MREE and HREE. These geochemical classifications used for these thesis best suits the purpose of description and provide a consistent and logical treatment of the rocks.

The geochemical classification of the Lofdal carbonatites provides a better basis for discussion of their characteristics than field observation and petrographic

characteristics, which did not provide a basis for classification of the carbonatite types using conventional methods such as their colour, mineralogy, texture and structure.

6.3.2 Major element composition of Carbonatites

Silica contents are generally low (<3%) in the calcio-carbonatite plugs and in some of the dykes. The highest SiO_2 concentrations are observed in the dolomite carbonatites, which contain up to 30 wt% SiO_2 and show secondary alteration, mainly due to albititisation and fluid-infiltration in the brecciated ankerite dolomite rocks. One sample of Type 1 Dyke rocks (sample 813) has a similarly high SiO_2 content (24.5 wt %) and a representative of Type 3 Dyke has similarly high SiO_2 concentration and contains substantial amounts of albite and quartz.

Na_2O and K_2O are variable although Na_2O is usually greater than K_2O. This variation is reflected in the presence of minerals such as albite (high Na_2O).

MgO contents are low, generally < 1 Wt %, except for the dolomite carbonatite (8.6 – 10 wt % MgO) and the Type 2 dyke (1.6 – 1.7 wt % MgO). Fe_2O_3 is often high but very variable.

Harker diagrams showing variations in major element contents among the carbonatites are presented in Fig 6.9. Na_2O and Al_2O_3 are strongly correlated with SiO_2, which almost certainly reflects the presence of variable amounts of albite.

The other major elements are generally variable and do not display any clear trends that might be related to fractionation or alteration processes.

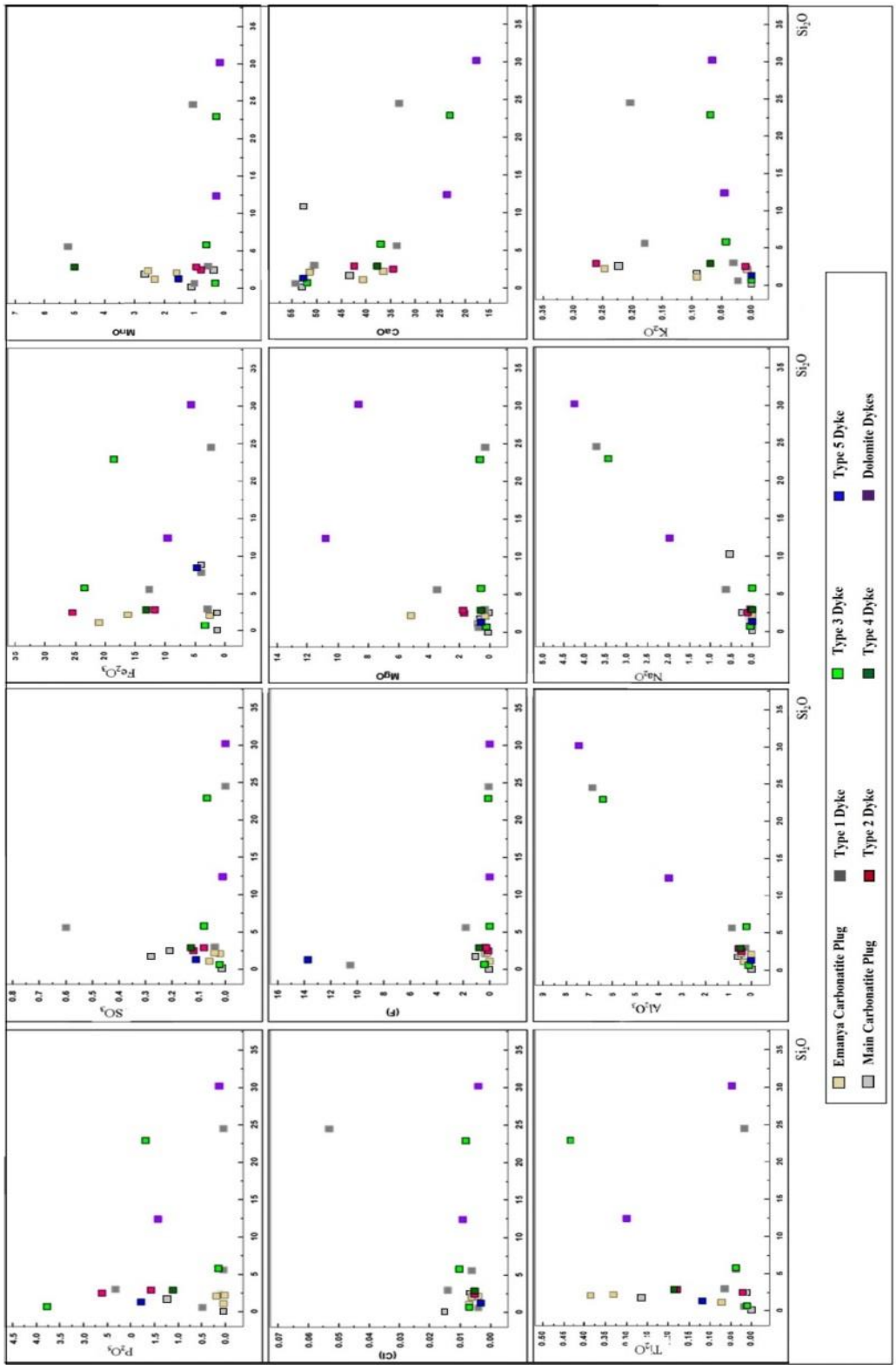

Figure 6.9 Harker diagrams showing variations of major elements among the carbonatite types with relation to SiO_2.

6.3.2.1 Classification of Lofdal Carbonatites

The Lofdal carbonatites are classified as calciocarbonatites, ferrocarbonatites and magnesiocarbonatites (Figure 6.10), based on the presence and abundance of carbonate minerals as recommended by the IUGS (Le Maitre et al. 2002). The use of whole rock major elements was also considered in the classification by Woolley and Kempe (1989). Samples 927, 189, 914 and 924 belonging to Types 2, 4 and 5 dykes have highest Fe values and are classified as ferrocarbonatites according to Le Maitre et al. (2002) and as ferruginous calcite carbonatite according to Gittins and Harmer (1997). The ferruginous monazite-(Ce) - xenotime-(Y)-bearing calcite carbonatite described by Wall et al. (2008) belongs to this group.

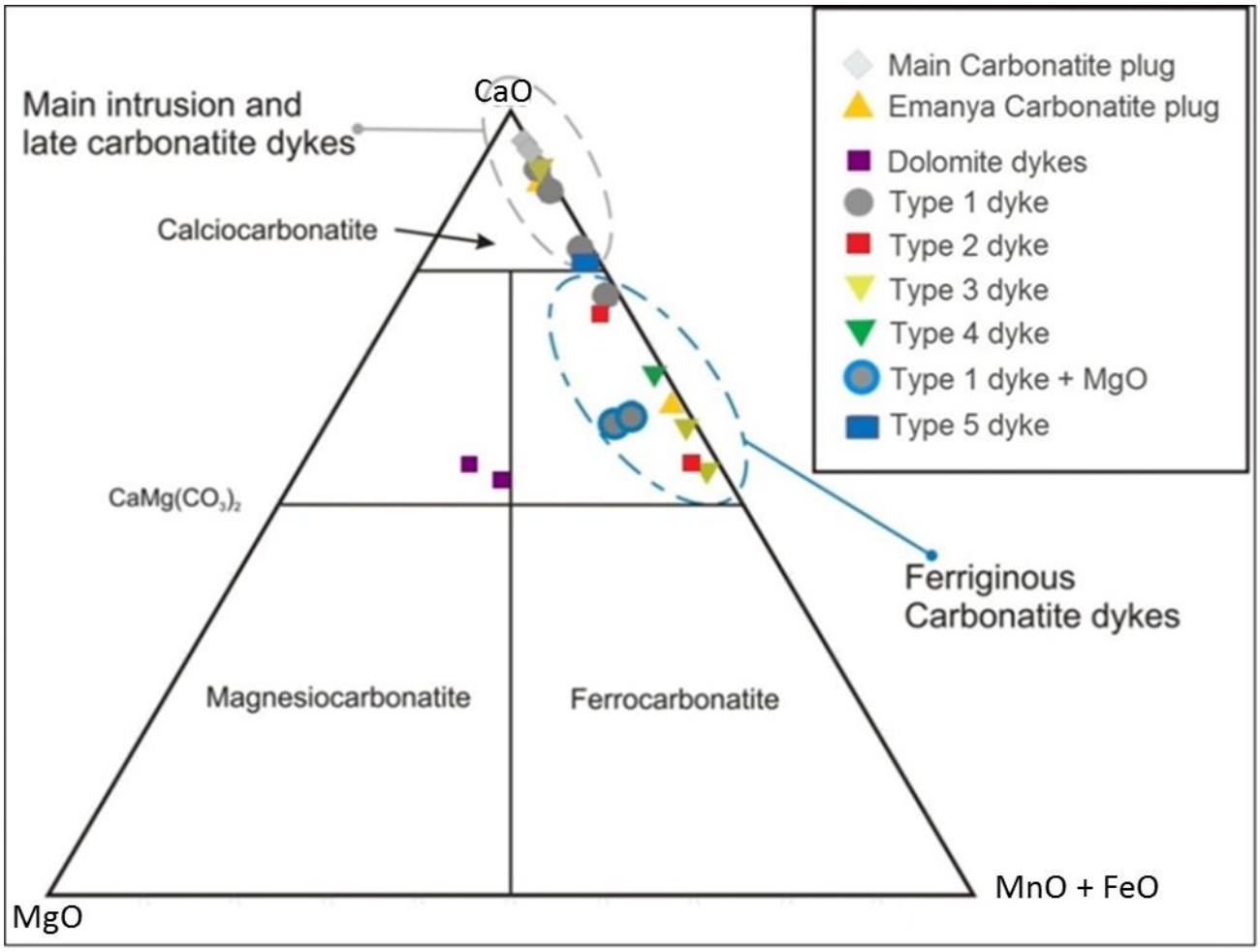

Figure 6.10 Lofdal samples displayed in the classification diagram for carbonatite using wt. % oxide (after Woolley and Kempe 1989).

6.3.3 Geochemical Characteristics of the Lofdal complex carbonatite groups

The different groups of carbonatites at Lofdal are here presented individually and their description given with relation to their REE pattern as well as their specific geochemical behaviour (Figure 6.11).

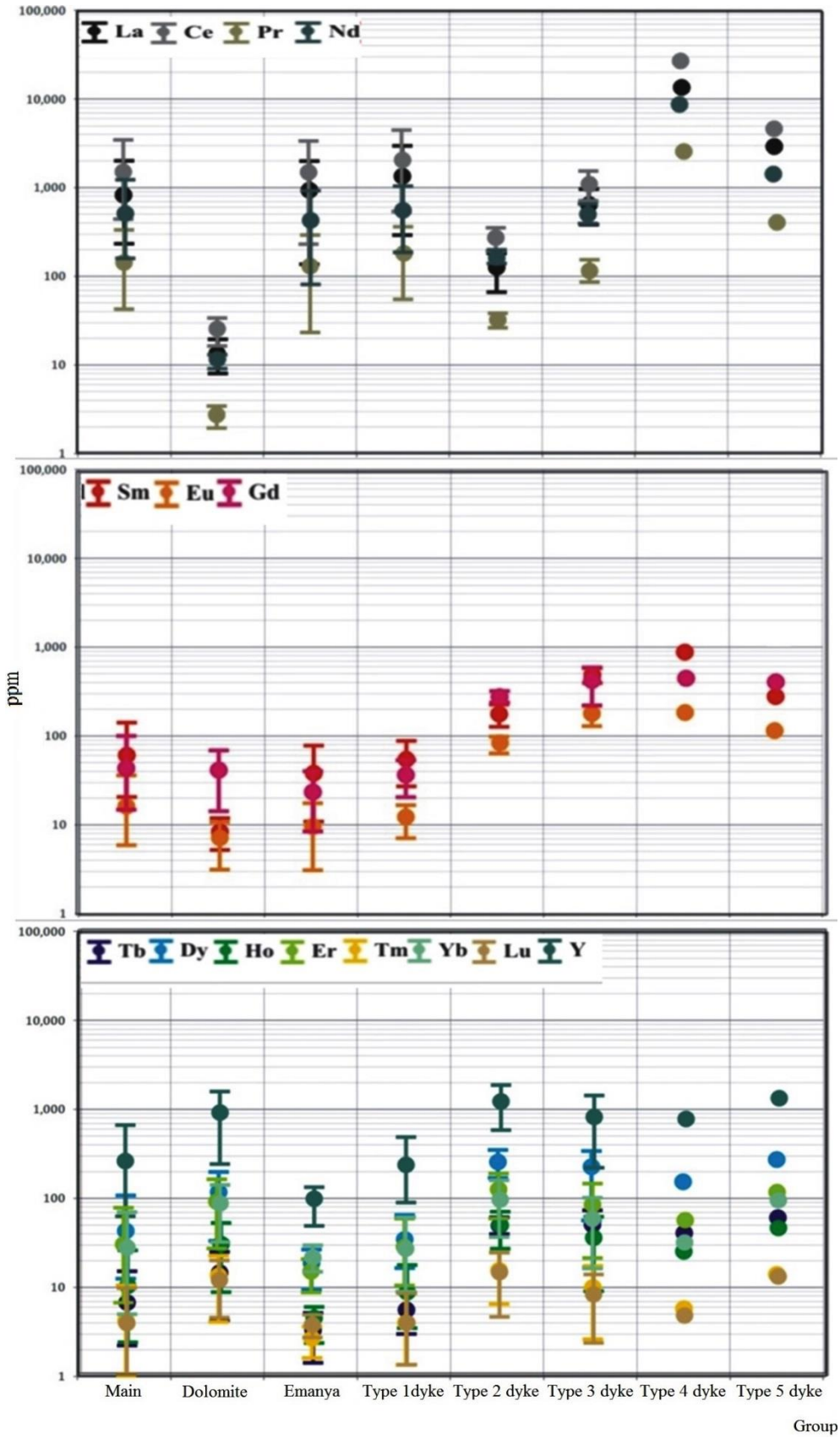

Figure 6.11 LREE, MREE and HREE distribution in the Lofdal carbonatite rocks.

6.3.3.1 Main carbonatite intrusion

The “Main carbonatite” group contains rocks from the main calciocarbonatite intrusive plug (samples FRC 08_58, 326). It also includes one of the calcite carbonatite dykes (269 or Zero sample) that exhibits a geochemical pattern similar to that of the Main carbonatite and appears to be the least altered of all the dykes outside the Main and Emanya carbonatite intrusions. Despite this similarity in the geochemical element patterns of the Zero sample with the main plug, the concentration of REE and incompatible elements are much higher than in the carbonatite plugs. Hf, Ta and U concentrations are consistent with the values in the main carbonatite plug. CaO showed highest values of > 50 wt% in the main carbonatite plug, whilst in the Zero sample the CaO content reached only 43 wt%.

The carbonatites of this group are coarse-grained with well-formed rhombohedral white crystals. The group plots in the field of calciocarbonatite and specifically into the sövite field (Figure 6.10). The Zero sample shows more alteration and higher REE concentrations than the plugs, but considering the geochemical context and isotopic characteristics, the Zero sample is assigned to the group of the Main carbonatite plug.

The distinctive geochemical characteristic of the Main carbonatite group is the relatively low ΣREE concentration. The LREE are enriched relative to the HREE (Figure 6.12), a common trend of most carbonatites worldwide. The average ΣREE concentration of the Main calcio-carbonatite plug is approximately 0.3 wt % and thus slightly lower than the average calcite carbonatite ΣREE concentration of Woolley and Kempe (1989). The ΣREE concentrations in the Main carbonatite type range between 0.1 – 0.8 wt %. The maximum HREE values are consistently higher than the values of average carbonatite (Woolley and Kempe 1989). The lower values are consistent with the limits of the calciocarbonatites worldwide.

Samples from the Main carbonatite plug show the lowest concentrations of trace elements of all carbonatite groups at Lofdal, particularly the high field strength lithophile elements (HFSE), as defined by Chakhmouradian (2006). Elements such Hf, Ta, Nb and U are below the detection limits of 5 and 8 ppm in all samples of this group, although samples from the immediate area of the Main carbonatite contact locally contain higher values of Hf, Ta, Nb and (sample 228d).

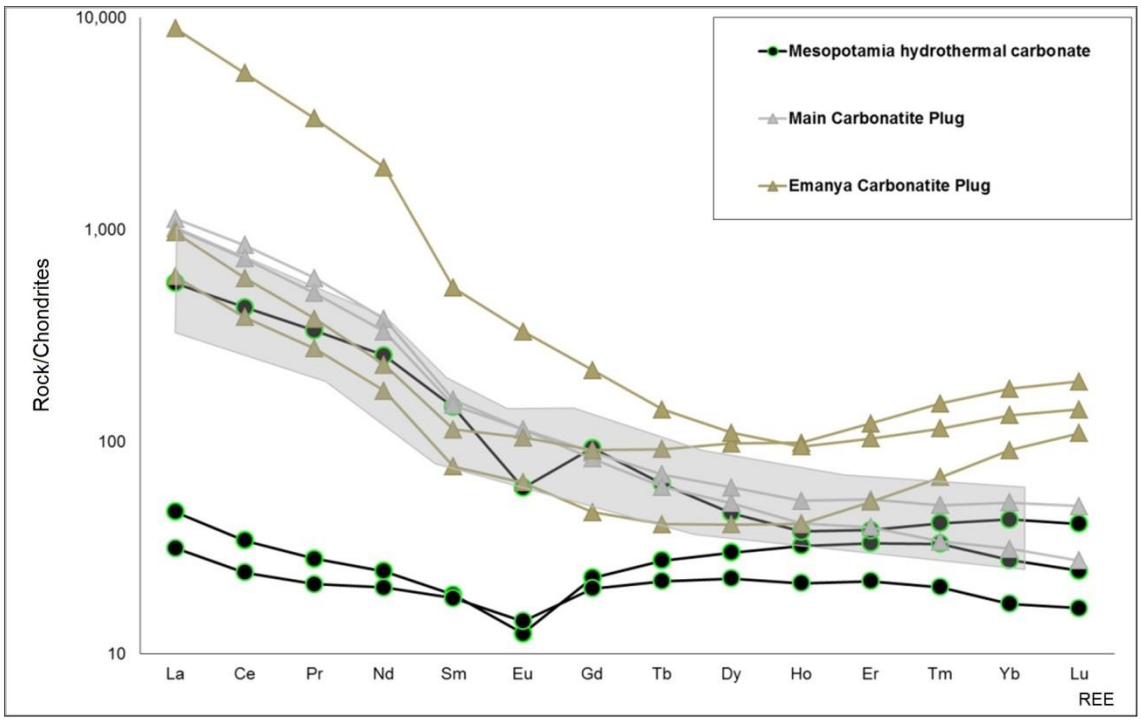

Figure 6.12 Chondrite-normalized REE-pattern of the Mesopotamie hydrothermal carbonate, Main and Emanya calciocarbonatite plugs

Anomalous concentrations of incompatible elements and REE at the contact zone between the carbonatite and syenite are interpreted to represent a zone where a REE rich phase was precipitated in the carbonatite due to interaction with the syenite. Precipitation of apatite and pyrochlore in these zones was a result of temperature and/or chemical change experienced by these fluids through interaction with the syenite.

Apatite content in the contact zone can reach up to 40 vol % and there is a large amount of pyrochlore that shows a high degree of alteration and replacement. The centres of the pyrochlore crystals contain significant U and Th. The thorium concentration ranges between 30 and 40 ppm in the Main carbonatite and is much higher in the Zero sample, reaching 190 ppm. In comparison to the values in the Main carbonatite plugs, Nb, Y, Zn, Ho and Zr concentrations are very low but increase by a hundred times in the Zero sample. Sr content ranges between 1.1 to 1.8 wt% in this group, with lowest values observed in the Main carbonatite plug and the highest values in the Zero sample. This group of rocks records the highest Sr concentration at Lofdal.

La shows enrichment in the Main calciocarbonatite. The group shows low concentrations of K, Ti and Zr (Figure 6.17), indicated by the negative anomalies. The Main carbonatite is especially enriched with Th, La, Pr, Dy and Lu.

In comparison to Emanya calciocarbonatite, the Main carbonatite is enriched in U, Nb, Sm, Dy, Y and Yb, while the Emanya plug shows enrichment in Ce, Nd and Eu.

6.3.3.2 Emanya carbonatite plug

Most of the Emanya carbonatite plug samples consist of pure calcite or a mixture of fine-grained calcite and Fe-oxide and pure (secondary) calcite, except for sample 949 that consists of calcite with Fe-oxide veinlets. Sample 949 has a bluish red appearance in the field caused by weathering and iron oxidation. The Emanya carbonatite plug is LREE- rich with LREE average, minimum and maximum values within the global values for calcite carbonatite (Woolley and Kempe 1989). The MREE values are below the average concentration of these elements in calcite carbonatite, although the minimum and maximum concentration values are within the limit of the values of calcite carbonatite (Woolley and Kempe 1989).

Although the Emanya REE concentrations are relatively higher than of the Main calciocarbonatite plug, these are slightly lower in comparison to the calciocarbonatite averages (Woolley and Kempe 1989), see Table 6.3 and Figure 6.12. They are also among the rocks with the lowest REE rock concentrations at Lofdal. Like the Main carbonatite, Emanya REE show steep, but linear LREE patterns and with a less pronounced HREE plateau.

Among the HREE, Tb is far below the average concentration of calciocarbonatite while Tm and Yb could not be compared to the concentration of an average calciocarbonatite due to limited data availability.

The concentration of elements such as Y, Ho, ΣHREE and ΣREE in the Emanya carbonatite plug are consistent with world average concentrations of these elements, though Yb and Lu conform within the range in their chondrite values, their upper limits are relatively higher compared to the maximum values of calciocarbonatite worldwide (Woolley and Kempe, 1989).

Fe_2O_3 is elevated in the Emanya samples and is highest in sample 949 that shows a high degree of alteration.

The Emanya type is also enriched in La, Pr, Dy, and Lu relative to the Main calciocarbonatite plug. The difference in element distribution between the Main and Emanya calciocarbonatite is that the Main plug is additionally enriched in U, Nb, Sm, Dy, Y and Yb, while the Emanya plug shows enrichment in Ce, Nd and Eu. The observed enrichment could be possibly influenced by samples from the contact phase that are more enriched in these elements. The differences in depletion of elements between the two carbonatite plugs mainly concern the depletion of Ba and Sr at Emanya and of Pb at the Main carbonatite (Zero sample), otherwise they are identical. The Emanya carbonatite also shows slight Ti enrichments.

Nb concentration is variable in the group ranging between 38 and 1858 ppm with an average concentration of 1198 ppm, compared with an average Nb concentration of 112 ppm in Lofdal carbonatites. Th, U and Y concentrations are within the ranges of the average calcite carbonatites and are consistent with the minimum and maximum values. Emanya Zr/Hf and Y/Ho average ratio is 18 and 14 times, respectively, lower than the primitive mantle values of 37 and 29 respectively, and lower than that of the average carbonatite worldwide of 60. Emanya Zr/Hf average ratios are also lower than the Lofdal average of 29. Th/U ratios are variable, ranging between 3 and 11 with an average ratio of 8. La/Yb ratios are lowest in this group with average of 0.3.

6.3.3.3 Dolomite carbonatites dykes

This type of carbonatite is represented by brecciated xenotime-(Y)-bearing dolomite-ankerite carbonatite (samples 119, 114). The breccias are nested, indicating that they formed through a number of events. The rocks are made up of two different types of dolomite: (1) dolomite with abundant iron and (2) dolomite with little iron.

The main geochemical characteristic of the Dolomite dykes at Lofdal is their moderate concentration of REE, where the LREE are very low compared to the HREE (Figure 6.13). The Fe_2O_3 contents are more variable ranging between 0.1 to 1.4 wt percent. While sodium concentrations are generally exceptionally low at Lofdal, the bulk rock analyses of the Dolomite dykes have values of up to 2 wt% Na_2O.

The Dolomite dykes show more enrichment than depletion of elements relative to other carbonatites at Lofdal. The enriched elements in the dolomite dykes are Pr, Eu, Y, Yb and Lu, while Ba, K and Ti are depleted. Dolomite dykes also show extreme depletion indicated by negative anomalies shown by K, Ti and Zr. Dy shows slight depletion in dolomite rocks. Slight levels of Sm enrichments are observed in the dolomite dykes. Zn amounts in the Dolomite dykes were generally higher, ranging between 1117 and 13980 ppm. The Dolomite dykes are most enriched in Y compared to other representative samples in this study, with Y contents reaching 1.4 wt% in sample 119. Nb values range between 22 and 73 ppm and are lower than the worldwide carbonatite averages, but are still within the minimum Nb ranges. Ta is mostly below the detection limit of 5ppm. This is, however, consistent with Ta average values in most carbonatites (Woolley and Kempe 2000).

The Zr/Hf ratio of Lofdal Dolomite dykes ranges between 30 and 66, thus within and exceeding the mantle value of 37 (Sun and McDonough 1995). Zr/Hf and Nb/Ta are within the standards for the average world-wide carbonatite of 60 and 35, respectively (Chakhmouradian 2006).

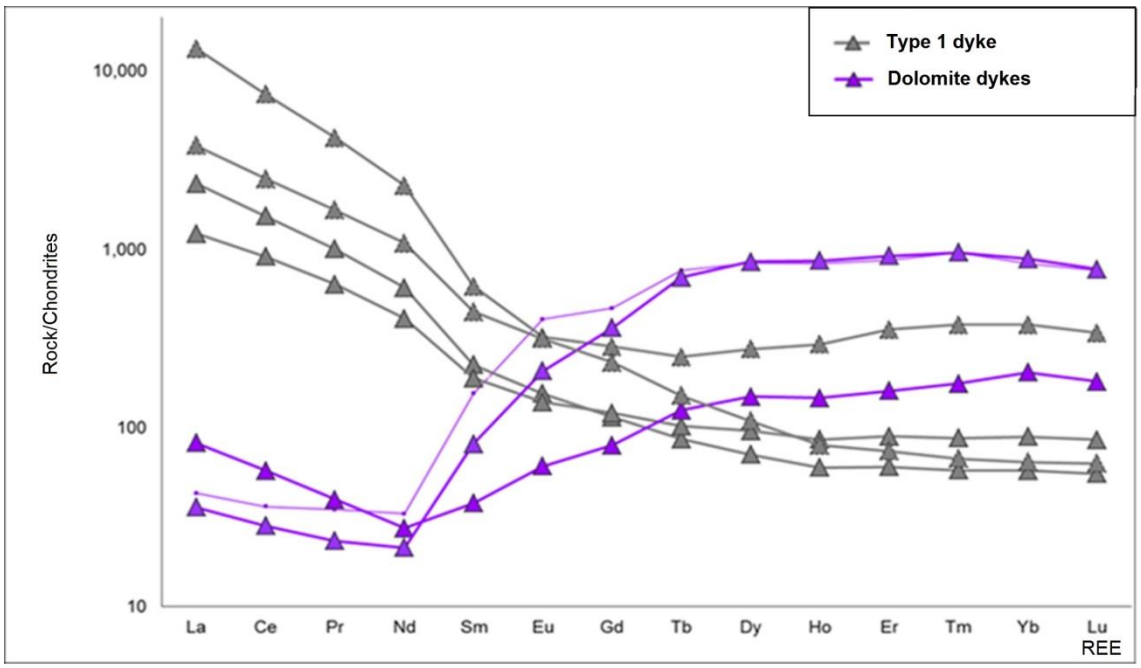

Figure 6.13 Chondrite-normalized REE-pattern of Dolomite dykes and Type 1 dyke carbonatites from Lofdal.

The Nb/Ta and Y/Ho ratios are subchondritic with values of 4-12 and 7-16, respectively. The Y/Ho primitive ratio is 29. The Th/U ratios range between 10 and 20. The values are very low, giving the dolomite group the lowest Th/U ratio in comparison to other HREE-bearing carbonatite groups at Lofdal.

6.3.3.4 Type 1 Dyke

Type 1 dykes are the most common type of dykes at Lofdal. They consist of intensely sheared dark calciocarbonatite rock. The group is represented by samples 115, 15769G, 813 and 907 that locally contains sulphides, magnetite, Mn-oxide and fluorite. Type 1 dykes have very high LREE and relatively low HREE concentrations. This is a typical pattern of carbonatites worldwide and shows a similar REE pattern to the groups of the Main and Emanya carbonatite plugs. These types of carbonatites are also enriched in LREE, Sr and Ba. The average concentrations of the LREE in the representative samples are consistent and in agreement with the average values of calciocarbonatites (Woolley and Kempe 1989).

Samples from Type 1 dykes show higher REE contents compared to most of the samples from the Main and the Emanya carbonatite plugs. Total REE concentrations are slightly lower in comparison to the global calciocarbonatite averages see Table 6.9; (Woolley and Kempe 1989).

Like the Emanya plug, Type 1 dykes show steep but linear LREE patterns and with a less pronounced HREE plateau (Figure 6.13).

The average ΣMREE values and the minimum and maximum values of this group are below the recorded concentration of MREE in calciocarbonatite worldwide (Woolley and Kempe 1989). The ΣHREE content in Type 1 dyke is 0.03 ppm, thus higher than the average 0.01ppm HREE content in calciocarbonatites. The ΣREE concentration in this group ranges from 0.1 wt% to 1wt %.

Primitive mantle-normalized trace element patterns (spider diagrams) are presented in Fig 6.18. The group has the highest amount of Nb (sample 813), reaching 713ppm. The high content of Nb can possibly be traced to pyrochlore. The Sr content is high, ranging from 0.1 wt. % to 1.7 wt %. The highest Sr value of all the samples studied from Lofdal is recorded in sample 115 belonging to this carbonatite dyke group.

Some samples belonging to this group recorded the second highest fluorine content reaching up to 10 wt% in the whole rock analysis. They have the highest Pb and Zn contents of 1461ppm and 4404 ppm respectively, in comparison to all other carbonatite types at Lofdal. The normal Lofdal Pb and Zn amounts are about 40 ppm and 50 ppm, respectively.

Concentrations of Hf and Ta are low, reaching 5 ppm, which is consistent with the Main and the Emanya carbonatite plugs and the dolomite dykes. Th and U are both at 20ppm, but are slightly higher in sample 813. Yttrium concentration ranges from 87 to 483 ppm. Zr/Hf ratios are low ranging between 5 and 15 in most representative samples of the group and far below average mantle values of 37. Sample 813 has Zr/Hf and Nb/Ta ratio of 97 and 101, respectively, which is above average mantle values and the average world carbonatite values of 60 and 35 respectively. These values are also higher compared to the average Lofdal Zr/Hf and Nb/Ta values of 29 and 20 respectively. Y/Ho values are about 2 for the whole group, and thus are very low. The La/Yb ratios are second highest with an average of about 50.

6.3.3.5 Type 2 Dyke

Type 2 dykes are represented by intensely sheared and altered carbonatite samples with a high iron content and high level of oxidation. These rock types are composed of ferruginous calciocarbonatite and are enriched in MREE and HREE. REE patterns of this type of dykes are characterised by high HREE/LREE ratios (Figure 6.14). There seems to be a relationship between the extent of shearing in type 2 dykes and the MREE concentration. The group is represented by samples 189 and 927.

The most important characteristic of this group are the extremely low LREE concentrations, which are lower than the concentrations in the Main intrusion but similar to Emanya concentrations of the carbonatites.

The minimum and maximum LREE concentrations are also generally lower than other known calciocarbonatites (Woolley and Kempe 1989).

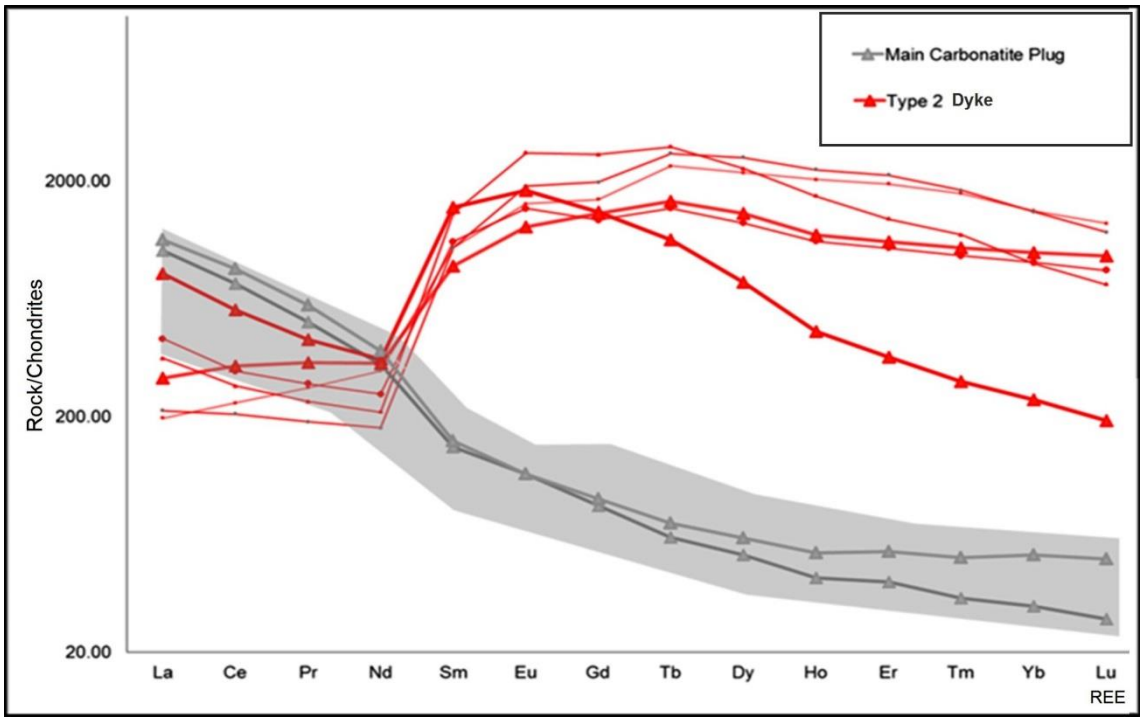

Figure 6.14 Chondrite-normalized REE-pattern of Lofdal carbonatite Type 2 dykes and Main carbonatite plug.

In contrast, the concentration of MREE and HREE are far above averages, as well as minimum and maximum recorded concentration values in carbonatites. The average ΣHREE value is 0.2 wt% and individual values range between 0.2 and 0.3 wt% ΣHREE. This REE composition has resulted in unusually high HREE/LREE ratios.

The high concentration of HFSE in this group is distinct in comparison with other dyke types at Lofdal. The group records the highest values of Hf, Th, U and Zr concentrations at Lofdal. Although Hf is high in the Lofdal context, Hf and Ta are relatively low and consistent with the rest of the groups at Lofdal. Zr/Hf ratio reached the highest value of 164. The value is 2.7 times above the average world carbonatite Zr/Hf values of 60. Nb/Ta ratios are 44, which is 2.4 times above the primitive mantle values of calciocarbonatites (18). Th/U ratio reaches 39 and is below the Lofdal Th/U ratio of 53. Sample 927 is highly enriched in Y and does not contain LREE-minerals (bastnäsite mineral group or monazite) but xenotime-(Y), zircon, apatite, thorite, fluorite, rutile and phlogopite. A slightly negative Eu-anomaly is observed.

6.3.3.6 Type 3 Dyke

The group is represented by samples15769, 15769LG and 15796. They have high overall REE concentrations and LREE is equal to/or higher than HREE concentrations.

These late calciocarbonatite dykes, that locally cut earlier ferruginous dykes (e.g. sample 189), contain xenotime-(Y).

The amount of Nb, Th and U is higher in the group compared to earlier discussed carbonatite rocks types at Lofdal. The element Co has the highest values in one of the representative sample of this group of up to 93 ppm, otherwise it is generally low.

The content of sodium reaches 3.42wt% in sample 15796. This can be a result of possible inclusions of the country rocks in these carbonatites, since aluminium was also high in the said sample reaching 13.13wt% in the whole rock analysis. High sodium content might also reflect metasomatism with growth of albite (or incorporation of albitite in the sample as both xenoliths rocks with albite and albite minerals were observed.)

LREE concentration are consistent with the averages, minimum and maximum LREE concentration in average calciocarbonatite (Woolley and Kempe 1989). MREE and HREE are highly enriched in the Type 3 dykes, in a similar trend to that observed in the Type 2 dykes (Figure 6.15). The difference between the two groups is that in type 2 dykes the LREE were consistently below the calciocarbonatite averages, while in type 3 dykes, the level of LREE is higher and within the levels of calciocarbonatites (Woolley and Kempe, 1989).

The group records the highest Th/U ratio at Lofdal ranging from (121 to 244). The Th/U ratios are much higher than the average Th/U ratio, making this group 2.3 to 4.6 times higher in Th/U ratios than the Lofdal average (53).

Sr content ranges between 445 and 2133 ppm and is generally lower, with only few samples with high values. Zr/Hf and Nb/Ta ratios are variable. For most samples these ratios are sub-chondritic, ranging between 2 and 5, respectively. Sample 15796 has the highest Zr/Hf and Nb/Ta ratios 70 and 33, respectively. These values are above the average chondrite values. The Nb/Ta ratio is relatively consistent with average world carbonatite values, but Zr/Hf is above these average values. In contrast to Type 2 dyke, Type 3 dyke contains both HREE- and LREE-bearing minerals.

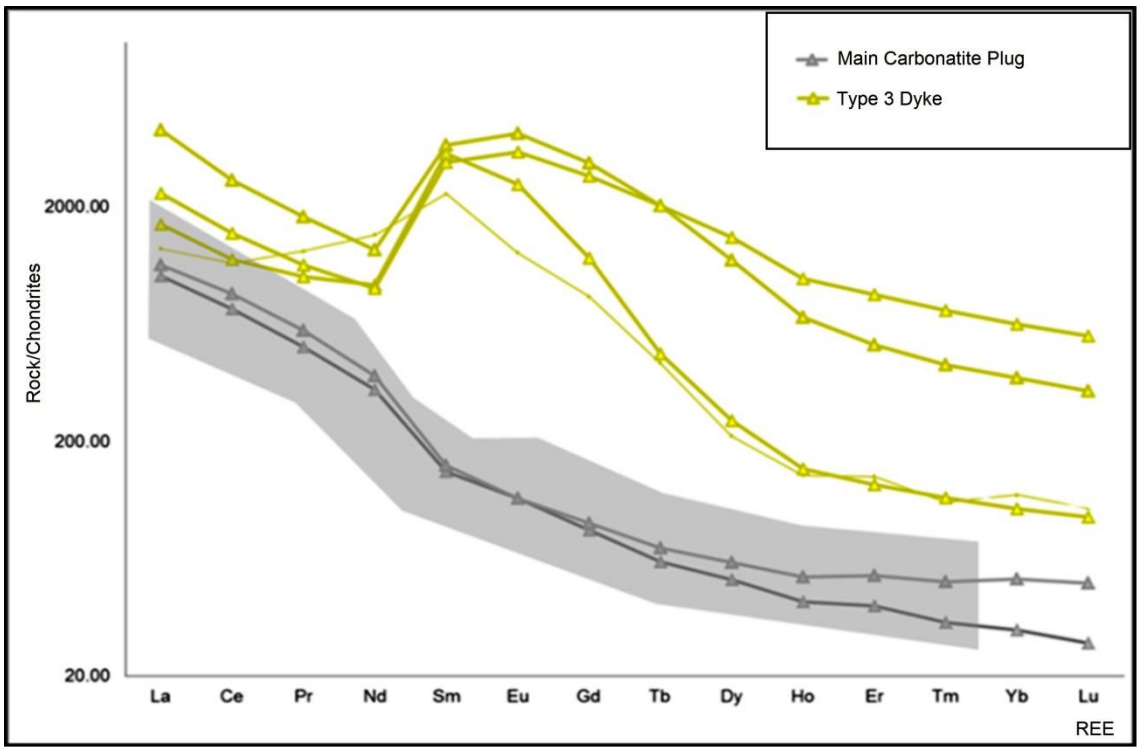

Figure 6.15 Chondrite-normalized REE-pattern of Lofdal carbonatite Type 3 dykes and Main carbonatite plug.

6.3.3.7 Type 4 Dyke

The group is characterised by very high LREE and relatively low HREE concentrations. Sample 914 is representative of this group (Figure 6.16). Its matrix contains calcite with Fe-oxide veinlets. The Type 4 dykes are extremely enriched in LREE and have relatively high concentrations of MREE and HREE. Type 4 dyke contain the highest total REE content of 5.3 wt % followed by dyke type 5 with 1.2 wt %.

Pb, La and Ce are enriched in Type 4 dyke. Lu is also specially enriched, making this carbonatite type remarkably different to other groups of carbonatites at Lofdal. The group shows a K, Ti and Zr depletion, indicated by the negative anomalies in the mantle-normalized spider graph. Like the dolomite and Type 2 dyke, the group shows slight depletion of Dy and Yb. F is highest in this group, reaching 13.7 wt% of the bulk rock analysis. The group has highest La/Yb ratios reaching 294. The La/Yb is more than 200 higher than the next highest of 67 belonging to Type 1 dyke.

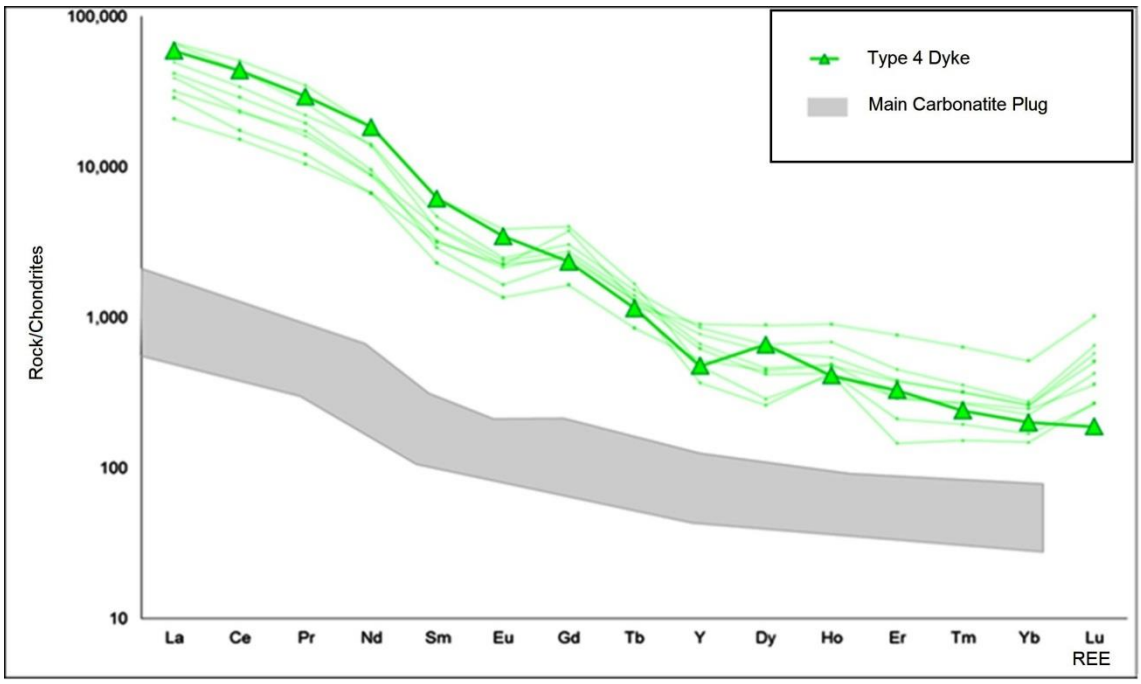

Figure 6.16 Chondrite-normalized REE-pattern of Lofdal carbonatite Type 4 dyke and the Main Carbonatite plug.

6.3.3.8 Type 5 Dyke

A number of samples from NRE clearly define this group as a separate entity (Figure 5.17). The group is represented by sample 924. The group characteristic is the high overall REE content forming a flat REE pattern with a slightly positive slope.

In comparison to Type 4 dykes, this group contains the same amount and at times much higher LREE concentrations. The MREE concentrations are higher than the HREE, although the MREE are also considered to be very high.

The sharp drop at Nd and sudden rise in the MREE on the chondrite normalized diagram make this group distinctive. Type 5 dyke showed the second highest ΣREE enrichment of 1.2wt %) Although Type 5 dyke shows a flat pattern, the HREE at this level are high.

Pb, La and Ce are enriched in the Type 5 dyke. Hf and Sr are especially enriched in the calciocarbonatites of the Emanya plug. Ta enrichment is only observed in Type 5 dyke, while Lu is enriched in Types 4 and 5 dykes. La/Yb ratios are 21 sitting on the Lofdal average.

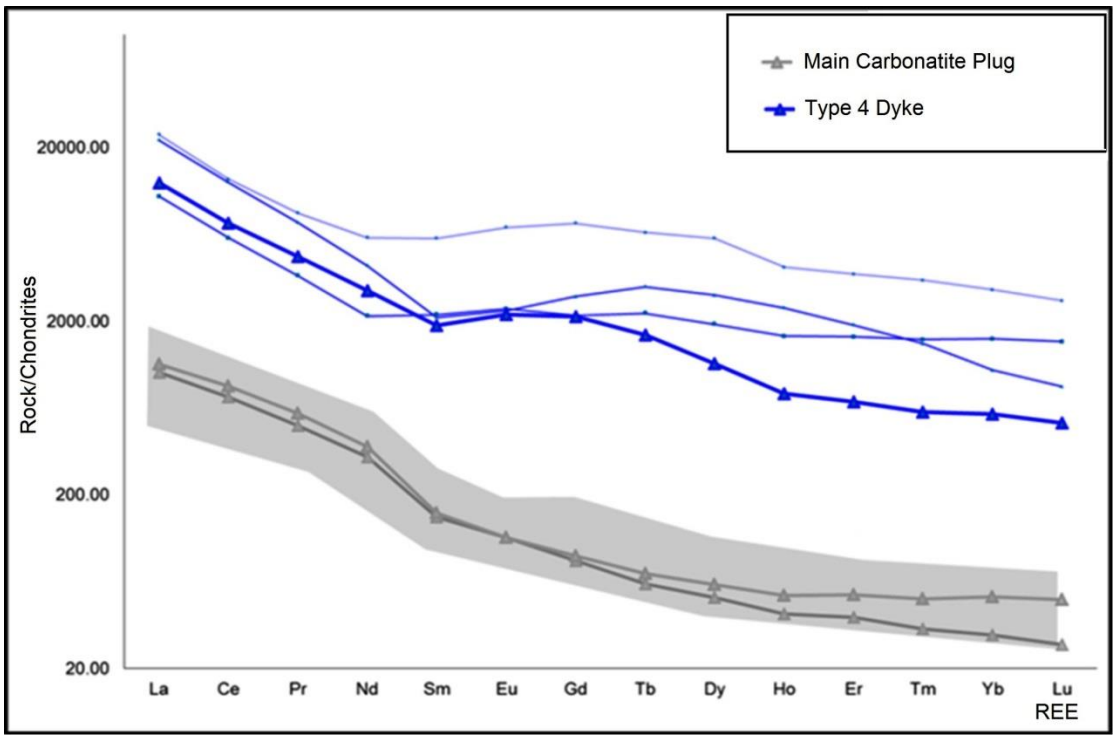

Figure 6.17 Chondrite-normalized REE-pattern of Lofdal carbonatite Type 5 dykes and Main carbonatite plug.

6.3.4 Trace Element Characteristics of the Lofdal carbonatites

Lofdal carbonatites cover an extensive range of HFSE compositions. The average Nb, Ta and Zn values for all Lofdal carbonatite types are significantly lower and the Zr values are higher, than those reported by Woolley and Kempe (1989).

The compatible element (Cr, Co, Ni and Sc) concentrations are low throughout the complex. The chalcophile elements (As, Bi, Cu, In, Ge, Mo, Sn, Sb and Zn,) are also very low, although some samples are locally enriched in these elements.

La shows enrichment in the main carbonatite, while Pb, La and Ce are enriched in dyke types 1, 4 and 5. The HFSE ratio compositions of incompatible elements are given in Table 6.6. The data shows wide variation among groups of Lofdal carbonatite rocks, and even within the members of the same group.

Sr ranges between 357 ppm to 1.8 wt% in the Lofdal sövite carbonatite plugs, whereas it ranges between 429 ppm and 1.7 wt% in the rest of the Lofdal carbonatite dykes. Sr is generally elevated in samples of the Main carbonatite and those that show high levels of LREE. Incompatible elements in the mantle-normalized spider graph (Figure 6.18), show distinct positive anomalies of Th, Pr, Eu and Lu in all Lofdal carbonatite types.

The primitive mantle normalized plots exhibit significant negative anomalies in K, Ti and Zr, observed across all the Lofdal carbonatite groups. Rb and Ba show a general depletion, although in some groups either only Rb is depleted or Ba. Sr is depleted in

Type 2 and 3 dykes. Type 1 dyke and the Main sövite carbonatite plug show Pb depletion. Type 3 dyke shows depletion in most elements including Rb, Ba, Nb and Sr. Dolomite dykes show more enrichment than depletion of elements. The enriched elements in the dolomite dykes are Th, U, Nb, Pr, Eu, Y, Yb and Lu, while Ba, K and Ti are depleted.

Table 6.6 HFSE ratio compositions of carbonatites (after Chakhmouradian 2006)

Sample:	Zr/Hf	Nb/Ta	Th/U
58	12.1	15.6	8.0
326	4.7	1.6	6.0
269	44.0	27.7	38.0
881G	2.0	37.0	8.5
881R	1.6	6.3	3.2
949	1.5	22.5	11.4
114	65.7	4.4	9.8
119	30.0	12.2	19.6
914	1.4	9.3	66.0
924	4.8	24.2	57.6
813	97.3	101.9	1.3
907	5.3	26.7	2.3
115	11.6	3.3	85.4
15769G	15.7	7.2	18.2
189	22.0	2.9	80.1
927	163.7	44.3	39.3
15769L	4.3	2.8	244.3
15796	69.6	33.7	184.3
15769	3.5	4.5	121.7

The carbonatite plugs show differences in the depletion and enrichment of trace elements. The primitive mantle-normalized spider plots show positive anomalies in Th, La, Pr, Dy, and Lu (Fig6.18). The Main carbonatite also has positive anomalies in enriched U, Nb, Sm, Dy, Y, Yb and the Emanya plug shows enrichment in Ce, Nd and Eu. All Lofdal carbonatites have strong negative anomalies in K, Zr and Ti (Table 6.7). The differences in trace element compositions between the two carbonatite plugs are the lower concentrations of Ba at Emanya and the Main carbonatite. Types 1 and 2 dyke are enriched with the same elements Th, U, Pr, Eu, Yb and Lu, and differ only in Ce enrichment in Type 1 dyke and Y enrichment in Dyke type 2. Slight levels of U, Sm, Ti, Y, Yb enrichments are observed in the Main and Emanya carbonatite plugs as well as in the dolomite dykes.

Sr is distinctively enriched in the Main carbonatite and the Type 5 dyke. Ta enrichment is only observed in Type 5 dyke, while Lu is enriched in Type 4 and 5 dykes. There is a significant depletion of Ba, K, Ti, Zr, Pb and Sr, whereas Th, U, Pr, Eu, Yb, Lu and Y are more enriched in higher REE concentrations in the Lofdal carbonatite than in the average calcio-carbonatite (Table 6.8) (Woolley and Kempe 1989).

Sr, Ba and Ti proportions can be used in conjunction with the REE to discriminate the different carbonatite groups at Lofdal using ternary diagrams (Figure 6.20). Sr is elevated in samples of the Main carbonatite and those that show high level of LREE.

Table 6.7 Summary of trace element positive and negative anomalies in primitive mantle-normalized plots in the Lofdal carbonatites

Type of Carbonatite	**Trace Elements Enrichment**	**Low Enrichment**	**Trace Elements Depletion**
Main Plug	**Th, U,** Nb, La, **Pr,** Sm ,Dy, **Y, Yb, Lu**		**K,** Pb, **Zr, Ti**
Emanya Plug	**Th,** La, Ce, **Pr,** Nd, **Eu, Dy, Lu**		Ba, **K, Zr, Ti,**
Dolomite	**Th,** Nb, **Pr, Eu, Y, Yb, Lu**		Ba, **K, Ti,**
Type 1 dyke	**Th, U,** Ce, **Pr, Eu, Yb, Lu**	Nd, Hf, Y	Rb, **K, Zr**, Pb, **Ti**
Type 2 dyke	**Th, U, Pr, Eu,** Y, **Yb, Lu**	Pb, Pr	**K, Zr,** Sr, **Ti**
Type 3 dyke	**Th, Pr, Eu, Lu**		Rb, Ba, Nb, **K,** Sr, Zr, Ti
Type 4 dyke	**Th, U,** La, Ce, **Pr,** Nd, **Eu,** Dy, **Y, Yb, Lu**		Rb, Ba, Th, Nb, **K, Zr, Ti**
Type 5 dyke	**Th, U, Pr**, Nd, **Eu, Dy, Y, Yb, Lu**		Ba, Th, Nb, **Zr, Ti**
Lofdal common Features	**Th, U, Eu, Yb, Pr, Y, Yb, Lu**		**K, Zr, Ti**

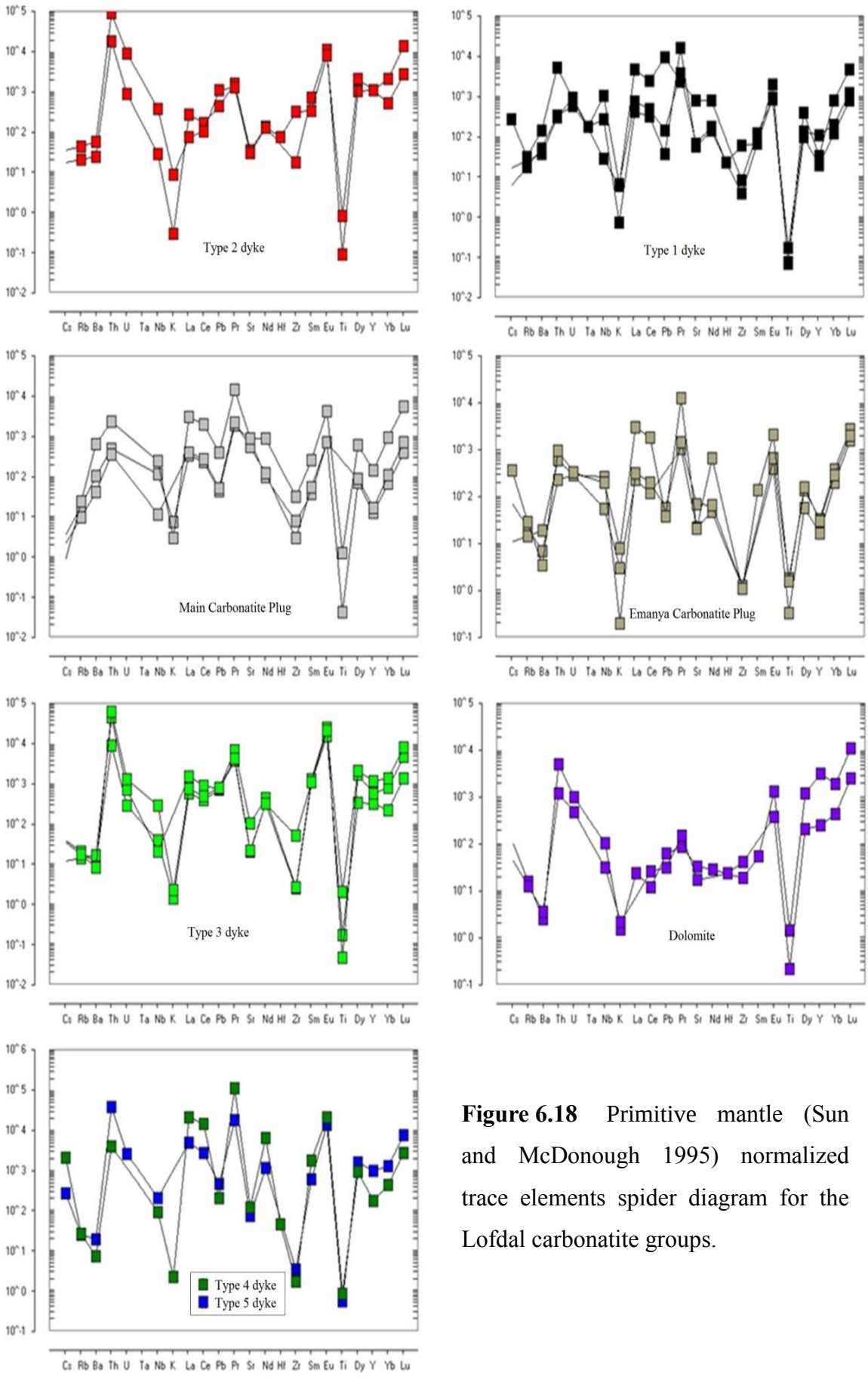

Figure 6.18 Primitive mantle (Sun and McDonough 1995) normalized trace elements spider diagram for the Lofdal carbonatite groups.

6.3.5 Analysis of Rare Earth Elements characteristics

The REE content can be used to distinguish between carbonate of sedimentary origin and those of igneous origin. Studies by Möller et al. (1980) and Mariano (1989) indicate that the ΣREE of sedimentary carbonate rarely exceeds 200 ppm while in carbonatites the ΣREE content exceeds 500ppm but is less than 10 000 ppm. A study by Samoilov, (1984) showed that carbonatites may be distinguished as a separate group based on geochemical features of their isotopic characteristics. Main features required to classify carbonatite geochemically are their content of P, Nb, Sr, Ba, Pb, Zn, REE and Y.

The most distinguishing features are consistent enrichment of Sr > 700 ppm, Ba>500 ppm, high LREE relative to HREE and Y (Table 6.7). (ΣCe/ Σ Y > 4); ΣCe = La+Ce+Pr+Nd+Sm+Eu, Σ Y= Gd+Tb+Dy+Ho+Er+Yb+Lu+Y). The Lofdal ΣREE contents are here evaluated according to these criteria and the results are summarised in Table 6.10. Based on the geochemical features and isotopic characteristics, Lofdal carbonatites are consistent with distinguished features of carbonatites in general, where Sr, Ba, V, and the REE + Y are variable outside the range and in many instances far above the concentration limits. The ratio of LREE to HREE is also below 4 in most samples that show variability of the other trace elements. The geochemical differences among different groups of Lofdal carbonatites are great.

The Main carbonatite together with the Zero samples is the closest fit to Samoilov (1984) geochemical composition. Based on the ratio of Ba/Nb versus Zn/Pb, other samples plotted in the field of formation of near fault carbonatites and alkali metasomatites. The rare elements of near fault carbonatites are said to be specifically rich in Nb and depleted in Ba. They also have the highest average values Sr/Ba and Nb/Ba (Samoilov 1984); the trend seems to fit well with the Lofdal setting.

Table 6.8 Showing a comparison of traces and REE values generally observed in carbonatite Worldwide and at Lofdal after Samoilov 1984.

Sample	Ba >250	REE + Y > 500	Sr >700	*ΣLREE/ΣHREEE > 4*	V >20	Y	Ba/Nb	ΣLREE	ΣHREE	ΣREE
58	717	3275	16810	***6.63***	4	59	9.19	2846	429	3216
326	290	3779	11490	***5.8***	5	77	36.25	3223	556	3702
269	4472	26734	18640	***5.36***	37	662	26.94	22530	4204	26072
881G	132	3571	1465	2.04	44	150	0.71	2394	1175	3421
881R	48	2148	457	2.79	40	76	1.26	1581	567	2072
949	24	21781	427	***17.21***	19	135	0.18	20586	1196	21646
114	25	2646	357	0.13	36	1117	1.14	305	2342	1529
119	17	20680	676	0.02	73	13980	0.23	397	20282	6700
189	396	18132	638	0.23	228	4869	1.49	3436	14696	13263
927	169	15357	744	0.56	239	4966	8.45	5511	9844	10391
115	1010	31183	16940	***9.28***	32	483	50.5	28148	3034	30700
813	261	6496	1443	***9.02***	4	87	0.37	5846	648	6409
907	352	4414	1214	3.85	13	153	1.88	3504	910	4261
15769	74	23718	429	1.08	167	1445	2.74	12331	11385	22273
15769G	668	10811	7823	***9.55***	11	184	18.56	9786	1025	10627
15769L	115	28832	2133	1.59	131	2558	8.21	17708	11124	26274
15796	59	18427	445	1.38	26	5238	0.29	10670	7758	13189
914	51	166308	2482	***25.42***	37	808	0.78	160893	6330	165500
924	134	44235	1585	2.63	241	4327	0.92	32717	12441	39908

The ΣREE values of the Lofdal carbonatites are highly variable, varying between 446 ppm and 53725 ppm with an average ΣREE content of 0.6 wt%. Samples with low LREE concentrations are below the average calciocarbonatite LREE concentrations as defined by Woolley and Kempe (1989).

The REE concentrations of the representative Lofdal carbonatite samples are presented in Table 6.3. The different carbonatite groups are highlighted with their corresponding colours according to their LREE, MREE and HREE classifications and the total values of the ΣREE, LREE, MREE and HREE for the representative samples. Additionally, La/Lu ratios and the mantle normalized values of $(La/Yb)_n$ ratios are presented.

Type 4 and 5 dykes have the highest ΣREE abundances (5.3 wt. % and 1.2 wt. %, respectively) of all groups at Lofdal. Lofdal carbonatites show a general variable REE enrichment distribution pattern with no obvious negative Eu anomaly.

Type 5 dyke shows element enrichment from Sm, while Type 4 dyke is extremely enriched in the LREE and has relatively high amounts of MREE and HREE. Samples from the Main carbonatite and from the Emanya plug have slightly lower ΣREE

abundances in comparison to the carbonatite averages for the calcite carbonatite (Table 6.8); (Woolley and Kempe 1989). These have also the lowest REE concentrations in comparison to all other Lofdal carbonatite groups. Samples from the plugs (Main and Emanya carbonatites) and Type 1 dyke show steep, but linear LREE patterns with a less pronounced HREE plateau.

The REE patterns (Table. 6.3) indicate that the HREE are enriched in the carbonatite dykes, relative to the carbonatite plug intrusions. Average, minimum and maximum values for the REE in different carbonatite rocks from Lofdal are presented in Figure 6.18, according to their LREE, MREE and HREE grouping.

There are distinctly lower LREE and higher HREE in Lofdal xenotime-(Y)-bearing calciocarbonatite (Types 2 to 5 and the Dolomite dykes) compared with average calciocarbonatite (Woolley and Kempe 1989) (Figure 6.19). Lofdal rocks have slightly lower LREE, but higher MREE and HREE concentrations compared to average sövites and alvikite. All the MREE and HREE are well above the maximum values listed by Le Bas (1997), except for Tm which looks anomalously low in the Le Bas data set. Lofdal carbonatites are thus outside of the range of, or on the extreme margins of those observed values for carbonatites.

While some groups are LREE-enriched, other groups are enriched in the MREE and HREE. As illustrated in Figure 6.20, elements such as Ti, Ba and Sr also help to geochemically discriminate the various carbonatites in the Lofdal complex, in agreement with the proposed division of the different carbonatite groups suggested by the REE distributions (Figs.6.19 and 6.20). The HREE discriminate the LREE-enriched from the HREE-enriched groups, Ti separates Emanya from otherwise similar Main and Type 1 dyke.

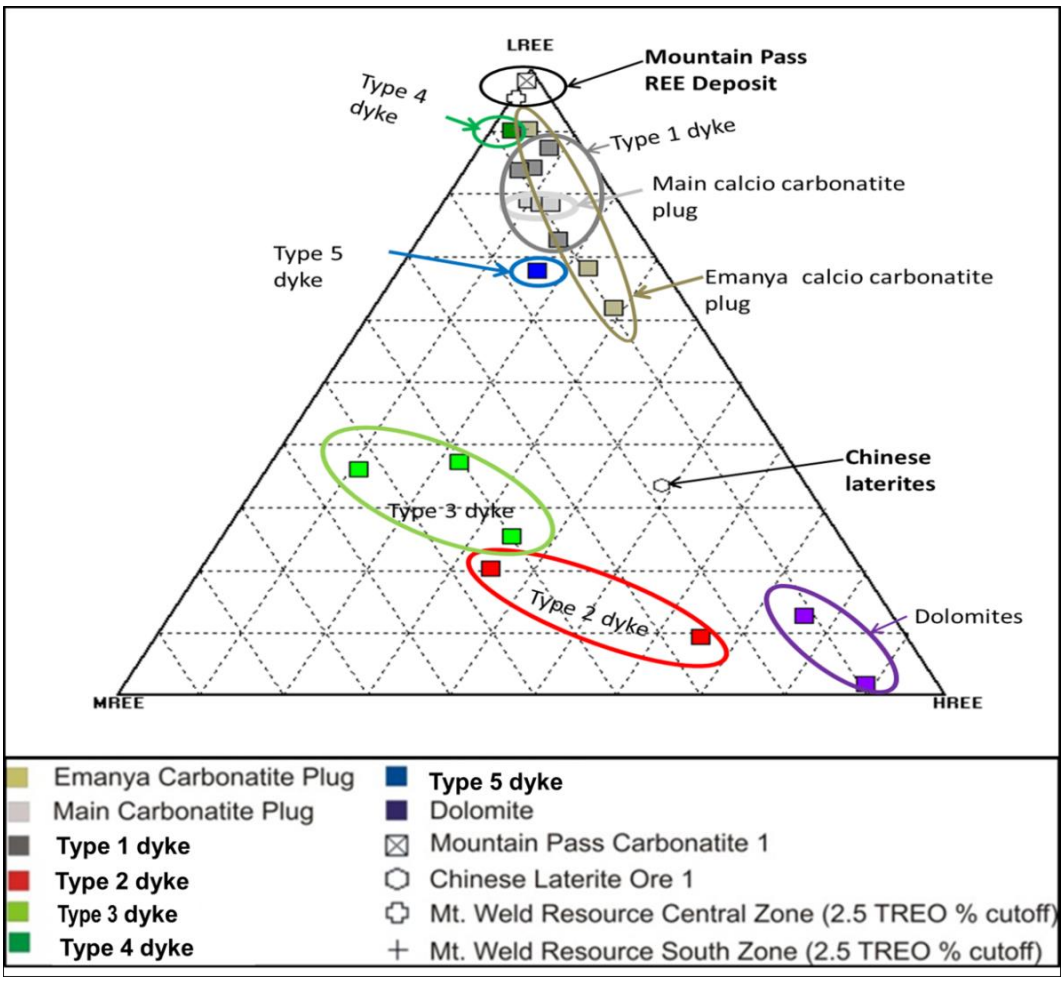

Figure 6.19 Diagram showing the proportions of LREE, MREE and HREE in the Lofdal carbonatites, compared with known REE deposits.

The chondrite-normalized La/Yb and $(La/Yb)_n$ ratios range from 0.04 to 294.15, (Table 6.7). The Dolomite dykes display the lowest $(La/Yb)_n$ ratios (0.04 to 0.40), while Type 5 dyke shows the extreme highest $(La/Yb)_n$ ratio of 295.

Sövites from the Lofdal carbonatite plugs show roughly parallel chondrite-normalized patterns, which flatten towards the HREE, resulting in a $(La/Yb)_n$ ratios ranging from 20 to 32.

Dolomite dykes show inverted patterns compared to the REE distribution generally observed in carbonatites. The REE patterns of the dolomite dykes show low LREE, and steeply increase from Sm to the HREE field.

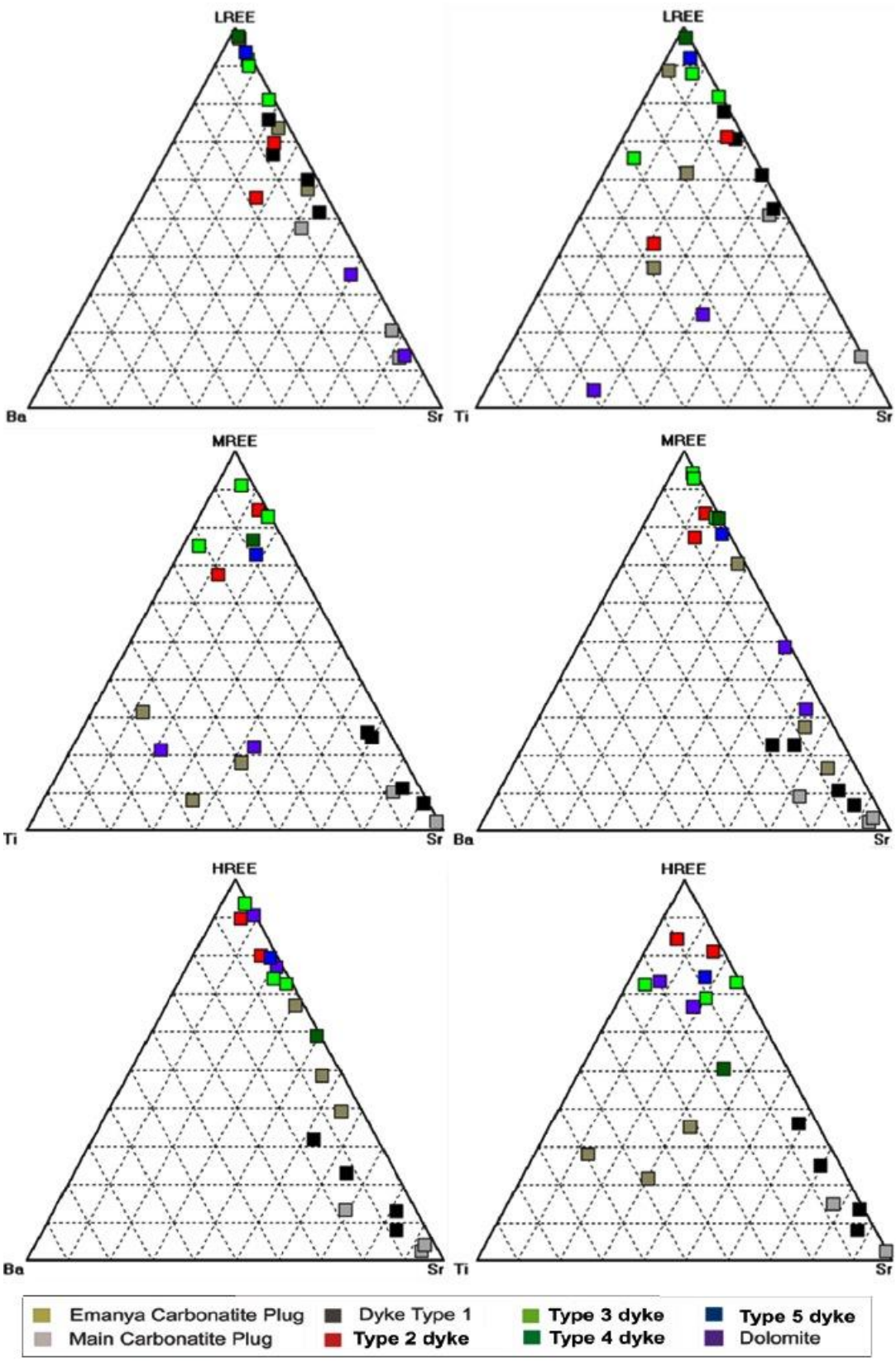

Figure 6.20 Graphs showing the discrimination of groups based on Ba, Ti and Sr versus LREE, MREE and HREE in the Lofdal carbonatites.

Dyke type 5 is characterized by relatively flat patterns that are slightly uniform in REE abundance and in the distribution pattern of LREE and HREE.

The calciocarbonatite Types 2 and 3 dykes show abundances and similar enrichment patterns on the LREE side, but the HREE patterns differ in amounts and trends. These two types of dykes are similar and in good agreement with previously published total REE and distribution patterns (Wall et al. 2008).

Lofdal carbonatites are 1 to 3 times higher than the maximum values in the Le Bas data set and 2 to 5.9 times higher than the Le Bas suggested standard median values. A 't' test of all available Lofdal whole rock data and the Le Bas datasets showed conclusively that the samples come from two different populations because the significance was p = 0.00. Le Bas (1997) does not give Y values (Wall et al. 2008). The Main and the Emanya carbonatite plug have REE concentrations that approach general REE contents in carbonatite, while Types 2, 4, 5 and the dolomite dykes have REE values approaching world-class levels of enrichment. The Emanya carbonatite plug records the lowest Th values between 19 and 80 ppm in the whole rock analyses, with an average of 50 ppm. Ferruginous and ferrocarbonatites have very high ranges of ThO_2 ranging from 0.04 to 34.4 wt%. Barbour (1982) noted that ThO_2 values range from 0.17 to 14.4 wt%.

There is a positive correlation between the concentration of P and HREE (Figure 5.22). This relationship is particularly apparent for the Types 2, 4, 5 and the dolomite dykes which contain abundant apatite, fluorite, xenotime-(Y) and as much as 150 ppm Yb, a proxy for the HREE.

The Main and the Emanya carbonatites are however depleted relative to the Dolomite dykes and Type 2,3, dykes in fluorite, apatite and xenotime-(Y) (having 0.1–0.3 wt % P_2O_5 and 0.5 – 0.03 wt % REE) and contain less than 100 ppm ΣREE in samples studied in details of the group. Yttrium contents are highest in the rocks with highest REE, but the Y content increases with a decreasing La/Yb ratio, i.e. with a decreasing degree of LREE-enrichment.

Type 2 dykes have the highest Y content and also the highest degree of HREE enrichment (Figure 6.21). There is quite a difference in the LREE-contents of the Dolomite dykes, Type 2, 3 and 5 dykes but all have high Y along with their HREE-enrichment. The LREE concentrations are generally low in these dykes. The Y/Ho ratio is 4.3 for average Lofdal carbonatites, ranging from 1.5 to 16.2 (Figure 6.22), which is below the chondritic ratio of 28 (Anders and Grevesse, 1989). The same applies to the Th/U ratio of 5.7 and 2.9 in the carbonatite dykes, given a chondritic ratio of 3.8.

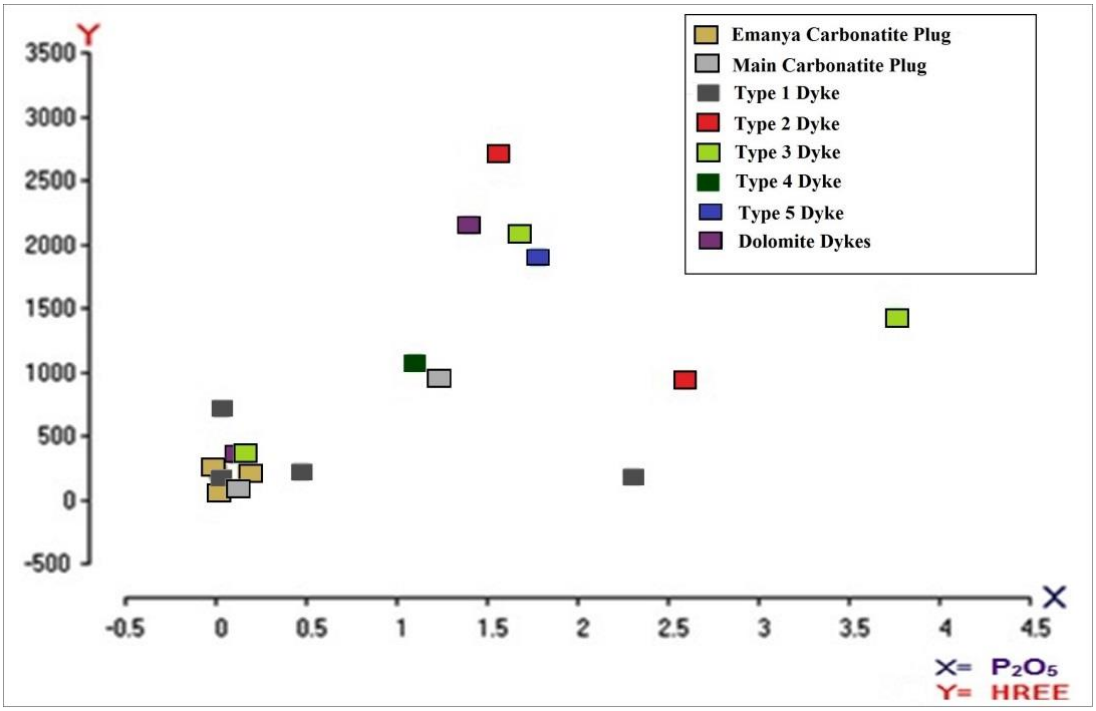

Figure 6.21 Binary plot indicating the positive correlation between the concentration of P_2O_5 and HREE

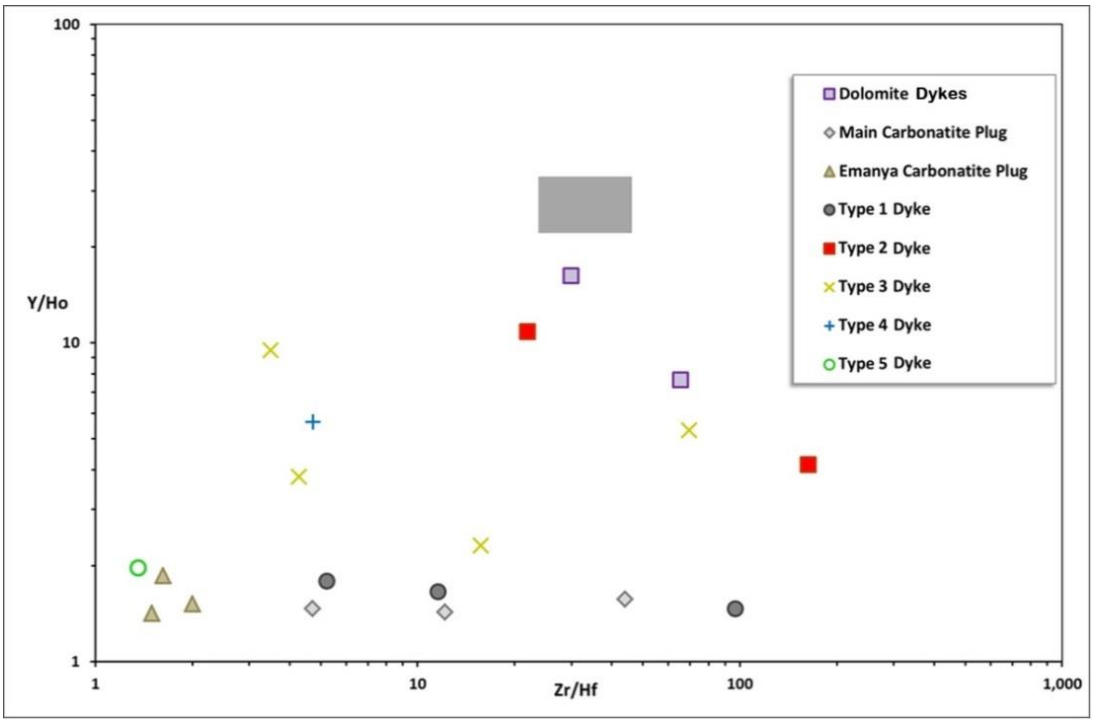

Figure 6.22 Zr/Hf versus Y/Ho diagram of different carbonatites at Lofdal. The field in gray represents the CHARAC range of Zr/Hf (CHARAC = CHArge and RAdius Controlled cation behaviour; Bau 1996).

6.4 Comparison with other Namibian carbonatites

There are a variety of carbonatite rock intrusions in the immediate area of the Lofdal complex, including one that is within the same geological setting as Lofdal, in the Tsumas Mountains. No geochemical data is available for this carbonatite.

The Epembe and the Swartbooidrift carbonatites north of Lofdal fall under the same large structure geophysically defined by Corner (2003) although the Epembe and Swartbooidrift carbonatites are directly related to the Kunene complex dated at 1.1 Ga (Littmann 2000). The Swartbooisdrift ferrocarbonatite is reported to have a closer geochemical composition to Lofdal (Thompson et al. 2002, Wall et al. 2008).

Namibian carbonatite geochemistry is scarce and recent analyses have been selectively focused mainly on the economic viability of their contained REE. Even in this study, although a number of carbonatites were sampled, only a few were analysed for the whole rock geochemistry. Their REE distribution presented in comparison to Lofdal carbonatites (Fig 6.23).

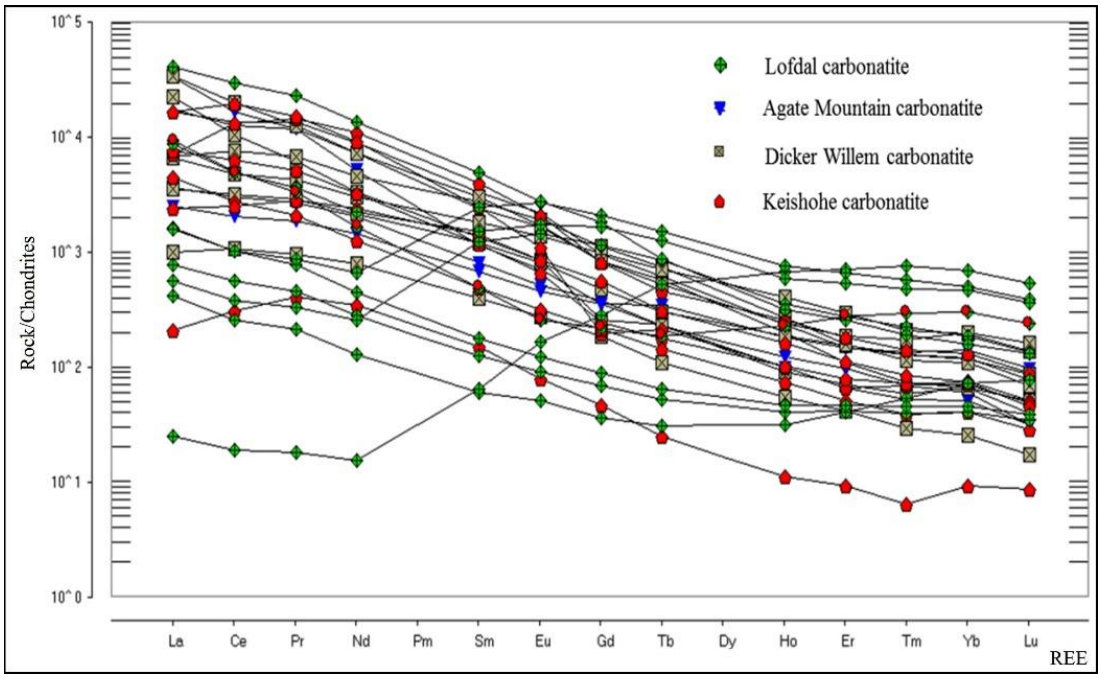

Figure 6.23 Comparisons of chondrite-normalised REE (ppm) compositions of the Namibian carbonatites sampled.

The most remarkable features of carbonatite magmas globally are their low SiO_2 contents, exceptional enrichment in highly incompatible elements, and their very steep chondrite-normalized REE patterns (Woolley and Kempe 1989).

Most Namibian carbonatites display these characteristics, but Lofdal is an exception to this rule and many samples show MREE and HREE enrichment in comparison to the data presented (Table 6.9). Lofdal LREE is also high, similar to the Keishöhe carbonatite and Agate Mountain carbonatites.

Le Roex and Lanyon (1998) reported trace element data for five Cretaceous alkaline complexes: Osongombo, Kalkfeld, Ondurakorume, Okorusu and Okenyenya. These define a broad northeasterly-trending linear feature which extends from Cape Cross on the Atlantic coast to Okorusu some 350 km inland, with emplacement between ~137 and 123 Ma (Milner et al. 1995). Their emplacement coincides with the eruption of the voluminous Paraná-Etendeka flood basalts of Brazil and northwest Namibia and the opening of the South Atlantic Ocean (Siedner & Mitchell, 1976; Renne et al., 1992; Turner et al. (1994) and are suggested to be a product of thermal activity associated with the break-up of western Gondwana (Milner et al. 1995, Milner and le Roex 1996).

Cretaceous carbonatites are characterized by enrichment of highly incompatible elements up to ~10 000 times primitive mantle values, with LREE abundances 4000 to 40 000 times of the chondrite values, and La/Yb_n ratios of >400 (Le Roux et al. 1996).

It is widely acknowledged that zirconium and hafnium are closely coupled during magmatic differentiation, because of their very similar partitioning behavior, as both elements are tetravalent and have very similar effective ionic radii (in VI-fold coordination 0.84 and 0.83Å, respectively; Shannon 1976). As a result, basic, intermediate, most other silicate magmatic rocks, and clastic sediments show Zr/Hf ratios close to the chondritic ratio of 38 (C1-chondrite from Anders & Grevesse, 1989) (e.g., Goldschmidt 1937, Jochum et al. 1986, Bau 1996). Super-chondritic Zr/Hf ratios are said to be typical for carbonatite melts (e.g. Dupuy et al. 1992,; Rudnick et al. 1993, Yaxley et al. 1991 and Nelson et al. 1988), but non-chondritic Zr/Hf in carbonatites are reported in alkaline and carbonatite rocks, and have been interpreted to be the consequence of heterogeneities of their source in the mantle (Andrade et al. 2002).
The Lofdal carbonatites have variable Zr contents ranging between 12 and 3602 ppm, with an average of 519 ppm. Hf content is below the detection limit of 7 ppm in most samples and the maximum Hf values of 22 ppm are recorded in all samples of dyke group 2. Group 4 recorded the second highest Hf values of 14 ppm. Both groups with very high Hf content are REE mineralised and are highly altered.

Sample 189 of group 2, which is mineralised with HREE, recorded the highest Zr values, while dyke type 4, which is highly mineralised with light REE, has lower Zr values. The Zr/Hf ratio ranges between1.5 to 165 and is extremely variable even in the carbonatite groups (Fig 6.24 and Table 6.10).

Lofdal carbonatites show a great degree of fractionation, and this cannot be explained simply by the charge and ionic radius that controls the geochemical behaviour of these elements. Other factors played a role in the heterogeneities of the Zr/Hf ratio at Lofdal, considering that even geochemically similar carbonatite groups displayed different Zr/Hf ratio. The degree of alteration and the heterogeneities of their origin plus the composition of their source region could explain the non chondritic and superchondritic behaviours of the Lofdal rocks, as those conditions are important in precipitation of Zr and/or Hf-bearing minerals.

Most carbonatites at Lofdal are subchondritic with Zr/Hf values very low and below a chondritic ratio of 38 (C1-chondrite from Anders and Grevesse 1989). Sample119 of the dolomite group, 813 of Type 1 dyke and rich in zircon, 15796 of Type 3 dyke and sample 927 of Type 2 dyke show super chondritic values ranging between 66 and 163.

In comparison to other Namibian carbonatites Lofdal rocks are rather similar to other carbonatites with regard to rock associations and major element distribution. It is the presence of the HREE-rich groups that makes them unique as these have not been reported from other carbonatites.

Also Lofdal carbonatites show the widest Zr/Hf ratios spreading far below and above the chondritic levels. The values below the chondrite level could be the result from low and below detection Zr/Hf values of some of the Lofdal carbonatites.

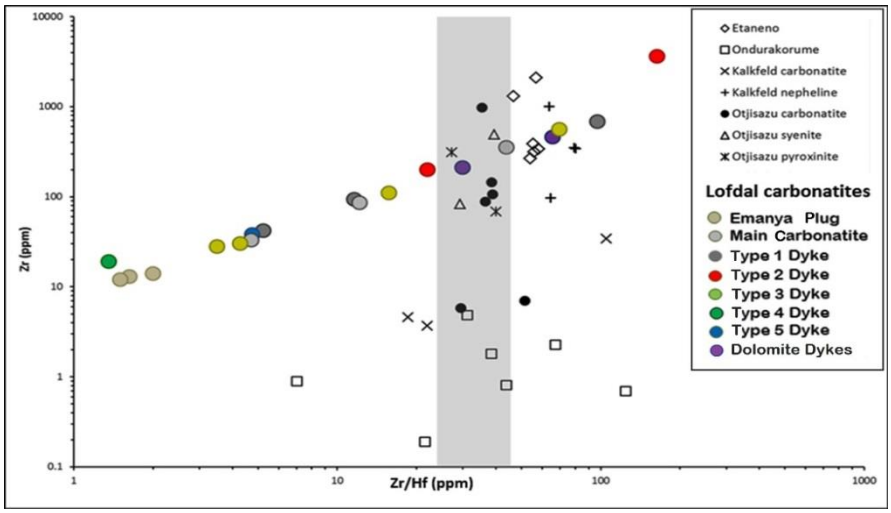

Figure 6.24 Zr/Hf versus Zr (ppm) of the Lofdal carbonatites, against Zr/Hf versus Zr (ppm) of carbonatites and alkaline rocks, data from the literature (Woolley et al. 1995, De Andrade et al. 2002). Chondrite C1 (+) after Anders and Grevesse (1989). The field in gray represents the CHARAC range of Zr/Hf (CHARAC = CHArge and RAdius Controlled cation behaviour; Bau 1996). Note: The plots on the left side of the gray field have very low values approaching the detection limits, thus these might not necessarily represent the indicated trend. Note that Zr separates types 4 and 5 clearly6.5 Comparison with REE-rich carbonatites

Table 6.9 Comparison of incompatible elements and their ratio values of various trace elements in some of the Namibian carbonatites.

Location	Otjisazu										Kalkfeld									
Sample	OS59	OS90	OS65	OS85	OS155	OS158	OS67	OS95	OS156	OS159	KF50	KF54	KF94	KF115	KF200	KF201	KF208	KF60	KF97	KF99
Rock type	pxt	pxt	syen	syen	carb	carb	carb	carb	carb	carb	carb	carb	carb	neph	neph	neph	neph	carb	carb	carb
Zr (ppm)	313	68.9	83.2	494	7	107	88.5	5.8	145	976	22.9	11.3	9.3	1001	96.6	350	339	4.6	34.4	3.7
Hf uncorrected	11.7	1.88	3.01	12.7	0.23	2.83	2.53	0.34	3.84	28.1				15.8	1.6	4.47	4.28	0.77	0.6	0.33
Hf corrected	11.5	1.72	2.85	12.5	0.14	2.76	2.42	0.2	3.76	27.5				15.7	1.5	4.4	4.21	0.25	0.33	0.17
Y	87.6	53	66.6	87.2	9.28	85	104	140	80.3	802	137	435	504	30.3	7.63	4.02	4.98	474	307	232
Ho	3.29	2.16	0.58	3.12	0.34	3.4	3.85	5.24	2.96	33.6	5.07	16.5	19.2	1.05	0.29	0.15	0.2	19.7	11.7	6.08
Sr	787	1080	5470	2170	7080	3410	12900	24000	4940	3720	20000	20000	6180	2260	1220	963	685	24000	24000	7150
Zr/Hf corrected	27.2	40.1	29.2	39.4	51.5	38.8	36.5	29.4	38.5	35.5				63.9	64.6	79.6	80.6	18.5	105	21.9
Y/Ho	26.6	24.5	25.8	27.9	27.3	25	27	26.7	23.9	27	27	26.4	26.3	28.9	26.4	26.8	24.9	24.1	26.2	38.2
Location	Ondurakorume										Etaneno									
Sample	ON57	ON58	ON60	ON62a	ON62b	ON65	N76	ON78	ON50		ET5	ET151	ET152	ET153	ET163	ET169				
Rock type	carb	carb	carb	carb	carb	carb	carb	carb	carb		neph	neph	neph	neph	neph	neph				
Zr (ppm)			4.85	1.81	0.81	0.191	2.29	0.7	0.9		389	268	342	314	1321	2099				
Hf uncorrected			0.3	0.11	0.07	0.29	0.33	0.19	0.35		7.13	5.05	6	5.74	28.5	37.1				
Hf corrected			0.16	0.05	0.02	0.01	0.03	0.01	0.13		7.03	4.95	5.9	5.64	28.3	37				
Y	141	123	82.3	46.2	57.6	230	268	169	137		41.4	35.1	40.5	36.1	120	109				
Ho	5.64	5.8	3.23	1.79	1.94	9.27	10.7	6.8	5.81		1.53	1.27	1.47	1.24	4.36	4.01				
Sr	20000	20000	31440	4290	4990	25150	25860	18330	24000		888	816	805	396	405	509				
Zr/Hf corrected			31.1	38.3	43.8	21.5	67.3	124	7		55.3	54	58	55.7	46.6	56.8				
Y/Ho	25	21.2	5.5	25.8	29.7	24.8	25	24.9	23.6		27.1	27.6	27.6	29.1	27.5	27.2				
Location	Lofdal																			
Sample	114	119	881G	881R	949	15769	15769G	15769L	15796	RC 08_0	269	326	115	813	907	914	924	927	189	
Rock type	dol	dol	carb	carb	carb	carb	carb	carb	carb	carb	carb	carb	carb	carb	carb	carb	carb	carb	carb	
Zr (ppm)	460	210	14	13	12	28	110	30	557	85	352	33	93	681	42	19	38	3602	198	
Hf uncorrected	7	<7	<7	<8	<8	<8	<7	<7	<8	<7	<8	<7	<8	7	<8	14	<8	22	<9	
Hf corrected	7	7	7	8	8	8	7	7	8	7	8	7	8	7	8	14	8	22	9	
Y																				
Ho																				
Sr																				
Zr/Hf corrected	65.714	30	2	1.625	1.5	3.5	15.714	4.2857	69.625	12.143	44	4.7143	11.625	97.286	5.25	1.3571	4.75	163.73	22	
Y/Ho																				

6.5 Comparison with REE-rich carbonatites

Carbonatites of about 750 Ma have been described elsewhere on the African continent. For example, Midende et al., (1986) report ΣREE from 500 to 2500 ppm and strong LREE enrichment with La/Yb 80-140 in the 740 Ma Matongo Bandaga carbonatite (Burundi), and at Lueshe, (D.R. Congo), which is of similar age.

Table 6.10 Showing a comparison of REE between average calciocarbonatite (Woolley and Kempe, 1989) and the Lofdal carbonatite.

	Av Ca-carb	Min – max	Av Ca-Carb (Main plug and Zero)	Min-max	Ave	Min - Max	Ave	Min-max	Ave	Min - Max	Average	Min - Max	NAM - 914	NAM - 924
La	608	90 - 1600	845	238-2032	938	141 - 2089	1377	287-3126	663	394 - 998	129	68.2 - 190	13850	2952
Ce	1687	74 - 4152	1481	442-3488	1490	234 - 3312	2073	548 - 4462	1098	719 - 1562	270	198 - 341	26334	4458
Pr	219	50 - 389	150	44.9-351	136	25 - 299	184	56 - 376	120	89 - 161	34	30 - 38	2612	420
Nd	883	190 - 1550	485	150-1133	409	79 - 892	531	185 - 1027	483	404 - 594	155	152 - 158	8305	1362
TLREE	3397	219 -6691	3352	875-7004	2973	478 - 6592	4165	1076 - 8991	2367	1622 - 3315	588	448 - 727	51101	9192
Sm	130	95 - 164	63	22-143	39.3	11 – 79	56	28 - 91	496	455 - 536	178	128 - 227	908	280
Eu	39	29 - 48	17	6-38	10.1	4 -19	13	8 - 18	186	139 - 230	87	71.3 - 102	194	123
Gd	105	91 - 119	46	16-103	24.4	9 - 43	38	22.5 - 55.9	442	237 - 602	289	286 - 291	461	419
TMREE	274	29 - 164	141	45-28387	73.7	24 -140	107	59.4 - 165.2	1132	874 - 1367	553	485 - 620	1563	822
Tb			7	2-16	3.33	1 -5	6	3.13 - 9.04	50.7	17 - 73	50	41 - 59.6	41.7	60.8
Dy	34	22 - 46	45	12-107	19.5	10 - 27	36	17.2 - 67.1	225	59 - 359	267	180 - 353	160	278
Y	119	25 - 346	258	60-642	98	50 - 130	231	87.6 - 473	789	216 - 1325	1210	584 - 1835	742	1276
Ho	6	3 -9	10	2-23	4	2 - 5	8	3.32 - 16.3	32.8	8 - 55	45	25 - 66	22.9	42.6
Er			29	6-72	14	8 - 19	26	9.6 - 56.4	78.3	21 - 134	116	56.8 - 175	52.1	109
Tm			4	1-11	3	2 - 4	4	1.4 - 9.12	10.2	3 - 17	16	6.81 - 25.2	5.82	14.6
Yb	5	1.5 - 12	28	5-70	21.9	15 - 29	28	9.33 - 61.3	59.9	17 - 103	100	38.3 - 161	32.6	95.1
Lu	1		4	1-9	3.64	3 - 5	4	1.34 - 8.26	7.98	2 - 14	14	4.68 - 23.4	4.57	12.7
THREE	164.7	0 -346	384	90-951	167	91 - 224	343	132.92 - 700.52	1253	344 - 2079	1817	937.19 - 2697.8	1061.69	1888.8
TREE	3835.7	918 - 10632	3931	1009-8238	3211	593 - 6944	4628	1346.68 - 9856.72	4621	2840 - 6102	3182	2284 - 3631.4	53725.69	11902.8

Exceed limit
Within carbonatite average and Min-Max
below average and Min-Max
Far above averageand Min-Max
Far Below average and Min-Max

Another interesting but different comparison is with highly REE-rich carbonatites at Kangankunde, Malawi, which are ferroan dolomite carbonatites containing over 10 wt% RE_2O_3 and rock-forming quantities of the REE minerals such as monazite-(Ce), bastnäsite-(Ce) and florencite-(Ce) (Wall 2000, Wall et al. 2008).

The absolute concentrations of the HREE at Bayan Obo and Mountain Pass are high relative to LREE. The HREE values of the Dyke type-1 and Dyke type-2 mineralized dykes at Lofdal are high relative to the ores from Bayan Obo and Mountain Pass (Figure 6.25).

The LREE concentrations from Bayan Obo and Mountain Pass are orders of magnitude higher than at Lofdal but the values for MREE and HREE are similar and below Lofdal values, thus explaining why carbonatites with high amounts of LREE and discreet REE minerals do not usually contain xenotime-(Y) (Wall et al. 2008).

When Lofdal ferrocarbonatite (Type 2, 4 and 5) dykes are compared with Woolley and Kempe (1989) average ferrocarbonatite, Lofdal type 4 once again has markedly lower

LREE concentrations, MREE and HREE values that are just on the lower edge of the maximum values in the data set (Table 9.8).

However, the Woolley and Kempe (1989) data set was rather limited for HREE, with as few as one or two values for some elements and a much greater number of REE analyses were available to Le Bas (1997, 1999) but these are also limited on the Lofdal MREE and HREE concentrations context. The data set for some elements, such as Tm, is still small but for elements such as Yb, Le Bas has 96 values from 29 localities for the standard sövite calculation. The Lofdal calcite carbonatites (Zero sample, Main and Emanya carbonatite plugs) are comparable with the Le Bas standard (median) values for sövite (sövite = coarse-grained calciocarbonatite) and alvikite (alvikite = fine-grained calciocarbonatite) on Table 5.9.

In comparison to the Mountain Pass and Bayan Obo REE deposits, Lofdal carbonatites show a wide distribution of Sr in relation to LREE. There is a positive correlation between Sr and LREE-enriched carbonatite types 1 and 5 dykes. There is also a positive correlation with the poorly REE-enriched Main and Emanya carbonatite plugs. These carbonatites are rich in LREE-Sr-carbonate minerals such as strontianite and carbo cerianite. Such a correlation may indicate the tendencies of LREE to substitute for strontium in primary carbonate minerals.

The relation between the LREE and HREE, represented by La and Yb respectively, is shown in Figure 6.25. The Lofdal carbonatite plugs and the dyke type 1 are on the low end of the LREE and HREE enrichment field in comparison to Mountain Pass, Bayan Obo and other carbonatite dykes at Lofdal.

For the Main and Emanya carbonatite plugs, the light blue shaded area in Figure 6.25 represents the different calciocarbonatite dykes and the purple circle represents the dolomite carbonatite samples. The colour used for the sample points is consistent with the colours of representative samples used for Lofdal rocks in the thesis. Also shown are the minimum, mean, and maximum grades of the REE ores from Mountain Pass (Castor 2008) and Bayan Obo (Yuan et al., 1992; Yang et al. 2009), (A) Sr versus La (ppm) and (B) Yb versus La (ppm). Note the logarithmic scale.

Lofdal Type 1 to 6 dykes show extreme enrichment of HREE compared to the Lofdal carbonatite plugs and by far exceed the average HREE concentrations of Mountain Pass and Bayan Obo (Figure 6.25 and 6.26).

Most importantly, Lofdal carbonatite plugs are enriched with REE similar to carbonatites worldwide (Woolley and Kempe 1989), while the dykes are highly enriched in the HREE above the recorded values of carbonatites.

Most Lofdal carbonatite samples show low concentrations of Sr and La in comparison to Mountain Pass ores and the Bayan Obo carbonatite dykes, although a small number of samples from Lofdal are dispersed and are comparable to Mountain Pass ores and the Bayan Obo carbonatite dykes (Figure6.23). The Dolomite dykes have the lowest Sr and La content compared to other carbonatite rocks from Lofdal.

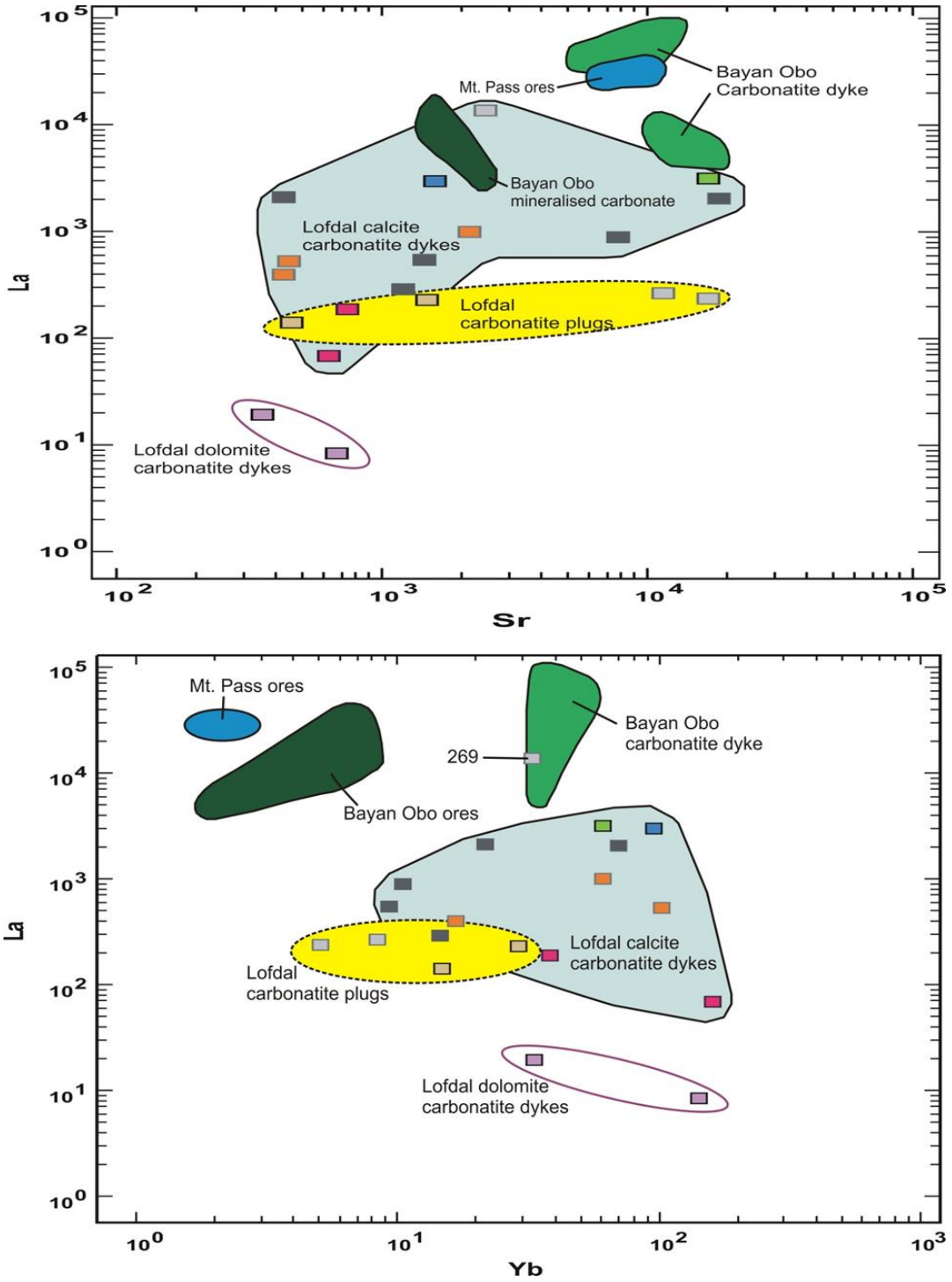

Figure 6.25 Diagrams illustrating the magnitude and significance of REE enrichment in the dykes of the Lofdal carbonatite complex.

Yellow oval shaded areas represent the On the plot of La versus Yb (ppm) (Figure 6.25), all Lofdal samples fall on the HREE side with the dykes showing more LREE and HREE than the plugs and the dolomite samples. Mountain Pass samples have the highest values of LREE compared to both Lofdal and Bayan Obo carbonatites. The Bayan Obo carbonatite dykes and ore samples also have high LREE above those recorded in Lofdal carbonatites, but the Bayan Obo HREE are comparable with the Lofdal Emanya carbonatite plug. Types 2,3,4,5 dykes and the dolomite dykes show higher HREE values than those at Bayan Obo dykes and the Bayan Obo ores are lowest.

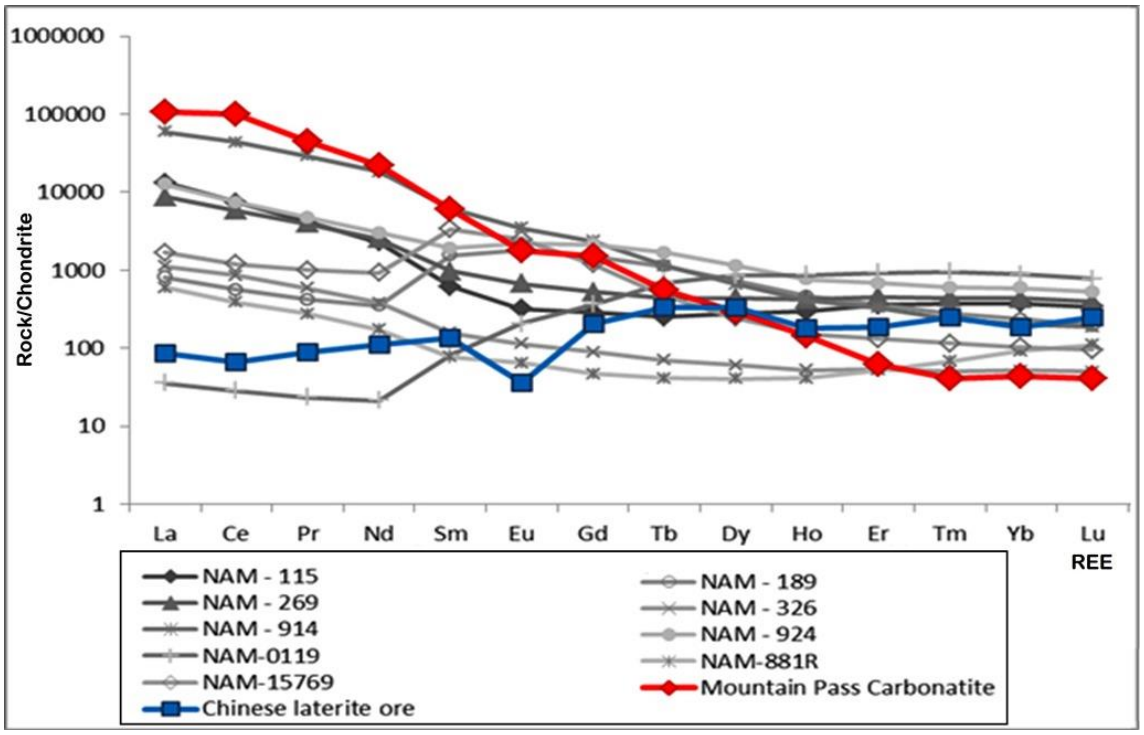

Figure 6.26 Chondrite-normalized values of REE pattern (Nakamura 1974), showing comparison of Lofdal carbonatites to the Chinese laterite ore and the Mountain Pass carbonatites.

There are noticeable differences among Lofdal carbonatites when compared to the Chinese laterites and the Mountain Pass carbonatites.

The Lofdal carbonatites are variable and bimodal with respect to enrichment in LREE, MREE and HREE, showing distinct variations in the REE concentrations among the dykes and the carbonatite plugs. Lofdal is comparable with world class REE-enriched deposits which are enriched in LREE such as Mountain Pass, and with Bayan Obo that is enriched in both LREE and HREE.

6.6 Conclusions

The conclusions drawn from the Lofdal carbonatite geochemistry are that:

1. Lofdal carbonatites are classified as calciocarbonatites, ferrocarbonatites and magnesiocarbonatites according to the IUGS carbonatite classification.
2. Lofdal carbonatites are consistent with other known carbonatites worldwide as far as their association with alkaline silicate rocks is concerned.
3. Lofdal carbonatites can be grouped into eight distinctive groups according to their LREE, MREE and HREE distribution.
4. Some Lofdal carbonatites show REE-enrichment especially in the MREE and HREE, which are all above the average calciocarbonatite (Woolley and Kempe 1989), making these different to all other known carbonatites.
5. Incompatible elements such as Sr, Ti and Ba are consistent with the groupings based on the REE distribution in the Lofdal carbonatite rocks.

Further conclusions and discussion are left until after the mineralogical and additional geochemical results presented in the following chapters.

Chapter 7: Mineralogy of the Lofdal carbonatites

7.1 Introduction

This chapter has four main emphases:

1. Mineral assemblage description of the Lofdal carbonatites according to their classifications, based on the REE distribution as discussed in the previous chapters.
2. Listing of minerals found at Lofdal including the REE hosting minerals.
3. Description of the mineral compositions for xenotime, monazite, synchysite, parisite, thorite, apatite, zircon, fluorite, pyrochlore, calcite and dolomite.
4. Comparison of the whole rock and mineral compositions and discussion of minerals formation in the carbonatites at Lofdal.

Fifteen rock samples have been used for the study of mineral characteristics. The samples were selected based on the different geochemical characteristics observed among the Lofdal carbonatites. Different methods were used on different samples for the understanding of mineralogy of Lofdal carbonatites (see appendix 7).

Hand specimens were described and later pulverised for the XRD and parallel thin sections were prepared for the petrographic study. Later the samples were analysed using SEM, EDS and EPMA. A selection of minerals depending on the grain sizes and suitability were analysed for trace elements using the LA-ICP-MS (see method details in Chapter 4).

7.2 The mineral assemblages at Lofdal

Lofdal carbonatites have variable textural characteristics and contain a wide range of mineral assemblages. The samples studied are coarse, medium to fine-grained calciocarbonatites, ferrocarbonatites and dolomitic carbonatites overprinted by a widespread hydrothermal assemblage. Iron oxide staining is abundant in the calciocarbonatite with a characteristic dark brown, red to yellow colour.

At Lofdal, the mineralogy varies spatially within the same rock and even within the same thin section sample and often the chemistry of a mineral species displays a large compositional ranges. A wide variety of different minerals have typically formed within a single rock type. Forty one minerals have been identified in the eight main carbonatite groups at Lofdal.

The mineral groups identified include phosphates, oxides, carbonates, silicates, sulphates and halides. The list of minerals found in the carbonatites at Lofdal is presented in Table 7.1 and an attempt has been made to quantify major mineral constituents in these rocks. The minor and accessory phases are listed but not their amounts. REE hosting minerals are listed in Table 7.3 according to their mineral classes.

The carbonate in Lofdal carbonatites is mainly calcite and this is the most widespread mineral at Lofdal but there is also minor dolomite and ankerite. Apatite, synchysite, fluorite, Fe- oxide and xenotime-(Y) are found as major components in some carbonatite samples but they are mostly present as accessory minerals. Fe oxide includes magnetite, hematite and amorphous iron oxide phases. Thorite/hutonite, zircon, baryte and biotite are accessory minerals. Rare accessory minerals include celestine, smithsonite, galena, quartz, rutile, strontianite and amphibole. These minerals occur mainly in the calciocarbonatite matrix and in the calciocarbonatite veins that cut earlier ferruginous calcite carbonatites. Thus, these are secondary minerals forming during the late hydrothermal phase.

The hydrothermal assemblage in these rocks consists of both LREE and HREE-bearing minerals. Apatite, quartz, albite and fluorite are important gangue minerals in REE-bearing carbonatite dykes. Both LREE and HREE minerals occur in significant amounts of up to 10 vol % in the rock sample.

Apatite is a typical magmatic mineral in carbonatites that is used to mark the end of the magmatic phase (Wall et al. 2000). At Lofdal apatite occurs as a magmatic mineral but when in association with xenotime-(Y) II, it is clearly a post magmatic mineral (Table 7.2). It marks the transition phase forming a dissolution-reprecipitation with xenotime-(Y) II in some samples (Figure7.20).

Minerals Content in Lofdal carbonatite (%)																			
Carbonattite Type	**Dolomite**		**Main Carbonatite plug**			**Emanya carbonatite plug**			**Type 1 dyke**				**Type 2 dyke**		**Type 3 dyke**			**Type 4 dyke**	**Type 5 dyke**
Sample NO.	**114**	**119**	**N08-58**	**326**	**269**	**881G**	**881R**	**949**	**813**	**15769G**	**907**	**115**	**927**	**189**	**15769**	**15769LG**	**15796**	**924**	**914**
Mineral																			
amphibole													_					_	
aegirine						_	_			_		XX			_	_	_		
allanite												_							
ancylite (Ce)				_	_														
apatite	_	X	_		_	_		X	_	XX	XX	X	3	2		3	1	2	XX
barite			_		_	_				_								_	
biotite	_	_			_	_						_			_	_			
bismuth						_													
celestine					_							_							
carbonate (ankerite)	15	22										_	5	5	x				10
carbonate (calcite)	2	3	99.5	99	97	98	97	94	65	98	80	40	34	52	65	95	72	85	32
carbonate (dolomite)	80	75											15	10					15
cerianite				_	_														
chlorite								_								_			
Fe-hydroxide (amormph)												_		_					
fluorite					_	_	_	_	_		7	_	X	XX	X		XX	1	52
galena									_		_	_							
hematite	0.5				_	_	_	5		_	_	_	20	30	XX	_	21	XX	6
ilmenite					1														
k-feldspar								_	_			_	1	7					2
magnetite	_	_			_	_	_	X	_	_	_	_	0.5	3	2	_	_	_	3
Mn oxide									_			1	XX	XX	XX		XX		XX
Mn rich calcite												3							
kutnahorite												1							
monazite	X	_		XX														_	
sychysite (Ce)				_	_		_	_	_	_	_	3	_	_	_		_		5
parisite (Ce)				_	_		_	_	_	_	_	2	_	_	_		_		2
phlogopite											_	_	_					_	
plagioclase + albite	2	_							32			_						_	
pyrite				_			_									_			
pyrochlore									XX				XX	XX				_	
quartz	X	X				_			_	_		_					XX	1	
riebeckite												_	_						
rutile						_		_				_	_		_		_		
smithonite									_			XX							
sphalerite					_														
strontianite			_	_	0.5					_		1							
thorite/hutonite						_				_	_	_	X	2	_	_	1	XX	
xenotime	0.8	3					_	_		_			3	1	_	_	0.8	_	
zircon	_	_							XXX				_			_	_		

Table 7.1 Lofdal minerals with their modal composition %

Note: The number represents percentage of mineral in the rock, ***X****= accesory* ***XX****= abundant and - = trace*

Table 7.2 Mineral paragenetic sequences of the Lofdal carbonatite rocks

Magmatic	Transition	Hydrothermal
aegirine		
albite		
allanite		
ancylite		
ankerite		
apatite		
amphibole		
baryte		
biotite		
bismuth		
calcite		
carbocernite		
cerianite		
chlorite		
dolomite		
Fe-oxide		
fluorite		
galena		
hematite		
ilmenite		
Mn oxide		
monazite-(Ce)		
parisite-(Ce)		
phlogopite		
pyrite		
pyrochlore		
quartz		
rutile		
smithsonite		
sphalerite		
strontianite		
synchysite-(Ce)		
thorite/huttonite		
xenotime-(Y)		
zircon		

Note: Solid lines in the table indicate observations that clearly define the precipitation phase, while dashed lines indicate a gradational stage from one phase into another.

Transitional minerals were formed immediately after the magmatic phase but before the hydrothermal phase.

Associations such as synchysite-(Ce) replacing calcite are certainly sub-solidus reactions and appear to be the product of low temperature hydrothermal activity. The observed synchysite-(Ce) - xenotime-(Y) association is also considered to occur in the hydrothermal phase, similar to the xenotime-(Y)-monazite-(Ce) association described by Wall et al. (2008).

Boundaries from one paragenetic phase into another are gradational and this is even more prominent between the transitional and hydrothermal phases, thus making it difficult definitively separate the two phases. Despite the gradational nature and the arbitrary boundaries between phases, some minerals are observed to crystallise at specific time before other minerals have precipitated and it is for this reason that a transitional phase is used to define the paragenetic position of such minerals.

7.3 Petrographic and mineral association of different carbonatite types at Lofdal

Mineral descriptions are presented according to the eight (8) carbonatite groups identified in chapter 6 based on geochemical criteria, particularly the chondrite-normalised REE patterns and LREE, MREE and HREE ratios.

7.3.1 Petrography and Mineralogy of the Main Carbonatite Intrusion Plugs

Samples 58, 326 and 269 represent the main intrusive carbonatite plug. Sample 269, having a low degree of alteration and light colour compared to other carbonatite dykes (Figure7.1), is considered to have similar characteristics to the main intrusion plug and therefore, forms part of this carbonatite group even though it is a dyke.

The calciocarbonatites of the Main carbonatite plug are characterized by a coarse-grained, rhombohedral white crystal of massive non-mineralised sövite. Some veinlets of younger calcite crosscut the sample. Some of these late veinlets are magnesium-rich and contain hydrothermal REE-bearing minerals. Accessory minerals such as synchysite-(Ce), parisite-(Ce), monazite-(Ce), strontianite, apatite, baryte, fluorite strontianite, pyrite and magnetite are encountered. Monazite-(Ce), magnetite, carbocernaite and cerianite-(Ce) show igneous textures and form elongated and euhedral crystals in the calcite matrix, while other LREE bearing minerals observed in the main calcite carbonatite occur mainly along the edges of calcite grains, in the calcite cleavage fractures and altered calcite zones. These secondary minerals also form tiny areas up to 30 μm long found mostly in cavities within the calcite. Synchysite-(Ce) occasionally forms needle-like textures that radiate outwards and are in contact with strontianite.

Table 7.3 List of REE hosting minerals in the Lofdal carbonatites

Mineral class	**Mineral**	**Chemical formula**	**Mode of occurrence**
Phosphates	Monazite-(Ce) xenotime-(Y) apatite	(Ce, La, Th, Nd, Y)PO_4 YPO_4 $CaPO_4$	Magmatic, fracture filling and replacement magmatic, vein, fracture filling and replacement magmatic and vein
Carbonates	ancylite-(Ce) synchysite -(Ce) parisite-(Ce) carbocernite, -(Ce)	Ce,Sr, Ca)$(CO_3)(OH,H_2O)$ $Ca(Ce, La)(CO_3)_2F$ $Ca(Ce, La)_2(CO_3)_3F_2$ $(Ca,Na)(Sr,Ce, Ba)(CO_3)_2$	fracture filling veins, fracture filling and replacement veins, fracture filling and replacement hydrothermal
oxides	cerianite -(Ce) pyrochlore	$(Ce,ThO_2$ $(Na, REE, K,U)_2 (Nb, Ta, Ti)_2 (O,OH,F)$	Magmatic Magmatic
Silicates	allanite-(Ce) zircon	{Ca, Ce}{Al $_2Fe^{+2}$}$(Si_2O_7)(SiO_4)O(OH)$ (Zr, REE) SiO_4	Cavities Magmatic
Halides	Fluorite	(Ca, REE) F	Magmatic and veins

Note: Mineral formulae from Mindat.org (IMA approved).

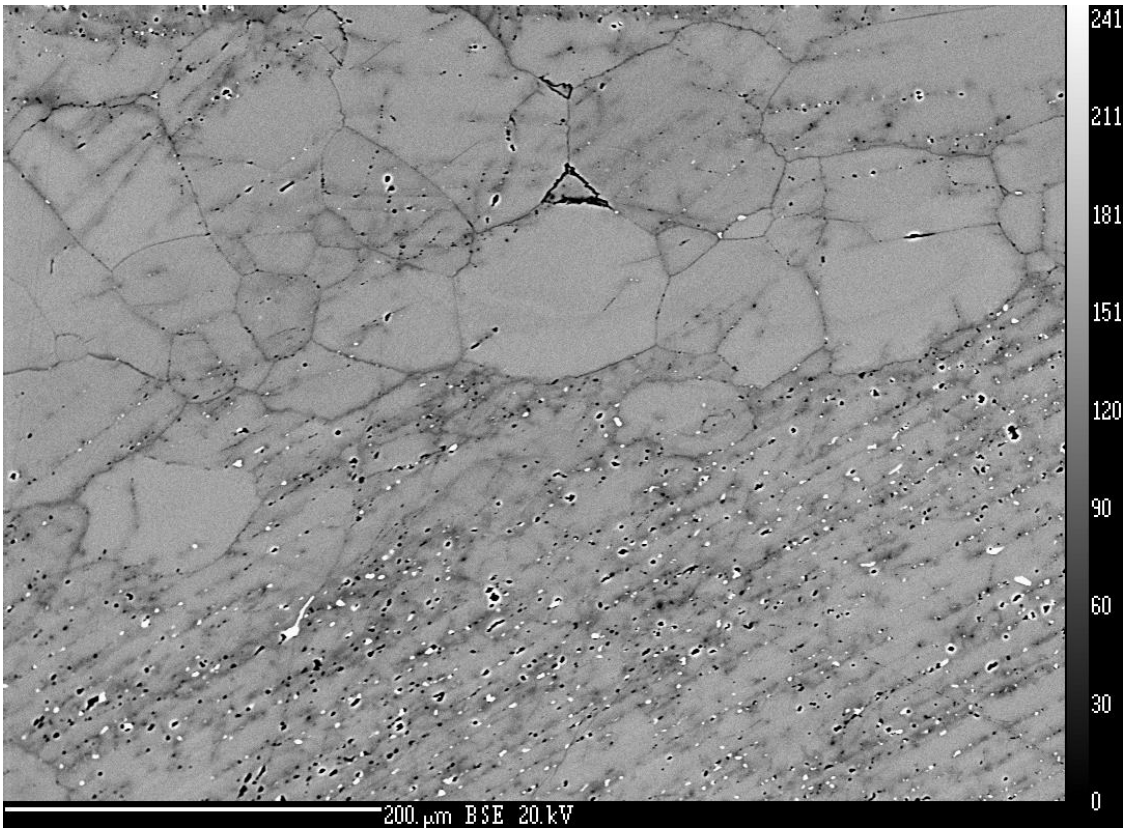

figure 7.1 Sövite of the Main carbonatite showing weak alteration and replacement of calcite

Strontianite and **apatite** may occur as single grains within the calcite grains and also along the cracks and lamellae of the calcite.

Baryte was observed to form only along the veinlets within the calcite lamellae. The location of these minerals in the altered and fractured zones indicates their late precipitation in the system, possibly, during the hydrothermal phase, when the fluids concentrated in the open spaces of the cavities.

The non-rock forming minerals in dyke 269 exceed those in the main carbonatite plug. These include barytocalcite, albite, biotite sphalerite, ilmenite, ancylite-(La), fluorite and celestine. Other accessory minerals are aegirine, apatite, strontianite, pyrite and synchysite-(Ce). All accessory minerals are localised in veinlets and cavities, rather than in the calcite matrix of the early magmatic phase and therefore are here interpreted to have formed during late-stage processes of the hydrothermal phase.

Celestine is intergrown with ancylite while baryte is intergrown in the calcite matrix, but not in the lamellae structures as observed in the rocks of the Main calciocarbonatite plug.

Magnetite forms subhedral large grains in association with ilmenite. Ilmenite is at times enclosed within magnetite, forming inclusions. Anhedral and elongated subhedral grains of ilmenite reach up to 100 μm wide and are set in the calcite matrix.

Fluorite forms single and aggregated anhedral large grains in the calcite matrix and in areas rich in synchysite-(Ce), parisite-(Ce) and magnetite.

Apatite occurs as anhedral grains in the calcite matrix, concentrated in areas rich in Fe-oxide, following bands of flow textures.

Celestine occurs as grains in the calcite matrix and in contact with elongated ilmenite.

Synchysite-(Ce) and parisite-(Ce) form large grains in close association with largely sized fluorite in the calcite matrix.

Hematite is the main iron oxide observed forming stains in the calcite matrix. **Calcite** is in places homogenous but is mostly altered and stained with Fe-oxide.

Some flow banding or mineral zonation is marked by enrichment of synchysite-(Ce), parisite-(Ce), and magnetite that are clearly observed on backscattered electron images.

Sphalerite occurs in zones with flow banding, occurring as minute grains up to15 μm.

Biotite is encountered in the matrix close to ancylite, while anhedral-shaped baryte crystals are in the matrix surrounded by calcite.

Ancylite-(La) forms anhedral grains and in places, form needles, that are closely associated with strontianite and bordered by calcite.

7.3.2 Petrography and mineralogy of the Emanya carbonatite plug

The Emanya carbonatite plug has three main rock types;

1. Pure calcite with very little alteration.
2. A mixture of fine-grained calcite and albite mixed with small grains of fluorite, xenotime-(Y), magnetite, apatite and Fe-oxide and a secondary pure calcite, forming part of the rock matrix.
3. Brown with a bluish tint and iron stained calciocarbonatite represented by sample 949.

This rock consists of calcite with iron oxide veinlets in areas rich in fluorite. Calcite forms euhedral grains. One sample shows flow texture and mineral zonation marked by enrichment of synchysite-(Ce) and magnetite.

Accessory minerals in the Emanya calciocarbonatite are baryte, rutile, apatite, synchysite-(Ce), parisite-(Ce), native bismuth, magnetite/hematite, fluorite, quartz, thorite, magnetite, K-feldspar, rutile, phlogopite, xenotime-(Y) and aegirine.

Under the scanning electron microscope synchysite-(Ce) and parisite-(Ce) show zonations that are marked by light and dark grey areas. Brighter areas contain more Ce than darker areas (Figure7.9). Synchysite-(Ce) and parisite-(Ce) are in contact with resorbed apatite, rutile and anhedral grains of iron oxide. In some representative samples of the Emanya carbonatite group, synchysite-(Ce) and parisite-(Ce) form anhedral mineral grains, especially in the heterogeneous calcite that is Fe-oxide rich, but not in the late pure calcite carbonatite areas. Magnetite forms single subhedral small grains in the oxidised calcite matrix, while in the sample 949, it forms zones, that are magnetite rich and are closely associated with synchysite-(Ce) and fluorite.

In samples 881G and 881R, hematite occurs as stains on the calcite grains and also as an alteration product of magnetite in cracks and areas with flow textures.

Fluorite forms anhedral large grains up to 50 μm scattered in the calcite matrix and in places associated with the pyroxene mineral aegirine. Quartz is anhedral up to 10 μm and is scattered within the oxidized calcite matrix.

K-feldspar forms anhedral grains in the calcite matrix in areas rich in Fe-oxide alteration and in contact with rutile.

Rutile forms highly resorbed grains that are dispersed in the calcite matrix and are associated with LREE in less altered samples of 881R and 881G. In sample 949 rutile forms up to 100 μm wide euhedral grains in calcite that is homogenous. Rutile in altered calcite with Fe-oxide occurs as small aggregated grains and/or along the magnetite grains. Rutile was also observed in vugs and in contact with the synchysite-(Ce) and albite. Other minerals found in the homogenous calcite areas are euhedral grains of xenotime-(Y) and magnetite.

Baryte forms up to 80 μm anhedral resorbed and broken grains in the oxidized calcite matrix.

Thorite/hutonite forms single crystals in the calcite matrix and small grains within and at the edge of synchysite-(Ce) and parisite-(Ce).

Native Bismuth occurs as subhedral 10 μm grains in the calcite matrix. Bismuth is uncommon in carbonatites with only two localities reported to contain bismuth minerals in carbonatites (Mindat.org). These are Phalaborwa, South Africa and Fuerte Aventura, Canary Islands. On farm Mesopotamia 504 at about 7 km NW from Lofdal, bismuth is reported from an old Cu mine known as the Mesopotamie Copper Valley. This is a polymetallic hydrothermal quartz-vein deposit of Cu, Bi, W, Pb, V and Ag.

Xenotime-(Y) forms euhedral grains in the highly oxidized calcite carbonatite sample 949 but surrounded by pure late calcite that is fluorite rich and in association with

magnetite. Xenotime-(Y) is also observed infilling cracks in the magnetite grains, located in pure calcite and fluorite rich areas. No xenotime-(Y) was observed in the heterogeneous and altered calcite Fe-oxide areas in rocks of the Emanya.

7.3.3 Petrography and mineralogy of the dolomite carbonatites

This type of carbonatite is represented by ferruginous cataclastically brecciated xenotime-(Y)-bearing dolomite-ankerite carbonatite (Samples 119, 114). The matrix of the dolomite carbonatites consists of two different types of dolomite;

(1) Dolomite that is iron rich (brighter areas) and

(2) Dolomite that is iron poor (darker areas) (Figure 7.2 and 7.4).

The iron poor dolomite is brecciated by the iron rich dolomite. Healing of the cracks of the early dolomite is observed. Brecciation of the Dolomite dykes is followed by the infiltration of albite that forms large grains in the matrix. The two dolomite dykes and the albite breccia are later re-brecciated and filled with late calcite, xenotime-(Y) and phlogopite that fill in the fractures and form the matrix of some earlier breccias. These mineral mixtures form veinlets that crosscut the rock section (Fig 7.2 and 7.3).

Dolomite, xenotime-(Y) and late calcite form the major mineral assemblage in the dolomitic/ankeritic carbonatites. Other accessory minerals are hematite, magnetite, apatite, phlogopite, synchysite-(Ce), parisite-(Ce), zircon and thorite/huttonite.

The main mineralogical characteristics of the dolomite dykes at Lofdal is their carbonate mineral compositions, which are mainly dolomite-ankerite solid solutions (Ca (Mg, Fe^{+2}) (CO_3). Structurally, these rocks are intensely brecciated and crosscut by veinlets rich in calcite and xenotime-(Y).

Xenotime-(Y) has several mineral paragenesis and assemblages in the dolomite carbonatites:

- Very fine-grained fibrous xenotime-(Y) occurs in veinlets and forms a major mineral component of the rock (up to 3%).
- Xenotime-(Y) segregations, nests and veins cut earlier dolomitic/ankeritic carbonatites;
- Xenotime-(Y) occurs in a heterogeneous matrix and in contact with synchysite-(Ce) and parisite-(Ce);
- As small veins with inclusions of zircon and magnetite and along the darker coloured grains of the carbonates (dolomite1).

- At times xenotime-(Y) shows complex internal zoning textures, when mantling the zircons. Zircons mantled by xenotime-(Y) are euhedral, while isolated zircon grains are largely altered.

Xenotime-(Y) is the main carrier of the HREE mineralisation in the dolomite carbonatite dykes, causing the observed characteristic chondrite normalised REE pattern (Figure 8.3). The observed texture in the dolomite dykes points to a hydrothermal process of secondary HREE-enrichment. Xenotime-(Y) does not exhibit any magmatic texture in these rocks.

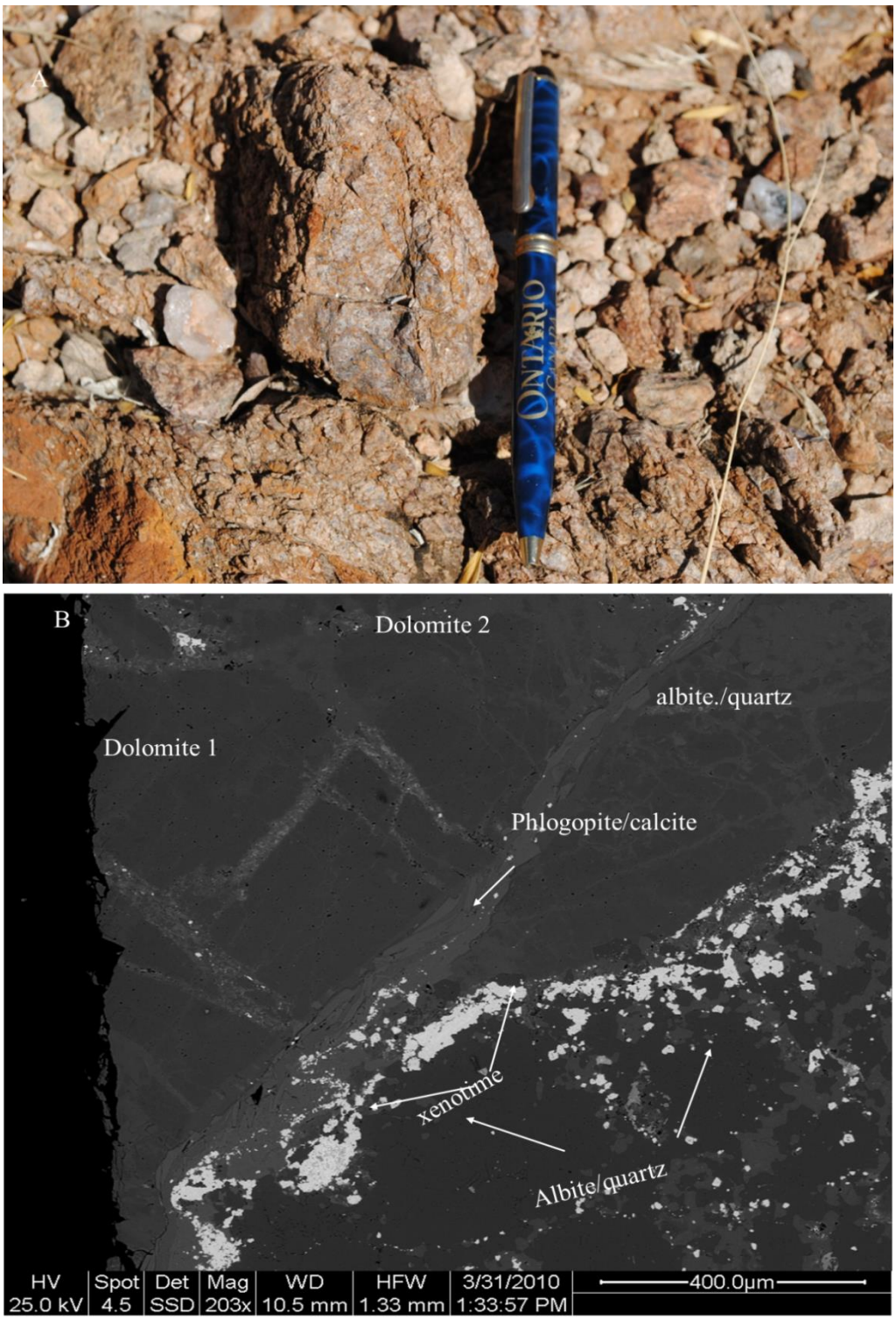

Figure 7.2 Lofdal dolomitic carbonatites: A) Rock outcrop of the dolomite sample 114 showing the micro breccia of the dolomitic carbonatite; B) Dolomitic/ankeritic rock with xenotime-(Y) veinlets (white areas), filling fractures of dolomite 1, 2 and albite breccias.

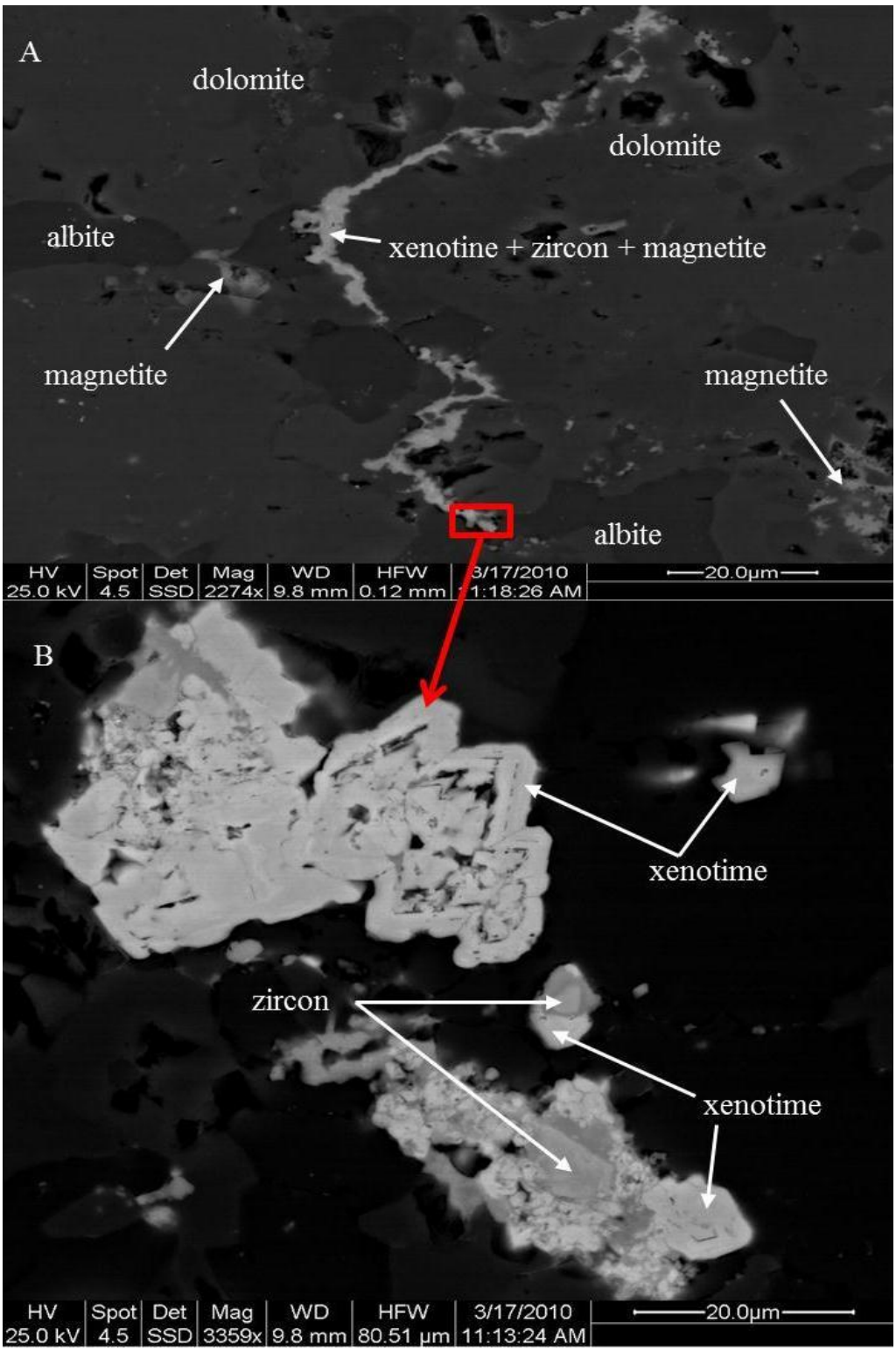

Figure 7.3 Back scattered electron image showing A) Dolomite/ankerite carbonatite cut by calcite and xenotime-(Y)-rich veinlets; B) Close view of the dolomitic carbonatite showing veinlets with xenotime-(Y) enclosing zircon. Note the complex xenotime-(Y) internal textures and zircon mantled by xenotime-(Y).

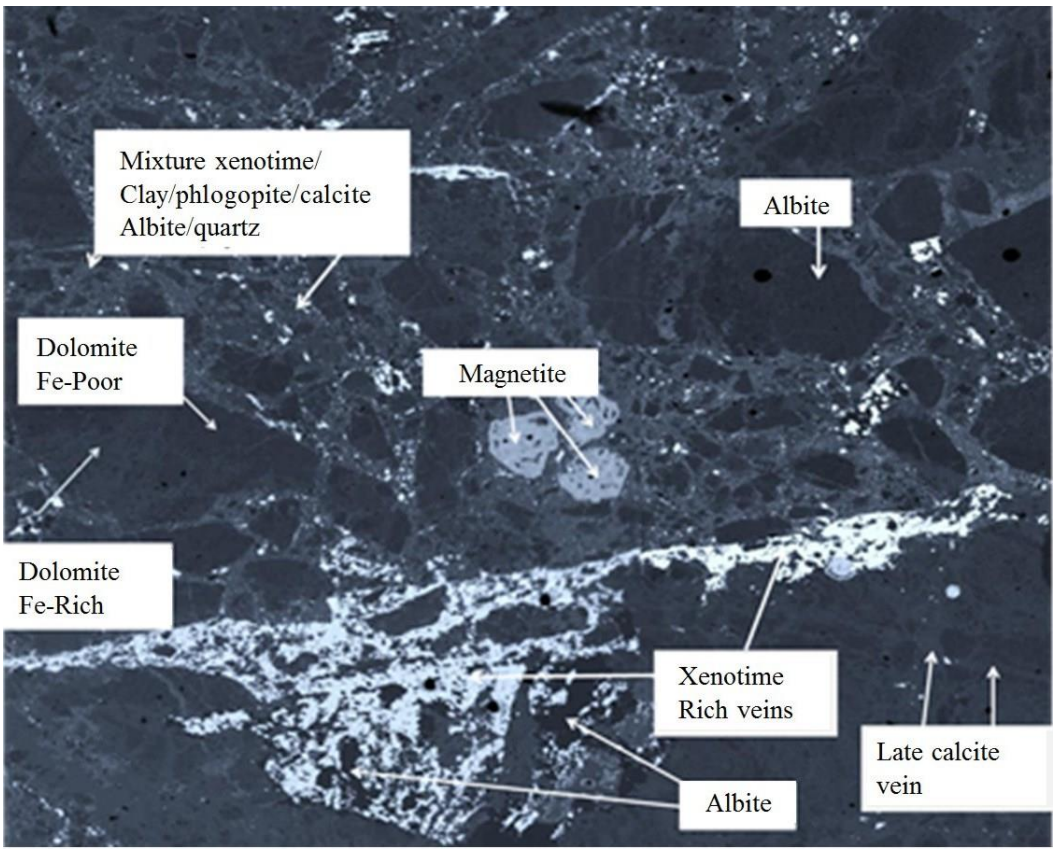

Figure 7.4 BSE showing the internal textures of the dolomite/ankerite carbonatite at Lofdal. Note the very fine grained fibrous xenotime-(Y) mineral in the veinlets, iron-rich-dolomite (brighter areas) iron-poor dolomite (darker areas).

The following minerals are found in Lofdal dolomite carbonatite:

Apatite is subhedral forming grains up to 20 μm that are scattered in the matrix and mostly aggregated with a heterogeneous texture in the late calcite and in contact with magnetite and the dolomite matrix. Apatite contains abundant inclusions of xenotime-(Y) and thorite/huttonite inclusions.

Magnetite forms euhedral to subhedral grains, which are scattered in the iron stained calcite matrix and in contact with calcite and apatite. Magnetite grains are strongly altered to hematite.

Quartz is highly resorbed in the calcite matrix indicating disequilibrium in such an environment. Quartz was also observed in contact with synchysite-(Ce) and parisite-(Ce).

Calcite constitutes the lighter grey areas observed in the breccia crack filling areas of the section and in the veinlets that intruded late into the system during the hydrothermal phase. The evidence of late calcite intrusion is also confirmed by the Cathodoluminescence image observation (Figure 7. 12).

Monazite forms small anhedral grains in the calcite matrix and is particularly found in areas rich in apatite and xenotime-(Y).

Biotite and **phlogopite** form part of the observed flow texture in areas that are rich in albite, quartz and calcite. Both minerals are but different mafic micas. This observation suggests that biotite and phlogopite are part of the albitisation, which preceded the HREE enrichment process. The presence of two mafic micas is either a replacement/reaction between them.

Albite forms large anhedral grains scattered in the dolomite/ankerite.

Synchysite-(Ce) and parisite-(Ce) are highly altered and show some zoning, occurring in single grains that reach up to 40μm, located between fluorite and calcite and sometimes associated with ilmenite. Lofdal dolomite type carbonatite contains needle-like parisite- (Ce) in close association with celestine and Sr-baryte.

7.3.4 Petrography and mineralogy of Type 1 dykes

The group is represented by samples 115, 15769G, 813 and 907. Most carbonatite dykes at Lofdal are Type 1, consisting of sheared dark grey calciocarbonatite dykes rich in sulphides, magnetite, iron-manganese-oxides, albite and fluorite. These carbonatite dykes are mostly heterogeneous, altered and stained with Fe-oxide. Some flow texture or mineral bands marked by zones rich in synchysite-(Ce), parisite-(Ce) fluorite and magnetite are generally observed.

All samples of this group display variable mineralogy and similar REE patterns. Accessory minerals in Type 1 dykes are strontianite, synchysite-(Ce), parisite-(Ce), thorite/huttonite, fluorite, apatite, albite, ilmenite, galena, amphibole, hematite, baryte, sphalerite, pyrite, zircon, allanite, phlogopite-annite, aegirine, barite (enclosing magnetite subhedral crystals), willemite, pyrochlore and rutile. These minerals occur only locally and can be absent in some samples of the group.

Synchysite-(Ce) and parisite-(Ce) in the calcite veinlets are zoned and form anhedral grains that are in contact with anhedral chlorite, calcite and apatite.

Sample 813 is different with very heterogeneous matrix made up of calcite with Fe-oxide, large albite, zircon and pyrochlore minerals (Figure 7.5).

Sample 115 is the most heterogeneous of the group with recrystallised areas that have Mn-bearing calcite, locally with a very fine-grained mixture of Fe-Mn-oxides and pure calcite all forming the rock matrix. Locally nests of Fe-Mn-oxides form very fine-grained mixtures of ankerite-kutnahorite with calcite (Figure7.6).The rock exhibits massive veins and veinlets marked by synchysite-(Ce), parisite-(Ce), and strontianite

(Figure 7.7). TiO_2 polymorphs (anatase, brookite or rutile) are common in the late-stage paragenesis locally as a replacement product of ilmenite.

The description of the mineral occurring in Type 1 dykes is as follows;

Synchysite-(Ce), parisite-(Ce) occur together with strontianite and in association with sulphides, (galena and sphalerite), Fe-Mn-oxides and phlogopite in veinlets, clearly indicating that strontianite together with REE-fluorocarbonate minerals (synchysite-(Ce) and parisite-(Ce)) are late-stage minerals formed at metasomatic/autometasomatic stage. Parisite-(Ce) and synchysite-(Ce) are found as single crystals, aggregates and chains similar to those earlier discussed in the Main carbonatite group (sample 269).

Albite is found in calcite together with small grains of fluorite, xenotime-(Y), magnetite and apatite.

Magnetite forms single euhedral small grains in the calcite matrix Fe-oxides (hematite) replace magnetite.

Baryte occurs as anhedral grain inclusions in the calcite matrix in contact with anhedral magnetite and at places forming the matrix around the anhedral magnetite although most magnetite forms euhedral crystals in this rock, similar to cumulate texture.

Quartz occurs as anhedral grains in the calcite matrix.

Apatite forms elongated strings indicating flow textures and at places forming subhedral aggregated grains in calcite.

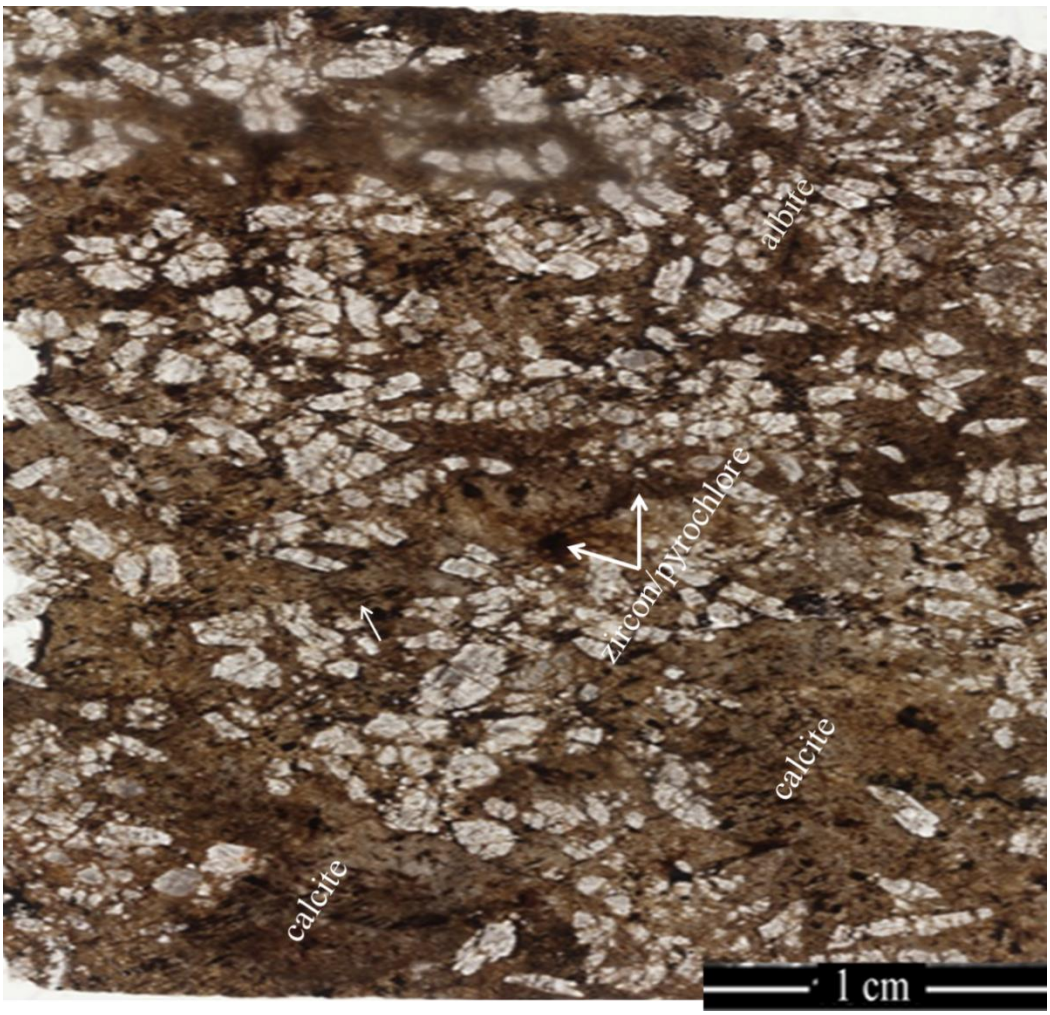

Figure 7.5 Thin section of calciocarbonatite from a Type 1 dyke (Sample 813) with albite, pyrochlore and zircon.

Galena forms up to 20 μm wide euhedral grains in the heterogeneous part of the matrix and occurs only in the dark coloured part of the sample, which is rich in calcite veinlets crosscutting the section (Fig 7.6). Fluorite and calcite of primary origin are cut and resorbed by these veins.

Fluorite shows simple zoning with bright colour in the centre of the mineral and darker colours on the boundaries. Fluorite anhedral grains in calcite exceed 1mm in size (sample 907) and are closely associated with synchysite-(Ce) and parisite-(Ce). These large fluorite grains indicate early formation possibly at the end of magmatic phase. The fluorite grains associated with Fe-oxides are grouped in chains or veins cutting the whole slide as in sample 269 at the late stage of the carbonatite formation and are clear secondary minerals.

Phlogopite occurs as anhedral grains in the calcite matrix in areas rich in Fe-oxide and in associated with altered synchysite-(Ce) and parisite-(Ce).

Thorite\huttonite is found as minute grains in the calcite matrix and at the edge of synchysite-(Ce) and parisite-(Ce). It also occurs as small grains between magnetite aggregates in the calcite matrix.

Zircon forms large, up to 30mm grains (Fig 7.19). New age determinations were carried out on zircon and pyrochlore from this type of carbonatite and the results are presented in Chapter 8.

Calcite is variable in composition with homogeneous unaltered areas containing minor Mn and Fe. Where alteration is observed, calcite contains abundant Mn and Fe oxides. Sometimes calcite forms large homogenous crystals but typically is altered and stained with Fe-oxides (Fig 7.7). Flow banding or mineral zonation is marked by enrichment of synchysite-(Ce), parisite-(Ce) and magnetite.

Xenotime-(Y) forms up to 20 μm wide strings of aggregates made of individual subhedral and poorly zoned grains in younger calcite veinlets crosscutting the calcite matrix. In places xenotime-(Y) can be found disseminated as single grains in the matrix and as inclusions in the magnetite mineral, similar to those observed in sample 949 of the Emanya calciocarbonatite plug. Such textural features suggest an early paragenesis.

Pyrochlore was only found in Type 1 Dykes (sample 813).

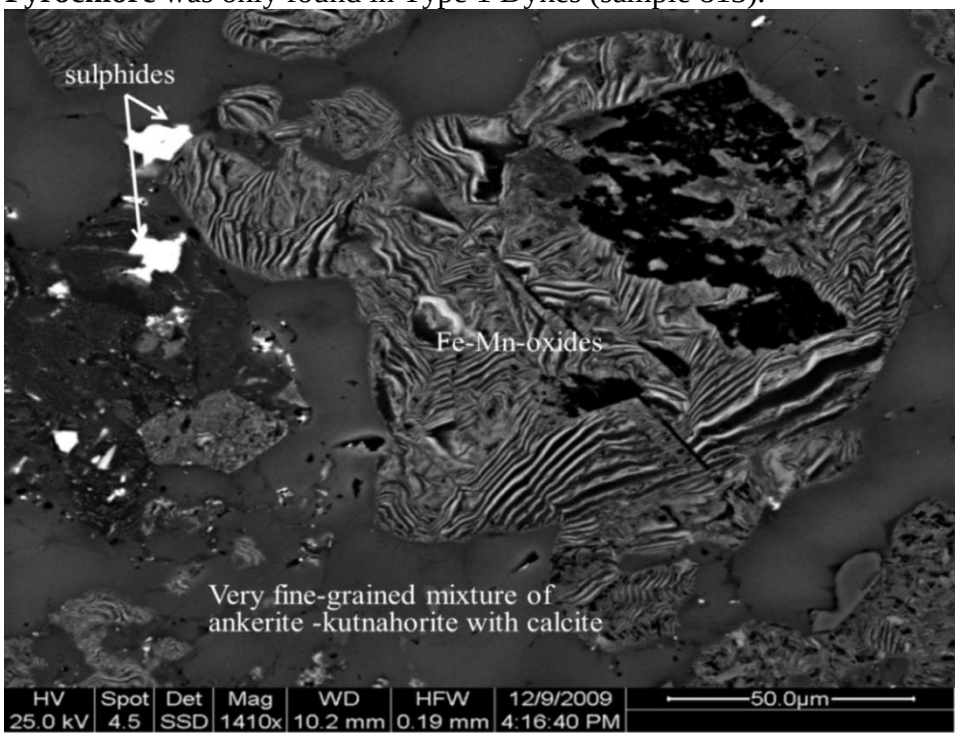

Figure 7.6 Iron-manganese-oxide pseudomorphs in the calcite matrix

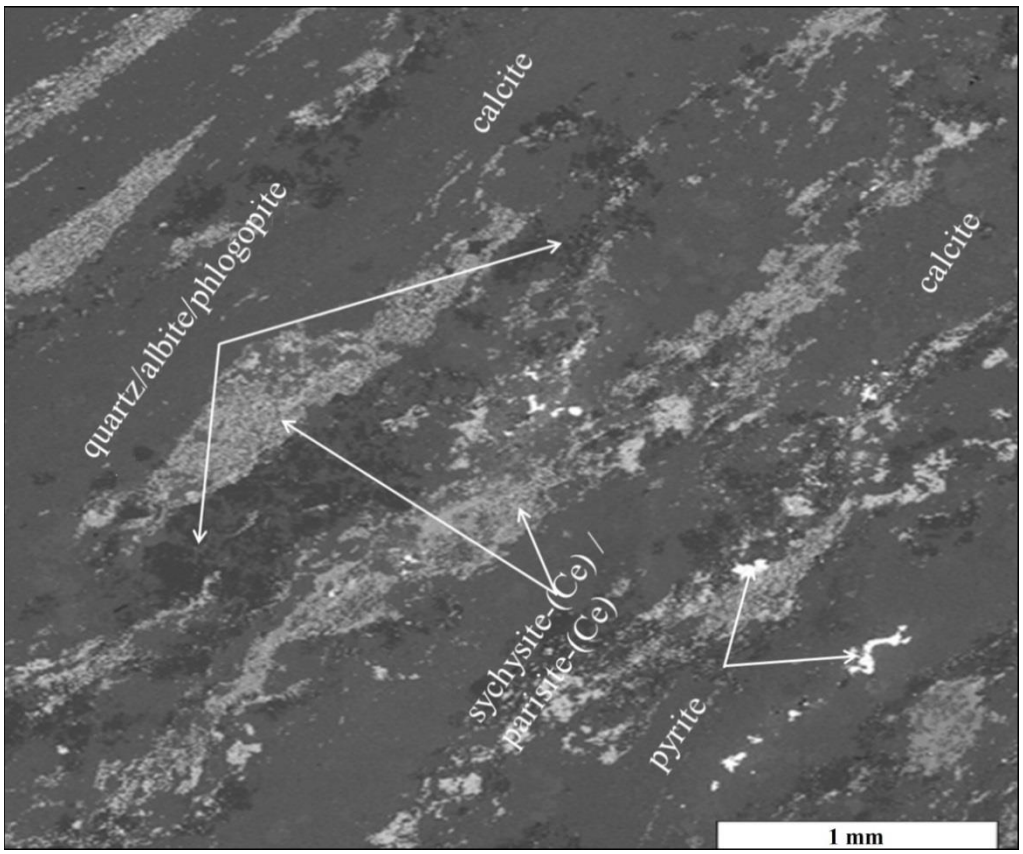

Figure 7.7 Flow texture and mineral zonation in sheared Type 1 dyke calciocarbonatite shown by synchysite and parisite (light colours); the grey areas are calcite

7.3.5 Petrography and Mineralogy of Type 2 dyke

The group is represented by samples 189 and 927. Type 2 dykes consist of the most sheared and altered calcite-carbonatite dykes. These rocks are highly ferruginous with colours ranging from dark brown, bright orange-brown to yellow and are generally silicified calciocarbonatite, with abundant mica of the phlogopite-annite series. These dykes are crosscut by two other carbonatite generations after their emplacement. The matrix of the samples belonging to this group consists of Fe-oxide and calcite that is very heterogeneous and crosscut by various generations of Fe-oxide veinlets.

The rock-forming minerals in Type 2 dykes are calcite, Fe-Mn-oxides, albite, Na-Fe-amphibole and phlogopite. Accessory minerals are apatite, xenotime-(Y), magnetite, fluorite, parisite-(Ce) and thorite. Sample 927 has additional accessory minerals including zircon and rutile. The group is enriched in Y and LREE minerals are limited to small quantities of parisite-(Ce), synchysite-(Ce) and monazite.

The most important mineralogical characteristics observed in the group are:

1. The existence of two generations of xenotime-(Y) and

2. The close relationship and co-existence of the minerals xenotime-(Y) and synchysite-(Ce), parisite-(Ce) and xenotime-(Y)-apatite, where synchysite-(Ce), parisite-(Ce) are replacing earlier formed xenotime-(Y).

Magnetite forms large subhedral grains in the homogenous calcite and is associated with synchysite-(Ce), parisite-(Ce), thorite/huttonite and xenotime-(Y).

Fe-oxides and/or hematite are seen as bright areas under BSE in calcite, forming schlieren textures (Figure7.4).

Calcite is variable in composition with areas that are stable showing homogeneity of the calcite matrix. Where alteration is observed, calcite contains abundant Mn and Fe - oxides. Sometimes calcite forms large homogenous crystals but typically is altered and stained with Fe oxides.

Thorite/huttonite is found within and at the edge of synchysite-(Ce), parisite-(Ce) and in contact with resorbed xenotime-(Y) that is being replaced by synchysite-(Ce), parisite-(Ce). Replacement of xenotime-(Y) by synchysite-(Ce) and parisite-(Ce) resulted in the enrichment of LREE (e.g. dyke type 5).

Synchysite-(Ce) and parisite-(Ce) form anhedral grains in the calcite matrix and are in close association with magnetite.

Xenotime-(Y) occurs as euhedral grains about 30μm wide in the iron oxide rich calcite matrix (e.g. in sample 189). Such xenotime-(Y) exhibits a primary characteristic of multiple internal zoning. Where xenotime-(Y) is in contact with synchysite-(Ce) and parisite-(Ce), it is anhedral and lacks zonation. When xenotime-(Y) is in contact with calcite, it is zoned and the mineral faces are well preserved. Samples of type 2 dykes contain two xenotime-(Y) and apatite generations referred to as xenotime-(Y) I and xenotime-(Y) II and apatite I and II respectively. Xenotime-(Y) I forms euhedral particles in the Fe-oxide-rich calcite matrix and is associated with thorite/huttonite, magnetite and phlogopite forming occeli textures (Fig 7.8). The zonation texture observed in xenotime-(Y) I and its relationship with other minerals indicates a magmatic origin for xenotime-(Y) I. Xenotime-(Y) II is strongly related to apatite II, forming aggregated clouds, elongated segregations and veinlets in the Mn-Fe-oxide and Mn-oxide rich matrix. The two minerals appear to be co-genetic. Both xenotime-(Y) II and apatite II are finer-grained in comparison to xenotime-(Y) I, reaching only up to 7 μm in size. This makes it difficult to conduct a detailed mineral analysis using LA-ICP-MS.

The existence of xenotime-(Y) I, apatite I and thorite/huttonite, as well as clouds of xenotime-(Y) II and apatite II in the calcite matrix seem to indicate that these clusters

were crystallized while the magma intruded into the fault/dyke zones rather than being transported from a deeper magma chamber, thus the association is interpreted as magmatic.

Apatite forms anhedral grains in the altered calcite matrix and is in contact with altered calcite and thorite/huttonite.

Albite occurs as anhedral grains in the calcite matrix, in altered areas rich in Fe-oxide and in contact with rutile.

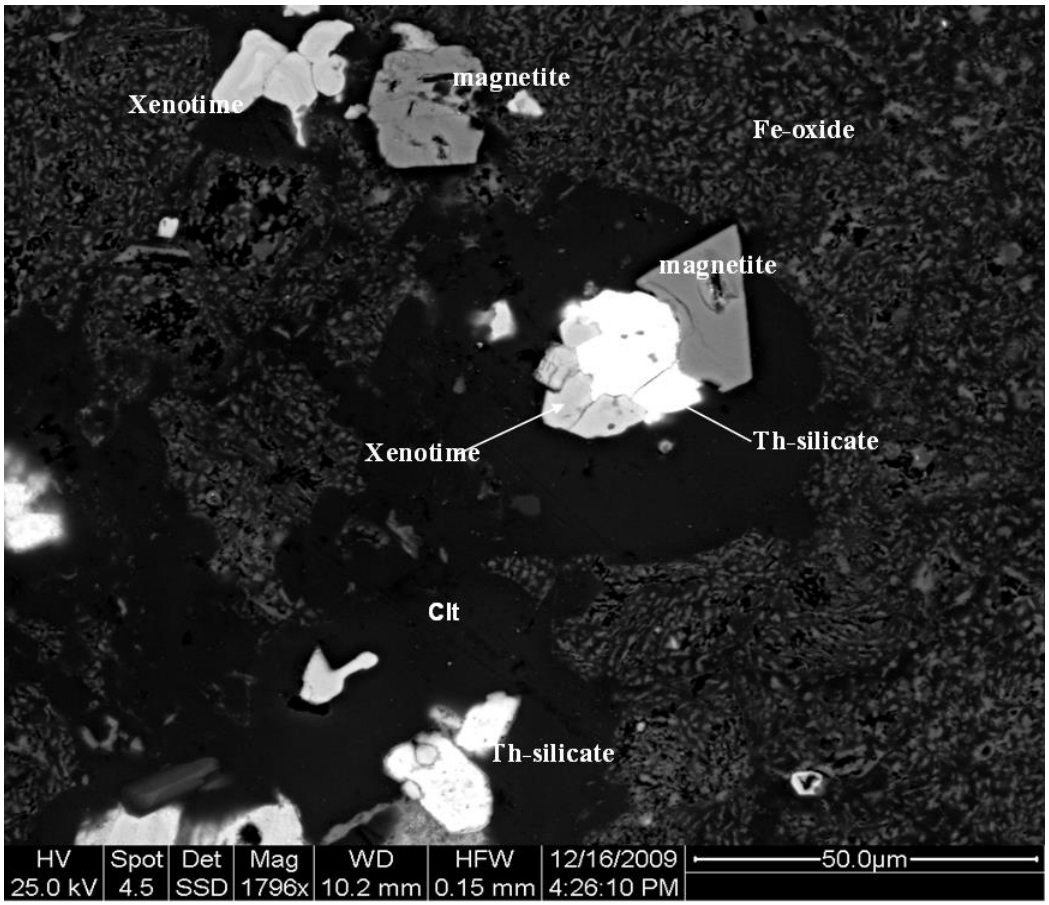

Figure 7.8 Type 2 carbonatite dyke sample with heterogeneous matrix of calcite, Fe oxide, magnetite, thorite/huttonite and xenotime-(Y) in pure calcite matrix forming occelli textures.

Thorite/huttonite grains occur in the calcite matrix and at the edge of synchysite-(Ce) and parisite-(Ce) according to microscopic observations. Thorite/huttonite has many habits in type 2 dykes. It is observed forming anhedral inclusion patches, aggregates on xenotime-(Y) 1 and rarely at xenotime-(Y) grain boundaries.

Fluorite forms anhedral large grains in the calcite matrix, especially in the regions altered by Fe-oxides.

Fluorite reaches up to 500μm in size forming elongated grains in the regions with a Mn-Fe-oxide-rich calcite matrix and in contact with xenotime-(Y) II, apatite II aggregated and in contact with thorite/huttonite.

Rutile forms 20 μm anhedral grains in the Fe- Mn oxide-rich calcite matrix and is in contact with apatite I, xenotime-(Y) II and apatite II aggregates, calcite and thorite. Rutile is overgrown by xenotime-(Y) II and thorite/huttonite minerals. Thorite/huttonite, apatite and xenotime-(Y) are at times observed in vugs and cracks in rutile.

Zircon forms large anhedral grains in regions where xenotime-(Y) II and apatite II aggregates are found and in contact with the two minerals.

Phlogopite occurs as large anhedral grains in the calcite carbonate matrix and in contact with xenotime-(Y) II and apatite II aggregate clouds, thorite/huttonite and Mn- and Fe-Mn-oxide.

7.3.6 Petrography and mineralogy of the Type 3 dykes

This group is represented by samples15769, 15769LG and 15796. Type 3 dykes mainly consist of crystalline calciocarbonatite enriched in LREE. Calcite carbonatite inclusions of the earlier carbonatite phases, which are highly altered and contain xenotime-(Y), are found in this carbonatite group. This mode of occurrence supports the field observations where these rocks crosscut earlier ferruginous calciocarbonatite (e.g. sample 189 of the type 2 dykes).

The matrix of the calciocarbonatite in this group variably consists of;

1. Fine-grained calcite-Fe-oxide-mixture (samples 15769).
2. Well-developed pure calcite forming large grains up to 200 μm in the slightly iron oxidised matrix and with late veinlets that contain LREE (sample15769LG).
3. A mixture of pure calcite, fine-grained oxidized zones of calciocarbonatite and a combination of both with small grains of fluorite, xenotime-(Y), magnetite and/or pure calcite that contains apatite, albite (sample 15796).

Accessory minerals are Fe-oxide, xenotime-(Y), rutile, fluorite, synchysite-(Ce), calcite, thorite/huttonite, biotite, aegirine, apatite and zircon.

Synchysite-(Ce) and parisite-(Ce) are observed only in pure calcite and veinlets of secondary origin. The two minerals are zoned and form up to 1 mm anhedral grains in the veinlets of younger calcite.

Xenotime-(Y) forms aggregates in sample 15769 where Fe-oxide veinlets and secondary calcite-veins are abundant. Xenotime-(Y) in places encloses euhedral zircon and/or forms aggregates while elsewhere it is closely associated with apatite. In some of

the type 3 dykes, xenotime-(Y) constitutes a major mineral component of the rock, forming a reaction front along compositional domains (Figure 7.9). The reaction front could have been a result of the early magmatic event possibly later fluid flow fronts.

Magnetite forms individual subhedral grains found as inclusions in the calcite matrix and in veinlets cutting through the section. Hematite is an alteration product of magnetite in these rocks.

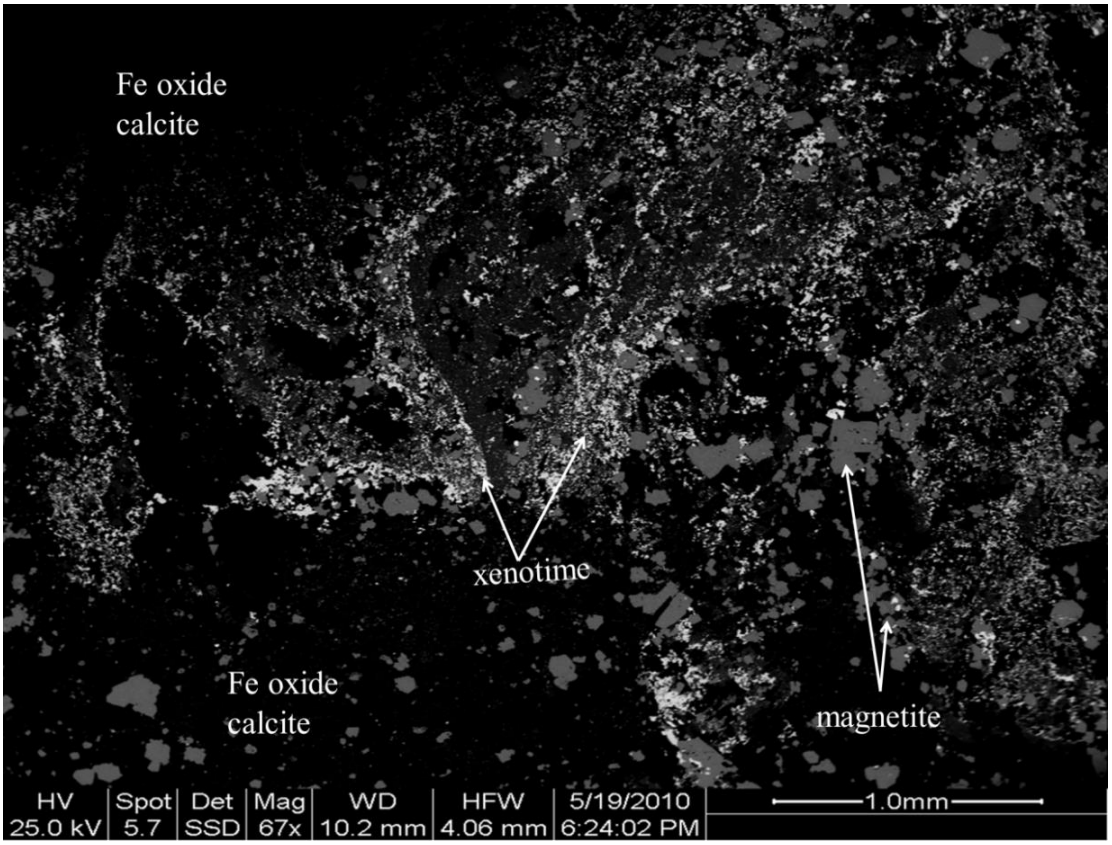

Figure 7.9 Backscattered electron images showing the texture formed by xenotime-(Y) in the calcite carbonatite of a Type 3 dyke. Note the aggregates of xenotime-(Y) grains and the reaction front.

Synchysite-(Ce), parisite-(Ce) and aegirine form large anhedral grains in the calcite matrix and contain inclusions of the thorite/hutonite. Synchysite-(Ce), parisite-(Ce) and xenotime-(Y) are also found as inclusions in the magnetite and in zones that are rich in fluorite.

Xenotime-(Y) is in contact with calcite, apatite and anhedral magnetite, found between magnetite grains as aggregates and as inclusions forming subhedral and poorly zoned minerals. In places xenotime-(Y) mantles zircon occurring as single scattered crystals in the calcite matrix. It is also observed forming inclusions in apatite in zones that are apatite II rich.

Apatite occurs as large anhedral grains, disseminated in the calcite matrix and aggregated in areas that are rich in xenotime-(Y) and magnetite. In places apatite encloses xenotime-(Y).

Rutile forms up to 500 µm long grains observed in the hematite rich veinlets and containing inclusions of thorite/huttonite.

Zircon grains are up to 50 µm long and are mantled by xenotime-(Y).

Fluorite is found as veinlets cutting through the heterogeneous Fe oxide - calcite mixture, **Pyrite** occurs as euhedral single grains up to 10 µm in the calcite matrix.

Thorite/huttonite has a positive weathering red lustrous colour on the surface of the carbonatite dykes, which makes it easy to recognize in the field (Figure7.10). Unfortunately, very little data was obtained from samples that contained thorite crystals, as the samples were considered unsafe for human handling. Cross observations using the backscattered images show thorite/huttonite to occur mainly as inclusions in the synchysite-(Ce) and parisite-(Ce), forming large single crystals of up to 100 µm at the edges of rutile, xenotime-(Y) and between magnetite aggregates in the calcite.

Biotite forms anhedral large grains in contact with anhedral aegirine augite, possibly as an alteration product of the pyroxenes forming corona texture, which is set in the calcite-Fe oxide matrix.

Figure 7.10 pink carbonatite with red, lustrous positively weathered thorite on the surface

7.3.7. Petrography and mineralogy of the Type 4 dyke

A number of samples from NRE clearly define this group as a separate entity (Fig 6.8). The group is here represented by sample 914. The calcite carbonatite of type 4 dykes contains very fine-grain Mn-Fe- oxides and magnetite/hematite causing the dark grey or brown colors in rock outcrop thin section.

Synchysite-(Ce) and **parisite-(Ce)** intergrown sporadically and are major mineral components reaching up to 4% in Type 4 dykes. These minerals form grains up to 0.5mm long in zones that show flow banding (Figure 7.11). Accessory minerals are hematite, pyrite, apatite, zircon, phlogopite, xenotime-(Y), thorite, and baryte.

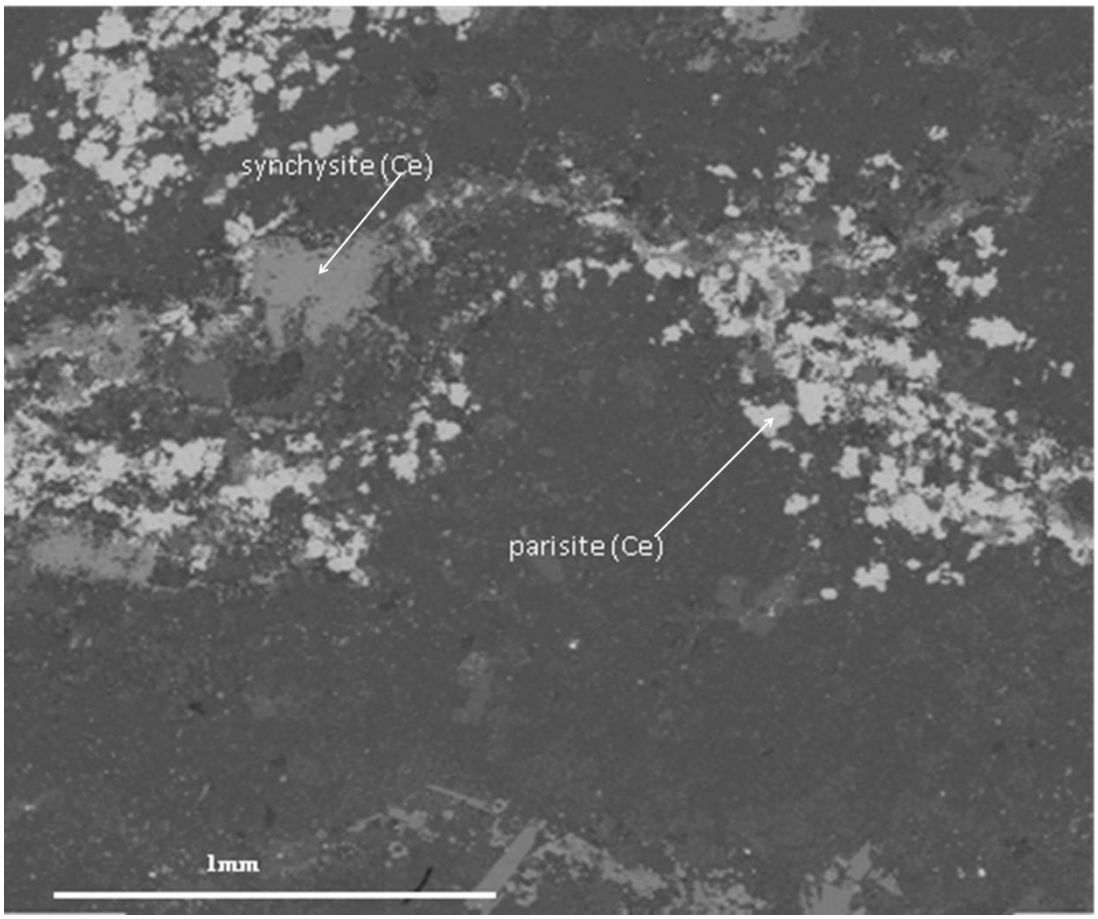

Figure 7.11 Backscattered image overview of the section of type 4 dyke, showing the rock textures. White synchysite-(Ce) and parisite-(Ce) form veinlets cutting through the section.

Xenotime-(Y), a HREE-bearing mineral occurs separately from synchysite-(Ce) and parisite-(Ce) which are LREE-bearing minerals. Calcite, fluorite, phenocysts of albite and quartz forms the matrix (Figure 7.11).

Magnetites up to 100 μm diameter occurs as scattered grains in the calcite matrix and are abundant in areas with flow banding. There is a close relation of magnetite with REE as these occur in the same regions and at most in contacts.

Phlogopite is associated with synchysite-(Ce), parisite-(Ce), magnetite and hematite.

Quartz forms large crystals up to 70 µm long. It is strongly resorbed on the grain boundaries and encloses synchysite-(Ce), parisite-(Ce) and calcite.

Zircon forms euhedral grains in the calcite and in proximity with synchysite-(Ce) and parisite-(Ce) rich areas.

7.3.8 Petrography and Mineralogy of the Type 5 dykes

Type 5 dyke is represented by sample 924. The matrix of the sample is mainly made up of fluorite and calcite.

Fluorite: There are two generations of fluorite;

Fluorite of the first generation forming large subhedral grains up to1.2 mm (Figure 7.12 and 7.13); and fluorite of the second generation, that is medium to fine grained, found in the veinlets that cut across the section (Figure 7.12 and 7.13).

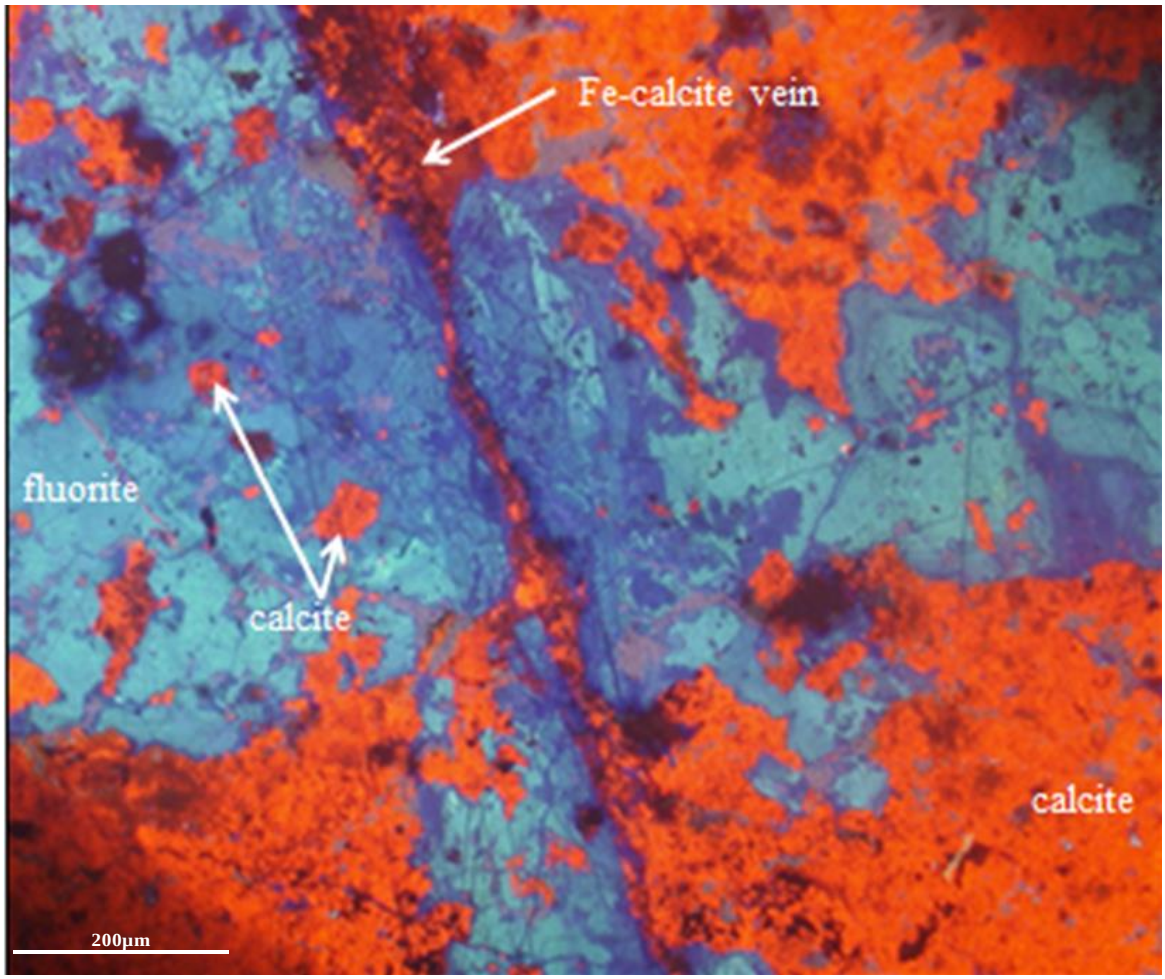

Figure 7.12 Cathodoluminescence image showing Fe-rich calcite veinlet cutting the big fluorite grains of first generation inclusions of pyrochlore, quartz, albite and xenotime-(Y) (Sample 924).

Large fluorite grains contain inclusions of quartz, pyrochlore, albite and calcite. The secondary fluorite grains are small in size and do not exceed 20 μm. They form veinlets that cut through the first generation of large grained fluorite and are found between the grains of the first generation fluorite.

Quartz occurs as abundant anhedral patches.

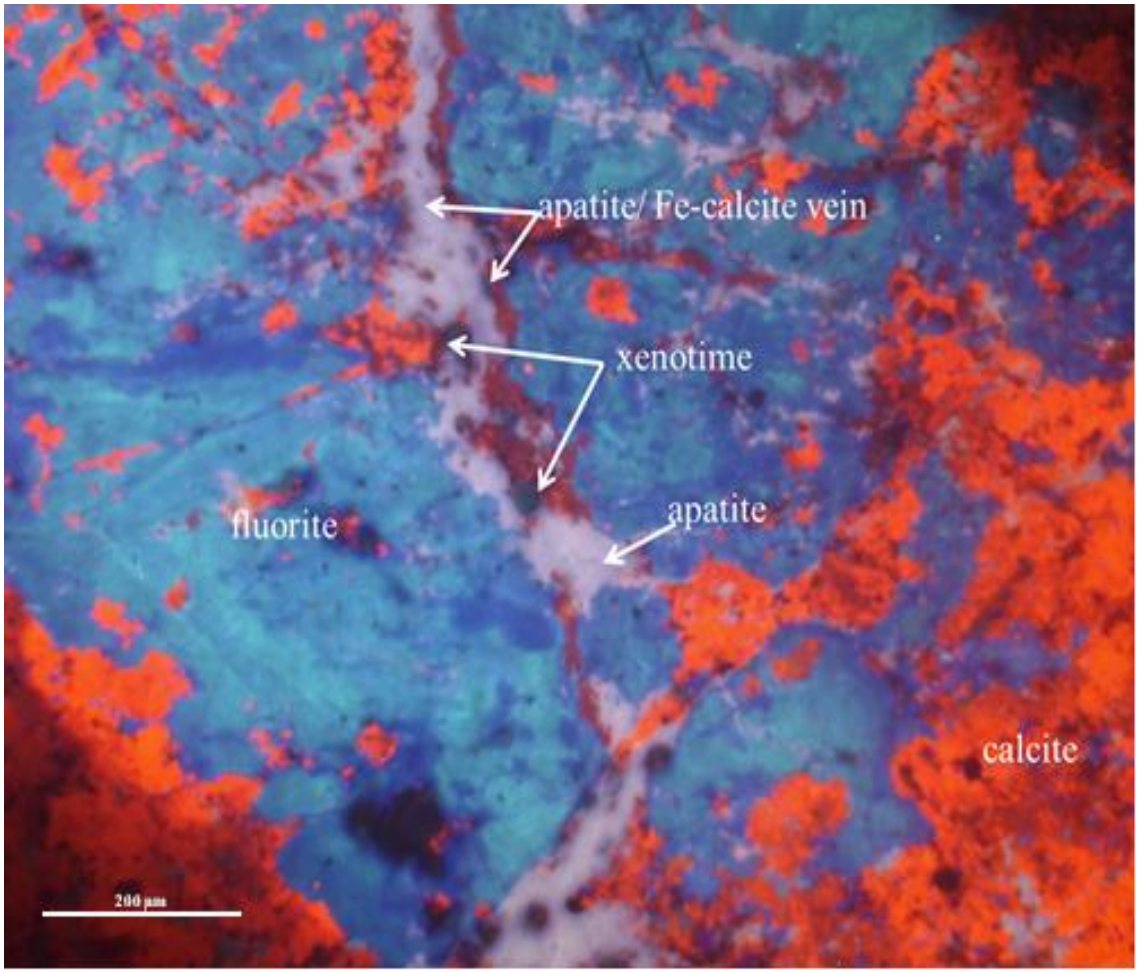

Figure 7.13 Cathodoluminescence image illustrating fluorite-calcite-apatite-hematite veins, cutting the first generation fluorite grains (Sample 924).

7.4 The mineral paragenetic sequence at Lofdal

The paragenetic sequences were worked out through detailed microscopic studies of polished petrographic thin sections, cathodoluminescence petrography and back scattered electron images. The cathodoluminescence method proved very helpful in textural observations of the carbonate minerals. A summary of the Lofdal mineral paragenesis and paragenetic sequence is presented in Table 7.2. The paragenetic scheme builds on the observations in Wall et al. (2008) and incorporating results from 15 new samples.

Mineral sequences indicate that some minerals in the Lofdal carbonatites have formed during the magmatic phase, some minerals formed at the transitional stage and majority formed during the hydrothermal stage. Specific minerals are used to define the phases. The magmatic stage marks the formation and precipitation of magmatic minerals before the onset of transitional and hydrothermal stage mineral precipitation started. Zircon is used in this paragenetic sequence to mark the magmatic phase that ends before the transitional phase, which is marked by the precipitation of xenotime-(Y) II and apatite II. Some minerals occur throughout the sequence. The minerals forming in the hydrothermal stage constitute mainly the alteration minerals at Lofdal.

Other magmatic minerals are calcite, xenotime-(Y) and apatite (when in absence of xenotime-(Y) II and apatite II), magnetite, dolomite, pyrochlore, albite, and carbocernaite. Xenotime-(Y) is observed as a magmatic mineral but it is most abundant in the transitional and hydrothermal phases; sometimes xenotime-(Y) is intergrown with apatite. Xenotime-(Y) is also observed being replaced by synchysite-(Ce) and parisite-(Ce). In several rock samples from different carbonatite type dykes, it is replacing zircon. Magmatic xenotime-(Y) occurs in the Fe – rich calcite matrix.

Monazite-(Ce) is magmatic and occurs also in hydrothermal veinlets.

The mineral paragenesis at Lofdal is variable owing to multiple combinations of magmatic and hydrothermal processes during multi stage dyke emplacement. Hydrothermal alteration is evident in the dykes at Lofdal. The majority of REE minerals formed during the hydrothermal / carbothermal stages of carbonatite formation. While some minerals are of clearly magmatic origin (such as calcite, pyrochlore, xenotime-(Y), zircon and albite), others are clearly of hydrothermal origin (such as monazite, synchysite, parisite, thorite, apatite and fluorite). Note that albite occur as both primary in some carbonatite dykes while in others is a result of hydrothermal alteration.

The majority of REE minerals formed during the hydrothermal/carbonathermal stage of carbonatite formation.

A large number of minerals have formed by processes of metasomatism and alteration leading overall to a complicated picture of mineral assemblages.

7.5 REE hosting minerals at Lofdal

At Lofdal REE-bearing minerals occur in all phases: magmatic, transitional and hydrothermal (see Table 7.3). Most REE hosting minerals are hydrothermal, making Lofdal a hydrothermal rather than a primary magmatic deposit as defined by Mariano (1989). The list of REE hosting minerals at Lofdal is given in Table 7.3 and these are presented according to their mineral classes.

Primary mineralisation occurs in mineral classes belonging to the phosphates, oxides and silicates. The primary REE-bearing minerals are xenotime-(Y) apatite, pyrochlore, monazite-(Ce) and cerianite-(Ce). Hydrothermal mineralisation is most widespread at Lofdal in the carbonatite dykes and it is seen in all mineral classes such as the phosphates, carbonates, sulphates, oxides, silicates and halides. The most common hydrothermal minerals are synchysite, parisite-(Ce) and monazite-(Ce). Other hydrothermal minerals present are allanite-(Ce), carbocernaite-(Ce) and ancylite-(Ce). It is important to note that minerals such as calcite and thorite, which are generally considered not important hosts for REE, can contain elevated amounts of LREE, MREE and HREE.

7.6 Mineral chemistry of LREE minerals

The most abundant LREE hosting minerals at Lofdal are monazite, synchysite-(Ce), parisite-(Ce), apatite, fluorite and calcite. Mineral compositions of the LREE-bearing minerals at Lofdal are considered in detail below.

7.6.1 Synchysite-(Ce)

Abundant synchysite [(La,Ce,Nd)Ca(CO_3)$_2$) F] is found in veins and matrix of the calcite carbonatites of Type 1, 2, 3 and 4 dyke with subordinate amounts of parisite. Synchysite-(Ce) occurs as fibrous fringes around monazite and when in vugs it forms fibro-radial aggregates (e.g. Main Carbonatite plug (Fig 7.14). Table 7.4 shows chemical analyses of synchysite-(Ce) in Type 3 dykes. Synchysite-(Ce) and parisite-(Ce) are sometimes intergrown forming syntaxial intergrowth structures that differ in colours with parisite-(Ce) showing dark grey areas and synchysite-(Ce) having lighter grey colour in backscatter images (Figure 7.15) . Synchysite-(Ce) predominates over parisite-(Ce) in the Lofdal carbonatite rocks.

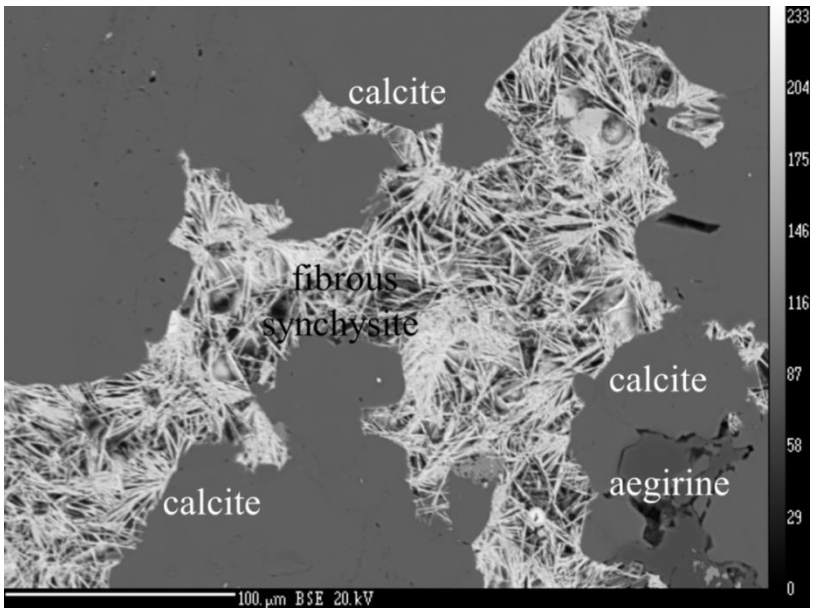

Figure 7.14 Backscattered image showing mineral syntaxial intergrowth structures indicated by synchysite –(Ce) lighter grey colour and parisite-(Ce) dark grey areas from Type dyke 1 (sample 326).

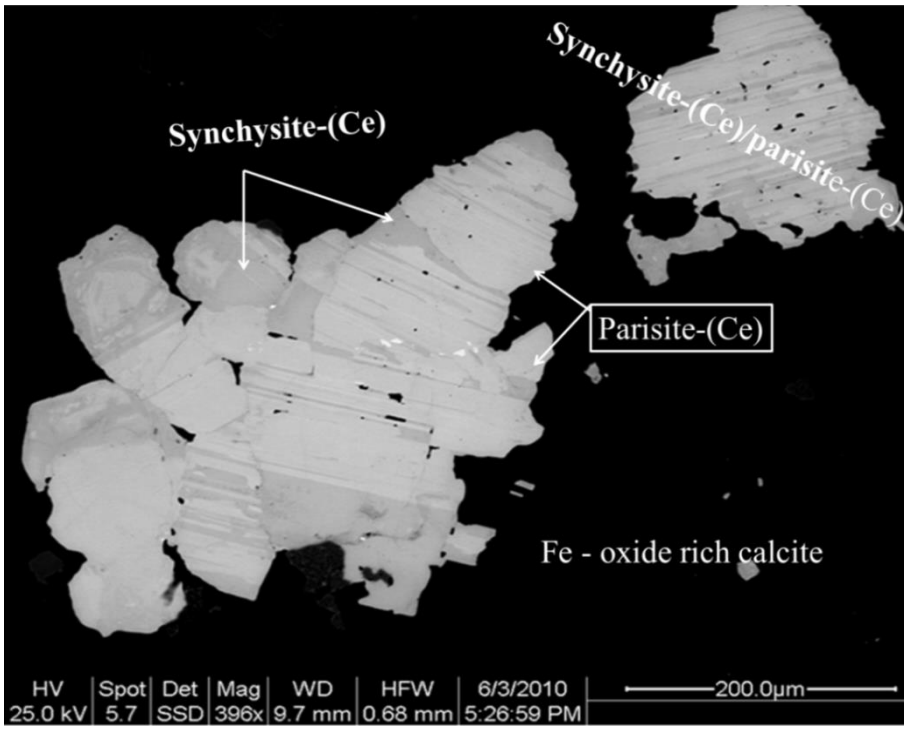

Figure 7.15 Synchysite-(Ce) and parisite-(Ce) from calciocarbonatites Type 4 dyke (sample 914), showing syntaxial intergrowths. Note synchysite-(Ce) is darker and parisite-(Ce) is lighter in colour.

Table 7.4 Electron microprobe analyses of synchysite-(Ce) in sample 15769LG of Type 3 dyke. CO_2 is determined using stoichiometry calculation.

Sample Anal. No.	5	7	36	37	38	52	55	57	58
Wt%									
Al_2O_3	b.d.	b.d.	0.08	0.08	b.d.	b.d.	0.12	b.d.	b.d.
SiO_2	0.43	0.74	0.12	1.65	0.00	0.18	0.23	0.17	0.30
P_2O_5	b.d.	b.d.	b.d.	0.24	b.d.	b.d.	b.d.	b.d.	b.d.
SO_3	b.d.	b.d.	b.d.	b.d.	b.d.	0.12	0.10	b.d.	0.15
CaO	9.55	9.96	8.71	6.25	10.66	10.24	6.04	16.80	11.74
TiO_2	b.d.	b.d.	0.08	b.d.	b.d.	b.d.	b.d.	b.d.	b.d.
MnO	b.d.	0.40	b.d.	b.d.	b.d.	b.d.	b.d.	b.d.	b.d.
FeO	b.d.	b.d.	2.43	b.d.	b.d.	b.d.	1.95	b.d.	b.d.
SrO	0.25	0.32	1.06	b.d.	b.d.	0.71	1.10	0.21	0.40
Y_2O_3	1.27	1.24	1.04	0.94	1.03	0.80	0.63	1.43	0.91
BaO	0.23	b.d.	b.d.	b.d.	b.d.	b.d.	b.d.	b.d.	b.d.
La_2O_3	16.04	14.78	15.12	17.68	16.08	20.77	18.71	13.57	18.57
Ce_2O_3	24.30	28.44	26.88	34.36	28.77	28.18	32.30	23.04	30.08
Nd_2O_3	8.07	7.52	7.94	8.17	8.50	6.01	5.99	6.61	6.69
ThO_2	1.05	1.23	2.31	1.51	b.d.	1.31	2.83	0.00	2.19
CO_2	28.81	30.79	30.60	33.04	30.40	31.95	31.39	31.71	33.74
F	5.39	5.17	5.84	4.17	5.50	5.12	5.79	4.13	4.83
Total	95.37	100.59	102.23	108.09	100.94	105.39	107.18	97.67	109.59
O=F	93.10	98.41	99.77	106.34	98.63	103.24	104.74	95.93	107.56
Al			0.004	0.004			0.006		
S						0.006	0.005		0.007
Ca	0.530	0.524	0.390	0.271	0.483	0.447	0.264	0.755	0.491
Ti			0.003						
Mn		0.016	0.000						
Fe			0.085				0.067		
Sr	0.008	0.009	0.026			0.017	0.026	0.005	0.009
Y	0.035	0.033	0.023	0.020	0.023	0.017	0.014	0.032	0.019
Ba	0.005	0.000							
La	0.307	0.268	0.233	0.263	0.251	0.312	0.282	0.210	0.268
Ce	0.461	0.511	0.411	0.508	0.445	0.421	0.483	0.354	0.430
Nd	0.149	0.132	0.118	0.118	0.128	0.088	0.087	0.099	0.093
Th	0.012	0.014	0.022	0.014		0.012	0.026		0.019
C	2.039	2.066	1.743	1.823	1.755	1.780	1.751	1.817	1.801
Total	3.546	3.573	3.057	3.021	3.086	3.101	3.010	3.273	3.139
P				0.008					
Si	0.022	0.036	0.005	0.067		0.008	0.009	0.007	0.012
Total	0.022	0.036	0.005	0.075	0.000	0.008	0.009	0.007	0.012
F	0.883	0.803	0.770	0.532	0.735	0.660	0.748	0.548	0.597

Na, Mn, Cl, SO_3, Mg, K, Sr and Ba are below detection limit of about 0.05 wt%
b.d. = below detection limit of 0.05 wt%

Bastnäsite is absent in all rocks analysed which may mean that there was a progressive supply of both Ca^{2+} and CO_2^{-3} in the fluids from which synchysite-(Ce) and parisite-(Ce) mineral suites precipitated. Synchysite-(Ce) is one of the few REE carbonate minerals that hosts Ce, La and Nd.

7.6.2 Parisite

Subordinate amounts of parisite [$(La,Ce,Nd)_2Ca(CO_3)_3F_2$] occur in most carbonatite dykes at Lofdal, closely associated with synchysite-(Ce), forming thin light grey layers within the large dark grey laths of synchysite-(Ce) (Figure 7.15) and at times forming complex syntaxial intergrowth structures with synchysite-(Ce and rarely as randomly oriented anhedral laths. Parisite-(Ce) occurs also as anhedral aggregates filling the fractures and resorbed grains associated with xenotime-(Y) in the matrix of the fractured and fragmented Dolomite dykes (sample 114) rocks. Type 4 dykes have the largest grains and contents. Parisite-(Ce) dimensions range from 20 μm up to 1 mm wide.

The CaO content in parisite-(Ce from Lofdal ranges between 6.25 and 16.80 wt %, with an average of 10 wt %, possibly with synchysite-(Ce) amounts. The mineral contains substantial amounts of Y_2O_3 shown in all samples analysed and ranging between 0.63 to 1.27 wt% with an average content of 1.03 wt%.

7.6.3 Allanite-(Ce)

Allanite-(Ce) occurs in sample 115 representing Type 1 calciocarbonatite dyke. Grains are about 15 μm forming anhedral and highly resorbed grain in the iron oxide rich matrix forming part of the minerals forming the REE rich veinlets (Fig 7.16). This mineral constitutes a trace constituent of the rock and was only observed in one sample. The allanite-(Ce) shows dark rings possibly the result of radiation damage. Allanite is known as a host for REE in other carbonatite environments.

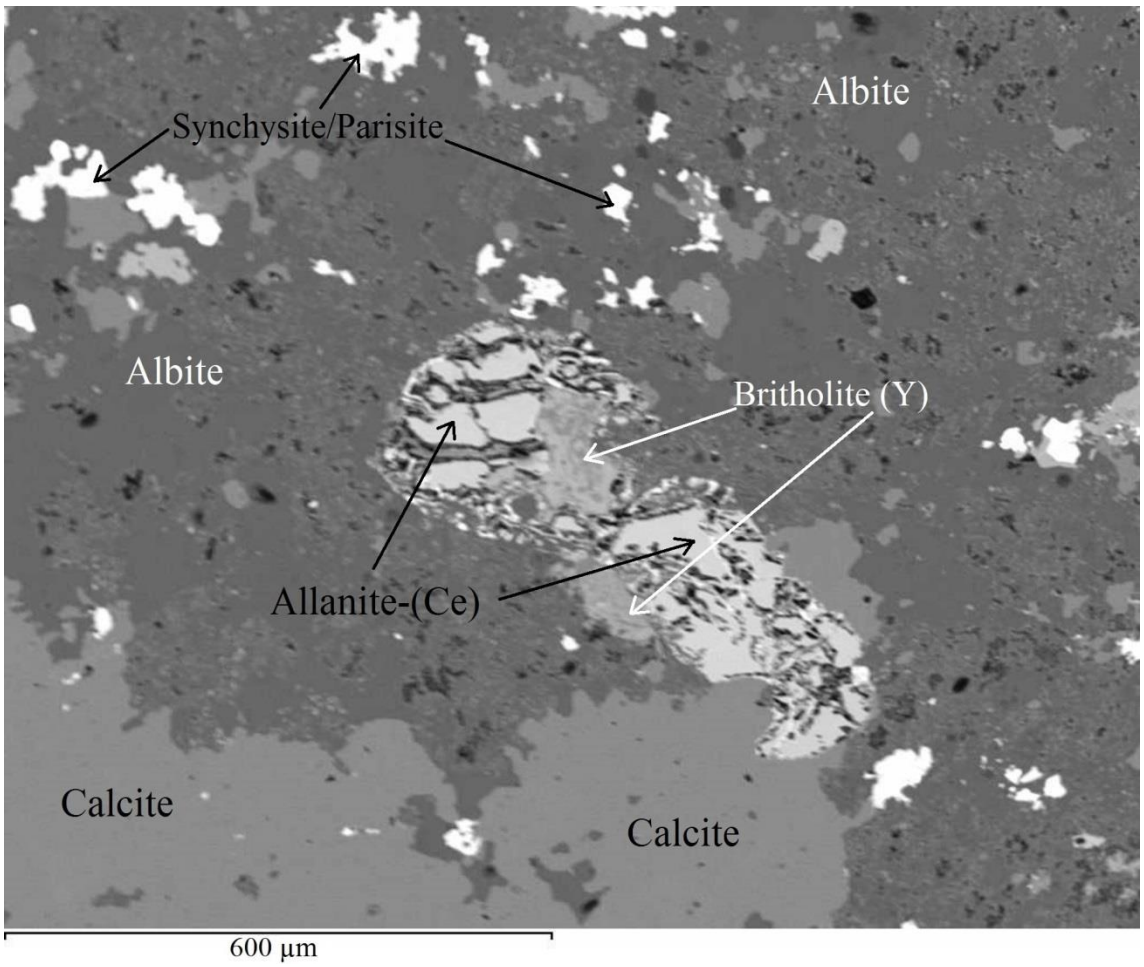

Figure 7.16 Anhedral allanite-(Ce) from the Lofdal calciocarbonatites Type 1 dyke (sample 115), showing dark alteration rings.

7.6.4 Monazite-(Ce)

Monazite-(Ce) forms grains of about 15µm – 100 µm as observed with SEM/EDS, forming crystals in the calcite matrix of the Main calcite carbonatite plug and at times occurring in veinlets closely associated with synchysite-(Ce) and parisite-(Ce). Monazite-(Ce) in the matrix appears to be of primary origin but in the veinlets it may result from hydrothermal processes (Figure 7.17). Monazite-(Ce) from Lofdal has high Th and U contents (Table 7.5). Its chemical composition is presented below and a comparison is made to the monazite-(Ce) analyses from Lofdal carbonatites by Wall et al. (2008). Table 7.5 also shows chemical compositions of monazite-(Ce) from other carbonatites. Monazite is a common accessory mineral in carbonatite and at Lofdal the monazite-(Ce) is light REE-enriched but with higher Nd, Eu and other mid REE compared to some other carbonatitic monazite (Wall et al. 2008). Sm is the heaviest REE detected in many carbonatitic monazite crystals and Ce/Sm ratios vary from about 2 -15 in Table 10.6 of Wall and Zaitsev (2004), compared with 1.8 – 9 at Lofdal.

Monazite-(Ce) directly associated with xenotime-(Y) has higher Y, Th, Dy and Ca than monazite-(Ce) elsewhere at Lofdal.

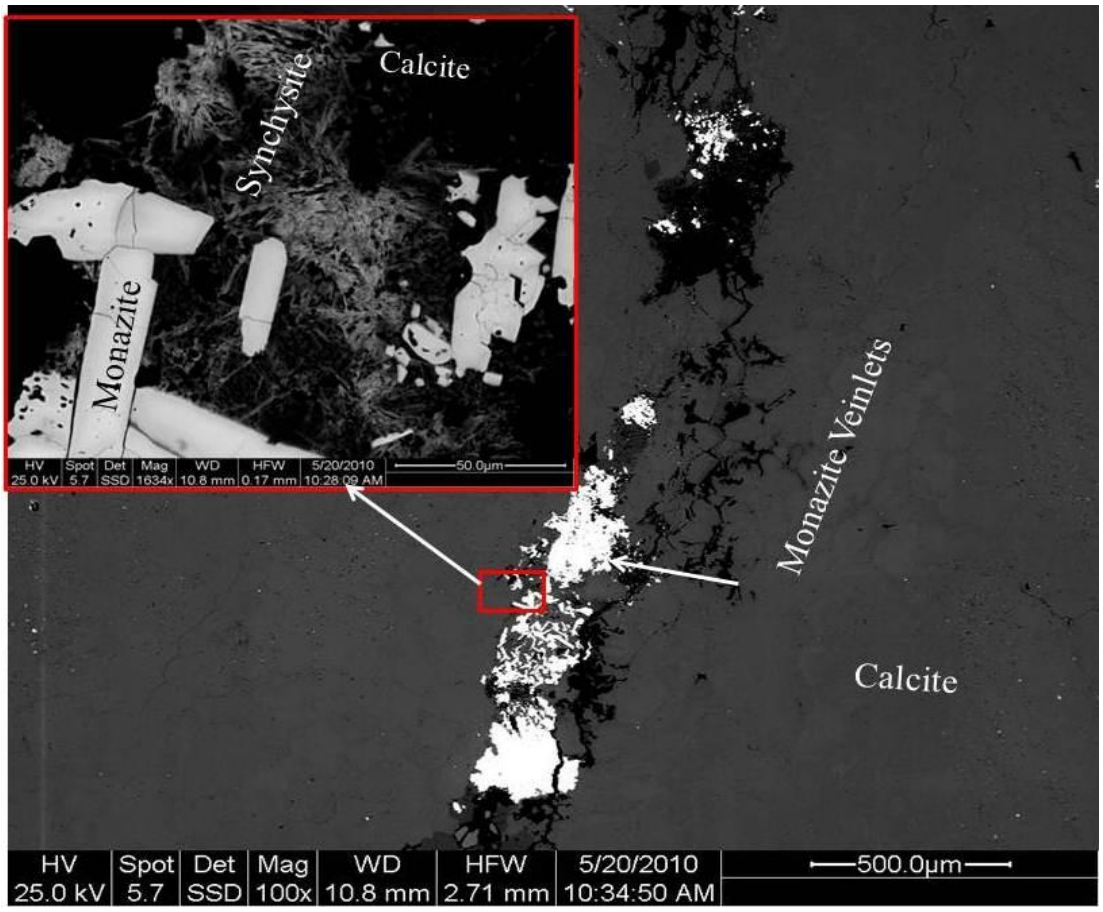

Figure 7.17 Backscattered electron images: showing the monazite veining in the main carbonatite and monazite-(Ce) with synchysite-(Ce).

Lofdal monazite has lower SrO than most other carbonatitic monazite (<0.16 wt%, c.f. Wall and Zaitsev 2004) and is also low in Th (0.2 –1.7 wt %), which is consistent with most carbonatitic monazite and different from typical monazite-(Ce) from granitic rocks. There are no signs of the extreme conditions of REE remobilisation that produce highly variable and occasionally La-depleted REE patterns (Wall and Zaitsev 2004).

Table 7.5 Electron microprobe compositions of monazite-(Ce) from Lofdal carbonatite

	15769LG			326		In vein cutting xenotime-bearing carbonatite (VNP130)		In carbonatite with zircon but no xenotime (VNP78b)		< 10 µm aggregates with xenotime (VNP21)	
Sample anal. Point	41	48	1	2	20	#1	#3	#1	#5	#11	#13
SiO_2	0.23	0.24	0.21	0.13	0.10	0.4	0.35	0.34	0.92	0.91	0.54
P_2O_5	30.20	29.50	29.67	30.36	29.71	30.71	30.98	31.11	31	30.28	30.92
CaO	0.47	0.46	n.d	0.14	0.40	-	0.09	0.5	0.23	0.79	2.1
FeO^t	0.20	n.d	n.d	n.d	n.d	0.06	0.09	0.15	0.51	1.2	0.3
SrO	0.17	n.d	n.d	n.d	n.d	0.16	0.13	0.05	0.11	0.15	0.08
Y_2O_3	0.31	n.d	n.d	n.d	n.d	0.14	0.16	-	0.12	0.99	1.06
La_2O_3	17.99	15.84	16.81	15.89	18.24	14.52	14.57	17.31	19.09	14.79	14.08
Ce_2O_3	35.45	34.99	41.41	40.64	40.96	29.74	28.18	35.45	33.96	31.49	29.22
Pr_2O_3	_	_	_	_	_	3.32	3.21	3.65	3.19	3.45	3.51
Nd_2O_3	8.11	9.10	10.48	12.29	9.84	14.27	15.4	11.58	10.6	12.23	12.15
Sm_2O_3	_	_	_	_	_	4.05	4.82	0.88	1.01	1.75	1.93
Eu_2O_3	_	_	_	_	_	0.75	0.72	0.08	0.21	0.32	0.37
Gd_2O_3	_	_	_	_	_	1.69	2.09	0.55	0.66	1.35	1.48
Tb_2O_3	_	_	_	_	_	0.06	0.14	0.05	0.09	0.08	0.17
Dy_2O_3	_	_	_	_	_	0.06	0.18	-	-	0.38	0.5
ThO_2	2.22	1.62	1.92	1.33	1.35	0.84	0.24	-	-	1.78	1.7
Total	95.84	92.06	100.91	101.19	100.94	100.75	101.33	101.69	101.7	101.95	100.1
O=F	95.64	91.93	100.74	101.05	100.80						
F	0.49	0.32	0.40	0.33	0.34						
	Formula to 4(O)					Formula to 16(O)					
Ca	0.020	0.020		0.006	0.017	0.006	0.014	0.081	0.037	0.128	0.342
Fe						0.007	0.011	0.019	0.064	0.152	0.038
Sr	0.004					0.014	0.012	0.004	0.01	0.013	0.007
Y	0.007					0.011	0.013		0.01	0.08	0.086
Ba	0.003										
La	0.261	0.238	0.241	0.225	0.261	0.826	0.824	0.97	1.06	0.827	0.79
Ce	0.511	0.523	0.589	0.571	0.582	1.679	1.581	1.971	1.872	1.747	1.626
Pr						0.186	0.179	0.202	0.175	0.19	0.194
Nd	0.114	0.133	0.145	0.168	0.136	0.786	0.844	0.628	0.57	0.663	0.66
Sm	_	_	_	_	_	0.215	0.255	0.046	0.052	0.092	0.101
Eu	_	_	_	_	_	0.04	0.038	0.004	0.011	0.017	0.019
Gd	_	_	_	_	_	0.086	0.106	0.028	0.033	0.068	0.074
Tb	_	_	_	_	_	0.003	0.007	0.003	0.004	0.004	0.008
Dy	_	_	_	_	_	0.003	0.009			0.019	0.024
Th	0.020	0.015	0.017	0.012	0.012	0.029	0.008			0.062	0.059
Total	0.939	0.929	0.992	0.981	1.008	3.893	3.9	3.957	3.898	4.06	4.029
P	1.006	1.019	0.975	0.986	0.976	4.01	4.021	4.003	3.953	3.887	3.98
Si	0.009	0.010	0.008	0.005	0.004	0.061	0.054	0.052	0.139	0.138	0.081
Total	1.015	1.029	0.984	0.991	0.980	4.071	4.076	4.056	4.092	4.025	4.061
F	0.061	0.041	0.049	0.040	0.041						

- = below detection limit of about 0.05 wt.%

Al, Mn, Er, U and Pb also analysed but below detection

Total Fe as FeO

Table 7.6 Electron microprobe compositions of monazite-(Ce) from other carbonatites

	Kanda-guba	---Vuoriyarvi---		Lesnaya Veraka		------Sokli-----		Sallan-latvi	Tamazert	Mountain Pass	Kizilçaö-ren
	Av. 13	1 wet						Av. of 4			
	1	**2**	**3**	**4**	**5**	**6**	**7**	**8**	**9**	**10**	**11**
Al_2O_3	0.11	0.06	0.10	-	-	0.15	0.32	0.60	-	-	-
SiO_2	0.07	0.70	0.49	-	-	-	-	0.27	0.14	0.61	-
P_2O_5	30.36	25.84	26.59	29.00	29.06	28.39	30.01	26.41	29.03	29.91	27.72
CaO	1.23	4.60	2.89	0.92	2.81	4.11	5.69	2.16	0.35	0.31	2.99
FeO	-	-	-	-	-	2.27	0.81	0.55	-	-	-
Fe_2O_3	0.51	6.10	2.20	-	-	-	-	-	-	-	-
SrO	2.66	-	3.97	5.17	8.33	1.71	1.12	2.83	0.95	-	11.20
Y_2O_3	-	-	0.24	-	-	0.15	0.04	-	0.04	-	-
BaO	-	-	-	-	-	0.36	0.47	-	0.02	-	0.43
La_2O_3	17.94	4.31	11.32	15.14	0.62	16.42	12.04	16.00	24.49	18.33	19.46
Ce_2O_3	31.18	32.70	25.47	29.18	14.78	31.69	28.79	30.60	33.76	34.13	25.39
Pr_2O_3	4.10	3.40	4.30	3.85	2.96	2.26	2.87	2.89	2.26	2.73	6.27
Nd_2O_3	10.41	5.94	12.19	8.77	5.50	6.66	10.07	10.45	7.53	10.43	4.38
Sm_2O_3	-	2.56	2.54	-	-	-	0.41	1.29	0.70	1.06	-
Gd_2O_3	-	1.65	-	-	-	-	-	0.10	0.14	-	-
ThO_2	1.62	5.77	1.40	9.74	34.94	0.16	0.65	0.10	0.57	2.62	0.10
UO_2	-	-	-	-	-	0.18	0.21	-	0.10	-	
F	-	-	-	-	-	-	-	-	-	-	0.74
SO_3	0.12	3.12	-	-	-	-	-	-	-	-	-
O=F	-	-	-			-	-	-	-	-	0.31
Total	**100.31**	**100.47**	**94.55**	**101.77**	**99.00**	**94.51**	**93.50**	**96.41**	**100.00**	**100.13**	**99.30**
	Formula calculated to 16(O)										
Ca	0.199	0.759	0.504	0.156	0.488	0.709	0.959	0.383	0.060	0.053	0.508
Fe	-	0.872	0.268	-	-	0.306	0.106	0.076	-	-	-
Sr	0.381	-	0.372	0.476	0.788	0.160	0.102	0.272	0.087	-	1.036
Y	-	-	0.020	-	-	0.013	0.003	-	-	-	-
Ba	-	-	-	-	-	0.023	0.029	-	-	-	-
La	0.998	0.245	0.680	0.884	0.036	0.975	0.698	0.977	1.433	1.047	1.144
Ce	1.720	1.842	1.516	1.692	0.880	1.868	1.657	1.854	1.960	1.933	1.480
Pr	0.225	0.191	0.256	0.224	0.176	0.133	0.164	0.174	0.133	0.153	0.364
Nd	0.561	0.327	0.708	0.496	0.320	0.383	0.566	0.618	0.427	0.580	0.248
Sm	-	-	-	-	-	-	0.022	0.074	0.04	0.060	-
Gd	-	-	-	-	-	-	-	-	-	-	-
Th	0.056	0.202	0.052	0.352	1.296	0.006	0.023	0.004	0.02	0.093	0.004
U	-	-	-	-	-	0.006	0.007	-	-	-	-
Total	**4.139**	**4.657**	**4.520**	**4.280**	**3.984**	**4.581**	**4.337**	**4.471**	**4.294**	**3.920**	**4.784**
P	3.875	3.367	3.656	3.890	4.000	3.870	4.000	3.702	3.900	3.927	3.872
S	0.014	0.360	0.104	-	-	-	-	-	-	-	-
Al	0.020	0.011	0.020	-	-	0.030	0.060	0.117	-	-	-
Si	0.011	0.108	0.080	-	-	-	-	0.045	0.020	0.093	-
Total	**3.919**	**3.846**	**3.860**	**3.890**	**4.000**	**3.900**	**4.050**	**3.864**	**3.920**	**4.020**	**3.872**

: - = below detection limit of about 0.05 wt.%

Al, Mn, Er, U and Pb also analysed but below detection limits of about 0.05 wt%

Total Fe as FeO

- = below detection limit of about 0.05 wt.%

7.6.5. Strontianite

Strontianite was encountered in the Type 1 dykes and the Main carbonatite plug. In the dykes strontianite is encountered in areas that are calcite rich and at times surrounded by albite. In such an environment strontianite forms channel interfingering textures and reactions with albites and or infilling of the joints in the albite (Figure 7.18).

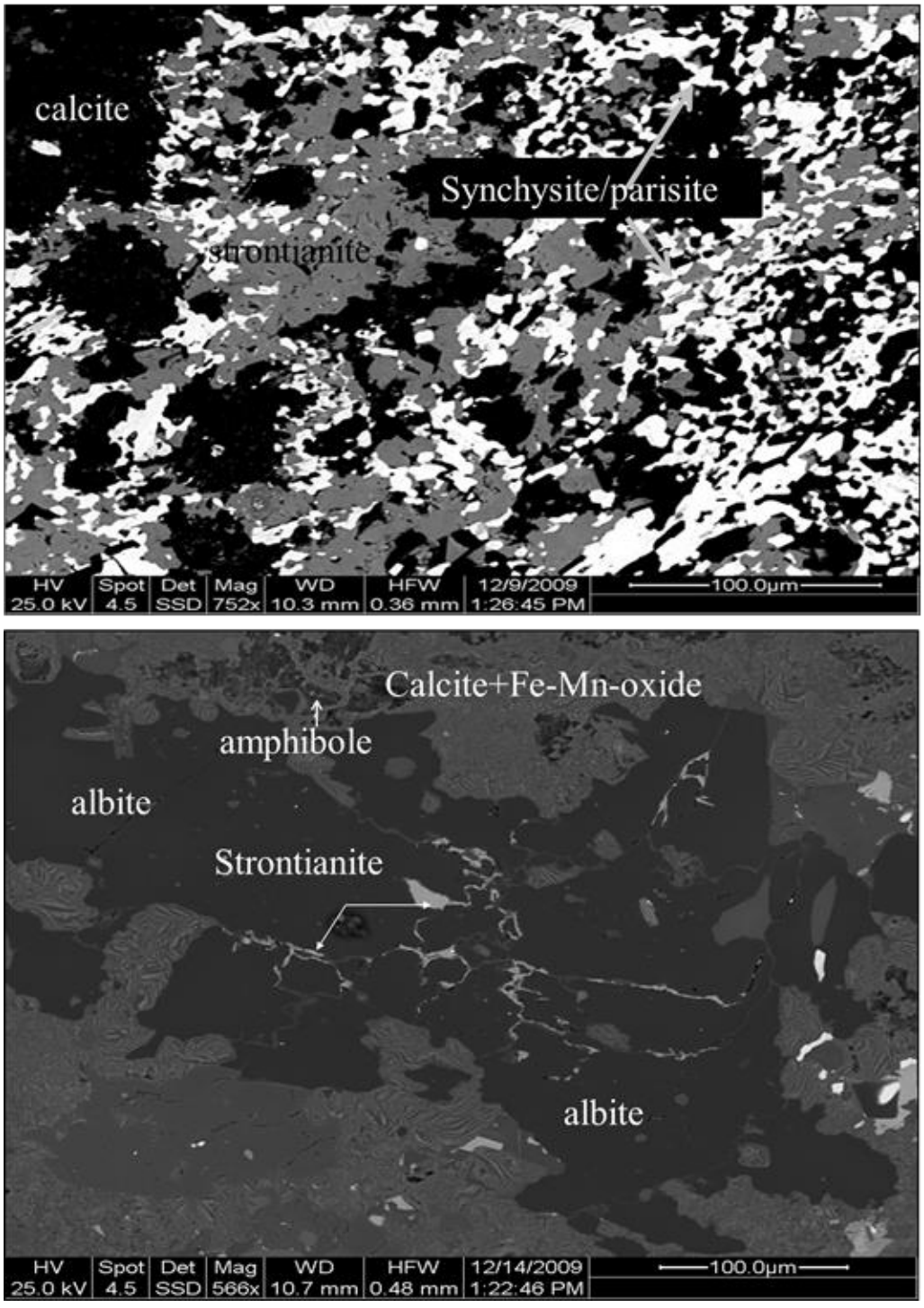

Figure 7.18 Strontianite in the Lofdal carbonatite

Strontianite is also observed forming large grains up to 100 µm, which are closely intergrown with fibrous ancylite and baryte (Figure 7.19), possibly pseudomorphs of strontianite. These large grains are set in the pure calcite matrix. In sample 269 of the Main carbonatite plug group strontianite forms anhedral and highly resorbed grains up to 100µm, which are closely associated with synchysite, parisite and calcite. These minerals are at times also found as inclusions in strontianite.

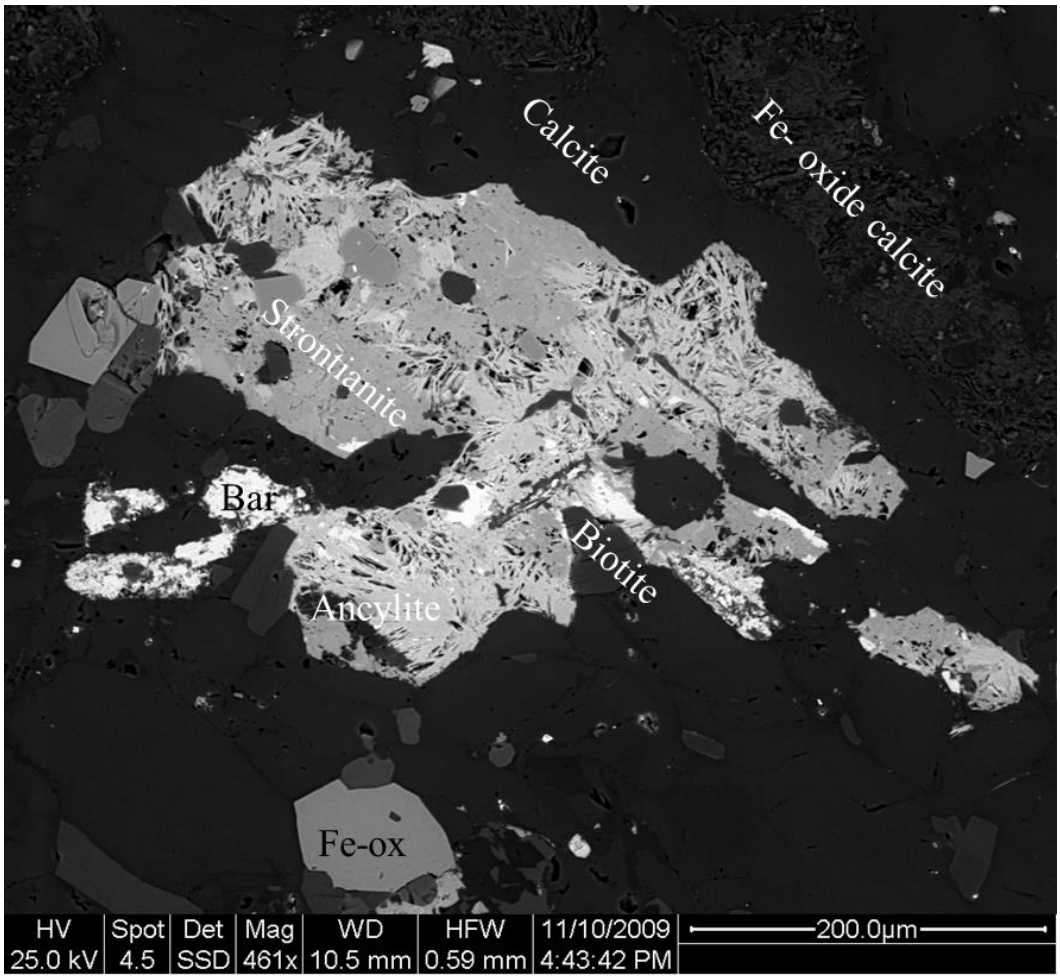

Figure 7.19 Strontianite grains that are closely intergrown with fibrous ancylite and baryte Type 1 dyke (sample 269).

Strontianite has SrO content ranging from 66.12 – 74.37 and CaO ranging from2.84 to 5.71 as Ca substitutes for Sr (Table 7.7).

Table 7.7 Electron microprobe compositions of strontianite from Lofdal carbonatites

Sample	326	
Anal. No.	19.00	23.00
CaO	5.71	2.84
SrO	66.12	74.37
BaO	0.94	
CO_2	32.83	33.81
Total	105.60	111.02
	Formula 3(O)	
Ca	0.136	0.066
Sr	0.855	0.934
Ba	0.008	
C	1.000	1.000
Total	2.000	2.000

F, Cl, Al_2O_3, SO_3, K_2O, TiO_2, MnO, SiO_2, FeO, P_2O_5, Y_2O_3, La_2O_3, Ce_2O_3, Nd_2O_3, ThO_2 are below detection limit of about 0.05 wt%. CO_2 calculated from the stoichiometry.

7.6.6 Apatite

Apatite and fluorite are important gangue minerals that are associated with REE minerals at Lofdal. Apatite occurs as euhedral stubby to acicular prisms and lozenge-shaped, slightly resorbed at the contact between the Main calciocarbonatite plug and the syenite.

Single crystals and aggregates of apatite are commonly found intergrown with xenotime-(Y) and calcite, indicating an early formation in the crystallization sequence. Apatite is also found in areas that are rich in fluorite and these are interpreted as formed during the hydrothermal phase. In the dolomite dykes, apatite in Type 2 and 3 dykes is observed forming disseminated grains associated with xenotime-(Y) II in the matrix (Figure 7.20). These clouds consist of minute apatite II and xenotime-(Y) II minerals that are closely intergrown indicating dissolution-reprecipitation of the two minerals from the iron oxide rich matrix, as a result of disequilibrium. The association is interpreted as a reworking of apatite I-xenotime-(Y) I-calcite carbonatite by low temperature solutions, during the low temperature hydrothermal fluid phase. Both minerals are phosphates and important hosts of the REE in a variety of environments including the alkaline and carbonatite environments (Clark 1984, Mariano 1989, Spear and Pyle 2002). Apatite has the formula $Ca_5(PO_4)_3F$, and is usually LREE enriched with a monoclinic structure, whereas xenotime-(Y) has the formula YPO_4, and is HREE-selective with an orthorhombic structure, thus they both phosphates that compete for different kind of REE.

The observed dissolution-re-precipitation mechanisms between xenotime-(Y) II and apatite II (Figure 7.20) are important in understanding possible model dissolution and precipitation of the two mineral phases in crustal fluids.

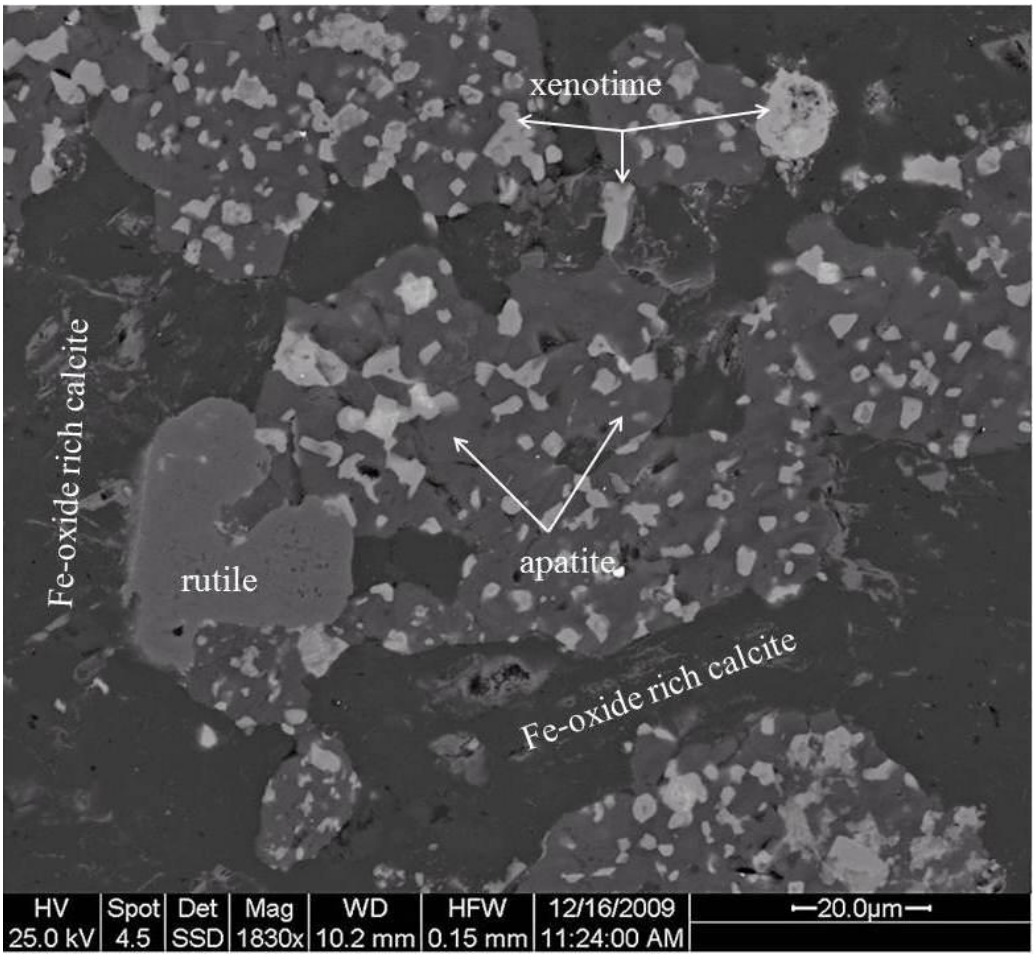

Figure 7.20 Backscattered image showing intergrowth between xenotime-(Y) II and apatite II in a Type 2 dyke (sample 927).

In the Lofdal samples two different luminescence types of apatite were found (Figure 7.21). Relatively large euhedral crystals (0.2 – 1 mm) showing primary oscillatory growth zoning with bluish green shades occur in sample 130. The small apatites (10 – 80 µm) of sample 52 have patchy pink to bluish CL. The crystals form batches or clusters of crystals. According to Mariano (1988) bluish CL is most commonly encountered in primary apatite from carbonatites and their genetically related igneous rocks. The spectra of both apatite types are dominated by the activation of Sm^{3+} and Dy^{3+} and to a lesser extent of Nd^{3+} and probably Tb^{3+} and Eu^{2+}. The position of emission bands is identical in both crystals. According to Kempe and Götze (2002) the peak between 865 and 880 nm is attributed to Nd^{3+}.

The Sm^{3+} activation is more pronounced than the Dy^{3+} activation in the pinkish apatite which points to higher Sm concentration in apatite from sample 130. Thus, the apatites

of sample 130 crystallised in an environment which was more enriched in MREE and probably LREE than the environment of sample 52. Minor Mn^{2+} activation between 562 and 580 nm may also be present, which may cause the loss in resolution between the principal emission bands of Sm^{3+} and Dy^{3+} (Mariano 1988).

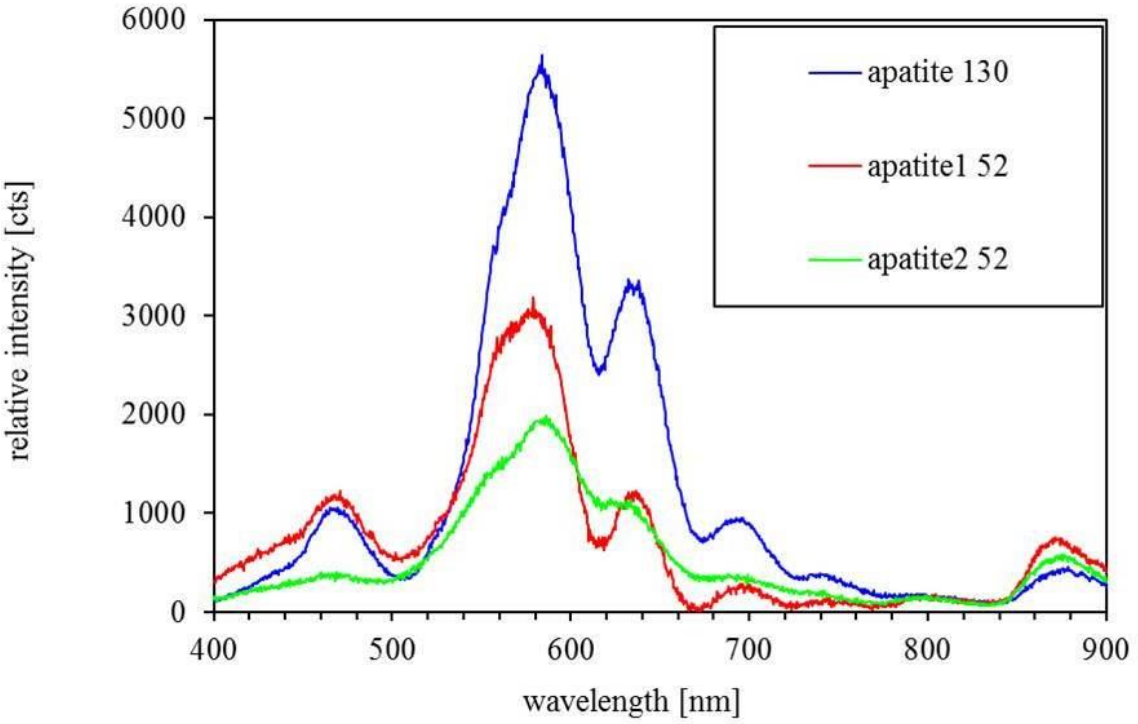

Figure 7.21 Cathodoluminescence scan of apatite

Table 7.8 displays a compositional range of apatite from Lofdal; CaO (48.45–56.47 wt.%), P_2O_5 (38.90–43.88 wt.%;) with substantial fluorine (up to 4.90 wt.%, Y_2O_3 3.97 wt.%,) and minor strontium (SrO: 0.27–1.29. wt.%). La_2O_3 (0.17–0.18 wt.%) and Ce_2O_3 (0.17–0.56 wt.%). Apatite grains with lowest P_2O_5 and F contain the highest amounts of Y and Na. This is partially consistent with a coupled substitution of Na and REE commonly observed in apatite. In consistence with the cathodoluminescence spectra analysis, the geochemical analyses indicate a high content of REE such as Y, La, Ce and Nd in apatite.

Table 7.8 Electron microprobe analyses of apatite in sample 15769LG of Type 3 dykes.

Sample													
Anal. No.	1	11	12	15	16	17	24	27	28	44	45	50	51
wt%													
Na_2O	0.18	2.01	0.40	0.27	0.54	0.91	0.40	0.74	0.56	0.26	0.24	0.20	1.61
MgO	b.d	b.d	b.d	0.05	b.d	b.d	b.d	b.d	b.d	b.d	b.d	b.d	b.d
Al_2O_3	b.d	b.d	b.d	0.13	0.06	0.08	0.00	0.24	b.d	b.d	b.d	b.d	b.d
SiO_2	0.05	0.00	0.08	0.48	0.16	0.31	0.00	0.70	0.10	b.d	b.d	b.d	b.d
P_2O_5	43.52	40.24	43.14	40.84	41.60	40.87	42.33	38.90	42.72	43.88	42.47	42.42	39.85
SO_3	b.d	b.d	b.d	b.d	b.d	b.d	0.11	b.d	b.d	b.d	b.d	b.d	b.d
K_2O	b.d	b.d	b.d	0.08	b.d	0.06	b.d	0.08	b.d	b.d	b.d	b.d	b.d
CaO	56.47	48.45	54.49	52.47	52.82	50.53	54.50	49.76	54.63	55.29	55.68	55.46	49.04
FeO	b.d	b.d	0.50	0.81	0.99	0.57	b.d	b.d	b.d	b.d	b.d	b.d	b.d
SrO	0.46	0.84	0.71	0.79	0.41	0.64	0.76	0.68	0.36	1.29	0.27	0.28	0.47
Y_2O_3	0.16	3.97	0.48	0.37	0.88	1.45	0.58	0.96	0.95	0.26	0.25	0.21	3.28
La_2O_3	b.d	b.d	b.d	b.d	b.d	b.d	b.d	0.17	b.d	b.d	b.d	b.d	0.18
Ce_2O_3	b.d	0.37	b.d	b.d	b.d	0.28	b.d	0.33	0.20	b.d	0.24	0.17	0.56
Nd_2O_3	b.d	0.38	b.d	b.d	b.d	b.d	0.21	b.d	b.d	b.d	b.d	b.d	0.45
ThO_2	b.d	b.d	b.d	b.d	b.d	0.99	b.d	0.91	b.d	b.d	b.d	b.d	b.d
F	2.31	1.76	4.51	4.20	4.06	4.78	4.59	3.71	4.90	3.65	4.28	2.80	3.89
Total	103.16	98.03	104.30	100.48	101.52	101.55	103.56	97.17	104.41	104.64	103.42	101.54	99.31
O=F	102.19	97.29	102.40	98.71	99.81	99.54	101.63	95.61	102.35	103.10	101.62	100.36	97.68
						Formula 26 (O)							
Na	0.055	0.683	0.121	0.084	0.169	0.287	0.124	0.246	0.169	0.080	0.073	0.063	0.524
Mg				0.012									
Al				0.025	0.011	0.016		0.048					
S				0.000			0.021						
K				0.017		0.012		0.017					
Ca	9.794	9.079	9.160	9.197	9.186	8.786	9.232	9.131	9.154	9.341	9.469	9.737	8.854
Fe			0.065	0.111	0.134	0.077							
Sr	0.043	0.085	0.065	0.075	0.039	0.060	0.070	0.067	0.032	0.118	0.025	0.027	0.046
Y	0.014	0.370	0.040	0.032	0.076	0.126	0.048	0.088	0.079	0.022	0.021	0.018	0.294
La								0.011					
Ce		0.024				0.017		0.020	0.011		0.014	0.010	0.035
Nd		0.024					0.012	0.000					0.027
Th						0.036		0.036					
Total	9.907	10.265	9.451	9.553	9.615	9.417	9.507	9.664	9.445	9.561	9.602	9.854	9.780
Si	0.009		0.013	0.079	0.026	0.050	0.000	0.121	0.015				
P	5.965	5.958	5.731	5.655	5.717	5.616	5.666	5.640	5.656	5.858	5.708	5.885	5.686
Total	5.974	5.958	5.744	5.734	5.743	5.666	5.666	5.760	5.671	5.858	5.708	5.885	5.686
F	1.184	0.974	2.237	2.173	2.082	2.455	2.295	2.008	2.423	1.822	2.148	1.452	2.072

Ti, Ba, Mn, Cl, SO_3, are below detection limit of about 0.05 wt%

b.d. = below detection limit of 0.05 wt%

7.7 HREE and their host minerals– EPMA and LAICPMS

7. 7.1 Xenotime-(Y)

Xenotime-(Y) was originally described from a pegmatite locality in southern Norway (Berzelius 1824), Its occurrence in carbonatites is rare (Wall et al. 2008). In the Lofdal carbonatites, xenotime-(Y) is a common mineral and abundant in the carbonatite dykes and fenites. It occurs with calcite, dolomite and Mn-Fe-oxides. However, in the sövite plugs it is only observed in the Emanya plug and not in the Main calciocarbonatite plug. In few instances of intense hydrothermal overprinting in dykes it constitutes a major mineral component of the rock reaching up to 10% by volume. Xenotime-(Y) is the principal host of the (HREE) dysprosium, erbium, terbium and ytterbium.

Xenotime-(Y) shows a range of occurence:

a) Replacing early zircon, probably in the final magmatic stages of carbonatite emplacement, to late formation with monazite-(Ce), apatite and synchysite-(Ce) in hydrothermal carbonatite.
b) Coexisting with synchysite-(Ce) and parisite-(Ce), as small remnants in association and replaced by synchysite-(Ce) and parisite-(Ce).
c) Very fine-grained fibrous xenotime-(Y) occurring in veinlets that intrude the calciocarbonatite and dolomitic dykes. These can be very rich xenotime-(Y) (up to 3% of the thin section).
d) Association of xenotime-(Y)-apatite-thorite

All indicated occurrences above are secondary. In most cases xenotime-(Y) is associated with apatite; calcite, fluorite, zircon and thorite except for the variety were xenotime-(Y) is associated with apatite only. The association xenotime-(Y)-apatite-thorite is common at Lofdal and may be a result of carbonatite melt/fluid differentiation, the late-stage of the carbonatite formation, where at the end of differentiation processes the carbonatite melt became very rich in water, F, Cl, and finally practically a hydrothermal fluid. REE could be transported with F- and Cl- complexes which are stable until the latest stages of carbonatite-formation. Upon de-stabilisation of these complexes REE-minerals can precipitate from the fluid (Salvi and Williams-Jones 1990, Smith and Henderson 2000, Williams-Jones et al. 2000, Schönenberger et al. 2008).

Xenotime (Y) is common here in the albitised country rock and carbonatite-free shear zones. The presence of xenotime(Y) in albitised country rocks and carbonatite-free shear zones is evidence that most of the xenotime-(Y)-formed from a carbonatite-related hydrothermal system associated with the dykes.

It is important to note that at Lofdal xenotime-(Y) formed at both, the magmatic stage and as sub solidus hydrothermal phases during the evolution of the Lofdal alkaline complexes in a similar fashion as to that described by Mariano (1989), Wall and Zaitsev (2004). Late-stage carbonatites and the transition from magmatic to hydrothermal conditions are not very well understood and REE minerals often form at this stage and as subsolidus hydrothermal phases (Mariano 1989, Wall and Zaitsev 2004). For example in Type 2 dyke xenotime-(Y) crystallised at an early magmatic stage and also at the very last stage of hydrothermal activity pointing to a possible major source of yttrium and heavy REE right at the magmatic phase, rather than the usual early phase that is rich in LREE. The Lofdal occurrence points to a continuous LREE-depletion during the hydrothermal phase and a good supply REE and yttrium in the hydrothermal stage. The tracted process of LREE depletion and HREE enrichment could explain different varieties or typomorphs of xenotime-(Y) at Lofdal, as with time crystallisation conditions are likely to change. Seven distinguishable types at Lofdal are discussed below.

7.7.1.1 Xenotime-(Y) paragenesis

Xenotime-(Y) occurs in several different paragenesis within the Lofdal dyke samples. A summary of Lofdal paragenesis is given in Table 7.3.

The apatite associated with xenotime-(Y) in calcite carbonatite looks very similar to magmatic carbonatitic apatite elsewhere (such as Sokli, Finland) and some of the xenotime-(Y) may well have formed in association with magnetite, which is a typical magmatic mineral in carbonatite (Wall et al. 2008). Here apatite cannot be used to define phases of formation, since it precipitated during both magmatic and hydrothermal stages. Xenotime-(Y) has a gradation range of formation conditions and the boundary is somewhat arbitrary but associations such as synchysite-(Ce) replacing calcite and xenotime-(Y) are certainly sub-solidus reactions and appear to be the product of low temperature hydrothermal activity. The synchysite-(Ce) and xenotime-(Y) association has been placed as hydrothermal. Xenotime-(Y) replacing early zircon probably occurred in the final magmatic stage of carbonatite emplacement, to late formation with

monazite-(Ce) (Wall et al. 2008), while apatite and synchysite-(Ce) form during the hydrothermal carbonatite phase.

- **Segregations and aggregates**

Xenotime-(Y) is observed forming series of aggregate subhedral grains with an average size of up to 15 μm in veinlets of highly ferruginous bright orange-brown calcite carbonatite. It is concentrated particularly at the borders between albite and ankerite crystals. In places xenotime (Y) forms cumulate-like textures with hematite that replace earlier magnetite, giving an impression of white dots in large area of the BSE images (Figure 7.22). These rocks (e.g. sample 15769), have the largest concentration of xenotime-(Y). Highly ferruginous bright orange-brown calcite carbonatites have the highest concentration of xenotime-(Y) found as aggregates and surrounded by a fine grained Fe- oxide rich calcite, hematite and magnetite. Xenotime-(Y) occurs as segregates and in veins that cut earlier coarse-grained (non-cathodoluminescent) carbonatite. The observed textures are clearly of magmatic character.

Small thorite crystals occur also at the boundary and in the middle of the xenotime-(Y). At times subhedral and euhedral xenotime-(Y) grains are observed in zones with pure calcite possibly a product of recrystallised calcite and/or possibly a late phase of calcite fluid infiltration into the inhomogeneous iron oxidized matrix.

- **Single euhedral and large subhedral xenotime-(Y) grains**

These types of xenotime-(Y) are mostly large individual grains up to 500 μm wide that occur in mottled pink-brown ankerite-calcite carbonatite Type 1, 3 dykes and the Emanya plug. The xenotime-(Y) from the Emanya plug is complete and euhedral with absent zoning and resorbed edges. The xenotime occur in nests of pure calcite (Figure 7.22a). The euhedral xenotime-(Y) is in places associated with magnetite and or enclosed in the magnetite grains.

Mineral zoning is a common characteristic among the subhedral and euhedral xenotime-(Y) grains that are large and located in the matrix. Zoning and the occurence of xenotime inclusions in the magnetite appears to indicate the magmatic character of the xenotime-(Y) formation. Some xenotime-(Y) crystal boundaries are resorbed and replaced and these could have been affected by the alteration processes.

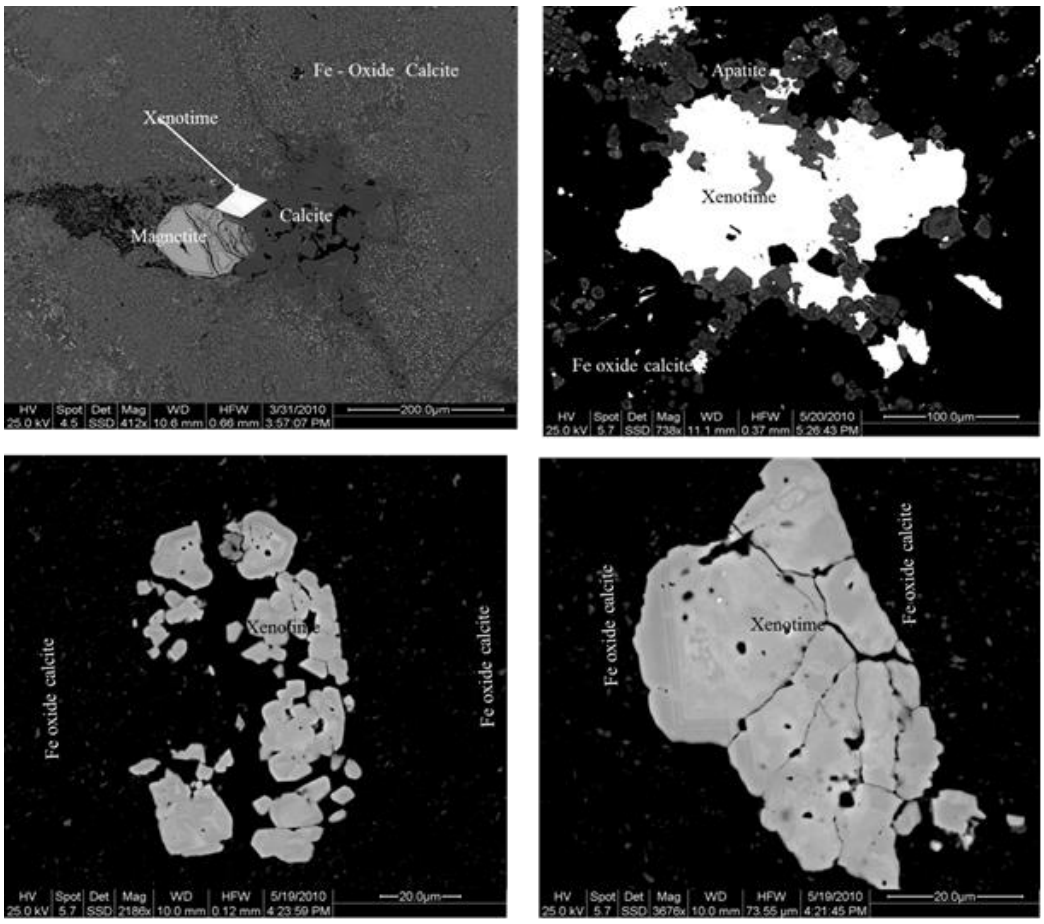

Figure 7.22 Backscattered electron images showing euhedral and anhedral xenotime-(Y). a) Xenotime (Y) in nests of pure secondary calcite, b) large xenotime (Y) grains associated with apatite b) and resorbed large xenotime-(Y) in the fine Fe oxide matrix C) (samples 881R, 15769LG and 189)

These are multiple-sized xenotime-(Y) grains, scattered in the calcite matrix, at the boundaries of large calcite- Fe oxide/ankerite grains, veinlets and at times forming strings. The calcite in this carbonatite contains large amounts of exsolved Fe oxides and gives an opaque characteristic under the microscope and using cathodoluminescence. Disseminated xenotime-(Y) grains are found in the calciocarbonatite dykes that are rich in albite and quartz (Figure 7.23). They are resorbed and do not show any zoning neither do they enclose zircons. The xenotime-(Y) grain sizes are generally small ranging up to 20µm. The largest xenotime-(Y) crystals are observed at the edge of a Fe oxide/ankerite vein, reaching up to 50 µm in size.

The presence of quartz and albite indicate late albitisation and silicification process of the carbonatite dykes.

The disseminated xenotime-(Y) occurrence indicates a secondary origin, mainly because it is found at the boundaries of the mineral grains and the veinlets as shown in Figure 7.23.

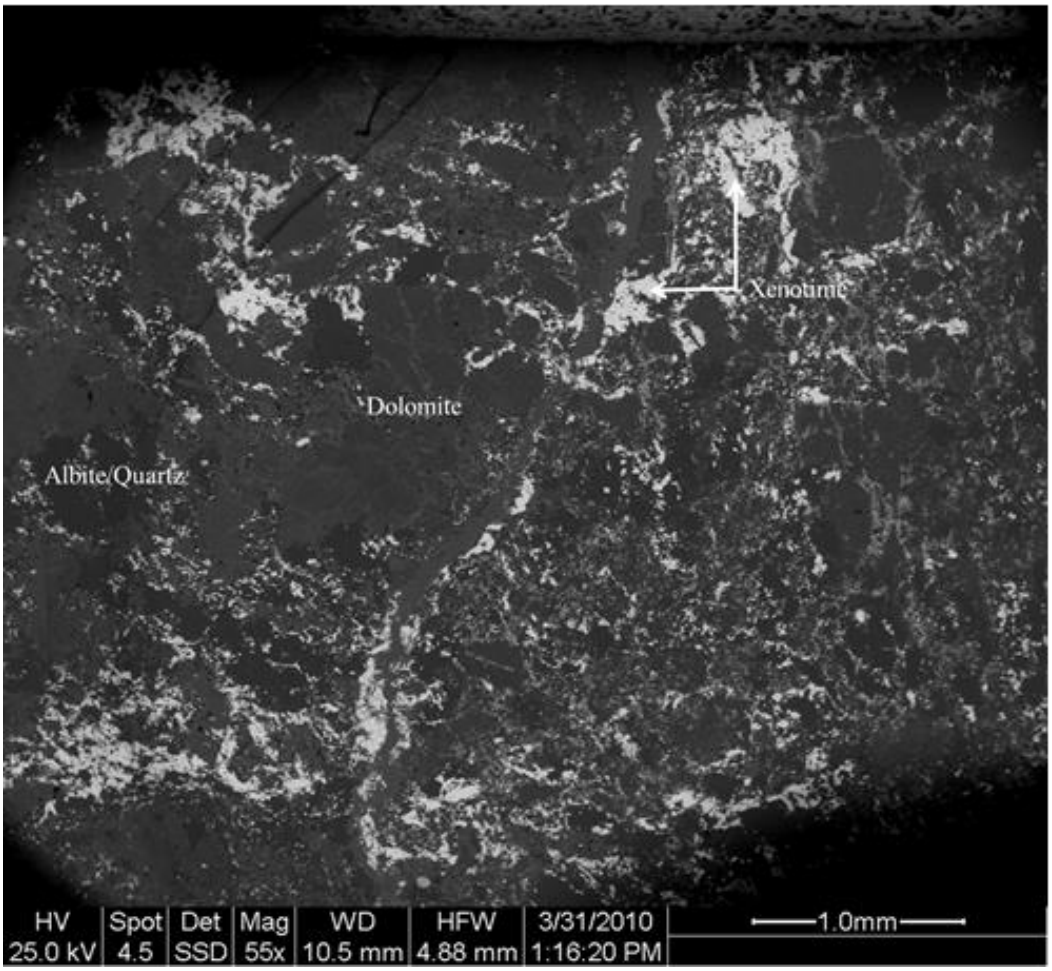

Figure 7.23 Backscattered image of disseminated xenotime-(Y) in dolomite carbonatite (sample 114)

- **Granular xenotime-(Y)**

Granular xenotime-(Y) is observed as individual grains in the oxidized calcite carbonatite. Xenotime-(Y) sits as individual grains in a heterogeneous calcite matrix, with some areas that are mostly opaque in thin section owing to finely disseminated Fe oxides plus accessory phlogopite-annite series mica and albite. The zones where xenotime-(Y) grains occur are rich in apatite and fluorite. Granular xenotime-(Y) is observed as concentrically zoned 10-20 μm euhedral crystals of xenotime-(Y) at the edge of 5 μm anhedral areas of synchysite-(Ce). Thorite is found along xenotime-(Y) and also covering the central parts of large grains of synchysite. Such large grains of synchysite are possible replacements of the coarse grained calcite as such rocks are medium grained rather than the usual fine grained xenotime-(Y) rich carbonatites. These xenotime-(Y) minerals are in zones that exhibit flow banding.

- **Xenotime-(Y) second generation**

Xenotime-(Y) occurrence referred to as xenotime-(Y) II, is most commonly found in highly ferruginous and altered bright orange-brown silicified calcite carbonatite, with abundant mica of the phlogopite-annite series (e.g. sample 927 and 189). Xenotime-(Y) II consists of anhedral xenotime-(Y) grains with an average size of 5 µm and completely enclosed in apatite II (Figure 7.24). Xenotime-(Y) II and apatite II occur in veins that cut earlier carbonatite, forming aggregate nests and are enclosed into the apatite I matrix and set into the iron- oxidized ferruginous carbonatite matrix with grains of xenotime-(Y) I.

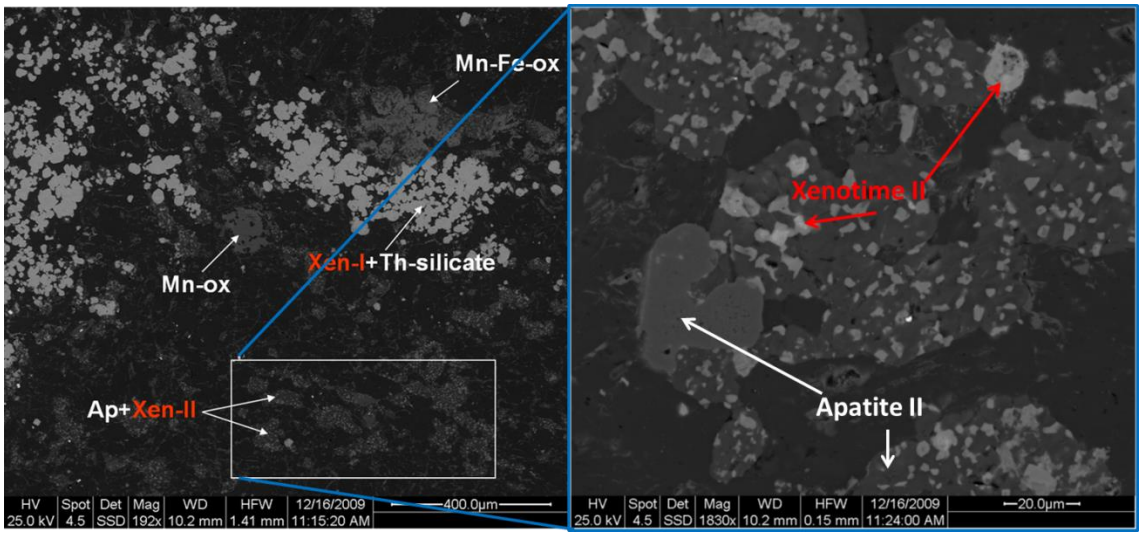

Figure 7.24 Backscattered image showing two generations of xenotime-(Y) of a Lofdal carbonatite dyke). Left: overview of the section showing primary and secondary crystallization of xenotime-(Y) in calcite matrix. Right: magnified Xenotime-(Y) II, closely associated with apatite.

Xenotime-(Y) apatite-thorite crystallisation is probably the result of carbonatite melt/fluid differentiation, the late-stage of the carbonatite formation. Due to the small grain size of the secondary xenotime-(Y) no mineral analysis was done. The apatite associated with secondary xenotime-(Y) showed high values of HREE. Other minerals associated with xenotime-(Y) II are Fe-Ox (iron oxide), calcite and rutile.

- **Xenotime-(Y) associated with LREE**

Parisite-(Ce) and synchysite-(Ce) are the LREE minerals associated with the xenotime-(Y) in Type 3 dykes. Coexisting xenotime-(Y) with LREE synchysite-(Ce) and parisite-(Ce) as small remnants in association and replaced by LREE- synchysite-(Ce) and

parisite (Ce) has been observed. The association occurs in the dark mottled brown ferruginous silicified calcite carbonatite. This is an unusual association in most known carbonatites and also at Lofdal. Partially resorbed zircons and small thorite crystals occur at the boundary between the zircon and xenotime-(Y). Monazite has been encountered in association with xenotime-(Y) in distinct and separate late ferruginous calcite veins that cut earlier calcio-carbonatite rocks (Wall et al. 2008).

The association of the LREE flour-carbonate appears to reflect a late stage process where the minerals parisite-(Ce) and synchysite-(Ce) are replacing xenotime-(Y). This process most likely took place during the hydrothermal phase, when parisite-(Ce) and synchysite-(Ce) became more stable under the hydrothermal conditions than xenotime-(Y) which precipitated during the magmatic phase.

- **Xenotime-(Y) mantling zircon**

Some xenotime-(Y) crystals have zircon cores, where xenotime-(Y) overgrow the zircon and imitates the original shape outline of the replaced zircon. Tiny (1 μm) thorite crystals mark the original zircon margins and all xenotime-(Y) shows the same stages of overgrowth, first euhedral following the original zircon and then a final anhedral stage. Xenotime-(Y) mantling zircon is observed in calcio-carbonatites of Type 2 dykes and the Dolomite group (Figure 7.25).

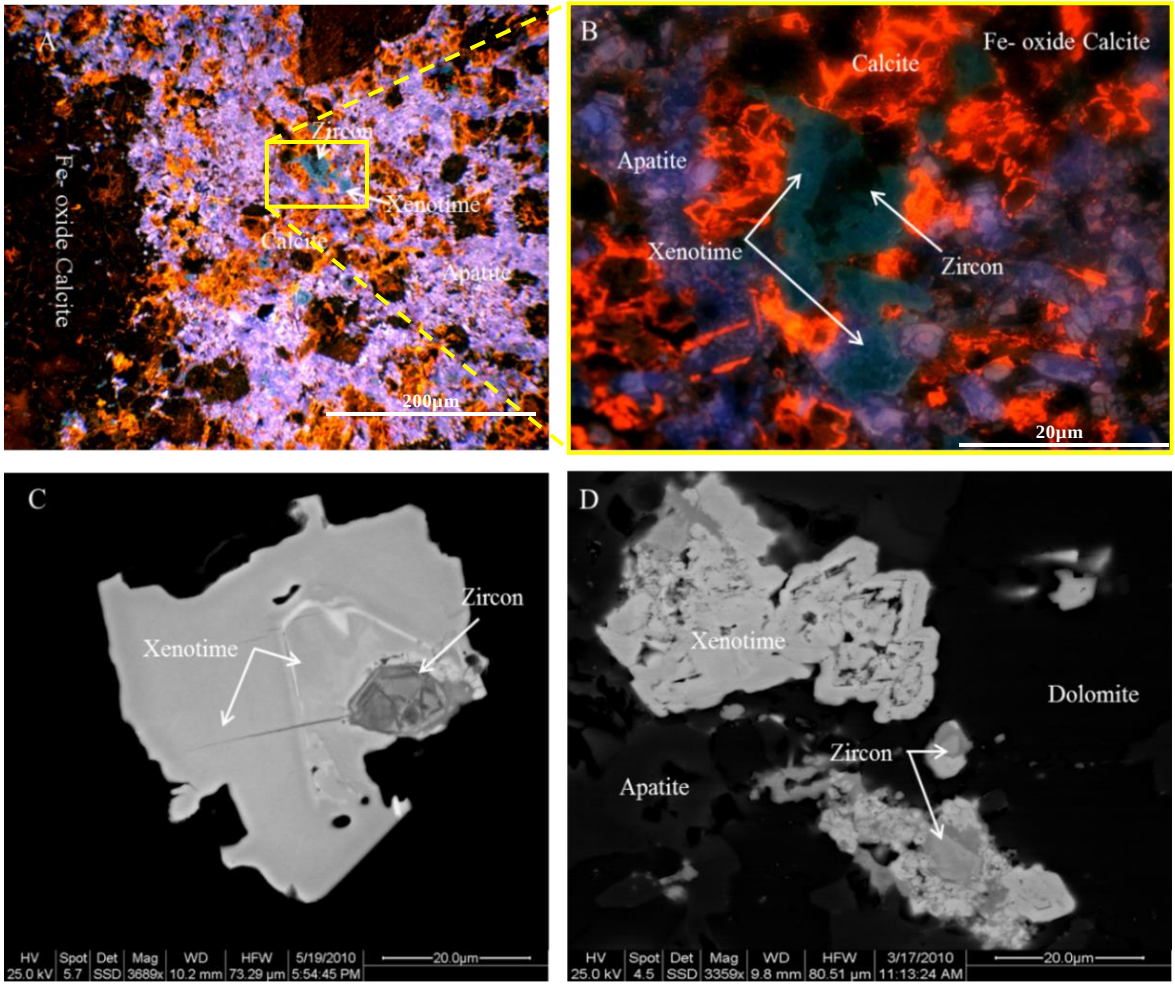

Figure 7.25 Xenotime-(Y) mantles zircon. A) Cathodoluminescence image showing the overview of the calcite veinlet that is rich in apatite, which is associated with the xenotime-(Y) enclosing zircon. The calcite veinlet cut through an early iron oxide rich calcite. B) Cathodoluminescence image close view of the minerals xenotime-(Y) zircon association. C) Backscattered image showing the xenotime-(Y) mantling zircon mineral. Note the original shape and size of original zircon mineral preserved after xenotime-(Y) replacement of the zircon. D) Xenotime-(Y) replacing zircon in dolomite carbonatite.

In some Lofdal carbonatites zircon is of particular interest because of the way it acts as a substrate for, and is replaced by the xenotime-(Y) (Figure 7.25). Zircon and xenotime-(Y) are isostructural (Finch and Hanchar 2003) and zircon/xenotime-(Y) overgrowths are relatively common in metamorphic rocks and in granites (e.g. Corfu et al. 2003). This overgrowth has also been seen in trachyte at the Chagatai carbonatite (Wall et al. 2008). The Y substitution from the mineral xenotime-(Y) predominantly involves replacement of Zr in the larger triangular dodecahedral sites of the zircon.

Coupled substitution of REEs and PO_4 into the zircon structure (Speer 1980, Romans et al. 1975) can lead to substantial enrichment in the REEs as is the case at Lofdal.

7.7.1.2 Xenotime-(Y) composition

Lofdal xenotime-(Y) is mid and heavy-REE enriched. Observed concentric zoning in xenotime-(Y) represents small changes in REE versus Y, especially Dy and Gd, Th, Fe and Ca (Wall et al. 2008) and no consistent difference overall between brighter and darker zones on BSE images(Fig 7.25).

The xenotime-(Y) has a dull turquoise colour under cathodoluminescence. The relatively low CL intensity and the small sampling area due to small grain size required an acquisition time of 120s. Xenotime (Y) spectra of the Lofdal carbonatite show strong emission at 473 and 565 nm, which is attributed to Dy^3+ (Gorobets and Rogojine 2002). The low but distinct emission band at 535 nm is probably related to activation by Tb^3+. The set of minor peaks at 690 nm and the emission at 590-610 and 630-650 nm probably indicates the presence of Sm3+ in the xenotime-(Y) lattice.

A difference exist between Lofdal carbonatite xenotime-(Y) and xenotime-(Y) from granites, showing consistent large Eu anomaly in granitic xenotime-(Y) (Förster 1998) and lack of any anomaly at Lofdal (Wall et al. 2008) or in xenotime-(Y) from a hydrothermal quartz rock associated with carbonatite at Kangankunde, Malawi (Wall and Mariano 1996). It is conclusive that the characteristics of carbonatitic xenotime-(Y) are lack of an Eu anomaly, higher Gd (variable but reaches >6 wt%) and lower Yb (below 4 wt%) (Wall et al. 2008). Chondrite-normalised values for Y and Ho are usually similar because of their similar size and charge. However, decoupling of Y from Ho is occasionally seen as a result of probable deuteric alteration during the final stages of crystallization of evolved granites (Förster 1998).

Although there is great variation between the ratio of light to heavy REE with (La/Yb)n at Lofdal; ranging from 0.04 to 294.15 in dolomite rock to 294.15 in Type 5 dykes there is no evidence decoupling of Y and Ho.

There is up to 1 wt% ThO_2 in magmatic xenotime-(Y) and usually lower, about 0.3 wt% ThO_2. Despite the variation in the paragenesis of xenotime-(Y) at Lofdal, their geochemical patters are rather similar with only a small variation in MREE for some xenotime-(Y) groups (Figure7.26). The chondrite-normalized REE pattern of xenotime-(Y) coincides with that of Dolomite dykes (Figure 7.26).

Table 7.9 Electron microprobe analyses of xenotime-(Y) in Type 3 dyke (Sample 15769LG) and other carbonatites dykes from Lofdal.

	VNP130		**VNP21**		**15769LG**		
Anal. No.	13	11	2	6	9	40	56
wt%							
SiO_2	-	0.28	0.77	0.49	0.54	0.89	
P_2O_5	35.19	35.03	35.61	35.84	29.31	28.55	27.84
CaO	-	0.10	-	0.21	0.23	0.22	0.18
FeO	-	0.06	0.10	0.15	0	0.26	0
Y_2O_3	47.51	47.04	48.54	47.04	38.67	35.85	34.45
ThO_2	0.07	0.37	1.27	1.00	1.86	1.55	0.72
	Formula 4(O)						
Ca		0.014	0.000	0.030	0.01	0.011	0.0009
Fe		0.007	0.010	0.016			
Y	3.343	3.302	3.335	3.231	0.857	0.836	0.826
Th	0.002	0.011	0.037	0.029	0.018	0.015	0.007
P	3.939	3.912	3.891	3.916	1.033	1.059	1.063
Si		0.037	0.100	0.063	0.041	0.024	0.04

F, Cl, Al_2O_3, SO_3, K_2O, TiO_2, MnO, SiO_2, BaO, Ce_2O_3, Nd_2O_3 all below detection limit of about 0.05 wt% b.d. = below detection limit of 0.05 wt%. Total Fe is expressed as FeO

At Lofdal xenotime-(Y) is observed very occasionally coexisting with monazite (Wall, et al. 2008). Coexisting monazite-xenotime-(Y) pairs have been proposed as a geothermometer in metamorphic rocks, specifically metapelites. The application of these geothermometers was tested for an average coexisting monazite-(Ce)-xenotime-(Y) composition in ferruginous calcite carbonatite (VNP21) from Lofdal (Wall et al. 2008). The Lofdal monazite-(Ce) gives a temperature of 450 – 500°C at 5-2 kbar when plotted on the monazite limb of the (Ce-Y) PO4 binary plot determined experimentally by Gratz and Heinrich (1997). Temperatures for the Lofdal xenotime-(Y) were about 600°C which is higher than expected for mineralization in the Fe-rich carbonatite (Wall et al. 2008). The carbonatitic system is rather different from metapelites but they provide at least a potential hypothesis that xenotime-(Y) formed at temperatures >450° (Wall et al. 2008).

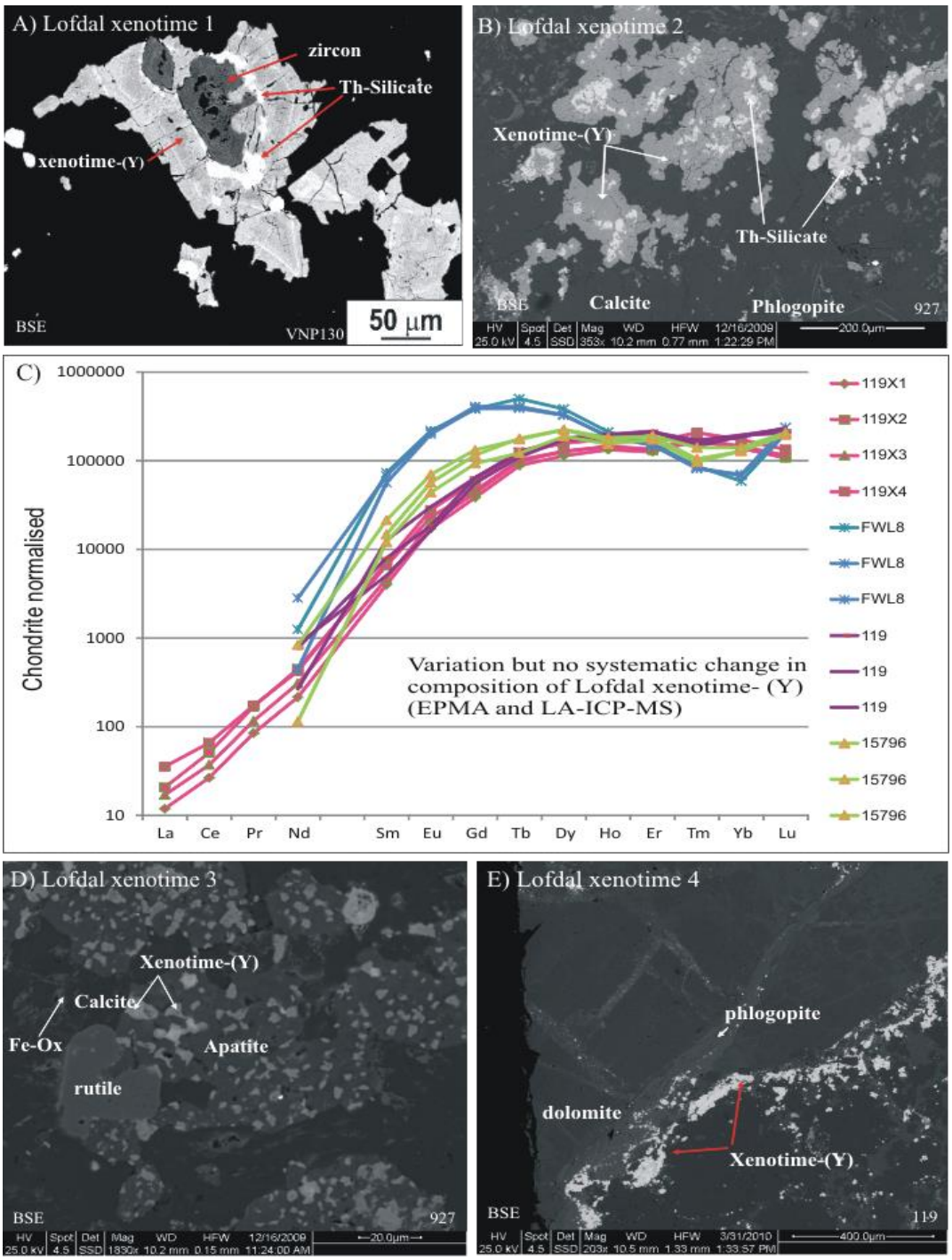

Figure 7.26 a) subhedral xenotime-(Y) in the calcite and albite matrix of the carbonatite dyke type 1, b) xenotime-(Y) I granular, c) Chondrite-normalized REE patterns from Lofdal carbonatites. Chondrite values are from McDonough and Sun (1995); d) xenotime-(Y) II associated with apatite II xenotime-(Y) disseminated, and e) veinlets in dolomitic carbonatite.

7.7.2 Zircon

Zircon ($ZrSiO_4$) is a common accessory mineral found in igneous and metamorphic rocks and is generally in an amorphous state due to self-irradiation from radioactive impurities.

Zircon in Lofdal carbonatites ranges from 0.5 to 4 mm in diameter with an average of 1 mm and has a greater variety of shapes, from well-rounded grains to those with angular margins. Zircons in syenites are larger, with an average diameter of about 2 mm. The larger zircons are subhedral to well-rounded. Occasional euhedral grains of pyrochlore were observed as inclusions in large zircon grains.

Alteration and radiation-damaged (metamict) crystals are revealed using cathodoluminescence (CL) and back-scattered electron (BSE) images. Metamict zircon is chemically and physically less stable than its crystalline equivalent, causing enhanced susceptibility to alteration by aqueous fluids (Pidgeon et al. 1966, Trocellier and Delmas 2001, Geisler et al. 2003a, 2007, Hoskin, 2005). Hydrothermal alteration of metamict zircon results in the structural recovery of amorphous areas and enrichment in hydrous species and the non-formula elements Al, Mg, Ca, Fe, Mn, Y and P (Speer 1982, Geisler et al. 2003a, 2003b, 2007).

Zircon always contains a certain amount of hafnium: the HfO_2/ZrO_2 ratio varies but is normally about 0.01. The highest ratio is found in metamict varieties (0.06) while it increases from 0.015 for zircons in nepheline-syenites to 0.04 for those in granites (Rankama and Sahama 1950). Phosphorus may be present in some varieties, probably replacing Si, the structure maintaining electrostatic neutrality by the entry of rare earths.

The chondrite-normalised REE concentrations for zircon increase rapidly from Sm to Lu even in rocks which have significant LREE enrichment. Calculated partition coefficients between zircon and melt (based on measured concentrations of mineral separates and interstitial glass from volcanic rocks or whole rocks) are high for the heavy REEs (HREEs), falling rapidly towards the light REEs (LREEs; approx. 400 for Lu and 4 for Ce; Hendersen 1984).

Despite the relatively high concentrations of the HREEs in zircon, it generally does not have a significant effect on the bulk rock REE chemistry due to its low abundance (Gromet and Silver 1983, Exley 1980). Experimental studies have also demonstrated zircon's preference for the HREE (Watson 1980). However, the measured variations in the partition coefficients between the HREE and the LREE are much lower than those observed in the natural samples. It has been shown that Ce can be anomalously high in

zircon compared to other LREEs (Murali et al. 1983). The experimental studies suggest that significant partitioning of the LREEs into zircon is possible.

All the zircon suites analysed show a preference for concentrating the HREE.

Sample 813 and 78 contain common euhedral zircons with concentric oscillatory growth zoning. The zoning is visualised by shades of very weak greenish CL. The outermost growth zone (<3 μm) has a very bright green luminescence. The spectra of the zircon show strong emission bands at 473 and 565 nm activated Dy^{3+}. Mariano (1978) pointed out that zircon strongly favours the incorporation of the HREE, in particular Dy, due to its very restricted crystal chemistry compared to other host minerals. As a result zircon often shows Dy3+ emission bands, normally indicative of an HREE environment, regardless of whether it has crystallised in a HREE-rich or an LREE-rich environment.

Scanning electron microscope studies of the Lofdal carbonatite showed that both pyrochlore and zircon contain an appreciable amount of uranium. The centre of some pyrochlore and zircon grains is totally resolved and the amount of uranium at such points is very high with up 5 wt%.

7.7.2.1 Zircon composition and mobility

The zircons are euhedral as observed in the field. They are brown in colour and porous. It is evident that zircon crystallised in the silica-rich calcite carbonatite (VNP 813) enclosing calcite in calcite-rich areas. The outer margins of the crystals appear clean and uncorroded; however, in CL there are signs of internal zircon corrosion and infiltration by calcite. Backscattered electron, cathodolumeniscence, LA-ICP-MS show that Lofdal zircon is internally altered and porous and has gone through a mictimisation, a process of self-radiation of zircon from radioactive impurities.

After zircon formation, thorite formed at the crystal margins. The zircon appears out of equilibrium in the calcite system, as predicted from thermodynamic considerations (Barker 2001) and is easily altered and even removed. Although most zircons show different alterations recognized under the reflected light microscope and cathodoluminiscence, their REE geochemistry exhibits remarkable similarities. It means that REE geochemistry cannot be used to determine the degree of alteration of the carbonatites.

Zircons in this study have small Ce and Yb positive anomalies. All other zircon populations have Zr/Hf values that range across and near the chondritic value. They contain appreciable P and Y. The compositions have consistent but low HfO2 (Wall et

al. 2008). In general, zircon contains about 1 % HfO2 and Hf becomes increasingly enriched with differentiation of granite (Deer et al. 1992).

The Lofdal values of <1 wt% HfO_2 (Table7.10) are consistent with the 0.5-1.7 wt% HfO_2 reported in zircon from Kola Peninsula carbonatites and alkaline rocks by Chakhmouradian and Williams (2004). There is no evidence from zircon compositions, textures, inclusions or the LAICP-MS dating to indicate that any of the Lofdal zircon crystals are xenocrysts picked up from granitic wall rocks. The REE composition of the zircon from Lofdal is attached as appendix.

Table 7.10 Electron microprobe analyses of zircon (sample VNP 130 and VNP 78b) dykes from Lofdal (Wall et al. 2008).

Sample	VNP 130 Zircon in centre of xenotime crystal			VNP 78b Large crystals of zircon, no xenotime		
				with "thorite	no "thorite"	
Anal.	#2	#3	#1	#1	#3	#9
No.	1	2	3	4	5	6
ZrO_2 wt%	64.24	64.06	64.35	65.42	65.42	65.55
HfO_2	0.68	0.76	0.81	0.39	0.29	0.2
Y_2O_3	0.79	0.83	0.66	0.29	0.63	0.42
Dy_2O_3	0.09	0.06	_	_	0.07	_
P_2O_5	0.33	0.33	0.28	n.d.	n.d.	n.d.
FeO	0.14	0.21	0.09	0.22	0.06	0.05
UO_2	_	_	_	0.06	_	0.04
ThO_2	_	_	_	0.31	0.07	_
PbO	_	_	_	_	0.18	0.13
SiO_2	32.24	32.12	32.37	32.66	32.52	32.33
Total	**98.51**	**98.37**	**98.56**	**99.35**	**99.24**	**98.72**

n.d.: not determined.

-: below detection limits of about 0.05 wt%.

Gd and Ce were also sought, but found to be below detection limits of the electron microprobe.

7.7.3 Pyrochlore

Pyrochlore (Na, REE, $Ca)_2$ Nb_2 $(O,OH)_6F$ occurs in the Lofdal carbonatites concentrated at the contacts between the carbonatite and the syenite plugs at the top contact zone. It is also encountered in the carbonatite of Dyke Type 1 (sample 813), mainly the albite rich variety. It occurs as large up to 200μm euhedral to subhedral crystals (Figure 7.27) with irregular zonings or more frequently in corroded crystals with somewhat higher REE, ThO_2 and UO_2 contents (Table 7.11). It occurs also as inclusions in the calcite and zircon crystals, indicating its early phase of crystallisation.

The geochemical composition of Lofdal pyrochlore is variable with different zones indicating different mineral content. The bright colour and highly altered zone in the centre of the crystal contain most incompatible elements while the least altered have a more uniform composition (Figure 7.27).

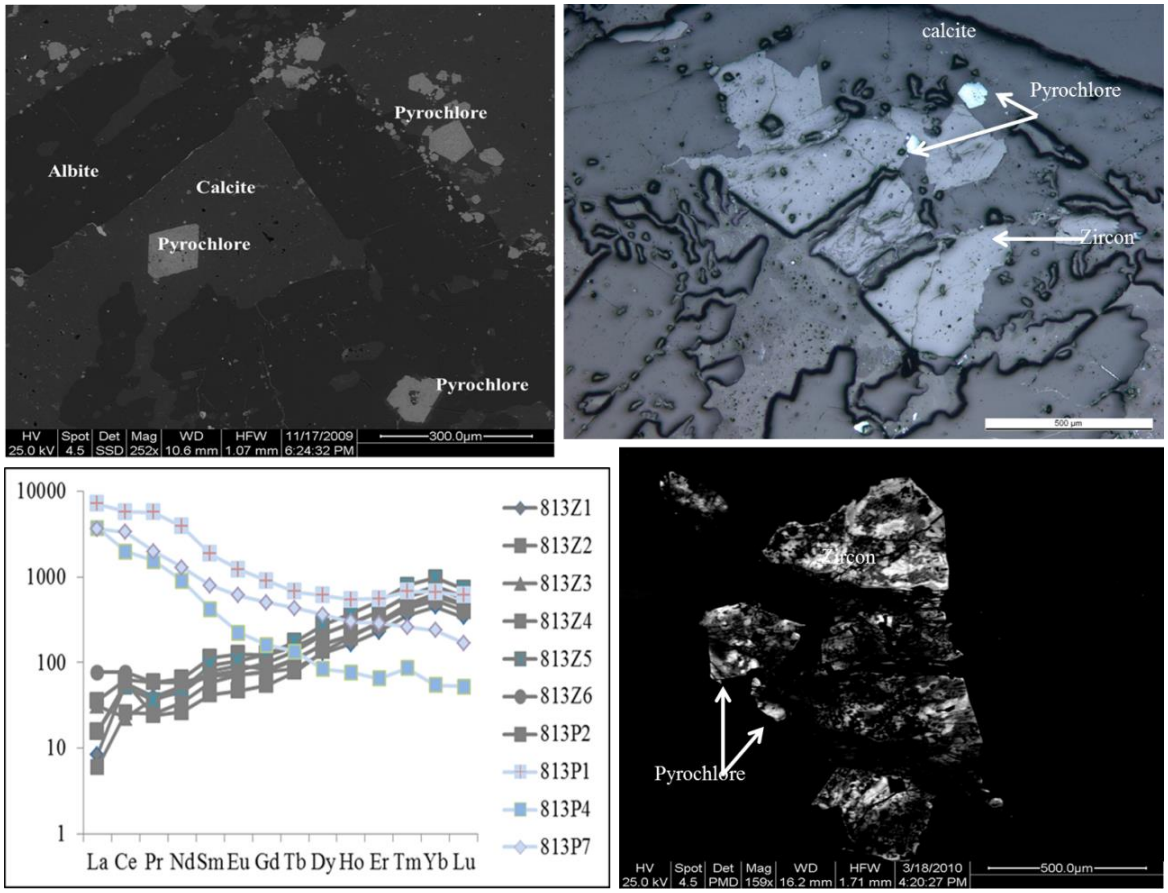

Figure 7.27 Backscattered image showing pyrochlore mineral in the albite rich calcite (sample 813). Note LA-ICP-MS data for zircon (Z1 –Z6)) and pyrochlore (P1, P2, P4 and P7).

Table 7.11 Electron microprobe compositions of pyrochlore in the Lofdal carbonatite

Comment 288a	Bright alteration	Grey zone 10µm	dark zone	Homogenous zone	Light colour	Outermost zone	Broken pieces in matrix
No. point analyses	4	4	2	3	3	4	3
SiO_2	4.66	1.46	4.84	0.55	0.64	0.46	0.46
Na_2O	0.34	0.10	0.83	5.27	3.11	4.68	4.68
CaO	6.31	1.04	9.43	15.26	13.80	14.12	14.12
MnO	2.72	7.82	0.58	0.21	1.00	0.14	0.14
Y_2O_3	b.d	b.d	b.d	b.d	b.d	b.d	b.d
BaO	0.56	0.47	0.67	b.d	0.16	b.d	b.d
FeO	5.70	17.22	1.77	0.66	2.64	0.30	0.30
Al_2O_3	0.87	0.49	0.93	b.d	b.d	b.d	b.d
SrO	3.48	0.79	5.90	2.67	2.85	3.55	3.55
La_2O_3	0.18	b.d	0.21	0.21	0.14	b.d	b.d
TiO_2	6.37	8.30	3.76	5.55	5.71	5.44	5.44
Ce_2O_3	2.63	0.26	0.92	0.88	0.48	1.35	1.35
Nb_2O_5	48.42	46.77	47.66	60.40	59.84	61.21	61.21
Ta_2O_5	b.d	b.d	b.d	b.d	b.d	b.d	b.d
ThO_2	1.60	0.22	0.18	0.09	0.14	0.06	0.06
ZrO_2	b.d	0.06	0.38	b.d	0.08	b.d	b.d
UO_2	1.20	0.24	1.73	0.11	0.13	0.13	0.13
PbO	0.33	0.27	0.30	0.30	0.34	0.27	0.27
F	0.13	b.d	0.89	4.41	3.27	3.67	3.67
Total	85.49	85.57	80.60	94.86	92.97	94.16	94.16

7.8 Other cathodoluminescence spectra of minerals in the Lofdal carbonatites

Various cathodoluminescence images have been presented in the descriptions above and the cathodoluminiscence study of the minerals from Lofdal is summarised below.

The recorded CL spectra of fluorite, apatite, xenotime-(Y) and zircon in carbonatites from Lofdal are dominated by REE-activated luminescence, particularly, Dy^{3+} in fluorite, xenotime-(Y) and zircon and Sm^{3+} in apatite (Table 7.12). The approximate positions of the emission bands and their activators are listed in Table 7.12. The general similarity of the CL pattern of the four accessory minerals points to a very high abundance of REE of the crystallising fluid/magma.

These accessory minerals have a strong affinity for lanthanides and, thus, they are an effective host for REE in magmatic systems (Marshall 1988 and references therein).

Typical activators in these minerals are the REE Sm^{3+}, Dy^{3+}, Tb^{3+}, Eu^{2+} and, rarely, Eu^{3+} (Monod-Herzen 1966, Mariano 1988, Götze et al. 2001, Gorobets and Rogojine 2002, Kempe and Götze 2002). These elements cause unique sets of narrow emission

bands when they are either the major or minor components in the minerals (Monod-Herzen 1966).

Lofdal carbonatites reflect the high abundance of HREE in the system. However, there are also distinct bands of the MREE Nd^{3+}, Eu^{2+} and Sm^{3+}. The strongest band for Tb^{3+} and Sm^{3+} at 540 nm and 580-585 nm, respectively, form peak shoulders next to the strong green Dy^{3+} band. According to Gorobets and Rogojine (2002), the peak at 865 nm is activated by Nd^{3+}.

Fluorite is either a rock forming (up to 30%) or an accessory in highly mineralized dykes at Lofdal. Only few dykes have possibly economic amounts of fluorite and these are restricted to an area SW and north of the Emanya intrusion. The specific location of fluorite raises important question of whether there is an underlying differentiated intrusive complex from which the mineralizing fluids had derived and the fluorite rich area is a sign of the fluid source.

Fluorite in Type 5 dykes indicates veining in cracks of the carbonatites together with apatite, celestine and magnetite. Such association may suggest that all these minerals crystallized at the same time. The relationships between the phases indicate that the minerals grew in equilibrium.

Microscopic studies show that large earlier formed fluorite crystals contain up to 500μm irregular shaped fluid inclusion (Fig 7.28). The study of these fluid inclusions would give insight into the hydrothermal environment that existed during the formation of fluorite. Other inclusions were identified as quartz.

Table 7.12 Wavelengths of CL bands (nm) of fluorite, apatite, xenotime-(Y) and zircon from the Lofdal carbonatites and their most possible activators according to literature (Mariano and Ring 1975, Mariano 1988, Mariano 1978, Götze et al. 2001, Gorobets and Rogojine 2002, Kempe and Götze 2002).

colour	**violet**	**Blue**	**green**	**green**	**yel-low**	**red**	**Red**	**red**	**red**	**infra-red**	**infra-red**
Fluorite											
Peak position	420-430	470	535-540	565	580-585	-	650-660	-	745-755	-	865
activator	Eu^{2+}	Dy^{3+}	Tb^{3+}	Dy^{3+}	Sm^{3+}	-	Dy^{3+}	-	Dy^{3}	-	Nd^{3+}
Apatite											
Peak position	415-435	470	525	560	580 - 585	638	-	695	745	800-810	865-880
activator	?Eu^{2+}	Dy^{3+}	Tb^{3+}	Dy^{3+}	Sm^{3+}	Sm^{3+}	-	Sm^{3+}	Dy^{3+}	Sm^{3+}	Nd^{3+}
xenotime-(Y)											
Peak position	-	473	535	565	590-610	630-650	-	690	740-755	-	-
activator	-	Dy^{3+}	?Tb^{3+}	Dy^{3+}	?Sm^{3+}	?Sm^{3+}	-	?Sm^{3+}	Dy^{3+}	-	-
Zircon											
Peak position	-	473	520-530	565	-	-	-	-	-	-	-
activator	-	Dy^{3+}	Tb^{3+}	Dy^{3+}	-	-	-	-	-	-	-

The study of apatite showed strong blue luminescence and an emission band of at 565, 650-660 and 745-755 nm (Figure29). Mariano (1988) reported that the Sm^{3+} peak is almost invariably greater in intensity than the Dy^{3+} peak in fluorite of alkaline rocks. The dominance of Dy^{3+} in fluorite from the Lofdal carbonatites probably indicates the high abundance of HREE in the system. However, there are also distinct bands of the MREE Nd^{3+}, Eu^{2+} and Sm^{3+}. The strongest band for Tb^{3+} and Sm^{3+} at 540 nm and 580-585 nm, respectively, form peak shoulders next to the strong green Dy^{3+} band. According to Gorobets & Rogojine (2002) the peak at 865 nm is activated by Nd^{3+}.

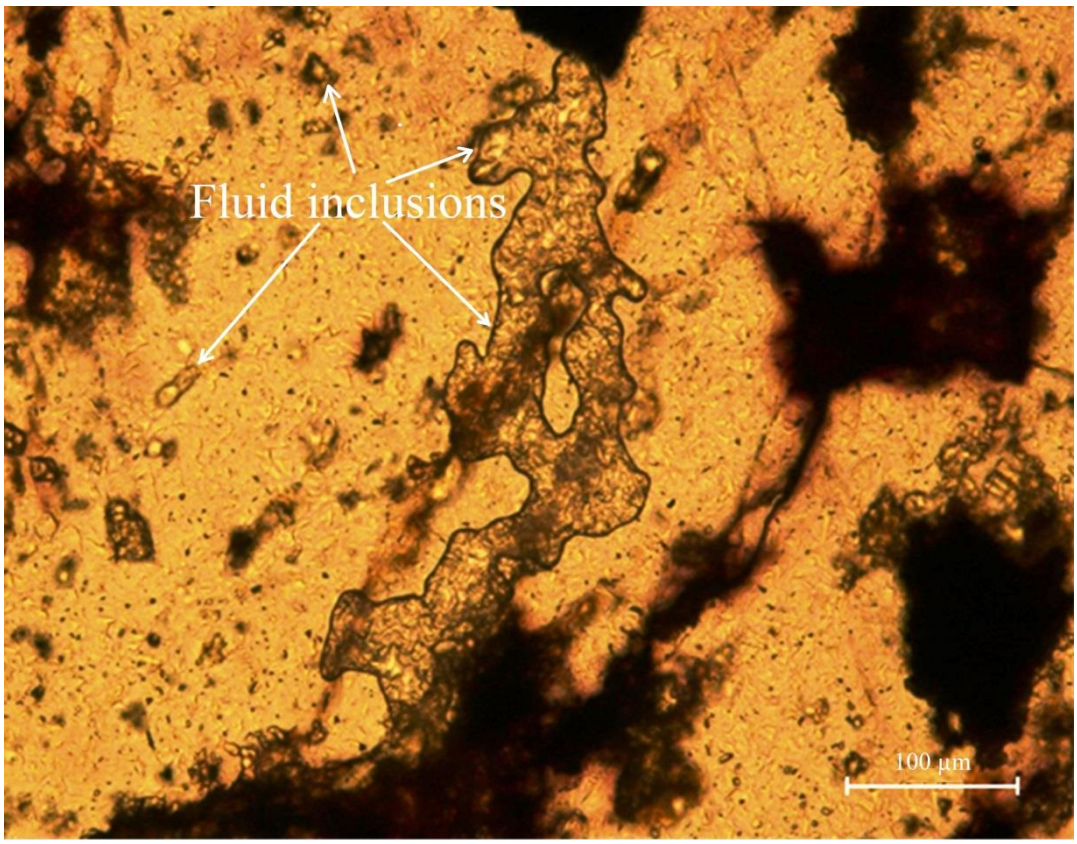

Figure 7.28 Petrographic image showing irregular-shaped fluid inclusions in fluorite from Lofdal carbonatite.

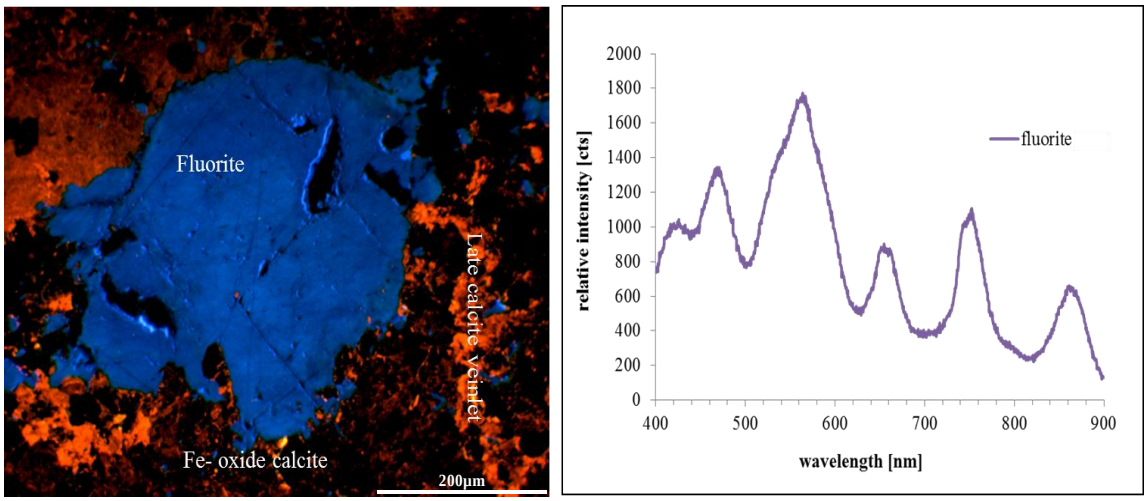

Figure 7.29 Cathodoluminescence spectra of fluorite from Lofdal carbonatites.

Moreover, the blue emission range is accompanied by the emission band of Dy^{3+} at 470 nm. Dy^{3+} causes also the strong bands which appear at 565, 650-660 and 745-755 nm. Mariano (1988) reported that the Sm^{3+} peak is almost invariably greater in intensity than the Dy^{3+} peak in fluorite of alkaline rocks.

7.8.1 Calcite and dolomite

Calcitic carbonatite dominates by far in the Lofdal intrusions. It occurs as an abundant primary and secondary phase. Veins of calcite are also observed locally in both the carbonatite dykes and plugs.

Dolomite constitutes the main carbonate component in some dykes. Dolomitic carbonatite show intense brecciation multiple generations of dolomite intrusions followed by albitisation and later the intrusion of calcite accompanied by xenotime-(Y) mineralisation. The composition of calcite and dolomite are provided in Table, 7.13, while their mineralogical scans are presented in Fig 7.31. Dolomite mineral analysis was unsuccessful using LA-ICP-MS however dolomite crystals were used for stable isotope studies and the results are presented in a later chapter.

Dolomite crystals range in size from very fine in highly sheared carbonatite dykes to 10 cm long in the carbonatites plugs. Calcite is observed in association with other primary carbonatite minerals such as aegirine and magnetite in the less altered carbonatite plugs but in variable associations in the altered carbonatite dykes.

Compositionally, calcite is REE-rich in the xenotime-(Y)-rich dykes (Fig 7.30)

Table 7.13 Electron microprobe compositions of calcite and dolomite from the Lofdal carbonatite [sample 119 is a dolomite/ankerite, 1569LG and 15769 are Type 3 dykes and 326 is from the Main calciocarbonatite.

	Calcite					Dolomite-ankerite					
Sample no.	**15769LG**	**326**	**15769**	**119**		**119**					
No.of analyses	N=16	N=39	N=15	b.d	42	N=52	45	46	53	54	19
Na_2O	b.d	b.d	b.d	0.119	b.d	b.d	0.052	b.d	0.043	b.d	0.062
MgO	0.173	0.097	0.293	56.147	0.055	14.968	19.271	20.297	18.517	19.094	8.358
CaO	54.419	52.412	51.027	0.104	54.988	29.489	32.436	32.109	29.328	29.449	27.685
MnO	0.177	1.000	0.633		0.101	0.275	0.359	0.415	0.107	0.000	0.709
FeO	1.038	0.982	5.931		0.28	9.853	0.189	0.198	5.372	4.177	19.574
SrO	0.311	1.470	0.298		b.d	0.153	b.d	b.d	b.d	b.d	b.d
CO_2	43.387	43.008	44.545	44.257	43.448	45.587	46.869	47.737	46.620	46.516	43.325
Total	**98.831**	**98.841**	**102.237**	**100.627**	**98.872**	**100.021**	**99.17557079**	**100.756**	**99.986**	**99.235**	**99.713**
Formula 3(O)				Formula 6(O)		Formula 6(O)					
Mg	0.004	0.002	0.007	0.006	0.003	0.715	0.898	0.928	0.867	0.896	0.421
Ca	0.984	0.956	0.902	1.991	1.986	1.016	1.086	1.056	0.987	0.994	1.003
Mn	0.003	0.014	0.010	0.003	0.003	0.008	0.009	0.011	0.003	0.000	0.020
Fe	0.010	0.014	0.078		0.008	0.265	0.005	0.005	0.141	0.110	0.553
Sr	0.003	0.015	0.003			0.001					
C	1.000	1.000	1.000	2.000	2.000	2.000	2.000	2.000	2.000	2.000	2.000
Total	1.000	1.000	0.995	2.000	2.000	2.000	2.001	2.000	2.001	2.000	2.002

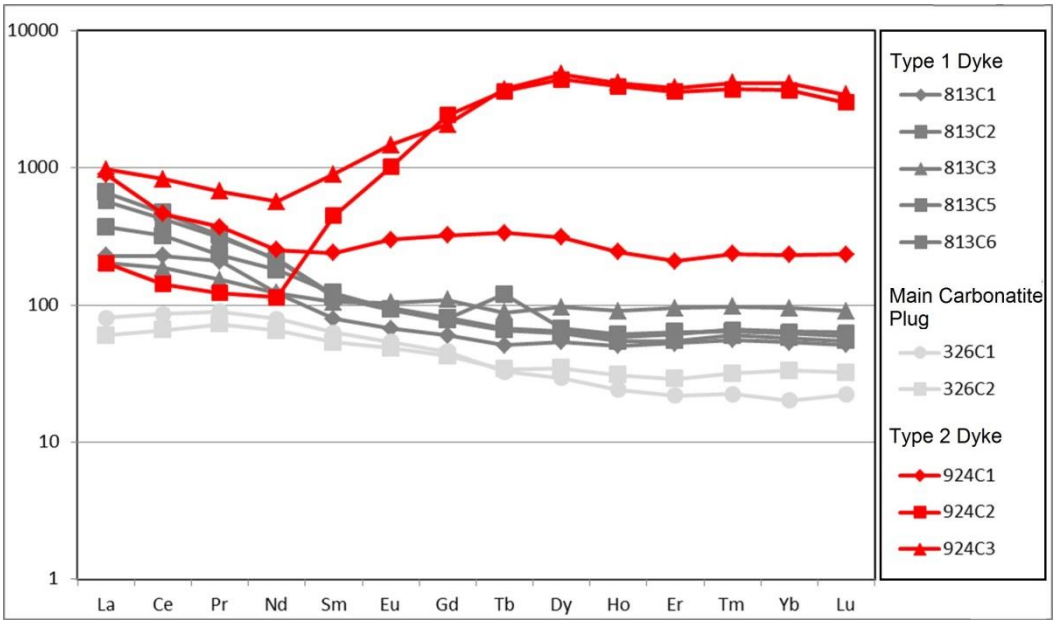

Figure 7.30 LA-ICP-MS analyses **o**f calcite. Note enrichment of REE in altered and xenotime-rich Type 2 dykes.

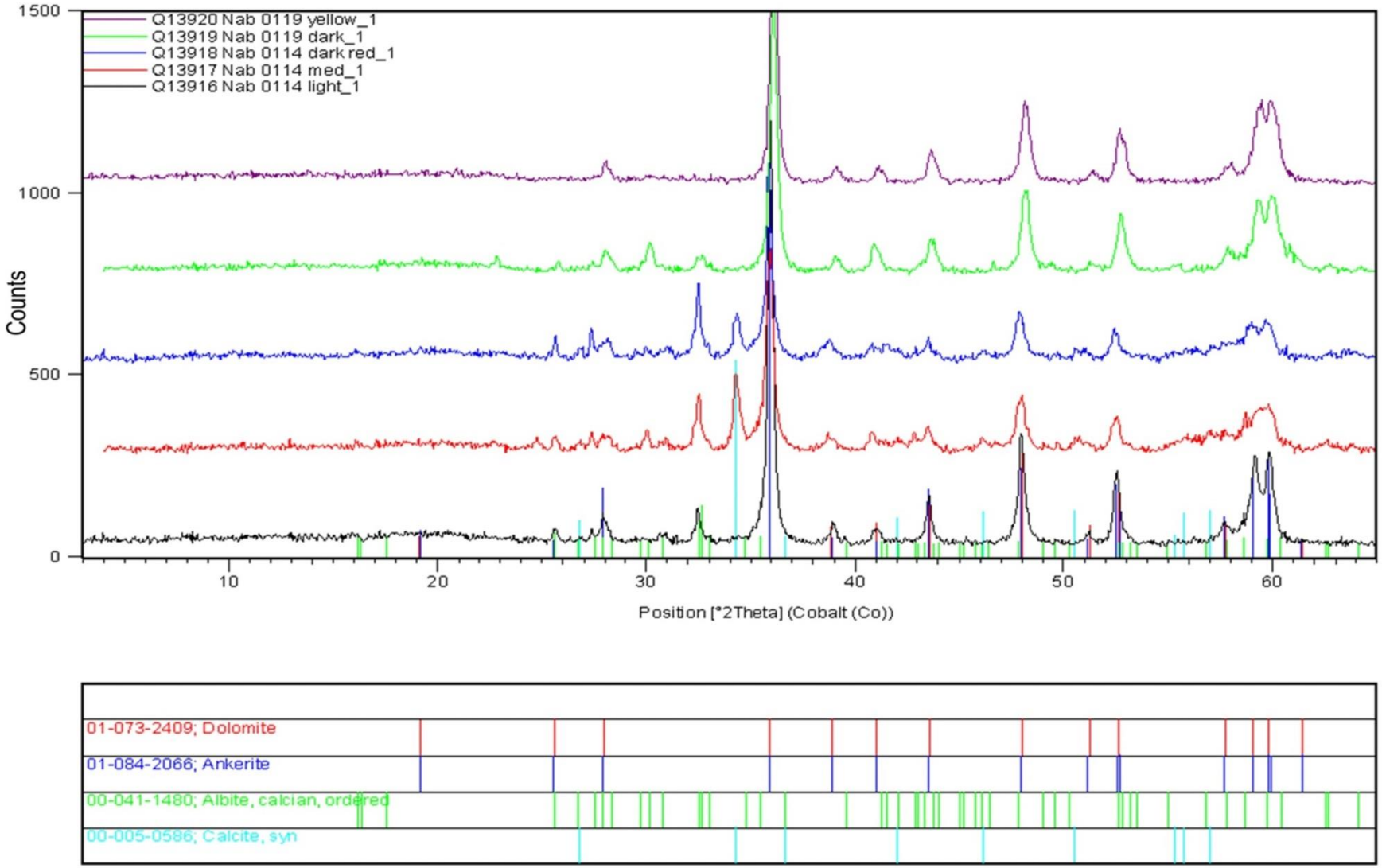

Figure 7.31 X-ray diffraction of dolomite from Lofdal carbonatites.

7.9 Relative distribution of REE in the Lofdal carbonatites, their economic potential and comparison with other carbonatites

The sövite plugs have low REE concentrations in comparison to the dykes, although, there is some iron oxide veining and locally fluorite, indicating that some hydrothermal alteration has occurred in the plugs.

Hydrothermal alteration is evident in the dykes at Lofdal. The majority of REE minerals formed during the hydrothermal / carbothermal stages of carbonatite formation. These minerals include fluorite along fractures, apatite, xenotime-(Y), bastnäesite group of minerals, accompanied by late calcite veining and re-precipitation of Fe oxides (hematite).

High Th, U, Zr and HREE are associated with carbonatites that have high levels of Na_2O (Chapter 6). The main mineral host for Na_2O is albite and this may indicate a subsolidus hydrothermal process of albitisation.

MREE and HREE are mainly found enriched in the mineral xenotime-(Y) in carbonatite dykes. At Lofdal xenotime-(Y) is relatively coarse in some and should be amenable to concentration. In highly altered dykes the xenotime-(Y) grain sizes are rather fine and concentrated in late veins, clearly indicating a hydrothermal origin.

HREE are the most valuable of the REE, thus Lofdal has the potential to become a source of HREE supply.

While xenotime-(Y) is the major HREE host, apatite and fluorite may constitute important HREE-bearing minerals as well. Thus, recovery of fluorite, calcite and apatite might significantly add to the economics of a future Lofdal mine.

Spatially related deposits within 10 km of the Lofdal carbonatite are small mineral deposits. These are mainly tantalite, extracted from pegmatites in the Huab basement, within 3 km from the main carbonatite plug. Most work in the area concentrated on the copper found at Mesopotamie copper valley, a copper deposit that was mined underground until 1970.

At Lofdal copper showings are found within the carbonatite and phonolite dykes as chalcopyrite clusters. Apatite constituting up to 40% of the rock as well as pyrochlore are noted at the contacts between the Main intrusion carbonatites and the syenites.

Like other known carbonatites world-wide, Lofdal is largely a calciocarbonatite with late stage REE mineralisation but limited dolomite-ankerite and ferruginous calcite carbonatite. Substantial REE enrichments are limited to carbonatite dykes at Lofdal.

The most significant aspect of REE distribution at Lofdal is the mix of LREE, MREE and HREE.

The total REE content of Type 1, 3, 4, 5 dykes and the plugs compares with a number of known REE deposits e.g. Mount Weld in Australia, which carries LREE and some of the HREE, Mountain Pass in California which carries LREE but does not have HREE and Hoidas Lake which carries LREE but only a few of the HREE.

At Lofdal the MREE and HREE contents are uniquely high making the deposit exceptionally different and economically important as these commodities are highly priced and occurring rarely in the World.

7.10 Formation of REE minerals in the Lofdal carbonatites

Autometasomatism is marked by albitisation of the carbonatite and in a thin layer of syenite where large crystals of albite are observed.

Apatite and pyrochlore were mostly observed at the contacts of carbonatites and syenites, possibly resulting from the contact metasomatism of carbonatite fluids precipitating on interaction with the syenite country rocks. It is apparent that fluid interaction is bound to pathways in the carbonatite with the example of monazite rich veins and the fracture zones within the carbonatite body where red and yellow patches are observed along fractures in the top-zone of the Main and Emanya carbonatite.

The hydrothermal activity has mineralized alteration lithologies including albitites and fenites by leakage into the country rocks rather than just in the carbonatite dykes, making the country rock potentially prospective for HREE deposit in addition to the carbonatite dykes.

Mineralised country rock exhibits a red brown colour possibly from carbonatite and/or iron oxides, pointing to the involvement of oxidized fluids in the mineralisation of REE at Lofdal.

REE minerals occur mainly in the carbonatite dykes in open spaces filling hydrothermal veins, showing several stages of hydrothermal activities and different generations of veining.

REE-mineralisation in the plugs appears to be limited to metasomatic reaction zones (red, brown, yellow carbonates) which form irregular bodies along fracture zones, e.g. in the Emanya carbonatite plug.

Mineralisation in carbonatite dykes (Type 1, 2, 3, 4, and 5 dykes) is highly variable following sub-parallel zones. Such mineralisation formed probably by variably intense multiple hydrothermal/metasomatic overprint of the primary carbonatite in a solid or

liquid stage by fluids. These metasomatic overprints are either contemporaneous with the main stage carbonatite intrusion in the dykes by an accompanying fluid phase (perhaps resulting in fine grained grey, magnetite-rich carbonatite or they are post-intrusive but in very close temporal relationship with the intrusion (yellow and brown varieties).

The hydrothermal veining stages are associated mainly with calcite carbonatite.

Apatite and fluorite are two important gangue minerals and possible played an important role in the transportation and deposition of the REE at Lofdal. Information on the chemical nature of fluid inclusion in these minerals could give important information about their depositional environment. At Lofdal it is difficult to distinguish between syn- and post-intrusive metasomatism due to successive overprinting of carbonatite by metasomatism. This process makes it quite difficult for exploration approaches, compared to a model of pulses of different magmatic carbonatite intrusions from a possible underlying highly differentiated carbonatite complex.

The amount and type of mineral deposition is controlled by pre-existing fault fissures and the permeability of the earlier carbonatites and the surrounding country rocks. This is best observed in the Emanya carbonatite plug, which is fractured and more mineralised than the homogenous Main Carbonatite plug.

REE minerals commonly develop in the late stage of carbonatite emplacement. This frequently makes it difficult to determine whether the minerals were precipitated directly from the carbonatite magma or from hydrothermal fluid (Wall and Mariano 1996). The fluid appears to relate to the intrusion of the alkaline rocks in the region and most likely to the carbonatites. The fluid originated from the evolution and extended fractional differentiation of the carbonatite and silicate magma forming the hydrothermal fluid phase of the intrusion and precipitated at the late stage. Leaching of the carbonatite indicates a characteristic pattern of most carbonatites.

Minerals that are a product of alteration were probable dissolved by later fluids and no LREE mineral was observed (Fig 7.32), thus the results confirm the fractionation of REE during hydrothermal activities.

REE minerals present include LREE-rich fluorocarbonates (synchysite-(Ce), parisite-(Ce)), monazite-(Ce) and apatite while HREE are mainly enriched in xenotime-(Y).

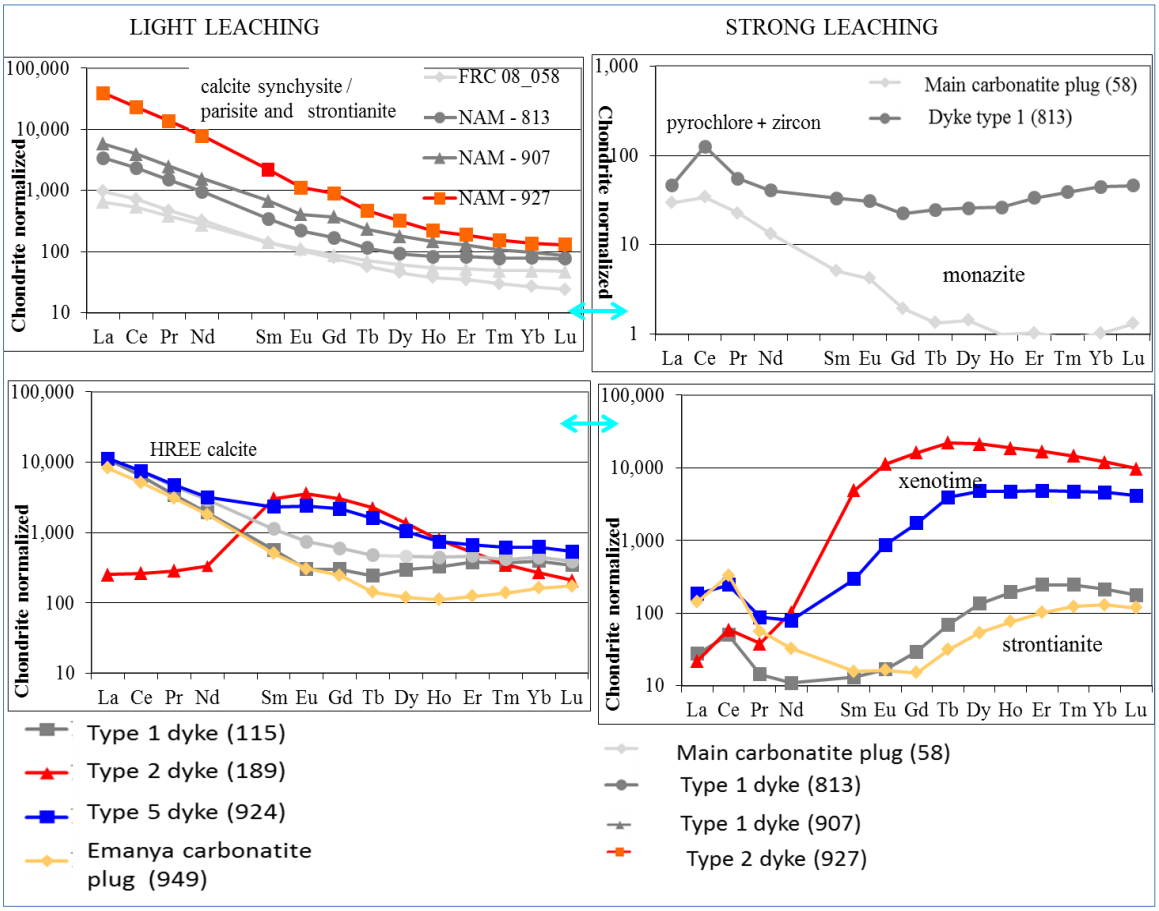

Figure 7.32 Different REE patterns observed after light and strong leaching of the Lofdal carbonatite.

The chemical composition of REE minerals from the Lofdal carbonatites varies with LREE, MREE and HREE-enriched species, forming a deposit with widely variable mineral paragenesis and concentrations. Under these conditions the stability of REE complexes increases with atomic number, leading to greater MREE to HREE solubility in hydrothermal fluids. Late stage alteration of all the earlier paragenetic stages by phosphate-bearing fluids lead to the release of Y into solution. This process was probably controlled by the relative solubility of REE minerals as well as speciation in the hydrothermal fluid. In addition, fractionation of REE during hydrothermal activities can produce an enrichment of mid-atomic number REEs and Y in carbonatites (Mariano, 1989).This hydrothermal fractionation seems to have caused the unusual high HREE/LREE ratios in the Lofdal carbonatites.

7.11 Comparison of whole rock compositions and REE minerals in the Lofdal carbonatites

The whole rock geochemical composition is used to match the rocks from which the minerals have been analysed. The characteristic patterns of the whole rock data in the Lofdal carbonatites relate closely to the observed profiles of the common REE minerals (Figure 7.34). It can be concluded that the observed geochemical pattern in the carbonatites at Lofdal are directly controlled by the relative amounts of each mineral in the carbonatite rock (Figure 7.32 and 7.33).

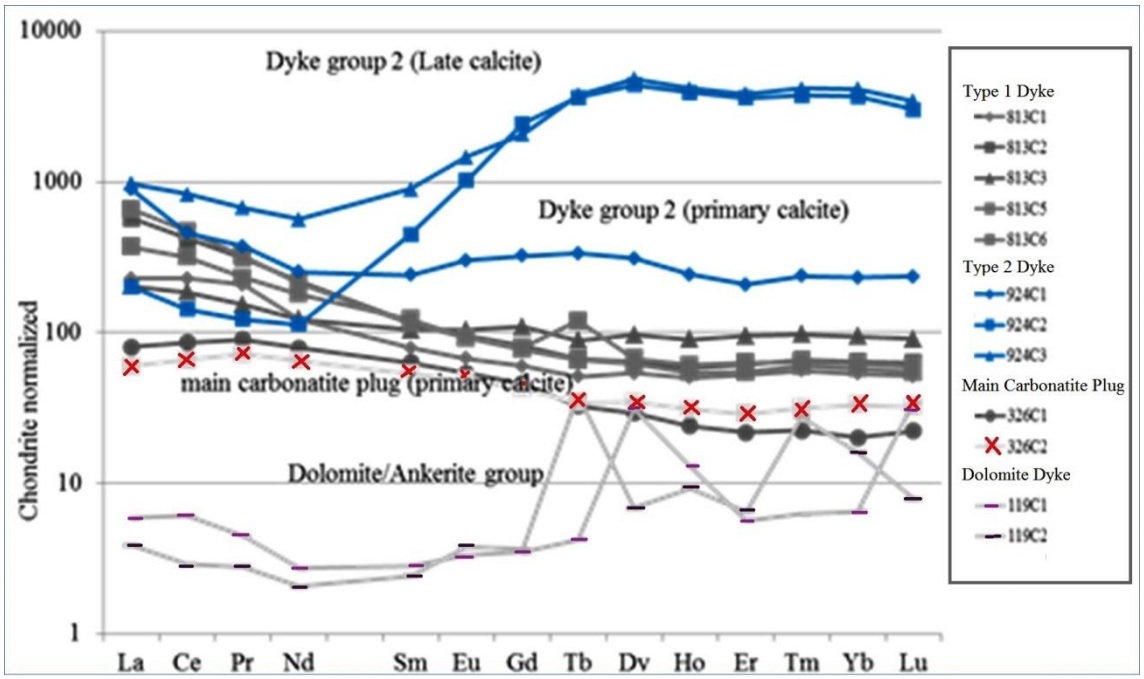

Figure 7.33 REE hosts minerals patterns of the Lofdal carbonatites.

REE occur in the minerals xenotime-(Y), thorite/hutonite, monazite, bastnäesite, parisite, allanite, calcite and apatite. The REO content ranges from tens of ppm up to 12 wt.% total REE.

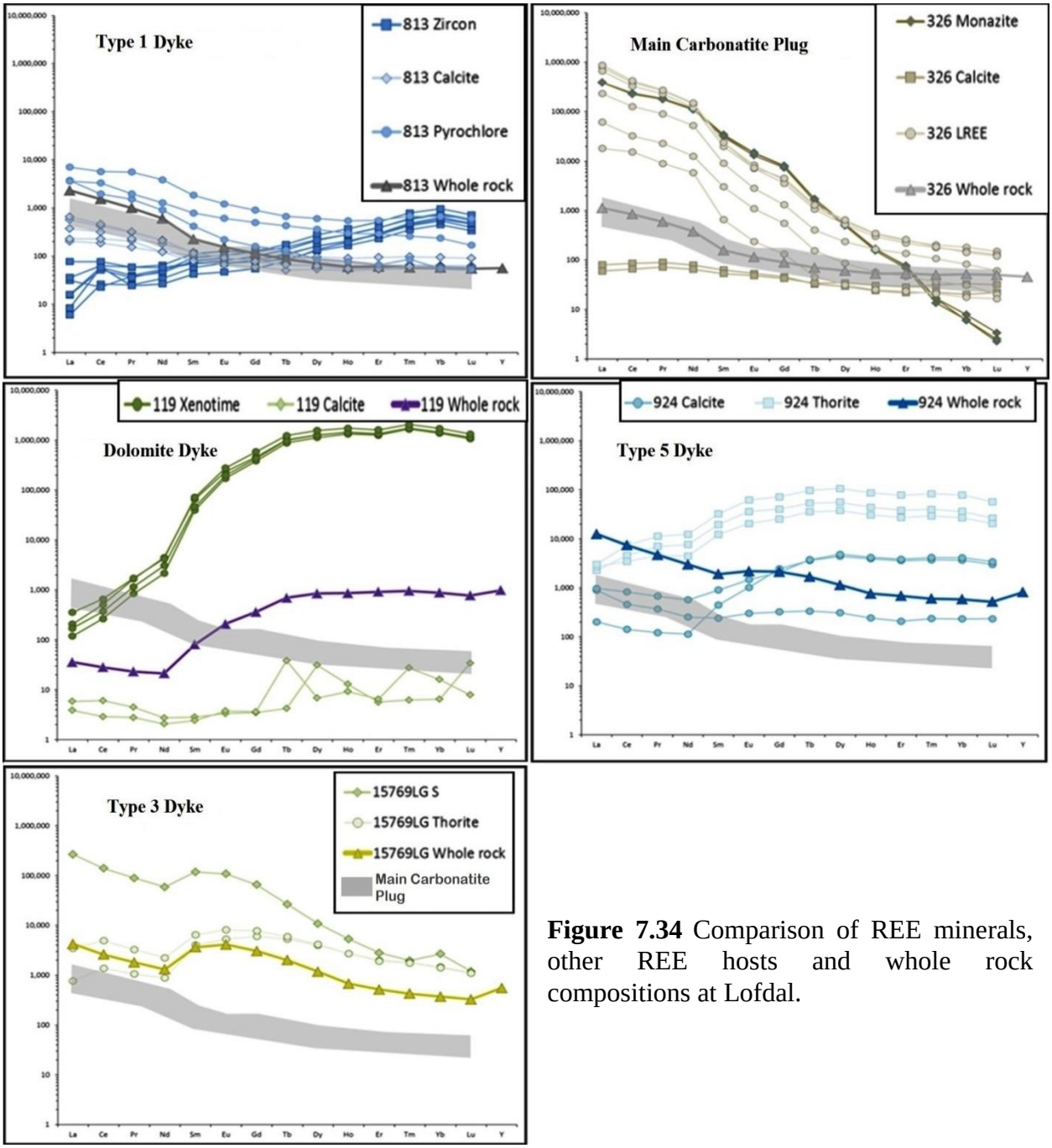

Figure 7.34 Comparison of REE minerals, other REE hosts and whole rock compositions at Lofdal.

7.12 Conclusions

- The various mineral and rock textures suggest only minor formation of HREE-minerals during the magmatic phases but the majority of minerals formed during the hydrothermal / carbothermal stages of mineralisation with the formation of minerals such as fluorite along fractures, apatite, xenotime-(Y), bastnäsite group of minerals, accompanied by late calcite veining and reprecipitation of Fe oxides (hematite). This is consistent with the common mineral paragenesis in carbonatites where LREE (and much more rarely HREE) -enriched minerals form during magmatic and hydrothermal stages.
- Phlogopite is a common mineral in REE- enriched and altered carbonatite rocks at Lofdal. Its presence in these rocks is important for their petrogenesis.
- The Main calciocarbonatite plug of the LACC represents an early magmatic phase with only minor LREE and HREE mineralisation.
- Mineralisation in carbonatite dykes (Type 1, 2, 3, 4, and 5 dykes) is highly variable following sub-parallel zones. Such mineralisation formed probably by variably intense multiple hydrothermal/metasomatic overprint of the primary carbonatite in a solid or liquid stage by fluids. These metasomatic overprints are either contemporaneous with the main stage carbonatite intrusion in the dykes by an accompanying fluid phase (perhaps resulting in fine grained grey, magnetite-rich carbonatite or they are post-intrusive but in very close temporal relationship with the intrusion (yellow and brown varieties).
- HREE-mineralisation is strongly controlled by intensive shearing within the carbonatites dykes and the surrounding fenitised country rocks.
- At Lofdal HREE are mainly hosted in minerals such as xenotime-(Y), thorite, zircon, apatite and fluorite while pyrochlore, parisite-Ce), synchysite-(Ce) and monazite host LREE.
- HREE precipitation partly took place in the fractured albitised country rocks and carbonatite-free shear zones, indicating intensive interaction of an HREE-rich hydrothermal fluid with the country rocks.
- HREE- enrichment increases from the early magmatic to the late hydrothermal stages of mineralisation.
- At contacts between the carbonatite and the syenites metasomatism and autometasomatism is observed reflected in apatite and pyrochlore mineralisation.

- There is a close relation between the albitites, REE and xenotime-(Y) enrichment in all carbonatite types at Lofdal. At Lofdal the MREE and HREE contents are uniquely high making the deposit exceptionally different and economically important as these commodities are highly priced and occurring rarely in the World.

Chapter 8: Stable isotope and geochronology studies of the Lofdal carbonatite rocks

This chapter presents the results of isotopic studies carried out by collaborators in Germany, Hungary and the UK. Stable isotopes of carbon and oxygen were measured to test the possible role of externally-derived fluids in the HREE mineralisation. A number of radiogenic isotope determinations were made to check the geochronology of zircon, xenotime and pyrochlore and to test if the HREE mineralisation has the expected carbonatite mantle source characteristics or shows evidence of the involvement of crustally-derived components, such as hydrothermal fluids.

8.1 Carbon and oxygen isotopes of the Lofdal carbonatites

Carbon and oxygen isotope analyses of 15 samples from the Lofdal carbonatite complex are presented in Table 8.1. The calcite and ankerite mineral samples (Figure 8.1B) were drilled out and analysed depending on their lithological characteristics. The carbon and oxygen isotope analyses have been corrected to VPDB and VSMOW, respectively and are expressed in delta notation. The data are presented for the individual Lofdal carbonatite types using colour codes for the group consistent with previous chapters.

The results exhibit a broad variation in both ^{13}C and ^{18}O (Table. 8.1), displaying distinct isotope trends that are characterized by a moderate rise in $\delta\,^{13}C$ coupled with a sizeable increase in $\delta^{18}O$. The oxygen and carbon isotopic compositions of samples from carbonatite plugs vary only slightly compared to those of the dykes.

The Main carbonatite, which is the least differentiated sövite, has an average $\delta^{13}C$ of -5.13 ± 0.6 ‰ [PDB] and $\delta^{18}O$ ‰ of 8.08 [SMOW]. The oxygen and carbon isotopic compositions of the Main and Emanya calciocarbonatite plugs suggest that these carbonatites are isotopically homogeneous, plotting in the primary carbonatite field as defined by Taylor et al. (1967) with a range in $\delta^{18}O$ of 6.0 to 8.5) and $\delta^{13}C$ of -5.1 to -7.3 characteristic of carbonatite rocks (Figure 8.1).

Table 8.1 Carbon and oxygen isotope data for the Lofdal carbonatite dykes and plugs.

Sample No.	δ18O o/oo (VPDB)	δ18O o/oo (SMOW)	δ13C o/oo (VPDB)
RC08-058 whitish-grey rock	-23.87	6.43	-5.72
115 dark brown rock	-14.01	16.60	-2.86
189 orange rock	-0.11	30.93	0.16
269 dark grey rock	-20.11	10.30	-4.58
326 white rock	-22.82	7.51	-5.08
813 light brown rock	-7.05	23.77	-5.18
907 purple rock	-7.94	22.85	-5.03
914 dark grey rock	-8.52	22.26	-3.99
924 brown rock	-11.69	18.98	-3.66
927 purple rock	-4.89	26.00	-3.07
949 brown rock	-12.91	17.73	-3.11
114 light red ankerite	-19.06	11.27	-3.12
114 dark red ankerite	-4.59	26.18	-3.52
114 medium ankerite	-10.45	20.14	-3.15
119 yellow ankerite	-20.85	9.42	-3.15
119 dark red ankerite	-21.49	8.76	-3.45
188 red-black calcite	-7.27	23.42	-5.49
188 coarse crystal calcite	-7.51	23.17	-7.35
188 dark red calcite	-8.44	22.21	-6.75
15769 dark red calcite	-21.49	8.76	-5.50
15769 yellow calcite	-12.17	18.36	-4.82

The samples from the carbonatite plugs have a narrow $\delta^{18}O$ range and have not been extensively affected by fenitization. The carbonatites from the dykes have a wide range of $\delta^{18}O$, which points to intense hydrothermal overprint and fenitisation. These carbonatites are accompanied by pervasive sodic-fenitization and plot away from the primitive magmatic field.

The carbon isotope variations in Lofdal carbonatites are generally low. Values of $\delta^{13}C$ are highest in the least altered carbonatites. These values decrease with increasing degree of weathering and alteration of the rocks. The averages $\delta^{13}C$ in these types of dykes and plugs range from -5.68 to -1.46 ‰, with the highest $\delta^{13}C$ value of 0.16‰ observed in Type 2 carbonatite dykes. The isotopic variation of both carbon and oxygen is highest in Type 2 dykes, thus exhibiting a noticeable spread away from the primary field, low-temperature hydrothermal and towards the field for carbonate in weathering solutions of meteoric water.

The observation is consistent with the observed high degree of weathering on the outcrop of these carbonatites, giving rise to a deep yellowish brown colour.

The six dolomite carbonatite samples from Lofdal have very similar $\delta^{13}C$ composition ranging from 3.12 to 3.52‰ with an average of 3.28 ‰ whereas; their $\delta^{18}O$ is highly variable with values ranging from 8.76 to 20.14‰ with an average value of 15.15 ‰.

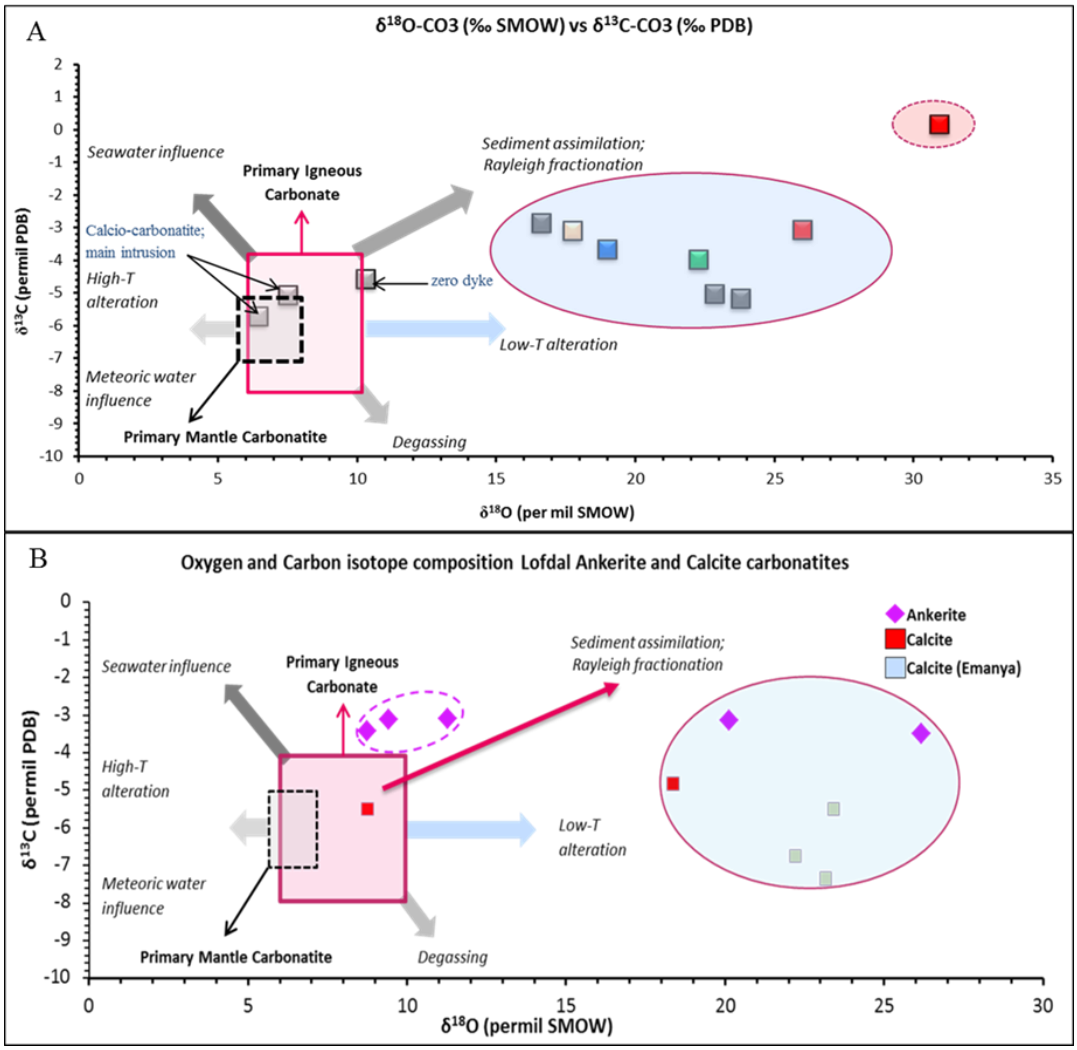

Figure 8.1 Carbon and oxygen isotope compositions in ‰ relative to VPDB and SMOW, expressed in delta notation for a) Lofdal carbonatites rock types (the red squares belong to Type 2 dykes carbonatite. Other dyke types are noted with designated colours in previous chapters b) ankerite is from the dolomite carbonatites. The graph indicates the primary carbonatite field (Taylor et al. 1967) and the field of sediment assimilation and direction of Rayleigh fractionation (after Deines 1989 and Demeny et al. 2004).

Notably, an increase of $\delta^{18}O$ is also observed in the Types 1, 3, 4, and 5 dykes. These dykes plot within the secondary field of Flay and O'Neil (1983), midway between the primary and secondary fields. They are interpreted as related to a late phase of low-temperature hydrothermal activity involving large-scale participation of $\delta^{18}O$-depleted ground waters.

The results of the analyses of calcite and ankerite from Lofdal carbonatites show that the differences in mineralogy correspond to differences in the isotope composition of carbon but not of oxygen (Figure 8.1B). The ankerite samples have a narrow range of carbon isotope compositions and the calcite samples a wider range. It is also interesting that different aliquots of both calcite and ankerite from the same sample can have different oxygen isotope composition. These preliminary results on different phases within individual samples are interesting in terms of defining the origin of these phases.

A range of explanations is typically applied to isotope variations in magmatic carbonates, including heterogeneities in the source, age, tectonic setting, isotopic exchange with isotopically different systems, mineralogy, fractionation between carbonate and a gaseous phase, and truly secondary processes involving meteoric water and wall rock alteration.

Variations in $\delta^{13}C$ and $\delta^{18}O$ in carbonatite complexes may also be attributed to differences in the main characteristics of carbonatites. Stable isotope compositions of type 1 dykes $\delta^{13}C$ (-5.18 ‰V-PDB) and $\delta^{18}O$ (22.92 ‰V-SMOW), plot in the field of "low temperature alteration" (Figure 8.1) after Deines (1989), Demeny et al. (1998) and Demeny et al. (2004). Again carbon and oxygen isotope compositions of Type 2 dyke are consistent with these results with values of $\delta^{13}C$ = -3.66 ‰VPDB and $\delta^{18}O$ =18.14 ‰SMOW and plot in the field of low temperature alteration. These dyke types are located in shear zones and associated with calcite and xenotime-(Y).

Large carbon isotope differences among the samples are interpreted in terms of magmatism, contamination by country rocks, and hydrothermal processes.

This study concludes that although fractional crystallization and liquid immiscibility may affect the oxygen and carbon isotopic composition of the Lofdal carbonatites, it is mainly hydrothermal alteration that affects the oxygen and carbon isotopic composition causing a shift from the magmatic to the hydrothermal meteoric fields. Thus, the variability in $\delta^{13}C$ and $\delta^{18}O$ at Lofdal reflects low temperature hydrothermal alteration.

8.2 Strontium isotopes

Strontium isotope analyses were carried out in the samples representing the Main calciocarbonatite, Types 1 and Type 4 dykes. The initial $^{87}Sr/^{86}Sr$ isotope ratio of the calcite is 0.70274 for the Main calciocarbonatite, which corresponds to a mantle signature (Bell and Blenkinsop 1989).

The initial strontium isotope ratio of calcite is consistent with the stable carbon and oxygen isotope compositions discussed previously, where the $\delta^{13}C$ -5.72 ‰ VPDB and $\delta^{18}O$ 5.58 ‰ SMOW, plot in the "primary carbonatite field" as outlined by Taylor et al. (1967) and Keller and Höefs (1995), thus indicating a magmatic origin.

The initial Sr isotopic ratio of the calcite in Type 1 dyke is 0.70392 which corresponds to a mantle signature. The calcite in Type 2 dykes shows $^{87}Sr/^{86}Sr$ of 0.70804 and thus is much higher than in samples of the Main calciocarbonatite. This suggests a slightly enriched ^{87}Sr source pointing to assimilation of crustal materials possibly during shearing and brecciation of gneissic country rocks in similar fashion as those described by Bell and Blenkinsop (1989).

8.3 In situ U-Pb dating of zircon, xenotime-(Y) and pyrochlore

8.3.1 Pb-U in zircon

Age determinations were carried out on zircon and pyrochlore from Type 1 calciocarbonatite by collaborators at the University of Frankfurt using LA-SF-ICP-MS, see Chapter 4 for analytical details. Twenty one spot analyses on zircon yielded a concordia age of 765.9±5.4 Ma (Figure 8.2, Table 8.2), which is in agreement with the Lofdal zircon age (775 ± 41 Ma) and xenotime-(Y) age (765 ±16 Ma) of Wall et al. (2008).

The age obtained relates in space and time to the anorogenic alkaline magmatism in the region such the Naauwpoort formation rocks, the Oas and Lofdal syenites. There is also a close association in time with the last Damara rifting events at about 700 Ma (Miller 2008), which was accompanied by regional extensional tectonics.

Table 8.2 Xenotime-(Y) and zircon U-Pb LA-ICP-MS results.

				Isotopic ratios and errors †						Ages and errors			
Analysis	Mineral (*)	Beam diameter (µm)	Line length (µm)	$^{207}Pb/^{235}U$	+/- 2σ (%)	$^{206}Pb/^{238}U$	+/- 2σ (%)	$^{207}Pb/^{206}Pb$	+/- 2σ (%)	$^{207}Pb/^{235}U$	+/- 2σ	$^{206}Pb/^{238}U$	+/- 2σ
oc07b08	x	9	17	1.149	9.4	0.122	5.2	0.068	7.1	776.5	72.8	744.4	39
oc07b09	x	9	17	1.013	7.5	0.116	2.3	0.068	4.3	710.2	53.4	710.3	16.2
oc07b10	x	9	17	1.071	9	0.128	3.4	0.061	10.1	739	66.4	776.4	26.3
oc07b11	z	9	17	1.146	8.7	0.128	5.6	0.074	8.5	775.4	67.5	775.4	43.3
oc07b13	x	9	17	1.137	30.3	0.127	7.7	0.072	18.3	771	233.4	771	59
oc07b14	x	18	20	0.995	7	0.115	4	0.07	2.6	701.1	49.2	701.1	28.1

* x - xenotime, z - zircon

† normalised to zircon 91500, bold text have had 207Pb correction applied

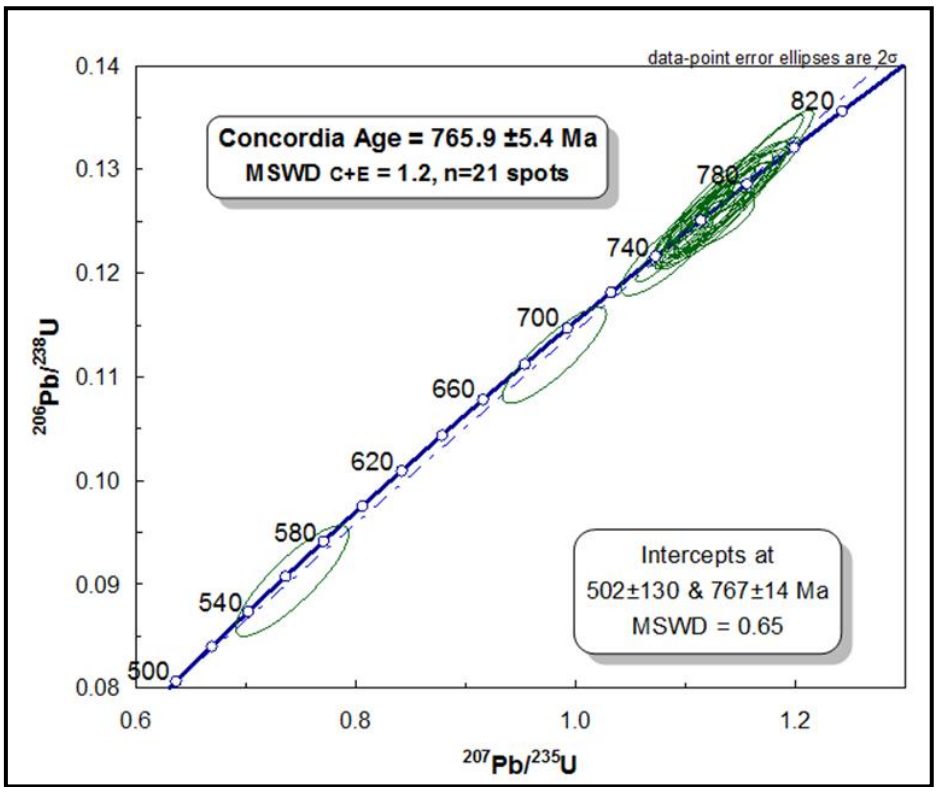

Figure 8.2 LA-ICP-MS Concordia diagram for the zircons from the Lofdal carbonatite

8.3.2 LA-ICP-MS U-Pb dating of xenotime-(Y)

Earlier studies gave a concordant age of 765 ± 16 Ma Wall et. al., (2008) (Figure 8.3). Two xenotime-(Y) analyses plot slightly younger and discordant with a weighted average $^{206}Pb/^{238}U$ age of 713 ± 14 Ma (2σ). A ^{207}Pb correction on these analyses leads to a concordant age of 709 ±9 Ma (2σ), again within error of the uncorrected $^{206}Pb/^{238}U$ age. It is possible that these two analyses have suffered minor Pb loss, resulting in the slightly younger ages.

The age for xenotime-(Y) growth is therefore interpreted as 765 + 16 Ma, reflecting the bulk of the xenotime-(Y) analyses (Wall et al. 2008). The calculated age for xenotime-(Y) crystallisation is consistent with the 764+/- 60 Ma determined for the Lofdal nepheline syenite (Hawkesworth et al. 1983).

The ages obtained using xenotime-(Y) tie the production of the xenotime-(Y) to the main carbonatite-forming event rather than any later Damara metamorphism or hydrothermal activity, clearly distinguishing the Lofdal carbonatites from the ca. 135 Ma continental rifting magmatism that constitutes most of the alkaline and carbonatite complexes in this region of Namibia (Milner et al. 1995), such as Okorusu, Kalkfeld, etc.

It suggests that the xenotime-(Y)-bearing dykes might be compared with Neoproterozoic carbonatitic activity elsewhere, such as monazite-bearing dykes at Eureka (Burger et al. 1965, Dunai et al. 1989).

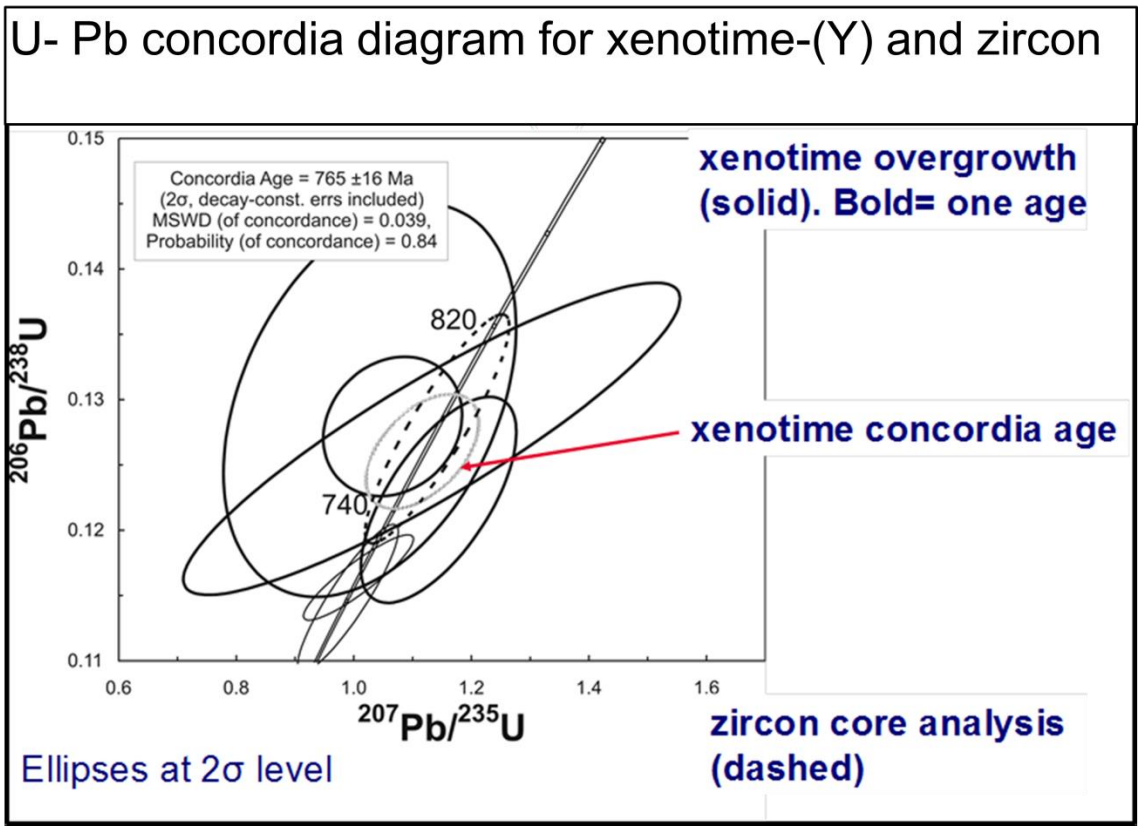

Figure 8.3 Plot of U-Pb xenotime-(Y) data for the carbonatites Wall et. al, (2008)

8.3.3 Pb U- isotopes in pyrochlore

A few analyses of pyrochlore show similar ages to that of zircon but most spots yielded ages in the range between 600 and 480 Ma. Interestingly, the histogram diagram and probability plots (Figure8.4) show multiple different peaks yielding an older age of 780±74 Ma and a younger age of 496±36 Ma. The multiple peaks possibly indicate phases of recrystallisation, which changed (re-started) the U-Pb-system. This observation is interpreted as an indication of disturbances of the U-Pb system of pyrochlore, probably by Pb-loss, during a later alteration event. This conclusion is consistent with the known crystal chemical behaviour of pyrochlore in which sub-solidus alteration and cation exchange is common. Lumpkin (1992) experimented that Pb decreased in some samples while the divalent cations Ca, Mn, and Fe increased during alteration. He also concluded that the U-Pb systematics indicated that radiation-induced micro-fracturing plays an important role in controlling the long-term loss of radiogenic Pb in microlite.

The most likely explanation for the variable pyrochlore ages is a result of a range of pyrochlore closing temperatures during the late deformation phases that resulted in multiphase recrystallisation at about 600 to 480 Ma. These ages can be related to regional geological events (Fig 8.5) around Lofdal. The pronounced recrystallisation phase is at around 565 Ma, coinciding with the peak metamorphism of the Damara Orogen, mainly, the Kaoko and the Damara Belts.

The period coincides also with the syenitic, dioritic magmatism and metamorphism in the central zone of the Damara Belt. Other major age phases in the order of peak magnitudes are those at 525, 482, 600 and 648 Ma. These ages can be correlated with different cooling and metamorphism stages recorded at different regions of the branches of the Damara belt.

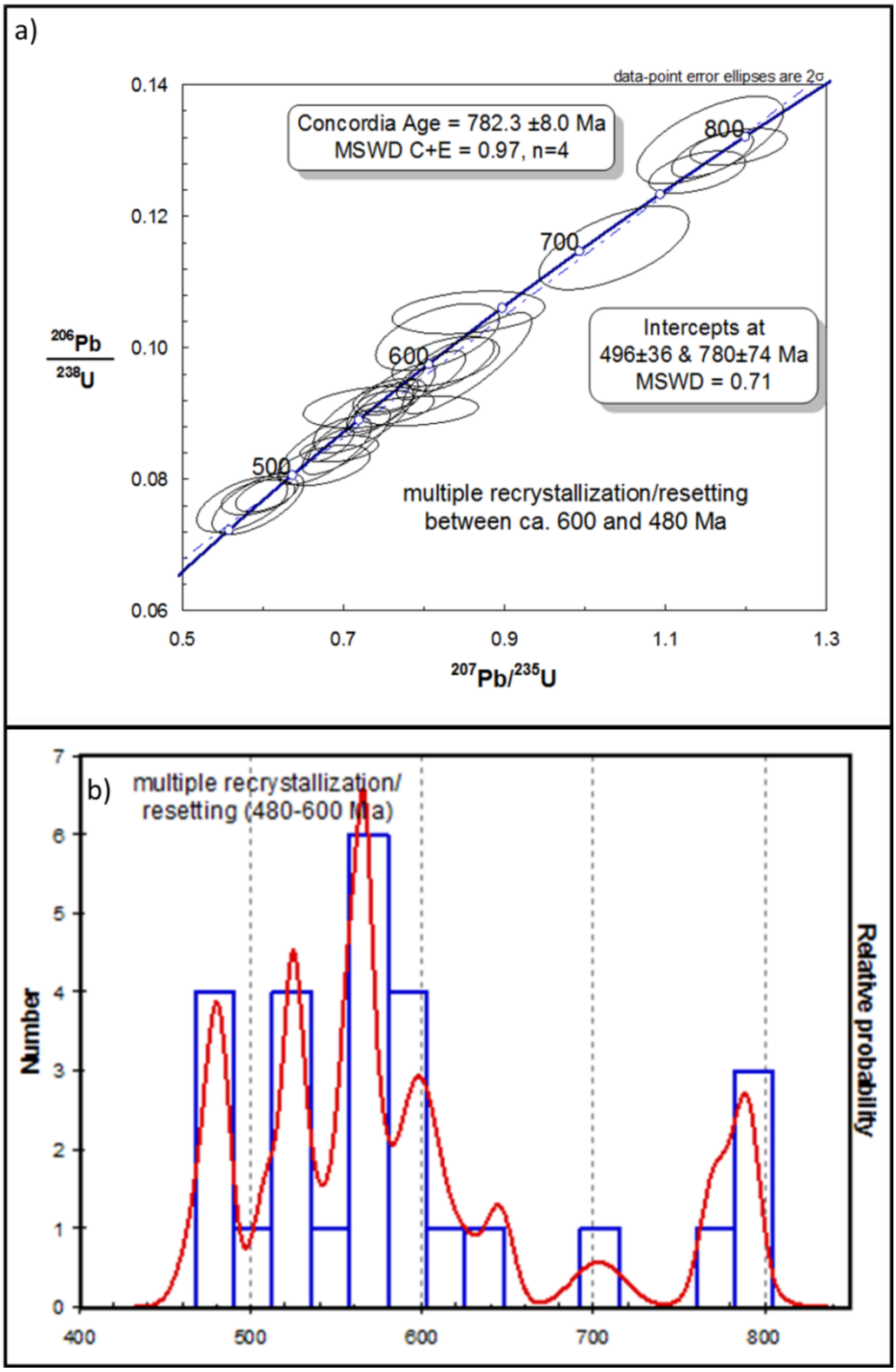

Figure 8.4 a) Concordia diagram for pyrochlore b) Histogram showing the distribution of ages recorded in pyrochlore

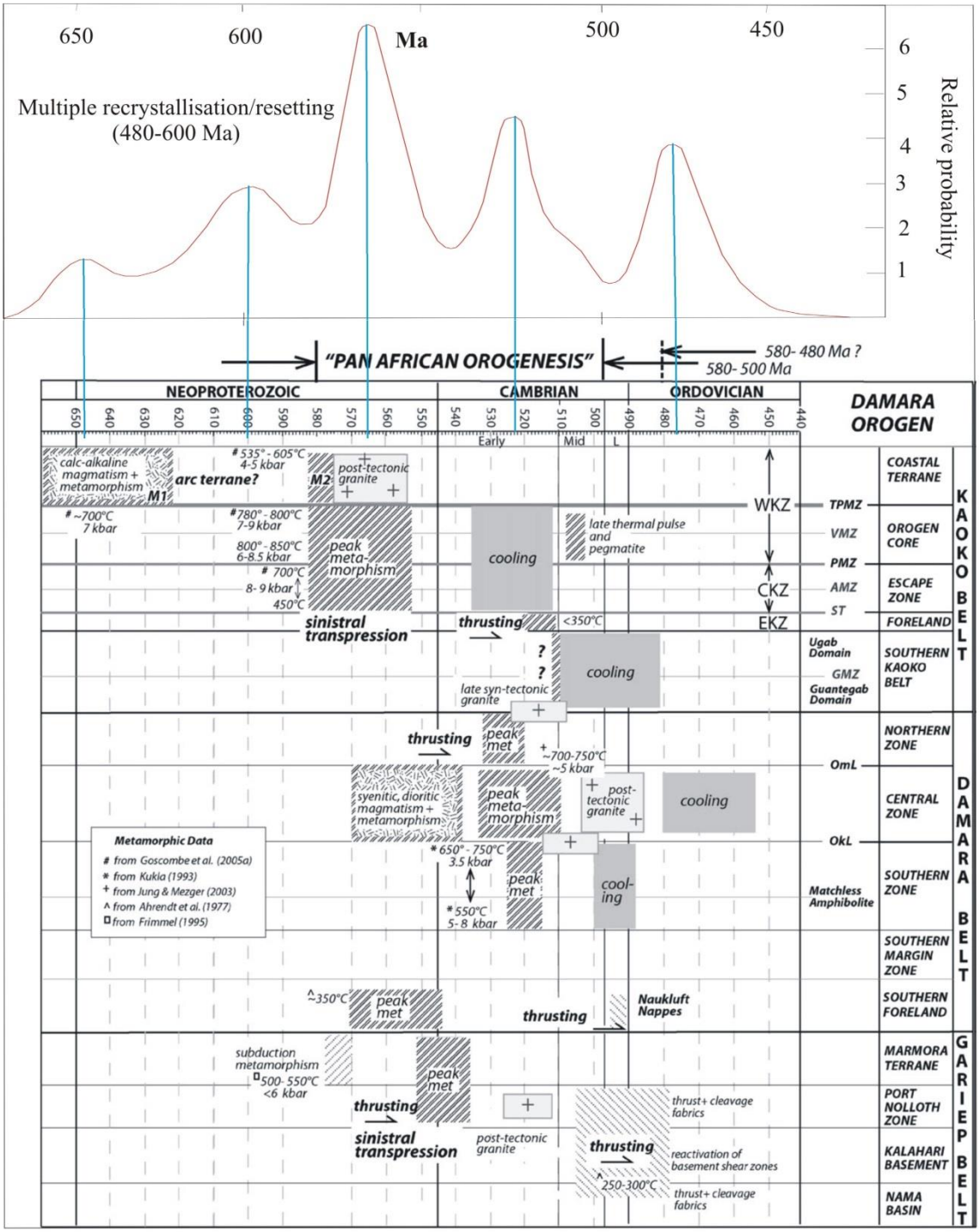

Figure 8.5 Damara Orogen main deformation events after Goscombe (2004) compared with multiple recrystallisation ages recorded in Lofdal pyrochlore.

8.4 K-Ar dating of the silicate rocks associated with carbonatites at Lofdal

K-Ar data record ages ranging from 699 ± 21Ma to 426 ±12.8 Ma (Table 8.3). Although field observation indicates that silicate intrusive rocks are older than the carbonatites, the obtained ages are younger than those of the carbonatite. These ages are consistent with deformation phases of the Pan African Orogenesis, thus these ages possibly represent the syn- and post-tectonic events in the region after the emplacement of the igneous rocks.

Table 8.3 K-Ar of the silicate rocks associated with carbonatites at Lofdal

No. of K-Ar	sample No.	Dated fraction	K (%) 1	K (%) 2	K (%) mean	40 Ar rad (%)	40 Ar rad (ccSTP/g) *10-4	K-Ar age (Ma)
6428	VNP 28	Whole rock	4.93	4.84	4.88	96.9	0.9117	426.1±12.8
6429	VNP 31	Whole rock	4.61	4.49	4.55	97.8	1.5101	699.0±21.0
6430	VNP 36	Whole rock	4.25	4.18	4.22	98.2	1.1953	612.0±18.3
6431	VNP 58	Whole rock	7.77	7.60	7.69	97.8	1.8764	538.6±16.1
		Biotite	6.41	6.39	6.40	93.6	1.5034	521.2±15.7
6432	VNP 80	Whole rock	6.14	6.02	6.08	97.7	1.2861	475.6±14.3
6433	VNP 91	Whole rock	4.08	4.00	4.04	97.3	1.2086	640.9+/-19.2

8.5 Leach Sm-Nd and residue isochrons

Sm-Nd analyses were carried out on leached fractions of sample of Lofdal carbonatites (see Chapter 4 for method details). The "easily resorbed fraction" ε–Nd values are relatively homogeneous compared to initial $^{87}Sr/^{86}Sr$ isotope ratios (0, 0274 – 0, 71165). The residue fraction ε –Nd values (for 760 Ma age) vary significantly, arguing that the Sm-Nd isotope system was disturbed by alteration processes (Table 8.4).

The calculations for the individual samples are as follows in Table 8.4 and Figures 8.6 and 8.7).

Table 8.4 Calculated ages of the leaches and residues of the Lofdal carbonatite.

Sample	**Calculated age (Ma)**	**Initial $^{143}Nd/^{144}Nd$**
Nam-115	No variation in $^{147}Sm/^{144}Nd$	
Nam-189	673±8	0.51275±0.00013
Nam-269	395±87	0.51191±0.00005
Nam-813	420±58	0.51194±0.00005
Nam-924	643±11	0.51185±0.00002
Nam-949	495±130	0.51185±0.00006

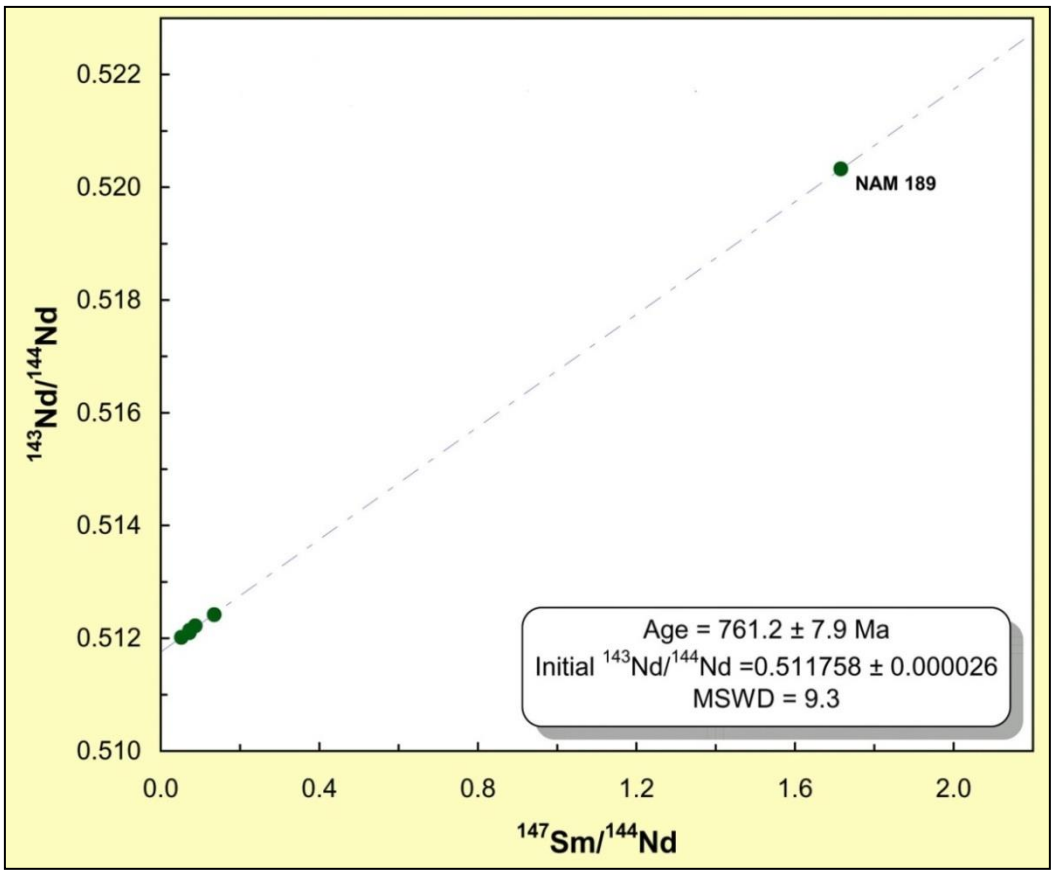

Figure 8.6 $^{143}Nd/^{144}Nd$ vs $^{147}Sm/^{144}Nd$ data for Lofdal carbonatites. Note that altered sample 189 Type 2 dyke shows very high values.

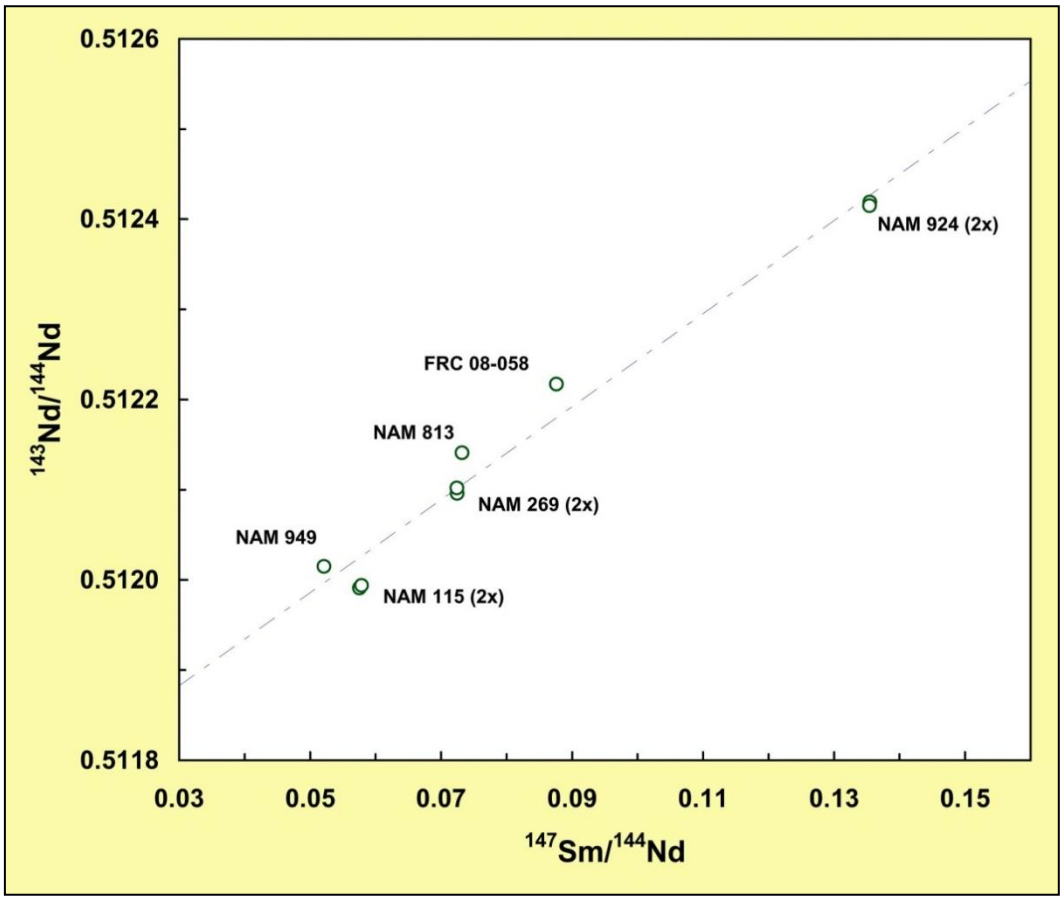

Figure 8.7 $^{143}Nd/^{144}Nd$ vs $^{147}Sm/^{144}Nd$ data for Lofdal carbonatites. Note that altered sample 189 Type 2 dyke with very high values age is removed.

Internal isochron calculations for easily resorbed fractions and residue fractions within sample 189 of Type 2 dyke demonstrate disperse ages between 680 Ma and 310 Ma. Calculated errors for the isochron ages vary significantly (from 8 to 130 Ma) and depend on relative difference in $^{147}Sm/^{144}Nd$ ratios (Figs 8.6 and 8.7). The results show that the carbonatites underwent some alteration, which re-set their Sm-Nd and Rb-Sr isotope systems, similar to information recorded from pyrochlore and K-Ar dating.

A study by Jung et al. (2008) indicated that the nepheline-normative samples from Lofdal, the unradiogenic Sr and radiogenic Nd isotope composition and low $\delta^{18}O$ values suggest derivation of these samples from a moderately depleted lithospheric upper mantle with crustal-like U/Pb ratios ($^{87}Sr/^{86}Sr$: 0.7031–0.7035, εNd: ca. +1, $\delta^{18}O$: 7‰, $^{206}Pb/^{204}Pb$: ca.18.00, $^{207}Pb/^{204}Pb$: 15.58–15.60).

8.6 Conclusions

- Lofdal carbonatite $\delta^{13}C$ and $\delta^{18}O$ values exhibit a broad variation characterized by a moderate rise in $\delta^{13}C$ coupled with a sizeable increase in $\delta^{18}O$.
- The oxygen and carbon isotopic compositions of samples from the Main calciocarbonatite plug are relatively homogeneous compared to those of the dykes and plot in the range of values expected for mantle-derived calcite carbonatite.
- Low temperature hydrothermal alteration significantly affected the oxygen, and to a lesser extent the carbon isotopic composition of Lofdal carbonatite dykes.
- The initial Sr isotopic ratio of the calcite in Type 1 dyke corresponds to a mantle signature, while the calcite in Type 2 dykes suggests a highly enriched mantle source or more likely incorporation of a crustal signature as a result of shearing into the Sr structure.
- The xenotime-(Y) at Lofdal is the same age as the main carbonatite (765 ± 16 Ma).
- Zircon yielded a concordia age of 765.9 ± 5.4 Ma which is in agreement with the Lofdal zircon (775+/ 41 Ma) and xenotime-(Y) age (765 ±16 Ma).
- The pyrochlore dating indicates that the carbonatites were affected by regional geological events related to Pan African Orogenesis between 900 and 400 Ma.
- K –Ar dating also recorded the deformation events of the Damaran Orogen.
- The Sm-Nd isochron indicates that the Sm-Nd isotope system was disturbed by alteration processes.
- The ages obtained show that the Lofdal complex is part of intense magmatic activity and initial rifting stages in the Kaoko and Damara belts (730-770 Ma) and altered by the Early Pan-African orogeny responsible for the Damara Orogen (±650 Ma).

Chapter 9: Discussion and interpretation of the evolution and formation of the Lofdal HREE-enriched carbonatites

This chapter brings together the results and interpretations from each previous chapter, plus information from the literature and comparison with other localities, to give an overall view of the formation and evolution of the HREE-enriched Lofdal carbonatites.

9.1 Structural and tectonic evolution

The Lofdal Alkaline Carbonatite Complex REE deposit occurs in an intracontinental extensional setting formed by pull-apart tectonics. The sequence of structural and evolution of events can be summarised as follows:

- The Damara orogen commenced about 900 Ma and culminated at about 400 Ma.
- At about 780 Ma the region around Lofdal underwent regional rifting and a transition period from rifting to spreading plus extension (Miller 2008). The structural setting of Lofdal can be related to the consequences of this event, considering its age of 765 Ma (Wall et al. 2008). Structural mapping indicates that thrusting and faulting was developed in response to the strain developed during the extension regime.
- Further rifting of the cratonic basement at about 770-750 Ma, may well have led to the ascent of silicate and carbonatite magmas, which form the LACC. These rocks intruded into the Huab Metamorphic Complex, which had been variably metamorphosed at amphibolite grade and deformed before the intrusion of Fransfontein Granite Suite much earlier, at 1.8 Ga. However, there are other alkaline igneous rocks that have similar dates to LACC and are therefore likely to be related to the same geodynamic event. These are the Naauwpoort volcanics (Miller 2008) and the Oas syenites and quartz porphyries (Table 9.1).

Table 9.1 Summary of published ages for Lofdal syenites and carbonatites, Oas syenites and rhyolites of the Naauwpoort Formation

Intrusion	Age	Technique	Reference
Lofdal nepheline-normative syenite	764±60 Ma	Rb–Sr whole rock	Hawkesworth et al. 1983
Oas quartz-normative syenite	840±13 and 652±11 Ma	Rb–Sr whole rock	Hawkesworth et al. 1983
Oas quartz normative syenite	783 +133/-141	U-Pb zircon	Tegtmeyer and Kröner, 1985
Alkali rhyolite (Naauwpoort Formation)	728 ± 40 and 750 ± 65	U-Pb zircon	Miller and Burger, 1983
Oas quartz normative syenite	756 ± 2 Ma	U-Pb zircon	Hoffman et al. 1996
Oas quartz porphyries	752 ± 7 Ma	U-Pb zircon	De Kock et al. 2000
Lofdal syenites	715 ± 9 to 751 ± 4 Ma	U-Pb titanite	Jung et al. 2007
Lofdal nepheline syenites	754 ± 8 Ma	U-Pb titanite	Jung et al. 2007
Oas syenites	737 ± 5 to 758 ± 7 Ma	U-Pb titanite	Jung et al. 2007
Oas quartz syenites	758 ± 4 Ma	U-Pb titanite	Jung et al. 2007
Lofdal carbonatite dyke	765 ± 16 Ma	U-Pb xenotime	Wall et al. 2008
Lofdal carbonatite dyke	765.9 ± 5.4 Ma	U-Pb zircon	this thesis
Lofdal carbonatite dyke	761.2 ± 7.9 Ma	Sm-Nd mineral concentrates	this thesis

- The fault systems that bound the LACC have been (re-)activated subsequent to the emplacement of the LACC. There is evidence that these events have affected the LACC, e.g. the multiphase recrystallization recorded by pyrochlore geochronology that gives dates between 600 and 480 Ma. Regionally these ages are coincident with subsequent crustal convergence between Congo and Kalahari Craton from 600-580 Ma to the final collision at 550-540 Ma (Miller 2008).

  The ages also spatially and temporally relate to episodic high-temperature metamorphic events and granitic intrusions that followed in the northern and central part of the Damara Belt and the youngest pan-African metamorphic

rocks which are dated at 465 Ma. The final uplift of the central parts of the orogen is said to have taken place from 470 - 465 Ma (Miller 1983).

The LACC occurs in a rift-related continental province, similar to other carbonatite occurrences, that are also associated with volcanic sequences and dykes that can differentiate into phonolite and carbonatite melts (Mitchell and Jambor 1996). The LACC is interpreted to fit to the rift-related continental provinces as supported by the regional geological settings, the ages and the geochemical composition set by Samoilov (1984). Based on the ratio of Ba/Nb versus Zn/Pb, most samples from Lofdal carbonatites plotted though in the field of formation of near fault carbonatites and alkali metasomatites. The rare elements of near fault carbonatites are said to be specifically rich in Nb and depleted in Ba. They also have the highest average values Sr/Ba and Nb/Ba (Samoilov 1984).

The Neoproterozoic age of the LACC and therefore its relationship to the Damara origin sets it apart from the better known ca. 130 Ma Cretaceous alkaline and carbonatite intrusive centres in Damaraland, the formation of which was related to the Gondwana break up and the opening of the now South Atlantic Ocean (Chapter 3; Marsh 1972, Pirajno 2004a). There are however, a significant number of Damaran-related alkaline and carbonatite complexes in Namibia (Chapter 3) and these deserve further research to determine how they might be related.

9.2 Emplacement and origin of the Lofdal alkaline and carbonatite complex

The mode of emplacement of the LACC is interpreted based on field observations complemented by mineral textures and geochemistry. It was associated with regional fracturing of the metamorphic basement rocks, mainly along NNE/SSW to NE/SW structures, which indicate local reactivation of older basement structures. A suite of granite, phonolite, carbonatite dykes and later hydrothermal fluids were emplaced in these fractures. The emplacement is considered to be facilitated by the thinning of the continental lithosphere observed by the existence of formation of grabens and crustal faulting systems.

These processes enabled decompressional melting of the mantle and emplacement of a wide spectrum of the alkaline magmas that form the LACC and other local complexes. Minor faulting accompanied the major strike faulting, possibly during the extensional and compressional tectonics, to produce the pattern of faults shown today by the dyke swarm (Figure 9.2 a,b). The most abundant and longest faults traverse in a NE-SW shear zone over a strike length of 30km. smaller faults crosscut these in N-S directions.

The structures developed and the fracture systems were activated episodically over a large period of time giving rise to different rock types at different times and hydrothermal activities as observed by the diverse compositions of the rocks, minerals and the multiple deformation activities recorded in the area. The faults were intruded by earlier granite, phonolite syenites, possibly mafic (lamprophyre) dykes, plus the syenite and carbonatite plugs (Figure 9.2 c and e). None of the mafic or other alkaline rocks cut the carbonatites, indicating that carbonatites are the youngest intrusive rocks of the LACC. Regionally, there are prominent shear zones at or near the footwall, which are variably albitised and carbonatised. The shear zones range from centimeters to as much as several meters wide and the shear fabrics are cut by both albitite and carbonatite suggesting that they represent structures that pre-date the intrusion. There is a main footwall shear zone developed locally, which may be the controlling structure for much of the alteration and mineralisation (Figure 9.2 d). Syenitic and carbonatite magmas intruded into the hinge zone of the pull-apart basin. Extensional step over and a releasing bend along a strike slip fault zone as seen at Lofdal is a feature commonly localised in the shallow crust (Dooley and McClay 1998). The geological succession of these intrusions is indicated in Table 9.2.

Table 9.2 Summary of the geological succession and rock types in the LACC and at Oas

No.	Rock type	Comments
6	lamprophyre	One 20 cm dyke
5	carbonatite plugs and dykes	calcite carbonatite, ferroan calcite carbonatite
4	polylithic breccias	Lithic fragments of syenite, amphibolites, gneisses from the local area
3	Oas and Lofdal syenite, nepheline-syenite plugs	
2	Lofdal phonolite dykes	
1	granitic pegmatite dykes	

The intrusion of the LACC was accompanied by significant brecciation and alteration, mainly the intrusion of the carbonatite dykes. The alteration associated to these intrusions extended to preexisting silicate intrusive and the adjacent metamorphic wall rocks, producing sometimes wide zones of variable carbonatite and silicate alterations accompanied by carbonatised, altered rocks and breccia.

The level of erosion at Lofdal has exposed the top of the carbonatite pipes of Main and Emanya intrusions and hundreds of phonolite and carbonatite dykes. The intrusive centre for the system seems to be in the area of the Main intrusion, which is exposed over an area of about 2 km x 0.8 km. The complex has a general ENE trend and most carbonatite and related intrusions are considered to be preserved underneath cover, extending for at least 2 km to the SSW. The complex overall length is 6.5 km, as indicated by the radiometric and gravimetric data **(**Figure 9.1). The observed undercover structure is potential prospect for undiscovered carbonatite plug with HREE enrichment.

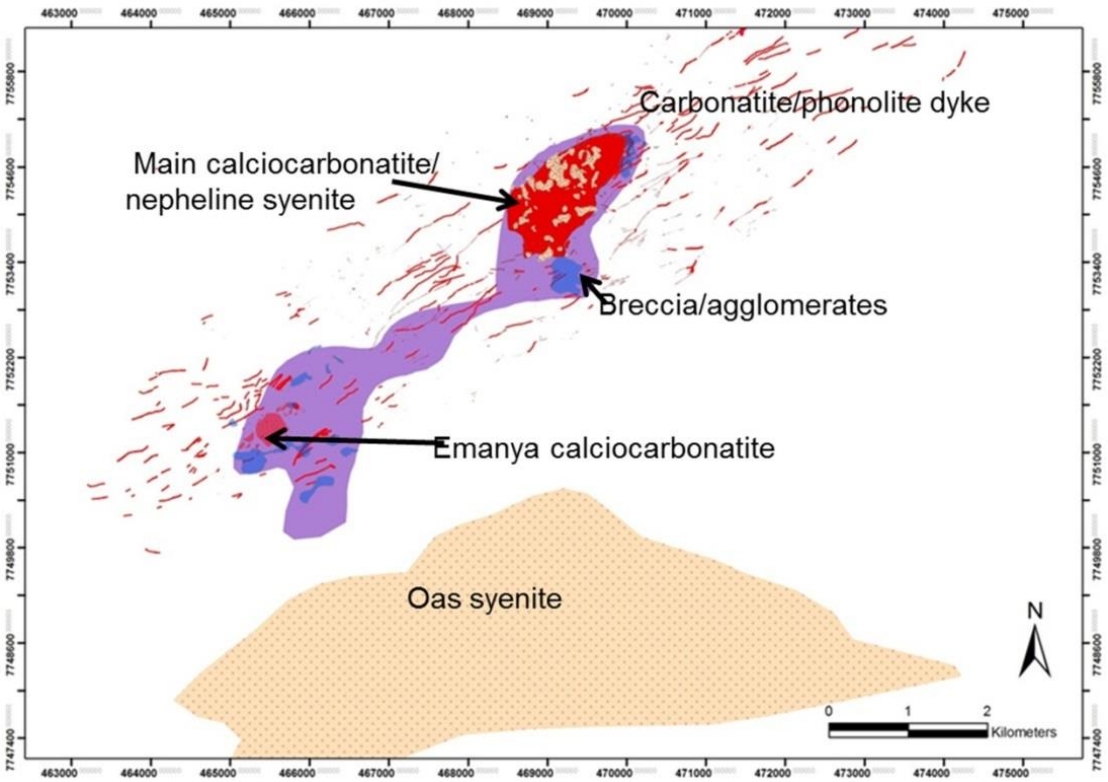

Figure 9.1 Possible sub-surface extension of the Lofdal alkaline carbonatite complex. The purple colour indicates the geophysical anomalies and/or alteration zone related to the intrusion. The structural and evolution of events is illustrated below:

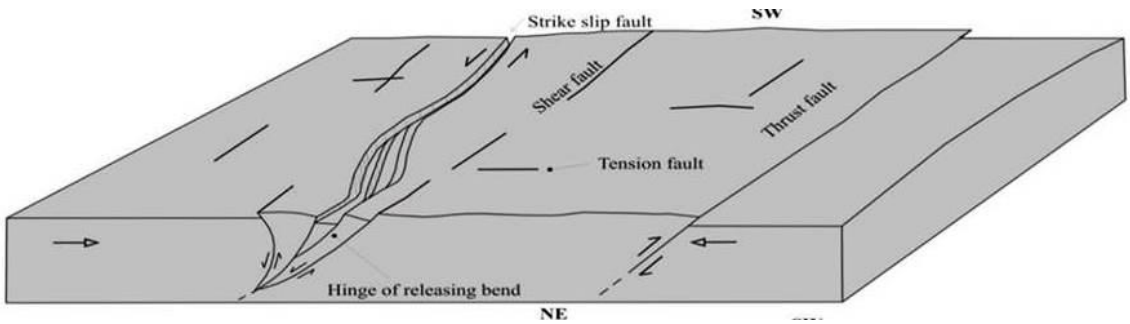

Figure 9.2 a) Schematic illustrations of thrusting and faulting developed in s to the strain developed during the rifting and extensional regime.

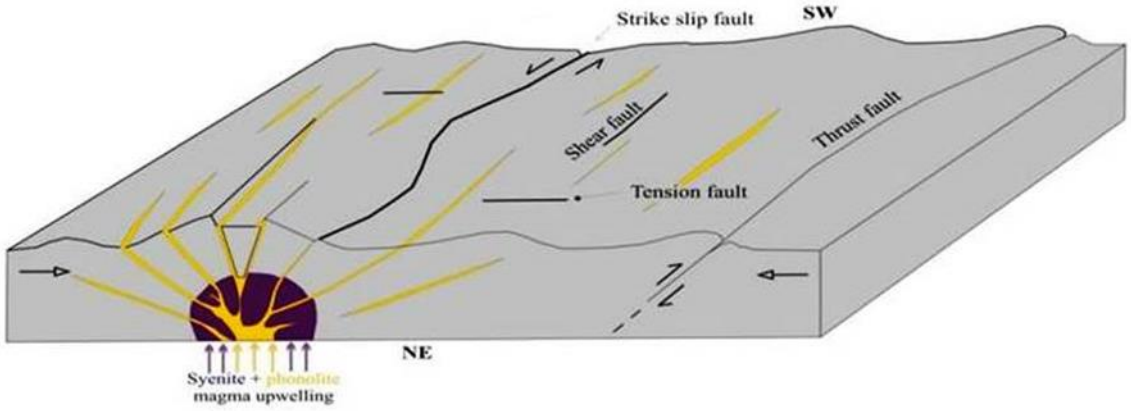

Figure 9.2 b) Syenite and phonolite intrusion along regional fracture systems. Carbonatites plugs and dykes intrude accompanied by hydrothermal fluids utilising the same conduits of dilation fracture systems.

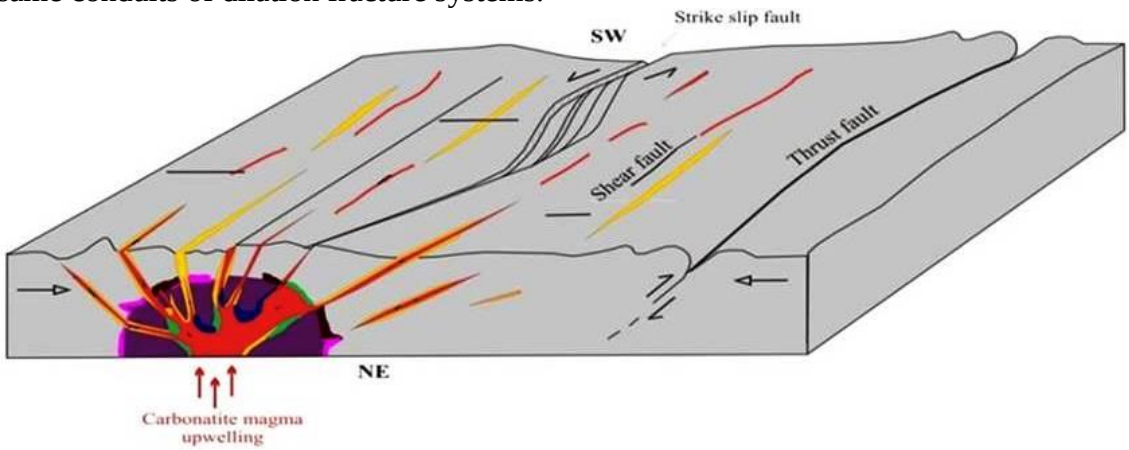

Figure 9.2 c) release bend and or stepover feature formed along the sinistral strike slip zone, producing a duplex structure, allowing alkaline and carbonatite magmas passage through the two echelons left lateral strike slip fault into country rock.

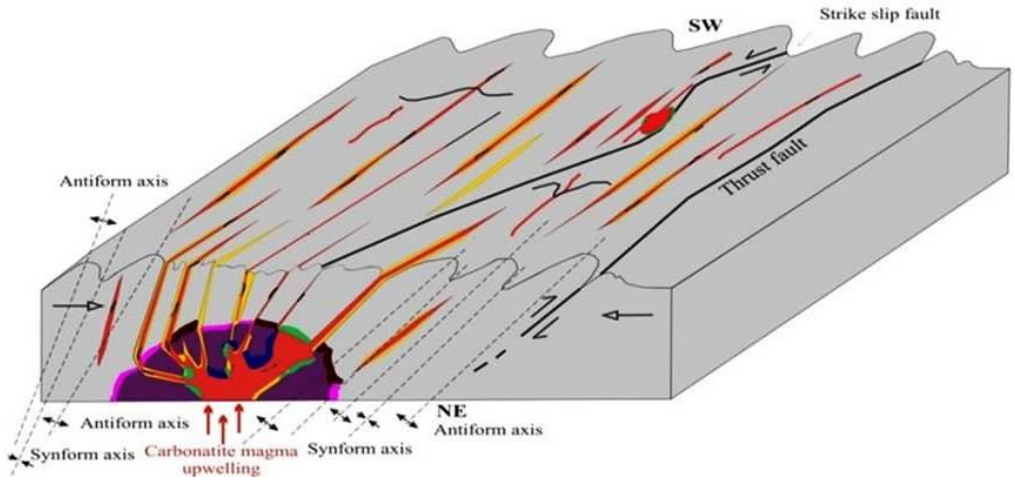

Figure 9.2 d) Syenites and carbonatites magma intruded into the hinge zone of the pull-apart basin.

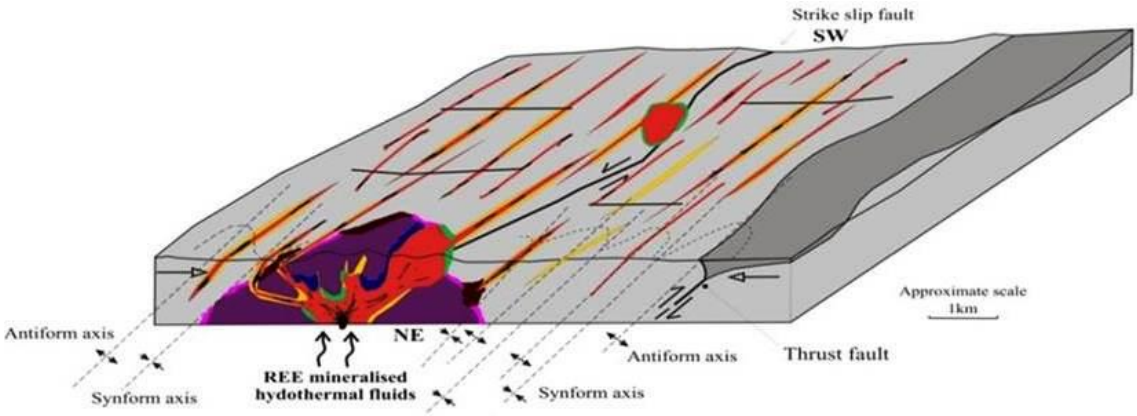

Figure 9.2 e) The carbonatite dykes are later REE mineralised with by hydrothermal fluids– presumably carbonatite-derived.

The shallow emplacement of the LACC is in line with the nepheline syenite- carbonatite complexes that are generally considered components of relatively shallow complexes of subvolcanic origin (Figure 9.3) Woolley and Kjarsgaard (2008). The intrusive nature of the LACC with regard to the absence of mantle xenoliths, variability of rock types and the geochemical composition possibly indicate their origin by high level differentiation (Figure 9.3). However, the presence of mafic and ultramafic rocks, especially the lamprophyre, associated with LACC intrusions indicates that some may have come from a deeper mantle source of the magma. Phlogopite, the presence of which at Lofdal may be indicative of K-bearing magma, is known from many metasomatised mantle assemblages (e.g. Johnson et al. 1997; Lloyd et al. 2002) and is considered the most likely K-bearing phase in the melting assemblage because of its potential to produce silica-undersaturated melts with high K/Na ratios Brady and Moore (2012). Thus, the origin of high level differentiation does not produce all of the observed rock assemblages. It is considered that the origins of the LACC magma were possibly having a deeper origin than the depth postulated by Woolley and Kjarsgaard (2008). The possible origin of the LACC magma is indicated with red dashed line in Figure 9.3. This theory supports the unusual high concentration of the REE and in particularly the HREE as these form part of the rocks with deep mantle source.

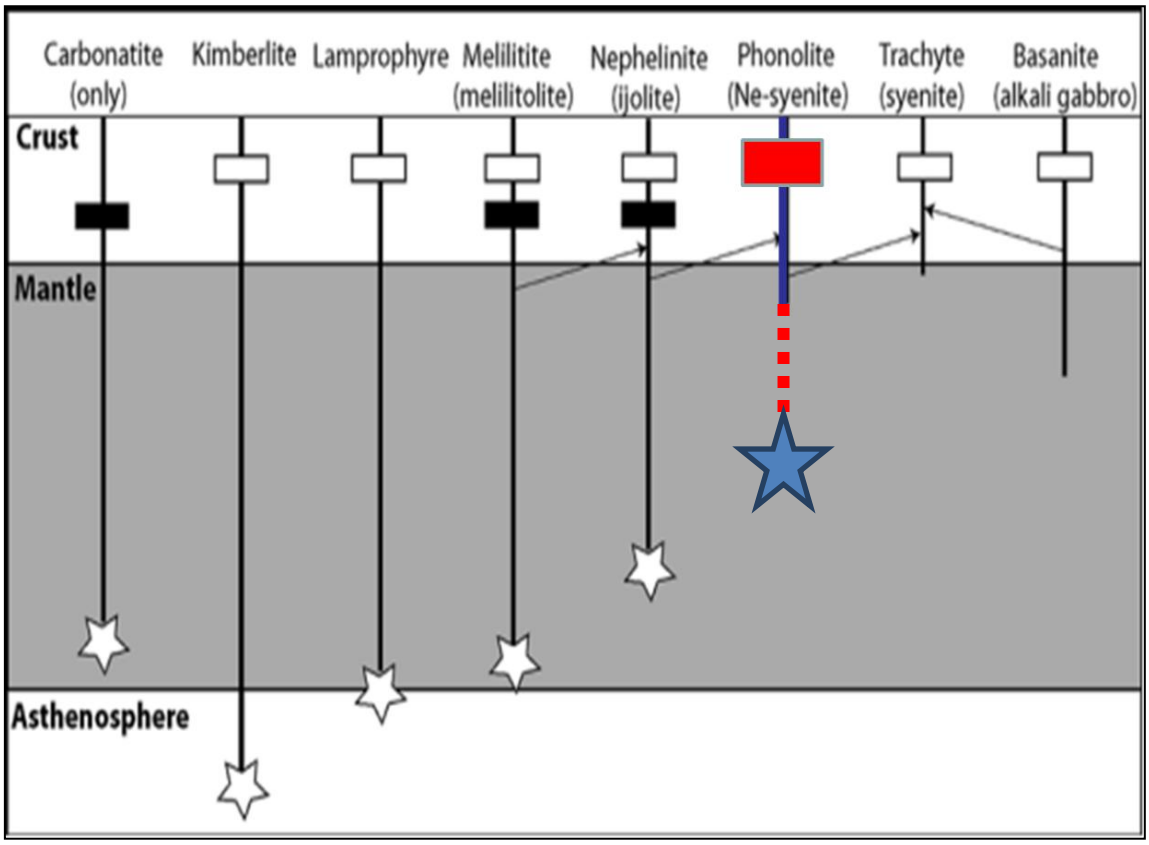

Figure 9.3 Schematic diagram illustrating the carbonatite only association and seven alkali silicate rock associations occurring with carbonatite Woolley and Kjarsgaard (2008). Relative depths of magma generation in the mantle and, in particular, two levels of carbonatite generation are also illustrated, i.e., directly in the mantle (stars) and by differentiation processes at shallower depths (open white boxes). Note that carbonatite originating in the mantle can pass directly to the surface, and need not be involved in differentiation at a higher level (open white boxes). Ultramafic cumulate rocks are depicted by the solid black rectangles. Known alkali silicate differentiation series are represented by the thin black lines with arrowheads indicating the sequence from primary magma to differentiate. The red box indicates the fit to the Lofdal Alkaline Carbonatite Complex. The red dashed line indicates the possible source region of the LACC magma.

The LACC is similar to many other carbonatite complexes in terms of its multiple varieties of carbonatite, with low REE contents in the earlier members of the complex and high REE in the late-stage carbonatites, coupled with evidence for subsolidus alteration. The association with syenites and phonolites is also seen elsewhere. The main distinctive feature of the LACC is its emplacement as a large dyke swarm and small plugs rather than as a composite pluton (Barker 1989). The intrusion of dykes into

shear zones may have permitted a much higher fluid flow around, and in, the dykes than can take place in the more usual situation where the later dykes penetrate earlier carbonatite.

9.3 Hydrothermal processes in the Lofdal Alkaline Carbonatite Complex

Although carbonatites are igneous rocks, there is much mineralogical and geochemical evidence of hydrothermal activity in and around the carbonatites in the LACC. Hydrothermal processes appear to have played an important role in the formation of the HREE-enriched rocks.

9.3.1 Evidence for hydrothermal modification

Petrographic, mineralogical and isotopic data presented in previous chapters demonstrate that the Lofdal carbonatites were subject to significant hydrothermal activity. Mineralisation in most of the Lofdal carbonatite dykes is highly variable following sub-parallel zones that may reflect a variable intensity of multiple hydrothermal and /or metasomatic overprints of the primary carbonatite. The Main carbonatite and Emanya plugs represent an early magmatic phase with only minor LREE and HREE mineralisation.

The petrographic and mineralogical evidence for hydrothermal fluids includes veinlets of xenotime, mainly in the carbonatite dykes that are far away from the main carbonatite intrusions, altered and REE-enriched, especially by the LREE and HREE. Representative samples from the highly altered carbonatite types, e.g. Type 2 carbonatite dykes, are highly enriched in Y and do not contain LREE-minerals but only xenotime-(Y), zircon, apatite, thorite, fluorite, rutile and phlogopite. At Lofdal xenotime is observed as dissolution-reactions on highly altered rocks of dyke type 2. This occurrence indicates that the fluid flux must have been generally high enough to mobilise relatively insoluble essential constituents. The xenotime-bearing veins display brecciation and a relatively weak foliation but there is little evidence for metamorphic overprinting. The low thorium concentration in most REE minerals suggests that they are secondary in origin, and were deposited by hydrothermal fluids. This paragenesis contracts with the large bastnäsite deposit in carbonatite at Mountain Pass, USA, which is thought to be in large part magnatic (Wall and Mariano 1996) and with Kangankunde, Malawi, which although produced by subsolidus alteration has distinctive hexagonal pseudomorphs seen in a number of REE-rich carbonatites (Wigu Hill Tanzania, Bear Lodge USA, Khibina Russia (Wall and Zaitsev 2004; Zaitsev et al. 2008). No similar features were seen in Lofdal.

Regional mapping and the results of extensive sampling and analysis support the idea that REE mineralisation is structurally controlled by migration paths of fluid phases and not necessarily dyke-specific. Recent drilling by Namibia Rare Earth Ltd indicates that hydrothermal alteration and brecciation is widespread in association with the carbonatites, and that dyke intrusions are associated with wide alteration and breccia haloes characterized by albitite, fenite, iron oxides, carbonate and fluorite. This concept is supported by geochemical data in this thesis, showing that the more altered and Fe-rich rocks contain high levels of REE concentrations. The mineralization is interpreted to be late in the alteration sequence, based on the apparent REE mineralization in late fracture veinlets, breccia fill, and alteration streams that cross cut the albitite, the albitite crackle breccias and the carbonatites.

The characteristic lithology of alteration zones around the LACC is albitite, which frequently displays an intense, variably developed, brittle brecciation ranging from slight cracking and infusion by brown carbonatite and iron oxide veinlets, to complete brecciation with angular fragments surrounded by a matrix of later albitite and/or carbonatite. Thus the widespread hydrothermal alteration appears to have been volatile-rich and the origin of the albitites can be explained from the evolution of fluids in the Lofdal system, which may have played an important role on the deposition of the HREE.

The dates obtained from Lofdal xenotime coincide with those from syenite (Table 9.1 and Chapter 8) and were concluded to represent the main age of emplacement of the carbonatite. In contrast pyrochlore records younger ages suggesting the carbonatites were affected by the regional geological events related to the Pan African Orogen that occurred post intrusion until 400 Ma. K –Ar dating also recorded the deformation events of the Damaran Orogen. Therefore an important point is that the HREE mineralization at Lofdal, as recorded by the xenotime, is coincident with the emplacement of the carbonatite complex.

This makes the LACC similar to most other REE-rich carbonatites (e.g. Mountain Pass, USA, Kangankunde, Malawi, Wall and Mariano 1996) and different to Bayan Obo, China. At Bayan Obo, the World's largest REE deposit, the REE minerals in the ore bodies give much younger dates than the carbonatite dykes in the area and formed some 900 Ma after emplacement of the original carbonatites (Kynicky et al. 2012).

9.3.2 Origin of fluids (stable and radioisotope evidence)

Lofdal $\delta^{13}C$ values are distinctively lower than in sedimentary carbonate and consistent with a magmatic origin. The $\delta^{13}C$ and $\delta^{18}O$ isotopes exhibit a broad variation characterized by a moderate rise in $\delta^{13}C$ coupled with a sizeable increase in $\delta^{18}O$. The oxygen and carbon isotopic compositions of samples from carbonatite plugs are more homogeneous than those of the dykes of the complex, indicating the mantle origin of the carbonatites. The investigation of the carbonatite dykes showed that $\delta^{18}O$ values are higher than those representing mantle-related primary carbonatites i.e. 6 -8 % (Taylor et al. 1967). The oxygen and carbon isotopic compositions of the dykes are significantly affected by hydrothermal alteration. The observed $\delta^{18}O$ enrichment probably reflects re-equilibrium during hydrothermal processes implying interaction with meteoric water. Such interactions took place at possible lower to mid temperature ranges from dominantly aqueous fluids as indicated by the stable isotope studies. Variations in $\delta^{l8}O$ not necessarily accompanied by variations in $\delta^{13}C$, suggest that the mineralising fluids were at least partly sourced from meteoric water in a subvolcanic settings. Variations in $\delta^{13}C$ are usually attributed to interaction of carbonatites with non-igneous carbonate wall-rocks, interaction with CO_2-rich vapors or fluids derived from external sources, or magma degassing (Santos and Clayton 1995, Demény et al. 2004). Crustal contamination is responsible for the isotope variation in many continental magmatic rocks.

The presence of oxygen isotopic disequilibrium between calcite and dolomite minerals (chapter 8), in many instances addresses the isotopic variations associated with processes involving H_2O-bearing and H_2O~O-CO_2-bearing fluids.

The initial Sr isotopic ratio of the calcite in Type 1 dykes corresponds to a mantle signature, while the calcite in Type 2 dykes suggests a highly enriched mantle source or a crustal contamination by assimilation (or by reaction of hydrothermal fluid with wall rocks). These isotopic characteristics indicate that the source of the carbonatitic magma was in the sub-continental lithospheric mantle.

At temperatures below 270°C, calcite-water $\delta^{l8}O$ fractionation becomes larger than 6 (O'Neil et al. 1969). Hence, it may also be concluded that high temperature fluids derived from the main carbonatite intrusion (>>300°C) played a major role. The presence of magmatic water in carbonatites is supported by experimental studies (Wyllie and Tuttle 1960, Wyllie 1989) and studies of natural samples (Treiman and

Essene 1984), which suggest that water is an important component in the fluid phase of carbonatites, in particular, in the late stages of the evolution of the magma.

A carbonatitic origin for much of the fluid activity is consistent with the geochemical evidence. Over time, however, flow of heated fluid would subside and it is plausible that influx of meteoric water would then be able to influence the hydrothermal system.

9.3.3. Fluid chemistry

Fluid inclusion studies were not carried out as part of this study at Lofdal. However, it is possible to make some statements about possible compositions of fluids in and around the LACC. Firstly, the magmatic system which formed the LACC must have been CO_2–rich because of the abundance of carbonatite, and therefore it is highly likely that hydrothermal fluids exsolved from the magma would also have been CO_2-rich, and certainly CO_2-bearing. Carbonate components are found in veins within the carbonate-free country rock. Secondly, at Lofdal, fluorocabonates are the dominant REE minerals in LREE-rich carbonatite rocks, including dykes and plugs and fluorite is found in widespread, at times in the same rocks as the REE fluorcarbonates. It is thus likely that fluorine as well as the more usual chlorine may have had a role in fluid transport of cations. A more detailed discussion of the role of ligands is given in section 9.4 below.

9.4 Comparisons with other HREE ore deposits and origins of the HREE mineralization

Given the discussion above, it is possible to review some of the fundamental questions about the formation of the HREE deposit at Lofdal. The carbonatite complex itself has many features in common with most other carbonatites: its emplacement in an extensional setting, its range of carbonatite compositions, the accompanying silicate intrusions, its radiogenic and stable isotopic signatures and the magmatic emplacement followed by subsolidus hydrothermal activity. The unusual features are the linear dyke swarm rather than the more usual concentrically shaped intrusions, the presence of so much xenotime, and also the extent of the HREE mineralization now being found by the Namibia Rare Earths exploration programme outside of the carbonatite dykes in the surrounding altered (fenitised) country rocks.

The difference in REE mineralisation at Lofdal tells us that the history or conditions at Lofdal were different to other carbonatites.

The factors that may have contributed to this difference are: the initial REE enrichment in the magma, such as the source mineralogy, the degree of melting, the fractional crystallisation history and crustal contamination, or changes in physical–chemical parameters (Eh, pH, temperature, available fluids, REE fluid activities and REE complexation that produced hydrothermal distribution/redistribution in and around the complex.

Three possibilities for the formation of xenotime are (1) that the magma was originally particularly enriched in HREE either from its production in the mantle or as a result of crustal differentiation or contamination. This HREE-enriched magma then produced the magmatic and hydrothermal xenotime mineralization, (2) that a hydrothermal fluid evolved, e.g. cooled, to become progressively LREE through to HREE-enriched or (3) that a particular combination of ligands were able to mobilize or remobilize and concentrate HREE.

9.4.1 An original HREE-enriched magma?

The first possibility for magmatic enrichment of HREE is enrichment of the original mantle-derived melt. The presence of lamprophyre and the mineral phlogopite in the Lofdal carbonatites may have significance here in showing that the parental magma segregated from a metasomatised mantle source rich in an early melting hydrous K-bearing phase, possibly in a similar system to the dolomite silico-carbonates described by Brady and Moore (2012). The problem is that carbonatites derived from such sources are not necessarily at all enriched in REE. Other possibilities for enrichment in the mantle source were discussed by Wall et al. (2008). For example, the REE-chondrite normalized profile of Lofdal dykes is similar to garnet-bearing pyroxenite in the Neoproterozoic carbonatite at Otjisazu, Namibia (Bühn et al. 2001). If extensive metasomatism had fluxed a garnet mantle component to melt or reworked cumulate garnet, such as in the pyroxenite at Otjisazu, this may be a way of producing a more HREE-rich carbonatitic magma.

The next possibility is that fractionation processes in the crust produced an HREE-enriched carbonatite magma. There are a variety of carbonatites present at Lofdal, ranging from calcite carbonatite of the Main intrusion with low REE content to the LREE in Emanya and LREE and HREE-enrichments in the dykes. They include coarse, medium to fine-grained calciocarbonatites, ferrocarbonatites and dolomitic carbonatites overprinted by a widespread hydrothermal assemblage. Wyllie and Tuttle (1960a)

demonstrated that synthetic carbonatite magmas are extremely fluid and that crystal settling occurs within a few minutes. This would provide abundant opportunities for the separation of magma batches or accumulated crystal fractions of different composition from carbonatite magma (Keller 1989). The LACC provides an example of small scale differentiation illustrated by the development of xenotime-rich bands and lenses in the carbonatite dykes. The mineralogy varies spatially within the same rock and even within the same thin section sample and often the chemistry of a mineral species displays a large compositional ranges. Crystallization of the first generation of xenotime is characterised by coarse grain size and generally euhedral morphology.

At Lofdal elements such as TiO_2, MgO, CaO, FeO, Al_2O_3 and P_2O_5 decrease with decreasing molar Al/(Na+K) ratio in the nepheline syenites and the associated carbonatites. This implies fractionation of early forming minerals i.e., clinopyroxene, amphibole, plagioclase or nepheline, Fe–Ti oxides and apatite. Nb and Zr abundances increase with decreasing molar Al/(Na+K) ratio indicating that titanite and zircon which are important hosts for these elements were not important during fractional crystallization processes. Zircon is observed in abundance in some carbonatite dykes that contain albite. Such evolution may have caused the concentration of REE to remain in the melt and intrude at late stage with the carbonatites.

There is no particular evidence of magmatic crystal contamination at Lofdal. The isotope data are more consistent with late contamination during hydrothermal processes. Although the magmatic processes are likely to have been a key factor in producing a magma with levels of HREE higher than usual for carbonatite, the field and petrographic evidence for extensive hydrothermal mobilization/remobilization is strong and this must have also played a key role in the formation of the xenotime deposit.

9.4.2 Evolution of the mineralising fluid (closed system REE mineral crystallisation from an evolving hydrothermal fluid)

Other REE-rich carbonatites do exhibit a temporal evolution, with decreasing temperature of hydrothermal fluids (or ‘carbo-hydrothermal fluids’), to more HREE-rich mineral compositions (Van Wambeke 1977, Walter et al. 1995, Zaitsev et al. 1998, Smith et al. (2000).). The formation of xenotime-(Y) inclusions in apatite (chapter 7) could also be interpreted as the result of dissolution-reprecipitation processes that occurred in an effectively closed chemical system. The reaction was possibly initiated

by interaction between the early crystallizing xenotime-(Y) I and apatite I and the evolving HREE-rich fluid. This fluid may have been dominated by H_2O, but also contained F and significant quantities of dissolved Na+ and K+ as these rocks have elevated alkali content. This may be interpreted as an example of auto-metasomatism. However, xenotime occurs throughout the paragenetic sequence at Lofdal, in contrast to a locality such as Khibina, for example, where HREE minerals only occur in the latest zeolite-bearing veins Zaitsev et al. (1998) and a simple fluid evolution therefore seems unlikely as an overall explanation for HREE enrichment. In hydrothermal systems, the relative REE abundance in minerals will be related to fractionation during precipitation Möller and Morteani (1983); Möller, (1991); Möller (1998), sorption on to mineral surfaces (Bau, 1991), and to the relative abundance of the various REE in the hydrothermal fluid. These factors will be controlled in turn by the REE source, the P-T conditions and fluid chemistry but also by the speciation and availability of ligands (Wood, 1990a,b; Haas et al. 1995).

9.4.3 Fluid chemical effects (ligand availability and temperature effects)

Hydrothermal transport and precipitation of REE can be strongly influenced by the ligands available. Experimental studies of monazite and xenotime solubility in H_2O show that solubilities rise with pressure and temperature, but are generally very low over a wide range of igneous and metamorphic conditions (Tropper et al. 2012). The low monazite and xenotime solubilities returned by experimental studies make it difficult to explain their natural associations with metasomatic features in igneous rocks, such as hydrothermal alteration assemblages, veins and skarns (Cesbron 1989, Philippot and Selverstone 1991, Bingen et al. 1996, Gieré 1996, Poitrasson et al. 1996, 2000, Townsend et al. 2000, Seydoux-Guillaume et al. 2002, Roland et al. 2003, Hetherington and Harlov 2008, Bosse et al. 2009). An alternative mechanism for the dissolution and transportation of orthophosphate components is a high alkali halide concentration in the fluid phase as indicated by the presence of fluorite and chlorine. It has been proposed that REE (and by extension, Y) mobility may be enhanced by dissolved halogens (Pan and Fleet 2002, Schmidt et al. 2007, Antignano and Manning 2008a, Pourtier et al. 2010).

The behavior of REE at elevated temperatures has been investigated theoretically by Wood (1990) and Haas et al. (1995). Based on chemistry of fluids and mineralogy of deposits, Wood (1990) and Haas et al. (1995) indicate that possible ligands involved in the transport of the REE are F^-, CO_3^{2-}, OH^-, Cl^-, SO_4^{2-}, and HCO_3 According to data

presented by Wood (1990), F^- forms the strongest complex with REE. REE dissolution in natural fluids is controlled by ligands other than H_2O or phosphate, such as chloride, fluoride and sulfate, all of which can be expected to occur in varying proportions Tropper et al. (2011).

Pearson's rules (Pearson 1963, Willian-Jones et.al. 2012), state that hard cations such as the REE which have relatively small ionic and usually a +3 charge, will bond preferentially with hard anions and soft cations will bond preferentially with soft anions. The order of monovalent inorganic ligands with which the REEs should form their most stable aqueous complexes if $F^- > OH^- > NO_3^- > Cl^- > Br^-$ Pearson (1963). For complexes involving divalent ligands, the order should be $CO_3^{2-} > SO_4^{2-} > P_2O_5^{2-}$. Based on Pearson's rules, the stability of complexes of the trivalent REE involving a hard ligand like F- or CO_3^{2-} is predicted to increase systematically along the lanthanide series from La to Lu, with Y occupying a place between Ho and Er and Sc situated beyond Lu. The stability of REE complexes with hard ligands such as F- and CO_3^{2-} is an order of magnitude greater than with ligands of intermediate hardness, like Cl^-, and the stability for a particular ligand increases with the hardness of the REE (Schijf and Byrne 1999, Luo and Byrne 2001).Significantly, however, the stability of complexes of the REE with $SO_4^{2-,}$ which ranks behind F^- and CO_3^{2-} in terms of hardness, varies little with the hardness of the corresponding REE, and complexes with the borderline ligand Cl^- decrease in stability with increasing REE hardness (Luo and Byrne 2001).

Chloride species are assumed to transport the REE in most hydrothermal systems. For example, the Gallinas Mountains deposit, New Mexico, containing a fluorite–bastnäsite-(Ce) assemblage cemented by quartz syenite and sandstone breccias (Williams-Jones et al. 2000) is interpreted to have formed between 300 and 400 ºC from brines containing 12 to 18 wt% NaCl equivalent. Another example is the Karonge deposit in Burundi, 1 – 10 cm wide bastnäsite-(Ce) veins and stockworks in granitic gneiss (Lehmann et al. 1994) proposed to have formed at >420 ºC from a brine containing >25 wt% NaCl equivalent. The hydrothermal REE deposits described above are all LREE-enriched.

The deposition of the REE as bastnäsite-(Ce) can be described by the reaction:

$REECl^{2+} + HF + HCO_3^- = REECO_3F + 2H^+ + Cl^-$, where $REECO_3F$ is bastnäsite-(Ce),

and thus any mechanism that leads to an increase in pH and/or HCO_3^- activity or a decrease in Cl^- activity will lead to deposition of bastnäsite-(Ce) (Williams-Jones et al. 2013). The strong enhancement of $CePO_4$ and YPO_4 solubilities by NaCl points to major REE mobility at neutral pH, even at only modest salinity. Where concentrated NaCl brines occur, REE mobility may be profound Tropper et al. (2011).

At Lofdal, xenotime is more common than monazite. Tropper et al. (2011) found that YPO_4 is at least 1.5 times more soluble than $CePO_4$ in pure H_2O at 800°C and 1 GPa. Although such a result is in conflict with the general observation that monazite is more common than xenotime generally in hydrothermal veins and other metasomatic features, it fits well with the Lofdal deposit where xenotime is more common than monazite. This might imply greater solubility of HREE relative to LREE, contrary to observation by Schmidt et al. (2007). It also probably highlights the fact that REE solubilities are a complex function of the concentrations of a range of ligands in natural fluids.

Evidence from REE deposits show that besides chloride, the fluids involved in REE transport and deposition can have high fluoride activity (Williams-Jones et al. 2013). There is also commonly a close association between hydrothermal REE mineralisation and fluorite. Fluorite is a common mineral in the Lofdal phonolites, syenites and carbonatites. It is important to note that the Lofdal REE mineralisation is not observed directly related to the fluorite but some dykes that are mineralised also contain significant amounts of fluorite. Like the REE fluorcarbonate minerals, fluorite is extremely insoluble, and thus any free fluoride will deposit as fluorite when brought into contact with a source of calcium. The presence of fluorite is a common indicator of mineralization in some highly oxidized dykes, which indicate that hydrothermal concentration of REE occurs mainly when fluids containing these complexes interact with cooler, pH-neutralising rocks, or mix with cooler, pH-neutralising fluids. According to Richardson and Holland (1979), massive fluorites are precipitated either as a consequence of changes in temperature and pressure along the flow path of hydrothermal solutions or due to fluid mixing, or as the result of the interaction of hydrothermal solutions with wall rocks. Thus the mixture of F-rich fluid with the Ca-, CO_2-bearing carbonatite derived fluid cause deposition of REE minerals and later fluorites. Given the abundance of F-bearing minerals at Lofdal, it may well have been an important ligand in transporting REE, and in the preferential transport of HREE. Xenotime is seen to precipitate when in contact with phosphate (e.g. in apatite) and in carbonate veins. Calcite in a HREE-rich vein has been shown to be HREE-rich and so consistent with precipitation from the same fluid as the xenotime. Carbonate ligands may also have a role in carrying REE.

Various studies have shown that the high-temperature behaviour (>150 ºC) of the REE differs in important respects from that inferred from theoretical models (Migdisov et al. 2009, Williams-Jones 2012). Experimental determinations show that $LREEF^{2+}$ species

are more stable than $HREEF^{2+}$ species at elevated temperature (Migdisov et al. 2009). This change in the relative stability of $LREEF^{2+}$ and $HREEF^{2+,}$ from that at ambient temperature, occurs at approximately 150ºC. Since the xenotime-(Y) formed at temperatures >450°C at Lofdal (Wall et al. 2008) LREE concentrations should be higher than HREE because $LREEF^{2+}$ species are more stable than $HREEF^{2+}$ species at elevated temperature according to Migdisov et al. (2009). This is not the case for some dykes at Lofdal where HREE concentrations are higher than LREE. Possible explanations are that the xenotime-precipitating fluids are below 150°C but this seems unlikely for all cases, given the long range of paragenesis. In the Nechalacho deposit, Northwest Territories, Canada (indicated resource of 88 million tonnes grading 1.53 wt% REE_2O_3), the host rock is a layered, silica-undersaturated alkaline complex in which the magmatic REE minerals such as eudialyte (a complex zirconosilicate containing ~7 wt% REE_2O_3) and zircon (containing ~3 wt% REE_2O_3.) were altered. The LREE were preferentially hydrothermally mobilised to significantly greater distances from their magmatic source than the HREE. This observation is in marked contrast to the situation at Lofdal, where dykes and shear zones outside of the main carbonatite plugs are most likely to be HREE enriched. If Cl- is an important transporting agent at Nechalacho, it is likely to be preferentially transport the LREE but not the HREE. It is possible to hypothesise that at in and around the Lofdal carbonatites, CO_3^{2-} is more important as a transporting ligand and Cl- is less important than in silicate complexes such as Nechalacho. Better HREE transport would also be expected at fluid temperatures <150°C when F also becomes a good transporting ligand, and this may also help to explain some of the high HREE values in fenitized shear zones some distance away from the carbonatite dykes.

Preferential transport of LREE rather than HREE has also been proposed in the silicate system at Browns Range, Australia, which hosts multiple generations of granites proposed as potential sources of REE contained in its mineralisation. Granites are well-known sources of REE and these are readily released from a granitic magma into a hydrothermal fluid (Lottermoser 1992, Migdisov et al. 2009, Monecke et al. 2003), possibly via unmixing during the final stages of granite crystallization (Bottrell and Yardley 1988). With the exception of negligible Nb, the element association (Y-REE-Zr = (F)) is, however consistent with rare-element NYF pegmatites formed in anorogenic settings and associated with A- and I-type granites (Cerny, 1991). Hydrothermal fluids subsequently dissolved these minerals and reprecipitated the REE as fergusonite-(Y), secondary zircon, allanite-(Ce), bastnäsite-(Ce) and monazite-(Ce).

The HREE were deposited proximal to the precursor minerals, whereas the LREE were mobilised on a scale of metres and perhaps tens of metres (Ngwenya 1994, Gieré 1996, Oliver et al. 1999 and Rankin 2005).

9.5 Implications

The large majority of carbonatite complexes are LREE-enriched, with limited potential for production of HREE. What is unique at Lofdal is the significant enrichment in HREE associated with the carbonatites, and the dominance of xenotime as a principal REE-bearing mineral. The REE at Lofdal come from ore deposits of magmatic, carbonatitic origin, which have been affected by hydrothermal processes. In most respects, the LACC is not particularly different from other REE-rich carbonatite complexes. The distinctive features are the emplacement as a major dyke swarm in an area of shearing, which as mentioned above may have permitted higher fluid flow in and around the dykes and almost certainly, an original magma composition enriched in HREE compared with more usual carbonatites. Other Neoproterozoic carbonatites in Namibia have similar REE patterns but lower overall REE abundances as discussed in section 6.4.

9.5.1 Exploration for bedrock HREE enriched systems

The limited analogues elsewhere in the World for this style of REE-mineralisation constrains development of a comprehensive exploration model find other bedrocks of HREE enriched systems like that of Lofdal. It is, however important to explore alkaline complexes (e.g., alkaline-or carbonatite-associated), that show characteristics of better constrained types of REE deposits and reworking of late stage hydrothermal activities. These systems can represent both magmatic and/or hydrothermal ore types. Independent of the source or type of mineralizing fluid, a tentative model can be put forward to account for the petrographic evidence, such as the presence of REE-bearing minerals. Fluid infiltration into the country rocks and fracture structure of the host rocks and the intrusions of the dyke systems are the features to search for. One may speculate that these units are the main host for mineralisation in regions where alkaline rocks are present as they may allow the passage of mineralised hydrothermal fluids and may operate as a trap for reduced fluids.

Radioactivity constitutes an issue faced by many REE exploration projects but is very useful in exploration. At Lofdal elevated levels of thorium provide an excellent guide for exploration and often pinpoint areas of high HREE potential. A key point about

exploration targeting is not to be constrained to the main plutonic areas of carbonatite, because large, fresh-looking, plutons of calcite carbonatite are rarely enriched in either light or heavy REE. However, searching for slightly abnormal REE profiles (above average those described by Wooley and Kempe 1989, even if concentrations are low may be useful. In addition searching away from the main area of intrusions, following shear zones and fault structures may be fruitful in finding the next Lofdal.

Chapter 10: Conclusions

The Lofdal alkaline carbonatite complex is situated on the southern rift margin of the Congo craton, at the intersection of the Northern Platform Zone of the central Damara belt with both the eastern Kaoko Zone and the Northern Margin Zone, but more specifically between the Northern zone and the Ugab tectono-zone.

The LACC occurs in a rift-related continental province as supported by the regional geological settings, the ages and the geochemical composition and is similar to other carbonatite occurrences, that are also associated with volcanic sequences and dykes that can differentiate into phonolite and carbonatite melts It has Neoproterozoic age, therefore its relationship to the Damara origin sets it apart from the better known ca. 130 Ma Cretaceous alkaline and carbonatite intrusive centres in Damaraland,

The emplacement of the LACC is associated with regional fracturing of the metamorphic basement rocks, mainly along NNE/SSW to NE/SW structures, which indicate local reactivation of older basement structures.
The complex consists of a swarm of carbonatite veins and associated plugs on the Bergville and Lofdal farms northwest of Khorixas, Namibia, intruding the basement rocks following a NE-SW shear zone over 30 km distance. The complex has an ellipsoidal shape in plan with a NE-trending elongation. Carbonatites are spatially associated with earlier phonolites, syenites and mafic rocks. The lack of mantle xenoliths observation and the carbonatite association with syenite, phonolites and mafic rocks was interpreted to indicate that the Lofdal alkaline complex is a shallow intrusion.

The carbonatite dykes and plugs are predominantly calcite carbonatites with associated ferric iron oxides. Two calciocarbonatite bodies were discovered during the mapping programme: both sövite carbonatite referred to as the Main and Emanya calciocarbonatite plugs. A thin marginal zone of alkali metasomatised syenite and basement rocks forms the contact zone between the calciocarbonatite and the syenite intrusion and or the country rocks, extending several meters from the carbonatite intrusions.

Like most carbonatite complexes, silicate rocks were emplaced before the carbonatites, which are the last phase to be emplaced at Lofdal. Several breccia pipes are localized within the Huab metamorphic basement, around the main syenite/carbonatite intrusions,

in the syenite plug and along the contact with the syenites and the carbonatite plugs. The breccias are chaotic and contain a wide variety of different rocks types, sizes and colours.

Carbonatite dykes and fine-grained and porphyritic phonolite dykes have a general North-East direction with a steep dip (60^{o}C) towards the south. The phonolites are younger than the basement rocks and the syenites, but older than the carbonatite plugs and dykes. Common minerals in the phonolites are potassium feldspars, pyroxenes, biotite, chlorite, cancrinite, fluorite, magnetite and others.

Carbonatite dykes exhibit variable characteristics with colours ranging from white to grey, through shades of brown, red and yellow. The variable colours are interpreted to reflect the abundance, state of iron oxidation and the relative degree of hydrothermal alteration.

Fenitisation occurs at the immediate contacts with varied wall rocks. Dissolution of carbonate and residual concentration of iron oxide are the dominant secondary phases. Precipitation of apatite and pyrochlore is also observed at the contact between the carbonatite and syenite. Other lithological alteration zones are albitite, localized zones of green phlogopite fenite; brown stained albitite breccias infused with carbonatites in the country rocks, calcite and altered schist that has been carbonatised and chloritised. Hyperspectral images revealed a wide zone of iron and argillic alteration south and southeast of the main intrusion.

Field mapping and hyperspectral imaging were used to consider structural geologic including the extend of deformation and alteration in individual dykes, that are related to the following sequences of events, the mineralogy and the presented isotope values;

- Uplift and extension regime associated with faulting and brecciation. Some faults and regional structures record also a compressional deformation regime.
- Intrusion of phonolite dykes.
- Intrusion of syenite and carbonatite plugs and subsequently carbonatite dyke intrusions associated with further brecciation.
- Hydrothermal processes related to carbonatite and/or syenite intrusions. Fluids derived from the carbonatite and syenite intrusions are responsible for the origin of the REE deposits.

The rock textures, mineralogy and geochemistry indicate that the magmatic and hydrothermal processes affected both the alkaline intrusive and the country rock.

Based on different geochemical characteristics and REE trends the carbonatites are classified as calciocarbonatites, ferrocarbonatites and magnesiocarbonatites according to the IUGS carbonatite chemical classification and are grouped into eight (8) main groups. Some Lofdal carbonatites show extreme REE-enrichment especially in the MREE and HREE, which are all above the average calciocarbonatite (Woolley and Kempe 1989), making these different to all other known carbonatites. Incompatible elements such as Sr, Ti and Ba are consistent with the groupings based on the REE distribution in the Lofdal carbonatite rocks.

HREE-mineralisation is strongly controlled by intensive shearing within the carbonatites dykes and the surrounding fenitised country rocks. The HREE are mainly hosted in minerals such as xenotime-(Y), thorite, zircon, apatite and fluorite while pyrochlore, parisite-(Ce), synchysite-(Ce) and monazite-(Ce) host LREE. HREE precipitation is observed to take place in the fractured albitised country rocks and carbonatite-free shear zones, indicating intensive interaction of an HREE-rich hydrothermal fluid with the country rocks.

The petrographic and mineralogical evidence for hydrothermal modification includes veinlets of xenotime, different levels of alterations and REE-enriched. The characteristic lithology of alteration zones around the LACC is albitite, displaying an intense, variably developed, brittle brecciation ranging from slight cracking and infusion by brown carbonatite and iron oxide veinlets, to complete brecciation with angular fragments surrounded by a matrix of later albitite and/or carbonatite.

There is a general HREE- enrichment increase from the early magmatic to late hydrothermal stages of mineralisation. Metasomatism and autometasomatism is observed reflected by apatite and pyrochlore mineralisation at contacts between the syenites and the carbonatites. There is a close relationship between the albitites, REE and xenotime-(Y) enrichment in all carbonatite types at Lofdal is observed. The MREE and HREE contents are uniquely high making the deposit exceptionally different and economically important as these commodities are highly priced and occurring rarely in the World.

The $\delta^{18}O$ and $\delta^{13}C$ and $^{87}Sr/^{86}Sr$ isotopic compositions of the Lofdal Alkaline Carbonatite Complex have been studied in order to determine primary compositions and the effects of rock alteration processes. The $\delta^{18}O$ and $\delta^{13}C$ isotopic compositions of the least altered carbonatites plugs and dykes indicate a mantle origin while highly altered carbonatite dykes indicated strong influence by secondary processes involving meteoric water. The results indicate that the carbonatite plugs and least altered dykes formed from primary carbonatite magma while the altered carbonatite dykes are affected by hydrothermal alteration and crustal contamination. The deposit shows a significant contribution of meteoric water to the mineralised fluids that intruded the dykes and the country rocks along existing fractures at different geological times. Variations in $\delta^{18}O$ not necessarily accompanied by variations in $\delta^{13}C$, suggest that the mineralising fluids were at least partly sourced from meteoric water in a shallow tectonic setting.

The oxygen and carbon isotopic compositions of the dykes are significantly affected by hydrothermal alteration. The observed $\delta^{18}O$ enrichment probably reflects re-equilibrium during hydrothermal processes implying interaction with meteoric water.
Sr – Nd isotopes ratios also indicate a mantle source for the least altered carbonatites and crustal influence for the altered carbonatite dykes, in agreement with the C and O isotope studies. The calculated isotopic compositions of the interacting fluids indicate a meteoric water origin.

The Lofdal xenotime-(Y) has the same age as the main carbonatite (765 ± 16 Ma). Zircon from the carbonatites yielded a concordia age of 765.9 ± 5.4 Ma which is in agreement with the Lofdal zircon from the syenites (775+/ 41 Ma). The pyrochlore and K –Ar dating were affected by regional geological events related to Pan African Orogenesis between 900 and 400 Ma.

The initial Sr isotopic ratio of the calcite in Type 1 dykes corresponds to a mantle signature, while the calcite in Type 2 dykes suggests a highly enriched mantle source or a crustal contamination by assimilation (or by reaction of hydrothermal fluid with wall rocks). These isotopic characteristics indicate that the source of the carbonatitic magma was in the sub-continental lithospheric mantle.
A Sm-Nd isochron indicated also that the Sm-Nd isotope system was disturbed by an alteration processes. These interpretation of results is that the Lofdal complex is part of an intense magmatic activity and initial rifting stages in the Kaoko and Damara belts

(730-770 Ma) and altered by the Early Pan-African orogeny responsible for the Damara Orogen (±650 Ma).

A carbonatitic origin for much of the fluid activity is consistent with the geochemical evidence. Over time, however, flow of heated fluid subsided and it is plausible that influx of meteoric water then influenced the hydrothermal system.

Fluid inclusion studies were not carried out as part of this study at Lofdal. However, it seems that, the magmatic system which formed the LACC must have been CO_2–rich because of the abundance of carbonatite, and therefore it is highly likely that hydrothermal fluids exsolved from the magma would also have been CO_2-rich, and certainly CO_2-bearing.

At Lofdal, fluorocabonates are the dominant REE minerals in LREE-rich carbonatite rocks, including dykes and plugs and fluorite is found in widespread, It is thus likely that fluorine as well as the more usual chlorine may have had a role in fluid.

The LACC has many features in common with most other carbonatites such as: its emplacement in an extensional setting, its range of carbonatite compositions, the accompanying silicate intrusions, its radiogenic and stable isotopic signatures and the magmatic emplacement followed by subsolidus hydrothermal activity. The unusual features are the linear dyke swarm rather than the more usual concentrically shaped intrusions, the presence of so much xenotime, and also the extent of the HREE mineralization now being found by the Namibia Rare Earths exploration programme outside of the carbonatite dykes in the surrounding altered (fenitised) country rocks.

The difference in REE mineralisation at Lofdal tells us that the history or conditions at Lofdal were different to other carbonatites. The factors that may have contributed to this difference are: the initial REE enrichment in the magma, such as the source mineralogy, the degree of melting, the fractional crystallisation history and crustal contamination, or changes in physical–chemical parameters (Eh, pH, temperature, available fluids, REE fluid activities and REE complexation that produced hydrothermal distribution/redistribution in and around the complex.

The first possibility for magmatic enrichment of HREE is enrichment of the original mantle-derived melt.

The next possibility is that fractionation processes in the crust produced a HREE-enriched carbonatite magma. There is no particular evidence of magmatic crystal contamination at Lofdal. The isotope data are more consistent with late contamination during hydrothermal processes.

Hydrothermal transport and precipitation of REE seem to be strongly influenced by the ligands available.

The large majority of carbonatite complexes are LREE-enriched, with limited potential for production of HREE. What is unique at Lofdal is the significant enrichment in HREE associated with the carbonatites, and the dominance of xenotime as a principal REE-bearing mineral.

The REE at Lofdal come from ore deposits of magmatic, carbonatitic origin, which have been affected by hydrothermal processes. In most respects, the LACC is not particularly different from other REE-rich carbonatite complexes. The distinctive features are the emplacement as a major dyke swarm in an area of shearing, which as mentioned above may have permitted higher fluid flow in and around the dykes and almost certainly, an original magma composition enriched in HREE compared with more usual carbonatites.

Thus, the overall conclusion is that the HREE mineralisation at Lofdal is mainly related to a post-magmatic hydrothermal process which led to HREE-mineralisation in intensively fractured carbonatite dykes as well as in fenitised country rocks by mixing of hot magmatic-derived fluids with a cool meteoric fluid.

Exploration for bedrock HREE enriched systems can represent both magmatic and/or hydrothermal ore types, independent of the source or type of mineralizing fluid, a tentative model is put forward to account for the petrographic evidence, such as the presence of REE-bearing minerals. Fluid infiltration into the country rocks and fracture structure of the host rocks and the intrusions of the dyke systems are the features to search for. It is also important to explore alkaline complexes (e.g., alkaline-or carbonatite-associated), that show characteristics of better constrained types of REE deposits and reworking of late stage hydrothermal activities.

Radioactivity was very useful in exploration at Lofdal as elevated levels of thorium provided an excellent guide for exploration and often pinpoints areas of high HREE potential. A key point about exploration targeting is to not be constrained to the main plutonic areas of carbonatite, searching away from the main area of intrusions, following shear zones and fault structures may be fruitful in finding the next Lofdal.

Abbreviations

BGR – Bundesanstalt für Geowissenschaften und Rohstoffe (BGR)

CL - Cathodoluminescence

EPMA - Electron probe microanalysis

FCC - Fluid Catalytic Cracking

GSN - Geological Survey of Namibia

HREE - Heavy Rare Earth Elements

LREE - Light Rare Earth Elements

IAGS - The Institute for the Analysis of Global Security

IMCOA - Industrial Minerals Company of Australia Pty Ltd

IUGS - International Union of Geological Sciences

IUPAC - International Union of Pure and Applied Chemistry

MREE - Medium Rare Earth Elements

NdFeB - Neodymium Iron Boron magnets

NHM - Natural History Museum

NiMH - Nickel–Metal Hydride

NRE – Namibia Rare Earths

PDB - Peedee Belemnite

REE- Rare Earth Elements

REO - Rare Earth Oxide

SMOW - Standard Mean Ocean Water

SEM - Scanning Electron Microscope

TMR - Technology Metals Research

USGS – United States Geological Survey

VPDB - Vienna Pee Dee Belemnite

VSMOW - Vienna Standard Mean Ocean Water

List of Appendices

Appendix 1 List of samples collected by the author and methods used for the mineral studies

Appendix 2 a) Chemical composition analysis of samples collected by Etruscan and Namibia Rare Earth (Pty) Ltd (NRE) and used in this study (see attached CD).

Appendix 2 b) Trace elements analysis of samples collected by Etruscan and Namibia Rare Earth (Pty) Ltd (NRE) and used in this study (see attached CD).

Appendix 3 a) Descriptions of VNP samples; collected by the author based on carbonatite and alkalic rocks lithologies (see attached CD).

Appendix 3 b) Descriptions and radiometric data of VNP samples collected by the author based on carbonatite and alkalic rocks lithologies (see attached CD).

Appendix 4 Chemical composition analysis of Lofdal samples

Appendix 5 Chemical composition analysis of Mesopotamia Lofdal samples

Appendix 6 Chemical composition analysis of Minerals from Lofdal samples

Appendix 7 Laser ablation analysis of trace elements for Lofdal mineral samples

Appendix 8 Lofdal carbonatite samples 114, 119, 881G, 881R, 1569, 15769G, 15769LG, ZC and ZS sent to BGR for analysis_22Feb10

Appendix 9 Lofdal carbonatite samples 08_058, 115, 189, 269, 326, 813, 907, 914, 924, 927 and 949 sent to BGR for analysis_10Aug09

Appendix 10 Chemical composition analysis of Dicker Willem and Keishohe samples

Appendix 11 Chemical composition analysis of Agate Mountain and Teufelskuppe samples

Appendix 12 Reference data and December xenotimesö

Appendix 13 Mineral crystallization sequence in the syenites

References

Allsopp, H.L., Köstlin, E.O., Welke, H.J. (1979). Rb-Sr and U-Pb geochronology of the Late Precambrian – Early Paleozoic igneous activity in the Richterveld (South Africa) and South West Africa. Trans.geol.Soc. South Africa, vol. 82, pp. 185-204.

Allsopp, H.L., Manton, W.I., Bristow, J.W., and Erlank A.J. (1984b). Rb-Sr geochronology of Karoo felsic volcanics, in Petrogenesis of the Volcanic Rocks of the Karoo Province, edited by A.J. Erlank, Spec. Publ. Geol. Soc. .S. Afr., vol. 13, pp. 273-280.

Anders, E. and Grevesse, N. (1989). Abundances of the elements: Meteoritic and solar. Geochimica et Cosmochimica Acta, vol. 53, pp. 197–214.

Andrade, F.R.D.D., Moller, P., Dulski, P. (2002). Zr/Hf in carbonatites and alkaline rocks: new data and a re-evaluation. Rev. Brasil. Geocience vol. 32 (3), pp. 361–370.

Antignano, A., Manning, C.E., 2008a. Fluorapatite solubility in H2O and H2O–NaCl at 700 to 900 °C amd at 0.7 to 2.0 GPa. Chemical Geology 251, 112–119.

Airborne Earth Science Workshop, JPL Pub. 96-4, Vol. 1. AVIRIS Workshop, Jet Propulsion Laboratory, California Institute of Technology, Pasadena, Calif., p.63-66

Bailey, D.K. (1993). Carbonate magmas. J. Geol. Soc., London, vol. 150, pp. 637-651.

Barker, D.S. (1989) Field relations of carbonatites. Pp 38 – 69 in: K. Bell, editor, Carbonatites: genesis and evolution, Unwin Hyman, London.

Barker, D.S. and Nixon, P.H. (1989). High-Ca, low-alkali carbonatite volcanism at Fort Portal, Uganda. Contributions to Mineralogy and Petrology, vol. 103, pp. 166-177.

Barbour, E.A. (1982). Lofdal project-prospecting grant M46/3/1320, Khorixas area, Damaraland. Unpublished Report, 7 pp.

Barker D. S. (1989). Field-relations of carbonatite. K. Bell (Ed.), *Carbonatites: Genesis and Evolution* London: Unwin Hyma, pp. 38-69.

Barker, D.S. (2001). Calculated silica activities in carbonatite liquids. Contributions to Mineralogy and Petrology, vol. 141, pp. 704-709.

Bau, M. (1996). Controls on the fractionation of isovalent trace elements in magmatic and aqueous systems; evidence from Y/Ho, Zr/Hf, and lanthanide tetrad effect. Contributions to Mineralogy and Petrology, vol. 123, pp. 323-333.

Bauer, D., Diamond, D., Li, J., Sandalow, D., Telleen, P. and Wanner, B. (2010). Critical Materials Strategy, Department of Energy,

http://www.energy.gov/news/documents/criticalmaterialsstrategy.pdf

Bell, K. and Blenkinsop, J. (1989). Neodymium and strontium isotope geochemistry of carbonatites. In: Bell K., editor. Carbonatites: Genesis and Evolution. Unwin Hyman, London, pp. 278-300.

Bell, K. (1998). Radiogenic Isotope Constraints on Relationships between Carbonatites and Associated Silicate Rocks—a Brief Review Petrology, vol. 39 (11-12), 1987-1996.

Bell, K. and Rukhlov, A.S. (2004). Carbonatites from the Kola Alkaline Province: origin, evolution and source characteristics. In F. Z. Wall (Ed.), *Phoscorites and Carbonatites from Mantle to Mine: the Key Example of the Kola Alkaline Province.* Mineralogical Society of Great Britain & Ireland, pp. 433-468.

Bernard-Griffiths, J., Peucat, J-J., Fourcade, S. (1988). Origin and evolution of 2 Ga old carbonatite complex (Ihouhaouene, Ahaggar, Algeria): Nd and Sr isotopic evidence. Contribution to mineralogy and petrology vol. 100 (3), pp. 339 – 348, DOI: 10. 1007/BF00379743.

Bingen, B., Demaiffe, D., Hertogen, J., 1996. Redistribution of rare earth elements, thorium and uranium over accessory minerals in the course of amphibolite to granulite-facies metamorphism: the role of apatite and monazite in orthogneisses from southwestern Norway. Geochimica et Cosmochimica Acta 60, 1341–1354.

Birkett, T.C. and Simandl, G.J. (1999). Carbonatite-associated Deposits: Magmatic, Replacement and Residual; in Selected British Columbia Mineral Deposit Profiles, British Columbia Ministry of Energy and Mines, Industrial Minerals, vol. 3.

Boardman, J. W. and Kruse, F. A. (1994). Automated spectral analysis: a geologic example using AVIRIS data, north Grapevine Mountains, Nevada. Proceedings of the Tenth Thematic Conference on Geologic Remote Sensing Ann Arbor, Environ. Res. Inst. Of Michigan, pp. I407 – I418.

Boardman, J.W. and Huntington, J.H. (1996). Mineral mapping with 1995 AVIRIS data: in Summaries of the 6th Annual JPL Airborne Earth Science Workshop, AVIRIS Workshop, Jet Propulsion Laboratory, California Institute of Technology, Pasadena, Calif., JPL Pub. 96-4, vol. 1, pp. 9-11.

Boctor, N.Z., Nixon, P.H., Bukley, F. and Boyd, F. R. (1984). Proceedings of "The Third International Kimberlite Conference" "Petrology of Carbonate Tuff from Melkfontein, East Griqualand, Southern Africa". Elsevier Amsterdam- Oxford- New York- Tokyo, vol. 1.

Bosse, V., Boulvais, P., Gautier, P., Tiepolo, M., Ruffet, G., Devidal, J.L., Cherneva, Z., Gerdjikov, I., Paquette, J.L., 2009. Fluid-induced disturbance of the monazite Th–Pb chronometer: in situ dating and element mapping in pegmatites from the Rhodope (Greece, Bulgaria). Chemical Geology 261, 286–302.

Bottrell, S.H., Yardley, B.W.D., 1988. The composition of a primary granite-derived ore fluid from S.W. England, determined by fluid inclusion analysis. Geochimica et Cerny, P., 1991. Rare-element granitic pegmatites. Part I: anatomy and internal evolution of pegmatite deposits. Geoscience Canada 18, 49–67.

Brady A. E. and Moore K. R. (*2012)* A mantle-derived dolomite silicocarbonatite from the southwest coast of Ireland *Mineralogical Magazine, April 2012, Vol. 76(2), pp. 357–376.*

British Geological Survey, (2010). Rare Earth Elements: Mineral profile. 45pp. http://www.bgs.ac.uk/mineralsuk/home.html

Bühn, B., Dorr, W. & Brauns, C.M. (2001): Petrology and age of the Otjisazu carbonatite complex, Namibia: implications for the pre-and synorogenic Damaran evolution. *J.Afr. Earth Sci.* **32**, 1-17.

Burger, A.J., Von Knorr, O. and Clifford, T.N. (1965). Mineralogical and Radiometric Studies of Monazite and Sphene Occurrences in Namib Desert South-West Africa. Mineral. Mag., vol. **35**, pp. 519-528.

Campbell, L.S. (1998). Zircon-fluid interaction in the Bayan Obo REE-Nb-Fe ore deposit, Inner Mongolia, China. *In* Water-Rock Interaction (G.B. Arehart & J.R. Hulston, eds) Proceedings of the 9th International Symposium on Water-Rock Interaction, Balkema, Rotterdam, pp. 521-523.

Castor, S.B ,(2008), The Mountain Pass rare-earth carbonatite and associated ultrapotassic rocks, California: Canadian Mineralogist, v. 46, no. 4, p. 779-806.

Cesbron, F., 1989. Mineralogy of the rare-earth elements. In: Möller, P., Cerny, P., Saupe, F. (Eds.), Lanthanides, Tantalum and Niobium. Mineralogy, Geochemistry, Characteristics of Primary Ore Deposits, Prospecting, Processing, and Applications. Springer-Verlag, pp. 3–26.

Chakhmouradian, A. R. (2004). Crystal chemistry and paragenesis of compositionally unique (Al-, Fe-, Nb-, and Zr-rich) titanite from Afrikanda, Russia. American Mineralogist, vol. 89 (11-12), pp. 1752-1762.

Chakhmouradian, A. R. (2006). High-field-strength elements in carbonatitic rocks; geochemistry, crystal chemistry and significance for constraining the sources of carbonatites. Chemical Geology, vol. 235 (1-2), pp. 138-160.

Chakhmouradian, A. R. and Zaitsev, A. N. (2002). Calcite-amphibole-clinopyroxene rock from the Afrikanda Complex, Kola Peninsula, Russia; mineralogy and a possible link to carbonatites; III, Silicate minerals. The Canadian Mineralogist, vol. 40 (5), pp. 1347-1274.

Chao, E.C.T., Back, J.M., Minkin, J.A., Tatsumoto, M., Wang Junwen, Conrad, J.E., McKee, E.H., Hou Zonglin, Meng Qingrun, and Huang Shengguang, 1997, The sedimentary carbonate-hosted giant Bayan Obo REE-Fe-Nb ore deposit of Inner

Mongolia, China - a cornerstone.example for giant polymetallic ore deposits of hydrothermal origin: U.S. Geological Survey Bulletin 2143, 65 p.

China Rare Earth Industry Report, (2006). Research in China, http://www.researchinchina.com/report/Material/3536.html

Clark, A.M. (1984). Mineralogy of the rare earth elements. In: Henderson, P. (Ed.), Rare Earth Element Geochemistry, Developments in Geochemistry, Elsevier, Amsterdam, vol. 2, pp. 33–61.

Clark, R. N., Swayze, G. A., Rowan, L. C., Livo, K.E. and Watson, K. (1996). Mapping surficial geology, vegetation communities, and environmental materials in our national parks: The USGS imaging spectroscopy integrated geology, ecosystems, and environmental mapping project: in Summaries of the 6th Annual JPL Airborne Earth Science Workshop.. AVIRIS Workshop, Jet Propulsion Laboratory, California Institute of Technology, Pasadena, Calif., JPL Pub. 96-4, vol. 1, pp. 55-56.

Concept paper on Rare Earth Element, source:

www.c-tempo.org/studies/Rare_Earth_paper.pdf

Comin-Chiaramonti, P. & Gomes, C.B., 1996. Alkaline magmatism in Central-Eastern Paraguay. Relationships with coeval magmatism in Brazil. Edusp/Fapesp, São Paulo, Brazil, 432 pp.

Cooper, A.F. and Reid, D.L. (1998). Nepheline sövites as parental magmas in carbonatite complexes: evidence from Dicker Willem, Southwest Namibia. Journal of Petrology, vol. 39 (11-12), pp. 2123-2136.

Corfu, F., Hanchar, J.M., Hoskin, P.W.O. and Kinny, P. (2003). Atlas of zircon textures. Reviews in Mineralogy and Geochemistry, vol. 53, pp. 469-500.

Coward, M.P. (1981). The junction between Panafrican mobile belts in Namibia: its structural history. Tectonophysics, vol. 76, pp. 59-73.

Cox K.G., Bell, J.D. and Pankhurst, R.J. (1979). The interpretation of igneous rocks. London, Alien, Unwin. 450pp.

Crowley, J. K. (1993). Mapping playa evaporite minerals with AVIRIS data: a first report from Death Valley, CA. Remote Sensing of Environment, vol. 44, pp. 337– 356.

Crowley, J. K., and Zimbelman, d. R.,(1996) Mapping hydrothermally altered rock on Mount Rainier, Washington: Application of AVIRIS data to volcanic hazard assessments: in Summaries of the 6th Annual JPL

Cullers, R.L., Graf, J.L. (1984). Rare earth elements in igneous rocks of thecontinental crust: predominantly basic and ultrabasicrocks. In: Henderson, P. (ed) Rare earth element geochemistry, Developments in geochemistry, Elsevier Amsterdam, vol. 2, pp. 237–274.

Dawson, J.B. (1966). Oldoinyo Lengai – an active volcano with sodium carbonatite lava flows, In: Tuttle, O.F., and Gittins, J., Ed's, 1966, Carbonatites, John Wiley and Sons Ltd., Great Britain.

Dean B. Peter and Dean I. Kirsti (1996), Sir Johan Gadolin of Turku: The Grandfather of Gadolinium [Published in *Academic Radiology*, 1996, Aug;3 Suppl 2:S165-9.

De Aza A.H., Pena P., and De Aza S., "Ternary System Al_2O_3–MgO–CaO: Part I, Primary Phase Field of Crystallization of Spinel in the Subsystem $MgAl_2O$–$CaAl_4O_7$–CaO–MgO," J. Am. Ceram. Soc., 82 [8] 2193–203 (1999).

De Kock, G.S., Eglington, B., Armstrong, R.A., Harmer, R.E. and Walraven, F., (2000). U–Pb and Pb–Pb ages of the Naauwpoort rhyolite, Kawakeup leptite and Okongava diorite: implications for the onset of rifting and orogenesis in the Damara belt, Namibia. Commun. Geol. Surv. Namib., vol. 12, pp. 81–88.

Deer. W.A., Howie, R.A. and Zussman, J. (1992). An introduction to the rockforming minerals (2nd ed.), Longman, Essex, UK.

Deines, P. (1989). Stable isotope variations in carbonatites. In Carbonatites: Genesis and Evolution (K. Bell, Ed.). Unwin Hyman, London, pp. 301-359.

Demény, A., Sitnikova, M.A. and Karchevsky, P.I. (2004). Stable C and O isotope compositions of carbonatite complexes of the Kola Alkaline Province: phoscorite–carbonatite relationships and source compositions. In F. Z. Wall (Ed.), Phoscorites and Carbonatites from Mantle to Mine: the Key Example of the Kola Alkaline Province, Mineralogical Society, London, pp. 407-431.

Dempster, T.J., Hay, D.C., Gordon, S.H. and Kelly, N.M. (2008). Micro-zircon: origin and evolution during metamorphism. Journal of Metamorphic Geology, vol. 26, pp. 499-507.

Dooley, T. and McClay, K. R. (1997). Analog modeling of pull-apart basins. AAPG Bulletin, vol. 81(11), pp. 1804–1826.

Ducea, M.N., Saleeby, J., Morrison, J., Valencia, V.A., 2005.љ Subducted carbonates, metasomatism of mantle wedges, and possible connections to diamond formation: An example from California.љ American Mineralogist 90, 864-870.

Dunai, T., Stoessel, G.F.U. and Ziegler, U.R.F. (1989). A Sr isotope study of the Eureka Carbonatite, Damaraland, Namibia. Communications of the Geological Survey of South West Africa/Namibia = Mededelinge van die Geologiese Opname van Suidwes-Afrika/Namibe, vol. 5, pp. 89-90.

Dupuy, C., Liotard, J.M. and Dostal, J. (1992). Zr/Hf fractionation in intraplate basaltic rocks: carbonate metasomatism in the mantle source. Geochim. Cosmochin. Acta, vol. 56, pp. 2417-2423.

D¨urr, S.B. and Dingeldey, D.P. (1996). The Kaoko belt (Namibia): part of a late Neoproterozoic continental-scale strike-slip system. Geology, vol. 24, pp. 503–506.

Ehlers E . G. and Blatt H. (1982) -Petrology. Freeman, San Francisco.

Eriksson, S.C., (1989), Phalaborwa: A saga of magmatism, metasomatism and miscibility, in Bell, K., ed., Carbonatites: Genesis and evolution: London, Unwin Hyman, p. 221–254.

Exley, R. A. (1980). Microprobe studies of REE-rich accessory minerals: Implications for Skye granite petrogenesis and REE mobility in hydrothermal systems. Earth Planet. Sci. Lett., vol. 48, pp. 97-110.

Ferguson, J., Martin, H., Nicolaysen, L.O. and Dunchin, R.V. (1975). Gross Brukkaros: a kimberlite-carbonatite volcano. Physics and Chemistry of the Earth, vol. 9, pp. 219-234.

Finch, R.J. and Hanchar, J.M. (2003). Structure and Chemistry of Zircon and Zircon-Group Minerals. In Zircon (J.M. Hanchar and P.W.O. Hoskin, eds.), Rev. Mineral., vol. 53, pp. 1-25.

Fletcher, I.R., Mcnaughton, N.J., Aleinikoff, J.A., Rasmussen, B. and Kamo, S.L (2004). Improved calibration procedures and new standards for U-Pb and Th-Pb dating of Phanerozoic xenotime-(Y) by ion microprobe. Chemical Geology, vol. 209, pp. 295-314.

Foley, S.F., Venturelli, G., Green, D.H. and Toscani, L. (1987). The ultrapotassic rocks: characteristics, classification, and constraints for petrogenetic models. Earth Sci. Rev., vol. 24, pp. 81–134.

Förster, H-J. (1998).The chemical composition of REE-Y-Th-U-rich accessory minerals in peraluminous granites of the Erzgebirge-Fichtelgebirge region, Germany. Part II: Xenotime-(Y). Am. Mineral., vol. 83, pp.1302-1315.

Frets, D.C. (1969). Geology and structure of the Huab-Welwitschia area, South West Africa. Bulletin Precambrian Research Unit, University of Cape Town, vol.5, pp. 1-235.

Frezzotti, M.L., Touret, J. L.R. and Neumann, E. R. (2002). Ephemeral carbonate melts in the upper mantle: carbonate-silicate immiscibility in microveins and inclusions within spinel peridotite xenoliths, La Gomera, Canary Islands. European Journal of Mineralogy, vol.14 (5), pp. 891-904.

Frimmel, H.E., and Hartnady, C.J.H. (1992). The significance of blue amphiboles for the metamorphic history of the Pan-African Gariep Belt, Namibia. Precambrian Research Unit Information Circular No. 5, pp. 1 – 27.

Gadolin J. (1794), Examination of a black, dense mineral from the Ytterby Quarry in Roslagen. Proceedings of the Royal Academy (Stockholm, new series) (in the original Swedish: Undersökning af en svart tung Stenart ifrån Ytterby Stenbrott i Roslagen. K Vetenskaps-akad nya handl) 1794;15:137-155.

Geisler, T., Rashwan, A. A., Rahn, M.K., Poller, U., Zwingmann, H., Pidgeon, R.T., Schleicher, H. and Tomaschenk, F. (2003). Low-temperature hydrothermal alteration of natural metamict zircons from the Eastern Desert, Egypt. Mineralogical Magazine, vol. 67 (3), pp. 485–508.

Geisler, T., Schaltegger, U. and Tomaschek, F. (2007). Re equilibration of zircon in aqueous fluids and melts. Elements, vol. 3 (1), pp. 43–50.

Gieré R (1996). Formation of rare earth minerals in hydrothermal systems. In: Jones AP, Wall F, Williams T (eds) Rare Earth Minerals: Chemistry, Origin and Ore deposits. Mineralogical Society Series 7, pp 105-150.

Gittins. J. and Harmer, R.E. (1997). What is ferrocarbonatite? A revised classification, J. Afr. Earth Sci., vol. 25, pp. 159-168.

Gittins, J., and Harmer, R. E. (2003). Myth and reality in the carbonatite – silicate rock "association". Periodico di Mineralogia, vol. 72, pp. 19-26.

Gleason, J.D., Miller, C.V., Wooden, J.L. and Bennett, V.C. (1994). Petrogenesis of the highly potassic 1.42 Ga Barrel Spring pluton, southeastern California, with implications for mid-Proterozoicmagma genesis in the southwestern USA. Contributions to Mineralogy and Petrology, vol. 118, pp. 182–197.

Goetz, A. F. H., Vane, G., Solomon, J. E., and Rock, B. N.,(1985), Imaging spectrometry for earth remote sensing: Science, 228, 1147-1153.

Goldschmidt V.M. (1937). The principles of distribution of chemical elements in minerals and rocks. J. Chem. Soc., pp. 655-673.

Goodfellow W.D. 2006 Natural Resources Canada Http://gsc.nrcan.gc.ca/mindep/

Gordon, B.H., James, B. H. and Greta, J.O. (2002). Rare Earth Elements—Critical Resources for High Technology. U.S. Geological Survey Fact Sheet 087-02.

Gorobets, B.S. Androgojine, A.A. (2002). Luminescent spectra of minerals. Moscow, 300 pp.

Goscombe, B.D., Hand, M. and Gray, D. (2003a). Structure of the Kaoko Belt, Namibia: progressive evolution of a classic transpressional orogen. J. Struct. Geol., vol. 25, pp. 1049–1081.

Goscombe, B.D., Hand, M., Gray, D. and Mawby, J. (2003b). The metamorphic architecture of a transpressional orogen: the Kaoko Belt, Namibia. J. Petrol., vol. 44, pp. 676–711.

Gratz, R., Heinrich, W., (1997). Monazite–xenotime thermobarometry: experimental calibration of the miscibility gap in the binary system CePO4–YPO4. American Mineralogist 82, 772–780.

Great Western Minerals Group (Rare Earth Elements), The Crow Bar Financial Forum, http://crowlee.proboards.com/index.cgi?board=miningcompanies&action=display&thread=1027

Gromet, L.P. and Silver, L.T. (1983). Rare-earth element distributions among minerals in a granodiorite and their petrogenetic implications. Geochimica et Cosmochimica Acta, vol. 47, pp. 925-939.

Gunthorpe, R.J., Buerger, A.D., (1986). Geology and economic evaluation of the Otjisazu alkaline igneous complex, central South West Africa/Namibia. In: Anhaeusser, C.R., Maske, S. (Eds.), Mineral Deposits of Southern Africa. Geological Society South Africa, Johannesburg, pp. 2255-2260.

Gupta K. C. and Krishnamurthy N. (2004), Extractive Metallurgy of Rare Earths, CRC Press Print ISBN: 978-0-415-33340-5.

Haas J. R., Shock E. L. and Sassani D. C. (1995) Rare earth elements in hydrothermal systems: estimates of standard partial molar thermodynamic properties of aqueous complexes of the rare earth elements at high pressures and temperatures. Geochim. Cosmochim. Acta 59, 4329–4350.

Hamilton D L, Kjarsgaard B A. The immiscibility of silicate and carbonate melts. South Africa Journal of Geology 1993;96:139-142.

Harmer, R. E. (1999). The petrogenetic association of carbonatite and alkaline magmatism: constraints from the Spitskop Complex, South Africa. Journal of Petrology, vol. 40 (4), pp. 525-548.

Harmer, R. E. and Gittins, J. (1998). The case of primary, mantle-derived carbonatite magma. Journal of Petrology, vol. 39 (11-12), pp. 1895-1903.

Harrison, T. M. and Watson, E.B. (1983): Kinetics of zircon dissolution and zirconium diffusion in granitic melts of variable water content. Contrib. Mineral. Petrol. Vol. 84, pp. 66-72.

Hawkesworth, C.J., Gledhill, A.R., Roddick, J.C., Miller, R. MCG. and Kröner, (1983). Rb-Sr and 40Ar/39Ar studies bearing on models for the thermal evolution of the Damara Belt, Namibia. *In*: Evolution of the Damara Orogen of South West Africa/Namibia (R. McG. Miller, ed.) Publication of the Geological Society of South Africa, Johannesburg, S.A., vol. 11, pp. 323-338.

Heath, D. C., and Toerien, D. K., (1965). A cryptovolcanic structure on Hatzium II 28, South West. Africa: South Africa Geol. Survey, Annals, v. 1, for 1962, p. 81-85.

Hetherington, C.J., Harlov, D.E., 2008. Metasomatic thorite and uraninite inclusions in xenotime and monazite from granitic pegmatites, Hidra anorthosite massif, southwestern Norway: mechanics and fluid chemistry. American Mineralogist 93, 806–820.

Hoffman, P.F., Hawkins, D.P., Isachsen, C.E. and Bowring, S.A. (1996). Precise U-Pb zircon ages for early Damaran magmatism in the Summas Mountains and Welwitschia Inlier, northern Damara belt, Namibia: Geol. Surv. Namibia Commun., vol. 11, pp. 47-52**.**

Horstwood, M.S.A., Foster, G.L., Parrish, R.R., Noble, S.R. and Nowell, G.M. (2003). Common-Pb corrected in situ U-Pb accessory mineral geochronology by LA-MC-ICP-MS. Journal of Analytical Atomic Spectrometry, vol. 8, pp. 837-846.

Hoskin, P.W.O. (2005). Trace-element composition of hydrothermal zircons and the alteration of Hadean zircon from the Jack Hills, Australia. Geochimica et Cosmochimica Acta, vol. 69 (3), pp. 637–648.

Hurst, C. (2010). China's Grip Tightens on Rare-Earth Metal Neodymium. Asia Times, June 29, 2009. fmso.leavenworth.army.mil/documents/rareearth.pdf

http://www.etruscan.com/i/pdf/2009-01-15_NR.pdf

Janse, A.A (1969). Gross Brukkaros, a probable carbonative volcano in the Nama plateau of South West Africa. Bull. Geol. Soc. Am., 80: 573-586.

Japan International Cooperation Agency - Metal Mining Agency of Japan, (1995). Report on the mineral exploration in the Orange and Kalkfeld areas, the Republic of Namibia.

Jeffries, T.E., Fernandez-Suarez, J., Corfu, F., and Alonso, G.G. (2003): Advances in U-Pb geochronology using a frequency quintupled Nd : YAG 25 based laser ablation system (lambda=213 nm) and quadrupole based ICP-MS. *Journal of Analytical Atomic Spectrometry*, **18**, 847-855.

Jochum, K.P., Seufert, M.H., Spettel, B., Palme, H., 1986. The solar system abundances of Nb, Ta and Y and the relative abundances of refractory lithophile elements in differentiated planetary bodies. Geochim. Cosmochim. Acta 50, 1173–1183.

Johnson, L.H., Jones, A.P., Church, A.A. and Taylor, W.R. (1997) ultramafic xenoliths and megacrysts from a melilitite tuff cone, Deeti, northern Tanzania.*Journal of African Earth Sciences*, 25, 29 - 42.

Judith Chegwidden, and Suzanne Shaw, (2011). Rare Earths: The Uncertainities of Supply. Roskill Information Services Ltd., Institute for the Analysis of Global Security (IAGS), http://www.iags.org/

Jung, S. and Mezger, K. (2003). Petrology of basement-dominated terranes: I. Regional metamorphic T-t path from U–Pb monazite and Sm–Nd garnet chronology (Central Damara orogen, Namibia). Chem. Geol., vol. 198, pp. 223–247.

Jung, S., Hoffer, E. and Hoernes S. (2007). Neo-Proterozoic rift-related syenites (Northern Damara Belt, Namibia): Geochemical and Nd–Sr–Pb–O isotope constraints for mantle sources and petrogenesis. Lithos, vol. 96, pp. 415–435.

Kanazawa, Y. and Kamitani, M. (2006). Rare earth minerals and resources in the world. Journal of alloys and compounds, vol 408 – 412, pp. 1339 – 1343.

Keller, J. (1981). Carbonatitic volcanism in the Kaiserstuhl alkaline complex: Evidence for highly fluid carbonatitic melts at the Earth's surface: Journal of Volcanology and Geothermal Research, vol. 9, pp. 423-431.

Keller, J. (1989). Extrusive carbonatites and their significance. In: Bell, K. (Ed.), Carbonatites: Genesis and Evolution. Unwin Hyman, London, pp. 70– 88.

Kempe, U. and Götze, J. (2002). Cathodoluminescence (CL) behaviour and crystal chemistry of apatite from rare-metal deposits. Mineralogical Magazine, vol. 66, pp. 135-156.

Kempe, U., Gruner, T., Renno, A.D., Wolf, D. and Rene, M. (2004). Discussion on Wang et al. (2000) 'Chemistry of Hf-rich zircons from the Laoshan I- and A-type granites, Eastern China'. Mineral. Mag, vol. 68, pp. 669-675.

Kjarsgaard, B.A. and Hamilton, D.L. (1989). The genesis of carbonatites by immiscibility. In K. Bell (Ed.), Carbonatites; Genesis and Evolution, Unwin Hyman, London, pp. 388-404.

King, B.C. and Sutherland, D.L. (1960). Alkaline rocks of eastern and southern Africa. Science Progress vol. 47, pp. 298–321, 504–524 and 709–720.

Kröner, A. (1982). Rb – Sr geochronology and tectonic evolution of the pan African Damara Belt of Namibia, southwestern Africa. Am. J. Sci., vol. 282, pp. 1471-1507.

Kruse, F. A. (1988). Use of airborne imaging spectrometer data to map minerals associated with hydrothermally altered rocks in the northern Grapevine Mountains, Nevada– California. Remote Sensing of Environment, vol. 24, pp. 31– 52.

Kruse, F. A., Lefkoff, A. B., Boardman, J. B., Heidebreicht, K. B., Shapiro, A. T., Barloon, P. J. and Goetz, A.F.H. (1993). The Spectral Image Processing System (SIPS)—interactive visualization and analsis of imaging spectrometer data. Remote Sensing of Environment, vol. 44, pp. 145– 163.

Kynicky, J., Smith, M.P. and Xu, C. (2012) Diversity of rare earth deposits: the key example of China. Elements, 8, 361-367.

Lang, H. R., Adams, S. L., Conel, J. E., McGuffie, B. A., Paylor, E. D., and Walker, R. E., 1987,Multispectral remote sensing as stratigraphic tool, Wind River Basin and Big Horn Basin areas, Wyoming: American Association of Petroleum Geologists Bulletin, 71, 4, 389-402.

Lapido-Loureiro, F.E. (1973). Carbonatitos de Angola. Memórias e Trabalhos do Instituto de Investigação Cientifica de Angola, vol. 11.

Lapin, A.V. and Vartiainen, H. (1983). Orbicular and spherulitic carbonatites from Sokli and Vuorijärvi. Lithos, vol. 16, pp. 53-60.

Le Bas, M. J. (1987). Nephelinites and carbonatites. In J. G. Fitton, and B. G. Upton (Eds.) Proceedings of Rare Earths'04 MS. International Journal of Mass Spectrometry, vol. 253, pp. 87-97.

Le Bas, M.J. (1997): Standard Rare Earth Element Compositions for Sovitic and Alvikitic Carbonatites. In: Geochemical Studies on Synthetic and Natural Rock Systems. (Felicitation volume in honour of Professor Kenzo Yagi), (A.K. Gupta, K. Onuma and M. Arima, eds.), Allied Publishers, New Delhi, India, pp. 104-125.

Le Bas, M.J. (1999). Sovite and alvikite; two chemically distinct calciocarbonatites C1 and C2. S. Afr. J. Geol., vol.102, pp.109 – 121.

Le Bas, M.J. (1980). The east African Cenozoic magmatic province., Academia Nazionale dei Lincei, v. 47, p. 111 – 122.

Lee, W.-J., Wyllie, P. J. & Rossman, G. R. (1994). CO2-rich glass, round calcite crystals and no liquid immiscibility in the system CaO–SiO2–CO2 at 2·5 GPa. American Mineralogist 79, 1135–1144.

Lee, W.L. and Wyllie, P.J. (1997). Liquid immiscibility between nephelinite and carbonatite from 1.0 to 2.5 Ga compared with mantle melt compositions. Contrib. Mineral. Petrol., vol. 127, pp. 1-16.

Lee, W.J. and Wyllie, P.J. (1998a). Petrogenesis of carbonatite magmas from mantle to crust, constrained by the system CaO–(MgO+FeO□)–(Na_2O+K_2O)–(SiO_2+Al_2O_3+TiO_2)–CO_2. J. Petrol., vol. 39, pp. 495–517.

Lee, W.J. and Wyllie, P.J. (1998b). Processes of crustal carbonatite formation by liquid immiscibility and differentiation, elucidated bymodel systems. J. Petrol., vol. 39, pp. 2005–2013.

Lehmann B, Nakai S, Höhndorf A, Brinckmann J, Dulski P, Hein UF, Masuda A (1994) REE mineralization at Gakara, Burundi: Evidence for anomalous upper mantle in the western Rift Valley. Geochimica et Cosmochimica Acta 58: 985-992.

Le Maitre, R. (Ed.). (2002). Igneous Rocks: A Classification and Glossary of Terms. Cambridge University Press, Cambridge.

Le Roex, A.P., Watkins, R.T. and Reid, A.M. (1996). Geochemical evolution of the Okenyenya sub-volcanic ring complex, northwestern Namibia. Geol. Mag., vol. 133, pp. 645-670.

Le Roex, A.P. and Lanyon, R. (1998). Isotope and Trace Element Geochemistry of Cretaceous Damaraland Lamprophyres and Carbonatites, Northwestern Namibia: Evidence for Plume-Lithosphere Interactions. J. Petrol., vol. 39, pp. 1117-1146.

Littmann, S., Romer, R. L. & Okrusch, M. (2000). Nephelinsyenite der Epembe–Swartbooisdrif-Alkali-Provinz (ESAP)/NW Namibia. Berichte der Deutschen Mineralogischen Gesellschaft, Beihefte zum European Journal of Mineralogy 12, 115.

Lloyd, F.E., Woolley, A.R., Stoppa, F. and Eby, G.N. (2002) Phlogopite-biotite parageneses from the K-mafic-carbonatite effusive magmatic association of Katwe-Kikorongo, SW Uganda. *Mineralogy andPetrology*, 74, 299- 322.

Lottermoser, B.G., 1992. Rare earth elements and hydrothermal ore formation processes. Ore Geology Reviews 7, 25–41.

Luo Y. R. and Byrne R. H. (2001) Yttrium and rare earth element complexation by chloride ions at 25 _C. J. Solut. Chem. 30, 837–845.

Mariano, A.N. and Ring, P.J. (1975). Europium-activated cathodoluminescence in minerals. Geochim. Cosmochim. Acta, vol. 39, pp. 649-660.

Mariano, A.N. (1988). Cathodoluminescence spectra of rare earth element activators in minerals. In: Marshall, D.J., Cathodoluminescence of geological materials, Unwin Hyman, Boston, pp. 339-348.

Mariano, A.N. (1989). Nature of economic mineralisation in carbonatites and related rocks. *In* Carbonatites Genesis and Evolution (K. Bell, ed.) Unwin Hyman, Ltd., London, U.K., pp. 149-176.

Mariano, A.N. (1989b): Economic Geology of Rare Earth Minerals. In Geochemistry and Mineralogy of Rare Earth Elements (B.R. Lipman and G.A. KcKay, Eds), Reviews in Mineralogy, Mineralogical Society of America, vol. 21, pp. 303-337.

Mariano, A.N. (1989). Cathodoluminescence emission spectra of rare earth elements activators in minerals, Geochemistry and Mineralogy of Rare Earth Elements. Reviews in Mineralogy, Mineralogical Society of America, vol. 21, pp. 309–-348.

Marc Humphries, (2012). Rare Earth Elements: The Global Supply Chain. Congressional Research Service, www.crs.gov.

Marsh JS (1972). Relationships between transform directions and alkaline igneous rock lineaments in Africa and South America. Earth Planet. Lett., 18:317-323.

Marsh, J.S. (1973). Relationships between transform directions and alkaline igneous rock lineaments in Africa and South America. Earth and Planetary Science Letters, vol. 18, pp. 317-323.

Marshall, D.J. (1988). Cathodoluminescence of geological Materials. Unwin Hyman, Boston, 146 pp.

McDonough, W. F. and Sun, S.S. (1995). The composition of the Earth. Chemical Geology, vol. 120 (3-4), pp. 223-253.

McCulloch, M. T., JacquesA, . L, Nelson, D. R. and Lewis, J. D. (1983) Nd and Sr isotopes in kimberlites and lamproites from Western Australia: an enriched mantle origin. Nature, 3O2,4W- 403.

Meinert, L. (2012). Mineral Resources Supply and Information with a Focus on Rare Earth Elements, Workshop on: "Informed policy-making through improved mineral raw materials data". Mineral Resources Program, USGS, US-EU, http://ec.europa.eu/enterprise/policies/raw-materials/files/docs/eu-us-meinert2_en.pdf

Menge, G.F.W. (1986). Sodalite carbonatite deposits of Swartbooisdrif, South West Africa/Namibia. In: Anhaeuser CR, (S. Maske, ed.) Mineral deposits of southern Africa, Geol. Soc. S. Afr., Johannesburg, pp. 2261–2268.

Migdisov AA, Williams-Jones AE, Wagner T (2009) An experimental study of the solubility and speciation of the Rare Earth Elements (III) in fl uoride- and chloride-bearing aqueous solutions at temperatures up to 300 ºC. Geochimica et Cosmochimica Acta 73: 7087-7109.

Miller, C., Schuster, R., Klözli, U., Frank, W. and Purtscheller, F. (1999). Post-collisional potassic and ultrapotassic magmatism in SW Tibet: geochemical and Sr–Nd–Pb–O isotopic constraints for mantle source characteristics and petrogenesis. J. Petrol., vol. 40, pp. 1399–1424.

Miller, R. McG. (1980). Geology of a portion of central Damaraland, South West Africa/Namibia. Mem. Geol. Surv. S. Afr., S.W.Afr., ser. 6, 78 pp.

Miller, R. McG. (1983). The Pan-African Damara orogen of South West Africa/Namibia. In Evolution of the Damara Orogen of South West Africa/Namibia (R. McG., Miller, Ed., 1983), Special Publication, Geological Society of South Africa, No. 11, pp. 431-515.

Miller, R. McG. and Burger, A.J. (1983). U-Pb zircon age of the early Damaran Naauwpoort formation. In Evolution of the Damara Orogen of South West Africa/Namibia (R. McG., Miller, Ed., 1983), Special Publication, Geological Society of South Africa, , No.11, pp. 267-272.

Miller, R. McG. (2008). The geology of Namibia. Ministry of Mines and Energy, Geological Survey of Namibia, Namibia, vol. 1,2 and 3.

Milner, S.C., Le Roex, A.P. and O'Connor, J.M. (1995). Age of Mesozoic Igneous Rocks in Northwestern Namibia, and Their Relationship to Continental Breakup. J. Geol. Soc., vol. 152, pp. 97-104.

Milner S.C. and Le Roex, A.P. (1996). Isotope characteristics of the Okenyenya igneous complex northwestern Namibia: constraints on the composition of the early Trisan plume and the origin of the EMI mantle component. Earth and Planetary Science Letters, vol. 141, pp. 277-291.

Ministry of Industry and Information Technology (August 17, 2009). Ministry of Industry and Information Technology Draws Red Line for Rare Earth Exports; Elementary Materials Remain Prohibited for Export," http://www.Sina.com/ [Chinese].

Mineral prices, (31 December 2012). http://www.mineralprices.com/

Mitchell, R. (2005). Carbonatites and carbonatites and carbonatites. The Canadian Mineralogist, vol. 43 (6), pp. 2049-2068. Alkaline Igneous Rocks, Geological Society Special Publications, Geological Society of London, London, vol.30, pp. 53-83.

Monecke, T., Herzig, P.M., Kempe, U., Dulski, P., 2003. Rare earth element mobility during hydrothermal alteration in the footwall of the Waterloo VHMS deposit, Australia. In: Eliopoulos, D.G., et al. (Ed.), Mineral Exploration and Sustainable Development. Vol. 1. Millpress, Rotterdam, pp. 163–166.

Moore, Meghan, Chakhmouradian, Anton, Mariano, Anthony, Sidhu, Ravinder, Evolution of rare-earth mineralization in the Bear Lodge Carbonatite, Wyoming: Mineralogical and isotopic evidence, *Ore Geology Reviews* (2014.

Murali, A.V., Parthasarathy, R., Mahadevan, T.M. and Sankar Das, M. (1983). Trace element characteristics, REE patterns and partition coefficients of zircons from different geological environments – a case study on Indian zircons. Geoch.

Murkowski Lisa, (2009). Reliable domestic rare earths supply critical to US clean energy development. Washington, D.C. im. Cosmochim Acta, vol. 47, pp. 2047–2052.

Nakamura N. (1974), "Determination of REE, Ba, Fe, Mg, Na, and K in carbonaceous and ordinary chondrites", Geochimica et Cosmochimica Acta 38, 757-775.

Ngwenya, TB (1994). Hydrothermal rare earth mineralisation in carbonatites of the Tundulu complex, Malawi: Processes at the fluid/rock interface Geochim Cosmochim Acta 58, 2061-2072.

Nelson, D.R., Chivas, A.R., Chappell, B.V. and McCulloch, M.T. (1988). Geochemical and isotopic systematic in carbonatites and implications for the evolution of ocean-island sources. Geochim. Cosmochim. Acta, vol. 52, pp. 1-17.

Neumann, H. (1985). Norges Mineraler, Norges Geologiske Undersøkelse – Universitetesforlaget, Skrifter 68.

Nielsen, T.F. and Veksler, I.V. (2002). Is natrocarbonatite a cognate fluid condensate? Contrib. Mineral Petrol., vol. 142 (4), pp. 425- 435.

Notholt, A.J.G., Highley, D.E. and Deans, T., (1990). Economic minerals in carbonatites and associated alkaline rocks. Trans. Inst. Min. Metall., 99: B59-B80.

O'Connor, D. 2010. Petrogenesis of Nepheline Syenites and Phonolites from the Lofdal Intrusive Complex, Kunene Region, Namibia. Unpublished B.Sc (Honours) Thesis., Dalhousie University, Halifax, NS, Canada 103p.

O'Neil, J.R. (1983). Water-rock interactions along active fault zones in California. Symposium on Water-Rock Interaction, Misasa, Japan (extended abstract), pp. 381-384.

Oliver NHS, Pearson PJ, Holcombe RJ, Ord A (1999) Mary Kathleen metamorphic hydrothermal uranium – rare-earth element deposit: Ore genesis and numerical model of coupled deformation and fluid flow. Australian Journal of Earth Sciences 46: 467-484.

Orris, G.J. and Grauch, R.I. (2002). Rare Earth Element Mines, Deposits, and Occurrences. USGS Open-File Rep., 174, pp. 2-189.

Pan, Y.M., Fleet, M.E., 2002. Compositions of the apatite-group minerals: substitution mechanisms and controlling factors. Reviews in Mineralogy and Geochemistry 48, 13–49.

Panina and Motorina, Geochemistry International, 2008, Vol. 46, No. 5, pp. 448-464

Passchier, C.W., Trouw, R.A.J., Ribeiro, A. and Paciullo, F.V.P. (2002). Tectonic evolution of the southern Kaoko Belt, Namibia. J. Afr. Earth Sci., vol. 35, pp. 61–75.

Pearson RG (1963) Hard and soft acids and bases. Journal of the American Chemical Society 85: 3533-3539.

Peccerillo, A. & Taylor, S. R. (1976). Geochemistry of Eocene calc-alkaline volcanic rocks from the Kastamonu area, Northern Turkey. Contributions to Mineralogy and Petrology 58,

Pell, J. (1996). Mineral deposits associated with carbonatites and related alkaline igneous rocks. In Undersaturated Alkaline Rocks; Mineralogy, Petrogenesis, and Economic Potential (R. Mitchell, Ed.), Mineralogical Association of Canada Short Course, pp. 271-310.

Pell, J. and Hey, T. (1989). Carbonatites in a continental margin environment - the Canadian Cordillera. In Carbonatites - Genesis and evolution (K. Bell, Ed.), Unwin Hyman, London, pp. 200-220.

Pidgeon, R.T., O'Neil, J.R. and Silver, L.T. (1966). Uranium and lead isotopic stability in metamict zircon under experimental hydrothermal conditions. Science, vol. 154, pp. 1538-1540.

Pieters, C. M., and Mustard, J. M., (1988), Exploration of Crustal/Mantle Material for the Earth and Moon Unsing Reflectance Spectroscopy: Remote Sensing of Environment, v. 24, p. 151 - 178.

Pieterse G. M. (2011). Rare Earths Elements Letter, a publication by Goldletter International, P.O. Box 76988, 1070 KG Amsterdam, the Netherlands.

Philippot, P., Selverstone, J., 1991. Trace element-rich brines in eclogitic veins: implications for fluid compositions and transport during subduction. Contributions to Mineralogy and Petrology 106, 417–430.

Pirajno F (1994). Mineral resources of anorogenic alkaline complexes in Namibia: A review. Austral. J. Earth Sci., 41:157-168.

Pirajno F (1998) Geology and mineral deposits of Namibia, Australian Institute of Geoscience Bulletin 25: 61 -66.

Pirajno, F. (2004a). Hotspots and mantle plumes: Global intraplate tectonics, magmatism and ore deposits. Mineralogy and Petrology, vol. 82, pp. 183-216.

Poitrasson, F., Chenery, S., Bland, D.J., 1996. Contrasted monazite hydrothermal alteration mechanisms and their geochemical implications. Earth and Planetary Science Letters 145, 79–96.

Poitrasson, F., Chenery, S., Shepherd, T.J., 2000. Electron microprobe and LA-ICP-MS study of monazite hydrothermal alteration: implications for U–Th–Pb geochronology and nuclear ceramics. Geochimica et Cosmochimica Acta 64, 3283–3297.

Potts, P. J., Bowles, J. F., Reed, S. J. and Cave, M. R. (1995). Microprobe Techniques in the Earth Sciences. The Mineralogical Society Series, Chapman and Hall, vol. 6.

Pourtier, E., Devidal, J.L., Gibert, F., 2010. Solubility measurements of synthetic neodymium monazite as a function of temperature ar 2 kbars, and aqueous neodymium speciation in equilibrium with monazite. Geochimica et Cosmochimica Acta 74, 1872–1891.

Prins, P. (1981). The geochemical evolution of the alkaline and carbonatite complexes of the Damaraland igneous province, South West Africa. Annales Universiteit Stellenbosch, vol.3 (A1), pp. 145–278.

Pui-Kwan, T. (2011). China's Rare-Earth Industry. Open–File Report, USGS, pp. 2011–1042.

Rankama, K. and Sahama, Th.G. (1950). Geochemistry 4th Edition, 1960. University of Chicago Press, Chicago, 912 pp.

Rankin AH (2005) Carbonatite-associated rare metal deposits: composition and evolution of ore-forming fluids – the fluid inclusion evidence. In: Linnen RL, Samson IM (eds) Geological Association of Canada, Short Course Notes 17, pp 299-314.

Rasmussen, B. (2005). Zircon growth in very low grade metasedimentary rocks: evidence for zirconium mobility at ~250 ºC. Contributions to Mineralogy and Petrology, vol. 150, pp. 146-155.

Rass, I.T. (1998). Geochemical features of carbonatite indicative of the composition, evolution, and differentiation of their mantle magmas. Geochem. Int., vol. 36, pp. 107-116.

Reeder, R.J. (1983). Carbonates: mineralogy and geochemistry. Reviews in Mineralogy and Geochemistry, vol. 11, p. 367.

Reid, D.L, Cooper, A., Rex, D.C., and Harmer, R.E (1990). Timing of alkaline magmatism in southern Namibia. Geological Magazine, vol. 129, pp. 400-409.

Reguir E.P., Chakhmouradian A.R., Halden N.M., Malkovets V.G. & Yang P. (2009) Major- and trace-element compositional variation of phlogopite from kimberlites and carbonatites as a petrogenetic indicator. Lithos, 112S, 372-384.

Renne, P. R., Ernesto, M., Pacc, I. G., Coe, R. S., Glen, J. M., Prevot, M. and Perrin, M. (1992). The age of Paraná flood volcanism, rifting of Gondwanaland, and the Jurassic-Crateceous boundary. Science, vol. 258, pp. 975-979.

Roland, Y., Cox, S., Boullier, A.M., Pennacchioni, G., Mancktelow, N., 2003. Rare earth and trace element mobility in mid-crustal shear zones: insights from the Mont Blanc Massif (Western Alps). Earth and Planetary Science Letters 214, 203–219.

Romans, P, A., Brown, L. L., and White, J. C. (1975). An electron microprobe study of yttrium, rare earth, and phosphorus distributions in zoned and ordinary zircon. Amer. Mineral., vol. 60, pp. 475.

Roskill, (2007). The economics of rare earths and yttrium. Roskill information Services Limited, 13th edition.

Rudnick, R. L., McDonough, W. F. and Chappell, B. W. (1993). Carbonatite metasomatism in the northern Tanzanian mantle: petrographic and geochemical characteristics. Earth and Planetary ScienceLetters vol. 114, pp. 463–476.

Salvi S. and Williams-Jones A. E. (1990) The role of hydrothermal processes in the granite-hosted Zr, Y, REE deposit at Strange Lake, Quebec/Labrador: Evidence from fluid inclusions. Geochim. Cosmochim. Acta 54, 2403–2418.

Samoilov, V.S. (1984). Geochemistry of Carbonatites. Nauka, Moscow, Russia.

Santos, R. V. and Clayton, R. N. (1995). Variations of oxygen and carbon isotopes in carbonatites: A study of Brazilian alkaline complexes. Geochimica et Cosmochimica Acta, vol. 59 (7), pp. 1339-1352.

Schijf J, Byrne RH (1999) Determination of stability constants for the mono- and difluoro-complexes of Y and the REE, using a cation-exchange resin and ICP-MS. Polyhedron 18: 2839-2844.

http://www.mineweb.com/mineweb/content/en/mineweb-whats-new?oid=91107&sn=Detail

Schmidt, C., Rickers, K., Bilderback, D.H., Huang, R., 2007. In situ synchrotron radiation XRF study of REE phosphate dissolution in aqueous fluids to 800 °C. Lithos 95, 87–102.

Schneider, G. (2008). The Roadside Geology of Namibia. Gebrüder Borntraeger, Stuttgart, Germany, 2nd edition.

Schommarz, R.E. (1988). Preliminary report on the Marinkas Quelle carbonatite complex. Unpubl. Economic Mineral rep., Geol. Surv. Namibia.

Schönenberger J., Köhler J. and Markl G. (2008) REE systematics of fluorides, calcite and siderite in peralkaline plutonic rocks from the Gardar Province, South Greenland. Chem. Geol. 247, 16–35.

Schreuder, C.P. (1975). Carbonate-bearing eruptives between the Great Karas Mountains and the Bremen Igneous Complex, South West Africa. Unpubl. M.Sc. thesis, Univ. Stellenbosch, 66 pp.

Scogings, A.J. and Forster, I.F. (1989). Gneissose carbonatites in the Bulls Run Complex, Natal. S. Afr. J. Geol., 92, 1-10.

Seth, B., Kröner, A., Mezger, K., Nemchin, A.A., Pidgeon, R.T. and Okrusch, M. (19980. Archaean to Neoproterozoic magmatic events in the Kaoko belt of NW Namibia and their geodynamic significance. Precambrian Res., vol. 92, pp. 341–363.

Seydoux-Guillaume, A.-M., Paquette, J.-L., Wiedenbeck, M., Montel, J.-M., Heinrich, W., 2002. Experimental resetting of the U–Th–Pb systems in monazite. Chemical Geology 191, 165–181.

Shannon, R.D. (1976). Revised effective ionic radii and systematic studies of interatomic distances in halides and chalcogenides. Acta Crystallogr., A32, pp. 751-767.

Shaw Suzanne and Chegwidden Judith (2011) Global drivers for rare earth demand, Roskill Information Services.

Siedner G. and Mitchell J. G. (1976) Episodic Mesozoic volcanism in Namibia and Brazil: a K–Ar isochron study bearing on the opening of the South Atlantic. Earth and Planetary Science Letters, vol. 30, pp. 292-302.

Silva, L.C., Le Bas, M.J., Robertson, A.H.F., 1981. An oceanic carbonatite volcano on São Tiago, Cape Verde Islands. Nature 294, 644–645. Staudacher, T., Allègre, C.J., 1982. Terrestrial xenology. Earth Planet. Sci. Lett. 60, 389–406.

Sindern, S., Zaitsev, A. N., Demény, A., Bell, K., Chakhmouradian, A. R., Kramm, U., et al. (2004). Mineralogy and geochemistry of silicate dyke rocks associated with carbonatites from the Khibina complex (Kola, Russia) - isotope constraints on genesis and small-scale mantle sources. Contributions to Mineralogy and Petrology, vol. 80, pp. 215-239.

Smith, M.P., and Henderson, P., 2000, Preliminary fluid inclusion constraints on fluid evolution in the Bayan Obo Fe- REE-Nb deposit, Inner Mongolia, China: Economic Geology, v. 95, p. 1371-1388.

Smith, M.P., Henderson, P and Campbell L. S. (2000). Fractionation of the REE during hydrothermal processes: Constraints from the Bayan Obo Fe-REE-Nb deposit, Inner Mongolia, China. Geochimica et Cosmochimica Acta, Vol. 64, No. 18, pp. 3141–3160.

Smith, S.R., Foster, G.L., Romer, R.L., Tindle, A.G., Kelley, S.P., Noble, S.R., Horstwood, M. and Breaks, F.W. (2004). U-Pb columbite-tantalite chronology of rare-

element pegmatites using TIMS and laser ablation-multi collector-ICP-MS. Contrib. Mineral. Petrol., vol. 147, pp. 549-564.

Smithies, R.H., Marsh, J.S. (1998) The Marinkas Quellen carbonatite complex, southern Namibia: carbonatite magmatism with an uncontaminated depleted mantle signature in a continental setting. Chem Geol, vol. 148, pp. 201–212.

Spear, F.S. and Pyle, J.M. (2002). Apatite, monazite, and xenotime-(Y) in metamorphic rocks. In Phosphates - Geochemical, Geobiological, and Materials Importance (Kohn, M.J., Rakovan, J., Hughes, J.M., Eds.), Reviews in Mineralogy and Geochemistry, vol. 48, pp. 293– 335.

Speer, J. A. (1980). Zircon. Reviews in Mineralogy (P. H. Ribbe, ed.), Mineral. Soc. Amer., vol. 5, pp. 67-112.

Storey, C.D., Jeffries, T.E. and Smith, M. (2006). Common lead corrected laser ablation ICP-MS systematics and geochronology of titanite. Chemical Geology, vol. 227, pp. 37-52.

Taylor, H. P., Frechen, J. and Degens, E.T. (1967). Oxygen and carbon isotope studies of carbonatites from the Laacher See District, West Germany and the Alnö District, Sweden. Geochimica et Cosmochimica Acta, vol. 31 (3), pp. 407-430.

Technology Metals Research, LLC (2011). Rare Earth Demand Rises, No Supply Increase Seen Outside China. *www.techmetalsresearch.com*

Tegtmeyer, A., Kröner, A., 1985. U–Pb zircon ages for granitoid gneisses in northern Namibia and their significance for Proterozoic crustal evolution of southwestern Africa. Precambrian Res., vol. 28, pp. 311–326.

Thompson, R.N., Smith, P.M., Gibson, S.A., Mattey, D.P. and Dicken, A.P. (2002). Ankerite carbonatite from Swartbooisdrif, Namibia: the first evidence for magmatic ferrocarbonatite. Contrib. Mineral. Petrol., vol. 143, pp. 377-395.

Tom Vulcan (04 November 2008) “Rare Earth Metals: Not So Rare, But Still Valuable”, Features and Interviews *www.HardAssetsInvestor.com*

Townsend, K.J., Miller, C.F., D'Andrea, J.L., Ayers, J.C., Harrison, T.M., Coath, C.D., 2000. Low-temperature replacement of monazite in the Ireteba granite, southern Nevada: geochronological implications. Chemical Geology 172, 95–112.

Treiman, A.H. and Essene, E.J. (1984). A periclase-dolomite-calcite carbonatite from the Oka complex, Quebec, and its calculated volatile composition. Contrib. Mineral. Petrol., vol. 85, pp. 149–157.

Treiman, A.H. (1989). Carbonatite magma: properties and processes. InCarbonatites: genesis and evolution (K. Bell, ed). Unwin Hyman, London, pp. 89–104.

Trocellier, P. and Delmas, R. (2001). Chemical durability of Zircon. Nucl. Instr. and Meth. in Phys. Res., vol. 181, pp. 408-412.

Tropper Peter a,b,□, Manning Craig E. b and Harlov Daniel E. (2011). Solubility of CePO4 monazite and YPO4 xenotime in H2O and H2O–NaCl at 800 °C and 1 GPa: Implications for REE and Y transport during high-grade metamorphism Chemical Geology 282 58–66.

Turner, S.P., Regelous, M., Kelley, S., Hawkesworth, C.J., and Mantovani, M.S.M. (1994). Magmatism and continental break-up in the South Atlantic: high precision $^{40}Ar/^{39}Ar$ geochronology. Earth Planet. Sci. Lett.., vol. 121, pp. 333-348.

Vallini, D., Rasmussen, B., Krapez, B., Fletcher, I. R. and McNaughton, N. J. (2002). Obtaining diagenetic ages from metamorphosed sedimentary rocks: U-Pb-dating of unusually coarse xenotime-(Y) cement in phosphatic sandstone. Geology, vol. 30 (12), pp. 1083–1086.

Van Alstine, R. E. and Schruben, P. G. (1980). Fluorspar re-sources of Africa. Geol Surv. Bull., no. 1487, pp. 1–25.

Van Wambeke L. (1977), The Karonge rare earth deposits, Republic of Burundi: New mineralogy-geochemical data and origin of the mineralisation. Mineralum Deposita, 12, 373 – 380.

Van Zijl, P.J. (1962). The Geology, structure and petrology of the alkaline intrusions of Kalkfeld and Okorusu and the invaded Damara rocks. Ann. Univ. Stellenbosch., Ser. A37, pp. 237-340.

Verwoerd, W.J. (1967). The carbonatites of South Africa and South West Africa. Department of Mines, Government Printer, Pretoria, Handbook 6.

Verwoerd, W. J., (1986) Mineral deposits associated with carbonatites and alkaline rocks. In: Mineral deposits of Southern Africa. Vol. II. 2173-2191. Edited by: Annhaeusser and Maske, Geological Society of South Africa.

Verwoerd, W.J. (1993). Update on carbonatites of South Africa and Namibia, South African Journal of Geology, vol. 96 (3), pp. 75-95.

Vichi, G., Stoppa, F. and Wall, F. (2005). The carbonate fraction in carbonatitic Italian lamprophyres. Lithos, vol. 85, pp. 154-170.

Voloshin, A.V., Subbotin, V.V., Yakovenchuk, V.V., Paghomovsky, YA.A., Men'shikov, Y.U.P. and Zaitsev, A.N. (1990). Mckelveyite from carbonatites and hydrothermalites of alkaline rocks, the Kola Peninsula (the first findings in the USSR). Zapiski Vserossiskogo Mineralogicheskogo Obshchestva, vol. 119(6), pp. 76-86.

Von Eckermann, H. (1948). The alkaline district of Alno¨ Island. Sveriges Geologiska Undersoekning, Serie Ca 36.

von Seckendorff, V., Drüppel, K., Okrusch, M., Cook, N.J., and Littmann, S. (2000): Mineralium Deposita 35, 430-450.; Drüppel, K., Hoefs, J., & Okrusch, M. (2005). Fenitizing processes induced by ferrocarbonatite magmatism at Swartbooisdrif, NW Namibia. Journal of Petrology, 46(2), 377-406.

Wall, F. and Mariano, A.N. (1996). Rare earth minerals in carbonatites: a discussion centred on the Kangankunde carbonatite, Malawi. In Rare Earth Minerals: chemistry, origin and ore deposits (A.P. Jones, F. Wall and C.T. Williams, Eds), Chapman and Hall, London, UK.

Wall, F., Bulakh, A.G., Nesterov, A.R., Zaitsev, A.N., Pilipiuk, N. and Kirillov, A.S. (2000). Sulfur-containing monazite-(Ce) from late-stage mineral assemblages at the Kandaguba and Vuoriyarvi carbonatite complexes, Kola peninula, Russia. Neues Jahrbuch fuer Mineralogie Monatschefte, vol. 2000, pp. 217-233.

Wall, F. and Zaitsev, A.N. (2004). Rare earth minerals in Kola carbonatites. In Phoscorites and Carbonatites from Mantle to Mine: the key example of the Kola

Alkaline Province (F. Wall and A.N. Zaitsev, eds.) Mineralogical Society Series, London, U.K., vol. 10, pp. 341-373.

Wall, F., Rosatelli, G. and Stoppa, F. (2005). Carbonatites plus: A special issue arising from the 'EuroCarb' ESF network. Special issue, Lithos, vol. 85 (1-4), pp. vii-viii.

Wall, F., Niku-Paavola, V.N., Storey, C., Müller, A. and Jeffries, T. (2008). Xenotime-(Y) from carbonatite dykes at Lofdal, Namibia: Unusually low LREE:HREE ratio in carbonatite, and the first dating of xenotime-(Y) overgrowths on zircon. Canadian Mineralogist, vol. 46 (4), pp. 861-877, 1251-1268.

Wallace, M.E. and Green, D.H. (1988). An experimental determination of primary carbonatite magma composition. Nature, vol. 335 (6188), pp. 343-346.

Walter A.-V., Flicoteaux R., Parron C., Loubet M., and Nahon D. (1995) Rare-earth elements and isotopes (Sr, Nd, O, C) in minerals from the Juquia carbonatite (Brazil): Tracers of a multistage evolution. *Chem. Geol.* 120, 27–44.

Walter, M.J., Bulanova, G.P., Armstrong, L.S., Keshav, S., Blundy, J.D., Gudfinnsson, G., Lord, O.T., Lennie, A.R., Clark, S.M., Smith, C.B. and Gobbo, L. (2008). Primary carbonatite melt from deeply subducted oceanic crust. Nature, vol. 454 (7204), pp. 622-625.

Wang Caifeng (2009). Speech at the 2009 Minor Metals and Rare Earths Conference, Beijing, China, September 2-3, 2009.

Watson, E.B. (1980). Some experimentally determined zircon/liquid partition coefficients for the rare earth elements. Geochim Cosmochim Acta, vol. 44, pp. 895–897.

Wayne M. Morrison, and Rachel Tang, (2012). China’s Rare Earth Industry and Export Regime: Economic and Trade Implications for the United States, CRS.

Wiendenbeck, M., Alle P., Corfu, F., Griffin, W.L., Meier, M., Oberli, F., Vonquadt, A., Roddick, J.C., and Speigel, W. (1995). 3 Natural Zircon Standards for U-Th-Pb, Lu-Hf, Trace-Element and REE Analyses. Geostandards Newsletter, vol. 19, pp. 1-23.

Williams C.T. (1996). Analysis of rare earth minerals. In Rare Earth Minerals: Chemistry, Origin and Ore Deposits (A.P. Jones, F. Wall and C.T. Williams, Eds.) Mineralogical Society Series, London, U.K. vol. 7, pp. 327-348.

Williams, I.S. (1998). Chapter 1, U-Th-Pb geochronology by ion microprobe. *In* Applications of Microanalytical Techniques to Understanding Mineralizing processes, (Mckibben, M.A., Shanks III, W.C., and Ridley, W.I., eds.) Littleton, CO. Reviews in Economic Geology, Soc. Econom. Geol. Inc., vol. 7.

Williams-Jones A. E., Samson I. M. and Olivo G. R. (2000) The genesis of hydrothermal fluorite-REE deposits in the Gallinas Mountains, New Mexico. Econ. Geol. 95, 327–341.

Williams-Jones Anthony E., Migdisov Artashes A. and Samson Iain M. (2013) Hydrothermal Mobilisation of the Rare Earth Elements – a Tale of "Ceria" and "Yttria"Cosmochimica Acta 52, 585–588.

Wood S. A. (1990a) The aqueous geochemistry of the rare-earth elements and yttrium. Theoretical predictions of speciation in hydrothermal solutions to 350 ^{C} at saturation water vapor pressure. Chem. Geol. 88, 99–125.

Wood S. A. (1990b). The aqueous geochemistry of the rare-earth elements [REE] and yttrium. 1. Review of available low temperature data for inorganic complexes and the inorganic REE speciation of natural waters. Chem. Geol. 82, 159–186.

Woolley, A.R. (1989). The spatial and temporal distribution of carbonatites. In Carbonatites: Genesis and Evolution (K. Bell, ed.), Unwin Hyman, London, pp. 15-35.

Woolley, A.R. and Kempe, D.R. (1989). Carbonatites: nomenclature, average chemical compositions, and element distribution. In Carbonatites: Genesis and Evolution (K. Bell, ed.), Unwin Hyman Ltd., London, UK, pp. 1-14.

Woolley, A.R. (1991). Extrusive carbonatites from the Uyaynah Area, United Arab Emirates. J. Petrol., vol. 32, pp. 1143- 1167.

Woolley, A.R. (2001). Alkaline Rocks and Carbonatites of the World. Part 3: Africa. Geological Society, London, UK.

Woolley, A.R. (2003). Igneous silicate rocks associated with carbonatites: their diversity, relative abundances and implications for carbonatite genesis. Periodico di Mineralogia, vol. 72, pp. 9–17.

Woolley, A.R. and Church, A.A. (2005). Extrusive carbonatites: A brief review Lithos, vol. 85(1-4), pp. 1-14.

Woolley Alan R. and Kjarsgaard Bruce A. (2008) Paragentic types of carbonatites as indicated by the diversity and relative abundances of associated silicate rocks: Evidence from global database.The Canadian Mineralogist Vol. 46, pp. 741-752

Wyllie, P.J. and Tuttle, O.F. (1960). The system $CaO-CO_2-H_2O$ and the origin of carbonatites. J. Petrol., vol. 1, pp. 1-46.

Wyllie, P.J. and Huang, W.L. (1976). Carbonation and melting reactions in the system CaO-MgO-SiO2-CO2 at mantle pressures with geophysical and petrological applications. Contributions to Mineralogy and Petrology, vol. 54, pp. 79-107.

Wyllie, P.J. (1989). Origin of carbonatites: evidence from phase equilibrium studies. In Carbonatites: genesis and evolution (K. Bell, ed). Unwin Hyman, London, pp. 500–545.

Xuewu L. aAnd Byrne Robert H. (1997) Rare earth and yttrium phosphate solubilities in aqueous solution. Geochirnica et Cosmochimica Acta, Vol. 61, No. 8, pp. 1625-1633.

Yaxley, G.M., Crawford, A.J. and Green, D.H. (1991). Evidence for carbonatite metasomatism in spinel peridotite xenoliths from western Victoria, Australia. Earth and Planetary Science Letters, vol. 107, pp. 305–317.

Yuan, Z., Bai, G. and Wu, C. (1992) Geological features and genesis of the Bayan Obo REE ore deposit, Inner Mongolia, China. Appl. Geochem., 7, 429-42.

Zaitsev, A.N., Wall, F. and Le Bas, M.J. (1998). REE-Sr-Ba minerals from the Khibina carbonatites, Kola Peninsula, Russia: their mineralogy, paragenesis and evolution. Mineralogical Magazine, vol. 62, pp. 225–250.

Zaitsev A N, Keller J, Spratt J, Jeffries T E, Sharygin V V (1980) Chemical composition of nyerereite and gregoryite from natrocarbonatites of Oldoinyo Lengai volcano, Tanzania. Geology of Ore Deposits 2009;51:608-616.

Appendix 1 List of samples collected by the author and methods used for the mineral studies

Group	Sample No.	Analytical used Methods*								
		CL	XRD	XRF	SEM	EPMA	LA-ICPMS	O, C Isotope	$^{147}Sm/^{144}Nd$	U-Pb Dating
Main-carbonatite plug and sample 269	326		X	X	X	X	X	X		
	58		X	X	X	X		X		
	269		X	X	X	X		X	X	
Emanya plug	881g		X	X	X	X	X	X		
	881R		X	X	X			X		
	949		X	X	X			X	X	
Dyke type1	813		X	X	X	X	X	X	X	xx
	15769G	X	X	X			X			
	907	X	X	X		X		X		
	115	X	X	X	X	X	X	X	X	
Dolomite	114	X	X	X	X					
	119		X	X	X	X	X	X		
Dyke type2	189		X	X	X	X	X	X	X	
	927	X	X	X	X	X	X	X		
Dyke type3	15796		X	X	X			X		
	15796G	X	X	X						
	15769		X	X	X			X		
Dyke type4	914	X	X	X	X	X		X		
Dyke type5	924				X	X		X	X	

* See chapter 5 for further details of methods used.

Appendix 2 b) Trace elements analysis of samples collected by Etruscan and NRE and used in this study

Sample No.	ER12528	ER12529	ER12530	ER12531	ER12532	ER12533	ER12534	ER12535	ER12536	ER12537	ER12538	ER12539	ER12540	ER12541	ER12542	ER12543	ER12544	ER12545
Ba	146.50	1940.00	511.00	579.00	62.20	666.00	574.00	465.00	1490.00	373.00	2070.00	426.00	446.00	581.00	1695.00	550.00	337.00	352.00
Ga	21.60	29.20	5.00	9.90	4.20	10.00	9.40	8.40	34.20	10.70	26.90	3.20	4.40	5.20	28.50	6.30	5.60	3.00
Hf	11.70	23.80	3.80	3.50	0.80	27.90	6.40	3.20	14.90	4.40	36.60	2.90	0.20	0.30	7.50	1.80	5.20	0.30
Nb	970.00	1510.00	72.30	75.40	59.80	1465.00	44.70	166.50	866.00	4720.00	2800.00	77.30	49.60	706.00	215.00	325.00	204.00	14.00
Rb	11.00	160.00	2.60	23.50	0.40	52.20	22.30	6.80	215.00	57.70	202.00	7.00	32.40	24.50	186.00	14.80	2.10	4.30
Sr	898.00	520.00	364.00	6170.00	70.40	8570.00	6560.00	9740.00	1190.00	9130.00	1920.00	15300.00	564.00	10900.00	1275.00	12500.00	11600.00	8830.00
Ta	17.70	23.90	0.90	0.50	0.40	30.20	0.70	2.40	12.50	13.40	67.50	1.10	1.10	8.20	8.20	10.00	2.00	0.20
Th	17.85	15.80	3.15	3.15	3.67	3.80	1.28	4.76	7.52	84.10	12.90	2.25	6.62	7.26	2.69	3.70	6.09	1.73
U	14.80	8.47	47.40	3.24	0.66	1.73	9.00	12.15	34.60	118.00	37.30	2.44	3.72	55.60	7.65	124.00	23.20	8.71
Zr	906.00	1870.00	270.00	137.00	29.00	2330.00	351.00	262.00	1070.00	453.00	2960.00	245.00	9.00	29.00	447.00	147.00	350.00	11.00
La	96.80	104.50	74.00	248.00	34.90	177.00	149.00	253.00	66.20	212.00	77.10	256.00	81.50	207.00	18.50	206.00	203.00	133.50
Ce	210.00	237.00	128.50	499.00	58.50	366.00	314.00	524.00	141.50	502.00	154.50	519.00	148.50	414.00	42.80	428.00	423.00	280.00
Pr	24.20	27.90	13.70	53.10	6.19	40.20	34.80	57.00	16.45	57.60	16.55	55.60	15.50	43.30	4.65	46.90	46.60	30.60
Nd	89.10	105.50	43.10	184.50	21.40	144.00	122.50	201.00	61.80	211.00	53.70	199.00	51.40	144.00	16.80	168.00	166.00	104.50
Sm	13.90	16.75	4.97	26.00	3.16	21.50	19.70	29.00	10.45	33.30	6.94	29.40	7.29	20.30	2.72	24.30	24.80	16.70
Eu	3.06	4.24	1.21	6.70	0.82	6.10	5.54	7.71	2.95	8.59	1.81	8.15	1.84	5.74	0.80	6.74	7.13	5.06
Gd	11.70	14.20	5.07	25.20	2.99	20.70	19.55	27.30	9.63	30.50	6.65	29.20	7.63	20.60	2.46	23.80	24.60	17.30
Tb	1.23	1.59	0.56	2.92	0.33	2.51	2.59	3.13	1.23	3.64	0.73	3.45	0.96	2.55	0.31	2.74	3.12	2.26
Dy	5.20	6.92	2.77	14.45	1.51	12.75	14.05	14.50	6.05	17.05	3.49	17.15	5.04	13.20	1.54	13.25	15.45	11.70
Ho	0.94	1.17	0.55	2.74	0.27	2.48	2.77	2.68	1.15	3.09	0.70	3.27	1.04	2.56	0.28	2.45	2.93	2.33
Er	2.54	3.09	1.58	7.31	0.68	6.64	7.46	6.99	2.97	7.86	2.02	8.37	3.03	7.07	0.76	6.29	7.72	6.30
Tm	0.35	0.42	0.25	1.04	0.10	0.99	1.14	0.92	0.43	1.02	0.32	1.11	0.48	1.03	0.14	0.78	1.10	0.93
Yb	2.42	3.01	1.79	6.90	0.58	6.92	7.56	5.60	2.75	6.25	2.26	6.49	3.40	6.63	0.96	4.77	7.20	6.07
Lu	0.37	0.50	0.30	0.99	0.09	1.15	1.13	0.78	0.43	0.92	0.39	0.84	0.54	0.99	0.18	0.66	1.08	0.91
Y	22.60	27.10	13.70	70.30	7.10	62.40	69.20	67.20	28.50	76.10	17.70	82.30	25.20	64.90	6.80	61.40	71.60	57.30
La/Yb	40.00	34.72	41.34	35.94	60.17	25.58	19.71	45.18	24.07	33.92	34.12	39.45	23.97	31.22	19.27	43.19	28.19	21.99

Appendix 2 b) Trace elements analysis of samples collected by Etruscan and NRE and used in this study

Sample No.	ER12546	ER12547	ER12548	ER12549	ER12550	ER12551	ER12552	ER12553	ER12554	ER12555	ER12556	ER12557	ER12558	ER12559	ER12560	ER12561	ER12562	ER12563
Ba	732.00	256.00	1320.00	244.00	583.00	782.00	385.00	641.00	537.00	1040.00	372.00	222.00	553.00	211.00	267.00	837.00	1085.00	605.00
Ga	50.50	16.60	40.30	10.40	23.40	7.00	32.00	9.00	8.50	23.50	3.90	57.10	61.70	13.40	5.00	11.60	25.60	11.20
Hf	21.00	1.20	41.20	0.60	0.40	1.70	1.90	10.40	3.30	1.20	0.60	2.00	1.00	0.70	1.60	2.30	11.60	1.60
Nb	1000.00	16.00	2620.00	76.60	5.80	5.80	98.70	225.00	222.00	146.00	100.00	26.00	40.00	5.00	40.70	69.40	344.00	51.00
Rb	325.00	24.90	232.00	70.10	23.20	12.30	2.90	33.60	3.60	7.50	2.50	9.00	77.00	4.60	1.00	9.30	21.60	0.20
Sr	4960.00	5660.00	3990.00	1370.00	2220.00	2400.00	2190.00	1320.00	2610.00	2160.00	8860.00	8710.00	8630.00	5770.00	7510.00	957.00	856.00	5730.00
Ta	16.70	0.30	73.90	0.90	0.20	0.20	0.50	1.10	1.40	0.80	0.30	1.00	0.50	0.30	0.40	1.40	3.70	0.10
Th	10.70	135.50	12.30	4.09	73.90	150.50	242.00	120.50	9.95	574.00	21.00	664.00	423.00	253.00	9.33	64.90	212.00	314.00
U	23.60	3.57	110.00	1.84	2.01	9.20	5.79	5.82	5.77	15.10	1.88	2.20	2.00	2.09	3.39	13.40	25.00	12.85
Zr	1820.00	71.00	3790.00	57.00	5.00	121.00	80.00	302.00	48.00	37.00	16.00	150.00	130.00	17.00	150.00	215.00	711.00	93.00
La	108.50	1695.00	103.50	210.00	3910.00	560.00	5920.00	633.00	816.00	3700.00	229.00	10750.00	9130.00	1625.00	282.00	765.00	348.00	1805.00
Ce	230.00	3390.00	206.00	423.00	6130.00	905.00	9210.00	1115.00	1350.00	6430.00	506.00	17500.00	14350.00	3040.00	561.00	1340.00	591.00	3150.00
Pr	26.30	349.00	22.20	45.00	499.00	87.30	739.00	102.50	118.00	571.00	58.30	1740.00	1430.00	290.00	58.90	143.00	61.30	317.00
Nd	93.70	1235.00	76.00	148.50	1415.00	282.00	2120.00	372.00	403.00	1820.00	213.00	4430.00	3700.00	987.00	200.00	477.00	204.00	1065.00
Sm	14.65	149.50	11.50	19.15	141.50	40.50	199.50	69.50	53.80	257.00	34.60	414.00	421.00	147.50	31.70	72.30	37.10	156.00
Eu	4.15	22.40	3.19	2.54	37.60	12.50	44.60	20.20	14.20	66.40	9.47	93.50	106.00	36.00	8.10	24.80	11.75	43.90
Gd	14.10	119.00	11.15	18.70	177.50	49.30	247.00	79.30	56.80	264.00	32.50	417.00	428.00	148.50	32.30	84.60	47.20	154.50
Tb	1.82	9.10	1.43	2.18	16.90	9.20	22.50	13.65	6.19	31.20	4.27	41.20	41.30	19.75	4.32	10.80	8.81	20.70
Dy	9.81	25.20	7.81	11.10	71.50	74.00	107.00	87.20	28.40	167.50	22.20	220.00	170.00	116.50	23.80	49.50	59.50	116.00
Ho	1.96	4.31	1.65	2.34	12.75	19.20	23.10	17.65	5.16	34.20	4.30	52.20	30.00	25.40	5.00	8.76	13.20	25.40
Er	5.44	14.40	4.87	6.86	33.50	63.20	68.90	47.20	13.40	95.00	11.60	153.50	78.90	73.30	13.85	23.70	41.00	80.80
Tm	0.84	1.51	0.79	1.06	3.85	11.75	9.93	6.75	1.78	13.80	1.69	21.60	9.32	11.65	2.10	2.95	5.80	11.25
Yb	5.43	10.30	5.55	7.38	22.90	87.90	65.60	39.50	10.95	88.00	11.35	101.50	44.70	80.50	13.80	17.80	35.20	66.50
Lu	0.79	1.51	0.87	1.10	3.07	13.10	9.44	5.01	1.48	12.35	1.62	13.50	5.86	11.65	1.93	2.33	4.54	8.50
Y	50.00	110.50	40.90	66.30	350.00	535.00	578.00	436.00	124.00	1010.00	112.00	1660.00	874.00	697.00	120.50	203.00	376.00	739.00
La/Yb	19.98	164.56	18.65	28.46	170.74	6.37	90.24	16.03	74.52	42.05	20.18	105.91	204.25	20.19	20.43	42.98	9.89	27.14

Appendix 2 b) Trace elements analysis of samples collected by Etruscan and NRE and used in this study

Sample No.	ER12564	ER12565	ER12566	ER12567	ER12568	ER12569	ER12570	ER12571	ER12572	ER12573	ER12574	ER12575	ER12576	ER12577	ER12578	ER12579	ER12580	ER12581
Ba	1125.00	52.50	498.00	21.50	2290.00	540.00	790.00	393.00	679.00	71.70	482.00	242.00	49.20	658.00	504.00	338.00	140.00	297.00
Ga	10.50	14.30	17.80	0.40	8.80	1.40	14.20	14.10	24.00	7.80	8.30	7.90	8.60	37.40	34.90	15.20	1.70	6.80
Hf	0.50	0.20	2.00	0.30	0.50	1.10	1.40	4.00	0.90	0.30	1.50	1.90	0.80	0.50	1.00	5.20	8.80	0.30
Nb	8.60	0.70	209.00	5.90	14.30	5.90	18.90	46.70	12.20	2.30	194.50	143.00	5.40	5.00	3.00	413.00	52.50	64.30
Rb	5.90	1.10	2.00	1.30	0.60	0.40	36.10	2.40	14.40	6.60	1.30	2.50	1.00	7.00	2.00	4.40	11.50	24.80
Sr	5890.00	699.00	10000.00	477.00	3290.00	1180.00	345.00	1115.00	3540.00	917.00	1460.00	1825.00	632.00	1265.00	1895.00	1590.00	1185.00	2310.00
Ta	0.10	0.05	0.60	0.10	0.20	0.30	0.20	0.20	0.10	0.10	0.70	0.80	0.10	0.25	0.25	7.60	0.30	0.80
Th	158.00	220.00	249.00	10.50	299.00	79.10	7.79	88.50	127.00	159.00	214.00	516.00	168.00	230.00	213.00	655.00	6940.00	28.80
U	3.45	4.66	36.30	0.63	6.70	3.38	3.87	9.46	7.80	1.81	15.30	36.60	6.35	2.60	3.40	15.80	59.90	1.73
Zr	13.00	1.00	90.00	20.00	10.00	67.00	57.00	271.00	42.00	20.00	82.00	107.00	22.00	90.00	100.00	168.00	726.00	12.00
La	1185.00	1070.00	2990.00	17.40	2000.00	15.50	8.00	1975.00	5940.00	1840.00	683.00	967.00	1085.00	6280.00	6300.00	666.00	29.60	192.50
Ce	2600.00	3080.00	4950.00	33.20	2690.00	55.60	26.10	3700.00	7320.00	2430.00	1420.00	1730.00	1970.00	11000.00	10500.00	1245.00	79.30	382.00
Pr	298.00	402.00	475.00	3.69	230.00	8.76	3.24	404.00	577.00	197.00	162.50	177.50	219.00	1205.00	1075.00	132.00	11.90	40.60
Nd	1115.00	1475.00	1490.00	13.90	627.00	43.20	13.40	1370.00	1460.00	532.00	573.00	587.00	780.00	3320.00	2790.00	453.00	68.40	134.50
Sm	162.00	213.00	181.00	5.47	65.60	31.80	4.67	177.00	112.50	49.60	88.60	78.30	146.50	405.00	310.00	126.50	177.50	22.40
Eu	40.70	54.80	49.50	2.51	22.90	12.05	1.95	43.80	28.70	14.70	26.80	25.70	36.10	91.60	75.80	65.60	93.30	6.74
Gd	137.00	160.50	181.50	6.63	102.00	34.40	6.02	148.50	143.50	61.50	80.10	93.60	120.00	358.00	332.00	223.00	268.00	22.30
Tb	16.55	13.95	19.60	1.36	20.40	5.47	1.32	16.45	10.80	7.27	12.85	17.75	18.60	28.20	33.00	44.30	44.40	3.30
Dy	82.30	41.80	86.40	9.42	145.00	25.70	8.29	69.10	40.20	36.90	76.10	111.00	125.50	89.90	140.50	234.00	213.00	17.35
Ho	17.10	6.17	16.00	2.24	34.50	4.16	1.79	12.65	8.38	7.85	16.75	24.40	32.60	15.45	27.70	40.90	35.30	3.46
Er	55.10	18.10	46.80	7.44	117.50	10.55	5.33	36.80	31.00	27.00	52.70	75.80	120.00	43.70	77.70	101.00	83.00	10.20
Tm	7.60	1.61	6.32	1.25	19.90	1.34	0.72	4.26	4.57	4.59	8.08	11.85	20.60	5.39	10.75	13.10	10.35	1.44
Yb	46.90	10.05	39.60	8.75	134.00	8.60	4.77	25.00	31.40	35.60	51.70	75.40	140.50	27.90	52.70	78.90	59.50	8.95
Lu	6.27	1.32	5.32	1.30	18.15	1.15	0.69	3.25	4.32	5.42	7.17	10.10	19.20	3.94	7.25	10.30	7.69	1.17
Y	409.00	176.00	376.00	65.20	934.00	107.00	48.40	327.00	276.00	243.00	446.00	661.00	987.00	385.00	806.00	1105.00	843.00	87.10
La/Yb	25.27	106.47	75.51	1.99	14.93	1.80	1.68	79.00	189.17	51.69	13.21	12.82	7.72	225.09	119.54	8.44	0.50	21.51

Appendix 2 b) Trace elements analysis of samples collected by Etruscan and NRE and used in this study

Sample No.	ER125582	ER125583	ER125584	ER125585	ER125586	ER125587	ER125588	ER125589	ER125590	ER125591	ER125592	ER125593	ER125594	ER125595	ER125596	ER125597	ER125598	ER125599
Ba	160.50	381.00	795.00	53.00	145.50	594.00	815.00	156.50	64.70	82.70	454.00	356.00	483.00	46.00	59.00	2500.00	374.00	3410.00
Ga	7.90	3.60	20.20	1.00	12.80	6.60	11.90	6.00	8.90	22.10	15.50	8.10	12.80	1.70	1.40	5.20	6.40	19.50
Hf	0.10	8.20	1.00	2.40	2.40	0.60	1.60	1.80	1.70	3.60	0.60	1.00	2.00	0.60	0.40	1.00	0.30	3.00
Nb	1.00	59.30	22.90	7.20	2.60	95.60	160.00	102.50	138.50	70.10	25.60	191.00	153.50	13.10	6.50	28.00	1.00	159.00
Rb	3.40	41.60	11.80	2.30	3.50	4.50	62.10	12.10	2.20	0.80	8.10	8.00	8.30	3.20	5.00	0.50	2.80	10.00
Sr	2670.00	1420.00	1150.00	477.00	2140.00	5070.00	10200.00	2720.00	1815.00	3460.00	1005.00	10000.00	1685.00	469.00	311.00	3370.00	921.00	10000.00
Ta	0.05	1.40	0.30	0.20	0.40	1.90	2.70	1.40	1.00	0.70	0.20	1.20	0.40	0.10	0.05	0.25	0.10	1.50
Th	80.70	778.00	562.00	16.30	743.00	229.00	38.80	329.00	753.00	612.00	469.00	81.40	596.00	10.70	16.00	3490.00	148.50	1550.00
U	0.82	17.20	7.01	9.34	4.56	27.20	13.20	5.01	5.25	9.02	7.03	12.30	10.25	0.65	0.87	19.20	3.11	18.20
Zr	2.00	556.00	28.00	291.00	30.00	30.00	148.00	133.00	53.00	102.00	6.00	20.00	57.00	39.00	32.00	70.00	3.00	210.00
La	1125.00	49.70	2440.00	21.20	2470.00	718.00	684.00	414.00	1005.00	3490.00	2830.00	1310.00	1850.00	13.90	116.00	860.00	1185.00	3160.00
Ce	2080.00	123.50	5220.00	59.10	3650.00	1405.00	1325.00	738.00	2100.00	5490.00	4240.00	1710.00	2950.00	24.40	211.00	1250.00	1770.00	5080.00
Pr	216.00	16.90	642.00	9.01	326.00	158.00	144.00	77.60	240.00	510.00	384.00	147.00	279.00	2.57	23.40	110.00	159.50	491.00
Nd	735.00	81.00	2550.00	43.60	970.00	557.00	501.00	278.00	925.00	1585.00	1145.00	448.00	905.00	9.60	86.20	333.00	471.00	1575.00
Sm	96.00	153.50	618.00	20.80	322.00	93.10	73.40	87.10	214.00	226.00	144.00	70.60	156.00	4.37	25.30	59.30	55.00	236.00
Eu	18.15	106.50	114.00	7.52	132.50	31.00	19.05	41.40	79.00	76.70	39.70	23.80	56.20	1.94	18.45	26.50	16.25	74.70
Gd	75.90	389.00	397.00	23.70	425.00	92.90	62.40	96.40	242.00	282.00	154.50	79.60	202.00	5.90	26.70	109.00	65.60	288.00
Tb	7.34	95.10	43.10	4.63	80.80	14.35	7.21	16.20	40.80	48.20	20.00	10.25	33.70	1.17	3.64	27.40	9.65	50.00
Dy	30.00	610.00	176.50	28.50	468.00	74.20	31.10	83.70	209.00	282.00	115.00	51.80	190.50	7.73	17.50	217.00	66.00	329.00
Ho	6.23	124.00	31.20	5.97	91.60	14.05	5.49	14.75	37.20	56.10	25.10	10.30	34.80	1.69	3.03	54.80	16.95	70.70
Er	21.90	337.00	88.90	18.05	259.00	39.40	14.90	36.90	92.20	155.00	79.50	27.80	89.50	5.26	8.04	186.50	62.50	203.00
Tm	3.33	44.20	11.25	2.79	38.10	5.19	1.63	4.58	11.05	20.10	11.45	3.62	10.50	0.79	1.05	31.40	10.50	28.80
Yb	23.60	240.00	71.60	19.00	258.00	31.90	9.67	26.60	62.50	114.50	73.20	20.10	58.60	5.27	6.55	210.00	73.80	174.50
Lu	3.42	29.50	9.65	2.75	37.10	4.32	1.30	3.45	7.96	14.65	10.05	2.58	7.43	0.75	0.87	27.00	10.55	22.50
Y	223.00	3370.00	889.00	167.00	2790.00	397.00	144.00	441.00	1020.00	1740.00	790.00	278.00	895.00	48.50	102.50	1590.00	493.00	1890.00
La/Yb	47.67	0.21	34.08	1.12	9.57	22.51	70.73	15.56	16.08	30.48	38.66	65.17	31.57	2.64	17.71	4.10	16.06	18.11

Appendix 2 b) Trace elements analysis of samples collected by Etruscan and NRE and used in this study

Sample No.	ER12600	ER12601	ER12602	ER12603	ER12604	ER12605	ER12606	ER12607	ER12608	ER12609	ER12610	ER12611	ER12612	ER12613	ER12614	ER12615	ER12616	ER12617
Ba	184.00	2110.00	457.00	241.00	794.00	600.00	1425.00	984.00	400.00	1910.00	338.00	1460.00	520.00	593.00	705.00	1910.00	463.00	209.00
Ga	10.90	8.80	8.10	7.20	9.70	3.70	29.10	35.40	9.60	13.60	31.40	11.00	11.90	5.30	21.00	15.50	16.00	32.30
Hf	1.20	1.20	1.50	0.40	6.00	2.50	5.70	2.90	39.00	3.00	4.00	2.20	4.10	3.20	2.50	1.70	9.70	3.00
Nb	2.90	138.00	108.50	3.80	96.00	122.50	74.30	110.50	188.00	242.00	88.00	65.50	20.90	110.00	127.00	23.60	175.00	52.00
Rb	0.80	1.30	0.90	0.90	15.00	27.70	6.80	9.80	2.00	3.00	4.00	11.30	2.00	2.30	7.50	7.30	3.60	6.00
Sr	391.00	981.00	3190.00	1475.00	875.00	684.00	850.00	1475.00	1220.00	1200.00	1615.00	835.00	4980.00	1575.00	8010.00	1475.00	669.00	2030.00
Ta	0.10	0.10	0.10	0.05	2.10	0.40	0.40	1.00	1.30	3.60	0.90	0.40	0.30	0.90	0.40	0.20	1.60	0.80
Th	354.00	152.50	169.50	123.00	1785.00	172.00	664.00	752.00	2740.00	1610.00	741.00	227.00	29.00	175.00	25.30	336.00	308.00	749.00
U	4.82	7.69	5.21	3.12	12.60	5.43	31.20	9.13	21.90	10.20	12.20	11.15	2.81	7.95	61.60	14.95	12.10	15.90
Zr	76.00	226.00	268.00	22.00	140.00	72.00	338.00	81.00	2050.00	50.00	170.00	126.00	155.00	275.00	98.00	82.00	853.00	190.00
La	1865.00	1895.00	1460.00	1245.00	567.00	61.80	4630.00	2740.00	917.00	1500.00	6350.00	1500.00	1295.00	604.00	3030.00	2890.00	2070.00	5750.00
Ce	2930.00	2580.00	2140.00	1860.00	965.00	176.00	8630.00	6260.00	1550.00	2670.00	9960.00	2440.00	2250.00	962.00	5600.00	4230.00	4050.00	9640.00
Pr	295.00	213.00	191.50	168.50	99.40	27.90	822.00	774.00	165.50	294.00	944.00	234.00	216.00	96.70	570.00	383.00	438.00	940.00
Nd	1040.00	599.00	571.00	500.00	384.00	152.00	2550.00	3100.00	697.00	1125.00	2600.00	776.00	687.00	322.00	1910.00	1170.00	1535.00	2610.00
Sm	203.00	63.50	78.20	59.60	205.00	105.00	330.00	682.00	1220.00	426.00	282.00	119.00	93.60	52.20	298.00	169.50	232.00	307.00
Eu	56.00	17.00	23.90	14.45	137.00	62.00	107.50	171.50	515.00	173.50	83.20	38.30	23.50	17.20	77.30	50.90	66.80	101.50
Gd	210.00	72.10	92.30	63.50	523.00	218.00	389.00	539.00	1400.00	547.00	366.00	130.50	93.60	60.30	288.00	207.00	244.00	435.00
Tb	30.30	7.56	13.95	7.83	138.50	50.00	57.80	70.40	154.50	101.50	63.10	17.70	10.90	9.96	34.90	35.20	35.70	79.80
Dy	168.50	39.10	88.40	46.10	870.00	287.00	312.00	340.00	598.00	630.00	382.00	93.80	51.90	64.60	169.00	227.00	195.00	468.00
Ho	33.80	8.29	19.45	10.85	157.50	48.10	58.00	62.00	91.50	123.00	81.00	18.35	9.98	15.00	31.10	47.10	38.00	98.70
Er	96.90	28.10	61.00	38.50	355.00	97.80	153.50	170.00	216.00	300.00	210.00	53.20	30.00	51.20	85.40	132.50	109.50	249.00
Tm	12.70	4.34	8.75	6.30	40.30	8.71	18.65	20.90	28.10	35.00	28.40	6.89	3.94	8.40	10.35	17.55	14.65	32.00
Yb	76.50	30.30	53.70	43.70	203.00	36.90	109.50	124.50	170.00	171.50	139.50	37.50	24.90	55.40	60.50	104.00	89.50	153.00
Lu	10.05	4.43	7.24	6.39	23.80	4.06	14.45	15.95	20.70	19.65	18.25	4.57	3.38	7.39	7.50	13.70	12.15	19.50
Y	1015.00	254.00	535.00	290.00	4110.00	1110.00	1415.00	1675.00	2420.00	2980.00	1960.00	520.00	244.00	451.00	709.00	1230.00	1020.00	2440.00
La/Yb	24.38	62.54	27.19	28.49	2.79	1.67	42.28	22.01	5.39	8.75	45.52	40.00	52.01	10.90	50.08	27.79	23.13	37.58

Appendix 2 b) Trace elements analysis of samples collected by Etruscan and NRE and used in this study

Sample No.	ER12618	ER12619	ER12620	ER12621	ER12622	ER12623	ER12624	ER12625	ER12626	ER12627	ER12628	ER12629	ER12630	ER12631	ER12632	ER12633	ER12634	ER12635
Ba	178.00	286.00	446.00	10000.00	865.00	539.00	40.10	88.40	560.00	2120.00	565.00	408.00	379.00	1075.00	634.00	123.00	34.30	1025.00
Ga	36.80	29.20	5.80	35.80	14.30	8.20	2.70	3.80	3.50	8.80	15.30	5.90	18.20	24.40	11.80	12.80	15.90	7.10
Hf	5.00	5.90	0.20	13.00	0.50	2.00	2.20	70.70	1.60	1.20	2.00	9.10	6.50	1.60	4.50	2.50	2.10	1.30
Nb	27.00	548.00	2.80	51.00	12.70	131.00	19.70	349.00	38.70	27.60	74.40	122.00	313.00	5.60	200.00	280.00	188.00	5.40
Rb	4.00	122.00	17.50	8.00	6.50	35.90	0.80	10.70	12.80	22.40	8.80	4.30	30.10	2.10	0.80	1.00	6.50	0.70
Sr	1490.00	309.00	9420.00	10000.00	2380.00	3210.00	524.00	625.00	506.00	1845.00	731.00	379.00	4620.00	501.00	14100.00	662.00	653.00	4160.00
Ta	0.25	2.40	0.05	0.50	0.20	0.80	0.10	1.00	0.30	0.20	0.60	0.20	4.00	0.10	0.80	1.40	1.20	0.20
Th	474.00	87.00	4.51	1150.00	43.50	1.35	26.00	725.00	24.20	107.00	980.00	477.00	101.00	581.00	270.00	468.00	714.00	466.00
U	9.80	9.04	1.76	16.30	4.31	24.20	4.27	15.40	1.93	17.10	10.10	9.55	28.60	5.20	26.40	70.50	30.60	8.62
Zr	300.00	378.00	4.00	1070.00	24.00	109.00	204.00	3890.00	52.00	21.00	32.00	547.00	486.00	82.00	400.00	110.00	81.00	82.00
La	6650.00	311.00	715.00	8420.00	3150.00	318.00	56.90	638.00	254.00	1235.00	3490.00	483.00	981.00	3890.00	1525.00	1785.00	2840.00	917.00
Ce	11000.00	467.00	1090.00	11350.00	4400.00	573.00	93.80	1060.00	460.00	2300.00	5260.00	950.00	1465.00	6620.00	2680.00	3080.00	4810.00	1355.00
Pr	1070.00	43.20	99.10	921.00	354.00	57.70	9.03	107.00	48.90	241.00	465.00	108.00	155.00	705.00	285.00	344.00	471.00	143.50
Nd	3010.00	133.50	297.00	2370.00	960.00	187.50	30.30	371.00	175.00	831.00	1370.00	411.00	450.00	1945.00	948.00	962.00	1310.00	401.00
Sm	333.00	20.40	43.90	259.00	92.80	28.00	6.06	105.50	33.20	160.50	150.50	198.00	70.20	234.00	172.00	136.50	173.50	72.20
Eu	91.30	7.11	12.60	104.50	22.70	7.87	2.56	53.10	8.69	52.10	44.50	78.50	21.90	71.90	50.60	47.40	50.00	27.50
Gd	382.00	26.00	48.70	444.00	112.00	30.50	8.93	206.00	34.00	189.00	191.00	238.00	79.70	320.00	177.00	189.00	217.00	107.00
Tb	48.70	3.99	6.50	78.00	10.60	3.86	1.93	57.10	5.74	34.50	42.90	39.00	10.05	38.00	23.50	32.20	35.50	23.50
Dy	250.00	23.80	34.90	432.00	47.20	19.25	14.00	437.00	36.20	224.00	378.00	212.00	50.40	159.50	119.00	188.50	210.00	179.00
Ho	52.60	4.94	7.04	76.30	9.32	3.89	3.42	96.30	7.91	49.50	91.50	39.40	9.79	24.10	24.10	38.00	41.30	43.20
Er	145.50	14.75	21.70	182.00	30.00	11.90	11.05	280.00	25.10	156.00	268.00	108.00	25.70	51.30	67.30	104.50	107.00	128.00
Tm	19.85	2.09	3.13	21.90	3.96	1.66	1.66	37.80	3.88	23.10	33.40	14.60	3.30	4.53	9.38	16.10	15.65	19.20
Yb	101.50	13.15	20.60	118.00	26.20	10.70	10.10	208.00	26.40	145.50	165.50	87.20	17.05	21.50	50.30	92.60	92.80	105.00
Lu	14.05	1.86	2.96	14.50	3.73	1.53	1.32	26.10	3.78	18.75	18.30	11.30	2.37	2.80	6.87	13.50	14.50	15.05
Y	1400.00	136.00	180.50	1860.00	246.00	97.40	112.50	2720.00	210.00	1185.00	2960.00	1280.00	243.00	510.00	572.00	894.00	975.00	1150.00
La/Yb	65.52	23.65	34.71	71.36	120.23	29.72	5.63	3.07	9.62	8.49	21.09	5.54	57.54	180.93	30.32	19.28	30.60	8.73

Appendix 2 b) Trace elements analysis of samples collected by Etruscan and NRE and used in this study

Sample No.	ER12636	ER12637	ER12638	ER12639	ER12640	ER12641	ER12642	ER12643	ER12644	ER12645	ER12646	ER12647	ER12648	ER12649	ER12650	ER12651	ER12652	ER12653
Ba	270.00	54.20	532.00	84.20	50.40	815.00	203.00	193.00	78.80	512.00	361.00	407.00	217.00	368.00	363.00	237.00	666.00	2920.00
Ga	10.90	15.30	7.90	10.70	2.70	12.10	10.30	9.70	7.10	20.90	2.90	3.30	10.40	4.50	3.00	8.00	7.00	5.90
Hf	3.00	0.90	0.50	0.60	0.70	4.30	1.00	0.70	0.60	0.40	0.20	0.20	2.30	0.20	0.80	2.20	0.50	1.60
Nb	101.50	24.60	63.90	112.50	6.20	81.30	16.60	69.10	38.70	4.00	2.10	1.30	464.00	2.60	215.00	61.30	3.00	85.10
Rb	20.80	1.00	0.20	17.10	2.70	1.70	10.10	5.90	15.80	1.60	0.60	7.50	1.60	1.40	2.20	2.70	2.40	6.70
Sr	2780.00	2330.00	17400.00	726.00	441.00	13000.00	356.00	567.00	411.00	869.00	15600.00	16300.00	3810.00	6910.00	4190.00	6020.00	2120.00	31200.00
Ta	2.00	0.10	0.60	0.20	0.20	0.80	0.20	0.20	0.20	0.10	0.05	0.30	4.70	0.05	0.30	0.30	0.10	0.40
Th	94.30	137.00	130.00	251.00	3.34	170.00	75.40	50.90	113.00	216.00	70.00	80.00	92.80	29.30	56.20	15.00	92.40	220.00
U	19.90	7.03	20.10	37.40	0.81	30.30	5.41	9.91	2.64	3.63	0.55	0.49	24.30	0.44	3.30	17.05	4.39	8.52
Zr	176.00	27.00	26.00	18.00	17.00	203.00	36.00	34.00	23.00	5.00	5.00	4.00	161.00	6.00	24.00	146.00	19.00	105.00
La	942.00	3000.00	982.00	1425.00	63.70	1345.00	1875.00	1660.00	665.00	4160.00	280.00	345.00	1745.00	510.00	219.00	1060.00	1075.00	1100.00
Ce	1525.00	4470.00	1950.00	2500.00	144.50	2330.00	2720.00	2530.00	1220.00	6490.00	509.00	595.00	2840.00	889.00	451.00	1890.00	1650.00	1325.00
Pr	172.50	415.00	229.00	261.00	20.80	252.00	250.00	244.00	144.50	622.00	60.50	61.50	272.00	89.80	55.00	199.00	157.00	118.00
Nd	536.00	1110.00	816.00	822.00	83.50	837.00	727.00	724.00	463.00	1680.00	183.00	187.00	836.00	279.00	206.00	647.00	469.00	355.00
Sm	98.10	159.00	141.50	117.50	39.30	146.50	142.50	114.50	89.80	204.00	32.60	28.70	105.50	42.70	49.00	100.50	67.10	59.00
Eu	26.40	43.40	35.80	31.50	13.15	45.10	47.70	34.10	23.30	49.70	10.05	9.01	31.40	13.10	15.70	31.10	20.40	20.20
Gd	100.50	179.50	115.00	122.00	54.40	159.00	194.50	138.00	91.80	213.00	34.70	31.60	114.00	45.70	45.50	101.50	75.50	68.90
Tb	11.50	19.15	14.75	15.30	12.60	26.10	28.10	17.10	13.40	18.30	4.86	4.55	14.20	6.21	7.17	13.40	11.25	9.51
Dy	48.70	88.60	74.70	76.80	84.30	158.00	147.50	80.60	76.60	61.30	25.70	23.60	67.80	30.70	38.60	63.20	65.60	46.20
Ho	8.67	18.40	15.45	14.75	18.85	33.80	29.20	15.20	16.50	10.35	5.34	4.91	13.40	6.07	7.90	12.10	15.15	9.02
Er	23.10	55.20	45.30	40.10	55.90	90.40	80.10	41.20	47.50	31.00	15.15	14.10	38.10	17.10	22.40	32.80	48.10	23.70
Tm	3.03	7.86	6.63	5.39	9.39	11.45	11.70	5.48	7.19	3.34	2.31	2.09	5.05	2.39	3.36	4.15	7.74	2.99
Yb	18.20	45.60	37.80	31.90	58.00	52.70	66.50	30.40	42.00	19.30	13.40	13.20	30.40	15.05	21.30	23.40	51.00	16.45
Lu	3.24	6.94	5.34	4.96	9.26	6.54	9.69	4.51	6.39	2.90	2.07	1.87	4.21	2.19	3.00	3.06	7.37	2.07
Y	209.00	466.00	334.00	337.00	454.00	763.00	675.00	327.00	369.00	279.00	120.50	115.50	310.00	150.50	201.00	310.00	500.00	243.00
La/Yb	51.76	65.79	25.98	44.67	1.10	25.52	28.20	54.61	15.83	215.54	20.90	26.14	57.40	33.89	10.28	45.30	21.08	66.87

Appendix 2 b) Trace elements analysis of samples collected by Etruscan and NRE and used in this study

Sample No.	ER12654	ER12655	ER12656	ER12657	ER12658	ER12659	ER12660	ER12661	ER12662	ER12663	ER12664	ER12665	ER12666	ER12667	ER12668	ER12669	ER12670	ER12671
Ba	51.50	31.70	96.90	45.40	63.00	255.00	1150.00	92.90	25.70	215.00	254.00	106.50	13.70	579.00	179.50	530.00	137.00	1540.00
Ga	7.50	1.30	4.10	17.20	1.60	7.10	10.40	6.40	3.80	11.00	14.30	4.90	3.50	5.30	9.40	9.60	5.10	8.90
Hf	2.40	0.10	1.30	1.00	1.00	2.70	2.20	0.50	0.80	2.90	1.20	1.20	0.20	0.50	0.20	0.10	0.10	0.10
Nb	44.40	20.00	40.20	25.00	107.50	385.00	126.00	7.00	199.50	88.10	302.00	60.90	44.70	3.70	299.00	95.00	1.40	18.50
Rb	5.20	1.20	22.90	1.00	12.40	7.40	12.50	0.80	11.10	8.00	30.30	0.80	1.80	4.20	25.30	57.70	2.40	10.00
Sr	324.00	552.00	397.00	394.00	441.00	4660.00	2560.00	2840.00	401.00	261.00	1000.00	1985.00	213.00	1585.00	3580.00	1015.00	1270.00	2260.00
Ta	0.30	0.10	0.40	0.25	0.90	2.30	1.80	0.20	1.00	0.70	1.30	0.30	0.10	0.30	1.00	1.50	0.20	0.20
Th	7.31	86.80	71.30	1405.00	68.50	1360.00	1030.00	35.20	63.40	192.50	138.50	18.10	6.10	179.50	119.00	27.30	1.91	109.50
U	1.29	1.56	2.13	12.60	4.03	26.30	12.80	1.10	12.35	8.73	3.15	8.83	1.02	2.48	4.86	3.53	5.85	2.70
Zr	141.00	12.00	98.00	60.00	102.00	94.00	114.00	40.00	98.00	187.00	49.00	127.00	19.00	42.00	27.00	8.00	9.00	10.00
La	13.80	247.00	227.00	4690.00	78.00	1365.00	1030.00	1285.00	815.00	26.00	2480.00	867.00	12.90	1275.00	1450.00	419.00	404.00	1005.00
Ce	26.60	370.00	330.00	9350.00	148.50	2390.00	1700.00	2140.00	1395.00	46.60	4240.00	1540.00	22.70	1825.00	2680.00	767.00	898.00	2610.00
Pr	2.99	36.40	30.80	990.00	16.65	265.00	175.50	213.00	140.50	5.33	432.00	160.50	2.51	167.50	290.00	84.00	101.50	346.00
Nd	11.40	114.00	94.40	2910.00	62.50	1055.00	571.00	638.00	468.00	21.20	1385.00	536.00	9.30	495.00	963.00	285.00	337.00	1290.00
Sm	5.56	20.00	22.10	343.00	22.70	333.00	92.60	73.80	79.40	15.35	197.50	78.30	2.51	105.00	139.00	54.00	45.10	179.00
Eu	2.51	5.86	7.74	92.50	6.98	94.90	33.70	16.15	25.50	17.90	51.50	19.95	1.07	36.80	39.40	16.60	12.00	40.50
Gd	8.18	18.35	23.00	364.00	19.75	305.00	112.00	68.80	75.10	80.00	180.50	70.80	3.36	120.50	129.50	59.10	40.20	134.00
Tb	1.89	2.44	3.56	43.30	3.47	45.20	20.30	7.95	9.54	30.80	20.00	7.76	0.62	18.85	14.10	10.20	4.77	13.45
Dy	12.60	12.75	18.75	187.00	19.70	224.00	128.00	42.40	45.00	254.00	82.90	30.80	3.71	106.00	56.00	59.20	22.80	49.90
Ho	2.85	2.69	3.63	33.60	3.78	43.10	29.20	10.20	8.66	61.80	14.65	5.38	0.78	22.60	9.77	12.65	4.85	9.27
Er	8.41	8.02	9.81	83.60	10.60	112.50	88.30	36.00	24.20	185.50	42.20	14.30	2.21	64.80	26.40	37.30	15.60	29.20
Tm	1.29	1.17	1.32	9.60	1.62	14.55	13.20	5.90	3.17	26.20	5.39	1.51	0.34	9.05	2.89	5.47	2.20	3.66
Yb	8.32	7.48	7.79	45.30	10.40	80.70	79.90	40.20	17.90	141.50	32.80	8.60	2.20	53.70	17.00	35.90	14.80	24.40
Lu	1.18	1.09	1.06	5.68	1.54	10.45	10.70	6.00	2.38	19.30	4.45	1.21	0.32	7.48	2.25	5.26	2.35	3.55
Y	83.70	72.70	104.00	827.00	86.50	1170.00	891.00	305.00	214.00	1745.00	350.00	130.00	20.80	610.00	234.00	308.00	138.50	224.00
La/Yb	1.66	33.02	29.14	103.53	7.50	16.91	12.89	31.97	45.53	0.18	75.61	100.81	5.86	23.74	85.29	11.67	27.30	41.19

Appendix 2 b) Trace elements analysis of samples collected by Etruscan and NRE and used in this study

Sample No.	ER12672	ER12673	ER12674	ER12675	ER12676	ER12677	ER12678	ER12679	ER12680	ER12681	ER12682	ER12683	ER12684	ER12685	ER12686	ER12687	ER12688	ER12689
Ba	551.00	547.00	221.00	465.00	373.00	1575.00	1100.00	313.00	544.00	436.00	370.00	612.00	859.00	291.00	943.00	265.00	111.00	624.00
Ga	5.70	7.00	17.20	8.90	4.70	9.70	11.60	7.60	46.10	7.80	9.70	8.00	4.60	5.60	4.80	4.40	36.80	7.60
Hf	7.80	2.60	1.90	0.20	0.10	0.20	0.30	0.30	0.50	0.40	1.60	16.70	0.60	0.40	0.70	0.20	0.50	0.20
Nb	36.50	44.50	93.60	39.70	0.90	32.60	11.30	60.00	24.00	12.00	69.30	236.00	8.20	11.30	23.70	3.90	20.00	10.50
Rb	4.40	6.50	4.00	58.70	10.60	6.50	5.90	13.40	6.00	12.80	23.50	16.50	7.50	5.30	10.00	1.60	1.00	1.50
Sr	5290.00	4330.00	2050.00	2690.00	1225.00	1190.00	1310.00	1415.00	1340.00	1290.00	1165.00	2260.00	2670.00	2810.00	916.00	1585.00	586.00	1370.00
Ta	0.50	0.70	0.30	0.20	0.20	0.40	0.20	0.60	0.25	0.10	0.70	1.20	0.10	0.10	0.10	0.10	0.25	0.10
Th	78.00	476.00	229.00	85.90	3.02	116.00	48.50	89.10	232.00	51.70	18.75	94.30	23.00	29.30	8.31	27.60	189.50	56.70
U	2.76	3.71	9.65	3.70	4.32	3.88	4.74	3.35	2.60	2.36	7.87	13.35	2.17	2.56	9.71	2.80	13.70	2.57
Zr	287.00	103.00	139.00	27.00	6.00	23.00	10.00	6.00	20.00	18.00	106.00	935.00	33.00	17.00	30.00	8.00	20.00	9.00
La	430.00	935.00	2850.00	616.00	263.00	1795.00	1660.00	911.00	9470.00	899.00	768.00	354.00	412.00	541.00	214.00	448.00	7740.00	1095.00
Ce	891.00	1660.00	6060.00	1300.00	546.00	3400.00	2580.00	1465.00	13800.00	1460.00	1225.00	716.00	782.00	920.00	388.00	770.00	11000.00	1690.00
Pr	102.50	170.00	672.00	159.00	61.90	357.00	262.00	158.50	1260.00	159.00	123.00	95.40	96.70	103.50	42.70	90.40	983.00	174.00
Nd	359.00	539.00	2310.00	582.00	215.00	1090.00	737.00	469.00	3330.00	471.00	370.00	339.00	316.00	305.00	143.00	287.00	2550.00	486.00
Sm	64.90	90.10	307.00	90.80	34.60	113.00	69.10	59.60	249.00	56.60	46.60	69.10	49.80	33.40	26.40	41.60	197.00	49.00
Eu	22.10	34.80	67.80	22.20	11.65	26.90	15.50	17.35	56.60	14.20	12.90	22.40	13.45	7.96	8.99	11.20	46.40	11.00
Gd	69.30	126.00	245.00	76.30	34.50	105.00	75.80	70.90	340.00	59.80	48.60	78.20	48.60	34.50	28.50	41.80	265.00	51.50
Tb	9.81	21.40	18.60	8.30	4.73	8.93	6.95	10.85	19.55	7.33	5.75	14.75	6.53	3.77	4.47	5.26	15.20	4.55
Dy	48.80	112.00	48.20	33.10	24.10	32.60	27.70	63.60	48.50	37.00	27.30	90.30	31.80	17.90	23.10	24.90	36.40	18.15
Ho	9.54	20.60	8.72	6.16	4.81	6.75	5.53	13.20	8.05	7.64	5.49	18.75	6.06	3.85	4.54	4.94	5.66	4.00
Er	28.10	52.70	33.90	17.85	14.10	22.90	19.30	39.40	31.80	23.60	16.65	53.00	18.20	13.35	13.20	15.40	23.10	15.95
Tm	3.96	6.78	4.20	2.26	2.03	3.02	2.72	5.35	2.76	3.22	2.17	7.08	2.57	2.20	1.81	2.18	2.01	2.83
Yb	25.50	41.00	28.30	14.25	12.55	19.90	18.30	30.10	19.00	19.20	12.65	38.00	15.90	15.85	11.40	13.65	16.30	21.80
Lu	3.60	5.73	4.12	2.14	1.88	3.00	3.07	4.53	2.79	2.91	1.85	5.42	2.48	2.76	1.77	2.14	2.56	3.95
Y	255.00	590.00	218.00	170.00	122.00	172.50	140.00	323.00	184.00	192.00	157.50	379.00	153.00	104.00	131.00	125.00	132.00	103.00
La/Yb	16.86	22.80	100.71	43.23	20.96	90.20	90.71	30.27	498.42	46.82	60.71	9.32	25.91	34.13	18.77	32.82	474.85	50.23

Appendix 2 b) Trace elements analysis of samples collected by Etruscan and NRE and used in this study

Sample No.	ER12690	ER12691	ER12692	ER12693	ER12694	ER12695	ER12696	ER12697	ER12698	ER12699	ER12700	ER12701	ER12702	ER12703	ER12704	ER12705	ER12706	ER12707
Ba	751.00	252.00	139.00	1280.00	1390.00	938.00	593.00	1010.00	448.00	801.00	565.00	75.60	91.50	37.10	133.50	34.90	187.50	47.10
Ga	8.50	6.00	31.00	20.90	12.00	4.10	4.10	4.70	15.60	5.20	22.50	2.80	3.60	2.60	1.00	1.20	3.70	1.00
Hf	0.30	1.10	0.90	3.30	0.50	0.20	0.90	0.20	4.40	0.50	0.80	0.50	1.00	0.20	0.30	0.40	0.90	0.30
Nb	3.90	19.90	81.00	569.00	4.30	5.00	5.00	1.50	53.00	10.00	354.00	33.40	97.90	1.30	0.70	1.00	2.40	0.50
Rb	4.20	5.70	20.50	114.00	10.10	5.20	0.50	5.80	28.30	5.20	96.90	4.60	1.30	0.50	1.80	2.60	15.30	0.80
Sr	1715.00	403.00	724.00	1870.00	1530.00	2930.00	2550.00	4350.00	1380.00	1375.00	1515.00	105.00	102.00	72.00	105.50	92.40	106.00	119.00
Ta	0.05	0.10	0.30	2.10	0.05	0.10	0.10	0.10	0.60	0.10	1.40	0.60	1.00	0.05	0.05	0.05	0.10	0.05
Th	50.60	31.80	128.00	23.20	9.66	11.35	2.35	4.37	60.60	38.60	69.90	37.70	23.00	1.41	2.88	2.51	5.33	2.27
U	1.83	3.04	8.26	8.57	2.50	2.32	1.00	1.28	10.30	4.13	4.64	4.23	5.14	3.59	2.58	3.38	2.80	2.00
Zr	9.00	54.00	44.00	152.00	20.00	9.00	28.00	10.00	267.00	26.00	49.00	86.00	100.00	25.00	36.00	24.00	33.00	36.00
La	938.00	394.00	3540.00	594.00	1960.00	342.00	295.00	369.00	1940.00	423.00	1685.00	11.30	241.00	9.60	2.10	2.50	6.00	2.00
Ce	1755.00	745.00	6530.00	1165.00	2840.00	564.00	479.00	728.00	3030.00	767.00	2640.00	18.50	394.00	19.00	5.50	6.40	14.00	5.30
Pr	202.00	79.50	763.00	128.00	285.00	63.20	59.40	89.30	326.00	91.50	235.00	2.08	38.90	2.15	0.76	0.84	1.81	0.69
Nd	623.00	253.00	2330.00	390.00	763.00	188.50	190.50	286.00	948.00	297.00	800.00	8.20	130.50	8.30	3.80	4.10	7.70	3.10
Sm	70.30	35.40	241.00	41.40	67.10	25.90	28.00	41.00	116.00	49.00	90.10	2.59	23.60	2.97	1.82	1.84	2.54	1.24
Eu	16.65	9.47	47.70	9.62	14.90	7.26	7.82	10.40	27.70	13.25	19.90	1.56	6.27	0.95	0.61	0.53	0.64	0.37
Gd	70.30	34.30	215.00	41.40	75.30	28.20	26.90	39.30	119.00	48.30	92.30	3.33	24.20	3.78	2.62	2.46	2.73	1.56
Tb	7.42	4.00	17.65	4.52	6.40	3.75	3.75	4.97	12.30	6.48	8.16	0.62	3.32	0.74	0.52	0.47	0.48	0.32
Dy	31.10	16.95	53.40	20.30	23.50	18.90	19.20	24.30	50.10	31.90	27.90	3.37	15.90	4.27	3.03	2.54	2.63	2.10
Ho	6.05	3.10	9.09	3.96	4.75	3.88	3.98	4.86	9.25	6.27	5.03	0.68	2.99	0.87	0.60	0.51	0.53	0.43
Er	19.45	9.33	31.20	12.55	17.10	11.75	11.95	15.05	28.30	18.70	16.45	2.01	8.26	2.47	1.65	1.43	1.58	1.25
Tm	2.69	1.24	3.04	1.66	2.47	1.65	1.66	2.14	3.65	2.69	2.01	0.30	1.32	0.38	0.26	0.23	0.24	0.18
Yb	17.50	8.09	17.95	9.54	17.00	10.30	9.60	13.20	21.90	17.15	13.05	2.27	6.98	2.51	1.80	1.69	1.71	1.20
Lu	2.84	1.28	2.72	1.47	2.82	1.58	1.47	2.02	3.47	2.80	2.08	0.35	0.88	0.36	0.26	0.24	0.25	0.17
Y	153.50	84.50	209.00	105.50	116.00	102.00	93.80	127.00	273.00	159.00	145.50	18.90	77.90	22.70	16.20	13.40	13.30	12.40
La/Yb	53.60	48.70	197.21	62.26	115.29	33.20	30.73	27.95	88.58	24.66	129.12	4.98	34.53	3.82	1.17	1.48	3.51	1.67

Appendix 2 b) Trace elements analysis of samples collected by Etruscan and NRE and used in this study

Sample No.	ER12708	ER12709	ER12710	ER12711	ER12712	ER12713	ER12714	ER12715	ER12716	ER12717	ER12718	ER12719	ER12720	ER12721	ER12722	ER12723	ER12724	ER12725
Ba	51.10	32.70	46.30	25.60	42.60	254.00	100.00	10000.00	655.00	819.00	996.00	247.00	232.00	105.50	298.00	36.80	188.00	75.90
Ga	5.50	3.30	1.00	1.20	1.90	2.90	1.70	6.00	5.10	2.70	6.00	3.10	3.10	3.00	1.90	1.30	1.70	1.70
Hf	0.90	0.50	0.30	0.40	1.70	0.80	0.40	1.90	1.50	0.40	2.20	1.70	0.80	0.70	0.10	0.20	0.80	0.50
Nb	6.70	2.80	1.30	1.10	1.10	7.00	4.10	14.20	22.00	6.60	53.80	6.60	2.60	6.70	2.70	1.10	6.50	1.80
Rb	7.50	8.70	4.10	4.20	2.20	8.50	5.80	39.40	36.60	10.60	39.00	70.00	16.70	16.40	12.30	3.20	8.70	7.90
Sr	164.50	259.00	126.00	210.00	78.40	47.60	125.00	553.00	146.50	165.50	98.70	282.00	47.80	67.10	81.70	102.00	147.50	110.00
Ta	0.20	0.10	0.05	0.10	0.05	0.40	0.20	0.80	0.90	0.30	2.30	0.30	0.10	0.30	0.10	0.05	0.20	0.10
Th	1.71	1.94	15.70	4.69	4.56	12.00	13.70	14.00	6.28	4.24	53.40	22.70	7.16	3.89	0.93	3.07	14.80	0.59
U	1.59	2.11	2.01	1.30	11.30	2.71	2.75	1.74	4.09	2.23	4.06	3.09	1.96	2.34	0.51	2.49	4.68	2.09
Zr	53.00	22.00	35.00	28.00	244.00	45.00	26.00	67.00	69.00	23.00	102.00	63.00	31.00	27.00	11.00	28.00	97.00	60.00
La	6.40	6.40	1.80	9.20	4.50	7.20	9.10	24.60	25.40	6.80	34.70	15.80	5.30	10.20	6.90	2.90	18.30	3.00
Ce	13.70	14.80	5.70	21.20	10.90	17.30	17.70	51.70	46.10	13.50	71.30	33.00	11.80	22.00	15.50	7.90	34.90	7.80
Pr	1.86	1.95	0.82	2.63	1.42	2.00	2.41	6.62	5.82	1.84	8.59	4.04	1.52	2.95	2.12	1.17	3.94	1.19
Nd	7.60	8.40	3.70	9.80	5.80	7.30	9.70	25.20	21.60	7.80	31.80	15.20	6.40	12.10	9.10	5.50	14.00	5.40
Sm	2.20	2.50	1.33	2.64	2.35	2.26	2.83	5.88	4.65	2.37	7.36	3.71	1.55	3.26	3.09	2.40	3.05	2.48
Eu	0.57	0.54	0.36	0.40	0.82	0.69	0.72	1.67	1.04	0.82	1.55	0.60	0.37	0.72	0.97	0.67	0.86	0.81
Gd	2.84	2.97	1.90	2.86	3.86	3.35	3.28	5.09	4.47	2.84	8.47	4.12	1.87	3.37	3.50	3.24	3.20	3.17
Tb	0.53	0.51	0.40	0.56	0.85	0.74	0.63	0.89	0.69	0.52	1.60	0.78	0.35	0.57	0.68	0.60	0.54	0.65
Dy	3.05	2.86	2.38	3.29	5.14	4.56	3.64	5.15	3.59	2.76	9.97	4.75	2.04	3.15	3.88	3.39	2.86	3.89
Ho	0.66	0.58	0.55	0.76	1.18	1.02	0.74	1.15	0.72	0.54	2.20	0.99	0.41	0.63	0.76	0.66	0.58	0.78
Er	1.94	1.56	1.55	2.17	3.55	2.89	2.23	3.28	2.09	1.57	6.50	2.97	1.26	1.84	2.22	1.89	1.75	2.20
Tm	0.30	0.21	0.24	0.33	0.54	0.42	0.36	0.52	0.30	0.24	0.99	0.43	0.20	0.28	0.34	0.28	0.26	0.34
Yb	1.94	1.35	1.44	2.01	3.37	2.49	2.38	3.20	1.89	1.51	6.16	2.69	1.46	1.97	2.47	1.93	1.64	2.38
Lu	0.31	0.21	0.23	0.31	0.51	0.37	0.36	0.47	0.28	0.22	0.88	0.39	0.23	0.28	0.39	0.28	0.24	0.36
Y	17.90	16.60	13.10	18.10	31.50	36.00	21.70	31.70	20.50	16.10	74.20	26.70	12.20	16.70	19.90	19.20	16.50	20.90
La/Yb	3.30	4.74	1.25	4.58	1.34	2.89	3.82	7.69	13.44	4.50	5.63	5.87	3.63	5.18	2.79	1.50	11.16	1.26

Appendix 2 b) Trace elements analysis of samples collected by Etruscan and NRE and used in this study

Sample No.	ER12726	ER12727	ER12728	ER12729	ER12730	ER12731	ER12732	ER12733	ER12734	ER12735	ER12736	ER12737	ER12738	ER12739	ER12740	ER12741	ER12742	ER12743
Ba	60.90	50.50	185.50	89.10	95.60	44.90	52.10	13.70	1220.00	801.00	230.00	683.00	102.00	46.20	13.50	116.00	294.00	89.90
Ga	2.70	1.00	9.80	3.60	3.70	2.00	8.10	0.80	21.20	9.40	14.30	7.70	2.80	1.80	2.40	9.70	18.90	12.90
Hf	1.00	0.20	2.60	2.50	0.90	0.90	2.40	0.10	1.60	2.10	0.40	7.20	0.90	0.60	1.70	3.00	0.90	1.40
Nb	3.90	0.30	9.40	4.60	3.40	1.90	8.40	0.20	20.00	47.90	3.20	24.60	4.20	7.10	25.50	41.80	67.90	325.00
Rb	6.10	4.00	27.10	15.10	5.70	4.50	10.60	3.70	3.70	1.40	0.30	1.10	3.20	6.20	1.10	14.80	1.50	1.20
Sr	125.00	107.50	149.00	101.00	131.00	162.50	142.50	95.90	3320.00	2960.00	487.00	429.00	296.00	374.00	324.00	1005.00	820.00	1190.00
Ta	0.50	0.05	0.40	0.60	0.10	0.10	1.30	0.05	0.10	0.10	0.10	0.20	0.20	0.10	0.30	0.30	0.20	0.60
Th	1.96	0.45	6.86	7.67	4.03	1.21	9.90	0.55	211.00	33.10	301.00	401.00	779.00	16.00	37.60	577.00	458.00	292.00
U	3.66	1.89	3.78	1.37	1.45	3.90	4.59	0.81	6.05	22.70	3.76	6.52	8.58	1.51	1.62	10.35	65.30	52.30
Zr	55.00	31.00	96.00	84.00	40.00	105.00	79.00	11.00	156.00	187.00	8.00	781.00	17.00	49.00	126.00	187.00	54.00	75.00
La	3.00	2.30	33.60	16.30	19.30	2.80	21.30	4.40	5360.00	1290.00	3430.00	668.00	43.70	26.60	219.00	911.00	2960.00	2220.00
Ce	6.90	5.20	68.60	34.40	39.10	6.80	43.40	9.50	7300.00	2310.00	4920.00	1600.00	96.20	49.20	455.00	1575.00	5020.00	3710.00
Pr	0.93	0.73	8.40	4.61	4.76	0.87	5.20	1.19	627.00	253.00	448.00	202.00	15.15	5.71	57.70	170.50	497.00	364.00
Nd	3.90	3.40	30.60	18.40	18.00	3.90	18.80	4.80	1690.00	831.00	1270.00	736.00	112.50	20.70	216.00	563.00	1485.00	1120.00
Sm	1.43	1.30	5.63	4.72	3.87	1.23	3.94	1.21	185.00	133.00	155.50	156.50	174.00	7.19	62.00	125.50	171.00	161.00
Eu	0.52	0.50	1.32	0.82	0.98	0.48	0.97	0.39	43.70	35.90	42.00	42.20	56.40	4.25	18.30	33.50	44.70	45.60
Gd	1.87	1.78	5.66	4.96	3.99	1.61	4.13	1.34	209.00	132.00	171.00	178.00	167.00	7.98	62.80	131.00	186.00	173.50
Tb	0.36	0.36	0.87	0.87	0.65	0.28	0.67	0.20	23.40	19.05	20.50	32.70	33.50	1.55	10.45	17.75	25.30	26.50
Dy	2.20	2.34	4.77	4.78	3.35	1.64	3.72	1.06	113.50	99.50	101.00	192.00	226.00	10.20	59.00	78.40	137.00	141.50
Ho	0.45	0.48	0.99	0.94	0.68	0.32	0.76	0.19	24.40	20.60	22.30	42.10	50.30	2.31	12.15	13.60	28.20	27.30
Er	1.31	1.40	2.90	2.83	2.05	0.94	2.24	0.52	77.20	60.10	72.10	127.50	137.50	7.03	33.60	34.60	77.80	75.10
Tm	0.20	0.20	0.42	0.43	0.28	0.12	0.32	0.07	10.80	8.24	11.10	19.70	18.70	1.12	4.70	4.17	10.50	9.80
Yb	1.38	1.32	2.65	2.87	1.91	0.91	2.19	0.44	67.70	48.60	73.90	130.50	113.00	7.55	27.60	23.80	68.20	57.50
Lu	0.21	0.18	0.40	0.42	0.30	0.13	0.33	0.07	9.36	6.42	10.75	18.30	16.50	1.09	3.65	3.14	10.55	8.01
Y	13.60	13.60	26.90	26.90	18.20	10.00	21.20	5.60	700.00	549.00	608.00	1270.00	1405.00	68.50	380.00	356.00	700.00	645.00
La/Yb	2.17	1.74	12.68	5.68	10.10	3.08	9.73	10.00	79.17	26.54	46.41	5.12	0.39	3.52	7.93	38.28	43.40	38.61

Appendix 2 b) Trace elements analysis of samples collected by Etruscan and NRE and used in this study

Sample No.	ER12744	ER12745	ER12746	ER12747	ER12749	ER12750	ER12751	ER12752	ER12753	ER12754	ER12755	ER12756	ER12757	ER12758	ER12759	ER12760	ER12761	ER12762
Ba	43.10	35.90	995.00	406.00	1415.00	279.00	422.00	1715.00	746.00	941.00	401.00	508.00	450.00	405.00	801.00	672.00	147.00	984.00
Ga	23.00	1.30	15.70	32.00	32.30	22.80	8.40	16.90	11.20	6.10	9.10	14.60	5.10	6.50	6.70	0.90	3.10	6.00
Hf	1.70	1.00	1.10	2.20	5.70	1.40	1.00	1.40	0.90	0.30	0.30	4.20	2.90	2.50	1.50	0.20	0.80	0.50
Nb	11.90	8.30	184.50	334.00	164.50	138.50	20.50	32.70	27.00	89.20	18.30	188.00	91.10	164.50	186.50	2.90	10.10	24.50
Rb	0.50	0.50	3.60	8.30	44.80	6.00	22.20	7.50	16.80	8.90	16.20	42.00	17.50	39.70	12.50	1.10	5.70	20.20
Sr	440.00	392.00	16700.00	846.00	1970.00	1080.00	1490.00	996.00	1090.00	896.00	768.00	1120.00	10000.00	2700.00	6460.00	132.00	405.00	4750.00
Ta	0.30	0.05	1.40	1.50	1.20	0.30	0.10	0.20	0.10	0.30	0.10	1.20	0.70	0.70	0.60	0.05	0.10	0.10
Th	2020.00	33.70	230.00	406.00	272.00	461.00	47.30	65.70	111.00	9.66	24.70	34.50	14.10	37.90	75.00	4.35	13.20	2.49
U	6.19	3.66	13.95	32.70	5.99	37.50	4.77	7.45	5.55	3.49	6.60	5.12	5.18	9.32	5.15	2.34	7.60	1.44
Zr	27.00	129.00	43.00	133.00	260.00	73.00	67.00	102.00	37.00	16.00	18.00	206.00	195.00	130.00	76.00	24.00	65.00	15.00
La	5000.00	112.50	1580.00	3710.00	2640.00	3540.00	564.00	2170.00	966.00	502.00	326.00	352.00	243.00	303.00	958.00	7.20	68.90	687.00
Ce	7780.00	181.50	2780.00	6230.00	4070.00	5870.00	943.00	3130.00	1670.00	811.00	711.00	665.00	466.00	589.00	1700.00	14.70	115.50	1320.00
Pr	736.00	19.35	277.00	591.00	367.00	556.00	95.00	319.00	188.50	89.40	85.50	74.90	51.10	66.30	175.00	1.71	10.95	136.00
Nd	2160.00	65.20	943.00	1780.00	1080.00	1685.00	295.00	888.00	561.00	262.00	307.00	260.00	172.50	239.00	575.00	6.80	33.80	421.00
Sm	416.00	16.20	150.00	210.00	138.00	202.00	42.50	92.50	67.80	27.70	46.50	46.70	27.70	44.30	79.00	2.12	5.03	47.90
Eu	164.50	5.33	43.80	52.80	39.30	57.50	9.84	22.90	18.50	6.61	10.05	15.00	8.72	15.05	21.30	0.64	1.32	12.00
Gd	601.00	16.10	151.00	214.00	158.00	242.00	42.40	103.50	74.70	29.20	37.90	45.30	27.30	43.60	70.90	2.90	5.09	44.30
Tb	91.00	2.25	19.65	22.80	19.25	35.10	4.91	10.20	8.05	2.83	4.35	6.28	3.67	6.55	7.88	0.53	0.72	4.77
Dy	415.00	11.20	95.60	108.00	96.60	191.50	23.10	41.20	33.80	11.35	18.50	31.20	18.40	35.50	34.20	3.11	3.65	20.30
Ho	69.80	2.08	18.80	23.50	20.00	36.70	4.44	7.67	6.28	2.20	3.56	5.94	3.67	7.43	7.04	0.61	0.77	4.04
Er	164.50	5.80	54.30	76.60	60.80	95.90	13.40	24.00	19.05	7.11	11.20	15.50	10.20	20.10	21.70	1.75	2.46	12.15
Tm	18.80	0.82	7.18	10.20	8.31	11.85	1.83	2.99	2.35	0.89	1.50	2.06	1.39	2.78	3.20	0.29	0.38	1.57
Yb	98.60	5.21	42.50	62.50	49.90	70.50	12.20	18.30	14.90	5.48	9.87	11.95	8.47	16.55	21.10	2.07	2.87	10.10
Lu	12.65	0.75	5.40	8.69	6.55	9.46	2.01	2.97	2.33	0.84	1.62	1.71	1.22	2.31	3.14	0.31	0.47	1.52
Y	1620.00	53.90	519.00	769.00	622.00	934.00	120.00	216.00	202.00	66.30	85.80	159.50	98.70	189.00	316.00	17.80	23.10	104.00
La/Yb	50.71	21.59	37.18	59.36	52.91	50.21	46.23	118.58	64.83	91.61	33.03	29.46	28.69	18.31	45.40	3.48	24.01	68.02

Appendix 2 b) Trace elements analysis of samples collected by Etruscan and NRE and used in this study

Sample No.	ER12763	ER12764	ER12765	ER12766	ER12767	ER12768	ER12769	ER12770	ER12771	ER12772	ER12773	ER12774	ER12775	ER12776	ER12777	ER12778	ER12779	ER12780
Ba	480.00	831.00	796.00	134.50	759.00	74.50	189.50	223.00	43.70	924.00	460.00	276.00	262.00	1035.00	274.00	774.00	2150.00	1335.00
Ga	7.30	5.50	11.20	9.20	6.10	7.90	8.10	7.80	7.70	10.80	8.30	28.30	14.90	13.30	9.80	12.30	2.80	3.20
Hf	0.30	0.40	5.70	0.30	0.20	0.30	0.20	0.60	0.30	0.60	2.10	4.00	5.20	0.90	1.30	1.70	0.40	0.30
Nb	42.30	94.60	143.00	7.70	6.90	23.20	41.40	46.90	538.00	23.20	24.40	24.00	98.70	14.90	41.00	367.00	10.90	6.90
Rb	1.70	4.70	22.10	10.10	4.10	2.90	1.50	8.30	3.50	9.80	5.10	8.00	9.50	75.60	17.10	16.90	3.60	4.10
Sr	3070.00	5580.00	5700.00	1330.00	1485.00	1050.00	2020.00	1730.00	587.00	2630.00	1795.00	1840.00	1615.00	3470.00	2260.00	2920.00	562.00	10000.00
Ta	0.30	0.10	0.40	0.05	0.05	0.10	0.20	0.20	0.90	0.10	0.10	0.25	0.60	0.20	0.20	4.60	0.10	0.05
Th	14.65	24.00	178.50	139.00	4.33	57.80	68.20	75.30	47.40	63.60	97.10	248.00	233.00	197.00	166.00	101.00	7.56	8.23
U	3.30	3.91	6.68	5.87	3.53	9.45	2.62	2.22	5.04	4.00	2.08	8.30	8.87	2.23	2.86	12.35	1.22	1.72
Zr	2.00	10.00	349.00	1.00	1.00	12.00	2.00	16.00	5.00	25.00	138.00	220.00	349.00	42.00	53.00	97.00	9.00	9.00
La	1210.00	1040.00	792.00	1160.00	1525.00	847.00	1340.00	1240.00	1435.00	1515.00	1705.00	7130.00	3440.00	2080.00	1170.00	2630.00	236.00	386.00
Ce	2140.00	1635.00	1375.00	1685.00	2160.00	1655.00	2380.00	1840.00	2320.00	3170.00	2820.00	10650.00	5120.00	3050.00	2330.00	3970.00	461.00	757.00
Pr	206.00	153.00	140.00	156.50	185.00	177.50	234.00	166.00	213.00	340.00	261.00	994.00	455.00	277.00	266.00	331.00	52.60	84.60
Nd	623.00	457.00	448.00	448.00	500.00	581.00	724.00	476.00	615.00	1165.00	790.00	2770.00	1365.00	897.00	1015.00	935.00	189.50	303.00
Sm	68.70	55.70	65.20	42.30	46.70	80.20	88.00	49.30	54.40	136.00	103.00	303.00	210.00	155.00	198.00	101.50	36.50	60.30
Eu	18.10	14.75	19.15	9.64	11.80	21.70	23.30	12.45	12.20	30.20	24.90	72.70	54.90	42.00	52.80	29.60	11.15	18.80
Gd	70.00	54.50	65.10	40.50	50.80	72.50	83.80	50.10	53.00	107.50	100.50	346.00	207.00	146.50	170.50	120.00	32.60	56.50
Tb	8.71	6.07	8.83	3.31	4.40	7.96	9.03	5.47	3.92	10.50	11.70	28.40	25.40	19.95	22.60	14.40	4.09	7.76
Dy	47.50	28.40	46.30	12.00	16.70	32.30	38.30	28.60	11.40	42.30	59.00	120.00	126.50	105.50	104.50	73.10	19.45	37.90
Ho	10.90	5.78	9.55	2.54	3.16	5.88	7.43	6.98	2.24	8.49	12.95	24.20	27.00	22.10	19.25	15.20	3.78	7.48
Er	35.70	17.60	28.20	9.04	10.15	16.05	22.10	25.70	7.92	26.60	41.30	83.60	80.50	63.20	51.20	43.60	11.20	21.20
Tm	5.58	2.68	4.07	1.37	1.41	2.02	3.06	4.51	1.07	3.54	6.22	9.48	11.25	8.39	6.89	5.78	1.69	3.06
Yb	35.30	18.85	25.50	10.20	10.45	12.80	20.00	31.70	8.15	22.40	40.40	57.10	65.50	46.80	43.80	33.90	11.45	19.05
Lu	5.12	2.97	3.70	1.77	1.70	1.90	3.07	4.76	1.35	3.30	5.62	7.49	8.84	5.95	6.20	4.63	1.75	2.79
Y	257.00	139.00	246.00	74.10	78.10	169.00	211.00	216.00	60.90	254.00	440.00	814.00	878.00	724.00	551.00	398.00	99.10	191.50
La/Yb	34.28	55.17	31.06	113.73	145.93	66.17	67.00	39.12	176.07	67.63	42.20	124.87	52.52	44.44	26.71	77.58	20.61	20.26

Appendix 2 b) Trace elements analysis of samples collected by Etruscan and NRE and used in this study

Sample No.	ER12781	ER12782	ER12783	ER12784	ER12785	ER12786	ER12787	ER12788	ER12789	ER12790	ER12791	ER12792	ER12793	ER12794	ER12795	ER12796	ER12797	ER12798
Ba	1085.00	154.00	368.00	415.00	184.00	1085.00	498.00	1645.00	691.00	174.00	10000.00	541.00	975.00	1350.00	1090.00	1090.00	797.00	1115.00
Ga	7.40	9.50	6.50	14.50	8.70	11.40	7.90	9.00	11.90	4.90	14.50	5.00	11.80	14.80	3.80	9.90	3.90	4.70
Hf	0.50	0.80	2.10	1.90	0.20	0.40	8.90	3.10	1.90	0.30	0.70	0.20	6.60	3.50	1.50	0.30	1.30	0.40
Nb	8.80	1.00	81.70	62.00	6.80	47.70	232.00	269.00	459.00	8.60	8.60	5.60	354.00	58.40	41.40	10.90	74.90	4.70
Rb	5.70	2.10	11.40	17.80	6.60	19.40	10.10	17.30	12.30	3.20	9.70	1.20	10.50	2.40	6.70	23.90	5.30	2.90
Sr	5230.00	1540.00	1190.00	684.00	618.00	1660.00	6210.00	1440.00	994.00	1680.00	1475.00	2460.00	1330.00	1840.00	1775.00	521.00	1475.00	1020.00
Ta	0.10	0.05	0.40	0.20	0.05	0.20	4.00	0.60	0.60	0.05	0.05	0.05	1.80	0.10	0.20	0.05	0.60	0.05
Th	150.00	147.00	30.10	103.00	109.50	53.40	12.75	30.60	97.90	59.70	267.00	3.34	48.30	165.00	61.00	25.20	45.00	125.50
U	2.55	0.60	13.05	7.51	6.44	2.37	5.69	17.70	12.50	2.38	11.85	1.76	3.96	4.15	2.17	4.38	2.82	3.66
Zr	4.00	35.00	133.00	105.00	1.00	13.00	704.00	181.00	112.00	8.00	9.00	1.00	114.00	152.00	41.00	1.00	64.00	5.00
La	933.00	2220.00	907.00	1885.00	1820.00	1945.00	325.00	961.00	1810.00	532.00	1995.00	383.00	429.00	2110.00	234.00	695.00	305.00	426.00
Ce	2100.00	3380.00	1525.00	2900.00	2500.00	2820.00	581.00	1545.00	2910.00	937.00	3380.00	847.00	693.00	3630.00	419.00	1410.00	579.00	931.00
Pr	254.00	307.00	164.50	295.00	235.00	260.00	66.30	158.00	291.00	101.00	348.00	107.00	73.80	373.00	47.40	171.00	67.40	125.50
Nd	995.00	976.00	516.00	856.00	628.00	722.00	221.00	482.00	894.00	316.00	1015.00	385.00	233.00	1195.00	162.00	628.00	227.00	514.00
Sm	202.00	171.50	72.70	89.10	56.10	67.40	32.40	62.80	128.50	46.40	110.50	64.30	37.90	172.50	33.40	135.00	43.30	139.50
Eu	55.30	47.50	20.50	20.10	13.50	16.20	9.71	19.30	39.30	14.15	28.90	17.30	12.55	48.70	11.15	40.40	14.40	44.00
Gd	158.00	160.00	67.10	81.30	60.30	71.20	32.00	64.20	132.50	46.50	123.00	55.10	41.90	164.00	34.30	120.00	46.10	119.50
Tb	18.25	18.25	8.42	7.51	6.17	6.87	3.65	7.38	16.10	5.42	14.00	6.38	6.12	18.85	4.85	12.90	6.62	14.50
Dy	77.10	76.30	43.70	29.20	32.50	33.10	17.00	34.80	79.20	25.10	67.00	29.10	34.00	82.50	25.50	50.80	36.10	64.30
Ho	14.25	13.30	8.58	5.42	7.34	7.15	2.98	6.60	15.00	4.75	13.15	5.37	6.53	14.45	4.90	8.25	6.99	10.50
Er	39.20	34.50	25.70	18.00	25.60	25.30	8.46	19.15	43.30	14.75	40.30	16.10	18.10	40.20	14.30	23.10	19.45	27.80
Tm	5.09	4.44	3.77	2.45	4.25	4.20	1.08	2.52	5.88	2.55	5.65	2.34	2.62	5.02	2.25	3.27	2.74	3.87
Yb	30.90	28.90	24.10	17.00	29.30	29.60	6.65	14.70	33.70	19.00	33.00	15.55	15.70	29.50	14.55	22.30	16.60	25.20
Lu	4.27	4.25	3.43	2.45	4.38	4.49	0.96	1.97	4.30	2.98	4.42	2.23	2.15	3.77	2.13	3.28	2.21	3.64
Y	349.00	404.00	221.00	131.00	192.00	177.00	80.90	185.00	391.00	128.50	352.00	134.00	169.50	385.00	142.00	210.00	185.00	259.00
La/Yb	30.19	76.82	37.63	110.88	62.12	65.71	48.87	65.37	53.71	28.00	60.45	24.63	27.32	71.53	16.08	31.17	18.37	16.90

Appendix 2 b) Trace elements analysis of samples collected by Etruscan and NRE and used in this study

Sample No.	ER12799	ER12800	ER12801	ER12802	ER12803	ER12804	ER12805	ER12806	ER12807	ER12808	ER12809	ER12810	ER12811	ER12812	ER12813	ER12814	ER12815	ER12816
Ba	275.00	80.10	315.00	544.00	404.00	390.00	713.00	1245.00	1790.00	856.00	355.00	149.00	279.00	296.00	380.00	205.00	1010.00	853.00
Ga	6.00	4.10	5.70	3.60	10.50	11.10	9.20	21.50	16.20	10.30	6.30	2.40	15.80	12.10	8.70	4.30	19.80	11.30
Hf	0.30	0.30	0.60	0.60	0.60	7.10	3.30	0.70	0.80	2.20	1.40	0.50	3.20	5.80	1.10	0.20	2.30	2.10
Nb	45.30	5.00	127.50	44.20	26.70	290.00	200.00	21.30	21.10	85.40	78.50	4.80	35.10	478.00	6.10	5.10	89.10	14.10
Rb	18.40	1.20	24.70	11.00	63.00	59.80	24.60	35.30	15.90	45.00	9.60	4.90	7.00	85.50	7.40	5.90	43.60	31.90
Sr	907.00	1015.00	10000.00	6420.00	6740.00	7080.00	7220.00	4040.00	1530.00	1805.00	3310.00	5050.00	336.00	377.00	2510.00	1620.00	3940.00	1540.00
Ta	0.20	0.05	0.80	0.60	0.30	1.50	0.50	0.20	0.10	0.80	0.70	0.10	0.30	3.50	0.10	0.05	0.50	0.10
Th	29.60	66.00	19.15	28.20	20.10	16.90	22.30	177.00	48.90	174.00	101.00	109.50	11.40	120.00	52.70	8.85	92.20	40.00
U	3.19	3.77	19.25	3.14	1.86	21.30	18.45	8.42	3.93	9.88	9.16	4.00	1.40	40.80	2.51	4.68	8.64	7.15
Zr	6.00	16.00	20.00	26.00	16.00	307.00	180.00	22.00	36.00	171.00	96.00	15.00	116.00	314.00	74.00	4.00	143.00	109.00
La	84.20	393.00	327.00	341.00	456.00	230.00	606.00	2960.00	2250.00	767.00	801.00	99.10	11.50	1225.00	1135.00	369.00	3010.00	1625.00
Ce	170.50	691.00	585.00	561.00	798.00	434.00	994.00	5770.00	3870.00	1610.00	1320.00	200.00	23.50	2140.00	1855.00	604.00	4600.00	2440.00
Pr	20.70	75.90	67.00	60.50	108.50	48.60	118.50	646.00	436.00	226.00	155.50	23.00	3.34	266.00	213.00	76.90	488.00	265.00
Nd	76.00	244.00	217.00	187.50	367.00	157.00	359.00	2350.00	1290.00	794.00	490.00	75.20	14.30	860.00	625.00	242.00	1420.00	761.00
Sm	18.95	41.60	37.60	30.90	61.40	25.10	53.00	315.00	131.50	135.00	79.20	14.30	5.90	131.00	77.20	37.80	160.00	86.30
Eu	6.88	10.90	12.50	10.25	18.65	8.06	15.40	71.30	31.70	33.30	23.50	5.18	2.79	34.90	21.10	10.95	37.80	20.60
Gd	20.90	38.40	38.90	33.10	58.20	26.30	52.00	249.00	125.50	101.50	75.40	20.30	6.48	116.50	74.60	37.20	145.00	78.50
Tb	3.61	4.54	5.68	5.21	8.22	3.80	7.20	20.40	11.10	12.10	10.35	4.99	1.17	15.15	8.60	5.26	13.20	7.16
Dy	21.90	23.20	29.10	29.70	43.50	20.10	37.90	61.20	41.70	58.00	53.70	37.90	6.83	71.60	40.60	27.50	48.00	26.30
Ho	4.58	4.94	6.02	6.66	9.35	4.35	7.96	12.45	9.23	12.70	11.10	9.98	1.54	14.00	8.52	6.08	9.38	5.49
Er	13.85	17.05	16.10	19.25	27.40	12.10	22.10	46.90	30.40	37.70	30.20	33.50	4.29	37.00	25.30	17.90	29.40	17.65
Tm	2.18	3.01	2.31	2.94	4.26	1.80	3.23	7.70	3.98	5.54	4.30	6.65	0.69	4.94	3.70	2.83	4.16	2.74
Yb	13.85	20.90	13.75	17.85	27.30	10.70	19.45	59.40	23.70	32.40	25.40	48.90	4.47	27.10	23.40	17.60	28.40	18.85
Lu	1.96	3.03	2.05	2.75	4.44	1.66	3.11	10.15	3.71	4.83	4.04	8.74	0.75	3.99	3.74	2.83	4.90	3.14
Y	126.50	171.00	134.50	156.00	236.00	94.40	202.00	329.00	264.00	367.00	308.00	268.00	36.30	323.00	256.00	150.50	235.00	141.50
La/Yb	6.08	18.80	23.78	19.10	16.70	21.50	31.16	49.83	94.94	23.67	31.54	2.03	2.57	45.20	48.50	20.97	105.99	86.21

Appendix 2 b) Trace elements analysis of samples collected by Etruscan and NRE and used in this study

Sample No.	ER12817	ER12818	ER12819	ER12820	ER12821	ER12822	ER12823	ER12824	ER12825	ER12826	ER12827	ER12828	ER12829	ER12830	ER12831	ER12832	ER12833	ER12834
Ba	2240.00	760.00	754.00	1335.00	1400.00	490.00	593.00	231.00	1160.00	1790.00	337.00	220.00	668.00	756.00	537.00	704.00	482.00	194.00
Ga	13.30	3.70	4.00	11.20	7.40	7.10	5.90	11.80	17.60	26.70	9.60	11.90	61.20	19.20	5.50	11.90	24.00	4.60
Hf	2.40	0.20	0.40	1.10	0.60	0.60	1.10	1.90	1.60	3.20	2.00	2.40	2.00	2.00	0.80	3.40	3.40	0.50
Nb	105.50	7.40	6.30	74.40	30.00	16.10	20.80	26.70	16.20	277.00	113.50	89.90	87.00	27.40	182.50	506.00	69.60	4.20
Rb	17.10	5.60	4.00	13.80	7.30	18.50	8.50	3.60	12.10	27.50	17.50	14.90	1.00	2.60	5.20	11.30	5.90	9.10
Sr	1595.00	5010.00	4560.00	2270.00	3520.00	1840.00	2790.00	2830.00	767.00	938.00	1375.00	946.00	526.00	1025.00	1125.00	1770.00	279.00	517.00
Ta	0.30	0.10	0.10	0.30	0.10	0.10	0.20	0.10	0.30	0.50	0.40	0.50	0.25	0.30	0.20	3.50	0.10	0.05
Th	151.00	37.60	12.60	45.50	14.70	76.50	28.80	88.20	207.00	340.00	83.30	151.00	342.00	332.00	68.10	36.70	287.00	34.60
U	26.30	1.66	0.30	7.06	3.25	2.23	2.15	4.78	7.85	4.43	3.30	5.40	5.00	4.81	3.55	8.80	13.55	8.36
Zr	103.00	3.00	8.00	52.00	25.00	21.00	28.00	114.00	77.00	148.00	94.00	194.00	90.00	58.00	30.00	181.00	119.00	43.00
La	1485.00	324.00	312.00	1525.00	701.00	577.00	553.00	1795.00	2310.00	6490.00	671.00	1095.00	16200.00	4380.00	407.00	1225.00	5750.00	226.00
Ce	2660.00	596.00	588.00	2400.00	1375.00	1160.00	803.00	3110.00	4080.00	7650.00	1020.00	1925.00	21400.00	5970.00	611.00	2060.00	8070.00	452.00
Pr	334.00	68.70	69.20	262.00	184.00	154.00	88.00	345.00	456.00	593.00	113.00	238.00	1715.00	510.00	74.60	248.00	659.00	47.00
Nd	1105.00	225.00	229.00	738.00	626.00	514.00	246.00	976.00	1330.00	1605.00	320.00	779.00	4390.00	1500.00	232.00	766.00	1820.00	152.00
Sm	164.00	38.80	37.60	76.50	89.00	82.00	33.20	91.40	128.00	142.50	38.30	126.00	305.00	145.50	41.70	106.00	187.50	25.60
Eu	48.50	12.00	11.85	20.60	23.40	21.80	9.59	21.20	29.20	41.20	10.75	37.10	72.40	48.70	14.95	30.60	51.10	6.89
Gd	150.00	37.40	38.20	82.40	72.80	69.00	35.30	94.20	130.00	201.00	44.20	121.00	438.00	221.00	49.20	95.80	218.00	28.30
Tb	17.45	5.26	5.66	9.68	8.91	8.80	4.60	8.70	12.75	20.10	6.75	16.35	29.30	38.00	9.15	11.50	23.40	4.31
Dy	72.00	27.10	31.30	44.60	38.10	41.90	24.10	33.40	49.70	78.50	39.90	79.80	83.40	233.00	55.30	50.90	104.00	26.00
Ho	13.40	5.84	6.98	8.86	7.14	8.72	5.20	6.93	9.87	13.60	8.83	15.55	12.35	48.50	12.50	9.54	17.45	5.14
Er	35.00	17.40	20.70	24.70	18.75	25.00	15.10	22.30	29.80	36.90	24.90	39.20	45.70	119.50	38.30	24.70	50.50	15.70
Tm	4.23	2.87	3.26	3.43	2.19	3.87	2.39	3.24	3.81	4.63	4.00	4.96	3.94	15.25	6.93	3.00	6.81	2.40
Yb	22.40	18.95	20.50	21.20	12.05	25.20	15.70	23.20	23.70	31.50	26.50	26.40	26.30	78.30	47.60	16.40	47.70	16.20
Lu	3.12	3.18	3.26	3.40	1.71	4.05	2.44	3.94	3.78	5.28	4.57	3.74	4.12	11.20	8.04	2.35	7.26	2.40
Y	262.00	132.00	190.00	218.00	164.00	215.00	130.50	164.50	299.00	323.00	240.00	354.00	295.00	988.00	283.00	226.00	403.00	135.50
La/Yb	66.29	17.10	15.22	71.93	58.17	22.90	35.22	77.37	97.47	206.03	25.32	41.48	615.97	55.94	8.55	74.70	120.55	13.95

Appendix 2 b) Trace elements analysis of samples collected by Etruscan and NRE and used in this study

Sample No.	ER12835	ER12836	ER12837	ER12838	ER12839	ER12840	ER12841	ER12842	ER12843	ER12844	ER12845	ER12846	ER12847	ER12848	ER12849	ER12850	ER12851	ER12852
Ba	129.50	165.00	210.00	584.00	821.00	296.00	2270.00	450.00	3350.00	3180.00	644.00	226.00	840.00	1880.00	983.00	1465.00	927.00	1070.00
Ga	7.50	2.90	3.30	6.30	7.40	2.80	11.10	2.70	12.80	10.60	14.10	10.10	9.10	23.50	24.80	7.50	12.70	5.00
Hf	0.70	0.30	0.30	0.50	0.70	0.30	1.00	0.30	0.40	4.70	6.00	3.70	4.70	0.90	10.60	2.10	0.80	0.30
Nb	41.20	13.80	44.80	21.80	71.70	3.40	129.00	71.40	10.00	159.00	372.00	374.00	95.80	137.00	472.00	51.90	64.30	100.00
Rb	25.50	0.80	1.60	5.10	20.90	1.80	28.00	11.80	12.50	2.00	6.40	11.40	9.90	71.30	2.30	0.60	11.10	4.00
Sr	1835.00	1805.00	4950.00	5600.00	5320.00	3430.00	4120.00	6610.00	1435.00	3530.00	1640.00	10000.00	5190.00	4120.00	3430.00	10000.00	1725.00	973.00
Ta	0.05	0.10	0.20	0.20	0.20	0.05	0.90	0.20	0.10	0.50	5.20	2.50	0.40	12.50	0.80	0.40	0.40	0.30
Th	25.60	12.55	19.30	9.51	56.90	10.30	23.30	7.97	181.00	56.20	40.00	48.20	36.30	17.55	127.00	39.10	140.00	60.30
U	3.52	2.04	4.76	2.37	1.91	2.06	13.75	9.10	12.25	20.30	19.85	16.75	15.20	7.24	19.35	10.25	2.69	2.89
Zr	51.00	5.00	8.00	12.00	29.00	6.00	81.00	8.00	6.00	400.00	424.00	345.00	454.00	59.00	613.00	165.00	28.00	12.00
La	251.00	224.00	262.00	470.00	585.00	217.00	938.00	254.00	2510.00	1410.00	619.00	1105.00	906.00	444.00	7750.00	997.00	3890.00	794.00
Ce	472.00	428.00	510.00	804.00	938.00	434.00	1565.00	475.00	3690.00	2570.00	947.00	2080.00	1700.00	772.00	9560.00	2120.00	5280.00	1290.00
Pr	48.40	46.40	57.40	102.00	116.50	48.20	183.00	53.40	397.00	319.00	116.50	266.00	221.00	104.00	752.00	291.00	453.00	130.00
Nd	160.00	145.00	183.00	326.00	384.00	155.50	561.00	172.50	1225.00	1055.00	371.00	894.00	752.00	354.00	2050.00	1045.00	1225.00	398.00
Sm	29.20	25.00	32.00	55.20	72.50	27.70	79.50	29.40	186.50	149.00	55.70	131.00	111.50	49.90	162.00	159.50	119.50	56.10
Eu	9.62	6.77	8.75	15.45	18.65	7.62	20.50	8.64	46.60	37.40	14.35	33.00	28.70	12.55	38.50	38.80	28.70	15.15
Gd	33.80	22.40	29.00	52.10	57.80	24.10	65.70	28.50	153.00	119.00	47.50	103.50	89.30	39.60	194.00	119.00	118.50	51.30
Tb	5.42	4.01	4.91	8.49	8.16	3.97	8.45	4.45	14.60	13.85	6.16	13.90	11.45	4.64	15.60	13.30	12.00	7.04
Dy	33.30	24.10	27.80	45.20	39.60	22.30	38.70	24.80	45.30	57.00	29.00	63.60	51.70	18.45	54.60	48.20	51.70	37.40
Ho	6.75	5.01	5.67	8.38	7.57	4.55	7.12	4.90	6.88	9.80	5.22	11.10	9.21	3.06	10.65	7.33	9.58	7.54
Er	20.40	16.05	17.75	23.60	23.70	14.25	20.50	15.55	22.20	28.60	15.75	31.30	26.40	8.52	38.40	20.80	27.50	21.60
Tm	3.03	2.64	2.73	3.46	3.87	2.23	2.74	2.36	2.86	3.52	2.21	3.83	3.25	0.98	4.67	2.32	3.62	3.28
Yb	19.90	17.15	17.40	21.00	28.00	13.95	15.75	14.45	20.30	20.20	13.40	21.30	18.10	6.01	27.70	13.75	21.30	19.60
Lu	2.85	2.64	2.78	3.18	4.95	2.14	2.27	2.22	3.36	2.82	2.02	2.87	2.54	1.03	4.08	1.94	3.06	2.87
Y	207.00	154.00	162.50	229.00	240.00	131.50	219.00	127.00	162.00	244.00	142.50	290.00	222.00	75.20	319.00	160.00	224.00	195.00
La/Yb	12.61	13.06	15.06	22.38	20.89	15.56	59.56	17.58	123.65	69.80	46.19	51.88	50.06	73.88	279.78	72.51	182.63	40.51

Appendix 2 b) Trace elements analysis of samples collected by Etruscan and NRE and used in this study

Sample No.	ER12853	ER12854	ER12855	ER12856	ER12857	ER12858	ER12859	ER12860	ER12861	ER12862	ER12863	ER12864	ER12865	ER12866	ER12867	ER12868	ER12869	ER12870
Ba	311.00	75.80	401.00	319.00	1085.00	171.00	223.00	133.00	497.00	352.00	984.00	330.00	273.00	1100.00	953.00	646.00	930.00	1755.00
Ga	14.80	5.90	10.20	20.50	6.00	5.90	3.90	6.20	5.20	6.10	5.10	3.00	4.00	9.40	38.10	5.30	9.00	6.50
Hf	3.50	1.60	3.50	2.20	0.20	0.40	0.30	0.30	0.10	1.70	4.30	2.10	1.30	1.10	1.00	0.80	0.80	0.50
Nb	30.60	13.50	89.30	21.60	6.60	12.60	33.00	40.70	1.90	49.50	19.10	3.60	174.50	18.50	40.00	35.40	55.10	23.40
Rb	11.00	3.80	30.30	4.70	2.10	9.80	1.10	15.80	8.40	11.80	15.50	1.40	7.30	12.00	4.00	5.70	15.10	4.50
Sr	1030.00	2410.00	931.00	900.00	2500.00	708.00	1960.00	877.00	694.00	1975.00	2650.00	6060.00	7920.00	588.00	1385.00	997.00	1170.00	1285.00
Ta	0.10	0.10	0.80	0.05	0.10	0.10	0.20	0.20	0.05	0.30	0.10	0.05	0.80	0.20	0.25	0.10	0.30	0.20
Th	59.50	64.00	85.00	175.00	20.60	30.50	9.91	28.80	14.00	12.65	41.60	10.50	27.10	50.50	56.70	51.90	45.60	6.56
U	11.50	1.72	5.07	12.80	3.31	5.90	1.43	7.33	3.90	3.05	3.32	1.88	4.07	6.11	1.40	1.91	7.30	1.61
Zr	250.00	70.00	162.00	100.00	5.00	11.00	10.00	9.00	4.00	95.00	175.00	98.00	82.00	115.00	30.00	34.00	43.00	18.00
La	3040.00	1215.00	1135.00	5050.00	468.00	375.00	247.00	339.00	435.00	452.00	227.00	235.00	289.00	865.00	8130.00	378.00	927.00	665.00
Ce	4320.00	1885.00	1720.00	8350.00	863.00	662.00	459.00	603.00	722.00	813.00	463.00	459.00	564.00	1575.00	11400.00	740.00	1615.00	1230.00
Pr	399.00	183.50	161.00	811.00	92.60	72.30	51.10	64.10	72.60	88.20	57.50	53.20	69.30	165.00	1025.00	83.50	159.00	126.50
Nd	1115.00	551.00	486.00	2360.00	290.00	238.00	169.00	202.00	212.00	282.00	215.00	181.50	247.00	553.00	2620.00	305.00	505.00	415.00
Sm	118.00	74.60	62.50	230.00	40.10	37.70	27.70	29.60	23.90	40.10	46.10	30.50	42.20	80.90	186.00	47.60	65.70	65.00
Eu	28.20	19.45	15.95	39.10	11.60	10.85	9.04	9.13	7.11	12.15	14.70	9.66	11.90	21.60	46.10	12.65	17.10	19.25
Gd	110.50	63.40	55.20	186.50	41.50	36.20	31.30	31.80	28.80	43.50	44.00	32.40	38.80	74.40	275.00	41.60	64.80	65.20
Tb	11.85	6.95	6.58	14.40	5.16	4.27	4.43	4.32	3.67	5.56	6.00	4.28	5.02	8.18	16.80	5.14	7.23	8.28
Dy	56.90	30.60	31.10	44.30	25.30	19.10	23.80	21.70	20.90	27.20	31.10	21.20	24.40	35.70	41.30	25.20	32.70	42.60
Ho	12.45	6.00	6.29	7.95	5.02	3.48	4.60	4.25	4.61	5.20	6.10	3.93	4.69	6.64	6.52	4.89	6.26	8.21
Er	38.20	17.80	17.65	27.40	16.10	10.50	14.20	13.75	16.40	15.80	18.85	11.50	14.40	19.90	26.90	14.65	18.70	23.70
Tm	5.74	2.79	2.36	3.35	2.55	1.43	2.10	2.00	2.80	2.24	2.83	1.53	1.98	2.59	2.96	2.17	2.59	3.43
Yb	35.30	19.20	15.45	20.80	17.80	9.06	13.75	13.75	20.10	15.00	18.70	8.86	12.80	16.15	21.40	13.80	16.10	21.40
Lu	5.17	3.00	2.27	3.08	2.90	1.43	2.04	2.27	3.19	2.27	2.88	1.28	1.90	2.38	3.47	2.07	2.37	3.21
Y	322.00	140.00	160.50	184.50	125.50	86.20	121.50	109.50	137.00	132.00	171.50	104.50	127.50	172.00	141.00	131.50	157.00	211.00
La/Yb	86.12	63.28	73.46	242.79	26.29	41.39	17.96	24.65	21.64	30.13	12.14	26.52	22.58	53.56	379.91	27.39	57.58	31.07

Appendix 2 b) Trace elements analysis of samples collected by Etruscan and NRE and used in this study

Sample No.	ER12871	ER12872	ER12873	ER12874	ER12875	ER12876	ER12877	ER12878	ER12879	ER12880	ER12881	ER12882	ER12883	ER12884	ER12885	ER12886	ER12887	ER12888
Ba	260.00	105.50	136.50	155.00	162.00	368.00	357.00	1240.00	271.00	685.00	475.00	299.00	92.80	61.50	259.00	282.00	1100.00	156.00
Ga	12.40	6.90	4.90	12.80	60.00	4.40	3.30	3.60	3.70	26.40	25.50	3.10	34.50	17.00	2.40	3.30	3.20	7.20
Hf	5.80	0.70	1.30	3.20	69.70	0.40	0.20	0.20	4.60	13.00	2.00	1.50	1.00	1.20	1.20	1.30	1.70	0.80
Nb	129.00	107.00	272.00	14.80	1590.00	4.60	0.90	1.00	44.10	74.00	43.00	13.50	20.00	7.40	1.00	5.50	134.00	5.80
Rb	2.60	0.60	1.00	5.30	12.10	3.70	0.70	5.70	5.50	2.00	3.00	6.20	3.00	0.50	4.60	6.70	5.40	2.50
Sr	582.00	2100.00	440.00	216.00	1100.00	294.00	365.00	596.00	130.00	621.00	3770.00	6760.00	3030.00	1570.00	2060.00	847.00	1255.00	1605.00
Ta	1.30	0.60	3.80	0.50	70.70	0.10	0.05	0.05	0.50	0.50	0.25	0.10	0.25	0.10	0.10	0.10	0.20	0.10
Th	1000.00	53.00	58.10	4.36	61.60	4.77	2.03	1.14	60.30	537.00	200.00	56.40	427.00	243.00	16.35	43.50	113.50	94.10
U	7.32	16.25	8.01	0.90	55.40	3.62	1.83	3.66	4.10	17.70	4.90	1.84	4.60	7.11	4.99	3.06	13.40	7.08
Zr	264.00	52.00	98.00	105.00	4450.00	20.00	10.00	10.00	265.00	710.00	60.00	31.00	50.00	60.00	22.00	30.00	49.00	57.00
La	4010.00	1435.00	792.00	41.30	117.50	29.70	13.50	20.80	835.00	9310.00	8270.00	458.00	12600.00	6100.00	343.00	453.00	416.00	2220.00
Ce	5190.00	2400.00	1280.00	86.40	218.00	53.00	24.80	43.10	1145.00	12650.00	11950.00	750.00	17100.00	8140.00	566.00	758.00	761.00	2960.00
Pr	467.00	268.00	148.50	10.40	23.50	6.06	2.88	5.32	113.00	1060.00	1015.00	74.70	1385.00	694.00	56.70	76.70	83.80	272.00
Nd	1315.00	858.00	497.00	38.40	77.20	22.80	10.20	20.80	325.00	2940.00	2730.00	233.00	3640.00	1810.00	176.00	240.00	288.00	751.00
Sm	405.00	114.50	77.30	6.75	12.90	5.88	2.81	5.34	42.60	324.00	220.00	34.80	297.00	157.00	27.40	39.00	70.50	91.60
Eu	184.50	29.10	19.85	1.86	4.19	2.46	1.22	2.55	11.65	91.80	49.50	9.59	74.70	35.80	7.80	12.35	21.90	24.30
Gd	632.00	107.00	75.90	6.46	13.20	7.46	3.38	6.75	47.20	399.00	270.00	37.90	385.00	187.50	32.80	46.50	76.80	105.50
Tb	104.50	10.90	9.08	0.90	1.95	1.21	0.62	1.11	5.03	40.40	20.40	5.41	31.20	14.75	5.38	7.13	12.65	10.25
Dy	573.00	47.40	42.60	4.86	11.10	7.13	3.82	6.71	26.40	185.00	75.00	32.50	123.50	61.70	36.60	43.40	87.90	43.10
Ho	102.00	8.25	7.39	0.95	2.27	1.38	0.76	1.26	5.59	37.30	14.55	7.02	22.90	12.90	8.52	9.03	20.40	7.43
Er	257.00	23.40	20.10	2.72	6.92	3.94	2.25	3.78	17.55	126.00	52.40	22.60	77.10	46.70	27.50	26.60	65.30	23.90
Tm	32.80	2.85	2.54	0.42	1.10	0.55	0.38	0.64	2.59	17.25	6.09	3.46	8.18	7.62	4.44	3.91	9.77	3.97
Yb	180.50	16.05	14.40	3.00	7.03	3.85	2.73	4.40	16.65	105.50	38.60	22.10	46.80	56.70	28.70	23.70	58.50	31.60
Lu	23.30	2.15	1.80	0.58	1.08	0.57	0.42	0.66	2.31	14.30	5.59	3.07	6.59	8.91	4.01	3.17	7.74	5.11
Y	2240.00	198.50	151.50	25.30	59.00	39.30	18.80	35.80	312.00	1110.00	391.00	192.00	654.00	349.00	222.00	241.00	585.00	209.00
La/Yb	22.22	89.41	55.00	13.77	16.71	7.71	4.95	4.73	50.15	88.25	214.25	20.72	269.23	107.58	11.95	19.11	7.11	70.25

Appendix 2 b) Trace elements analysis of samples collected by Etruscan and NRE and used in this study

Sample No.	ER12889	ER12890	ER12891	ER12892	ER12893	ER12894	ER12895	ER12896	ER12897	ER12898	ER12899	ER12900	ER12901	ER12902	ER12903	ER12904	ER12905	ER12906
Ba	99.00	246.00	777.00	725.00	330.00	767.00	121.50	732.00	1415.00	513.00	955.00	557.00	1160.00	497.00	564.00	95.80	577.00	2230.00
Ga	10.30	16.40	21.60	5.80	4.30	35.00	3.20	33.10	43.50	20.80	37.00	19.70	26.40	4.20	5.80	7.10	11.30	7.50
Hf	0.90	1.10	9.60	2.90	0.20	11.70	0.30	0.40	0.40	0.40	0.40	0.80	3.20	0.40	2.20	1.00	3.30	2.00
Nb	39.50	3.20	98.70	21.10	3.50	115.50	3.20	74.50	41.80	7.20	4.90	6.00	48.40	1.60	16.80	28.60	169.00	67.10
Rb	1.30	9.90	85.40	17.20	1.60	143.50	4.10	18.20	33.60	10.50	29.00	19.50	33.00	1.10	16.40	11.20	39.20	24.70
Sr	1985.00	678.00	309.00	838.00	1310.00	507.00	1375.00	1500.00	1605.00	1195.00	1475.00	1980.00	10000.00	1725.00	2760.00	1100.00	945.00	736.00
Ta	0.20	0.05	2.10	0.10	0.05	2.00	0.05	0.40	0.20	0.10	0.05	0.05	0.10	0.05	0.10	0.20	0.80	0.50
Th	89.80	179.00	5.18	135.50	20.90	11.30	6.87	96.60	89.30	74.80	31.80	17.75	100.50	61.40	99.20	94.20	72.40	47.60
U	7.70	7.52	2.25	9.22	4.23	1.93	1.97	8.48	4.38	11.20	1.72	5.19	33.70	3.14	3.96	4.51	5.93	4.77
Zr	69.00	88.00	618.00	324.00	5.00	777.00	12.00	10.00	7.00	10.00	18.00	32.00	665.00	16.00	58.00	65.00	211.00	121.00
La	2650.00	3390.00	49.60	270.00	190.50	180.00	65.70	3760.00	5850.00	2280.00	5950.00	3050.00	1620.00	227.00	368.00	486.00	350.00	216.00
Ce	4240.00	6180.00	83.00	499.00	389.00	288.00	159.50	6340.00	9140.00	3810.00	7310.00	4050.00	3100.00	402.00	662.00	764.00	620.00	416.00
Pr	438.00	686.00	9.23	52.90	42.10	26.30	19.40	600.00	814.00	363.00	555.00	326.00	332.00	40.10	66.60	72.60	63.10	43.10
Nd	1320.00	2240.00	32.80	185.50	148.00	81.30	74.40	1870.00	2420.00	1135.00	1415.00	860.00	1185.00	132.50	219.00	238.00	216.00	150.00
Sm	138.50	241.00	5.94	33.10	26.50	10.15	17.15	199.00	233.00	134.50	102.50	70.00	171.50	22.50	36.20	49.90	37.20	30.30
Eu	30.10	47.00	1.78	8.50	7.63	2.64	6.44	47.70	53.50	34.20	24.80	16.35	48.30	6.99	9.52	17.95	9.68	9.33
Gd	130.50	198.50	6.08	34.40	25.60	10.40	21.90	198.00	246.00	132.00	146.00	88.10	163.00	25.80	41.70	65.70	38.40	32.80
Tb	10.80	14.70	0.87	5.30	3.40	1.09	4.41	16.55	18.80	11.95	9.13	6.30	18.85	4.41	5.87	12.35	4.99	4.78
Dy	46.30	49.00	5.09	38.20	22.40	5.25	31.80	67.20	67.70	52.90	28.00	22.90	91.40	29.90	33.30	90.40	28.50	30.10
Ho	10.75	9.21	1.02	9.75	5.85	1.04	7.09	13.30	12.70	10.55	5.64	4.39	16.50	6.62	6.41	20.00	6.14	6.73
Er	43.70	32.90	3.35	39.20	23.60	3.44	22.50	46.50	44.40	36.10	23.70	15.75	45.30	22.60	18.55	65.20	20.80	23.00
Tm	7.84	4.16	0.58	7.30	4.49	0.48	3.53	5.75	4.69	4.69	3.18	1.84	4.91	3.74	2.53	10.70	3.35	3.87
Yb	57.60	27.70	5.13	54.50	37.10	3.39	24.10	36.70	27.70	31.10	25.30	12.90	27.20	27.20	16.35	77.40	25.40	28.30
Lu	8.90	4.04	1.01	7.79	5.88	0.50	3.44	5.09	3.58	4.39	4.07	1.87	3.26	3.87	2.26	11.60	3.90	4.30
Y	397.00	254.00	27.50	422.00	203.00	30.00	213.00	463.00	412.00	369.00	174.50	159.50	406.00	207.00	149.50	569.00	190.50	198.00
La/Yb	46.01	122.38	9.67	4.95	5.13	53.10	2.73	102.45	211.19	73.31	235.18	236.43	59.56	8.35	22.51	6.28	13.78	7.63

Appendix 2 b) Trace elements analysis of samples collected by Etruscan and NRE and used in this study

Sample No.	ER12907	ER12908	ER12909	ER12910	ER12911	ER12912	ER12913	ER12914	ER12915	ER12916	ER12917	ER12918	ER12919	ER12920	ER12921	ER12922	ER12923	ER12924
Ba	448.00	303.00	483.00	215.00	578.00	1575.00	1050.00	785.00	777.00	400.00	1230.00	1605.00	1895.00	702.00	99.10	294.00	588.00	1170.00
Ga	14.40	9.30	4.40	7.40	7.30	6.40	21.30	5.00	7.20	12.50	7.30	7.70	19.70	5.70	3.60	6.70	6.10	17.10
Hf	1.10	0.80	0.50	1.60	5.40	0.30	3.60	0.20	0.90	1.30	0.40	0.30	2.20	0.40	0.60	2.80	0.40	9.90
Nb	195.50	102.50	10.90	6.10	9.10	4.40	35.70	6.00	2.30	65.30	7.50	6.90	165.00	11.70	4.80	35.70	8.60	155.50
Rb	32.50	19.10	6.10	16.40	17.30	10.90	22.50	4.30	2.20	19.70	3.70	2.20	47.40	4.40	3.10	31.90	13.10	14.40
Sr	836.00	870.00	9900.00	1080.00	779.00	2580.00	809.00	1045.00	948.00	715.00	3180.00	10000.00	9950.00	4220.00	1090.00	786.00	1030.00	503.00
Ta	0.50	0.20	0.10	0.05	0.05	0.05	0.20	0.05	0.05	0.20	0.10	0.10	1.20	0.10	0.05	0.20	0.10	2.50
Th	113.50	167.00	14.45	20.80	23.20	1.97	78.70	2.62	10.95	38.40	53.80	55.00	77.80	45.40	12.00	17.70	20.30	110.00
U	15.20	3.39	0.71	1.97	2.00	3.13	7.71	2.70	6.84	4.17	1.77	1.25	3.66	1.54	3.52	4.71	8.44	8.33
Zr	82.00	62.00	26.00	105.00	349.00	7.00	270.00	5.00	75.00	77.00	9.00	8.00	160.00	20.00	44.00	227.00	11.00	424.00
La	909.00	409.00	256.00	191.50	301.00	189.00	2400.00	121.00	120.50	911.00	399.00	589.00	1035.00	288.00	106.00	291.00	181.00	1385.00
Ce	1225.00	711.00	482.00	338.00	551.00	388.00	3640.00	254.00	195.50	1705.00	883.00	1115.00	1490.00	596.00	207.00	519.00	353.00	2660.00
Pr	101.00	72.90	49.20	34.50	57.10	42.10	325.00	28.20	22.10	185.50	106.00	117.00	130.00	67.60	22.30	53.20	36.80	277.00
Nd	277.00	258.00	164.00	120.00	193.00	153.50	970.00	100.50	75.40	649.00	416.00	399.00	382.00	247.00	75.30	176.00	125.50	883.00
Sm	39.50	53.80	26.60	26.10	34.00	33.00	122.00	18.40	13.60	99.40	83.30	62.50	50.40	48.00	12.60	26.00	25.40	113.00
Eu	11.60	15.85	7.83	8.33	10.30	10.70	32.90	5.47	4.31	27.50	26.10	18.50	16.35	13.95	3.55	6.69	9.19	24.40
Gd	53.00	55.90	28.20	26.60	36.50	36.00	138.50	19.10	14.85	99.60	81.50	64.20	65.50	47.00	14.35	26.40	33.30	114.00
Tb	8.34	8.29	3.77	3.28	5.09	5.81	13.95	2.93	2.25	12.45	11.00	7.93	8.37	6.51	2.27	3.51	6.25	13.75
Dy	51.60	48.50	21.70	17.60	29.30	36.70	61.80	20.00	13.75	67.00	60.20	39.20	43.50	31.80	14.00	19.20	38.60	69.10
Ho	9.96	9.84	4.45	3.90	6.01	7.61	11.10	4.81	2.94	13.10	12.05	7.09	7.87	6.19	3.15	4.20	8.05	14.05
Er	28.50	31.00	13.85	14.80	20.00	23.60	33.60	17.95	9.56	37.50	39.20	21.80	22.80	19.35	10.15	13.80	24.40	44.70
Tm	3.93	4.93	1.97	2.89	3.41	3.58	4.40	3.29	1.46	4.39	5.71	3.33	3.23	3.00	1.47	1.98	3.59	6.24
Yb	26.10	36.50	12.95	25.20	25.10	24.50	30.60	25.60	10.70	25.10	36.80	26.00	23.00	22.80	9.65	13.50	24.40	43.40
Lu	3.53	5.78	1.82	4.29	3.80	3.47	4.62	4.04	1.62	3.29	4.93	4.18	3.50	3.41	1.31	1.83	3.34	6.16
Y	261.00	283.00	117.00	124.00	177.50	241.00	332.00	137.00	88.40	365.00	365.00	177.50	199.50	163.50	108.50	133.00	208.00	417.00
La/Yb	34.83	11.21	19.77	7.60	11.99	7.71	78.43	4.73	11.26	36.29	10.84	22.65	45.00	12.63	10.98	21.56	7.42	31.91

Appendix 2 b) Trace elements analysis of samples collected by Etruscan and NRE and used in this study

Sample No.	ER12925	ER12926	ER12927	ER12928	ER12929	ER12930	ER12931	ER12932	ER12933	ER12934	ER12935	ER12936	ER12937	ER12938	ER12939	ER12940	ER12941	ER12942
Ba	4490.00	361.00	542.00	6550.00	754.00	942.00	847.00	612.00	953.00	455.00	5230.00	690.00	440.00	504.00	237.00	192.00	350.00	287.00
Ga	113.50	10.40	3.30	11.60	38.60	16.00	4.80	7.60	8.20	10.00	13.40	14.70	6.30	17.30	7.00	4.20	11.70	6.60
Hf	2.00	0.90	0.40	0.50	2.80	3.80	0.20	0.40	9.40	7.50	0.70	2.60	4.10	0.50	0.60	0.50	2.00	2.20
Nb	59.00	31.30	2.00	57.00	39.60	287.00	7.80	139.50	125.00	160.00	72.50	14.50	65.50	9.00	50.60	31.90	183.00	128.50
Rb	1.00	17.60	1.70	5.10	12.90	74.30	3.00	7.40	44.90	13.70	5.20	16.80	30.90	16.40	8.90	6.50	16.50	14.80
Sr	10000.00	91.60	426.00	10000.00	1130.00	2550.00	3100.00	10000.00	10000.00	2630.00	6960.00	1860.00	2910.00	4090.00	4490.00	7200.00	3610.00	2980.00
Ta	1.30	0.20	0.10	0.70	0.10	3.20	0.05	0.20	0.80	0.50	0.80	0.10	0.30	0.10	0.20	0.20	0.50	0.30
Th	240.00	17.85	3.78	12.80	240.00	8.12	2.78	1.29	6.93	18.15	105.50	18.25	7.63	7.53	4.06	10.05	17.90	24.80
U	4.20	1.13	3.63	14.85	3.15	3.87	1.96	8.35	19.45	20.20	18.50	3.28	4.64	5.17	1.70	0.94	9.86	3.34
Zr	80.00	31.00	7.00	32.00	124.00	138.00	4.00	15.00	535.00	763.00	26.00	143.00	274.00	30.00	28.00	17.00	135.00	169.00
La	17700.00	177.50	128.50	1145.00	5930.00	195.50	389.00	270.00	247.00	887.00	1370.00	1610.00	187.00	2700.00	276.00	227.00	1090.00	472.00
Ce	23200.00	293.00	218.00	1920.00	7830.00	365.00	685.00	558.00	469.00	1525.00	2330.00	2400.00	350.00	3200.00	443.00	393.00	1625.00	677.00
Pr	1875.00	29.70	24.80	192.50	648.00	39.00	68.90	59.60	50.10	153.50	233.00	220.00	37.00	243.00	42.40	39.30	151.00	61.10
Nd	4850.00	98.90	100.50	652.00	1755.00	135.50	224.00	205.00	175.00	516.00	742.00	652.00	126.50	611.00	132.50	126.50	473.00	185.50
Sm	344.00	15.10	26.20	85.40	162.50	21.70	33.60	30.50	26.80	71.70	93.80	76.10	19.80	43.00	18.55	18.45	63.10	28.20
Eu	75.10	3.88	6.92	22.70	42.90	5.81	9.36	8.50	7.46	18.40	23.40	18.75	5.67	10.35	5.30	5.31	18.25	9.67
Gd	471.00	13.90	35.50	81.80	210.00	20.70	33.90	30.50	27.00	72.20	99.20	84.30	21.10	66.90	20.60	20.20	70.30	38.10
Tb	33.90	1.53	7.12	8.27	18.70	2.72	4.42	3.92	3.42	8.59	14.50	8.78	3.05	4.32	2.54	2.66	8.82	6.19
Dy	108.00	7.21	46.60	31.80	65.50	13.20	21.90	19.15	16.25	38.00	88.90	38.10	16.85	11.40	12.55	14.10	44.90	37.30
Ho	19.00	1.54	10.45	5.55	10.60	2.50	4.33	3.68	3.09	7.09	19.30	7.66	3.42	2.15	2.54	3.01	9.00	7.92
Er	70.70	5.04	32.10	16.25	32.40	7.32	12.95	11.10	8.92	21.10	58.60	25.00	10.15	8.33	8.11	9.45	26.60	25.20
Tm	6.88	0.69	4.74	1.64	3.28	0.94	1.71	1.46	1.14	2.52	8.07	3.31	1.32	0.81	1.09	1.29	3.16	3.63
Yb	38.80	4.69	31.80	10.10	22.40	6.30	10.65	9.49	6.94	14.95	52.90	22.30	8.19	5.42	7.20	8.16	18.60	23.90
Lu	4.70	0.65	4.34	1.26	3.21	0.88	1.36	1.26	0.99	1.83	6.86	3.11	1.07	0.70	0.98	1.09	2.27	3.19
Y	576.00	47.70	318.00	152.50	441.00	60.30	111.50	88.00	81.10	193.00	474.00	204.00	94.20	65.60	65.10	84.50	251.00	272.00
La/Yb	456.19	37.85	4.04	113.37	264.73	31.03	36.53	28.45	35.59	59.33	25.90	72.20	22.83	498.15	38.33	27.82	58.60	19.75

Appendix 2 b) Trace elements analysis of samples collected by Etruscan and NRE and used in this study

Sample No.	ER12943	ER12944	ER12945	ER12946	ER12947	ER12948	ER12949	ER12950	ER12951	ER12952	ER12953	ER12954	ER12955	ER12956	ER12957	ER12958	ER12959	ER12960
Ba	333.00	163.00	1015.00	168.00	153.00	1830.00	981.00	652.00	703.00	1530.00	1255.00	573.00	276.00	840.00	404.00	854.00	1030.00	1030.00
Ga	9.20	9.70	12.00	18.30	17.00	19.60	62.40	4.40	50.10	9.80	14.10	10.20	16.80	22.40	12.50	6.50	16.10	13.80
Hf	1.40	0.90	0.40	4.00	3.60	0.90	2.00	0.70	3.90	1.30	1.00	1.00	0.40	1.10	0.30	7.30	5.00	2.20
Nb	83.10	48.00	5.70	142.50	132.50	10.00	29.00	9.00	16.90	13.10	30.50	27.30	8.40	144.00	15.90	228.00	258.00	457.00
Rb	25.70	14.10	26.20	7.40	11.00	4.60	23.00	3.90	14.50	18.80	30.00	22.30	5.90	19.10	4.70	10.00	15.40	5.70
Sr	2410.00	4640.00	1750.00	336.00	333.00	2510.00	1820.00	6240.00	3140.00	1760.00	1610.00	2110.00	933.00	639.00	1740.00	707.00	3840.00	1065.00
Ta	0.40	0.30	0.05	2.40	0.80	0.10	0.50	0.10	0.40	0.10	0.40	0.20	0.10	0.40	0.10	2.20	8.30	4.00
Th	11.90	9.95	9.00	28.00	11.65	64.40	373.00	84.50	268.00	15.05	82.80	51.70	30.30	481.00	158.50	43.20	80.80	206.00
U	11.75	3.42	5.56	4.36	3.15	6.94	5.10	2.63	8.76	4.26	3.00	6.14	1.77	10.85	4.53	42.90	8.41	19.20
Zr	85.00	44.00	22.00	276.00	208.00	47.00	110.00	35.00	194.00	61.00	18.00	34.00	16.00	52.00	9.00	924.00	276.00	96.00
La	479.00	924.00	1125.00	637.00	54.90	2990.00	7020.00	257.00	6340.00	628.00	761.00	657.00	2180.00	7930.00	5010.00	943.00	601.00	772.00
Ce	780.00	1335.00	1470.00	979.00	90.90	3790.00	10600.00	508.00	9620.00	1045.00	1525.00	949.00	3010.00	9880.00	6290.00	1550.00	1190.00	1670.00
Pr	76.60	120.00	119.50	90.10	9.39	302.00	992.00	55.70	868.00	103.00	177.50	86.20	259.00	774.00	476.00	165.00	139.50	222.00
Nd	247.00	355.00	311.00	271.00	31.00	798.00	3190.00	204.00	2570.00	343.00	679.00	275.00	729.00	1795.00	1120.00	518.00	541.00	956.00
Sm	34.80	40.50	29.30	32.20	5.37	98.60	493.00	51.80	310.00	70.50	156.00	68.00	70.50	196.00	96.10	82.50	111.00	233.00
Eu	10.10	10.40	8.29	8.66	1.69	31.40	133.50	17.70	88.50	24.10	49.50	26.10	16.80	67.00	26.00	25.40	28.80	60.30
Gd	37.30	46.60	41.50	35.70	6.15	138.50	458.00	57.00	375.00	83.70	160.50	90.60	86.20	287.00	126.50	84.70	96.10	190.50
Tb	4.50	4.70	4.13	3.57	0.99	17.05	48.00	9.40	44.30	13.60	25.60	15.35	7.61	33.80	12.40	12.00	12.60	26.40
Dy	21.60	19.40	19.40	14.45	5.60	90.70	218.00	51.60	211.00	77.00	140.50	91.50	30.40	137.00	53.20	56.80	57.50	122.50
Ho	4.17	3.73	4.23	2.70	1.17	18.90	36.30	10.20	38.90	15.45	27.40	19.10	6.10	24.20	11.35	11.05	10.10	20.60
Er	12.80	11.65	14.70	8.17	3.56	59.60	98.30	30.70	112.50	46.50	81.00	58.10	20.40	59.50	35.20	29.40	27.90	54.20
Tm	1.61	1.35	2.13	0.95	0.49	8.13	10.35	4.38	13.30	6.71	11.05	8.38	2.45	7.54	5.19	4.10	3.27	6.43
Yb	10.10	8.49	14.80	5.70	3.27	53.20	60.00	28.80	81.80	45.10	67.10	53.80	16.25	44.20	32.40	24.70	19.40	39.10
Lu	1.32	1.11	2.05	0.77	0.48	7.16	8.60	3.86	10.65	6.18	7.76	6.95	2.11	6.66	4.88	3.53	2.50	4.99
Y	115.00	93.90	117.00	72.40	32.90	600.00	1040.00	260.00	1070.00	438.00	845.00	540.00	164.50	648.00	324.00	280.00	258.00	490.00
La/Yb	47.43	108.83	76.01	111.75	16.79	56.20	117.00	8.92	77.51	13.92	11.34	12.21	134.15	179.41	154.63	38.18	30.98	19.74

Appendix 2 b) Trace elements analysis of samples collected by Etruscan and NRE and used in this study

Sample No.	ER12961	ER12962	ER12963	ER12964	ER12965	ER12966	ER12967	ER12968	ER12969	ER12970	ER12971	ER12972	ER12973	ER12974	ER12975	ER12976	ER12977	ER12978
Ba	822.00	2660.00	5010.00	770.00	3050.00	1125.00	671.00	938.00	1380.00	945.00	271.00	503.00	2150.00	1205.00	540.00	528.00	137.50	949.00
Ga	12.40	95.40	31.50	22.90	24.10	31.60	15.20	19.60	18.70	41.50	6.60	34.80	9.70	37.30	6.00	17.50	6.60	17.60
Hf	1.30	2.00	5.20	1.10	5.50	1.30	2.80	5.30	2.20	1.50	0.60	3.30	0.40	1.20	0.70	1.10	4.00	0.60
Nb	6.50	230.00	461.00	18.30	110.50	13.80	156.50	273.00	252.00	15.30	70.50	33.20	5.00	7.80	65.60	20.00	114.00	12.70
Rb	9.20	2.00	37.90	5.50	24.70	3.20	11.10	28.40	13.20	5.10	22.80	9.80	5.20	9.70	7.30	11.40	5.30	4.90
Sr	856.00	7880.00	1545.00	1565.00	3050.00	2050.00	2790.00	2860.00	7730.00	289.00	921.00	1090.00	2120.00	3510.00	7440.00	2060.00	861.00	3930.00
Ta	0.10	1.20	4.10	0.10	1.50	0.20	1.00	2.10	1.40	0.20	0.20	0.20	0.05	0.20	0.20	0.10	0.50	0.10
Th	87.00	511.00	453.00	163.00	253.00	245.00	109.00	169.00	135.50	82.00	13.50	187.50	14.30	119.00	15.15	133.50	41.20	147.00
U	1.71	7.10	18.15	14.00	31.20	6.88	44.50	9.00	20.40	7.88	3.10	16.40	3.31	7.01	5.12	10.40	4.65	2.70
Zr	116.00	90.00	177.00	38.00	514.00	63.00	347.00	220.00	62.00	85.00	31.00	244.00	17.00	36.00	36.00	43.00	260.00	21.00
La	1085.00	14150.00	1465.00	1580.00	2080.00	3540.00	1315.00	827.00	982.00	6260.00	250.00	3480.00	784.00	4230.00	258.00	1130.00	325.00	2020.00
Ce	1735.00	18200.00	3710.00	3440.00	3580.00	5660.00	2230.00	1335.00	2320.00	8330.00	464.00	6200.00	1240.00	6720.00	514.00	2270.00	536.00	2990.00
Pr	168.00	1470.00	509.00	385.00	376.00	543.00	221.00	144.00	292.00	674.00	48.20	621.00	120.50	615.00	57.40	259.00	52.30	269.00
Nd	517.00	3900.00	2190.00	1295.00	1305.00	1720.00	725.00	570.00	1145.00	1765.00	158.50	1970.00	391.00	1850.00	205.00	935.00	168.00	783.00
Sm	64.40	357.00	523.00	166.00	216.00	220.00	99.70	198.50	236.00	153.50	24.40	254.00	60.00	218.00	34.60	141.50	24.50	84.50
Eu	15.90	82.90	135.50	40.80	62.10	59.40	25.90	62.90	63.40	36.10	7.05	61.70	16.00	57.70	10.15	34.90	6.30	22.40
Gd	66.60	440.00	455.00	167.50	212.00	232.00	106.00	211.00	211.00	202.00	26.40	251.00	58.60	247.00	35.30	127.50	26.10	102.00
Tb	7.81	42.20	61.00	21.00	26.70	24.90	12.00	32.40	27.90	14.50	3.82	25.10	6.82	28.30	4.91	16.05	3.70	12.20
Dy	41.40	191.00	276.00	110.00	133.00	106.50	51.10	160.50	127.50	41.90	21.20	107.00	34.50	141.50	25.50	77.00	24.70	66.90
Ho	9.93	36.20	47.40	24.30	27.20	19.50	8.73	27.60	22.50	7.62	4.45	21.10	7.55	28.90	5.09	15.50	6.49	15.15
Er	39.30	115.00	126.00	83.10	88.40	57.40	24.20	69.50	63.70	29.10	14.30	68.60	26.80	87.70	15.35	48.80	26.40	52.70
Tm	7.01	13.30	14.45	12.55	12.30	6.51	2.70	8.38	8.02	3.31	2.04	8.19	4.22	10.40	2.05	6.63	5.19	7.88
Yb	54.60	75.50	81.60	86.90	77.80	38.80	16.45	49.40	49.40	24.40	13.85	47.30	29.80	58.90	13.05	44.70	41.50	53.20
Lu	8.37	9.84	9.83	12.30	10.40	5.02	2.20	6.13	6.23	3.59	1.94	5.83	4.34	7.29	1.77	6.59	6.49	7.32
Y	284.00	1150.00	1205.00	750.00	821.00	508.00	204.00	656.00	525.00	231.00	134.00	697.00	224.00	854.00	139.00	437.00	169.50	515.00
La/Yb	19.87	187.42	17.95	18.18	26.74	91.24	79.94	16.74	19.88	256.56	18.05	73.57	26.31	71.82	19.77	25.28	7.83	37.97

Appendix 2 b) Trace elements analysis of samples collected by Etruscan and NRE and used in this study

Sample No.	ER12979	ER12980	ER12981	ER12982	ER12983	ER12984	ER12985	ER12986	ER12987	ER12988	ER12989	ER12990	ER12991	ER12992	ER12993	ER12994	ER12995	ER12996
Ba	41.70	146.00	296.00	44.70	79.60	185.50	213.00	215.00	82.50	66.40	132.50	318.00	130.50	133.50	321.00	832.00	551.00	401.00
Ga	6.40	10.80	11.90	22.60	27.40	17.90	33.70	32.00	8.80	4.20	30.80	6.50	19.90	81.00	20.70	5.20	6.40	11.80
Hf	0.70	0.90	5.70	3.80	0.60	0.70	1.40	1.10	1.10	1.50	2.00	5.30	5.50	3.00	1.10	0.30	0.30	1.40
Nb	25.10	10.70	128.00	18.90	3.70	37.70	291.00	74.20	63.60	10.80	65.00	6.50	10.90	3.00	2.10	4.20	12.30	205.00
Rb	17.70	6.70	13.90	24.20	7.00	13.60	15.90	18.40	8.60	14.40	7.60	3.20	25.00	7.00	12.60	1.10	0.90	9.10
Sr	1225.00	2320.00	2850.00	1050.00	1225.00	2010.00	1600.00	1225.00	2560.00	707.00	4950.00	4520.00	1900.00	1690.00	4660.00	2980.00	10000.00	6010.00
Ta	0.10	0.10	2.10	0.10	0.05	0.10	0.80	0.20	0.40	0.05	0.40	0.05	0.10	0.25	0.05	0.05	0.10	0.50
Th	21.10	19.80	17.40	209.00	50.60	17.50	26.50	18.85	15.90	13.80	87.50	17.80	97.60	212.00	25.30	13.15	11.95	16.70
U	4.01	10.70	10.90	8.17	3.51	10.60	17.30	29.30	12.85	8.81	2.04	5.16	4.56	4.30	1.33	2.73	1.25	38.10
Zr	49.00	32.00	318.00	317.00	22.00	27.00	83.00	64.00	45.00	160.00	85.00	423.00	432.00	170.00	43.00	11.00	17.00	105.00
La	263.00	675.00	518.00	1980.00	3400.00	1375.00	3150.00	3090.00	406.00	100.50	4380.00	505.00	2570.00	19600.00	3920.00	611.00	954.00	1215.00
Ce	519.00	1220.00	763.00	3480.00	5030.00	2660.00	5820.00	5420.00	827.00	176.50	5680.00	746.00	3300.00	22800.00	4800.00	895.00	1330.00	1840.00
Pr	55.00	127.50	71.60	358.00	442.00	278.00	568.00	516.00	89.00	18.60	451.00	68.20	265.00	1700.00	346.00	78.60	113.50	168.50
Nd	185.00	435.00	227.00	1160.00	1220.00	885.00	1695.00	1525.00	292.00	65.70	1200.00	203.00	706.00	4040.00	863.00	228.00	318.00	505.00
Sm	32.40	72.10	30.50	144.50	121.50	95.60	146.50	131.50	43.90	14.45	114.50	28.10	90.60	319.00	71.30	26.40	32.90	61.50
Eu	9.34	19.95	9.49	37.60	30.60	20.60	34.70	32.00	13.25	4.67	25.50	7.87	27.70	81.70	18.35	6.80	8.59	16.85
Gd	37.00	78.40	34.00	147.50	151.00	102.00	178.00	162.50	54.40	14.45	153.50	31.90	118.50	457.00	103.50	28.00	38.30	66.60
Tb	5.73	11.65	4.06	16.10	13.10	10.10	16.05	14.35	8.62	1.92	11.85	3.92	12.60	35.60	8.18	2.71	3.81	7.58
Dy	32.90	65.30	21.30	71.70	50.00	39.50	63.00	52.80	50.70	9.07	39.50	21.90	56.50	129.00	30.30	12.05	17.40	38.10
Ho	6.89	13.65	4.49	14.45	9.88	7.38	12.40	9.64	10.65	1.72	7.53	5.03	11.35	21.40	6.31	2.67	3.68	8.11
Er	21.60	41.30	15.15	47.10	34.50	23.80	42.00	31.50	33.00	5.36	27.20	18.60	36.80	65.80	22.40	9.39	12.15	24.70
Tm	3.05	5.71	2.16	6.00	4.28	2.88	4.77	3.24	4.53	0.79	3.38	3.22	5.19	5.87	3.16	1.43	1.75	3.06
Yb	19.35	35.50	13.70	38.90	29.30	20.00	29.60	20.10	29.20	5.73	24.40	25.70	36.00	33.70	23.00	10.10	11.95	16.65
Lu	2.68	4.73	1.77	5.46	4.08	2.94	3.84	2.62	4.12	0.83	3.62	4.13	5.31	4.70	3.49	1.43	1.70	2.04
Y	185.50	373.00	143.00	430.00	286.00	220.00	376.00	284.00	379.00	48.10	246.00	139.00	341.00	662.00	198.50	82.20	106.50	241.00
La/Yb	13.59	19.01	37.81	50.90	116.04	68.75	106.42	153.73	13.90	17.54	179.51	19.65	71.39	581.60	170.43	60.50	79.83	72.97

Appendix 2 b) Trace elements analysis of samples collected by Etruscan and NRE and used in this study

Sample No.	ER12997	ER12998	ER12999	ER13000	ER13451	ER13452	ER13453	ER13454	ER13455	ER13456	ER13457	ER13458	ER13459	ER13460	ER13461	ER13462	ER13463	ER13464
Ba	153.50	1260.00	506.00	1260.00	663.00	279.00	263.00	211.00	91.50	325.00	259.00	683.00	110.50	256.00	354.00	128.50	83.50	269.00
Ga	6.10	10.20	3.90	19.20	42.70	8.10	5.90	10.80	25.00	26.50	13.00	13.60	10.20	7.40	21.10	4.40	7.10	5.70
Hf	0.10	0.50	0.40	9.20	2.00	0.20	0.30	19.50	0.70	0.60	1.10	1.70	0.90	7.60	12.80	0.60	0.60	0.40
Nb	5.70	256.00	25.90	472.00	47.00	0.90	3.40	2240.00	16.30	33.20	184.00	159.50	13.00	174.00	921.00	71.80	41.40	18.30
Rb	0.50	16.70	2.30	9.50	56.00	2.40	3.50	11.50	19.20	12.70	47.20	79.60	20.00	17.50	34.10	2.40	9.70	4.00
Sr	8220.00	9330.00	9180.00	5910.00	1245.00	1590.00	1300.00	1320.00	1075.00	1600.00	3130.00	1980.00	1265.00	4020.00	1800.00	2410.00	1520.00	5670.00
Ta	0.05	0.30	0.10	1.60	0.25	0.05	0.05	26.10	0.20	0.20	1.40	0.30	0.10	0.60	9.80	0.40	0.20	0.10
Th	9.41	21.30	4.87	636.00	146.00	1.78	60.30	26.70	25.90	56.00	109.00	137.00	52.60	42.20	32.30	18.00	37.40	83.40
U	0.75	56.10	7.47	6.17	5.30	3.19	3.14	31.90	7.01	11.45	2.38	8.90	6.30	4.57	21.20	2.51	9.67	2.79
Zr	5.00	37.00	24.00	455.00	90.00	9.00	8.00	942.00	38.00	24.00	66.00	116.00	48.00	433.00	996.00	38.00	25.00	18.00
La	898.00	744.00	290.00	2910.00	6880.00	1395.00	687.00	186.50	4120.00	4210.00	604.00	700.00	622.00	423.00	650.00	343.00	339.00	444.00
Ce	1290.00	1190.00	484.00	4040.00	11100.00	2080.00	1055.00	356.00	6310.00	6860.00	1450.00	1450.00	1070.00	845.00	1390.00	585.00	663.00	840.00
Pr	110.00	110.50	46.70	337.00	1075.00	175.50	95.60	36.80	546.00	595.00	177.50	162.50	107.50	94.60	155.00	57.80	72.00	89.60
Nd	302.00	346.00	146.00	995.00	2940.00	487.00	281.00	125.50	1485.00	1710.00	674.00	576.00	347.00	335.00	544.00	180.00	246.00	307.00
Sm	28.80	45.00	20.00	166.00	238.00	44.60	31.80	22.40	110.00	159.50	113.00	90.00	50.40	57.10	80.10	23.10	45.60	53.20
Eu	7.04	12.70	5.64	62.50	50.30	10.90	9.29	7.44	24.20	37.00	31.60	26.40	12.30	17.05	22.00	6.37	15.90	15.85
Gd	32.90	48.50	20.20	242.00	277.00	50.70	36.70	24.40	128.50	173.00	104.00	95.30	50.30	55.30	73.20	22.90	46.70	52.90
Tb	2.91	6.12	2.48	45.40	15.75	4.16	4.59	3.76	7.69	13.45	13.55	14.60	5.66	7.66	8.22	2.67	6.59	7.34
Dy	12.05	33.50	12.25	293.00	37.70	15.20	29.10	23.30	14.40	42.20	68.50	88.90	26.10	40.80	35.60	13.30	32.50	38.40
Ho	2.56	7.32	2.65	62.50	6.38	3.05	7.38	4.91	2.32	7.47	13.05	18.80	4.39	8.08	6.42	2.75	5.90	7.36
Er	9.21	22.30	9.44	181.50	25.80	11.55	28.30	14.40	11.55	25.80	37.30	56.70	12.65	22.80	18.90	8.66	15.45	20.90
Tm	1.41	2.89	1.52	24.60	2.20	1.85	5.17	2.12	1.04	2.63	4.73	8.17	1.79	3.13	2.34	1.26	2.28	2.96
Yb	10.15	17.00	10.95	136.00	14.10	14.65	37.00	12.65	8.15	15.75	25.50	47.80	11.15	18.70	14.15	7.99	13.05	18.95
Lu	1.48	2.20	1.57	16.40	2.03	2.55	5.83	1.80	1.43	2.16	3.29	6.62	1.58	2.65	2.01	1.24	1.89	2.82
Y	74.00	230.00	80.30	1870.00	140.00	72.60	203.00	137.00	60.20	190.00	366.00	496.00	108.50	196.50	159.50	77.60	146.50	182.00
La/Yb	88.47	43.76	26.48	21.40	487.94	95.22	18.57	14.74	505.52	267.30	23.69	14.64	55.78	22.62	45.94	42.93	25.98	23.43

Appendix 2 b) Trace elements analysis of samples collected by Etruscan and NRE and used in this study

Sample No.	ER13465	ER13466	ER13467	ER13468	ER13469	ER13470	ER13471	ER13472	ER13473	ER13474	ER13475	ER13476	ER13477	ER13478	ER13479	ER13480	ER13481	ER13482
Ba	494.00	832.00	305.00	387.00	1630.00	726.00	235.00	264.00	1020.00	509.00	674.00	695.00	607.00	434.00	203.00	536.00	199.50	124.00
Ga	8.70	8.00	5.40	5.30	9.80	33.80	18.70	17.20	7.50	8.80	6.80	8.80	4.10	4.10	17.70	2.70	3.50	12.10
Hf	0.30	0.60	1.00	0.70	0.80	1.00	0.30	0.60	0.40	10.60	10.30	1.20	9.00	0.40	0.80	0.30	0.20	0.60
Nb	22.00	49.00	298.00	61.40	15.40	71.00	92.90	14.60	23.40	108.50	90.20	93.70	11.30	25.20	58.40	7.70	8.00	21.60
Rb	14.80	14.70	8.40	6.90	3.30	4.00	1.70	12.50	16.50	24.50	17.10	29.20	9.30	5.30	0.80	5.70	3.30	5.40
Sr	2160.00	2070.00	1435.00	1490.00	1750.00	1270.00	1280.00	2070.00	2160.00	2200.00	2630.00	1650.00	3090.00	2270.00	1865.00	8590.00	1295.00	735.00
Ta	0.10	0.20	1.20	0.50	0.10	0.25	0.80	0.10	0.20	0.20	0.70	0.50	0.10	0.10	0.10	0.10	0.05	0.05
Th	98.30	23.40	67.90	9.70	44.80	243.00	119.50	191.50	94.30	42.20	102.50	62.70	32.30	86.40	196.00	7.10	26.30	86.20
U	2.18	2.49	4.42	3.52	3.18	10.30	5.45	4.73	2.05	12.80	6.78	4.50	1.04	3.46	12.00	1.16	4.76	20.30
Zr	8.00	22.00	39.00	28.00	39.00	30.00	7.00	18.00	9.00	661.00	637.00	63.00	399.00	18.00	34.00	11.00	10.00	29.00
La	1105.00	1005.00	492.00	597.00	1700.00	6090.00	3530.00	3050.00	1245.00	469.00	468.00	355.00	234.00	679.00	4440.00	279.00	363.00	3150.00
Ce	1935.00	1670.00	845.00	889.00	2450.00	9610.00	5530.00	4600.00	2060.00	914.00	880.00	631.00	417.00	1145.00	7550.00	508.00	622.00	4360.00
Pr	186.50	157.00	82.30	78.60	205.00	912.00	468.00	383.00	213.00	106.50	102.50	69.00	46.00	120.50	754.00	57.00	68.90	380.00
Nd	575.00	474.00	264.00	223.00	554.00	2440.00	1335.00	1090.00	644.00	351.00	342.00	219.00	148.00	362.00	2070.00	185.50	217.00	1010.00
Sm	71.50	60.30	46.50	24.60	45.80	191.00	122.00	108.00	82.60	52.90	57.80	36.00	23.80	48.50	170.00	29.90	31.50	85.60
Eu	18.85	16.90	16.00	7.09	10.40	44.80	29.10	29.70	24.70	15.60	19.90	12.65	7.69	15.50	35.10	9.58	10.00	21.00
Gd	73.50	64.20	55.50	28.90	53.80	252.00	140.50	140.00	87.90	51.30	63.70	42.20	24.70	55.40	166.50	30.90	32.80	94.10
Tb	8.98	7.68	8.65	3.56	4.09	18.20	12.15	17.65	12.65	7.30	11.40	7.83	3.57	8.85	11.55	4.54	4.44	6.75
Dy	44.50	36.00	49.70	20.80	15.30	67.00	49.60	104.50	67.70	38.60	70.40	49.50	18.95	51.30	31.80	23.60	22.10	19.40
Ho	8.44	6.70	9.92	4.79	3.18	12.45	9.61	22.90	14.15	8.26	15.60	10.90	3.98	11.05	5.84	4.74	4.50	3.63
Er	24.90	20.50	29.70	16.00	12.85	42.40	30.60	69.80	37.60	23.70	45.70	31.10	11.45	31.40	18.95	13.60	12.90	12.80
Tm	3.46	3.00	4.68	2.63	2.11	4.10	3.69	9.65	4.90	3.51	6.70	4.54	1.71	4.66	1.71	2.03	1.87	1.77
Yb	22.40	19.75	31.50	18.65	16.75	24.90	21.40	54.80	27.00	21.70	37.60	26.20	10.75	29.40	10.20	12.80	12.50	13.55
Lu	3.30	3.02	4.87	3.05	2.95	3.45	3.03	7.46	3.67	3.22	5.14	3.68	1.64	4.42	1.35	1.88	1.98	2.39
Y	216.00	156.00	298.00	150.00	82.40	321.00	238.00	571.00	306.00	189.00	345.00	248.00	96.30	267.00	127.00	118.50	121.00	79.20
La/Yb	49.33	50.89	15.62	32.01	101.49	244.58	164.95	55.66	46.11	21.61	12.45	13.55	21.77	23.10	435.29	21.80	29.04	232.47

Appendix 2 b) Trace elements analysis of samples collected by Etruscan and NRE and used in this study

Sample No.	ER13483	ER13484	ER13485	ER13486	ER13487	ER13488	ER13489	ER13490	ER13491	ER13492	ER13493	ER13494	ER13495	ER13496	ER13497	ER13498	ER13499	ER13500
Ba	996.00	167.00	132.00	485.00	41.40	165.50	221.00	579.00	703.00	162.00	659.00	381.00	293.00	1750.00	271.00	296.00	734.00	493.00
Ga	6.20	4.30	3.30	2.90	9.80	3.80	8.50	2.70	17.00	4.80	4.90	6.70	6.30	10.20	5.10	5.20	5.10	6.80
Hf	0.20	0.20	0.20	0.20	0.50	0.30	1.90	0.10	4.00	0.50	2.40	0.50	0.50	1.80	0.40	0.30	0.20	5.20
Nb	13.00	23.40	6.90	9.30	52.60	13.00	28.40	2.50	170.00	21.40	120.50	17.50	99.10	325.00	45.60	10.90	4.80	65.10
Rb	0.40	7.30	4.30	0.80	21.40	1.20	14.40	1.20	31.30	5.40	13.30	25.60	19.10	16.30	8.80	10.30	5.80	15.50
Sr	4860.00	574.00	1670.00	6720.00	520.00	1165.00	2590.00	3280.00	946.00	722.00	1725.00	2240.00	1615.00	2420.00	792.00	947.00	525.00	2220.00
Ta	0.10	0.10	0.05	0.10	0.30	0.10	0.30	0.05	0.80	0.10	0.70	0.10	0.40	1.20	0.20	0.05	0.05	0.20
Th	53.90	14.60	10.40	26.10	34.30	24.90	62.40	2.58	147.50	48.80	32.70	30.40	50.50	94.50	36.70	35.90	26.00	53.10
U	2.91	7.59	2.41	1.64	7.69	1.68	5.14	1.26	16.85	7.62	10.65	3.95	4.94	16.05	2.49	6.33	2.84	6.10
Zr	12.00	10.00	6.00	9.00	28.00	12.00	97.00	5.00	246.00	42.00	145.00	28.00	25.00	152.00	17.00	13.00	5.00	292.00
La	1990.00	351.00	416.00	283.00	1105.00	461.00	1060.00	447.00	3080.00	629.00	362.00	497.00	593.00	1775.00	721.00	517.00	697.00	544.00
Ce	2780.00	616.00	716.00	545.00	2000.00	930.00	2290.00	706.00	4720.00	1055.00	637.00	854.00	1020.00	2770.00	1160.00	921.00	1160.00	1290.00
Pr	248.00	68.40	76.00	62.70	208.00	112.00	273.00	71.60	467.00	111.00	71.30	92.00	109.00	270.00	119.00	100.50	123.50	166.00
Nd	658.00	217.00	232.00	204.00	613.00	378.00	926.00	209.00	1380.00	339.00	230.00	287.00	339.00	819.00	353.00	317.00	378.00	586.00
Sm	59.80	32.30	31.50	31.40	54.90	55.90	116.00	26.40	175.00	47.20	36.50	43.50	51.00	108.00	45.60	43.10	49.60	79.70
Eu	15.45	10.15	9.85	9.51	13.20	15.45	27.30	8.08	47.70	13.20	11.75	12.85	15.30	30.60	13.45	12.35	14.75	19.90
Gd	65.60	31.90	33.00	31.10	53.80	50.40	97.60	28.90	174.00	45.50	38.20	43.30	52.50	107.50	47.90	41.60	50.30	65.20
Tb	5.52	3.76	4.13	4.33	4.68	6.58	10.15	3.76	19.50	5.26	5.57	5.46	6.79	11.55	5.89	4.89	6.20	7.67
Dy	20.60	16.10	19.25	22.00	17.40	32.70	40.80	18.90	85.40	23.40	28.00	25.50	32.30	48.80	27.40	21.70	28.70	34.30
Ho	4.38	3.04	3.81	4.72	3.71	6.67	8.01	3.94	16.65	4.75	5.52	5.15	6.74	9.12	5.46	4.39	5.60	7.04
Er	16.10	8.35	11.40	14.10	13.30	19.25	23.50	11.75	46.10	14.30	15.40	14.70	19.15	24.90	16.50	13.45	16.25	21.30
Tm	2.89	1.17	1.64	2.26	2.16	2.72	3.00	1.74	5.98	2.25	2.15	2.17	2.80	3.11	2.56	2.03	2.35	3.05
Yb	23.50	7.70	11.15	15.40	16.45	17.00	18.85	11.20	36.20	15.45	13.15	14.25	18.00	17.95	17.50	14.00	15.40	19.55
Lu	4.14	1.24	1.71	2.44	2.95	2.56	2.74	1.73	5.03	2.49	1.95	2.21	2.77	2.46	2.82	2.26	2.40	2.85
Y	108.00	77.20	94.00	110.50	85.90	161.00	186.50	95.60	429.00	110.00	132.00	125.50	173.00	236.00	133.50	112.50	133.00	198.50
La/Yb	84.68	45.58	37.31	18.38	67.17	27.12	56.23	39.91	85.08	40.71	27.53	34.88	32.94	98.89	41.20	36.93	45.26	27.83

Appendix 2 b) Trace elements analysis of samples collected by Etruscan and NRE and used in this study

Sample No.	ER13748	ER13749	ER13750	ER13864	ER13865	ER13866	ER13867	ER13868	ER13869	ER13870	ER13871	ER13872	ER13873	ER13874	ER13875	ER13876	ER13877	ER13878
Ba	326.00	205.00	208.00	116.00	331.00	241.00	136.00	660.00	2180.00	572.00	555.00	421.00	883.00	620.00	217.00	1015.00	98.70	247.00
Ga	53.60	43.90	40.80	1.70	5.40	19.00	8.10	4.30	12.00	6.20	13.50	17.90	10.30	20.40	7.50	6.50	7.40	6.20
Hf	2.00	6.00	2.00	0.10	2.90	0.30	0.40	0.20	4.00	1.80	0.20	0.40	0.20	0.40	0.30	0.20	0.60	1.50
Nb	7.00	130.00	36.00	7.30	42.40	2.90	14.40	8.90	680.00	3.70	6.20	4.40	3.30	59.90	13.90	5.90	44.50	631.00
Rb	1.00	1.00	7.00	0.80	5.60	7.60	2.30	1.30	61.70	1.10	3.90	11.80	1.50	19.30	3.10	8.50	3.70	8.80
Sr	1295.00	1650.00	1525.00	75.20	600.00	2450.00	2100.00	1390.00	1020.00	2280.00	2030.00	911.00	1875.00	1905.00	761.00	1400.00	1030.00	917.00
Ta	0.25	1.90	0.25	0.05	0.20	0.05	0.10	0.10	7.50	0.05	0.10	0.05	0.05	0.30	0.05	0.05	0.20	3.10
Th	1775.00	2540.00	1230.00	3.94	17.80	98.10	41.20	11.50	64.20	13.25	38.10	162.00	26.60	124.00	8.23	76.20	22.50	48.30
U	6.20	9.40	3.40	0.59	8.47	3.31	1.89	2.52	10.80	2.59	4.00	9.89	2.98	4.05	8.24	2.64	9.29	10.05
Zr	40.00	90.00	60.00	9.00	208.00	15.00	24.00	6.00	328.00	192.00	9.00	25.00	5.00	18.00	5.00	6.00	40.00	88.00
La	8750.00	6600.00	5800.00	70.30	351.00	5170.00	2430.00	903.00	636.00	931.00	4270.00	6020.00	2960.00	6180.00	954.00	1205.00	594.00	665.00
Ce	14600.00	11200.00	9730.00	123.50	552.00	7830.00	3350.00	1355.00	1075.00	1510.00	5630.00	8200.00	4120.00	8750.00	1560.00	1965.00	1240.00	1225.00
Pr	1435.00	1095.00	948.00	12.60	55.50	710.00	295.00	129.00	111.50	151.50	468.00	692.00	360.00	757.00	162.00	196.50	145.50	135.50
Nd	4650.00	3710.00	3170.00	39.00	167.00	1920.00	786.00	363.00	338.00	440.00	1195.00	1725.00	965.00	1930.00	476.00	575.00	480.00	427.00
Sm	662.00	702.00	475.00	5.66	21.70	164.00	63.00	38.60	49.10	47.10	93.10	131.00	87.80	163.00	60.70	62.90	67.70	57.30
Eu	163.00	243.00	115.00	1.75	6.76	36.00	15.30	10.30	15.45	11.40	23.10	30.80	22.40	40.60	17.00	16.50	19.30	17.55
Gd	632.00	1010.00	445.00	5.89	21.50	172.50	73.40	41.20	52.90	45.20	117.00	162.50	99.90	196.50	65.20	64.70	63.50	59.20
Tb	68.60	179.50	49.60	0.75	2.75	12.50	5.56	4.47	6.72	4.30	8.99	10.80	8.60	16.00	7.72	6.51	7.87	7.66
Dy	325.00	1165.00	253.00	3.59	13.45	39.20	18.40	21.50	31.50	17.95	29.90	28.00	32.50	58.00	34.10	29.20	37.30	39.40
Ho	59.50	236.00	49.30	0.73	2.69	8.00	3.80	4.84	6.07	4.06	5.65	5.00	6.39	11.00	6.35	6.58	7.41	8.18
Er	176.00	660.00	151.50	2.02	8.11	29.50	14.10	16.10	16.95	13.90	19.05	18.30	21.50	34.70	17.65	23.30	21.60	23.60
Tm	20.80	75.10	18.35	0.29	1.22	4.13	2.37	2.84	2.42	2.40	2.62	2.03	3.12	4.27	2.34	3.80	3.05	3.38
Yb	124.50	382.00	107.50	1.81	8.66	28.70	19.20	21.80	15.55	18.20	18.85	14.20	22.20	26.40	15.30	26.10	19.45	20.00
Lu	16.10	42.50	13.55	0.27	1.38	4.53	3.45	3.73	2.38	3.20	3.15	2.34	3.68	3.98	2.34	4.05	2.86	2.80
Y	1770.00	6860.00	1460.00	18.30	65.10	177.50	86.60	115.50	131.50	94.90	123.00	114.50	158.00	263.00	149.00	283.00	197.50	208.00
La/Yb	70.28	17.28	53.95	38.84	40.53	180.14	126.56	41.42	40.90	51.15	226.53	423.94	133.33	234.09	62.35	46.17	30.54	33.25

Appendix 2 b) Trace elements analysis of samples collected by Etruscan and NRE and used in this study

Sample No.	ER13879	ER13880	ER13881	ER13882	ER13883	ER13884	ER13885	ER13886	ER13887	ER13888	ER13889	ER13890	ER13891	ER13892	ER13893	ER13894	ER13895	ER13896
Ba	345.00	357.00	436.00	1120.00	394.00	2160.00	109.00	409.00	10000.00	2470.00	1145.00	259.00	441.00	98.00	333.00	706.00	249.00	735.00
Ga	4.70	4.90	2.90	10.60	3.50	16.10	13.20	5.30	29.20	18.50	22.40	8.00	7.50	4.20	9.10	5.00	32.10	11.50
Hf	0.20	0.60	0.20	0.30	0.10	3.10	4.60	0.40	2.00	0.50	0.60	0.20	3.80	0.40	0.40	0.20	0.50	0.70
Nb	26.80	36.20	7.60	8.10	20.60	79.40	7.80	26.50	30.00	5.90	12.00	11.60	781.00	41.60	101.50	18.70	34.00	130.00
Rb	2.80	10.00	3.20	2.70	8.00	12.50	10.50	4.80	9.00	3.10	18.80	3.20	9.40	2.80	5.50	11.20	8.00	29.10
Sr	6900.00	3730.00	5830.00	2290.00	1810.00	410.00	941.00	1180.00	1235.00	3090.00	809.00	1440.00	3070.00	775.00	572.00	5200.00	1155.00	1445.00
Ta	0.20	0.30	0.10	0.10	0.10	0.30	0.05	0.10	0.25	0.05	0.10	0.10	4.60	0.05	0.30	0.10	0.25	0.80
Th	18.70	26.80	16.85	77.30	6.08	317.00	210.00	26.80	267.00	137.50	131.00	83.10	44.10	16.65	83.80	2.38	145.00	42.60
U	0.94	1.52	0.45	1.22	4.04	10.35	3.33	7.31	8.90	3.24	13.05	3.82	18.15	24.60	5.71	5.15	2.60	2.50
Zr	4.00	36.00	6.00	8.00	3.00	188.00	324.00	19.00	90.00	24.00	30.00	6.00	156.00	16.00	17.00	4.00	10.00	44.00
La	517.00	512.00	286.00	3820.00	730.00	5060.00	2580.00	757.00	8040.00	5580.00	5430.00	1590.00	643.00	263.00	2090.00	736.00	9340.00	2190.00
Ce	996.00	1150.00	554.00	5040.00	1090.00	7020.00	4480.00	1615.00	12800.00	8550.00	7640.00	2740.00	1155.00	488.00	3160.00	1265.00	13550.00	3200.00
Pr	112.50	148.00	66.70	418.00	105.00	617.00	463.00	191.50	1255.00	773.00	660.00	274.00	127.00	54.90	298.00	127.00	1230.00	285.00
Nd	361.00	532.00	231.00	1095.00	305.00	1645.00	1455.00	642.00	3440.00	2010.00	1705.00	795.00	404.00	176.50	857.00	363.00	3180.00	771.00
Sm	49.40	83.50	41.30	107.00	44.20	187.00	198.50	83.60	286.00	166.00	141.50	79.00	60.80	28.30	83.90	44.70	223.00	64.70
Eu	13.55	21.90	12.45	31.70	13.80	52.40	52.00	21.20	62.80	38.70	32.70	20.90	18.45	7.43	19.45	13.85	50.70	16.20
Gd	47.50	69.80	39.00	141.50	49.20	211.00	187.50	75.00	342.00	199.00	166.50	88.10	63.10	30.00	87.00	51.60	318.00	78.20
Tb	5.64	8.47	5.29	15.25	6.15	19.95	19.00	8.34	22.20	15.20	10.90	8.80	8.06	4.12	7.08	5.82	17.10	6.13
Dy	26.10	37.70	25.50	69.30	29.70	65.80	71.10	36.00	64.30	51.60	26.00	35.70	37.60	19.85	24.10	24.50	35.70	20.50
Ho	5.32	7.56	5.13	13.80	6.02	9.53	12.40	7.30	10.15	9.72	4.15	6.81	7.06	3.74	4.72	4.48	5.41	4.26
Er	15.95	22.30	14.50	40.40	17.30	24.40	35.10	22.70	35.50	31.20	15.55	20.90	19.70	9.93	15.90	13.15	24.40	15.80
Tm	2.23	3.16	2.07	5.44	2.54	2.55	4.34	3.30	2.73	3.60	1.44	2.90	2.62	1.31	2.15	1.76	2.06	2.53
Yb	14.45	20.30	13.25	33.50	15.85	17.25	26.90	22.00	16.70	23.40	9.62	19.55	15.85	8.00	15.05	12.10	16.50	19.10
Lu	2.12	2.92	1.96	4.79	2.28	2.62	3.96	3.33	2.19	3.39	1.51	2.98	2.23	1.17	2.42	1.87	2.74	3.23
Y	134.50	200.00	131.00	326.00	157.50	219.00	323.00	186.00	240.00	225.00	114.00	167.00	171.00	99.60	114.00	92.60	115.00	100.50
La/Yb	35.78	25.22	21.58	114.03	46.06	293.33	95.91	34.41	481.44	238.46	564.45	81.33	40.57	32.88	138.87	60.83	566.06	114.66

Appendix 2 b) Trace elements analysis of samples collected by Etruscan and NRE and used in this study

Sample No.	ER13897	ER13898	ER13899	ER13900	ER14753	ER14754	ER14755	ER14756	ER14757	ER14758	ER14759	ER14760	ER14761	ER14762	ER14763	ER14764	ER14765	ER14766
Ba	70.70	490.00	540.00	617.00	526.00	397.00	706.00	1570.00	389.00	337.00	391.00	571.00	442.00	499.00	3380.00	2830.00	883.00	251.00
Ga	3.30	8.00	2.80	3.80	18.40	21.10	4.20	29.90	3.30	4.00	6.60	20.90	16.60	11.10	9.30	9.40	5.30	9.50
Hf	0.10	0.80	0.20	0.30	5.90	6.80	0.70	9.40	0.10	1.70	3.40	1.00	2.50	0.40	2.20	0.70	2.40	1.00
Nb	33.60	30.00	10.10	8.30	65.20	126.50	7.80	536.00	5.90	306.00	44.70	259.00	23.30	34.50	12.10	21.10	90.30	53.30
Rb	2.20	16.00	2.00	2.60	25.70	52.50	3.20	177.50	1.70	8.20	4.30	20.10	11.60	4.40	5.70	10.10	12.80	22.20
Sr	97.30	571.00	3120.00	1305.00	941.00	834.00	11900.00	961.00	10000.00	8860.00	1955.00	957.00	2960.00	10000.00	1115.00	3380.00	10000.00	1045.00
Ta	0.20	0.20	0.05	0.05	0.80	2.30	0.05	4.90	0.05	0.40	0.20	2.10	0.20	0.20	0.10	0.20	0.20	0.40
Th	8.48	16.60	8.38	37.30	6.45	19.90	8.54	12.20	3.12	18.60	35.50	344.00	129.50	174.50	150.00	162.50	18.45	185.00
U	2.40	4.66	1.24	4.21	2.06	4.35	0.11	15.05	0.48	10.40	1.33	4.64	4.27	5.04	2.08	2.55	8.83	8.02
Zr	5.00	58.00	4.00	7.00	277.00	287.00	27.00	687.00	5.00	139.00	79.00	29.00	97.00	12.00	68.00	17.00	175.00	63.00
La	439.00	671.00	257.00	559.00	223.00	482.00	390.00	63.10	289.00	222.00	321.00	3560.00	1395.00	1335.00	1180.00	1025.00	404.00	394.00
Ce	653.00	1245.00	475.00	886.00	407.00	818.00	705.00	135.00	536.00	430.00	547.00	5850.00	3500.00	3000.00	2470.00	2170.00	701.00	737.00
Pr	62.00	136.00	54.50	87.70	45.10	88.60	77.80	15.60	60.00	49.30	59.10	568.00	435.00	340.00	263.00	247.00	70.60	78.90
Nd	167.00	434.00	183.00	256.00	148.00	271.00	245.00	54.30	197.50	165.50	187.50	1695.00	1560.00	1245.00	896.00	919.00	236.00	269.00
Sm	15.10	60.90	32.80	30.90	21.90	34.10	32.20	8.99	30.90	25.90	30.60	202.00	193.00	171.50	137.00	157.00	37.90	46.60
Eu	3.93	17.75	10.55	9.86	4.93	7.62	8.30	2.46	8.40	7.44	10.20	48.40	44.50	36.80	40.90	46.80	11.80	15.75
Gd	17.55	60.80	34.60	40.10	18.70	30.50	30.40	7.98	29.50	24.80	33.50	189.50	160.00	122.50	135.00	150.50	37.40	47.30
Tb	1.48	6.70	5.08	6.81	2.08	3.05	3.37	0.98	3.58	3.02	4.76	15.85	17.80	11.10	18.20	19.65	5.01	6.41
Dy	5.33	26.80	26.70	43.70	9.09	12.05	14.90	4.43	16.55	13.60	26.90	51.30	67.00	37.60	98.30	89.00	25.80	31.40
Ho	1.04	4.80	5.43	9.87	1.84	2.42	2.99	0.87	3.26	2.67	5.35	8.56	10.55	6.40	19.40	14.60	4.82	5.67
Er	3.22	13.65	15.95	29.60	5.61	7.65	9.19	2.42	8.96	7.25	15.15	28.90	29.30	23.60	61.80	40.40	14.55	16.60
Tm	0.45	1.81	2.41	4.31	0.85	1.07	1.28	0.33	1.15	0.94	2.20	3.86	3.20	3.32	8.61	4.88	1.95	2.19
Yb	3.07	11.45	15.40	26.40	6.09	7.16	8.21	2.28	6.81	5.76	13.40	27.40	19.45	26.10	53.90	30.70	12.40	13.80
Lu	0.45	1.67	2.29	3.89	1.07	1.17	1.24	0.45	0.98	0.93	1.82	4.18	2.69	4.15	7.42	4.12	1.63	1.88
Y	22.70	125.00	139.00	256.00	51.20	67.70	80.40	22.30	88.80	69.20	134.00	208.00	248.00	170.00	604.00	358.00	145.50	163.50
La/Yb	143.00	58.60	16.69	21.17	36.62	67.32	47.50	27.68	42.44	38.54	23.96	129.93	71.72	51.15	21.89	33.39	32.58	28.55

Appendix 2 b) Trace elements analysis of samples collected by Etruscan and NRE and used in this study

Sample No.	ER14767	ER14768	ER14769	ER14770	ER14771	ER14772	ER14773	ER14774	ER14775	ER14776	ER14777	ER14778	ER14779	ER14780	ER14781	ER14782	ER14783	ER14784
Ba	336.00	4950.00	208.00	561.00	2420.00	172.00	1425.00	620.00	437.00	2540.00	487.00	10000.00	910.00	1700.00	920.00	289.00	837.00	358.00
Ga	11.10	14.10	16.80	9.20	8.80	5.10	9.20	6.10	9.60	9.70	6.80	64.80	5.30	2.90	10.10	2.00	9.90	5.90
Hf	12.30	7.30	1.20	1.00	2.00	2.10	0.80	0.40	0.50	0.50	0.30	1.00	4.80	0.30	2.50	0.40	1.00	0.50
Nb	403.00	261.00	12.40	3.90	39.50	51.70	330.00	38.90	5.00	3.70	17.90	56.00	23.10	4.50	17.10	7.50	89.90	4.50
Rb	45.00	50.20	7.40	1.30	55.90	15.60	9.20	4.30	9.20	0.40	14.00	2.00	3.10	1.30	7.20	4.40	31.60	12.10
Sr	2040.00	685.00	5240.00	1340.00	340.00	523.00	5510.00	2710.00	1070.00	939.00	917.00	1220.00	2560.00	6920.00	2000.00	973.00	4690.00	1695.00
Ta	2.20	0.30	0.10	0.10	0.40	0.10	2.70	0.30	0.10	0.10	0.10	0.25	0.10	0.05	0.20	0.05	1.00	0.10
Th	67.50	76.60	158.00	154.50	29.90	59.20	102.50	41.00	72.00	167.50	18.70	743.00	1000.00	42.00	318.00	2.60	4.59	43.90
U	45.20	9.72	3.17	0.98	3.95	8.20	15.35	4.64	1.92	2.05	5.10	5.00	5.55	2.11	5.66	1.55	4.22	1.72
Zr	842.00	531.00	55.00	40.00	91.00	123.00	44.00	13.00	13.00	15.00	11.00	40.00	197.00	8.00	88.00	14.00	39.00	13.00
La	615.00	1080.00	3430.00	961.00	277.00	486.00	300.00	530.00	808.00	862.00	457.00	13750.00	402.00	235.00	970.00	122.00	622.00	502.00
Ce	1210.00	2060.00	5200.00	2080.00	507.00	798.00	606.00	1180.00	1785.00	1955.00	897.00	19700.00	851.00	427.00	1980.00	175.50	1255.00	933.00
Pr	133.50	218.00	445.00	244.00	53.10	76.10	68.20	138.50	216.00	236.00	96.60	1835.00	103.00	46.00	233.00	16.00	137.50	96.50
Nd	467.00	753.00	1275.00	944.00	173.00	239.00	248.00	526.00	846.00	927.00	323.00	5050.00	427.00	163.50	946.00	49.40	484.00	319.00
Sm	77.70	101.00	127.50	192.50	28.00	33.50	47.70	104.00	165.00	186.50	47.30	518.00	213.00	37.80	260.00	8.05	78.20	46.00
Eu	22.90	23.80	37.00	59.30	6.88	8.85	20.70	31.60	46.10	57.40	13.25	134.00	91.00	13.95	90.90	2.68	26.60	14.05
Gd	76.50	94.80	163.00	172.50	27.50	34.60	65.40	92.60	135.00	164.50	47.00	604.00	235.00	42.30	251.00	9.23	84.40	50.70
Tb	10.40	12.45	19.70	20.50	3.35	4.36	11.45	11.40	13.90	17.65	5.87	45.00	29.50	6.17	31.60	1.31	11.60	6.43
Dy	52.60	66.80	93.50	88.10	16.15	22.00	59.30	51.70	48.80	66.10	30.90	129.00	122.00	32.10	136.50	7.48	58.00	32.30
Ho	9.44	13.35	16.20	14.00	2.94	4.03	9.92	8.73	7.18	9.82	6.26	16.90	17.70	5.92	21.90	1.59	10.00	6.27
Er	27.40	43.70	46.20	37.40	9.33	12.40	26.50	24.80	19.65	26.60	20.70	48.80	43.20	17.30	58.20	5.26	26.70	20.60
Tm	3.61	6.26	5.30	4.10	1.30	1.64	3.43	3.01	1.95	2.82	2.97	3.38	5.31	2.41	7.24	0.79	3.01	3.12
Yb	22.70	40.80	33.30	24.00	9.37	10.25	21.30	18.65	12.30	17.35	19.50	20.30	33.30	15.55	45.20	5.42	17.25	21.50
Lu	3.17	5.68	4.56	3.14	1.45	1.38	2.77	2.50	1.55	2.25	2.87	2.79	4.40	2.19	5.81	0.81	2.23	3.18
Y	260.00	372.00	460.00	406.00	94.70	120.50	271.00	233.00	170.00	249.00	173.50	358.00	605.00	179.50	521.00	60.90	234.00	202.00
La/Yb	27.09	26.47	103.00	40.04	29.56	47.41	14.08	28.42	65.69	49.68	23.44	677.34	12.07	15.11	21.46	22.51	36.06	23.35

Appendix 2 b) Trace elements analysis of samples collected by Etruscan and NRE and used in this study

Sample No.	ER14785	ER14786	ER14787	ER14788	ER14789	ER14790	ER14791	ER14792	ER14793	ER14794	ER14795	ER14796	ER14797	ER14798	ER14799	ER14800	ER18001	ER18002
Ba	94.90	439.00	280.00	372.00	431.00	252.00	169.50	266.00	146.00	388.00	525.00	393.00	2890.00	313.00	100.50	687.00	809.00	1005.00
Ga	5.10	4.10	2.80	14.10	2.90	3.50	37.50	11.20	36.50	4.30	12.50	7.90	3.00	3.50	5.70	36.10	13.80	11.00
Hf	0.40	0.30	0.50	0.90	0.70	5.10	2.10	0.70	1.00	2.70	2.50	3.80	0.50	0.70	0.90	0.60	12.70	3.50
Nb	10.80	82.80	12.00	4.70	15.60	175.50	125.50	66.50	5.00	31.50	43.70	20.20	1.20	0.80	10.40	6.40	181.00	172.50
Rb	4.40	7.80	0.60	19.90	1.90	6.80	6.20	0.50	1.00	5.70	21.70	33.00	4.40	2.80	4.40	5.20	46.50	7.20
Sr	366.00	2460.00	3330.00	1320.00	3360.00	2080.00	1265.00	790.00	1305.00	2440.00	1730.00	1045.00	5630.00	825.00	1085.00	2740.00	3930.00	5570.00
Ta	0.20	0.70	0.10	0.10	0.10	0.30	0.60	0.50	0.25	0.30	0.30	0.20	0.10	0.05	0.10	0.05	1.60	0.50
Th	33.90	2.16	9.75	72.30	9.98	5.46	555.00	35.50	52.50	106.00	124.00	39.10	44.20	28.40	39.20	114.00	965.00	343.00
U	2.28	1.90	1.15	2.48	0.62	1.50	3.92	4.97	2.70	4.47	3.78	2.09	1.41	5.36	0.82	4.52	16.60	5.15
Zr	13.00	8.00	15.00	42.00	23.00	420.00	103.00	39.00	50.00	191.00	156.00	205.00	15.00	44.00	63.00	21.00	805.00	177.00
La	311.00	219.00	129.50	1890.00	137.00	167.00	6390.00	985.00	7210.00	245.00	899.00	625.00	142.00	349.00	499.00	7260.00	1140.00	2190.00
Ce	629.00	415.00	296.00	2870.00	237.00	273.00	9630.00	2070.00	10050.00	419.00	1980.00	956.00	259.00	560.00	958.00	9900.00	2130.00	3010.00
Pr	71.60	44.40	37.60	249.00	23.10	26.60	855.00	219.00	879.00	44.70	237.00	91.00	26.70	54.70	97.30	824.00	291.00	307.00
Nd	258.00	151.00	155.50	737.00	74.80	85.20	2700.00	722.00	2230.00	157.00	961.00	293.00	93.20	173.50	318.00	2380.00	1180.00	840.00
Sm	43.60	26.00	40.00	86.30	15.65	14.20	413.00	78.70	157.00	30.00	198.50	51.20	24.20	31.50	49.30	262.00	481.00	111.00
Eu	13.10	8.80	14.20	22.50	6.50	5.28	141.50	19.85	35.20	10.20	61.00	19.90	11.00	9.43	13.70	64.10	153.50	34.00
Gd	42.70	28.60	46.60	103.50	23.80	18.65	482.00	80.80	231.00	35.80	174.50	66.30	36.00	34.20	49.10	264.00	502.00	134.50
Tb	5.22	3.81	8.55	10.80	5.81	3.25	54.40	7.46	12.90	5.03	20.50	9.34	7.23	5.58	6.12	19.05	103.50	23.10
Dy	24.50	19.80	55.80	54.90	51.30	21.70	241.00	27.80	30.00	26.40	94.80	49.80	48.50	35.00	28.60	41.80	608.00	140.50
Ho	4.55	3.79	11.70	12.00	13.75	4.46	41.50	5.28	5.03	4.89	17.60	9.16	10.30	8.04	5.43	5.94	111.50	29.10
Er	14.05	11.65	38.60	42.70	54.30	13.95	117.00	18.30	21.20	15.20	51.40	26.50	33.60	29.80	18.15	25.70	277.00	90.10
Tm	2.01	1.59	6.17	6.13	9.83	2.07	12.80	2.07	1.92	2.19	5.94	3.46	5.30	4.71	2.38	2.00	32.70	13.70
Yb	13.65	10.30	41.90	39.20	68.60	13.05	74.20	13.25	14.80	15.50	33.30	21.60	35.50	38.40	18.35	17.50	153.50	80.70
Lu	2.05	1.46	6.02	5.21	9.45	1.75	9.39	1.87	2.27	2.32	4.11	2.91	4.95	5.13	2.29	2.39	19.40	11.85
Y	133.00	109.00	295.00	398.00	440.00	130.00	1170.00	151.50	139.00	176.00	469.00	250.00	314.00	233.00	188.50	157.00	2820.00	832.00
La/Yb	22.78	21.26	3.09	48.21	2.00	12.80	86.12	74.34	487.16	15.81	27.00	28.94	4.00	9.09	27.19	414.86	7.43	27.14

Appendix 2 b) Trace elements analysis of samples collected by Etruscan and NRE and used in this study

Sample No.	ER18003	ER18004	ER18005	ER18006	ER18007	ER18008	ER18009	ER18010	ER18011	ER18012	ER18013	ER18014	ER18015	ER18016	ER18017	ER18018	ER18019	ER18020
Ba	1350.00	543.00	522.00	653.00	855.00	369.00	1245.00	925.00	535.00	260.00	50.30	169.00	136.50	67.40	204.00	364.00	290.00	174.50
Ga	4.70	5.00	7.30	13.20	8.60	5.90	19.00	21.70	25.10	11.90	4.90	2.70	35.20	5.80	20.30	27.60	8.10	12.20
Hf	2.00	0.80	4.10	6.20	1.10	1.70	15.00	8.10	7.40	0.70	4.70	0.20	0.80	0.50	1.10	3.00	4.50	9.20
Nb	83.40	28.50	92.80	50.10	56.40	98.10	122.50	190.00	234.00	7.70	12.10	14.70	23.80	14.40	36.20	7.00	139.50	93.00
Rb	0.90	2.10	2.20	4.40	1.40	1.30	1.10	2.00	4.10	4.20	4.30	1.90	13.30	15.50	30.50	11.00	17.70	1.20
Sr	3380.00	5750.00	2500.00	10000.00	9570.00	4130.00	1535.00	2390.00	1810.00	1380.00	640.00	740.00	3010.00	1250.00	3150.00	1295.00	1120.00	3650.00
Ta	0.20	0.20	0.20	0.10	0.20	0.20	0.20	1.20	1.60	0.10	0.10	0.10	0.10	0.10	0.10	0.25	0.80	1.60
Th	112.00	162.00	19.80	49.10	303.00	121.00	106.50	167.50	162.50	51.50	24.50	4.23	53.70	18.00	73.90	176.00	36.30	6.77
U	1.80	1.30	12.70	4.23	1.58	1.25	19.50	5.36	6.41	3.90	4.18	1.35	1.77	2.20	5.44	4.50	30.90	2.60
Zr	132.00	31.00	377.00	904.00	59.00	88.00	3330.00	415.00	466.00	54.00	294.00	13.00	40.00	41.00	46.00	160.00	392.00	720.00
La	489.00	659.00	967.00	1560.00	1575.00	497.00	4460.00	1415.00	2770.00	3110.00	537.00	100.50	5920.00	268.00	5570.00	8420.00	1375.00	153.50
Ce	758.00	912.00	1475.00	3160.00	2220.00	683.00	6210.00	2360.00	3930.00	4050.00	759.00	170.00	7610.00	450.00	6980.00	10650.00	2290.00	252.00
Pr	92.40	103.00	163.50	411.00	234.00	78.20	535.00	275.00	387.00	375.00	64.10	16.70	577.00	43.30	545.00	841.00	254.00	25.60
Nd	294.00	303.00	478.00	1410.00	679.00	235.00	1605.00	864.00	1040.00	955.00	186.50	54.00	1485.00	140.50	1490.00	2120.00	808.00	79.80
Sm	53.40	49.10	55.80	212.00	102.50	42.80	163.00	112.00	106.50	86.20	25.90	8.72	119.00	22.30	132.50	188.50	107.00	12.85
Eu	16.00	15.05	13.00	50.00	30.80	14.15	35.00	23.10	24.80	18.60	7.02	2.76	29.80	6.59	32.30	50.50	31.30	4.97
Gd	58.20	56.00	49.50	158.00	117.50	52.80	149.50	90.20	108.50	91.70	31.60	11.00	180.50	25.90	162.00	251.00	108.00	14.35
Tb	13.45	12.20	5.80	19.00	22.40	11.85	12.35	11.80	13.05	8.78	3.73	1.91	14.05	3.67	15.20	20.30	11.65	2.01
Dy	102.50	88.40	27.60	77.50	140.50	85.60	37.50	61.50	67.90	37.20	20.70	12.65	53.30	22.30	62.00	75.90	52.90	11.50
Ho	25.10	21.40	5.37	12.70	29.00	20.40	6.61	12.55	14.20	7.45	4.80	2.89	11.00	5.28	11.85	13.30	9.25	2.35
Er	89.10	78.10	17.50	34.00	87.10	71.70	23.30	40.30	46.00	25.70	16.00	9.38	36.90	17.55	39.50	44.20	25.50	7.46
Tm	15.95	14.35	2.47	3.62	12.90	12.90	2.82	5.93	6.74	3.64	2.55	1.43	4.42	2.89	5.27	5.05	3.04	1.25
Yb	103.50	95.90	14.80	18.70	78.20	87.30	18.90	36.80	39.60	22.50	18.35	9.50	28.00	20.80	32.00	34.00	18.15	10.25
Lu	15.80	14.65	2.23	2.43	11.55	13.60	3.02	5.90	5.81	3.37	2.70	1.31	3.73	3.03	4.76	4.99	2.52	2.03
Y	788.00	690.00	169.00	332.00	834.00	636.00	218.00	363.00	421.00	262.00	161.00	97.50	326.00	166.00	352.00	422.00	230.00	61.90
La/Yb	4.72	6.87	65.34	83.42	20.14	5.69	235.98	38.45	69.95	138.22	29.26	10.58	211.43	12.88	174.06	247.65	75.76	14.98

Appendix 2 b) Trace elements analysis of samples collected by Etruscan and NRE and used in this study

Sample No.	ER18021	ER18022	ER18023	ER18024	ER18025	ER18026	ER18027	ER18028	ER18029	ER18030	ER18031	ER18032	ER18033	ER18034	ERN15101	ERN15102	ERN15103	ERN15104
Ba	178.50	278.00	809.00	570.00	475.00	380.00	300.00	408.00	222.00	372.00	855.00	44.40	700.00	802.00	330.00	308.00	784.00	336.00
Ga	4.70	1.80	5.70	1.80	1.80	7.50	3.50	2.20	2.90	6.40	7.80	2.40	20.90	8.20	3.30	9.00	13.50	19.80
Hf	0.40	0.20	0.90	0.30	0.20	5.80	1.80	1.00	0.30	2.60	6.90	1.50	24.30	2.20	0.20	13.40	3.70	12.70
Nb	17.10	1.30	6.10	0.80	3.90	239.00	371.00	138.50	5.40	220.00	23.70	38.50	742.00	80.30	2.50	237.00	140.00	747.00
Rb	1.60	0.70	19.40	0.40	1.20	51.30	5.40	0.40	5.10	2.10	3.60	2.30	2.20	9.60	3.80	11.70	86.10	42.90
Sr	209.00	3880.00	467.00	7280.00	10000.00	1920.00	609.00	10000.00	690.00	3260.00	7510.00	879.00	461.00	1495.00	12100.00	11000.00	8510.00	1045.00
Ta	0.10	0.05	0.10	0.05	0.10	5.80	2.20	0.60	0.05	2.40	0.40	0.50	1.80	0.60	0.20	7.90	1.90	13.50
Th	19.90	4.23	10.95	2.89	3.59	9.22	12.95	9.11	7.61	64.70	3.52	5.87	295.00	90.60	1.87	9.56	7.45	8.03
U	5.28	1.03	4.79	0.32	0.52	8.73	6.27	6.29	8.02	8.13	1.50	2.55	7.06	16.65	0.99	65.80	18.45	16.55
Zr	15.00	11.00	36.00	10.00	6.00	464.00	89.00	45.00	11.00	131.00	172.00	85.00	2010.00	136.00	5.00	773.00	344.00	909.00
La	544.00	332.00	815.00	308.00	263.00	354.00	339.00	220.00	290.00	339.00	807.00	123.50	1480.00	1535.00	205.00	288.00	199.00	102.00
Ce	915.00	571.00	1315.00	532.00	478.00	715.00	595.00	420.00	536.00	672.00	1425.00	244.00	2690.00	2550.00	455.00	693.00	457.00	205.00
Pr	92.90	56.40	143.50	53.40	50.00	85.70	65.00	45.70	57.70	80.30	165.00	28.70	306.00	286.00	48.10	78.70	50.30	20.70
Nd	274.00	171.50	454.00	163.50	162.50	306.00	219.00	157.50	191.50	298.00	541.00	107.00	1015.00	931.00	152.50	266.00	166.00	61.80
Sm	36.60	24.40	76.50	24.70	27.30	53.30	41.00	29.70	36.20	65.00	80.60	24.00	147.50	124.00	23.00	39.40	25.90	8.51
Eu	10.30	6.75	24.70	7.11	8.18	16.00	12.55	10.15	9.85	20.40	19.85	7.73	32.20	34.70	7.09	12.15	7.68	2.49
Gd	35.20	26.80	81.10	27.60	29.10	53.20	43.10	35.80	35.10	70.80	80.50	27.80	125.00	124.50	23.10	38.10	24.60	8.73
Tb	3.40	3.53	9.90	3.77	4.09	6.96	6.27	6.07	4.31	10.95	9.54	4.56	11.85	14.80	3.13	4.73	3.34	1.11
Dy	13.95	19.65	46.00	21.20	23.10	36.00	33.30	36.20	19.90	64.00	45.60	26.00	47.40	75.70	14.70	19.10	15.45	5.16
Ho	2.59	4.10	8.05	4.46	4.75	6.54	5.95	7.18	3.46	12.20	8.63	4.99	9.10	14.45	3.01	3.40	3.07	1.03
Er	7.80	12.75	22.80	13.60	14.10	17.80	15.60	19.95	9.99	34.10	24.90	13.95	37.80	42.00	8.77	9.14	8.65	3.21
Tm	1.06	1.90	3.05	2.01	2.07	2.37	2.04	2.76	1.36	4.69	3.30	2.05	9.65	5.57	1.09	0.97	1.07	0.42
Yb	6.58	12.25	18.75	12.40	12.95	13.90	11.95	16.20	8.50	27.50	20.30	12.85	113.00	34.00	6.75	5.79	6.90	2.75
Lu	0.90	1.76	2.64	1.71	1.76	1.98	1.61	2.05	1.21	3.71	2.72	1.88	24.50	4.68	0.99	0.92	1.06	0.42
Y	76.20	95.80	201.00	108.00	110.00	147.00	122.50	166.50	89.90	303.00	203.00	125.50	219.00	413.00	80.60	83.80	78.80	30.10
La/Yb	82.67	27.10	43.47	24.84	20.31	25.47	28.37	13.58	34.12	12.33	39.75	9.61	13.10	45.15	30.37	49.74	28.84	37.09

Appendix 2 b) Trace elements analysis of samples collected by Etruscan and NRE and used in this study

Sample No.	ERN15105	ERN15106	ERN15107	ERN15108	ERN15109	ERN15110	ERN15111	ERN15112	ERN15113	ERN15114	ERN15115	ERN15116	ERN15117	ERN15118	ERN15119	ERN15120	ERN15121	ERN15122
Ba	392.00	429.00	376.00	426.00	589.00	387.00	304.00	275.00	297.00	333.00	832.00	317.00	588.00	817.00	511.00	877.00	331.00	170.50
Ga	2.80	3.10	5.10	14.30	3.70	9.00	18.00	4.70	10.90	10.20	3.60	3.70	17.00	5.10	10.40	23.00	8.10	6.30
Hf	0.20	0.20	1.80	10.50	0.50	1.30	1.40	0.20	6.70	13.40	0.80	0.20	15.90	0.70	2.00	12.30	3.40	0.50
Nb	11.60	33.60	65.60	328.00	13.60	38.00	162.00	65.70	328.00	64.00	184.50	16.80	952.00	102.00	245.00	1505.00	149.50	51.70
Rb	2.70	3.90	11.60	33.20	6.30	12.30	115.50	18.60	34.60	11.20	1.40	13.80	91.00	26.70	51.60	147.00	23.50	9.80
Sr	20900.00	20800.00	12400.00	9660.00	16700.00	1005.00	6960.00	10800.00	7200.00	7560.00	2950.00	12800.00	5340.00	6580.00	11000.00	5330.00	9860.00	314.00
Ta	0.20	0.40	0.40	6.90	0.30	0.70	0.80	0.30	1.10	0.20	0.70	0.10	15.50	1.30	1.10	18.20	3.10	0.40
Th	1.55	1.72	5.82	4.30	17.45	2.93	4.02	2.66	10.55	19.40	5.24	3.20	7.51	6.27	1.66	11.20	3.57	7.99
U	0.64	2.22	1.61	4.07	2.13	34.70	25.10	2.32	3.40	2.28	9.66	0.84	42.20	4.85	8.70	75.40	12.55	2.93
Zr	11.00	14.00	80.00	930.00	40.00	98.00	64.00	5.00	468.00	513.00	30.00	13.00	1140.00	43.00	121.00	998.00	316.00	21.00
La	205.00	195.50	206.00	189.50	190.50	35.00	188.00	153.00	233.00	204.00	202.00	142.50	152.00	180.00	199.50	143.00	278.00	257.00
Ce	444.00	404.00	471.00	414.00	416.00	99.80	429.00	333.00	562.00	455.00	399.00	267.00	301.00	362.00	414.00	267.00	560.00	522.00
Pr	45.10	41.20	51.20	43.70	43.80	11.90	45.80	34.60	63.50	48.00	46.60	30.40	33.70	41.90	48.80	29.80	65.30	59.10
Nd	139.00	126.00	166.50	139.50	136.50	45.80	145.50	108.00	216.00	152.00	163.00	101.50	112.50	143.00	168.00	99.20	227.00	200.00
Sm	20.40	17.75	26.10	21.10	20.30	11.90	21.20	16.60	34.80	21.70	26.50	15.60	16.40	22.90	25.00	14.90	34.20	28.10
Eu	6.72	5.74	8.11	6.43	6.35	4.30	6.69	5.17	10.70	6.87	7.79	4.44	4.70	6.63	6.98	4.14	9.79	5.43
Gd	21.40	18.65	26.70	21.40	20.70	11.85	21.90	17.55	34.00	22.70	26.10	15.50	16.60	23.20	24.40	14.85	34.10	27.40
Tb	2.97	2.40	3.65	2.89	2.85	1.96	2.88	2.49	4.64	3.07	3.53	2.05	2.12	3.15	3.11	1.96	4.28	3.31
Dy	14.40	11.05	16.50	13.70	13.45	11.20	12.85	12.15	20.90	14.40	17.40	10.10	10.05	15.45	13.90	9.39	19.40	15.00
Ho	2.96	2.25	3.22	2.79	2.76	2.31	2.51	2.46	4.04	2.95	3.36	1.97	1.97	3.05	2.64	1.85	3.70	2.95
Er	8.58	6.49	8.91	7.93	8.16	6.52	7.27	7.09	10.90	8.73	9.67	5.98	5.83	9.13	7.85	5.56	10.55	8.99
Tm	1.08	0.80	1.04	0.98	1.05	0.92	0.86	0.88	1.24	1.09	1.25	0.78	0.74	1.23	0.98	0.74	1.26	1.14
Yb	6.76	4.86	6.25	6.09	6.80	6.21	5.53	5.47	7.36	6.93	7.72	4.94	4.43	8.02	6.05	4.59	7.40	7.02
Lu	1.03	0.70	0.93	0.91	1.06	0.97	0.83	0.82	1.07	1.11	1.02	0.65	0.60	1.09	0.82	0.63	0.95	0.91
Y	74.70	58.90	81.20	75.30	71.70	60.60	63.90	64.90	104.50	77.30	89.30	50.70	51.40	77.70	64.10	49.10	95.40	74.50
La/Yb	30.33	40.23	32.96	31.12	28.01	5.64	34.00	27.97	31.66	29.44	26.17	28.85	34.31	22.44	32.98	31.15	37.57	36.61

Appendix 2 b) Trace elements analysis of samples collected by Etruscan and NRE and used in this study

Sample No.	ERN15123	ERN15124	ERN15125	ERN15126	ERN15127	ERN15128	ERN15129	ERN15130	ERN15131	ERN15132	ERN15133	ERN15134	ERN15135	ERN15136	ERN15137	ERN15138	ERN15139	ERN15140
Ba	37.70	192.00	1240.00	97.80	157.50	266.00	371.00	931.00	246.00	226.00	2560.00	141.50	759.00	38.90	88.80	184.50	170.00	187.50
Ga	10.30	18.20	70.30	28.90	28.50	3.30	3.00	4.10	4.10	3.50	50.60	11.80	17.10	2.40	1.00	38.50	5.90	17.40
Hf	1.10	1.40	4.00	0.60	1.00	0.30	0.90	0.20	0.60	0.30	14.00	1.10	8.50	3.00	16.10	2.40	0.40	0.30
Nb	5.80	17.00	110.00	0.80	14.10	152.00	99.80	3.20	103.50	14.20	1170.00	55.80	305.00	7.00	53.00	38.70	5.70	154.50
Rb	2.10	16.50	0.50	35.20	5.60	0.60	1.00	0.80	0.80	4.70	22.00	2.70	6.50	0.50	1.10	2.90	0.40	39.10
Sr	3100.00	6150.00	3630.00	684.00	1555.00	9710.00	9920.00	10500.00	178.00	195.50	3890.00	703.00	2190.00	16.90	255.00	422.00	1635.00	2670.00
Ta	0.30	0.10	0.25	0.10	0.20	0.60	0.20	0.10	0.10	0.10	8.10	0.40	3.60	0.20	0.40	0.70	0.10	9.60
Th	364.00	239.00	733.00	421.00	737.00	6.39	2.02	20.30	7.36	98.30	249.00	87.00	418.00	126.50	631.00	198.50	29.00	11.65
U	4.75	5.28	28.80	7.82	13.50	7.17	2.52	0.65	4.55	4.64	57.40	5.35	27.60	4.27	10.60	6.04	2.16	8.50
Zr	65.00	100.00	420.00	8.00	15.00	9.00	15.00	3.00	15.00	10.00	400.00	23.00	452.00	350.00	1720.00	32.00	10.00	13.00
La	1425.00	3040.00	11600.00	5180.00	5080.00	228.00	204.00	455.00	176.50	218.00	8050.00	1430.00	1420.00	8.30	10.10	4140.00	461.00	244.00
Ce	2600.00	4510.00	20500.00	7930.00	7990.00	459.00	434.00	902.00	263.00	430.00	12950.00	2660.00	2630.00	13.80	21.80	7560.00	819.00	438.00
Pr	267.00	406.00	1965.00	744.00	764.00	50.00	50.10	97.70	24.10	48.20	1345.00	296.00	273.00	1.68	3.09	740.00	89.50	46.60
Nd	903.00	1220.00	5990.00	2260.00	2340.00	171.50	178.50	328.00	81.30	177.50	3610.00	1075.00	928.00	7.20	14.90	2320.00	284.00	146.00
Sm	128.50	149.50	650.00	304.00	284.00	27.10	29.80	47.40	15.20	31.80	382.00	183.00	175.00	8.03	22.90	438.00	43.10	24.40
Eu	32.00	37.90	142.00	85.20	72.30	7.64	8.02	12.30	5.03	6.97	85.80	46.40	61.20	7.32	22.70	133.50	12.60	8.34
Gd	118.50	150.50	608.00	293.00	269.00	25.70	25.90	41.10	16.20	28.50	354.00	158.00	219.00	33.60	91.70	513.00	48.70	30.00
Tb	17.15	18.25	55.70	31.30	35.00	3.58	3.61	5.41	2.54	4.42	24.30	21.60	34.20	9.91	27.50	59.90	6.00	4.02
Dy	95.80	96.30	223.00	131.50	202.00	18.50	18.30	28.00	13.55	25.90	61.90	110.00	198.50	73.70	204.00	261.00	30.00	20.10
Ho	20.50	20.80	41.60	24.10	45.60	3.74	3.53	5.92	2.62	5.85	9.59	21.60	41.50	16.85	46.30	48.80	6.42	4.02
Er	66.20	66.40	109.50	69.90	147.50	11.10	10.25	18.70	6.75	19.30	29.80	61.20	117.00	50.30	138.00	141.50	20.80	11.85
Tm	10.30	9.81	12.70	8.81	21.50	1.54	1.44	2.74	0.92	2.84	3.25	7.93	16.55	8.24	23.10	20.30	3.38	1.82
Yb	69.30	64.50	59.20	54.00	133.50	9.73	9.24	18.05	4.76	18.25	20.20	45.80	86.80	48.60	135.50	123.50	22.30	11.45
Lu	9.72	8.92	7.53	7.33	18.05	1.33	1.29	2.50	0.63	2.54	3.04	5.42	10.35	6.54	18.45	16.80	3.18	1.62
Y	605.00	646.00	1020.00	758.00	1495.00	100.00	92.70	175.50	84.40	236.00	212.00	589.00	1065.00	482.00	1240.00	1105.00	171.50	105.50
La/Yb	20.56	47.13	195.95	95.93	38.05	23.43	22.08	25.21	37.08	11.95	398.51	31.22	16.36	0.17	0.07	33.52	20.67	21.31

Appendix 2 b) Trace elements analysis of samples collected by Etruscan and NRE and used in this study

Sample No.	ERN15141	ERN15142	ERN15143	ERN15144	ERN15145	ERN15146	ERN15147	ERN15148	ERN15149	ERN15151	ERN15152	ERN15153	ERN15154	ERN15155	ERN15156	ERN15157	ERN15158	ERN15159
Ba	139.50	393.00	152.50	541.00	470.00	486.00	790.00	1180.00	466.00	793.00	134.50	239.00	260.00	1045.00	1765.00	1905.00	1925.00	1495.00
Ga	4.60	5.30	21.40	3.30	39.40	39.20	3.40	20.50	32.90	11.80	10.10	23.90	48.60	42.00	12.30	44.50	19.70	19.20
Hf	0.30	0.20	0.50	0.20	0.30	0.30	5.50	2.50	0.70	1.10	0.70	8.80	10.10	7.60	0.80	1.00	5.00	4.00
Nb	3.10	28.90	1.80	1.70	1.40	0.40	40.80	49.80	1.60	190.00	595.00	931.00	81.00	50.30	65.40	82.00	250.00	233.00
Rb	9.20	22.50	4.50	0.80	2.40	5.80	7.90	44.10	0.40	0.80	1.10	6.40	11.70	37.80	26.70	16.60	47.20	29.60
Sr	3650.00	2980.00	1435.00	1330.00	4200.00	3140.00	447.00	6830.00	20600.00	19300.00	5010.00	483.00	1850.00	1965.00	2400.00	3140.00	1640.00	8130.00
Ta	0.10	0.10	0.10	0.05	0.10	0.10	1.10	0.90	0.20	1.00	2.10	13.90	0.80	2.50	0.40	0.30	2.70	3.70
Th	7.73	2.59	264.00	1.93	35.40	37.30	13350.00	759.00	186.00	142.50	21.90	1610.00	239.00	2190.00	92.50	473.00	216.00	631.00
U	1.41	4.30	2.81	10.65	0.95	1.21	88.30	3.01	0.51	10.80	13.75	53.80	4.23	19.20	8.49	11.00	6.54	10.15
Zr	7.00	3.00	4.00	3.00	2.00	3.00	146.00	42.00	2.00	48.00	62.00	397.00	399.00	168.00	3.00	3.00	296.00	158.00
La	181.50	257.00	2410.00	186.00	6760.00	6530.00	83.00	2200.00	4340.00	934.00	824.00	1810.00	4870.00	5200.00	918.00	4680.00	965.00	714.00
Ce	363.00	509.00	3820.00	375.00	9060.00	8580.00	162.50	3150.00	6560.00	1770.00	1580.00	3180.00	9160.00	7620.00	1525.00	8540.00	1485.00	1065.00
Pr	41.10	55.90	368.00	41.50	699.00	659.00	20.60	266.00	561.00	182.50	162.00	365.00	932.00	661.00	152.50	814.00	150.00	105.50
Nd	134.00	174.50	1190.00	132.00	1725.00	1625.00	94.60	783.00	1540.00	640.00	558.00	1820.00	3030.00	1900.00	456.00	2360.00	479.00	330.00
Sm	23.80	26.30	212.00	21.90	125.50	128.50	215.00	132.00	160.00	91.30	71.50	810.00	463.00	311.00	65.20	245.00	83.70	63.30
Eu	7.60	8.38	57.70	7.34	32.20	34.10	147.50	58.40	42.50	28.70	21.10	237.00	126.50	129.00	22.50	71.30	27.90	25.50
Gd	27.40	32.40	213.00	25.80	238.00	234.00	509.00	229.00	227.00	103.50	80.30	591.00	488.00	546.00	93.30	353.00	99.20	94.90
Tb	3.88	4.43	19.00	3.43	13.65	14.25	101.50	39.60	20.30	12.40	8.04	72.70	47.10	115.00	15.15	34.30	13.50	18.15
Dy	20.10	23.20	60.60	16.95	31.20	34.60	547.00	230.00	84.40	56.50	29.70	280.00	150.50	687.00	93.70	117.00	70.20	104.00
Ho	4.18	4.80	10.40	3.40	6.85	6.99	95.90	45.40	17.85	10.75	5.35	41.50	23.30	133.00	20.80	19.35	13.55	19.35
Er	12.60	14.05	34.30	10.30	32.00	29.80	219.00	121.50	59.40	31.10	15.75	98.60	67.70	304.00	63.70	59.30	36.50	49.60
Tm	1.97	2.09	4.47	1.56	4.37	3.54	28.60	17.50	8.31	4.11	1.70	11.75	7.02	36.10	10.35	6.85	4.93	7.28
Yb	12.20	12.30	30.60	10.05	31.00	23.30	144.50	98.90	51.20	23.70	9.29	70.20	44.10	170.00	64.90	42.10	27.30	43.30
Lu	1.71	1.64	4.27	1.41	4.54	3.26	17.70	12.90	6.97	3.00	1.12	8.49	6.00	20.50	8.99	5.91	3.46	6.05
Y	108.50	114.00	268.00	79.40	215.00	196.50	2140.00	1220.00	513.00	298.00	130.50	897.00	560.00	3260.00	498.00	407.00	364.00	461.00
La/Yb	14.88	20.89	78.76	18.51	218.06	280.26	0.57	22.24	84.77	39.41	88.70	25.78	110.43	30.59	14.14	111.16	35.35	16.49

Appendix 2 b) Trace elements analysis of samples collected by Etruscan and NRE and used in this study

Sample No.	ERN15160	ERN15161	ERN15162	ERN15163	ERN15164	ERN15165	ERN15166	ERN15167	ERN15168	ERN15169	ERN15170	ERN15171	ERN15172	ERN15173	ERN15174	ERN15175	ERN15176	ERN15177
Ba	1685.00	1450.00	832.00	187.00	456.00	1220.00	229.00	448.00	290.00	254.00	267.00	334.00	322.00	291.00	1195.00	362.00	630.00	271.00
Ga	13.80	110.50	21.90	11.10	7.80	6.60	5.80	4.40	8.30	20.80	4.90	4.10	6.60	3.40	38.10	7.50	22.90	3.60
Hf	1.50	0.50	7.20	2.20	1.20	0.80	0.20	0.20	0.20	4.20	0.50	0.20	0.30	0.20	0.50	0.40	0.40	0.10
Nb	126.50	13.00	356.00	3.90	9.00	2.80	4.20	62.80	66.40	783.00	37.40	36.50	803.00	10.80	78.00	3.80	65.90	1.00
Rb	2.90	24.00	43.20	0.70	2.90	1.00	11.00	12.70	16.00	8.20	1.20	2.90	2.00	1.10	41.00	3.70	14.10	2.80
Sr	13800.00	10000.00	2160.00	3830.00	2530.00	938.00	5280.00	7320.00	10900.00	3390.00	11100.00	6710.00	1785.00	6430.00	3230.00	1605.00	1745.00	7930.00
Ta	1.10	0.25	3.70	0.60	0.30	0.20	0.10	0.30	0.40	9.60	0.30	0.10	4.30	0.30	0.25	0.20	0.30	0.10
Th	50.50	204.00	354.00	547.00	110.00	64.80	9.18	1.88	7.67	3.44	3.36	10.65	30.10	2.61	53.10	10.70	141.00	1.54
U	16.05	2.70	26.00	9.72	4.45	3.89	1.82	2.84	1.86	8.69	1.19	1.37	23.60	0.47	4.20	1.70	3.61	0.30
Zr	41.00	400.00	371.00	4.00	25.00	4.00	3.00	4.00	3.00	452.00	12.00	5.00	6.00	3.00	120.00	11.00	2.00	1.00
La	1395.00	15600.00	1515.00	1235.00	662.00	479.00	481.00	203.00	650.00	215.00	232.00	194.00	188.50	215.00	6340.00	818.00	1880.00	172.50
Ce	2430.00	26100.00	2030.00	1875.00	1165.00	790.00	793.00	414.00	1090.00	433.00	462.00	387.00	425.00	449.00	10550.00	1535.00	5140.00	407.00
Pr	242.00	2350.00	174.00	169.00	123.50	84.00	79.70	47.00	111.00	49.40	52.90	43.60	45.50	46.90	1120.00	140.00	571.00	44.50
Nd	788.00	6810.00	558.00	558.00	389.00	266.00	234.00	152.00	335.00	161.50	173.50	141.50	147.00	146.50	2960.00	455.00	1975.00	144.00
Sm	135.00	584.00	109.50	141.00	67.10	53.80	31.80	27.10	44.80	25.70	26.50	22.70	23.70	23.20	300.00	67.30	273.00	24.40
Eu	38.50	118.50	40.90	62.30	24.00	19.65	9.09	8.40	12.70	8.07	7.52	6.69	6.97	6.56	71.40	20.10	62.90	7.62
Gd	145.00	569.00	154.00	227.00	91.80	72.40	38.40	30.30	51.80	28.40	29.20	24.80	22.60	23.70	304.00	68.60	210.00	23.60
Tb	16.40	36.40	26.50	45.70	16.10	13.80	4.23	4.32	5.54	3.55	3.56	3.13	3.42	3.53	26.20	10.45	21.30	3.71
Dy	69.80	95.60	159.00	282.00	105.50	98.00	19.35	22.50	23.90	16.85	16.45	15.15	17.35	18.30	94.40	59.50	70.80	18.60
Ho	12.80	15.50	32.20	57.30	25.20	25.10	3.97	4.61	4.57	3.26	3.24	2.98	3.58	3.85	16.35	14.25	13.00	3.86
Er	36.80	52.70	86.40	160.50	86.80	88.30	12.55	13.70	13.65	9.48	9.50	8.88	10.25	11.20	44.40	46.50	41.00	11.15
Tm	4.99	5.58	12.20	25.80	16.20	17.25	1.92	2.05	1.83	1.33	1.30	1.27	1.34	1.53	5.01	7.08	4.46	1.48
Yb	30.40	29.70	66.30	155.50	105.00	115.50	12.20	12.50	10.95	8.00	7.75	7.81	8.61	9.90	26.40	46.50	29.60	9.63
Lu	4.10	4.17	8.28	21.40	14.60	16.45	1.67	1.70	1.48	1.07	1.04	1.06	1.35	1.54	3.70	7.37	4.66	1.51
Y	303.00	444.00	827.00	1330.00	730.00	788.00	100.50	117.50	113.50	83.60	82.00	79.00	93.10	94.30	312.00	387.00	383.00	92.50
La/Yb	45.89	525.25	22.85	7.94	6.30	4.15	39.43	16.24	59.36	26.88	29.94	24.84	21.89	21.72	240.15	17.59	63.51	17.91

Appendix 2 b) Trace elements analysis of samples collected by Etruscan and NRE and used in this study

Sample No.	ERN15178	ERN15179	ERN15180	ERN15181	ERN15182	ERN15183	ERN15184	ERN15185	ERN15186	ERN15187	ERN15188	ERN15189	ERN15190	ERN15191	ERN15194	ERN15195	ERN15196	ERN15197
Ba	1860.00	595.00	339.00	690.00	563.00	460.00	108.50	236.00	2090.00	646.00	325.00	2350.00	1295.00	309.00	703.00	1885.00	1660.00	741.00
Ga	24.40	6.90	18.40	45.70	8.10	36.20	11.30	6.70	15.00	17.10	110.50	14.20	16.00	19.80	12.90	13.30	12.30	9.40
Hf	0.30	0.50	0.50	1.00	1.20	2.00	1.50	14.90	1.90	1.70	0.50	0.70	0.70	8.10	5.40	3.00	2.00	0.30
Nb	1.90	27.40	96.30	140.00	8.50	4.60	16.10	173.50	10.40	27.90	196.00	3.80	402.00	116.50	13.00	61.70	11.90	4.70
Rb	7.40	14.80	38.70	14.00	2.30	0.30	1.40	8.60	0.30	5.40	27.00	4.60	10.90	35.70	62.50	16.40	10.70	6.20
Sr	1875.00	1155.00	6740.00	3070.00	3960.00	11500.00	7250.00	4200.00	13100.00	11000.00	2290.00	2260.00	837.00	1605.00	1740.00	1985.00	6920.00	3010.00
Ta	0.20	0.30	0.70	0.25	0.30	0.50	0.80	1.60	0.60	0.50	2.20	0.30	2.50	1.40	0.10	0.20	0.10	0.05
Th	114.00	52.40	5.78	158.50	24.40	350.00	469.00	395.00	465.00	360.00	395.00	145.00	16.10	780.00	766.00	168.50	183.00	13.20
U	13.05	4.39	3.44	6.70	1.76	2.24	1.83	2.65	3.83	5.98	5.10	1.97	10.25	9.49	12.00	15.85	4.20	5.49
Zr	10.00	12.00	8.00	170.00	53.00	23.00	22.00	911.00	12.00	41.00	140.00	6.00	41.00	765.00	353.00	149.00	171.00	3.00
La	3190.00	459.00	188.00	8600.00	633.00	5210.00	1275.00	537.00	1430.00	1380.00	15650.00	1875.00	664.00	1900.00	716.00	2040.00	1640.00	2270.00
Ce	5880.00	912.00	401.00	12250.00	1320.00	9400.00	2300.00	1080.00	3080.00	2860.00	30700.00	3040.00	1340.00	3550.00	1365.00	3130.00	2820.00	3020.00
Pr	522.00	90.20	41.80	1165.00	130.50	828.00	203.00	102.00	304.00	270.00	3100.00	244.00	120.50	323.00	150.00	290.00	280.00	240.00
Nd	1550.00	283.00	132.50	2860.00	457.00	2480.00	617.00	346.00	1010.00	853.00	9130.00	689.00	385.00	1015.00	552.00	914.00	906.00	637.00
Sm	188.00	43.90	21.60	327.00	86.60	364.00	104.00	61.60	179.00	129.50	1140.00	98.70	54.10	196.00	138.00	128.00	119.00	63.90
Eu	42.00	13.60	6.67	89.70	29.00	117.00	40.20	29.00	68.30	42.70	204.00	34.40	15.15	73.60	52.80	37.20	29.10	16.60
Gd	166.00	45.00	21.20	373.00	92.00	418.00	148.00	103.00	236.00	150.00	800.00	127.50	55.50	263.00	175.00	133.00	108.50	79.00
Tb	14.00	6.50	3.17	46.00	18.10	67.40	38.20	31.30	54.70	27.30	53.00	20.50	7.36	50.50	25.60	17.95	12.15	8.55
Dy	36.30	31.20	16.35	230.00	110.50	333.00	275.00	243.00	328.00	152.50	121.00	120.50	34.80	289.00	121.00	101.50	61.40	42.00
Ho	5.92	6.11	3.29	42.30	24.00	63.10	65.20	60.90	67.40	31.60	16.80	27.50	7.15	59.70	20.70	21.00	12.90	8.12
Er	21.40	17.45	9.50	105.00	71.90	158.00	189.00	188.00	169.00	87.60	54.70	82.90	21.50	157.50	55.60	65.90	43.70	25.10
Tm	2.23	2.28	1.24	13.40	10.15	17.10	25.90	28.00	20.40	11.35	4.35	11.70	2.92	19.40	7.54	9.26	7.12	3.51
Yb	16.65	14.95	8.25	65.00	65.20	89.80	151.50	174.00	112.00	69.70	25.90	75.20	19.20	106.00	48.30	56.70	53.90	23.10
Lu	2.79	2.41	1.30	8.86	10.20	12.40	22.20	26.60	16.25	10.65	3.61	11.95	3.22	14.50	6.46	7.37	8.45	3.25
Y	141.00	144.00	82.10	970.00	626.00	1455.00	1810.00	1880.00	1755.00	839.00	475.00	705.00	160.50	1595.00	574.00	621.00	349.00	204.00
La/Yb	191.59	30.70	22.79	132.31	9.71	58.02	8.42	3.09	12.77	19.80	604.25	24.93	34.58	17.92	14.82	35.98	30.43	98.27

Appendix 2 b) Trace elements analysis of samples collected by Etruscan and NRE and used in this study

Sample No.	ERN15198	ERN15199	ERN15201	ERN15202	ERN15203	ERN15204	ERN15205	ERN15206	ERN15207	ERN15208	ERN15209	ERN15210	ERN15211	ERN15212	ERN15213	ERN15214	ERN15215	ERN15216
Ba	584.00	348.00	514.00	424.00	1185.00	140.00	348.00	132.00	54.90	115.00	554.00	1250.00	266.00	725.00	514.00	365.00	85.50	49.50
Ga	12.10	4.50	2.60	13.90	11.80	6.20	9.30	15.60	28.70	7.80	7.10	17.20	8.60	25.60	32.10	6.20	1.40	0.70
Hf	0.40	2.50	1.40	2.70	1.50	0.50	2.90	1.00	1.00	1.70	4.60	4.60	2.30	4.90	1.00	1.70	3.70	9.30
Nb	8.20	30.20	6.00	81.00	10.20	12.70	289.00	60.00	28.00	182.50	636.00	108.50	90.50	481.00	15.00	9.70	9.60	26.20
Rb	1.10	13.00	3.10	10.40	6.70	0.50	10.10	4.00	4.00	0.40	6.10	10.80	2.80	28.70	2.00	6.00	1.30	1.80
Sr	2200.00	956.00	3850.00	2520.00	1315.00	2900.00	5930.00	1900.00	1050.00	4120.00	2910.00	2130.00	8090.00	6020.00	3320.00	668.00	405.00	508.00
Ta	0.10	0.10	0.10	0.20	0.10	0.10	1.30	1.40	0.25	1.70	2.00	0.50	0.40	11.70	0.25	0.10	0.05	0.20
Th	74.40	359.00	401.00	189.00	419.00	234.00	83.80	1220.00	1195.00	60.50	21.90	245.00	37.50	43.00	34.00	276.00	123.50	215.00
U	2.70	5.57	6.39	11.70	6.83	2.69	18.20	5.70	6.80	15.50	19.30	6.36	4.74	41.40	2.80	7.38	6.67	6.79
Zr	2.00	147.00	91.00	184.00	75.00	13.00	178.00	20.00	20.00	81.00	157.00	159.00	65.00	370.00	90.00	170.00	413.00	917.00
La	2870.00	363.00	446.00	2780.00	2640.00	1040.00	1020.00	2190.00	5070.00	1080.00	461.00	2460.00	295.00	496.00	7320.00	1190.00	27.10	26.00
Ce	4130.00	706.00	718.00	4400.00	3870.00	1790.00	1365.00	3880.00	8930.00	1570.00	967.00	3220.00	564.00	981.00	9960.00	1615.00	51.50	58.70
Pr	366.00	74.20	69.00	418.00	347.00	179.50	123.00	445.00	909.00	147.50	109.50	264.00	59.00	110.00	830.00	141.50	6.31	7.52
Nd	1075.00	259.00	216.00	1310.00	1045.00	589.00	387.00	1685.00	2820.00	472.00	391.00	731.00	200.00	396.00	2000.00	421.00	25.80	32.40
Sm	132.50	59.80	35.10	172.00	139.00	83.70	59.20	366.00	333.00	71.20	62.70	78.10	31.40	59.80	135.50	63.00	17.55	31.50
Eu	30.80	21.60	19.35	45.70	39.90	22.90	20.60	107.00	98.70	24.30	17.30	22.80	8.68	16.50	29.30	21.00	10.40	22.60
Gd	136.00	77.70	77.00	163.00	149.50	86.70	67.50	322.00	386.00	76.80	59.80	97.20	31.50	53.60	177.50	84.10	38.10	87.70
Tb	16.40	15.05	22.50	17.70	20.50	12.90	9.66	36.80	61.40	10.20	7.91	13.15	4.40	6.57	11.35	15.55	8.95	24.00
Dy	91.50	101.50	167.00	84.30	123.00	75.10	61.00	151.50	347.00	56.20	39.40	74.20	24.20	31.50	31.40	114.00	60.00	179.50
Ho	19.60	21.80	34.40	16.35	24.50	15.35	13.05	24.70	65.00	11.90	7.39	14.30	4.90	5.59	6.40	27.20	13.00	40.30
Er	61.70	64.90	91.40	51.40	67.60	46.70	38.60	66.90	168.00	36.70	20.50	40.20	14.85	15.55	24.10	94.40	40.80	126.00
Tm	8.54	9.19	11.00	7.01	9.53	6.87	5.29	9.04	21.20	4.88	2.72	5.31	2.14	1.90	2.94	15.75	6.52	18.85
Yb	53.70	56.20	56.50	43.60	69.10	45.70	33.00	60.50	122.00	28.20	16.60	33.50	13.90	11.15	17.80	111.50	44.30	118.50
Lu	6.75	7.52	6.51	5.81	10.40	6.27	4.31	8.84	16.25	3.53	2.32	4.60	1.95	1.41	2.49	16.35	6.23	15.90
Y	730.00	628.00	877.00	506.00	691.00	459.00	385.00	660.00	1600.00	379.00	188.00	408.00	129.50	150.50	197.00	720.00	366.00	1135.00
La/Yb	53.45	6.46	7.89	63.76	38.21	22.76	30.91	36.20	41.56	38.30	27.77	73.43	21.22	44.48	411.24	10.67	0.61	0.22

Appendix 2 b) Trace elements analysis of samples collected by Etruscan and NRE and used in this study

Sample No.	ERN15217	ERN15218	ERN15219	ERN15220	ERN15221	ERN15222	ERN15223	ERN15224	ERN15225	ERN15227	ERN15229	ERN15230	ERN15231	ERN15232	ERN15233	ERN15234	ERN15235	ERN15236
Ba	685.00	385.00	809.00	662.00	362.00	2430.00	421.00	109.50	217.00	65.50	474.00	837.00	839.00	174.50	619.00	425.00	482.00	546.00
Ga	10.90	6.30	6.10	5.00	15.60	15.00	19.30	20.00	20.90	17.90	42.50	9.80	9.60	8.00	67.80	12.20	4.40	4.30
Hf	1.10	0.80	1.00	1.90	6.00	4.20	16.00	3.10	2.30	12.90	4.00	4.60	1.20	1.90	0.50	0.40	13.50	16.20
Nb	26.80	2.10	322.00	62.90	16.80	231.00	576.00	38.10	7.40	291.00	120.00	99.80	60.00	6.70	12.00	4.80	126.50	86.00
Rb	25.70	2.10	2.00	6.60	3.90	3.60	1.00	1.30	2.00	6.40	4.00	0.50	59.90	0.80	19.00	8.40	17.10	48.40
Sr	1995.00	5150.00	10000.00	891.00	4460.00	13300.00	3070.00	2220.00	1360.00	431.00	1690.00	4580.00	521.00	1675.00	1060.00	478.00	1470.00	721.00
Ta	0.20	0.10	1.30	1.40	0.90	2.00	3.10	0.40	0.50	1.10	1.30	0.80	0.50	0.50	0.25	0.10	1.20	1.30
Th	638.00	138.50	81.90	76.30	1250.00	788.00	4720.00	445.00	723.00	188.50	4340.00	430.00	341.00	372.00	373.00	63.50	2580.00	2530.00
U	8.31	1.86	16.30	10.15	14.85	17.95	10.20	5.71	2.64	6.07	43.20	0.93	12.20	3.95	1.70	8.82	34.10	85.20
Zr	30.00	12.00	40.00	189.00	188.00	148.00	750.00	63.00	25.00	1130.00	300.00	126.00	62.00	13.00	90.00	5.00	1310.00	1280.00
La	1975.00	700.00	810.00	529.00	1685.00	1105.00	536.00	2160.00	711.00	235.00	5740.00	849.00	311.00	598.00	8180.00	1005.00	100.50	46.20
Ce	3240.00	1300.00	1430.00	930.00	2640.00	1860.00	1700.00	3140.00	2400.00	561.00	8330.00	1385.00	692.00	951.00	13900.00	1775.00	188.00	138.00
Pr	314.00	140.00	150.50	95.90	251.00	185.00	356.00	275.00	357.00	76.90	897.00	133.50	115.00	101.00	1540.00	177.50	24.60	23.60
Nd	1015.00	484.00	507.00	325.00	842.00	661.00	2350.00	841.00	1570.00	321.00	2860.00	468.00	685.00	354.00	4410.00	628.00	112.50	141.50
Sm	153.50	84.20	78.70	59.50	193.00	109.50	2340.00	146.00	368.00	86.30	944.00	112.00	333.00	123.50	611.00	88.50	162.50	154.00
Eu	45.60	26.20	24.40	19.35	86.60	44.70	1275.00	54.80	95.60	30.10	426.00	52.40	71.10	57.60	140.00	21.80	85.60	89.60
Gd	171.50	93.40	77.50	68.50	309.00	162.00	4580.00	196.00	344.00	94.00	1445.00	182.50	162.50	187.50	542.00	87.10	269.00	328.00
Tb	26.30	16.95	9.84	9.50	72.90	32.80	933.00	30.80	57.40	15.35	275.00	39.40	15.65	40.10	50.90	10.45	55.70	84.10
Dy	149.50	114.00	49.00	46.30	481.00	188.00	4800.00	176.50	307.00	75.70	1460.00	257.00	51.10	246.00	186.00	53.30	322.00	527.00
Ho	30.40	25.50	9.19	7.93	96.60	34.60	803.00	35.70	57.70	13.70	269.00	56.20	7.98	50.70	30.00	11.75	61.60	113.00
Er	96.20	80.10	24.70	21.10	241.00	86.10	1660.00	101.00	152.50	37.90	670.00	174.00	22.50	145.50	76.30	37.50	165.00	309.00
Tm	14.85	11.85	3.15	2.71	26.90	10.35	191.50	13.45	17.95	5.42	98.40	27.40	2.66	21.80	8.86	4.96	23.30	42.90
Yb	101.00	74.80	17.40	17.05	126.00	56.70	812.00	81.30	99.40	36.90	506.00	181.50	19.20	142.00	45.50	29.70	147.00	243.00
Lu	14.25	10.10	2.30	2.30	13.90	6.96	97.00	10.70	11.95	5.28	70.80	25.00	2.52	19.60	6.32	3.86	20.30	32.10
Y	840.00	846.00	242.00	193.50	2370.00	804.00	15350.00	913.00	1655.00	332.00	5670.00	1410.00	210.00	1285.00	772.00	364.00	1420.00	3090.00
La/Yb	19.55	9.36	46.55	31.03	13.37	19.49	0.66	26.57	7.15	6.37	11.34	4.68	16.20	4.21	179.78	33.84	0.68	0.19

Appendix 2 b) Trace elements analysis of samples collected by Etruscan and NRE and used in this study

Sample No.	ERN15237	ERN15238	ERN15239	ERN15240	ERN15241	ERN15242	ERN15243	ERN15244	ERN15245	ERN15246	ERN15247	ERN15301	ERN15302	ERN15303	ERN15304	ERN15305	ERN15306	ERN15307
Ba	79.50	574.00	462.00	59.00	158.00	1985.00	910.00	593.00	808.00	327.00	657.00	589.00	745.00	734.00	929.00	2460.00	943.00	611.00
Ga	37.70	8.70	7.90	37.80	4.00	4.30	7.40	54.20	13.90	33.00	9.40	20.50	15.20	23.80	14.30	28.00	59.10	26.90
Hf	2.70	8.00	1.50	1.50	11.60	0.20	0.40	0.50	2.60	2.40	1.90	2.50	5.90	519.00	1.90	1.00	4.00	2.90
Nb	46.20	17.20	15.10	18.40	130.00	3.70	163.00	4.00	182.00	127.50	8.50	227.00	61.90	412.00	5.60	4.00	16.00	119.50
Rb	1.80	31.40	13.50	0.70	3.00	2.40	62.50	5.00	29.40	7.10	9.50	2.30	9.70	57.00	6.60	2.00	16.00	7.10
Sr	508.00	410.00	639.00	2810.00	618.00	5150.00	10950.00	2810.00	3550.00	1455.00	364.00	6590.00	4190.00	2200.00	1945.00	10000.00	10000.00	3490.00
Ta	0.70	1.00	0.20	0.40	0.80	0.10	0.90	0.25	6.90	3.10	0.20	1.40	0.60	2.00	0.20	0.25	0.25	0.60
Th	241.00	116.00	16.90	578.00	117.00	3.87	2.07	29.00	580.00	530.00	45.10	761.00	504.00	2250.00	453.00	1015.00	1080.00	212.00
U	3.05	31.20	13.30	12.45	36.30	1.24	12.65	4.90	14.55	10.05	2.48	23.00	15.15	1250.00	5.25	14.70	10.50	23.40
Zr	11.00	740.00	51.00	33.00	1330.00	8.00	8.00	90.00	54.00	35.00	66.00	86.00	483.00	50000.00	37.00	60.00	470.00	211.00
La	3140.00	207.00	308.00	5390.00	20.60	322.00	213.00	10250.00	761.00	2230.00	607.00	4370.00	3280.00	2350.00	1815.00	4780.00	13200.00	4060.00
Ce	6820.00	771.00	636.00	7680.00	40.60	596.00	461.00	13250.00	1455.00	5300.00	1155.00	7700.00	4740.00	3770.00	2820.00	7180.00	19900.00	6060.00
Pr	757.00	146.00	80.00	672.00	4.70	64.60	56.40	1170.00	180.50	684.00	131.50	772.00	409.00	339.00	295.00	635.00	1685.00	573.00
Nd	2750.00	785.00	306.00	1985.00	19.00	208.00	216.00	2640.00	853.00	2920.00	512.00	2620.00	1225.00	1055.00	879.00	1875.00	4560.00	1555.00
Sm	452.00	299.00	70.20	234.00	10.75	31.00	56.60	165.50	432.00	667.00	162.50	388.00	173.50	178.50	119.00	253.00	370.00	182.00
Eu	104.50	124.50	22.80	63.20	7.87	8.50	17.70	33.70	134.00	166.00	46.70	101.00	51.10	63.40	38.30	73.30	86.00	46.70
Gd	452.00	464.00	76.90	294.00	33.10	31.90	54.10	220.00	386.00	475.00	147.50	378.00	210.00	254.00	164.50	303.00	508.00	236.00
Tb	68.30	101.00	12.10	34.80	11.95	4.16	7.75	11.00	56.00	55.50	22.10	50.50	29.90	48.60	27.00	37.90	46.90	25.30
Dy	370.00	574.00	60.90	178.00	95.90	20.60	37.00	22.10	253.00	212.00	111.50	274.00	177.00	333.00	163.50	202.00	239.00	124.50
Ho	73.40	115.50	11.80	38.90	22.40	4.15	6.70	3.81	42.90	36.20	21.30	51.80	36.70	77.90	37.30	42.30	49.90	27.80
Er	199.00	297.00	34.50	125.50	70.60	12.65	18.05	15.40	108.50	103.50	62.20	153.00	113.00	273.00	120.00	136.50	144.50	87.80
Tm	23.40	38.10	5.13	17.90	11.40	1.71	2.30	1.43	13.80	11.80	9.31	18.55	15.10	47.30	19.25	21.00	15.65	12.90
Yb	128.50	213.00	36.80	117.00	75.00	11.20	14.95	7.80	85.10	74.60	65.70	116.50	97.10	338.00	125.50	147.00	88.40	80.50
Lu	15.95	27.90	5.34	16.30	10.45	1.51	2.03	1.08	10.80	9.68	9.70	14.60	12.25	49.80	18.35	20.10	11.40	11.20
Y	1950.00	3680.00	362.00	1105.00	620.00	100.50	140.50	101.00	1135.00	1000.00	445.00	1375.00	1190.00	2250.00	958.00	1085.00	1230.00	709.00
La/Yb	24.44	0.97	8.37	46.07	0.27	28.75	14.25	1314.10	8.94	29.89	9.24	37.51	33.78	6.95	14.46	32.52	149.32	50.43

Appendix 2 b) Trace elements analysis of samples collected by Etruscan and NRE and used in this study

Sample No.	ERN15308	ERN15309	ERN15310	ERN15311	ERN15312	ERN15313	ERN15314	ERN15315	ERN15316	ERN15317	ERN15318	ERN15319	ERN15320	ERN15321	ERN15322	ERN15323	ERN15324	ERN15325
Ba	565.00	542.00	345.00	683.00	85.50	263.00	983.00	655.00	396.00	463.00	212.00	503.00	728.00	634.00	539.00	159.50	758.00	1425.00
Ga	13.30	30.40	15.00	20.60	65.50	10.30	8.50	7.00	22.70	14.30	9.70	15.60	16.70	13.90	16.00	16.30	44.50	28.70
Hf	0.70	3.40	0.60	1.60	5.00	2.00	3.20	3.00	2.80	14.30	0.60	7.00	10.30	7.70	1.90	1.10	2.00	16.70
Nb	5.70	85.20	1.80	6.30	115.00	340.00	65.70	43.20	455.00	150.00	12.10	89.60	222.00	207.00	66.10	9.00	54.00	839.00
Rb	4.90	10.70	0.40	7.90	3.00	5.00	1.10	40.60	2.40	1.60	8.40	2.20	18.30	19.20	1.80	0.50	5.00	0.60
Sr	4640.00	3650.00	2250.00	2030.00	2570.00	10000.00	5050.00	535.00	889.00	919.00	1660.00	630.00	826.00	814.00	1045.00	3870.00	4950.00	1175.00
Ta	0.10	0.50	0.10	0.30	0.90	3.60	0.40	2.10	5.40	1.50	0.10	0.70	5.20	5.80	0.40	0.10	0.25	14.40
Th	181.00	716.00	244.00	538.00	1265.00	48.40	474.00	7.88	582.00	736.00	629.00	291.00	300.00	58.70	841.00	543.00	561.00	235.00
U	8.88	11.00	2.65	7.19	23.80	11.30	57.00	3.92	14.90	11.50	3.63	17.10	8.68	4.50	20.20	4.38	17.80	29.70
Zr	21.00	118.00	12.00	35.00	360.00	200.00	390.00	113.00	105.00	1125.00	15.00	733.00	633.00	369.00	35.00	54.00	200.00	1295.00
La	2170.00	4610.00	1985.00	3550.00	12700.00	1085.00	970.00	43.80	2560.00	1615.00	332.00	461.00	266.00	79.70	1830.00	2510.00	8810.00	1185.00
Ce	3170.00	6880.00	2930.00	5570.00	20100.00	1860.00	1860.00	83.00	4160.00	2510.00	876.00	821.00	496.00	164.00	3630.00	3820.00	12600.00	2120.00
Pr	313.00	645.00	271.00	547.00	1815.00	184.50	218.00	10.00	429.00	258.00	140.00	92.60	65.60	21.10	433.00	365.00	1125.00	238.00
Nd	963.00	1765.00	725.00	1695.00	5110.00	604.00	746.00	37.40	1335.00	797.00	631.00	327.00	275.00	81.20	1485.00	1030.00	3350.00	758.00
Sm	136.00	224.00	72.10	238.00	513.00	78.40	118.50	8.18	188.50	168.00	165.50	71.90	100.50	18.70	233.00	121.50	395.00	116.50
Eu	31.00	69.20	22.20	62.10	133.00	21.20	37.20	2.69	62.40	69.30	34.30	22.40	27.10	6.95	64.40	28.90	88.60	32.50
Gd	150.50	336.00	110.00	279.00	652.00	75.80	136.50	9.58	258.00	281.00	126.00	79.20	88.40	24.00	265.00	151.00	407.00	139.50
Tb	17.15	55.60	15.55	39.00	86.20	7.36	22.10	1.55	45.40	69.60	15.15	11.90	11.55	4.10	43.10	17.20	40.20	24.50
Dy	84.20	356.00	102.50	231.00	477.00	29.10	132.50	8.07	273.00	550.00	66.30	66.50	58.10	21.80	255.00	90.50	191.50	155.00
Ho	18.20	73.00	23.80	49.50	88.90	4.81	28.30	1.51	52.80	131.00	12.25	13.65	11.35	4.11	51.00	19.90	37.40	31.70
Er	59.30	190.00	75.90	143.50	230.00	13.40	86.10	3.92	137.00	377.00	37.00	39.70	32.80	10.80	136.00	64.50	116.00	84.60
Tm	9.18	24.00	11.20	19.25	25.50	1.47	14.10	0.52	16.10	53.70	5.41	6.12	4.88	1.58	18.70	10.35	14.35	10.75
Yb	57.60	124.00	65.40	111.50	133.00	9.00	92.00	3.03	79.30	286.00	37.30	37.90	29.50	9.82	111.00	68.50	89.40	56.20
Lu	8.30	15.70	8.79	15.00	15.80	1.16	13.20	0.43	10.00	36.70	5.47	5.36	4.01	1.37	15.55	10.20	11.65	7.14
Y	502.00	1785.00	763.00	1235.00	2310.00	116.00	727.00	37.80	1270.00	3660.00	298.00	370.00	295.00	100.00	1310.00	571.00	1105.00	716.00
La/Yb	37.67	37.18	30.35	31.84	95.49	120.56	10.54	14.46	32.28	5.65	8.90	12.16	9.02	8.12	16.49	36.64	98.55	21.09

Appendix 2 b) Trace elements analysis of samples collected by Etruscan and NRE and used in this study

Sample No.	ERN15326	ERN15327	ERN15328	ERN15329	ERN15330	ERN15331	ERN15332	ERN15333	ERN15334	ERN15335	ERN15336	ERN15337	ERN15338	ERN15339	ERN15340	ERN15341	ERN15342	ERN15343
Ba	26.00	74.10	58.90	159.00	47.30	124.50	455.00	651.00	635.00	10000.00	2630.00	138.00	252.00	140.50	150.50	140.00	167.00	89.40
Ga	1.00	13.60	6.90	3.80	17.50	14.10	7.10	9.20	3.00	3.60	4.30	3.90	18.60	15.50	13.20	11.70	4.70	2.70
Hf	1.10	9.70	3.10	32.40	4.90	2.40	2.40	0.90	1.60	0.50	0.30	2.20	3.40	10.20	3.70	2.60	59.50	4.60
Nb	6.30	101.00	7.20	74.90	161.00	60.90	199.50	85.90	16.20	3.00	6.00	30.90	228.00	95.20	87.10	227.00	122.00	14.00
Rb	0.20	1.40	2.60	15.10	3.30	7.60	24.10	1.20	4.00	9.00	29.30	2.70	5.20	2.40	13.10	11.20	18.10	6.20
Sr	507.00	135.50	493.00	585.00	331.00	357.00	512.00	2810.00	303.00	909.00	295.00	349.00	179.50	364.00	371.00	354.00	168.00	179.50
Ta	0.10	1.40	0.10	0.20	0.50	0.70	0.60	0.70	0.20	0.25	0.50	0.50	0.70	0.40	0.70	0.90	1.30	0.50
Th	22.70	35.40	34.30	117.00	43.60	23.30	204.00	147.50	115.50	2.40	1.50	65.40	22.90	84.90	37.20	38.50	196.50	113.50
U	2.88	6.58	11.65	27.70	5.33	1.49	2.67	24.20	2.51	0.90	0.87	4.35	5.23	20.80	3.32	4.63	46.20	6.33
Zr	95.00	356.00	379.00	3520.00	345.00	110.00	147.00	51.00	101.00	10.00	17.00	149.00	178.00	866.00	180.00	140.00	6480.00	433.00
La	61.10	39.80	8.30	7.10	29.60	16.10	18.90	1220.00	32.40	13.00	17.30	15.70	10.80	9.80	17.60	9.10	15.20	24.30
Ce	90.20	82.80	13.90	21.80	59.90	32.70	49.80	2140.00	73.00	25.00	33.90	30.80	20.80	20.40	34.20	19.40	26.10	43.70
Pr	8.84	10.40	1.53	4.95	7.67	4.06	9.34	235.00	11.35	2.70	4.01	3.58	2.38	2.56	4.08	2.53	3.47	5.21
Nd	27.90	40.20	5.70	36.00	30.90	15.70	59.30	754.00	50.60	11.00	16.00	13.80	8.90	10.60	15.50	10.70	17.70	22.90
Sm	6.55	10.10	2.06	27.80	11.50	4.15	46.20	108.50	22.20	3.80	5.92	5.27	2.58	3.91	4.92	4.57	23.10	13.00
Eu	3.31	3.14	1.47	13.10	4.33	1.49	18.45	32.00	10.85	1.70	2.82	3.27	1.38	2.09	2.13	2.83	17.10	5.78
Gd	12.30	11.65	6.06	39.40	15.50	6.07	62.50	118.00	43.30	4.90	7.26	12.80	6.05	9.02	8.16	11.50	58.50	16.60
Tb	2.77	1.88	1.95	8.49	3.49	1.54	12.65	14.00	10.25	0.82	1.42	3.69	2.19	2.95	2.06	3.95	13.85	3.03
Dy	19.20	10.90	16.55	53.10	24.30	11.85	78.60	68.80	64.10	5.00	7.80	26.70	18.30	22.40	14.60	31.00	96.40	16.65
Ho	4.14	2.24	3.89	10.80	5.18	2.76	15.35	14.30	12.15	0.92	1.46	5.84	4.26	4.93	3.19	7.02	21.80	3.23
Er	11.75	6.59	11.85	31.70	14.95	8.57	39.50	40.30	28.20	2.50	4.00	18.25	14.25	15.95	10.25	22.20	76.60	10.75
Tm	1.88	1.00	1.95	5.33	2.46	1.47	5.40	4.97	3.34	0.50	0.66	2.89	2.41	2.72	1.66	3.57	14.00	1.88
Yb	11.35	6.87	12.20	34.60	16.25	9.48	29.20	27.60	16.50	2.70	4.24	18.70	16.30	20.20	11.60	22.70	109.50	14.25
Lu	1.56	1.07	1.72	5.30	2.39	1.44	3.91	3.48	2.08	0.42	0.58	2.61	2.33	2.95	1.79	3.11	17.85	2.20
Y	112.00	56.00	106.00	274.00	132.00	73.10	389.00	378.00	291.00	25.00	38.90	159.50	112.00	126.50	86.70	195.00	686.00	86.60
La/Yb	5.38	5.79	0.68	0.21	1.82	1.70	0.65	44.20	1.96	4.81	4.08	0.84	0.66	0.49	1.52	0.40	0.14	1.71

Appendix 2 b) Trace elements analysis of samples collected by Etruscan and NRE and used in this study

Sample No.	ERN15344	ERN15345	ERN15346	ERN15347	ERN15348	ERN15349	ERN15350	ERN15401	ERN15402	ERN15403	ERN15404	ERN15405	ERN15406	ERN15407	ERN15408	ERN15409	ERN15410	ERN15411
Ba	380.00	2770.00	240.00	4710.00	87.70	95.60	53.60	5280.00	1305.00	5180.00	477.00	451.00	1065.00	1240.00	1460.00	356.00	1540.00	184.00
Ga	17.40	6.10	6.30	17.80	4.80	5.20	9.20	41.30	5.90	14.90	4.80	22.20	18.50	9.40	8.70	5.50	22.10	6.10
Hf	0.80	1.70	4.40	0.90	14.10	5.30	2.00	2.00	1.30	5.00	6.80	1.50	1.40	3.60	2.00	0.70	29.50	5.70
Nb	1.10	61.60	60.20	2.90	140.50	133.00	16.00	35.00	30.60	623.00	80.00	31.40	33.80	295.00	98.30	6.90	1410.00	324.00
Rb	8.00	1.50	2.40	0.60	4.50	1.40	1.00	4.00	22.40	4.90	3.90	4.70	3.60	8.00	19.40	2.30	199.00	13.40
Sr	347.00	7560.00	5860.00	2840.00	719.00	601.00	259.00	1350.00	211.00	6840.00	54.90	3110.00	959.00	4370.00	1335.00	7920.00	2250.00	2440.00
Ta	0.40	0.50	0.70	0.50	1.50	1.00	0.25	0.25	0.40	4.20	0.40	0.30	0.20	1.00	0.70	0.05	20.50	1.70
Th	460.00	384.00	369.00	469.00	113.50	829.00	1270.00	292.00	13.35	1000.00	26.80	503.00	450.00	301.00	72.00	2.75	6.12	5.86
U	7.11	12.80	13.40	11.35	22.00	7.89	12.50	4.40	4.46	22.20	0.60	12.85	11.70	6.75	8.00	0.83	31.30	6.29
Zr	57.00	67.00	180.00	26.00	1430.00	276.00	110.00	40.00	58.00	193.00	432.00	64.00	69.00	190.00	89.00	31.00	2340.00	281.00
La	5890.00	1050.00	571.00	6140.00	82.60	1470.00	3060.00	4840.00	257.00	910.00	182.50	3950.00	3190.00	1150.00	1035.00	221.00	122.00	180.50
Ce	7660.00	1790.00	1070.00	8090.00	130.00	2060.00	4110.00	10400.00	479.00	2120.00	437.00	6080.00	5010.00	1725.00	1695.00	425.00	219.00	335.00
Pr	635.00	187.50	120.00	681.00	13.30	186.00	336.00	1240.00	53.50	338.00	49.30	633.00	529.00	182.00	195.00	45.00	21.70	35.00
Nd	1660.00	621.00	424.00	1805.00	46.70	574.00	1025.00	3890.00	184.00	1350.00	155.00	1730.00	1450.00	541.00	590.00	137.00	64.40	105.00
Sm	142.00	102.00	88.30	159.00	23.30	254.00	309.00	390.00	45.40	337.00	21.30	184.50	161.50	129.50	89.80	24.60	10.15	16.65
Eu	41.50	39.80	33.60	42.40	11.80	120.00	139.50	84.40	12.70	87.20	4.49	42.20	41.10	45.30	23.40	7.12	2.97	4.58
Gd	183.00	144.00	110.00	215.00	38.70	392.00	430.00	386.00	56.90	282.00	17.85	183.50	170.00	163.00	86.00	25.10	10.85	17.55
Tb	17.40	26.30	18.85	24.00	7.57	81.20	64.20	39.50	12.30	43.20	1.98	27.30	29.50	31.80	12.55	4.15	1.74	2.75
Dy	86.80	157.00	107.00	131.50	46.40	529.00	325.00	160.50	71.50	189.50	6.82	189.00	177.50	161.00	60.00	20.80	9.30	13.25
Ho	18.65	32.00	19.45	28.70	9.80	110.00	59.70	32.00	16.75	36.30	1.25	52.60	42.00	31.90	13.40	4.64	2.18	2.95
Er	65.60	90.00	52.10	100.50	32.50	321.00	166.00	106.50	44.60	87.50	3.77	152.50	113.00	72.10	37.50	12.40	6.33	7.88
Tm	9.88	11.70	6.25	15.40	5.43	44.40	23.00	12.95	6.85	11.85	0.63	22.40	16.70	9.43	5.99	1.83	1.03	1.16
Yb	65.70	67.50	35.60	105.50	39.50	265.00	154.50	76.90	39.50	65.10	5.49	113.50	90.90	48.00	35.40	10.50	6.39	6.66
Lu	9.26	8.76	4.70	14.85	6.04	35.50	21.60	10.15	5.90	8.92	1.28	15.05	13.05	6.40	5.15	1.55	0.99	1.01
Y	576.00	903.00	549.00	776.00	259.00	3070.00	1575.00	768.00	522.00	881.00	30.90	1330.00	1055.00	817.00	377.00	111.50	53.00	77.40
La/Yb	89.65	15.56	16.04	58.20	2.09	5.55	19.81	62.94	6.51	13.98	33.24	34.80	35.09	23.96	29.24	21.05	19.09	27.10

Appendix 2 b) Trace elements analysis of samples collected by Etruscan and NRE and used in this study

Sample No.	ERN15412	ERN15413	ERN15414	ERN15415	ERN15416	ERN15417	ERN15418	ERN15419	ERN15420	ERN15421	ERN15422	ERN15423	ERN15424	ERN15425	ERN15426	ERN15427	ERN15428	ERN15429
Ba	584.00	870.00	1055.00	719.00	762.00	799.00	1940.00	1055.00	1150.00	830.00	916.00	1680.00	10000.00	272.00	224.00	589.00	1690.00	1835.00
Ga	11.90	9.00	21.00	10.60	19.00	77.70	11.30	15.80	16.10	14.10	12.90	68.90	173.50	7.80	14.40	14.10	50.30	99.90
Hf	1.90	3.30	3.50	5.70	2.50	6.00	0.70	2.80	2.30	3.20	1.00	4.00	4.00	22.00	3.70	1.00	4.80	3.00
Nb	341.00	126.50	33.60	159.00	192.50	621.00	9.40	59.10	36.70	18.10	13.90	87.00	78.00	12.00	560.00	187.00	770.00	45.00
Rb	6.20	17.80	18.30	7.00	6.00	10.00	11.60	4.80	2.90	2.60	1.00	6.00	2.00	18.00	5.80	3.40	1.60	7.00
Sr	7170.00	504.00	1725.00	6210.00	1625.00	1860.00	1160.00	1690.00	1650.00	3200.00	8730.00	1785.00	2070.00	1590.00	3650.00	3650.00	616.00	887.00
Ta	0.80	0.70	0.30	1.40	1.60	2.10	0.10	0.20	0.90	0.40	0.60	1.50	0.80	4.20	2.50	1.40	8.80	0.25
Th	27.50	108.00	147.00	32.20	163.50	416.00	154.50	65.40	158.00	26.60	21.30	965.00	1405.00	2750.00	48.10	77.20	225.00	271.00
U	28.10	10.95	5.46	31.30	23.20	9.30	3.70	5.73	5.96	3.83	3.85	10.90	24.90	30.50	20.70	42.40	37.40	11.90
Zr	131.00	281.00	187.00	516.00	167.00	270.00	28.00	245.00	147.00	209.00	58.00	40.00	70.00	370.00	379.00	36.00	82.00	110.00
La	915.00	1010.00	3130.00	1310.00	2920.00	15450.00	1470.00	2240.00	1755.00	936.00	1005.00	9970.00	22400.00	525.00	1515.00	2110.00	3160.00	7360.00
Ce	1650.00	1475.00	4950.00	2130.00	4510.00	19850.00	2260.00	3410.00	3180.00	1995.00	2180.00	16850.00	44200.00	1030.00	2520.00	3310.00	8130.00	22800.00
Pr	179.00	139.50	479.00	218.00	435.00	1650.00	219.00	330.00	342.00	243.00	267.00	1640.00	4120.00	124.00	255.00	326.00	835.00	2640.00
Nd	560.00	394.00	1335.00	653.00	1215.00	4130.00	641.00	923.00	1045.00	841.00	934.00	4800.00	11100.00	523.00	759.00	950.00	2670.00	8200.00
Sm	77.40	52.50	142.00	82.60	130.50	379.00	85.40	95.30	141.00	120.50	135.50	603.00	1290.00	392.00	97.40	120.00	337.00	887.00
Eu	24.00	16.45	40.40	25.80	36.80	97.10	25.70	23.30	40.50	33.50	37.60	173.50	328.00	280.00	28.40	35.80	70.50	172.00
Gd	76.20	58.10	158.50	84.90	151.50	531.00	96.40	102.50	149.50	104.50	117.00	740.00	1500.00	1140.00	96.70	123.50	283.00	793.00
Tb	8.60	6.65	17.55	9.18	19.45	50.80	12.95	9.85	18.20	11.30	12.95	111.00	148.50	370.00	10.30	13.65	25.10	59.50
Dy	38.00	30.30	85.60	39.20	113.00	202.00	76.10	43.40	85.50	46.10	52.50	602.00	567.00	2770.00	46.00	64.60	91.80	141.00
Ho	7.50	5.97	18.65	7.55	26.00	36.10	17.40	9.50	16.60	8.39	9.66	110.50	96.40	603.00	8.96	12.95	16.70	21.20
Er	21.60	17.00	54.90	21.20	76.80	105.00	54.10	31.10	44.00	23.50	26.40	262.00	272.00	1680.00	25.30	36.70	50.30	77.70
Tm	2.63	2.19	6.48	2.41	10.20	11.15	7.67	4.29	5.02	2.55	2.99	23.50	26.40	221.00	2.96	4.29	5.29	5.10
Yb	14.55	13.25	32.30	13.55	56.10	62.40	45.60	27.10	26.70	14.15	16.90	106.00	136.00	1135.00	16.45	23.30	29.90	28.60
Lu	2.00	1.92	3.95	1.85	7.67	7.97	6.43	4.08	3.49	1.89	2.31	12.35	15.35	136.50	2.36	3.10	3.66	3.41
Y	191.00	161.00	617.00	202.00	732.00	913.00	584.00	306.00	413.00	189.50	216.00	2770.00	2300.00	16300.00	235.00	339.00	380.00	534.00
La/Yb	62.89	76.23	96.90	96.68	52.05	247.60	32.24	82.66	65.73	66.15	59.47	94.06	164.71	0.46	92.10	90.56	105.69	257.34

Appendix 2 b) Trace elements analysis of samples collected by Etruscan and NRE and used in this study

Sample No.	ERN15430	ERN15431	ERN15432	ERN15433	ERN15434	ERN15435	ERN15436	ERN15437	ERN15438	ERN15439	ERN15440	ERN15441	ERN15442	ERN15443	ERN15444	ERN15445	ERN15446	ERN15447
Ba	915.00	1010.00	436.00	1280.00	870.00	3510.00	1595.00	985.00	610.00	1050.00	535.00	345.00	136.50	1415.00	1950.00	1295.00	1005.00	546.00
Ga	14.30	40.00	10.20	13.80	10.40	40.70	7.70	13.70	13.30	29.50	16.20	13.00	10.00	99.10	150.50	47.00	5.00	7.00
Hf	5.70	1.60	1.00	3.20	2.30	5.90	1.80	2.50	2.30	3.30	6.40	1.30	9.00	2.00	6.00	4.00	1.10	8.70
Nb	167.00	406.00	274.00	301.00	77.30	27.50	45.90	44.60	107.50	786.00	71.40	306.00	45.00	208.00	188.00	64.00	4.70	12.80
Rb	9.90	1.00	7.80	10.10	6.50	3.40	6.40	15.10	19.00	12.70	21.40	2.80	1.00	115.00	61.00	9.00	3.10	14.40
Sr	498.00	303.00	1075.00	619.00	1135.00	1255.00	822.00	1080.00	839.00	928.00	572.00	1955.00	1025.00	1750.00	1340.00	1610.00	522.00	641.00
Ta	1.30	1.20	2.70	4.80	1.30	0.50	1.30	1.20	1.70	6.20	0.90	1.80	1.50	0.90	1.20	0.50	0.10	0.40
Th	101.00	403.00	189.50	231.00	672.00	538.00	634.00	1000.00	602.00	107.50	24.10	43.80	703.00	86.70	1690.00	1260.00	192.00	393.00
U	12.50	22.80	17.55	6.37	16.00	11.75	9.83	24.90	14.40	37.10	12.00	28.70	8.20	20.50	31.90	9.50	9.72	10.25
Zr	451.00	91.00	34.00	160.00	62.00	192.00	66.00	61.00	79.00	127.00	295.00	59.00	140.00	20.00	190.00	130.00	40.00	383.00
La	310.00	3860.00	1235.00	151.50	899.00	6070.00	752.00	1180.00	848.00	1530.00	44.10	1590.00	712.00	15750.00	21000.00	8210.00	255.00	257.00
Ce	725.00	8010.00	2110.00	318.00	1775.00	9810.00	1275.00	2070.00	1400.00	2540.00	90.80	2530.00	1340.00	25400.00	37200.00	11750.00	550.00	602.00
Pr	86.80	806.00	224.00	36.60	225.00	904.00	151.00	234.00	149.50	263.00	10.50	252.00	155.50	2160.00	3510.00	1080.00	66.30	75.80
Nd	303.00	2450.00	696.00	129.50	872.00	2750.00	563.00	812.00	495.00	806.00	37.50	746.00	618.00	6040.00	10600.00	3020.00	276.00	326.00
Sm	51.30	233.00	96.00	44.70	260.00	328.00	143.00	177.50	112.00	109.50	8.05	98.30	358.00	959.00	1690.00	524.00	125.00	156.00
Eu	14.85	48.90	28.50	22.50	93.60	97.60	51.90	69.80	41.60	32.10	2.53	27.60	213.00	225.00	364.00	168.50	51.20	67.00
Gd	49.40	227.00	97.20	70.60	294.00	385.00	170.00	227.00	135.50	106.00	9.05	100.50	788.00	915.00	1485.00	606.00	152.50	214.00
Tb	6.57	20.30	12.60	10.30	49.00	48.00	34.60	48.00	25.30	11.80	1.54	10.55	201.00	82.10	156.00	73.60	25.80	43.70
Dy	32.80	82.70	63.90	47.90	262.00	259.00	212.00	334.00	165.00	52.20	9.45	46.10	1160.00	291.00	587.00	328.00	132.50	265.00
Ho	6.48	17.30	13.05	8.29	48.60	59.20	43.50	75.00	37.00	9.96	2.12	9.07	195.00	49.10	92.60	58.60	22.30	52.30
Er	17.25	51.80	36.70	20.40	115.50	188.50	109.00	207.00	102.00	27.10	6.28	25.60	395.00	140.00	240.00	164.50	45.60	121.00
Tm	2.14	5.12	4.81	2.61	13.15	27.30	13.40	27.20	13.50	3.00	0.88	2.92	34.10	13.10	21.20	20.30	4.50	13.30
Yb	11.95	26.50	28.00	14.70	68.20	165.00	70.60	149.50	72.60	15.70	5.36	16.60	141.50	67.70	105.50	117.50	21.30	63.50
Lu	1.69	3.47	4.05	2.12	8.89	23.50	9.41	20.70	9.68	2.02	0.87	2.29	15.75	7.18	11.90	15.10	2.68	8.15
Y	163.00	510.00	346.00	213.00	1080.00	1860.00	1005.00	1850.00	879.00	256.00	59.00	244.00	4470.00	1210.00	2140.00	1450.00	522.00	1190.00
La/Yb	25.94	145.66	44.11	10.31	13.18	36.79	10.65	7.89	11.68	97.45	8.23	95.78	5.03	232.64	199.05	69.87	11.97	4.05

Appendix 2 b) Trace elements analysis of samples collected by Etruscan and NRE and used in this study

Sample No.	ERN15448	ERN15449	ERN15450	ERN15451	ERN15452	ERN15453	ERN15454	ERN15455	ERN15456	ERN15457	ERN15458	ERN15459	ERN15460	ERN15461	ERN15462	ERN15463	ERN15464	ERN15465
Ba	8970.00	494.00	505.00	1350.00	360.00	570.00	706.00	396.00	412.00	221.00	446.00	212.00	160.00	459.00	441.00	314.00	2380.00	403.00
Ga	110.50	22.80	46.20	102.00	4.60	7.00	4.00	20.70	18.10	2.80	39.10	26.60	32.60	5.00	3.60	18.10	26.60	28.40
Hf	4.00	0.80	4.00	10.00	1.00	2.10	1.10	2.30	7.40	0.30	2.00	1.50	2.00	0.50	0.20	1.10	0.30	0.60
Nb	126.00	63.50	49.00	212.00	3.40	16.90	8.10	180.50	54.70	23.20	10.00	8.90	19.00	5.10	10.00	16.80	26.20	6.80
Rb	7.00	10.70	6.00	18.00	7.40	4.90	8.50	4.00	6.80	0.80	0.50	8.10	7.00	2.70	5.30	11.60	9.10	11.10
Sr	2320.00	1495.00	1445.00	1250.00	995.00	1410.00	814.00	2350.00	2950.00	3080.00	997.00	1065.00	1785.00	1835.00	2350.00	1055.00	962.00	2200.00
Ta	0.70	0.60	0.25	1.90	0.40	0.50	0.40	1.30	0.60	0.10	0.25	0.40	0.25	0.40	0.20	0.50	0.50	0.50
Th	771.00	91.30	180.00	1130.00	29.90	100.00	36.10	176.00	102.50	15.35	58.10	35.70	362.00	37.90	9.47	33.00	92.50	124.00
U	24.60	10.10	20.90	27.60	6.09	2.45	11.35	7.03	23.80	1.92	3.40	4.74	6.20	1.30	1.33	3.26	7.21	3.08
Zr	120.00	40.00	250.00	310.00	85.00	128.00	80.00	175.00	1050.00	18.00	170.00	100.00	120.00	14.00	6.00	73.00	13.00	24.00
La	16450.00	3890.00	8150.00	19950.00	454.00	890.00	336.00	3190.00	2850.00	309.00	8950.00	6440.00	8130.00	325.00	405.00	3080.00	4150.00	4900.00
Ce	32600.00	6010.00	12200.00	31300.00	711.00	1525.00	634.00	5450.00	4130.00	596.00	12600.00	8330.00	10550.00	687.00	678.00	4640.00	6480.00	7770.00
Pr	3430.00	537.00	1155.00	2840.00	63.80	145.00	63.90	520.00	356.00	61.20	1100.00	631.00	907.00	77.10	64.20	400.00	575.00	696.00
Nd	10500.00	1585.00	3150.00	7760.00	190.00	457.00	210.00	1655.00	1065.00	202.00	2750.00	1560.00	2310.00	282.00	202.00	1125.00	1630.00	1965.00
Sm	1165.00	170.00	280.00	823.00	25.00	66.20	34.00	210.00	123.50	31.50	211.00	111.00	246.00	57.60	30.70	101.00	139.50	177.50
Eu	219.00	40.40	65.80	201.00	6.46	18.75	8.13	43.60	31.70	8.48	45.60	23.60	70.70	18.35	8.99	22.50	29.90	41.50
Gd	1050.00	159.00	330.00	952.00	26.10	72.40	34.00	196.00	125.00	31.30	277.00	141.50	306.00	60.40	32.40	105.00	139.50	189.00
Tb	84.00	12.95	28.50	90.10	3.07	10.25	4.58	20.10	12.80	4.23	17.95	10.10	29.10	9.70	4.57	8.44	9.90	17.55
Dy	252.00	47.00	109.50	353.00	15.80	55.30	27.10	93.20	59.30	24.20	51.20	37.00	110.00	62.50	27.00	33.00	31.60	81.60
Ho	42.40	7.89	21.20	63.70	3.06	10.05	5.54	17.30	10.70	4.76	10.55	6.68	18.20	13.15	5.55	6.03	5.23	15.65
Er	139.00	25.90	69.50	184.00	8.75	28.20	18.40	54.10	31.20	14.35	43.20	22.90	51.80	43.40	17.55	20.20	18.45	48.10
Tm	12.00	2.92	7.69	17.20	1.06	3.54	2.70	6.85	3.62	1.89	4.79	2.59	5.36	6.75	2.46	2.29	1.78	5.10
Yb	70.30	20.10	43.70	86.60	6.77	24.00	18.45	44.60	22.30	11.85	28.70	17.75	32.50	50.60	16.65	15.75	12.75	27.40
Lu	8.91	3.00	5.66	10.60	0.90	3.39	2.63	5.97	2.75	1.62	3.80	2.50	4.55	7.50	2.36	2.35	1.92	3.25
Y	1040.00	200.00	630.00	1660.00	92.10	267.00	155.50	444.00	284.00	118.50	336.00	190.50	510.00	365.00	145.50	183.50	145.00	464.00
La/Yb	234.00	193.53	186.50	230.37	67.06	37.08	18.21	71.52	127.80	26.08	311.85	362.82	250.15	6.42	24.32	195.56	325.49	178.83

Appendix 2 b) Trace elements analysis of samples collected by Etruscan and NRE and used in this study

Sample No.	ERN15466	ERN15467	ERN15468	ERN15469	ERN15470	ERN15471	ERN15472	ERN15473	ERN15474	ERN15475	ERN15476	ERN15477	ERN15478	ERN15479	ERN15480	ERN15481	ERN15482	ERN15483
Ba	822.00	557.00	987.00	2350.00	744.00	823.00	776.00	2330.00	273.00	1265.00	323.00	91.00	206.00	59.90	165.50	759.00	1680.00	1295.00
Ga	4.10	2.80	7.20	9.90	6.70	8.80	4.70	12.50	5.60	9.60	7.30	25.30	3.70	2.20	3.80	59.00	19.50	13.00
Hf	0.30	0.10	1.10	0.30	0.40	0.60	0.60	0.60	1.40	0.50	0.90	0.70	0.30	0.10	0.20	1.00	5.00	12.10
Nb	15.20	5.60	118.00	2.70	2.50	10.80	24.70	5.30	88.20	13.60	31.30	10.10	4.00	1.60	0.80	6.00	54.30	85.10
Rb	5.80	6.00	29.20	5.20	4.80	5.20	3.90	2.00	26.30	7.00	4.10	0.40	0.50	1.60	1.70	20.00	14.70	33.00
Sr	2440.00	1790.00	1930.00	1060.00	2100.00	1500.00	1570.00	2320.00	824.00	701.00	2570.00	2360.00	4470.00	1305.00	3330.00	2250.00	1825.00	271.00
Ta	0.20	0.20	0.40	0.40	0.20	0.20	0.20	0.50	0.60	0.20	0.50	0.50	0.20	0.10	0.40	0.25	0.70	0.80
Th	48.50	6.11	106.00	111.50	29.70	147.50	133.00	153.00	30.70	111.50	46.90	448.00	35.30	6.03	62.20	537.00	81.00	314.00
U	1.39	1.63	26.90	4.14	3.25	5.64	2.74	3.14	2.27	1.18	5.96	6.00	0.59	0.35	0.17	6.20	4.68	20.50
Zr	16.00	1.00	51.00	3.00	3.00	15.00	23.00	13.00	70.00	14.00	24.00	17.00	6.00	3.00	8.00	10.00	325.00	1060.00
La	350.00	123.50	389.00	1015.00	574.00	783.00	380.00	1190.00	109.50	983.00	750.00	4610.00	372.00	119.50	376.00	11950.00	2360.00	1365.00
Ce	608.00	267.00	853.00	2040.00	1235.00	1715.00	815.00	2760.00	214.00	2040.00	1355.00	7180.00	604.00	226.00	575.00	17400.00	3740.00	2290.00
Pr	59.80	30.80	100.50	228.00	147.00	202.00	97.40	336.00	23.60	220.00	132.50	646.00	55.40	23.40	50.70	1560.00	338.00	229.00
Nd	193.00	114.50	393.00	828.00	584.00	785.00	387.00	1335.00	82.90	748.00	420.00	1870.00	168.00	79.60	146.00	4030.00	982.00	801.00
Sm	29.30	24.40	98.10	146.50	143.00	175.50	86.80	258.00	15.75	87.90	56.60	225.00	23.50	13.80	17.35	362.00	102.00	149.50
Eu	8.83	8.40	38.30	46.00	50.50	58.20	27.00	77.20	5.37	21.40	15.35	57.10	7.41	4.07	5.01	84.70	24.90	41.90
Gd	30.50	26.40	114.00	137.00	145.50	167.50	78.30	223.00	18.25	80.80	58.90	232.00	30.10	15.80	21.40	461.00	107.00	163.00
Tb	4.20	3.90	16.15	15.10	18.90	20.70	10.25	25.40	3.23	9.16	8.32	23.90	5.80	2.71	3.36	43.40	11.80	25.50
Dy	24.70	22.30	83.70	63.20	88.30	94.60	50.80	106.00	21.00	45.00	53.40	111.50	47.30	18.85	24.40	177.00	66.20	150.00
Ho	5.03	4.29	14.50	9.97	14.15	15.30	8.72	16.15	4.34	8.24	12.30	20.80	11.90	4.33	6.00	32.80	14.40	28.10
Er	15.85	12.30	39.00	27.80	36.60	39.50	24.30	41.30	13.30	24.70	42.20	65.90	43.80	14.55	21.20	98.80	48.80	77.40
Tm	2.32	1.65	4.86	3.41	4.35	4.60	3.15	4.71	1.83	3.03	6.41	8.47	7.18	2.16	3.24	10.00	6.85	9.47
Yb	16.55	10.85	30.30	23.70	27.80	29.90	20.70	30.50	12.15	20.40	43.80	56.40	50.00	14.15	22.10	52.00	46.40	54.80
Lu	2.45	1.48	4.18	3.38	3.80	4.15	2.94	4.11	1.69	2.92	6.03	7.50	6.83	1.90	3.10	6.29	6.38	6.70
Y	133.00	101.50	369.00	243.00	316.00	359.00	230.00	385.00	116.50	212.00	370.00	550.00	342.00	146.50	179.50	904.00	430.00	735.00
La/Yb	21.15	11.38	12.84	42.83	20.65	26.19	18.36	39.02	9.01	48.19	17.12	81.74	7.44	8.45	17.01	229.81	50.86	24.91

Appendix 2 b) Trace elements analysis of samples collected by Etruscan and NRE and used in this study

Sample No.	ERN15484	ERN15485	ERN15486	ERN15487	ERN15488	ERN15489	ERN15490	ERN15491	ERN15492	ERN15493	ERN15494	ERN15495	ERN15496	ERN15497	ERN15498	ERN15499	ERN15500	ERN15501
Ba	467.00	83.60	244.00	54.50	246.00	640.00	143.00	2490.00	323.00	414.00	322.00	1100.00	502.00	961.00	174.50	302.00	1010.00	146.50
Ga	8.00	17.90	8.20	3.70	3.50	20.10	9.50	16.40	59.50	8.50	10.40	50.80	28.60	14.30	22.50	13.00	24.70	13.40
Hf	3.00	1.10	1.60	2.30	1.00	2.20	2.10	0.70	2.00	0.50	2.20	3.00	3.60	1.80	1.60	0.30	3.00	1.30
Nb	92.50	7.10	61.70	4.30	5.30	134.50	34.00	3.20	5.00	411.00	72.80	308.00	56.90	128.50	18.70	9.80	80.70	42.30
Rb	13.80	1.10	8.70	1.40	6.50	2.00	0.60	4.10	1.00	3.00	14.50	1.00	16.50	2.70	2.50	7.00	4.80	5.10
Sr	810.00	555.00	692.00	255.00	393.00	1825.00	1000.00	1915.00	10000.00	7210.00	1800.00	3490.00	3710.00	1345.00	2550.00	788.00	817.00	401.00
Ta	0.80	0.20	1.00	0.20	0.10	0.30	0.40	0.20	0.25	1.80	0.30	1.00	0.50	0.70	0.30	0.10	1.50	0.60
Th	256.00	600.00	96.00	288.00	195.00	133.00	529.00	308.00	648.00	23.20	158.50	271.00	443.00	99.20	452.00	36.10	600.00	686.00
U	10.95	7.05	16.20	7.34	4.12	3.97	8.88	5.91	3.90	20.00	4.72	12.70	16.60	18.25	9.12	6.82	10.10	7.96
Zr	172.00	23.00	158.00	259.00	95.00	190.00	144.00	9.00	80.00	38.00	92.00	70.00	149.00	145.00	39.00	16.00	79.00	4.00
La	791.00	1015.00	696.00	528.00	430.00	3200.00	1635.00	2420.00	13650.00	1035.00	912.00	9600.00	3490.00	2230.00	3320.00	1975.00	4170.00	2710.00
Ce	1175.00	3020.00	1295.00	781.00	645.00	5170.00	2240.00	3510.00	18500.00	1740.00	1610.00	15050.00	6110.00	3460.00	5050.00	2490.00	6550.00	4370.00
Pr	111.50	513.00	151.00	79.70	67.30	510.00	221.00	339.00	1460.00	186.50	175.50	1275.00	636.00	338.00	514.00	217.00	628.00	421.00
Nd	326.00	2490.00	489.00	238.00	222.00	1520.00	894.00	933.00	3800.00	573.00	555.00	3430.00	1830.00	1075.00	1505.00	544.00	1830.00	1335.00
Sm	63.30	539.00	63.70	45.90	58.80	203.00	274.00	112.00	324.00	75.80	98.20	302.00	222.00	142.00	207.00	48.40	264.00	190.50
Eu	24.30	106.50	17.25	13.85	12.50	47.50	60.80	30.40	79.60	21.40	23.30	67.70	61.90	38.80	54.80	12.35	70.40	56.90
Gd	93.00	341.00	61.00	71.00	64.10	207.00	213.00	141.50	441.00	78.50	94.70	369.00	282.00	152.50	244.00	65.80	329.00	240.00
Tb	17.25	41.80	6.51	17.45	10.60	20.40	28.00	19.95	37.80	8.37	11.10	32.10	41.40	16.95	33.50	5.15	50.50	47.30
Dy	111.00	167.50	25.40	130.00	61.60	78.90	150.00	121.00	148.50	35.30	47.50	149.50	237.00	76.50	183.00	18.00	295.00	322.00
Ho	26.50	30.90	4.45	31.00	13.15	13.85	33.50	27.70	26.40	6.34	8.86	31.10	49.20	15.05	37.90	3.36	63.30	68.80
Er	87.30	91.70	11.50	100.50	39.90	39.30	105.50	86.90	87.00	17.20	24.90	104.50	131.50	43.00	107.00	10.65	179.00	199.50
Tm	16.25	13.85	1.22	17.65	6.39	4.44	16.45	13.15	10.35	1.97	3.28	12.85	16.15	5.53	15.00	1.24	23.90	27.00
Yb	117.00	93.30	6.38	115.50	41.80	25.60	102.00	78.60	66.70	10.65	19.80	75.10	82.10	30.20	86.90	7.22	129.00	160.00
Lu	17.55	13.20	0.85	16.70	6.08	3.51	13.90	10.90	9.14	1.37	2.76	9.50	10.50	3.85	11.85	0.98	16.75	20.90
Y	832.00	1050.00	100.50	863.00	373.00	320.00	879.00	808.00	679.00	166.50	278.00	1010.00	1275.00	377.00	1035.00	96.90	1685.00	1925.00
La/Yb	6.76	10.88	109.09	4.57	10.29	125.00	16.03	30.79	204.65	97.18	46.06	127.83	42.51	73.84	38.20	273.55	32.33	16.94

Appendix 2 b) Trace elements analysis of samples collected by Etruscan and NRE and used in this study

Sample No.	ERN15502	ERN15503	ERN15504	ERN15505	ERN15506	ERN15507	ERN15508	ERN15509	ERN15510	ERN15511	ERN15512	ERN15513	ERN15514	ERN15515	ERN15516	ERN15517	ERN15518	ERN15519
Ba	87.20	2190.00	2270.00	517.00	1325.00	730.00	974.00	1265.00	826.00	114.00	262.00	39.90	222.00	67.90	132.50	53.90	36.90	361.00
Ga	6.10	13.90	6.50	12.70	8.70	8.70	17.90	16.70	6.00	8.80	16.10	1.00	0.80	25.50	9.70	1.90	1.30	10.20
Hf	0.80	4.70	2.00	2.00	2.00	1.40	8.70	0.80	1.40	4.00	1.40	5.60	0.30	0.80	8.50	0.30	0.30	0.70
Nb	49.30	223.00	159.00	111.00	354.00	111.00	124.00	6.20	65.20	551.00	34.80	18.60	1.00	10.00	133.00	13.50	12.20	11.40
Rb	1.30	53.60	8.00	0.50	6.00	7.40	219.00	4.50	23.10	35.00	2.30	1.80	3.30	1.10	0.60	3.10	1.10	1.60
Sr	4100.00	2970.00	10000.00	9050.00	9090.00	8200.00	445.00	1635.00	9260.00	448.00	5650.00	226.00	222.00	300.00	836.00	185.00	138.00	1450.00
Ta	0.60	3.70	2.60	1.00	2.50	0.60	5.70	0.10	0.70	1.80	0.80	0.10	0.05	0.10	0.20	0.10	0.10	0.10
Th	17.55	86.30	183.50	1145.00	1755.00	286.00	26.40	428.00	7.70	1285.00	702.00	14.70	12.40	178.50	296.00	2.71	3.04	502.00
U	8.53	7.85	13.00	10.90	39.40	8.58	5.03	5.50	9.84	71.00	4.75	2.51	0.91	4.23	16.00	1.14	1.08	11.15
Zr	64.00	194.00	120.00	10.00	20.00	27.00	343.00	15.00	76.00	270.00	17.00	375.00	6.00	27.00	417.00	11.00	8.00	11.00
La	757.00	505.00	803.00	1230.00	1070.00	1175.00	118.00	3910.00	460.00	750.00	1765.00	27.80	39.30	5220.00	1055.00	31.70	26.70	2320.00
Ce	1375.00	913.00	1480.00	2570.00	1820.00	1835.00	196.50	4550.00	804.00	1350.00	3110.00	44.40	82.00	7050.00	1940.00	48.40	59.70	2620.00
Pr	143.00	97.00	158.00	305.00	185.50	239.00	27.60	483.00	110.00	143.50	444.00	6.30	13.70	767.00	272.00	7.35	10.25	270.00
Nd	472.00	331.00	551.00	1195.00	643.00	776.00	98.90	1365.00	366.00	504.00	1610.00	24.10	61.20	2070.00	943.00	28.50	46.30	771.00
Sm	58.90	54.30	84.70	351.00	169.50	117.00	18.65	186.50	72.30	210.00	370.00	9.78	24.10	218.00	149.00	9.88	17.30	129.50
Eu	18.90	16.10	26.50	140.00	88.40	31.90	4.60	37.30	17.40	117.50	94.60	3.98	6.61	44.10	35.10	3.20	5.17	34.40
Gd	54.60	55.40	84.40	460.00	307.00	148.50	18.60	218.00	73.70	307.00	379.00	11.00	32.40	241.00	138.50	13.50	22.00	162.00
Tb	5.80	7.57	11.70	90.50	65.00	24.50	2.03	22.00	8.88	68.70	45.80	1.62	5.03	18.05	14.05	2.08	3.32	19.80
Dy	24.60	39.40	63.70	561.00	396.00	175.00	10.50	122.00	52.90	486.00	255.00	10.40	33.50	76.10	73.00	13.90	22.10	128.50
Ho	4.22	7.34	13.10	109.00	76.10	44.20	2.31	30.30	12.65	108.50	57.00	2.67	8.50	15.85	16.95	3.48	5.67	32.40
Er	11.65	20.30	38.60	284.00	193.00	109.00	5.46	82.60	31.70	325.00	136.50	7.36	22.10	40.20	43.60	9.17	14.85	83.20
Tm	1.31	2.59	5.44	36.40	24.70	14.65	0.73	12.30	4.55	49.10	18.35	1.19	3.46	4.64	5.93	1.43	2.34	12.30
Yb	7.74	15.45	33.00	204.00	138.00	82.60	4.50	79.40	28.70	288.00	109.00	8.18	22.90	27.90	35.20	9.89	15.90	77.40
Lu	1.02	1.99	4.26	25.70	16.75	10.80	0.60	11.45	4.01	37.30	14.85	1.25	3.28	3.93	4.60	1.57	2.40	10.75
Y	110.00	197.50	396.00	2780.00	1990.00	1210.00	56.70	824.00	303.00	2950.00	1440.00	71.40	245.00	398.00	429.00	102.00	173.50	804.00
La/Yb	97.80	32.69	24.33	6.03	7.75	14.23	26.22	49.24	16.03	2.60	16.19	3.40	1.72	187.10	29.97	3.21	1.68	29.97

Appendix 2 b) Trace elements analysis of samples collected by Etruscan and NRE and used in this study

Sample No.	ERN1 5520	ERN1 5521	ERN1 5522	ERN1 5523	ERN1 5524	ERN1 5525	ERN1 5526	ERN1 5527	ERN1 5528	ERN1 5529	ERN1 5530	ERN1 5531	ERN1 5532	ERN1 5534	ERN1 5535	ERN1 5536	ERN1 5537	ERN1 5538
Ba	771.00	265.00	23.50	54.50	117.50	1340.00	672.00	898.00	121.50	392.00	224.00	72.10	91.40	36.30	295.00	22.20	106.50	8430.00
Ga	24.90	12.60	0.80	29.00	18.40	21.10	28.50	11.70	12.20	11.40	9.30	1.30	12.80	9.20	18.50	2.60	12.40	24.90
Hf	2.90	2.40	1.90	1.00	3.00	1.50	2.70	3.30	33.60	1.50	2.20	4.50	2.70	3.80	2.00	1.50	0.90	3.10
Nb	108.50	99.90	8.80	14.60	667.00	48.80	336.00	43.60	203.00	70.50	53.60	50.60	493.00	62.60	184.00	80.90	116.00	227.00
Rb	3.90	2.80	5.40	11.60	19.00	15.30	24.70	63.80	16.90	34.90	40.90	5.60	10.00	1.10	10.80	2.90	2.60	13.40
Sr	1680.00	5160.00	515.00	202.00	814.00	2180.00	4030.00	165.50	781.00	3690.00	276.00	606.00	746.00	932.00	4300.00	392.00	285.00	2760.00
Ta	0.50	0.80	0.05	0.10	1.80	1.30	4.90	2.20	2.50	2.10	0.20	0.40	1.20	0.40	0.50	0.40	0.40	0.70
Th	380.00	176.00	37.70	580.00	1745.00	54.00	160.50	22.70	801.00	41.40	30.10	125.50	395.00	610.00	379.00	82.70	133.00	291.00
U	34.20	38.40	3.12	8.77	70.60	5.86	8.93	7.82	25.80	4.77	1.70	3.54	106.50	5.97	34.70	2.22	30.40	3.84
Zr	241.00	203.00	177.00	26.00	130.00	127.00	143.00	139.00	2270.00	143.00	119.00	393.00	161.00	222.00	105.00	112.00	31.00	84.00
La	4520.00	1980.00	48.90	5580.00	3000.00	1935.00	2360.00	41.20	600.00	507.00	21.00	25.90	1830.00	865.00	2790.00	292.00	2280.00	4230.00
Ce	6350.00	3070.00	73.70	7980.00	4680.00	3520.00	3950.00	73.10	1010.00	978.00	38.80	43.10	2940.00	1335.00	4040.00	466.00	3150.00	5780.00
Pr	753.00	391.00	9.45	909.00	423.00	371.00	383.00	9.13	116.50	115.50	6.43	6.30	378.00	175.00	494.00	61.70	375.00	676.00
Nd	2280.00	1275.00	32.30	2440.00	1215.00	1285.00	1230.00	38.70	454.00	393.00	34.80	25.20	1225.00	592.00	1580.00	209.00	1135.00	2060.00
Sm	320.00	211.00	11.70	207.00	141.50	183.50	166.00	13.70	209.00	60.40	34.80	11.60	191.00	217.00	245.00	65.00	154.00	282.00
Eu	63.40	48.90	3.23	43.80	50.50	42.40	44.30	4.32	73.80	16.20	8.57	3.87	43.90	60.60	54.10	15.05	38.10	56.40
Gd	306.00	215.00	13.10	288.00	206.00	168.00	176.50	12.85	263.00	53.10	31.10	15.50	194.50	239.00	244.00	62.80	157.50	271.00
Tb	26.00	23.20	1.89	33.70	37.40	17.35	19.50	1.96	57.10	6.09	4.13	2.75	20.30	26.50	24.20	7.37	13.75	22.50
Dy	122.00	118.00	11.85	164.50	212.00	62.90	78.40	10.95	369.00	25.20	25.10	20.10	100.00	132.00	121.50	37.80	63.00	93.30
Ho	28.00	25.20	2.91	26.60	37.50	11.05	14.60	2.45	76.80	4.57	6.00	5.50	21.10	26.80	26.10	7.37	13.50	18.20
Er	74.60	58.80	7.88	46.80	95.10	33.00	45.60	7.61	188.00	12.10	15.00	15.85	51.10	59.20	61.70	15.70	33.60	43.30
Tm	10.05	7.34	1.31	4.13	12.70	3.48	5.77	1.40	22.20	1.37	2.23	2.98	7.21	7.60	7.78	1.98	4.46	5.52
Yb	61.60	42.00	8.97	22.00	79.00	21.30	38.50	10.05	108.00	7.72	13.45	18.50	50.50	43.00	44.10	11.50	27.10	35.80
Lu	8.26	5.31	1.31	3.14	10.95	2.84	5.41	1.70	14.25	1.09	1.84	2.79	7.89	5.57	5.60	1.57	3.94	5.01
Y	759.00	584.00	76.80	458.00	946.00	264.00	396.00	74.60	2280.00	126.50	164.00	150.50	467.00	644.00	603.00	158.00	326.00	402.00
La/Yb	73.38	47.14	5.45	253.64	37.97	90.85	61.30	4.10	5.56	65.67	1.56	1.40	36.24	20.12	63.27	25.39	84.13	118.16

Appendix 2 b) Trace elements analysis of samples collected by Etruscan and NRE and used in this study

Sample No.	ERNI 5539	ERNI 5540	ERNI 5541	ERNI 5543	ERNI 5545	ERNI 5546	ERNI 5547	ERNI 5551	ERNI 5552	ERNI 5553	ERNI 5554	ERNI 5555	ERNI 5556	ERNI 5557	ERNI 5558	ERNI 5559	ERNI 5560	ERNI 5561
Ba	381.00	17.70	124.00	1100.00	217.00	1725.00	374.00	720.00	1110.00	434.00	35.60	1380.00	104.50	1025.00	534.00	1275.00	665.00	3360.00
Ga	8.40	0.30	6.90	13.60	16.70	37.50	2.70	7.70	17.60	4.60	1.20	8.90	12.20	11.20	10.70	30.40	27.70	4.30
Hf	5.50	0.10	1.00	3.30	5.20	13.00	0.80	1.70	1.30	7.90	5.90	0.50	2.10	38.20	4.70	3.90	6.80	1.80
Nb	769.00	3.70	2.10	179.50	32.20	369.00	32.20	139.00	17.50	80.40	4.90	17.60	120.00	158.00	127.50	55.70	641.00	148.50
Rb	1.90	0.40	12.70	9.60	6.80	21.00	1.50	6.70	7.10	4.30	0.50	6.20	10.70	87.80	9.90	14.50	21.40	5.10
Sr	7450.00	300.00	608.00	3120.00	796.00	308.00	293.00	8030.00	4840.00	598.00	323.00	905.00	182.00	619.00	1485.00	1205.00	1465.00	1390.00
Ta	4.60	0.05	0.05	0.70	0.30	4.50	0.20	0.80	0.20	0.90	0.40	0.10	2.10	1.20	2.70	0.40	21.90	1.70
Th	692.00	5.73	18.45	164.50	51.50	404.00	5.44	116.50	297.00	467.00	389.00	39.80	3.94	829.00	518.00	75.40	28.40	284.00
U	59.80	0.35	2.75	16.10	7.14	16.10	4.39	7.03	8.18	9.43	6.81	1.50	2.69	44.30	7.34	9.78	27.40	6.90
Zr	136.00	6.00	26.00	224.00	494.00	770.00	40.00	138.00	56.00	620.00	420.00	15.00	106.00	3270.00	301.00	165.00	398.00	164.00
La	979.00	8.90	893.00	2310.00	4680.00	5950.00	109.50	826.00	3720.00	384.00	71.90	1030.00	6.80	791.00	1005.00	5560.00	420.00	512.00
Ce	1545.00	14.30	1350.00	3230.00	4700.00	9800.00	151.50	1220.00	5030.00	618.00	137.50	1895.00	12.70	1290.00	1585.00	7720.00	714.00	831.00
Pr	205.00	1.99	160.00	381.00	412.00	954.00	17.90	126.50	457.00	86.20	19.55	223.00	1.63	159.50	171.00	699.00	81.10	93.10
Nd	697.00	7.50	480.00	1170.00	941.00	2800.00	54.50	405.00	1300.00	531.00	101.00	750.00	7.20	705.00	598.00	1950.00	269.00	310.00
Sm	239.00	3.58	75.40	169.50	69.30	331.00	9.03	67.40	153.00	350.00	79.20	100.50	2.55	312.00	142.50	211.00	37.80	61.70
Eu	100.50	1.24	16.90	34.60	13.40	77.30	2.26	18.20	40.20	93.30	38.40	23.60	1.16	96.60	62.30	47.20	10.20	21.10
Gd	402.00	4.73	83.20	175.50	109.50	329.00	9.90	71.60	193.50	400.00	164.00	91.30	4.02	358.00	262.00	254.00	37.70	74.20
Tb	58.50	0.62	8.43	16.75	6.77	36.50	1.14	9.61	22.20	76.90	44.30	8.72	0.73	52.40	51.30	23.50	4.12	10.35
Dy	339.00	3.46	44.80	86.00	29.90	156.00	6.62	52.90	121.00	510.00	351.00	35.90	4.63	275.00	299.00	108.50	18.55	51.60
Ho	71.40	0.73	10.50	19.40	7.49	29.00	1.72	10.40	25.40	106.00	82.40	6.85	0.98	46.50	50.10	21.90	3.32	8.90
Er	154.50	1.79	26.80	47.00	21.50	78.10	4.84	30.00	80.90	293.00	263.00	22.50	2.93	112.00	113.50	72.50	9.33	22.00
Tm	19.25	0.27	3.62	5.73	2.77	9.63	0.80	3.85	11.70	40.60	46.00	3.02	0.42	13.40	12.60	9.92	1.13	2.37
Yb	104.50	1.77	21.70	32.10	16.70	57.10	5.51	22.90	76.30	232.00	313.00	21.20	3.07	76.20	65.20	63.40	7.59	12.80
Lu	13.30	0.27	2.96	4.14	2.29	8.47	0.84	2.94	10.50	28.30	42.70	3.13	0.52	9.33	7.81	8.40	1.07	1.52
Y	1720.00	18.50	226.00	484.00	208.00	692.00	46.70	263.00	679.00	3630.00	2200.00	172.50	28.00	1065.00	1175.00	635.00	80.10	225.00
La/Yb	9.37	5.03	41.15	71.96	280.24	104.20	19.87	36.07	48.75	1.66	0.23	48.58	2.21	10.38	15.41	87.70	55.34	40.00

Appendix 2 b) Trace elements analysis of samples collected by Etruscan and NRE and used in this study

Sample No.	ERN15562	ERN15563	ERN15564	ERN15565	ERN15566	ERN15567	ERN15568	ERN15569	ERN15570	ERN15571	ERN15572	ERN15573	ERN15574	ERN15575	ERN15576	ERN15577	ERN15578	ERN15579
Ba	174.00	1340.00	607.00	241.00	1180.00	311.00	416.00	102.50	11.50	145.50	184.00	69.30	64.20	602.00	85.80	1075.00	903.00	586.00
Ga	5.30	72.00	45.90	29.50	34.60	23.20	45.00	18.60	22.10	8.70	17.80	5.20	5.00	29.10	10.30	76.20	35.60	54.90
Hf	0.80	2.00	1.90	1.70	2.10	9.00	1.10	1.30	1.00	5.10	6.20	1.30	1.70	3.00	0.50	1.80	3.80	1.20
Nb	9.60	7.00	4.00	151.50	11.80	342.00	51.20	31.80	13.40	76.10	138.00	3.50	23.30	175.00	6.20	82.70	106.00	8.50
Rb	15.00	1.00	15.40	1.50	2.50	14.00	4.40	5.00	0.40	4.40	24.60	21.20	7.10	21.60	4.20	9.40	19.60	2.80
Sr	424.00	3110.00	1420.00	2210.00	9850.00	668.00	358.00	648.00	168.50	290.00	299.00	493.00	445.00	1545.00	555.00	881.00	1725.00	1345.00
Ta	0.10	0.25	0.10	0.60	0.50	14.00	0.30	0.30	0.30	0.70	1.90	0.10	0.50	1.70	0.10	0.80	0.90	0.30
Th	49.10	242.00	209.00	148.50	728.00	52.90	995.00	254.00	1000.00	333.00	206.00	121.50	525.00	123.00	184.00	300.00	50.70	207.00
U	2.02	2.70	10.30	5.37	6.05	8.16	17.30	5.24	22.70	15.40	6.64	4.20	13.00	48.90	4.41	6.13	23.40	4.67
Zr	47.00	80.00	98.00	111.00	19.00	509.00	35.00	82.00	30.00	514.00	443.00	89.00	91.00	238.00	40.00	48.00	614.00	49.00
La	458.00	8030.00	2980.00	2090.00	3620.00	250.00	2780.00	1305.00	1225.00	37.40	98.20	11.80	45.00	1420.00	653.00	6250.00	2390.00	4600.00
Ce	679.00	10900.00	5600.00	3570.00	4590.00	475.00	4330.00	1725.00	2100.00	68.30	174.00	21.30	85.60	2400.00	935.00	8330.00	3420.00	6160.00
Pr	70.60	979.00	557.00	346.00	367.00	58.60	389.00	156.50	199.00	7.44	19.25	2.47	9.41	236.00	93.00	679.00	292.00	507.00
Nd	221.00	2250.00	1625.00	1110.00	986.00	200.00	1185.00	412.00	657.00	26.10	66.80	9.70	33.00	785.00	273.00	1780.00	858.00	1320.00
Sm	34.80	233.00	175.00	161.50	148.50	32.60	159.00	50.50	122.50	13.85	25.50	4.82	19.45	112.50	47.00	215.00	95.20	176.50
Eu	9.21	71.70	43.20	45.80	54.20	9.65	46.10	15.55	24.10	6.11	8.97	2.75	10.30	32.50	11.95	56.00	25.80	44.80
Gd	39.20	346.00	208.00	167.50	217.00	33.10	210.00	78.80	143.00	30.50	44.20	12.70	58.20	121.00	56.40	289.00	117.00	225.00
Tb	5.09	44.10	20.90	19.65	33.80	4.00	25.30	12.10	19.30	7.07	9.81	3.24	15.10	13.95	6.69	31.30	11.60	24.90
Dy	28.60	194.00	75.70	85.00	190.50	17.30	123.50	76.80	103.50	50.70	67.30	24.40	114.00	61.00	31.40	149.50	47.90	118.50
Ho	5.90	38.60	13.80	15.85	37.30	3.17	24.50	16.90	22.00	11.65	14.90	5.75	26.80	11.75	6.21	32.10	9.74	25.40
Er	18.85	96.50	44.10	46.40	106.00	8.85	75.00	50.60	67.30	36.40	45.00	17.80	81.00	36.00	18.10	102.50	32.40	79.50
Tm	2.88	11.95	4.55	5.41	14.10	0.99	10.10	7.48	9.16	6.18	7.04	2.90	12.80	4.44	2.29	13.30	4.23	10.25
Yb	20.10	60.10	28.50	32.00	85.80	5.65	59.90	46.10	52.30	39.70	42.30	18.85	77.90	25.50	13.20	76.30	25.20	59.10
Lu	3.06	8.13	3.73	4.03	11.20	0.77	8.12	6.65	7.41	6.02	6.06	2.99	11.10	3.47	1.74	10.30	3.45	7.74
Y	164.00	1140.00	398.00	436.00	1010.00	82.30	607.00	442.00	588.00	335.00	374.00	167.00	810.00	289.00	173.00	964.00	284.00	770.00
La/Yb	22.79	133.61	104.56	65.31	42.19	44.25	46.41	28.31	23.42	0.94	2.32	0.63	0.58	55.69	49.47	81.91	94.84	77.83

Appendix 2 b) Trace elements analysis of samples collected by Etruscan and NRE and used in this study

Sample No.	ERN15580	ERN15581	ERN15582	ERN15583	ERN15584	ERN15585	ERN15586	ERN15587	ERN15588	ERN15589	ERN15590	ERN15591	ERN15592	ERN15593	ERN15594	ERN15595	ERN15596	ERN15597
Ba	700.00	547.00	179.00	8170.00	580.00	559.00	6520.00	1030.00	1150.00	1895.00	398.00	660.00	1715.00	1585.00	493.00	884.00	908.00	153.00
Ga	9.60	4.70	2.40	39.00	16.30	23.80	27.30	23.90	5.60	34.10	16.10	17.50	23.10	25.00	12.90	6.90	25.40	21.40
Hf	1.20	3.70	0.40	1.20	1.60	0.90	6.00	11.40	2.10	2.90	0.60	0.60	2.50	1.10	5.50	2.10	1.50	1.20
Nb	7.70	14.80	2.90	251.00	27.40	279.00	248.00	513.00	15.80	142.00	144.00	32.40	125.00	173.50	75.70	8.60	2.60	119.50
Rb	31.80	31.60	0.60	123.00	3.00	3.50	81.70	13.40	62.50	4.30	14.20	6.80	7.70	5.50	5.20	26.20	1.90	1.80
Sr	472.00	895.00	568.00	6630.00	10000.00	5290.00	5340.00	10000.00	831.00	10000.00	4780.00	4500.00	1990.00	6310.00	609.00	468.00	1950.00	3660.00
Ta	0.50	0.40	0.05	3.50	0.70	0.50	8.10	8.90	0.30	0.80	1.00	0.80	0.40	0.60	0.50	0.10	0.20	0.50
Th	3.99	19.70	3.01	585.00	50.30	40.70	47.70	68.80	11.45	42.10	85.70	13.35	51.80	74.80	45.90	32.00	211.00	57.30
U	1.47	6.99	2.73	13.00	1.46	28.90	12.85	24.40	5.78	33.80	7.84	2.31	14.00	19.00	5.41	6.78	5.77	49.10
Zr	34.00	328.00	42.00	12.00	54.00	45.00	246.00	513.00	173.00	302.00	11.00	23.00	164.00	69.00	268.00	108.00	57.00	165.00
La	139.00	73.90	8.30	1230.00	657.00	1240.00	942.00	1025.00	15.10	2250.00	560.00	762.00	1080.00	1290.00	57.00	29.10	1560.00	1010.00
Ce	287.00	122.50	14.00	2280.00	1210.00	2020.00	1485.00	1690.00	34.80	3370.00	1155.00	1375.00	1835.00	2120.00	96.30	53.20	2350.00	1750.00
Pr	43.60	12.55	1.45	241.00	136.00	204.00	158.00	175.00	5.09	298.00	139.00	148.50	200.00	206.00	10.80	6.02	218.00	190.50
Nd	172.50	40.10	4.90	853.00	431.00	687.00	480.00	501.00	23.20	916.00	440.00	440.00	615.00	680.00	36.90	21.20	698.00	577.00
Sm	41.50	9.32	1.57	191.50	68.80	93.80	69.30	57.50	10.50	109.00	64.40	58.70	83.00	92.20	8.95	5.72	106.50	77.90
Eu	8.16	3.26	0.63	70.50	19.85	27.20	17.00	15.30	3.55	31.50	20.40	16.95	25.30	27.50	3.63	2.23	36.10	24.10
Gd	44.30	13.35	2.44	230.00	77.00	102.00	78.30	69.80	14.05	131.50	76.60	70.60	93.60	103.00	13.60	7.86	139.50	91.10
Tb	7.97	2.41	0.52	32.80	9.48	11.15	8.68	7.32	3.18	12.45	10.20	8.34	10.35	11.00	3.02	1.61	17.35	9.63
Dy	48.80	15.10	3.37	147.50	45.90	46.20	36.00	33.30	21.80	42.00	47.20	40.20	43.40	44.20	22.00	10.85	80.40	38.10
Ho	10.75	3.29	0.77	25.00	9.24	8.68	6.56	7.72	4.88	7.00	9.04	8.41	8.16	8.02	5.15	2.44	14.85	7.15
Er	31.40	9.78	2.44	65.80	26.60	26.30	19.00	26.60	14.45	22.20	27.60	27.40	24.60	23.90	16.10	7.39	42.60	22.40
Tm	4.41	1.50	0.41	8.69	3.06	2.94	2.13	3.62	2.25	2.27	3.87	3.95	2.77	2.55	2.46	1.13	5.28	2.64
Yb	25.70	9.31	2.63	54.30	15.40	16.65	12.40	20.80	13.65	14.00	24.80	26.20	16.05	14.05	14.50	7.00	31.70	15.25
Lu	3.60	1.33	0.39	7.71	1.81	2.25	1.68	2.79	1.89	2.03	3.83	4.01	2.19	1.85	2.11	0.99	4.35	2.11
Y	344.00	87.60	22.40	502.00	230.00	232.00	179.00	233.00	138.50	177.00	233.00	221.00	204.00	212.00	150.00	66.80	380.00	162.50
La/Yb	5.41	7.94	3.16	22.65	42.66	74.47	75.97	49.28	1.11	160.71	22.58	29.08	67.29	91.81	3.93	4.16	49.21	66.23

Appendix 2 b) Trace elements analysis of samples collected by Etruscan and NRE and used in this study

Sample No.	ERN15598	ERN15599	ERN15600	ERN15601	ERN15602	ERN15603	ERN15604	ERN15605	ERN15606	ERN15607	ERN15608	ERN15609	ERN15610	ERN15611	ERN15612	ERN15613	ERN15614	ERN15615
Ba	1530.00	879.00	3180.00	890.00	1380.00	820.00	916.00	2850.00	774.00	1640.00	1680.00	871.00	1320.00	84.30	37.20	357.00	2720.00	982.00
Ga	28.00	4.30	33.10	6.40	10.60	12.30	8.50	10.40	2.80	6.80	11.30	5.00	8.10	0.70	0.70	3.20	5.70	9.80
Hf	0.70	3.80	1.70	1.00	2.00	1.60	2.00	5.30	0.50	0.50	0.90	0.50	2.40	0.10	0.20	0.30	5.00	2.00
Nb	47.50	19.90	17.80	7.90	467.00	219.00	28.80	268.00	6.30	36.90	123.50	2.60	14.10	1.60	2.50	18.60	73.00	24.10
Rb	0.70	6.30	31.70	4.30	7.50	19.30	2.40	9.40	5.80	27.10	59.20	2.60	14.70	0.80	1.70	2.90	52.00	2.60
Sr	6130.00	115.50	2400.00	2790.00	6180.00	950.00	5350.00	7210.00	786.00	2160.00	2420.00	4190.00	1600.00	1325.00	46.70	842.00	4720.00	7180.00
Ta	0.80	0.30	0.20	0.10	3.10	1.00	0.50	0.80	0.10	0.10	0.30	0.10	0.10	0.05	0.10	0.10	0.80	0.40
Th	111.50	10.85	119.00	59.00	48.90	57.00	133.00	45.60	41.50	26.80	78.20	87.00	22.30	5.53	4.99	6.29	1610.00	17.85
U	7.66	9.25	10.30	5.11	11.05	6.52	2.33	20.50	11.60	6.51	5.82	1.44	5.84	0.33	0.34	9.52	47.90	2.00
Zr	5.00	336.00	139.00	59.00	129.00	126.00	124.00	381.00	29.00	25.00	30.00	14.00	126.00	3.00	5.00	7.00	450.00	69.00
La	1760.00	28.00	4420.00	754.00	1315.00	1455.00	494.00	1135.00	27.40	243.00	707.00	590.00	697.00	39.90	5.30	461.00	434.00	398.00
Ce	2570.00	43.60	7900.00	1190.00	2260.00	2380.00	922.00	1930.00	52.00	418.00	1295.00	975.00	1265.00	56.30	9.10	832.00	802.00	732.00
Pr	227.00	5.14	770.00	116.50	222.00	231.00	97.90	188.50	6.11	42.10	132.50	97.20	130.50	5.07	0.98	86.20	83.00	73.00
Nd	687.00	19.20	2420.00	420.00	770.00	758.00	369.00	638.00	25.10	148.00	468.00	339.00	467.00	15.60	3.40	285.00	303.00	246.00
Sm	88.80	3.95	222.00	82.20	107.00	99.30	88.90	87.40	8.54	24.80	84.40	55.90	71.80	2.67	0.61	47.60	62.00	40.90
Eu	27.40	1.34	42.40	22.60	29.00	26.10	29.60	24.00	3.20	7.66	23.40	14.70	18.50	1.19	0.20	12.30	21.50	11.35
Gd	121.50	4.77	211.00	78.10	98.90	91.70	101.00	84.50	12.15	25.10	89.00	55.90	65.80	4.13	0.76	49.80	83.60	41.80
Tb	14.75	0.87	16.50	11.65	11.60	10.00	16.70	9.94	2.93	3.65	13.90	8.10	8.48	0.77	0.12	6.13	14.70	5.75
Dy	72.20	5.74	49.80	63.10	50.10	38.10	92.00	42.90	20.80	18.45	70.20	42.90	39.30	6.77	0.72	30.60	84.10	32.00
Ho	14.40	1.24	9.23	13.20	8.90	6.64	18.05	7.66	4.61	3.62	12.90	8.90	7.19	2.46	0.15	5.96	16.20	6.52
Er	44.00	3.98	33.60	40.60	25.10	19.70	53.50	22.40	14.10	10.65	34.70	27.50	21.30	13.25	0.41	17.05	42.60	19.30
Tm	5.65	0.56	3.43	5.57	2.81	2.14	7.30	2.52	2.16	1.40	4.15	3.93	2.54	2.76	0.06	2.05	5.31	2.47
Yb	33.80	3.84	21.50	35.50	17.25	13.15	43.80	14.75	13.85	8.65	24.10	25.70	15.40	22.90	0.41	11.70	31.60	14.35
Lu	4.61	0.54	2.81	4.48	2.26	1.69	5.30	1.90	1.86	1.18	2.98	3.45	1.96	3.85	0.05	1.40	3.86	1.74
Y	378.00	59.00	211.00	390.00	234.00	182.00	520.00	216.00	129.50	93.80	309.00	226.00	187.00	93.90	3.80	162.00	380.00	170.50
La/Yb	52.07	7.29	205.58	21.24	76.23	110.65	11.28	76.95	1.98	28.09	29.34	22.96	45.26	1.74	12.93	39.40	13.73	27.74

Appendix 2 b) Trace elements analysis of samples collected by Etruscan and NRE and used in this study

Sample No.	ERN15616	ERN15617	ERN15618	ERN15619	ERN15620	ERN15621	ERN15622	ERN15623	ERN15624	ERN15625	ERN15626	ERN15627	ERN15628	ERN15629	ERN15630	ERN15631	ERN15632	ERN15633
Ba	3840.00	531.00	1050.00	3650.00	878.00	770.00	2740.00	502.00	852.00	525.00	1020.00	2070.00	243.00	570.00	246.00	454.00	1555.00	1450.00
Ga	12.60	10.50	6.70	11.00	5.80	7.10	6.00	4.30	21.90	2.90	7.30	10.50	5.30	37.70	12.00	26.60	22.60	17.20
Hf	6.00	17.00	2.00	3.20	2.90	1.50	0.90	1.00	2.10	0.50	1.00	12.10	2.90	3.00	0.90	2.10	1.60	3.60
Nb	378.00	2580.00	221.00	103.00	91.70	85.90	24.20	247.00	28.40	4.00	89.00	68.90	390.00	165.00	17.10	410.00	18.60	77.80
Rb	23.00	7.30	2.00	17.30	6.90	6.70	23.60	13.00	20.40	0.50	1.00	38.70	17.50	2.00	7.30	14.70	4.20	3.30
Sr	10000.00	4330.00	10000.00	6920.00	9190.00	7050.00	318.00	10000.00	658.00	10000.00	10000.00	575.00	5040.00	1585.00	673.00	1320.00	3630.00	586.00
Ta	4.30	22.70	2.20	0.40	0.90	0.90	0.20	0.60	0.50	0.25	1.20	0.60	0.60	0.50	0.10	0.50	0.20	0.70
Th	87.30	117.50	76.20	376.00	394.00	86.20	15.10	10.50	560.00	2.30	16.30	8.23	96.30	1095.00	232.00	223.00	319.00	407.00
U	24.50	448.00	5.70	9.67	9.83	22.20	4.31	4.30	28.60	0.30	5.50	10.75	16.60	13.10	3.68	34.60	3.05	10.50
Zr	300.00	912.00	70.00	146.00	159.00	64.00	42.00	50.00	57.00	10.00	150.00	773.00	189.00	120.00	29.00	77.00	35.00	186.00
La	1040.00	318.00	883.00	923.00	851.00	780.00	152.50	273.00	4970.00	552.00	750.00	168.00	802.00	9800.00	1900.00	3680.00	6210.00	4190.00
Ce	2050.00	627.00	1520.00	1610.00	1495.00	1295.00	301.00	546.00	7920.00	978.00	1090.00	289.00	1360.00	15500.00	3570.00	8060.00	9300.00	5900.00
Pr	220.00	67.00	149.00	176.50	159.00	133.00	31.50	56.70	760.00	91.60	98.00	30.20	138.50	1425.00	384.00	923.00	820.00	527.00
Nd	799.00	225.00	495.00	662.00	551.00	445.00	104.00	199.00	2330.00	296.00	308.00	104.50	458.00	4490.00	1315.00	3240.00	2280.00	1615.00
Sm	129.50	37.20	72.20	151.00	120.00	71.70	17.85	31.30	305.00	43.80	45.70	19.55	75.10	722.00	206.00	453.00	245.00	245.00
Eu	34.20	10.15	21.90	53.50	50.00	22.90	4.45	9.10	77.30	12.80	12.90	5.51	25.50	210.00	55.30	87.60	58.00	70.40
Gd	119.00	36.60	72.40	176.00	184.50	75.00	17.40	32.00	335.00	49.10	47.30	22.60	82.90	798.00	193.50	354.00	287.00	267.00
Tb	13.90	4.84	9.29	29.00	37.20	9.26	2.23	4.12	46.70	6.91	5.53	3.48	11.80	87.90	21.50	32.00	28.60	31.70
Dy	64.20	25.50	53.10	161.50	243.00	45.70	11.55	21.00	291.00	38.30	26.50	21.40	66.50	369.00	88.50	121.50	126.50	145.00
Ho	11.55	4.88	11.45	30.00	47.90	8.38	2.09	4.11	66.50	7.96	5.08	4.31	12.70	58.60	14.90	21.80	23.20	25.40
Er	31.70	14.65	33.50	79.90	129.00	23.70	6.40	11.90	214.00	23.80	13.50	13.95	35.90	145.50	46.90	71.60	71.60	71.30
Tm	3.78	2.16	4.34	10.45	16.10	2.83	0.88	1.50	31.60	2.92	1.54	2.16	4.99	14.25	6.53	8.62	9.36	9.18
Yb	22.70	17.60	26.60	65.40	94.80	16.85	6.66	10.10	204.00	17.00	9.90	17.35	33.80	78.60	48.50	57.20	64.10	60.20
Lu	2.84	3.05	3.48	8.62	11.75	2.13	0.97	1.36	26.80	1.96	1.35	2.95	4.88	9.64	7.19	7.72	8.75	7.89
Y	296.00	115.50	334.00	822.00	1400.00	227.00	64.70	102.00	1795.00	206.00	140.00	121.00	343.00	1375.00	423.00	705.00	566.00	642.00
La/Yb	45.81	18.07	33.20	14.11	8.98	46.29	22.90	27.03	24.36	32.47	75.76	9.68	23.73	124.68	39.18	64.34	96.88	69.60

Appendix 2 b) Trace elements analysis of samples collected by Etruscan and NRE and used in this study

Sample No.	ERN15634	ERN15635	ERN15636	ERN15637	ERN15638	ERN15639	ERN15640	ERN15641	ERN15642	ERN15643	ERN15644	ERN15645	ERN15646	ERN15647	ERN15648	ERN15649	ERN15651	ERN15652
Ba	3150.00	371.00	795.00	46.40	142.00	106.00	46.10	409.00	52.90	144.50	85.70	5190.00	347.00	1150.00	654.00	195.50	22.60	682.00
Ga	2.20	7.90	15.00	1.10	2.30	11.50	5.50	24.50	1.40	7.30	3.10	5.10	9.80	12.90	13.60	8.60	1.70	6.40
Hf	3.40	42.80	4.60	0.80	2.60	1.10	0.60	1.00	0.30	1.90	2.20	0.70	1.80	14.70	2.80	1.90	0.20	0.40
Nb	9.20	120.00	576.00	3.60	38.50	33.20	73.40	8.00	10.30	84.80	9.10	55.30	14.50	308.00	140.50	137.50	1.40	23.10
Rb	6.30	8.30	29.60	2.80	5.60	10.20	6.90	10.00	3.10	19.50	0.60	2.00	5.40	75.50	3.50	15.00	2.10	2.00
Sr	804.00	1910.00	2110.00	583.00	292.00	544.00	273.00	466.00	181.50	326.00	333.00	661.00	3070.00	1950.00	1860.00	2560.00	256.00	6750.00
Ta	0.05	0.20	5.10	0.05	0.20	0.50	0.10	0.25	0.10	1.60	0.10	0.30	0.20	1.30	0.80	1.10	0.05	0.30
Th	29.70	66.00	22.50	21.10	209.00	761.00	528.00	770.00	43.40	76.20	37.80	96.80	615.00	103.00	321.00	72.20	7.35	11.50
U	22.80	18.90	25.80	2.52	8.31	12.05	7.90	7.60	1.77	14.95	10.25	4.91	9.24	20.90	9.07	24.10	0.82	1.78
Zr	473.00	3820.00	442.00	84.00	344.00	111.00	42.00	120.00	12.00	177.00	289.00	60.00	72.00	1260.00	225.00	153.00	4.00	5.00
La	68.00	1230.00	1030.00	48.60	167.50	3770.00	1160.00	7660.00	102.50	1545.00	15.70	1330.00	2750.00	2000.00	3550.00	1125.00	29.60	694.00
Ce	98.80	2010.00	1830.00	74.90	320.00	4870.00	1815.00	10450.00	172.00	2500.00	32.90	2080.00	3700.00	3000.00	5390.00	1910.00	67.90	1180.00
Pr	9.55	197.50	189.50	7.16	34.90	401.00	177.00	861.00	18.50	237.00	4.18	194.50	321.00	272.00	491.00	187.00	9.56	129.00
Nd	32.30	624.00	621.00	22.50	121.50	1100.00	558.00	2390.00	67.40	745.00	16.90	579.00	971.00	816.00	1485.00	596.00	43.80	412.00
Sm	8.13	83.30	83.50	4.47	27.50	139.00	91.60	262.00	26.50	100.50	5.89	72.10	162.00	102.50	196.00	77.90	16.20	76.40
Eu	3.14	22.00	23.50	1.39	5.66	37.70	22.70	64.80	8.30	28.00	2.35	20.60	52.90	28.60	50.90	21.90	5.28	21.60
Gd	11.50	83.20	78.90	5.60	35.00	165.50	106.50	305.00	39.60	106.50	11.25	80.50	222.00	111.50	212.00	82.60	19.85	80.60
Tb	2.23	8.81	8.25	0.97	6.01	16.90	13.00	29.70	6.75	11.95	2.75	8.55	36.40	11.50	23.60	9.96	3.81	11.20
Dy	16.10	39.80	35.70	6.40	36.20	68.30	63.90	139.00	39.50	51.30	20.30	37.70	210.00	49.90	112.00	47.80	24.30	56.20
Ho	3.73	7.17	6.22	1.39	7.73	10.70	12.05	25.50	7.91	8.79	4.75	7.00	40.90	9.14	22.00	8.80	5.54	10.90
Er	12.35	20.30	17.55	4.47	23.50	30.00	34.60	78.90	23.70	23.80	15.55	20.70	112.00	25.60	66.30	24.90	16.85	30.30
Tm	1.93	2.27	1.98	0.68	3.47	3.57	4.72	9.40	3.69	2.65	2.36	2.50	14.00	2.78	8.40	2.92	2.67	4.29
Yb	12.95	13.45	12.60	5.06	23.90	23.50	30.80	60.50	26.40	15.00	15.80	15.50	78.40	16.50	50.10	17.25	17.25	24.80
Lu	1.78	1.72	1.70	0.69	3.71	3.04	4.06	7.96	3.83	1.86	2.11	2.09	9.47	1.98	6.23	2.13	2.64	3.35
Y	122.00	179.00	153.00	40.00	220.00	288.00	315.00	734.00	261.00	207.00	141.50	207.00	1215.00	259.00	631.00	226.00	186.00	308.00
La/Yb	5.25	91.45	81.75	9.60	7.01	160.43	37.66	126.61	3.88	103.00	0.99	85.81	35.08	121.21	70.86	65.22	1.72	27.98

Appendix 2 b) Trace elements analysis of samples collected by Etruscan and NRE and used in this study

Sample No.	ERNI 5653	ERNI 5654	ERNI 5655	ERNI 5656	ERNI 5657	ERNI 5658	ERNI 5659	ERNI 5660	ERNI 5661	ERNI 5662	ERNI 5663	ERNI 5664	ERNI 5665	ERNI 5666	ERNI 5667	ERNI 5668	ERNI 5669	ERNI 5670
Ba	1415.00	3790.00	5750.00	3190.00	4960.00	1760.00	782.00	546.00	1680.00	94.20	98.40	112.50	3330.00	150.50	795.00	2460.00	677.00	326.00
Ga	12.80	10.10	10.80	22.40	20.00	11.40	2.90	3.90	7.30	42.00	27.10	12.00	23.90	11.10	11.70	25.00	26.60	24.30
Hf	0.50	0.70	0.70	2.90	2.60	1.50	0.30	0.60	5.40	3.00	2.00	3.40	2.50	0.60	2.20	4.20	9.70	16.10
Nb	22.40	24.70	11.90	336.00	133.00	228.00	3.50	49.30	121.50	81.00	33.80	102.00	103.00	59.20	88.60	625.00	374.00	361.00
Rb	4.70	2.10	0.70	1.20	1.60	1.60	3.20	8.70	4.90	25.00	8.80	13.30	1.60	5.50	6.90	2.20	63.30	21.60
Sr	10000.00	10000.00	1030.00	3860.00	1995.00	7540.00	7950.00	9600.00	7570.00	615.00	890.00	182.00	10000.00	1930.00	5610.00	10000.00	1945.00	2050.00
Ta	0.30	0.30	0.05	3.20	0.90	1.30	0.10	0.10	0.70	0.25	0.20	0.30	0.90	0.50	1.30	3.30	26.90	2.40
Th	22.10	66.80	1.74	164.00	337.00	20.60	1.67	2.90	133.50	187.50	289.00	34.30	1000.00	57.90	189.00	240.00	50.50	1000.00
U	3.67	5.73	2.71	11.50	13.50	15.85	1.33	5.10	6.45	4.70	5.33	3.68	22.00	6.85	18.55	26.00	11.45	11.20
Zr	5.00	13.00	22.00	159.00	89.00	96.00	13.00	24.00	220.00	190.00	64.00	188.00	59.00	17.00	121.00	184.00	446.00	1260.00
La	1690.00	1150.00	33.70	2370.00	3240.00	1370.00	185.50	268.00	860.00	10200.00	4860.00	23.20	3650.00	904.00	1055.00	1460.00	258.00	1155.00
Ce	2830.00	2150.00	60.90	4740.00	5000.00	2290.00	333.00	451.00	1375.00	12200.00	6930.00	45.00	4700.00	1520.00	1835.00	2350.00	504.00	1885.00
Pr	282.00	235.00	7.50	520.00	483.00	232.00	38.70	50.60	144.00	876.00	640.00	5.38	389.00	157.50	193.50	238.00	59.00	198.00
Nd	909.00	817.00	26.30	1700.00	1455.00	755.00	125.00	161.50	431.00	2080.00	1640.00	19.70	1150.00	523.00	645.00	789.00	221.00	731.00
Sm	142.00	127.00	6.02	275.00	257.00	96.50	23.50	26.30	59.70	149.00	137.00	4.61	141.50	77.10	96.20	125.50	37.80	327.00
Eu	38.00	33.00	2.01	66.70	80.10	26.90	6.97	7.63	15.95	39.50	36.70	1.60	40.20	14.90	25.30	33.60	9.56	106.50
Gd	144.50	126.00	7.10	262.00	307.00	99.70	25.90	28.00	66.70	246.00	209.00	5.81	189.00	77.90	97.70	130.50	33.70	329.00
Tb	17.25	16.20	1.43	29.00	43.80	10.20	3.91	3.69	8.95	16.95	23.30	1.31	29.60	8.30	12.50	16.30	4.18	57.40
Dy	79.40	82.50	9.54	118.00	222.00	40.30	21.30	18.05	49.30	59.40	117.50	9.41	181.50	35.30	64.40	88.10	18.40	342.00
Ho	15.10	17.05	2.19	21.10	43.30	7.11	4.27	3.55	10.70	9.75	23.40	2.42	37.30	6.70	13.20	18.70	3.28	66.40
Er	42.50	51.20	7.12	58.90	117.50	19.25	12.15	10.10	32.20	31.00	66.30	8.02	105.00	20.40	39.60	56.00	9.18	171.50
Tm	5.51	7.45	1.08	7.57	15.25	2.13	1.79	1.39	4.78	2.85	8.15	1.52	15.70	2.55	5.44	8.02	1.10	24.30
Yb	31.50	44.10	6.31	44.20	81.90	11.45	10.20	7.93	28.80	18.00	45.30	9.79	98.30	15.75	30.90	48.30	6.71	142.50
Lu	4.22	5.98	0.89	5.97	9.81	1.52	1.36	1.07	3.98	2.42	6.35	1.57	13.10	2.01	3.74	5.95	0.86	17.95
Y	377.00	452.00	65.60	472.00	1195.00	176.50	113.50	94.70	294.00	265.00	622.00	78.20	1020.00	212.00	379.00	540.00	86.90	1770.00
La/Yb	53.65	26.08	5.34	53.62	39.56	119.65	18.19	33.80	29.86	566.67	107.28	2.37	37.13	57.40	34.14	30.23	38.45	8.11

Appendix 2 b) Trace elements analysis of samples collected by Etruscan and NRE and used in this study

Sample No.	ERN15671	ERN15672	ERN15673	ERN15674	ERN15675	ERN15676	ERN15677	ERN15678	ERN15679	ERN15680	ERN15681	ERN15682	ERN15683	ERN15684	ERN15685	ERN15686	ERN15687	ERN15688
Ba	326.00	726.00	436.00	1080.00	89.20	141.00	113.50	109.50	326.00	195.50	397.00	725.00	248.00	93.10	688.00	304.00	50.90	188.50
Ga	23.20	22.70	15.80	25.90	17.70	17.90	12.70	12.80	9.80	12.10	17.50	26.30	11.60	15.00	15.50	15.50	3.80	13.80
Hf	6.20	7.40	3.50	6.70	2.70	1.10	7.00	1.40	1.90	2.60	2.30	1.80	1.90	2.10	4.90	3.30	0.50	2.00
Nb	547.00	563.00	532.00	122.50	252.00	123.00	514.00	281.00	133.50	215.00	819.00	73.90	101.50	276.00	360.00	227.00	7.10	39.20
Rb	5.90	64.10	4.90	193.00	10.10	2.70	7.60	5.60	1.00	26.50	6.90	26.40	25.40	6.30	19.00	5.00	6.40	14.30
Sr	2500.00	4770.00	3550.00	259.00	189.50	2850.00	1765.00	3700.00	7030.00	1720.00	10000.00	1555.00	6700.00	1065.00	2290.00	4280.00	293.00	3140.00
Ta	7.00	4.50	4.40	5.80	0.60	0.70	6.20	2.40	3.50	6.80	7.00	0.90	1.90	8.20	8.10	1.10	0.10	0.50
Th	986.00	64.60	435.00	18.05	40.80	169.50	1000.00	37.80	94.30	40.60	80.90	379.00	133.50	144.50	1000.00	138.00	1.94	295.00
U	31.50	42.90	26.20	11.70	1.93	33.00	38.40	22.60	15.65	5.06	34.70	9.59	15.45	13.40	59.20	26.50	1.17	11.95
Zr	282.00	623.00	90.00	317.00	104.00	26.00	145.00	58.00	90.00	158.00	144.00	23.00	74.00	69.00	31.00	177.00	17.00	37.00
La	901.00	1255.00	1560.00	126.00	30.30	1940.00	1320.00	896.00	647.00	705.00	1420.00	2850.00	868.00	1010.00	992.00	1325.00	26.30	1560.00
Ce	1660.00	1985.00	2550.00	229.00	57.40	3080.00	2100.00	1450.00	1220.00	1270.00	2290.00	4420.00	1550.00	1715.00	1680.00	2240.00	44.70	2270.00
Pr	181.00	191.00	257.00	25.70	6.54	294.00	206.00	147.00	138.50	139.50	231.00	411.00	165.50	183.00	181.50	230.00	5.19	214.00
Nd	628.00	623.00	851.00	99.70	25.60	983.00	693.00	481.00	496.00	481.00	769.00	1290.00	554.00	615.00	647.00	776.00	20.30	670.00
Sm	157.50	84.40	162.00	19.65	6.56	150.50	252.00	73.30	85.20	75.60	109.50	180.00	83.40	105.50	165.00	122.00	4.98	95.90
Eu	71.40	21.90	54.00	5.29	2.15	39.00	131.50	19.85	24.90	19.80	29.30	47.00	22.50	30.50	68.00	29.90	2.73	26.90
Gd	281.00	89.50	213.00	18.05	10.45	159.00	457.00	76.70	83.40	72.50	111.50	227.00	86.60	111.00	281.00	117.00	5.55	109.50
Tb	55.60	9.14	33.00	2.47	2.96	19.30	82.70	9.40	11.15	8.56	12.25	31.80	11.30	16.10	79.00	12.55	0.91	14.20
Dy	322.00	35.90	175.50	11.35	23.50	94.90	428.00	44.00	56.00	38.10	54.50	192.00	60.40	85.90	586.00	50.80	5.55	79.40
Ho	57.50	6.49	33.50	2.06	5.16	18.85	71.90	7.90	11.10	7.12	10.70	43.00	12.70	16.75	118.00	9.78	1.20	16.90
Er	137.00	18.70	85.00	5.52	13.40	55.20	161.50	21.00	31.40	20.30	31.30	123.50	37.90	45.10	285.00	33.10	3.54	49.70
Tm	17.95	2.00	10.85	0.66	1.81	7.21	19.75	2.36	4.23	2.49	3.61	16.25	5.21	5.63	35.80	5.12	0.59	6.84
Yb	98.50	11.45	60.60	3.78	10.10	40.00	103.50	12.50	25.10	14.55	19.95	86.90	29.80	29.40	176.00	34.80	4.11	39.90
Lu	12.05	1.38	7.08	0.52	1.34	4.77	11.70	1.49	3.16	1.82	2.45	9.73	3.60	3.52	19.90	4.63	0.64	4.93
Y	1415.00	175.00	805.00	54.30	139.50	493.00	1650.00	191.00	318.00	205.00	294.00	1190.00	381.00	475.00	3170.00	269.00	36.70	505.00
La/Yb	9.15	109.61	25.74	33.33	3.00	48.50	12.75	71.68	25.78	48.45	71.18	32.80	29.13	34.35	5.64	38.07	6.40	39.10

Appendix 2 b) Trace elements analysis of samples collected by Etruscan and NRE and used in this study

Sample No.	ERN15689	ERN15690	ERN15691	ERN15692	ERN15693	ERN15694	ERN15695	ERN15696	ERN15697	ERN15698	ERN15699	ERN15700	ERN15701	ERN15702	ERN15703	ERN15704	ERN15705	ERN15706
Ba	79.60	699.00	647.00	83.50	1265.00	646.00	432.00	191.50	36.80	17.60	18.00	14.00	68.10	142.00	54.40	92.10	133.50	59.10
Ga	11.30	12.80	32.40	9.00	16.80	20.10	14.20	18.70	4.30	5.20	1.20	5.10	5.30	6.60	20.10	23.00	4.70	2.10
Hf	1.40	1.60	4.90	0.80	8.40	58.00	3.30	2.70	6.80	2.60	0.90	4.80	14.00	0.90	2.00	2.30	0.30	0.20
Nb	4.00	2.80	62.80	18.70	668.00	217.00	58.00	1115.00	86.20	44.20	5.30	69.80	70.00	370.00	85.80	70.00	5.10	1.80
Rb	0.40	0.60	51.70	0.80	4.70	15.80	63.20	9.80	1.10	5.00	0.60	0.90	3.00	2.60	6.80	8.70	9.60	1.90
Sr	4960.00	870.00	471.00	5410.00	4590.00	966.00	269.00	4950.00	552.00	302.00	240.00	344.00	256.00	3220.00	1945.00	1570.00	97.30	149.00
Ta	0.50	0.30	1.00	0.30	5.10	1.70	0.50	6.50	0.20	0.20	0.05	0.30	3.40	7.80	1.20	0.70	0.10	0.10
Th	625.00	823.00	401.00	154.00	1000.00	49.00	13.20	80.80	104.00	59.90	11.30	35.10	5000.00	215.00	417.00	434.00	6.98	2.59
U	8.98	16.05	7.72	2.29	44.90	21.90	1.19	69.50	45.50	12.00	2.26	21.20	36.80	10.65	6.92	5.40	1.28	1.99
Zr	9.00	34.00	161.00	12.00	205.00	2770.00	156.00	169.00	1010.00	243.00	77.00	461.00	180.00	70.00	60.00	45.00	12.00	6.00
La	1085.00	663.00	2180.00	94.80	1085.00	798.00	6.10	961.00	8.90	5.10	5.60	26.20	225.00	487.00	2820.00	2870.00	30.90	20.80
Ce	1680.00	996.00	3520.00	152.50	1840.00	1575.00	13.10	1665.00	24.60	18.20	13.70	57.00	450.00	965.00	4760.00	4560.00	56.60	38.10
Pr	163.00	94.10	343.00	15.60	192.50	174.50	1.66	173.50	4.00	3.51	1.95	7.17	56.00	107.00	455.00	420.00	6.17	4.26
Nd	521.00	293.00	1140.00	65.60	763.00	606.00	7.40	569.00	21.40	21.50	9.00	30.00	246.00	406.00	1480.00	1340.00	23.70	17.00
Sm	102.00	57.80	182.50	52.10	495.00	92.40	4.42	78.50	12.60	16.40	6.82	8.83	607.00	73.30	183.50	169.50	5.46	4.40
Eu	33.50	21.40	48.60	19.15	158.50	27.30	3.01	22.90	4.45	7.59	2.98	3.00	414.00	27.80	47.90	52.20	2.36	2.51
Gd	131.00	90.90	191.00	54.50	445.00	92.10	9.29	85.70	19.65	35.80	9.61	14.35	1355.00	78.20	207.00	220.00	6.57	5.40
Tb	25.20	20.00	24.30	11.05	68.50	10.90	2.37	10.30	4.85	9.83	1.79	3.48	331.00	13.60	32.40	41.00	1.25	1.13
Dy	177.00	152.50	136.50	69.60	350.00	47.40	17.15	50.20	33.70	64.70	10.30	24.10	1985.00	76.80	177.00	248.00	7.92	7.31
Ho	41.30	36.00	30.30	13.80	58.80	8.63	3.72	10.25	7.01	11.85	1.95	4.92	378.00	14.95	34.40	50.10	1.70	1.61
Er	131.50	106.50	97.70	38.90	136.50	25.50	11.00	31.10	21.90	28.30	5.25	14.35	951.00	42.30	95.50	139.00	5.14	5.08
Tm	23.10	17.00	15.45	6.26	17.95	2.87	1.62	3.82	3.59	3.49	0.74	2.37	126.00	5.44	11.90	18.15	0.72	0.76
Yb	149.00	102.50	98.00	41.00	103.50	17.10	10.10	21.90	26.10	20.50	5.08	16.70	689.00	33.00	73.70	111.00	4.95	5.31
Lu	19.70	13.10	12.65	5.68	12.60	2.34	1.42	2.84	4.10	2.96	0.76	2.65	86.40	4.30	9.87	14.85	0.70	0.80
Y	1205.00	1070.00	874.00	354.00	1560.00	202.00	97.50	265.00	183.00	269.00	48.30	119.50	9700.00	408.00	937.00	1390.00	51.90	49.00
La/Yb	7.28	6.47	22.24	2.31	10.48	46.67	0.60	43.88	0.34	0.25	1.10	1.57	0.33	14.76	38.26	25.86	6.24	3.92

Appendix 2 b) Trace elements analysis of samples collected by Etruscan and NRE and used in this study

Sample No.	ERNI 5707	ERNI 5708	ERNI 5709	ERNI 5710	ERNI 5711	ERNI 5712	ERNI 5713	ERNI 5714	ERNI 5715	ERNI 5716	ERNI 5717	ERNI 5718	ERNI 5719	ERNI 5720	ERNI 5721	ERNI 5722	ERNI 5723	ERNI 5724
Ba	48.10	280.00	255.00	1145.00	4060.00	325.00	144.50	63.90	126.50	228.00	215.00	783.00	198.50	518.00	845.00	692.00	124.00	132.00
Ga	1.60	11.20	10.10	8.30	8.50	13.60	22.60	13.90	18.80	23.50	23.50	8.90	22.40	23.10	20.50	14.70	14.40	6.60
Hf	0.30	4.30	1.60	1.70	2.30	1.10	2.30	8.90	7.90	4.90	4.30	1.00	4.60	1.50	8.80	2.80	2.60	0.70
Nb	2.50	651.00	78.10	44.80	116.00	20.80	9.00	198.00	237.00	106.50	105.00	7.30	30.20	12.40	87.80	329.00	564.00	19.80
Rb	2.50	8.40	2.10	12.60	21.70	31.20	100.50	4.70	3.30	3.90	3.50	15.80	1.90	9.10	208.00	10.60	17.20	10.00
Sr	168.50	2750.00	1595.00	1075.00	1370.00	772.00	71.00	1515.00	3970.00	873.00	933.00	388.00	1040.00	563.00	185.00	10000.00	4320.00	1400.00
Ta	5.40	10.40	2.00	2.50	1.40	2.50	4.30	7.60	2.10	6.20	2.30	1.30	0.30	0.40	5.60	1.70	2.40	0.80
Th	0.58	265.00	56.30	27.70	27.50	623.00	13.05	819.00	451.00	279.00	299.00	119.00	294.00	673.00	9.68	56.80	68.00	625.00
U	0.24	31.50	4.25	12.80	11.40	40.00	2.15	29.50	21.90	8.67	8.48	3.71	14.00	13.30	21.50	24.10	25.30	1.73
Zr	6.00	326.00	76.00	52.00	108.00	41.00	41.00	279.00	611.00	231.00	203.00	40.00	197.00	22.00	385.00	108.00	170.00	12.00
La	38.50	597.00	851.00	908.00	887.00	633.00	10.90	1310.00	2250.00	1650.00	1850.00	167.50	2740.00	3100.00	73.30	1250.00	1480.00	441.00
Ce	94.80	1125.00	1280.00	1340.00	1310.00	1245.00	18.60	2190.00	3040.00	2750.00	3030.00	332.00	4610.00	5060.00	146.50	2220.00	2330.00	771.00
Pr	13.75	117.00	120.50	122.50	121.00	181.50	2.15	220.00	261.00	262.00	287.00	45.50	440.00	488.00	18.00	224.00	214.00	83.20
Nd	68.90	422.00	393.00	410.00	408.00	1230.00	9.00	819.00	814.00	845.00	945.00	248.00	1450.00	1595.00	72.40	775.00	689.00	385.00
Sm	20.10	62.00	58.20	59.80	59.60	403.00	3.28	269.00	137.50	104.50	114.50	71.10	180.00	224.00	13.10	108.00	89.00	222.00
Eu	6.68	18.10	17.95	18.65	18.35	81.10	0.65	74.00	46.60	29.00	30.90	15.95	44.60	61.70	3.99	29.60	25.90	69.10
Gd	21.70	65.30	62.90	63.20	62.20	210.00	4.26	283.00	160.50	113.00	120.50	49.40	183.50	248.00	12.15	106.00	99.10	189.50
Tb	3.94	11.00	8.12	7.63	7.59	21.80	0.89	37.80	19.85	14.40	15.25	7.46	22.30	37.40	1.65	12.05	12.65	23.50
Dy	23.70	73.80	38.90	35.80	33.60	70.60	5.54	166.50	89.80	81.10	84.30	37.40	104.50	218.00	7.29	50.80	61.70	84.90
Ho	5.20	17.40	7.33	7.71	6.59	10.95	1.09	27.60	15.90	18.60	19.35	7.13	21.10	47.30	1.33	9.23	11.45	10.75
Er	15.20	57.60	21.60	27.50	20.40	33.60	3.25	71.10	42.90	63.30	66.70	20.90	68.40	147.00	3.58	27.10	31.70	21.80
Tm	2.16	8.58	2.79	4.03	2.62	4.32	0.48	8.61	5.07	9.41	9.83	2.85	9.28	20.10	0.41	3.09	3.53	2.14
Yb	13.75	57.80	17.70	26.20	16.80	34.00	3.27	55.20	31.40	61.10	63.30	18.70	62.60	122.50	2.56	18.35	19.90	13.85
Lu	1.85	7.77	2.31	3.39	2.27	5.14	0.46	7.39	4.05	8.19	8.56	2.59	8.84	16.35	0.34	2.30	2.38	1.72
Y	162.50	525.00	214.00	235.00	202.00	332.00	31.30	757.00	473.00	581.00	627.00	230.00	666.00	1345.00	36.70	249.00	281.00	250.00
La/Yb	2.80	10.33	48.08	34.66	52.80	18.62	3.33	23.73	71.66	27.00	29.23	8.96	43.77	25.31	28.63	68.12	74.37	31.84

Appendix 2 b) Trace elements analysis of samples collected by Etruscan and NRE and used in this study

Sample No.	ERNI 5725	ERNI 5726	ERNI 5727	ERNI 5728	ERNI 5729	ERNI 5730	ERNI 5731	ERNI 5732	ERNI 5733	ERNI 5734	ERNI 5735	ERNI 5736	ERNI 5737	ERNI 5738	ERNI 5739	ERNI 5740	ERNI 5741	ERNI 5742
Ba	33.80	310.00	43.60	267.00	121.50	130.00	315.00	800.00	28.80	35.80	460.00	257.00	134.50	406.00	734.00	2490.00	1335.00	1440.00
Ga	10.40	18.60	20.80	19.00	12.10	12.40	11.10	31.50	1.70	14.20	12.30	4.30	3.40	5.00	44.30	12.50	12.40	6.60
Hf	0.50	0.70	0.60	0.40	1.20	1.10	3.30	8.70	0.70	14.00	1.00	0.40	0.40	6.20	2.00	1.00	2.10	0.50
Nb	291.00	238.00	73.70	22.20	332.00	228.00	222.00	74.20	10.20	76.70	6.50	1.20	1.10	1035.00	11.00	125.50	10.00	3.50
Rb	0.20	0.90	6.40	1.40	4.00	4.60	8.00	7.60	2.40	1.10	2.10	3.40	3.10	2.60	16.00	21.80	13.20	1.90
Sr	4100.00	2840.00	769.00	1280.00	5030.00	5960.00	6800.00	9080.00	442.00	194.00	661.00	1795.00	1350.00	226.00	800.00	2620.00	1375.00	4510.00
Ta	1.70	1.10	0.40	0.10	1.30	1.30	2.90	1.40	0.30	1.90	0.10	0.10	0.05	2.50	0.25	0.40	0.20	0.20
Th	48.30	27.60	337.00	487.00	197.50	116.50	40.50	1000.00	32.30	101.50	44.10	8.72	12.70	10.20	282.00	251.00	111.00	4.17
U	5.02	15.95	5.60	9.45	33.30	22.80	21.60	8.35	1.33	14.55	3.33	1.11	1.43	35.30	3.70	9.22	2.88	1.74
Zr	37.00	43.00	5.00	5.00	33.00	47.00	333.00	124.00	56.00	1210.00	56.00	21.00	16.00	422.00	90.00	36.00	56.00	5.00
La	1470.00	2770.00	2870.00	2070.00	1365.00	1375.00	924.00	3970.00	56.30	224.00	1620.00	384.00	216.00	43.60	8030.00	1455.00	880.00	439.00
Ce	2200.00	4190.00	4630.00	3370.00	2180.00	2250.00	1735.00	6380.00	97.50	408.00	2390.00	561.00	405.00	67.20	10550.00	2200.00	1900.00	988.00
Pr	190.00	365.00	427.00	327.00	202.00	208.00	177.50	599.00	10.40	41.90	204.00	47.80	40.80	6.21	928.00	192.50	226.00	115.50
Nd	567.00	1090.00	1290.00	1145.00	633.00	659.00	586.00	2050.00	39.00	145.50	586.00	138.50	139.00	19.80	2510.00	584.00	908.00	447.00
Sm	63.60	124.00	152.00	364.00	83.70	89.70	80.20	565.00	12.45	38.70	66.30	17.10	24.10	4.38	327.00	85.10	198.50	98.50
Eu	18.50	33.70	37.00	90.90	28.70	29.10	23.40	250.00	4.68	11.40	15.75	4.90	6.83	1.60	93.00	30.40	63.50	34.90
Gd	77.30	138.00	172.50	255.00	104.50	109.00	81.90	818.00	20.10	50.50	82.40	22.40	27.60	5.66	404.00	112.50	186.50	103.50
Tb	8.37	13.25	19.25	19.80	15.00	14.80	8.90	117.50	4.03	8.78	7.71	3.19	4.14	1.10	34.90	16.75	24.50	14.15
Dy	37.30	50.70	91.10	47.70	78.60	74.90	36.40	506.00	23.40	49.40	29.80	19.25	23.40	7.29	120.50	104.00	106.50	64.40
Ho	6.95	8.85	18.10	5.85	14.80	13.80	6.50	73.30	4.24	9.66	5.80	4.38	5.05	1.62	22.00	23.00	17.55	11.10
Er	21.30	27.00	56.30	17.95	41.70	37.20	19.45	167.50	11.20	29.60	20.00	15.55	16.60	4.96	68.60	73.20	46.10	30.40
Tm	2.56	2.85	6.96	1.86	5.19	4.30	2.20	18.20	1.43	4.48	2.74	2.59	2.62	0.71	7.36	10.65	5.29	3.93
Yb	16.05	17.25	41.30	16.40	31.50	24.80	13.00	101.50	8.31	31.30	19.90	19.20	18.65	5.06	45.30	67.40	33.70	26.00
Lu	2.06	2.22	5.14	2.26	4.06	3.09	1.76	12.25	1.07	4.46	2.92	2.89	2.65	0.73	6.34	9.00	4.49	3.63
Y	202.00	247.00	552.00	146.50	399.00	358.00	169.50	1715.00	109.00	262.00	170.00	124.00	159.00	42.60	622.00	674.00	455.00	252.00
La/Yb	91.59	160.58	69.49	126.22	43.33	55.44	71.08	39.11	6.77	7.16	81.41	20.00	11.58	8.62	177.26	21.59	26.11	16.88

Appendix 2 b) Trace elements analysis of samples collected by Etruscan and NRE and used in this study

Sample No.	ERN15743	ERN15744	ERN15745	ERN15746	ERN15747	ERN15748	ERN15749	ERN15750	ERN15751	ERN15752	ERN15753	ERN15754	ERN15755	ERN15756	ERN15757	ERN15758	ERN15759	ERN15760
Ba	322.00	415.00	153.50	134.50	108.00	470.00	235.00	362.00	348.00	241.00	351.00	114.00	68.70	2100.00	258.00	124.00	665.00	257.00
Ga	19.60	10.30	6.60	13.30	16.00	14.00	22.80	23.00	21.10	24.60	23.60	28.00	36.10	16.50	25.40	12.50	16.90	8.50
Hf	3.10	5.50	1.80	34.00	2.80	9.10	8.80	16.20	9.80	9.20	2.60	1.70	2.20	5.40	0.80	0.50	5.40	2.00
Nb	206.00	197.00	231.00	424.00	148.00	170.50	458.00	324.00	621.00	1275.00	92.70	28.00	6.90	349.00	23.70	11.70	556.00	321.00
Rb	15.20	7.20	12.00	3.00	7.30	18.20	19.90	35.00	5.00	10.00	4.00	15.10	2.30	45.70	1.20	5.80	23.90	3.10
Sr	4020.00	5360.00	2640.00	410.00	2580.00	2870.00	2500.00	3780.00	6230.00	4880.00	6660.00	614.00	2640.00	5430.00	2850.00	472.00	2590.00	2460.00
Ta	1.80	3.60	2.80	8.00	2.20	2.70	4.40	3.40	6.10	14.00	1.30	0.60	0.50	5.10	0.30	0.50	5.10	1.60
Th	933.00	468.00	499.00	1640.00	724.00	261.00	326.00	646.00	768.00	160.50	619.00	509.00	713.00	519.00	812.00	432.00	398.00	315.00
U	21.10	9.56	10.80	43.50	4.98	23.00	22.60	25.50	39.60	81.40	26.50	7.90	10.15	16.30	8.46	5.61	37.10	59.50
Zr	43.00	382.00	78.00	1080.00	13.00	351.00	437.00	665.00	387.00	487.00	97.00	10.00	12.00	197.00	10.00	7.00	379.00	69.00
La	1950.00	732.00	425.00	250.00	1155.00	1330.00	1180.00	2100.00	2250.00	1210.00	2840.00	3750.00	4930.00	551.00	4560.00	1775.00	958.00	757.00
Ce	3470.00	1415.00	802.00	450.00	2360.00	2240.00	1930.00	3370.00	3700.00	2060.00	4270.00	6160.00	8080.00	957.00	5960.00	2490.00	1670.00	1410.00
Pr	341.00	153.00	83.00	53.00	259.00	215.00	177.00	317.00	343.00	197.50	369.00	571.00	735.00	97.10	459.00	213.00	162.50	141.00
Nd	1145.00	558.00	295.00	220.00	948.00	710.00	571.00	1045.00	1145.00	644.00	1135.00	1840.00	2250.00	332.00	1225.00	623.00	545.00	489.00
Sm	169.00	100.00	55.70	583.00	147.50	110.50	94.00	210.00	219.00	96.00	146.50	243.00	291.00	78.00	120.50	76.00	116.00	127.00
Eu	62.20	38.80	22.30	524.00	54.60	36.20	33.80	70.70	76.70	31.40	47.50	76.60	89.10	39.50	34.90	24.10	47.30	47.20
Gd	253.00	139.50	87.90	1910.00	223.00	131.00	126.00	259.00	288.00	118.50	199.00	298.00	367.00	148.00	181.50	95.10	158.50	127.50
Tb	52.60	31.60	19.50	547.00	60.40	20.10	18.95	37.90	46.90	17.95	27.20	44.40	58.00	35.30	21.90	12.20	26.00	15.65
Dy	352.00	214.00	128.00	3730.00	434.00	117.50	90.60	183.50	254.00	99.80	145.50	266.00	343.00	230.00	115.50	65.40	138.50	66.80
Ho	74.20	44.10	25.80	790.00	88.80	23.70	14.95	31.10	45.50	18.75	28.90	55.60	69.40	44.40	22.20	13.80	24.90	11.45
Er	217.00	124.50	73.00	2150.00	244.00	67.80	41.60	81.90	120.00	50.30	83.10	174.00	200.00	115.50	65.40	43.60	66.30	33.40
Tm	29.20	15.45	9.86	303.00	32.30	8.43	5.62	9.79	14.25	5.84	10.35	24.50	25.70	14.45	8.12	5.88	8.09	4.70
Yb	169.00	82.00	59.20	1655.00	190.00	47.40	37.90	59.40	78.70	32.10	61.70	153.50	148.50	78.10	50.30	36.90	48.10	34.00
Lu	21.00	9.81	7.62	219.00	24.80	5.73	5.13	7.70	9.54	3.87	7.68	20.40	18.80	9.46	6.65	4.81	6.06	4.77
Y	2180.00	1285.00	692.00	20600.00	2490.00	661.00	362.00	806.00	1195.00	479.00	810.00	1600.00	2010.00	1205.00	622.00	448.00	623.00	395.00
La/Yb	11.54	8.93	7.18	0.15	6.08	28.06	31.13	35.35	28.59	37.69	46.03	24.43	33.20	7.06	90.66	48.10	19.92	22.26

Appendix 2 b) Trace elements analysis of samples collected by Etruscan and NRE and used in this study

Sample No.	ERN15761	ERN15762	ERN15763	ERN15764	ERN15765	ERN15766	ERN15767	ERN15768	ERN15769	ERN15770	ERN15771	ERN15772	ERN15773	ERN15774	ERN15775	ERN15776	ERN15777	ERN15778
Ba	111.00	2060.00	439.00	49.50	21.70	110.50	88.70	181.50	103.50	78.10	202.00	708.00	339.00	208.00	434.00	1505.00	651.00	3570.00
Ga	17.80	12.20	20.20	5.70	13.60	34.70	16.50	12.30	2.70	7.20	10.00	14.40	10.30	16.60	13.90	15.00	21.60	12.80
Hf	7.70	2.70	22.80	3.50	8.70	2.60	2.50	21.00	7.90	2.50	4.00	2.10	4.00	2.30	20.30	13.80	2.70	2.20
Nb	208.00	705.00	119.00	30.70	78.80	79.40	3.10	116.00	5.20	504.00	949.00	235.00	70.10	399.00	725.00	1010.00	234.00	178.00
Rb	10.60	0.90	91.20	5.30	1.90	4.00	2.40	3.00	0.80	0.40	2.60	28.50	106.50	2.30	6.30	0.50	11.80	26.40
Sr	3050.00	10000.00	115.50	214.00	133.00	1405.00	4120.00	696.00	586.00	5930.00	5650.00	8920.00	589.00	2430.00	4120.00	4790.00	4620.00	10000.00
Ta	1.50	2.70	2.80	0.40	1.60	0.90	0.60	4.10	1.80	7.90	10.30	3.20	3.00	4.00	9.60	9.50	2.00	1.50
Th	390.00	237.00	159.00	25.40	39.90	625.00	686.00	5000.00	960.00	597.00	956.00	177.50	29.60	233.00	291.00	173.00	168.50	134.00
U	6.62	4.30	37.60	3.41	7.14	2.60	0.95	69.00	23.60	17.65	27.40	6.80	6.54	16.25	50.60	38.20	28.30	12.30
Zr	173.00	223.00	2180.00	224.00	574.00	63.00	11.00	960.00	75.00	80.00	90.00	81.00	223.00	122.00	784.00	532.00	111.00	124.00
La	1325.00	881.00	242.00	35.00	31.40	3240.00	1245.00	632.00	74.10	489.00	505.00	535.00	45.10	1305.00	879.00	866.00	1770.00	809.00
Ce	2140.00	1530.00	406.00	66.60	63.70	5130.00	2190.00	1200.00	137.00	963.00	990.00	996.00	89.50	2200.00	1510.00	1555.00	2830.00	1185.00
Pr	208.00	173.50	51.10	7.51	7.71	551.00	256.00	149.00	16.60	108.00	112.50	107.50	10.40	219.00	153.00	158.50	262.00	111.50
Nd	658.00	545.00	176.00	26.80	27.30	1600.00	815.00	631.00	73.80	377.00	403.00	361.00	38.90	704.00	488.00	513.00	827.00	345.00
Sm	115.00	88.20	46.00	10.40	9.28	229.00	121.50	938.00	175.50	63.30	73.80	54.50	7.66	104.50	83.40	79.90	112.50	51.30
Eu	38.10	32.10	14.00	3.22	2.53	77.70	47.00	551.00	133.50	24.50	33.50	16.40	3.35	35.20	30.00	27.80	33.80	16.45
Gd	156.00	116.50	64.60	11.40	11.85	284.00	204.00	1805.00	433.00	80.80	104.00	56.70	8.38	126.50	108.50	98.90	130.50	57.60
Tb	28.90	21.50	14.45	2.00	2.41	44.10	52.70	421.00	116.50	19.40	28.00	8.30	1.47	19.35	20.60	16.95	17.85	7.42
Dy	174.50	120.50	95.40	11.15	15.05	241.00	349.00	2610.00	780.00	154.50	227.00	45.90	8.52	109.50	131.50	97.20	94.10	39.00
Ho	34.90	24.10	22.80	2.30	3.34	53.40	74.80	511.00	162.00	38.60	55.60	10.35	1.76	22.60	27.40	19.45	19.60	8.23
Er	92.20	59.90	69.50	6.22	9.75	152.50	196.50	1390.00	438.00	118.00	174.50	32.00	5.74	64.60	74.70	54.80	57.40	24.30
Tm	11.10	7.88	12.80	1.04	1.80	22.70	29.50	178.50	60.50	17.40	27.00	4.35	0.88	8.10	9.29	6.88	7.19	3.16
Yb	59.40	39.50	79.80	6.60	12.00	129.00	165.50	978.00	325.00	98.10	157.00	25.60	5.84	43.40	47.70	38.10	39.00	19.25
Lu	7.60	5.27	12.65	1.04	1.93	18.40	24.00	123.00	42.00	12.40	20.30	3.37	0.82	5.48	5.98	4.93	4.87	2.61
Y	936.00	586.00	570.00	60.00	88.70	1475.00	1635.00	13650.00	4420.00	1140.00	1580.00	313.00	55.10	640.00	751.00	534.00	551.00	237.00
La/Yb	22.31	22.30	3.03	5.30	2.62	25.12	7.52	0.65	0.23	4.98	3.22	20.90	7.72	30.07	18.43	22.73	45.38	42.03

Appendix 2 b) Trace elements analysis of samples collected by Etruscan and NRE and used in this study

Sample No.	ERNI 5779	ERNI 5780	ERNI 5781	ERNI 5782	ERNI 5783	ERNI 5784	ERNI 5785	ERNI 5786	ERNI 5787	ERNI 5788	ERNI 5789	ERNI 5790	ERNI 5791	ERNI 5792	ERNI 5793	ERNI 5794	ERNI 5795	ERNI 5796
Ba	140.50	355.00	850.00	1540.00	206.00	613.00	654.00	408.00	329.00	624.00	191.50	247.00	244.00	14.90	109.00	15.80	288.00	173.50
Ga	18.80	17.80	22.60	30.80	11.00	11.80	14.70	9.70	17.80	34.40	12.10	12.10	24.30	4.60	8.40	1.60	14.10	32.50
Hf	0.90	3.90	2.40	2.50	2.50	3.60	1.30	1.30	3.70	9.80	1.90	2.20	4.80	2.40	2.80	0.50	3.00	2.10
Nb	13.10	166.50	138.50	418.00	282.00	123.00	512.00	216.00	173.00	299.00	1005.00	1135.00	308.00	12.10	18.70	3.50	223.00	13.20
Rb	3.20	6.90	7.20	59.10	0.70	2.40	15.10	20.60	3.50	17.90	2.60	0.80	58.50	9.20	34.20	2.40	10.20	1.60
Sr	867.00	2040.00	2390.00	7730.00	10000.00	1810.00	10000.00	426.00	10000.00	720.00	5430.00	3410.00	1125.00	314.00	169.00	291.00	7870.00	1975.00
Ta	0.40	2.00	0.80	1.90	1.80	1.50	5.60	0.50	1.50	8.80	4.40	5.40	4.40	0.50	0.70	0.10	1.90	0.60
Th	410.00	520.00	181.50	133.50	158.00	113.50	115.50	114.00	947.00	804.00	286.00	393.00	24.00	27.20	25.80	8.22	61.60	562.00
U	3.71	23.80	26.20	21.20	51.50	6.89	14.30	2.72	25.50	61.80	45.10	50.30	5.90	3.12	2.47	0.67	6.95	35.80
Zr	25.00	237.00	133.00	124.00	259.00	112.00	41.00	49.00	101.00	635.00	93.00	118.00	288.00	169.00	132.00	26.00	182.00	8.00
La	828.00	982.00	1430.00	2280.00	721.00	689.00	782.00	13.00	1575.00	1695.00	731.00	772.00	266.00	37.10	59.20	7.20	1170.00	3550.00
Ce	1395.00	1485.00	2410.00	3310.00	1295.00	1290.00	1365.00	28.50	2430.00	2930.00	1385.00	1475.00	463.00	80.10	116.50	16.40	1435.00	5220.00
Pr	162.00	150.50	241.00	289.00	134.50	139.50	139.50	3.76	234.00	287.00	147.50	160.50	48.60	9.25	13.20	2.07	119.50	452.00
Nd	847.00	524.00	781.00	850.00	430.00	464.00	445.00	16.70	724.00	945.00	489.00	538.00	156.00	33.10	48.50	8.20	341.00	1310.00
Sm	353.00	148.00	116.50	104.50	57.30	65.00	58.80	13.30	114.50	149.00	80.00	84.80	22.80	8.51	16.70	4.38	45.60	162.00
Eu	83.40	53.30	33.10	30.60	17.10	18.60	18.75	7.02	39.70	55.80	30.00	34.90	6.87	2.06	4.70	1.78	14.45	47.90
Gd	195.00	188.00	121.50	129.00	63.20	68.20	69.00	21.60	159.00	175.00	101.00	120.50	25.20	10.30	18.00	6.11	57.00	214.00
Tb	19.70	32.30	15.55	14.30	8.77	9.23	10.15	4.29	31.90	27.00	15.45	20.50	3.27	1.80	2.99	1.30	6.67	31.10
Dy	54.70	168.50	72.30	62.10	47.90	44.50	54.40	22.90	211.00	148.50	78.10	106.00	15.50	10.65	15.20	8.11	31.80	205.00
Ho	7.46	30.80	14.55	12.55	10.85	8.80	12.15	4.02	46.00	29.60	14.55	20.10	3.05	2.15	2.69	1.67	6.75	49.80
Er	23.20	76.30	43.60	38.90	34.10	25.40	37.10	10.05	127.50	85.40	38.30	53.00	8.92	6.13	7.04	4.66	21.30	158.50
Tm	2.85	9.54	5.29	4.75	4.89	3.17	5.20	1.40	16.55	11.40	4.50	6.59	1.10	0.91	0.94	0.70	2.81	21.40
Yb	24.40	52.90	29.10	27.70	29.80	18.90	32.10	8.38	85.30	66.80	25.00	38.50	6.56	6.16	6.01	4.47	16.40	112.00
Lu	3.77	6.81	3.61	3.56	3.87	2.52	4.40	1.15	10.40	8.94	3.20	5.17	0.91	0.91	0.83	0.60	2.11	12.80
Y	183.50	732.00	416.00	354.00	304.00	248.00	356.00	104.00	1305.00	809.00	370.00	514.00	80.80	58.20	71.40	45.60	207.00	1500.00
La/Yb	33.93	18.56	49.14	82.31	24.19	36.46	24.36	1.55	18.46	25.37	29.24	20.05	40.55	6.02	9.85	1.61	71.34	31.70

Appendix 2 b) Trace elements analysis of samples collected by Etruscan and NRE and used in this study

Sample No.	ERN15797	ERN15798	ERN15799	ERN15800	ERN15801	ERN15802	ERN15803	ERN15804	ERN15805	ERN15806	ERN15807	ERN15808	ERN15809	ERN15810	ERN15811	ERN15812	ERN15813	ERN15814
Ba	138.50	778.00	293.00	2270.00	302.00	48.20	569.00	974.00	292.00	779.00	483.00	294.00	207.00	311.00	588.00	148.50	114.00	259.00
Ga	24.80	14.70	11.90	18.80	12.30	11.40	16.90	15.00	17.10	21.30	28.30	93.40	30.30	12.20	19.20	14.20	32.10	27.60
Hf	1.20	2.20	1.00	2.00	0.70	0.60	0.80	0.90	0.40	9.20	9.50	1.00	1.00	1.70	5.60	1.00	8.40	4.00
Nb	442.00	161.00	121.00	276.00	150.00	177.00	357.00	961.00	479.00	145.50	623.00	2.00	10.00	58.20	454.00	227.00	3.60	57.40
Rb	1.00	6.40	9.10	33.80	7.20	10.00	0.40	3.30	0.80	20.70	1.20	0.50	2.90	9.70	22.60	0.50	4.20	1.30
Sr	3890.00	5330.00	6230.00	473.00	10000.00	714.00	6630.00	10000.00	514.00	1835.00	8770.00	1745.00	293.00	6080.00	714.00	5710.00	1560.00	745.00
Ta	1.80	2.20	2.30	15.20	1.60	0.70	1.60	4.80	2.30	2.50	10.20	0.25	0.30	0.60	2.90	1.00	1.80	0.80
Th	157.00	384.00	105.00	24.00	24.60	131.00	32.30	22.10	32.30	412.00	44.20	487.00	381.00	31.20	46.90	47.30	1000.00	902.00
U	23.10	16.60	45.00	8.26	21.40	9.52	18.20	53.80	55.40	31.60	25.20	11.90	7.64	11.60	19.60	39.80	12.75	7.21
Zr	37.00	53.00	23.00	130.00	65.00	13.00	59.00	76.00	18.00	309.00	686.00	20.00	5.00	103.00	415.00	59.00	15.00	83.00
La	3000.00	1055.00	694.00	286.00	758.00	1140.00	1400.00	1045.00	1555.00	792.00	1125.00	9640.00	3260.00	1265.00	1590.00	1070.00	3120.00	2760.00
Ce	4280.00	1810.00	1290.00	525.00	1365.00	1615.00	2410.00	1875.00	2710.00	1255.00	2120.00	15100.00	5270.00	1665.00	2110.00	2010.00	4950.00	4180.00
Pr	360.00	183.50	137.00	55.40	142.50	142.50	238.00	193.00	277.00	122.00	225.00	1405.00	484.00	145.00	187.50	210.00	466.00	378.00
Nd	1080.00	616.00	474.00	191.50	479.00	423.00	779.00	656.00	932.00	403.00	796.00	4250.00	1565.00	447.00	594.00	719.00	1565.00	1225.00
Sm	126.50	96.30	68.20	27.00	63.80	49.50	93.60	88.10	123.00	75.30	121.50	460.00	212.00	63.70	90.40	90.40	303.00	188.00
Eu	33.30	35.30	20.00	7.45	17.80	15.70	24.50	25.10	30.20	29.40	33.30	114.00	54.80	19.65	29.60	23.50	146.00	69.70
Gd	140.50	123.00	68.80	26.10	60.90	61.20	93.80	87.20	113.00	99.80	109.50	516.00	220.00	72.10	97.50	85.90	582.00	268.00
Tb	14.55	23.30	9.40	3.09	7.07	8.60	9.84	10.05	11.05	19.00	13.70	52.50	25.00	8.94	11.60	9.43	144.00	43.70
Dy	63.00	140.50	48.50	13.40	27.70	54.90	36.40	39.20	34.50	114.00	58.80	187.00	102.50	41.60	51.30	37.20	880.00	231.00
Ho	13.25	28.00	9.89	2.48	4.94	12.80	6.69	6.72	5.52	21.60	11.10	41.00	20.50	8.11	9.67	7.34	157.50	43.10
Er	44.30	77.90	29.40	7.49	15.15	40.80	22.20	19.15	17.80	55.30	32.50	127.50	71.90	23.80	27.70	24.30	374.00	116.00
Tm	5.98	10.25	3.76	0.86	1.57	5.86	2.54	1.78	1.53	6.64	3.76	17.05	11.05	2.91	3.22	2.79	45.80	14.70
Yb	35.30	53.10	19.50	4.93	8.58	31.40	15.00	8.85	8.10	32.40	19.90	92.10	73.00	15.65	17.20	14.80	221.00	76.30
Lu	4.96	7.13	2.72	0.70	1.23	4.30	2.09	1.10	1.02	4.25	2.76	12.25	11.50	2.20	2.34	1.90	29.80	10.25
Y	338.00	682.00	271.00	62.30	124.50	346.00	179.00	159.50	132.50	524.00	261.00	1140.00	508.00	228.00	243.00	207.00	3890.00	1110.00
La/Yb	84.99	19.87	35.59	58.01	88.34	36.31	93.33	118.08	191.98	24.44	56.53	104.67	44.66	80.83	92.44	72.30	14.12	36.17

Appendix 2 b) Trace elements analysis of samples collected by Etruscan and NRE and used in this study

Sample No.	ERNI S815	ERNI S816	ERNI S817	ERNI S818	ERNI S819	ERNI S820	ERNI S821	ERNI S822	ERNI S823	ERNI S824	ERNI S825	ERNI S826	ERNI S827	ERNI S828	ERNI S829	ERNI S830	ERNI S831	ERNI S832
Ba	708.00	334.00	5470.00	144.00	211.00	318.00	165.00	135.50	89.20	252.00	627.00	1345.00	300.00	809.00	43.70	234.00	447.00	1120.00
Ga	13.10	15.30	26.20	65.40	3.80	16.20	6.60	14.90	1.70	12.90	14.50	22.40	45.20	18.40	25.00	4.30	21.20	12.90
Hf	7.20	8.20	1.10	1.00	0.10	9.40	5.70	8.90	0.20	1.30	1.00	6.40	1.50	11.00	1.70	0.60	9.70	4.70
Nb	62.80	522.00	597.00	6.00	1.00	726.00	727.00	530.00	2.80	521.00	68.10	217.00	18.30	310.00	11.40	10.50	266.00	242.00
Rb	2.80	84.40	232.00	1.00	8.50	12.40	29.20	7.20	1.90	6.80	11.90	85.90	27.20	70.30	18.00	9.80	16.20	0.50
Sr	1175.00	395.00	591.00	3670.00	161.50	8120.00	396.00	367.00	195.00	3250.00	3750.00	1050.00	75.00	2350.00	383.00	521.00	2700.00	7540.00
Ta	2.00	1.10	17.50	0.25	0.10	9.20	1.20	2.90	0.05	5.40	0.90	4.50	0.40	4.10	0.40	0.40	3.00	4.70
Th	1000.00	171.00	278.00	1745.00	9.58	296.00	65.90	1000.00	4.11	118.00	203.00	61.40	678.00	677.00	573.00	22.10	558.00	426.00
U	47.40	26.30	10.35	1.50	2.83	49.40	8.44	16.20	3.90	15.30	18.80	10.90	12.55	32.40	12.00	4.30	12.10	14.70
Zr	87.00	648.00	23.00	40.00	4.00	452.00	380.00	158.00	5.00	40.00	9.00	326.00	17.00	232.00	8.00	10.00	352.00	150.00
La	1040.00	9.80	699.00	6720.00	47.70	1075.00	23.50	121.50	9.50	738.00	897.00	291.00	3100.00	693.00	2280.00	84.00	1095.00	902.00
Ce	1615.00	18.90	1205.00	10050.00	82.90	1780.00	44.20	254.00	18.90	1320.00	1570.00	482.00	6830.00	1300.00	3800.00	151.50	1920.00	1625.00
Pr	167.00	2.34	122.00	1050.00	7.87	172.50	4.70	31.70	2.25	138.50	161.00	49.00	681.00	137.50	358.00	15.65	195.50	175.50
Nd	661.00	11.20	414.00	2920.00	28.80	556.00	18.60	144.00	10.40	478.00	552.00	165.50	2260.00	494.00	1185.00	55.50	652.00	633.00
Sm	756.00	25.00	61.10	394.00	6.24	74.90	12.30	235.00	4.19	72.00	87.40	26.40	259.00	84.40	167.50	10.60	100.50	112.50
Eu	360.00	25.20	17.40	126.00	2.40	22.60	5.56	149.00	1.59	20.20	26.20	8.28	63.50	32.10	48.80	4.21	31.40	38.80
Gd	838.00	86.30	61.50	484.00	7.61	84.70	16.20	449.00	5.54	70.30	96.80	29.10	287.00	116.00	191.00	16.15	114.00	128.00
Tb	151.00	27.30	9.91	54.00	1.42	14.65	3.78	115.00	1.31	9.74	15.70	4.90	32.10	28.40	28.30	5.03	19.45	25.40
Dy	725.00	195.00	63.30	146.50	9.12	91.50	23.90	765.00	9.15	50.00	94.80	29.60	109.00	195.50	163.50	44.70	110.00	160.50
Ho	113.00	40.70	14.45	16.90	2.03	18.85	4.78	155.00	2.11	10.15	20.10	6.07	16.55	40.90	35.70	11.25	22.10	31.00
Er	264.00	115.50	44.90	35.60	6.21	54.50	13.65	416.00	6.78	30.70	57.20	17.45	49.50	110.00	119.50	35.70	64.60	81.00
Tm	34.80	17.90	6.22	2.60	0.99	7.47	2.19	59.20	1.20	4.05	7.49	2.34	4.26	14.05	18.90	5.51	9.14	9.87
Yb	189.00	97.80	31.70	15.90	5.90	40.90	13.70	298.00	8.44	22.70	37.40	12.45	25.00	67.00	117.50	29.90	52.70	46.80
Lu	25.30	13.85	4.28	2.48	0.99	5.68	2.12	40.50	1.45	3.17	4.92	1.78	3.59	8.56	17.70	4.32	7.70	6.08
Y	2570.00	1140.00	432.00	340.00	55.90	481.00	117.50	4100.00	63.50	266.00	557.00	157.50	374.00	1025.00	936.00	334.00	569.00	789.00
La/Yb	5.50	0.10	22.05	422.64	8.08	26.28	1.72	0.41	1.13	32.51	23.98	23.37	124.00	10.34	19.40	2.81	20.78	19.27

Appendix 2 b) Trace elements analysis of samples collected by Etruscan and NRE and used in this study

Sample No.	ERN15833	ERN15834	ERN15835	ERN15836	ERN15837	ERN15838	ERN15839	ERN15840	ERN15841	ERN15842	ERN15843	ERN15844	ERN15845	ERN15846	ERN15847	ERN15848	ERN15849	ERN15850
Ba	130.50	58.30	3020.00	468.00	120.00	245.00	942.00	934.00	140.00	320.00	135.50	194.00	377.00	675.00	135.50	107.00	22.50	261.00
Ga	36.70	25.40	17.70	43.10	12.90	54.80	16.00	16.40	18.80	7.50	20.60	28.60	25.20	16.90	17.60	10.50	3.00	35.60
Hf	1.40	5.50	4.80	2.90	7.30	0.80	5.10	2.50	1.10	0.10	0.70	5.20	5.50	1.30	4.30	2.10	11.10	2.50
Nb	11.30	364.00	253.00	73.60	163.50	40.90	138.50	91.10	58.30	5.60	82.20	747.00	1000.00	415.00	111.50	105.00	112.50	427.00
Rb	1.60	21.20	1.50	7.50	3.20	23.80	5.50	2.60	7.10	7.40	2.30	1.10	18.30	8.40	5.00	7.60	2.70	2.40
Sr	1980.00	945.00	9720.00	1835.00	3050.00	4320.00	5010.00	7420.00	3550.00	453.00	1230.00	5020.00	1230.00	4270.00	523.00	484.00	585.00	1590.00
Ta	0.40	3.20	1.10	0.70	0.30	0.30	1.50	0.60	0.90	0.05	0.40	3.60	12.40	4.40	1.10	0.80	0.20	0.20
Th	770.00	1000.00	264.00	412.00	65.90	224.00	1000.00	1000.00	81.40	254.00	30.10	149.00	42.10	34.20	135.00	307.00	63.90	156.00
U	11.80	36.10	67.70	10.30	20.80	1.19	10.60	15.65	10.20	2.01	20.40	27.70	37.40	45.20	11.35	18.35	49.60	23.00
Zr	16.00	127.00	268.00	63.00	314.00	11.00	100.00	67.00	37.00	4.00	19.00	239.00	446.00	165.00	357.00	90.00	1140.00	131.00
La	2750.00	1750.00	1025.00	5330.00	650.00	4370.00	801.00	1155.00	1165.00	21.50	1650.00	1010.00	530.00	600.00	758.00	640.00	83.30	3490.00
Ce	4750.00	2830.00	1940.00	8380.00	1175.00	7480.00	1450.00	1950.00	2100.00	59.20	2650.00	1875.00	1040.00	1170.00	1395.00	1100.00	142.50	5020.00
Pr	490.00	288.00	205.00	812.00	122.50	764.00	154.50	198.50	218.00	16.30	253.00	197.00	116.50	128.00	143.00	115.50	15.50	440.00
Nd	1600.00	1045.00	690.00	2590.00	409.00	2410.00	540.00	659.00	725.00	141.00	797.00	652.00	400.00	434.00	467.00	399.00	55.50	1275.00
Sm	224.00	464.00	91.60	355.00	59.50	322.00	158.00	98.20	94.00	63.70	105.00	94.30	60.70	64.90	69.00	85.60	12.10	146.50
Eu	53.80	164.00	24.30	91.20	15.55	66.50	77.10	38.90	19.60	12.00	27.20	26.90	16.15	16.45	17.55	27.60	3.75	35.50
Gd	251.00	483.00	99.30	387.00	63.20	319.00	288.00	157.50	87.20	32.80	116.00	103.00	60.50	62.00	75.20	125.00	16.45	179.00
Tb	37.80	67.10	13.75	44.60	8.25	32.60	64.00	33.00	8.04	4.47	12.60	14.75	7.16	7.22	10.05	29.20	3.52	17.70
Dy	196.50	259.00	74.00	217.00	39.70	111.00	370.00	196.00	25.00	18.50	48.20	80.30	27.70	29.00	49.40	201.00	25.30	67.30
Ho	39.60	38.40	16.65	44.10	8.21	20.60	70.00	41.20	4.91	3.07	8.83	17.10	4.88	5.34	9.51	42.90	6.43	13.25
Er	124.50	100.50	56.40	135.50	27.00	70.30	188.50	127.00	20.50	9.32	28.10	54.60	15.15	16.80	30.20	119.00	24.30	44.50
Tm	15.30	13.15	7.65	18.95	3.35	6.78	22.60	16.30	2.60	1.22	2.79	6.43	1.57	1.85	3.53	13.40	4.09	4.64
Yb	93.30	96.40	48.30	119.00	20.90	38.60	123.00	93.20	18.95	9.16	15.90	34.80	9.86	10.70	21.10	64.30	28.70	26.60
Lu	12.65	14.40	6.58	15.25	2.73	4.60	15.70	12.25	2.80	1.52	2.08	4.19	1.52	1.54	2.80	7.27	4.37	3.46
Y	1020.00	1000.00	448.00	1295.00	218.00	748.00	1990.00	1200.00	145.50	91.40	226.00	495.00	119.50	136.50	276.00	1235.00	189.50	348.00
La/Yb	29.47	18.15	21.22	44.79	31.10	113.21	6.51	12.39	61.48	2.35	103.77	29.02	53.75	56.07	35.92	9.95	2.90	131.20

Appendix 2 b) Trace elements analysis of samples collected by Etruscan and NRE and used in this study

Sample No.	ERN15851	ERN15852	ERN15853	ERN15854	ERN15855	ERN15856	ERN15857	ERN15858	ERN15859	ERN15860	ERN15861	ERN15862	ERN15863	ERN15864	ERN15865	ERN15866	ERN15867	ERN15868
Ba	61.60	841.00	413.00	85.10	1050.00	800.00	1050.00	644.00	124.00	44.20	99.80	718.00	139.50	169.50	1330.00	1600.00	247.00	253.00
Ga	3.00	25.10	42.10	30.60	17.00	16.90	19.90	16.80	94.60	9.20	6.60	5.50	11.20	6.80	6.30	6.60	8.20	7.40
Hf	2.90	2.00	2.80	0.30	0.30	0.60	0.70	1.50	2.00	4.00	1.00	1.30	0.80	1.80	1.30	1.00	3.00	3.50
Nb	25.30	102.00	23.80	7.60	83.40	86.70	84.50	484.00	289.00	74.00	402.00	73.80	14.80	345.00	139.00	86.00	243.00	78.30
Rb	0.60	7.30	16.20	3.40	0.80	8.60	2.10	1.30	4.00	6.00	0.50	16.60	2.30	16.20	2.20	6.00	1.00	23.20
Sr	315.00	10000.00	3940.00	1555.00	1665.00	5390.00	10000.00	7130.00	3130.00	850.00	6550.00	6650.00	4050.00	3810.00	7700.00	10000.00	10000.00	1035.00
Ta	0.20	0.50	0.40	0.10	0.50	0.50	0.30	1.30	1.80	1.20	1.00	1.70	0.10	1.70	0.80	0.25	1.10	1.40
Th	33.70	601.00	397.00	206.00	99.00	102.50	159.50	44.70	346.00	1380.00	1115.00	53.50	379.00	63.10	279.00	226.00	1080.00	182.00
U	8.67	27.30	8.06	1.98	15.30	12.15	11.65	21.20	20.30	5.20	31.80	5.43	3.65	5.53	25.60	14.50	21.40	12.30
Zr	291.00	115.00	88.00	8.00	6.00	14.00	18.00	78.00	30.00	100.00	90.00	42.00	29.00	147.00	38.00	30.00	80.00	239.00
La	16.10	1750.00	3260.00	2500.00	971.00	1000.00	1250.00	1185.00	7280.00	1480.00	958.00	623.00	2550.00	883.00	931.00	804.00	1160.00	525.00
Ce	31.80	2440.00	5480.00	4200.00	1820.00	1845.00	2210.00	1960.00	12400.00	2830.00	1600.00	1160.00	3610.00	1495.00	1705.00	1395.00	2140.00	1010.00
Pr	3.99	230.00	547.00	397.00	198.50	195.00	237.00	194.50	1280.00	299.00	154.50	123.50	312.00	148.00	181.50	139.50	217.00	110.50
Nd	16.70	709.00	1725.00	1190.00	692.00	672.00	803.00	614.00	4040.00	1065.00	513.00	424.00	877.00	480.00	625.00	476.00	748.00	392.00
Sm	5.81	122.00	270.00	117.00	104.00	98.50	117.00	82.50	488.00	367.00	83.20	63.10	106.00	57.80	98.20	72.50	144.00	62.40
Eu	1.66	40.90	71.10	24.80	27.80	27.40	31.60	23.00	107.00	160.50	28.10	19.45	36.20	14.70	30.10	24.40	68.30	16.70
Gd	8.04	160.00	295.00	138.00	102.50	102.50	119.50	91.40	515.00	480.00	110.50	64.00	154.00	56.30	102.00	86.60	248.00	67.60
Tb	2.25	26.00	41.20	13.10	12.60	11.90	15.00	10.15	46.30	63.50	24.60	7.82	21.90	6.18	15.55	12.70	49.80	9.49
Dy	18.20	145.00	210.00	48.90	55.80	50.20	66.20	40.40	137.50	335.00	215.00	38.10	116.00	34.00	89.20	73.40	297.00	50.80
Ho	4.79	28.80	44.50	10.40	10.85	9.48	13.20	7.55	21.90	67.10	51.60	7.20	22.60	8.02	18.25	14.45	53.70	10.05
Er	18.30	82.20	149.00	39.20	35.20	30.70	43.50	24.00	69.80	201.00	149.50	20.80	65.80	26.60	51.90	44.40	145.00	28.50
Tm	3.25	9.27	19.75	4.64	4.21	3.54	5.01	2.48	6.17	25.30	16.90	2.69	9.18	3.65	6.53	5.97	17.25	3.57
Yb	23.30	48.50	118.00	31.70	25.20	21.60	31.00	14.00	38.80	150.50	83.20	16.95	62.70	22.80	36.60	36.60	95.90	21.30
Lu	3.67	6.07	15.65	4.63	3.37	2.90	4.17	1.77	5.06	18.95	9.57	2.25	8.75	2.88	4.55	4.64	12.15	2.72
Y	155.50	794.00	1250.00	352.00	312.00	250.00	372.00	213.00	516.00	2270.00	1540.00	204.00	607.00	225.00	527.00	403.00	1325.00	291.00
La/Yb	0.69	36.08	27.63	78.86	38.53	46.30	40.32	84.64	187.63	9.83	11.51	36.76	40.67	38.73	25.44	21.97	12.10	24.65

Appendix 2 b) Trace elements analysis of samples collected by Etruscan and NRE and used in this study

Sample No.	ERN15869	ERN15870	ERN15871	ERN15872	ERN15873	ERN15874	ERN15875	ERN15876	ERN15877	ERN15878	ERN15879	ERN15880	ERN15881	ERN15882	ERN15883	ERN15884	ERN15885	ERN15886
Ba	32.60	204.00	79.40	309.00	402.00	183.50	238.00	68.90	416.00	117.00	134.00	74.50	70.40	338.00	50.80	48.00	421.00	318.00
Ga	2.40	6.40	10.20	12.80	19.30	6.80	20.40	20.90	5.30	12.30	19.60	8.20	8.70	8.10	5.20	5.00	12.80	7.30
Hf	11.20	1.40	1.00	1.20	3.30	1.80	2.90	1.30	0.30	6.00	0.70	2.00	3.00	2.00	3.80	1.20	3.50	2.00
Nb	222.00	141.50	30.50	404.00	244.00	44.40	12.50	95.00	58.90	238.00	9.30	136.00	266.00	152.50	86.30	6.60	582.00	124.00
Rb	3.20	0.70	28.20	28.50	100.50	12.50	67.10	2.10	2.50	5.00	39.70	13.00	7.00	0.70	1.80	2.90	23.50	5.20
Sr	585.00	2820.00	1790.00	2270.00	1690.00	1540.00	172.50	719.00	6060.00	2370.00	90.30	397.00	291.00	4360.00	4770.00	230.00	4290.00	3920.00
Ta	1.60	1.20	0.60	5.90	3.30	0.70	0.70	0.40	1.10	2.70	0.50	0.60	1.00	0.50	0.90	0.30	10.50	1.50
Th	22.10	214.00	894.00	427.00	710.00	545.00	13.90	916.00	63.00	1445.00	6.36	1580.00	1275.00	97.90	59.60	24.20	306.00	588.00
U	10.85	21.80	20.90	9.74	12.30	18.00	4.75	26.90	9.41	20.10	1.93	24.20	11.80	15.05	9.91	3.69	66.80	40.70
Zr	548.00	46.00	11.00	34.00	145.00	95.00	52.00	17.00	2.00	150.00	14.00	80.00	100.00	132.00	261.00	90.00	281.00	40.00
La	254.00	956.00	1740.00	870.00	853.00	614.00	14.40	5400.00	872.00	1215.00	10.50	61.00	1200.00	1375.00	158.00	21.80	464.00	1000.00
Ce	519.00	1695.00	2720.00	1640.00	1590.00	1220.00	28.60	8130.00	1580.00	1985.00	18.90	138.00	2060.00	2680.00	343.00	41.10	898.00	1795.00
Pr	58.10	179.50	262.00	177.00	168.00	135.50	3.21	738.00	165.50	194.50	2.02	16.70	206.00	293.00	40.60	4.73	94.80	188.00
Nd	210.00	607.00	835.00	621.00	585.00	481.00	12.60	2090.00	559.00	650.00	6.80	63.90	736.00	1015.00	152.00	19.70	327.00	667.00
Sm	34.30	96.60	120.50	110.00	114.00	146.50	3.76	213.00	87.00	123.50	2.13	27.70	241.00	150.00	36.50	6.47	52.50	127.00
Eu	12.15	30.40	37.60	40.80	50.30	81.10	0.99	60.70	26.80	47.70	0.41	15.20	95.00	41.70	17.40	2.62	19.15	50.60
Gd	36.50	105.50	155.50	147.50	189.00	305.00	6.21	269.00	93.10	212.00	3.23	64.50	358.00	145.50	57.50	10.90	67.10	180.50
Tb	4.91	15.95	28.90	25.00	38.20	66.40	1.46	40.90	12.50	43.10	0.73	14.60	47.60	21.30	12.30	2.24	11.90	42.30
Dy	25.80	91.00	191.50	137.50	222.00	394.00	10.20	262.00	64.90	278.00	4.52	99.00	235.00	126.50	74.80	14.70	66.00	334.00
Ho	4.90	18.40	41.50	24.40	40.30	73.40	2.31	53.80	12.65	55.20	0.82	19.60	40.10	26.90	13.65	2.75	11.75	76.20
Er	13.80	51.80	121.50	60.10	98.50	175.50	7.08	145.50	35.70	149.00	2.00	55.30	103.50	78.60	36.50	7.80	33.30	234.00
Tm	1.79	6.36	16.15	6.68	10.75	19.25	1.00	16.75	4.28	17.10	0.23	7.00	11.70	9.30	4.52	1.04	4.54	29.70
Yb	11.45	37.60	91.00	35.50	54.50	99.80	6.72	89.40	24.20	88.70	1.38	38.90	68.80	49.00	28.60	6.59	31.80	162.00
Lu	1.57	4.74	11.10	4.28	6.44	12.05	0.99	10.40	2.96	10.50	0.17	4.63	8.36	5.67	3.91	0.90	4.56	18.15
Y	139.50	493.00	1245.00	642.00	1110.00	1890.00	68.00	1415.00	364.00	1515.00	23.20	550.00	1050.00	720.00	420.00	80.40	316.00	2370.00
La/Yb	22.18	25.43	19.12	24.51	15.65	6.15	2.14	60.40	36.03	13.70	7.61	1.57	17.44	28.06	5.52	3.31	14.59	6.17

Appendix 2 b) Trace elements analysis of samples collected by Etruscan and NRE and used in this study

Sample No.	ERN15887	ERN15888	ERN15889	ERN15890	ERN15892	ERN15893	ERN15894	ERN15895	ERN15896	ERN15897	ERN15898	ERN15899	ERN15900	ERN15901	ERN15902	ERN15903	ERN15904	ERN15905
Ba	76.20	698.00	99.70	177.50	72.70	151.00	197.00	417.00	174.50	198.00	448.00	684.00	362.00	916.00	994.00	380.00	350.00	351.00
Ga	14.80	6.80	6.30	5.60	4.10	1.20	8.60	5.70	10.70	11.60	3.90	10.30	6.00	3.30	13.40	6.60	4.60	8.30
Hf	2.90	0.70	5.30	0.40	3.20	0.30	2.70	0.60	0.90	0.90	1.80	0.70	1.40	1.20	1.20	1.50	1.00	0.90
Nb	134.00	84.30	128.50	276.00	16.80	0.90	139.00	2.40	19.60	3.20	5.00	14.80	6.90	0.60	12.80	53.40	16.50	18.50
Rb	4.50	15.90	28.10	17.60	1.30	0.40	29.20	4.60	19.50	4.90	17.70	3.40	3.60	3.30	2.70	7.10	2.30	3.00
Sr	296.00	7080.00	303.00	375.00	347.00	298.00	369.00	222.00	471.00	476.00	241.00	8980.00	376.00	280.00	646.00	1115.00	449.00	348.00
Ta	0.50	0.20	0.40	1.60	0.50	0.10	0.40	0.40	0.20	0.05	0.10	0.10	0.10	0.05	0.40	0.40	0.20	0.60
Th	28.90	48.90	45.90	20.20	6.26	0.53	61.50	10.05	114.50	124.00	5.55	204.00	74.20	79.00	182.00	14.25	81.90	160.50
U	1.94	15.80	21.20	9.88	4.00	2.44	19.10	4.17	4.53	3.97	7.66	7.73	4.97	3.46	8.96	14.45	3.59	4.42
Zr	126.00	55.00	821.00	29.00	197.00	17.00	201.00	26.00	47.00	71.00	119.00	23.00	132.00	101.00	78.00	60.00	82.00	64.00
La	59.40	1415.00	10.30	1015.00	13.80	5.20	1200.00	140.00	2790.00	2410.00	23.70	2380.00	1180.00	134.50	2930.00	1255.00	528.00	1305.00
Ce	94.10	2190.00	22.60	1635.00	27.60	8.90	2020.00	221.00	4000.00	4250.00	42.60	3470.00	1680.00	269.00	4480.00	1855.00	904.00	1950.00
Pr	8.80	205.00	2.92	158.00	3.16	1.37	200.00	24.80	343.00	418.00	5.05	325.00	152.50	30.80	388.00	164.00	86.80	170.00
Nd	26.90	634.00	13.10	513.00	12.90	6.10	673.00	85.40	1000.00	1235.00	20.20	961.00	445.00	111.50	1140.00	514.00	282.00	502.00
Sm	5.76	80.30	4.16	66.40	3.25	1.66	93.20	11.05	129.00	111.50	4.42	124.00	54.30	22.50	139.00	64.30	41.30	66.70
Eu	3.41	23.50	1.56	18.00	0.98	0.57	25.50	2.97	31.60	24.80	1.11	34.40	15.20	7.42	41.10	18.25	12.00	20.50
Gd	12.25	82.20	5.84	62.50	3.95	2.03	92.40	9.22	139.50	121.50	4.72	142.50	63.60	28.50	166.00	65.60	41.90	76.80
Tb	2.90	8.76	1.27	6.58	0.75	0.38	10.95	1.04	15.20	9.39	0.83	17.90	7.33	5.94	20.50	7.07	5.15	9.12
Dy	19.40	39.60	9.01	27.90	4.71	2.24	51.80	4.44	76.40	34.10	5.21	97.80	40.40	40.30	112.50	32.80	26.40	44.70
Ho	3.88	7.12	1.97	4.61	1.02	0.44	9.33	0.82	15.15	6.36	1.11	20.00	8.29	8.15	20.90	6.07	5.23	8.33
Er	11.65	20.10	6.52	12.60	3.29	1.27	26.40	2.22	49.20	21.20	3.58	60.40	26.10	23.20	60.50	17.40	15.95	23.80
Tm	1.61	2.15	0.99	1.16	0.47	0.16	3.05	0.27	6.61	2.45	0.48	8.45	3.78	3.43	7.09	1.98	2.18	3.04
Yb	10.95	12.90	7.27	6.49	3.29	1.16	17.85	2.01	43.00	16.20	3.20	54.70	24.10	23.60	40.60	11.75	14.25	20.70
Lu	1.55	1.56	1.01	0.67	0.46	0.17	2.10	0.28	5.63	2.19	0.46	7.23	3.30	3.32	5.18	1.39	1.94	2.69
Y	104.00	205.00	61.90	123.50	27.00	11.10	231.00	19.70	450.00	164.00	31.50	549.00	236.00	223.00	609.00	160.50	151.00	225.00
La/Yb	5.42	109.69	1.42	156.39	4.19	4.48	67.23	69.65	64.88	148.77	7.41	43.51	48.96	5.70	72.17	106.81	37.05	63.04

Appendix 2 b) Trace elements analysis of samples collected by Etruscan and NRE and used in this study

Sample No.	ERNI 5906	ERNI 5907	ERNI 5908	ERNI 5909	ERNI 5910	ERNI 5911	ERNI 5912	ERNI 5913	ERNI 5914	ERNI 5915	ERNI 5916	ERNI 5917	ERNI 5918	ERNI 5919	ERNI 5920	ERNI 5921	ERNI 5922	ERNI 5923
Ba	53.90	223.00	111.00	95.80	10000.00	542.00	198.50	408.00	491.00	650.00	148.50	71.90	220.00	123.50	291.00	178.00	492.00	323.00
Ga	1.70	9.70	25.20	14.70	8.80	31.60	8.10	10.70	25.70	17.00	7.20	4.60	7.20	13.10	6.30	6.10	4.70	23.10
Hf	0.20	5.50	8.00	1.20	1.00	5.00	2.70	0.60	1.60	1.20	0.90	0.40	0.90	1.20	1.70	1.40	1.80	5.20
Nb	9.90	32.50	44.00	2.10	207.00	52.00	304.00	7.10	33.60	3.30	107.50	4.60	7.80	41.20	10.20	173.00	103.50	144.50
Rb	5.80	49.10	12.00	1.40	4.00	30.00	6.50	2.10	4.90	1.30	3.80	0.60	3.80	14.50	6.80	4.60	5.20	43.40
Sr	368.00	434.00	556.00	554.00	3120.00	321.00	710.00	1140.00	477.00	2170.00	533.00	904.00	675.00	413.00	259.00	7030.00	1845.00	4860.00
Ta	0.10	0.70	0.25	0.20	1.00	0.25	0.70	0.40	0.40	0.20	0.30	0.10	0.30	0.20	0.40	0.80	0.30	0.70
Th	2.91	38.80	335.00	282.00	64.20	454.00	287.00	113.00	393.00	253.00	104.50	57.10	413.00	407.00	125.50	27.20	150.00	132.50
U	0.62	6.43	7.20	13.70	37.40	7.40	22.80	3.99	16.15	18.15	7.94	2.48	5.34	7.25	4.25	19.60	14.05	26.70
Zr	13.00	350.00	770.00	97.00	110.00	330.00	227.00	30.00	86.00	57.00	56.00	28.00	26.00	90.00	98.00	117.00	176.00	546.00
La	54.60	155.00	7410.00	3010.00	1250.00	4390.00	1355.00	1745.00	4950.00	4370.00	1145.00	545.00	1090.00	3540.00	633.00	909.00	829.00	3280.00
Ce	77.20	261.00	9590.00	5030.00	2190.00	9840.00	2200.00	2820.00	8700.00	6500.00	2000.00	931.00	1865.00	4820.00	970.00	1495.00	1275.00	4550.00
Pr	6.85	25.10	755.00	462.00	219.00	1125.00	209.00	255.00	854.00	569.00	200.00	88.10	185.00	391.00	89.60	141.50	118.50	373.00
Nd	22.30	84.30	2030.00	1440.00	729.00	4120.00	674.00	776.00	2780.00	1675.00	682.00	280.00	632.00	1100.00	281.00	455.00	374.00	1090.00
Sm	3.80	13.30	199.50	174.50	102.50	549.00	104.50	94.10	359.00	193.00	92.80	42.00	136.00	124.50	39.00	63.50	49.10	126.50
Eu	0.99	3.70	47.50	41.60	28.80	101.50	30.00	24.90	83.90	50.10	17.95	10.85	42.90	35.20	10.55	19.05	15.60	33.70
Gd	4.76	13.70	237.00	185.00	98.90	400.00	117.50	103.50	308.00	215.00	92.60	41.90	168.50	147.50	43.70	65.10	51.30	134.50
Tb	0.67	1.71	21.30	23.30	10.70	33.70	18.50	12.80	28.10	29.30	11.65	5.61	27.60	16.45	5.43	7.52	6.79	13.25
Dy	3.78	9.73	97.50	134.00	49.90	111.50	121.50	75.40	111.50	176.00	60.50	32.30	167.00	81.60	29.00	38.10	40.30	58.80
Ho	0.76	2.04	20.10	28.30	8.85	18.35	26.60	16.25	19.30	36.10	11.90	6.81	34.20	15.65	5.65	7.11	7.83	10.25
Er	2.22	6.65	66.80	89.10	23.90	55.50	85.20	55.30	62.10	107.50	36.20	22.20	106.50	47.80	16.50	21.00	22.90	28.80
Tm	0.30	0.96	9.69	11.90	2.56	5.65	11.95	8.04	7.33	13.35	4.64	3.15	15.55	6.10	2.15	2.53	2.92	3.03
Yb	2.00	6.96	69.50	75.00	15.00	35.80	73.00	55.30	48.20	77.50	28.90	21.40	104.50	37.80	13.55	15.55	18.55	17.30
Lu	0.28	0.98	9.86	9.74	1.83	4.57	9.02	7.63	6.69	9.33	3.83	2.94	14.20	4.95	1.76	1.98	2.28	2.08
Y	23.60	60.90	656.00	973.00	234.00	497.00	823.00	516.00	576.00	1015.00	300.00	213.00	1050.00	430.00	162.50	202.00	226.00	274.00
La/Yb	27.30	22.27	106.62	40.13	83.33	122.63	18.56	31.56	102.70	56.39	39.62	25.47	10.43	93.65	46.72	58.46	44.69	189.60

Appendix 2 b) Trace elements analysis of samples collected by Etruscan and NRE and used in this study

Sample No.	ERN15924	ERN15925	ERN15926	ERN15927	ERN15928	ERN15929	ERN15930	ERN15931	ERN15932	ERN15933	ERN15934	ERN15935	ERN15936	ERN15937	ERN15938	ERN15939	ERN15940	ERN15941
Ba	49.60	43.90	639.00	39.30	533.00	1330.00	142.00	577.00	427.00	141.50	541.00	219.00	527.00	414.00	461.00	217.00	274.00	958.00
Ga	13.10	2.20	11.70	13.30	9.00	5.10	4.60	13.80	9.00	4.50	6.70	6.80	6.80	11.60	15.50	4.60	4.80	10.10
Hf	1.70	0.40	1.70	1.30	1.00	1.60	0.60	1.30	5.50	0.50	0.40	7.40	1.70	0.90	0.70	1.70	1.90	0.60
Nb	126.50	3.70	224.00	41.00	14.60	97.60	6.70	2.00	10.40	28.50	10.20	196.00	27.40	6.40	3.80	8.40	31.40	53.60
Rb	0.50	0.30	8.10	5.70	7.20	3.40	0.50	0.40	9.70	5.10	3.50	9.20	7.70	1.00	9.40	13.50	1.70	3.10
Sr	260.00	491.00	816.00	768.00	380.00	2490.00	883.00	6140.00	964.00	496.00	1185.00	3780.00	239.00	913.00	2210.00	1365.00	644.00	736.00
Ta	0.20	0.10	0.90	0.60	0.20	0.40	0.40	0.40	0.20	0.20	0.50	1.20	0.30	0.20	0.50	0.40	0.60	0.20
Th	102.50	46.10	311.00	350.00	345.00	39.00	134.50	359.00	376.00	124.50	94.60	48.90	280.00	235.00	274.00	49.10	293.00	21.10
U	8.88	2.07	12.05	7.60	3.90	10.15	7.58	5.37	12.60	1.32	2.61	49.80	5.88	11.25	2.84	4.13	23.20	3.69
Zr	239.00	42.00	174.00	114.00	87.00	126.00	41.00	12.00	396.00	39.00	14.00	705.00	178.00	33.00	18.00	122.00	139.00	15.00
La	3350.00	28.50	2800.00	3510.00	2280.00	984.00	513.00	3450.00	1985.00	933.00	712.00	1260.00	1680.00	2310.00	4310.00	282.00	605.00	1375.00
Ce	4870.00	54.10	4140.00	5030.00	3190.00	1475.00	900.00	4910.00	3310.00	1385.00	1220.00	2030.00	2510.00	4530.00	6470.00	442.00	1080.00	2850.00
Pr	423.00	6.06	371.00	424.00	266.00	134.00	86.00	416.00	336.00	130.00	122.50	197.00	236.00	460.00	566.00	41.30	112.50	333.00
Nd	1240.00	23.20	1160.00	1210.00	776.00	425.00	281.00	1205.00	1100.00	391.00	390.00	622.00	737.00	1425.00	1545.00	130.50	380.00	1235.00
Sm	147.00	6.73	151.50	131.50	96.00	56.50	44.60	221.00	170.50	48.70	61.70	76.70	102.00	159.50	158.50	23.80	76.90	187.00
Eu	33.60	2.36	42.50	34.60	23.10	17.60	11.90	79.10	50.60	13.00	17.40	21.30	28.20	31.30	46.50	8.68	34.50	51.10
Gd	146.50	10.30	164.00	154.50	111.00	59.60	51.50	302.00	198.50	56.40	66.30	80.20	115.50	171.00	217.00	32.90	132.50	168.50
Tb	12.95	2.20	18.90	17.05	13.15	7.05	7.59	51.40	26.10	6.69	9.20	8.25	14.15	17.70	24.90	5.70	26.10	19.10
Dy	53.10	15.50	93.50	87.20	68.20	37.00	46.00	331.00	127.50	35.00	54.40	36.00	71.10	78.40	128.00	38.80	172.00	78.70
Ho	9.72	3.51	17.25	16.80	13.30	7.40	9.71	68.00	23.50	7.23	12.50	6.86	14.15	14.10	26.50	9.44	36.70	13.30
Er	32.00	11.45	50.40	49.30	38.80	22.20	32.90	204.00	66.90	23.10	43.30	20.10	41.80	39.90	83.40	31.90	107.00	35.30
Tm	4.15	1.71	6.14	6.06	4.75	2.75	5.39	28.60	9.60	3.67	7.90	2.65	5.92	5.00	13.00	5.37	16.45	4.28
Yb	27.40	11.70	37.00	37.40	29.00	15.95	39.30	187.50	55.20	22.80	50.70	14.10	33.40	27.50	75.20	30.50	94.20	21.80
Lu	3.67	1.57	4.64	4.72	3.85	1.99	5.51	25.30	7.49	3.31	7.27	1.79	4.27	3.64	10.05	4.10	12.60	2.59
Y	266.00	109.50	499.00	469.00	375.00	206.00	284.00	2130.00	657.00	204.00	371.00	177.00	385.00	357.00	701.00	328.00	1020.00	300.00
La/Yb	122.26	2.44	75.68	93.85	78.62	61.69	13.05	18.40	35.96	40.92	14.04	89.36	50.30	84.00	57.31	9.25	6.42	63.07

Appendix 2 b) Trace elements analysis of samples collected by Etruscan and NRE and used in this study

Sample No.	ERNI 9942	ERNI 9943	ERNI 9944	ERNI 9945	ERNI 9946	ERNI 9947	ERNI 9948	ERNI 9949	ERNI 9950	ERNI 9951	ERNI 9952	ERNI 9953	ERNI 9954	ERNI 9955	ERNI 9956	ERNI 9957	ERNI 9958	ERNI 9959
Ba	818.00	871.00	993.00	820.00	2910.00	1665.00	264.00	824.00	752.00	304.00	290.00	156.50	3470.00	431.00	962.00	660.00	136.00	178.00
Ga	6.60	6.90	17.60	12.20	7.10	5.60	6.70	10.00	26.90	35.50	8.90	3.50	32.70	23.60	11.40	21.00	16.30	50.90
Hf	2.80	2.70	0.50	163.00	2.00	1.70	0.90	1.60	2.00	1.80	3.30	0.70	1.00	2.50	1.90	11.90	2.80	1.30
Nb	30.50	8.70	15.70	108.00	79.00	90.30	3.50	176.00	27.00	3.00	19.50	3.00	35.50	3.80	23.10	276.00	36.60	1.20
Rb	3.90	2.70	8.10	7.00	1.00	2.50	0.90	8.10	5.00	6.70	6.00	1.60	10.50	5.00	18.00	102.00	2.10	10.30
Sr	4610.00	391.00	1490.00	562.00	10000.00	7750.00	214.00	4240.00	2610.00	3710.00	1800.00	105.00	10000.00	2010.00	320.00	181.50	887.00	627.00
Ta	0.30	1.10	0.50	0.25	0.25	0.30	0.40	0.50	0.25	0.30	0.50	0.05	0.40	0.30	0.40	9.10	0.40	0.20
Th	266.00	204.00	219.00	1275.00	71.50	117.50	259.00	54.30	1325.00	444.00	255.00	172.50	913.00	1000.00	151.00	23.80	241.00	221.00
U	7.41	8.44	4.01	95.80	9.50	15.50	4.98	7.99	6.00	4.35	5.10	1.84	13.70	14.65	3.69	9.67	5.42	9.22
Zr	174.00	30.00	17.00	11900.00	190.00	153.00	57.00	54.00	60.00	31.00	122.00	66.00	7.00	136.00	81.00	838.00	151.00	27.00
La	1070.00	1620.00	4790.00	2740.00	1350.00	1100.00	1350.00	1325.00	6910.00	4190.00	240.00	106.50	3560.00	1670.00	223.00	186.00	1440.00	4060.00
Ce	2200.00	2560.00	7080.00	4750.00	2390.00	1915.00	2110.00	2370.00	10650.00	5250.00	463.00	220.00	4840.00	2890.00	364.00	297.00	2210.00	6930.00
Pr	255.00	252.00	628.00	476.00	240.00	202.00	207.00	248.00	959.00	416.00	52.10	25.70	417.00	298.00	35.80	31.40	207.00	685.00
Nd	905.00	813.00	1730.00	1640.00	811.00	675.00	646.00	806.00	2940.00	1100.00	195.50	95.90	1220.00	1005.00	117.50	102.50	616.00	2070.00
Sm	133.00	133.50	171.50	329.00	118.50	101.50	93.00	105.50	417.00	127.00	64.90	26.80	182.00	188.50	22.40	15.70	89.50	238.00
Eu	37.60	47.70	45.30	95.90	34.20	31.90	24.60	29.90	131.00	39.10	28.10	7.90	54.50	61.50	8.10	4.54	25.70	60.10
Gd	129.50	216.00	203.00	375.00	120.50	110.50	108.00	106.00	516.00	192.50	104.00	29.40	227.00	222.00	34.10	16.85	122.50	283.00
Tb	16.65	63.20	18.70	59.10	15.25	14.95	14.10	12.95	78.50	25.90	26.20	3.62	26.40	34.90	6.95	2.13	20.40	30.60
Dy	90.00	563.00	84.00	366.00	80.00	77.30	68.40	64.60	441.00	159.00	196.00	15.75	119.00	185.00	47.90	10.20	135.50	141.00
Ho	18.60	145.50	17.25	82.10	15.75	14.90	12.30	13.25	82.10	35.90	45.10	2.70	21.90	33.40	9.93	2.00	31.10	29.80
Er	58.40	462.00	58.00	274.00	43.60	41.10	32.60	39.70	212.00	113.00	138.00	7.31	65.90	91.70	28.30	6.39	98.00	103.00
Tm	9.12	69.80	8.62	44.90	5.30	5.52	4.12	5.90	25.20	15.15	20.30	0.90	8.33	12.50	3.83	0.90	14.00	14.35
Yb	55.40	358.00	50.80	319.00	28.20	29.10	21.70	33.20	139.50	89.20	124.00	5.57	53.50	83.80	22.40	6.08	82.70	96.50
Lu	7.61	44.80	6.58	45.70	3.15	3.55	2.87	4.36	17.70	11.60	16.15	0.77	7.19	12.00	2.99	0.90	10.75	13.80
Y	500.00	5020.00	568.00	2210.00	407.00	378.00	310.00	357.00	2100.00	1050.00	1095.00	72.40	521.00	788.00	268.00	50.80	1030.00	824.00
La/Yb	19.31	4.53	94.29	8.59	47.87	37.80	62.21	39.91	49.53	46.97	1.94	19.12	66.54	19.93	9.96	30.59	17.41	42.07

Appendix 2 b) Trace elements analysis of samples collected by Etruscan and NRE and used in this study

Sample No.	ERN15960	ERN15961	ERN15962	ERN15963	ERN15964	ERN15965	ERN15966	ERN15967	ERN15968	ERN15969	ERN15970	ERN15971	ERN15972	ERN15973	ERN15974	ERN15975	ERN15976	ERN15977
Ba	73.30	148.50	10000.00	673.00	2940.00	145.50	203.00	133.00	92.70	273.00	578.00	419.00	59.60	137.50	106.50	210.00	364.00	127.00
Ga	58.60	55.00	2.20	2.60	1.90	4.70	20.60	12.30	36.10	41.00	19.00	11.70	7.90	15.80	10.70	57.20	14.30	13.50
Hf	1.90	5.00	0.40	0.40	0.30	1.90	17.40	0.90	2.40	2.10	1.30	6.30	0.50	4.60	9.00	2.30	0.70	1.00
Nb	2.10	123.00	1.10	2.00	0.40	21.50	194.00	207.00	70.50	1.30	163.50	1150.00	6.10	230.00	271.00	8.80	127.50	531.00
Rb	4.20	1.30	3.60	27.20	8.00	4.90	37.90	0.60	6.60	1.90	1.30	82.20	15.50	1.40	17.00	1.60	2.10	3.50
Sr	445.00	513.00	815.00	462.00	353.00	420.00	402.00	481.00	591.00	435.00	4100.00	352.00	255.00	1100.00	345.00	2010.00	7650.00	4290.00
Ta	0.30	0.50	0.05	0.10	0.05	0.10	12.40	1.50	0.60	0.40	0.90	2.00	0.10	1.50	2.10	0.30	1.40	1.50
Th	330.00	884.00	9.88	4.72	1.67	78.60	23.90	66.10	533.00	530.00	47.70	106.00	29.50	1000.00	5000.00	840.00	57.10	29.90
U	8.99	15.55	1.18	0.53	0.90	5.17	3.79	5.04	10.10	8.09	16.90	7.47	2.20	7.56	61.80	15.45	11.65	8.59
Zr	101.00	532.00	22.00	20.00	9.00	153.00	785.00	83.00	154.00	42.00	83.00	473.00	17.00	174.00	390.00	64.00	33.00	45.00
La	5510.00	6240.00	39.10	18.90	8.30	48.30	181.00	1065.00	4050.00	4040.00	1685.00	42.60	237.00	369.00	382.00	5630.00	1020.00	1030.00
Ce	9140.00	9440.00	60.20	31.60	14.10	103.00	367.00	1745.00	6050.00	6480.00	2790.00	88.60	464.00	507.00	724.00	8910.00	1840.00	1550.00
Pr	871.00	856.00	5.92	3.29	1.58	12.60	44.10	193.00	555.00	690.00	309.00	10.90	54.50	54.60	87.40	955.00	219.00	168.50
Nd	2610.00	2420.00	19.20	11.50	5.80	47.50	159.50	584.00	1710.00	1940.00	939.00	39.00	196.00	175.50	341.00	2790.00	704.00	513.00
Sm	281.00	373.00	4.09	3.06	1.76	10.75	27.20	82.70	244.00	230.00	129.50	12.40	45.40	107.50	289.00	394.00	97.70	69.80
Eu	76.40	106.50	1.77	1.20	0.76	3.08	7.33	21.30	67.10	56.70	37.00	3.86	11.65	53.00	205.00	100.50	26.40	21.80
Gd	357.00	459.00	5.79	4.09	2.79	11.95	25.60	89.70	295.00	326.00	141.50	12.60	46.50	150.50	745.00	425.00	96.80	75.80
Tb	38.20	52.40	0.96	0.77	0.65	2.40	3.21	10.25	35.50	45.90	15.70	2.26	7.38	28.60	201.00	43.90	10.70	8.44
Dy	170.00	212.00	5.31	4.63	4.02	16.05	13.20	43.70	162.00	236.00	61.20	12.90	36.60	156.00	1275.00	162.00	41.80	31.50
Ho	34.00	39.50	1.17	1.00	0.89	3.95	2.38	8.62	33.20	49.00	11.70	2.76	7.53	30.20	242.00	29.70	8.11	5.77
Er	112.00	107.00	3.41	2.91	2.53	12.10	5.91	24.60	93.10	132.50	31.90	8.60	20.50	77.50	673.00	86.00	23.50	15.95
Tm	14.25	12.85	0.49	0.50	0.43	2.00	0.64	3.19	12.45	18.35	3.65	1.65	3.15	12.15	88.00	10.60	2.98	1.77
Yb	92.10	67.30	3.62	3.37	2.88	11.90	3.81	17.40	64.60	101.50	19.60	12.20	19.20	70.20	501.00	65.30	17.30	9.58
Lu	12.70	9.03	0.63	0.52	0.42	1.72	0.54	2.31	8.38	13.85	2.61	2.13	2.82	9.86	62.90	9.27	2.45	1.39
Y	905.00	933.00	34.40	23.70	23.20	114.50	58.90	179.50	813.00	1315.00	301.00	72.30	226.00	736.00	6710.00	843.00	201.00	150.00
La/Yb	59.83	92.72	10.80	5.61	2.88	4.06	47.51	61.21	62.69	39.80	85.97	3.49	12.34	5.26	0.76	86.22	58.96	107.52

Appendix 2 b) Trace elements analysis of samples collected by Etruscan and NRE and used in this study

Sample No.	ERN1 5978	ERN1 5979	ERN1 5980	ERN1 5981	ERN1 5982	ERN1 5983	ERN1 5984	ERN1 5985	ERN1 5986	ERN1 5987	ERN1 5988	ERN1 5989	ERN1 5990	ERN1 5991	ERN1 5992	ERN1 5993	ERN1 5994	ERN1 5995
Ba	345.00	445.00	30.70	147.00	120.00	279.00	116.00	46.70	595.00	1685.00	211.00	235.00	37.50	7.90	49.60	50.10	233.00	743.00
Ga	64.20	45.00	25.20	20.80	9.40	6.70	8.20	14.50	17.20	9.80	5.20	6.50	2.10	2.70	3.20	5.20	6.10	4.00
Hf	2.00	1.30	14.50	6.00	2.40	2.50	2.20	3.80	3.00	6.00	2.90	0.70	1.20	1.60	3.20	18.80	4.40	0.70
Nb	6.00	59.10	123.50	649.00	70.50	265.00	115.00	54.00	230.00	411.00	69.40	84.30	19.90	39.20	36.40	86.10	96.90	57.30
Rb	0.50	5.20	1.80	18.30	2.90	5.50	8.00	2.40	17.20	1.00	0.30	0.40	0.50	0.90	4.10	17.20	2.70	0.70
Sr	4300.00	5730.00	1850.00	4950.00	3540.00	4760.00	1845.00	472.00	7790.00	10000.00	3080.00	6170.00	420.00	432.00	317.00	427.00	5330.00	6650.00
Ta	0.50	0.50	0.40	2.50	1.00	1.10	1.60	0.90	1.60	1.30	0.60	1.10	0.20	0.40	0.70	0.50	0.60	0.70
Th	1585.00	800.00	207.00	110.50	278.00	175.00	114.50	56.20	206.00	141.00	406.00	633.00	17.30	108.00	33.90	164.50	52.40	508.00
U	2.90	1.09	30.80	32.70	8.81	18.05	14.95	6.49	15.65	36.80	31.80	38.60	3.31	4.89	4.81	57.60	15.95	16.80
Zr	20.00	7.00	906.00	292.00	73.00	147.00	63.00	178.00	100.00	390.00	124.00	9.00	113.00	140.00	281.00	2230.00	601.00	47.00
La	6090.00	4560.00	2350.00	1450.00	1320.00	1320.00	976.00	122.50	3380.00	1295.00	554.00	1105.00	30.00	208.00	45.30	37.70	588.00	576.00
Ce	9160.00	6550.00	3790.00	2340.00	2370.00	2120.00	1710.00	232.00	4860.00	2220.00	1035.00	1940.00	54.90	296.00	79.60	80.70	1165.00	1165.00
Pr	891.00	656.00	373.00	251.00	242.00	206.00	187.50	25.30	436.00	210.00	113.50	205.00	6.15	27.80	8.92	9.99	130.50	133.00
Nd	2690.00	1780.00	1235.00	732.00	818.00	633.00	626.00	90.80	1295.00	682.00	393.00	667.00	22.50	88.40	32.60	40.80	443.00	467.00
Sm	355.00	197.00	171.50	92.80	125.00	84.00	98.10	19.00	146.50	88.60	113.00	99.20	5.30	17.65	7.35	13.70	62.90	68.50
Eu	95.60	57.30	48.70	27.10	37.50	28.70	29.30	7.22	41.00	23.00	67.30	34.00	1.84	6.08	2.76	6.62	18.40	22.10
Gd	442.00	264.00	198.50	113.50	139.50	104.50	99.60	27.90	170.00	83.80	258.00	125.00	6.72	25.20	9.16	30.90	61.50	78.30
Tb	66.70	33.90	24.90	14.10	15.65	14.75	12.75	5.52	19.95	8.23	55.60	22.00	1.14	4.16	1.56	8.97	7.16	12.40
Dy	374.00	163.50	119.00	65.60	65.50	84.70	68.30	33.10	104.50	34.50	299.00	141.50	6.47	23.30	9.31	68.70	32.50	74.10
Ho	71.40	31.30	25.00	13.55	12.15	17.85	14.15	6.41	21.00	6.66	47.40	29.30	1.32	4.32	2.01	15.70	6.04	15.25
Er	190.00	82.00	71.90	39.40	35.60	50.80	43.50	17.70	56.90	21.60	105.50	81.00	3.81	11.65	6.20	50.20	17.40	43.50
Tm	19.60	10.80	9.91	5.73	4.85	6.74	6.58	2.64	7.09	3.30	13.55	10.75	0.60	1.73	1.05	9.24	2.42	6.07
Yb	99.10	62.70	53.80	34.00	29.40	31.50	34.80	15.50	35.80	23.40	71.50	52.70	3.68	9.54	6.86	60.90	14.40	32.00
Lu	11.90	9.23	7.44	4.97	4.05	3.52	4.34	2.30	4.28	3.37	9.55	6.24	0.53	1.26	1.03	9.08	2.04	4.09
Y	1940.00	757.00	598.00	377.00	315.00	480.00	367.00	150.00	538.00	180.00	1070.00	837.00	35.50	113.50	57.00	424.00	154.50	426.00
La/Yb	61.45	72.73	43.68	42.65	44.90	41.90	28.05	7.90	94.41	55.34	7.75	20.97	8.15	21.80	6.60	0.62	40.83	18.00

Appendix 2 b) Trace elements analysis of samples collected by Etruscan and NRE and used in this study

Sample No.	ERN15996	ERN15997	ERN15998	ERN15999	ERN16000	ERN18051	ERN18052	ERN18053	ERN18054	ERN18055	ERN18056	ERN18057	ERN18058	ERN18059	ERN18060	ERN18061	ERN18062	ERN18063
Ba	164.00	250.00	210.00	412.00	819.00	415.00	972.00	879.00	3020.00	10000.00	10000.00	10000.00	901.00	668.00	1900.00	476.00	1485.00	295.00
Ga	9.00	7.00	10.20	9.80	8.70	15.70	9.70	9.00	13.70	2.40	2.80	19.70	3.60	35.00	42.80	27.30	18.10	8.20
Hf	4.00	1.00	8.40	1.10	0.40	4.40	2.80	1.80	3.90	0.10	0.10	1.70	0.20	2.00	3.00	3.40	3.80	0.40
Nb	318.00	211.00	72.20	94.50	34.40	51.90	72.40	45.10	68.80	0.40	0.60	9.60	0.40	77.00	112.00	34.90	79.20	5.40
Rb	3.00	2.00	2.90	21.30	4.10	17.70	2.00	7.10	2.60	1.40	2.10	2.60	6.40	1.00	6.00	15.60	15.80	0.70
Sr	4610.00	10000.00	4340.00	2170.00	1120.00	726.00	845.00	881.00	8070.00	906.00	845.00	1290.00	430.00	2380.00	1280.00	1130.00	476.00	883.00
Ta	1.10	1.00	0.40	0.60	0.50	0.50	0.90	1.30	1.20	0.05	0.05	0.30	0.05	0.50	1.70	0.50	1.00	0.05
Th	1285.00	99.30	366.00	785.00	204.00	48.00	404.00	656.00	21.40	2.40	2.85	393.00	4.22	132.00	1000.00	513.00	128.50	16.15
U	34.70	26.90	45.00	53.80	13.00	3.83	22.40	25.30	5.00	2.06	1.01	5.17	1.81	13.80	12.70	10.70	6.07	4.67
Zr	70.00	60.00	340.00	8.00	1.00	228.00	92.00	38.00	325.00	5.00	4.00	29.00	8.00	250.00	130.00	171.00	215.00	18.00
La	1415.00	1355.00	706.00	799.00	1395.00	245.00	1350.00	1265.00	1245.00	11.80	19.50	3470.00	32.50	8330.00	6570.00	3300.00	381.00	62.30
Ce	2600.00	2300.00	1365.00	1485.00	2680.00	437.00	2290.00	2190.00	2610.00	21.80	37.10	5840.00	67.40	11900.00	11050.00	6080.00	679.00	98.60
Pr	267.00	219.00	148.00	158.00	289.00	46.80	242.00	225.00	283.00	2.41	3.61	517.00	6.98	1090.00	1075.00	655.00	74.80	9.07
Nd	923.00	720.00	510.00	536.00	987.00	159.00	803.00	733.00	1040.00	8.40	12.40	1540.00	23.80	2890.00	3120.00	2200.00	270.00	28.60
Sm	172.50	94.90	82.90	116.50	148.50	26.30	123.00	113.50	154.50	2.19	2.92	206.00	6.21	230.00	465.00	425.00	59.80	5.78
Eu	72.30	26.90	29.40	59.90	39.00	7.04	41.10	42.10	42.50	1.20	1.46	60.50	3.08	49.40	129.00	125.00	15.85	2.28
Gd	294.00	92.60	101.00	217.00	137.00	26.80	155.50	164.50	143.00	3.07	3.62	275.00	8.72	265.00	488.00	439.00	53.80	7.82
Tb	74.20	10.45	17.85	42.80	15.70	3.47	27.70	36.40	16.90	0.68	0.66	41.70	1.80	18.95	59.60	56.60	7.06	1.35
Dy	558.00	50.20	103.50	234.00	82.90	17.45	168.00	258.00	67.20	4.26	3.61	225.00	10.15	66.20	262.00	257.00	32.00	7.53
Ho	119.00	9.68	19.35	39.70	17.80	3.42	33.90	57.80	11.75	0.95	0.77	45.40	1.83	12.50	48.00	47.40	6.08	1.42
Er	311.00	29.80	51.80	99.00	58.90	10.20	94.70	165.00	30.20	2.93	2.25	117.00	4.41	39.90	115.00	124.00	16.60	3.51
Tm	35.50	3.79	6.62	13.20	8.60	1.42	12.65	23.10	3.08	0.47	0.35	14.00	0.60	4.61	11.50	16.05	2.20	0.45
Yb	171.50	23.50	41.20	86.80	58.90	9.27	77.70	130.50	15.75	3.19	2.52	72.40	3.50	29.50	54.70	92.20	13.15	2.57
Lu	18.30	3.04	5.51	12.25	7.79	1.36	10.90	17.95	1.89	0.49	0.41	9.06	0.52	3.93	6.98	12.10	1.81	0.34
Y	3140.00	267.00	503.00	997.00	511.00	101.00	948.00	1540.00	269.00	29.00	23.50	1210.00	51.20	345.00	1120.00	1310.00	168.50	40.50
La/Yb	8.25	57.66	17.14	9.21	23.68	26.43	17.37	9.69	79.05	3.70	7.74	47.93	9.29	282.37	120.11	35.79	28.97	24.24

Appendix 2 b) Trace elements analysis of samples collected by Etruscan and NRE and used in this study

Sample No.	ERNI 8064	ERNI 8065	ERNI 8066	ERNI 8067	ERNI 8068	ERNI 8069	ERNI 8070	ERNI 8071	ERNI 8072	ERNI 8073	ERNI 8074	ERNI 8075	ERNI 8076	ERNI 8077	ERNI 8078	ERNI 8079	ERNI 8080	ERNI 8081
Ba	982.00	359.00	830.00	124.00	212.00	6860.00	2300.00	795.00	291.00	65.70	73.20	467.00	165.50	226.00	110.50	576.00	503.00	1345.00
Ga	24.20	4.70	7.00	10.40	6.10	19.80	5.20	9.00	3.80	4.10	3.90	3.90	64.20	26.20	6.50	24.10	25.70	34.80
Hf	10.30	1.40	1.80	14.40	2.80	30.60	1.00	1.40	3.70	0.70	0.30	0.80	6.00	11.30	0.40	0.80	1.10	2.00
Nb	297.00	5.40	29.40	178.50	155.50	237.00	14.60	6.00	3.30	10.80	1.80	31.10	26.00	101.00	63.80	30.00	132.00	484.00
Rb	125.00	28.10	0.60	4.40	0.60	60.20	17.30	8.00	4.20	2.30	1.70	7.20	5.00	10.60	6.20	7.50	9.30	15.00
Sr	1345.00	625.00	430.00	904.00	1995.00	1430.00	387.00	638.00	4250.00	1110.00	1875.00	839.00	1795.00	474.00	1030.00	1540.00	2250.00	1310.00
Ta	12.10	0.10	1.10	2.20	2.40	2.10	0.10	0.10	0.05	0.05	0.05	0.10	0.25	2.10	0.60	0.10	0.20	0.60
Th	19.45	15.90	278.00	1000.00	380.00	226.00	12.80	42.40	24.20	44.40	7.04	16.00	395.00	5.18	20.10	112.50	307.00	368.00
U	8.96	2.01	12.90	12.50	11.45	26.50	9.75	5.23	2.62	2.08	1.64	2.13	4.00	3.28	7.97	4.88	7.92	5.90
Zr	626.00	78.00	112.00	1110.00	143.00	1680.00	50.00	45.00	110.00	53.00	14.00	53.00	780.00	614.00	15.00	72.00	94.00	210.00
La	123.50	11.80	875.00	439.00	807.00	1940.00	164.50	1590.00	310.00	302.00	226.00	79.60	12850.00	76.20	413.00	4060.00	4700.00	7620.00
Ce	234.00	21.70	1635.00	993.00	1375.00	3220.00	250.00	2440.00	527.00	442.00	367.00	167.50	20800.00	140.50	691.00	6490.00	7230.00	10750.00
Pr	24.40	2.33	189.00	143.00	144.50	316.00	23.00	220.00	53.40	43.60	34.60	18.95	2010.00	14.90	73.60	594.00	649.00	961.00
Nd	85.90	8.50	733.00	758.00	497.00	1075.00	69.60	620.00	167.50	131.50	105.50	67.20	6040.00	50.10	240.00	1755.00	1880.00	2540.00
Sm	14.40	2.34	229.00	499.00	131.00	133.50	10.35	72.30	27.00	18.90	14.10	12.95	657.00	8.20	39.80	181.00	193.50	224.00
Eu	4.43	0.75	50.00	169.00	62.00	32.00	3.11	16.75	7.47	4.81	3.44	4.07	144.50	3.56	11.45	39.20	45.60	53.80
Gd	14.60	2.88	162.00	495.00	227.00	139.50	12.55	82.80	30.20	20.40	13.50	14.55	607.00	8.02	39.60	167.00	196.50	262.00
Tb	1.93	0.54	19.40	68.20	46.40	15.75	1.69	8.50	4.44	3.04	1.73	2.82	46.00	1.13	5.67	12.90	18.30	19.40
Dy	9.01	3.27	79.20	300.00	254.00	69.20	8.52	37.50	23.90	17.30	10.25	19.85	166.50	6.20	31.60	45.10	73.40	66.30
Ho	1.67	0.68	13.50	48.30	46.40	13.80	1.76	7.85	5.22	3.95	2.58	5.00	32.50	1.25	6.89	8.80	13.65	11.05
Er	4.50	2.01	33.70	105.50	105.50	39.90	5.08	24.10	15.65	13.45	9.68	17.10	110.00	3.99	22.20	29.60	41.20	33.30
Tm	0.59	0.32	3.91	11.85	12.35	5.18	0.72	3.15	2.27	2.57	1.97	3.02	13.40	0.76	3.83	3.66	5.49	3.77
Yb	3.72	2.32	21.80	61.70	59.70	30.30	4.67	18.45	14.10	18.95	14.85	19.95	75.70	6.54	25.90	22.70	35.10	27.20
Lu	0.53	0.39	2.85	7.59	7.03	4.09	0.70	2.45	1.91	3.12	2.55	3.11	9.69	1.37	4.13	3.48	5.86	4.27
Y	43.80	18.60	366.00	1160.00	1180.00	399.00	53.20	241.00	140.00	142.50	95.40	163.00	969.00	34.60	228.00	291.00	446.00	303.00
La/Yb	33.20	5.09	40.14	7.12	13.52	64.03	35.22	86.18	21.99	15.94	15.22	3.99	169.75	11.65	15.95	178.85	133.90	280.15

Appendix 2 b) Trace elements analysis of samples collected by Etruscan and NRE and used in this study

Sample No.	ERN18082	ERN18083	ERN18084	ERN18085	ERN18086	ERN18087	ERN18088	ERN18089	ERN18090	ERN18091	ERN18092	ERN18093	ERN18094	ERN18095	ERN18096	ERN18097	ERN18098	ERN18099
Ba	931.00	601.00	1245.00	610.00	1420.00	994.00	2540.00	1500.00	273.00	1965.00	1400.00	1190.00	1425.00	1825.00	444.00	146.50	228.00	215.00
Ga	7.90	9.50	26.30	6.60	42.90	26.70	28.00	12.40	4.00	13.10	4.60	3.20	11.90	10.00	7.50	4.90	8.10	17.60
Hf	0.60	2.10	4.00	2.70	1.00	0.80	0.30	12.80	0.30	2.40	0.30	0.20	1.40	3.10	4.90	2.00	3.40	2.50
Nb	77.80	177.00	245.00	226.00	14.00	34.80	12.40	71.40	12.50	52.70	5.60	1.80	230.00	26.20	34.00	44.50	30.80	8.60
Rb	23.40	18.70	53.00	23.10	20.00	16.70	12.80	12.90	3.60	7.70	5.70	2.90	43.20	12.10	18.90	24.70	8.60	9.80
Sr	4970.00	5850.00	909.00	909.00	1545.00	1705.00	5890.00	1990.00	7390.00	8380.00	5110.00	6080.00	1850.00	3430.00	892.00	349.00	907.00	635.00
Ta	0.80	0.40	0.90	0.60	0.25	0.05	0.10	0.20	0.10	0.40	0.05	0.05	1.70	0.20	0.30	0.50	0.40	0.05
Th	59.10	37.10	12.50	7.82	85.40	81.00	84.40	91.50	5.39	61.00	50.40	6.59	5.05	76.90	20.80	13.40	45.00	48.50
U	6.99	21.00	7.87	8.52	9.60	5.29	4.34	8.76	0.87	21.30	1.22	0.99	4.87	9.27	2.78	2.66	1.53	4.19
Zr	26.00	101.00	133.00	60.00	170.00	47.00	12.00	912.00	12.00	111.00	13.00	3.00	64.00	188.00	240.00	97.00	118.00	119.00
La	351.00	329.00	310.00	294.00	8730.00	4850.00	5120.00	1560.00	197.50	1380.00	545.00	239.00	413.00	886.00	406.00	266.00	1005.00	3060.00
Ce	569.00	588.00	524.00	489.00	13450.00	6980.00	8260.00	2510.00	360.00	2600.00	835.00	476.00	804.00	1740.00	672.00	428.00	1685.00	4640.00
Pr	62.20	66.60	52.00	53.60	1245.00	646.00	756.00	257.00	41.10	298.00	78.40	51.60	85.50	229.00	65.70	40.80	168.50	420.00
Nd	202.00	221.00	169.50	173.00	3360.00	1740.00	2200.00	800.00	135.00	1035.00	245.00	176.50	276.00	858.00	203.00	124.00	526.00	1170.00
Sm	35.90	35.30	27.20	26.30	250.00	155.00	198.50	107.00	23.30	150.50	38.60	32.00	38.90	133.50	28.00	16.70	63.10	104.50
Eu	12.55	10.75	9.65	7.67	50.40	33.20	40.00	29.60	7.25	39.80	12.35	9.85	12.05	37.40	7.92	5.33	16.15	24.20
Gd	42.40	37.10	27.30	26.30	277.00	154.00	190.00	102.00	24.40	130.50	42.30	32.20	41.80	112.50	30.10	18.70	63.80	112.50
Tb	6.67	5.53	3.51	3.59	15.35	10.90	13.30	11.15	3.73	15.30	5.95	4.71	5.86	13.20	4.16	2.62	7.60	9.13
Dy	35.60	30.60	17.35	18.50	34.00	31.70	39.70	47.20	21.10	67.50	30.60	26.00	31.70	56.90	23.70	14.75	39.30	34.10
Ho	7.12	6.23	3.30	3.83	5.43	5.50	7.31	8.99	4.50	12.00	5.51	5.01	6.36	9.76	5.12	3.08	7.92	6.28
Er	20.90	17.90	9.73	11.15	20.90	19.60	27.40	27.00	13.35	30.80	15.20	15.50	19.45	28.40	16.65	9.36	24.80	20.20
Tm	3.45	2.72	1.35	1.63	1.75	2.23	3.47	3.81	2.05	3.49	2.10	2.26	2.83	3.70	2.51	1.32	3.56	2.53
Yb	22.90	16.75	8.52	9.90	13.20	16.00	22.50	22.60	12.45	18.05	14.40	15.05	19.00	24.70	16.05	9.19	24.50	17.35
Lu	3.63	2.58	1.30	1.47	1.90	2.48	3.48	3.24	1.86	2.35	2.02	2.19	2.74	3.54	2.26	1.29	3.55	2.66
Y	191.00	169.00	88.20	105.50	152.00	228.00	257.00	251.00	117.00	299.00	139.50	133.50	166.50	232.00	146.50	90.10	221.00	184.00
La/Yb	15.33	19.64	36.38	29.70	661.36	303.13	227.56	69.03	15.86	76.45	37.85	15.88	21.74	35.87	25.30	28.94	41.02	176.37

Appendix 2 b) Trace elements analysis of samples collected by Etruscan and NRE and used in this study

Sample No.	ERN18100	ERN18101	ERN18102	ERN18103	ERN18104	ERN18105	ERN18106	ERN18107	ERN18108	ERN18109	ERN18110	ERN18111	ERN18112	ERN18113	ERN18114	ERN18115	ERN18116	ERN18117
Ba	183.00	3060.00	382.00	463.00	254.00	331.00	4410.00	455.00	2430.00	5350.00	1110.00	1120.00	1385.00	1160.00	674.00	1080.00	38.40	208.00
Ga	7.30	16.00	28.80	38.60	4.70	12.00	19.70	17.40	12.70	25.90	151.00	129.50	34.50	99.10	11.20	11.90	5.70	12.00
Hf	4.50	3.90	14.30	5.00	1.50	2.20	8.80	4.80	1.90	6.00	3.00	11.00	1.10	6.00	2.00	0.80	15.50	1.70
Nb	4.40	61.30	299.00	144.00	5.60	4.50	207.00	33.70	112.50	349.00	110.00	67.00	16.40	232.00	225.00	89.60	56.10	120.50
Rb	2.10	15.20	12.10	4.00	4.80	7.40	11.40	6.80	8.10	20.10	15.00	2.00	11.10	15.00	5.90	2.60	11.80	22.00
Sr	779.00	2690.00	1260.00	783.00	588.00	598.00	6000.00	1595.00	10000.00	3190.00	2700.00	1815.00	1290.00	1670.00	6010.00	8720.00	971.00	6780.00
Ta	0.05	0.40	1.90	0.60	0.20	0.20	2.50	0.30	0.70	9.00	0.90	1.10	0.20	1.10	1.50	0.40	0.50	0.70
Th	130.00	170.50	281.00	591.00	352.00	215.00	114.00	777.00	402.00	192.00	194.50	278.00	425.00	1465.00	39.70	29.00	54.50	4.26
U	2.88	26.30	16.10	18.00	8.52	7.68	5.25	8.67	15.00	17.15	22.40	14.60	9.10	18.10	26.00	20.30	8.71	29.80
Zr	227.00	222.00	821.00	290.00	60.00	148.00	411.00	404.00	92.00	288.00	100.00	260.00	43.00	270.00	171.00	51.00	1540.00	149.00
La	1225.00	1795.00	4110.00	6730.00	285.00	1740.00	1050.00	2600.00	771.00	658.00	24300.00	21700.00	5200.00	16750.00	1085.00	1495.00	591.00	308.00
Ce	1735.00	2720.00	6610.00	9970.00	573.00	2610.00	1645.00	3810.00	1695.00	1800.00	38600.00	33600.00	7490.00	25800.00	1745.00	2330.00	964.00	599.00
Pr	145.00	276.00	711.00	855.00	71.20	246.00	173.50	354.00	204.00	238.00	3690.00	3210.00	646.00	2310.00	166.50	217.00	99.20	66.70
Nd	380.00	820.00	2210.00	2450.00	254.00	753.00	548.00	1080.00	795.00	950.00	10700.00	9530.00	1815.00	6240.00	536.00	674.00	296.00	207.00
Sm	37.50	129.50	326.00	269.00	56.70	105.50	98.30	213.00	183.50	278.00	1150.00	1085.00	187.00	594.00	67.80	86.20	41.80	33.00
Eu	13.20	41.00	77.20	69.40	16.80	29.50	27.70	75.00	57.30	84.10	205.00	210.00	53.60	151.00	20.50	26.70	11.75	9.90
Gd	60.50	155.50	306.00	324.00	73.60	125.00	104.50	272.00	179.50	252.00	1030.00	1010.00	237.00	750.00	70.80	92.10	42.20	34.80
Tb	10.05	22.30	29.90	33.50	16.85	16.30	14.35	44.40	26.30	35.50	70.50	80.80	29.90	77.80	8.04	10.20	4.80	4.85
Dy	60.70	116.00	116.00	157.50	117.50	87.00	69.50	211.00	127.50	157.50	172.00	261.00	149.00	342.00	34.50	42.10	21.00	23.70
Ho	11.15	22.80	20.00	28.60	26.20	18.25	13.15	38.20	25.80	29.10	29.20	46.60	32.90	63.20	6.82	8.16	4.42	5.03
Er	30.90	62.50	57.90	80.60	73.10	51.80	35.20	95.50	71.40	75.00	111.00	152.00	100.00	179.50	19.70	23.10	14.30	14.80
Tm	4.13	7.94	7.23	9.43	10.60	6.86	4.73	12.20	9.21	8.97	8.20	13.95	13.15	18.75	2.30	2.50	2.05	1.95
Yb	27.90	43.80	44.70	56.50	62.60	38.60	27.80	74.00	51.90	49.30	43.20	74.50	76.10	96.20	12.70	13.80	13.15	11.30
Lu	3.90	5.79	6.45	7.92	9.12	5.24	3.83	11.10	6.99	6.38	4.97	8.92	10.55	11.65	1.70	1.88	1.93	1.61
Y	395.00	684.00	542.00	890.00	692.00	510.00	346.00	857.00	681.00	610.00	782.00	1190.00	849.00	1500.00	173.00	199.50	121.50	126.00
La/Yb	43.91	40.98	91.95	119.12	4.55	45.08	37.77	35.14	14.86	13.35	562.50	291.28	68.33	174.12	85.43	108.33	44.94	27.26

Appendix 2 b) Trace elements analysis of samples collected by Etruscan and NRE and used in this study

Sample No.	ERN18118	ERN18119	ERN18120	ERN18121	ERN18122	ERN18123	ERN18124	ERN18125	ERN18126	ERN18127	ERN18128	ERN18129	ERN18130	ERN18131	ERN18132	ERN18133	ERN18134	ERN18135
Ba	525.00	168.50	2250.00	2950.00	161.00	373.00	27.60	726.00	5120.00	217.00	2490.00	992.00	1005.00	1420.00	972.00	2090.00	3700.00	2260.00
Ga	40.70	13.50	20.10	38.80	9.30	4.90	1.50	18.30	38.50	8.40	14.60	5.30	17.60	21.30	15.50	11.00	7.70	10.40
Hf	2.20	0.90	1.00	1.80	2.90	3.10	0.10	4.10	20.30	0.20	1.40	2.60	7.00	4.10	3.40	0.70	19.30	0.50
Nb	44.00	121.50	29.30	72.10	40.90	186.00	2.00	81.10	843.00	31.40	299.00	27.10	111.50	19.30	156.00	36.10	381.00	48.90
Rb	92.00	67.40	1.70	9.50	38.70	5.60	0.50	5.20	72.60	0.50	3.50	73.40	7.80	5.30	21.10	5.10	7.70	2.80
Sr	1515.00	7600.00	10000.00	10000.00	1630.00	8430.00	456.00	1315.00	1660.00	1225.00	3780.00	1065.00	6800.00	1075.00	6470.00	7270.00	5420.00	6400.00
Ta	0.50	1.10	0.20	0.60	0.05	1.40	0.05	0.20	14.40	0.70	1.90	0.20	0.80	0.70	1.40	1.40	2.80	1.20
Th	887.00	9.11	393.00	714.00	7.80	10.80	0.68	202.00	431.00	13.75	108.50	145.00	203.00	1000.00	1000.00	66.00	384.00	31.50
U	9.41	15.90	5.53	10.75	23.30	11.20	0.21	14.15	103.00	5.53	23.20	3.91	8.90	17.45	7.98	9.94	22.20	8.29
Zr	96.00	57.00	41.00	49.00	181.00	149.00	5.00	345.00	1470.00	10.00	97.00	321.00	417.00	223.00	61.00	44.00	593.00	24.00
La	4610.00	235.00	3370.00	6670.00	478.00	219.00	73.80	2330.00	256.00	914.00	1815.00	23.30	887.00	3090.00	1400.00	1365.00	426.00	1250.00
Ce	7760.00	475.00	4690.00	9310.00	808.00	426.00	194.50	3820.00	396.00	1605.00	3010.00	45.30	1265.00	4630.00	2200.00	2180.00	918.00	2020.00
Pr	743.00	54.40	394.00	773.00	86.50	48.70	25.00	373.00	41.50	166.00	294.00	5.49	119.50	439.00	223.00	210.00	131.00	197.00
Nd	2230.00	172.50	1035.00	1940.00	266.00	159.50	86.60	1130.00	133.00	567.00	903.00	22.30	327.00	1350.00	836.00	685.00	556.00	643.00
Sm	445.00	28.90	113.00	199.50	40.60	31.60	15.60	163.00	34.70	74.50	128.50	12.10	44.20	303.00	349.00	93.00	241.00	86.10
Eu	156.50	8.69	32.80	63.70	13.35	10.35	5.51	47.40	15.30	19.20	34.40	6.06	15.85	129.50	126.00	27.00	84.00	24.80
Gd	500.00	29.80	142.00	293.00	43.00	36.00	15.65	166.00	53.40	70.90	129.00	26.20	64.10	483.00	438.00	92.50	245.00	84.60
Tb	53.10	3.98	18.55	43.90	5.51	5.99	2.29	21.00	11.45	7.97	15.40	6.57	12.60	95.80	71.40	10.85	38.90	9.51
Dy	171.00	18.55	101.00	260.00	25.50	32.10	12.20	98.30	72.40	32.80	66.50	43.80	90.10	543.00	349.00	46.80	201.00	40.90
Ho	24.70	3.84	23.40	58.70	5.20	6.89	2.83	20.70	16.65	6.45	13.15	9.83	23.90	111.00	68.20	9.22	42.10	8.11
Er	56.00	11.00	75.30	174.50	15.25	19.40	9.04	61.80	49.10	19.05	37.20	26.80	78.20	289.00	178.50	26.50	120.00	23.10
Tm	4.77	1.41	11.15	23.20	1.94	2.61	1.44	8.09	7.14	2.25	4.37	3.62	11.60	37.10	23.40	3.18	17.35	2.59
Yb	27.00	8.47	71.60	131.50	12.05	14.95	9.95	45.90	41.90	12.65	24.10	19.70	70.50	201.00	133.00	18.10	109.50	14.20
Lu	3.59	1.21	10.75	18.85	1.70	2.12	1.61	6.26	5.77	1.77	3.17	2.60	9.88	27.10	17.60	2.49	16.30	2.00
Y	533.00	90.70	683.00	1615.00	128.00	159.00	117.00	537.00	433.00	174.00	320.00	258.00	955.00	2550.00	2170.00	234.00	896.00	204.00
La/Yb	170.74	27.74	47.07	50.72	39.67	14.65	7.42	50.76	6.11	72.25	75.31	1.18	12.58	15.37	10.53	75.41	3.89	88.03

Appendix 2 b) Trace elements analysis of samples collected by Etruscan and NRE and used in this study

Sample No.	ERN18136	ERN18137	ERN18138	ERN18139	ERN18140	ERN18141	ERN18142	ERN18143	ERN18144	ERN18145	ERN18146	ERN18147	ERN18148	ERN18149	ERN18150	ERN18151	ERN18152	ERN18153
Ba	5080.00	4710.00	456.00	1125.00	548.00	4460.00	5180.00	2130.00	2720.00	2410.00	4050.00	670.00	2710.00	1315.00	997.00	1675.00	3270.00	3250.00
Ga	23.20	20.10	5.90	10.80	2.00	14.50	20.50	11.40	29.30	7.00	10.80	2.60	6.00	10.60	16.10	10.50	7.70	13.10
Hf	6.90	7.30	3.90	1.00	1.40	4.50	5.60	1.80	3.30	1.30	11.00	2.90	2.60	0.80	0.30	0.40	3.60	5.90
Nb	325.00	559.00	31.70	111.50	15.90	199.50	321.00	74.00	113.50	156.00	232.00	13.90	15.10	25.60	33.00	3.40	402.00	280.00
Rb	48.50	27.70	24.80	8.90	3.70	31.60	16.50	4.80	5.90	0.60	8.70	15.30	73.30	1.20	0.70	4.10	2.90	22.10
Sr	10000.00	8970.00	1155.00	7780.00	520.00	2510.00	4540.00	10000.00	2920.00	6610.00	1690.00	884.00	555.00	7000.00	3400.00	7900.00	10000.00	5150.00
Ta	4.70	4.60	0.20	1.20	0.10	1.10	4.50	1.30	1.20	0.50	2.70	0.20	0.30	0.20	0.10	0.10	1.30	2.70
Th	385.00	1000.00	239.00	40.00	8.77	145.50	396.00	299.00	619.00	47.20	1000.00	483.00	56.60	162.50	87.50	189.50	1000.00	929.00
U	18.50	30.50	7.59	18.35	1.56	16.30	17.65	6.70	10.65	24.00	8.19	4.47	2.74	7.20	5.84	3.79	38.10	12.60
Zr	562.00	349.00	457.00	62.00	102.00	169.00	272.00	97.00	230.00	80.00	572.00	181.00	203.00	23.00	13.00	15.00	172.00	293.00
La	588.00	541.00	423.00	1245.00	10.80	396.00	829.00	1045.00	6050.00	966.00	706.00	16.80	85.60	1335.00	2770.00	1235.00	885.00	546.00
Ce	1180.00	857.00	718.00	2010.00	22.30	1010.00	1860.00	2240.00	7610.00	1635.00	1390.00	39.60	119.50	2300.00	4080.00	2280.00	1460.00	882.00
Pr	144.50	95.80	76.30	197.00	2.85	171.50	292.00	261.00	617.00	168.00	191.00	5.71	11.70	242.00	374.00	247.00	155.50	91.20
Nd	513.00	336.00	227.00	647.00	11.60	781.00	1465.00	940.00	1685.00	571.00	1085.00	27.40	42.50	828.00	1145.00	855.00	564.00	336.00
Sm	128.00	137.00	44.60	88.40	4.23	162.50	400.00	188.50	188.00	82.20	607.00	27.80	11.15	127.50	126.50	123.00	173.00	143.50
Eu	45.80	70.40	16.30	26.00	1.83	41.20	103.50	54.00	49.90	25.20	161.50	12.60	3.65	37.40	28.40	31.50	80.40	65.10
Gd	152.50	256.00	66.90	89.30	6.81	131.00	310.00	186.50	231.00	84.40	461.00	52.40	13.90	131.50	122.00	111.00	303.00	229.00
Tb	29.90	59.50	13.85	10.60	1.62	20.90	44.10	27.00	28.80	11.55	56.60	9.06	2.51	19.40	11.50	13.00	71.50	44.10
Dy	171.00	340.00	83.80	44.50	10.35	103.50	196.00	143.00	162.00	62.80	250.00	44.60	15.55	118.00	51.60	65.90	489.00	251.00
Ho	34.90	65.80	17.65	8.59	2.25	20.70	36.60	26.50	33.10	11.50	37.10	6.92	3.14	25.00	10.70	13.95	97.40	42.50
Er	91.80	158.50	45.90	23.60	6.28	56.10	97.20	72.60	97.90	30.30	80.20	15.95	9.19	74.50	35.70	49.10	270.00	99.50
Tm	11.75	19.70	5.73	2.63	0.90	6.96	11.95	9.19	12.80	3.46	8.23	1.99	1.35	9.56	4.98	8.49	36.50	11.80
Yb	63.90	106.50	30.20	14.55	5.52	40.00	68.60	53.60	77.30	18.50	45.20	11.55	8.65	51.10	32.70	64.20	216.00	63.80
Lu	8.30	14.35	4.04	1.95	0.81	5.45	9.17	6.73	9.93	2.26	5.62	1.45	1.19	6.01	4.50	9.61	26.80	7.61
Y	832.00	1455.00	431.00	203.00	59.30	404.00	871.00	759.00	1025.00	303.00	664.00	175.00	90.10	744.00	325.00	390.00	2610.00	1010.00
La/Yb	9.20	5.08	14.01	85.57	1.96	9.90	12.08	19.50	78.27	52.22	15.62	1.45	9.90	26.13	84.71	19.24	4.10	8.56

Appendix 2 b) Trace elements analysis of samples collected by Etruscan and NRE and used in this study

Sample No.	ERN18154	ERN18155	ERN18156	ERN18157	ERN18158	ERN18159	ERN18160	ERN18161	ERN18162	ERN18163	ERN18164	ERN18165	ERN18166	ERN18167	ERN18168	ERN18169	ERN18170	ERN18171
Ba	2740.00	2410.00	10000.00	3260.00	1975.00	1255.00	980.00	325.00	131.00	605.00	982.00	171.00	513.00	507.00	794.00	241.00	149.00	977.00
Ga	11.70	19.80	57.60	19.70	15.10	10.10	25.00	14.20	12.60	33.60	8.10	11.50	13.10	12.10	11.50	7.30	5.10	88.10
Hf	1.20	3.10	3.00	10.30	6.20	0.60	4.40	0.80	0.70	1.50	0.40	8.10	4.90	1.00	4.90	1.50	2.00	7.00
Nb	17.60	38.10	167.00	409.00	232.00	16.40	29.00	5.10	87.00	10.00	110.00	93.20	388.00	141.00	20.70	4.20	442.00	94.00
Rb	20.20	11.20	7.00	4.20	2.90	3.00	12.20	10.90	10.80	16.10	3.20	6.20	12.60	1.80	12.00	8.70	14.20	4.00
Sr	2340.00	10000.00	5430.00	9480.00	7430.00	10000.00	1185.00	936.00	726.00	738.00	10000.00	1265.00	1480.00	1090.00	796.00	1220.00	1910.00	1060.00
Ta	0.20	0.50	1.20	4.00	1.90	0.20	0.60	0.20	0.40	0.40	0.80	0.60	1.20	0.40	0.10	0.10	0.70	0.60
Th	723.00	649.00	728.00	362.00	539.00	223.00	710.00	511.00	699.00	941.00	33.60	900.00	886.00	121.00	274.00	79.00	18.95	2200.00
U	9.68	3.84	34.60	13.80	14.20	12.30	19.70	6.56	7.48	8.06	7.50	14.30	9.14	9.24	4.83	4.08	15.15	27.30
Zr	27.00	79.00	120.00	378.00	213.00	12.00	327.00	7.00	7.00	20.00	11.00	599.00	188.00	38.00	383.00	84.00	109.00	370.00
La	1100.00	3120.00	9510.00	2050.00	1950.00	1430.00	4810.00	2120.00	1810.00	4910.00	863.00	970.00	1260.00	1450.00	1080.00	665.00	282.00	22200.00
Ce	1840.00	4330.00	14350.00	3120.00	2920.00	2220.00	6760.00	3290.00	2920.00	7990.00	1490.00	1995.00	2530.00	2650.00	1910.00	1205.00	521.00	26300.00
Pr	214.00	392.00	1370.00	301.00	267.00	209.00	601.00	317.00	288.00	787.00	155.00	230.00	290.00	284.00	202.00	128.00	54.70	2060.00
Nd	912.00	1260.00	3820.00	970.00	812.00	662.00	1745.00	993.00	922.00	2490.00	518.00	847.00	1070.00	988.00	734.00	435.00	187.50	4960.00
Sm	275.00	227.00	403.00	168.00	123.00	96.10	192.50	122.50	114.50	321.00	71.40	150.50	180.00	146.00	258.00	65.30	31.10	382.00
Eu	78.70	64.00	101.00	47.80	40.70	26.70	54.30	30.30	32.50	86.00	19.75	57.90	69.80	42.40	80.30	18.25	9.32	113.00
Gd	265.00	240.00	448.00	177.50	168.00	107.00	241.00	128.00	126.50	345.00	66.70	215.00	281.00	149.00	226.00	65.10	32.30	644.00
Tb	40.50	31.90	52.00	26.20	31.70	15.90	47.90	23.20	23.10	53.60	6.92	54.80	80.60	22.20	23.80	8.86	4.46	76.50
Dy	216.00	170.50	282.00	158.00	222.00	101.00	397.00	180.50	170.00	336.00	28.80	430.00	618.00	140.00	103.00	47.60	24.40	339.00
Ho	39.00	33.20	63.50	33.90	49.60	22.10	95.60	41.60	36.90	67.00	4.83	94.70	119.00	30.90	18.85	9.63	4.79	49.50
Er	105.50	100.50	205.00	111.00	153.50	70.50	303.00	119.50	108.50	181.00	13.10	279.00	283.00	100.50	57.10	30.40	13.85	106.00
Tm	14.20	14.45	26.30	17.25	22.90	10.60	41.50	15.05	15.05	21.00	1.46	35.80	29.00	14.75	8.39	4.61	1.88	8.15
Yb	87.10	94.00	142.50	113.50	143.00	69.00	231.00	80.40	93.40	107.00	8.98	180.50	125.50	87.60	58.20	30.80	11.25	39.40
Lu	11.25	12.25	17.85	15.35	19.05	9.02	27.20	9.29	12.35	12.15	1.20	19.90	13.65	11.25	7.92	4.39	1.53	4.87
Y	958.00	877.00	1870.00	983.00	1300.00	702.00	3880.00	1340.00	1020.00	1825.00	126.00	2730.00	3230.00	909.00	658.00	291.00	130.00	930.00
La/Yb	12.63	33.19	66.74	18.06	13.64	20.72	20.82	26.37	19.38	45.89	96.10	5.37	10.04	16.55	18.56	21.59	25.07	563.45

Appendix 2 b) Trace elements analysis of samples collected by Etruscan and NRE and used in this study

Sample No.	ERN18172	ERN18173	ERN18174	ERN18175	ERN18176	ERN18177	ERN18178	ERN18179	ERN18180	ERN18181	ERN18182	ERN18183	ERN18184	ERN18185	ERN18186	ERN18187	ERN18188	ERN18189
Ba	413.00	461.00	568.00	306.00	1715.00	776.00	1655.00	935.00	638.00	386.00	970.00	638.00	243.00	1115.00	768.00	843.00	1800.00	3350.00
Ga	7.80	7.50	16.90	13.60	24.70	22.10	17.40	15.20	5.80	8.80	14.30	19.20	15.10	4.40	29.90	5.20	23.10	28.70
Hf	0.70	4.60	3.20	2.40	0.80	2.40	2.60	1.30	0.20	0.60	0.70	17.30	1.90	21.30	1.70	2.40	9.90	1.80
Nb	40.10	148.50	10.40	91.40	15.00	204.00	243.00	46.30	6.10	13.40	54.40	332.00	123.50	135.00	53.00	27.70	52.30	35.20
Rb	5.80	4.70	18.90	12.50	30.70	12.30	39.40	5.50	5.70	8.10	8.00	73.70	4.70	22.00	6.90	3.40	80.50	8.20
Sr	778.00	6890.00	624.00	640.00	1045.00	1265.00	704.00	972.00	3340.00	1830.00	2260.00	4150.00	791.00	485.00	1020.00	3660.00	118.00	1385.00
Ta	0.20	0.60	0.10	0.80	0.20	0.80	0.90	0.20	0.10	0.20	0.40	5.70	0.20	0.70	0.20	0.20	1.10	0.30
Th	79.60	14.40	107.00	102.00	273.00	169.00	490.00	117.00	6.85	23.50	175.50	6.30	128.00	212.00	346.00	19.45	19.90	198.00
U	11.20	2.50	25.90	10.75	7.13	9.76	8.49	14.75	3.14	4.18	8.23	12.50	10.45	11.05	8.99	1.41	3.58	9.87
Zr	44.00	249.00	274.00	195.00	34.00	161.00	104.00	65.00	4.00	17.00	34.00	1560.00	183.00	2150.00	116.00	108.00	444.00	112.00
La	773.00	287.00	2360.00	955.00	3520.00	3400.00	2010.00	2500.00	529.00	910.00	2320.00	336.00	2850.00	224.00	6070.00	372.00	148.00	4240.00
Ce	1315.00	512.00	3410.00	1395.00	5080.00	5380.00	2860.00	3470.00	863.00	1590.00	3020.00	550.00	3840.00	353.00	8230.00	670.00	198.50	6970.00
Pr	136.00	52.50	320.00	128.00	459.00	509.00	257.00	304.00	89.00	175.50	242.00	52.10	319.00	34.00	673.00	71.00	17.85	690.00
Nd	446.00	171.00	942.00	387.00	1380.00	1575.00	772.00	873.00	257.00	554.00	660.00	164.00	864.00	111.50	1810.00	267.00	54.00	2260.00
Sm	63.90	26.30	102.00	51.40	169.50	181.50	144.00	110.00	38.20	87.90	84.80	23.70	83.80	23.90	155.00	67.60	7.20	301.00
Eu	16.70	7.58	24.10	14.75	45.70	49.60	58.40	30.90	10.75	24.40	29.20	6.98	23.50	9.90	40.20	22.70	1.88	70.80
Gd	61.40	28.30	102.00	56.90	182.00	202.00	206.00	136.00	43.90	91.10	123.00	27.00	108.00	40.70	213.00	79.90	7.90	291.00
Tb	7.42	3.88	9.77	7.20	21.30	22.30	30.90	15.50	5.79	12.15	15.15	3.42	11.65	9.12	21.50	13.30	0.87	31.00
Dy	37.80	21.30	45.90	37.30	116.50	95.80	161.50	74.10	30.70	63.70	70.50	17.95	60.70	64.60	97.80	77.50	4.13	137.00
Ho	7.36	4.37	9.16	6.95	24.60	16.70	29.90	15.35	6.49	13.40	12.50	3.62	12.30	14.05	18.50	15.90	0.83	25.40
Er	22.50	13.25	29.90	19.60	78.70	48.40	84.90	46.70	20.30	42.20	35.30	10.95	38.00	39.40	56.50	46.10	2.93	74.40
Tm	2.97	1.92	4.03	2.48	11.35	6.19	11.85	6.75	3.15	6.72	4.82	1.54	5.06	5.21	7.39	6.42	0.55	9.01
Yb	18.50	12.85	27.00	15.40	75.50	40.70	78.00	41.70	20.20	45.30	32.00	9.69	31.30	30.00	47.80	39.20	5.25	54.10
Lu	2.41	1.81	3.91	2.05	10.35	5.71	10.95	5.92	3.03	6.90	4.50	1.32	4.24	4.01	6.44	5.03	1.06	7.05
Y	226.00	117.00	310.00	163.00	789.00	430.00	646.00	407.00	169.00	355.00	309.00	93.80	314.00	394.00	495.00	344.00	24.00	716.00
La/Yb	41.78	22.33	87.41	62.01	46.62	83.54	25.77	59.95	26.19	20.09	72.50	34.67	91.05	7.47	126.99	9.49	28.19	78.37

Appendix 2 b) Trace elements analysis of samples collected by Etruscan and NRE and used in this study

Sample No.	ERN18190	ERN18191	ERN18192	ERN18193	ERN18194	ERN18195	ERN18196	ERN18197	ERN18198	ERN18199	ERN18200	ERN18202	ERN18203	ERN18204	ERN18205	ERN18206	ERN18207	ERN18208
Ba	1425.00	863.00	737.00	2080.00	3990.00	5640.00	10000.00	2930.00	2960.00	2330.00	748.00	273.00	1040.00	370.00	101.50	165.00	287.00	343.00
Ga	22.70	9.40	6.90	75.60	6.00	13.20	1.80	1.40	113.50	16.00	27.70	4.30	26.00	6.40	17.60	8.30	13.70	3.90
Hf	28.30	2.00	0.90	2.00	0.40	2.60	0.20	0.10	8.00	9.10	4.70	0.50	3.40	8.80	4.90	1.30	2.60	1.10
Nb	75.00	131.50	5.00	29.00	6.90	178.00	0.60	0.20	233.00	65.30	117.00	107.00	7.60	18.60	5.50	9.20	10.00	6.00
Rb	14.50	11.10	7.00	13.00	4.90	4.10	1.40	1.00	15.00	2.00	6.00	1.30	1.30	2.60	1.50	0.90	4.60	3.70
Sr	2960.00	453.00	6920.00	1065.00	1315.00	2040.00	3750.00	1180.00	2100.00	10000.00	665.00	2050.00	1200.00	1040.00	4040.00	2120.00	2030.00	1720.00
Ta	0.50	1.70	0.10	0.50	0.05	0.50	0.05	0.05	2.10	0.30	0.30	0.20	0.10	0.20	0.50	0.20	0.10	0.05
Th	550.00	23.20	32.60	145.00	95.30	552.00	5.61	1.97	4170.00	37.00	64.10	21.30	69.30	59.10	156.00	143.00	109.00	25.20
U	23.90	9.48	2.95	5.60	3.77	6.60	3.01	0.66	36.10	4.26	5.70	2.81	3.26	1.02	4.58	1.99	1.44	1.02
Zr	2770.00	156.00	56.00	60.00	19.00	218.00	11.00	2.00	130.00	661.00	330.00	16.00	264.00	581.00	277.00	52.00	173.00	67.00
La	3720.00	801.00	545.00	11300.00	410.00	1720.00	21.40	23.50	22000.00	1625.00	2860.00	342.00	5940.00	846.00	3310.00	832.00	1675.00	214.00
Ce	5370.00	1250.00	1055.00	19600.00	676.00	2730.00	37.40	39.20	33700.00	3180.00	5480.00	633.00	8170.00	1295.00	5000.00	1770.00	2900.00	397.00
Pr	471.00	118.50	119.50	2080.00	68.80	259.00	3.94	3.99	3110.00	347.00	604.00	62.60	673.00	121.50	440.00	192.00	292.00	40.50
Nd	1465.00	374.00	443.00	6490.00	232.00	812.00	14.80	13.10	8780.00	1245.00	2180.00	211.00	1795.00	377.00	1330.00	674.00	956.00	139.00
Sm	247.00	48.80	73.10	819.00	40.80	108.00	3.67	2.41	1220.00	172.50	333.00	36.40	148.50	53.00	181.50	122.50	143.50	27.00
Eu	77.80	15.20	21.10	149.50	13.00	31.90	2.88	0.90	403.00	45.30	89.50	10.80	36.50	16.75	61.20	38.20	38.60	8.25
Gd	308.00	53.80	74.00	675.00	46.90	132.00	4.70	2.84	1630.00	150.50	304.00	40.20	214.00	71.60	270.00	141.50	149.00	28.90
Tb	40.50	5.97	11.25	53.50	7.01	19.95	0.73	0.46	232.00	15.05	27.40	5.56	15.90	13.20	46.30	22.10	17.20	4.70
Dy	194.00	25.90	67.60	158.00	41.10	113.00	3.96	2.95	1045.00	57.40	81.70	32.10	56.80	89.90	295.00	107.00	75.50	30.30
Ho	35.50	4.53	14.95	27.10	8.53	22.40	0.77	0.76	167.50	9.73	10.90	6.67	12.25	21.40	62.90	19.25	14.60	7.00
Er	99.10	12.15	47.80	90.30	25.30	66.40	2.24	2.95	396.00	27.60	27.70	19.25	43.80	66.60	180.00	49.90	44.90	24.20
Tm	13.20	1.34	7.56	8.20	3.63	9.73	0.36	0.54	38.10	2.96	2.18	2.87	5.70	10.65	25.30	7.39	6.78	4.32
Yb	82.20	7.65	50.70	46.40	23.00	62.50	2.73	4.62	178.00	17.55	13.60	17.85	32.80	65.00	126.50	46.30	43.40	28.20
Lu	11.15	0.99	6.78	5.49	3.05	8.58	0.44	0.98	20.20	2.17	1.76	2.40	4.46	9.10	15.30	6.50	6.03	3.95
Y	920.00	118.00	440.00	648.00	268.00	677.00	24.20	23.40	3810.00	226.00	300.00	175.00	408.00	707.00	1915.00	501.00	414.00	225.00
La/Yb	45.26	104.71	10.75	243.53	17.83	27.52	7.84	5.09	123.60	92.59	210.29	19.16	181.10	13.02	26.17	17.97	38.59	7.59

Appendix 2 b) Trace elements analysis of samples collected by Etruscan and NRE and used in this study

Sample No.	ERNI8209	ERNI8210	ERNI8211	ERNI8212	ERNI8213	ERNI8214	ERNI8215	ERNI8216	ERNI8217	ERNI8218	ERNI8219	ERNI8220	ERNI8221	ERNI8222	ERNI8223	ERNI8224	ERNI8225	ERNI8226
Ba	426.00	244.00	179.50	587.00	282.00	341.00	339.00	4230.00	161.00	446.00	1440.00	309.00	1095.00	355.00	309.00	602.00	201.00	360.00
Ga	2.80	3.30	3.80	15.00	13.60	3.10	16.20	14.40	43.20	3.00	11.60	22.80	6.20	4.70	10.80	7.30	30.60	23.70
Hf	0.30	0.40	0.30	4.00	0.50	1.10	1.30	27.90	2.00	0.20	0.20	2.00	0.20	0.80	0.70	5.40	1.00	1.80
Nb	33.40	0.80	2.50	91.00	4.90	30.00	22.70	492.00	35.00	2.50	1.20	3.10	57.60	14.60	99.10	3.10	1.90	5.90
Rb	0.10	0.30	0.70	13.50	0.40	1.30	0.60	18.20	1.00	0.10	3.80	3.90	4.60	7.80	4.50	5.50	1.90	18.00
Sr	3710.00	3250.00	1790.00	2310.00	1670.00	7350.00	2190.00	7730.00	1995.00	2010.00	1300.00	798.00	1145.00	1080.00	3930.00	947.00	1460.00	946.00
Ta	0.05	0.10	0.05	0.80	0.10	0.20	0.20	2.40	0.25	0.05	0.05	0.10	0.20	0.10	0.40	0.10	0.10	0.10
Th	14.15	7.54	6.13	589.00	165.00	82.10	260.00	97.10	506.00	12.30	41.70	212.00	18.15	10.70	23.80	116.00	383.00	75.70
U	1.79	0.03	0.03	10.65	7.13	5.24	14.50	31.50	5.10	0.43	7.60	1.87	1.80	3.66	4.75	2.82	2.52	3.63
Zr	14.00	6.00	8.00	205.00	25.00	32.00	45.00	1940.00	90.00	12.00	12.00	100.00	11.00	47.00	35.00	331.00	43.00	80.00
La	301.00	102.50	57.90	2700.00	3070.00	395.00	3570.00	1605.00	8830.00	85.90	1305.00	4930.00	891.00	292.00	1585.00	767.00	7140.00	5860.00
Ce	570.00	188.00	124.00	3510.00	3800.00	622.00	5030.00	2580.00	13200.00	157.00	2590.00	6890.00	1150.00	573.00	2570.00	1275.00	9520.00	6840.00
Pr	56.30	18.85	13.75	295.00	305.00	58.00	408.00	245.00	1195.00	16.35	277.00	579.00	91.20	58.10	244.00	129.50	793.00	515.00
Nd	180.50	63.60	52.10	847.00	808.00	190.00	1095.00	790.00	3190.00	57.90	907.00	1605.00	248.00	197.50	742.00	454.00	2210.00	1270.00
Sm	30.10	14.40	15.05	144.50	85.40	36.00	96.90	107.50	340.00	11.70	95.30	197.00	29.30	34.10	91.90	89.80	240.00	94.60
Eu	8.76	5.88	5.77	53.50	22.10	9.99	24.90	30.30	92.90	3.90	19.80	57.90	8.91	9.71	25.00	27.20	66.40	23.00
Gd	34.00	22.60	21.70	228.00	115.50	40.20	148.00	114.00	470.00	13.70	88.40	253.00	40.60	39.00	101.50	102.00	310.00	155.00
Tb	4.75	6.56	5.56	42.40	12.00	6.04	14.60	13.35	43.90	2.69	6.59	29.60	4.90	6.10	10.30	14.65	29.00	11.10
Dy	26.90	58.50	43.10	270.00	66.00	34.50	73.70	61.70	175.00	19.30	18.20	140.00	27.50	37.30	44.00	73.80	101.50	36.50
Ho	5.91	17.45	11.35	58.50	16.70	7.48	16.45	12.40	31.70	4.79	3.30	28.20	6.39	8.51	8.54	15.40	16.55	6.48
Er	17.55	63.30	39.10	160.50	61.60	22.20	52.10	33.80	101.00	16.90	13.25	79.00	21.20	26.50	25.90	47.70	45.20	20.50
Tm	2.71	11.85	6.73	22.70	11.25	3.50	7.72	4.21	11.15	3.28	1.75	10.75	3.59	4.18	3.56	7.89	4.93	2.35
Yb	16.90	75.90	42.20	122.00	72.60	20.70	47.50	21.70	64.00	23.00	13.40	64.60	24.40	27.00	22.90	50.20	29.30	15.45
Lu	2.32	10.55	6.01	14.80	10.00	2.72	6.46	2.56	8.07	3.58	2.13	8.97	3.59	3.81	3.11	7.38	4.21	2.37
Y	150.00	562.00	331.00	1730.00	586.00	189.50	443.00	320.00	914.00	128.00	84.30	934.00	170.00	243.00	214.00	469.00	420.00	210.00
La/Yb	17.81	1.35	1.37	22.13	42.29	19.08	75.16	73.96	137.97	3.73	97.39	76.32	36.52	10.81	69.21	15.28	243.69	379.29

Appendix 2 b) Trace elements analysis of samples collected by Etruscan and NRE and used in this study

Sample No.	ERNI 8227	ERNI 8228	ERNI 8229	ERNI 8230	ERNI 8231	ERNI 8232	ERNI 8233	ERNI 8234	ERNI 8235	ERNI 8236	ERNI 8237	ERNI 8238	ERNI 8239	ERNI 8240	ERNI 8241	ERNI 8242	ERNI 8243	ERNI 8244
Ba	398.00	160.50	254.00	116.00	275.00	403.00	10000.00	174.00	377.00	734.00	322.00	692.00	489.00	4260.00	213.00	903.00	671.00	388.00
Ga	38.80	34.90	6.10	7.80	8.90	54.00	19.50	5.30	24.10	10.00	2.30	24.30	5.30	9.10	4.10	7.00	7.80	18.40
Hf	3.00	6.00	0.80	0.70	1.00	3.00	7.60	0.50	13.90	17.30	1.00	0.50	0.90	1.00	0.50	0.40	0.30	2.20
Nb	7.00	7.00	5.60	4.70	622.00	56.00	110.00	26.20	327.00	193.50	2.40	11.70	14.30	19.60	2.20	1.80	7.90	23.00
Rb	4.00	5.00	3.10	3.20	4.70	15.00	2.40	10.20	11.20	21.20	4.10	17.10	16.50	17.10	3.90	9.50	25.90	39.30
Sr	1455.00	866.00	788.00	1590.00	1895.00	4430.00	933.00	3160.00	414.00	889.00	1210.00	3030.00	1210.00	1870.00	1295.00	1235.00	2850.00	578.00
Ta	0.25	0.25	0.05	0.05	1.40	0.25	1.00	0.10	3.60	1.00	0.05	0.10	0.10	0.10	0.05	0.05	0.10	0.10
Th	123.00	282.00	21.90	44.90	46.40	631.00	919.00	7.28	18.90	34.90	10.75	106.50	3.55	177.00	24.90	40.20	7.57	138.00
U	5.40	4.00	2.63	3.70	8.31	3.20	21.10	0.81	7.03	2.91	2.47	1.81	1.65	2.38	4.27	2.83	1.23	4.37
Zr	190.00	360.00	35.00	36.00	52.00	150.00	495.00	21.00	726.00	785.00	67.00	14.00	36.00	32.00	23.00	12.00	2.00	99.00
La	7370.00	9110.00	853.00	1495.00	1810.00	14300.00	1915.00	335.00	263.00	292.00	68.10	5100.00	315.00	1815.00	342.00	1010.00	289.00	972.00
Ce	11500.00	11000.00	1290.00	2100.00	2510.00	18550.00	4710.00	681.00	440.00	493.00	137.00	7100.00	516.00	2410.00	532.00	1380.00	601.00	1925.00
Pr	1080.00	856.00	116.50	174.00	208.00	1515.00	565.00	69.60	43.40	50.70	16.15	611.00	52.10	206.00	51.70	122.50	69.90	228.00
Nd	2920.00	2050.00	349.00	493.00	571.00	3770.00	2140.00	230.00	139.00	170.50	58.50	1635.00	160.50	562.00	154.50	335.00	245.00	812.00
Sm	226.00	231.00	43.30	64.10	62.20	315.00	456.00	31.30	19.40	31.60	12.10	132.00	22.80	63.90	19.45	31.20	45.30	121.50
Eu	51.90	88.90	10.90	17.60	16.65	85.50	119.50	8.58	5.47	10.05	4.08	33.90	6.53	24.10	5.36	8.30	13.70	33.10
Gd	314.00	433.00	49.20	78.60	81.00	532.00	407.00	34.10	19.65	33.20	13.75	195.50	25.80	106.00	22.00	43.10	45.50	116.00
Tb	19.70	55.40	5.20	8.21	8.95	48.00	48.60	4.20	2.10	4.45	2.27	13.40	3.17	13.55	2.31	3.80	5.95	13.65
Dy	43.60	268.00	24.00	35.10	46.40	184.00	210.00	20.40	9.05	23.00	13.45	40.20	16.20	55.70	11.05	15.60	29.60	50.20
Ho	7.55	44.40	4.69	6.95	10.80	31.90	37.30	4.24	1.69	4.50	2.89	6.58	3.31	8.56	2.45	3.13	5.75	7.64
Er	31.90	109.00	14.20	20.40	35.20	95.50	99.80	13.05	5.68	13.25	9.24	21.90	10.15	24.70	9.24	10.85	17.75	20.80
Tm	2.41	11.75	2.07	3.07	5.71	10.05	13.40	1.88	0.88	1.90	1.42	2.21	1.45	3.78	1.52	1.52	2.60	2.47
Yb	16.60	77.10	13.95	20.50	36.60	59.90	75.80	11.75	6.36	11.95	9.91	15.75	9.47	29.50	11.45	10.60	17.65	17.55
Lu	2.34	11.10	2.04	2.94	5.17	7.21	9.73	1.70	1.02	1.66	1.45	2.34	1.35	4.46	1.71	1.59	2.61	2.74
Y	236.00	1200.00	138.00	207.00	353.00	854.00	980.00	99.50	53.10	120.00	95.90	178.00	90.70	206.00	104.00	126.00	159.50	189.00
La/Yb	443.98	118.16	61.15	72.93	49.45	238.73	25.26	28.51	41.35	24.44	6.87	323.81	33.26	61.53	29.87	95.28	16.37	55.38

Appendix 2 b) Trace elements analysis of samples collected by Etruscan and NRE and used in this study

Sample No.	ERN18245	ERN18246	ERN18247	ERN18248	ERN18249	ERN18250	ERN18251	ERN18252	ERN18253	ERN18254	ERN18255	ERN18256	ERN18257	ERN18258	ERN18259	ERN18260	ERN18261	ERN18262
Ba	60.90	58.70	390.00	581.00	2120.00	314.00	58.50	441.00	61.40	1860.00	247.00	271.00	112.00	47.10	914.00	177.00	185.50	66.70
Ga	3.90	7.40	18.30	7.10	12.50	9.20	27.70	6.90	4.10	7.50	5.10	6.60	18.70	6.10	5.60	7.00	21.60	46.40
Hf	0.30	0.60	3.70	0.50	1.00	0.70	2.00	0.80	16.60	2.40	1.40	4.70	2.70	3.70	2.50	21.60	6.40	2.00
Nb	1.80	119.50	8.80	6.60	11.00	384.00	8.00	48.70	31.20	234.00	64.80	65.50	219.00	56.50	146.00	232.00	183.50	11.00
Rb	5.20	3.10	5.20	2.40	4.20	2.40	0.50	9.70	1.00	1.40	5.50	5.00	1.70	2.20	1.00	17.30	4.60	6.00
Sr	622.00	1740.00	2350.00	10000.00	2430.00	2260.00	1735.00	6130.00	472.00	6950.00	476.00	4350.00	443.00	164.00	7340.00	153.50	670.00	606.00
Ta	0.05	0.20	0.60	0.20	0.20	1.90	0.50	0.20	0.30	0.60	0.10	0.40	9.50	0.50	0.50	1.70	1.00	0.25
Th	19.45	86.80	822.00	167.50	519.00	32.00	1875.00	83.40	286.00	38.70	73.10	528.00	53.00	39.70	671.00	321.00	241.00	586.00
U	3.51	19.65	6.32	19.10	3.45	16.45	18.20	15.90	48.30	7.28	2.56	17.70	13.25	4.92	30.90	34.60	24.50	11.50
Zr	8.00	9.00	44.00	3.00	36.00	47.00	10.00	52.00	1570.00	165.00	89.00	181.00	210.00	209.00	126.00	2030.00	563.00	140.00
La	198.50	602.00	2440.00	830.00	2210.00	1270.00	6590.00	1265.00	155.00	1085.00	78.70	587.00	36.50	33.00	559.00	261.00	2140.00	8510.00
Ce	365.00	1030.00	4060.00	1320.00	3090.00	2140.00	10900.00	2120.00	270.00	2120.00	172.00	1075.00	69.10	55.70	1065.00	470.00	4370.00	13350.00
Pr	38.80	114.00	469.00	134.00	277.00	227.00	1030.00	212.00	31.00	232.00	21.40	120.00	8.21	7.01	119.50	51.60	534.00	1290.00
Nd	130.50	384.00	1985.00	440.00	790.00	737.00	3290.00	684.00	113.00	804.00	85.90	395.00	30.70	25.80	399.00	182.00	1865.00	3710.00
Sm	21.50	72.70	734.00	65.70	98.80	99.60	459.00	94.90	34.20	114.50	26.70	76.60	8.94	6.19	113.00	46.10	275.00	432.00
Eu	6.61	22.80	246.00	18.75	27.10	28.90	145.50	26.80	21.10	29.10	9.73	29.80	2.67	2.26	60.00	23.30	66.50	102.50
Gd	20.80	88.40	852.00	75.60	133.00	106.50	613.00	98.60	96.90	105.00	31.20	109.50	12.80	10.05	193.00	105.50	237.00	415.00
Tb	3.45	16.60	145.50	11.25	17.35	11.70	101.00	11.40	26.60	12.15	5.06	19.15	3.01	2.59	37.40	29.30	25.80	42.10
Dy	21.20	104.00	781.00	71.70	99.30	48.70	588.00	52.40	177.50	51.90	27.00	106.00	20.50	18.70	220.00	199.50	90.30	189.00
Ho	4.76	22.80	141.00	17.70	22.60	8.82	106.50	9.66	36.10	8.86	5.14	22.40	4.66	4.18	46.00	43.00	15.40	34.10
Er	14.75	71.80	330.00	63.80	80.30	24.90	278.00	27.10	103.00	24.00	14.50	65.10	14.75	11.25	125.50	118.50	47.00	91.70
Tm	2.47	12.25	39.50	10.55	13.45	2.70	28.90	3.11	14.70	2.57	2.00	9.39	2.37	1.45	17.00	16.50	5.47	9.72
Yb	16.15	77.30	191.50	70.40	92.70	15.40	141.00	19.10	96.10	14.20	13.95	58.70	16.10	8.26	98.30	99.10	35.30	57.60
Lu	2.71	11.80	24.40	9.54	12.95	1.90	15.90	2.45	13.50	1.69	1.99	8.30	2.41	1.16	12.50	13.50	4.87	7.33
Y	133.00	533.00	3610.00	567.00	685.00	235.00	2870.00	251.00	963.00	220.00	138.50	543.00	125.00	103.50	1080.00	1070.00	355.00	905.00
La/Yb	12.29	7.79	12.74	11.79	23.84	82.47	46.74	66.23	1.61	76.41	5.64	10.00	2.27	4.00	5.69	2.63	60.62	147.74

Appendix 2 b) Trace elements analysis of samples collected by Etruscan and NRE and used in this study

Sample No.	ERN18263	ERN18264	ERN18265	ERN18266	ERN18267	ERN18268	ERN18269	ERN18270	ERN18271	ERN18272	ERN18273	ERN18274	ERN18275	ERN18276	ERN18277	ERN18278	ERN18279	ERN18280
Ba	497.00	114.50	764.00	1145.00	75.70	1680.00	172.50	906.00	148.50	81.10	54.20	108.50	57.50	78.20	24.10	119.00	10000.00	40.80
Ga	27.80	3.70	6.50	7.40	5.70	29.70	12.50	13.80	2.50	4.10	2.70	10.90	10.30	11.20	1.00	3.90	8.50	1.20
Hf	1.70	0.20	2.30	0.70	2.30	8.10	0.80	1.90	0.40	0.90	0.30	1.20	5.20	6.60	0.20	0.70	1.00	2.60
Nb	25.80	1.60	11.30	23.10	18.90	208.00	10.70	51.30	7.10	11.70	5.00	9.20	80.40	100.50	0.60	8.50	278.00	8.70
Rb	26.40	7.50	19.30	2.00	4.10	1.50	4.70	1.50	1.80	9.80	6.50	4.70	2.40	11.50	2.00	7.90	7.00	4.20
Sr	679.00	150.00	349.00	337.00	442.00	430.00	375.00	539.00	506.00	199.50	180.00	253.00	264.00	470.00	211.00	573.00	819.00	597.00
Ta	0.30	0.05	0.20	0.10	0.20	0.30	0.10	0.20	0.05	0.10	0.10	0.10	4.40	5.20	0.05	0.10	1.40	0.05
Th	472.00	3.41	7.14	91.60	161.00	131.50	159.00	66.60	26.10	10.80	1.08	255.00	29.30	13.10	4.38	3.83	103.50	12.85
U	9.19	2.82	1.54	4.56	6.76	12.85	9.73	24.10	1.31	4.52	0.83	8.92	13.30	14.20	1.66	1.62	19.70	3.25
Zr	48.00	18.00	101.00	54.00	182.00	512.00	49.00	225.00	28.00	87.00	16.00	97.00	311.00	386.00	11.00	42.00	220.00	308.00
La	5290.00	11.90	24.20	704.00	814.00	5290.00	2090.00	1790.00	172.50	90.60	8.50	1870.00	91.60	116.50	5.50	35.00	1240.00	25.40
Ce	8030.00	19.80	42.00	1180.00	1280.00	8260.00	3050.00	3030.00	272.00	146.00	15.00	2830.00	175.00	231.00	12.10	62.50	2010.00	41.30
Pr	733.00	2.01	4.55	122.50	132.50	772.00	292.00	328.00	26.80	14.55	1.65	278.00	20.60	28.30	1.65	6.54	201.00	4.21
Nd	2140.00	7.10	15.10	382.00	400.00	2240.00	824.00	1045.00	84.10	47.20	6.10	807.00	74.70	105.50	6.90	22.70	623.00	13.90
Sm	275.00	1.74	3.56	57.80	58.90	209.00	91.20	150.00	12.80	7.84	1.56	97.30	12.45	19.10	2.45	4.20	76.00	3.09
Eu	65.50	0.74	1.23	16.30	16.45	39.50	24.60	37.00	3.73	2.04	0.59	27.40	3.54	5.11	0.79	1.21	20.40	1.17
Gd	322.00	2.78	5.07	66.60	67.30	259.00	117.00	152.50	14.50	8.91	2.07	119.00	12.75	17.70	2.97	5.04	70.70	4.65
Tb	41.60	0.64	1.21	9.80	9.10	23.90	13.55	18.15	1.87	1.33	0.41	14.90	1.58	2.39	0.61	0.88	7.78	1.10
Dy	205.00	4.39	8.77	51.80	44.40	88.80	61.20	77.10	9.06	6.64	2.27	71.90	6.67	10.40	3.22	5.20	37.20	7.95
Ho	42.40	1.00	2.08	10.85	9.11	18.50	12.75	14.30	1.82	1.40	0.48	15.05	1.25	2.00	0.63	1.17	7.04	1.89
Er	120.00	2.96	6.75	29.80	26.60	64.30	40.30	40.70	5.34	4.07	1.36	46.00	3.23	5.72	1.74	3.55	19.50	5.67
Tm	15.90	0.41	1.06	3.96	3.62	8.56	5.59	4.69	0.73	0.53	0.17	6.06	0.25	0.77	0.27	0.50	2.29	0.85
Yb	89.00	3.12	6.65	20.80	20.90	56.40	35.40	26.70	4.86	3.41	1.26	39.30	2.44	5.32	2.10	3.38	14.40	5.39
Lu	11.65	0.47	1.06	2.86	2.86	7.70	4.87	3.50	0.68	0.51	0.20	5.18	0.35	0.81	0.35	0.48	1.79	0.71
Y	1075.00	26.90	61.70	291.00	248.00	513.00	374.00	355.00	45.30	36.50	11.60	426.00	28.30	47.00	14.20	30.50	195.00	54.70
La/Yb	59.44	3.81	3.64	33.85	38.95	93.79	59.04	67.04	35.49	26.57	6.75	47.58	37.54	21.90	2.62	10.36	86.11	4.71

Appendix 2 b) Trace elements analysis of samples collected by Etruscan and NRE and used in this study

Sample No.	ERN18281	ERN18282	ERN18283	ERN18284	ERN18285	ERN18286	ERN18287	ERN18288	ERN18289	ERN18290	ERN18291	ERN18292	ERN18293	ERN18294	ERN18295	ERN18296	ERN18297	ERN18298
Ba	78.50	192.00	330.00	1825.00	123.50	2370.00	167.00	1060.00	59.70	972.00	222.00	166.00	40.50	74.10	10000.00	2230.00	662.00	1265.00
Ga	8.90	4.90	9.10	10.60	10.80	9.00	9.80	9.20	37.30	17.80	10.90	8.60	23.30	12.30	16.70	25.50	5.60	17.20
Hf	0.50	3.00	1.00	0.60	0.70	2.00	1.30	0.80	1.00	1.00	1.10	1.70	0.70	1.80	1.00	4.00	0.60	0.50
Nb	83.40	11.90	7.30	142.00	14.00	55.60	6.10	19.80	3.00	11.40	123.50	63.80	10.90	646.00	20.00	19.00	25.80	27.10
Rb	10.20	7.50	8.70	3.10	2.40	1.10	7.40	2.90	1.00	7.10	16.60	9.50	1.80	1.50	2.00	8.00	0.40	1.60
Sr	674.00	500.00	730.00	712.00	841.00	7600.00	582.00	7160.00	1635.00	457.00	926.00	1000.00	753.00	1175.00	1760.00	1600.00	5130.00	2770.00
Ta	0.10	0.10	0.10	0.20	0.10	0.30	0.20	0.10	0.25	0.20	0.80	0.30	0.20	4.20	0.60	1.00	0.20	0.30
Th	84.50	333.00	102.50	37.30	106.00	40.20	101.00	171.50	320.00	466.00	194.50	38.00	177.00	129.00	256.00	1015.00	47.00	202.00
U	1.69	13.60	1.97	9.79	14.80	8.54	7.23	4.34	4.30	3.75	16.00	12.45	3.56	21.00	37.20	19.80	5.32	12.55
Zr	18.00	232.00	44.00	41.00	31.00	80.00	36.00	26.00	100.00	26.00	69.00	174.00	31.00	218.00	70.00	120.00	19.00	5.00
La	1525.00	598.00	916.00	1155.00	930.00	1555.00	1025.00	1110.00	7970.00	3080.00	1885.00	991.00	4270.00	1490.00	2530.00	2830.00	479.00	2740.00
Ce	2140.00	909.00	1555.00	2070.00	1540.00	2140.00	1770.00	1790.00	10600.00	4660.00	2680.00	1630.00	6150.00	2490.00	3830.00	4950.00	763.00	3860.00
Pr	205.00	90.30	176.00	236.00	158.50	207.00	192.50	188.00	888.00	451.00	259.00	171.00	556.00	273.00	377.00	540.00	81.40	352.00
Nd	590.00	279.00	624.00	769.00	494.00	604.00	632.00	589.00	2270.00	1350.00	774.00	535.00	1655.00	928.00	1170.00	1845.00	266.00	967.00
Sm	71.30	46.90	113.00	105.00	78.70	72.60	94.70	86.20	181.00	188.00	105.50	75.20	171.50	170.50	151.00	340.00	48.50	103.00
Eu	19.45	11.20	30.10	29.90	21.40	22.20	25.90	26.40	47.50	55.10	28.50	20.30	37.90	55.40	41.00	126.50	14.45	24.20
Gd	86.10	64.60	115.50	105.50	95.10	87.60	102.00	99.90	231.00	232.00	117.00	76.30	201.00	187.00	172.50	485.00	55.40	129.50
Tb	10.40	13.00	16.15	12.15	14.15	9.27	13.80	13.05	21.70	30.00	14.65	8.48	21.00	26.50	26.20	111.50	8.76	13.85
Dy	50.20	84.10	79.50	50.00	78.50	42.10	69.80	60.80	101.00	141.00	72.50	35.10	92.60	127.00	173.50	800.00	51.60	75.00
Ho	10.70	18.60	16.55	9.36	18.45	8.87	15.40	12.45	18.70	28.50	14.85	6.48	20.40	23.70	39.20	177.00	11.75	18.70
Er	32.40	53.00	50.30	28.00	60.30	28.90	47.90	35.80	55.90	83.10	43.70	17.95	65.90	62.00	120.50	506.00	39.30	64.70
Tm	4.26	7.10	7.21	3.40	9.23	4.12	7.10	4.85	6.49	11.10	5.54	1.99	8.88	7.56	16.80	65.70	6.36	9.73
Yb	25.00	41.50	46.10	19.55	61.50	27.60	46.10	30.40	40.50	68.50	32.90	11.85	55.70	43.70	102.00	376.00	44.60	64.90
Lu	3.34	5.46	6.31	2.54	8.54	4.02	6.55	4.26	5.28	9.42	4.27	1.60	7.51	5.62	12.90	47.10	6.89	9.36
Y	256.00	495.00	457.00	230.00	543.00	233.00	429.00	332.00	514.00	748.00	427.00	173.50	575.00	549.00	994.00	4360.00	332.00	583.00
La/Yb	61.00	14.41	19.87	59.08	15.12	56.34	22.23	36.51	196.79	44.96	57.29	83.63	76.66	34.10	24.80	7.53	10.74	42.22

Appendix 2 b) Trace elements analysis of samples collected by Etruscan and NRE and used in this study

Sample No.	ERN18299	ERN18300	ERN18301	ERN18302	ERN18303	ERN18304	ERN18305	ERN18306	ERN18307	ERN18308	ERN18309	ERN18310	ERN18311	ERN18312	ERN18313	ERN18314	ERN18315	ERN18316
Ba	489.00	178.00	27.30	271.00	93.60	28.40	199.00	319.00	63.10	81.50	28.10	190.50	110.00	148.00	385.00	304.00	1210.00	356.00
Ga	23.50	21.90	29.80	3.50	8.30	28.90	10.50	26.20	8.20	29.70	9.10	8.90	12.00	6.60	6.10	9.30	13.10	5.30
Hf	1.10	2.70	0.60	0.50	0.60	4.90	0.50	13.50	0.90	3.00	0.90	2.50	1.00	1.40	0.40	21.00	0.60	0.90
Nb	5.00	27.30	3.80	0.30	46.50	5.50	58.20	294.00	87.00	2.60	93.00	105.00	58.90	40.10	163.50	593.00	37.90	35.80
Rb	2.50	7.10	1.30	11.30	1.80	0.70	10.90	97.50	0.70	0.80	2.60	6.60	17.60	32.50	1.20	34.00	10.90	6.00
Sr	1480.00	1060.00	1065.00	349.00	455.00	166.50	1220.00	273.00	2590.00	198.50	1445.00	627.00	351.00	690.00	3680.00	745.00	916.00	3050.00
Ta	0.20	0.40	0.10	0.05	0.30	0.40	0.30	17.30	0.30	0.10	0.40	2.60	0.90	0.20	0.40	1.30	0.10	0.20
Th	474.00	480.00	264.00	1.61	204.00	24.80	83.20	26.20	23.90	11.85	17.95	592.00	499.00	177.50	77.40	1450.00	71.10	41.80
U	6.25	21.70	2.50	6.27	12.05	1.59	16.70	13.45	17.45	1.83	11.20	19.10	11.35	3.98	13.30	28.70	2.71	1.94
Zr	17.00	204.00	9.00	18.00	9.00	171.00	13.00	1015.00	53.00	108.00	63.00	38.00	13.00	68.00	17.00	2060.00	17.00	34.00
La	4130.00	3190.00	4380.00	11.10	651.00	48.60	1225.00	104.50	916.00	63.50	1090.00	1075.00	1145.00	494.00	680.00	634.00	1525.00	285.00
Ce	5630.00	5080.00	7700.00	21.70	1060.00	88.80	2030.00	208.00	1600.00	108.50	1845.00	1825.00	1920.00	892.00	1145.00	1165.00	3150.00	563.00
Pr	491.00	495.00	750.00	2.95	112.00	9.71	212.00	23.80	173.50	11.55	201.00	197.50	205.00	97.50	114.00	125.00	379.00	61.50
Nd	1425.00	1605.00	2170.00	12.80	370.00	34.60	679.00	81.60	563.00	38.50	651.00	649.00	661.00	341.00	361.00	491.00	1415.00	216.00
Sm	178.00	243.00	185.50	4.38	63.20	6.32	96.60	13.50	80.60	6.35	88.90	105.00	133.50	90.40	53.20	234.00	221.00	41.90
Eu	49.70	66.10	40.50	1.54	22.90	1.63	27.50	3.87	22.40	1.39	22.70	45.20	47.80	30.60	14.45	98.10	56.40	12.35
Gd	236.00	278.00	240.00	5.60	89.20	8.05	108.00	13.50	82.70	7.01	94.60	188.00	194.00	99.50	54.80	311.00	180.50	43.90
Tb	32.10	37.00	20.90	1.08	15.70	1.68	13.40	1.88	9.19	1.05	10.25	54.40	29.80	13.00	7.45	46.60	20.20	6.75
Dy	181.00	183.00	78.90	6.26	87.60	10.85	68.30	8.78	34.60	5.40	40.00	403.00	131.00	66.20	41.10	258.00	85.30	38.60
Ho	38.90	36.90	17.10	1.26	16.65	2.27	15.35	1.71	5.97	1.12	7.37	88.60	21.10	12.40	8.11	50.40	13.80	7.72
Er	114.00	106.50	56.90	3.50	43.10	6.09	50.90	4.85	16.80	3.41	20.90	233.00	47.40	34.80	24.80	150.50	35.90	23.70
Tm	15.60	12.75	5.99	0.51	5.03	0.73	7.27	0.64	1.71	0.48	2.22	27.00	4.48	4.54	3.47	22.10	3.50	3.49
Yb	96.10	71.00	34.60	3.69	25.60	3.73	44.10	4.08	10.05	3.10	12.85	128.00	21.80	30.30	24.00	137.50	19.90	23.70
Lu	13.25	9.01	4.40	0.52	2.99	0.48	5.74	0.58	1.31	0.46	1.65	14.70	2.51	4.00	3.19	18.10	2.26	3.16
Y	989.00	1050.00	463.00	34.30	380.00	60.20	403.00	42.70	147.00	30.10	184.50	2200.00	455.00	339.00	202.00	1440.00	311.00	195.50
La/Yb	42.98	44.93	126.59	3.01	25.43	13.03	27.78	25.61	91.14	20.48	84.82	8.40	52.52	16.30	28.33	4.61	76.63	12.03

Appendix 2 b) Trace elements analysis of samples collected by Etruscan and NRE and used in this study

Sample No.	ERNI8317	ERNI8318	ERNI8319	ERNI8320	ERNI8321	ERNI8322	ERNI8323	ERNI8324	ERNI8325	ERNI8326	ERNI8327	ERNI8328	ERNI8329	ERNI8330	ERNI8331	ERNI8332	ERNI8333	ERNI8334
Ba	769.00	636.00	497.00	103.00	289.00	1110.00	190.00	442.00	395.00	930.00	346.00	531.00	230.00	343.00	2540.00	626.00	662.00	1265.00
Ga	7.20	10.40	11.90	11.70	12.60	11.30	2.90	11.70	18.20	9.70	7.10	6.50	4.80	12.70	13.70	10.10	12.10	13.70
Hf	0.70	2.80	0.90	6.40	14.10	3.10	2.70	1.10	7.30	6.30	6.10	4.20	2.30	96.00	3.00	1.00	1.00	0.70
Nb	78.00	111.50	64.60	8.80	222.00	28.60	30.50	75.30	73.00	72.40	16.60	119.50	78.90	119.00	545.00	190.00	51.10	4.80
Rb	18.10	1.30	5.30	2.70	6.60	3.90	11.50	8.80	3.70	3.30	3.80	22.10	4.00	32.00	1.00	2.00	8.90	1.10
Sr	1255.00	7400.00	4170.00	328.00	610.00	1310.00	621.00	4030.00	952.00	580.00	6780.00	713.00	724.00	3780.00	10000.00	10000.00	1350.00	2990.00
Ta	0.30	0.60	0.10	0.50	1.10	0.20	0.10	0.10	0.20	0.20	0.10	1.60	0.40	0.60	5.70	1.30	0.80	0.50
Th	30.90	431.00	68.10	12.30	371.00	137.00	31.00	105.50	964.00	239.00	413.00	361.00	105.50	4590.00	117.00	355.00	184.00	256.00
U	4.93	16.35	4.83	2.17	15.20	11.35	4.47	7.61	10.50	8.09	9.39	4.46	3.59	121.00	26.20	22.10	5.70	8.13
Zr	30.00	140.00	43.00	233.00	1080.00	210.00	248.00	47.00	649.00	494.00	491.00	138.00	146.00	8830.00	190.00	90.00	18.00	16.00
La	1205.00	1605.00	2330.00	47.50	266.00	1865.00	127.00	1115.00	3660.00	1225.00	1155.00	644.00	233.00	860.00	629.00	1700.00	2060.00	2650.00
Ce	1910.00	2850.00	3230.00	96.80	536.00	2660.00	227.00	2490.00	5830.00	1975.00	1785.00	1070.00	403.00	1825.00	1180.00	2660.00	3180.00	4080.00
Pr	185.00	300.00	285.00	11.75	64.60	247.00	24.80	310.00	566.00	197.50	168.50	108.50	43.80	237.00	128.00	253.00	357.00	423.00
Nd	561.00	987.00	808.00	45.60	256.00	745.00	86.20	1195.00	1715.00	641.00	513.00	352.00	160.00	1055.00	448.00	791.00	1220.00	1335.00
Sm	73.40	139.50	88.20	9.65	68.50	95.50	17.05	196.50	217.00	102.50	86.60	66.70	59.50	402.00	66.40	108.50	181.00	139.00
Eu	19.65	36.90	23.30	2.41	24.30	26.40	5.61	53.50	58.90	26.50	31.20	20.70	19.30	146.00	19.70	33.10	48.20	30.40
Gd	74.80	145.00	97.10	10.10	92.60	102.00	20.10	165.50	260.00	106.50	120.50	76.80	61.80	499.00	68.70	127.00	187.00	133.00
Tb	8.83	21.50	10.20	1.67	18.25	13.35	3.38	19.80	31.70	11.25	18.85	12.05	9.40	89.90	9.36	17.85	32.00	17.65
Dy	43.70	134.50	50.40	9.95	116.00	79.90	21.60	90.90	130.00	43.00	98.00	68.90	55.10	458.00	53.20	101.50	219.00	114.50
Ho	8.15	29.50	10.05	2.08	22.90	17.75	4.62	16.45	18.90	6.69	17.15	13.00	10.85	74.00	11.00	19.60	47.60	27.10
Er	24.30	91.50	32.20	6.45	65.00	59.30	15.05	48.50	46.90	18.70	49.40	35.40	30.30	172.00	31.20	54.10	131.50	88.20
Tm	3.10	12.70	4.30	0.91	8.59	8.59	2.21	6.01	4.88	2.49	7.28	4.46	4.02	21.30	4.14	7.07	17.75	13.85
Yb	19.55	82.20	28.20	6.23	50.10	56.80	15.15	36.30	29.60	18.00	50.30	27.00	25.30	135.50	23.90	41.70	90.40	85.50
Lu	2.48	10.70	3.66	0.89	6.25	7.59	2.09	4.22	3.77	2.55	6.93	3.38	3.23	19.10	3.06	5.41	9.95	11.10
Y	197.50	797.00	307.00	57.00	604.00	488.00	127.50	444.00	413.00	152.00	426.00	335.00	313.00	1705.00	290.00	494.00	1320.00	769.00
La/Yb	61.64	19.53	82.62	7.62	5.31	32.83	8.38	30.72	123.65	68.06	22.96	23.85	9.21	6.35	26.32	40.77	22.79	30.99

Appendix 2 b) Trace elements analysis of samples collected by Etruscan and NRE and used in this study

Sample No.	ERN18335	ERN18336	ERN18337	ERN18338	ERN18339	ERN18340	ERN18341	ERN18342	ERN18343	ERN18344	ERN18345	ERN18346	ERN18347	ERN18348	ERN18349	ERN18350	ERN18351	ERN18352
Ba	2030.00	474.00	432.00	333.00	926.00	590.00	138.00	793.00	2370.00	548.00	1935.00	1785.00	1435.00	446.00	4420.00	193.50	270.00	542.00
Ga	15.40	37.70	32.50	19.00	26.60	28.20	3.40	26.90	8.00	20.20	8.60	7.50	25.00	13.10	8.90	9.80	42.00	18.70
Hf	6.10	5.70	1.00	4.00	7.00	384.00	3.40	1.10	2.00	1.90	0.90	6.50	1.00	10.70	9.20	2.00	1.00	0.60
Nb	45.20	537.00	12.00	19.00	12.00	181.00	60.10	3.70	237.00	158.50	28.10	465.00	52.60	100.00	90.10	370.00	14.00	50.50
Rb	4.10	26.10	25.00	2.00	9.00	49.00	6.70	0.30	2.00	3.00	6.50	1.40	0.40	6.90	5.20	1.00	16.00	13.00
Sr	9420.00	2040.00	10000.00	10000.00	1315.00	3740.00	176.50	6690.00	10000.00	5430.00	1295.00	9880.00	4110.00	1315.00	9000.00	10000.00	1895.00	1595.00
Ta	0.70	3.20	0.25	0.25	0.25	0.50	0.30	0.50	1.30	1.30	0.50	3.40	1.50	2.00	0.50	2.80	0.25	0.40
Th	924.00	72.50	1100.00	1845.00	1490.00	257.00	36.10	362.00	241.00	267.00	358.00	471.00	335.00	221.00	302.00	55.50	547.00	230.00
U	16.40	18.75	8.10	13.10	20.70	26.70	1.61	5.74	14.50	10.85	11.40	27.10	10.55	9.93	25.50	12.30	9.90	9.77
Zr	397.00	471.00	60.00	410.00	620.00	22800.00	273.00	42.00	140.00	95.00	37.00	371.00	24.00	629.00	768.00	220.00	50.00	10.00
La	3510.00	2300.00	7690.00	4100.00	6920.00	1065.00	250.00	5650.00	1460.00	4690.00	1220.00	854.00	6730.00	2320.00	1380.00	980.00	6430.00	2960.00
Ce	4710.00	2990.00	10550.00	6180.00	10150.00	1915.00	519.00	9410.00	1900.00	6810.00	1920.00	1560.00	8490.00	3310.00	2500.00	1685.00	13450.00	5890.00
Pr	394.00	239.00	865.00	585.00	916.00	198.00	58.00	939.00	164.00	600.00	204.00	166.50	795.00	358.00	271.00	168.00	1530.00	669.00
Nd	1095.00	622.00	2340.00	1860.00	2750.00	687.00	206.00	3080.00	489.00	1695.00	637.00	581.00	2200.00	1155.00	944.00	541.00	5340.00	2440.00
Sm	147.50	54.80	250.00	349.00	404.00	119.00	29.70	408.00	63.10	185.50	80.80	99.70	206.00	147.50	132.00	69.00	763.00	370.00
Eu	44.20	12.15	65.30	106.00	127.00	31.90	5.84	80.80	18.40	44.50	19.85	30.20	46.00	37.80	32.70	19.30	161.00	72.80
Gd	194.50	64.30	325.00	404.00	507.00	114.00	21.90	333.00	74.20	190.00	82.80	113.50	231.00	153.50	113.50	68.70	572.00	291.00
Tb	33.20	5.89	34.10	53.90	62.40	14.45	2.34	33.00	9.11	19.50	12.20	21.50	27.90	23.20	13.80	6.92	50.80	28.80
Dy	196.00	28.50	162.00	238.00	270.00	82.60	9.60	137.50	56.40	93.90	73.40	147.50	168.50	145.50	72.60	29.50	177.00	112.50
Ho	37.40	6.26	30.80	35.40	40.60	19.30	1.76	25.50	13.85	18.50	14.70	32.40	39.40	31.60	15.40	5.33	28.70	20.30
Er	100.00	20.80	90.40	84.20	93.70	72.80	5.32	75.20	49.40	54.70	40.20	92.10	126.50	89.30	48.40	15.10	84.40	58.80
Tm	14.55	3.26	11.65	10.35	9.55	13.25	0.81	10.20	7.51	7.69	5.68	13.30	19.50	12.45	8.20	1.74	8.52	7.47
Yb	90.50	21.50	73.60	67.80	55.40	99.00	6.52	63.50	42.50	50.70	33.60	73.60	114.50	69.60	60.90	9.90	53.60	49.30
Lu	11.60	3.04	9.55	9.35	7.05	14.95	1.23	8.10	5.23	7.00	4.36	8.85	14.05	8.39	9.11	1.25	7.02	6.38
Y	931.00	198.00	713.00	736.00	910.00	567.00	45.30	757.00	464.00	588.00	412.00	896.00	1205.00	923.00	410.00	132.00	794.00	592.00
La/Yb	38.78	106.98	104.48	60.47	124.91	10.76	38.34	88.98	34.35	92.50	36.31	11.60	58.78	33.33	22.66	98.99	119.96	60.04

Appendix 2 b) Trace elements analysis of samples collected by Etruscan and NRE and used in this study

Sample No.	ERN18353	ERN18354	ERN18355	ERN18356	ERN18357	ERN18358	ERN18359	ERN18370	ERN18371	ERN18372	ERN18373	ERN18374	ERN18375	ERN18376	ERN18377	ERN18378	ERN18379	ERN18380
Ba	68.00	88.80	133.50	88.20	274.00	2480.00	585.00	332.00	2460.00	521.00	1010.00	286.00	475.00	620.00	102.50	542.00	526.00	608.00
Ga	12.40	21.20	10.40	10.70	11.10	17.00	5.50	9.60	6.30	26.10	16.60	10.30	14.20	8.40	12.60	16.20	6.90	13.70
Hf	0.60	0.70	1.70	0.80	1.00	1.00	0.80	2.50	1.20	13.00	4.10	3.00	1.70	0.40	3.00	2.00	1.50	4.00
Nb	7.40	58.40	47.10	53.40	9.80	8.00	3.70	169.00	9.70	383.00	404.00	402.00	79.20	4.30	6.00	441.00	78.10	257.00
Rb	4.50	31.60	12.50	3.80	11.00	2.00	3.40	7.70	1.70	62.90	23.60	22.00	2.90	2.40	0.50	7.00	7.70	14.00
Sr	3880.00	1960.00	2710.00	1500.00	1115.00	10000.00	1615.00	4050.00	1065.00	845.00	5300.00	4820.00	2590.00	1690.00	2430.00	4270.00	8950.00	3910.00
Ta	0.10	0.40	0.20	0.70	0.20	0.25	0.30	3.00	0.60	8.50	1.80	1.90	2.10	0.40	0.70	3.40	0.50	2.80
Th	340.00	355.00	187.50	164.50	203.00	264.00	254.00	32.00	272.00	873.00	283.00	1555.00	198.00	159.00	1735.00	2080.00	356.00	1365.00
U	3.00	10.30	5.28	11.15	2.42	1.50	7.56	11.60	23.20	13.45	10.05	42.40	16.55	4.30	9.60	35.40	20.80	13.30
Zr	13.00	4.00	83.00	11.00	48.00	40.00	7.00	174.00	15.00	809.00	194.00	170.00	67.00	15.00	10.00	30.00	61.00	280.00
La	2940.00	3960.00	1530.00	1155.00	1245.00	1935.00	326.00	892.00	423.00	529.00	1205.00	1400.00	1260.00	867.00	3180.00	1415.00	966.00	1060.00
Ce	4280.00	6190.00	2660.00	2140.00	2540.00	4430.00	879.00	1550.00	1345.00	1060.00	1890.00	2250.00	3240.00	2190.00	5070.00	2690.00	1760.00	1665.00
Pr	412.00	615.00	298.00	244.00	313.00	572.00	118.50	164.00	210.00	135.50	187.50	207.00	416.00	272.00	490.00	293.00	189.00	173.00
Nd	1290.00	2020.00	1130.00	937.00	1205.00	2190.00	484.00	530.00	920.00	591.00	614.00	665.00	1565.00	941.00	1615.00	1135.00	627.00	577.00
Sm	178.50	344.00	270.00	239.00	251.00	401.00	154.00	70.50	212.00	248.00	121.50	125.00	230.00	117.50	400.00	429.00	93.00	128.50
Eu	48.00	90.10	54.60	61.60	55.30	103.00	53.00	18.85	60.80	84.80	38.70	48.20	52.10	24.20	178.50	193.50	29.40	49.50
Gd	182.50	315.00	213.00	222.00	178.00	327.00	151.50	70.40	198.50	255.00	130.50	180.50	194.50	90.80	726.00	667.00	105.00	162.00
Tb	21.40	36.10	24.80	31.40	21.20	35.30	30.00	8.07	33.40	40.40	18.60	35.80	24.30	7.90	150.50	112.00	16.80	30.20
Dy	98.40	170.00	112.50	163.50	90.20	140.50	182.50	38.80	199.50	208.00	93.40	235.00	133.00	24.60	878.00	561.00	98.70	191.00
Ho	19.75	33.30	21.20	31.60	16.65	23.50	38.40	7.60	42.50	38.50	16.95	48.30	29.90	4.05	153.00	92.80	21.00	37.30
Er	56.50	93.80	58.70	82.30	49.60	63.40	116.50	22.90	130.50	105.00	45.40	134.00	93.90	13.90	365.00	222.00	64.70	98.20
Tm	7.70	12.50	7.95	11.00	6.21	7.50	15.30	2.93	18.25	13.40	5.38	18.20	12.70	1.68	41.90	25.90	9.01	12.30
Yb	50.50	79.80	52.30	66.50	40.50	47.90	90.60	17.10	113.00	73.30	31.00	108.00	76.70	12.50	238.00	146.00	54.90	75.70
Lu	6.72	10.45	6.90	8.81	5.41	6.33	10.95	2.25	15.70	8.87	4.09	13.90	10.60	2.04	29.90	18.15	7.18	9.50
Y	543.00	945.00	573.00	883.00	458.00	544.00	1190.00	205.00	1555.00	1205.00	471.00	1335.00	1110.00	107.50	3900.00	2450.00	626.00	997.00
La/Yb	58.22	49.62	29.25	17.37	30.74	40.40	3.60	52.16	3.74	7.22	38.87	12.96	16.43	69.36	13.36	9.69	17.60	14.00

Appendix 2 b) Trace elements analysis of samples collected by Etruscan and NRE and used in this study

Sample No.	ERN18381	ERN18382	ERN18383	ERN18384	ERN18385	ERN18386	ERN18387	ERN18388	ERN18389	ERN18390	ERN18392	ERN18393	ERN18394	ERN18395	ERN18396	ERN18397	ERN18398	ERN18399
Ba	138.50	252.00	106.00	369.00	2610.00	97.70	21.80	691.00	1155.00	573.00	224.00	214.00	351.00	1005.00	372.00	527.00	140.00	189.00
Ga	8.20	7.80	20.70	13.20	10.80	28.80	7.00	11.90	9.20	7.40	11.10	10.00	4.40	8.70	12.10	7.10	13.10	8.80
Hf	2.00	2.20	2.50	2.00	0.80	1.00	0.80	3.90	2.00	4.60	0.80	2.60	0.10	3.20	0.70	1.10	3.80	2.40
Nb	332.00	74.80	33.70	121.00	63.70	66.00	72.00	305.00	300.00	35.70	330.00	109.50	1.60	102.00	23.60	70.20	341.00	87.10
Rb	8.00	0.80	11.10	15.00	16.00	0.50	0.90	0.50	10.90	5.00	14.30	8.70	1.20	16.80	2.40	2.10	1.60	7.70
Sr	2660.00	4760.00	5030.00	5480.00	3210.00	1985.00	3090.00	8570.00	6920.00	8110.00	7140.00	3790.00	360.00	4160.00	8370.00	5690.00	1895.00	2500.00
Ta	2.30	0.60	0.80	1.20	0.70	0.25	0.60	2.50	3.60	1.00	2.00	0.60	0.30	1.50	0.50	0.70	5.80	0.20
Th	1615.00	644.00	987.00	1320.00	589.00	1655.00	159.00	720.00	290.00	923.00	198.00	217.00	34.40	50.40	503.00	157.00	646.00	154.50
U	30.50	14.40	4.64	11.50	5.01	26.50	16.45	13.70	12.55	10.35	10.75	8.49	1.95	5.10	4.75	14.55	24.90	16.85
Zr	50.00	44.00	45.00	30.00	7.00	10.00	22.00	207.00	104.00	113.00	27.00	94.00	6.00	235.00	6.00	53.00	251.00	151.00
La	1875.00	1220.00	5780.00	2500.00	1450.00	8340.00	959.00	877.00	1000.00	1005.00	1040.00	1185.00	260.00	477.00	1465.00	633.00	841.00	772.00
Ce	3000.00	2470.00	8710.00	4010.00	2880.00	12750.00	2040.00	1655.00	1715.00	1945.00	2220.00	2380.00	549.00	899.00	3160.00	1430.00	1580.00	1120.00
Pr	282.00	306.00	826.00	379.00	342.00	1140.00	253.00	201.00	176.50	227.00	273.00	270.00	62.90	101.00	383.00	184.50	199.00	108.00
Nd	943.00	1200.00	2410.00	1220.00	1325.00	3290.00	989.00	848.00	578.00	862.00	1045.00	968.00	208.00	350.00	1400.00	717.00	883.00	352.00
Sm	194.00	297.00	301.00	210.00	275.00	343.00	202.00	283.00	96.70	242.00	206.00	197.50	29.50	55.90	216.00	160.00	288.00	62.80
Eu	75.00	89.70	100.00	89.30	87.50	82.20	49.40	90.10	36.10	86.60	54.00	51.60	8.18	17.25	58.90	48.20	92.00	21.50
Gd	265.00	290.00	392.00	346.00	266.00	349.00	174.00	256.00	126.00	297.00	163.50	156.50	25.80	54.80	193.00	141.50	285.00	69.60
Tb	43.30	43.50	58.60	74.90	34.90	37.10	23.10	30.60	21.40	58.20	19.95	18.45	3.57	8.28	32.20	20.70	47.30	10.05
Dy	247.00	218.00	352.00	506.00	164.00	206.00	110.50	124.50	123.00	334.00	88.80	75.40	20.40	42.90	181.00	104.00	249.00	53.10
Ho	48.70	39.40	75.10	102.00	29.80	49.20	19.75	20.10	24.90	62.10	16.20	13.20	4.74	8.49	37.00	19.40	42.90	9.88
Er	139.50	109.00	240.00	271.00	86.00	174.00	57.00	56.50	71.80	159.50	45.90	38.80	16.55	23.60	108.50	53.00	105.50	28.60
Tm	18.75	13.90	34.70	32.80	11.30	26.30	7.62	7.38	9.45	20.70	5.97	5.54	2.75	3.07	15.70	6.82	12.00	3.71
Yb	110.50	82.40	217.00	175.00	68.60	176.50	47.50	49.70	56.50	120.00	37.10	38.80	20.90	19.10	100.00	42.10	71.00	22.60
Lu	14.25	10.75	29.40	20.90	8.89	24.40	6.48	6.77	7.30	15.60	5.06	5.52	3.26	2.64	13.50	5.38	8.89	2.84
Y	1350.00	1165.00	2400.00	2830.00	862.00	1685.00	588.00	570.00	727.00	1590.00	466.00	349.00	125.00	218.00	946.00	509.00	1300.00	296.00
La/Yb	16.97	14.81	26.64	14.29	21.14	47.25	20.19	17.65	17.70	8.38	28.03	30.54	12.44	24.97	14.65	15.04	11.85	34.16

Appendix 2 b) Trace elements analysis of samples collected by Etruscan and NRE and used in this study

Sample No.	ERN18400	ERN18401	ERN18402	ERN18403	ERN18404	ERN18405	ERN18406	ERN18407	ERN18408	ERN18409	ERN18410	ERN18411	ERN18412	ERN18413	ERN18414	ERN18501	ERN18502	ERN18503
Ba	782.00	461.00	269.00	181.00	78.90	541.00	84.10	979.00	515.00	319.00	215.00	103.00	625.00	86.60	353.00	4600.00	1525.00	1400.00
Ga	12.70	16.10	11.20	66.60	27.80	9.50	19.10	9.90	26.70	27.30	17.90	11.80	12.30	29.00	11.90	16.90	13.90	20.00
Hf	1.70	1.40	1.90	6.00	2.00	2.00	1.30	0.90	1.20	2.60	2.40	1.60	0.50	2.00	1.90	2.10	1.00	3.00
Nb	376.00	69.40	364.00	130.00	33.00	74.70	64.60	93.00	17.10	139.50	7.90	6.30	376.00	58.00	9.60	8.80	2.00	116.00
Rb	26.00	6.70	5.10	30.00	9.00	1.50	3.40	3.50	1.10	6.90	1.00	2.40	1.00	6.00	2.70	20.20	3.00	6.00
Sr	215.00	4010.00	8960.00	927.00	926.00	8980.00	620.00	2410.00	3630.00	539.00	1910.00	2470.00	10000.00	912.00	5130.00	2630.00	10000.00	10000.00
Ta	8.10	0.50	1.70	1.80	0.70	0.90	0.70	1.80	0.20	1.00	0.60	0.40	3.50	0.60	0.30	0.50	0.25	0.60
Th	711.00	580.00	123.50	2350.00	1565.00	106.00	409.00	342.00	550.00	481.00	841.00	937.00	131.50	1235.00	566.00	181.50	429.00	366.00
U	25.70	11.25	19.50	15.10	17.00	12.75	5.45	11.60	11.50	6.60	12.35	12.70	13.70	18.40	5.49	41.70	14.50	14.70
Zr	63.00	18.00	117.00	140.00	60.00	109.00	41.00	21.00	33.00	86.00	17.00	17.00	40.00	50.00	51.00	117.00	20.00	150.00
La	966.00	2980.00	1535.00	12850.00	5770.00	736.00	736.00	1125.00	4990.00	2750.00	3490.00	1580.00	628.00	6420.00	971.00	3040.00	2200.00	3970.00
Ce	1880.00	4870.00	2460.00	21300.00	9640.00	1330.00	1455.00	1875.00	8120.00	4540.00	5320.00	2950.00	1220.00	10500.00	1725.00	4810.00	3830.00	6090.00
Pr	262.00	485.00	234.00	2150.00	974.00	138.50	214.00	189.50	794.00	433.00	508.00	330.00	139.00	1060.00	185.00	454.00	398.00	558.00
Nd	1375.00	1550.00	747.00	6630.00	2970.00	464.00	1125.00	630.00	2560.00	1335.00	1550.00	1285.00	479.00	3260.00	619.00	1365.00	1325.00	1680.00
Sm	396.00	228.00	94.40	914.00	388.00	66.40	339.00	93.50	388.00	172.00	220.00	374.00	67.30	409.00	123.00	142.50	181.50	215.00
Eu	91.50	67.80	26.80	287.00	115.00	20.30	87.70	29.90	102.50	49.60	77.80	121.00	19.60	118.00	51.50	32.40	48.70	56.70
Gd	237.00	254.00	95.70	976.00	422.00	66.80	238.00	105.50	371.00	178.50	313.00	385.00	62.70	443.00	183.50	146.50	181.00	237.00
Tb	25.00	44.40	11.40	151.50	70.60	9.37	28.60	18.25	44.40	21.90	74.80	65.50	8.62	67.50	39.80	15.25	23.60	27.80
Dy	92.80	292.00	58.00	827.00	468.00	49.40	111.50	119.00	206.00	108.50	595.00	372.00	51.10	422.00	257.00	77.10	127.50	146.00
Ho	14.95	63.10	11.85	150.00	99.00	9.25	17.95	26.00	36.60	20.60	133.50	69.50	10.70	85.10	52.80	16.00	26.70	29.90
Er	42.60	191.50	37.10	384.00	285.00	26.50	48.20	83.30	108.50	61.60	394.00	182.50	31.50	235.00	161.00	49.60	84.50	89.30
Tm	5.03	25.20	4.72	42.60	36.10	3.16	5.76	11.55	13.65	7.20	48.00	21.20	3.92	28.50	23.50	7.17	12.55	11.25
Yb	35.70	150.50	30.10	227.00	198.00	18.10	41.40	71.30	91.00	43.70	258.00	118.50	22.40	158.00	160.00	46.20	84.60	65.10
Lu	4.64	19.40	3.88	26.80	23.50	2.28	5.84	8.99	11.85	5.44	29.50	14.35	2.65	19.20	22.20	6.06	11.40	8.30
Y	423.00	1855.00	348.00	3780.00	2780.00	254.00	532.00	832.00	952.00	593.00	3660.00	2040.00	297.00	2320.00	1360.00	534.00	706.00	1015.00
La/Yb	27.06	19.80	51.00	56.61	29.14	40.66	17.78	15.78	54.84	62.93	13.53	13.33	28.04	40.63	6.07	65.80	26.00	60.98

Appendix 2 b) Trace elements analysis of samples collected by Etruscan and NRE and used in this study

Sample No.	ERN18504	ERN18505	ERN18506	ERN18507	ERN18508	ERN18509	ERN18510	ERN18511	ERN18512	ERN18513	ERN18514	ERN18515	ERN18516	ERN18517	ERN18518	ERN18519	ERN18520	ERN18521
Ba	1245.00	327.00	2380.00	880.00	1165.00	145.00	407.00	416.00	250.00	179.00	522.00	98.80	2840.00	720.00	867.00	3330.00	2700.00	5810.00
Ga	20.20	8.10	7.30	8.20	12.30	5.10	8.90	7.30	11.90	5.20	33.20	16.60	12.30	8.80	6.80	10.70	10.20	11.20
Hf	1.50	1.70	3.00	1.80	0.90	0.60	1.00	0.50	0.70	2.90	1.00	2.70	0.80	2.60	1.40	3.00	2.00	1.20
Nb	24.90	13.20	49.00	112.00	11.10	3.70	110.00	20.00	3.50	68.00	13.00	62.70	5.70	31.00	723.00	112.50	9.30	112.00
Rb	2.80	2.10	6.00	5.70	0.90	2.50	7.60	3.80	1.00	5.10	4.00	1.30	9.10	11.50	12.40	7.70	7.40	25.80
Sr	3270.00	2570.00	10000.00	2310.00	3040.00	1500.00	1150.00	1465.00	1645.00	2890.00	805.00	3310.00	2070.00	1415.00	1045.00	2530.00	1320.00	1665.00
Ta	0.80	0.50	0.80	0.30	0.50	0.50	0.70	0.20	0.50	0.50	0.25	0.50	0.10	0.30	2.60	0.60	0.30	0.20
Th	645.00	191.50	545.00	24.00	260.00	155.00	291.00	92.80	153.50	150.00	557.00	18.60	170.00	455.00	30.00	436.00	660.00	301.00
U	13.25	5.54	3.90	40.70	3.04	2.16	2.92	5.83	2.87	16.10	13.70	7.27	7.89	10.35	38.60	13.60	5.49	4.49
Zr	21.00	86.00	90.00	201.00	24.00	12.00	25.00	18.00	16.00	413.00	50.00	190.00	39.00	143.00	123.00	164.00	57.00	63.00
La	4920.00	1090.00	991.00	809.00	2660.00	406.00	969.00	1050.00	1930.00	753.00	6550.00	2450.00	2560.00	1595.00	562.00	1685.00	2520.00	1995.00
Ce	6880.00	1995.00	1550.00	1475.00	3870.00	680.00	1755.00	1670.00	2960.00	1125.00	11350.00	4020.00	4160.00	2390.00	1145.00	2810.00	3710.00	2690.00
Pr	602.00	208.00	146.50	172.00	344.00	75.60	186.00	159.50	295.00	107.00	1115.00	405.00	415.00	229.00	138.00	290.00	351.00	229.00
Nd	1720.00	702.00	470.00	611.00	990.00	267.00	641.00	503.00	996.00	343.00	3520.00	1370.00	1285.00	709.00	506.00	944.00	1030.00	630.00
Sm	238.00	118.00	74.00	89.00	121.50	44.90	90.30	75.40	156.50	45.20	383.00	178.00	170.50	109.50	76.60	141.50	155.00	73.70
Eu	81.70	34.60	33.00	24.00	35.90	13.90	26.00	20.40	37.50	14.00	78.30	41.90	42.90	35.30	20.00	49.40	49.90	22.70
Gd	348.00	129.00	129.50	79.00	157.00	60.50	109.50	82.70	154.50	51.40	382.00	164.00	171.50	141.00	70.60	186.00	211.00	102.00
Tb	55.60	19.10	29.90	9.01	24.40	13.10	21.10	12.35	19.95	7.28	32.60	17.20	16.30	23.60	8.43	34.30	36.90	14.75
Dy	322.00	116.00	206.00	39.30	138.50	94.40	145.00	74.00	101.50	43.00	115.50	72.70	66.80	139.00	37.50	217.00	236.00	92.30
Ho	60.20	24.90	41.00	6.77	26.30	22.70	32.80	15.75	20.10	8.70	19.35	12.30	13.25	26.10	6.55	42.90	50.00	20.80
Er	150.00	77.10	108.50	18.05	69.90	77.30	103.50	50.20	62.30	24.60	58.70	32.60	46.90	68.10	18.25	118.00	145.00	67.90
Tm	18.90	12.30	13.65	2.23	9.51	14.80	18.40	8.66	9.69	3.61	6.36	3.71	7.93	8.06	2.32	15.40	20.20	11.10
Yb	101.00	83.80	78.80	13.25	54.60	112.00	126.50	61.10	61.80	21.50	38.10	20.40	62.20	45.20	14.65	94.40	120.50	77.20
Lu	12.15	12.15	10.15	1.83	7.08	17.05	18.25	8.68	8.36	2.70	5.14	2.35	9.27	5.59	2.11	12.65	15.70	11.45
Y	1840.00	1065.00	1120.00	172.50	744.00	526.00	1035.00	444.00	602.00	243.00	543.00	304.00	331.00	640.00	151.00	996.00	1370.00	511.00
La/Yb	48.71	13.01	12.58	61.06	48.72	3.63	7.66	17.18	31.23	35.02	171.92	120.10	41.16	35.29	38.36	17.85	20.91	25.84

Appendix 2 b) Trace elements analysis of samples collected by Etruscan and NRE and used in this study

Sample No.	ERN18522	ERN18523	ERN18524	ERN18525	ERN18526	ERN18527	ERN18528	ERN18529	ERN18530	ERN18531	ERN18532	ERN18533	ERN18534	ERN18535	ERN18536	ERN18537	ERN18538	ERN18539
Ba	1155.00	201.00	845.00	1135.00	82.20	152.00	611.00	120.00	210.00	497.00	7750.00	218.00	61.10	99.40	368.00	335.00	3270.00	779.00
Ga	9.90	6.20	7.70	13.00	3.40	13.60	13.80	2.30	1.60	10.20	6.20	20.70	5.60	1.60	24.10	6.90	9.30	27.50
Hf	3.10	0.90	4.90	5.80	31.10	11.00	6.40	1.40	0.40	4.80	1.00	2.00	1.70	0.90	1.00	0.60	1.10	1.00
Nb	122.00	66.80	296.00	726.00	252.00	119.00	21.50	5.80	11.90	266.00	102.00	18.30	26.80	10.70	11.10	721.00	42.20	18.00
Rb	17.80	3.80	16.00	51.90	5.30	2.70	3.90	1.90	3.40	26.60	3.00	2.00	1.80	4.60	6.60	1.80	5.30	3.00
Sr	8170.00	1470.00	794.00	927.00	228.00	662.00	264.00	198.50	590.00	558.00	10000.00	951.00	440.00	423.00	1020.00	2280.00	1665.00	10000.00
Ta	1.90	0.20	1.40	6.50	1.50	6.50	0.50	0.10	0.10	2.60	1.30	0.10	0.10	0.10	0.10	1.10	0.30	0.25
Th	13.55	34.60	78.70	32.30	99.70	17.05	12.70	37.60	62.00	58.80	28.70	525.00	207.00	46.80	333.00	42.60	326.00	535.00
U	2.87	5.55	28.10	23.90	9.78	12.05	5.28	1.90	2.14	21.40	5.90	5.95	2.91	1.25	3.24	19.80	9.96	16.80
Zr	148.00	77.00	625.00	485.00	2910.00	599.00	268.00	93.00	36.00	491.00	160.00	220.00	143.00	89.00	48.00	63.00	53.00	110.00
La	549.00	407.00	1160.00	895.00	315.00	125.50	31.70	27.20	59.90	906.00	839.00	5310.00	1025.00	119.00	7120.00	1010.00	2520.00	7430.00
Ce	849.00	682.00	1850.00	1535.00	577.00	243.00	62.20	51.50	118.00	1450.00	1395.00	8070.00	1655.00	183.00	9400.00	1880.00	3370.00	10000.00
Pr	83.60	67.80	183.50	162.50	65.80	29.30	7.76	6.18	13.95	143.00	142.50	771.00	164.00	17.65	788.00	207.00	297.00	864.00
Nd	265.00	210.00	572.00	541.00	233.00	113.50	29.90	24.30	56.00	443.00	458.00	2340.00	521.00	55.30	2040.00	701.00	819.00	2360.00
Sm	34.50	28.20	74.80	77.00	38.90	20.90	6.95	6.13	14.75	59.20	60.20	281.00	76.40	9.21	166.00	103.00	91.50	223.00
Eu	10.90	8.10	22.30	26.60	8.38	6.19	1.26	1.63	4.18	17.05	18.30	66.40	20.50	2.99	39.60	28.90	26.90	58.20
Gd	38.30	32.90	79.80	79.70	40.20	21.20	7.41	7.70	19.25	62.00	58.70	297.00	83.10	12.95	229.00	96.00	121.00	264.00
Tb	4.21	4.92	9.00	9.75	5.80	2.86	1.44	1.49	3.96	6.81	6.30	33.00	10.45	2.71	21.20	10.90	18.45	27.40
Dy	19.95	31.60	41.00	47.20	29.70	14.20	8.70	9.37	24.50	31.10	27.90	161.50	52.90	20.10	107.50	47.90	119.50	148.50
Ho	3.71	7.28	7.61	8.49	5.45	2.62	1.97	2.02	4.83	5.58	4.88	31.00	10.25	4.76	23.70	8.25	25.30	32.10
Er	10.50	24.60	21.20	23.60	14.80	7.09	6.21	6.43	13.50	16.20	13.10	89.70	31.50	15.75	72.50	22.50	73.70	104.50
Tm	1.27	3.73	2.59	2.88	1.92	0.94	0.91	0.97	1.81	1.93	1.45	10.70	4.47	2.47	9.12	2.53	10.35	14.30
Yb	7.91	24.60	14.75	17.10	11.90	5.68	6.24	6.94	11.50	11.95	8.20	59.90	30.30	16.80	57.40	14.50	65.70	90.60
Lu	1.07	3.38	1.86	2.23	1.62	0.80	0.86	0.97	1.61	1.55	1.21	7.33	4.12	2.30	7.48	1.79	9.34	12.05
Y	95.30	215.00	213.00	226.00	131.50	62.70	53.70	55.30	153.50	128.00	129.00	897.00	258.00	125.50	619.00	204.00	715.00	954.00
La/Yb	69.41	16.54	78.64	52.34	26.47	22.10	5.08	3.92	5.21	75.82	102.32	88.65	33.83	7.08	124.04	69.66	38.36	82.01

Appendix 2 b) Trace elements analysis of samples collected by Etruscan and NRE and used in this study

Sample No.	ERN18522	ERN18523	ERN18524	ERN18525	ERN18526	ERN18527	ERN18528	ERN18529	ERN18530	ERN18531	ERN18532	ERN18533	ERN18534	ERN18535	ERN18536	ERN18537	ERN18538	ERN18539
Ba	1155.00	201.00	845.00	1135.00	82.20	152.00	611.00	120.00	210.00	497.00	7750.00	218.00	61.10	99.40	368.00	335.00	3270.00	779.00
Ga	9.90	6.20	7.70	13.00	3.40	13.60	13.80	2.30	1.60	10.20	6.20	20.70	5.60	1.60	24.10	6.90	9.30	27.50
Hf	3.10	0.90	4.90	5.80	31.10	11.00	6.40	1.40	0.40	4.80	1.00	2.00	1.70	0.90	1.00	0.60	1.10	1.00
Nb	122.00	66.80	296.00	726.00	252.00	119.00	21.50	5.80	11.90	266.00	102.00	18.30	26.80	10.70	11.10	721.00	42.20	18.00
Rb	17.80	3.80	16.00	51.90	5.30	2.70	3.90	1.90	3.40	26.60	3.00	2.00	1.80	4.60	6.60	1.80	5.30	3.00
Sr	8170.00	1470.00	794.00	927.00	228.00	662.00	264.00	198.50	590.00	558.00	10000.00	951.00	440.00	423.00	1020.00	2280.00	1665.00	10000.00
Ta	1.90	0.20	1.40	6.50	1.50	6.50	0.50	0.10	0.10	2.60	1.30	0.10	0.10	0.10	0.10	1.10	0.30	0.25
Th	13.55	34.60	78.70	32.30	99.70	17.05	12.70	37.60	62.00	58.80	28.70	525.00	207.00	46.80	333.00	42.60	326.00	535.00
U	2.87	5.55	28.10	23.90	9.78	12.05	5.28	1.90	2.14	21.40	5.90	5.95	2.91	1.25	3.24	19.80	9.96	16.80
Zr	148.00	77.00	625.00	485.00	2910.00	599.00	268.00	93.00	36.00	491.00	160.00	220.00	143.00	89.00	48.00	63.00	53.00	110.00
La	549.00	407.00	1160.00	895.00	315.00	125.50	31.70	27.20	59.90	906.00	839.00	5310.00	1025.00	119.00	7120.00	1010.00	2520.00	7430.00
Ce	849.00	682.00	1850.00	1535.00	577.00	243.00	62.20	51.50	118.00	1450.00	1395.00	8070.00	1655.00	183.00	9400.00	1880.00	3370.00	10000.00
Pr	83.60	67.80	183.50	162.50	65.80	29.30	7.76	6.18	13.95	143.00	142.50	771.00	164.00	17.65	788.00	207.00	297.00	864.00
Nd	265.00	210.00	572.00	541.00	233.00	113.50	29.90	24.30	56.00	443.00	458.00	2340.00	521.00	55.30	2040.00	701.00	819.00	2360.00
Sm	34.50	28.20	74.80	77.00	38.90	20.90	6.95	6.13	14.75	59.20	60.20	281.00	76.40	9.21	166.00	103.00	91.50	223.00
Eu	10.90	8.10	22.30	26.60	8.38	6.19	1.26	1.63	4.18	17.05	18.30	66.40	20.50	2.99	39.60	28.90	26.90	58.20
Gd	38.30	32.90	79.80	79.70	40.20	21.20	7.41	7.70	19.25	62.00	58.70	297.00	83.10	12.95	229.00	96.00	121.00	264.00
Tb	4.21	4.92	9.00	9.75	5.80	2.86	1.44	1.49	3.96	6.81	6.30	33.00	10.45	2.71	21.20	10.90	18.45	27.40
Dy	19.95	31.60	41.00	47.20	29.70	14.20	8.70	9.37	24.50	31.10	27.90	161.50	52.90	20.10	107.50	47.90	119.50	148.50
Ho	3.71	7.28	7.61	8.49	5.45	2.62	1.97	2.02	4.83	5.58	4.88	31.00	10.25	4.76	23.70	8.25	25.30	32.10
Er	10.50	24.60	21.20	23.60	14.80	7.09	6.21	6.43	13.50	16.20	13.10	89.70	31.50	15.75	72.50	22.50	73.70	104.50
Tm	1.27	3.73	2.59	2.88	1.92	0.94	0.91	0.97	1.81	1.93	1.45	10.70	4.47	2.47	9.12	2.53	10.35	14.30
Yb	7.91	24.60	14.75	17.10	11.90	5.68	6.24	6.94	11.50	11.95	8.20	59.90	30.30	16.80	57.40	14.50	65.70	90.60
Lu	1.07	3.38	1.86	2.23	1.62	0.80	0.86	0.97	1.61	1.55	1.21	7.33	4.12	2.30	7.48	1.79	9.34	12.05
Y	95.30	215.00	213.00	226.00	131.50	62.70	53.70	55.30	153.50	128.00	129.00	897.00	258.00	125.50	619.00	204.00	715.00	954.00
La/Yb	69.41	16.54	78.64	52.34	26.47	22.10	5.08	3.92	5.21	75.82	102.32	88.65	33.83	7.08	124.04	69.66	38.36	82.01

Appendix 2 b) Trace elements analysis of samples collected by Etruscan and NRE and used in this study

Sample No.	ERN18558	ERN18559	ERN18560	ERN18561	ERN18562	ERN18563	ERN18564	ERN18565	ERN18566	ERN18567	ERN18568	ERN18569	ERN18570	ERN18571	ERN18572	ERN18573	ERN18574	ERN18575
Ba	248.00	131.50	872.00	142.00	130.00	85.50	10000.00	315.00	155.00	383.00	308.00	315.00	267.00	384.00	244.00	371.00	345.00	160.50
Ga	8.70	4.70	25.70	27.50	8.90	12.50	4.50	12.20	10.00	5.40	3.70	8.60	8.20	6.50	4.20	2.70	9.80	11.70
Hf	1.40	1.20	1.10	2.30	1.60	1.00	0.50	0.90	0.80	0.50	1.00	0.60	0.70	2.40	1.60	0.50	1.30	0.50
Nb	6.50	10.50	0.60	28.10	222.00	66.50	2.00	99.60	327.00	776.00	98.50	7.50	371.00	122.00	33.00	58.00	342.00	18.50
Rb	2.40	1.20	4.10	0.60	5.50	3.00	13.00	1.90	3.50	4.00	0.80	71.80	26.10	2.00	1.00	0.50	4.80	4.50
Sr	646.00	2260.00	382.00	338.00	348.00	967.00	3280.00	5430.00	1595.00	10000.00	9250.00	3700.00	1865.00	4440.00	7730.00	10000.00	1370.00	1365.00
Ta	0.50	0.30	0.50	0.70	0.30	0.30	0.25	0.80	1.40	1.50	0.50	0.50	1.50	1.00	0.60	0.25	2.00	0.20
Th	134.00	172.50	303.00	528.00	192.50	99.10	4.70	6.39	72.70	3.10	2.34	1.52	2.54	11.55	2.47	3.30	3.88	11.00
U	6.04	3.18	7.41	6.82	9.83	3.58	0.90	1.65	6.04	31.10	15.00	1.17	4.88	4.00	2.88	3.30	3.41	1.80
Zr	57.00	30.00	20.00	123.00	88.00	63.00	10.00	20.00	15.00	20.00	29.00	10.00	7.00	71.00	29.00	10.00	33.00	14.00
La	714.00	527.00	4130.00	6210.00	1300.00	1835.00	13.00	155.50	368.00	173.00	182.50	154.00	172.50	162.00	228.00	174.00	441.00	610.00
Ce	1065.00	841.00	6890.00	8070.00	1995.00	3110.00	24.00	314.00	657.00	369.00	386.00	296.00	344.00	332.00	463.00	367.00	725.00	1060.00
Pr	105.50	90.30	715.00	744.00	215.00	348.00	2.40	35.30	70.60	39.10	47.60	32.60	39.60	38.60	53.70	37.40	76.70	101.00
Nd	321.00	295.00	2140.00	2120.00	698.00	1150.00	9.20	119.00	229.00	137.00	170.00	109.00	131.00	135.00	184.50	132.50	236.00	323.00
Sm	53.30	51.90	229.00	296.00	105.50	158.50	2.70	18.75	33.00	22.70	28.10	16.75	20.90	26.00	28.60	22.00	31.20	43.00
Eu	16.90	14.60	44.90	74.00	23.60	36.90	0.90	5.31	9.35	6.60	7.74	5.07	6.15	7.75	8.01	6.40	8.98	11.35
Gd	63.90	62.50	247.00	350.00	110.00	147.50	3.60	18.70	36.10	21.90	27.70	18.45	22.40	26.70	29.80	23.40	35.60	44.80
Tb	10.75	12.55	21.50	37.60	13.85	14.65	0.52	2.43	4.28	2.96	3.45	2.28	2.80	3.63	3.59	2.99	3.95	4.85
Dy	74.20	98.60	86.20	179.50	63.60	52.70	2.90	12.50	20.20	15.30	17.40	11.40	13.40	19.65	17.35	15.30	18.95	20.30
Ho	17.40	24.70	18.70	35.10	11.25	9.20	0.58	2.50	4.09	2.96	3.40	2.20	2.71	3.87	3.33	3.06	3.65	3.85
Er	53.80	78.60	66.70	105.50	29.80	28.40	1.90	7.13	12.05	8.50	9.36	6.34	7.71	10.05	9.75	8.80	10.85	12.85
Tm	8.92	13.00	10.70	14.35	3.83	3.52	0.20	1.00	1.66	1.13	1.24	0.82	1.04	1.40	1.26	1.17	1.48	1.62
Yb	57.60	77.10	77.50	84.80	23.10	21.60	2.10	6.24	10.65	7.50	7.30	5.08	6.47	8.37	7.23	7.70	9.41	11.10
Lu	8.71	10.50	12.45	11.95	3.30	2.99	0.34	0.97	1.69	1.00	1.07	0.74	0.93	1.20	1.09	1.11	1.33	1.53
Y	489.00	999.00	497.00	990.00	294.00	232.00	18.00	61.50	98.00	74.00	84.20	51.50	64.20	92.60	81.70	76.00	88.30	103.50
La/Yb	12.40	6.84	53.29	73.23	56.28	84.95	6.19	24.92	34.55	23.07	25.00	30.31	26.66	19.35	31.54	22.60	46.87	54.95

Appendix 2 b) Trace elements analysis of samples collected by Etruscan and NRE and used in this study

Sample No.	ERNI8576	ERNI8577	ERNI8578	ERNI8579	ERNI8580	ERNI8581	ERNI8582	ERNI8583	ERNI8584	ERNI8585	ERNI8586	ERNI8587	ERNI8588	ERNI8589	ERNI8590	ERNI8591	ERNI8592	ERNI8593
Ba	355.00	504.00	471.00	488.00	242.00	1240.00	332.00	388.00	371.00	409.00	511.00	321.00	160.00	429.00	409.00	306.00	2270.00	352.00
Ga	12.10	2.80	5.40	16.50	5.60	12.10	7.70	4.20	4.40	12.20	12.90	8.00	10.20	3.50	2.50	2.20	25.30	1.70
Hf	0.30	0.20	0.30	6.10	1.00	0.40	1.50	0.20	0.60	2.50	1.00	0.80	0.30	1.60	0.50	0.20	11.10	0.20
Nb	4.50	7.70	66.90	475.00	84.40	547.00	94.00	76.60	622.00	122.50	181.00	122.50	20.30	83.60	211.00	104.50	429.00	5.90
Rb	0.70	0.40	3.70	40.70	3.50	88.60	1.80	0.70	8.80	7.10	78.90	19.40	31.70	2.00	4.20	3.40	278.00	0.90
Sr	2050.00	7840.00	3350.00	5470.00	955.00	874.00	4090.00	1530.00	5210.00	3930.00	1995.00	8220.00	4420.00	5920.00	1865.00	7410.00	330.00	9680.00
Ta	0.10	0.10	0.20	6.00	0.20	6.70	1.20	0.60	4.40	0.70	3.30	0.60	0.20	0.20	0.30	0.10	13.50	0.10
Th	7.71	1.66	7.92	6.40	11.95	9.94	7.96	9.27	11.10	21.40	4.80	9.00	9.05	5.46	1.31	2.34	3.60	1.47
U	1.17	1.04	8.38	17.20	4.37	10.50	3.44	2.40	67.70	7.56	4.30	2.61	0.50	7.03	2.84	1.69	3.36	0.99
Zr	11.00	4.00	7.00	456.00	184.00	16.00	91.00	7.00	19.00	164.00	54.00	39.00	13.00	32.00	14.00	11.00	774.00	6.00
La	933.00	168.50	259.00	235.00	47.80	95.50	166.00	240.00	214.00	303.00	275.00	339.00	1035.00	218.00	150.50	150.00	30.50	216.00
Ce	1455.00	346.00	506.00	485.00	117.00	198.00	328.00	472.00	452.00	608.00	483.00	659.00	1350.00	461.00	325.00	319.00	64.40	424.00
Pr	133.00	36.20	53.30	52.50	16.10	21.10	35.20	51.70	52.00	68.10	50.90	72.20	114.00	52.30	37.40	36.20	7.53	45.30
Nd	388.00	124.00	180.50	187.00	68.80	74.10	120.00	176.00	185.00	235.00	170.50	251.00	314.00	184.00	130.50	128.50	27.90	154.00
Sm	46.90	20.20	27.10	30.00	22.60	12.90	19.05	26.80	31.80	41.30	25.60	38.80	30.60	29.70	20.80	21.30	4.79	22.90
Eu	13.15	6.26	7.92	8.21	8.62	3.99	5.76	7.95	9.67	12.95	7.32	11.25	8.10	8.82	6.23	6.71	1.53	6.99
Gd	55.30	22.40	28.40	29.40	25.50	13.65	20.40	28.10	32.50	45.60	25.90	39.50	37.00	29.90	21.10	22.50	4.71	24.50
Tb	5.90	3.19	3.62	3.74	4.95	1.95	2.83	3.49	4.18	6.80	3.17	4.89	3.11	3.83	2.74	3.06	0.64	3.19
Dy	25.40	16.55	17.10	17.45	28.00	9.92	14.90	17.90	20.80	38.20	15.65	23.40	12.45	19.30	14.00	15.95	2.99	16.55
Ho	5.00	3.38	3.29	3.31	4.92	2.04	3.04	3.42	3.80	7.56	2.98	4.41	2.51	3.66	2.74	3.07	0.56	3.29
Er	15.90	10.30	9.81	9.83	12.55	6.05	9.09	10.10	10.70	21.80	8.83	12.85	8.55	10.65	7.95	8.94	1.64	9.66
Tm	1.98	1.41	1.23	1.20	1.46	0.78	1.26	1.35	1.31	3.00	1.20	1.63	1.13	1.37	1.03	1.19	0.23	1.25
Yb	13.45	9.45	7.93	7.71	8.83	5.13	7.88	8.77	8.20	19.35	7.98	10.60	7.85	8.98	6.75	7.53	1.58	8.01
Lu	1.95	1.29	1.09	1.06	1.16	0.71	1.09	1.18	1.10	2.58	1.11	1.41	1.07	1.21	0.88	0.98	0.24	1.04
Y	124.50	84.40	82.00	83.20	116.00	50.10	76.70	85.00	91.00	192.50	72.50	107.50	74.30	90.40	70.20	76.30	13.60	83.60
La/Yb	69.37	17.83	32.66	30.48	5.41	18.62	21.07	27.37	26.10	15.66	34.46	31.98	131.85	24.28	22.30	19.92	19.30	26.97

Appendix 2 b) Trace elements analysis of samples collected by Etruscan and NRE and used in this study

Sample No.	ERNI8594	ERNI8595	ERNI8596	ERNI8597	ERNI8598	ERNI8599	ERNI8600	ERNI8601	ERNI8602	ERNI8603	ERNI8604	ERNI8605	ERNI8606	ERNI8607	ERNI8608	ERNI8609	ERNI8610	ERNI8611
Ba	369.00	322.00	175.50	269.00	403.00	371.00	1095.00	395.00	594.00	170.00	550.00	586.00	723.00	1320.00	728.00	1315.00	785.00	593.00
Ga	2.60	3.20	2.90	3.30	2.50	2.30	14.40	5.00	2.60	3.50	6.30	8.20	11.00	36.00	18.70	13.80	5.40	4.70
Hf	0.60	0.20	0.20	0.80	1.30	0.20	0.40	2.90	1.00	1.70	0.20	0.30	0.50	0.50	0.50	0.30	0.90	1.20
Nb	86.20	110.50	90.50	163.00	88.50	19.80	383.00	1030.00	141.00	122.50	20.30	48.10	15.00	7.00	1.40	0.40	72.70	19.10
Rb	2.60	12.60	6.10	4.50	2.80	3.40	164.50	18.30	1.00	3.70	25.30	1.80	1.00	5.00	2.10	3.30	8.30	11.70
Sr	3920.00	3730.00	2700.00	9720.00	2770.00	917.00	2750.00	6220.00	10000.00	6450.00	3910.00	1800.00	10000.00	4870.00	1965.00	1615.00	8580.00	3990.00
Ta	0.20	0.30	0.10	0.20	0.20	0.20	5.30	2.20	0.25	0.20	0.10	0.40	0.25	0.25	0.40	0.40	0.80	0.50
Th	3.60	2.42	4.90	5.57	6.85	6.69	5.04	5.13	8.00	1.97	18.90	71.70	13.80	67.70	26.20	14.45	15.20	13.75
U	1.31	1.39	1.85	2.30	2.40	2.25	10.90	17.50	4.50	7.39	2.27	2.32	1.20	0.70	1.72	1.89	6.33	1.26
Zr	19.00	8.00	11.00	45.00	45.00	6.00	14.00	100.00	20.00	38.00	5.00	8.00	10.00	10.00	14.00	11.00	21.00	40.00
La	205.00	170.00	193.50	296.00	205.00	140.50	99.60	239.00	274.00	249.00	829.00	1635.00	1720.00	7130.00	3840.00	2690.00	387.00	200.00
Ce	424.00	335.00	393.00	572.00	426.00	280.00	208.00	535.00	538.00	528.00	1205.00	2540.00	2740.00	10900.00	5860.00	4150.00	785.00	406.00
Pr	47.60	36.60	43.60	62.80	48.20	31.40	22.90	63.70	56.40	60.70	110.00	240.00	253.00	933.00	532.00	383.00	100.00	48.10
Nd	165.50	123.50	151.00	215.00	172.00	107.50	77.90	233.00	198.00	219.00	317.00	713.00	778.00	2610.00	1520.00	1090.00	368.00	167.50
Sm	25.70	19.65	23.70	32.20	27.70	18.50	11.95	37.90	30.70	34.90	34.50	82.20	99.50	215.00	132.50	95.10	71.50	29.10
Eu	7.99	6.27	7.17	9.60	8.56	5.75	3.70	11.15	9.50	10.35	8.60	21.30	26.70	43.80	30.00	21.80	21.70	8.33
Gd	27.50	21.40	24.70	34.20	29.10	19.75	12.65	38.20	32.80	36.40	41.40	94.60	110.50	237.00	155.50	111.50	78.40	30.30
Tb	3.57	2.78	3.13	4.20	3.75	2.78	1.65	4.81	4.10	4.42	4.19	9.22	11.70	14.45	10.70	8.32	13.05	4.10
Dy	18.15	14.35	15.85	20.10	19.00	14.90	8.57	23.30	20.30	21.10	20.00	38.90	56.90	40.00	32.60	28.40	76.70	22.70
Ho	3.46	2.81	3.08	3.77	3.61	2.99	1.65	4.28	4.04	3.88	4.00	7.14	10.60	7.14	6.13	5.39	15.00	4.65
Er	10.10	8.26	9.05	10.85	10.50	8.79	4.90	12.05	12.00	11.25	12.50	21.20	34.00	27.20	22.70	18.90	39.20	13.05
Tm	1.28	1.11	1.18	1.33	1.32	1.22	0.66	1.47	1.47	1.40	1.63	2.53	4.31	2.82	2.60	2.25	5.10	1.92
Yb	8.17	6.98	7.48	8.29	8.62	8.02	4.28	9.14	9.20	8.65	10.70	15.80	27.10	19.00	18.35	15.55	28.80	12.20
Lu	1.05	0.95	0.97	1.05	1.15	1.09	0.59	1.23	1.25	1.16	1.44	2.02	3.71	2.69	2.62	2.16	3.94	1.75
Y	87.60	70.10	76.10	92.80	90.90	75.40	40.60	105.50	103.00	92.40	124.50	199.00	274.00	188.00	208.00	183.00	341.00	123.00
La/Yb	25.09	24.36	25.87	35.71	23.78	17.52	23.27	26.15	29.78	28.79	77.48	103.48	63.47	375.26	209.26	172.99	13.44	16.39

Appendix 2 b) Trace elements analysis of samples collected by Etruscan and NRE and used in this study

Sample No.	ERNI8612	ERNI8613	ERNI8614	ERNI8615	ERNI8616	ERNI8617	ERNI8618	ERNI8619	ERNI8620	ERNI8621	ERNI8622	ERNI8623	ERNI8624	ERNI8625	ERNI8626	ERNI8627	ERNI8628	ERNI8629
Ba	277.00	257.00	2260.00	714.00	243.00	803.00	302.00	394.00	392.00	1655.00	9570.00	7840.00	523.00	606.00	551.00	504.00	1330.00	413.00
Ga	4.60	4.40	21.70	6.90	3.10	5.10	3.80	4.40	9.00	4.50	20.40	41.90	11.40	3.80	2.00	19.90	24.90	5.90
Hf	1.20	1.20	6.70	0.50	0.40	0.30	0.30	0.20	1.00	0.50	0.70	0.70	0.90	1.30	0.20	0.30	0.20	0.20
Nb	243.00	118.00	270.00	87.00	15.50	309.00	38.60	60.90	76.70	8.00	55.50	734.00	74.70	60.60	7.30	12.90	8.60	4.10
Rb	6.70	9.10	230.00	42.00	4.10	24.60	11.70	4.10	11.30	9.00	0.80	8.40	4.80	8.50	0.90	1.50	48.50	11.80
Sr	7410.00	7220.00	2540.00	10000.00	5380.00	7940.00	3830.00	8840.00	3480.00	10000.00	9680.00	2520.00	2780.00	2690.00	986.00	3740.00	1415.00	1095.00
Ta	0.70	0.30	12.00	0.25	0.10	1.70	0.20	0.50	0.20	0.25	0.90	9.60	0.40	0.10	0.10	0.10	0.10	0.05
Th	2.94	3.71	4.67	8.40	1.73	2.37	2.44	8.91	14.55	5.90	25.20	103.00	125.50	16.25	3.96	65.40	33.60	4.53
U	1.81	4.48	1.95	2.60	3.69	9.94	7.84	4.48	7.01	0.30	2.54	47.90	22.10	11.95	4.04	0.57	2.59	4.47
Zr	35.00	35.00	415.00	10.00	13.00	13.00	18.00	11.00	33.00	20.00	17.00	8.00	29.00	62.00	12.00	19.00	4.00	3.00
La	230.00	206.00	45.80	198.00	220.00	196.00	261.00	416.00	1050.00	89.00	2850.00	4380.00	1200.00	233.00	188.50	6740.00	6940.00	1225.00
Ce	458.00	421.00	94.20	409.00	423.00	413.00	518.00	682.00	1675.00	184.00	4590.00	7630.00	2120.00	481.00	374.00	8480.00	9030.00	1620.00
Pr	52.80	50.70	11.35	43.60	46.30	48.40	59.40	75.70	157.00	21.90	401.00	725.00	216.00	54.00	40.00	665.00	734.00	135.00
Nd	182.00	174.00	40.50	155.00	156.00	166.50	201.00	241.00	476.00	88.20	1195.00	2250.00	732.00	190.50	135.00	1680.00	1920.00	353.00
Sm	28.90	29.20	6.48	26.70	23.20	25.80	31.90	32.50	55.00	18.10	103.00	247.00	118.00	30.10	21.10	110.00	146.50	32.70
Eu	8.22	8.20	1.97	8.10	6.78	7.80	9.42	9.38	15.30	5.50	26.00	61.20	37.80	8.52	6.26	24.00	31.20	8.10
Gd	29.00	29.30	6.38	27.50	24.50	25.70	33.00	35.00	69.40	17.10	141.00	281.00	131.50	29.50	21.10	154.00	183.00	42.00
Tb	3.81	3.69	0.78	3.42	3.20	3.34	4.32	4.37	6.93	2.52	11.35	23.90	18.10	3.82	2.88	8.75	11.20	4.15
Dy	18.10	18.95	3.64	17.70	15.70	16.00	21.20	21.70	26.20	14.60	31.50	68.20	86.70	19.30	14.70	21.30	30.60	20.30
Ho	3.56	3.65	0.69	3.43	3.19	3.08	4.29	4.33	5.00	3.18	6.11	12.30	17.30	3.75	3.05	3.94	5.49	4.41
Er	10.15	10.20	2.08	10.30	9.45	9.03	12.90	13.40	16.15	10.70	23.30	44.00	50.30	10.05	8.45	14.80	19.95	13.90
Tm	1.31	1.42	0.27	1.28	1.26	1.14	1.67	1.84	1.92	1.54	2.28	4.27	6.27	1.27	1.13	1.42	1.98	1.88
Yb	8.08	8.05	2.05	8.30	7.66	7.12	10.60	11.50	12.05	10.30	15.40	27.50	37.70	8.19	7.67	9.61	13.55	12.85
Lu	1.11	1.16	0.35	1.11	1.00	0.94	1.36	1.55	1.66	1.38	2.06	3.61	4.69	1.07	1.04	1.24	1.79	1.83
Y	88.20	92.80	17.10	88.00	79.90	75.30	108.00	110.50	125.00	101.00	170.50	328.00	420.00	90.70	72.90	96.50	155.50	125.50
La/Yb	28.47	25.59	22.34	23.86	28.72	27.53	24.62	36.17	87.14	8.64	185.06	159.27	31.83	28.45	24.58	701.35	512.18	95.33

Appendix 2 b) Trace elements analysis of samples collected by Etruscan and NRE and used in this study

Sample No.	ERNI8630	ERNI8631	ERNI8632	ERNI8633	ERNI8634	ERNI8635	ERNI8636	ERNI8637	ERNI8638	ERNI8639	ERNI8640	ERNI8641	ERNI8642	ERNI8643	ERNI8644	ERNI8645	ERNI8646	ERNI8647
Ba	126.00	239.00	91.60	485.00	520.00	1015.00	736.00	738.00	925.00	369.00	498.00	105.00	685.00	254.00	345.00	1710.00	5500.00	287.00
Ga	31.20	65.60	22.60	5.80	7.00	18.00	7.20	8.40	10.40	23.40	41.10	49.10	6.30	6.40	4.60	10.20	9.00	7.10
Hf	0.50	0.50	0.10	1.70	0.50	5.60	1.30	2.80	1.10	1.00	6.00	1.00	1.00	0.30	0.30	4.90	2.00	1.00
Nb	3.00	8.00	0.60	84.40	76.00	251.00	75.40	69.30	70.30	90.00	16.00	25.00	76.60	1.20	1.70	126.50	117.00	31.00
Rb	9.00	5.00	1.80	6.90	6.40	101.00	12.20	12.50	7.10	10.00	12.00	6.00	5.40	12.60	2.10	17.90	23.00	18.30
Sr	1035.00	2880.00	2810.00	2900.00	1190.00	3980.00	5270.00	7870.00	5650.00	887.00	2280.00	771.00	8130.00	1475.00	3750.00	9830.00	10000.00	1440.00
Ta	0.25	0.25	0.05	1.00	1.50	3.90	0.90	1.10	0.90	0.60	0.90	0.90	0.50	0.10	0.10	3.80	1.30	0.40
Th	34.30	72.40	26.30	7.19	9.59	429.00	72.10	62.00	76.10	1450.00	2190.00	362.00	24.80	37.90	19.00	453.00	427.00	86.70
U	2.00	1.70	0.62	4.58	3.09	21.20	4.19	3.36	4.88	12.10	6.00	2.90	8.83	1.91	1.77	10.30	11.00	8.45
Zr	90.00	70.00	1.00	133.00	23.00	284.00	64.00	153.00	45.00	50.00	60.00	60.00	34.00	4.00	5.00	124.00	110.00	50.00
La	9560.00	20300.00	7180.00	645.00	393.00	2100.00	719.00	573.00	1410.00	5170.00	10300.00	11850.00	483.00	847.00	547.00	754.00	749.00	1280.00
Ce	12600.00	26900.00	9360.00	1095.00	693.00	3260.00	1235.00	1125.00	2520.00	7750.00	14750.00	18000.00	886.00	1600.00	1050.00	1330.00	1160.00	1905.00
Pr	1035.00	2250.00	762.00	114.50	71.90	318.00	131.00	129.00	272.00	736.00	1340.00	1710.00	95.60	175.00	116.00	151.50	118.50	183.00
Nd	2650.00	5930.00	2010.00	372.00	239.00	1000.00	435.00	467.00	925.00	2260.00	3850.00	4990.00	331.00	607.00	411.00	579.00	414.00	566.00
Sm	192.50	418.00	151.50	52.40	36.30	155.50	67.40	91.40	157.00	499.00	975.00	491.00	56.90	100.00	75.80	193.00	98.40	79.30
Eu	41.50	87.60	31.70	13.25	9.94	55.60	20.20	27.20	41.90	159.50	466.00	101.50	16.45	22.60	15.90	98.80	37.60	22.20
Gd	234.00	506.00	188.50	50.10	37.00	210.00	70.10	92.90	150.50	568.00	1605.00	492.00	57.40	88.20	71.20	347.00	121.00	82.10
Tb	13.00	26.90	11.30	5.69	4.75	34.30	9.07	14.40	18.90	68.90	252.00	37.90	7.62	10.45	9.72	64.60	21.40	8.98
Dy	29.90	49.50	28.10	26.10	24.50	187.50	44.80	77.60	89.30	300.00	1235.00	113.50	36.60	50.50	52.10	327.00	130.00	39.40
Ho	5.02	7.18	4.93	5.14	5.16	36.30	8.63	15.60	16.85	47.30	190.50	16.30	6.86	10.25	11.20	56.50	24.70	7.15
Er	19.60	32.30	18.00	14.55	14.65	97.00	23.20	41.90	45.50	114.00	411.00	46.60	17.90	30.50	33.00	133.50	68.20	19.50
Tm	1.52	1.85	1.62	1.83	2.05	13.45	2.92	5.44	5.94	12.95	41.10	3.63	2.30	4.22	4.67	17.20	8.86	2.46
Yb	10.40	11.80	10.85	12.30	14.05	91.20	18.40	33.70	37.20	80.70	211.00	23.60	14.55	27.80	30.90	104.00	54.70	15.95
Lu	1.39	1.46	1.45	1.63	1.90	12.50	2.41	4.42	4.81	10.70	25.00	3.20	1.91	3.83	4.37	13.15	7.11	2.14
Y	157.00	194.00	156.50	122.00	129.00	751.00	217.00	400.00	417.00	1200.00	4520.00	464.00	168.00	272.00	270.00	1255.00	690.00	178.00
La/Yb	919.23	1720.34	661.75	52.44	27.97	23.03	39.08	17.00	37.90	64.06	48.82	502.12	33.20	30.47	17.70	7.25	13.69	80.25

Appendix 2 b) Trace elements analysis of samples collected by Etruscan and NRE and used in this study

Sample No.	ERN18648	ERN18649	ERN18650	ERN18651	ERN18652	ERN18653	ERN18654	ERN18655	ERN18656	ERN18657	ERN18658	ERN18659	ERN18660	ERN18661	ERN18662	ERN18663	ERN18664	ERN18665
Ba	130.00	249.00	3170.00	324.00	288.00	261.00	669.00	487.00	133.50	38.30	79.50	37.20	268.00	269.00	398.00	592.00	483.00	613.00
Ga	39.20	9.20	14.20	15.40	2.60	2.90	21.30	10.40	4.10	3.90	2.80	9.10	4.30	5.30	6.60	3.80	4.20	11.00
Hf	0.50	1.10	3.00	42.90	0.40	1.30	1.10	6.40	1.40	1.60	0.20	0.80	1.50	4.00	3.70	0.50	0.80	1.10
Nb	8.00	101.50	296.00	357.00	4.00	32.70	26.20	632.00	34.00	120.00	11.60	14.40	191.50	337.00	82.10	13.00	109.50	1135.00
Rb	2.00	18.60	6.00	13.70	1.80	1.20	3.30	8.10	0.60	0.50	0.40	0.60	4.10	3.00	12.20	3.00	6.50	3.70
Sr	1675.00	978.00	10000.00	1575.00	1405.00	4830.00	2330.00	9070.00	917.00	517.00	322.00	367.00	4250.00	10000.00	5860.00	10000.00	5020.00	1420.00
Ta	0.25	0.60	6.70	4.30	0.05	0.20	0.10	1.20	0.10	0.30	0.05	0.10	0.40	0.25	0.10	0.25	0.20	1.00
Th	280.00	176.50	215.00	5.04	1.22	1.67	151.00	13.20	3.03	2.55	7.25	152.50	2.94	2.60	4.02	5.40	3.88	32.50
U	4.60	7.52	7.80	7.22	1.33	5.24	10.10	7.10	1.06	2.91	1.00	2.99	26.40	1.30	7.88	2.20	14.50	43.00
Zr	50.00	40.00	90.00	2540.00	14.00	46.00	57.00	236.00	39.00	54.00	5.00	48.00	66.00	180.00	139.00	20.00	38.00	45.00
La	7400.00	1270.00	870.00	93.70	159.00	154.00	2170.00	168.00	311.00	206.00	149.00	883.00	172.50	214.00	277.00	266.00	242.00	491.00
Ce	13300.00	2120.00	1645.00	211.00	320.00	311.00	4960.00	336.00	611.00	439.00	317.00	2040.00	343.00	439.00	554.00	510.00	474.00	932.00
Pr	1385.00	213.00	192.00	25.80	37.10	35.70	592.00	38.80	70.50	52.60	37.90	255.00	39.60	47.60	67.00	53.90	54.70	103.50
Nd	4360.00	694.00	729.00	93.40	123.00	122.00	2050.00	132.00	236.00	181.50	130.50	886.00	131.50	169.00	228.00	181.00	188.50	342.00
Sm	462.00	131.00	167.00	15.15	19.90	19.10	250.00	21.40	33.30	27.60	18.70	107.50	20.50	25.10	34.30	27.30	28.40	52.10
Eu	107.00	37.00	45.90	4.01	5.86	5.76	47.40	6.06	8.59	6.54	3.50	20.80	5.69	6.90	9.08	7.80	8.30	15.90
Gd	401.00	156.50	133.50	13.45	19.70	21.10	195.00	21.30	32.40	26.00	17.35	98.10	20.60	24.30	32.90	28.30	28.70	58.30
Tb	29.50	25.10	15.90	1.74	2.63	2.68	15.10	2.70	3.90	3.22	2.06	10.50	2.50	3.02	3.90	3.38	3.52	7.44
Dy	78.40	133.00	72.00	7.91	13.20	13.05	36.00	13.05	18.10	14.05	9.41	42.00	11.70	14.30	17.30	16.30	15.90	35.40
Ho	10.75	25.40	12.30	1.53	2.62	2.57	6.04	2.54	3.66	2.45	1.92	8.54	2.28	2.60	3.21	3.28	2.97	6.70
Er	34.10	60.70	33.80	5.35	7.88	7.59	24.00	7.53	11.05	7.10	6.33	27.40	6.56	7.30	9.79	9.70	8.61	19.40
Tm	2.61	7.13	4.14	0.86	1.06	1.03	1.88	0.98	1.48	0.82	0.91	3.16	0.81	1.03	1.18	1.37	1.02	2.51
Yb	18.30	41.00	26.00	8.41	6.93	6.76	12.25	6.07	9.58	5.06	6.44	18.55	5.14	5.90	8.03	8.90	6.56	15.65
Lu	2.50	5.20	3.44	2.02	1.04	1.02	1.57	0.93	1.50	0.74	1.05	2.54	0.75	0.83	1.18	1.23	0.90	2.12
Y	313.00	693.00	321.00	40.00	63.10	62.50	161.50	60.30	95.00	51.00	49.00	229.00	53.60	61.00	78.10	83.00	70.20	165.00
La/Yb	404.37	30.98	33.46	11.14	22.94	22.78	177.14	27.68	32.46	40.71	23.14	47.60	33.56	36.27	34.50	29.89	36.89	31.37

Appendix 2 b) Trace elements analysis of samples collected by Etruscan and NRE and used in this study

Sample No.	ERNI8666	ERNI8667	ERNI8668	ERNI8669	ERNI8670	ERNI8671	ERNI8672	ERNI8673	ERNI8674	ERNI8675	ERNI8676	ERNI8677	ERNI8678	ERNI8679	ERNI8680	ERNI8701	ERNI8702	ERNI8703
Ba	638.00	92.80	193.00	258.00	120.00	1940.00	443.00	603.00	116.50	490.00	1920.00	283.00	136.50	178.50	790.00	2950.00	631.00	1220.00
Ga	16.00	3.90	4.80	4.00	30.80	16.90	21.50	17.00	45.80	18.90	46.50	30.70	20.60	10.40	12.60	24.20	4.10	31.80
Hf	3.70	11.00	4.00	4.80	1.20	3.00	0.70	3.00	0.50	0.90	0.50	2.00	2.00	0.60	1.10	11.50	1.90	16.00
Nb	197.00	411.00	2240.00	156.00	9.10	56.00	2.60	47.00	2.00	38.10	422.00	70.00	10.60	5.30	103.50	274.00	60.70	521.00
Rb	46.70	3.40	9.40	2.80	4.70	4.00	0.60	9.00	2.00	6.10	30.00	4.00	8.70	35.40	9.60	159.00	3.90	190.00
Sr	7510.00	1730.00	4540.00	8540.00	1975.00	1390.00	1615.00	9490.00	3140.00	6910.00	1705.00	1775.00	4450.00	1895.00	4670.00	1435.00	6100.00	1180.00
Ta	2.70	2.70	11.80	0.70	0.20	0.80	0.10	0.70	0.25	0.70	2.90	1.30	0.60	0.20	1.80	13.20	0.50	8.30
Th	6.55	7.41	40.30	8.08	636.00	1765.00	186.00	1610.00	231.00	141.50	167.00	1400.00	495.00	43.00	178.50	4.33	5.01	4.01
U	6.26	23.00	79.00	29.30	3.57	12.20	4.01	8.10	1.00	7.40	12.40	10.80	2.70	2.26	10.45	1.03	1.71	1.07
Zr	313.00	1205.00	336.00	266.00	15.00	20.00	9.00	50.00	30.00	34.00	50.00	30.00	24.00	9.00	34.00	709.00	185.00	1135.00
La	245.00	229.00	241.00	280.00	5340.00	1640.00	3210.00	2080.00	7760.00	2470.00	5920.00	6160.00	2690.00	972.00	814.00	49.80	339.00	40.00
Ce	463.00	418.00	511.00	547.00	8600.00	3540.00	5690.00	4150.00	13950.00	4610.00	11400.00	8880.00	4430.00	1925.00	1505.00	105.50	652.00	83.60
Pr	52.40	46.80	62.90	62.60	827.00	412.00	607.00	465.00	1380.00	509.00	1160.00	795.00	467.00	231.00	172.50	12.10	68.80	9.40
Nd	176.50	152.50	223.00	208.00	2410.00	1515.00	2000.00	1670.00	4180.00	1600.00	3640.00	2350.00	1535.00	741.00	577.00	44.00	239.00	34.10
Sm	26.60	22.50	35.50	31.60	256.00	261.00	243.00	365.00	394.00	202.00	366.00	326.00	243.00	111.00	108.00	7.11	35.60	5.21
Eu	7.71	7.66	10.30	9.08	72.00	103.00	45.20	156.50	77.00	53.00	74.50	102.50	75.10	30.60	38.00	2.01	9.73	1.51
Gd	27.50	23.60	34.00	31.50	345.00	402.00	259.00	583.00	386.00	212.00	332.00	414.00	286.00	112.00	127.00	6.28	33.80	4.89
Tb	3.30	2.91	4.34	3.84	42.10	92.60	26.50	117.50	27.00	21.30	22.90	59.70	48.30	13.50	19.05	0.75	4.01	0.59
Dy	15.00	13.70	19.90	16.60	212.00	601.00	110.00	663.00	86.10	80.30	65.80	321.00	323.00	64.10	99.40	3.56	19.55	2.89
Ho	2.87	2.67	3.58	3.20	40.80	115.50	21.80	112.50	16.05	15.05	11.30	59.50	73.80	13.00	18.70	0.61	3.61	0.54
Er	8.18	7.98	10.30	9.61	112.50	287.00	69.80	270.00	58.90	49.30	40.50	168.50	231.00	41.00	52.00	1.82	10.80	1.76
Tm	1.01	1.06	1.18	1.20	12.20	33.40	8.08	30.90	7.29	5.93	4.41	23.70	33.90	5.91	7.06	0.26	1.37	0.29
Yb	5.95	7.05	7.11	7.39	65.20	177.50	48.30	175.00	49.30	38.80	31.50	159.50	225.00	38.30	42.10	2.20	9.11	2.43
Lu	0.84	1.19	0.98	1.05	8.26	21.60	6.55	21.60	6.80	5.69	4.42	21.80	32.10	6.01	5.91	0.39	1.23	0.44
Y	68.90	74.20	86.90	79.10	1055.00	2720.00	714.00	2550.00	487.00	406.00	345.00	1595.00	1920.00	369.00	530.00	14.80	88.80	13.10
La/Yb	41.18	32.48	33.90	37.89	81.90	9.24	66.46	11.89	157.40	63.66	187.94	38.62	11.96	25.38	19.33	22.64	37.21	16.46

Appendix 2 b) Trace elements analysis of samples collected by Etruscan and NRE and used in this study

Sample No.	ERN18704	ERN18705	ERN18706	ERN18707	ERN18708	ERN18709	ERN18710	ERN18711	ERN18712	ERN18713	ERN18714	ERN18715	ERN18716	ERN18717	ERN18718	ERN18719	ERN18720	ERN18721
Ba	4360.00	2070.00	714.00	2970.00	3460.00	1945.00	2080.00	3500.00	1125.00	983.00	1970.00	1050.00	944.00	1400.00	1665.00	331.00	1620.00	1585.00
Ga	24.70	34.60	9.50	25.50	23.10	14.10	25.10	23.30	37.90	41.40	27.20	32.00	26.60	17.00	26.30	5.10	24.50	23.50
Hf	5.40	28.60	0.50	12.70	9.20	3.40	9.80	9.30	7.40	24.40	7.90	8.10	9.60	2.00	6.70	0.20	5.20	7.60
Nb	563.00	1085.00	49.40	640.00	319.00	3430.00	367.00	337.00	95.60	757.00	168.00	502.00	172.50	250.00	280.00	13.10	269.00	184.50
Rb	249.00	211.00	64.90	212.00	183.00	120.00	229.00	201.00	326.00	267.00	230.00	188.50	183.50	100.00	244.00	16.00	128.50	165.00
Sr	1990.00	1020.00	6850.00	1640.00	1295.00	9310.00	1720.00	1285.00	139.50	567.00	918.00	619.00	1665.00	4680.00	1450.00	6750.00	710.00	1110.00
Ta	8.50	19.30	0.20	12.50	13.10	43.80	8.30	12.20	3.10	15.30	1.50	4.40	4.60	5.20	6.80	0.10	9.00	9.40
Th	4.46	9.16	3.78	11.45	5.14	32.10	4.04	5.37	5.28	7.43	3.13	8.57	5.84	9.74	3.91	24.10	5.36	3.96
U	2.69	11.90	2.74	2.81	2.04	404.00	1.44	3.06	2.06	59.50	3.31	11.25	1.66	86.30	5.04	1.32	4.20	1.53
Zr	411.00	1930.00	29.00	1010.00	563.00	250.00	658.00	577.00	451.00	1790.00	483.00	425.00	614.00	165.00	435.00	9.00	311.00	426.00
La	39.20	109.00	202.00	82.90	37.50	296.00	30.50	82.60	40.60	27.60	19.60	45.00	26.00	212.00	46.20	192.50	34.20	38.80
Ce	80.30	223.00	405.00	145.50	87.50	692.00	60.40	157.50	70.70	51.00	38.90	91.80	50.80	442.00	88.10	405.00	65.90	83.90
Pr	8.91	25.40	41.70	14.55	10.85	81.00	6.63	17.40	7.27	5.05	4.20	10.35	5.56	49.00	9.38	44.70	7.06	9.59
Nd	31.90	93.60	143.00	47.70	41.50	300.00	23.80	61.70	23.60	16.70	14.70	39.00	19.70	174.50	31.90	159.50	24.30	34.20
Sm	4.89	15.55	21.80	6.79	6.96	50.00	3.88	9.27	3.21	2.26	2.31	7.13	3.20	26.90	4.44	27.20	3.78	5.30
Eu	1.41	4.41	6.10	1.97	2.11	13.15	1.13	2.60	0.93	0.67	0.71	2.09	0.93	7.63	1.19	7.98	1.06	1.42
Gd	4.58	14.20	20.90	7.09	6.29	41.90	3.47	8.36	3.20	2.33	2.24	6.90	2.93	25.20	4.04	26.50	3.56	4.54
Tb	0.54	1.77	2.57	0.95	0.77	4.88	0.43	0.98	0.42	0.28	0.27	0.93	0.35	3.03	0.45	3.79	0.44	0.54
Dy	2.55	8.68	12.65	4.90	3.67	22.40	2.21	4.63	2.33	1.40	1.45	4.68	1.84	14.40	2.16	20.20	2.18	2.40
Ho	0.46	1.56	2.42	0.93	0.65	3.98	0.42	0.81	0.50	0.29	0.28	0.89	0.36	2.65	0.40	3.88	0.42	0.42
Er	1.28	4.46	7.14	2.65	1.82	11.35	1.34	2.52	1.54	0.99	0.91	2.61	1.21	7.67	1.22	11.25	1.23	1.34
Tm	0.16	0.57	0.90	0.33	0.25	1.36	0.21	0.34	0.24	0.18	0.15	0.36	0.20	1.00	0.17	1.50	0.17	0.21
Yb	1.03	3.83	6.03	2.20	1.88	8.89	1.70	2.58	1.72	1.13	1.13	2.36	1.75	6.44	1.16	9.58	1.12	1.72
Lu	0.14	0.58	0.81	0.32	0.31	1.19	0.31	0.42	0.26	0.20	0.19	0.32	0.30	0.91	0.16	1.31	0.16	0.32
Y	11.20	38.20	61.30	22.90	15.10	98.50	10.50	20.50	13.30	7.20	7.40	21.50	9.20	63.70	9.90	99.90	10.20	10.60
La/Yb	38.06	28.46	33.50	37.68	19.95	33.30	17.94	32.02	23.60	24.42	17.35	19.07	14.86	32.92	39.83	20.09	30.54	22.56

Appendix 2 b) Trace elements analysis of samples collected by Etruscan and NRE and used in this study

Sample No.	ERN18722	ERN18723	ERN18724	ERN18725	ERN18726	ERN18727	ERN18728	ERN18729	ERN18730	ERN18731	ERN18732	ERN18733	ERN18734	ERN18735	ERN18736
Ba	2670.00	1295.00	3450.00	446.00	1955.00	4670.00	359.00	2070.00	504.00	1345.00	446.00	3550.00	325.00	410.00	100.50
Ga	38.40	24.70	22.70	3.20	31.50	25.80	3.10	34.30	3.00	25.00	2.20	31.60	22.80	25.60	2.60
Hf	21.90	1.30	6.70	0.50	31.90	9.10	0.30	9.30	0.20	13.20	1.60	19.20	11.60	13.20	0.40
Nb	1045.00	128.50	404.00	6.00	1670.00	231.00	13.00	618.00	52.40	2940.00	4.40	670.00	130.50	163.00	107.50
Rb	279.00	49.20	220.00	9.00	257.00	242.00	5.00	183.00	5.80	184.50	1.80	159.50	5.30	8.10	1.30
Sr	2010.00	5390.00	2080.00	10000.00	1595.00	1805.00	6250.00	380.00	8420.00	552.00	4240.00	2030.00	338.00	181.50	8290.00
Ta	15.40	1.10	12.30	0.25	22.00	10.90	0.20	13.90	0.30	28.90	0.05	14.30	0.90	0.90	0.50
Th	7.83	52.20	6.60	2.60	4.52	2.39	2.16	5.40	15.60	14.95	2.52	3.30	6.55	8.15	6.90
U	2.98	75.80	3.93	0.60	6.41	3.55	0.96	12.90	1.66	40.80	1.42	4.14	2.26	3.12	5.40
Zr	1645.00	80.00	448.00	10.00	2420.00	531.00	14.00	580.00	12.00	1095.00	74.00	1620.00	692.00	574.00	13.00
La	67.20	5420.00	90.60	176.00	64.40	26.00	153.50	91.80	153.50	114.00	173.00	30.50	46.40	62.90	275.00
Ce	139.00	7240.00	181.00	364.00	125.00	48.90	317.00	153.00	352.00	224.00	356.00	63.70	92.30	122.00	554.00
Pr	15.25	586.00	20.10	36.90	12.70	5.28	33.10	14.60	42.60	23.50	38.70	7.09	10.85	13.25	59.10
Nd	55.30	1565.00	72.20	130.50	42.60	18.30	112.50	46.00	173.00	81.10	135.00	25.00	40.00	47.10	200.00
Sm	8.62	135.00	11.50	20.50	6.49	2.73	17.40	5.72	41.60	11.70	21.40	3.94	6.85	7.72	32.40
Eu	2.39	34.10	3.27	6.00	1.76	0.87	4.94	1.67	11.70	2.95	6.08	1.18	2.40	2.13	9.86
Gd	7.77	163.50	10.50	20.70	6.17	2.63	17.20	5.81	35.90	10.55	20.60	3.73	7.55	7.58	33.30
Tb	0.95	13.55	1.26	2.74	0.74	0.30	2.22	0.60	4.36	1.23	2.66	0.48	1.04	1.01	4.66
Dy	4.66	49.70	5.80	13.70	3.86	1.46	11.35	2.82	19.95	5.75	13.15	2.52	5.63	5.20	24.80
Ho	0.85	8.09	1.03	2.73	0.77	0.26	2.15	0.51	3.53	1.01	2.49	0.51	1.04	1.05	4.73
Er	2.59	23.70	2.83	8.00	2.48	0.80	6.49	1.56	9.94	3.04	7.17	1.76	2.92	2.89	14.00
Tm	0.37	2.31	0.35	1.06	0.37	0.14	0.87	0.22	1.27	0.36	0.94	0.31	0.39	0.37	1.73
Yb	2.64	14.00	2.23	8.00	2.87	1.14	5.69	1.51	8.26	2.52	6.26	2.63	3.06	2.96	11.40
Lu	0.42	1.80	0.31	1.09	0.46	0.23	0.82	0.26	1.14	0.35	0.91	0.46	0.55	0.49	1.46
Y	21.10	190.00	24.20	67.00	18.80	6.60	54.00	12.80	83.60	24.40	63.20	12.00	26.40	27.10	116.00
La/Yb	25.45	387.14	40.63	22.00	22.44	22.81	26.98	60.79	18.58	45.24	27.64	11.60	15.16	21.25	24.12

Appendix 3 a) Descriptions of VNP samples; collected by the author based on carbonatite and alkalic rocks lithologies

Sample No.	Coordinates		Description
	Lat (S)	Long (E)	
VNP1	20° 21.392'	014° 56.715'	Mafic dyke intruded into the amphibolites partly migmatitic country rock. Calcitic micro dykes cutting the mafic dykes. NE direction
VNP2	20° 17.866'	014° 43.516'	Alkaline dyke with light minerals accentuated by weathering. Sample and photo to be taken. NE Direction
VNP3	20° 17.866'	014° 43.516'	Mafic rock with black inclusions (lamprophyre??. Located at 6 m E of VNP2. VNP3 cross cutting VNP2 (sketch)
VNP4	20° 17.892'	014° 43.407'	CARBONATITE DYKES 5 – 10 cm wide. The dyke can be followed for few meters and has dark to red brown colour.
VNP5	20° 18.087'	014° 43.329'	Carbonatite dyke of 5 cm wide. It is grey colour and intrudes into the light coloured rock (quartzite)
VNP7	20° 18.101'	014° 43.323'	Carbonatites with black reddish and yellow colour. magnetite layers in the carbonatites.
VNP8	20° 18.123'	014° 43.324'	Mafic dyke with mafic xenoliths (lamprophyre). The body has eastern-western direction and can be followed for kms. This unit lies parallel to the carbonatites (VNP7) for kms keeping the distance between the two fairly constant. The inclusions (mafic) are subangular to rounded and has a size up to 3 cm. The inclusions weather creating holes in the rock. The feldspar which are accentuated by the weathering have a direction following the dyke.Schist layer between the amphibole near the point (VNP 8). The schist contains blebs of cordierite and at the sides the feldspar growth can be seen indicating high temperature at about (6000C)
VNP9	20° 18.144'	014° 43.333'	Carbonatite intruding the schist. The carbonatite is grey in colour and containing fragments of the country rock.
VNP10	20° 18.163'	014° 43.352'	Mafic dyke intruding the country rock. The dyke is brecciated at the central part by fluids. The fragments are in place photo taken. These fragments are observed only on weathered parts of the dyke.
VNP11	20° 18.271'	014° 43.311'	Carbonatite dyke of about 1 m wide containing magnetite layers on the margins. Show some kind of layering.
VNP12	20° 18.306'	014° 43.299'	Carbonatite dyke with a N-S direction, clearly cutting the pegmatites and the fine grained felsic dyke. At five (5) meters the carbonatites direction follows the local foliation
VNP13	20° 18.307'	014° 43.293'	Flow-textures observed on the rocks that are intruding. Dyke size 80 cm. Rocks next to the carbonatite dykes that fractured and filled with secondary black (magnetite) fluids mingling and mostly parallel to the carbonatite dyke (read plume tectonics).
VNP14	20° 18.467'	014° 43.204'	Fault?? With a NS direction and filled with carbonatite. The carbonatite contain quartzite fragments. Sample taken
VNP15	20° 18.475'	014° 43.175'	Ryolite? 2m dyke following the local textures (schistosity). This rock cuts the pegmatites of the Huab formation. Lithofuse texture observed.
VNP16	20° 18.367'	014° 42.921'	A large body of brecciated country rock. At places carbonatites are found with joints /cracks brecciated cutting the dyke. At places fractures are filled with magnetite veins. Sample to be taken at this place (carbonatite)Alteration of clasts. Clast are angular shapes up to 0.5 m Fragments are closely packed, angular varying in size between 1 – 50cm. Carbonatites have intruded the breccia, and are embedded in a fine grained facies of syenites??.
VNP17	20° 19.304'	014° 39.193'	LOFDAL Mafic dyke cutting granitic rocks, these rock show strong schcistocity EW direction and also NS direction, younger facies
VNP17a	21° 19.304'	015° 39.193'	Carbonatites materials filling the cavities created by schistocity. VNP17a CARBONATITE? CARBONATITE FILLING JOINTS OF a mafic rock.
VNP18	21° 19.304'	015° 39.193'	Sample of the mafic rock.
VNP19	21° 19.304'	015° 39.193'	Carbonatite dyke up to 30 cm wide and 40 m long.
VNP20	20° 19.513'	014° 42.530'	dark brown colour carbonatite

Appendix 3 a) Descriptions of VNP samples; collected by the author based on carbonatite and alkalic rocks lithologies

Sample No.	Coordinates		Description
	Lat (S)	Long (E)	
VNP21	20° 19.036'	014° 41.067'	Sample taken of a brecciated country rock fragments with angular (granitic schist. Fragments at contact of each other or cemented by dark mineral (hematite).
VNP22	20° 19.036'	014° 41.067'	grey coloured carbonatite
VNP23	20° 19.061'	014° 41.067'	Small dykes – mafic dyke cutting granitic gneisses. If these dykes are bigger than 5 cm they clearly cut the country rock following the local foliation. Smaller dykes < 5 cm show mingling fillinn fractures in all directions.
VNP24	20° 19.153'	014° 41.050'	Felsic dyke cutting the granitic gneisses, which covers most of the hill. The dyke show porphyritic texture observed on the weathered surface, indicated by white patches that are randomly distributed.
VNP25	20° 19.145'	014° 41.052'	Mafic dyke adjacent 5 m to VNP 24. Greenish brown coloured on the weathered surface. Agglomeratic texture observed on the weathered surface marked by the green mineral. The minerals are oriented towards one direction see drawing.
VNP26	20° 19.139'	014° 41.105'	Carbonatite dyke observed on the lower side hill extending EW direction. Light brown in colour on the weathered surface. A sample was taken.
VNP27	20° 19.151'	014° 41.154'	Dyke with a thickness of about 30 cm and an EW direction cutting the amphibole rich layer into the granitic gneiss. Felsic mineral minerals direction follow the direction of the dyke. Light brown colour on the weathered surface and grey on the fresh surface.
VNP28	20° 19.282'	014° 41.205'	Carbonatite dyke 5 m wide with an EW direction. This carbonatite is red brown in colour at the weathered surface. Some red colours indicating late veining into carbonatite can be observed.
VNP29	20° 19.315'	014° 41.234'	Carbonatite dyke 4 m wide extending EW direction. Calcite show re-crystalisation marked by large crystals of calcite at places.
VNP29a	20° 19.315'	014° 41.234'	A large grained calcite mixed with magnetite. The carbonatite intrude amphibolites and contacts are observed.
VNP30	20° 19.380'	014° 41.210'	Sample from the Lofdal syenite pegmatite. 0.5 KM across body of syenite. The syenites are cut by pegmatitic syenites ranging from few centimeters across to 3 meters. These micro dykes have an EW direction. Inclusions of mafic rocks similar to VNP 25 are observed. There are also inclusions of granite gneisses.
VNP31	20° 19.380'	014° 41.210'	Sample of the mafic inclusion found in the syenite 4 m south of VNP 30
VNP32	20° 19.380'	014° 41.210'	Sample taken from the common syenite viewed around VNP 30 at about 7 m north. The syenite is coarse-grained, generally equi-granular with some porphyritic grains of feldspars (nepheline up to 10 cm large) set into the syenite. The feldspars are accentuated by weathering.
VNP33	20° 19.422'	014° 41.135'	Coarse-grained syenite with a different texture compared to VNP 32. Blue coloured felsic mineral. Later identified as sodalite.
VNP34	20° 19.490'	014° 41.133'	Porphyritic syenite. The porphyritic texture is marked by the dark minerals.
VNP35	20° 19.424'	014° 41.133'	Carbonatite dyke cutting the porphyritic syenite. Carbonatite cut by a tree!
VNP36	20° 19.413'	014° 41.129'	Felsic dyke cutting the syenites dyke.
VNP37	20° 19.465'	014° 41.120'	Fine grained syenites found next to the coarse grained syenites ro the east.
VNP38	20° 19.468'	014° 41.135'	Phonolite? Dyke cutting the fine grained version of the syenites. The dyke has 2 m wide and an EW direction.
VNP39	20° 19.468'	014° 41.167'	2 m thick phonolite dyke cutting the fine syenites and has an EW direction.
VNP40	20° 19.425'	014° 41.147'	Mafic dyke at places in contact with VNP 40 . contain inclusions of the coarse grained syenites and orthogneises.

Appendix 3 a) Descriptions of VNP samples; collected by the author based on carbonatite and alkalic rocks lithologies

Sample No.	Coordinates		Description
	Lat (S)	Long (E)	
VNP41	20° 19.425'	014° 41.147'	Chilled margins between the porphyritic dyke and the syenites.
VNP42	20° 19.425'	014° 41.147'	Porphyritic dyke cutting the fine grained syenites and a mafic dyke containing coarse syenites fragments. The dyke has an EW direction and is 1 m wide. Feldspar minerals are accentuated by weathering and are parallel to the dyke length. The rock contains fluorite phenocrysts.
VNP42a	20° 19.425'	014° 41.147'	Light coloured inclusions of syenites?
VNP44	20° 18.539'	014° 40.665'	Mafic dyke containing inclusions of granitic material? That is fine grained and with an EW direction. Chloritisation is observed in the cracks.
VNP45	20° 18.555'	014° 40.718'	A Carbonatite dyke intruding into the amphibolites and the gneisses. At times it seems that carbonatites fill in the fractures within the country rock. Fragments of the country rock form inclusions into the carbonatites.
VNP46	20° 18.572'	014° 40.737'	0.5 m carbonatite dyke with an EW direction. A 25 cm another carbonatite intrude the schist north (3 m) from this point.
VNP47	20° 17.292'	014° 42.549'	Yellow coloured carbonatite dyke ranging from 5 – 10 m thick. At places the carbonatite has yellow colour and at places the colour is brown reddish.
VNP48	20° 17.292'	014° 42.549'	Sample taken from the brown reddish color. These two carbonatites are found in contact with each other and no clear relationship can be observed. The carbonatites has breacciated the country rock, indicating a forceful act of emplacement. The dyke has a NS direction.
VNP49	20° 19.435'	014° 41.303'	Grey coloured carbonatite on the weathered and fresh surfaces syenites. Coarse grained with same feldspar mineral forming rock weak porphyritic textures.
VNP50	20° 19.425'	014° 41.301'	Fine-grained brown coloured dyke (weathered surface, cutting the grey coarse grained syenite. The dyke has an EW direction on the south contact the country rock shows shearing/fenitisisation zone of up to 10 – 50 cm wide
VNP51	20° 19.425'	014° 41.301'	A dyke that is brown in colour intruding dyke VNP 50. The dyke shows flow banding on the weathered surface marked by aligned vugs.
VNP52	20° 19.404'	014° 41.296'	Carbonatite dyke that is 10 cm wide with an EN direction. The dyke cuts the grey coarse grained syenites. Fluorite crystals set in the matrix ranging up to 2 cm.
VNP53	20° 19.423'	014° 41.344'	Black coloured chilled surface next to the carbonatited. Chilled margins?
VNP113	20° 20.208'	014° 40.648'	Carbonatite body between the brecciated country rock. The carbonatite is coarse-grained, white to brown in colour, 5m wide and extends 10m.
VNP114	20° 19.237'	014° 41.300'	3-4m wide felsic dyke showing porphyritic texture marked by light minerals on the weathered surface with N-W direction. The same
VNP115	20° 19.225'	014° 41.304'	Brown-black carbonatite dyke cut by a felsic dyke with E-W direction
VNP116	20° 19.225'	014° 41.304'	The felsic dyke that cuts the carbonatite dyke
VNP117	20° 19.225'	014° 41.306'	Light brown to white carbonatite dyke cutting the brown-black
Note:	20° 17.776'	014° 42.164'	Hydrothermally altered granitic gneiss hill 50x20m outcrops the surrounding N of the breccia, VNP16
VNP118	20° 17.685'	014° 42.069'	Porhyritic mafic dyke intruded into the amphibolite marked by white minerals on the weathered surface
VNP119	20° 17.638'	014° 42.038'	Carbonatite dyke with E-W direction intruded into the granitic
VNP120	20° 18.798'	014° 40.506'	Black and brown colour dyke striking E-W direction, the weathered surface is grey with porphyritic texture marked with euhedral minerals
VNP121	20° 20.719'	014° 37.370'	Carbonatite dyke mingled /intruded into the granitic pegmatite up to 10m wide with N-S direction. White quartz veins cutting the carbonatite. The
VNP122	20° 21.664'	014° 35.644'	Fine-grained mafic rock (phonolite?) forming boulders on the low relief surface, equigrenular and hard

Appendix 3 a) Descriptions of VNP samples; collected by the author based on carbonatite and alkalic rocks lithologies

Sample No.	Coordinates		Description
	Lat (S)	Long (E)	
VNP123	20° 20.749'	014° 37.795'	E-W striking carbonatite dyke up to 20m wide extending for up to 8km. Dark and light-brown in colour with trenching done in theses carbonatites. Black minerals (hematite?) filling fractures with calcitic materials
VNP124	21° 20.749'	015° 37.795'	Sample of iron rich? Found within the carbonatites at VNP123.
VNP125	20° 18.006'	014° 40.788'	30cm wide carbonatite dyke with E-W direction intruding the amphibolites and the schist with some well developed crenulation on the country rock.
VNP126	20° 17.493'	014° 43.445'	3-5m wide carbonatite dyke intruded into the gneisses. The dyke can be followed up to 3km's with E-W direction.
VNP127	20° 17.503'	014° 43.446'	Felsic dyke striking parallel to the carbonatite with E-W direction. Dark brown on the weathered surface and grey in colour on the fresh surface.
VNP128	20° 17.544'	014° 43.470'	4m wide dyke running parallel to VNP126&127 with an E-W direction. Brown to dark brown on the surface, grey when fresh, fine-grained and non-porphyritic.
VNP129	20° 17.563'	014° 43.461'	Brown dyke extending in E-W direction. Poorly porphyritic formed by
VNP130	20° 17.559'	014° 43.472'	15-30cm wide carbonatite dykes with E-W direction intruded into the amphibolite schist and forming many veinlets in the country rock.
VNP130b	20° 17.556'	014° 43.478'	Light coloured carbonatite sample
VNP130c	20° 17.568'	014° 43.468'	Brown-yellow veinlets
VNP130d	20° 17.568'	014° 43.470'	Carbonatite similar to VNP130
VNP130e	20° 17.563'	014° 43.470'	Black and red colour carbonatite tha is iron rich
VNP131	20° 16.844'	014° 43.420'	Dark bown rock with black porphiritic minerals. The direction of the dyke is N-S.
VNP132			Porphyritic dyke with violet feldspars forming the porphyritic texture North of Lofdal settlement, 3m south of the road.
VNP133			Magnetite? Dark coloured minerals found on the cleavage joints of the dyke VNP132
VNP134			Coarse-grained calcitic? Carbonatite.
VNP135			Breccia rock at the boundry between Tussenby and Lofdal.
VNP136			Coarse-grained syenite- common rock for the first syenite hill at Lofdal.
VNP137			Sample with yellow coloured mineral found in the pegmatite-syenite.
VNP138			Fine-grained dyke next to the VNP136 syenite with E-W direction.
VNP139			Sample taken from the porphyritic dyke with purple flourite crystals.
VNP140			Mafic dyke with many inclusions- syenite, granitic gneiss (orthoclase) and mafic inclusions.
VNP141			Magnetite crystals
VNP142			Quartz with magnetite veins
VNP143			Quartz vein with multiple cracking heeling as observed around the brecciated in matrix pieces of quartz.
VNP144a & b			Breccia - most likely from the pegmatite around which have been subjected to hydrothermal alteration. The rock is found in contact with carbonatites , having the same E-W direction that forms elevated ridges south of Bergville.
VNP 164	20° 19.467'	014° 41.077'	Grey colour carbonatite cutting the nepheline syenite at Lofdal
VNP 165	20° 19.731'	014° 40.591'	Dark grey phonolite hill with coarse grained nepheline syenite downhill
VNP 166	20° 19.731'	014° 40.591'	A carbonatite dyke E of Lofdal settlement intruding the country rock
VNP 170	20° 18.327'	014° 42.403'	Carbonatite dyke cutting the coarse grained grey syenite body
VNP 171	20° 18.327'	014° 42.403'	Carbonatite dyke cutting the nepheline syenites

Appendix 3 a) Descriptions of VNP samples; collected by the author based on carbonatite and alkalic rocks lithologies

Sample No.	Coordinates		Description
	Lat (S)	Long (E)	
VNP 172	20° 18.512'	014° 42.233'	Flat area of nepheline syenite with mica (muscovite) rich layers and carbonatite dykes
VNP 173	20° 18.620'	014° 42.235'	Breciatted nepheline syenite hill with green contact minerals
VNP 174	20° 18.862'	014° 42.196'	Hill with carbonatite layers invading the pegmatites. Thick carbonatite body ~10m wide at the base with the green contact mineral
VNP 175	20° 18.772'	014° 42.213'	Carbonatite body, ~50m wide
VNP 181	20° 19.053'	014° 42.056'	Yellowish reddish carbonatite dyke ~22cm wide with E-W direction
VNP 183	20° 18.833'	014° 42.123'	Carbonatite brecciated nepheline syenite. At places ferritisation has developed within the contacts
VNP 185	20° 18.780'	014° 42.122'	Sample taken on the calcitic carbonatite at the ferritised zone S of the intrusions
VNP 188	20° 18.996'	014° 42.183'	Fenite zone consisting of large blocks of nepheline syenites, granitic gneissess and alkaline dykes that are all strongly brecciated and calcitic carbonatites filling in the fractures and a scree of magnetite observed
VNP 193	20° 17.465'	014° 43.763'	Carbonatite breccia observed at quartz veins down hill
VNP 199	20° 15.856'	014° 46.801'	An alkaline dyke that continues E of the road at Bergville main post
VNP 200	20° 16.420'	014° 47.728'	Reddish strongly brecciated pegmatite dyke with carbonatite filled fractures
VNP 201	20° 16.629'	014° 48.940'	Carbonatite breccia on the pegmatite dyke
VNP 208	20° 16.619'	014° 41.870'	Closed Lofdal copper mine area with granitic pegmatites, quartz veins and most minerals observed are malachite and cuprite.
VNP 209	20 19 225	014 41 304	Sample of late veining ~3m consisting of coarse calcitic materials and finer grained carbonatite taken from a place of VNP116
VNP 210	20° 19.232'	014° 41.278'	Coarse-grained carbonatite that has large zoned brown and white in the centre crystals
VNP 211	20° 18.957'	014° 42.207'	White carbonatite cutting the nepheline syenite
VNP 212	20° 18.879'	014° 42.188'	Flat area of carbonatite body extending ~300-400m across with magnetite calcite veins cutting through the carbonatite
VNP 213	20° 18.858'	014° 42.173'	Highly porphyritic dykes cutting through the breccia with 25cm wide carbonatites
VNP 214	20° 18.907'	014° 42.186'	Red carbonatite dyke, ~25cm wide cutting through the nepheline syenite and sovite carbonatites
VNP 215	20° 18.933'	014° 42.206'	Sample taken from the sovite carbonatite body
VNP 216	20° 18.808'	014° 42.125'	Carbonatite dykes in contact with nepheline syenite with features of black minerals forming parallel joints perpendicular to the contact
VNP 217	20° 18.790'	014° 42.093'	Homogeneous grey nepheline syenite body, ideal for dating?
VNP 218	20° 20.982'	014° 42.013'	Reddish with black patches syenite body of the Oas. The rock is highly weathered, coarse-grained and pegmatitic at places
VNP 219	20° 21.417'	014° 42.143'	Brown reddish Oas syenite with more mafic rocks (with respect to VNP218) sample taken south of the trail road
VNP 220	20° 21.792'	014° 41.535'	Much more mafic Oas syenite than the previous Oas syenite sample
VNP 221	20° 22.233'	014° 41.803'	Yellow brown (cinamon) carbonatite?
VNP 222	20° 22.233'	014° 41.803'	Grey carbonates found next to VNP221 carbonatites?
VNP 223	20° 17.564'	014° 43.470'	Carbonate/tite filling in fractures of an igneous dyke that is highly porphyritic and at parts strongly sheared in the Nauport formation
VNP 224	20° 24.294'	014° 37.138'	30cm wide light-brown coloured dyke cutting the larger VNP223 dyke with a S-N direction
	20° 28.000'	014° 25.000'	Volcanics at Austerlitz
VNP 225	20° 27.387'	014° 26.896'	Sample of a fine-grained silica rich rock of an unknown origin (volcanic or sedimentary).
VNP 250	20° 17.175'	014° 43.355'	Granite hill about 40m wide
VNP 251 A	20° 18.627'	014° 43.233'	Reddish brown homogeneous carbonatite extending E-W direction

Appendix 3 a) Descriptions of VNP samples; collected by the author based on carbonatite and alkalic rocks lithologies

Sample No.	Coordinates		Description
	Lat (S)	Long (E)	
VNP 251 B	20° 18.627'	014° 43.233'	Carbonatite with magnetite intruding VNP 251 C
VNP 251 C	20° 18.627'	014° 43.233'	Brecciated carbonatite
VNP 252	20° 19.416'	014° 41.141'	Nepheline syenite, S of Lofdal settlement. 4 large (~20m) separate hills
VNP 253	20° 19.416'	014° 41.141'	Bluish coloured nepheline synite
VNP 255	20° 16.034'	014° 46.310'	Sedimental rock with pegmatite
VNP 256 A	20° 16.133'	014° 46.253'	Carbonatite with less inclusions
VNP 256 B	20° 16.133'	014° 46.253'	Calcite, remobilised from the carbonatite
VNP 256 C	20° 16.133'	014° 46.253'	Carbonatite
VNP 257	20° 16.141'	014° 43.230'	More dark coloured rock, fine-grained and homogeneous
VNP 258 A	20° 17.471'	014° 43.487'	Coarse-grained carbonatite dyke with siderite, extremely overprinted with quartz veins cutting
VNP 258 B	20° 17.471'	014° 43.487'	Fine-grained carbonatite dyke with siderite, extremely overprinted with quartz veins cutting
VNP 258 C	20° 17.471'	014° 43.487'	Quartz crystal for fluid inclusion studies
VNP 259	20° 17.471'	014° 43.487'	Yellow-brown coloured carbonatite cut by a brownish coloured carbonatite
VNP 260	20° 17.437'	014° 43.611'	Large dyke, 4m wide of porphyritic rocks
VNP 261	20° 17.437'	014° 43.611'	Oas synite
VNP 262	20.30912°	014.70234°	2m wide dyke of Carbonatite with pyrite, pyrotite, charcopyrite
VNP 263 A	20.30912°	014.70234°	Brown coloured carbonatite at Ruimnte, magnetite concentrated on top due to weathering
VNP 263 B	20.30912°	014.70234°	Magnetite rich carbonetite
VNP 263 C	20.30912°	014.70234°	Yellow coloured carbonatite
VNP 264	20° 21.603'	014° 40.239'	Coarse grained syenite body, 20m from the road
VNP 265 A	20° 17.274'	014° 42.540'	Red coloured carbonatite with a S-N direction, strongly brecciated surrounding country rock
VNP 265 B	20° 17.274'	014° 42.540'	Yellow coloured carbonatite with a S-N direction
VNP 266	20° 18.092'	014° 41.322'	Coarse-grained, red-brown coloured carbonatite that has a N-S direction
VNP 267	20° 16.536'	014° 39.107'	A stop at a Sandstone of the Damara, little deformation with E-W and N-S cleavage
VNP 268 A	20° 19.258'	014° 41.268'	Homogeneous carbonatite intruded by carbonatite veinlets E of the Lofdal syenite
VNP 268 B	20° 19.258'	014° 41.268'	Remobilised coarse-grained carbonatite that lies next to A.
VNP 268 C	20° 19.258'	014° 41.268'	Yellow coloured carbonatite that forms a dyke conforming with A
VNP 268 D	20° 19.258'	014° 41.268'	Contact between A and B
VNP 269			Greyish carbonatite showing no hydrothermal activities, "ZERO samples", 40m from carbonatite containing a pebble of Lofdal syenite.
VNP 270 A	20° 19.522'	014° 41.135'	Youngest porhyritic dyke of the alkaline rocks that forms a hill at the end of the Lofdal syenite, with mineral accentuated by weathering and aligned parellel to the direction of the dyke.
VNP 270 B	20° 19.522'	014° 41.135'	Phonolite that is representative of the hill, cutting the dense syenite
VNP 270 C	20° 19.522'	014° 41.135'	The dyke that has several inclusions of the coarse-grained syenite
VNP 271	20° 19.102'	014° 43.237'	Grey carbonatite dyke with E-W direction, ~50m wide and can be traced for 100's of metres
VNP 272	20° 19.102'	014° 43.237'	Carbonatites that cantain minerals such as pyrite, chalcopyrite intruding brecciated syenite country rock everywhere.
VNP 273	20° 18.354'	014° 42.212'	Hill made of brecciated syenite that forms the top of the carbonatitie body, with amphibole minerals formed crystals
VNP 274	20° 18.885'	014° 42.194'	Spongy rock found on the contact of the carbonatite body and overlying country rock

Appendix 3 a) Descriptions of VNP samples; collected by the author based on carbonatite and alkalic rocks lithologies

Sample No.	Coordinates		Description
	Lat (S)	Long (E)	
VNP 275	20° 18.891'	014° 42.204'	Subvolcanic breccia similar to VNP 270, with syenite pebbles and some hollow spaces
VNP 276 B	20° 18.781'	014° 42.233'	Carbonatite body below the nephelin syenite with many amphibole minerals
VNP 276 A	20° 18.781'	014° 42.233'	Carbonatite body below the nephelin syenite with few amphibole minerals
VNP 277	20° 19.362'	014° 45.040'	A stop at a brecciated amphibolite schist country rock with carbonatite in fillings
VNP 278	20° 18.205'	014° 46.421'	Phonolite dykes with a ENE/WSW trend
VNP 279 A	20° 17.452'	014° 46.826'	Carbonatite dyke with ENE trend
VNP 279 B	20° 17.452'	014° 46.826'	Nodules-like that are found with the carbonatite
VNP 280	20° 16.422'	014° 47.732'	A hill 300m E of the road with carbonatite filling in the fractures of the country rock
VNP 281 A	20° 16.422'	014° 47.732'	Carbonatite from the veins filling into the Quartzite
VNP 281 B	20° 16.422'	014° 47.732'	Carbonatite veins in the schist country rock
VNP 281 C	20° 16.422'	014° 47.732'	Schist country rock
VNP 282	20° 18.121'	014° 42.835'	A metre wide red carbonatite with NE/SW direction showing remobilisation of calcitic materials
VNP 283	20° 18.109'	014° 42.865'	Iron-rich carbonatite dyke with N-S direction cutting the breccia material
VNP 284	20° 18.109'	014° 42.865'	A hill made of breccia with pebbles/boulders of coarse-grained nepheline syenite and amphibolite schist and carbonatites crosscutting the braccia in the S-N direction
VNP 285	20° 18.109'	014° 42.865'	Light coloured carbonatite at the bottom of the previous sample; up to 4m wide and 20m thick
VNP 286	20° 18.170'	014° 42.755'	Breccia materials containing inclusions of carbonatites and porphyritic
VNP 287	20° 18.179'	014° 42.734'	Recrystallised calcitic carbonatite that has a bluish appearance
VNP 288 A	20° 18.210'	014° 42.687'	Carbonatite containing two minerals (amphibolites and feldspar) from the contact with the breccia
VNP 288 B	20° 18.210'	014° 42.687'	Bluish grey mineral shown as the calcitic carbonate
VNP 288 C	20° 18.210'	014° 42.687'	Pumice like rock found on top of the carbonatite body with the breccia contact found at some places
VNP 288 D	20° 18.210'	014° 42.687'	Fine grained carbonatite unit at the contact between breccia and carbonatite
VNP 288 E	20° 18.210'	014° 42.687'	Unit that intruded the carbonatite body
VNP 289	20° 18.326'	014° 42.555'	Medium-grained syenite at the hill top and broken blocks at the bottom on top of the carbonatite boby
VNP 290	20° 18.046'	014° 42.669'	Area at low level covered by debris of brecciated materials and at places carbonatites, thought to be on top of the carbonatite body
VNP 291 A	20° 18.033'	014° 42.441'	Grey carbonatite dyke with NW/SE direction, ~20cm wide and can be followed for 10's of metres intruded into the syenites
VNP 291 B	20° 18.033'	014° 42.441'	Another carbonatite dyke ~50m away from A, striking the same direction
VNP 292	20° 18.710'	014° 42.278'	A hill made up of nepheline syenite that at the bottom shows increased brecciation and carbonatite bodies at lower units
VNP 293	20° 18.695'	014° 42.339'	Nepheline syenite hill cut by a grey carbonatite dyke ~15cm wide and 10's of metres long
VNP 294	20° 18.862'	014° 42.398'	Relatively massive syenite outcrop with few carbonatite dykes intruding
VNP 295	20° 18.662'	014° 42.513'	Strongly brecciated and hydrothermal altered rock that appear to be original a syenite
VNP 296	20° 18.527'	014° 42.466'	Coarse grained and strongly altered syenite body ~50m diameter and cut by carbonatite dykes
VNP 297	20° 18.381'	014° 42.409'	Highly porphyritic dyke with a N-S direction cutting the nepheline syenite ~2m thick and at places brecciated

Appendix 3 a) Descriptions of VNP samples; collected by the author based on carbonatite and alkalic rocks lithologies

Sample No.	Coordinates		Description
	Lat (S)	Long (E)	
VNP 298	20° 18.406'	014° 42.264'	Syenite body that is brecciated at places. Sample taken for dating
VNP 299	20° 18.515'	014° 42.067'	Dark coloured fine grained xenoliths found in the syenites
VNP 300	20° 18.516'	014° 42.067'	Carbonatite body ~500m wide at places covered with breccia materials
VNP 301	20° 18.626'	014° 42.194'	Breccia hill in the middle, altered syenite top and at the bottom is carbonatite rich in pyrite, charcopyrite and pyrotite
VNP 302	20° 19.980'	014° 40.866'	One metre mafic dyke with E-W direction. The country rock is altered marked by greeen mineral in veins and joints
VNP 303 A	20° 20.225'	014° 40.617'	Breccia material for composition of fragments study
VNP 303 B	20° 20.225'	014° 40.617'	White coloured carbonatite
VNP 303 C	20° 20.225'	014° 40.617'	Brown coloured carbonatite at Ruimnte, magnetite concentrated on top due to weathering
VNP 303 D	20° 20.225'	014° 40.617'	Carbonatite rich in amphibole/pyroxene?? Mineral and containing pyrotite
VNP 304 A	20° 20.246'	014° 40.583'	A 1m thick N-S direction carbonatite dyke that is strongly altered
VNP 304 B	20° 20.246'	014° 40.583'	A NE-SW direction carbonatite dyke that is ten metres away from VNP 304 A.
VNP 305	20° 20.246'	014° 40.583'	A carbonatite dyke 20m W of 304 with a NE/SW direction containing
VNP 306	20° 20.174'	014° 40.565'	Schist country rock that is strongly brecciated and carbonatite dykes concentrate South of this area
VNP 307	20° 19.701'	014° 40.786'	Dark grey carbonatite dyke with E-W direction and about 0.5m long
VNP 308 A	20° 18.706'	014° 40.753'	~15m diametre of carbonatite body exposed at ground level
VNP 308 B	20° 18.706'	014° 40.753'	Remobilised calcitic materials that form up to 20cm crystals
VNP 309	20° 19.636'	014° 40.626'	Syenite body with mafic xenoliths and intruded by carbonatite dykes
VNP 310 A	20° 19.636'	014° 40.626'	Dark syenite forming subparallel crystal laths of a grey subhedral mineral.
VNP 310 B	20° 19.636'	014° 40.626'	Pink vein of pink mineral crosscutting the syenite
VNP 310 C	20° 19.636'	014° 40.626'	Red mineral in the dark syenite
VNP 311 A	20° 19.650'	014° 40.591'	Fine grained porphyritic dyke with grains aligned showing flow textures parallel to the dyke direction (NE-SW) cutting the coarse grained dark syenite.
VNP 311 B	20° 19.650'	014° 40.591'	Black mineral in the fine grained porpyritic dyke
VNP 312 A	20° 19.664'	014° 40.581'	Greenish fine-grained agglomerate dyke with a NE-SW direction
VNP 312 B	20° 19.664'	014° 40.581'	Greyish colour agglomerate
VNP 313	20° 19.698'	014° 40.526'	4m wide greyish to yellowish carbonatite dyke with E-W direction
VNP 314	20° 19.714'	014° 40.591'	Agglomeritic materials cut by the pink coloured vein.
VNP 315 A	20° 19.813'	014° 40.438'	A lower level carbonatite dyke cutting through the brecciated material hill
VNP 315 B	20° 19.813'	014° 40.438'	Highly porphyritic and medium grained dyke cutting the breccia with NE-SW direction
VNP 316	20° 19.813'	014° 40.438'	The breccia hill showing a NE jointing, following the direction of the intruding carbonatites
VNP 317	20° 19.665'	014° 40.950'	Breccia material cut by carbonatite dyke of 0.5m wide
VNP 318	20° 19.665'	014° 40.950'	Carbonatite dyke with NE-Sw direction cutting through 317 breccia hill
VNP 319	20° 18.707'	014° 41.019'	Carbonatite dyke cutting the second hill of brecciated materials with NE-SW direction
VNP 320	20° 14.355'	014° 42.073'	Carbonatite/nate?? 20-40cm wide and following the rock folliation
VNP 321	20° 13.961'	014° 42.130'	15m wide E-W direction quartzite vein cutting through the Huab metamorphic rocks
VNP 322	20° 13.883'	014° 41.827'	Massive conglomerate unit
VNP 323	20° 12.729'	014° 41.068'	E-W direction quartzite vein intruded into the amphibolite gneiss, a unit that follows after the conglomerates units

Appendix 3 a) Descriptions of VNP samples; collected by the author based on carbonatite and alkalic rocks lithologies

Sample No.	Coordinates		Description
	Lat (S)	Long (E)	
VNP 324	20° 12.182'	014° 40.743'	Cordierite-amphibolite schist
VNP 325	20° 15.541'	014° 43.714'	Quartzite ridge ~5-7m wide with carbonatites filling the fractures in this quartzite
VNP 326 A	20° 18.718'	014° 42.237'	Carbonatite body exposed in the river, sample considered "zero" from the bottom of the intrusion
VNP 326 B	20° 18.718'	014° 42.237'	Green contact minerals between the carbonatite and the brecciated material of the syenite
VNP 326 C	20° 18.718'	014° 42.237'	Porphyritic dyke
VNP 326 D	20° 18.718'	014° 42.237'	Carbonatite with amorphous brown mineral that gives yellowish colour on the weathered surface
VNP 327 A	20° 18.790'	014° 42.241'	Younger carbonatite dyke cutting the syenite and carbonatites
VNP 327 B	20° 18.790'	014° 42.241'	Older carbonatite cutting only the syenite
VNP 328	20° 18.709'	014° 42.155'	Valley area altitude of 3203m covered with carbonatite body at the soil level
VNP 329 A	20° 18.875'	014° 42.055'	Dark colour medium-grained syenite
VNP 329 B	20° 18.875'	014° 42.055'	Light colour medium-grained syenite
VNP 330	20° 18.885'	014° 41.908'	Breccia material with carbonatite at the base of intrusion
VNP 331 A	20° 18.736'	014° 42.027'	Fine-grained syenite forming a hill
VNP 331 B	20° 18.736'	014° 42.027'	Carbonatite at the base showing radiating features marked by the calcite
VNP 332	20° 18.734'	014° 42.033'	Mafic porphyritic dyke cutting the syenites. N-S direction carbonatite vein cut through
VNP 333	20° 19.449'	014° 42.503'	Place where mining of the breccia is taking place
VNP 334	20° 20.732'	014° 37.319'	Quartz vein intermingled with carbonatite, have a N-S direction
VNP 335 A	20° 21.754'	014° 37.319'	Carbonatite dyke intruding a mafic body of the Huab
VNP 335 B	20° 21.754'	014° 37.319'	Carbonatites associated with Quartz veins. A mafic dyke has been cut by the quartz-carbonatite veins
VNP 336	20° 23.369'	014° 34.636'	Outcrop strongly brecciated and filled in by carbonatites cut by the road
VNP 337 A	20° 23.999'	014° 35.347'	Carbonatite dykes folded with the schist at places showing pink colour and crosscut by quartz veins
VNP 337 B	20° 23.999'	014° 35.347'	Grey carbonatites
VNP 337 C	20° 23.999'	014° 35.347'	Carbonatite that is brown showing bluish purple colours (apetite ?)
VNP 337 D	20° 23.999'	014° 35.347'	Speciman showing crenulation
VNP 338	20° 21.871'	014° 56.718'	Carbonate?? At the T-junction from Khorixas to the rest camp
VNP 339	20° 23.999'	014° 35.347'	Carbonatite in the schist forming as fillings
VNP 340	20° 20.044'	014° 46.677'	Carbonatite dykes forming breccia and filling in the fractures with E-W direction
VNP 341	20° 17.417'	014° 43.578'	Carbonatite that has E-W direction and is brown coloured ~2m wide and extends for kilometers
VNP 342	20° 17.431'	014° 43.568'	Carbonatite that is bright yellow and red cutting the brown carbonatite

Appendix 4 Chemical composition analysis of Lofdal samples

SAMPLE	08_58	326	269	119	114	881R	881G	949	907	115
SiO_2	2.57	0.18	1.72	12.47	30.29	1.13	2.13	2.24	0.66	5.62
TiO_2	0.01	<0.001	0.26	0.30	0.05	0.07	0.39	0.33	0.02	0.04
Al_2O_3	0.47	<0.05	0.51	3.53	7.42	0.31	<0.05	0.45	0.12	0.83
Fe_2O_3	1.48	1.35	9.51	9.62	5.56	20.96	2.53	16.16	9.44	12.66
MnO	0.41	1.10	2.74	0.27	0.15	2.45	1.59	2.59	0.97	5.19
MgO	0.08	0.13	0.71	10.79	8.62	0.72	0.29	5.14	0.67	3.44
CaO	50.87	52.91	43.41	23.48	17.63	40.60	51.33	36.45	54.23	33.80
Na_2O	0.21	<0.01	0.08	1.96	4.23	<0.01	<0.01	<0.01	<0.01	0.62
K_2O	0.22	<0.005	0.09	0.05	0.07	0.09	0.01	0.25	0.02	0.18
P_2O_5	0.11	0.04	1.23	1.41	0.12	0.03	0.17	0.02	0.48	0.03
(SO_3)	0.21	0.01	0.28	0.01	<0.01	0.06	0.02	0.04	0.02	0.60
(Cl)	0.01	0.02	0.01	0.01	0.00	0.01	0.01	0.00	0.00	0.01
(F)	0.08	0.08	1.08	<0.05	<0.05	<0.05	0.28	0.15	10.51	1.74
LOI	41.00	42.63	34.85	33.84	25.39	33.29	40.87	35.26	26.74	31.79
Total (%)	**97.73**	**98.44**	**96.47**	**97.74**	**99.52**	**99.69**	**99.65**	**99.06**	**103.89**	**96.54**
(As)	<2	<2	43.00	27.00	9.00	8.00	8.00	13.00	17.00	13.00
Ba	717.00	290.00	4472.00	17.00	25.00	48.00	132.00	24.00	352.00	1010.00
Bi	<3	<3	20.00	<3	<2	4.00	4.00	<3	<3	51.00
Ce	400.00	471.00	3408.00	21.00	46.00	210.00	353.00	3129.00	552.00	4276.00
Co	<3	<3	8.00	239.00	40.00	28.00	6.00	12.00	9.00	12.00
Cr	<5	<5	<5	122.00	58.00	<5	<5	<5	<5	8.00
Cs	<4	<4	<4	<3	<3	<4	<4	8.00	<4	6.00
Cu	28.00	19.00	22.00	<3	3.00	52.00	34.00	25.00	18.00	26.00
Ga	2.00	<2	3.00	<2	7.00	<2	<2	<2	<2	<2
Hf	<7	<7	<8	<7	7.00	<8	<7	<8	<8	<8
La	235.00	263.00	2115.00	16.00	<15	152.00	217.00	2081.00	287.00	3194.00
Mo	<3	<3	46.00	<4	<3	10.00	<3	21.00	21.00	<3
Nb	78.00	8.00	166.00	73.00	22.00	38.00	185.00	135.00	187.00	20.00
Nd	126.00	159.00	1157.00	37.00	<13	63.00	87.00	878.00	189.00	1040.00
Ni	<3	<3	<3	51.00	34.00	6.00	<3	8.00	6.00	13.00
Pb	7.00	8.00	64.00	10.00	5.00	<4	9.00	6.00	6.00	1461.00
Rb	12.00	6.00	15.00	10.00	8.00	14.00	9.00	18.00	11.00	20.00
Sb	<12	<12	<12	<9	<9	<11	<12	<11	<13	<11
Sc	<3	<3	5.00	17.00	12.00	8.00	6.00	6.00	<3	3.00
Sm	16.00	23.00	110.00	23.00	<15	<20	<16	60.00	28.00	53.00
Sn	<5	<5	<5	<4	<4	<5	<5	5.00	<5	<5
Sr	16810.00	11490.00	18640.00	676.00	357.00	457.00	1465.00	427.00	1214.00	16940.00
Ta	<5	<5	<6	<6	<5	<6	<5	<6	7.00	<6
Th	40.00	30.00	190.00	412.00	98.00	19.00	51.00	80.00	28.00	427.00
U	<5	<5	<5	21.00	10.00	6.00	6.00	7.00	12.00	<5
W	7.00	<7	31.00	n/a	n/a	n/a	n/a	20.00	41.00	8.00
V	<4	<5	37.00	73.00	36.00	40.00	44.00	19.00	13.00	32.00
Y	59.00	77.00	662.00	13980.00	1117.00	76.00	150.00	135.00	153.00	483.00
Zn	11.00	9.00	864.00	19.00	18.00	65.00	16.00	31.00	152.00	4404.00
Zr	85.00	33.00	352.00	210.00	460.00	13.00	14.00	12.00	42.00	93.00
La	1014.06	1129.10	8657.86	35.82	82.25	602.59	971.33	8900.72	13319.13	1222.84
Ce	732.76	848.81	5782.49	28.23	57.46	387.33	592.35	5490.72	7397.21	908.49
Pr	503.93	592.59	3939.39	23.28	39.69	275.79	380.87	3355.78	4219.98	635.24
Nd	331.56	380.19	2504.42	21.25	27.34	174.23	230.68	1971.71	2270.11	408.93
Sm	148.88	157.72	972.13	81.30	37.72	76.63	114.33	533.65	620.67	189.67
Eu	114.29	114.29	675.00	207.87	60.84	64.30	105.09	332.14	321.43	139.29
Gd	83.42	89.52	523.91	363.61	79.57	46.68	91.33	217.70	284.33	120.55
Tb	61.43	70.25	432.51	695.01	125.08	40.91	92.42	142.42	249.04	102.20
Dy	51.50	60.98	440.87	850.43	149.01	40.81	98.36	110.42	276.47	96.00
Ho	41.37	52.70	422.66	863.22	146.82	40.95	98.91	95.32	293.17	85.79
Er	39.65	53.49	454.37	919.39	161.17	52.10	122.06	103.84	354.94	89.36
Tm	33.88	50.41	442.15	957.16	176.84	68.16	151.96	115.70	376.86	87.60
Yb	31.32	51.75	432.00	880.36	204.03	91.48	178.09	133.54	377.23	89.23
Lu	27.57	49.79	392.59	773.51	181.55	110.17	193.08	142.39	339.92	85.60
Y	38.53	45.96	411.54	986.12	151.04	31.82	82.83	83.33	303.21	93.59
La/Yb	32.37	21.82	20.04	0.04	0.40	6.59	5.45	66.65	35.31	13.70

Appendix 4 Chemical composition analysis of Lofdal samples

SAMPLE	813	15769G	927	189	15796	15769LG	15769	914	924
SiO_2	24.53	3.02	2.92	2.54	22.96	0.71	5.81	2.96	1.30
TiO_2	0.02	0.06	0.18	0.02	0.43	0.01	0.04	0.19	0.12
Al_2O_3	6.85	0.24	0.54	0.38	6.40	0.11	0.22	0.48	<0.05
Fe_2O_3	2.23	2.84	11.81	25.40	18.40	3.30	23.43	13.13	10.09
MnO	1.03	0.55	0.92	0.79	0.29	0.31	0.59	5.02	1.53
MgO	0.26	0.32	1.70	1.64	0.60	0.21	0.53	0.58	0.55
CaO	33.18	50.42	42.32	34.50	23.01	51.73	36.88	37.63	52.55
Na_2O	3.72	0.03	0.02	0.09	3.42	0.04	<0.01	<0.01	<0.01
K_2O	0.20	0.03	0.26	0.01	0.07	<0.005	0.04	0.07	<0.005
P_2O_5	0.03	2.31	1.56	2.60	1.67	3.76	0.15	1.10	1.78
(SO_3)	<0.01	0.04	0.08	0.12	0.07	0.02	0.08	0.13	0.11
(Cl)	0.05	0.01	0.01	0.01	0.01	0.01	0.01	0.01	0.00
(F)	0.06	0.28	0.23	0.10	0.13	0.35	<0.05	0.75	13.68
LOI	26.97	38.50	35.08	30.46	20.51	38.02	31.42	31.82	21.43
Total (%)	**99.15**	**98.65**	**97.63**	**98.63**	**97.99**	**98.57**	**99.19**	**93.81**	**103.18**
(As)	5.00	3.00	23.00	162.00	590.00	70.00	51.00	<2	133.00
Ba	261.00	668.00	396.00	169.00	59.00	115.00	74.00	51.00	134.00
Bi	<3	<3	<3	4.00	9.00	6.00	<3	<3	4.00
Ce	870.00	1433.00	185.00	292.00	874.00	1528.00	682.00	25450.00	4721.00
Co	<3	5.00	68.00	86.00	113.00	34.00	20.00	<6	67.00
Cr	8.00	<5	25.00	64.00	27.00	<5	93.00	<6	47.00
Cs	<4	<4	<4	<4	<3	<4	<4	45.00	6.00
Cu	21.00	18.00	<4	<4	<4	4.00	18.00	14.00	<4
Ga	36.00	<2	<2	<2	3.00	<2	<2	<3	<2
Hf	7.00	<7	22.00	<9	<8	<7	<8	14.00	<8
La	526.00	940.00	52.00	190.00	518.00	1031.00	398.00	14160.00	3375.00
Mo	<3	7.00	17.00	29.00	15.00	5.00	<3	19.00	165.00
Nb	713.00	36.00	266.00	20.00	202.00	14.00	27.00	65.00	145.00
Nd	237.00	467.00	169.00	177.00	417.00	591.00	423.00	8525.00	1503.00
Ni	<3	<3	17.00	28.00	37.00	6.00	10.00	<4	12.00
Pb	23.00	6.00	171.00	68.00	129.00	119.00	112.00	32.00	71.00
Rb	16.00	9.00	28.00	13.00	11.00	9.00	13.00	17.00	16.00
Sb	<11	<12	<12	<11	<10	<12	<11	<11	<13
Sc	5.00	<3	42.00	70.00	32.00	16.00	46.00	7.00	33.00
Sm	29.00	66.00	143.00	304.00	479.00	539.00	478.00	754.00	262.00
Sn	<5	<5	<5	<5	<4	<5	<5	<5	<5
Sr	1443.00	7823.00	638.00	744.00	445.00	2133.00	429.00	2482.00	1585.00
Ta	7.00	<5	<6	<7	<6	<5	<6	<7	<6
Th	25.00	91.00	7424.00	1521.00	5160.00	3664.00	730.00	330.00	3224.00
U	20.00	<5	189.00	19.00	28.00	15.00	6.00	<5	56.00
W	9.00	n/a	90.00	187.00	n/a	n/a	n/a	17.00	64.00
V	<4	26.00	228.00	239.00	131.00	11.00	167.00	37.00	241.00
Y	87.00	184.00	4869.00	4966.00	5238.00	2558.00	1445.00	808.00	4327.00
Zn	55.00	12.00	92.00	83.00	20.00	<2	55.00	18.00	31.00
Zr	681.00	110.00	3602.00	198.00	557.00	30.00	28.00	19.00	38.00
La	2326.37	3803.65	290.58	809.54	2270.41	4251.35	1678.45	59011.50	12577.76
Ce	1530.17	2476.47	328.25	565.32	1533.48	2590.06	1192.56	43657.16	7390.58
Pr	1001.12	1661.51	337.82	423.12	1126.38	1806.06	1003.21	29315.38	4713.80
Nd	607.87	1081.29	335.99	349.25	893.62	1311.93	927.73	18357.65	3010.61
Sm	225.70	447.37	870.16	1543.17	3095.16	3640.93	3377.57	6172.67	1903.47
Eu	155.36	315.55	1273.21	1821.43	3413.33	4107.60	2490.30	3464.29	2196.43
Gd	114.45	232.51	1454.73	1480.16	2699.78	3061.32	1206.75	2344.86	2131.23
Tb	86.23	151.29	1641.87	1129.48	2015.63	2009.96	471.39	1148.76	1674.93
Dy	70.87	109.33	1454.47	741.66	1478.86	1179.74	244.98	659.25	1145.45
Ho	59.71	79.89	1179.86	460.43	986.27	674.71	152.67	411.87	766.19
Er	60.42	74.10	1101.32	357.46	843.37	516.49	130.66	327.88	685.97
Tm	57.85	67.19	1041.32	281.40	722.21	424.31	114.68	240.50	603.31
Yb	57.42	64.10	990.77	235.69	632.42	371.91	103.05	200.62	585.23
Lu	55.14	63.09	962.96	192.59	562.18	327.87	95.23	188.07	522.63
Y	56.15	74.61	1176.28	374.36	849.06	553.03	138.77	475.64	817.95
La/Yb	40.52	59.34	0.29	3.43	3.59	11.43	16.29	294.15	21.49

Appendix 5 Chemical composition analysis of Mesopotamia Lofdal samples

Sample	MES 06-001	MES 06-002	MES 06-003	MES 06-004	MES 06-005	MES 06-006	MES 06-007	MES 06-008	MES 06-009	MES 06-010	MES 06-011	MES 06-012	MES 06-013	MES 06-014	MES 06-015	MES 06-016
SiO_2	81.38	70.31	76.00	81.00	81.50	84.90	87.95	86.86	95.27	80.05	62.47	55.64	56.69	43.26	87.41	93.23
TiO_2	0.02	0.03	0.02	0.04	0.03	0.04	0.04	0.03	0.21	0.03	0.05	0.03	0.03	2.84	0.02	0.05
Al_2O_3	0.74	0.51	0.23	0.25	0.13	0.28	0.19	1.11	0.17	0.81	0.79	1.13	0.72	5.50	0.21	0.76
Fe_2O_3	16.44	21.02	22.66	18.30	17.51	8.39	10.54	10.72	4.03	16.30	30.45	7.96	8.26	35.46	11.31	5.30
MnO	0.34	0.79	0.03	0.04	0.17	0.31	0.29	0.11	0.01	0.68	1.65	0.31	0.29	0.67	0.17	0.08
MgO	0.15	0.12	0.03	0.05	0.03	0.10	0.07	0.18	0.02	0.20	0.32	9.97	5.22	0.56	0.20	0.07
CaO	0.50	6.88	0.11	0.07	0.06	5.79	0.67	0.56	0.06	1.74	4.02	24.42	28.40	9.25	0.49	0.18
K_2O	0.25	0.13	0.02	0.05	0.02	0.05	0.01	0.24	0.02	0.02	0.07	0.24	0.20	1.76	0.05	0.19
Na_2O	0.16	0.15	0.12	0.12	0.12	0.12	0.12	0.15	0.12	0.13	0.15	0.26	0.13	0.13	0.12	0.12
P_2O_5	0.02	0.05	0.10	0.11	0.02	0.01	0.13	0.03	0.09	0.03	0.03	0.03	0.04	0.57	0.02	0.01
Total(%)	**100.00**	**100.00**	**99.33**	**100.03**	**99.61**	**100.00**	**100.00**	**100.00**	**100.00**	**100.00**	**100.00**	**100.00**	**100.00**	**100.00**	**100.00**	**100.00**
S	200.00	2200.00	8500.00	1200.00	8000.00	2100.00	2200.00	11900.00	2900.00	200.00	600.00	100.00	500.00	100.00	4700.00	5900.00
V	85.00															
Cr	11.00															
Co	15.00															
Ni	38.00															
Cu	>10000															
Zn	312.00															
As	12.00															
Rb	183.00															
Sr	8.00															
Y	42.00															
Zr	306.00															
Nb	22.00															
Mo	11.00															
Ag	9.00															
Cd	1.00															
Sn	7.00															
Sb	14.00															

Appendix 6 Chemical composition analysis of Minerals from Lofdal samples

wt%, dl	Sample	1_AS9398_BSE1a	11_AS9398_BSE2c	12_AS9398_BSE2c	15_AS9398_BSE2a	16_AS9398_BSE2a	17_AS9398_BSE2a	24_AS9398_BSE3a	27_AS9398_BSE5a	28_AS9398_BSE5c	44_AS9398_BSE3f	45_AS9398_BSE3g	50_AS9398_BSE5d
	Mineral	Apatite											
	SiO_2	0.05	0.00	0.08	0.48	0.16	0.31	0.00	0.70	0.10	0.00	0.00	0.00
	TiO_2	0.00	0.00	0.00	0.00	0.00	0.00	0.00	0.00	0.00	0.00	0.00	0.00
	$Al2O_3$	0.00	0.00	0.00	0.13	0.06	0.08	0.00	0.24	0.00	0.00	0.00	0.00
	FeO	0.00	0.00	0.50	0.81	0.99	0.57	0.00	0.00	0.00	0.00	0.00	0.00
	MnO	0.00	0.00	0.00	0.00	0.00	0.00	0.00	0.00	0.00	0.00	0.00	0.00
	MgO	0.00	0.00	0.00	0.05	0.00	0.00	0.00	0.00	0.00	0.00	0.00	0.00
	CaO	56.47	48.45	54.49	52.47	52.82	50.53	54.50	49.76	54.63	55.29	55.68	55.46
	Na_2O	0.18	2.01	0.40	0.27	0.54	0.91	0.40	0.74	0.56	0.26	0.24	0.20
	K_2O	0.00	0.00	0.00	0.08	0.00	0.06	0.00	0.08	0.00	0.00	0.00	0.00
	P_2O_5	43.52	40.24	43.14	40.84	41.60	40.87	42.33	38.90	42.72	43.88	42.47	42.42
	F	2.31	1.76	4.51	4.20	4.06	4.78	4.59	3.71	4.90	3.65	4.28	2.80
	Cl	0.00	0.00	0.00	0.00	0.00	0.08	0.08	0.00	0.00	0.00	0.00	0.00
	SO_3	0.00	0.00	0.00	0.00	0.00	0.00	0.11	0.00	0.00	0.00	0.00	0.00
	SrO	0.46	0.84	0.71	0.79	0.41	0.64	0.76	0.68	0.36	1.29	0.27	0.28
	Y_2O_3	0.16	3.97	0.48	0.37	0.88	1.45	0.58	0.96	0.95	0.26	0.25	0.21
	BaO	0.00	0.00	0.00	0.00	0.00	0.00	0.00	0.00	0.00	0.00	0.00	0.00
	La_2O_3	0.00	0.00	0.00	0.00	0.00	0.00	0.00	0.17	0.00	0.00	0.00	0.00
	Ce_2O_3	0.00	0.37	0.00	0.00	0.00	0.28	0.00	0.33	0.20	0.00	0.24	0.17
	Nd_2O_3	0.00	0.38	0.00	0.00	0.00	0.00	0.21	0.00	0.00	0.00	0.00	0.00
	ThO_2	0.00	0.00	0.00	0.00	0.00	0.99	0.00	0.91	0.00	0.00	0.00	0.00
	CO_2	-	-	-	-	-	-	-	-	-	-	-	-
	Total	**103.16**	**98.03**	**104.30**	**100.48**	**101.52**	**101.55**	**103.56**	**97.17**	**104.41**	**104.64**	**103.42**	**101.54**
minus	$O=F_2Cl$	102.19	97.29	102.40	98.71	99.81	99.54	101.63	95.61	102.35	103.10	101.62	100.36
	Ox	26.00	26.00	26.00	26.00	26.00	26.00	26.00	26.00	26.00	26.00	26.00	26.00
apfu	F	1.18	0.97	2.24	2.17	2.08	2.46	2.30	2.01	2.42	1.82	2.15	1.45
	Al	0.00	0.00	0.00	0.03	0.01	0.02	0.00	0.05	0.00	0.00	0.00	0.00
	Ba	0.00	0.00	0.00	0.00	0.00	0.00	0.00	0.00	0.00	0.00	0.00	0.00
	C	-	-	-	-	-	-	-	-	-	-	-	-
	Ca	9.79	9.08	9.16	9.20	9.19	8.79	9.23	9.13	9.15	9.34	9.47	9.74
	Ce	0.00	0.02	0.00	0.00	0.00	0.02	0.00	0.02	0.01	0.00	0.01	0.01
	Cl	0.00	0.00	0.00	0.00	0.00	0.02	0.02	0.00	0.00	0.00	0.00	0.00
	Fe	0.00	0.00	0.07	0.11	0.13	0.08	0.00	0.00	0.00	0.00	0.00	0.00
	K	0.00	0.00	0.00	0.02	0.00	0.01	0.00	0.02	0.00	0.00	0.00	0.00
	La	0.00	0.00	0.00	0.00	0.00	0.00	0.00	0.01	0.00	0.00	0.00	0.00
	Mg	0.00	0.00	0.00	0.01	0.00	0.00	0.00	0.00	0.00	0.00	0.00	0.00
	Mn	0.00	0.00	0.00	0.00	0.00	0.00	0.00	0.00	0.00	0.00	0.00	0.00
	Na	0.06	0.68	0.12	0.08	0.17	0.29	0.12	0.25	0.17	0.08	0.07	0.06
	Nd	0.00	0.02	0.00	0.00	0.00	0.00	0.01	0.00	0.00	0.00	0.00	0.00
	P	5.96	5.96	5.73	5.66	5.72	5.62	5.67	5.64	5.66	5.86	5.71	5.88
	S	0.00	0.00	0.00	0.00	0.00	0.00	0.02	0.00	0.00	0.00	0.00	0.00
	Si	0.01	0.00	0.01	0.08	0.03	0.05	0.00	0.12	0.01	0.00	0.00	0.00
	Sr	0.04	0.09	0.07	0.07	0.04	0.06	0.07	0.07	0.03	0.12	0.03	0.03
	Th	0.00	0.00	0.00	0.00	0.00	0.04	0.00	0.04	0.00	0.00	0.00	0.00
	Ti	0.00	0.00	0.00	0.00	0.00	0.00	0.00	0.00	0.00	0.00	0.00	0.00
	Y	0.01	0.37	0.04	0.03	0.08	0.13	0.05	0.09	0.08	0.02	0.02	0.02

Appendix 6 Chemical composition analysis of Minerals from Lofdal samples

wt%, dl	Sample	1_AS9398_BSE1a	11_AS9398_BSE2c	12_AS9398_BSE2c	15_AS9398_BSE2a	16_AS9398_BSE2a	17_AS9398_BSE2a	24_AS9398_BSE3a	27_AS9398_BSE5a	28_AS9398_BSE5e	44_AS9398_BSE3f	45_AS9398_BSE3g	50_AS9398_BSE5d
	Mineral	Apatite											
	SiO_2	0.05	0.00	0.08	0.48	0.16	0.31	0.00	0.70	0.10	0.00	0.00	0.00
	TiO_2	0.00	0.00	0.00	0.00	0.00	0.00	0.00	0.00	0.00	0.00	0.00	0.00
	$Al2O_3$	0.00	0.00	0.00	0.13	0.06	0.08	0.00	0.24	0.00	0.00	0.00	0.00
	FeO	0.00	0.00	0.50	0.81	0.99	0.57	0.00	0.00	0.00	0.00	0.00	0.00
	MnO	0.00	0.00	0.00	0.00	0.00	0.00	0.00	0.00	0.00	0.00	0.00	0.00
	MgO	0.00	0.00	0.00	0.05	0.00	0.00	0.00	0.00	0.00	0.00	0.00	0.00
	CaO	56.47	48.45	54.49	52.47	52.82	50.53	54.50	49.76	54.63	55.29	55.68	55.46
	Na_2O	0.18	2.01	0.40	0.27	0.54	0.91	0.40	0.74	0.56	0.26	0.24	0.20
	K_2O	0.00	0.00	0.00	0.08	0.00	0.06	0.00	0.08	0.00	0.00	0.00	0.00
	P_2O_5	43.52	40.24	43.14	40.84	41.60	40.87	42.33	38.90	42.72	43.88	42.47	42.42
	F	2.31	1.76	4.51	4.20	4.06	4.78	4.59	3.71	4.90	3.65	4.28	2.80
	Cl	0.00	0.00	0.00	0.00	0.00	0.08	0.08	0.00	0.00	0.00	0.00	0.00
	SO_3	0.00	0.00	0.00	0.00	0.00	0.00	0.11	0.00	0.00	0.00	0.00	0.00
	SrO	0.46	0.84	0.71	0.79	0.41	0.64	0.76	0.68	0.36	1.29	0.27	0.28
	Y_2O_3	0.16	3.97	0.48	0.37	0.88	1.45	0.58	0.96	0.95	0.26	0.25	0.21
	BaO	0.00	0.00	0.00	0.00	0.00	0.00	0.00	0.00	0.00	0.00	0.00	0.00
	La_2O_3	0.00	0.00	0.00	0.00	0.00	0.00	0.00	0.17	0.00	0.00	0.00	0.00
	Ce_2O_3	0.00	0.37	0.00	0.00	0.00	0.28	0.00	0.33	0.20	0.00	0.24	0.17
	Nd_2O_3	0.00	0.38	0.00	0.00	0.00	0.00	0.21	0.00	0.00	0.00	0.00	0.00
	ThO_2	0.00	0.00	0.00	0.00	0.00	0.99	0.00	0.91	0.00	0.00	0.00	0.00
	CO_2	-	-	-	-	-	-	-	-	-	-	-	-
	Total	**103.16**	**98.03**	**104.30**	**100.48**	**101.52**	**101.55**	**103.56**	**97.17**	**104.41**	**104.64**	**103.42**	**101.54**
minus	O=F,Cl	102.19	97.29	102.40	98.71	99.81	99.54	101.63	95.61	102.35	103.10	101.62	100.36
	Ox	26.00	26.00	26.00	26.00	26.00	26.00	26.00	26.00	26.00	26.00	26.00	26.00
apfu	F	1.18	0.97	2.24	2.17	2.08	2.46	2.30	2.01	2.42	1.82	2.15	1.45
	Al	0.00	0.00	0.00	0.03	0.01	0.02	0.00	0.05	0.00	0.00	0.00	0.00
	Ba	0.00	0.00	0.00	0.00	0.00	0.00	0.00	0.00	0.00	0.00	0.00	0.00
	C	-	-	-	-	-	-	-	-	-	-	-	-
	Ca	9.79	9.08	9.16	9.20	9.19	8.79	9.23	9.13	9.15	9.34	9.47	9.74
	Ce	0.00	0.02	0.00	0.00	0.00	0.02	0.00	0.02	0.01	0.00	0.01	0.01
	Cl	0.00	0.00	0.00	0.00	0.00	0.02	0.02	0.00	0.00	0.00	0.00	0.00
	Fe	0.00	0.00	0.07	0.11	0.13	0.08	0.00	0.00	0.00	0.00	0.00	0.00
	K	0.00	0.00	0.00	0.02	0.00	0.01	0.00	0.02	0.00	0.00	0.00	0.00
	La	0.00	0.00	0.00	0.00	0.00	0.00	0.00	0.01	0.00	0.00	0.00	0.00
	Mg	0.00	0.00	0.00	0.01	0.00	0.00	0.00	0.00	0.00	0.00	0.00	0.00
	Mn	0.00	0.00	0.00	0.00	0.00	0.00	0.00	0.00	0.00	0.00	0.00	0.00
	Na	0.06	0.68	0.12	0.08	0.17	0.29	0.12	0.25	0.17	0.08	0.07	0.06
	Nd	0.00	0.02	0.00	0.00	0.00	0.00	0.01	0.00	0.00	0.00	0.00	0.00
	P	5.96	5.96	5.73	5.66	5.72	5.62	5.67	5.64	5.66	5.86	5.71	5.88
	S	0.00	0.00	0.00	0.00	0.00	0.00	0.02	0.00	0.00	0.00	0.00	0.00
	Si	0.01	0.00	0.01	0.08	0.03	0.05	0.00	0.12	0.01	0.00	0.00	0.00
	Sr	0.04	0.09	0.07	0.07	0.04	0.06	0.07	0.07	0.03	0.12	0.03	0.03
	Th	0.00	0.00	0.00	0.00	0.00	0.04	0.00	0.04	0.00	0.00	0.00	0.00
	Ti	0.00	0.00	0.00	0.00	0.00	0.00	0.00	0.00	0.00	0.00	0.00	0.00
	Y	0.01	0.37	0.04	0.03	0.08	0.13	0.05	0.09	0.08	0.02	0.02	0.02

Appendix 6 Chemical composition analysis of Minerals from Lofdal samples

Sample	51_AS9398_BSE5d	8_AS9398_BSE1a	13_AS9398_BSE1a	14_AS9398_BSE2a	19_AS9398_BSE3a	20_AS9398_BSE3k	21_AS9398_BSE3k	22_AS9398_BSE3m	23_AS9398_BSE3k	25_AS9398_BSE5a	26_AS9398_BSE5a	29_AS9398_BSE7a
Mineral	Apatite	Calcite										
SiO_2	0.00	0.06	0.00	0.00	0.00	0.00	0.00	0.00	0.00	0.00	0.00	0.07
TiO_2	0.00	0.00	0.00	0.00	0.00	0.00	0.00	0.00	0.00	0.00	0.00	0.00
Al2O_3	0.00	0.00	0.00	0.00	0.00	0.00	0.00	0.00	0.00	0.00	0.00	0.00
FeO	0.00	0.17	0.00	1.34	0.00	0.00	1.32	0.00	1.22	0.00	1.25	0.46
MnO	0.00	0.00	0.24	0.24	0.00	0.14	0.22	0.00	0.28	0.00	0.26	0.09
MgO	0.00	0.21	0.24	0.16	0.10	0.15	0.18	0.00	0.17	0.24	0.20	0.19
CaO	49.04	55.22	54.91	52.46	55.70	55.51	53.99	56.36	53.68	55.23	52.45	53.88
Na_2O	1.61	0.00	0.00	0.00	0.00	0.00	0.00	0.00	0.00	0.00	0.00	0.00
K_2O	0.00	0.00	0.00	0.00	0.00	0.00	0.00	0.00	0.00	0.00	0.00	0.00
P_2O_5	39.85	0.00	0.00	0.00	0.00	0.00	0.00	0.00	0.00	0.00	0.00	0.00
F	3.89	0.00	0.00	0.00	0.00	0.00	0.00	0.00	0.00	0.00	0.00	0.00
Cl	0.00	0.00	0.00	0.00	0.00	0.00	0.00	0.00	0.00	0.00	0.00	0.00
SO_3	0.00	0.00	0.00	0.00	0.00	0.00	0.00	0.00	0.00	0.00	0.00	0.00
SrO	0.47	0.16	0.00	0.30	0.00	0.23	0.26	0.00	0.42	0.00	0.46	0.33
Y_2O_3	3.28	0.00	0.00	0.00	0.00	0.00	0.00	0.00	0.00	0.00	0.00	0.00
BaO	0.00	0.00	0.00	0.00	0.00	0.00	0.00	0.00	0.00	0.00	0.00	0.00
La_2O_3	0.18	0.00	0.00	0.00	0.00	0.00	0.00	0.00	0.00	0.00	0.00	0.00
Ce_2O_3	0.56	0.00	0.00	0.00	0.00	0.00	0.00	0.00	0.00	0.00	0.00	0.00
Nd_2O_3	0.45	0.00	0.00	0.00	0.00	0.00	0.00	0.00	0.00	0.00	0.00	0.00
ThO_2	0.00	0.00	0.00	0.00	0.00	0.00	0.00	0.00	0.00	0.00	0.00	0.00
CO_2	-	43.82	43.51	42.44	43.82	43.91	43.62	44.23	43.41	43.61	42.50	43.08
Total	**99.31**	**99.63**	**98.91**	**96.95**	**99.62**	**99.95**	**99.58**	**100.59**	**99.19**	**99.08**	**97.12**	**98.10**
O=F,Cl	97.68	-	-	-	-	-	-	-	-	-	-	-
Ox	26.00	3.00	3.00	3.00	3.00	3.00	3.00	3.00	3.00	3.00	3.00	3.00
F	2.07	0.00	0.00	0.00	0.00	0.00	0.00	0.00	0.00	0.00	0.00	0.00
Al	0.00	0.00	0.00	0.00	0.00	0.00	0.00	0.00	0.00	0.00	0.00	0.00
Ba	0.00	0.00	0.00	0.00	0.00	0.00	0.00	0.00	0.00	0.00	0.00	0.00
C	-	1.00	1.00	1.00	1.00	1.00	1.00	1.00	1.00	1.00	1.00	1.00
Ca	8.85	0.99	0.99	0.97	1.00	0.99	0.97	1.00	0.97	0.99	0.97	0.98
Ce	0.03	0.00	0.00	0.00	0.00	0.00	0.00	0.00	0.00	0.00	0.00	0.00
Cl	0.00	0.00	0.00	0.00	0.00	0.00	0.00	0.00	0.00	0.00	0.00	0.00
Fe	0.00	0.00	0.00	0.02	0.00	0.00	0.02	0.00	0.02	0.00	0.02	0.01
K	0.00	0.00	0.00	0.00	0.00	0.00	0.00	0.00	0.00	0.00	0.00	0.00
La	0.01	0.00	0.00	0.00	0.00	0.00	0.00	0.00	0.00	0.00	0.00	0.00
Mg	0.00	0.01	0.01	0.00	0.00	0.00	0.00	0.00	0.00	0.01	0.01	0.00
Mn	0.00	0.00	0.00	0.00	0.00	0.00	0.00	0.00	0.00	0.00	0.00	0.00
Na	0.52	0.00	0.00	0.00	0.00	0.00	0.00	0.00	0.00	0.00	0.00	0.00
Nd	0.03	0.00	0.00	0.00	0.00	0.00	0.00	0.00	0.00	0.00	0.00	0.00
P	5.69	0.00	0.00	0.00	0.00	0.00	0.00	0.00	0.00	0.00	0.00	0.00
S	0.00	0.00	0.00	0.00	0.00	0.00	0.00	0.00	0.00	0.00	0.00	0.00
Si	0.00	0.00	0.00	0.00	0.00	0.00	0.00	0.00	0.00	0.00	0.00	0.00
Sr	0.05	0.00	0.00	0.00	0.00	0.00	0.00	0.00	0.00	0.00	0.00	0.00
Th	0.00	0.00	0.00	0.00	0.00	0.00	0.00	0.00	0.00	0.00	0.00	0.00
Ti	0.00	0.00	0.00	0.00	0.00	0.00	0.00	0.00	0.00	0.00	0.00	0.00
Y	0.29	0.00	0.00	0.00	0.00	0.00	0.00	0.00	0.00	0.00	0.00	0.00

Appendix 6 Chemical composition analysis of Minerals from Lofdal samples

Sample	30_AS9398_BSE7a	31_AS9398_BSE8a	32_AS9398_BSE8a	33_AS9398_BSE8a	54_AS9398_BSE5a	3_AS9102_BSE1a	4_AS9102_BSE1a	5_AS9102_BSE1a	6_AS9102_BSE1a	7_AS9102_BSE1e	8_AS9102_BSE1e	9_AS9102_BSE1e
Mineral	Calcite											
SiO_2	0.05	0.00	0.00	0.00	0.00	0.00	0.00	0.00	0.00	0.00	0.00	0.00
TiO_2	0.00	0.00	0.00	0.00	0.00	0.00	0.00	0.00	0.00	0.00	0.00	0.00
$Al2O_3$	0.00	0.00	0.00	0.00	0.00	0.00	0.00	0.00	0.00	0.00	0.00	0.00
FeO	0.00	1.22	0.00	0.00	1.32	0.91	0.94	1.15	0.93	0.97	0.00	0.94
MnO	0.00	0.33	0.00	0.00	0.32	1.06	1.07	1.09	1.08	0.97	0.00	1.09
MgO	0.10	0.16	0.24	0.08	0.17	0.07	0.09	0.10	0.10	0.10	0.07	0.11
CaO	55.35	52.38	55.41	55.62	52.55	52.83	52.00	51.66	52.67	52.66	55.45	52.72
Na_2O	0.00	0.00	0.00	0.00	0.07	0.00	0.00	0.00	0.00	0.00	0.00	0.00
K_2O	0.00	0.00	0.00	0.00	0.04	0.00	0.00	0.00	0.00	0.00	0.00	0.00
P_2O_5	0.00	0.00	0.00	0.00	0.00	0.00	0.00	0.00	0.00	0.00	0.10	0.00
F	0.00	0.00	0.00	0.00	0.00	0.00	0.00	0.00	0.00	0.00	0.00	0.00
Cl	0.00	0.00	0.00	0.00	0.00	0.00	0.00	0.00	0.00	0.00	0.00	0.00
SO_3	0.00	0.00	0.00	0.00	0.00	0.00	0.00	0.00	0.00	0.00	0.00	0.00
SrO	0.21	0.33	0.00	0.00	0.41	0.69	1.43	1.38	1.20	1.39	0.14	0.85
Y_2O_3	0.00	0.00	0.00	0.00	0.00	0.00	0.00	0.00	0.00	0.00	0.00	0.00
BaO	0.00	0.00	0.00	0.00	0.00	0.00	0.00	0.00	0.00	0.00	0.00	0.00
La_2O_3	0.00	0.00	0.00	0.00	0.00	0.00	0.00	0.00	0.00	0.00	0.00	0.00
Ce_2O_3	0.00	0.00	0.00	0.00	0.00	0.00	0.00	0.00	0.00	0.00	0.00	0.00
Nd_2O_3	0.00	0.00	0.00	0.00	0.00	0.00	0.00	0.00	0.00	0.00	0.00	0.00
ThO_2	0.00	0.00	0.00	0.00	0.00	0.00	0.00	0.00	0.00	0.00	0.00	0.00
CO_2	43.71	42.38	43.75	43.73	42.67	43.05	42.75	42.61	43.19	43.22	43.81	43.11
Total	**99.43**	**96.80**	**99.39**	**99.42**	**97.53**	**98.61**	**98.27**	**97.97**	**99.16**	**99.30**	**99.57**	**98.83**
O=F,Cl	-	-	-	-	-	-	-	-	-	-	-	-
Ox	3.00	3.00	3.00	3.00	3.00	3.00	3.00	3.00	3.00	3.00	3.00	3.00
F	0.00	0.00	0.00	0.00	0.00	0.00	0.00	0.00	0.00	0.00	0.00	0.00
Al	0.00	0.00	0.00	0.00	0.00	0.00	0.00	0.00	0.00	0.00	0.00	0.00
Ba	0.00	0.00	0.00	0.00	0.00	0.00	0.00	0.00	0.00	0.00	0.00	0.00
C	1.00	1.00	1.00	1.00	1.00	1.00	1.00	1.00	1.00	1.00	1.00	1.00
Ca	0.99	0.97	0.99	1.00	0.97	0.96	0.95	0.95	0.96	0.96	0.99	0.96
Ce	0.00	0.00	0.00	0.00	0.00	0.00	0.00	0.00	0.00	0.00	0.00	0.00
Cl	0.00	0.00	0.00	0.00	0.00	0.00	0.00	0.00	0.00	0.00	0.00	0.00
Fe	0.00	0.02	0.00	0.00	0.02	0.01	0.01	0.02	0.01	0.01	0.00	0.01
K	0.00	0.00	0.00	0.00	0.00	0.00	0.00	0.00	0.00	0.00	0.00	0.00
La	0.00	0.00	0.00	0.00	0.00	0.00	0.00	0.00	0.00	0.00	0.00	0.00
Mg	0.00	0.00	0.01	0.00	0.00	0.00	0.00	0.00	0.00	0.00	0.00	0.00
Mn	0.00	0.00	0.00	0.00	0.00	0.02	0.02	0.02	0.02	0.01	0.00	0.02
Na	0.00	0.00	0.00	0.00	0.00	0.00	0.00	0.00	0.00	0.00	0.00	0.00
Nd	0.00	0.00	0.00	0.00	0.00	0.00	0.00	0.00	0.00	0.00	0.00	0.00
P	0.00	0.00	0.00	0.00	0.00	0.00	0.00	0.00	0.00	0.00	0.00	0.00
S	0.00	0.00	0.00	0.00	0.00	0.00	0.00	0.00	0.00	0.00	0.00	0.00
Si	0.00	0.00	0.00	0.00	0.00	0.00	0.00	0.00	0.00	0.00	0.00	0.00
Sr	0.00	0.00	0.00	0.00	0.00	0.01	0.01	0.01	0.01	0.01	0.00	0.01
Th	0.00	0.00	0.00	0.00	0.00	0.00	0.00	0.00	0.00	0.00	0.00	0.00
Ti	0.00	0.00	0.00	0.00	0.00	0.00	0.00	0.00	0.00	0.00	0.00	0.00
Y	0.00	0.00	0.00	0.00	0.00	0.00	0.00	0.00	0.00	0.00	0.00	0.00

Appendix 6 Chemical composition analysis of Minerals from Lofdal samples

Sample	10_AS9102_BSE1e	12_AS9102_BSE5a	13_AS9102_BSE7b	14_AS9102_BSE7b	15_AS9102_BSE7b	16_AS9102_BSE7b	17_AS9102_BSE7b	18_AS9102_BSE7b	22_AS9102_BSE2b	25_AS9102_BSE4a	26_AS9102_BSE4a	27_AS9102_BSE6a
Mineral	Calcite											
SiO_2	0.00	0.00	0.00	0.00	0.00	0.00	0.00	0.00	0.00	0.00	0.00	0.00
TiO_2	0.00	0.00	0.00	0.00	0.00	0.00	0.00	0.00	0.00	0.00	0.00	0.00
$Al2O_3$	0.00	0.00	0.00	0.00	0.00	0.00	0.00	0.00	0.00	0.00	0.00	0.00
FeO	0.76	1.14	1.23	1.00	1.00	1.08	1.12	1.10	0.99	1.10	1.04	1.19
MnO	0.99	0.96	1.13	1.10	1.12	1.06	1.09	0.95	1.07	1.12	1.07	1.09
MgO	0.09	0.10	0.11	0.11	0.08	0.10	0.08	0.10	0.10	0.13	0.14	0.11
CaO	52.48	51.50	51.46	50.92	51.43	51.40	51.28	52.65	52.07	51.49	51.90	51.66
Na_2O	0.00	0.00	0.00	0.00	0.00	0.00	0.00	0.00	0.00	0.00	0.00	0.00
K_2O	0.00	0.00	0.00	0.00	0.00	0.00	0.00	0.00	0.00	0.00	0.00	0.00
P_2O_5	0.00	0.00	0.00	0.00	0.00	0.00	0.00	0.00	0.00	0.00	0.00	0.00
F	0.00	0.00	0.00	0.00	0.00	0.00	0.00	0.00	0.00	0.00	0.00	0.00
Cl	0.00	0.05	0.00	0.00	0.00	0.00	0.00	0.00	0.00	0.00	0.00	0.00
SO_3	0.00	0.00	0.00	0.00	0.00	0.00	0.00	0.00	0.00	0.00	0.00	0.00
SrO	0.90	2.20	1.88	2.01	2.01	2.01	1.79	1.64	1.87	2.07	2.15	1.50
Y_2O_3	0.00	0.00	0.00	0.00	0.00	0.00	0.00	0.00	0.00	0.00	0.00	0.00
BaO	0.00	0.00	0.00	0.00	0.00	0.00	0.00	0.00	0.00	0.00	0.00	0.00
La_2O_3	0.00	0.00	0.00	0.00	0.00	0.00	0.00	0.00	0.00	0.00	0.00	0.00
Ce_2O_3	0.00	0.00	0.00	0.00	0.00	0.00	0.00	0.00	0.00	0.19	0.00	0.00
Nd_2O_3	0.00	0.00	0.00	0.00	0.00	0.00	0.00	0.00	0.00	0.00	0.00	0.00
ThO_2	0.00	0.00	0.00	0.00	0.00	0.00	0.00	0.00	0.00	0.00	0.00	0.00
CO_2	42.75	42.75	42.75	42.23	42.61	42.62	42.46	43.38	43.04	42.88	43.10	42.70
Total	97.98	98.70	98.55	97.37	98.24	98.26	97.82	99.81	99.15	98.99	99.41	98.25
O=F,Cl	-	-	-	-	-	-	-	-	-	-	-	-
Ox	3.00	3.00	3.00	3.00	3.00	3.00	3.00	3.00	3.00	3.00	3.00	3.00
F	0.00	0.00	0.00	0.00	0.00	0.00	0.00	0.00	0.00	0.00	0.00	0.00
Al	0.00	0.00	0.00	0.00	0.00	0.00	0.00	0.00	0.00	0.00	0.00	0.00
Ba	0.00	0.00	0.00	0.00	0.00	0.00	0.00	0.00	0.00	0.00	0.00	0.00
C	1.00	1.00	1.00	1.00	1.00	1.00	1.00	1.00	1.00	1.00	1.00	1.00
Ca	0.96	0.94	0.94	0.95	0.95	0.95	0.95	0.95	0.95	0.94	0.94	0.95
Ce	0.00	0.00	0.00	0.00	0.00	0.00	0.00	0.00	0.00	0.00	0.00	0.00
Cl	0.00	0.00	0.00	0.00	0.00	0.00	0.00	0.00	0.00	0.00	0.00	0.00
Fe	0.01	0.02	0.02	0.01	0.01	0.02	0.02	0.02	0.01	0.02	0.01	0.02
K	0.00	0.00	0.00	0.00	0.00	0.00	0.00	0.00	0.00	0.00	0.00	0.00
La	0.00	0.00	0.00	0.00	0.00	0.00	0.00	0.00	0.00	0.00	0.00	0.00
Mg	0.00	0.00	0.00	0.00	0.00	0.00	0.00	0.00	0.00	0.00	0.00	0.00
Mn	0.01	0.01	0.02	0.02	0.02	0.02	0.02	0.01	0.02	0.02	0.02	0.02
Na	0.00	0.00	0.00	0.00	0.00	0.00	0.00	0.00	0.00	0.00	0.00	0.00
Nd	0.00	0.00	0.00	0.00	0.00	0.00	0.00	0.00	0.00	0.00	0.00	0.00
P	0.00	0.00	0.00	0.00	0.00	0.00	0.00	0.00	0.00	0.00	0.00	0.00
S	0.00	0.00	0.00	0.00	0.00	0.00	0.00	0.00	0.00	0.00	0.00	0.00
Si	0.00	0.00	0.00	0.00	0.00	0.00	0.00	0.00	0.00	0.00	0.00	0.00
Sr	0.01	0.02	0.02	0.02	0.02	0.02	0.02	0.02	0.02	0.02	0.02	0.01
Th	0.00	0.00	0.00	0.00	0.00	0.00	0.00	0.00	0.00	0.00	0.00	0.00
Ti	0.00	0.00	0.00	0.00	0.00	0.00	0.00	0.00	0.00	0.00	0.00	0.00
Y	0.00	0.00	0.00	0.00	0.00	0.00	0.00	0.00	0.00	0.00	0.00	0.00

Appendix 6 Chemical composition analysis of Minerals from Lofdal samples

Sample	28_AS9102_BSE7a	29_AS9102_BSE8a	30_AS9102_BSE9a	31_AS9102_BSE9a	36_AS9102_BSE10a	37_AS9102_BSE10a	38_AS9102_BSE11a	39_AS9102_BSE12a	40_AS9102_BSE13a	41_AS9102_BSE13a	5_AS9396_BSE3b	6_AS9396_BSE1a
Mineral	Calcite											
SiO_2	0.00	0.00	0.00	0.00	0.00	0.00	0.00	0.00	0.00	0.00	0.00	0.00
TiO_2	0.00	0.00	0.00	0.00	0.00	0.00	0.00	0.00	0.00	0.00	0.00	0.00
$Al2O_3$	0.00	0.00	0.00	0.00	0.00	0.00	0.00	0.00	0.00	0.00	0.00	0.00
FeO	1.15	1.01	1.13	1.05	0.00	1.17	0.88	0.44	0.00	1.09	0.18	0.97
MnO	1.03	1.10	0.97	1.11	0.08	1.03	1.02	0.37	0.00	1.17	0.00	0.26
MgO	0.08	0.08	0.12	0.12	0.06	0.10	0.12	0.11	0.05	0.09	0.27	0.21
CaO	52.29	51.97	51.89	51.29	56.15	51.57	51.91	55.46	55.71	51.47	55.79	53.09
Na_2O	0.00	0.00	0.00	0.00	0.00	0.00	0.00	0.00	0.00	0.00	0.00	0.00
K_2O	0.00	0.00	0.00	0.00	0.00	0.00	0.00	0.00	0.00	0.00	0.00	0.00
P_2O_5	0.00	0.00	0.00	0.00	0.00	0.00	0.00	0.00	0.00	0.00	0.00	0.00
F	0.00	0.00	0.00	0.00	0.00	0.00	0.00	0.00	0.00	0.00	0.00	0.00
Cl	0.00	0.00	0.00	0.00	0.00	0.00	0.00	0.00	0.00	0.00	0.00	0.00
SO_3	0.00	0.00	0.00	0.00	0.00	0.00	0.00	0.00	0.00	0.00	0.00	0.00
SrO	1.78	1.90	1.59	1.85	0.19	2.12	1.82	0.37	0.26	1.63	0.00	0.54
Y_2O_3	0.00	0.00	0.00	0.00	0.00	0.00	0.00	0.00	0.00	0.00	0.00	0.00
BaO	0.00	0.00	0.00	0.00	0.00	0.00	0.00	0.00	0.00	0.00	0.00	0.00
La_2O_3	0.00	0.00	0.00	0.00	0.00	0.00	0.00	0.00	0.00	0.00	0.00	0.00
Ce_2O_3	0.00	0.00	0.00	0.00	0.00	0.00	0.00	0.00	0.00	0.00	0.00	0.00
Nd_2O_3	0.00	0.00	0.00	0.00	0.00	0.00	0.00	0.00	0.00	0.00	0.00	0.00
ThO_2	0.00	0.00	0.00	0.00	0.00	0.00	0.00	0.00	0.00	0.00	0.00	0.00
CO_2	43.23	42.97	42.82	42.50	44.27	42.84	42.81	44.31	43.88	42.59	44.19	42.88
Total	**99.56**	**99.03**	**98.52**	**97.92**	**100.75**	**98.83**	**98.55**	**101.06**	**99.90**	**98.04**	**100.43**	**97.96**
O=F,Cl	-	-	-	-	-	-	-	-	-	-	-	-
Ox	3.00	3.00	3.00	3.00	3.00	3.00	3.00	3.00	3.00	3.00	3.00	3.00
F	0.00	0.00	0.00	0.00	0.00	0.00	0.00	0.00	0.00	0.00	0.00	0.00
Al	0.00	0.00	0.00	0.00	0.00	0.00	0.00	0.00	0.00	0.00	0.00	0.00
Ba	0.00	0.00	0.00	0.00	0.00	0.00	0.00	0.00	0.00	0.00	0.00	0.00
C	1.00	1.00	1.00	1.00	1.00	1.00	1.00	1.00	1.00	1.00	1.00	1.00
Ca	0.95	0.95	0.95	0.95	1.00	0.94	0.95	0.98	1.00	0.95	0.99	0.97
Ce	0.00	0.00	0.00	0.00	0.00	0.00	0.00	0.00	0.00	0.00	0.00	0.00
Cl	0.00	0.00	0.00	0.00	0.00	0.00	0.00	0.00	0.00	0.00	0.00	0.00
Fe	0.02	0.01	0.02	0.02	0.00	0.02	0.01	0.01	0.00	0.02	0.00	0.01
K	0.00	0.00	0.00	0.00	0.00	0.00	0.00	0.00	0.00	0.00	0.00	0.00
La	0.00	0.00	0.00	0.00	0.00	0.00	0.00	0.00	0.00	0.00	0.00	0.00
Mg	0.00	0.00	0.00	0.00	0.00	0.00	0.00	0.00	0.00	0.00	0.01	0.01
Mn	0.01	0.02	0.01	0.02	0.00	0.01	0.01	0.01	0.00	0.02	0.00	0.00
Na	0.00	0.00	0.00	0.00	0.00	0.00	0.00	0.00	0.00	0.00	0.00	0.00
Nd	0.00	0.00	0.00	0.00	0.00	0.00	0.00	0.00	0.00	0.00	0.00	0.00
P	0.00	0.00	0.00	0.00	0.00	0.00	0.00	0.00	0.00	0.00	0.00	0.00
S	0.00	0.00	0.00	0.00	0.00	0.00	0.00	0.00	0.00	0.00	0.00	0.00
Si	0.00	0.00	0.00	0.00	0.00	0.00	0.00	0.00	0.00	0.00	0.00	0.00
Sr	0.02	0.02	0.02	0.02	0.00	0.02	0.02	0.00	0.00	0.02	0.00	0.01
Th	0.00	0.00	0.00	0.00	0.00	0.00	0.00	0.00	0.00	0.00	0.00	0.00
Ti	0.00	0.00	0.00	0.00	0.00	0.00	0.00	0.00	0.00	0.00	0.00	0.00
Y	0.00	0.00	0.00	0.00	0.00	0.00	0.00	0.00	0.00	0.00	0.00	0.00

Appendix 6 Chemical composition analysis of Minerals from Lofdal samples

Sample	7_AS9396_BSE1a	12_AS9396_BSE2e	13_AS9396_BSE2e	16_AS9396_BSE3b	17_AS9396_BSE3a	19_AS9396_BSE3b	22_AS9396_BSE4b	25_AS9396_BSE5b	24_AS9396_BSE5b	8_AS9396_BSE1a	14_AS9396_BSE2e	18_AS9396_BSE3b
Mineral	Calcite									Calcite-(Fe)		
SiO_2	0.00	0.32	0.00	0.00	0.00	0.00	0.29	0.00	0.00	0.50	0.55	0.34
TiO_2	0.00	0.00	0.00	0.00	0.00	0.00	0.00	0.00	0.00	0.00	0.00	0.00
$Al2O_3$	0.00	0.23	0.00	0.00	0.00	0.00	0.00	0.00	0.00	0.00	0.00	0.00
FeO	0.84	0.26	0.00	0.24	0.43	0.24	0.33	0.55	0.25	19.90	19.33	19.72
MnO	0.29	0.54	0.00	1.23	1.01	0.83	0.00	0.66	0.00	0.43	1.05	0.54
MgO	0.13	0.05	0.14	0.08	0.23	0.16	0.55	0.21	0.06	0.58	0.54	0.50
CaO	53.29	54.47	56.34	53.37	53.77	53.97	55.47	54.19	55.92	41.75	40.49	41.72
Na_2O	0.00	0.00	0.00	0.00	0.00	0.00	0.00	0.00	0.00	0.00	0.00	0.00
K_2O	0.00	0.15	0.00	0.00	0.00	0.00	0.00	0.00	0.00	0.00	0.00	0.00
P_2O_5	0.00	0.00	0.00	0.00	0.00	0.00	0.00	0.00	0.00	0.00	0.00	0.00
F	0.00	0.00	0.00	0.00	0.00	0.00	0.00	0.00	0.00	0.00	0.00	0.00
Cl	0.00	0.00	0.00	0.00	0.00	0.00	0.00	0.00	0.00	0.00	0.00	0.00
SO_3	0.00	0.00	0.00	0.11	0.15	0.18	0.00	0.21	0.00	0.09	0.00	0.12
SrO	0.53	0.00	0.00	0.00	0.00	0.00	0.00	0.00	0.00	0.12	0.00	0.00
Y_2O_3	0.00	0.00	0.00	0.00	0.00	0.00	0.00	0.00	0.00	0.00	0.00	0.00
BaO	0.00	0.00	0.00	0.00	0.00	0.00	0.00	0.00	0.00	0.00	0.00	0.00
La_2O_3	0.00	0.00	0.00	0.00	0.00	0.00	0.00	0.00	0.00	0.00	0.00	0.00
Ce_2O_3	0.00	0.00	0.00	0.00	0.00	0.00	0.00	0.00	0.00	0.00	0.00	0.00
Nd_2O_3	0.00	0.00	0.00	0.00	0.00	0.00	0.00	0.00	0.00	0.00	0.00	0.00
ThO_2	0.00	0.00	0.00	0.00	0.00	0.00	0.00	0.00	0.00	0.00	0.00	0.00
CO_2	42.88	44.11	44.37	43.19	43.73	43.69	44.77	44.10	44.11	46.89	45.66	46.52
Total	**97.95**	**100.11**	**100.86**	**98.22**	**99.32**	**99.08**	**101.41**	**99.92**	**100.34**	**110.26**	**107.62**	**109.46**
O=F,Cl	-	-	-	-	-	-	-	-	-	-	-	-
Ox	3.00	3.00	3.00	3.00	3.00	3.00	3.00	3.00	3.00	3.00	3.00	3.00
F	0.00	0.00	0.00	0.00	0.00	0.00	0.00	0.00	0.00	0.00	0.00	0.00
Al	0.00	0.00	0.00	0.00	0.00	0.00	0.00	0.00	0.00	0.00	0.00	0.00
Ba	0.00	0.00	0.00	0.00	0.00	0.00	0.00	0.00	0.00	0.00	0.00	0.00
C	1.00	1.00	1.00	1.00	1.00	1.00	1.00	1.00	1.00	1.00	1.00	1.00
Ca	0.98	0.97	1.00	0.97	0.96	0.97	0.97	0.96	0.99	0.70	0.70	0.70
Ce	0.00	0.00	0.00	0.00	0.00	0.00	0.00	0.00	0.00	0.00	0.00	0.00
Cl	0.00	0.00	0.00	0.00	0.00	0.00	0.00	0.00	0.00	0.00	0.00	0.00
Fe	0.01	0.00	0.00	0.00	0.01	0.00	0.00	0.01	0.00	0.26	0.26	0.26
K	0.00	0.00	0.00	0.00	0.00	0.00	0.00	0.00	0.00	0.00	0.00	0.00
La	0.00	0.00	0.00	0.00	0.00	0.00	0.00	0.00	0.00	0.00	0.00	0.00
Mg	0.00	0.00	0.00	0.00	0.01	0.00	0.01	0.01	0.00	0.01	0.01	0.01
Mn	0.00	0.01	0.00	0.02	0.01	0.01	0.00	0.01	0.00	0.01	0.01	0.01
Na	0.00	0.00	0.00	0.00	0.00	0.00	0.00	0.00	0.00	0.00	0.00	0.00
Nd	0.00	0.00	0.00	0.00	0.00	0.00	0.00	0.00	0.00	0.00	0.00	0.00
P	0.00	0.00	0.00	0.00	0.00	0.00	0.00	0.00	0.00	0.00	0.00	0.00
S	0.00	0.00	0.00	0.00	0.00	0.00	0.00	0.00	0.00	0.00	0.00	0.00
Si	0.00	0.01	0.00	0.00	0.00	0.00	0.00	0.00	0.00	0.01	0.01	0.01
Sr	0.01	0.00	0.00	0.00	0.00	0.00	0.00	0.00	0.00	0.00	0.00	0.00
Th	0.00	0.00	0.00	0.00	0.00	0.00	0.00	0.00	0.00	0.00	0.00	0.00
Ti	0.00	0.00	0.00	0.00	0.00	0.00	0.00	0.00	0.00	0.00	0.00	0.00
Y	0.00	0.00	0.00	0.00	0.00	0.00	0.00	0.00	0.00	0.00	0.00	0.00

Appendix 6 Chemical composition analysis of Minerals from Lofdal samples

Sample	26_AS9396_BSE5a	10_AS9398_BSE1d	42_AS9398_BSE3e	43_AS9398_BSE3e	46_AS9398_BSE3i	49_AS9398_BSE3e	9_AS9398_BSE1d	40_AS9398_BSE3d	56_AS9398_BSE6b	41_AS9398_BSE3e	48_AS9398_BSE3i	1_AS9102_BSE1b
Mineral	Cal-(Fe)	Thorianite					Xenotime			Monazite		
SiO_2	0.37	12.38	13.01	13.26	14.96	14.15	1.00	0.54	0.89	0.23	0.24	0.21
TiO_2	0.00	0.00	0.09	0.00	0.00	0.00	0.00	0.00	0.00	0.00	0.00	0.00
$Al2O_3$	0.00	0.00	0.25	0.21	0.54	0.32	0.00	0.00	0.00	0.00	0.00	0.00
FeO	19.80	2.51	1.99	1.95	0.47	0.29	0.00	0.26	0.00	0.00	0.00	0.00
MnO	0.76	0.00	0.00	0.00	0.00	0.00	0.00	0.00	0.00	0.00	0.00	0.00
MgO	0.68	0.00	0.00	0.00	0.00	0.00	0.00	0.00	0.00	0.00	0.00	0.00
CaO	41.77	2.73	2.47	2.39	1.75	1.82	0.23	0.22	0.18	0.47	0.46	0.00
Na_2O	0.00	0.00	0.00	0.00	0.00	0.00	0.06	0.00	0.00	0.00	0.00	0.00
K_2O	0.00	0.00	0.00	0.00	0.00	0.00	0.00	0.00	0.00	0.00	0.00	0.00
P_2O_5	0.00	5.13	5.60	4.95	2.66	2.68	29.31	28.55	27.84	30.20	29.50	29.67
F	0.00	0.35	0.70	0.72	0.35	0.40	0.00	0.00	0.00	0.49	0.32	0.40
Cl	0.00	0.00	0.00	0.00	0.00	0.00	0.00	0.00	0.00	0.00	0.00	0.00
SO_3	0.15	0.00	0.00	0.00	0.00	0.00	0.00	0.00	0.00	0.00	0.00	0.00
SrO	0.00	0.00	0.00	0.00	0.00	0.00	0.00	0.00	0.00	0.17	0.00	0.00
Y_2O_3	0.00	4.92	6.27	5.23	3.08	2.55	38.67	35.85	34.45	0.31	0.00	0.00
BaO	0.00	0.00	0.00	0.00	0.00	0.00	0.00	0.00	0.00	0.20	0.00	0.00
La_2O_3	0.00	0.00	0.00	0.00	0.44	0.36	0.00	0.00	0.00	17.99	15.84	16.81
Ce_2O_3	0.00	0.50	0.51	0.36	0.22	0.43	0.00	0.00	0.00	35.45	34.99	41.41
Nd_2O_3	0.00	0.39	0.28	0.00	0.64	0.56	0.00	0.00	0.00	8.11	9.10	10.48
ThO_2	0.00	72.60	66.71	69.84	77.37	79.24	1.86	1.55	0.72	2.22	1.62	1.92
CO_2	47.08	-	-	-	-	-	-	-	-	-	-	-
Total	**110.62**	**101.51**	**97.88**	**98.90**	**102.47**	**102.81**	**71.13**	**66.98**	**64.08**	**95.84**	**92.06**	**100.91**
O=F,Cl	-	-	-		98.60	102.33	102.64	-	-		95.64	91.93	100.74
Ox	3.00	4.00	4.00	4.00	4.00	4.00	4.00	4.00	4.00	4.00	4.00	4.00
F	0.00	0.06	0.11	0.11	0.06	0.07	0.00	0.00	0.00	0.06	0.04	0.05
Al	0.00	0.00	0.01	0.01	0.03	0.02	0.00	0.00	0.00	0.00	0.00	0.00
Ba	0.00	0.00	0.00	0.00	0.00	0.00	0.00	0.00	0.00	0.00	0.00	0.00
C	1.00	0.00	0.00	0.00	0.00	0.00	0.00	0.00	0.00	0.00	0.00	0.00
Ca	0.70	0.15	0.13	0.13	0.10	0.10	0.01	0.01	0.01	0.02	0.02	0.00
Ce	0.00	0.01	0.01	0.01	0.00	0.01	0.00	0.00	0.00	0.51	0.52	0.59
Cl	0.00	0.00	0.00	0.00	0.00	0.00	0.00	0.00	0.00	0.00	0.00	0.00
Fe	0.26	0.11	0.08	0.08	0.02	0.01	0.00	0.01	0.00	0.00	0.00	0.00
K	0.00	0.00	0.00	0.00	0.00	0.00	0.00	0.00	0.00	0.00	0.00	0.00
La	0.00	0.00	0.00	0.00	0.01	0.01	0.00	0.00	0.00	0.26	0.24	0.24
Mg	0.02	0.00	0.00	0.00	0.00	0.00	0.00	0.00	0.00	0.00	0.00	0.00
Mn	0.01	0.00	0.00	0.00	0.00	0.00	0.00	0.00	0.00	0.00	0.00	0.00
Na	0.00	0.00	0.00	0.00	0.00	0.00	0.00	0.00	0.00	0.00	0.00	0.00
Nd	0.00	0.01	0.00	0.00	0.01	0.01	0.00	0.00	0.00	0.11	0.13	0.15
P	0.00	0.22	0.23	0.21	0.12	0.12	1.03	1.06	1.06	1.01	1.02	0.98
S	0.00	0.00	0.00	0.00	0.00	0.00	0.00	0.00	0.00	0.00	0.00	0.00
Si	0.01	0.62	0.64	0.66	0.76	0.74	0.04	0.02	0.04	0.01	0.01	0.01
Sr	0.00	0.00	0.00	0.00	0.00	0.00	0.00	0.00	0.00	0.00	0.00	0.00
Th	0.00	0.83	0.75	0.79	0.90	0.94	0.02	0.02	0.01	0.02	0.02	0.02
Ti	0.00	0.00	0.00	0.00	0.00	0.00	0.00	0.00	0.00	0.00	0.00	0.00
Y	0.00	0.13	0.17	0.14	0.08	0.07	0.86	0.84	0.83	0.01	0.00	0.00

Appendix 6 Chemical composition analysis of Minerals from Lofdal samples

Sample	2_AS9102_BSE1b	20_AS9102_BSE1c	11_AS9102_BSE5a	19_AS9102_BSE5b	23_AS9102_BSE3a	1_AS9393_BSE1b	2_AS9393_BSE1b	3_AS9393_BSE1a	4_AS9393_BSE1b	5_AS9393_BSE1b	6_AS9393_BSE1b	7_AS9393_BSE1a
Mineral	Monazite		Calciobur	Strontianite		Dolomite-Ankerite						
SiO_2	0.13	0.10	0.00	0.00	0.00	0.00	0.00	0.00	0.05	0.00	0.00	0.00
TiO_2	0.00	0.00	0.00	0.00	0.00	0.00	0.00	0.00	0.00	0.00	0.00	0.00
$Al2O_3$	0.00	0.00	0.00	0.00	0.00	0.00	0.00	0.00	0.00	0.00	0.00	0.00
FeO	0.00	0.00	0.00	0.00	0.00	13.20	12.26	12.46	11.99	7.96	6.74	9.07
MnO	0.00	0.00	0.00	0.00	0.00	0.40	0.40	0.43	0.39	0.22	0.23	0.20
MgO	0.00	0.00	0.00	0.00	0.00	13.20	13.19	13.51	13.74	16.66	17.47	15.89
CaO	0.14	0.40	6.19	5.71	2.84	29.18	28.32	28.38	29.35	29.27	29.78	29.08
Na_2O	0.00	0.00	10.11	0.00	0.00	0.00	0.00	0.00	0.00	0.00	0.04	0.00
K_2O	0.00	0.00	0.00	0.00	0.00	0.00	0.00	0.00	0.00	0.00	0.00	0.00
P_2O_5	30.36	29.71	0.00	0.00	0.00	0.00	0.00	0.00	0.00	0.00	0.00	0.00
F	0.33	0.34	0.00	0.00	0.00	0.00	0.00	0.00	0.00	0.00	0.00	0.00
Cl	0.00	0.00	0.00	0.00	0.00	0.00	0.00	0.00	0.00	0.00	0.00	0.00
SO_3	0.08	0.00	0.00	0.00	0.00	0.00	0.00	0.00	0.00	0.00	0.00	0.00
SrO	0.00	0.00	29.45	66.12	74.37	0.14	0.23	0.00	0.21	0.00	0.00	0.00
Y_2O_3	0.00	0.00	0.00	0.00	0.00	0.00	0.00	0.00	0.00	0.00	0.00	0.00
BaO	0.00	0.00	1.58	0.94	0.00	0.00	0.00	0.00	0.00	0.00	0.00	0.00
La_2O_3	15.89	18.24	6.30	0.00	0.00	0.00	0.00	0.00	0.00	0.00	0.00	0.00
Ce_2O_3	40.64	40.96	12.63	0.00	0.00	0.00	0.00	0.00	0.00	0.00	0.00	0.00
Nd_2O_3	12.29	9.84	3.31	0.00	0.00	0.00	0.00	0.00	0.00	0.00	0.00	0.00
ThO_2	1.33	1.35	0.00	0.00	0.00	0.00	0.00	0.00	0.00	0.00	0.00	0.00
CO_2	-	-	33.93	32.83	33.81	45.70	44.48	44.92	45.79	46.18	46.75	45.86
Total	**101.19**	**100.94**	**103.49**	**105.60**	**111.02**	**101.82**	**98.87**	**99.71**	**101.52**	**100.29**	**101.02**	**100.11**
$O=F_2Cl$	101.05	100.80	-	-	-	-	-	-	-	-	-	-
Ox	4.00	4.00	15.00	3.00	3.00	6.00	6.00	6.00	6.00	6.00	6.00	6.00
F	0.04	0.04	0.00	0.00	0.00	0.00	0.00	0.00	0.00	0.00	0.00	0.00
Al	0.00	0.00	0.00	0.00	0.00	0.00	0.00	0.00	0.00	0.00	0.00	0.00
Ba	0.00	0.00	0.07	0.01	0.00	0.00	0.00	0.00	0.00	0.00	0.00	0.00
C	0.00	0.00	5.00	1.00	1.00	2.00	2.00	2.00	2.00	2.00	2.00	2.00
Ca	0.01	0.02	0.72	0.14	0.07	1.00	1.00	0.99	1.01	0.99	1.00	1.00
Ce	0.57	0.58	0.50	0.00	0.00	0.00	0.00	0.00	0.00	0.00	0.00	0.00
Cl	0.00	0.00	0.00	0.00	0.00	0.00	0.00	0.00	0.00	0.00	0.00	0.00
Fe	0.00	0.00	0.00	0.00	0.00	0.35	0.34	0.34	0.32	0.21	0.18	0.24
K	0.00	0.00	0.00	0.00	0.00	0.00	0.00	0.00	0.00	0.00	0.00	0.00
La	0.22	0.26	0.25	0.00	0.00	0.00	0.00	0.00	0.00	0.00	0.00	0.00
Mg	0.00	0.00	0.00	0.00	0.00	0.63	0.65	0.66	0.66	0.79	0.82	0.76
Mn	0.00	0.00	0.00	0.00	0.00	0.01	0.01	0.01	0.01	0.01	0.01	0.01
Na	0.00	0.00	2.12	0.00	0.00	0.00	0.00	0.00	0.00	0.00	0.00	0.00
Nd	0.17	0.14	0.13	0.00	0.00	0.00	0.00	0.00	0.00	0.00	0.00	0.00
P	0.99	0.98	0.00	0.00	0.00	0.00	0.00	0.00	0.00	0.00	0.00	0.00
S	0.00	0.00	0.00	0.00	0.00	0.00	0.00	0.00	0.00	0.00	0.00	0.00
Si	0.00	0.00	0.00	0.00	0.00	0.00	0.00	0.00	0.00	0.00	0.00	0.00
Sr	0.00	0.00	1.84	0.86	0.93	0.00	0.00	0.00	0.00	0.00	0.00	0.00
Th	0.01	0.01	0.00	0.00	0.00	0.00	0.00	0.00	0.00	0.00	0.00	0.00
Ti	0.00	0.00	0.00	0.00	0.00	0.00	0.00	0.00	0.00	0.00	0.00	0.00
Y	0.00	0.00	0.00	0.00	0.00	0.00	0.00	0.00	0.00	0.00	0.00	0.00

Appendix 6 Chemical composition analysis of Minerals from Lofdal samples

Sample	8_AS9393_BSE1c	9_AS9393_BSE1c	10_AS9393_BSE1c	11_AS9393_BSE1c	12_AS9393_BSE1c	13_AS9393_BSE1c	14_AS9393_BSE1c	15_AS9393_BSE1c	16_AS9393_BSE1d	17_AS9393_BSE1d	18_AS9393_BSE1d	19_AS9393_BSE1d
Mineral	Dolomite-Ankerite											
SiO_2	0.00	0.00	0.00	0.00	0.00	0.00	0.00	0.00	0.00	0.00	0.00	0.00
TiO_2	0.00	0.00	0.00	0.00	0.00	0.00	0.00	0.00	0.00	0.00	0.00	0.00
$Al2O_3$	0.00	0.00	0.00	0.00	0.00	0.00	0.00	0.00	0.00	0.00	0.00	0.00
FeO	8.86	5.56	6.14	10.23	8.56	9.31	7.06	8.13	14.08	4.83	4.94	19.57
MnO	0.29	0.14	0.12	0.29	0.24	0.31	0.19	0.18	0.45	0.15	0.15	0.71
MgO	15.88	17.99	17.88	14.67	15.85	15.59	17.24	16.42	12.51	18.39	18.65	8.36
CaO	29.01	29.36	29.20	29.20	29.51	28.94	29.62	29.13	28.55	29.61	29.41	27.69
Na_2O	0.00	0.00	0.00	0.00	0.00	0.00	0.00	0.00	0.00	0.00	0.00	0.06
K_2O	0.00	0.00	0.00	0.00	0.00	0.00	0.00	0.00	0.00	0.00	0.00	0.00
P_2O_5	0.00	0.00	0.00	0.00	0.00	0.00	0.00	0.00	0.00	0.00	0.00	0.00
F	0.00	0.00	0.00	0.00	0.00	0.00	0.00	0.00	0.00	0.00	0.00	0.00
Cl	0.00	0.00	0.00	0.00	0.00	0.00	0.00	0.00	0.00	0.00	0.00	0.00
SO_3	0.00	0.00	0.00	0.00	0.00	0.00	0.00	0.00	0.00	0.00	0.00	0.00
SrO	0.00	0.00	0.00	0.10	0.00	0.00	0.00	0.00	0.00	0.00	0.00	0.00
Y_2O_3	0.00	0.00	0.00	0.00	0.00	0.00	0.00	0.00	0.00	0.00	0.00	0.00
BaO	0.00	0.00	0.00	0.00	0.00	0.00	0.00	0.00	0.00	0.00	0.00	0.00
La_2O_3	0.00	0.00	0.00	0.00	0.00	0.00	0.00	0.00	0.00	0.00	0.00	0.00
Ce_2O_3	0.00	0.00	0.00	0.00	0.00	0.00	0.00	0.00	0.00	0.00	0.00	0.00
Nd_2O_3	0.00	0.00	0.00	0.00	0.00	0.00	0.00	0.00	0.00	0.00	0.00	0.00
ThO_2	0.00	0.00	0.00	0.00	0.00	0.00	0.00	0.00	0.00	0.00	0.00	0.00
CO_2	45.70	46.18	46.26	45.42	45.86	45.63	46.51	45.88	44.97	46.36	46.56	43.32
Total	**99.73**	**99.25**	**99.60**	**99.91**	**100.02**	**99.77**	**100.61**	**99.75**	**100.57**	**99.34**	**99.71**	**99.71**
O=F,Cl	-	-	-	-	-	-	-	-	-	-	-	
Ox	6.00	6.00	6.00	6.00	6.00	6.00	6.00	6.00	6.00	6.00	6.00	6.00
F	0.00	0.00	0.00	0.00	0.00	0.00	0.00	0.00	0.00	0.00	0.00	0.00
Al	0.00	0.00	0.00	0.00	0.00	0.00	0.00	0.00	0.00	0.00	0.00	0.00
Ba	0.00	0.00	0.00	0.00	0.00	0.00	0.00	0.00	0.00	0.00	0.00	0.00
C	2.00	2.00	2.00	2.00	2.00	2.00	2.00	2.00	2.00	2.00	2.00	2.00
Ca	1.00	1.00	0.99	1.01	1.01	1.00	1.00	1.00	1.00	1.00	0.99	1.00
Ce	0.00	0.00	0.00	0.00	0.00	0.00	0.00	0.00	0.00	0.00	0.00	0.00
Cl	0.00	0.00	0.00	0.00	0.00	0.00	0.00	0.00	0.00	0.00	0.00	0.00
Fe	0.24	0.15	0.16	0.28	0.23	0.25	0.19	0.22	0.38	0.13	0.13	0.55
K	0.00	0.00	0.00	0.00	0.00	0.00	0.00	0.00	0.00	0.00	0.00	0.00
La	0.00	0.00	0.00	0.00	0.00	0.00	0.00	0.00	0.00	0.00	0.00	0.00
Mg	0.76	0.85	0.84	0.71	0.75	0.75	0.81	0.78	0.61	0.87	0.87	0.42
Mn	0.01	0.00	0.00	0.01	0.01	0.01	0.01	0.00	0.01	0.00	0.00	0.02
Na	0.00	0.00	0.00	0.00	0.00	0.00	0.00	0.00	0.00	0.00	0.00	0.00
Nd	0.00	0.00	0.00	0.00	0.00	0.00	0.00	0.00	0.00	0.00	0.00	0.00
P	0.00	0.00	0.00	0.00	0.00	0.00	0.00	0.00	0.00	0.00	0.00	0.00
S	0.00	0.00	0.00	0.00	0.00	0.00	0.00	0.00	0.00	0.00	0.00	0.00
Si	0.00	0.00	0.00	0.00	0.00	0.00	0.00	0.00	0.00	0.00	0.00	0.00
Sr	0.00	0.00	0.00	0.00	0.00	0.00	0.00	0.00	0.00	0.00	0.00	0.00
Th	0.00	0.00	0.00	0.00	0.00	0.00	0.00	0.00	0.00	0.00	0.00	0.00
Ti	0.00	0.00	0.00	0.00	0.00	0.00	0.00	0.00	0.00	0.00	0.00	0.00
Y	0.00	0.00	0.00	0.00	0.00	0.00	0.00	0.00	0.00	0.00	0.00	0.00

Appendix 6 Chemical composition analysis of Minerals from Lofdal samples

Sample	20_AS9393_BSE1d	21_AS9393_BSE3b	22_AS9393_BSE3b	23_AS9393_BSE3b	24_AS9393_BSE3b	25_AS9393_BSE3b	26_AS9393_BSE3b	27_AS9393_BSE4c	28_AS9393_BSE4c	29_AS9393_BSE4c	30_AS9393_BSE4c	31_AS9393_BSE4c
Mineral	Dolomite-Ankerite											
SiO_2	0.00	0.00	0.00	0.00	0.00	0.00	0.00	0.00	0.00	0.00	0.00	0.00
TiO_2	0.00	0.00	0.00	0.06	0.00	0.00	0.00	0.00	0.00	0.00	0.00	0.00
$Al2O_3$	0.00	0.00	0.00	0.00	0.00	0.00	0.00	0.00	0.00	0.00	0.00	0.00
FeO	12.25	12.48	12.19	4.90	7.51	11.14	10.93	12.58	8.88	10.07	9.65	9.80
MnO	0.38	0.39	0.43	0.00	0.17	0.45	0.44	0.41	0.17	0.15	0.16	0.16
MgO	13.62	13.63	13.27	19.03	17.14	13.89	14.31	13.59	16.24	15.61	15.88	15.79
CaO	28.59	29.04	28.23	29.40	29.33	29.07	28.46	28.54	28.63	28.21	28.70	28.62
Na_2O	0.00	0.00	0.00	0.00	0.00	0.00	0.00	0.00	0.00	0.00	0.00	0.00
K_2O	0.00	0.00	0.00	0.00	0.00	0.03	0.00	0.00	0.00	0.00	0.00	0.00
P_2O_5	0.00	0.00	0.00	0.00	0.00	0.00	0.00	0.00	0.00	0.00	0.00	0.00
F	0.00	0.00	0.00	0.00	0.00	0.00	0.00	0.00	0.00	0.00	0.00	0.00
Cl	0.00	0.00	0.00	0.00	0.00	0.00	0.00	0.00	0.00	0.00	0.00	0.00
SO_3	0.00	0.00	0.00	0.00	0.00	0.00	0.00	0.00	0.00	0.00	0.00	0.00
SrO	0.14	0.11	0.13	0.20	0.00	0.00	0.14	0.16	0.00	0.18	0.00	0.17
Y_2O_3	0.00	0.00	0.00	0.00	0.00	0.00	0.00	0.00	0.00	0.00	0.00	0.00
BaO	0.00	0.00	0.00	0.00	0.00	0.00	0.00	0.00	0.00	0.00	0.00	0.00
La_2O_3	0.00	0.00	0.00	0.00	0.00	0.00	0.00	0.00	0.00	0.00	0.00	0.00
Ce_2O_3	0.00	0.00	0.00	0.00	0.00	0.00	0.00	0.00	0.00	0.00	0.00	0.00
Nd_2O_3	0.00	0.00	0.00	0.00	0.00	0.00	0.00	0.00	0.00	0.00	0.00	0.00
ThO_2	0.00	0.00	0.00	0.00	0.00	0.00	0.00	0.00	0.00	0.00	0.00	0.00
CO_2	45.10	45.60	44.42	47.00	46.43	45.10	44.99	45.25	45.74	45.52	45.88	45.87
Total	100.08	101.25	98.66	100.59	100.58	99.68	99.28	100.52	99.65	99.75	100.27	100.41
O=F,Cl	-	-	-	-	-	-	-	-	-	-	-	-
Ox	6.00	6.00	6.00	6.00	6.00	6.00	6.00	6.00	6.00	6.00	6.00	6.00
F	0.00	0.00	0.00	0.00	0.00	0.00	0.00	0.00	0.00	0.00	0.00	0.00
Al	0.00	0.00	0.00	0.00	0.00	0.00	0.00	0.00	0.00	0.00	0.00	0.00
Ba	0.00	0.00	0.00	0.00	0.00	0.00	0.00	0.00	0.00	0.00	0.00	0.00
C	2.00	2.00	2.00	2.00	2.00	2.00	2.00	2.00	2.00	2.00	2.00	2.00
Ca	0.99	1.00	1.00	0.98	0.99	1.01	0.99	0.99	0.98	0.97	0.98	0.98
Ce	0.00	0.00	0.00	0.00	0.00	0.00	0.00	0.00	0.00	0.00	0.00	0.00
Cl	0.00	0.00	0.00	0.00	0.00	0.00	0.00	0.00	0.00	0.00	0.00	0.00
Fe	0.33	0.34	0.34	0.13	0.20	0.30	0.30	0.34	0.24	0.27	0.26	0.26
K	0.00	0.00	0.00	0.00	0.00	0.00	0.00	0.00	0.00	0.00	0.00	0.00
La	0.00	0.00	0.00	0.00	0.00	0.00	0.00	0.00	0.00	0.00	0.00	0.00
Mg	0.66	0.65	0.65	0.88	0.81	0.67	0.69	0.66	0.78	0.75	0.76	0.75
Mn	0.01	0.01	0.01	0.00	0.00	0.01	0.01	0.01	0.00	0.00	0.00	0.00
Na	0.00	0.00	0.00	0.00	0.00	0.00	0.00	0.00	0.00	0.00	0.00	0.00
Nd	0.00	0.00	0.00	0.00	0.00	0.00	0.00	0.00	0.00	0.00	0.00	0.00
P	0.00	0.00	0.00	0.00	0.00	0.00	0.00	0.00	0.00	0.00	0.00	0.00
S	0.00	0.00	0.00	0.00	0.00	0.00	0.00	0.00	0.00	0.00	0.00	0.00
Si	0.00	0.00	0.00	0.00	0.00	0.00	0.00	0.00	0.00	0.00	0.00	0.00
Sr	0.00	0.00	0.00	0.00	0.00	0.00	0.00	0.00	0.00	0.00	0.00	0.00
Th	0.00	0.00	0.00	0.00	0.00	0.00	0.00	0.00	0.00	0.00	0.00	0.00
Ti	0.00	0.00	0.00	0.00	0.00	0.00	0.00	0.00	0.00	0.00	0.00	0.00
Y	0.00	0.00	0.00	0.00	0.00	0.00	0.00	0.00	0.00	0.00	0.00	0.00

Appendix 6 Chemical composition analysis of Minerals from Lofdal samples

Sample	32_AS9393_BSE4c	33_AS9393_BSE4c	34_AS9393_BSE4c	35_AS9393_BSE4d	36_AS9393_BSE4d	37_AS9393_BSE4d	38_AS9393_BSE4d	39_AS9393_BSE4d	40_AS9393_BSE5a	41_AS9393_BSE5a	42_AS9393_BSE5b	43_AS9393_BSE5b
Mineral	Dolomite-Ankerite											
SiO_2	0.00	0.00	0.00	0.00	0.00	0.00	0.00	0.00	0.00	0.00	0.00	0.00
TiO_2	0.00	0.00	0.00	0.00	0.00	0.00	0.00	0.00	0.00	0.00	0.00	0.00
$Al2O_3$	0.00	0.00	0.00	0.00	0.00	0.00	0.00	0.09	0.00	0.00	0.00	0.00
FeO	8.23	8.85	12.46	12.35	6.51	11.67	12.71	8.16	8.36	12.24	0.28	0.00
MnO	0.17	0.15	0.35	0.39	0.11	0.43	0.39	0.16	0.18	0.36	0.10	0.10
MgO	16.51	16.20	13.48	13.62	17.92	14.26	13.41	16.54	16.24	13.93	0.06	0.16
CaO	28.54	28.91	28.31	28.76	29.10	28.48	28.51	28.52	28.89	28.72	54.99	55.78
Na_2O	0.00	0.04	0.00	0.06	0.00	0.00	0.00	0.00	0.00	0.00	0.00	0.00
K_2O	0.00	0.00	0.00	0.00	0.00	0.00	0.00	0.00	0.00	0.00	0.00	0.00
P_2O_5	0.00	0.00	0.00	0.00	0.00	0.00	0.00	0.00	0.00	0.00	0.00	0.00
F	0.00	0.00	0.00	0.00	0.00	0.00	0.00	0.00	0.00	0.00	0.00	0.00
Cl	0.00	0.00	0.00	0.00	0.00	0.00	0.00	0.00	0.00	0.00	0.00	0.00
SO_3	0.00	0.00	0.00	0.00	0.00	0.00	0.00	0.00	0.00	0.00	0.00	0.00
SrO	0.00	0.00	0.17	0.16	0.00	0.17	0.13	0.14	0.00	0.16	0.00	0.00
Y_2O_3	0.00	0.00	0.00	0.00	0.00	0.00	0.00	0.00	0.00	0.00	0.00	0.00
BaO	0.00	0.00	0.00	0.00	0.00	0.00	0.00	0.00	0.00	0.00	0.00	0.00
La_2O_3	0.00	0.00	0.00	0.00	0.00	0.00	0.00	0.00	0.00	0.00	0.00	0.00
Ce_2O_3	0.00	0.00	0.00	0.00	0.00	0.00	0.00	0.00	0.00	0.00	0.00	0.00
Nd_2O_3	0.00	0.00	0.00	0.00	0.00	0.00	0.00	0.00	0.00	0.00	0.00	0.00
ThO_2	0.00	0.00	0.00	0.00	0.00	0.00	0.00	0.00	0.00	0.00	0.00	0.00
CO_2	45.57	45.91	44.85	45.35	46.46	45.40	45.10	45.71	45.64	45.53	43.45	44.01
Total	**99.02**	**100.05**	**99.61**	**100.68**	**100.09**	**100.41**	**100.25**	**99.31**	**99.31**	**100.94**	**98.87**	**100.06**
O=F,Cl	-	-	-	-	-	-	-	-	-	-	-	-
Ox	6.00	6.00	6.00	6.00	6.00	6.00	6.00	6.00	6.00	6.00	6.00	6.00
F	0.00	0.00	0.00	0.00	0.00	0.00	0.00	0.00	0.00	0.00	0.00	0.00
Al	0.00	0.00	0.00	0.00	0.00	0.00	0.00	0.00	0.00	0.00	0.00	0.00
Ba	0.00	0.00	0.00	0.00	0.00	0.00	0.00	0.00	0.00	0.00	0.00	0.00
C	2.00	2.00	2.00	2.00	2.00	2.00	2.00	2.00	2.00	2.00	2.00	2.00
Ca	0.98	0.99	0.99	1.00	0.98	0.98	0.99	0.98	0.99	0.99	1.99	1.99
Ce	0.00	0.00	0.00	0.00	0.00	0.00	0.00	0.00	0.00	0.00	0.00	0.00
Cl	0.00	0.00	0.00	0.00	0.00	0.00	0.00	0.00	0.00	0.00	0.00	0.00
Fe	0.22	0.24	0.34	0.33	0.17	0.31	0.35	0.22	0.22	0.33	0.01	0.00
K	0.00	0.00	0.00	0.00	0.00	0.00	0.00	0.00	0.00	0.00	0.00	0.00
La	0.00	0.00	0.00	0.00	0.00	0.00	0.00	0.00	0.00	0.00	0.00	0.00
Mg	0.79	0.77	0.66	0.66	0.84	0.69	0.65	0.79	0.78	0.67	0.00	0.01
Mn	0.00	0.00	0.01	0.01	0.00	0.01	0.01	0.00	0.00	0.01	0.00	0.00
Na	0.00	0.00	0.00	0.00	0.00	0.00	0.00	0.00	0.00	0.00	0.00	0.00
Nd	0.00	0.00	0.00	0.00	0.00	0.00	0.00	0.00	0.00	0.00	0.00	0.00
P	0.00	0.00	0.00	0.00	0.00	0.00	0.00	0.00	0.00	0.00	0.00	0.00
S	0.00	0.00	0.00	0.00	0.00	0.00	0.00	0.00	0.00	0.00	0.00	0.00
Si	0.00	0.00	0.00	0.00	0.00	0.00	0.00	0.00	0.00	0.00	0.00	0.00
Sr	0.00	0.00	0.00	0.00	0.00	0.00	0.00	0.00	0.00	0.00	0.00	0.00
Th	0.00	0.00	0.00	0.00	0.00	0.00	0.00	0.00	0.00	0.00	0.00	0.00
Ti	0.00	0.00	0.00	0.00	0.00	0.00	0.00	0.00	0.00	0.00	0.00	0.00
Y	0.00	0.00	0.00	0.00	0.00	0.00	0.00	0.00	0.00	0.00	0.00	0.00

Appendix 6 Chemical composition analysis of Minerals from Lofdal samples

Sample	44_AS9393_BSE5a	45_AS9393_BSE5b	46_AS9393_BSE5b	47_AS9393_BSE6a	48_AS9393_BSE6a	49_AS9393_BSE7b	50_AS9393_BSE7b	51_AS9393_BSE7b	52_AS9393_BSE7b	53_AS9393_BSE7a	54_AS9393_BSE7a	32_AS9102_BSE6a
Mineral	Dolomite-Ankerite											Celestine
SiO_2	0.00	0.00	0.00	0.00	0.00	0.00	0.00	0.00	0.00	0.00	0.00	0.00
TiO_2	0.00	0.00	0.00	0.00	0.00	0.00	0.00	0.00	0.00	0.00	0.00	0.00
$Al2O_3$	0.00	0.00	0.00	0.00	0.00	0.00	0.00	0.00	0.00	0.00	0.00	0.00
FeO	0.00	0.19	0.20	0.00	0.00	13.92	14.21	13.17	6.35	5.37	4.18	0.00
MnO	0.12	0.36	0.42	0.10	0.13	0.42	0.45	0.46	0.20	0.11	0.00	0.00
MgO	0.07	19.27	20.30	0.13	0.10	12.56	12.34	13.05	17.83	18.52	19.09	0.00
CaO	56.70	32.44	32.11	55.96	56.13	28.64	28.09	28.00	29.27	29.33	29.45	0.30
Na_2O	0.00	0.05	0.00	0.00	0.00	0.00	0.00	0.00	0.00	0.04	0.00	0.00
K_2O	0.00	0.00	0.00	0.00	0.00	0.00	0.00	0.00	0.00	0.00	0.00	0.00
P_2O_5	0.00	0.00	0.00	0.00	0.00	0.00	0.00	0.00	0.00	0.00	0.00	0.00
F	0.00	0.00	0.00	0.00	0.00	0.00	0.00	0.00	0.00	0.00	0.00	0.00
Cl	0.00	0.00	0.00	0.00	0.00	0.00	0.00	0.00	0.00	0.00	0.00	0.00
SO_3	0.00	0.00	0.00	0.00	0.00	0.00	0.00	0.00	0.00	0.00	0.00	42.10
SrO	0.00	0.00	0.00	0.00	0.00	0.12	0.13	0.14	0.00	0.00	0.00	57.83
Y_2O_3	0.00	0.00	0.00	0.00	0.00	0.00	0.00	0.00	0.00	0.00	0.00	0.00
BaO	0.00	0.00	0.00	0.00	0.00	0.00	0.00	0.00	0.00	0.00	0.00	0.23
La_2O_3	0.00	0.00	0.00	0.00	0.00	0.00	0.00	0.00	0.00	0.00	0.00	0.17
Ce_2O_3	0.00	0.00	0.00	0.00	0.00	0.00	0.00	0.00	0.00	0.00	0.00	0.57
Nd_2O_3	0.00	0.00	0.00	0.00	0.00	0.00	0.00	0.00	0.00	0.00	0.00	0.00
ThO_2	0.00	0.00	0.00	0.00	0.00	0.00	0.00	0.00	0.00	0.00	0.00	0.00
CO_2	44.64	46.87	47.74	44.12	44.23	45.02	44.56	44.64	46.45	46.62	46.52	-
Total	**101.53**	**99.18**	**100.76**	**100.30**	**100.59**	**100.69**	**99.78**	**99.47**	**100.10**	**99.99**	**99.24**	**101.21**
O=F,Cl	-	-	-	-	-	-	-	-	-	-	-	-
Ox	6.00	6.00	6.00	6.00	6.00	6.00	6.00	6.00	6.00	6.00	6.00	4.00
F	0.00	0.00	0.00	0.00	0.00	0.00	0.00	0.00	0.00	0.00	0.00	0.00
Al	0.00	0.00	0.00	0.00	0.00	0.00	0.00	0.00	0.00	0.00	0.00	0.00
Ba	0.00	0.00	0.00	0.00	0.00	0.00	0.00	0.00	0.00	0.00	0.00	0.00
C	2.00	2.00	2.00	2.00	2.00	2.00	2.00	2.00	2.00	2.00	2.00	0.00
Ca	1.99	1.09	1.06	1.99	1.99	1.00	0.99	0.98	0.99	0.99	0.99	0.01
Ce	0.00	0.00	0.00	0.00	0.00	0.00	0.00	0.00	0.00	0.00	0.00	0.00
Cl	0.00	0.00	0.00	0.00	0.00	0.00	0.00	0.00	0.00	0.00	0.00	0.00
Fe	0.00	0.00	0.01	0.00	0.00	0.38	0.39	0.36	0.17	0.14	0.11	0.00
K	0.00	0.00	0.00	0.00	0.00	0.00	0.00	0.00	0.00	0.00	0.00	0.00
La	0.00	0.00	0.00	0.00	0.00	0.00	0.00	0.00	0.00	0.00	0.00	0.00
Mg	0.00	0.90	0.93	0.01	0.00	0.61	0.60	0.64	0.84	0.87	0.90	0.00
Mn	0.00	0.01	0.01	0.00	0.00	0.01	0.01	0.01	0.01	0.00	0.00	0.00
Na	0.00	0.00	0.00	0.00	0.00	0.00	0.00	0.00	0.00	0.00	0.00	0.00
Nd	0.00	0.00	0.00	0.00	0.00	0.00	0.00	0.00	0.00	0.00	0.00	0.00
P	0.00	0.00	0.00	0.00	0.00	0.00	0.00	0.00	0.00	0.00	0.00	0.00
S	0.00	0.00	0.00	0.00	0.00	0.00	0.00	0.00	0.00	0.00	0.00	1.10
Si	0.00	0.00	0.00	0.00	0.00	0.00	0.00	0.00	0.00	0.00	0.00	0.00
Sr	0.00	0.00	0.00	0.00	0.00	0.00	0.00	0.00	0.00	0.00	0.00	0.70
Th	0.00	0.00	0.00	0.00	0.00	0.00	0.00	0.00	0.00	0.00	0.00	0.00
Ti	0.00	0.00	0.00	0.00	0.00	0.00	0.00	0.00	0.00	0.00	0.00	0.00
Y	0.00	0.00	0.00	0.00	0.00	0.00	0.00	0.00	0.00	0.00	0.00	0.00

Appendix 6 Chemical composition analysis of Minerals from Lofdal samples

Sample	2_AS9398_BSE1c	3_AS9398_BSE1c	4_AS9398_BSE1c	5_AS9398_BSE1b	6_AS9398_BSE1c	7_AS9398_BSE1b	18_AS9398_BSE2b	34_AS9398_BSE2b	35_AS9398_BSE3c	36_AS9398_BSE3c	37_AS9398_BSE3c	38_AS9398_BSE3c
Mineral	Synchisite?											
SiO_2	0.32	0.19	0.07	0.43	0.09	0.74	0.41	0.41	0.00	0.12	1.65	0.00
TiO_2	0.00	0.00	0.00	0.00	0.00	0.00	0.00	0.00	0.00	0.08	0.00	0.00
$Al2O_3$	0.00	0.00	0.00	0.00	0.00	0.00	0.00	0.00	0.00	0.08	0.08	0.00
FeO	0.00	0.00	0.00	0.00	0.00	0.00	0.00	0.65	0.00	2.43	0.00	0.00
MnO	0.00	0.00	0.00	0.00	0.00	0.40	0.00	0.00	0.00	0.00	0.00	0.00
MgO	0.00	0.00	0.00	0.00	0.00	0.00	0.00	0.00	0.00	0.00	0.00	0.00
CaO	15.68	11.77	17.48	9.55	17.69	9.96	16.38	15.28	17.09	8.71	6.25	10.66
Na_2O	0.00	0.00	0.00	0.00	0.00	0.00	0.10	0.00	0.00	0.00	0.00	0.00
K_2O	0.00	0.00	0.00	0.00	0.00	0.00	0.00	0.00	0.00	0.00	0.00	0.00
P_2O_5	0.00	0.00	0.00	0.00	0.00	0.00	0.00	0.00	0.00	0.00	0.24	0.00
F	5.73	5.02	5.14	5.39	5.19	5.17	5.04	5.52	3.92	5.84	4.17	5.50
Cl	0.00	0.00	0.00	0.00	0.00	0.00	0.07	0.00	0.00	0.00	0.00	0.00
SO_3	0.00	0.00	0.00	0.00	0.00	0.00	0.00	0.00	0.19	0.00	0.00	0.00
SrO	0.21	0.26	0.00	0.25	0.00	0.32	0.27	0.42	0.00	1.06	0.00	0.00
Y_2O_3	1.49	1.40	1.47	1.27	1.73	1.24	1.21	1.34	1.03	1.04	0.94	1.03
BaO	0.00	0.00	0.00	0.23	0.00	0.00	0.20	0.00	0.00	0.00	0.00	0.00
La_2O_3	10.15	14.14	10.97	16.04	10.75	14.78	12.29	12.33	13.00	15.12	17.68	16.08
Ce_2O_3	19.02	25.29	18.98	24.30	18.50	28.44	21.54	21.37	24.09	26.88	34.36	28.77
Nd_2O_3	7.50	8.11	7.45	8.07	7.73	7.52	6.66	6.87	8.28	7.94	8.17	8.50
ThO_2	1.39	1.01	0.00	1.05	0.00	1.23	2.88	2.25	0.94	2.31	1.51	0.00
CO_2	28.91	29.87	29.68	28.81	29.85	30.79	31.62	31.00	33.04	30.60	33.04	30.40
Total	**90.40**	**97.07**	**91.23**	**95.37**	**91.53**	**100.59**	**98.67**	**97.45**	**101.56**	**102.23**	**108.09**	**100.94**
O=F,Cl	87.99	94.96	89.07	93.10	89.34	98.41	96.55	95.13	99.91	99.77	106.34	98.63
Ox	7.00	7.00	7.00	7.00	7.00	7.00	7.00	6.00	6.00	6.00	6.00	6.00
F	0.93	0.80	0.83	0.88	0.83	0.80	0.77	0.72	0.50	0.77	0.53	0.74
Al	0.00	0.00	0.00	0.00	0.00	0.00	0.00	0.00	0.00	0.00	0.00	0.00
Ba	0.00	0.00	0.00	0.00	0.00	0.00	0.00	0.00	0.00	0.00	0.00	0.00
C	2.02	2.07	2.06	2.04	2.06	2.07	2.08	1.76	1.83	1.74	1.82	1.76
Ca	0.86	0.64	0.95	0.53	0.96	0.52	0.84	0.68	0.74	0.39	0.27	0.48
Ce	0.36	0.47	0.35	0.46	0.34	0.51	0.38	0.32	0.36	0.41	0.51	0.45
Cl	0.00	0.00	0.00	0.00	0.00	0.00	0.01	0.00	0.00	0.00	0.00	0.00
Fe	0.00	0.00	0.00	0.00	0.00	0.00	0.00	0.02	0.00	0.08	0.00	0.00
K	0.00	0.00	0.00	0.00	0.00	0.00	0.00	0.00	0.00	0.00	0.00	0.00
La	0.19	0.26	0.21	0.31	0.20	0.27	0.22	0.19	0.19	0.23	0.26	0.25
Mg	0.00	0.00	0.00	0.00	0.00	0.00	0.00	0.00	0.00	0.00	0.00	0.00
Mn	0.00	0.00	0.00	0.00	0.00	0.02	0.00	0.00	0.00	0.00	0.00	0.00
Na	0.00	0.00	0.00	0.00	0.00	0.00	0.01	0.00	0.00	0.00	0.00	0.00
Nd	0.14	0.15	0.14	0.15	0.14	0.13	0.11	0.10	0.12	0.12	0.12	0.13
P	0.00	0.00	0.00	0.00	0.00	0.00	0.00	0.00	0.00	0.00	0.01	0.00
S	0.00	0.00	0.00	0.00	0.00	0.00	0.00	0.00	0.01	0.00	0.00	0.00
Si	0.02	0.01	0.00	0.02	0.00	0.04	0.02	0.02	0.00	0.01	0.07	0.00
Sr	0.01	0.01	0.00	0.01	0.00	0.01	0.01	0.01	0.00	0.03	0.00	0.00
Th	0.02	0.01	0.00	0.01	0.00	0.01	0.03	0.02	0.01	0.02	0.01	0.00
Ti	0.00	0.00	0.00	0.00	0.00	0.00	0.00	0.00	0.00	0.00	0.00	0.00
Y	0.04	0.04	0.04	0.03	0.05	0.03	0.03	0.03	0.02	0.02	0.02	0.02

Appendix 6 Chemical composition analysis of Minerals from Lofdal samples

Sample	39_AS9398_BSE3c	47_AS9398_BSE3i	52_AS9398_BSE5b	53_AS9398_BSE5b	55_AS9398_BSE6b	57_AS9398_BSE6b	58_AS9398_BSE7b	59_AS9398_BSE7b	60_AS9398_BSE8b	23_AS9396_BSE4b	20_AS9396_BSE4a	21_AS9396_BSE4a
Mineral	Synchisite?									Barite	Quartz	
SiO_2	0.00	0.00	0.18	0.36	0.23	0.17	0.30	0.23	0.39	0.00	100.30	100.76
TiO_2	0.00	0.00	0.00	0.00	0.00	0.00	0.00	0.00	0.00	0.31	0.00	0.00
$Al2O_3$	0.00	0.00	0.00	0.00	0.12	0.00	0.00	0.00	0.00	0.00	0.11	0.17
FeO	0.00	0.00	0.00	0.00	1.95	0.00	0.00	0.00	0.00	0.00	0.00	0.00
MnO	0.00	0.00	0.00	0.00	0.00	0.00	0.00	0.00	0.00	0.00	0.00	0.00
MgO	0.00	0.00	0.00	0.00	0.00	0.00	0.00	0.00	0.00	0.00	0.00	0.00
CaO	16.17	17.58	10.24	15.65	6.04	16.80	11.74	17.26	11.22	0.38	0.00	0.00
Na_2O	0.00	0.00	0.00	0.00	0.00	0.00	0.00	0.00	0.00	0.10	0.04	0.00
K_2O	0.00	0.00	0.00	0.00	0.00	0.00	0.00	0.00	0.00	0.00	0.00	0.03
P_2O_5	0.00	0.00	0.00	0.00	0.00	0.00	0.00	0.00	0.00	0.00	0.00	0.00
F	4.60	4.62	5.12	4.13	5.79	4.13	4.83	4.65	4.78	0.00	0.00	0.00
Cl	0.00	0.00	0.00	0.00	0.00	0.00	0.00	0.00	0.00	0.00	0.00	0.00
SO_3	0.00	0.00	0.12	0.00	0.10	0.00	0.15	0.09	0.00	34.19	0.00	0.00
SrO	0.00	0.00	0.71	0.27	1.10	0.21	0.40	0.30	0.19	2.25	0.00	0.00
Y_2O_3	1.15	1.39	0.80	2.29	0.63	1.43	0.91	1.63	1.28	0.00	0.00	0.00
BaO	0.00	0.00	0.00	0.00	0.00	0.00	0.00	0.00	0.00	63.68	0.00	0.00
La_2O_3	12.91	10.97	20.77	11.49	18.71	13.57	18.57	10.64	15.44	0.00	0.00	0.00
Ce_2O_3	25.05	21.26	28.18	21.04	32.30	23.04	30.08	19.26	26.32	4.53	0.00	0.00
Nd_2O_3	7.71	7.57	6.01	7.24	5.99	6.61	6.69	7.94	8.45	0.00	0.00	0.00
ThO_2	0.00	0.00	1.31	0.91	2.83	0.00	2.19	1.76	0.70	0.00	0.00	0.00
CO_2	31.70	30.58	31.95	30.52	31.39	31.71	33.74	30.96	30.60	-	-	-
Total	**99.29**	**93.97**	**105.39**	**93.89**	**107.18**	**97.67**	**109.59**	**94.71**	**99.37**	**105.44**	**100.45**	**100.96**
O=F,Cl	97.35	92.03	103.24	92.15	104.74	95.93	107.56	92.76	97.36	-	-	-
Ox	6.00	6.00	6.00	6.00	6.00	6.00	6.00	6.00	6.00	3.00	2.00	2.00
F	0.60	0.63	0.66	0.57	0.75	0.55	0.60	0.62	0.65	0.00	0.00	0.00
Al	0.00	0.00	0.00	0.00	0.01	0.00	0.00	0.00	0.00	0.00	0.00	0.00
Ba	0.00	0.00	0.00	0.00	0.00	0.00	0.00	0.00	0.00	0.47	0.00	0.00
C	1.80	1.79	1.78	1.81	1.75	1.82	1.80	1.79	1.78	0.00	0.00	0.00
Ca	0.72	0.81	0.45	0.73	0.26	0.76	0.49	0.78	0.51	0.01	0.00	0.00
Ce	0.38	0.33	0.42	0.33	0.48	0.35	0.43	0.30	0.41	0.03	0.00	0.00
Cl	0.00	0.00	0.00	0.00	0.00	0.00	0.00	0.00	0.00	0.00	0.00	0.00
Fe	0.00	0.00	0.00	0.00	0.07	0.00	0.00	0.00	0.00	0.00	0.00	0.00
K	0.00	0.00	0.00	0.00	0.00	0.00	0.00	0.00	0.00	0.00	0.00	0.00
La	0.20	0.17	0.31	0.18	0.28	0.21	0.27	0.17	0.24	0.00	0.00	0.00
Mg	0.00	0.00	0.00	0.00	0.00	0.00	0.00	0.00	0.00	0.00	0.00	0.00
Mn	0.00	0.00	0.00	0.00	0.00	0.00	0.00	0.00	0.00	0.00	0.00	0.00
Na	0.00	0.00	0.00	0.00	0.00	0.00	0.00	0.00	0.00	0.00	0.00	0.00
Nd	0.11	0.12	0.09	0.11	0.09	0.10	0.09	0.12	0.13	0.00	0.00	0.00
P	0.00	0.00	0.00	0.00	0.00	0.00	0.00	0.00	0.00	0.00	0.00	0.00
S	0.00	0.00	0.01	0.00	0.01	0.00	0.01	0.00	0.00	0.81	0.00	0.00
Si	0.00	0.00	0.01	0.02	0.01	0.01	0.01	0.01	0.02	0.00	1.00	1.00
Sr	0.00	0.00	0.02	0.01	0.03	0.01	0.01	0.01	0.00	0.02	0.00	0.00
Th	0.00	0.00	0.01	0.01	0.03	0.00	0.02	0.02	0.01	0.00	0.00	0.00
Ti	0.00	0.00	0.00	0.00	0.00	0.00	0.00	0.00	0.00	0.00	0.00	0.00
Y	0.03	0.03	0.02	0.05	0.01	0.03	0.02	0.04	0.03	0.00	0.00	0.00

Appendix 6 Chemical composition analysis of Minerals from Lofdal samples

Sample	51_AS9398_BSE5d	8_AS9398_BSE1a	13_AS9398_BSE1a	14_AS9398_BSE2a	19_AS9398_BSE3a	20_AS9398_BSE3k	21_AS9398_BSE3k	22_AS9398_BSE3m	23_AS9398_BSE3k	25_AS9398_BSE5a	26_AS9398_BSE5a	29_AS9398_BSE7a
Mineral	Apatite	Calcite										
SiO_2	0.00	0.06	0.00	0.00	0.00	0.00	0.00	0.00	0.00	0.00	0.00	0.07
TiO_2	0.00	0.00	0.00	0.00	0.00	0.00	0.00	0.00	0.00	0.00	0.00	0.00
$Al2O_3$	0.00	0.00	0.00	0.00	0.00	0.00	0.00	0.00	0.00	0.00	0.00	0.00
FeO	0.00	0.17	0.00	1.34	0.00	0.00	1.32	0.00	1.22	0.00	1.25	0.46
MnO	0.00	0.00	0.24	0.24	0.00	0.14	0.22	0.00	0.28	0.00	0.26	0.09
MgO	0.00	0.21	0.24	0.16	0.10	0.15	0.18	0.00	0.17	0.24	0.20	0.19
CaO	49.04	55.22	54.91	52.46	55.70	55.51	53.99	56.36	53.68	55.23	52.45	53.88
Na_2O	1.61	0.00	0.00	0.00	0.00	0.00	0.00	0.00	0.00	0.00	0.00	0.00
K_2O	0.00	0.00	0.00	0.00	0.00	0.00	0.00	0.00	0.00	0.00	0.00	0.00
P_2O_5	39.85	0.00	0.00	0.00	0.00	0.00	0.00	0.00	0.00	0.00	0.00	0.00
F	3.89	0.00	0.00	0.00	0.00	0.00	0.00	0.00	0.00	0.00	0.00	0.00
Cl	0.00	0.00	0.00	0.00	0.00	0.00	0.00	0.00	0.00	0.00	0.00	0.00
SO_3	0.00	0.00	0.00	0.00	0.00	0.00	0.00	0.00	0.00	0.00	0.00	0.00
SrO	0.47	0.16	0.00	0.30	0.00	0.23	0.26	0.00	0.42	0.00	0.46	0.33
Y_2O_3	3.28	0.00	0.00	0.00	0.00	0.00	0.00	0.00	0.00	0.00	0.00	0.00
BaO	0.00	0.00	0.00	0.00	0.00	0.00	0.00	0.00	0.00	0.00	0.00	0.00
La_2O_3	0.18	0.00	0.00	0.00	0.00	0.00	0.00	0.00	0.00	0.00	0.00	0.00
Ce_2O_3	0.56	0.00	0.00	0.00	0.00	0.00	0.00	0.00	0.00	0.00	0.00	0.00
Nd_2O_3	0.45	0.00	0.00	0.00	0.00	0.00	0.00	0.00	0.00	0.00	0.00	0.00
ThO_2	0.00	0.00	0.00	0.00	0.00	0.00	0.00	0.00	0.00	0.00	0.00	0.00
CO_2	-	43.82	43.51	42.44	43.82	43.91	43.62	44.23	43.41	43.61	42.50	43.08
Total	**99.31**	**99.63**	**98.91**	**96.95**	**99.62**	**99.95**	**99.58**	**100.59**	**99.19**	**99.08**	**97.12**	**98.10**
O=F,Cl	97.68	-	-	-	-	-	-	-	-	-	-	
Ox	26.00	3.00	3.00	3.00	3.00	3.00	3.00	3.00	3.00	3.00	3.00	3.00
F	2.07	0.00	0.00	0.00	0.00	0.00	0.00	0.00	0.00	0.00	0.00	0.00
Al	0.00	0.00	0.00	0.00	0.00	0.00	0.00	0.00	0.00	0.00	0.00	0.00
Ba	0.00	0.00	0.00	0.00	0.00	0.00	0.00	0.00	0.00	0.00	0.00	0.00
C	-	1.00	1.00	1.00	1.00	1.00	1.00	1.00	1.00	1.00	1.00	1.00
Ca	8.85	0.99	0.99	0.97	1.00	0.99	0.97	1.00	0.97	0.99	0.97	0.98
Ce	0.03	0.00	0.00	0.00	0.00	0.00	0.00	0.00	0.00	0.00	0.00	0.00
Cl	0.00	0.00	0.00	0.00	0.00	0.00	0.00	0.00	0.00	0.00	0.00	0.00
Fe	0.00	0.00	0.00	0.02	0.00	0.00	0.02	0.00	0.02	0.00	0.02	0.01
K	0.00	0.00	0.00	0.00	0.00	0.00	0.00	0.00	0.00	0.00	0.00	0.00
La	0.01	0.00	0.00	0.00	0.00	0.00	0.00	0.00	0.00	0.00	0.00	0.00
Mg	0.00	0.01	0.01	0.00	0.00	0.00	0.00	0.00	0.00	0.01	0.01	0.00
Mn	0.00	0.00	0.00	0.00	0.00	0.00	0.00	0.00	0.00	0.00	0.00	0.00
Na	0.52	0.00	0.00	0.00	0.00	0.00	0.00	0.00	0.00	0.00	0.00	0.00
Nd	0.03	0.00	0.00	0.00	0.00	0.00	0.00	0.00	0.00	0.00	0.00	0.00
P	5.69	0.00	0.00	0.00	0.00	0.00	0.00	0.00	0.00	0.00	0.00	0.00
S	0.00	0.00	0.00	0.00	0.00	0.00	0.00	0.00	0.00	0.00	0.00	0.00
Si	0.00	0.00	0.00	0.00	0.00	0.00	0.00	0.00	0.00	0.00	0.00	0.00
Sr	0.05	0.00	0.00	0.00	0.00	0.00	0.00	0.00	0.00	0.00	0.00	0.00
Th	0.00	0.00	0.00	0.00	0.00	0.00	0.00	0.00	0.00	0.00	0.00	0.00
Ti	0.00	0.00	0.00	0.00	0.00	0.00	0.00	0.00	0.00	0.00	0.00	0.00
Y	0.29	0.00	0.00	0.00	0.00	0.00	0.00	0.00	0.00	0.00	0.00	0.00

Appendix 6 Chemical composition analysis of Minerals from Lofdal samples

Sample	30_AS9398_BSE7a	31_AS9398_BSE8a	32_AS9398_BSE8a	33_AS9398_BSE8a	54_AS9398_BSE5a	3_AS9102_BSE1a	4_AS9102_BSE1a	5_AS9102_BSE1a	6_AS9102_BSE1a	7_AS9102_BSE1e	8_AS9102_BSE1e	9_AS9102_BSE1e
Mineral	Calcite											
SiO_2	0.05	0.00	0.00	0.00	0.00	0.00	0.00	0.00	0.00	0.00	0.00	0.00
TiO_2	0.00	0.00	0.00	0.00	0.00	0.00	0.00	0.00	0.00	0.00	0.00	0.00
Al2O_3	0.00	0.00	0.00	0.00	0.00	0.00	0.00	0.00	0.00	0.00	0.00	0.00
FeO	0.00	1.22	0.00	0.00	1.32	0.91	0.94	1.15	0.93	0.97	0.00	0.94
MnO	0.00	0.33	0.00	0.00	0.32	1.06	1.07	1.09	1.08	0.97	0.00	1.09
MgO	0.10	0.16	0.24	0.08	0.17	0.07	0.09	0.10	0.10	0.10	0.07	0.11
CaO	55.35	52.38	55.41	55.62	52.55	52.83	52.00	51.66	52.67	52.66	55.45	52.72
Na_2O	0.00	0.00	0.00	0.00	0.07	0.00	0.00	0.00	0.00	0.00	0.00	0.00
K_2O	0.00	0.00	0.00	0.00	0.04	0.00	0.00	0.00	0.00	0.00	0.00	0.00
P_2O_5	0.00	0.00	0.00	0.00	0.00	0.00	0.00	0.00	0.00	0.00	0.10	0.00
F	0.00	0.00	0.00	0.00	0.00	0.00	0.00	0.00	0.00	0.00	0.00	0.00
Cl	0.00	0.00	0.00	0.00	0.00	0.00	0.00	0.00	0.00	0.00	0.00	0.00
SO_3	0.00	0.00	0.00	0.00	0.00	0.00	0.00	0.00	0.00	0.00	0.00	0.00
SrO	0.21	0.33	0.00	0.00	0.41	0.69	1.43	1.38	1.20	1.39	0.14	0.85
Y_2O_3	0.00	0.00	0.00	0.00	0.00	0.00	0.00	0.00	0.00	0.00	0.00	0.00
BaO	0.00	0.00	0.00	0.00	0.00	0.00	0.00	0.00	0.00	0.00	0.00	0.00
La_2O_3	0.00	0.00	0.00	0.00	0.00	0.00	0.00	0.00	0.00	0.00	0.00	0.00
Ce_2O_3	0.00	0.00	0.00	0.00	0.00	0.00	0.00	0.00	0.00	0.00	0.00	0.00
Nd_2O_3	0.00	0.00	0.00	0.00	0.00	0.00	0.00	0.00	0.00	0.00	0.00	0.00
ThO_2	0.00	0.00	0.00	0.00	0.00	0.00	0.00	0.00	0.00	0.00	0.00	0.00
CO_2	43.71	42.38	43.75	43.73	42.67	43.05	42.75	42.61	43.19	43.22	43.81	43.11
Total	**99.43**	**96.80**	**99.39**	**99.42**	**97.53**	**98.61**	**98.27**	**97.97**	**99.16**	**99.30**	**99.57**	**98.83**
O=F,Cl	-	-	-	-	-	-	-	-	-	-	-	-
Ox	3.00	3.00	3.00	3.00	3.00	3.00	3.00	3.00	3.00	3.00	3.00	3.00
F	0.00	0.00	0.00	0.00	0.00	0.00	0.00	0.00	0.00	0.00	0.00	0.00
Al	0.00	0.00	0.00	0.00	0.00	0.00	0.00	0.00	0.00	0.00	0.00	0.00
Ba	0.00	0.00	0.00	0.00	0.00	0.00	0.00	0.00	0.00	0.00	0.00	0.00
C	1.00	1.00	1.00	1.00	1.00	1.00	1.00	1.00	1.00	1.00	1.00	1.00
Ca	0.99	0.97	0.99	1.00	0.97	0.96	0.95	0.95	0.96	0.96	0.99	0.96
Ce	0.00	0.00	0.00	0.00	0.00	0.00	0.00	0.00	0.00	0.00	0.00	0.00
Cl	0.00	0.00	0.00	0.00	0.00	0.00	0.00	0.00	0.00	0.00	0.00	0.00
Fe	0.00	0.02	0.00	0.00	0.02	0.01	0.01	0.02	0.01	0.01	0.00	0.01
K	0.00	0.00	0.00	0.00	0.00	0.00	0.00	0.00	0.00	0.00	0.00	0.00
La	0.00	0.00	0.00	0.00	0.00	0.00	0.00	0.00	0.00	0.00	0.00	0.00
Mg	0.00	0.00	0.01	0.00	0.00	0.00	0.00	0.00	0.00	0.00	0.00	0.00
Mn	0.00	0.00	0.00	0.00	0.00	0.02	0.02	0.02	0.02	0.01	0.00	0.02
Na	0.00	0.00	0.00	0.00	0.00	0.00	0.00	0.00	0.00	0.00	0.00	0.00
Nd	0.00	0.00	0.00	0.00	0.00	0.00	0.00	0.00	0.00	0.00	0.00	0.00
P	0.00	0.00	0.00	0.00	0.00	0.00	0.00	0.00	0.00	0.00	0.00	0.00
S	0.00	0.00	0.00	0.00	0.00	0.00	0.00	0.00	0.00	0.00	0.00	0.00
Si	0.00	0.00	0.00	0.00	0.00	0.00	0.00	0.00	0.00	0.00	0.00	0.00
Sr	0.00	0.00	0.00	0.00	0.00	0.01	0.01	0.01	0.01	0.01	0.00	0.01
Th	0.00	0.00	0.00	0.00	0.00	0.00	0.00	0.00	0.00	0.00	0.00	0.00
Ti	0.00	0.00	0.00	0.00	0.00	0.00	0.00	0.00	0.00	0.00	0.00	0.00
Y	0.00	0.00	0.00	0.00	0.00	0.00	0.00	0.00	0.00	0.00	0.00	0.00

Appendix 6 Chemical composition analysis of Minerals from Lofdal samples

Sample	10_AS9102_BSE1e	12_AS9102_BSE5a	13_AS9102_BSE7b	14_AS9102_BSE7b	15_AS9102_BSE7b	16_AS9102_BSE7b	17_AS9102_BSE7b	18_AS9102_BSE7b	22_AS9102_BSE2b	25_AS9102_BSE4a	26_AS9102_BSE4a	27_AS9102_BSE6a
Mineral	Calcite											
SiO_2	0.00	0.00	0.00	0.00	0.00	0.00	0.00	0.00	0.00	0.00	0.00	0.00
TiO_2	0.00	0.00	0.00	0.00	0.00	0.00	0.00	0.00	0.00	0.00	0.00	0.00
$Al2O_3$	0.00	0.00	0.00	0.00	0.00	0.00	0.00	0.00	0.00	0.00	0.00	0.00
FeO	0.76	1.14	1.23	1.00	1.00	1.08	1.12	1.10	0.99	1.10	1.04	1.19
MnO	0.99	0.96	1.13	1.10	1.12	1.06	1.09	0.95	1.07	1.12	1.07	1.09
MgO	0.09	0.10	0.11	0.11	0.08	0.10	0.08	0.10	0.10	0.13	0.14	0.11
CaO	52.48	51.50	51.46	50.92	51.43	51.40	51.28	52.65	52.07	51.49	51.90	51.66
Na_2O	0.00	0.00	0.00	0.00	0.00	0.00	0.00	0.00	0.00	0.00	0.00	0.00
K_2O	0.00	0.00	0.00	0.00	0.00	0.00	0.00	0.00	0.00	0.00	0.00	0.00
P_2O_5	0.00	0.00	0.00	0.00	0.00	0.00	0.00	0.00	0.00	0.00	0.00	0.00
F	0.00	0.00	0.00	0.00	0.00	0.00	0.00	0.00	0.00	0.00	0.00	0.00
Cl	0.00	0.05	0.00	0.00	0.00	0.00	0.00	0.00	0.00	0.00	0.00	0.00
SO_3	0.00	0.00	0.00	0.00	0.00	0.00	0.00	0.00	0.00	0.00	0.00	0.00
SrO	0.90	2.20	1.88	2.01	2.01	2.01	1.79	1.64	1.87	2.07	2.15	1.50
Y_2O_3	0.00	0.00	0.00	0.00	0.00	0.00	0.00	0.00	0.00	0.00	0.00	0.00
BaO	0.00	0.00	0.00	0.00	0.00	0.00	0.00	0.00	0.00	0.00	0.00	0.00
La_2O_3	0.00	0.00	0.00	0.00	0.00	0.00	0.00	0.00	0.00	0.00	0.00	0.00
Ce_2O_3	0.00	0.00	0.00	0.00	0.00	0.00	0.00	0.00	0.00	0.19	0.00	0.00
Nd_2O_3	0.00	0.00	0.00	0.00	0.00	0.00	0.00	0.00	0.00	0.00	0.00	0.00
ThO_2	0.00	0.00	0.00	0.00	0.00	0.00	0.00	0.00	0.00	0.00	0.00	0.00
CO_2	42.75	42.75	42.75	42.23	42.61	42.62	42.46	43.38	43.04	42.88	43.10	42.70
Total	**97.98**	**98.70**	**98.55**	**97.37**	**98.24**	**98.26**	**97.82**	**99.81**	**99.15**	**98.99**	**99.41**	**98.25**
O=F,Cl	-	-	-	-	-	-	-	-	-	-	-	-
Ox	3.00	3.00	3.00	3.00	3.00	3.00	3.00	3.00	3.00	3.00	3.00	3.00
F	0.00	0.00	0.00	0.00	0.00	0.00	0.00	0.00	0.00	0.00	0.00	0.00
Al	0.00	0.00	0.00	0.00	0.00	0.00	0.00	0.00	0.00	0.00	0.00	0.00
Ba	0.00	0.00	0.00	0.00	0.00	0.00	0.00	0.00	0.00	0.00	0.00	0.00
C	1.00	1.00	1.00	1.00	1.00	1.00	1.00	1.00	1.00	1.00	1.00	1.00
Ca	0.96	0.94	0.94	0.95	0.95	0.95	0.95	0.95	0.95	0.94	0.94	0.95
Ce	0.00	0.00	0.00	0.00	0.00	0.00	0.00	0.00	0.00	0.00	0.00	0.00
Cl	0.00	0.00	0.00	0.00	0.00	0.00	0.00	0.00	0.00	0.00	0.00	0.00
Fe	0.01	0.02	0.02	0.01	0.01	0.02	0.02	0.02	0.01	0.02	0.01	0.02
K	0.00	0.00	0.00	0.00	0.00	0.00	0.00	0.00	0.00	0.00	0.00	0.00
La	0.00	0.00	0.00	0.00	0.00	0.00	0.00	0.00	0.00	0.00	0.00	0.00
Mg	0.00	0.00	0.00	0.00	0.00	0.00	0.00	0.00	0.00	0.00	0.00	0.00
Mn	0.01	0.01	0.02	0.02	0.02	0.02	0.02	0.01	0.02	0.02	0.02	0.02
Na	0.00	0.00	0.00	0.00	0.00	0.00	0.00	0.00	0.00	0.00	0.00	0.00
Nd	0.00	0.00	0.00	0.00	0.00	0.00	0.00	0.00	0.00	0.00	0.00	0.00
P	0.00	0.00	0.00	0.00	0.00	0.00	0.00	0.00	0.00	0.00	0.00	0.00
S	0.00	0.00	0.00	0.00	0.00	0.00	0.00	0.00	0.00	0.00	0.00	0.00
Si	0.00	0.00	0.00	0.00	0.00	0.00	0.00	0.00	0.00	0.00	0.00	0.00
Sr	0.01	0.02	0.02	0.02	0.02	0.02	0.02	0.02	0.02	0.02	0.02	0.01
Th	0.00	0.00	0.00	0.00	0.00	0.00	0.00	0.00	0.00	0.00	0.00	0.00
Ti	0.00	0.00	0.00	0.00	0.00	0.00	0.00	0.00	0.00	0.00	0.00	0.00
Y	0.00	0.00	0.00	0.00	0.00	0.00	0.00	0.00	0.00	0.00	0.00	0.00

Appendix 6 Chemical composition analysis of Minerals from Lofdal samples

Sample	28_AS9102_BSE7a	29_AS9102_BSE8a	30_AS9102_BSE9a	31_AS9102_BSE9a	36_AS9102_BSE10a	37_AS9102_BSE10a	38_AS9102_BSE11a	39_AS9102_BSE12a	40_AS9102_BSE13a	41_AS9102_BSE13a	5_AS9396_BSE3b	6_AS9396_BSE1a
Mineral	Calcite											
SiO_2	0.00	0.00	0.00	0.00	0.00	0.00	0.00	0.00	0.00	0.00	0.00	0.00
TiO_2	0.00	0.00	0.00	0.00	0.00	0.00	0.00	0.00	0.00	0.00	0.00	0.00
$Al2O_3$	0.00	0.00	0.00	0.00	0.00	0.00	0.00	0.00	0.00	0.00	0.00	0.00
FeO	1.15	1.01	1.13	1.05	0.00	1.17	0.88	0.44	0.00	1.09	0.18	0.97
MnO	1.03	1.10	0.97	1.11	0.08	1.03	1.02	0.37	0.00	1.17	0.00	0.26
MgO	0.08	0.08	0.12	0.12	0.06	0.10	0.12	0.11	0.05	0.09	0.27	0.21
CaO	52.29	51.97	51.89	51.29	56.15	51.57	51.91	55.46	55.71	51.47	55.79	53.09
Na_2O	0.00	0.00	0.00	0.00	0.00	0.00	0.00	0.00	0.00	0.00	0.00	0.00
K_2O	0.00	0.00	0.00	0.00	0.00	0.00	0.00	0.00	0.00	0.00	0.00	0.00
P_2O_5	0.00	0.00	0.00	0.00	0.00	0.00	0.00	0.00	0.00	0.00	0.00	0.00
F	0.00	0.00	0.00	0.00	0.00	0.00	0.00	0.00	0.00	0.00	0.00	0.00
Cl	0.00	0.00	0.00	0.00	0.00	0.00	0.00	0.00	0.00	0.00	0.00	0.00
SO_3	0.00	0.00	0.00	0.00	0.00	0.00	0.00	0.00	0.00	0.00	0.00	0.00
SrO	1.78	1.90	1.59	1.85	0.19	2.12	1.82	0.37	0.26	1.63	0.00	0.54
Y_2O_3	0.00	0.00	0.00	0.00	0.00	0.00	0.00	0.00	0.00	0.00	0.00	0.00
BaO	0.00	0.00	0.00	0.00	0.00	0.00	0.00	0.00	0.00	0.00	0.00	0.00
La_2O_3	0.00	0.00	0.00	0.00	0.00	0.00	0.00	0.00	0.00	0.00	0.00	0.00
Ce_2O_3	0.00	0.00	0.00	0.00	0.00	0.00	0.00	0.00	0.00	0.00	0.00	0.00
Nd_2O_3	0.00	0.00	0.00	0.00	0.00	0.00	0.00	0.00	0.00	0.00	0.00	0.00
ThO_2	0.00	0.00	0.00	0.00	0.00	0.00	0.00	0.00	0.00	0.00	0.00	0.00
CO_2	43.23	42.97	42.82	42.50	44.27	42.84	42.81	44.31	43.88	42.59	44.19	42.88
Total	**99.56**	**99.03**	**98.52**	**97.92**	**100.75**	**98.83**	**98.55**	**101.06**	**99.90**	**98.04**	**100.43**	**97.96**
O=F,Cl	-	-	-	-	-	-	-	-	-	-	-	-
Ox	3.00	3.00	3.00	3.00	3.00	3.00	3.00	3.00	3.00	3.00	3.00	3.00
F	0.00	0.00	0.00	0.00	0.00	0.00	0.00	0.00	0.00	0.00	0.00	0.00
Al	0.00	0.00	0.00	0.00	0.00	0.00	0.00	0.00	0.00	0.00	0.00	0.00
Ba	0.00	0.00	0.00	0.00	0.00	0.00	0.00	0.00	0.00	0.00	0.00	0.00
C	1.00	1.00	1.00	1.00	1.00	1.00	1.00	1.00	1.00	1.00	1.00	1.00
Ca	0.95	0.95	0.95	0.95	1.00	0.94	0.95	0.98	1.00	0.95	0.99	0.97
Ce	0.00	0.00	0.00	0.00	0.00	0.00	0.00	0.00	0.00	0.00	0.00	0.00
Cl	0.00	0.00	0.00	0.00	0.00	0.00	0.00	0.00	0.00	0.00	0.00	0.00
Fe	0.02	0.01	0.02	0.02	0.00	0.02	0.01	0.01	0.00	0.02	0.00	0.01
K	0.00	0.00	0.00	0.00	0.00	0.00	0.00	0.00	0.00	0.00	0.00	0.00
La	0.00	0.00	0.00	0.00	0.00	0.00	0.00	0.00	0.00	0.00	0.00	0.00
Mg	0.00	0.00	0.00	0.00	0.00	0.00	0.00	0.00	0.00	0.00	0.01	0.01
Mn	0.01	0.02	0.01	0.02	0.00	0.01	0.01	0.01	0.00	0.02	0.00	0.00
Na	0.00	0.00	0.00	0.00	0.00	0.00	0.00	0.00	0.00	0.00	0.00	0.00
Nd	0.00	0.00	0.00	0.00	0.00	0.00	0.00	0.00	0.00	0.00	0.00	0.00
P	0.00	0.00	0.00	0.00	0.00	0.00	0.00	0.00	0.00	0.00	0.00	0.00
S	0.00	0.00	0.00	0.00	0.00	0.00	0.00	0.00	0.00	0.00	0.00	0.00
Si	0.00	0.00	0.00	0.00	0.00	0.00	0.00	0.00	0.00	0.00	0.00	0.00
Sr	0.02	0.02	0.02	0.02	0.00	0.02	0.02	0.00	0.00	0.02	0.00	0.01
Th	0.00	0.00	0.00	0.00	0.00	0.00	0.00	0.00	0.00	0.00	0.00	0.00
Ti	0.00	0.00	0.00	0.00	0.00	0.00	0.00	0.00	0.00	0.00	0.00	0.00
Y	0.00	0.00	0.00	0.00	0.00	0.00	0.00	0.00	0.00	0.00	0.00	0.00

Appendix 6 Chemical composition analysis of Minerals from Lofdal samples

Sample	7_AS9396_BSE1a	12_AS9396_BSE2e	13_AS9396_BSE2e	16_AS9396_BSE3b	17_AS9396_BSE3a	19_AS9396_BSE3b	22_AS9396_BSE4b	25_AS9396_BSE5b	24_AS9396_BSE5b	8_AS9396_BSE1a	14_AS9396_BSE2e	18_AS9396_BSE3b
Mineral	Calcite									Calcite-(Fe)		
SiO_2	0.00	0.32	0.00	0.00	0.00	0.00	0.29	0.00	0.00	0.50	0.55	0.34
TiO_2	0.00	0.00	0.00	0.00	0.00	0.00	0.00	0.00	0.00	0.00	0.00	0.00
$Al2O_3$	0.00	0.23	0.00	0.00	0.00	0.00	0.00	0.00	0.00	0.00	0.00	0.00
FeO	0.84	0.26	0.00	0.24	0.43	0.24	0.33	0.55	0.25	19.90	19.33	19.72
MnO	0.29	0.54	0.00	1.23	1.01	0.83	0.00	0.66	0.00	0.43	1.05	0.54
MgO	0.13	0.05	0.14	0.08	0.23	0.16	0.55	0.21	0.06	0.58	0.54	0.50
CaO	53.29	54.47	56.34	53.37	53.77	53.97	55.47	54.19	55.92	41.75	40.49	41.72
Na_2O	0.00	0.00	0.00	0.00	0.00	0.00	0.00	0.00	0.00	0.00	0.00	0.00
K_2O	0.00	0.15	0.00	0.00	0.00	0.00	0.00	0.00	0.00	0.00	0.00	0.00
P_2O_5	0.00	0.00	0.00	0.00	0.00	0.00	0.00	0.00	0.00	0.00	0.00	0.00
F	0.00	0.00	0.00	0.00	0.00	0.00	0.00	0.00	0.00	0.00	0.00	0.00
Cl	0.00	0.00	0.00	0.00	0.00	0.00	0.00	0.00	0.00	0.00	0.00	0.00
SO_3	0.00	0.00	0.00	0.11	0.15	0.18	0.00	0.21	0.00	0.09	0.00	0.12
SrO	0.53	0.00	0.00	0.00	0.00	0.00	0.00	0.00	0.00	0.12	0.00	0.00
Y_2O_3	0.00	0.00	0.00	0.00	0.00	0.00	0.00	0.00	0.00	0.00	0.00	0.00
BaO	0.00	0.00	0.00	0.00	0.00	0.00	0.00	0.00	0.00	0.00	0.00	0.00
La_2O_3	0.00	0.00	0.00	0.00	0.00	0.00	0.00	0.00	0.00	0.00	0.00	0.00
Ce_2O_3	0.00	0.00	0.00	0.00	0.00	0.00	0.00	0.00	0.00	0.00	0.00	0.00
Nd_2O_3	0.00	0.00	0.00	0.00	0.00	0.00	0.00	0.00	0.00	0.00	0.00	0.00
ThO_2	0.00	0.00	0.00	0.00	0.00	0.00	0.00	0.00	0.00	0.00	0.00	0.00
CO_2	42.88	44.11	44.37	43.19	43.73	43.69	44.77	44.10	44.11	46.89	45.66	46.52
Total	**97.95**	**100.11**	**100.86**	**98.22**	**99.32**	**99.08**	**101.41**	**99.92**	**100.34**	**110.26**	**107.62**	**109.46**
O=F,Cl	-	-	-	-	-	-	-	-	-	-	-	-
Ox	3.00	3.00	3.00	3.00	3.00	3.00	3.00	3.00	3.00	3.00	3.00	3.00
F	0.00	0.00	0.00	0.00	0.00	0.00	0.00	0.00	0.00	0.00	0.00	0.00
Al	0.00	0.00	0.00	0.00	0.00	0.00	0.00	0.00	0.00	0.00	0.00	0.00
Ba	0.00	0.00	0.00	0.00	0.00	0.00	0.00	0.00	0.00	0.00	0.00	0.00
C	1.00	1.00	1.00	1.00	1.00	1.00	1.00	1.00	1.00	1.00	1.00	1.00
Ca	0.98	0.97	1.00	0.97	0.96	0.97	0.97	0.96	0.99	0.70	0.70	0.70
Ce	0.00	0.00	0.00	0.00	0.00	0.00	0.00	0.00	0.00	0.00	0.00	0.00
Cl	0.00	0.00	0.00	0.00	0.00	0.00	0.00	0.00	0.00	0.00	0.00	0.00
Fe	0.01	0.00	0.00	0.00	0.01	0.00	0.00	0.01	0.00	0.26	0.26	0.26
K	0.00	0.00	0.00	0.00	0.00	0.00	0.00	0.00	0.00	0.00	0.00	0.00
La	0.00	0.00	0.00	0.00	0.00	0.00	0.00	0.00	0.00	0.00	0.00	0.00
Mg	0.00	0.00	0.00	0.00	0.01	0.00	0.01	0.01	0.00	0.01	0.01	0.01
Mn	0.00	0.01	0.00	0.02	0.01	0.01	0.00	0.01	0.00	0.01	0.01	0.01
Na	0.00	0.00	0.00	0.00	0.00	0.00	0.00	0.00	0.00	0.00	0.00	0.00
Nd	0.00	0.00	0.00	0.00	0.00	0.00	0.00	0.00	0.00	0.00	0.00	0.00
P	0.00	0.00	0.00	0.00	0.00	0.00	0.00	0.00	0.00	0.00	0.00	0.00
S	0.00	0.00	0.00	0.00	0.00	0.00	0.00	0.00	0.00	0.00	0.00	0.00
Si	0.00	0.01	0.00	0.00	0.00	0.00	0.00	0.00	0.00	0.01	0.01	0.01
Sr	0.01	0.00	0.00	0.00	0.00	0.00	0.00	0.00	0.00	0.00	0.00	0.00
Th	0.00	0.00	0.00	0.00	0.00	0.00	0.00	0.00	0.00	0.00	0.00	0.00
Ti	0.00	0.00	0.00	0.00	0.00	0.00	0.00	0.00	0.00	0.00	0.00	0.00
Y	0.00	0.00	0.00	0.00	0.00	0.00	0.00	0.00	0.00	0.00	0.00	0.00

Appendix 6 Chemical composition analysis of Minerals from Lofdal samples

Sample	26_AS9396_BSE5a	10_AS9398_BSE1d	42_AS9398_BSE3e	43_AS9398_BSE3e	46_AS9398_BSE3i	49_AS9398_BSE3e	9_AS9398_BSE1d	40_AS9398_BSE3d	56_AS9398_BSE6b	41_AS9398_BSE3e	48_AS9398_BSE3i	1_AS9102_BSE1b
Mineral	Cal-(Fe)	Thorianite					Xenotime			Monazite		
SiO_2	0.37	12.38	13.01	13.26	14.96	14.15	1.00	0.54	0.89	0.23	0.24	0.21
TiO_2	0.00	0.00	0.09	0.00	0.00	0.00	0.00	0.00	0.00	0.00	0.00	0.00
$Al2O_3$	0.00	0.00	0.25	0.21	0.54	0.32	0.00	0.00	0.00	0.00	0.00	0.00
FeO	19.80	2.51	1.99	1.95	0.47	0.29	0.00	0.26	0.00	0.00	0.00	0.00
MnO	0.76	0.00	0.00	0.00	0.00	0.00	0.00	0.00	0.00	0.00	0.00	0.00
MgO	0.68	0.00	0.00	0.00	0.00	0.00	0.00	0.00	0.00	0.00	0.00	0.00
CaO	41.77	2.73	2.47	2.39	1.75	1.82	0.23	0.22	0.18	0.47	0.46	0.00
Na_2O	0.00	0.00	0.00	0.00	0.00	0.00	0.06	0.00	0.00	0.00	0.00	0.00
K_2O	0.00	0.00	0.00	0.00	0.00	0.00	0.00	0.00	0.00	0.00	0.00	0.00
P_2O_5	0.00	5.13	5.60	4.95	2.66	2.68	29.31	28.55	27.84	30.20	29.50	29.67
F	0.00	0.35	0.70	0.72	0.35	0.40	0.00	0.00	0.00	0.49	0.32	0.40
Cl	0.00	0.00	0.00	0.00	0.00	0.00	0.00	0.00	0.00	0.00	0.00	0.00
SO_3	0.15	0.00	0.00	0.00	0.00	0.00	0.00	0.00	0.00	0.00	0.00	0.00
SrO	0.00	0.00	0.00	0.00	0.00	0.00	0.00	0.00	0.00	0.17	0.00	0.00
Y_2O_3	0.00	4.92	6.27	5.23	3.08	2.55	38.67	35.85	34.45	0.31	0.00	0.00
BaO	0.00	0.00	0.00	0.00	0.00	0.00	0.00	0.00	0.00	0.20	0.00	0.00
La_2O_3	0.00	0.00	0.00	0.00	0.44	0.36	0.00	0.00	0.00	17.99	15.84	16.81
Ce_2O_3	0.00	0.50	0.51	0.36	0.22	0.43	0.00	0.00	0.00	35.45	34.99	41.41
Nd_2O_3	0.00	0.39	0.28	0.00	0.64	0.56	0.00	0.00	0.00	8.11	9.10	10.48
ThO_2	0.00	72.60	66.71	69.84	77.37	79.24	1.86	1.55	0.72	2.22	1.62	1.92
CO_2	47.08	-	-	-	-	-	-	-	-	-	-	-
Total	**110.62**	**101.51**	**97.88**	**98.90**	**102.47**	**102.81**	**71.13**	**66.98**	**64.08**	**95.84**	**92.06**	**100.91**
O=F,Cl	-	-	-	98.60	102.33	102.64	-	-	-	95.64	91.93	100.74
Ox	3.00	4.00	4.00	4.00	4.00	4.00	4.00	4.00	4.00	4.00	4.00	4.00
F	0.00	0.06	0.11	0.11	0.06	0.07	0.00	0.00	0.00	0.06	0.04	0.05
Al	0.00	0.00	0.01	0.01	0.03	0.02	0.00	0.00	0.00	0.00	0.00	0.00
Ba	0.00	0.00	0.00	0.00	0.00	0.00	0.00	0.00	0.00	0.00	0.00	0.00
C	1.00	0.00	0.00	0.00	0.00	0.00	0.00	0.00	0.00	0.00	0.00	0.00
Ca	0.70	0.15	0.13	0.13	0.10	0.10	0.01	0.01	0.01	0.02	0.02	0.00
Ce	0.00	0.01	0.01	0.01	0.00	0.01	0.00	0.00	0.00	0.51	0.52	0.59
Cl	0.00	0.00	0.00	0.00	0.00	0.00	0.00	0.00	0.00	0.00	0.00	0.00
Fe	0.26	0.11	0.08	0.08	0.02	0.01	0.00	0.01	0.00	0.00	0.00	0.00
K	0.00	0.00	0.00	0.00	0.00	0.00	0.00	0.00	0.00	0.00	0.00	0.00
La	0.00	0.00	0.00	0.00	0.01	0.01	0.00	0.00	0.00	0.26	0.24	0.24
Mg	0.02	0.00	0.00	0.00	0.00	0.00	0.00	0.00	0.00	0.00	0.00	0.00
Mn	0.01	0.00	0.00	0.00	0.00	0.00	0.00	0.00	0.00	0.00	0.00	0.00
Na	0.00	0.00	0.00	0.00	0.00	0.00	0.00	0.00	0.00	0.00	0.00	0.00
Nd	0.00	0.01	0.00	0.00	0.01	0.01	0.00	0.00	0.00	0.11	0.13	0.15
P	0.00	0.22	0.23	0.21	0.12	0.12	1.03	1.06	1.06	1.01	1.02	0.98
S	0.00	0.00	0.00	0.00	0.00	0.00	0.00	0.00	0.00	0.00	0.00	0.00
Si	0.01	0.62	0.64	0.66	0.76	0.74	0.04	0.02	0.04	0.01	0.01	0.01
Sr	0.00	0.00	0.00	0.00	0.00	0.00	0.00	0.00	0.00	0.00	0.00	0.00
Th	0.00	0.83	0.75	0.79	0.90	0.94	0.02	0.02	0.01	0.02	0.02	0.02
Ti	0.00	0.00	0.00	0.00	0.00	0.00	0.00	0.00	0.00	0.00	0.00	0.00
Y	0.00	0.13	0.17	0.14	0.08	0.07	0.86	0.84	0.83	0.01	0.00	0.00

Appendix 6 Chemical composition analysis of Minerals from Lofdal samples

Sample	2_AS9102_BSE1b	20_AS9102_BSE1c	11_AS9102_BSE5a	19_AS9102_BSE5b	23_AS9102_BSE3a	1_AS9393_BSE1b	2_AS9393_BSE1b	3_AS9393_BSE1a	4_AS9393_BSE1b	5_AS9393_BSE1b	6_AS9393_BSE1b	7_AS9393_BSE1a
Mineral	Monazite		Calciobur	Strontianite		Dolomite-Ankerite						
SiO_2	0.13	0.10	0.00	0.00	0.00	0.00	0.00	0.00	0.05	0.00	0.00	0.00
TiO_2	0.00	0.00	0.00	0.00	0.00	0.00	0.00	0.00	0.00	0.00	0.00	0.00
$Al2O_3$	0.00	0.00	0.00	0.00	0.00	0.00	0.00	0.00	0.00	0.00	0.00	0.00
FeO	0.00	0.00	0.00	0.00	0.00	13.20	12.26	12.46	11.99	7.96	6.74	9.07
MnO	0.00	0.00	0.00	0.00	0.00	0.40	0.40	0.43	0.39	0.22	0.23	0.20
MgO	0.00	0.00	0.00	0.00	0.00	13.20	13.19	13.51	13.74	16.66	17.47	15.89
CaO	0.14	0.40	6.19	5.71	2.84	29.18	28.32	28.38	29.35	29.27	29.78	29.08
Na_2O	0.00	0.00	10.11	0.00	0.00	0.00	0.00	0.00	0.00	0.00	0.04	0.00
K_2O	0.00	0.00	0.00	0.00	0.00	0.00	0.00	0.00	0.00	0.00	0.00	0.00
P_2O_5	30.36	29.71	0.00	0.00	0.00	0.00	0.00	0.00	0.00	0.00	0.00	0.00
F	0.33	0.34	0.00	0.00	0.00	0.00	0.00	0.00	0.00	0.00	0.00	0.00
Cl	0.00	0.00	0.00	0.00	0.00	0.00	0.00	0.00	0.00	0.00	0.00	0.00
SO_3	0.08	0.00	0.00	0.00	0.00	0.00	0.00	0.00	0.00	0.00	0.00	0.00
SrO	0.00	0.00	29.45	66.12	74.37	0.14	0.23	0.00	0.21	0.00	0.00	0.00
Y_2O_3	0.00	0.00	0.00	0.00	0.00	0.00	0.00	0.00	0.00	0.00	0.00	0.00
BaO	0.00	0.00	1.58	0.94	0.00	0.00	0.00	0.00	0.00	0.00	0.00	0.00
La_2O_3	15.89	18.24	6.30	0.00	0.00	0.00	0.00	0.00	0.00	0.00	0.00	0.00
Ce_2O_3	40.64	40.96	12.63	0.00	0.00	0.00	0.00	0.00	0.00	0.00	0.00	0.00
Nd_2O_3	12.29	9.84	3.31	0.00	0.00	0.00	0.00	0.00	0.00	0.00	0.00	0.00
ThO_2	1.33	1.35	0.00	0.00	0.00	0.00	0.00	0.00	0.00	0.00	0.00	0.00
CO_2	-	-	33.93	32.83	33.81	45.70	44.48	44.92	45.79	46.18	46.75	45.86
Total	**101.19**	**100.94**	**103.49**	**105.60**	**111.02**	**101.82**	**98.87**	**99.71**	**101.52**	**100.29**	**101.02**	**100.11**
O=F,Cl	101.05	100.80	-	-	-	-	-	-	-	-	-	
Ox	4.00	4.00	15.00	3.00	3.00	6.00	6.00	6.00	6.00	6.00	6.00	6.00
F	0.04	0.04	0.00	0.00	0.00	0.00	0.00	0.00	0.00	0.00	0.00	0.00
Al	0.00	0.00	0.00	0.00	0.00	0.00	0.00	0.00	0.00	0.00	0.00	0.00
Ba	0.00	0.00	0.07	0.01	0.00	0.00	0.00	0.00	0.00	0.00	0.00	0.00
C	0.00	0.00	5.00	1.00	1.00	2.00	2.00	2.00	2.00	2.00	2.00	2.00
Ca	0.01	0.02	0.72	0.14	0.07	1.00	1.00	0.99	1.01	0.99	1.00	1.00
Ce	0.57	0.58	0.50	0.00	0.00	0.00	0.00	0.00	0.00	0.00	0.00	0.00
Cl	0.00	0.00	0.00	0.00	0.00	0.00	0.00	0.00	0.00	0.00	0.00	0.00
Fe	0.00	0.00	0.00	0.00	0.00	0.35	0.34	0.34	0.32	0.21	0.18	0.24
K	0.00	0.00	0.00	0.00	0.00	0.00	0.00	0.00	0.00	0.00	0.00	0.00
La	0.22	0.26	0.25	0.00	0.00	0.00	0.00	0.00	0.00	0.00	0.00	0.00
Mg	0.00	0.00	0.00	0.00	0.00	0.63	0.65	0.66	0.66	0.79	0.82	0.76
Mn	0.00	0.00	0.00	0.00	0.00	0.01	0.01	0.01	0.01	0.01	0.01	0.01
Na	0.00	0.00	2.12	0.00	0.00	0.00	0.00	0.00	0.00	0.00	0.00	0.00
Nd	0.17	0.14	0.13	0.00	0.00	0.00	0.00	0.00	0.00	0.00	0.00	0.00
P	0.99	0.98	0.00	0.00	0.00	0.00	0.00	0.00	0.00	0.00	0.00	0.00
S	0.00	0.00	0.00	0.00	0.00	0.00	0.00	0.00	0.00	0.00	0.00	0.00
Si	0.00	0.00	0.00	0.00	0.00	0.00	0.00	0.00	0.00	0.00	0.00	0.00
Sr	0.00	0.00	1.84	0.86	0.93	0.00	0.00	0.00	0.00	0.00	0.00	0.00
Th	0.01	0.01	0.00	0.00	0.00	0.00	0.00	0.00	0.00	0.00	0.00	0.00
Ti	0.00	0.00	0.00	0.00	0.00	0.00	0.00	0.00	0.00	0.00	0.00	0.00
Y	0.00	0.00	0.00	0.00	0.00	0.00	0.00	0.00	0.00	0.00	0.00	0.00

Appendix 6 Chemical composition analysis of Minerals from Lofdal samples

Sample	8_AS9393_BSE1c	9_AS9393_BSE1c	10_AS9393_BSE1c	11_AS9393_BSE1c	12_AS9393_BSE1c	13_AS9393_BSE1c	14_AS9393_BSE1c	15_AS9393_BSE1c	16_AS9393_BSE1d	17_AS9393_BSE1d	18_AS9393_BSE1d	19_AS9393_BSE1d
Mineral	Dolomite-Ankerite											
SiO_2	0.00	0.00	0.00	0.00	0.00	0.00	0.00	0.00	0.00	0.00	0.00	0.00
TiO_2	0.00	0.00	0.00	0.00	0.00	0.00	0.00	0.00	0.00	0.00	0.00	0.00
$Al2O_3$	0.00	0.00	0.00	0.00	0.00	0.00	0.00	0.00	0.00	0.00	0.00	0.00
FeO	8.86	5.56	6.14	10.23	8.56	9.31	7.06	8.13	14.08	4.83	4.94	19.57
MnO	0.29	0.14	0.12	0.29	0.24	0.31	0.19	0.18	0.45	0.15	0.15	0.71
MgO	15.88	17.99	17.88	14.67	15.85	15.59	17.24	16.42	12.51	18.39	18.65	8.36
CaO	29.01	29.36	29.20	29.20	29.51	28.94	29.62	29.13	28.55	29.61	29.41	27.69
Na_2O	0.00	0.00	0.00	0.00	0.00	0.00	0.00	0.00	0.00	0.00	0.00	0.06
K_2O	0.00	0.00	0.00	0.00	0.00	0.00	0.00	0.00	0.00	0.00	0.00	0.00
P_2O_5	0.00	0.00	0.00	0.00	0.00	0.00	0.00	0.00	0.00	0.00	0.00	0.00
F	0.00	0.00	0.00	0.00	0.00	0.00	0.00	0.00	0.00	0.00	0.00	0.00
Cl	0.00	0.00	0.00	0.00	0.00	0.00	0.00	0.00	0.00	0.00	0.00	0.00
SO_3	0.00	0.00	0.00	0.00	0.00	0.00	0.00	0.00	0.00	0.00	0.00	0.00
SrO	0.00	0.00	0.00	0.10	0.00	0.00	0.00	0.00	0.00	0.00	0.00	0.00
Y_2O_3	0.00	0.00	0.00	0.00	0.00	0.00	0.00	0.00	0.00	0.00	0.00	0.00
BaO	0.00	0.00	0.00	0.00	0.00	0.00	0.00	0.00	0.00	0.00	0.00	0.00
La_2O_3	0.00	0.00	0.00	0.00	0.00	0.00	0.00	0.00	0.00	0.00	0.00	0.00
Ce_2O_3	0.00	0.00	0.00	0.00	0.00	0.00	0.00	0.00	0.00	0.00	0.00	0.00
Nd_2O_3	0.00	0.00	0.00	0.00	0.00	0.00	0.00	0.00	0.00	0.00	0.00	0.00
ThO_2	0.00	0.00	0.00	0.00	0.00	0.00	0.00	0.00	0.00	0.00	0.00	0.00
CO_2	45.70	46.18	46.26	45.42	45.86	45.63	46.51	45.88	44.97	46.36	46.56	43.32
Total	**99.73**	**99.25**	**99.60**	**99.91**	**100.02**	**99.77**	**100.61**	**99.75**	**100.57**	**99.34**	**99.71**	**99.71**
O=F,Cl	-	-	-	-	-	-	-	-	-	-	-	-
Ox	6.00	6.00	6.00	6.00	6.00	6.00	6.00	6.00	6.00	6.00	6.00	6.00
F	0.00	0.00	0.00	0.00	0.00	0.00	0.00	0.00	0.00	0.00	0.00	0.00
Al	0.00	0.00	0.00	0.00	0.00	0.00	0.00	0.00	0.00	0.00	0.00	0.00
Ba	0.00	0.00	0.00	0.00	0.00	0.00	0.00	0.00	0.00	0.00	0.00	0.00
C	2.00	2.00	2.00	2.00	2.00	2.00	2.00	2.00	2.00	2.00	2.00	2.00
Ca	1.00	1.00	0.99	1.01	1.01	1.00	1.00	1.00	1.00	1.00	0.99	1.00
Ce	0.00	0.00	0.00	0.00	0.00	0.00	0.00	0.00	0.00	0.00	0.00	0.00
Cl	0.00	0.00	0.00	0.00	0.00	0.00	0.00	0.00	0.00	0.00	0.00	0.00
Fe	0.24	0.15	0.16	0.28	0.23	0.25	0.19	0.22	0.38	0.13	0.13	0.55
K	0.00	0.00	0.00	0.00	0.00	0.00	0.00	0.00	0.00	0.00	0.00	0.00
La	0.00	0.00	0.00	0.00	0.00	0.00	0.00	0.00	0.00	0.00	0.00	0.00
Mg	0.76	0.85	0.84	0.71	0.75	0.75	0.81	0.78	0.61	0.87	0.87	0.42
Mn	0.01	0.00	0.00	0.01	0.01	0.01	0.01	0.00	0.01	0.00	0.00	0.02
Na	0.00	0.00	0.00	0.00	0.00	0.00	0.00	0.00	0.00	0.00	0.00	0.00
Nd	0.00	0.00	0.00	0.00	0.00	0.00	0.00	0.00	0.00	0.00	0.00	0.00
P	0.00	0.00	0.00	0.00	0.00	0.00	0.00	0.00	0.00	0.00	0.00	0.00
S	0.00	0.00	0.00	0.00	0.00	0.00	0.00	0.00	0.00	0.00	0.00	0.00
Si	0.00	0.00	0.00	0.00	0.00	0.00	0.00	0.00	0.00	0.00	0.00	0.00
Sr	0.00	0.00	0.00	0.00	0.00	0.00	0.00	0.00	0.00	0.00	0.00	0.00
Th	0.00	0.00	0.00	0.00	0.00	0.00	0.00	0.00	0.00	0.00	0.00	0.00
Ti	0.00	0.00	0.00	0.00	0.00	0.00	0.00	0.00	0.00	0.00	0.00	0.00
Y	0.00	0.00	0.00	0.00	0.00	0.00	0.00	0.00	0.00	0.00	0.00	0.00

Appendix 6 Chemical composition analysis of Minerals from Lofdal samples

Sample	20_AS9393_BSE1d	21_AS9393_BSE3b	22_AS9393_BSE3b	23_AS9393_BSE3b	24_AS9393_BSE3b	25_AS9393_BSE3b	26_AS9393_BSE3b	27_AS9393_BSE4c	28_AS9393_BSE4c	29_AS9393_BSE4c	30_AS9393_BSE4c	31_AS9393_BSE4c
Mineral	Dolomite-Ankerite											
SiO_2	0.00	0.00	0.00	0.00	0.00	0.00	0.00	0.00	0.00	0.00	0.00	0.00
TiO_2	0.00	0.00	0.00	0.06	0.00	0.00	0.00	0.00	0.00	0.00	0.00	0.00
$Al2O_3$	0.00	0.00	0.00	0.00	0.00	0.00	0.00	0.00	0.00	0.00	0.00	0.00
FeO	12.25	12.48	12.19	4.90	7.51	11.14	10.93	12.58	8.88	10.07	9.65	9.80
MnO	0.38	0.39	0.43	0.00	0.17	0.45	0.44	0.41	0.17	0.15	0.16	0.16
MgO	13.62	13.63	13.27	19.03	17.14	13.89	14.31	13.59	16.24	15.61	15.88	15.79
CaO	28.59	29.04	28.23	29.40	29.33	29.07	28.46	28.54	28.63	28.21	28.70	28.62
Na_2O	0.00	0.00	0.00	0.00	0.00	0.00	0.00	0.00	0.00	0.00	0.00	0.00
K_2O	0.00	0.00	0.00	0.00	0.00	0.03	0.00	0.00	0.00	0.00	0.00	0.00
P_2O_5	0.00	0.00	0.00	0.00	0.00	0.00	0.00	0.00	0.00	0.00	0.00	0.00
F	0.00	0.00	0.00	0.00	0.00	0.00	0.00	0.00	0.00	0.00	0.00	0.00
Cl	0.00	0.00	0.00	0.00	0.00	0.00	0.00	0.00	0.00	0.00	0.00	0.00
SO_3	0.00	0.00	0.00	0.00	0.00	0.00	0.00	0.00	0.00	0.00	0.00	0.00
SrO	0.14	0.11	0.13	0.20	0.00	0.00	0.14	0.16	0.00	0.18	0.00	0.17
Y_2O_3	0.00	0.00	0.00	0.00	0.00	0.00	0.00	0.00	0.00	0.00	0.00	0.00
BaO	0.00	0.00	0.00	0.00	0.00	0.00	0.00	0.00	0.00	0.00	0.00	0.00
La_2O_3	0.00	0.00	0.00	0.00	0.00	0.00	0.00	0.00	0.00	0.00	0.00	0.00
Ce_2O_3	0.00	0.00	0.00	0.00	0.00	0.00	0.00	0.00	0.00	0.00	0.00	0.00
Nd_2O_3	0.00	0.00	0.00	0.00	0.00	0.00	0.00	0.00	0.00	0.00	0.00	0.00
ThO_2	0.00	0.00	0.00	0.00	0.00	0.00	0.00	0.00	0.00	0.00	0.00	0.00
CO_2	45.10	45.60	44.42	47.00	46.43	45.10	44.99	45.25	45.74	45.52	45.88	45.87
Total	100.08	101.25	98.66	100.59	100.58	99.68	99.28	100.52	99.65	99.75	100.27	100.41
O=F,Cl	-	-	-	-	-	-	-	-	-	-	-	-
Ox	6.00	6.00	6.00	6.00	6.00	6.00	6.00	6.00	6.00	6.00	6.00	6.00
F	0.00	0.00	0.00	0.00	0.00	0.00	0.00	0.00	0.00	0.00	0.00	0.00
Al	0.00	0.00	0.00	0.00	0.00	0.00	0.00	0.00	0.00	0.00	0.00	0.00
Ba	0.00	0.00	0.00	0.00	0.00	0.00	0.00	0.00	0.00	0.00	0.00	0.00
C	2.00	2.00	2.00	2.00	2.00	2.00	2.00	2.00	2.00	2.00	2.00	2.00
Ca	0.99	1.00	1.00	0.98	0.99	1.01	0.99	0.99	0.98	0.97	0.98	0.98
Ce	0.00	0.00	0.00	0.00	0.00	0.00	0.00	0.00	0.00	0.00	0.00	0.00
Cl	0.00	0.00	0.00	0.00	0.00	0.00	0.00	0.00	0.00	0.00	0.00	0.00
Fe	0.33	0.34	0.34	0.13	0.20	0.30	0.30	0.34	0.24	0.27	0.26	0.26
K	0.00	0.00	0.00	0.00	0.00	0.00	0.00	0.00	0.00	0.00	0.00	0.00
La	0.00	0.00	0.00	0.00	0.00	0.00	0.00	0.00	0.00	0.00	0.00	0.00
Mg	0.66	0.65	0.65	0.88	0.81	0.67	0.69	0.66	0.78	0.75	0.76	0.75
Mn	0.01	0.01	0.01	0.00	0.00	0.01	0.01	0.01	0.00	0.00	0.00	0.00
Na	0.00	0.00	0.00	0.00	0.00	0.00	0.00	0.00	0.00	0.00	0.00	0.00
Nd	0.00	0.00	0.00	0.00	0.00	0.00	0.00	0.00	0.00	0.00	0.00	0.00
P	0.00	0.00	0.00	0.00	0.00	0.00	0.00	0.00	0.00	0.00	0.00	0.00
S	0.00	0.00	0.00	0.00	0.00	0.00	0.00	0.00	0.00	0.00	0.00	0.00
Si	0.00	0.00	0.00	0.00	0.00	0.00	0.00	0.00	0.00	0.00	0.00	0.00
Sr	0.00	0.00	0.00	0.00	0.00	0.00	0.00	0.00	0.00	0.00	0.00	0.00
Th	0.00	0.00	0.00	0.00	0.00	0.00	0.00	0.00	0.00	0.00	0.00	0.00
Ti	0.00	0.00	0.00	0.00	0.00	0.00	0.00	0.00	0.00	0.00	0.00	0.00
Y	0.00	0.00	0.00	0.00	0.00	0.00	0.00	0.00	0.00	0.00	0.00	0.00

Appendix 6 Chemical composition analysis of Minerals from Lofdal samples

Sample	32_AS9393_BSE4c	33_AS9393_BSE4c	34_AS9393_BSE4c	35_AS9393_BSE4d	36_AS9393_BSE4d	37_AS9393_BSE4d	38_AS9393_BSE4d	39_AS9393_BSE4d	40_AS9393_BSE5a	41_AS9393_BSE5a	42_AS9393_BSE5b	43_AS9393_BSE5b
Mineral	Dolomite-Ankerite											
SiO_2	0.00	0.00	0.00	0.00	0.00	0.00	0.00	0.00	0.00	0.00	0.00	0.00
TiO_2	0.00	0.00	0.00	0.00	0.00	0.00	0.00	0.00	0.00	0.00	0.00	0.00
$Al2O_3$	0.00	0.00	0.00	0.00	0.00	0.00	0.00	0.09	0.00	0.00	0.00	0.00
FeO	8.23	8.85	12.46	12.35	6.51	11.67	12.71	8.16	8.36	12.24	0.28	0.00
MnO	0.17	0.15	0.35	0.39	0.11	0.43	0.39	0.16	0.18	0.36	0.10	0.10
MgO	16.51	16.20	13.48	13.62	17.92	14.26	13.41	16.54	16.24	13.93	0.06	0.16
CaO	28.54	28.91	28.31	28.76	29.10	28.48	28.51	28.52	28.89	28.72	54.99	55.78
Na_2O	0.00	0.04	0.00	0.06	0.00	0.00	0.00	0.00	0.00	0.00	0.00	0.00
K_2O	0.00	0.00	0.00	0.00	0.00	0.00	0.00	0.00	0.00	0.00	0.00	0.00
P_2O_5	0.00	0.00	0.00	0.00	0.00	0.00	0.00	0.00	0.00	0.00	0.00	0.00
F	0.00	0.00	0.00	0.00	0.00	0.00	0.00	0.00	0.00	0.00	0.00	0.00
Cl	0.00	0.00	0.00	0.00	0.00	0.00	0.00	0.00	0.00	0.00	0.00	0.00
SO_3	0.00	0.00	0.00	0.00	0.00	0.00	0.00	0.00	0.00	0.00	0.00	0.00
SrO	0.00	0.00	0.17	0.16	0.00	0.17	0.13	0.14	0.00	0.16	0.00	0.00
Y_2O_3	0.00	0.00	0.00	0.00	0.00	0.00	0.00	0.00	0.00	0.00	0.00	0.00
BaO	0.00	0.00	0.00	0.00	0.00	0.00	0.00	0.00	0.00	0.00	0.00	0.00
La_2O_3	0.00	0.00	0.00	0.00	0.00	0.00	0.00	0.00	0.00	0.00	0.00	0.00
Ce_2O_3	0.00	0.00	0.00	0.00	0.00	0.00	0.00	0.00	0.00	0.00	0.00	0.00
Nd_2O_3	0.00	0.00	0.00	0.00	0.00	0.00	0.00	0.00	0.00	0.00	0.00	0.00
ThO_2	0.00	0.00	0.00	0.00	0.00	0.00	0.00	0.00	0.00	0.00	0.00	0.00
CO_2	45.57	45.91	44.85	45.35	46.46	45.40	45.10	45.71	45.64	45.53	43.45	44.01
Total	99.02	100.05	99.61	100.68	100.09	100.41	100.25	99.31	99.31	100.94	98.87	100.06
O=F,Cl	-	-	-	-	-	-	-	-	-	-	-	-
Ox	6.00	6.00	6.00	6.00	6.00	6.00	6.00	6.00	6.00	6.00	6.00	6.00
F	0.00	0.00	0.00	0.00	0.00	0.00	0.00	0.00	0.00	0.00	0.00	0.00
Al	0.00	0.00	0.00	0.00	0.00	0.00	0.00	0.00	0.00	0.00	0.00	0.00
Ba	0.00	0.00	0.00	0.00	0.00	0.00	0.00	0.00	0.00	0.00	0.00	0.00
C	2.00	2.00	2.00	2.00	2.00	2.00	2.00	2.00	2.00	2.00	2.00	2.00
Ca	0.98	0.99	0.99	1.00	0.98	0.98	0.99	0.98	0.99	0.99	1.99	1.99
Ce	0.00	0.00	0.00	0.00	0.00	0.00	0.00	0.00	0.00	0.00	0.00	0.00
Cl	0.00	0.00	0.00	0.00	0.00	0.00	0.00	0.00	0.00	0.00	0.00	0.00
Fe	0.22	0.24	0.34	0.33	0.17	0.31	0.35	0.22	0.22	0.33	0.01	0.00
K	0.00	0.00	0.00	0.00	0.00	0.00	0.00	0.00	0.00	0.00	0.00	0.00
La	0.00	0.00	0.00	0.00	0.00	0.00	0.00	0.00	0.00	0.00	0.00	0.00
Mg	0.79	0.77	0.66	0.66	0.84	0.69	0.65	0.79	0.78	0.67	0.00	0.01
Mn	0.00	0.00	0.01	0.01	0.00	0.01	0.01	0.00	0.00	0.01	0.00	0.00
Na	0.00	0.00	0.00	0.00	0.00	0.00	0.00	0.00	0.00	0.00	0.00	0.00
Nd	0.00	0.00	0.00	0.00	0.00	0.00	0.00	0.00	0.00	0.00	0.00	0.00
P	0.00	0.00	0.00	0.00	0.00	0.00	0.00	0.00	0.00	0.00	0.00	0.00
S	0.00	0.00	0.00	0.00	0.00	0.00	0.00	0.00	0.00	0.00	0.00	0.00
Si	0.00	0.00	0.00	0.00	0.00	0.00	0.00	0.00	0.00	0.00	0.00	0.00
Sr	0.00	0.00	0.00	0.00	0.00	0.00	0.00	0.00	0.00	0.00	0.00	0.00
Th	0.00	0.00	0.00	0.00	0.00	0.00	0.00	0.00	0.00	0.00	0.00	0.00
Ti	0.00	0.00	0.00	0.00	0.00	0.00	0.00	0.00	0.00	0.00	0.00	0.00
Y	0.00	0.00	0.00	0.00	0.00	0.00	0.00	0.00	0.00	0.00	0.00	0.00

Appendix 6 Chemical composition analysis of Minerals from Lofdal samples

Sample	44_AS9393_BSE5a	45_AS9393_BSE5b	46_AS9393_BSE5b	47_AS9393_BSE6a	48_AS9393_BSE6a	49_AS9393_BSE7b	50_AS9393_BSE7b	51_AS9393_BSE7b	52_AS9393_BSE7b	53_AS9393_BSE7a	54_AS9393_BSE7a	32_AS9102_BSE6a
Mineral	Dolomite-Ankerite											Celestine
SiO_2	0.00	0.00	0.00	0.00	0.00	0.00	0.00	0.00	0.00	0.00	0.00	0.00
TiO_2	0.00	0.00	0.00	0.00	0.00	0.00	0.00	0.00	0.00	0.00	0.00	0.00
$Al2O_3$	0.00	0.00	0.00	0.00	0.00	0.00	0.00	0.00	0.00	0.00	0.00	0.00
FeO	0.00	0.19	0.20	0.00	0.00	13.92	14.21	13.17	6.35	5.37	4.18	0.00
MnO	0.12	0.36	0.42	0.10	0.13	0.42	0.45	0.46	0.20	0.11	0.00	0.00
MgO	0.07	19.27	20.30	0.13	0.10	12.56	12.34	13.05	17.83	18.52	19.09	0.00
CaO	56.70	32.44	32.11	55.96	56.13	28.64	28.09	28.00	29.27	29.33	29.45	0.30
Na_2O	0.00	0.05	0.00	0.00	0.00	0.00	0.00	0.00	0.00	0.04	0.00	0.00
K_2O	0.00	0.00	0.00	0.00	0.00	0.00	0.00	0.00	0.00	0.00	0.00	0.00
P_2O_5	0.00	0.00	0.00	0.00	0.00	0.00	0.00	0.00	0.00	0.00	0.00	0.00
F	0.00	0.00	0.00	0.00	0.00	0.00	0.00	0.00	0.00	0.00	0.00	0.00
Cl	0.00	0.00	0.00	0.00	0.00	0.00	0.00	0.00	0.00	0.00	0.00	0.00
SO_3	0.00	0.00	0.00	0.00	0.00	0.00	0.00	0.00	0.00	0.00	0.00	42.10
SrO	0.00	0.00	0.00	0.00	0.00	0.12	0.13	0.14	0.00	0.00	0.00	57.83
Y_2O_3	0.00	0.00	0.00	0.00	0.00	0.00	0.00	0.00	0.00	0.00	0.00	0.00
BaO	0.00	0.00	0.00	0.00	0.00	0.00	0.00	0.00	0.00	0.00	0.00	0.23
La_2O_3	0.00	0.00	0.00	0.00	0.00	0.00	0.00	0.00	0.00	0.00	0.00	0.17
Ce_2O_3	0.00	0.00	0.00	0.00	0.00	0.00	0.00	0.00	0.00	0.00	0.00	0.57
Nd_2O_3	0.00	0.00	0.00	0.00	0.00	0.00	0.00	0.00	0.00	0.00	0.00	0.00
ThO_2	0.00	0.00	0.00	0.00	0.00	0.00	0.00	0.00	0.00	0.00	0.00	0.00
CO_2	44.64	46.87	47.74	44.12	44.23	45.02	44.56	44.64	46.45	46.62	46.52	-
Total	**101.53**	**99.18**	**100.76**	**100.30**	**100.59**	**100.69**	**99.78**	**99.47**	**100.10**	**99.99**	**99.24**	**101.21**
O=F,Cl	-	-	-	-	-	-	-	-	-	-	-	-
Ox	6.00	6.00	6.00	6.00	6.00	6.00	6.00	6.00	6.00	6.00	6.00	4.00
F	0.00	0.00	0.00	0.00	0.00	0.00	0.00	0.00	0.00	0.00	0.00	0.00
Al	0.00	0.00	0.00	0.00	0.00	0.00	0.00	0.00	0.00	0.00	0.00	0.00
Ba	0.00	0.00	0.00	0.00	0.00	0.00	0.00	0.00	0.00	0.00	0.00	0.00
C	2.00	2.00	2.00	2.00	2.00	2.00	2.00	2.00	2.00	2.00	2.00	0.00
Ca	1.99	1.09	1.06	1.99	1.99	1.00	0.99	0.98	0.99	0.99	0.99	0.01
Ce	0.00	0.00	0.00	0.00	0.00	0.00	0.00	0.00	0.00	0.00	0.00	0.00
Cl	0.00	0.00	0.00	0.00	0.00	0.00	0.00	0.00	0.00	0.00	0.00	0.00
Fe	0.00	0.00	0.01	0.00	0.00	0.38	0.39	0.36	0.17	0.14	0.11	0.00
K	0.00	0.00	0.00	0.00	0.00	0.00	0.00	0.00	0.00	0.00	0.00	0.00
La	0.00	0.00	0.00	0.00	0.00	0.00	0.00	0.00	0.00	0.00	0.00	0.00
Mg	0.00	0.90	0.93	0.01	0.00	0.61	0.60	0.64	0.84	0.87	0.90	0.00
Mn	0.00	0.01	0.01	0.00	0.00	0.01	0.01	0.01	0.01	0.00	0.00	0.00
Na	0.00	0.00	0.00	0.00	0.00	0.00	0.00	0.00	0.00	0.00	0.00	0.00
Nd	0.00	0.00	0.00	0.00	0.00	0.00	0.00	0.00	0.00	0.00	0.00	0.00
P	0.00	0.00	0.00	0.00	0.00	0.00	0.00	0.00	0.00	0.00	0.00	0.00
S	0.00	0.00	0.00	0.00	0.00	0.00	0.00	0.00	0.00	0.00	0.00	1.10
Si	0.00	0.00	0.00	0.00	0.00	0.00	0.00	0.00	0.00	0.00	0.00	0.00
Sr	0.00	0.00	0.00	0.00	0.00	0.00	0.00	0.00	0.00	0.00	0.00	0.70
Th	0.00	0.00	0.00	0.00	0.00	0.00	0.00	0.00	0.00	0.00	0.00	0.00
Ti	0.00	0.00	0.00	0.00	0.00	0.00	0.00	0.00	0.00	0.00	0.00	0.00
Y	0.00	0.00	0.00	0.00	0.00	0.00	0.00	0.00	0.00	0.00	0.00	0.00

Appendix 6 Chemical composition analysis of Minerals from Lofdal samples

Sample	2_AS9398_BSE1c	3_AS9398_BSE1c	4_AS9398_BSE1c	5_AS9398_BSE1b	6_AS9398_BSE1c	7_AS9398_BSE1b	18_AS9398_BSE2b	34_AS9398_BSE2b	35_AS9398_BSE3c	36_AS9398_BSE3c	37_AS9398_BSE3c	38_AS9398_BSE3c
Mineral	Synchisite?											
SiO_2	0.32	0.19	0.07	0.43	0.09	0.74	0.41	0.41	0.00	0.12	1.65	0.00
TiO_2	0.00	0.00	0.00	0.00	0.00	0.00	0.00	0.00	0.00	0.08	0.00	0.00
$Al2O_3$	0.00	0.00	0.00	0.00	0.00	0.00	0.00	0.00	0.00	0.08	0.08	0.00
FeO	0.00	0.00	0.00	0.00	0.00	0.00	0.00	0.65	0.00	2.43	0.00	0.00
MnO	0.00	0.00	0.00	0.00	0.00	0.40	0.00	0.00	0.00	0.00	0.00	0.00
MgO	0.00	0.00	0.00	0.00	0.00	0.00	0.00	0.00	0.00	0.00	0.00	0.00
CaO	15.68	11.77	17.48	9.55	17.69	9.96	16.38	15.28	17.09	8.71	6.25	10.66
Na_2O	0.00	0.00	0.00	0.00	0.00	0.00	0.10	0.00	0.00	0.00	0.00	0.00
K_2O	0.00	0.00	0.00	0.00	0.00	0.00	0.00	0.00	0.00	0.00	0.00	0.00
P_2O_5	0.00	0.00	0.00	0.00	0.00	0.00	0.00	0.00	0.00	0.00	0.24	0.00
F	5.73	5.02	5.14	5.39	5.19	5.17	5.04	5.52	3.92	5.84	4.17	5.50
Cl	0.00	0.00	0.00	0.00	0.00	0.00	0.07	0.00	0.00	0.00	0.00	0.00
SO_3	0.00	0.00	0.00	0.00	0.00	0.00	0.00	0.00	0.19	0.00	0.00	0.00
SrO	0.21	0.26	0.00	0.25	0.00	0.32	0.27	0.42	0.00	1.06	0.00	0.00
Y_2O_3	1.49	1.40	1.47	1.27	1.73	1.24	1.21	1.34	1.03	1.04	0.94	1.03
BaO	0.00	0.00	0.00	0.23	0.00	0.00	0.20	0.00	0.00	0.00	0.00	0.00
La_2O_3	10.15	14.14	10.97	16.04	10.75	14.78	12.29	12.33	13.00	15.12	17.68	16.08
Ce_2O_3	19.02	25.29	18.98	24.30	18.50	28.44	21.54	21.37	24.09	26.88	34.36	28.77
Nd_2O_3	7.50	8.11	7.45	8.07	7.73	7.52	6.66	6.87	8.28	7.94	8.17	8.50
ThO_2	1.39	1.01	0.00	1.05	0.00	1.23	2.88	2.25	0.94	2.31	1.51	0.00
CO_2	28.91	29.87	29.68	28.81	29.85	30.79	31.62	31.00	33.04	30.60	33.04	30.40
Total	**90.40**	**97.07**	**91.23**	**95.37**	**91.53**	**100.59**	**98.67**	**97.45**	**101.56**	**102.23**	**108.09**	**100.94**
O=F,Cl	87.99	94.96	89.07	93.10	89.34	98.41	96.55	95.13	99.91	99.77	106.34	98.63
Ox	7.00	7.00	7.00	7.00	7.00	7.00	7.00	6.00	6.00	6.00	6.00	6.00
F	0.93	0.80	0.83	0.88	0.83	0.80	0.77	0.72	0.50	0.77	0.53	0.74
Al	0.00	0.00	0.00	0.00	0.00	0.00	0.00	0.00	0.00	0.00	0.00	0.00
Ba	0.00	0.00	0.00	0.00	0.00	0.00	0.00	0.00	0.00	0.00	0.00	0.00
C	2.02	2.07	2.06	2.04	2.06	2.07	2.08	1.76	1.83	1.74	1.82	1.76
Ca	0.86	0.64	0.95	0.53	0.96	0.52	0.84	0.68	0.74	0.39	0.27	0.48
Ce	0.36	0.47	0.35	0.46	0.34	0.51	0.38	0.32	0.36	0.41	0.51	0.45
Cl	0.00	0.00	0.00	0.00	0.00	0.00	0.01	0.00	0.00	0.00	0.00	0.00
Fe	0.00	0.00	0.00	0.00	0.00	0.00	0.00	0.02	0.00	0.08	0.00	0.00
K	0.00	0.00	0.00	0.00	0.00	0.00	0.00	0.00	0.00	0.00	0.00	0.00
La	0.19	0.26	0.21	0.31	0.20	0.27	0.22	0.19	0.19	0.23	0.26	0.25
Mg	0.00	0.00	0.00	0.00	0.00	0.00	0.00	0.00	0.00	0.00	0.00	0.00
Mn	0.00	0.00	0.00	0.00	0.00	0.02	0.00	0.00	0.00	0.00	0.00	0.00
Na	0.00	0.00	0.00	0.00	0.00	0.00	0.01	0.00	0.00	0.00	0.00	0.00
Nd	0.14	0.15	0.14	0.15	0.14	0.13	0.11	0.10	0.12	0.12	0.12	0.13
P	0.00	0.00	0.00	0.00	0.00	0.00	0.00	0.00	0.00	0.00	0.01	0.00
S	0.00	0.00	0.00	0.00	0.00	0.00	0.00	0.00	0.01	0.00	0.00	0.00
Si	0.02	0.01	0.00	0.02	0.00	0.04	0.02	0.02	0.00	0.01	0.07	0.00
Sr	0.01	0.01	0.00	0.01	0.00	0.01	0.01	0.01	0.00	0.03	0.00	0.00
Th	0.02	0.01	0.00	0.01	0.00	0.01	0.03	0.02	0.01	0.02	0.01	0.00
Ti	0.00	0.00	0.00	0.00	0.00	0.00	0.00	0.00	0.00	0.00	0.00	0.00
Y	0.04	0.04	0.04	0.03	0.05	0.03	0.03	0.03	0.02	0.02	0.02	0.02

Appendix 6 Chemical composition analysis of Minerals from Lofdal samples

Sample	39_AS9398_BSE3c	47_AS9398_BSE3i	52_AS9398_BSE5b	53_AS9398_BSE5b	55_AS9398_BSE6b	57_AS9398_BSE6b	58_AS9398_BSE7b	59_AS9398_BSE7b	60_AS9398_BSE8b	23_AS9396_BSE4b	20_AS9396_BSE4a	21_AS9396_BSE4a
Mineral	Synchisite?									Barite	Quartz	
SiO_2	0.00	0.00	0.18	0.36	0.23	0.17	0.30	0.23	0.39	0.00	100.30	100.76
TiO_2	0.00	0.00	0.00	0.00	0.00	0.00	0.00	0.00	0.00	0.31	0.00	0.00
$Al2O_3$	0.00	0.00	0.00	0.00	0.12	0.00	0.00	0.00	0.00	0.00	0.11	0.17
FeO	0.00	0.00	0.00	0.00	1.95	0.00	0.00	0.00	0.00	0.00	0.00	0.00
MnO	0.00	0.00	0.00	0.00	0.00	0.00	0.00	0.00	0.00	0.00	0.00	0.00
MgO	0.00	0.00	0.00	0.00	0.00	0.00	0.00	0.00	0.00	0.00	0.00	0.00
CaO	16.17	17.58	10.24	15.65	6.04	16.80	11.74	17.26	11.22	0.38	0.00	0.00
Na_2O	0.00	0.00	0.00	0.00	0.00	0.00	0.00	0.00	0.00	0.10	0.04	0.00
K_2O	0.00	0.00	0.00	0.00	0.00	0.00	0.00	0.00	0.00	0.00	0.00	0.03
P_2O_5	0.00	0.00	0.00	0.00	0.00	0.00	0.00	0.00	0.00	0.00	0.00	0.00
F	4.60	4.62	5.12	4.13	5.79	4.13	4.83	4.65	4.78	0.00	0.00	0.00
Cl	0.00	0.00	0.00	0.00	0.00	0.00	0.00	0.00	0.00	0.00	0.00	0.00
SO_3	0.00	0.00	0.12	0.00	0.10	0.00	0.15	0.09	0.00	34.19	0.00	0.00
SrO	0.00	0.00	0.71	0.27	1.10	0.21	0.40	0.30	0.19	2.25	0.00	0.00
Y_2O_3	1.15	1.39	0.80	2.29	0.63	1.43	0.91	1.63	1.28	0.00	0.00	0.00
BaO	0.00	0.00	0.00	0.00	0.00	0.00	0.00	0.00	0.00	63.68	0.00	0.00
La_2O_3	12.91	10.97	20.77	11.49	18.71	13.57	18.57	10.64	15.44	0.00	0.00	0.00
Ce_2O_3	25.05	21.26	28.18	21.04	32.30	23.04	30.08	19.26	26.32	4.53	0.00	0.00
Nd_2O_3	7.71	7.57	6.01	7.24	5.99	6.61	6.69	7.94	8.45	0.00	0.00	0.00
ThO_2	0.00	0.00	1.31	0.91	2.83	0.00	2.19	1.76	0.70	0.00	0.00	0.00
CO_2	31.70	30.58	31.95	30.52	31.39	31.71	33.74	30.96	30.60	-	-	-
Total	**99.29**	**93.97**	**105.39**	**93.89**	**107.18**	**97.67**	**109.59**	**94.71**	**99.37**	**105.44**	**100.45**	**100.96**
O=F,Cl	97.35	92.03	103.24	92.15	104.74	95.93	107.56	92.76	97.36	-	-	-
Ox	6.00	6.00	6.00	6.00	6.00	6.00	6.00	6.00	6.00	3.00	2.00	2.00
F	0.60	0.63	0.66	0.57	0.75	0.55	0.60	0.62	0.65	0.00	0.00	0.00
Al	0.00	0.00	0.00	0.00	0.01	0.00	0.00	0.00	0.00	0.00	0.00	0.00
Ba	0.00	0.00	0.00	0.00	0.00	0.00	0.00	0.00	0.00	0.47	0.00	0.00
C	1.80	1.79	1.78	1.81	1.75	1.82	1.80	1.79	1.78	0.00	0.00	0.00
Ca	0.72	0.81	0.45	0.73	0.26	0.76	0.49	0.78	0.51	0.01	0.00	0.00
Ce	0.38	0.33	0.42	0.33	0.48	0.35	0.43	0.30	0.41	0.03	0.00	0.00
Cl	0.00	0.00	0.00	0.00	0.00	0.00	0.00	0.00	0.00	0.00	0.00	0.00
Fe	0.00	0.00	0.00	0.00	0.07	0.00	0.00	0.00	0.00	0.00	0.00	0.00
K	0.00	0.00	0.00	0.00	0.00	0.00	0.00	0.00	0.00	0.00	0.00	0.00
La	0.20	0.17	0.31	0.18	0.28	0.21	0.27	0.17	0.24	0.00	0.00	0.00
Mg	0.00	0.00	0.00	0.00	0.00	0.00	0.00	0.00	0.00	0.00	0.00	0.00
Mn	0.00	0.00	0.00	0.00	0.00	0.00	0.00	0.00	0.00	0.00	0.00	0.00
Na	0.00	0.00	0.00	0.00	0.00	0.00	0.00	0.00	0.00	0.00	0.00	0.00
Nd	0.11	0.12	0.09	0.11	0.09	0.10	0.09	0.12	0.13	0.00	0.00	0.00
P	0.00	0.00	0.00	0.00	0.00	0.00	0.00	0.00	0.00	0.00	0.00	0.00
S	0.00	0.00	0.01	0.00	0.01	0.00	0.01	0.00	0.00	0.81	0.00	0.00
Si	0.00	0.00	0.01	0.02	0.01	0.01	0.01	0.01	0.02	0.00	1.00	1.00
Sr	0.00	0.00	0.02	0.01	0.03	0.01	0.01	0.01	0.00	0.02	0.00	0.00
Th	0.00	0.00	0.01	0.01	0.03	0.00	0.02	0.02	0.01	0.00	0.00	0.00
Ti	0.00	0.00	0.00	0.00	0.00	0.00	0.00	0.00	0.00	0.00	0.00	0.00
Y	0.03	0.03	0.02	0.05	0.01	0.03	0.02	0.04	0.03	0.00	0.00	0.00

Appendix 7 Laser ablation analysis of trace elements for Lofdal mineral samples

Laser Ablation Analysis Results All values are reported in ppm								
	Zircon						Calcite	
Sample	813Z1	813Z2	813Z3	813Z4	813Z5	813Z6	813C1	813C2
Ca	0.13	0.13	0.13	0.13	0.13	0.13	28.59	28.59
Sc	60.94	14.33	2.40	4.43	9.99	3.13	0.50	0.82
Ti	4.31	1.04	0.16	0.31	0.71	0.22	0.00	0.00
V	0.10	0.01	0.00	0.01	0.03	0.01	0.01	0.18
Cr	0.00	0.00	0.00	0.01	0.04	0.00	0.00	0.00
Mn	0.03	0.02	0.13	0.03	0.02	0.02	5.24	4.31
Fe	0.01	0.00	0.00	0.00	0.00	0.00	0.02	0.07
Fe	0.01	0.00	0.00	0.00	0.00	0.00	0.02	0.09
Ni	0.00	0.00	0.00	0.00	0.00	0.00	0.00	0.00
Rb	0.11	0.03	0.01	0.02	0.04	0.04	0.05	0.03
Sr	2.98	3.06	1.22	1.62	3.54	3.23	242.11	246.11
Y	727.10	210.02	36.93	96.29	306.11	72.92	53.60	59.04
Zr	296548.75	72530.26	12888.87	24340.93	61044.44	18950.65	0.08	0.73
Nb	937.85	513.92	168.70	258.16	821.92	79.35	8.40	33.47
Cs	0.00	0.10	0.01	0.00	0.03	0.02	0.13	0.02
Ba	2.61	0.89	2.40	1.98	2.54	1.00	2.62	5.64
La	28.95	5.02	4.58	9.98	10.63	16.32	228.68	573.21
Ce	195.00	21.69	3.33	17.53	35.52	16.45	228.10	422.31
Pr	137.07	21.32	5.60	16.28	24.66	12.57	208.14	311.86
Nd	183.37	28.91	6.74	18.04	33.72	12.39	121.22	217.38
Sm	237.43	48.53	11.70	31.50	63.99	15.36	79.06	117.07
Eu	248.07	59.70	13.50	35.14	72.19	17.17	66.99	94.71
Gd	261.92	66.57	12.34	34.22	87.05	21.20	59.81	81.19
Tb	294.44	89.91	16.31	42.26	119.58	28.43	50.99	66.97
Dy	444.28	136.93	23.71	61.34	190.09	45.24	53.65	64.41
Ho	566.12	172.88	30.28	77.18	254.15	60.59	50.31	58.51
Er	786.29	235.01	42.47	107.35	354.47	83.08	52.57	61.44
Tm	1217.33	356.67	66.89	168.12	539.74	123.28	55.85	66.23
Yb	1537.07	449.32	86.00	212.89	661.94	153.95	53.44	63.96
Lu	1159.47	332.33	68.93	163.43	493.68	118.01	51.25	63.08
Hf	70511.68	16982.51	3059.39	5150.78	13109.17	4628.21	0.03	0.05
Ta	82.98	45.66	4.06	21.71	45.98	7.93	0.32	2.83
Pb	9.21	2.58	0.46	1.44	4.12	0.82	4.10	4.76
Th	17103.77	3830.04	680.20	2296.72	6302.43	1151.55	14.03	34.84
U	2634.52	648.67	160.08	345.36	747.15	288.47	27.80	234.95

Appendix 7 Laser ablation analysis of trace elements for Lofdal mineral samples

Laser Ablation Analysis Results All values are reported in ppm									
	Calcite					Pyrochlore			
Sample	813C3	813C5	813C6	326C1	326C2	813P1	813P2	813P3	813P4
Ca	28.59	28.59	28.59	28.59	28.59	4.24	0.13	4.24	4.24
Sc	0.64	0.59	0.73	0.03	0.03	22.22	29.52	0.41	3.72
Ti	0.00	0.00	0.01	0.00	0.00	17.02	2.10	0.20	98.81
V	0.59	0.05	0.16	0.01	0.02	46.05	0.02	5.68	2873.15
Cr	0.00	0.00	0.00	0.00	0.00	0.00	0.00	0.07	21.79
Mn	26.28	3.43	6.82	2.55	2.46	192.07	0.03	14.21	50.12
Fe	0.36	0.03	0.03	0.01	0.01	142.56	0.00	0.49	261.55
Fe	0.46	0.04	0.05	0.01	0.01	187.29	0.00	0.69	376.26
Ni	0.00	0.00	0.00	0.00	0.00	0.36	0.00	0.00	0.44
Rb	0.03	0.02	0.04	0.00	0.03	24.41	0.08	0.18	0.73
Sr	759.22	157.13	227.17	1097.38	940.15	1823.78	21.25	248.06	258.66
Y	126.76	63.62	55.41	23.08	28.63	362.48	439.34	19.22	49.85
Zr	1.90	229.49	168.45	0.01	0.01	341.37	164722.33	741.70	111.85
Nb	271.70	42.94	391.59	0.37	1.14	469860.59	5037.14	6742.47	532495.94
Cs	0.28	0.65	0.26	0.02	0.00	38.48	0.06	0.05	13.27
Ba	2217.33	5.43	188.82	63.61	57.06	793.61	4.14	1697.69	266.58
La	203.22	371.53	660.92	80.32	59.88	7109.76	29.63	110.10	3718.92
Ce	185.74	318.60	468.31	86.18	65.78	5744.95	109.30	72.31	1969.29
Pr	152.58	231.93	321.56	89.91	72.13	5620.23	45.44	73.49	1529.24
Nd	122.55	179.21	211.81	79.14	65.12	3858.71	49.48	54.02	904.85
Sm	104.50	122.24	114.00	63.10	53.19	1855.25	78.91	37.26	421.62
Eu	103.83	93.06	92.25	53.76	48.52	1222.62	87.58	33.14	222.16
Gd	109.16	79.72	77.13	45.79	42.39	903.82	102.41	28.32	160.60
Tb	88.45	119.55	65.48	32.60	34.12	674.10	146.00	23.64	133.91
Dy	96.63	67.21	62.22	29.24	34.53	608.05	255.61	23.91	84.49
Ho	90.13	60.84	54.20	24.00	30.92	544.01	365.38	20.55	77.53
Er	94.69	63.40	54.80	21.77	28.75	554.21	553.05	21.14	65.41
Tm	97.50	64.04	59.99	22.43	31.54	676.57	902.49	20.59	85.94
Yb	94.58	62.12	57.47	20.14	33.11	666.72	1185.98	19.23	54.95
Lu	90.66	59.34	54.78	22.16	32.05	608.00	901.84	17.92	52.97
Hf	0.23	43.28	29.35	0.06	0.09	148.38	32701.50	217.39	157.34
Ta	1.46	0.85	0.94	0.00	0.05	19150.55	622.99	227.99	54921.79
Pb	45.86	3.08	7.76	1.27	1.16	2188.91	8.73	12.87	573.00
Th	5.73	31.89	112.23	2.27	1.23	9215.33	9462.83	65.44	9904.52
U	1686.43	59.01	160.39	9.82	12.23	33474.02	4396.20	609.92	71461.60

Appendix 7 Laser ablation analysis of trace elements for Lofdal mineral samples

Laser Ablation Analysis Results All values are reported in ppm						
	Pyrochlore			Monazite		
Sample	813P5	813P6	813P7	326M1	326M2	326M3
Ca	4.24	4.24	4.24	8.89	8.89	8.89
Sc	17.62	0.83	6.61	10.67	3.57	5.99
Ti	126.98	3.95	76.70	281.95	63.42	33.23
V	1459.63	94.58	2712.61	154.77	90.69	34.31
Cr	7.54	0.09	1.77	0.00	0.00	0.00
Mn	29.10	4.68	426.11	4.43	2.35	1.04
Fe	90.21	10.20	184.70	3.52	3.50	1.55
Fe	128.73	16.59	312.91	4.59	4.54	2.12
Ni	0.11	0.01	0.06	0.03	0.00	0.00
Rb	7.37	2.46	3.39	18.94	54.68	20.52
Sr	5267.60	71.88	6378.61	23925.96	19733.37	14607.76
Y	670.16	20.87	168.85	26885.43	18289.15	16250.41
Zr	2177.22	18.54	324.54	458.56	204.63	236.71
Nb	2808420.75	101566.72	1214567.63	99397.09	21270.05	9338.68
Cs	81.80	1.97	96.04	0.00	26.27	126.55
Ba	1917.12	292.53	29776.49	54729.92	48027.74	38623.27
La	5166.36	400.81	3615.65	**	**	**
Ce	8443.80	222.35	3309.39	**	**	**
Pr	6091.21	283.38	1982.82	**	**	**
Nd	4185.07	191.19	1289.79	**	**	**
Sm	3213.25	118.12	791.26	**	7420975.00	6259742.50
Eu	2273.68	82.34	609.87	4704284.50	3084480.75	2776775.75
Gd	1626.56	59.66	501.11	2584391.00	1744710.63	1496049.75
Tb	1324.83	36.16	431.45	537451.81	359430.72	323504.97
Dy	1258.55	36.90	360.99	168122.88	116004.41	103042.29
Ho	902.66	32.96	299.85	52992.45	35928.62	30859.81
Er	1021.33	26.43	289.51	23405.89	16047.15	14576.03
Tm	979.42	24.22	260.63	5145.62	3162.35	3198.53
Yb	829.44	23.45	237.09	1867.16	1439.64	1475.54
Lu	761.28	26.45	168.78	704.87	590.56	636.54
Hf	1773.44	10.18	202.91	137.57	112.41	114.56
Ta	163910.17	275.79	5667.09	2145.57	582.45	323.86
Pb	579.90	33.04	972.62	17604.26	13507.40	10014.86
Th	46862.72	645.69	11111.68	**	**	**
U	684618.75	606.82	76895.32	38310.28	54204.86	86882.45

Appendix 7 Laser ablation analysis of trace elements for Lofdal mineral samples

Laser Ablation Analysis Results All values are reported in ppm							
	Sychysite-Parisite						Cerianite
Sample	326L1	326L2	326L3	326L4	326L5	326L6	326CE1
Ca	9.04	9.04	4.27	7.93	9.00	6.09	0.16
Sc	0.44	0.32	0.00	0.04	0.13	0.01	0.00
Ti	0.15	0.19	0.01	0.00	0.25	0.05	0.00
V	0.66	0.94	0.04	0.15	1.46	0.41	0.00
Cr	0.00	0.00	0.00	0.00	0.00	0.00	0.00
Mn	0.13	0.48	0.28	1.02	19.47	0.25	0.02
Fe	0.05	0.11	0.01	0.04	0.30	0.01	0.00
Fe	0.09	0.21	0.01	0.08	0.61	0.01	0.00
Ni	0.00	0.00	0.00	0.00	0.00	0.00	0.00
Rb	0.12	0.26	0.02	0.01	0.26	0.14	0.00
Sr	513.87	452.76	149.38	76.14	928.56	324.54	6.81
Y	371.84	344.95	64.33	21.97	310.75	210.06	0.30
Zr	150.83	95.60	0.58	0.23	4.00	0.86	0.01
Nb	1793.67	2781.58	25.23	13.62	2584.27	194.69	7.34
Cs	1.09	0.35	0.06	0.00	0.17	0.63	0.00
Ba	4.31	5.48	6.31	8.92	788.95	6.72	5.89
La	787359.88	667068.63	61570.72	18071.59	874999.81	232026.64	251.93
Ce	384200.66	329938.56	32335.41	15346.07	422600.22	127779.63	221.75
Pr	267818.09	228814.86	22917.66	8985.65	274667.78	90539.10	175.64
Nd	142439.14	120364.35	12661.20	5808.61	150026.11	52580.94	78.86
Sm	23707.14	19836.06	3036.62	654.79	23906.80	9056.17	13.67
Eu	8293.96	7141.50	1094.82	237.44	7362.85	2823.54	5.93
Gd	4121.18	3566.10	554.32	131.75	4542.34	1309.83	2.74
Tb	1189.43	1062.84	155.58	45.98	1296.87	406.07	0.87
Dy	590.32	523.94	86.02	31.75	646.61	236.74	0.49
Ho	333.99	301.30	57.57	25.05	346.27	165.85	0.30
Er	247.12	220.69	46.44	23.41	260.58	135.68	0.27
Tm	201.89	177.14	36.62	21.02	185.53	106.50	0.25
Yb	182.18	152.64	30.81	17.58	142.24	82.46	0.22
Lu	150.21	130.19	20.42	16.55	120.72	61.07	0.20
Hf	9.45	9.63	0.06	0.00	0.56	1.49	0.00
Ta	4.10	4.45	3.18	0.16	3.37	0.76	0.00
Pb	19.34	31.24	5.63	11.36	330.22	7.84	0.41
Th	43880.93	37190.43	3170.42	1814.84	39942.86	19430.25	12.62
U	12244.07	10992.20	4496.77	1206.33	26819.87	3786.47	3.27

Appendix 8 Loddal carbonatite samples 114, 119, 881G, 881R, 1569, 15769G, 15769LG, ZC and ZS sent to BGR for analysis_22Feb10

CARBONATITE ROCK SAMPLES LIST – 22 FEBRUARY 2010

Sample No.	Sample type	Colour	Structure	Description	Observable mineralogy	Analysis required
0114	Carbonatite dyke	White-Yellow	Fine with porphyritic texture	Porphyritic texture; veins up to 2mm thick, filled with dark and carbonate minerals; **high HREE**	Calcite, Fe-oxides	XRF, ICP, Electron Microprobe
0119	Carbonatite dyke	Light Brown	Fine to medium	Crystalline texture; small veins with two prominent directions; **high HREE**	Calcite, minor fe-oxides, clinopyroxene?	
881G	Carbonatite dyke	Yellow-Green	Fine	Tiny fractures prominent in most yellow part of rock and almost non-existent where green dominates; **Emanya intrusion**	Calcite, Fe-oxides?, pyroxenes?	
881R	Carbonatite dyke	Dark Red	Fine	Leached rock with up to 2cm wide orange-yellow minerals, and 2mm wide carbonate veins; **Emanya intrusion**	Fe-oxides (hematite?, limonite?), carbonates, quartz	
15769	Carbonatite dyke	Red	Fine	Massive texture with euhedral cubic minerals (possibly pyrite); carbonate veins; **early thorium dyke**	Carbonates, pyrite?, Fe-oxides	
15769G	Carbonatite dyke	Grey	Fine to medium	Crystalline calcite; slightly leached; ferruginous <1mm thick veins; **late thorium dyke**	Calcite, Fe-oxides	
15769LG	Carbonatite dyke	Yellowish-grey	Fine	Crystalline where calcite dominated; slightly leached where Fe-oxides dominate; **late, red dyke, thorium depleted**	Calcite, Fe-oxides	
15796	Carbonatite dyke	Orange-White	Fine	Calcite dominated clasts within Fe-rich calcitic matrix; **up to 2% REO + Y**	Fe-oxides , calcite	
ZC	Carbonatite	Brown	Medium to coarse	**Zircons (3mm) in carbonatite**; leached carbonatite with HCl	Albite, zircon	Dating
ZS	Syenite	Grey	Coarse	**Zircons (1.5cm) in syenite**; Feldspathoid	Zircon, Nepheline	

Appendix 9 Loddal carbonatite samples 08_058, 115, 189, 269, 326, 813, 907, 914, 924, 927 and 949 sent to BGR for analysis_10Aug09

CARBONATITE ROCK SAMPLES LIST AND, SAMPLE LOCALITY MAP (BELOW)

Sample No.	Sample type	Colour	Structure	Distinguishing criterion	Description	Observable mineralogy	Analysis Requested
NLOFRC 08_058	RC drill chips	Whitish-grey	Medium to coarse	carbonatite plug - ~170 m depth	Main carbonatite body	calcite, sulphides (pyrite), pyroxenes - aegerine?	- Whole rock analysis - ICP; - Stable isotopes (δ18O, δ13C); - Radiogenic isotopes (Sr); - Dating: zircons, U-Pb, Sm-Nd; - SEM-EDS to determine mineralogy (hosts of REEs)
115	Rock	Dark brown	fine	highly variable mineralogy	Layered; highly ferruginous	siderite?	
189	Rock	Orange	fine	radioactive	Highly ferruginous; high specific gravity;	Fe-oxides (siderite?), barite?, fluorite	
269	Rock	Dark grey	fine to medium	zero sample'	Magnetite bands; 'Zero' sample;		
326	Rock	White	Coarse	carbonatite plug - surface sample	Main carbonatite body, surface sample	carbonates, sulphides (pyrite)	
813	Rock	Light brown	Coarse	zircon content	Ferruginous rock	zircons, albite, calcite	
907	Rock	Purple	Coarse	fluorite-rich sample	Fluorite dominated; slightly ferruginous	fluorite, Fe-oxides	
914	Rock	Dark Grey	fine	High - LREE	Ferruginous	Fe-oxides	
924	Rock	Brown	Medium to coarse	High - REE	Highly ferruginous; carbonate veins	carbonates, Fe-oxides	
927	Rock	Purple	Medium	High - HREE	Fluorite rich; ferruginous material interstially	fluorite, Fe-oxides	
949	Rock	Brown	fine	Emanya' carbonatite	ferruginous and carbonate veins		

Map indicating samples' locality.

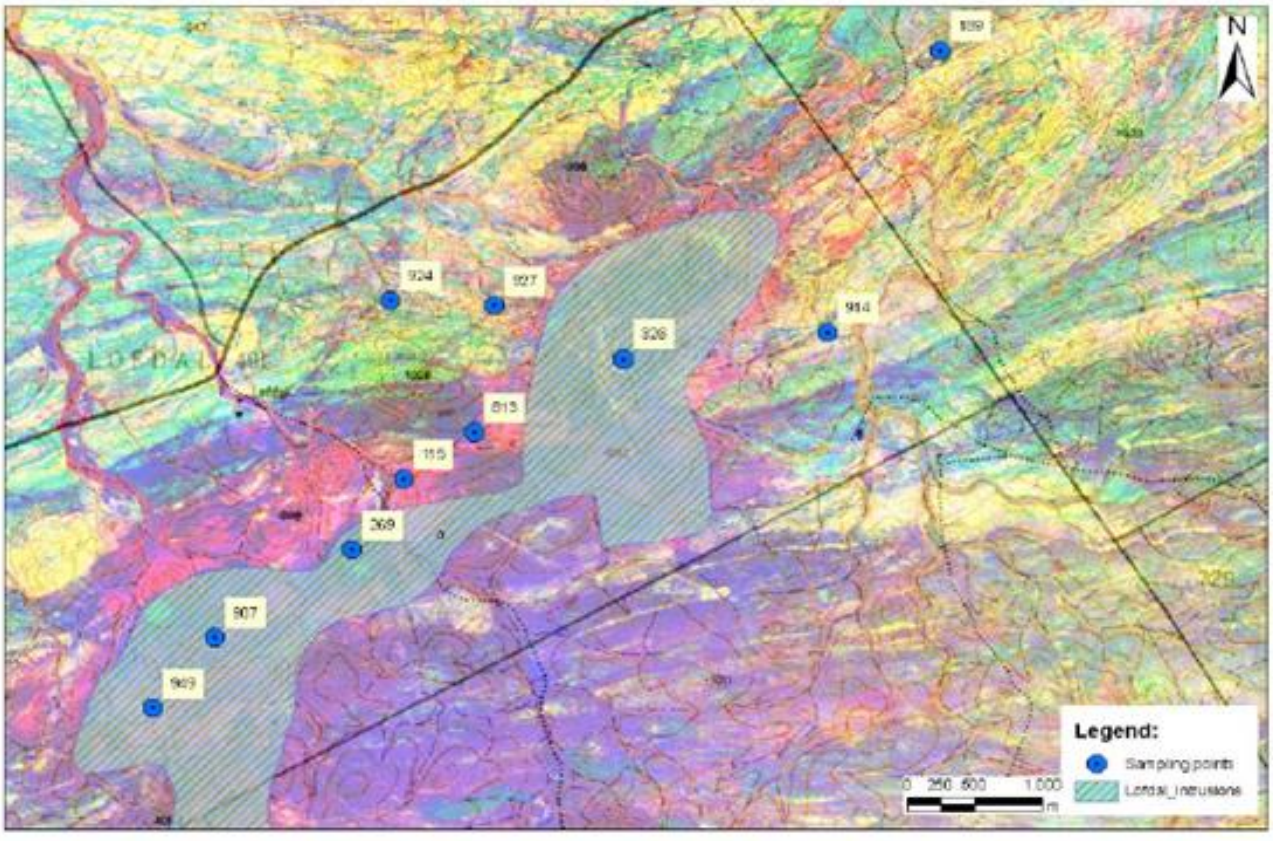

Appendix 10 Chemical composition analysis of Dicker Willem and Keishohe samples

ID	La	Ce	Pr	Nd	Sm	Eu	Gd	Tb	Dy	Ho	Er	Tm	Yb	Lu	La/Yb
D02	337.00	955.30	109.50	490.10	74.20	19.30	47.20	5.30	27.20	3.90	8.50	0.90	5.30	0.60	63.77
D03	>2000.00	>2000.000	956.60	>2000.00	248.80	59.60	66.20	11.30	48.00	6.50	14.50	1.80	13.60	1.80	>147.06
D04	1180.00	>2000.000	209.70	901.10	119.90	34.00	85.40	11.30	60.00	9.10	18.20	1.70	9.80	1.10	120.51
D05	>2000.00	>2000.000	442.20	1767.20	212.20	60.80	170.40	26.00	173.70	29.90	65.20	6.80	36.10	4.10	>55.40
D06	887.30	1851.86	206.70	1001.00	188.10	66.60	185.90	25.30	135.50	21.60	47.30	5.00	29.50	3.40	30.11
D07	735.90	1759.06	182.80	842.40	121.50	36.10	100.00	15.10	90.30	14.90	30.90	3.20	17.60	2.00	41.87
D08	506.00	1517.62	167.00	789.50	121.40	35.60	92.20	13.00	73.80	13.00	29.10	3.10	17.20	2.00	29.48
D09	1622.90	>2000.000	365.40	1665.80	223.90	58.00	122.70	14.60	77.90	13.30	32.00	4.00	24.10	3.00	67.38
D10	>2000.00	>2000.000	1024.20	>2000.00	510.90	133.70	284.30	35.30	160.70	19.10	32.50	3.50	22.70	2.40	>88.11
D11	1238.40	>2000.000	312.90	1492.20	240.10	72.90	203.80	26.40	133.50	18.60	37.20	3.60	21.80	2.60	56.85
D12	1650.90	>2000.000	423.10	1919.80	238.20	59.00	125.70	14.70	74.20	10.50	19.90	2.00	11.70	1.30	141.19
D13	1122.60	>2000.000	259.30	1200.10	165.50	45.70	118.90	16.30	92.00	14.20	28.60	2.90	17.10	2.00	65.71
D14	1090.70	>2000.000	267.30	1232.00	168.50	47.10	122.10	16.80	93.50	14.70	32.50	3.50	21.70	2.70	50.31
D15	>2000.00	>2000.000	622.20	>2000.00	174.50	41.70	85.30	12.10	65.40	12.20	29.50	3.40	20.60	2.50	>97.09
D16	108.30	271.67	35.00	137.80	18.90	4.70	12.90	1.60	8.30	1.30	2.80	0.30	2.50	0.30	43.72
D17	1370.10	>2000.000	352.00	1584.60	177.20	42.20	94.90	11.40	55.80	7.40	14.20	1.60	10.40	1.20	131.84
D18	1122.90	>2000.000	275.20	1293.10	172.40	46.00	111.10	12.90	64.70	9.20	18.50	1.90	12.60	1.50	89.20
D20	>2000.00	>2000.000	550.40	>2000.00	335.80	97.20	251.20	34.20	186.70	29.00	60.70	6.40	39.70	4.80	>50.38
D21	1530.20	>2000.000	340.60	1429.10	164.00	42.60	99.50	10.80	51.60	7.20	15.10	1.80	12.00	1.60	127.60
D22	395.40	798.43	69.90	251.30	32.60	8.90	22.90	3.30	19.90	3.60	8.50	0.90	5.90	0.70	67.19
D23	>2000.00	>2000.000	484.00	1895.30	179.20	41.50	85.40	10.30	48.00	6.30	12.10	1.30	9.10	1.20	>219.78
D25	1757.30	>2000.000	333.90	1475.20	217.50	55.40	159.50	23.70	147.80	28.60	80.70	11.10	77.70	10.20	22.63
D26	1781.80	>2000.000	306.70	1254.50	163.50	44.60	124.20	19.30	123.20	24.90	67.80	8.20	50.90	6.20	35.03
D27	>2000.00	>2000.000	>2000.00	>2000.00	560.70	119.60	210.30	25.40	116.80	17.10	38.20	5.30	40.60	5.70	>49.26
D28	1541.40	>2000.000	290.40	1247.90	188.90	58.30	179.70	32.90	233.70	50.00	144.10	20.30	148.30	21.20	10.40
D29	1758.80	>2000.000	312.80	1303.40	151.90	38.00	72.20	6.70	25.80	3.30	7.10	1.00	8.70	1.20	202.28
D50	1859.40	>2000.000	536.50	>2000.00	412.50	115.70	293.70	37.50	195.40	29.60	63.80	6.80	45.10	5.40	41.25
D51	1486.80	>2000.000	370.10	1773.20	245.30	64.60	147.60	18.20	95.40	14.90	30.60	3.30	21.20	2.50	70.18
K01	1831.40	>2000.000	>2000.00	>2000.00	981.70	172.10	219.60	17.60	81.90	9.50	15.70	2.30	16.90	1.90	108.43
K02	290.80	>2000.000	356.20	>2000.00	646.90	159.00	327.80	28.30	114.40	12.70	22.10	2.50	19.20	2.20	15.20
K03	>2000.00	>2000.000	>2000.00	>2000.00	733.60	146.30	208.70	22.10	123.80	18.40	37.50	4.30	27.00	3.10	>74.07
K04	70.70	275.72	47.20	212.20	27.80	5.60	11.80	1.20	6.00	0.80	1.90	0.20	1.90	0.30	37.74
K05	42.20	159.74	36.60	343.70	144.10	32.60	63.70	5.50	26.80	3.80	9.80	1.30	10.10	1.20	4.28
K06	>2000.00	>2000.000	>2000.00	>2000.00	456.80	78.00	49.60	10.40	60.20	7.10	13.60	2.10	15.40	1.80	>129.87
K07	>2000.00	>2000.000	714.90	>2000.00	219.40	46.20	62.80	8.50	51.50	7.40	16.30	2.20	14.60	1.70	>136.99
K08	128.60	400.49	58.70	340.50	63.70	11.30	20.60	1.20	5.20	0.40	1.00	0.10	1.20	0.10	108.00
K09	832.40	>2000.000	436.90	>2000.00	255.50	50.60	93.90	8.60	50.60	7.60	19.30	2.60	16.80	1.90	49.61
K10	>2000.00	>2000.000	1410.70	>2000.00	325.70	63.60	45.90	8.90	43.10	5.30	12.90	2.10	15.80	1.70	>126.58
K11	1883.10	>2000.000	250.70	956.90	91.70	22.40	54.70	6.90	35.40	5.30	10.50	1.20	8.30	1.00	227.00
K12	123.40	234.10	34.60	167.00	25.80	5.90	18.20	2.00	10.60	1.70	4.10	0.40	3.20	0.40	38.88
K13	785.10	>2000.000	652.70	>2000.00	259.50	49.50	94.70	7.20	39.40	4.70	8.70	1.30	9.10	1.10	86.38
K14	919.40	>2000.000	327.90	1872.50	261.80	60.40	142.70	15.00	80.90	11.60	22.90	2.60	15.00	1.60	61.36
K15	>2000.00	>2000.000	510.80	1756.80	117.10	23.60	42.70	4.70	21.40	2.40	3.60	0.50	4.10	0.40	>487.81

Appendix 11 Chemical composition analysis of Agate Mountain and Teufelskuppe

Sample	AMC1	AMC2	AMC3	AMC4	AMC5A	AMC5B	AMC5C	AMC5D	AMC6	T1	T2	T3
La	873.40	848.80	1238.60	1386.10	11226.00	17466.90	19802.60	13633.50	N.A.	5643.20	5929.00	571.30
Ce	1969.30	1840.60	2695.20	3259.00	14881.50	20234.90	23349.50	15512.10	N.A.	12060.60	11233.10	2002.00
Pr	242.50	212.30	306.10	380.50	1349.10	1586.90	1891.40	1367.70	2.00	1552.60	1336.00	301.40
Nd	988.40	878.50	1249.90	1466.00	3185.20	3357.20	4124.00	2753.20	N.A.	5456.60	4429.40	1699.80
Sm	148.90	126.30	149.50	187.10	211.50	158.40	181.70	152.50	0.90	617.20	440.70	295.10
Eu	37.10	32.40	36.50	47.50	49.80	31.70	32.00	33.70	0.30	156.00	118.50	78.90
Gd	105.20	89.70	96.20	129.10	90.90	49.50	<0.1	17.70	0.70	245.90	213.10	179.30
Tb	12.00	11.00	10.90	13.40	16.50	10.60	7.50	14.80	0.10	29.60	27.80	21.10
Dy	64.80	59.50	52.90	70.10	84.40	68.20	50.70	93.10	0.60	123.10	119.30	107.40
Ho	8.50	8.80	7.10	9.80	13.10	12.40	9.40	15.50	0.10	16.70	14.20	17.60
Er	17.40	19.80	13.40	19.20	30.00	27.80	21.10	36.90	0.30	30.60	22.50	39.00
Tm	2.00	2.10	1.60	2.00	4.10	3.80	3.20	4.10	<0.10	4.00	2.30	4.20
Yb	13.30	12.30	10.40	11.20	29.00	24.40	21.20	25.30	0.20	24.80	13.50	23.60
Lu	1.50	1.10	1.10	1.10	3.40	2.80	2.20	2.90	<0.10	2.70	1.40	2.50
La/Yb	65.67	69.01	119.10	123.76	387.10	715.86	934.08	538.87	-	227.55	439.19	24.21

Appendix 12 Reference data xenotime

McDonough and Sun (1995)	chondrite	PM	atomic weight	ox. To el.	el. To ox.
Si(%)	10.65	21.00	28.09	0.47	2.14
P			30.97	0.44	2.29
Ca(%)	0.93	2.53	40.08	0.71	1.40
Fe			55.85	0.78	1.29
Y	1.57	4.30	88.91	0.79	1.27
La	0.24	648.00	138.91	0.85	1.17
Ce	0.61	1675.00	140.21	0.85	1.17
Pr	0.09	254.00	140.91	0.85	1.17
Nd	0.46	1250.00	144.24	0.86	1.17
Sm	0.15	406.00	150.35	0.86	1.16
Eu	0.06	154.00	151.96	0.86	1.16
Gd	0.20	544.00	157.25	0.87	1.15
Tb	0.04	99.00	158.92	0.87	1.15
Dy	0.25	674.00	162.50	0.87	1.15
Ho	0.05	149.00	164.93	0.87	1.15
Er	0.16	438.00	167.26	0.87	1.14
Tm	0.02	68.00	168.93	0.70	1.14
Yb	0.16	441.00	173.04	0.88	1.14
Lu	0.02	67.50	174.97	0.88	1.14
Th	0.03	79.50	232.04	0.88	1.14
U	0.01	20.30	238.03	0.88	1.13
Pb	2.47	150.00	207.20	0.93	1.08
Hf	0.10	283.00			
Ta	0.01	37.00			
W	0.09	29.00			
Sc(ppm)	5.92	16.20			
Ti	440.00	1205.00			
V	56.00	82.00			
Cr	2650.00	2625.00			
Mn	1920.00	1045.00			
Co(ppm)	500.00	105.00			
Zn	310.00	55.00			
Ge	31.00	1.10			
Rb	2.30	0.60			
Sr	7.25	19.90	87.62	0.55	1.18
Zr	3.82	10.50			
Nb(ppm)	0.24	658.00			
Mo	0.90	50.00			
Cs	0.19	21.00			
Ba	2.41	6600.00	137.34	0.90	1.12
Mg(%)	9.65	22.80	24.31	0.60	1.66
F			19.00	1.00	1.00
Al			26.98	0.53	1.89
Sc			44.96	0.33	3.07
Ti			47.90	0.60	1.67

Appendix 12 Reference data xenotime

No.	1	2	3	4	5	6	7	8
Comment	FWL8_41	9393_1	9393_2	9393_3	FW8_41	9393_4	9393_5	9393_6
SiO_2	0.28	0.35	1.17	1.17	0.29	0.32	0.34	0.31
P_2O_5	36.07	36.80	35.32	34.85	35.82	37.19	36.97	37.41
CaO	0.15	0.07	0.11	0.12	0.17	0.07	0.08	0.20
FeO	0.09	0.13	0.14	0.16	0.16	0.07	0.10	0.25
Y_2O_3	39.20	49.28	50.53	51.01	38.33	50.19	49.90	49.52
La_2O_3	0.00	0.00	0.01	0.00	0.01	0.00	0.00	0.00
Ce_2O_3	0.03	0.07	0.03	0.03	0.01	0.05	0.03	0.06
Pr_2O_3	0.01	0.07	0.07	0.02	0.00	0.04	0.00	0.08
Nd_2O_3	0.07	0.00	0.05	0.07	0.04	0.04	0.01	0.00
Sm_2O_3	1.25	0.07	0.10	0.07	1.09	0.14	0.22	0.28
Eu_2O_3	1.42	0.11	0.14	0.12	1.50	0.12	0.20	0.29
Gd_2O_3	8.76	1.43	1.10	1.06	9.17	1.48	1.47	1.75
Tb_2O_3	2.08	0.48	0.30	0.29	2.02	0.50	0.53	0.44
Dy_2O_3	10.81	5.26	4.09	4.03	10.93	5.03	4.86	4.82
Ho_2O_3	1.32	1.19	1.05	1.00	1.41	1.24	1.21	0.98
Er_2O_3	2.83	4.12	4.14	4.08	2.80	3.93	3.84	3.97
Tm_2O_3	0.30	0.64	0.68	0.68	0.27	0.50	0.60	0.64
Yb_2O_3	1.08	4.14	4.49	4.50	0.92	3.53	3.57	3.86
Lu_2O_3	0.57	0.69	0.72	0.67	0.59	0.58	0.64	0.70
ThO_2	0.41	0.29	0.41	0.46	0.19	0.62	0.61	0.61
UO_2	0.00	0.01	0.05	0.06	0.03	0.04	0.03	0.03
PbO	0.24	0.35	0.47	0.47	0.26	0.42	0.35	0.42
Total	**106.96**	**105.54**	**105.17**	**104.91**	**106.00**	**106.10**	**105.55**	**106.62**

FW samples collected and analysed by F. Wall (2004)

Appendix 12 Reference data xenotime

No.	9	10	11	12	13	14	15	16
Comment	9393_7	9393_8	FWL8_41	9393_9	9393_10	9393_11	9393_12	9393_13
SiO_2	0.83	0.62	0.18	0.91	0.90	0.53	1.31	0.50
P_2O_5	36.42	36.20	36.35	35.55	35.21	35.48	34.25	36.36
CaO	0.11	0.12	0.09	0.61	0.09	0.18	0.08	0.09
FeO	0.21	0.18	0.08	0.89	0.16	0.28	0.14	0.10
Y_2O_3	49.33	49.37	39.61	47.31	51.04	50.59	50.40	49.47
La_2O_3	0.02	0.00	0.00	0.01	0.00	0.00	0.00	0.00
Ce_2O_3	0.07	0.05	0.04	0.06	0.05	0.03	0.04	0.02
Pr_2O_3	0.00	0.00	0.00	0.10	0.10	0.13	0.00	0.03
Nd_2O_3	0.05	0.00	0.15	0.03	0.02	0.06	0.08	0.00
Sm_2O_3	0.09	0.16	1.16	0.06	0.05	0.08	0.08	0.09
Eu_2O_3	0.11	0.15	1.37	0.11	0.09	0.05	0.06	0.08
Gd_2O_3	1.28	1.46	9.37	1.41	0.89	0.93	1.04	1.29
Tb_2O_3	0.46	0.51	1.69	0.38	0.33	0.35	0.43	0.42
Dy_2O_3	4.88	5.13	9.31	4.75	3.89	4.34	4.25	4.94
Ho_2O_3	1.07	1.16	1.17	1.03	1.07	1.10	1.03	1.04
Er_2O_3	3.90	3.86	2.74	3.73	3.92	3.87	3.81	3.76
Tm_2O_3	0.54	0.51	0.29	0.51	0.61	0.54	0.53	0.55
Yb_2O_3	3.40	3.41	1.28	3.47	4.31	3.26	3.65	3.36
Lu_2O_3	0.65	0.61	0.66	0.59	0.66	0.56	0.59	0.64
ThO_2	1.10	0.97	0.14	0.72	0.35	0.26	0.32	1.05
UO_2	0.05	0.06	0.01	0.04	0.06	0.03	0.05	0.02
PbO	0.38	0.47	0.24	0.30	0.36	0.40	0.41	0.38
Total	**104.94**	**104.98**	**105.93**	**102.58**	**104.16**	**103.05**	**102.53**	**104.19**

Appendix 12 Reference data xenotime

No.	17	18	19	20	21	22	23	24
Comment	FWL8_41	9393-14	9393-15	9393-16	9393-17	9393-18	9393-19	FWL8_41
SiO_2	0.18	0.70	0.29	0.44	0.11	0.34	1.81	0.19
P_2O_5	35.82	35.94	35.93	36.20	37.19	36.88	33.09	35.73
CaO	0.09	0.07	0.08	0.12	0.07	0.06	0.07	0.04
FeO	0.07	0.24	0.17	0.11	0.08	0.05	0.08	0.17
Y_2O_3	39.41	47.16	49.48	48.99	48.40	48.54	47.28	40.77
La_2O_3	0.01	0.00	0.02	0.00	0.00	0.01	0.00	0.00
Ce_2O_3	0.06	0.06	0.03	0.04	0.04	0.03	0.06	0.03
Pr_2O_3	0.05	0.03	0.04	0.07	0.00	0.00	0.00	0.00
Nd_2O_3	0.02	0.09	0.08	0.07	0.01	0.03	0.02	0.06
Sm_2O_3	0.96	0.21	0.09	0.09	0.09	0.15	0.14	0.92
Eu_2O_3	1.30	0.20	0.13	0.09	0.07	0.14	0.09	1.07
Gd_2O_3	8.92	1.69	1.32	1.21	1.46	1.40	1.25	7.90
Tb_2O_3	1.62	0.52	0.47	0.40	0.51	0.51	0.52	1.38
Dy_2O_3	9.19	5.48	4.89	4.68	5.15	5.12	5.13	8.45
Ho_2O_3	1.18	1.03	1.10	1.11	1.14	1.09	1.02	1.07
Er_2O_3	2.73	4.13	3.96	3.89	3.93	4.06	3.82	2.52
Tm_2O_3	0.29	0.61	0.52	0.60	0.55	0.56	0.55	0.32
Yb_2O_3	1.25	3.57	3.62	3.65	3.63	3.68	3.63	1.49
Lu_2O_3	0.56	0.72	0.61	0.62	0.62	0.61	0.68	0.57
ThO_2	0.15	0.60	0.20	0.87	0.18	0.27	1.10	0.29
UO_2	0.00	0.05	0.01	0.10	0.00	0.02	0.07	0.00
PbO	0.23	0.33	0.43	0.45	0.36	0.35	0.37	0.22
Total	**104.10**	**103.44**	**103.46**	**103.79**	**103.60**	**103.91**	**100.78**	**103.20**

Appendix 12 Reference data xenotime

No.	25	26	27	28	29	30	31	32
Comment	9399_20	9399_21	9399_22	9399_23	9399_24	9399_25	9399_26	FWL8_41
SiO_2	0.08	5.35	6.95	28.51	0.93	33.32	3.62	0.12
P_2O_5	36.12	32.24	33.07	3.54	33.02	13.25	35.50	35.92
CaO	0.03	0.09	0.09	0.10	0.15	0.06	0.13	0.10
FeO	0.05	0.17	1.24	1.14	0.08	0.21	0.34	0.05
Y_2O_3	45.87	40.48	41.03	4.67	42.61	13.75	44.29	39.03
La_2O_3	0.00	0.00	0.00	0.00	0.00	0.00	0.00	0.00
Ce_2O_3	0.04	0.03	0.02	0.00	0.06	0.01	0.05	0.06
Pr_2O_3	0.01	0.00	0.06	0.00	0.01	0.02	0.02	0.00
Nd_2O_3	0.00	0.00	0.01	0.01	0.04	0.01	0.00	0.01
Sm_2O_3	0.25	0.21	0.21	0.01	0.37	0.16	0.26	0.87
Eu_2O_3	0.37	0.34	0.29	0.00	0.46	0.20	0.36	1.03
Gd_2O_3	2.65	2.27	2.13	0.18	3.03	1.37	2.48	8.69
Tb_2O_3	0.74	0.61	0.51	0.00	0.72	0.38	0.63	1.63
Dy_2O_3	6.35	5.32	5.30	0.44	6.30	2.90	5.63	9.48
Ho_2O_3	1.14	1.00	0.96	0.08	1.05	0.50	1.09	1.03
Er_2O_3	3.45	2.92	3.15	0.09	3.51	1.56	3.34	2.56
Tm_2O_3	0.37	0.30	0.34	0.00	0.49	0.14	0.44	0.26
Yb_2O_3	2.34	2.09	2.36	0.18	2.58	1.06	2.49	1.06
Lu_2O_3	0.57	0.46	0.55	0.01	0.58	0.19	0.60	0.56
ThO_2	0.04	0.42	0.19	0.08	1.06	0.11	0.57	0.09
UO_2	0.00	0.00	0.02	0.00	0.01	0.00	0.01	0.00
PbO	0.37	0.27	0.32	0.07	0.23	0.07	0.34	0.27
Total	**100.85**	**94.57**	**98.78**	**39.11**	**97.29**	**69.26**	**102.18**	**102.84**

Appendix 12 Reference data xenotime

ELEMENT	1	2	3	4	5	6	7	8
wt. %	FWL8_41	9393_1	9393_2	9393_3	FW8_41	9393_4	9393_5	9393_6
Si(%)	0.13	0.16	0.55	0.55	0.14	0.15	0.16	0.15
P	15.74	16.06	15.41	15.21	15.63	16.23	16.13	16.32
Ca(%)	0.10	0.05	0.08	0.09	0.12	0.05	0.05	0.14
Fe	0.07	0.10	0.11	0.13	0.12	0.06	0.08	0.20
Y	30.87	38.81	39.79	40.17	30.18	39.52	39.29	39.00
La	0.00	0.00	0.01	0.00	0.01	0.00	0.00	0.00
Ce	0.02	0.06	0.02	0.03	0.01	0.04	0.03	0.05
Pr	0.01	0.06	0.06	0.02	0.00	0.04	0.00	0.06
Nd	0.06	0.00	0.04	0.06	0.03	0.04	0.01	0.00
Sm	1.08	0.06	0.09	0.06	0.94	0.12	0.19	0.24
Eu	1.23	0.09	0.12	0.10	1.30	0.10	0.17	0.25
Gd	7.60	1.24	0.95	0.92	7.96	1.28	1.28	1.52
Tb	1.81	0.41	0.26	0.25	1.75	0.43	0.46	0.38
Dy	9.42	4.58	3.56	3.51	9.52	4.38	4.23	4.20
Ho	1.15	1.04	0.92	0.87	1.23	1.08	1.06	0.86
Er	2.47	3.60	3.62	3.57	2.45	3.44	3.36	3.47
Tm	0.21	0.45	0.48	0.48	0.19	0.35	0.42	0.45
Yb	0.95	3.64	3.94	3.95	0.81	3.10	3.14	3.39
Lu	0.50	0.61	0.64	0.59	0.52	0.51	0.56	0.61
Th	0.36	0.25	0.36	0.41	0.16	0.54	0.54	0.54
U	0.00	0.01	0.05	0.05	0.02	0.04	0.03	0.03
Pb	0.22	0.32	0.44	0.44	0.24	0.39	0.33	0.39

Appendix 12 Reference data xenotime

ELEMENT	9	10	11	12	13	14	15	16
wt. %	9393_7	9393_8	FWL8_41	9393_9	9393_10	9393_11	9393_12	9393_13
Si(%)	0.39	0.29	0.09	0.43	0.42	0.25	0.61	0.23
P	15.89	15.80	15.86	15.51	15.36	15.48	14.95	15.87
Ca(%)	0.08	0.08	0.07	0.44	0.06	0.13	0.06	0.06
Fe	0.16	0.14	0.06	0.70	0.13	0.22	0.11	0.08
Y	38.85	38.88	31.19	37.25	40.19	39.84	39.69	38.96
La	0.02	0.00	0.00	0.01	0.00	0.00	0.00	0.00
Ce	0.06	0.05	0.03	0.05	0.04	0.02	0.04	0.02
Pr	0.00	0.00	0.00	0.09	0.09	0.11	0.00	0.02
Nd	0.04	0.00	0.13	0.03	0.02	0.05	0.07	0.00
Sm	0.08	0.14	1.00	0.06	0.05	0.07	0.07	0.08
Eu	0.09	0.13	1.18	0.10	0.08	0.04	0.05	0.07
Gd	1.11	1.27	8.13	1.22	0.77	0.81	0.90	1.12
Tb	0.40	0.44	1.47	0.33	0.28	0.30	0.38	0.36
Dy	4.25	4.47	8.11	4.14	3.39	3.78	3.70	4.30
Ho	0.94	1.01	1.02	0.90	0.94	0.96	0.90	0.91
Er	3.41	3.38	2.40	3.26	3.43	3.38	3.33	3.29
Tm	0.38	0.36	0.20	0.36	0.43	0.38	0.37	0.39
Yb	2.99	2.99	1.12	3.05	3.79	2.86	3.21	2.95
Lu	0.58	0.53	0.58	0.52	0.58	0.49	0.52	0.56
Th	0.97	0.85	0.12	0.63	0.31	0.23	0.28	0.92
U	0.04	0.05	0.01	0.04	0.05	0.03	0.04	0.02
Pb	0.35	0.43	0.22	0.28	0.33	0.37	0.38	0.35

Appendix 12 Reference data xenotime

ELEMENT	17	18	19	20	21	22	23	24
wt. %	FWL8_41	9393-14	9393-15	9393-16	9393-17	9393-18	9393-19	FWL8_41
Si(%)	0.08	0.33	0.13	0.20	0.05	0.16	0.85	0.09
P	15.63	15.68	15.68	15.80	16.23	16.09	14.44	15.59
Ca(%)	0.06	0.05	0.06	0.09	0.05	0.05	0.05	0.03
Fe	0.06	0.18	0.13	0.08	0.06	0.04	0.06	0.13
Y	31.03	37.14	38.96	38.58	38.11	38.22	37.23	32.10
La	0.01	0.00	0.02	0.00	0.00	0.01	0.00	0.00
Ce	0.05	0.05	0.02	0.04	0.03	0.03	0.05	0.02
Pr	0.04	0.02	0.04	0.06	0.00	0.00	0.00	0.00
Nd	0.02	0.08	0.07	0.06	0.01	0.03	0.01	0.05
Sm	0.83	0.18	0.08	0.08	0.08	0.13	0.12	0.79
Eu	1.12	0.17	0.11	0.08	0.06	0.12	0.07	0.93
Gd	7.74	1.47	1.15	1.05	1.27	1.21	1.08	6.85
Tb	1.41	0.45	0.41	0.35	0.44	0.44	0.45	1.20
Dy	8.01	4.77	4.26	4.08	4.49	4.46	4.47	7.36
Ho	1.03	0.90	0.96	0.97	1.00	0.95	0.89	0.93
Er	2.39	3.61	3.46	3.40	3.44	3.55	3.34	2.20
Tm	0.20	0.43	0.36	0.42	0.39	0.39	0.38	0.22
Yb	1.10	3.14	3.18	3.21	3.19	3.23	3.19	1.31
Lu	0.49	0.64	0.54	0.55	0.54	0.54	0.60	0.50
Th	0.13	0.53	0.17	0.76	0.16	0.23	0.97	0.25
U	0.00	0.05	0.01	0.09	0.00	0.02	0.07	0.00
Pb	0.21	0.31	0.40	0.41	0.34	0.32	0.35	0.20

Appendix 12 Reference data xenotime

ELEMENT	25	26	27	28	29	30	31	32
wt. %	9399_20	9399_21	9399_22	9399_23	9399_24	9399_25	9399_26	FWL8_41
Si(%)	0.04	2.50	3.25	13.33	0.43	15.58	1.69	0.06
P	15.76	14.07	14.43	1.54	14.41	5.78	15.49	15.67
Ca(%)	0.02	0.07	0.07	0.07	0.11	0.05	0.09	0.07
Fe	0.04	0.13	0.96	0.89	0.06	0.16	0.26	0.03
Y	36.12	31.88	32.31	3.68	33.55	10.83	34.88	30.73
La	0.00	0.00	0.00	0.00	0.00	0.00	0.00	0.00
Ce	0.03	0.03	0.02	0.00	0.05	0.01	0.04	0.05
Pr	0.01	0.00	0.05	0.00	0.01	0.01	0.02	0.00
Nd	0.00	0.00	0.01	0.01	0.04	0.01	0.00	0.01
Sm	0.22	0.19	0.18	0.01	0.32	0.14	0.22	0.75
Eu	0.32	0.30	0.25	0.00	0.40	0.17	0.31	0.89
Gd	2.30	1.97	1.85	0.15	2.63	1.19	2.15	7.54
Tb	0.64	0.53	0.44	0.00	0.63	0.33	0.55	1.42
Dy	5.53	4.64	4.62	0.38	5.49	2.53	4.91	8.26
Ho	0.99	0.88	0.84	0.07	0.92	0.43	0.95	0.90
Er	3.02	2.55	2.75	0.07	3.07	1.36	2.92	2.24
Tm	0.26	0.21	0.24	0.00	0.35	0.10	0.31	0.18
Yb	2.05	1.84	2.07	0.15	2.27	0.93	2.19	0.93
Lu	0.50	0.40	0.48	0.01	0.51	0.16	0.53	0.49
Th	0.04	0.37	0.17	0.07	0.93	0.10	0.50	0.08
U	0.00	0.00	0.02	0.00	0.01	0.00	0.01	0.00
Pb	0.35	0.25	0.29	0.07	0.21	0.06	0.31	0.25

Appendix 12 Reference data xenotime

Chondrite	1	2	3	4	5	6	7	8
normalised	FWL8_41	9393_1	9393_2	9393_3	FW8_41	9393_4	9393_5	9393_6
Y	19.66	24.72	25.34	25.59	19.23	25.17	25.03	24.84
La	0.00	0.00	0.05	0.00	0.02	0.00	0.00	0.00
Ce	0.04	0.09	0.04	0.05	0.01	0.07	0.04	0.08
Pr	0.10	0.66	0.60	0.17	0.00	0.41	0.00	0.70
Nd	0.12	0.00	0.09	0.14	0.07	0.08	0.03	0.00
Sm	7.28	0.42	0.57	0.39	6.38	0.80	1.26	1.65
Eu	21.78	1.67	2.17	1.85	23.01	1.84	3.03	4.40
Gd	38.19	6.23	4.78	4.62	39.98	6.45	6.41	7.63
Tb	50.06	11.49	7.28	6.90	48.61	12.03	12.73	10.57
Dy	38.29	18.63	14.49	14.27	38.71	17.82	17.21	17.07
Ho	21.11	19.03	16.83	15.95	22.54	19.83	19.35	15.67
Er	15.47	22.52	22.63	22.30	15.30	21.48	20.99	21.70
Tm	8.67	18.21	19.33	19.35	7.66	14.34	17.03	18.27
Yb	5.88	22.58	24.49	24.55	5.04	19.25	19.47	21.05
Lu	20.31	24.68	25.90	23.85	21.25	20.71	22.84	24.91

Appendix 12 Reference data xenotime

Chondrite	9	10	11	12	13	14	15	16
normalised	9393_7	9393_8	FWL8_41	9393_9	9393_10	9393_11	9393_12	9393_13
Y	24.74	24.76	19.87	23.73	25.60	25.37	25.28	24.81
La	0.07	0.00	0.00	0.02	0.00	0.00	0.00	0.00
Ce	0.10	0.08	0.06	0.08	0.07	0.04	0.06	0.03
Pr	0.00	0.00	0.00	0.93	0.94	1.15	0.00	0.26
Nd	0.08	0.00	0.28	0.06	0.05	0.12	0.15	0.00
Sm	0.51	0.91	6.75	0.38	0.31	0.48	0.44	0.54
Eu	1.63	2.32	21.02	1.76	1.39	0.75	0.85	1.27
Gd	5.58	6.37	40.85	6.15	3.88	4.07	4.52	5.62
Tb	11.03	12.18	40.67	9.22	7.83	8.43	10.41	10.09
Dy	17.28	18.17	32.98	16.82	13.78	15.37	15.05	17.50
Ho	17.17	18.55	18.71	16.54	17.13	17.56	16.42	16.58
Er	21.32	21.10	14.98	20.39	21.43	21.15	20.82	20.55
Tm	15.48	14.48	8.17	14.52	17.32	15.40	14.97	15.69
Yb	18.55	18.60	6.98	18.93	23.51	17.78	19.91	18.33
Lu	23.41	21.72	23.76	21.01	23.73	19.92	21.04	22.78

Appendix 12 Reference data xenotime

Chondrite	17	18	19	20	21	22	23	24
normalised	FWL8_41	9393-14	9393-15	9393-16	9393-17	9393-18	9393-19	FWL8_41
Y	19.77	23.65	24.82	24.57	24.28	24.35	23.71	20.45
La	0.04	0.00	0.07	0.00	0.00	0.04	0.00	0.00
Ce	0.08	0.09	0.04	0.06	0.06	0.04	0.09	0.04
Pr	0.47	0.24	0.41	0.61	0.00	0.00	0.00	0.00
Nd	0.04	0.17	0.15	0.14	0.02	0.06	0.03	0.12
Sm	5.62	1.25	0.51	0.51	0.52	0.88	0.83	5.34
Eu	19.94	3.10	2.02	1.45	1.13	2.18	1.32	16.49
Gd	38.89	7.37	5.75	5.28	6.37	6.10	5.45	34.44
Tb	38.99	12.48	11.28	9.70	12.20	12.26	12.47	33.21
Dy	32.55	19.41	17.32	16.58	18.24	18.13	18.17	29.93
Ho	18.87	16.45	17.57	17.74	18.29	17.36	16.24	17.12
Er	14.92	22.57	21.64	21.26	21.48	22.19	20.88	13.77
Tm	8.25	17.25	14.68	16.98	15.80	15.98	15.55	9.05
Yb	6.82	19.47	19.75	19.91	19.80	20.07	19.80	8.13
Lu	20.06	25.85	21.98	22.23	22.04	21.85	24.37	20.50

Appendix 12 Reference data xenotime

Chondrite	25	27	28	29	30	31	32
normalised	9399_20	9399_22	9399_23	9399_24	9399_25	9399_26	FWL8_41
Y	23.01	20.58		21.37		22.21	19.58
La	0.00	0.00		0.01		0.00	0.00
Ce	0.05	0.03		0.08		0.07	0.09
Pr	0.08	0.59		0.09		0.17	0.00
Nd	0.00	0.01		0.08		0.00	0.02
Sm	1.48	1.21		2.14		1.49	5.09
Eu	5.66	4.40		7.02		5.47	15.87
Gd	11.55	9.29		13.21		10.81	37.89
Tb	17.84	12.19		17.33		15.10	39.23
Dy	22.49	18.77		22.31		19.94	33.58
Ho	18.19	15.42		16.76		17.47	16.47
Er	18.86	17.22		19.18		18.26	13.99
Tm	10.49	9.60		14.05		12.61	7.34
Yb	12.76	12.87		14.07		13.58	5.78
Lu	20.38	19.51		20.71		21.50	20.12

Appendix 13 monazite

GLITTER4.4: Laser Ablation Analysis Results

D:\ICPCHEM\vdc\141210
Created: Wed Dec 15 12:21:48 2010

All values are reported in ppm

Monazite only, internal standard

GLITTER!: Trace Element Concentrations MDL filtered.

Element	NIST612A	NIST612B	NIST612C	NIST612D	NIST612E	NIST612F	NIST612G	NIST612H	NIST612I
Ca42	81926.48	81286.73	82009.91	89917.93	91406.6	87387.95	95949.27	91617.83	96753.28
Ca43	85999.45	86144.45	87358.64	84908.56	82945.06	80951.48	86017.23	84890.04	82251.63
Sc45	41.41	41.42	41.17	40.96	40.9	38.67	41.36	41.54	40.71
Ti47	48.22	48.6	49.37	50.62	46.18	44.94	47.28	48.35	46.23
V51	40.23	39.49	40.6	39.11	38.06	37.26	39.49	37.2	35.71
Cr53	43.04	41.59	42.51	40.61	42.99	25.36	40.64	40.53	36.78
Mn55	36.12	36.4	37.49	103.5	37.95	33.1	72.36	33.77	31.79
Fe56	63.29	29.83	41.31	239.84	90.85	220.98	20.57	48.54	101.97
Fe57	45.88	49.42	47.56	95.77	189.75	69.72	50.61	52.09	44.31
Ni60	40.76	38.59	40.02	36.97	37.37	36.38	36.92	36.75	34.9
Rb85	32.71	32.05	32.06	31.14	30	31.04	31.29	30.6	29.75
Sr88	76.3	77.05	77.27	75.69	77.26	73.94	74.67	74.36	74.71
Y89	38.65	37.98	37.6	37.56	38.33	37.69	38.15	38.16	39.29
Zr90	35.64	35.84	36.11	40.13	34.84	35.4	34.42	34.67	35.37
Nb93	37.39	36.57	36.92	36.87	77.87	36.48	36.83	35.44	35.24
Cs133	43.06	42.06	43.38	41.95	40.74	38.91	39.79	39.76	38.78
Ba137	37.89	38.01	37.69	37.28	38.24	37.14	37.55	37.45	37.37
La139	35.77	35.77	35.77	35.77	35.77	35.77	35.77	35.77	35.77
Ce140	38.64	38.67	39.78	37.97	38.11	37.89	37.48	37.24	36.26
Pr141	36.99	37.98	37.54	37.51	36.69	36.42	35.93	37.02	36.73
Nd146	35.07	36.38	36.3	35.22	34.33	34.62	33.73	35.99	34.57
Sm147	37.88	38.3	37.7	36.1	35.55	36.22	35.42	36.73	35.29
Eu153	34.13	35.64	34.36	36.43	33.22	33.3	33.56	34.29	33.64
Gd157	37.72	37.86	37.66	35.62	35.64	35.42	36.02	36.69	36.85
Tb159	35.78	36.19	35.71	36.19	35.32	35.88	35.59	37.6	36.68
Dy163	35.75	36.16	36.22	35.92	34.41	36.09	36.24	37.14	36.55
Ho165	37.8	38.44	37.03	38.67	36.78	37.12	37.98	39.83	38.69
Er166	37.39	37.81	36.79	37.72	36.13	37.24	37.15	39.83	38.13
Tm169	38.24	37.55	36.77	37.9	37.08	37.01	37	39.24	38.43
Yb172	41.17	40.08	38.88	39.1	38.68	38.75	39.98	44.43	40.34
Lu175	38.36	37.64	37.18	37.36	37.41	37.17	37.39	39.28	38.63
Hf178	35.39	34.72	34.25	34.61	34.39	34.19	34.69	35.63	36.16
Ta181	40.66	39.51	39.85	39.08	38.99	38.65	39.57	40.85	41
Pb208	45.58	40.26	40.01	39.32	39.9	27.39	38.78	38.46	36.36
Th232	36.02	35.32	35.18	271.18	72.13	33.77	36.47	35.82	36.08
U238	38.95	37.47	38.81	36.3	35.73	34.28	36.55	36.03	34.45

GLITTER!: 1 sigma error.

Appendix 13 monazite

Element	NIST612A	NIST612B	NIST612C	NIST612D	NIST612E	NIST612F	NIST612G	NIST612H	NIST612I
Ca42	12691.54	12717.3	12975.79	20540.25	21487.09	21149.13	23914.19	24993.04	27214.33
Ca43	5966.56	5992.14	6100.6	7476.35	7448.75	7419.33	8041.47	8449.63	8360.86
Sc45	2.21	2.22	2.22	2.66	2.7	2.59	2.82	2.99	2.99
Ti47	4.45	4.5	4.58	5.88	5.48	5.46	5.83	6.38	6.24
V51	4.88	4.8	4.94	6.02	5.98	5.97	6.46	6.47	6.34
Cr53	12.6	12.22	12.57	16.42	17.81	10.79	17.71	19.06	17.73
Mn55	19.29	19.5	20.16	73.38	27.52	24.56	54.92	27.46	26.45
Fe56	177.38	81.37	109.98	573.46	218.08	532.8	49.84	119.5	252.5
Fe57	45.47	48.69	46.69	110.26	222	82.93	61.2	66.19	57.24
Ni60	5.44	5.17	5.39	6.63	6.86	6.85	7.11	7.61	7.4
Rb85	3.81	3.72	3.73	4.46	4.38	4.62	4.74	4.91	4.87
Sr88	11.96	12.09	12.16	15.39	16.05	15.7	16.2	17.22	17.68
Y89	11.93	11.76	11.71	15.6	16.3	16.41	17	18.27	19.26
Zr90	5.72	5.76	5.83	8.46	7.51	7.8	7.76	8.36	8.72
Nb93	12.44	12.18	12.34	15.99	34.5	16.52	17.05	17.52	17.81
Cs133	5.63	5.49	5.66	6.8	6.73	6.55	6.83	7.24	7.2
Ba137	2.17	2.18	2.17	2.57	2.68	2.65	2.72	2.88	2.92
La139	1.16	1.16	1.16	1.16	1.16	1.16	1.16	1.17	1.17
Ce140	7.48	7.47	7.67	9.04	9.25	9.37	9.45	9.94	9.86
Pr141	9.12	9.37	9.28	11.96	11.95	12.12	12.22	13.43	13.62
Nd146	17.07	17.72	17.72	22.31	22.22	22.91	22.81	25.99	25.52
Sm147	6.32	6.4	6.31	7.74	7.78	8.1	8.09	8.94	8.78
Eu153	3.71	3.88	3.75	5.05	4.7	4.81	4.94	5.38	5.39
Gd157	5.34	5.37	5.35	6.55	6.69	6.8	7.06	7.68	7.89
Tb159	1.83	1.86	1.84	2.26	2.24	2.32	2.34	2.62	2.6
Dy163	1.96	1.98	1.99	2.41	2.35	2.52	2.57	2.79	2.8
Ho165	2.14	2.18	2.11	2.73	2.65	2.73	2.84	3.17	3.14
Er166	2.46	2.49	2.44	3.15	3.08	3.24	3.29	3.76	3.68
Tm169	2.07	2.04	2	2.54	2.53	2.57	2.62	2.94	2.94
Yb172	2.87	2.8	2.73	3.5	3.53	3.61	3.8	4.51	4.19
Lu175	2.05	2.02	2	2.46	2.51	2.54	2.6	2.89	2.9
Hf178	1.87	1.83	1.82	2.24	2.26	2.29	2.36	2.58	2.67
Ta181	2.27	2.21	2.23	2.69	2.73	2.76	2.88	3.15	3.23
Pb208	13.64	12.03	11.96	14.84	15.36	10.76	15.55	16.39	15.81
Th232	22.67	22.26	22.24	220.95	60.03	28.71	31.69	33.21	34.18
U238	5.25	5.04	5.21	5.96	5.98	5.84	6.34	6.61	6.44

GLITTER!: Minimum detection limits (99% confidence).

Element	NIST612A	NIST612B	NIST612C	NIST612D	NIST612E	NIST612F	NIST612G	NIST612H	NIST612I
Ca42	53.11	51.41	54.04	44.42	46.28	43.78	42.22	45.84	43.42
Ca43	33.84	29.98	35.36	35.72	39.56	34.16	32.83	41.87	34.17
Sc45	0.0628	0.0566	0.0688	0.0474	0.0563	0.0551	0.0539	0.0526	0.0518
Ti47	0.326	0.532	0.32	0.443	0.392	0.377	0.446	0.337	0.459
V51	0.0144	0.0248	0.0231	0.0275	0.028	0.0235	0.0214	0.0255	0.0307
Cr53	0.7	0.735	0.729	0.704	0.756	0.646	0.641	0.707	0.614
Mn55	0.109	0.107	0.114	0.0939	0.0961	0.0933	0.087	0.0943	0.0897

Appendix 13 monazite

Fe56	2.7	2.56	2.58	1.29	1.3	1.2	1.11	1.07	1.04
Fe57	3	2.73	3.12	2.51	2.11	2	1.83	2.19	1.98
Ni60	0.0723	0.0512	0.103	0.0807	0.0555	0.0796	0.0339	0.0365	0.0365
Rb85	0.011	0.0109	0.00676	0.0126	0.0106	0.00551	0.0117	0.0078	0.0155
Sr88	<0.00000	0.0117	<0.00000	0.00496	0.00931	<0.00000	0.00922	0.00696	0.00694
Y89	0.00846	0.00847	0.00647	0.00833	0.00905	0.01	<0.00000	0.00837	0.00592
Zr90	0.0118	0.0205	<0.00000	0.0114	0.0124	0.0158	0.0106	<0.00000	0.0114
Nb93	<0.00000	0.0062	0.00668	0.0102	<0.00000	0.00578	0.00549	0.00829	0.00827
Cs133	0.00439	0.00619	0.0047	0.00554	0.00518	0.0027	0.00722	<0.00000	0.00268
Ba137	0.0397	<0.00000	<0.00000	0.0525	0.0285	0.0257	<0.00000	<0.00000	<0.00000
La139	<0.00000	<0.00000	<0.00000	0.00377	<0.00000	0.00522	<0.00000	0.00373	0.00372
Ce140	0.00335	<0.00000	0.00358	0.00294	<0.00000	<0.00000	<0.00000	<0.00000	<0.00000
Pr141	0.00464	0.00378	0.00288	<0.00000	0.00382	0.00244	0.00401	0.00246	0.00245
Nd146	<0.00000	0.0157	0.0239	<0.00000	0.0275	<0.00000	<0.00000	0.0145	0.0144
Sm147	<0.00000	0.0184	0.0342	0.0171	0.0185	0.0167	0.0159	<0.00000	<0.00000
Eu153	<0.00000	0.00428	<0.00000	<0.00000	<0.00000	<0.00000	0.00372	0.00887	0.00395
Gd157	0.0186	<0.00000	0.0201	0.0177	<0.00000	<0.00000	0.0165	0.0352	0.0175
Tb159	0.00254	<0.00000	<0.00000	0.00246	0.00267	0.00242	<0.00000	0.0199	0.00492
Dy163	0.0107	<0.00000	0.0116	<0.00000	<0.00000	<0.00000	0.0137	0.0374	0.0207
Ho165	<0.00000	0.00263	0.00401	<0.00000	<0.00000	0.00254	<0.00000	0.0247	0.0172
Er166	<0.00000	<0.00000	<0.00000	<0.00000	<0.00000	<0.00000	<0.00000	0.0465	0.0446
Tm169	<0.00000	<0.00000	0.00378	0.00241	0.00371	0.00237	<0.00000	0.0241	0.0275
Yb172	0.0107	<0.00000	<0.00000	0.0149	0.0114	0.0146	0.00984	0.0597	0.0642
Lu175	<0.00000	0.00447	<0.00000	<0.00000	<0.00000	<0.00000	<0.00000	0.034	0.0315
Hf178	<0.00000	<0.00000	<0.00000	<0.00000	0.0127	0.00814	0.0109	0.0637	0.055
Ta181	0.00312	<0.00000	<0.00000	0.00302	<0.00000	<0.00000	<0.00000	0.0434	0.0377
Pb208	0.0195	0.0167	0.0251	0.0161	0.0195	0.0191	0.0148	0.115	0.106
Th232	<0.00000	0.00268	0.005	0.00359	0.00478	0.00499	0.00237	0.0486	0.042
U238	0.00426	0.00379	0.00406	0.00165	0.00309	0.00227	0.00339	0.0436	0.0453

GLITTER!: Trace element concentrations normalised to chondrite.

Element	NIST612A	NIST612B	NIST612C	NIST612D	NIST612E	NIST612F	NIST612G	NIST612H	NIST612I
Ca42	6.07	6.02	6.07	6.66	6.77	6.47	7.11	6.79	7.17
Ca43	6.37	6.38	6.47	6.29	6.14	6	6.37	6.29	6.09
Sc45	4.79	4.79	4.77	4.74	4.73	4.48	4.79	4.81	4.71
Ti47	0.0737	0.0743	0.0755	0.0774	0.0706	0.0687	0.0723	0.0739	0.0707
V51	0.473	0.465	0.478	0.46	0.448	0.438	0.465	0.438	0.42
Cr53	0.0108	0.0105	0.0107	0.0102	0.0108	0.0064	0.0102	0.0102	0.0093
Mn55	0.0123	0.0124	0.0128	0.035	0.0129	0.0113	0.025	0.0115	0.0108
Fe56	0.00023	0.00011	0.00015	0.0009	0.00033	0.0008	0.00007	0.00017	0.00037
Fe57	0.00017	0.00018	0.00017	0.00034	0.00068	0.00025	0.00018	0.00019	0.00016
Ni60	0.00247	0.00234	0.00243	0.00224	0.00226	0.00221	0.00224	0.00223	0.00211
Rb85	9.48	9.29	9.29	9.03	8.7	9	9.07	8.87	8.62
Sr88	6.41	6.48	6.49	6.36	6.49	6.21	6.28	6.25	6.28
Y89	17.18	16.88	16.71	16.69	17.03	16.75	16.95	16.96	17.46
Zr90	6.43	6.47	6.52	7.24	6.29	6.39	6.21	6.26	6.38
Nb93	99.72	97.51	98.45	98.31	207.65	97.29	98.23	94.49	93.96

Appendix 13 monazite

Cs133	154.32	150.77	155.47	150.35	146.01	139.45	142.6	142.51	139.01
Ba137	11.11	11.15	11.05	10.93	11.21	10.89	11.01	10.98	10.96
La139	97.47	97.47	97.47	97.47	97.47	97.47	97.47	97.47	97.47
Ce140	40.38	40.41	41.56	39.68	39.82	39.59	39.16	38.91	37.89
Pr141	269.98	277.21	274.03	273.76	267.84	265.82	262.26	270.22	268.13
Nd146	49.32	51.17	51.05	49.54	48.28	48.7	47.44	50.62	48.63
Sm147	163.98	165.82	163.21	156.3	153.88	156.8	153.34	159.01	152.78
Eu153	392.32	409.66	394.89	418.73	381.8	382.75	385.69	394.16	386.62
Gd157	123.27	123.74	123.09	116.42	116.46	115.75	117.71	119.89	120.43
Tb159	616.92	623.99	615.67	623.95	608.89	618.6	613.62	648.19	632.42
Dy163	93.83	94.91	95.06	94.27	90.31	94.72	95.12	97.48	95.92
Ho165	444.14	451.75	435.17	454.42	432.21	436.14	446.34	468.07	454.6
Er166	150.17	151.85	147.75	151.49	145.09	149.55	149.22	159.98	153.12
Tm169	1074.22	1054.65	1032.73	1064.54	1041.61	1039.65	1039.2	1102.23	1079.56
Yb172	166	161.61	156.78	157.66	155.98	156.25	161.21	179.13	162.66
Lu175	1006.7	988.02	975.81	980.45	981.93	975.48	981.47	1030.9	1013.78
Hf178	197.7	193.96	191.33	193.36	192.13	191.02	193.79	199.07	202.02
Ta181	1563.72	1519.45	1532.71	1503.18	1499.59	1486.45	1521.93	1571.33	1576.98
Pb208	12.49	11.03	10.96	10.77	10.93	7.51	10.62	10.54	9.96
Th232	847.49	831.14	827.76	6380.69	1697.19	794.56	858.17	842.85	848.96
U238	3192.3	3071.56	3181.44	2975.48	2928.7	2809.56	2995.88	2953.62	2823.93

Appendix 13 monazite

= 16wt% La2O3

NIST612J	NIST612K	NIST612L	NIST612M	NIST612N	326M1	326M2	326M3	326C1	326C2
98364.72	68483.12	68147.33	70445.07	68335.63	407.6	549.37	683.25	**********	**********
83026.94	97626.77	86977.41	90264.95	88008.09	1548.98	1696.19	1691.86	**********	**********
41.4	44.03	41.26	40.62	41.27	0.293	0.132	0.273	3779.24	6018.47
48.23	47.84	51.75	56.99	48.39	581.05	175.14	113.44	<8969.66	12868.42
36.78	43.71	44.51	48.75	44.97	40.93	32.11	15.01	6744.45	33411.64
38.29	47	51.38	61.7	56.47	<0.80	<0.71	<0.65	<16098.82	<18703.06
32.15	37.39	40.45	41.11	40.15	43.94	31.22	17.2	**********	**********
25.07	151.53	50.01	248.74	23.93	4069.08	5421.83	2952.49	**********	**********
33	98.89	38.22	46.98	51.95	4082.74	5401.11	3117.71	**********	**********
36.29	42.5	47.14	47.44	48.22	1.68	0.06	<0.054	5604.68	8815.75
29.55	34.78	37.75	38.62	37.3	0.203	0.78	0.364	<304.87	1812.09
74.08	76.91	78.91	81.77	77.45	899.91	994.5	910	**********	**********
39.1	38.83	36.33	288.1	38.64	194.43	177.42	195.09	824211.5	1372851
35.94	37.2	59.2	33.98	33.93	8.08	4.84	6.92	633.48	1412.48
36.26	36.26	38.32	39.9	39.89	121.51	34.87	18.94	2218.45	9231.52
38.71	47.52	51.05	51.2	48.3	<0.0066	0.0302	0.179	72.05	<115.59
36.56	39.39	42.3	37.46	39.39	591.09	695	690.85	3380271	4066704
35.77	35.77	35.77	35.77	35.77	143250.9	143250.9	143250.9	460449.4	460449.5
36.01	40.28	38.47	41.96	41.47	226950.6	223286.4	216947.4	1264229	1292682
36.29	36.54	39.53	38.69	39.11	25478.75	24446.17	24452.63	190514.1	204932.8
34.28	35.25	33.1	35.65	35.42	82455.66	77915.06	81087.51	882333.8	973886.6
35.6	36.23	33.88	35.57	34.67	7969.23	7199.71	7502.32	224544.5	253699.1
33.78	34.82	35.07	36.59	35.37	1291.2	1134.16	1261.84	72561.05	87831.42
36.34	37.53	34.01	35.69	58.5	2486.68	2249.04	2383.49	216721.5	269017.9
36.84	36.64	33.82	33.88	34.21	99.51	89.23	99.33	29759.98	41806.13
36.21	37.31	33.89	34.86	36.23	204.35	189.04	207.69	175210.3	277715.4
39.35	37.51	36.59	36.47	36.84	14.43	13.12	13.94	32246.41	55786.54
38.69	40.14	36.31	36.24	35.57	18.67	17.17	19.29	85651.25	151902.7
38.61	38.26	35.49	36.57	36.59	0.584	0.482	0.603	12565.19	23713.19
40.66	41.8	38.59	39.5	39.92	1.48	1.53	1.94	78763.02	173808.5
39.06	39.11	35.67	35.74	36.42	0.086	0.096	0.128	13285.49	25794.4
35.46	35.81	32.76	33.91	33.94	0.079	0.086	0.109	173.53	321.68
40.25	42.17	39	40.28	38.97	0.177	0.0645	0.0443	<71.04	24.39
36.78	47.43	53.77	53.98	54.27	196.5	201.59	184.36	69414.52	84698.96
35.73	36.39	34.04	33.16	33.66	7616.31	7545.2	7462.6	1651.57	1201.14
35.07	42.53	39.86	44.42	45.25	1.43	2.71	5.36	1795.01	2992.72

Appendix 13 monazite

NIST612J	NIST612K	NIST612L	NIST612M	NIST612N	326M1	326M2	326M3	326C1	326C2
28532.4	20498.48	21044.7	22444.46	22466.25	140.2	193.61	248.5	**********	**********
8614.96	10386.28	9456.58	10013.46	9961.34	184.15	204.32	213.02	**********	**********
3.09	3.41	3.26	3.27	3.37	0.043	0.03	0.049	783.35	1087.77
6.62	7	7.79	8.6	7.47	86.46	26.66	17.75	3362.82	6097.05
6.67	8.1	8.42	9.4	8.84	8.19	6.55	3.13	1543.04	7346.76
18.93	23.89	26.79	32.9	30.86	0.36	0.45	0.32	7081.51	9344.54
27.36	32.57	36.03	37.45	37.4	41.84	30.39	17.12	**********	**********
62.46	379.72	126.13	631	61.11	10450.24	14010.43	7676.44	**********	**********
43.34	131.99	52.25	64.85	72.78	5799.32	7790.36	4565.34	**********	**********
7.88	9.5	10.79	11.11	11.55	0.43	0.036	0.024	2173.21	3180.81
4.93	5.92	6.55	6.82	6.71	0.041	0.15	0.075	130.15	461.38
17.91	19.02	19.93	21.1	20.4	241.78	272.76	254.73	**********	**********
19.62	19.95	19.12	155.1	21.29	109.58	102.3	115.05	497122.7	846569.7
9.06	9.61	15.62	9.18	9.36	2.28	1.39	2.04	293.68	620.01
18.73	19.15	20.68	22	22.47	69.87	20.47	11.35	1393.83	5801.83
7.32	9.17	10.04	10.26	9.85	0.0028	0.0078	0.041	39.33	37.29
2.91	3.3	3.61	3.25	3.45	50.38	60.28	61.02	305519.3	374079.1
1.17	1.24	1.25	1.24	1.23	4530.02	4530.02	4530.05	15348.3	15469.47
9.98	11.38	11.07	12.3	12.37	68877.84	68969.3	68185.64	404348.8	420510.6
13.74	14.14	15.62	15.61	16.11	10703.78	10479.62	10693.94	85010.43	93248.19
25.85	27.16	26.06	28.66	29.08	69073.96	66617.24	70743.83	785377.1	884126
9.04	9.42	8.99	9.63	9.58	2239.15	2063.74	2193.4	67156.7	77354.59
5.52	5.83	5.99	6.38	6.29	233.43	209.14	237.3	13993.87	17262.2
7.95	8.42	7.8	8.35	13.95	603.76	557.52	603.15	56226.43	71188.3
2.66	2.72	2.57	2.61	2.69	7.86	7.18	8.15	2594.69	3685.96
2.83	3.02	2.81	2.94	3.1	17.4	16.41	18.38	16230.76	26038.87
3.26	3.19	3.18	3.23	3.32	1.32	1.22	1.33	3223.17	5632.12
3.81	4.07	3.76	3.83	3.83	2.04	1.91	2.2	10138.11	18199.43
3.01	3.07	2.9	3.05	3.11	0.053	0.045	0.06	1233.63	2304.98
4.31	4.57	4.32	4.51	4.65	0.18	0.19	0.26	10157.5	22567
2.99	3.08	2.86	2.92	3.03	0.01	0.011	0.017	1279.2	2453.95
2.66	2.79	2.61	2.74	2.79	0.015	0.015	0.023	101.32	185.57
3.23	3.47	3.28	3.45	3.4	0.019	0.009	0.0092	21.95	24.5
16.31	21.46	24.81	25.4	26.02	96	100.34	93.48	35866.8	44555.53
34.58	35.99	34.39	34.21	35.46	8192.42	8284.95	8363.28	1896.5	1410.77
6.67	8.25	7.87	8.93	9.25	0.3	0.57	1.15	416.88	693.55

NIST612J	NIST612K	NIST612L	NIST612M	NIST612N	326M1	326M2	326M3	326C1	326C2
42.07	172.88	370.82	190.17	188.61	54.1	49.36	46.01	1092029	1463737
36.01	130.94	289.87	146.95	158.14	43.04	36.47	35.76	803120.5	1117810
0.0468	0.21	0.306	0.209	0.192	0.0614	0.0538	0.0522	1163.94	1573.65
0.382	1.18	3.33	1.33	1.31	0.503	0.197	0.349	8969.66	10660.78
0.0232	0.0856	0.121	0.0736	0.103	0.0198	0.02	0.0259	427.88	813.96
0.589	2.54	5.08	2.52	2.88	0.797	0.709	0.653	16098.82	18703.06
0.0889	0.355	0.734	0.353	0.362	0.106	0.092	0.0897	2134.33	2629.08

Appendix 13 monazite

0.964	3.85	8.33	4.08	4	1.08	0.938	0.877	19874.15	25056.6
1.99	7.13	18.63	8.09	7.34	2.4	2.2	1.99	40877.64	56446.34
0.0694	0.24	0.68	0.223	0.339	0.0654	0.0572	0.0544	2471.46	3338.2
0.0544	0.0412	<0.00000	0.0462	0.0247	0.00948	0.0101	0.00955	304.87	236.33
0.0123	0.0321	<0.00000	<0.00000	0.0224	0.00862	0.00922	0.0101	114.18	217.41
0.00796	0.0389	<0.00000	0.0255	<0.00000	<0.00000	0.00923	0.0139	281.34	189.83
<0.00000	0.0746	<0.00000	0.0487	0.0741	0.0247	0.0176	0.0118	<0.00000	624.88
0.00785	0.0383	<0.00000	<0.00000	0.0465	0.00729	<0.00000	0.0104	236.65	<0.00000
0.0273	0.0175	0.0491	0.016	0.021	0.00656	0.00404	0.0066	<0.00000	115.59
<0.00000	0.138	<0.00000	0.11	0.167	<0.00000	0.028	0.0375	<0.00000	808.18
0.00353	0.014	<0.00000	0.0224	0.017	0.00653	<0.00000	<0.00000	<0.00000	<0.00000
<0.00000	0.0212	<0.00000	<0.00000	<0.00000	0.00344	<0.00000	0.00282	<0.00000	<0.00000
0.00465	0.016	<0.00000	<0.00000	<0.00000	0.00304	0.00265	0.00501	113.43	76.3
<0.00000	<0.00000	0.266	0.0868	0.132	0.0179	<0.00000	0.0148	<0.00000	<0.00000
<0.00000	0.0634	<0.00000	0.101	<0.00000	0.036	0.0181	0.0172	549.45	522.64
<0.00000	0.0149	<0.00000	<0.00000	0.0313	0.00693	<0.00000	0.00405	<0.00000	123.24
0.0288	<0.00000	<0.00000	<0.00000	0.114	0.0218	0.0191	<0.00000	409.36	551.31
0.00963	<0.00000	0.0456	0.0183	0.0196	0.00308	0.0027	0.00362	<0.00000	<0.00000
0.0295	0.0555	<0.00000	0.0444	0.0478	<0.00000	<0.00000	0.0187	244.23	<0.00000
0.0165	0.017	<0.00000	0.0111	0.012	0.00461	<0.00000	<0.00000	61.39	<0.00000
0.0277	<0.00000	<0.00000	<0.00000	<0.00000	<0.00000	<0.00000	0.00786	252.06	240.38
0.0262	0.0159	<0.00000	0.0104	<0.00000	<0.00000	0.00266	<0.00000	80.84	109.04
0.0744	<0.00000	<0.00000	<0.00000	0.0488	<0.00000	<0.00000	<0.00000	<0.00000	337.84
0.0377	0.0135	<0.00000	0.0108	0.0116	0.00315	0.00276	0.00262	59.32	<0.00000
0.0747	0.0444	<0.00000	0.0502	<0.00000	0.0104	<0.00000	0.00862	<0.00000	263.64
0.0532	0.0114	<0.00000	0.0129	0.0196	<0.00000	0.0033	0.00443	71.04	<0.00000
0.125	0.0743	0.133	0.0856	0.0569	0.0164	0.017	0.015	276.32	578.18
0.0512	0.019	<0.00000	<0.00000	0.0115	0.00444	0.00274	<0.00000	58.79	111.96
0.035	0.0103	<0.00000	0.00664	0.0123	0.00333	0.00289	0.00352	71.03	116.64

NIST612J	NIST612K	NIST612L	NIST612M	NIST612N	326M1	326M2	326M3	326C1	326C2
7.29	5.07	5.05	5.22	5.06	0.03	0.041	0.051	486398.2	656728.4
6.15	7.23	6.44	6.69	6.52	0.115	0.126	0.125	400942.2	549154
4.79	5.1	4.78	4.7	4.78	0.0339	0.0152	0.0316	437.41	696.58
0.074	0.073	0.079	0.087	0.074	0.89	0.268	0.173	0	19.68
0.433	0.514	0.524	0.57	0.53	0.481	0.378	0.177	79.35	393.08
0.0096	0.0118	0.0129	0.0155	0.0142	0	0	0	0	0
0.0109	0.013	0.014	0.014	0.014	0.015	0.011	0.0059	42589.03	55113.03
0.00009	0.0005	0.00018	0.0009	0.00009	0.015	0.02	0.011	215.15	284.94
0.00012	0.00036	0.00014	0.00017	0.00019	0.015	0.019	0.011	209.68	282.1
0.0022	0.00258	0.00286	0.00288	0.00292	0.0001	0	0	0.34	0.53
8.57	10.08	10.94	11.19	10.81	0.059	0.228	0.105	0	525.24
6.23	6.46	6.63	6.87	6.51	75.62	83.57	76.47	**********	**********
17.38	17.26	16.15	128.05	17.17	86.41	78.85	86.7	366316.2	610156
6.49	6.71	10.69	6.13	6.12	1.46	0.87	1.25	114.35	254.96
96.69	96.68	102.18	106.4	106.37	324.02	92.98	50.5	5915.88	24617.4

Appendix 13 monazite

138.74	170.32	182.99	183.52	173.13	0	0.108	0.64	258.23	0
10.72	11.55	12.4	10.98	11.55	173.34	203.81	202.59	991281.8	1192582
97.47	97.47	97.47	97.47	97.47	390329.5	390329.5	390329.5	1254631	1254631
37.63	42.09	40.2	43.84	43.33	237147.9	233319.1	226695.3	1321034	1350765
264.89	266.68	288.55	282.41	285.49	185976.3	178439.2	178486.3	1390614	1495860
48.21	49.58	46.55	50.13	49.82	115971.4	109585.2	114047.1	1240976	1369742
154.13	156.85	146.65	153.98	150.09	34498.83	31167.57	32477.57	972054.3	1098265
388.25	400.2	403.1	420.55	406.51	14841.39	13036.36	14503.9	834035.1	1009557
118.77	122.65	111.14	116.62	191.19	8126.4	7349.8	7789.19	708240.3	879143.6
635.24	631.66	583.15	584.16	589.88	1715.74	1538.41	1712.66	513103.1	720795.4
95.04	97.92	88.95	91.5	95.09	536.36	496.18	545.13	459869.5	728911.8
462.43	440.73	429.97	428.5	432.94	169.59	154.2	163.86	378923.7	655540.9
155.39	161.2	145.82	145.55	142.86	74.98	68.94	77.47	343980.9	610050.9
1084.69	1074.7	996.83	1027.13	1027.94	16.42	13.53	16.93	352954.7	666100.8
163.95	168.55	155.6	159.27	160.97	5.97	6.17	7.82	317592.8	700840.6
1025.33	1026.58	936.13	938.09	955.92	2.25	2.53	3.37	348700.6	677018.3
198.08	200.03	182.99	189.44	189.61	0.44	0.482	0.61	969.42	1797.08
1548.19	1622.05	1499.82	1549.37	1498.7	6.82	2.48	1.71	0	937.93
10.08	13	14.73	14.79	14.87	53.84	55.23	50.51	19017.68	23205.19
840.7	856.28	800.97	780.16	791.94	179207.2	177534	175590.5	38860.54	28262.18
2874.87	3485.71	3267.41	3641.1	3708.85	117.36	222.06	439.09	147132	245304.9

Appendix 13 monazite

326L1	326L2	326L3	326L4	NIST612O	NIST612P	NIST612Q	NIST612R	326L5	326L6
67920.58	80743.42	196256.1	2327579	9200125	77521.2	77958.55	84584.61	64638.46	112621.4
55128.1	66419.09	149487.1	1686242	*********	86776.27	89322.26	88720.05	75935.1	76994.67
1.91	1.67	0.117	6.19	5329.48	40.18	40.94	42.52	0.506	0.111
49.09	72.01	12.09	26.62	6528.51	44.85	47.24	48.47	73.66	35.94
27.76	46.34	11.04	243.09	5283.81	41.69	40.6	42.12	54.17	38.58
0.74	1.09	6.15	<7.85	5632.11	44.02	43.9	49.63	<0.78	0.89
207.3	899.43	2667.35	62388.99	4930.04	34.72	36.43	34.57	27984.39	920.39
9120.38	23597.34	6680.87	269870.8	12657.28	94.45	143.87	354.84	48302.64	3056.69
12313.46	33994.27	6538.53	431920.4	12833.26	57.75	38.53	117.33	75824.97	2963.28
0.34	0.135	0.35	2.67	5103.11	38.13	39.94	43.16	1.45	0.3
0.208	0.52	0.214	0.72	4028.2	32.32	32.87	34.01	0.385	0.54
3068.25	3190.78	5382.08	17370.56	10393.82	73.77	75.11	167.81	4964.68	4426.54
429.39	470.74	449.39	973.12	4760.73	36.4	35.69	39.42	324.72	560.76
423.33	316.87	9.77	25.21	3884.23	32.91	33.79	50.41	10.09	5.56
349.38	639.95	29.7	101.59	4417.75	36.33	35.91	40.13	453.31	87.18
0.148	0.055	0.05	<0.041	5313.38	43.27	46.68	45.17	0.0208	0.191
7.39	11.09	65.23	584.27	4829.98	36.14	36.73	41.23	1210.21	26.28
145638.5	145638.5	68726.35	127732.1	101723.7	35.77	35.77	35.77	144956.3	98058.68
181374.8	183596.3	91865.32	275685.6	186156.7	35.67	43.98	94.02	176637.4	136041.3
18296.2	18443.07	9440.34	23428.54	4310.2	302.4	40.79	38.26	16750.87	14080.06
51241.25	51108.4	27485.96	79846.9	4066.77	875.05	33.3	51.27	48328.99	43208.15
2718.25	2682.73	2098.29	2863.14	5499.15	37.8	33.74	52.93	2442.01	2358.32
361.03	366.83	287.44	394.64	4258.91	53.17	33.4	35.31	286.47	280.18
629.09	642.42	510.46	768.15	4402.78	44.91	35.87	41.93	620.42	456.36
35.08	37.02	27.72	51.92	4332.72	34.46	35.25	37.29	34.45	27.54
114.26	119.78	100.6	235.3	4205.37	38.32	35.4	38.08	112.7	105.34
14.51	15.46	15.12	41.7	4598.63	34.84	37.68	39.96	13.58	16.62
31.43	33.16	35.71	114.08	6373.19	33.89	37.2	40.57	29.91	39.78
3.65	3.79	4.01	14.57	4532.87	35.15	37.5	39.25	3.03	4.44
23.03	22.8	23.54	85.18	5042.64	37.54	39.05	42.18	16.23	24.04
2.91	2.98	2.39	12.28	4633.35	35.69	38.01	39.64	2.11	2.72
0.862	1.04	0.035	<0.096	4291.46	32.7	33.78	37.29	0.046	0.312
0.0539	0.069	0.252	0.082	4954.94	36.17	40.05	42.53	0.0398	0.0231
33.91	64.5	59.33	756.05	6013.61	43.45	47.57	49.2	509.57	30.79
1034.84	1036.64	452.43	1642.14	5270.41	32.27	34.43	36.31	852.67	1059.48
71.92	76.04	158.71	269.02	4840.52	37.46	43.23	42.09	138.66	49.83

Appendix 13 monazite

326L1	326L2	326L3	326L4	NIST612O	NIST612P	NIST612Q	NIST612R	326L5	326L6
27014.74	33164.15	83248.72	1019745	4163652	36253.34	37661.86	42221.23	33332.22	60018.64
7021.01	8634.41	19815.34	227955.7	1564199	12264.06	12851.73	13016.09	11312	11684.1
0.18	0.18	0.035	0.77	522.92	4.06	4.19	4.44	0.075	0.024
8.14	12.22	2.24	5.91	1209.8	8.62	9.09	9.51	14.2	7.04
6.11	10.39	2.53	56.53	1251.8	10.07	9.97	10.52	13.73	9.94
0.51	0.78	4.09	4.14	3885.51	31.07	31.64	36.54	0.49	0.71
219.85	974.01	2948.85	70398.61	5677.04	40.79	43.65	42.24	34860.59	1168.68
24147.89	62851.19	17899.45	727256.3	34306.06	257.46	394.36	977.98	133849.5	8515.53
18842.68	52765.99	10292.46	689342.3	20773.59	94.82	64.12	197.54	129233.7	5114.02
0.11	0.076	0.13	0.99	1530.17	11.71	12.5	13.79	0.5	0.11
0.044	0.11	0.05	0.19	858.62	7.01	7.24	7.6	0.092	0.13
911.91	967.02	1662.91	5470.31	3336.56	24.14	25.03	56.94	1713.87	1555.36
270.63	303.2	295.75	654.2	3269.26	25.53	25.55	28.8	242.03	426.4
132.31	101.09	3.19	8.43	1318.36	11.4	11.93	18.13	3.7	2.08
222.56	415.83	19.68	68.65	3043.01	25.51	25.68	29.24	336.27	65.85
0.035	0.015	0.014	0.024	1286.83	10.66	11.68	11.48	0.0071	0.051
0.71	1.1	6.34	57.59	498.19	3.85	3.92	4.47	128.52	2.85
4605.51	4605.54	2173.37	4039.63	3233.09	1.28	1.25	1.26	4583.97	3100.91
59969.18	61707.95	31379.67	95680.68	65630.85	12.78	16	34.71	66142.84	51684.59
8483.82	8716.21	4546.1	11493.38	2153.86	153.88	21.13	20.17	8982.82	7680.74
47427.3	48221.78	26429.88	78228.81	4059.58	889.4	34.46	54.01	51798.91	47115.35
842.09	846.9	674.83	937.95	1837.77	12.88	11.69	18.65	873.71	858.18
71.92	74.47	59.45	83.15	914.76	11.64	7.44	8.01	65.92	65.58
169.12	176.15	142.72	219.03	1283.21	13.34	10.85	12.92	194.05	145.32
3.04	3.27	2.5	4.8	405.68	3.31	3.44	3.7	3.45	2.8
10.7	11.44	9.79	23.44	430.76	4.02	3.77	4.12	12.21	11.6
1.46	1.59	1.59	4.49	502.29	3.9	4.29	4.64	1.6	1.99
3.78	4.08	4.48	14.65	833.09	4.55	5.07	5.64	4.21	5.69
0.35	0.37	0.4	1.49	462.54	3.68	3.99	4.25	0.34	0.5
3.01	3.05	3.21	11.93	717.9	5.48	5.79	6.38	2.49	3.75
0.27	0.29	0.24	1.24	462.49	3.65	3.95	4.2	0.23	0.3
0.086	0.11	0.012	0.064	422.02	3.31	3.46	3.88	0.013	0.039
0.0076	0.012	0.032	0.03	518.33	3.88	4.36	4.72	0.0087	0.0043
18.14	35.12	32.87	425.95	3445.28	25.31	28.16	29.59	311.25	19.1
1231.46	1257.99	559.76	2070.97	6773.72	42.25	45.93	49.32	1179.32	1491.67
16.23	17.44	36.97	63.66	1163.2	9.15	10.71	10.58	35.31	12.87

326L1	326L2	326L3	326L4	NIST612O	NIST612P	NIST612Q	NIST612R	326L5	326L6
31.37	38.66	49.11	515.7	26326.22	181.42	179.13	195.41	55.96	36.38
27.94	25.82	33.61	461	22588.69	152.87	138.56	134.53	50.91	30.39
0.0293	0.0419	0.0491	0.481	27.8	0.217	0.188	0.219	0.0642	0.0389
0.227	0.213	0.366	3.27	166.51	1.53	1.52	1.37	0.495	0.224
0.0162	0.02	0.0295	0.254	11.78	0.0923	0.0899	0.11	0.0258	0.0228
0.398	0.549	0.688	7.85	346.45	2.82	2.51	2.5	0.783	0.473
0.0624	0.07	0.1	1.03	52.83	0.344	0.332	0.371	0.109	0.066

Appendix 13 monazite

0.55	0.635	0.809	8.25	406.78	2.71	2.65	2.84	0.797	0.482
1.2	1.5	1.88	18.94	926.65	6.14	6.45	7.03	1.94	1.24
0.0471	0.094	0.0577	0.432	22.06	0.307	0.291	0.323	0.105	0.0851
0.00855	0.00877	0.00803	0.0597	5.25	0.0325	0.025	0.0516	0.0141	0.00897
0.00499	0.00702	0.00745	<0.00000	4.9	0.0248	0.0234	0.0259	0.00592	0.00758
<0.00000	0.0112	0.0113	0.12	3.53	0.0439	<0.00000	0.04	0.0106	0.00959
0.0166	<0.00000	<0.00000	0.131	9.44	<0.00000	0.0555	0.0615	0.0141	0.0127
0.00423	0.00486	0.00893	0.0666	7.58	0.021	0.0281	0.0382	0.0159	<0.00000
0.00324	0.00303	0.00481	0.0413	<0.00000	0.0205	0.0122	0.0135	0.00307	0.00339
<0.00000	0.0213	<0.00000	0.291	<0.00000	0.159	<0.00000	0.136	<0.00000	0.0198
0.00378	0.00307	<0.00000	<0.00000	3.02	0.0229	0.0125	<0.00000	0.00447	0.00405
0.00195	0.00316	0.00501	0.0304	1.54	0.0165	0.00898	0.0172	<0.00000	<0.00000
<0.00000	0.00402	0.00369	0.0389	1.4	0.00866	0.00818	0.00905	0.00292	<0.00000
0.0146	0.0167	<0.00000	0.28	8.23	0.051	0.0681	0.0533	0.0172	0.011
0.012	0.0138	0.0253	0.188	9.57	0.0593	0.0792	0.0876	<0.00000	<0.00000
0.00283	0.00459	0.00596	0.0444	<0.00000	0.014	0.0132	0.0146	<0.00000	<0.00000
0.0179	<0.00000	0.0189	0.345	17.59	0.063	0.0596	0.114	0.0213	<0.00000
0.00311	<0.00000	0.00269	<0.00000	<0.00000	<0.00000	0.017	0.00944	<0.00000	0.00196
<0.00000	0.00871	0.0113	0.12	<0.00000	0.0655	<0.00000	0.0562	0.0128	0.00823
0.00191	0.0031	0.00404	0.0302	1.54	0.00957	<0.00000	0.0201	<0.00000	<0.00000
<0.00000	0.00636	<0.00000	0.0874	<0.00000	<0.00000	0.0262	0.0291	<0.00000	<0.00000
<0.00000	0.00289	<0.00000	<0.00000	<0.00000	0.00888	0.0119	0.00933	<0.00000	0.00194
<0.00000	<0.00000	<0.00000	<0.00000	6.28	<0.00000	0.037	0.058	0.0265	0.00851
0.00184	<0.00000	<0.00000	<0.00000	1.48	<0.00000	0.0174	0.0137	0.00313	<0.00000
<0.00000	0.00697	<0.00000	0.0958	4.89	<0.00000	0.0406	<0.00000	<0.00000	<0.00000
<0.00000	<0.00000	0.00329	<0.00000	1.77	0.011	<0.00000	0.02	0.00647	<0.00000
0.00989	0.0116	0.0175	0.158	7.42	0.0545	0.0524	0.0655	0.0171	0.00981
0.00364	<0.00000	0.00384	0.0286	<0.00000	0.0128	0.0171	0.0164	0.00432	0.00277
0.00267	0.00216	0.00279	0.0293	<0.00000	0.0106	0.00706	0.0055	0.00433	0.00195

326L1	326L2	326L3	326L4	NIST612O	NIST612P	NIST612Q	NIST612R	326L5	326L6
5.03	5.98	14.54	172.41	681.49	5.74	5.77	6.27	4.79	8.34
4.08	4.92	11.07	124.91	839.12	6.43	6.62	6.57	5.62	5.7
0.221	0.194	0.0135	0.717	616.84	4.65	4.74	4.92	0.0585	0.0128
0.075	0.11	0.0185	0.0407	9.98	0.069	0.072	0.074	0.113	0.055
0.327	0.55	0.13	2.86	62.16	0.49	0.48	0.5	0.64	0.45
0.00019	0.00027	0.0015	0	1.42	0.0111	0.011	0.0125	0	0.00022
0.071	0.31	0.91	21.22	1.68	0.012	0.012	0.012	9.52	0.31
0.033	0.08	0.024	0.97	0.05	0.00034	0.0005	0.0013	0.17	0.011
0.044	0.12	0.024	1.55	0.046	0.00021	0.00014	0.00042	0.27	0.011
0.00002	0.00001	0.00002	0.00016	0.309	0.00231	0.00242	0.00262	0.00009	0.00002
0.06	0.152	0.062	0.209	1167.59	9.37	9.53	9.86	0.111	0.156
257.84	268.13	452.28	1459.71	873.43	6.2	6.31	14.1	417.2	371.98
190.84	209.22	199.73	432.5	2115.88	16.18	15.86	17.52	144.32	249.23
76.41	57.2	1.76	4.55	701.13	5.94	6.1	9.1	1.82	1
931.67	1706.53	79.2	270.91	11780.67	96.88	95.75	107.01	1208.83	232.48

Appendix 13 monazite

0.53	0.197	0.181	0	19044.38	155.09	167.33	161.89	0.075	0.68
2.17	3.25	19.13	171.34	1416.42	10.6	10.77	12.09	354.9	7.71
396835	396835	187265.3	348043.8	277176.2	97.47	97.47	97.47	394976.3	267189.8
189524.4	191845.6	95993.02	288072.7	194521.1	37.27	45.96	98.25	184574.1	142154
133548.9	134621	68907.59	171011.2	31461.29	2207.3	297.75	279.25	122269.1	102774.2
72069.26	71882.42	38658.17	112302.2	5719.78	1230.73	46.83	72.11	67973.27	60770.96
11767.29	11613.55	9083.5	12394.55	23805.82	163.65	146.05	229.14	10571.46	10209.18
4149.79	4216.45	3303.96	4536.1	48952.96	611.13	383.87	405.89	3292.79	3220.49
2055.84	2099.41	1668.18	2510.29	14388.17	146.77	117.23	137.01	2027.52	1491.37
604.76	638.26	478	895.14	74702.05	594.22	607.73	642.88	593.96	474.82
299.91	314.38	264.04	617.58	11037.73	100.59	92.91	99.94	295.81	276.49
170.47	181.69	177.67	490.06	54037.9	409.44	442.79	469.62	159.62	195.25
126.23	133.18	143.42	458.16	25595.15	136.11	149.4	162.95	120.14	159.75
102.63	106.37	112.51	409.23	127327.7	987.47	1053.44	1102.62	85.02	124.61
92.86	91.92	94.93	343.46	20333.21	151.37	157.48	170.08	65.46	96.92
76.37	78.18	62.73	322.19	121610.3	936.68	997.67	1040.38	55.31	71.43
4.81	5.8	0.198	0	23974.63	182.69	188.71	208.3	0.259	1.74
2.07	2.66	9.7	3.15	190574.7	1391.08	1540.41	1635.58	1.53	0.89
9.29	17.67	16.26	207.14	1647.56	11.9	13.03	13.48	139.61	8.44
24349.07	24391.51	10645.35	38638.61	124009.8	759.19	810.14	854.31	20062.93	24929.05
5894.74	6233.1	13008.75	22050.71	396764.2	3070.89	3543.24	3449.65	11365.45	4084.31

Appendix 13 monazite

326CE1	NIST612S	NIST612T	NIST612U	NIST612V	NIST612W	NIST612X	NIST612Y
52280.65	*********	*********	94100.57	*********	85644.46	85967.66	89825.02
36723	*********	*********	106755.7	*********	83579.67	83806.7	86722.21
0.087	126840.3	109546.9	42.82	38272.1	42.47	40.95	41.8
4.97	149554.6	127920.6	43.08	42198.05	55.33	54.85	55.17
2.1	118027.1	115231.7	63.23	45155.24	37.94	39.32	41.36
0.21	149980.1	126675.1	45.63	56115.94	46.35	38.53	49.25
1223.12	101937.6	92417.36	37.84	37162.93	34.43	32.46	66.91
7449.71	38219.84	34519.96	7.62	20107.91	136.54	16.16	11.98
11906.41	51352.5	267300.6	39.19	168700.4	35.39	26.7	35.28
0.072	118761.6	120499.9	48.81	49148.89	40.82	39.96	42.78
0.199	102175.5	95348.59	44.21	38686.36	31.59	30.53	31.34
1637.68	233730.3	224767.3	81.3	74711.89	70.86	62.31	74.95
14.04	89912.52	97579.54	41.64	47559.65	35.1	37.79	34.75
1.01	102203.9	83648.57	37.2	31873.04	32.32	29.34	35.68
57.94	98130.12	97633.74	37.02	37711.71	34.14	34.76	36.03
0.0162	124414	124366.1	52.38	48361.31	47.29	42.19	41.74
405.97	114174.2	98219.16	40.65	49561.1	36.89	35.98	38.36
1875.91	101723.7	101723.7	35.77	101723.7	35.77	35.77	35.77
4153.18	2179689	228126.6	52.02	80467.82	36.07	31.71	37.16
481.07	104783.1	98002.05	38.55	40156.32	32.22	35.33	35.16
1141.78	976209.3	7871594	325.68	40201.71	34.05	31.19	32.19
62.66	102822.8	281289.1	41.92	33575.87	61.8	78.57	34.71
10.37	105000.9	106577.7	36.95	33206.69	30.18	30.5	35.61
16.81	96717.34	99898.92	37.41	35719.96	34.88	33.88	37.08
1.05	92654.41	93238.48	38.41	34926.35	34.89	35.33	37.59
3.85	110924.5	90850.16	39.39	38135.25	33.75	32	34.99
0.53	104924.2	98505.52	38.24	38894.82	35.91	38.37	37.02
1.4	97430.37	96704.26	42.88	39240.4	33.33	35.58	37.2
0.182	111394.9	100385.3	40.01	36761.1	34.28	36.43	40.39
1.12	107224.8	104363	42.12	36806.87	38	38.41	39.81
0.155	104353.2	101916.7	41.57	39141.48	35.47	36.81	38.05
0.0081	94978.58	87872.47	35.64	32454.09	31.82	36.04	36.68
0.00096	109194	103841.3	44.68	39831.27	38.06	38.61	42.48
28.14	142587.8	121743.8	55.61	46836.75	43.06	45.66	48.57
12.14	94385.1	91061.66	37.51	32747.88	33.13	34.04	45.22
0.76	121744.3	109137.4	55.48	45992.26	42.27	35.98	39.88

Appendix 13 monazite

326CE1	NIST612S	NIST612T	NIST612U	NIST612V	NIST612W	NIST612X	NIST612Y
28797.64	*********	*********	57340.59	*********	55796.56	57950.66	62648.22
5678.47	*********	*********	17755.41	*********	14269.4	14596.69	15316.23
0.015	15435.49	12569	5.31	4759.81	5.23	5.19	5.32
1.02	36851.8	27469.62	10.89	10732.51	12.84	13.18	13.08
0.55	31859.76	31244.49	17.53	12687.76	10.81	11.38	12.13
0.18	121272.4	103595.3	38.39	48011.72	40.35	34.3	44.56
1582.72	134477.2	124130.9	51.77	51772.75	48.83	46.86	98.26
20862.98	107780.8	97711.09	21.76	57487.23	392.04	46.65	34.76
20801.96	93367.38	478571	71.5	309285.8	65.76	50.33	66.98
0.032	42355.59	42665.6	17.93	18334.42	15.42	15.44	16.76
0.048	24586.92	22955.43	10.89	9627.55	7.96	7.81	8.1
585.57	85429.66	83234.83	30.71	28641.87	27.6	24.68	30.14
10.89	71243.13	78706.22	34.26	39867.15	29.98	32.88	30.79
0.38	39976.08	33025.2	15.04	13102.73	13.48	12.47	15.39
44.55	76917.91	77756.58	30.02	31092.09	28.62	29.62	31.21
0.0048	33800.4	34034.85	14.61	13637.29	13.51	12.23	12.25
44.49	15363.48	11576.97	5.43	6416.61	4.7	4.76	4.97
59.33	5183.6	3623.64	1.73	3833.37	1.43	1.51	1.4
1600.52	854154.4	90445.41	20.96	32795.61	14.9	13.28	15.75
266.89	59227.48	56216.78	22.5	23797.31	19.4	21.6	21.83
1266.37	1101517	9026579	379.72	47653.56	41	38.15	39.98
23.19	39265.73	107677.5	16.46	13382.86	24.86	32.1	14.41
2.47	25757.42	26275.5	9.34	8493.17	7.83	8.05	9.51
5.45	32594.99	33637.05	12.97	12555.69	12.4	12.27	13.6
0.11	10355.04	10089.07	4.37	3966.67	4.01	4.15	4.44
0.44	13981.43	10749.89	5.03	4853.05	4.28	4.17	4.55
0.066	13573.6	12526.51	5.08	5178.13	4.85	5.29	5.16
0.21	15262.01	14736.44	6.84	6306.15	5.41	5.9	6.22
0.022	13459.45	11880.6	4.95	4557.7	4.31	4.67	5.23
0.18	18320.28	17353.46	7.35	6493.96	6.73	6.96	7.28
0.018	12363.76	11783.69	5.03	4739.79	4.35	4.61	4.81
0.003	11563.45	10006.64	4.38	3986.16	3.88	4.5	4.58
0.00056	13520.47	12564.67	5.65	5047.95	4.88	5.06	5.61
17.72	91297.37	79007.7	36.65	31294.5	29.17	31.37	33.82
17.39	137657.6	135071.3	56.59	50242.69	51.68	53.96	72.86
0.2	32555.86	29394.7	15.21	12731.05	11.85	10.22	11.46

326CE1	NIST612S	NIST612T	NIST612U	NIST612V	NIST612W	NIST612X	NIST612Y
13.5	642943.3	653656.2	260.97	227250.7	191.05	174.36	237.1
9.98	472241	1046114	219.81	164409.1	132.67	163.57	167.56
0.012	507.54	1056.98	0.223	214.97	0.199	0.146	0.24
0.12	3058.56	5133.49	1.01	2448.99	1.3	1.14	0.851
0.00385	314.31	891.47	0.117	108.36	0.0825	0.0809	0.0831
0.166	8354.52	6860.53	2.96	2805.8	2.15	2.56	2.89
0.0254	1082.97	1062.9	0.412	386.4	0.327	0.289	0.369

Appendix 13 monazite

0.175	8009.37	5940.62	2.96	2582.83	2.13	1.95	2.42
0.453	20997.72	15235.35	8.22	6935.44	5.21	5.39	5.7
0.0234	1063.58	2168.59	0.484	371.42	0.264	0.212	0.26
0.00196	156.66	625.58	0.0282	48.05	0.038	0.0383	<0.00000
0.00131	66.59	924.34	0.0381	39.87	0.04	0.0738	0.0319
0.00235	119.63	694.77	0.0344	41.65	0.0209	0.0194	<0.00000
0.00441	<0.00000	1125.12	0.0643	54.99	0.039	0.051	<0.00000
0.00353	160.12	666.48	<0.00000	<0.00000	0.034	0.0363	<0.00000
0.00068	48.4	493.73	0.0239	16.59	0.0186	0.0108	0.0114
<0.00000	<0.00000	1750.24	<0.00000	<0.00000	0.0852	<0.00000	<0.00000
<0.00000	71.07	556.52	0.0203	17.36	0.0174	<0.00000	0.017
0.00099	35.44	485.31	<0.00000	<0.00000	0.00857	0.0111	0.0118
0.00065	<0.00000	1000.49	0.0132	<0.00000	0.0113	0.0128	0.011
<0.00000	272.64	1040.45	<0.00000	<0.00000	0.0471	0.0869	<0.00000
<0.00000	<0.00000	1102.47	<0.00000	154.52	0.0948	<0.00000	0.0755
<0.00000	53.05	599.02	<0.00000	18.31	0.026	<0.00000	<0.00000
<0.00000	239.61	1063.26	0.097	<0.00000	0.0832	<0.00000	<0.00000
0.00068	48.74	460.87	<0.00000	<0.00000	<0.00000	0.0111	0.0118
<0.00000	144.86	961.45	<0.00000	<0.00000	<0.00000	0.033	<0.00000
0.00125	<0.00000	498.07	<0.00000	18.12	<0.00000	0.0188	<0.00000
0.00209	106.35	934.82	0.0432	<0.00000	0.0263	<0.00000	<0.00000
0.00067	48.24	461.23	<0.00000	20.54	0.0119	0.0135	<0.00000
0.00295	150.18	1092.85	<0.00000	<0.00000	<0.00000	0.0687	<0.00000
0.0007	<0.00000	478.62	0.0143	17.36	0.0174	<0.00000	<0.00000
0.00229	<0.00000	901.02	<0.00000	<0.00000	0.0287	0.0375	0.0398
<0.00000	59.6	585.22	0.0242	<0.00000	<0.00000	0.0096	0.0144
0.00273	195	1124.47	0.058	58.78	0.0494	0.0656	0.0571
0.00152	59.56	498.33	0.0197	<0.00000	0.0119	0.0174	0.0117
0.00067	19.65	409.76	0.0137	6.71	0.00949	0.00872	0.0145

326CE1	NIST612S	NIST612T	NIST612U	NIST612V	NIST612W	NIST612X	NIST612Y
3.87	18049.7	17224.33	6.97	6492.96	6.34	6.37	6.65
2.72	18494.84	18129.28	7.91	6920.97	6.19	6.21	6.42
0.0101	14680.59	12679.03	4.96	4429.64	4.92	4.74	4.84
0.0076	228.68	195.6	0.066	64.52	0.085	0.084	0.084
0.0247	1388.55	1355.67	0.74	531.24	0.45	0.46	0.49
0.00005	37.73	31.87	0.0115	14.12	0.012	0.0097	0.012
0.42	34.67	31.43	0.013	12.64	0.012	0.011	0.023
0.027	0.14	0.12	0.00003	0.07	0.0005	0.00006	0.00004
0.043	0.18	0.96	0.00014	0.61	0.00013	0.0001	0.00013
0	7.2	7.3	0.003	2.98	0.00247	0.00242	0.0026
0.058	29616.08	27637.27	12.81	11213.44	9.16	8.85	9.08
137.62	19641.2	18888.01	6.83	6278.31	5.95	5.24	6.3
6.24	39961.12	43368.68	18.51	21137.62	15.6	16.79	15.44
0.182	18448.36	15099.02	6.71	5753.26	5.83	5.3	6.44
154.52	261680.3	260356.6	98.71	100564.6	91.05	92.69	96.08

Appendix 13 monazite

0.058	445928.4	445756.4	187.73	173338	169.51	151.21	149.59
119.05	33482.17	28803.27	11.92	14534.05	10.82	10.55	11.25
5111.46	277176.2	277176.2	97.47	277176.2	97.47	97.47	97.47
4339.79	2277627	238376.8	54.36	84083.41	37.69	33.14	38.83
3511.46	764840.2	715343.5	281.38	293111.8	235.22	257.85	256.66
1605.88	1373009	*********	458.06	56542.49	47.9	43.87	45.28
271.25	445120.3	1217702	181.46	145350.1	267.55	340.11	150.25
119.19	1206907	1225031	424.67	381686.1	346.91	350.63	409.33
54.93	316069.8	326467.1	122.24	116731.9	113.98	110.73	121.16
18.03	1597490	1607560	662.31	602178.5	601.6	609.22	648.06
10.1	291140.4	238451.8	103.38	100092.5	88.59	83.99	91.83
6.23	1232952	1157527	449.36	457048.4	421.97	450.91	435.02
5.62	391286.6	388370.5	172.21	157592	133.87	142.9	149.4
5.12	3129069	2819813	1123.97	1032615	962.84	1023.42	1134.55
4.51	432358.2	420818.5	169.83	148414.8	153.22	154.88	160.54
4.06	2738930	2674978	1091	1027335	931.05	966.24	998.61
0.045	530606.6	490907.6	199.1	181307.8	177.74	201.31	204.9
0.037	4199771	3993895	1718.41	1531972	1463.83	1484.99	1633.67
7.71	39065.16	33354.45	15.24	12831.99	11.8	12.51	13.31
285.57	2220826	2142627	882.48	770538.3	779.62	800.88	1064.02
62.04	9979040	8945691	4547.5	3769857	3465.03	2949.21	3268.55

Appendix 13 synchysite

GLITTER4.4: Laser Ablation Analysis Results

D:\ICPCHEM\vdc\091210A
Created: Thu Dec 16 11:10:30 2010

All values are reported in ppm

Synchesite internal standard =9.8

GLITTER!: Trace Element Concentrations MDL filtered.

Element	NIST612O	NIST612P	NIST612Q	NIST612R	NIST612S	NIST612T	LGU1	LGS1	LGU2
Ca42	85262.52	85262.52	85262.52	85262.52	85262.52	85262.52	71470.1	70540.99	71470.1
Ca43	89582.73	91719.66	89644.8	86190.14	73287.14	76581.73	74287.55	62846.13	76328.59
Ti47	49.73	51.3	52.03	49.7	39.08	40.19	329.27	92.11	292.97
Mn55	38.42	44.78	38.41	36.48	31.67	36.16	466.69	159.87	1002.25
Fe56	23.39	22.61	180.45	46.75	<3.76	36.88	1875629	1670.67	3559990
Fe57	62.69	85.79	40	42.27	48.32	52.88	3249465	2122.48	6315774
Rb85	33.38	32.17	32.56	32.36	25.87	26.45	7.68	5.57	7.77
Sr88	83.85	96.17	85.58	84.19	56.85	61.97	1070.04	897.33	1811.44
Y89	434.17	47.98	39.2	37.75	23.45	669.92	421.32	10212.68	439.76
Zr90	40.76	42.77	41.79	40.01	24.2	30.02	109.5	33.53	84.64
Nb93	44.18	43.84	42.45	41.85	25.85	32.01	3.98	16.4	9.78
Ba137	44.67	44.64	44.59	41.9	24.08	28.68	299.89	51.27	383.29
La139	46.34	47.31	46.3	45.11	19.45	27.35	232.02	98179.55	185.42
Ce140	47.89	47.78	47.4	45.76	20.41	30.21	31.29	133711.5	31.41
Pr141	44.86	46.24	44.16	44.13	22.56	29.94	36.42	12212.23	28.14
Nd146	40.69	41.14	40.97	40.32	22.43	28.32	144.43	41853.85	117.54
Sm147	41.67	42.53	43.26	41.24	24	31.91	161.9	27473.65	127.9
Eu153	41.77	40.6	41.68	38.94	23.18	27.42	65	9394.4	95.99
Gd157	40.08	41.11	40.82	40.93	28.12	27.73	214.44	20040.58	299.39
Tb159	42.14	43.28	42.43	41.57	24.5	27.87	23.57	1540.38	24.93
Dy163	41.08	42.41	52.02	43.51	26.12	27.2	96.93	4147.23	172.16
Ho165	45.47	45.41	44.07	43.84	25.38	29.69	15.5	451.95	18.1
Er166	99.71	44.14	41.76	42.1	23.86	28.88	36.25	698.96	43.45
Tm169	43.31	44.56	44.14	43.76	27.16	29.51	6.1	70.11	16.24
Yb172	60.91	44.97	43.08	46.35	27.38	30.51	74.69	664.25	45.86
Lu175	45.23	47.01	46.22	45.53	25	29.62	17.05	45.38	7.26
Hf178	42.15	43.61	42.75	42.55	21.59	26.64	2.48	0.82	2.48
Ta181	48.66	49.81	49.07	48.36	24.79	30.74	0.18	0.18	0.33
Pb208	42.5	39.77	41.23	39.16	27.72	33.13	5504.15	134.81	10681.06
Th232	108.93	40.83	141.6	43.32	17.76	24.87	14.7	12617.45	364.46
U238	45.28	42.67	44.39	43.26	21.83	29.63	178.36	23.79	366.3

GLITTER!: 1 sigma error.

Element	NIST612O	NIST612P	NIST612Q	NIST612R	NIST612S	NIST612T	LGU1	LGS1	LGU2
Ca42	2711.46	2715.17	2710.83	2713.66	2706.9	2708.43	2317.16	2237.5	2332.43
Ca43	20631.67	21550.09	21482.73	21067.26	18265.5	19461.91	19261.75	16594.7	20560.28
Ti47	14.6	15.43	15.98	15.64	12.55	13.22	110.55	31.57	102.98
Mn55	7.61	9.06	7.95	7.72	6.86	7.99	105.25	36.82	235.82

Appendix 13 synchysite

Fe56	66.7	65.4	529.3	139.07	6.38	112.81	5815472	5250.88	*********
Fe57	56.53	79.17	37.85	40.95	47.84	53.57	3363632	2247.91	6842653
Rb85	9.64	9.53	9.88	10.07	8.25	8.65	2.59	1.92	2.75
Sr88	33.33	39.07	35.54	35.72	24.64	27.45	484.03	414.49	854.4
Y89	1138.37	128.22	106.74	104.74	66.28	1928.47	1235.14	30483.21	1336.2
Zr90	20.21	21.69	21.68	21.23	13.13	16.66	62.11	19.43	50.15
Nb93	18.54	18.83	18.64	18.8	11.87	15.03	1.92	8.05	4.91
Ba137	24.89	25.48	26.06	25.08	14.75	17.99	192.53	33.68	257.7
La139	34.15	35.72	35.81	35.75	15.79	22.74	197.59	85606.51	165.52
Ce140	66.6	68.26	69.55	68.97	31.6	48.02	51.08	224106.4	54.04
Pr141	27.16	28.67	28.05	28.71	15.03	20.43	25.44	8731.45	20.6
Nd146	22.2	22.96	23.38	23.53	13.39	17.28	90.05	26661.02	76.53
Sm147	20.86	21.76	22.61	22.02	13.09	17.77	92.07	15945.73	75.81
Eu153	20.9	20.77	21.79	20.81	12.66	15.3	37.05	5467.96	57.06
Gd157	15.81	16.57	16.79	17.2	12.06	12.14	95.8	9132.24	139.24
Tb159	21.1	22.15	22.19	22.21	13.38	15.54	13.42	895.43	14.8
Dy163	21.46	22.6	28.26	24.09	14.75	15.65	56.82	2476.14	104.72
Ho165	21.8	22.24	22.05	22.41	13.25	15.84	8.45	251.3	10.28
Er166	73.28	33.13	32.01	32.95	19.06	23.55	30.17	593.4	37.64
Tm169	19.44	20.43	20.67	20.92	13.26	14.71	3.11	36.38	8.6
Yb172	32.68	24.63	24.07	26.43	15.93	18.1	45.2	409.75	28.85
Lu175	24.63	26.16	26.28	26.44	14.83	17.94	10.55	28.64	4.68
Hf178	25.94	27.45	27.52	28	14.52	18.32	1.75	0.59	1.83
Ta181	29.49	30.89	31.13	31.39	16.46	20.88	0.13	0.13	0.25
Pb208	15.85	15.23	16.22	15.83	11.5	14.12	2409.34	60.59	4928.95
Th232	152.65	58.57	207.93	65.11	27.31	39.15	23.68	20788.47	614.22
U238	28.97	28.05	29.99	30.02	15.57	21.71	134.22	18.39	290.77

GLITTER!: Minimum detection limits (99% confidence).

Element	NIST612O	NIST612P	NIST612Q	NIST612R	NIST612S	NIST612T	LGU1	LGS1	LGU2
Ca42	77.41	78.31	71.11	72.8	170.91	73.26	214.21	34.58	298.43
Ca43	70.75	79.44	60.37	69.94	98.18	50.12	217.01	37.84	268.46
Ti47	0.92	0.894	0.639	0.948	0.488	0.557	2.44	0.415	2.57
Mn55	0.205	0.214	0.189	0.184	1.21	0.702	0.665	0.0957	0.82
Fe56	1.8	1.81	1.63	1.63	3.76	2.59	5.03	0.775	6.65
Fe57	5.13	5.57	4.54	4.55	5.18	4.02	14.26	2.34	20.14
Rb85	0.0111	0.025	0.0228	0.018	0.0191	0.014	0.0453	0.00742	0.099
Sr88	0.0137	0.0195	0.00888	0.0128	0.00675	0.00853	0.0674	0.00776	0.0533
Y89	0.0101	0.0143	<0.00000	<0.00000	0.00693	0.00617	0.0486	<0.00000	0.0382
Zr90	0.0315	0.0224	0.0204	0.0293	0.022	0.0278	<0.00000	0.0207	0.087
Nb93	0.0265	0.0119	<0.00000	0.0156	<0.00000	0.0148	0.0337	<0.00000	0.0463
Ba137	<0.00000	0.0757	<0.00000	<0.00000	0.0372	<0.00000	<0.00000	0.0431	0.21
La139	<0.00000	0.0111	0.00717	0.0103	0.00548	<0.00000	0.0317	<0.00000	0.0309
Ce140	0.00625	<0.00000	0.00579	0.00591	<0.00000	<0.00000	0.0367	0.003	<0.00000
Pr141	0.00895	0.00521	<0.00000	<0.00000	0.00363	<0.00000	0.0257	0.0042	0.0289
Nd146	<0.00000	<0.00000	0.0269	0.0386	<0.00000	0.0259	<0.00000	0.0192	0.115
Sm147	0.0674	0.0339	0.0617	<0.00000	0.0234	<0.00000	0.135	<0.00000	<0.00000

Appendix 13 synchysite

Eu153	0.00807	0.0141	<0.00000	0.0106	<0.00000	<0.00000	0.0323	0.00527	0.0627
Gd157	<0.00000	<0.00000	0.0309	<0.00000	<0.00000	0.0296	0.135	<0.00000	0.13
Tb159	0.00485	<0.00000	0.00443	0.0078	0.00674	<0.00000	0.0194	0.00223	<0.00000
Dy163	0.0199	0.0199	0.0313	<0.00000	<0.00000	<0.00000	<0.00000	<0.00000	0.0755
Ho165	0.0102	<0.00000	0.00465	0.00668	<0.00000	<0.00000	0.0144	0.00331	0.0279
Er166	<0.00000	0.0145	0.0186	<0.00000	<0.00000	0.0089	<0.00000	0.00933	0.0554
Tm169	<0.00000	<0.00000	<0.00000	0.00441	<0.00000	<0.00000	<0.00000	0.00309	0.0367
Yb172	0.0402	<0.00000	0.0183	<0.00000	<0.00000	<0.00000	0.0563	<0.00000	0.109
Lu175	0.01	0.00712	0.00647	0.00464	0.00347	<0.00000	<0.00000	<0.00000	<0.00000
Hf178	0.0237	<0.00000	<0.00000	<0.00000	<0.00000	<0.00000	0.0477	<0.00000	0.0925
Ta181	<0.00000	0.00617	<0.00000	0.00572	0.00428	<0.00000	0.0303	<0.00000	0.024
Pb208	0.0325	0.0285	0.023	0.0288	0.0164	0.0204	0.0617	0.0111	0.0897
Th232	0.00806	0.00813	0.00856	0.00974	0.00462	0.00507	0.0134	0.00378	0.026
U238	0.00586	0.00484	0.00627	0.00785	0.00341	0.00217	0.00995	0.00231	0.0239

GLITTER!: Trace element concentrations normalised to chondrite.

Element	NIST612O	NIST612P	NIST612Q	NIST612R	NIST612S	NIST612T	LGU1	LGS1	LGU2
Ca42	6.32	6.32	6.32	6.32	6.32	6.32	5.29	5.23	5.29
Ca43	6.64	6.79	6.64	6.38	5.43	5.67	5.5	4.66	5.65
Ti47	0.076	0.078	0.08	0.076	0.06	0.061	0.5	0.141	0.45
Mn55	0.0131	0.0152	0.0131	0.0124	0.0108	0.0123	0.159	0.054	0.341
Fe56	0.00008	0.00008	0.0006	0.00017	0	0.00013	6.75	0.006	12.81
Fe57	0.00023	0.00031	0.00014	0.00015	0.00017	0.00019	11.69	0.0076	22.72
Rb85	9.67	9.32	9.44	9.38	7.5	7.67	2.23	1.62	2.25
Sr88	7.05	8.08	7.19	7.07	4.78	5.21	89.92	75.41	152.22
Y89	192.97	21.33	17.42	16.78	10.42	297.74	187.26	4538.97	195.45
Zr90	7.36	7.72	7.54	7.22	4.37	5.42	19.77	6.05	15.28
Nb93	117.8	116.91	113.19	111.59	68.92	85.36	10.61	43.74	26.07
Ba137	13.1	13.09	13.08	12.29	7.06	8.41	87.94	15.04	112.4
La139	126.28	128.92	126.15	122.91	53.01	74.52	632.2	267519.2	505.24
Ce140	50.04	49.92	49.53	47.81	21.33	31.56	32.69	139719.4	32.82
Pr141	327.46	337.49	322.35	322.13	164.66	218.56	265.83	89140.37	205.43
Nd146	57.23	57.86	57.62	56.71	31.55	39.83	203.14	58866.17	165.31
Sm147	180.4	184.13	187.27	178.54	103.9	138.16	700.87	118933.5	553.69
Eu153	480.06	466.72	479.05	447.54	266.45	315.21	747.13	107981.7	1103.32
Gd157	130.99	134.36	133.38	133.77	91.91	90.62	700.8	65492.09	978.4
Tb159	726.49	746.15	731.56	716.73	422.49	480.47	406.36	26558.23	429.9
Dy163	107.81	111.32	136.55	114.19	68.57	71.4	254.41	10885.11	451.87
Ho165	534.33	533.62	517.82	515.12	298.2	348.91	182.14	5310.75	212.75
Er166	400.42	177.25	167.73	169.09	95.82	115.98	145.57	2807.08	174.52
Tm169	1216.54	1251.55	1239.96	1229.33	763.02	829.03	171.48	1969.36	456.14
Yb172	245.58	181.33	173.71	186.89	110.42	123.01	301.16	2678.41	184.9
Lu175	1187.15	1233.98	1213.1	1195.05	656.09	777.51	447.48	1191	190.57
Hf178	235.46	243.66	238.84	237.73	120.6	148.85	13.85	4.56	13.84
Ta181	1871.42	1915.88	1887.2	1859.86	953.6	1182.28	6.83	7	12.77
Pb208	11.64	10.9	11.3	10.73	7.59	9.08	1507.99	36.93	2926.32
Th232	2563.11	960.7	3331.76	1019.35	417.79	585.22	345.97	296881.1	8575.62
U238	3711.39	3497.42	3638.87	3545.6	1789.59	2428.87	14619.62	1949.93	30024.26

Appendix 13 synchysite

:7 Wt% CaO

LGT1	LGT2	LGT3	NIST612U	NIST612V	NIST612W	NIST612X
14294.02	15723.42	14294.02	85262.52	85262.52	85262.52	85262.52
15865.59	16977.06	15205.48	90694.3	89379.33	90261.47	90070.74
69.95	126.18	95.04	56.17	57.76	52.38	51.26
98.16	72.24	158.29	39.03	38.65	39.93	40.43
246.71	11447.01	19903.83	24.63	19.58	28.87	81.57
495.77	18658.92	38303.52	51.23	53.56	67.86	41.53
1.82	2.76	2.13	36.28	34.37	35.31	35.15
97.93	74.01	112.29	86.4	86.81	86.24	87.25
2.23	6350.23	6616.98	38.04	39.23	38.42	38.05
18.68	64.32	35.17	42.42	41.49	42.57	43.08
0.37	14.51	14.53	43.07	43.68	44.64	45.08
37.16	51.84	38.5	47.54	47.25	45.06	48.24
1.05	310.75	1270.7	48.6	47.98	48.25	48.02
4.53	1451.02	4722.25	50.53	51.04	54.51	52.95
0.26	159.12	448.12	46.22	46.94	47.74	48.16
0.96	687.5	1586.94	43.32	41.59	44.7	43.47
73.57	1025.31	1489.47	45.1	43.39	42.86	44.72
0.54	511.03	712.07	43.78	39.96	40.86	40.5
4.81	2023.2	2376.65	41.69	42.61	42.47	42.35
4.68	339.99	343.02	44.6	43.27	42.82	42.48
6.4	1665.88	1575.9	44.77	40.94	41.19	39.53
0.42	254.63	232.85	45.27	45.01	44.99	45.38
0.2	546.1	476.26	42.76	43.84	43	43.49
0.23	71.06	62.32	44.21	43.38	44	43.56
2.66	400.29	348.55	46.62	43.8	44.39	51.39
0.1	47.88	41.35	44.97	46.01	46.58	45.89
0.5	0.91	3.23	43.36	43.48	43.95	44.54
0.068	0.31	0.106	49.87	50.45	50.38	50.07
1.1	374.53	716.97	44.78	43.69	45.79	48.47
0.97	86452.8	<0.00	41.61	41.17	43.29	44.67
0.79	174.67	339.33	46.88	47.26	47.57	49.36

LGT1	LGT2	LGT3	NIST612U	NIST612V	NIST612W	NIST612X
456.93	503.1	456.5	2712.3	2712.96	2710.63	2710.07
4351.03	4742.98	4326.23	26271.84	26358.29	27092.05	27510.52
25.07	46.22	35.59	21.56	22.65	20.98	20.97
23.58	17.72	39.63	9.98	10.08	10.63	10.97

Appendix 13 synchysite

796.46	37443.43	65957.95	82.67	66.56	99.37	284.27
549.38	21143.47	44376.55	60.79	64.94	84.01	52.56
0.66	1.02	0.8	14.04	13.62	14.32	14.59
47.15	36.37	56.3	44.2	45.29	45.89	47.33
6.89	19982.26	21182.29	123.84	129.89	129.31	130.16
11.31	39.76	22.21	27.35	27.31	28.6	29.53
0.19	7.59	7.77	23.5	24.33	25.37	26.15
25.56	36.47	27.7	34.98	35.54	34.64	37.89
0.96	290.54	1215.58	47.56	48.02	49.38	50.24
8	2630.1	8783.38	96.43	99.93	109.46	109.03
0.2	121.89	351.11	37.04	38.45	39.98	41.22
0.64	466.85	1100.38	30.67	30.06	32.96	32.7
44.48	632.46	937.22	28.95	28.4	28.59	30.41
0.33	316.54	450.11	28.24	26.29	27.42	27.71
2.28	978.49	1171.96	20.96	21.84	22.18	22.53
2.83	210.12	216.27	28.68	28.38	28.63	28.95
3.96	1050.36	1011.4	29.24	27.21	27.84	27.17
0.24	150.48	140.37	27.84	28.22	28.76	29.56
0.18	491.86	437.3	40.02	41.81	41.78	43.03
0.12	39.14	34.99	25.31	25.31	26.15	26.38
1.71	261.44	231.92	31.6	30.23	31.19	36.75
0.066	32.1	28.28	31.36	32.71	33.75	33.89
0.38	0.7	2.52	34.56	35.36	36.47	37.7
0.051	0.23	0.083	39.45	40.75	41.55	42.15
0.52	182.1	357.76	22.93	22.96	24.68	26.8
1.67	152349.2	<0.00	76.62	77.48	83.23	87.73
0.64	146.18	291.52	41.34	42.77	44.18	47.03

LGT1	LGT2	LGT3	NIST612U	NIST612V	NIST612W	NIST612X
21.44	28.6	21.44	90.39	82.71	79.95	73.73
19.99	31.27	20.31	90.7	92.84	72.99	70.79
0.171	0.218	0.24	0.859	0.638	0.926	0.824
0.054	0.0802	0.0591	0.243	0.214	0.2	0.21
0.464	0.637	0.479	1.97	1.82	1.69	1.58
1.44	1.92	1.39	6.15	5.55	4.77	5.19
0.00555	0.00894	0.00939	0.028	0.0294	0.0214	0.022
0.00384	0.00654	0.00558	0.0166	0.011	<0.00000	0.0204
0.00274	0.00849	0.00485	0.0287	0.0155	0.0228	0.0128
0.00887	0.0151	<0.00000	0.0543	0.036	0.0238	0.0212
0.00334	0.00465	0.0091	0.0204	0.0136	0.022	0.0195
0.0262	0.0211	<0.00000	0.0658	0.0618	<0.00000	<0.00000
0.00316	0.00311	0.00231	0.0137	0.00913	0.0148	0.0108
0.0026	0.00257	0.00192	0.00808	0.00762	<0.00000	0.00641
0.00209	<0.00000	<0.00000	<0.00000	0.00853	<0.00000	0.00872
0.00825	0.0115	0.012	<0.00000	0.0335	<0.00000	<0.00000
0.0133	0.0185	0.0193	0.0405	0.0379	0.0355	0.0445

Appendix 13 synchysite

0.00226	0.00702	0.00402	0.00974	<0.00000	<0.00000	0.00759
0.0133	0.0184	<0.00000	0.0699	0.0378	0.0353	0.0313
<0.00000	0.00266	0.00139	<0.00000	0.00772	<0.00000	<0.00000
0.00542	0.0106	0.00555	<0.00000	0.0307	0.0202	<0.00000
0.00142	0.00279	0.00146	0.00611	0.0081	0.00535	0.00672
<0.00000	0.00554	<0.00000	<0.00000	<0.00000	0.03	<0.00000
0.00132	0.00183	<0.00000	<0.00000	0.00751	0.0086	<0.00000
0.00553	0.0109	0.00802	0.0411	0.0222	<0.00000	0.0184
0.00139	<0.00000	<0.00000	0.006	0.00794	0.00525	0.00807
0.00471	<0.00000	0.00485	0.0288	<0.00000	<0.00000	0.0224
<0.00000	0.00241	0.00253	0.0075	<0.00000	0.0132	0.0101
0.00707	0.011	0.00645	0.0333	0.039	0.0276	0.0246
0.00188	<0.00000	0.00137	0.00815	0.00766	0.00718	0.00783
<0.00000	0.0037	0.00233	<0.00000	0.00927	0.00552	0.00698

LGT1	LGT2	LGT3	NIST612U	NIST612V	NIST612W	NIST612X
1.059	1.165	1.059	6.32	6.32	6.32	6.32
1.18	1.26	1.13	6.72	6.62	6.69	6.67
0.107	0.193	0.145	0.086	0.088	0.08	0.078
0.0334	0.0246	0.054	0.0133	0.0131	0.0136	0.0138
0.0009	0.04	0.07	0.00009	0.00007	0.0001	0.0003
0.0018	0.067	0.14	0.00018	0.00019	0.00024	0.00015
0.53	0.8	0.62	10.52	9.96	10.24	10.19
8.23	6.22	9.44	7.26	7.29	7.25	7.33
0.99	2822.32	2940.88	16.9	17.44	17.07	16.91
3.37	11.61	6.35	7.66	7.49	7.68	7.78
0.99	38.69	38.76	114.86	116.48	119.05	120.22
10.9	15.2	11.29	13.94	13.85	13.21	14.15
2.86	846.72	3462.4	132.42	130.73	131.48	130.84
4.73	1516.21	4934.43	52.8	53.34	56.96	55.33
1.91	1161.48	3270.98	337.41	342.59	348.48	351.52
1.35	966.95	2231.98	60.92	58.5	62.88	61.14
318.47	4438.56	6447.93	195.26	187.85	185.53	193.6
6.18	5873.92	8184.66	503.18	459.25	469.67	465.53
15.71	6611.76	7766.84	136.23	139.26	138.79	138.4
80.68	5861.92	5914.17	769.03	746.12	738.26	732.35
16.8	4372.38	4136.21	117.5	107.44	108.1	103.75
4.88	2992.12	2736.15	532.02	528.93	528.73	533.22
0.81	2193.17	1912.7	171.74	176.05	172.68	174.64
6.35	1996.18	1750.43	1241.87	1218.67	1235.83	1223.69
10.74	1614.06	1405.45	187.96	176.6	179	207.21
2.62	1256.62	1085.42	1180.32	1207.56	1222.55	1204.58
2.8	5.08	18.02	242.23	242.88	245.54	248.85
2.61	11.78	4.09	1918.22	1940.2	1937.81	1925.67
0.3	102.61	196.43	12.27	11.97	12.55	13.28
22.77	2034183	0	979.05	968.8	1018.62	1051.03

64.44	14317	27813.92	3842.4	3873.63	3899.53	4046.09

Appendix 13 pyrochlore

GLITTER!: Trace Element Concentrations MDL filtered.												zircon	bad analysis	
Element	NIST612A	NIST612B	NIST612C	813Z1	813Z2	813C1	813C2	813C3	813P1	813Z3	813Z4	813P2	813P3	813P4
Ca42	85262.52	85262.52	85262.52	1786.75	1786.75	385938.5	385938.6	385938.5	57176.08	1786.75	1786.75	1786.75	57176.08	57176.08
Ca43	88641.65	89525.84	90035.25	3208.97	2760.39	611274.3	626725.9	625537.8	118983.7	2794.09	2915.68	3111.73	65700.76	79278.32
Sc45	42.81	43.17	42.55	526.56	123.78	4.36	7.07	5.57	192.01	20.76	38.23	255.06	3.58	32.15
Ti47	49.88	50.66	51.01	2817.84	683.05	0.56	0.27	0.89	11131.64	107.32	201.84	1375.48	132.02	64623.27
V51	41.5	41.06	41.84	8.06	0.94	1.09	15.26	49.75	3914.64	0.28	0.77	1.87	483.08	244217.9
Cr53	43.4	42.38	43.05	<1.54	1.66	1.06	0.76	1.21	<19.63	19.37	32.8	3.34	274.22	86611.09
Mn55	36.75	37.26	37.95	87.08	49.58	15402.56	12671.87	77249.99	564697.5	381.75	101.39	76.44	41780.58	147340.9
Fe56	61.93	28.61	38.32	3218.09	393.03	5158.11	19792.33	101428.8	*********	89.45	288.56	692.21	136861.3	*********
Fe57	49.29	53.22	50.52	2308.32	278.37	4145.48	24130.45	127254.6	*********	76.55	257.74	619.39	191842.5	*********
Ni60	41.74	39.89	41.05	2	0.21	0.4	1.68	7.34	5943.77	0.124	0.082	0.31	7.87	7255.25
Rb85	33.89	33.44	33.13	0.38	0.111	0.184	0.117	0.112	84.21	0.031	0.053	0.29	0.63	2.51
Sr88	79.3	80.65	80.11	35.48	36.38	2881.15	2928.72	9034.68	21702.99	14.49	19.24	252.87	2951.95	3078.08
Y89	40.36	39.93	39.15	1635.97	472.55	120.6	132.83	285.21	815.58	83.1	216.65	988.53	43.24	112.17
Zr90	37.15	37.63	37.55	1642880	401817.6	0.43	4.04	10.52	1891.21	71404.31	134848.8	912561.7	4109.01	619.65
Nb93	38.76	38.13	38.09	351.7	192.72	3.15	12.55	101.89	176197.7	63.26	96.81	1888.93	2528.43	199686
Cs133	44.28	43.59	44.56	<0.0087	0.029	0.037	0.0067	0.079	10.74	0.0031	0.00108	0.0161	0.0149	3.7
Ba137	39.46	39.85	39.12	8.9	3.05	8.93	19.22	7561.1	2706.2	8.2	6.76	14.13	5789.11	909.05
La139	37.23	37.48	37.11	10.63	1.84	83.93	210.37	74.58	2609.28	1.68	3.66	10.87	40.41	1364.84
Ce140	40.18	40.47	41.19	186.61	20.76	218.29	404.15	177.75	5497.91	3.18	16.78	104.6	69.2	1884.61
Pr141	38.41	39.71	38.88	18.78	2.92	28.52	42.72	20.9	769.97	0.77	2.23	6.23	10.07	209.51
Nd146	36.64	38.25	37.77	130.38	20.55	86.19	154.55	87.13	2743.54	4.79	12.83	35.18	38.41	643.35
Sm147	39	39.73	38.75	54.85	11.21	18.26	27.04	24.14	428.56	2.7	7.28	18.23	8.61	97.39
Eu153	35.45	37.28	35.59	21.58	5.19	5.83	8.24	9.03	106.37	1.17	3.06	7.62	2.88	19.33
Gd157	39.05	39.49	38.93	80.15	20.37	18.3	24.85	33.4	276.57	3.78	10.47	31.34	8.67	49.14
Tb159	37.21	37.9	37.04	17.08	5.21	2.96	3.88	5.13	39.1	0.95	2.45	8.47	1.37	7.77
Dy163	37.22	37.91	37.61	169.27	52.17	20.44	24.54	36.82	231.67	9.03	23.37	97.39	9.11	32.19
Ho165	39.33	40.29	38.44	48.18	14.71	4.28	4.98	7.67	46.3	2.58	6.57	31.09	1.75	6.6
Er166	39	39.71	38.26	195.79	58.52	13.09	15.3	23.58	138	10.57	26.73	137.71	5.26	16.29
Tm169	39.75	39.31	38.13	43.34	12.7	1.99	2.36	3.47	24.09	2.38	5.99	32.13	0.73	3.06
Yb172	42.83	42	40.36	381.19	111.43	13.25	15.86	23.46	165.35	21.33	52.8	294.12	4.77	13.63
Lu175	39.87	39.41	38.56	44.18	12.66	1.95	2.4	3.45	23.16	2.63	6.23	34.36	0.68	2.02
Hf178	36.83	36.38	35.55	12621.59	3039.87	0.0056	0.008	0.041	26.56	547.63	921.99	5853.57	38.91	28.16
Ta181	42.2	41.31	41.28	2.16	1.19	0.0082	0.074	0.038	497.91	0.106	0.56	16.2	5.93	1427.97
Pb208	45.92	40.92	40.35	33.6	9.43	14.96	17.38	167.37	7989.51	1.68	5.24	31.86	46.96	2091.44
Th232	36.35	35.8	35.23	726.91	162.78	0.6	1.48	0.24	391.65	28.91	97.61	402.17	2.78	420.94
U238	39.97	38.74	39.77	32.14	7.91	0.34	2.87	20.57	408.38	1.95	4.21	53.63	7.44	871.83

Appendix 13 pyrochlore

mixed analysis	GLITTER!: Trace Element Concentrations MDL filtered.									mixed analysis				
813P5	Element	813Z5	813Z6	813C5	813C6	NIST612D	NIST612E	NIST612F	NIST612G	813P6	813P7	NIST612H	NIST612I	NIST612J
57176.08	Ca42	1786.75	1786.75	385938.5	385938.5	85262.52	85262.52	85262.51	85262.52	57176.08	57176.08	85262.52	85262.52	85262.52
422899.8	Ca43	2852.59	2797.44	590995.5	572548.9	82323.2	79364.27	81293.11	78952.76	92924.27	153802.8	82564.05	76076.16	75872.88
152.21	Sc45	86.34	27.07	5.07	6.32	39.58	38.98	38.65	37.77	7.21	57.14	40.11	37.36	37.51
83046.39	Ti47	461.74	142.1	2.18	3.93	48.9	44.02	44.95	43.23	2583.88	50161.16	46.83	42.58	43.9
124069	V51	2.5	1.21	4.32	13.8	37.92	36.43	37.45	36.3	8039.25	230571.6	36.31	33.17	33.78
29960.71	Cr53	171.97	0.143	4.8	5.1	39.9	41.75	25.89	37.97	353.73	7036.1	40.3	34.82	35.87
85552.12	Mn55	56.57	44.4	10072.52	20044.52	95.17	34.38	31.42	62.68	13773.67	1252755	30.85	27.58	27.52
*********	Fe56	650.83	786.83	6974.61	9429.37	175.93	65.61	167.16	14.2	2834609	*********	35.43	70.79	17.2
*********	Fe57	655.63	827.28	10768.89	15050.32	91.19	178.15	68.65	45.52	4611009	*********	49.61	40.14	29.54
1792.98	Ni60	1.68	1.27	0.69	12.31	36.1	36.03	36.84	34.18	93.01	904.3	36.1	32.61	33.52
25.43	Rb85	0.145	0.153	0.056	0.152	30.13	28.66	31.14	28.71	8.49	11.69	29.82	27.6	27.11
62684.48	Sr88	42.12	38.48	1869.81	2703.34	72.95	73.45	73.77	68.08	855.33	75905.42	71.81	68.61	67.21
1507.86	Y89	688.74	164.06	143.15	124.67	36.04	36.26	37.38	34.54	46.96	379.92	36.51	35.7	35.07
12061.78	Zr90	338186.2	104986.6	1271.38	933.2	38.64	33.08	35.26	31.32	102.74	1797.93	33.37	32.36	32.47
1053158	Nb93	308.22	29.76	16.1	146.85	34.81	72.47	35.6	32.82	38087.52	455462.8	33.36	31.52	32.02
22.82	Cs133	0.0068	0.0044	0.181	0.073	40.77	39.12	39.25	36.73	0.55	26.8	39.05	36.27	35.82
6537.39	Ba137	8.66	3.4	18.5	643.87	35.86	36.29	36.98	34.17	997.52	101537.8	36.09	34.25	33.1
1896.06	La139	3.9	5.99	136.35	242.56	34.37	33.91	35.57	32.5	147.1	1326.94	34.42	32.73	32.33
8080.72	Ce140	33.99	15.75	304.9	448.17	36.57	36.23	37.82	34.21	212.79	3167.09	36.09	33.45	32.85
834.5	Pr141	3.38	1.72	31.77	44.05	36.18	34.93	36.38	32.81	38.82	271.65	35.84	33.82	33.02
2975.59	Nd146	23.98	8.81	127.42	150.6	33.77	32.46	34.34	30.56	135.94	917.04	34.52	31.53	30.88
742.26	Sm147	14.78	3.55	28.24	26.33	34.8	33.82	36.18	32.35	27.29	182.78	35.6	32.54	32.46
197.81	Eu153	6.28	1.49	8.1	8.03	35.1	31.58	33.23	30.6	7.16	53.06	33.14	30.91	30.68
497.73	Gd157	26.64	6.49	24.4	23.6	34.42	33.98	35.44	32.95	18.26	153.34	35.57	33.98	33.12
76.84	Tb159	6.94	1.65	6.93	3.8	34.76	33.45	35.65	32.3	2.1	25.02	36.09	33.46	33.19
479.51	Dy163	72.42	17.24	25.61	23.71	34.52	32.61	35.88	32.91	14.06	137.54	35.67	33.36	32.64
76.82	Ho165	21.63	5.16	5.18	4.61	37.15	34.84	36.87	34.46	2.81	25.52	38.2	35.26	35.41
254.31	Er166	88.26	20.69	15.79	13.65	36.21	34.2	36.96	33.68	6.58	72.09	38.17	34.71	34.78
34.87	Tm169	19.21	4.39	2.28	2.14	36.43	35.16	36.8	33.6	0.86	9.28	37.7	35.09	34.81
205.7	Yb172	164.16	38.18	15.41	14.25	37.59	36.67	38.52	36.3	5.81	58.8	42.65	36.8	36.62
29	Lu175	18.81	4.5	2.26	2.09	35.9	35.46	36.94	33.95	1.01	6.43	37.72	35.25	35.21
317.45	Hf178	2346.54	828.45	7.75	5.25	33.23	32.56	33.95	31.46	1.82	36.32	34.17	32.95	31.91
4261.66	Ta181	1.2	0.206	0.022	0.0244	37.62	37.02	38.5	36.01	7.17	147.34	39.35	37.54	36.4
2116.62	Pb208	15.03	2.98	11.26	28.32	38.11	38.24	27.6	35.78	120.59	3550.06	37.82	34.07	34.12
1991.67	Th232	267.85	48.94	1.36	4.77	243.33	63.74	31.25	30.79	27.44	472.25	31.87	30.47	29.76
8352.35	U238	9.12	3.52	0.72	1.96	35.26	34.3	34.58	33.75	7.4	938.12	35.43	32.27	32.52

Appendix 13 pyrochlore

GLITTER!: Trace Element Concentrations MDL filtered.

NIST612K	NIST612L	NIST612M	NIST612N	Element	326M1	326M2	326M3	326C1	326C2	326L1	326L2	326L3	326L4	NIST612O
85262.51	85262.52	85262.52	85262.52	Ca42	120069.8	120069.8	120069.8	385938.6	385938.5	122070.9	122070.9	57604.91	107062.2	85262.52
128739.8	115822	116867.7	118081.7	Ca43	493363.4	403117.4	325212.4	350113.9	357423.9	110458.3	112713.1	49600.39	88323.2	120458.5
57.52	54.39	52.01	54.72	Sc45	92.19	30.85	51.79	0.241	0.29	3.76	2.79	0.038	0.32	55.47
62.83	68.64	73.49	64.68	Ti47	184395.7	41478.72	21732.15	<0.58	0.62	98.09	121.89	4	1.39	69.3
57.96	59.66	63.59	60.83	V51	13155.87	7708.71	2916.69	0.44	1.63	56.43	79.87	3.72	12.96	57.27
63.62	70.32	82.2	78.07	Cr53	<261.88	<174.03	<129.81	<1.08	<0.93	1.54	1.92	2.12	<0.43	62.39
46.12	50.32	49.65	50.19	Mn55	13020.89	6894.32	3069.42	7508.54	7233.9	384.19	1410.26	816.85	3012.96	48.29
150.11	50.07	242.4	24.2	Fe56	978313.2	974384.3	429999.4	2937.6	2906.5	13942.46	30633.38	1700.51	10875.55	103.87
127.77	49.89	59.66	68.4	Fe57	1277182	1261852	589710	3714.32	3729.14	24365.19	57050.04	2148.69	22441.62	135.59
56.66	63.5	62.14	65.48	Ni60	542.32	14.56	<10.59	0.37	0.43	0.68	0.23	0.117	0.142	55.04
46.1	50.58	50.36	50.48	Rb85	65.35	188.64	70.81	<0.0200	0.089	0.42	0.91	0.072	0.039	43.86
100.7	104.34	105.14	103.2	Sr88	284718.9	234827.1	173832.4	13058.77	11187.75	6115.01	5387.88	1777.64	906.08	110.12
50.21	47.39	365.06	50.69	Y89	60492.21	41150.59	36563.42	51.94	64.42	836.64	776.13	144.75	49.44	49.06
48.47	77.86	43.44	44.93	Zr90	2540.4	1133.65	1311.37	0.04	0.067	835.6	529.6	3.19	1.3	40.66
46.17	49.24	49.81	51.58	Nb93	37273.91	7976.27	3502.01	0.138	0.43	672.62	1043.09	9.46	5.11	45.08
63.55	69.05	67.44	66.04	Cs133	<2.13	7.33	35.31	0.0048	<0.0057	0.31	0.096	0.0173	<0.0022	58.69
51.47	55.81	48.06	52.37	Ba137	186629	163774.6	131705.4	216.92	194.58	14.7	18.7	21.51	30.43	51.09
46.65	47.11	45.8	47.47	La139	**********	**********	**********	29.48	21.98	288961.1	244814.2	22596.46	6632.27	1072.74
53.08	51.25	54.41	55.8	Ce140	**********	**********	**********	82.47	62.95	367680	315751.2	30944.98	14686.19	2016.99
47.99	52.46	49.94	52.34	Pr141	8097405	5800246	4695195	12.32	9.88	36691.08	31347.63	3139.72	1231.03	46.02
45.81	43.43	45.48	46.83	Nd146	**********	**********	**********	56.27	46.3	101274.2	85579.05	9002.11	4129.92	42.72
47.69	45.06	46.03	46.53	Sm147	2540871	1714245	1446001	14.58	12.29	5476.35	4582.13	701.46	151.26	59.04
45.64	46.43	47.11	47.21	Eu153	409272.8	268349.8	241579.5	4.68	4.22	721.57	621.31	95.25	20.66	45.29
49.36	45.18	46.1	78.35	Gd157	790823.6	533881.4	457791.2	14.01	12.97	1261.08	1091.23	169.62	40.31	46.94
47.6	44.36	43.18	45.17	Tb159	31172.21	20846.98	18763.29	1.89	1.98	68.99	61.64	9.02	2.67	45.17
48.51	44.47	44.46	47.86	Dy163	64054.82	44197.68	39259.11	11.14	13.16	224.91	199.62	32.77	12.1	43.88
48.66	47.9	46.38	48.53	Ho165	4509.66	3057.53	2626.17	2.04	2.63	28.42	25.64	4.9	2.13	47.7
52.02	47.49	46.05	46.81	Er166	5828.07	3995.74	3629.43	5.42	7.16	61.53	54.95	11.56	5.83	66.07
49.75	46.57	46.63	48.34	Tm169	183.18	112.58	113.87	0.8	1.12	7.19	6.31	1.3	0.75	47.25
54.29	50.58	50.3	52.65	Yb172	463.06	357.03	365.93	4.99	8.21	45.18	37.86	7.64	4.36	52.38
50.84	46.79	45.57	48.09	Lu175	26.86	22.5	24.25	0.84	1.22	5.72	4.96	0.78	0.63	48.3
46.47	42.9	43.15	44.74	Hf178	24.62	20.12	20.51	0.011	0.0152	1.69	1.72	0.0115	<0.0049	44.63
55.02	51.36	51.57	51.68	Ta181	55.78	15.14	8.42	<0.0045	0.0012	0.107	0.116	0.083	0.0042	52
63.65	73.02	71.43	74.58	Pb208	64255.55	49302.03	36554.23	4.64	4.23	70.6	114.02	20.56	41.46	67.13
43.68	41.19	38.95	40.92	Th232	2195094	1620489	1294681	0.1	0.052	1864.94	1580.59	134.74	77.13	50.21
57.01	54.06	58.7	62.09	U238	467.39	661.3	1059.97	0.12	0.149	149.38	134.1	54.86	14.72	53.9

Appendix 13 pyrochlore

					bad analysis	GLITTER!: Trace Element Concentrations MDL filtered.							
NIST612P	NIST612Q	NIST612R	326L5	326L6	326CE1	Element	NIST612S	NIST612T	NIST612U	NIST612V	NIST612W	NIST612X	NIST612Y
85262.52	85262.52	85262.52	121499.2	82190.62	2144.1	Ca42	85262.52	85262.52	85262.52	85262.52	85262.52	85262.52	85262.52
110372.3	113894.2	105144	169276	67241.41	1819.1	Ca43	106543.8	110536.2	120373.6	114307.5	105810.2	106907.6	107128.6
49.96	50.98	49.16	1.1	0.094	0.0042	Sc45	52.55	47.97	46.76	45.28	51.93	50.39	49.74
56.96	60.17	57.4	164.14	31.39	0.25	Ti47	63.87	57.84	48.66	51.73	70.22	70.18	68.39
54.12	52.91	51.09	123.73	34.57	0.107	V51	51.83	53.64	73.59	57.11	49.72	52.01	53.07
58.38	58.42	61.44	<1.82	0.81	0.011	Cr53	67.09	60.02	54.02	72.13	61.7	51.71	64.06
40.63	42.7	37.63	57239.92	736.87	55.49	Mn55	39.81	38.17	38.98	41.51	39.77	37.75	75.29
93.01	142.5	327.78	84227.59	2095.76	290.8	Fe56	12.9	12.38	6.85	19.7	138.97	16.65	12
73.12	48.98	138.92	169203.6	2595.87	592.86	Fe57	22.08	121.89	44.72	209.38	45.56	34.73	44.54
49.19	51.66	51.89	3.28	0.27	0.0036	Ni60	51.42	55.22	55.84	61.01	52.44	51.71	53.61
42.17	43.07	41.5	0.88	0.49	0.0102	Rb85	45.25	44.79	51.95	49.44	41.86	40.85	40.71
93.53	95.51	198.45	11049.85	3862.01	81.09	Sr88	99.77	101.61	91.83	91.63	89.99	79.8	93.03
44.83	44.03	45.16	699.18	472.64	0.67	Y89	36.97	42.43	45.17	55.94	42.69	46.27	41.17
41.19	42.4	58.78	22.14	4.78	0.049	Zr90	42.9	37.16	41.26	38.36	40.26	36.82	43.37
44.33	43.92	45.62	969.1	73.01	2.75	Nb93	40.15	42.28	40.02	44.24	41.45	42.53	42.7
57.29	62.1	55.97	0.049	0.175	0.00084	Cs133	56.03	59.43	62.64	62.91	63.82	57.51	55.24
45.76	46.64	48.69	2690.32	22.9	20.08	Ba137	48.69	44.37	45.88	60.75	46.83	46.07	47.6
45.14	45.28	42.1	321124.9	85153.78	92.46	La139	43.22	45.77	40.21	124.17	45.22	45.6	44.19
46.32	57.37	114.21	404428.4	122285.1	212.21	Ce140	961.54	106.75	60.92	102.48	47.65	42.31	48.14
386.5	52.31	45.64	37629.48	12403.86	24.06	Pr141	45.2	44.79	44.04	49.83	41.43	45.82	44.22
1100.09	41.99	60.12	106668.6	37385.05	56.07	Nd146	413.29	3529.77	364.9	48.91	42.91	39.64	39.66
48.6	43.54	63.56	5522.47	2091.97	3.16	Sm147	44.68	129.55	48.26	42	80.12	102.78	44.03
67.67	42.65	41.94	640.57	245.65	0.52	Eu153	45.06	48.45	41.98	40.98	38.58	39.33	44.51
57.3	45.91	49.9	1389.96	400.81	0.84	Gd157	41.56	45.47	42.54	44.11	44.6	43.7	46.34
42.97	44.04	43.29	75.22	23.55	0.051	Tb159	38.7	41.22	42.39	41.81	43.22	44.1	45.42
47.83	44.27	44.26	246.36	90.2	0.187	Dy163	46.4	40.22	43.52	45.72	41.87	40	42.35
43.2	46.81	46.12	29.47	14.11	0.0255	Ho165	43.5	43.2	41.85	46.16	44.08	47.43	44.29
42	46.2	46.81	64.88	33.78	0.067	Er166	40.4	42.42	46.94	46.59	40.94	44.02	44.55
43.81	46.84	45.55	6.6	3.79	0.0088	Tm169	46.49	44.33	44.1	43.95	42.4	45.4	48.73
46.62	48.59	48.75	35.27	20.45	0.054	Yb172	44.53	45.85	46.17	43.76	46.73	47.57	47.73
44.48	47.48	46.01	4.6	2.33	0.0075	Lu175	43.57	45.03	45.84	46.82	43.9	45.9	45.93
40.66	42.09	43.17	0.101	0.266	0.00039	Hf178	39.55	38.72	39.2	38.72	39.27	44.81	44.16
45.39	50.39	49.73	0.088	0.0199	0.00005	Ta181	45.98	46.28	49.71	48.09	47.55	48.61	51.8
58.17	64.01	61.7	1205.31	28.61	1.49	Pb208	65.1	59	67.48	61.84	59	63.23	65.33
36.74	39.27	38.46	1697.57	825.79	0.54	Th232	35.9	36.64	37.66	35.66	37.32	38.61	49.66
50.03	58.03	52.65	327.2	46.19	0.04	U238	55.47	52.78	67.19	60.61	57.83	49.75	53.56

Appendix 13 Xenotime

D:\ICPCHEM\vdc\091210A
Created: Wed Dec 15 12:09:14 2010

All values are reported in ppm

GLITTER!: Trace Element Concentrations MDL filtered.

Element	NIST612F	NIST612G	NIST612H	NIST612J	NIST612K	NIST612M	NIST612N
Ca42	68557.05	883735.4	1107323	1321907	119495.7	1349889	1232068
Ca43	61900.82	797919.2	971278.4	949932.3	109957.4	1202817	1166763
Ti47	27.61	382.18	447.75	463.14	51.91	556.27	437.91
Mn55	26.15	347.64	458.48	436.86	47.82	535.54	496.58
Fe56	41.78	2417.42	388.32	6332.64	48.42	7942.51	4545.45
Fe57	41.98	249.15	815.6	465.25	41.24	963.88	428.99
Rb85	20.88	286.26	326.18	342.09	38.8	400.46	436.56
Sr88	54.97	684.92	706.48	774.09	94.19	870.24	900.81
Y89	38.25	38.25	38.25	38.25	38.25	38.25	38.25
Zr90	24.12	278.48	256.3	309.6	34.67	327.26	341.2
Nb93	25.4	332.77	339.91	382.05	44.49	431.3	464.5
Ba137	22.44	300.26	286.49	337.64	43.37	343.35	400.64
La139	24.67	328.32	259.39	361.84	41.4	334.05	341.5
Ce140	26.95	3687.67	319.05	412.09	50.92	398.59	423.68
Pr141	26.55	350.09	304.71	388.54	45.83	375.13	403.37
Nd146	21.97	302.07	255.95	305.84	39.08	313.27	353.25
Sm147	23.08	318.5	297.26	319	38.25	330.51	329.06
Eu153	23.38	304.92	291.42	329.28	41.22	350.48	372.61
Gd157	22.91	289.73	302.55	348.44	41.27	335.5	338.38
Tb159	25.72	354.97	296.76	382.95	43.29	381.81	406.28
Dy163	23.04	356.17	272.34	328.37	38.65	336.59	348.91
Ho165	27.11	356.66	347.75	405.78	45.34	408.96	407.67
Er166	23.64	370.31	303.19	327.44	40.62	363.16	351.79
Tm169	27.19	360.41	323.69	381.34	44.39	426.84	410.49
Yb172	25.06	435.98	328.8	386.06	44.14	389.17	377.94
Lu175	27.19	361.45	318.48	375.73	44.19	380.99	391.85
Hf178	22.63	291.65	238.83	307.12	37.65	305.93	322.63
Ta181	28.21	367.89	311.26	394.27	47.42	396.86	427.64
Pb208	26.96	401.18	441.64	497.09	54.75	584.62	598.06
Th232	23.98	930.44	405.59	604.28	176.5	586.36	369.81
U238	27.05	370.25	356.43	437.29	51.4	440.54	1120.89

D:\ICPCHEM\vdc\091210A
Created: Wed Dec 15 12:09:14 2010

Xenotime only, using 49.5 wt% Y2O3 as internal standard

GLITTER!: Trace Element Concentrations MDL filtered.

Element	119X1	119X2	119X3	119C1	119C2	119X4	NIST612O
Ca42	587136.4	2065404	771169.8	*********	*********	439179.9	106567.5
Ca43	553689.2	1347703	774239.7	*********	*********	447567.4	107339.7
Ti47	550.46	91924.64	2321.34	*********	7333812	457708.4	53.63
Mn55	4858.08	17978.78	5276.97	*********	*********	5492.4	41.2
Fe56	227310.2	789505.1	247125.8	*********	*********	151889.5	39.46
Fe57	95182.31	471227.2	113735.9	*********	*********	84192.29	54.23
Rb85	240.46	256.29	262.83	327044.9	233614.2	290.65	38.65
Sr88	1771.25	4202	4118.01	*********	*********	2493.1	100.95
Y89	391356.8	391356.8	391356.7	220482.7	220482.7	391356.8	38.25
Zr90	5555.08	18597.31	10605.45	2795410	2042032	32634.78	42.49
Nb93	49.3	9140.18	149.95	70543.81	75464.74	38646.95	49.75
Ba137	436.65	709.09	824.87	7777219	5553839	1356.94	48.28
La139	43.59	75.88	62.47	529576.5	239617.6	129.87	53.54
Ce140	254.27	487.96	355.56	1496117	482405.6	629.18	56.77
Pr141	115.99	229.06	159.06	156507.2	66137.24	237.06	53.02
Nd146	1529.76	3196.24	2190.32	439909.8	227951.3	3013.52	43.29
Sm147	9211.93	15171.99	10697.01	148576.4	86201.95	16618.64	43.55
Eu153	14958.67	20199.03	17118.57	72302.45	55595.43	24206.77	48.32
Gd157	117771	140681.4	132371.7	247197	176427.2	180473.3	44.13
Tb159	51217.84	59298.13	57269.84	64095.41	398417.8	72062.58	51.43
Dy163	432471.8	486839.8	483562.6	2926198	436198.5	597504.5	47.39
Ho165	113147.1	122437.6	123432.1	288336.3	139523.2	149088	55.11
Er166	313326.1	327702.4	336978.2	327292.5	254864.6	401439.5	107.28
Tm169	59469.71	59615.73	62852.49	58753.98	175105.5	73790.3	52.9
Yb172	347611.6	343714.1	359833.1	388118.5	654150.4	428604.7	68.41
Lu175	40884.35	41185.09	43858.27	338746.4	52868.32	50991.37	54.51
Hf178	53.67	137.82	82.17	74111.8	61239.47	222.08	46.64
Ta181	1.94	35.68	3.01	5682.25	3092.32	120.04	57.91
Pb208	1928.41	3254.05	2746.73	354931.4	190526.9	3786.34	52.23
Th232	33860.2	59728.53	51136.72	1255358	*********	75624.11	137.67
U238	2404.46	3449.91	2839.31	314016.4	20697.98	5496.34	56.11

Appendix 13 zircon

D:\ICPCHEM\vdc\141210
Created: Thu Dec 16 11:07:52 2010

Zircons only - internal standard = 65.5 wt% ZrO2

All values are reported in ppm

GLITTER!: Trace Element Concentrations MDL filtered.

Element	NIST612A	NIST612B	NIST612C	813Z1	813Z2	813C1	813C2	813C3	813P1	813Z3	813Z4	813P2	813P3	813P4	813P5	813Z5	813Z6	813C5
Ca42	82848.24	81943.84	82289.89	528.2	2164.93	**********	**********	**********	1833341	12372.52	6575.92	975.57	856880.1	5707153	294553.1	2680.41	8678.25	*********
Ca43	85595.52	85448.15	86225.84	940.39	3311.76	**********	**********	**********	3754230	19001.04	10515.71	1661.07	960233.7	7696404	2112812	4137.26	13093.13	*********
Sc45	41.34	41.19	40.73	154.2	148.37	4070810	702221.5	212650.4	6050.5	141.01	137.71	135.97	52.18	3117.51	759.55	125.08	126.58	1630.55
Ti47	48.04	48.21	48.71	823.16	816.71	520211	26337.07	33828.65	349607.2	726.15	724.01	729.91	1917.1	6230274	411800.4	664.29	659.31	693.99
V51	40.06	39.18	40.07	2.36	1.12	1014835	1517688	1901883	123409.5	1.9	2.79	0.99	7041.54	*********	617426.9	3.61	5.62	1379.49
Cr53	43.1	41.45	42.11	<0.46	2.02	998642.6	76431	46450.7	<619.82	131.41	117.64	1.77	3959.19	8279857	146930.4	244.06	0.65	1500.15
Mn55	35.96	36.12	37.01	26.05	60.87	**********	**********	**********	*********	2686.46	379.21	42.4	635765.8	*********	446723.8	85.91	218	3404941
Fe56	70.48	33.2	45.88	1208.55	617.8	**********	**********	**********	*********	863.77	1494.72	536.13	2928740	*********	*********	1412.13	5539.78	3391201
Fe57	47.37	50.65	48.33	676.46	334.3	**********	**********	**********	*********	521.49	930.61	330.74	2801808	*********	*********	946.19	3846.02	3434212
Ni60	40.78	38.44	39.62	0.59	0.253	375439.1	167729.1	280483.3	186938.1	0.84	0.293	0.165	113.9	695963.1	8836.04	2.39	5.84	216.36
Rb85	32.62	31.84	31.67	0.111	0.133	171605.1	11649.41	4269.44	2655.69	0.212	0.192	0.155	9.21	243.51	126.63	0.21	0.71	17.9
Sr88	77.64	78.01	77.71	10.53	44.15	**********	**********	**********	690329.5	99.22	69.82	135.65	43304.36	299569.4	313553.4	61.08	179.81	599718.6
Y89	38.66	37.86	37.3	477.58	565.53	**********	**********	**********	25806.54	567.42	785.58	531.2	637.02	10989.32	7611.27	1010.46	777.67	46689.19
Zr90	35.99	35.99	35.99	481201	481200.9	399766.9	399766.9	399767	59224.73	481200.9	481200.9	481200.9	59224.73	59224.73	59224.73	481200.9	481200.9	399766.9
Nb93	37.85	36.87	37.02	104.77	235.42	3004110	1275310	3985074	5692782	441.07	358.39	1036.16	38013.47	*********	5422810	461.12	143.78	5351.19
Cs133	42.76	41.61	42.69	<0.00254	0.0349	34943.44	669.78	3009.89	338.27	0.0213	0.0039	0.0086	0.216	357.52	113.25	0.0098	0.0204	57.64
Ba137	37.98	37.94	37.39	2.61	3.65	8338370	1911536	*********	85351.06	55.74	24.35	7.54	84535.42	88149.28	32611.8	12.54	15.87	5933.65
La139	35.61	35.49	35.32	3.1	2.21	**********	**********	2854384	82477.8	11.46	13.27	5.83	593.99	133386.9	9543.63	5.7	28.28	44279.28
Ce140	39.17	39.01	39.87	55.28	25.18	**********	**********	6870859	175245.9	21.86	61.05	56.29	1018.59	184070	40567.93	49.48	73.85	98138.62
Pr141	36.68	37.54	36.94	5.47	3.49	*********	4237620	797758.9	24264.66	5.22	8.05	3.33	147.42	20390.17	4181.92	4.92	8.09	10265.34
Nd146	35.09	36.26	35.98	38.06	24.6	**********	**********	3335382	86717.52	32.66	46.42	18.86	563.93	62777.49	14948.82	34.98	41.5	41252.52
Sm147	37.77	38.05	37.26	16.14	13.51	*********	2704445	927985	13592.4	18.48	26.38	9.78	126.39	9497.08	3723.57	21.52	16.66	9108.34
Eu153	33.89	35.26	33.83	6.28	6.2	5427165	817345.3	344743.1	3351.61	7.98	11.03	4.07	42.19	1880.03	990.65	9.13	7.01	2613.49
Gd157	37.7	37.71	37.32	23.52	24.49	*********	2478971	1281436	8754.8	25.77	37.9	16.79	127.13	4789.21	2496.08	38.78	30.47	7874.98
Tb159	35.68	35.98	35.33	4.99	6.25	2764826	386914.5	196659.5	1237.81	6.46	8.89	4.55	20.2	760.71	387.68	10.17	7.81	2258.85
Dy163	35.75	36.02	35.89	49.48	62.49	*********	2441912	1409300	7321.45	61.57	84.55	52.18	133.73	3140.34	2408.71	105.67	81.19	8294.17
Ho165	37.75	38.26	36.68	14.08	17.62	3999797	495545.8	293693.3	1463.87	17.58	23.78	16.68	25.71	644.77	386.67	31.63	24.35	1682.1
Er166	37.46	37.73	36.52	57.23	70.08	*********	1522106	902290.6	4359.79	72.06	96.66	73.75	77.23	1588.23	1276.91	128.72	97.41	5111.59
Tm169	38.18	37.36	36.4	12.68	15.22	1859503	234933.7	133075	762.55	16.26	21.7	17.26	10.79	299.46	175.79	28.15	20.76	741.99
Yb172	41.22	39.98	38.58	111.58	133.63	*********	1579737	898416	5227.82	145.43	191.03	157.6	70.02	1329.32	1033.14	239.47	179.81	4988.76
Lu175	38.32	37.48	36.84	12.93	15.19	1827530	239655.7	132545.5	734.04	17.95	22.6	18.48	10.06	197.74	146.37	27.58	21.29	736.46
Hf178	35.4	34.61	33.96	3692.94	3644.7	5250.19	800.89	1582.33	840.31	3737.11	3339.29	3140.08	571.9	2751.35	1596.87	3428.74	3908.65	2513.52
Ta181	40.64	39.35	39.49	0.63	1.43	7685.68	7331.07	1459.27	15765.04	0.72	2.05	8.69	87.15	139521.5	21439.36	1.75	0.97	7.13
Pb208	45.42	39.95	39.47	10.04	11.52	*********	1755693	6485931	254937.1	11.55	19.05	17.1	688.43	203216.6	10559.86	21.72	13.87	3590.08
Th232	36	35.19	34.88	221.06	203.41	582739	154557.2	9807.64	13049.56	208.26	374.1	228.82	43.45	43805.68	10695.46	418.68	247.5	472.19
U238	38.68	37.1	38.24	9.46	9.54	318813.4	286750.9	791138.6	12953.03	13.35	15.27	28.75	109.13	84872.09	41808.59	13.23	16.47	231.28

Appendix 14 Mineral crystal sequence in the syenite

Mineral	Primary	Late
zircon		
alkali feldspar		
nepheline		
plagioclase		
aegirine		
biotite		
cancrinite		
sodalite		
amphibole		
pyrochlore		
magnetite		
apatite		
hematite		